Mathematical modeling and simulation of waves in conducting poroelastic media using HDG method

Rose-Cloé Meyer

Thèse de Doctorat

Université de Pau et des Pays de l'Adour
Laboratoire de Mathématiques et de leurs Applications UMR CNRS 5142
Équipe-Projet Makutu INRIA E2S-UPPA CNRS

École Doctorale des Sciences et leurs Applications - ED 211

Rose-Cloé Meyer

Mathematical modeling and simulation of waves in conducting poroelastic media using HDG method

-

Modélisation mathématique et simulation de la propagation des ondes dans des milieux poro-conducteurs

Soutenue le 30 septembre 2021 devant le jury:

Hélène BARUCQ	Directrice de recherche, Inria Bordeaux Sud-Ouest	Directrice
Eric BONNETIER	Professeur, Université Joseph Fourier - Grenoble 1	Rapporteur
Daniel BRITO	Professeur, Université de Pau et des Pays de l'Adour	Président
Henri CALANDRA	Ingénieur de recherche expert, Total Energies	Examinateur
Julien DIAZ	Directeur de recherche, Inria Bordeaux Sud-Ouest	Directeur
Bruno LOMBARD	Directeur de recherche, CNRS	Rapporteur
Christina MORENCY	Professeure, Lawrence Livermore National Laboratory	Examinatrice
Ha PHAM	Chargée de recherche, Inria Bordeaux Sud-Ouest	Co-encadrante

Je tiens tout d'abord à adresser mes remerciements à mes encadrant·e·s qui m'ont permis de réaliser ce travail de thèse; mes deux directeurs de thèse Hélène Barucq et Julien Diaz, et Ha Pham. Je suis très reconnaissante d'avoir pu travailler avec eux·elles et de profiter de leurs compétences complémentaires et de leurs conseils pendant ces trois années, et je les remercie pour leur implication, même à distance.

Je souhaite remercier les membres de mon jury de thèse d'avoir accepté de participer à ma soutenance, notamment les rapporteurs Bruno Lombard et Eric Bonnetier pour leurs commentaires sur mon travail. Je remercie aussi Daniel Brito d'avoir présidé le jury, merci aussi pour les réunions en cours de la thèse. Je souhaite aussi remercier Christina Morency, et Henri Calandra pour leurs conseils.

Je tiens aussi à remercier Steve Pride de m'avoir accueillie à Berkeley, et de m'avoir aidée et conseillée sur mon sujet de thèse.

Je souhaite remercier tous les membres de l'équipe Magique 3D; Izar, Elvira, Justine, Alain, Yder, Victor, de l'équipe Makutu; Sébastien, Florian, Nathan, Chengyi, Aurélien, Margot, Stefano, Julien, Ibrahima, Arjeta, Johan, Nicolas, Sylvie, et les ingénieurs Algiane et Marc pour tous les bons moments que nous avons passé ensemble pendant mon stage et ma thèse. Merci à Vinduja, pour nos longues discussions, nos rigolades et ta gentillesse. Courage pour ta fin de thèse ! Merci à Pierre pour ton aide en fin de thèse, ton amitié, et surtout car sans toi je ne serais pas partie à Pau. Je vous souhaite à tou·te·s beaucoup de bonheurs et de réussites.

Merci à mes ami·e·s qui ont pu se connecter pour ma soutenance, et ceux·elles auprès de qui j'ai pu trouver du soutien pendant les années de la thèse et notamment pendant la crise que nous traversons. Votre amitié et votre présence ont été une aide importante pour réaliser ce travail.

Je tiens aussi à remercier mes parents qui m'ont permis de faire mes études et ma famille m'a soutenue pendant toutes ces années. Merci à mes parents et à mes soeurs Aude et Coralline pour leur présence et leur aide le jour de la soutenance. Une pensée particulière aussi à Lucas, Mathilde, la petite Hanaé, Théo, et Guillaume qui n'ont pas pu faire le déplacement.

Enfin, Mamadou, je ne peux pas exprimer à quel point je te suis reconnaissante. Je te remercie pour ton aide et tes conseils pendant ces années de thèse. Merci pour ta patience, ton soutien sans faille, ta confiance et ta gentillesse.

Contents

List of Figures

List of Tables

General Introduction

The sustainable exploration and exploitation of the natural resources of the Earth are fundamental for the socio-economic development in geothermic exploitation, CO2 storage and oil exploration. Hence, obtaining accurate images of water, mineral and energy sources deep below the surface is a key step for their management and exploitation. The exploration using wave propagation or seismic imaging has been investigated for many years and allows obtaining detailed maps of the Earth's interior using the information carried by the deformations and electromagnetic fields measured at the surface. Classically, for computational reasons, waves propagating in the subsurface are modeled as solutions to the elastic or acoustic equations. However, to improve the accuracy of the simulation, it is now necessary to consider more complex models such as conducting poroelastic media. The goal of this thesis is to develop a new software package based upon advanced numerical methods for simulating waves in porous conducting media. This implies to consider the coupling of the poroelastic wave equations with the Maxwell equations. At the beginning of the thesis, these two problems were not considered by the Hou10ni code developed in the team. Before realizing the coupling of the two physical models, it was therefore necessary to develop a code for each of them.

The shape and form of porous media can vary depending on the size of the pore and the structure of the solid skeleton. Porous media are found in nature (sandstone, volcanic rocks, ...) or can be manufactured (concrete, polyurethane foam, ...) as depicted in [29]. Instead of modeling such media as strongly heterogeneous, homogenization is used to describe the material on a macroscopic scale. Biot's theory [15, 18] describes the solid skeleton according to linear elasticity and adds to this the Navier-Stokes equation for a viscous fluid and Darcy's law governing the motion of the fluid [52]. For simplified linear elasticity, there are one equation of motion and one constitutive law, with the unknowns being the displacement field in solid and the solid stress. In poroelasticity, the added unknowns are the fluid displacement relative to the solid and the fluid pressure. There are two equations of motion, coupled with two constitutive laws. By plane wave analysis, one obtains three types of waves: S waves, fast P waves and slow P waves (Biot's waves). While the first two types are similar to those existing in elastic solids, the existence of a third type of wave with drastically smaller speed adds to the complications already encountered in elasticity.

The propagation of waves into conducting poroelastic media is a physical phenomenon involving mechanical waves interacting with electromagnetic waves. Electrokinetic effects arise from the relative displacement of the fluid in naturally charged porous media with a certain degree of fluid saturation. We focus on two kinds of electrokinetic effects: the seismoelectric effects and the electroseismic effects [105]. In naturally charged, fluid-saturated, porous media, a propagating seismic wave causes pore-fluid flow through deformation of the rock and generates an electrical current. This electrical current induces an electromagnetic field, referred to as a coseismic field, that propagates within the seismic waves. When this coseismic field impiges an heterogeneity (*e.g.*, a contrast in mechanical or electrical properties), an electric dipole is created, triggering an independent EM field [113, 78]. Conversely, an electric field acting on the layer causes the ions to move, which leads to a relative displacement of the fluid and solid frame, and hence a seismic wave propagates in the medium. By their nature, electrokinetic effects are highly sensitive to fluid properties, such as resistivity and dynamic fluid viscosity. The coupling between seismic and electromagnetic fields is natural, the coupling coefficient between seismic and electromagnetic energy is sensitive to permeability, porosity, salinity, and other crucial geothermal reservoir properties. In conducting poroelastic materials, four types of plane waves are sustained, the three types of waves similar to those in poroelastic media: S waves, fast P waves and slow P waves (Biot's waves), and electromagnetic (EM) waves [110]. The difference of speed between the EM wave and the seismic waves (fast and slow P, S) is even greater than the difference between the seismic waves which are indeed propagating much more slowly than electromagnetic waves. This is thus a multi-scale problem of propagation of waves with very different wavelengths, which is very challenging for the numerical representation. The wave propagation in conducting poroelastic media has been modeled by Pride [106, 110] and is expressed as the coupling of Biot's and Maxwell's equations. In this model, the coupling between seismic and electromagnetic fields is non-linearly dependent of the frequency.

This thesis is part of the multidisciplinary Chickpea project, supported by E2S-UPPA, a window of the I-Site label of excellence, of which the University of Pau and Pays de l'Adour is a laureate. The long-term objective of this project

is to demonstrate that Seismo-Electric Effects (SEE) should be taken into account for improving the definition of subsurface imaging. The fundamental goal of this PhD project is to provide a piece of software for simulating in 2D and 3D the electrokinetic equations using a numerical method allowing for hp-adaptivity to address the multi-scale feature of the problem. A bonus objective is the comparison of numerical data with experimental data. Another long-term objective of the project is to apply the numerical method to field experiments, and to use the numerical solver in an inverse problem using Full Waveform Inversion. The inversion is complex and requires a significant effort of development. To our knowledge, the most advanced works on this subject are the thesis of Xue [134], where the author proposes a method to inverse the source in Biot's equations, and the following paper [22] in which the authors study the stability of the inverse problem.

Regarding the numerical approximation of this wave propagation phenomenon, standard finite element methods coupled with time schemes have indeed difficulties to deliver accurate solutions because there is a need of adapting the time step discretization and the mesh size to the wave velocities. The numerical schemes must be able to reproduce in the same simulation waves with very different wavelengths. The size of the cells depends on the propagation velocity and the coverage of waves propagating at very different speeds would inevitably lead to huge computational costs if standard numerical methods are used. For time schemes, the mesh size is set in relation with the smallest wavelength, here the slow longitudinal wave. In addition, the time step depends on the ratio between the mesh size and the largest wavelengths, which is in fact the ratio of the smallest wavelength and the largest wavelength. Here, this ratio is of order 10^{-6}. Most works in time domain thus need to consider approximate equations, using for example quasi-static electromagnetic equations. To prevent the problem of time step, we work in the frequency domain. This also allows for the consideration of a wide variety of parameters which are non-linearly frequency dependent, and to take full account of Pride's equations and the electrokinetic effects. However, the large size of the system of equations increases the computation resources needed, in particular in frequency domain, which raises some linear algebra difficulties that will be described in this manuscript.

For computational methods, we use Discontinuous Galerkin (DG) methods. DG methods have proven their efficiency to solve wave problems in complex media [40, 50]. Besides being easy to implement in a massively parallel environment, they are h-p adaptive, which allows to reduce the computational costs while keeping a high level of accuracy. This is of great interest, particularly since the problem to be solved is multi-scale, combining electromagnetic and seismic wavelengths in the same simulation. Another interesting property is that DG methods are finite element methods usable in tetrahedral meshes, which is also usefull for the case of geophysical media, for example for appropriately capturing (sharp) topography and arbitrarily shaped fine layers, as they occur in realistic geothermal media. The method has been hybridized to Hybridizable Discontinuous Galerkin (HDG) methods in order to reduce the computational costs, costs that can be very high with classical DG discretizations [33, 21].

As previously indicated, the goal of the thesis is the development of numerical methods that are adapted to conducting poroelastic media. The first step has been the implementation of the solution of wave problems in porous media using Biot's harmonic equations. Then, we have developed a method to solve the full electrokinetic equations. This work of development has been carried out in the environment of the software Hou10ni, which already allows for the solution of elastic and acoustic wave problems in heterogeneous media, using Hybridizable Discontinuous Galerkin methods.

The accuracy of the numerical method has then been achieved thanks to the construction of analytical solutions that were not available neither in poroelastic or in conducting poroelastic media. These analytical solutions have been used as reference solutions to perform accuracy assessment.

Moreover, there is a challenging question about the boundary condition to be used for limiting the computational domain. This is in particular the case for the truncation of the computational domain when we consider infinite geophysical domain. In the thesis, we have proposed a low-order radiation boundary condition (RBC) both for poroelasticity and electrokinetic. The development of the RBC has been made using the form of the analytic solutions that we have developed.

Contributions

The contributions of this thesis are the following. First, we have constructed and analyzed analytical solutions in poroelastic and conducting poroelastic media in two dimensions. Those solutions are essential for the validation of the numerical method that we have developed. The results obtained for the poroelasticity are presented in Chapter 2. This is also published in a research report [7]. For the electrokinetic equations, we present the analytical solutions in Chapter 6. Secondly, we have developed a HDG method in two and three dimensions for the poroelastic and electrokinetic wave propagation, which is presented in Chapters 3 and 7 respectively for poroelasticity and electrokinetics. This method has been implemented in the software Hou10ni. We have published the HDG method for poroelasticity in IJNME [11], and an article on the method for electrokinetic effects is in preparation. The results have also been presented at the

AGU conference in 2018. Thirdly, we have built first-order Radiation Boundary Condition for poroelasticity (Chapter 4) and electrokinetics (Chapter 8) in two dimensions. We have studied the performance of this condition by comparing the corresponding numerical solution with an exact solution. In addition, we have implemented the condition in the HDG method, along with Perfectly Matched Layer, and we have compared RBC and PML performances. For poroelasticity, we have presented the results in a research report [10]. We have also implemented the HDG method for Maxwell's equations, see Appendix G. Eventually, we have also used the Inverse Fourier Transform to convert the results in frequency domain into seismograms and electrograms in time domain, see Chapter 9.

Outline

We now present an overview of the content of each chapter of this manuscript. This outline is meant to give a brief insight of the content of the dissertation. This thesis is composed of two parts. The first part focuses on the propagation of poroelastic waves, while the second deals with the electrokinetic waves propagation. The part on the poroelasticity is divided into four chapters. In the last five chapters we consider the electrokinetic coupling. We have also implemented a HDG formulation for time-harmonic Maxwell's equations. This achievement follows former works [85, 102] and since it does not contain any new contribution, we have decided to set it as an appendix of the dissertation (Appendix G).

In Chapter 1, **we present the parameters and the equations of poroelasticity**, which describe the wave propagation in a poroelastic medium. The equations of poroelasticity are given by the linear theory of deformation of a porous medium, called the theory of consolidation, first presented by Biot for the isotropic case in [16, 17]. In our work, we consider principally the **harmonic domain**. After introducing the physical parameters governing the poroelastic equations along with their meaning, we present the expression of the equations of poroelasticity, and propose a nondimensionalization of those equations. Then, we present **the explicit expression of the plane waves sustained in an isotropic poroelastic medium**. This chapter sets a framework for the rest of the developments given in the following chapters.

In Chapter 2, we focus on two-dimensional isotropic poroelastic equations. In this configuration, **we develop analytical solutions** that will be used in order to evaluate the accuracy of the discretization of poroelastic equations by Hybridizable Discontinuous Galerkin method. We first consider the homogeneous poroelastic equations on bounded domains, but also the scattering of plane wave by impenetrable and penetrable infinite cylindrical obstacles (thus with circular 2D cross-section), and a fluid-solid interaction problem in circular geometry. Finally, we present a test using point sources. In addition to the computation of analytic solutions for each considered problem, we go further and propose a definition of outgoing solutions, and **investigate numerically the well-posedness** for interaction problems with and without viscosity among others. The definition of outgoing solution is not covered in literature for poroelasticity. While this notion is well-established for elasticity with the Kudrapdze radiation condition [82], the mathematical analysis focus on bounded domain for poroelasticity, see [22]. Similarly, while the well-posedness of the interaction problem for acoustic fluid-elastic solid is covered in *e.g.* [51, 12, 77], this is not yet investigated for isotropic poroelasticity.

In Chapter 3, we focus on **the numerical simulation of the poroelastic equations using an Hybridizable Discontinuous Galerkin method**. This chapter is published in a reduced form in [11]. The HDG solution methodology relies on the possibility of relating local unknowns at the element level to a so-called hybrid variable defined only on the skeleton of the mesh (i.e., the set of edges in 2D and set of faces in 3D) by the mean of transmission conditions. In this way, the HDG solution is obtained by solving a smaller global system for the hybrid variables and the solution is reconstructed thanks to the solution of local systems in parallel. In two recent works, Fu [57] and Hungria [76] have implemented the HDG solution of poroelastic wave equations. Fu [57] considered the quasi-static Biot equations using a displacement-pressure formulation. Hungria [76] dealt with both the time-dependent and time-harmonic Biot equations using a displacement-stress-pressure formulation. Herein, we consider a formulation of Biot equations governing the frame velocity, the relative fluid velocity, the pressure field, and the solid stress tensor, written in the frequency domain. Our approach is closer to that of Hungria since we consider time-harmonic equations whereas Fu solved quasi-static equations. It is however worth noting that we do not solve the same formulation as Hungria. As an advantage, the first order formulation gives us access to velocities and stress tensor, which are the actual data displayed by experimental acquisition. This is very important if we want to use the code in an inversion loop for characterizing the propagation in the medium. Following Biot's model, we develop and implement an HDG method to simulate harmonic wave propagation in anisotropic poroelastic media in two and three dimensions. We provide a **detailed description of the numerical algorithm and the different steps required for its development**. Our HDG method is validated by comparing with reference solutions constructed in Chapter 2. In our numerical investigation, we show that the method depends on four stabilization parameters that are necessary for the method to

keep an optimal order of convergence $(p+1)$. We also **study numerically the condition number of the global and local problems**, and show that they remain in a good range that maintains stability for the geophysical material in consideration.

In Chapter 4, we extend the HDG formulation of time harmonic Biot's equations developed in Chapter 3 to infinite domains, that is to say, we introduce truncation methods in the HDG formulation. **We construct a Radiation Boundary Condition (RBC) which is obtained from the characterization of outgoing solutions of the 2D isotropic poroelastic equations.** This relation reads as:

$$\begin{cases} \boldsymbol{\tau}\,\boldsymbol{n} + \big(\mathbf{X}_1(\mathbf{u}\cdot\boldsymbol{n}) + \mathbf{X}_2(\mathbf{w}\cdot\boldsymbol{n})\big)\,\boldsymbol{n} + \mathbf{X}_3(\mathbf{u}\cdot\mathbf{t})\,\mathbf{t} = 0\,, \\ \mathrm{p} + \mathbf{X}_4(\mathbf{u}\cdot\boldsymbol{n}) + \mathbf{X}_5(\mathbf{w}\cdot\boldsymbol{n}) \;= 0\,, \end{cases}$$

with $\mathbf{u}$ the solid velocity, $\mathbf{w}$ the relative fluid velocity, $\boldsymbol{\tau}$ the stress tensor and p the fluid pressure. The obtained condition is comparable to Lysmer–Kuhlemeyer (LK) absorbing boundary condition for elasticity that has been investigated in [93]. It is worth noting that the derived RBC can be naturally coupled with HDG, since it resembles the transmission condition of numerical traces.

The performance of this RBC is evaluated in two groups of numerical investigations. In the first one, in the setting of planewave scattering by circular obstacles, we compare how well the reference solution associated to the RBC approximates the restriction of the true outgoing solution on the truncated domain. We have an overall conclusion that our RBC has comparable robustness to LK for elasticity and Sommerfeld condition for acoustic equation, in the sense that the error is less than 10 % for most cases. In the second investigation, the radiation condition is implemented in a hybridizable dicontinuous Galerkin (HDG) formulation. **We also apply perfectly matched layers (PML) on the HDG discretization of the poroelastic equations**. **We then compare the performance of our RBC with the PML technique on different configurations** (Section 4.6.2). PML can be an alternative to the radiation condition, but its performance depends on parameters that are specific to each experiment. If the size of the PML is not large enough, the performance is deteriorated. To obtain better results than RBC, the PML can be taken larger but this raises the degrees of freedom and incurs substantial increase of the computational time, while the gain in accuracy is not considerable.

After introducing the poroelasticity in the first part, the second part starts with Chapter 5 in which we present the principles of the electrokinetics, following Pride's theory, [105, 110]. The geophysical poroelastic materials are neutral media, however, the surface of the solid is usually negatively charged, and the fluid is an electrolyte, with ions in motion in the fluid, attracted by the opposite sign on the solid surface [111, 108, 113]. When a seismic wave propagates, the motion of the fluid in the porous media induces an electric current that creates electromagnetic signal. This is called the seismoelectric phenomenom [129, 79, 78]. The electromagnetic waves generated with a seismic source are composed by a co-seismic electric or magnetic field that propagates at the same speed as the produced seismic waves, and an electromagnetic converted wave generated at an interface between two media with different properties, that propagates at the electromagnetic wave speed. The converted waves are very interesting because they are heavily sensitive to the medium properties, and have potential applications in the detection of interfaces. **We introduce the physical parameters used to describe a conducting poroelastic material**, then **we present the expression of Pride's equations in harmonic domain** both in first and second-order formulation. **We determine the expression of the four kinds of plane waves sustained in a conducting poroelastic material**.

In Chapter 6, **we develop analytical solutions of Pride's equations in two dimensions** for different configurations; a homogeneous bounded domain, the scattering of a plane wave by impenetrable or penetrable obstacles, and the response to a point-source. Following what was formerly done for poroelasticity in Chapter 2, we express the fields in terms of potentials and **we investigate numerically the well-posedness** of the problems by studying the invertiblity of the analytical system. The results of this chapter will play a crucial role in the two following chapters where we validate a HDG formulation for solving Pride's equations in harmonic regime and we construct a low-order radiation boundary conditions for performing regional computations in bounded domains.

The aim of Chapter 7 is to **develop a HDG method to solve Pride's equations in harmonic domain**. We base the proposed method on what has been developed for poroelasticity in Chapter 3 and for Maxwell's equations in Appendix G. We first present the formulation of the HDG method. Then, **we detail the associated discretization in two dimensions, and we provide validations of the numerical simulations**. We also **investigate numerically the well-posedness of the problem**, and the formulation of the HDG method, especially the values of the stabilization parameters used to express the numerical traces. Next, **we describe the discretization of the proposed method in three dimensions**, and we perform numerical tests for the verification of the method.

In Chapter 8, we address the same problem as in Chapter 4 for Pride's equations. **We derive a low order RBC for Pride's equations**. For this, we first obtain an outgoing radiation condition at infinity by using the expression of the unknowns in potentials and the expansions of outgoing solutions given in Chapter 6. Then, when written in circular geometry, this exact condition is approximated to obtain the RBC, assuming the radius of the circular boundary is large enough. The resulting condition reads as:

$$\begin{cases} \boldsymbol{\tau}\,\boldsymbol{n} + \big(\mathbf{X}_1(\mathbf{u}\cdot\boldsymbol{n}) + \mathbf{X}_2(\mathbf{w}\cdot\boldsymbol{n})\big)\,\boldsymbol{n} + \mathbf{X}_3(\boldsymbol{n}\times\mathbf{u})\,\mathbf{t} + \mathbf{X}_4(\boldsymbol{n}\times\boldsymbol{E})\,\mathbf{t} = 0\,, \\ \mathrm{p} + \mathbf{X}_5(\mathbf{u}\cdot\boldsymbol{n}) + \mathbf{X}_6(\mathbf{w}\cdot\boldsymbol{n}) = 0\,, \\ \mathrm{H} + \mathbf{X}_7(\boldsymbol{n}\times\mathbf{u}) + \mathbf{X}_8\,(\boldsymbol{n}\times\boldsymbol{E}) = 0\,, \end{cases}$$

with the solid velocity $\mathbf{u}$, the relative fluid velocity $\mathbf{w}$, the solid stress tensor $\boldsymbol{\tau}$, the fluid pressure p the electric field $\boldsymbol{E}$, and the magnetic field $\boldsymbol{H}$. The relation is comparable to the relation obtained for poroelasticity in Chapter 4. **We investigate the performance of the condition**, by comparison of the associated solution with the outgoing solution that we obtained in Chapter 6. We implement the radiation condition in the HDG method presented in Chapter 7. In addition, we consider Perfectly Matched Layer (PML) to prevent the reflections on the artificial boundaries of the domain. **We also apply PML to the HDG discretization**. Finally, **we perform numerical tests to evaluate and compare the accuracy of the HDG method using the RBC and PML**, see Section 8.6. We study in particular if the PML can absorb all kinds of waves. In the considered configurations, we observe that the PML does not behave correctly for the electromagnetic wave. Indeed, Gao highlights in [61] the difficulty for the PML to absorb both the seismic and electromagnetic waves. This comes from the fact that the wavelengths of the seismic and electromagnetic waves have very different sizes.

The goal of Chapter 9 is to perform numerical experiments as a first step in the comparison between synthetic data and real data obtained in the laboratory. In particular, we want to verify if the developed code can simulate the converted waves created at interfaces. We study two conversions, the first one is the converted seismic wave obtained at an interface with an electromagnetic source. The second is the **converted electromagnetic wave** that appears at the interface when a coseismic wave is reflected. For that, the first step is to obtain the results in time domain. We hence run the code for several frequencies, then we use a Fourier transform to go to time domain, and we detail the method to obtain the results in time domain. We have succeeded in numerically reproducing the converted waves associated with an electroseismic case and a seismoelectric case.

Part I

Poroelasticity

Chapter 1

Introduction to poroelasticity

In this chapter, we present the parameters and the equations of poroelasticity, which describe the wave propagation in a poroelastic medium. A porous medium is a material composed of a solid frame, and pores filled with a fluid. The equations of poroelasticity are given by the linear theory of deformation of a porous medium, called the theory of consolidation, first presented by Biot for the isotropic case in [16] [17]. The Biot's model can be used when the following hypotheses are satisfied :

- The size of the pores is small in comparison with the wavelength.
- The displacements in the solid and fluid phases are small.
- The fluid phase is continuous.
- The solid frame is elastic.
- The thermo-mechanical effects are neglected.

In the following, we first introduce in Section 1.1 the physical parameters needed to study poroelastic equations and their meaning. In Section 1.2, we introduce the poroelastic equations in time and in frequency domain, and propose a nondimensionalization of those equations in Section 1.3. We present in Section 1.4 the boundary conditions used for harmonic poroelasticity. Then, Section 1.5 gives the explicit expression of the plane waves sustained in an isotropic poroelastic medium. We finally give properties of the slownesses in poroelastic media in Section 1.6.

1.1 Physical Parameters

We define the *porosity* of a material as the ratio of the fluid volume in the material and its total volume

$$\phi = \frac{V_f}{V_T}\,. \tag{1.1}$$

The geometry of pores is described in terms of *tortuosity* $\mathfrak{t}$. The tortuosity is a measure of the deviation of flow paths in the pores. The fluid is defined by the *incompressibility modulus* $\mathrm{k_f}$, the *fluid density* ρ_f, the *viscosity* η and the *permeability* κ_0. The *average density* of a poroelastic medium is defined as

$$\rho_a \;:=\; (1-\phi)\,\rho_s \;+\; \phi\,\rho_f\,. \tag{1.2}$$

We now have to introduce different notations, depending on whether the material is isotropic or not. An isotropic material has material parameters and properties that are the same in all directions. Conversely, the properties of an anisotropic material are directionally dependent.

Anisotropic material For an anisotropic poroelastic domain, the frame is described by the stiffness tensor $\mathbf{C}_{\mathrm{fr}}$ with components C_{ijkl} for $i,j,k,l = 1,2,3$, $\boldsymbol{\alpha}$ the effective-stress matrix, and M the fluid-solid coupling modulus, with all three given in Pa.

We can use Voigt notation, (cf [26], p13), to express the components C_{ijkl} using two indices I and J, for $I,J = 1,...,6$. The pairs of indices (i,j) or (k,l) are replaced by one capital index. The lowercase indices are connected to the capital ones by the following relations:

$$(1,1)\to 1\,,\qquad (2,2)\to 2\,,\qquad (3,3)\to 3\,,\qquad (2,3)\;=\;(3,2)\to 4\,,\qquad (1,3)\;=\;(3,1)\to 5\,,\qquad (1,2)\;=\;(2,1)\to 6\,.$$

In two dimensions the size of the stiffness tensor $\mathbf{C}_{\rm fr}$ is reduced, the lowercase indices i, j, k, l are taken between 1 and 2, and the capital indices I, J, are taken as $I, J = 1, 2, 3$. The connection between the indices is the following:

$$(1,1) \to 1\,, \qquad (2,2) \to 2\,, \qquad (1,2) \;=\; (2,1) \to 3\,.$$

In the general case, $\boldsymbol{\alpha}$ is given as:

$$\boldsymbol{\alpha}_I = 1 - \frac{C_{I1} + C_{I2} + C_{I3}}{3\mathrm{k_s}}\,, \qquad I = 1,2,3\,, \qquad \boldsymbol{\alpha}_4 = -\frac{C_{14} + C_{24} + C_{34}}{3\mathrm{k_s}}\,,$$
$$\boldsymbol{\alpha}_5 = -\frac{C_{15} + C_{25} + C_{35}}{3\mathrm{k_s}}\,, \qquad \boldsymbol{\alpha}_6 = -\frac{C_{16} + C_{26} + C_{36}}{3\mathrm{k_s}}\,,$$

where we have used Voigt notation; and the fluid-solid coupling modulus M is expressed as (see [26] [eqs. 7.137-7.140]):

$$M = \frac{\mathrm{k_s}}{1 - \frac{\mathrm{k}^\star}{\mathrm{k_s}} - \phi(1 - \frac{\mathrm{k_s}}{\mathrm{k_f}})}\,, \qquad \text{where} \quad \mathrm{k}^\star \;= \frac{1}{9}\left[C_{11} + C_{22} + C_{33} + 2\left(C_{12} + C_{13} + C_{23}\right)\right]\,.$$

Isotropic material In the case of isotropic poroelastic medium, the solid frame is defined by the *incompressibility modulus* $\mathrm{k_s}$, the *solid density* ρ_s, the *uncompressibility drained modulus* $\mathrm{k_{fr}}$, the *shear modulus* $\mu_{\rm fr}$ and the *consolidation parameter cs*. The solid skeleton has compressibility and shearing rigidity, and the fluid can be compressible. To describe a porous medium, we use a homogenization on the fluid and solid phases, to obtain an equivalent medium. For $\bullet$ = f, fr and s, corresponding respectively to the fluid, the frame, and the solid, the relation between the bulk modulus $\mathsf{k}_\bullet$ and the Lamé parameters $\lambda_\bullet$, $\mu_\bullet$ is

$$\lambda_\bullet = \mathrm{k}_\bullet - \tfrac{2}{3}\mu_\bullet \quad .$$

In this case, the stiffness tensor $\mathbf{C}_{\rm fr}$ is expressed in three dimensions as:

$$\mathbf{C}_{\rm fr} \;=\; \begin{pmatrix} \mathrm{k_{fr}} + \frac{4}{3}\mu_{\rm fr} & \mathrm{k_{fr}} - \frac{2}{3}\mu_{\rm fr} & \mathrm{k_{fr}} - \frac{2}{3}\mu_{\rm fr} & 0 & 0 & 0 \\ \mathrm{k_{fr}} - \frac{2}{3}\mu_{\rm fr} & \mathrm{k_{fr}} + \frac{4}{3}\mu_{\rm fr} & \mathrm{k_{fr}} - \frac{2}{3}\mu_{\rm fr} & 0 & 0 & 0 \\ \mathrm{k_{fr}} - \frac{2}{3}\mu_{\rm fr} & \mathrm{k_{fr}} - \frac{2}{3} & \mathrm{k_{fr}} + \frac{4}{3}\mu_{\rm fr}\mu_{\rm fr} & 0 & 0 & 0 \\ 0 & 0 & 0 & \mu_{\rm fr} & 0 & 0 \\ 0 & 0 & 0 & 0 & \mu_{\rm fr} & 0 \\ 0 & 0 & 0 & 0 & 0 & \mu_{\rm fr} \end{pmatrix}\,,$$

which is simplified in two dimensions as follows:

$$\mathbf{C}_{\rm fr} \;=\; \begin{pmatrix} \mathrm{k_{fr}} + \frac{4}{3}\mu_{\rm fr} & \mathrm{k_{fr}} - \frac{2}{3}\mu_{\rm fr} & 0 \\ \mathrm{k_{fr}} - \frac{2}{3}\mu_{\rm fr} & \mathrm{k_{fr}} + \frac{4}{3}\mu_{\rm fr} & 0 \\ 0 & 0 & \mu_{\rm fr} \end{pmatrix}\,.$$

We can consider two different conditions for the medium, drained or undrained. For the current discussion, we follow [26] and [30]. In undrained conditions, the fluid cannot flow out, or the fluid is viscous. In this case, there is a difference of pressure during the experiment, but no relative variation of fluid content ($\zeta = 0$). The moduli associated to this state are called the undrained ones, denoted by $\mu_{\rm undrained}$, $\lambda_{\rm undrained}$ and $\mathrm{k_{undrained}}$. They are also called Gassmann modulo,

$$\mu_G = \mu_{\rm undrained}\,, \quad \lambda_G = \lambda_{\rm undrained}\,, \quad \text{and } \mathrm{k}_G = \mathrm{k_{undrained}}\,.$$

A material has a drained response when the solid surface is exposed to the atmosphere, in this case, the fluid in the pores can flow out, but there is no variation of pressure inside the pores ($\Delta \mathrm{p} = 0$). The moduli associated to this state are denoted by $\mu_{\rm fr}$, $\lambda_{\rm fr}$ and $\mathrm{k_{fr}}$, also called the bulk modulus of the dry matrix or dry frame. The relations between the drained and undrained states are given by

$$\mu_G = \mu_{\rm fr}\,, \quad \text{and } \lambda_G = \lambda_{\rm fr} + \alpha^2 M\,. \tag{1.3}$$

In the above expression, the *effective-stress coefficient* α is defined as

$$\alpha \;=\; 1 - \frac{\mathsf{k_{fr}}}{\mathsf{k_s}}\,,$$

and the *fluid-solid coupling modulus* M as

$$\frac{1}{M} \;=\; \frac{\alpha}{\mathsf{k}_\mathrm{s}} + \phi\left(\frac{1}{\mathsf{k}_\mathrm{f}} - \frac{1}{\mathsf{k}_\mathrm{s}}\right).$$

With the physical assumption that

$$\mathsf{k}_\mathrm{s} \;>\; \mathsf{k}_\mathrm{fr} \quad , \quad \mathsf{k}_\mathrm{s} \;>\; \mathsf{k}_\mathrm{f}\,,$$

we have

$$\alpha \;>\; 0 \quad , \quad M \;>\; 0\,. \tag{1.4}$$

Using expressions (1.3), we obtain the relation between k_G and k_fr, *cf.* [27, eq.(4)]:

$$\mathrm{k}_G = \lambda_G + \tfrac{2}{3}\mu_G = \lambda_G + \tfrac{2}{3}\mu_\mathrm{fr} \overset{1.3}{=} \lambda_G - \lambda_\mathrm{fr} + \mathrm{k}_\mathrm{fr} = \mathrm{k}_\mathrm{fr} + \alpha^2 M\,.$$

We list the physical parameters of the specific isotropic porous media considered in this document in Table 1.1. The media are filled with brine, which is inviscid in the case of shale and sandstone materials.

Physical parameters	Sandstone	Sand 1	Shale	Sand 2
Porosity ϕ	0.2	0.3	0.16	0.3
Fluid Density ρ_f $(kg.L^{-1})$	1.04	1	1.04	1
Solid Density ρ_s $(kg.L^{-1})$	2.5	2.6	2.21	2.7
Viscosity η (mPa.s)	0	1	0	1
Permeability κ_0 (μm^2)	60	10	10	10
Tortuosity $\mathfrak{t}$	2	3	2	3
Solid Bulk Modulus k_s (GPa)	40	35	7.6	36
Fluid Bulk Modulus k_f (GPa)	2.5	2.2	2.5	2.2
Frame Bulk Modulus k_fr (GPa)	20	0.4	6.6	7
Frame Shear Modulus μ_fr (GPa)	12	0.5	3.96	5

Table 1.1: Summary of the physical parameters of media in consideration in the numerical experiments. The parameters for sand 1 are obtained from [64, Table 1], those for sandstone and shale from [39, Table 5], for sand 2 from [128, Table 1]. For the tests in sections 2.2 and after, we will use these materials. However, we will vary some of the parameters to highlight their effect on the solution.

We have introduced in the above our notations for physical parameters. For the sake of understanding, we compare in Table (1.5) our notations used with the ones used by Pride in formula [107, (9.15),(9.19)].

	Pride's notations	Our notation
Undrained bulk modulus	K_U	$\mathsf{k}_\mathrm{fr} + \alpha^2 M = \lambda_\mathrm{fr} + \frac{2}{3}\mu_\mathrm{fr} + \alpha^2 M = H - \frac{4}{3}\mu_\mathrm{fr}$
Undrained shear modulus	G	μ_fr
Biot incompressibilities	C	αM
constants [107, (9.18)]	$H = K_U + \frac{4}{3}G$	$\lambda_\mathrm{fr} + \frac{2}{3}\mu_\mathrm{fr} + \alpha^2 M + \frac{4}{3}\mu_\mathrm{fr} \;= \lambda_\mathrm{fr} + 2\mu_\mathrm{fr} + \alpha^2 M$

(1.5)

1.2 Equations

Now that we have introduced the physical parameters involved in the problem in consideration, we are going to present the equations of poroelasticity. In poroelastic equations, in addition to the nine unknowns already existing in elastic equation (with six for the stress tensor and three for the displacement of the particle), there are new quantities due to the presence of pore structure and fluid. These are the *pore pressure* p, and the three components of the *displacement of fluid relative to the solid displacement* w, *cf.* [26]. In this document we will mainly work in frequency domain, with the *pulsation* ω, and with the following unknowns:

u frame displacement in frequency-domain formulation,

w relative fluid displacement in frequency-domain formulation,

p fluid pressure,

$\boldsymbol{\tau}$ stress tensor.

For the purpose of introducing the equations of motion in time, we introduce briefly the time-dependent quantities,

$\mathtt{u}$ frame displacement in time-domain formulation,

$\mathtt{w}$ relative fluid displacement in time-domain formulation.

1.2.1 Equations of motion

We describe the equations of motion both in time and frequency domain, using the definition of two conventions for the time derivative in frequency domain. We next study the approximation models for vanishing viscosity.

Remark 1.1 (Convention of ∂_t). As we work in frequency domain, it is necessary to introduce a convention of the time derivative for the transformation in time domain.

- **Convention 1** This convention follows that of Pride and uses $\partial_t \to -\mathrm{i}\omega$. This is also employed in Dupuy [50]. Here, the time-harmonic part is represented by $e^{-\mathrm{i}\omega t}$, which is equivalent to using the Fourier transform convention

$$\mathcal{F}_1 g \;:=\; \int e^{\mathrm{i}\omega t} g(t)\, dt \quad \Rightarrow \quad \mathcal{F}_1 \dot{g} = -\mathrm{i}\omega\, \mathcal{F}_1 g\,. \tag{1.6}$$

  A plane wave is given by a multiple of

$$e^{-\mathrm{i}\omega t}\; e^{\mathrm{i}\mathbf{k}\cdot\boldsymbol{x}}\,\mathbf{d} \quad \text{, with } \mathbf{d} \text{ the polarization.}$$

- **Convention 2** : In this convention, one takes $\partial_t \to \mathrm{i}\omega$. The time-harmonic part is thus represented by $e^{\mathrm{i}\omega t}$, and is equivalent to using the Fourier transform convention,

$$\mathcal{F}_2 g \;:=\; \int e^{-\mathrm{i}\omega t} g(t)\, dt \quad \Rightarrow \quad \mathcal{F}_2 \dot{g} = \mathrm{i}\omega\, \mathcal{F}_2 g\,.$$

  A plane wave is given by a multiple of

$$e^{\mathrm{i}\omega t}\, e^{\mathrm{i}\mathbf{k}\cdot\boldsymbol{x}}\,\mathbf{d}.$$

  This form of plane wave was used in [52, Eq. 5.2.18]. △

We unify both conventions by writing

$$\partial_t \to \mathfrak{s}\,\mathrm{i}\,\omega \quad \text{with} \quad \mathfrak{s} = \begin{cases} -1 \quad , & \text{convention 1} \\ 1 \quad , & \text{convention 2} \end{cases}.$$

1.2.1.1 Equations of motion in time domain

The first equation of motion comes from balancing forces acting on each sample of the material [107],

$$\nabla\cdot\boldsymbol{\tau} \;+\; \mathfrak{f}_{\mathrm{u}} \;=\; \rho_a\,\ddot{\mathtt{u}} \;+\; \rho_f\ddot{\mathtt{w}}\,, \tag{1.7}$$

while the second one is a generalized Darcy's law that takes into account the dependence of the drag force (due to the viscosity of the fluid) on the frequency,

$$-\nabla \mathrm{p} \;+\; \mathfrak{f}_{\mathrm{w}} \;=\; \rho_f\ddot{\mathtt{u}} \;+\; \mathcal{V}(t)\star\dot{\mathtt{w}}. \tag{1.8}$$

In the above equation, $\mathfrak{f}_{\mathrm{w}}$ and $\mathfrak{f}_{\mathrm{u}}$ are external volume forces, and drag operator $\mathcal{V}$ is defined such that,

$$\mathcal{V}(t)\star g \;:=\; \mathcal{F}_1^{-1}\left(\frac{\eta}{k(\omega)}\;\mathcal{F}_1 g\right).$$

In the definition of $\mathcal{V}$, $\mathcal{F}_1$ is the Fourier transform defined in (1.6) in convention 1 in t (see remark 1.1), and $k(\omega)$ is Pride's dynamic permeability, *cf.* [106, Eq. 236],

$$\frac{1}{k(\omega)} = \frac{1}{k_0}\left(\sqrt{1-\mathrm{i}\frac{4}{m}\frac{\omega}{\omega_t}} - \mathrm{i}\frac{\omega}{\omega_t}\right).$$

Here, the (dimensionless) number m and the transition frequency ω_t are defined as

$$m := \frac{\phi}{\mathfrak{t} k_0}\lambda_{\rm fr}^2 \quad , \quad \omega_t := \frac{\phi}{\mathfrak{t} k_0}\frac{\eta}{\rho_f}\,.$$

The frequency ω_t separates the low-frequency viscous-flow behavior from the high-frequency inertial flow. The constant m is usually determined by experimental means with:

$$4 \le m \le 8\,.$$

We have also denoted by $\sqrt{\bullet}$, the square root branch that uses the principal value, i.e.for $z \in \mathbb{C}\setminus\{0\}$,

$$\sqrt{z} = \sqrt{|z|}\, e^{\mathrm{i}\,\mathrm{Arg}(z)/2} \quad , \quad \mathrm{Arg}\, z \in (-\pi, \pi]\,.$$

Thus $\mathrm{Re}\sqrt{\ } > 0$, while $\mathrm{Im}\sqrt{\ }$ can be positive or negative.

1.2.1.2 Equations of motion in the frequency domain

As mentioned above, we work in the frequency domain, i.e. with responses due to time-harmonic disturbances. The drag force described by the operator $\mathcal{V}$ has a simpler expression in this case. In particular, since

$$(\mathcal{F}_2\mathcal{V})(w) \;=\; (\mathcal{F}_1\mathcal{V})(-w) \;=\; \frac{\eta}{k(-\omega)} = \frac{\eta}{k_0}\left(\sqrt{1+\mathrm{i}\frac{4}{m}\frac{\omega}{\omega_t}} + \mathrm{i}\frac{\omega}{\omega_t}\right),$$

the contribution of the drag force is now written as,

$$\mathcal{F}_1\left(\mathcal{V}(t)\star\dot{\mathtt{w}}\right) \;=\; (\mathcal{F}_1\mathcal{V})(\omega)\,(\mathcal{F}_1\dot{\mathtt{w}})(\omega) \;=\; \frac{\eta}{k(\omega)}(-\mathrm{i}\omega)\;(\mathcal{F}_1\mathtt{w})\,,$$

$$\mathcal{F}_2\left(\mathcal{V}(t)\star\dot{\mathtt{w}}\right) \;=\; (\mathcal{F}_2\mathcal{V})(w)\,(\mathcal{F}_2\dot{\mathtt{w}})(\omega) = \frac{\eta}{k(-\omega)}\;(\mathrm{i}\omega)\;(\mathcal{F}_2\mathtt{w})\,.$$

The first equation of motion (1.7) is formally transformed to

$$\nabla\cdot\boldsymbol{\tau} + \mathbf{f}_{\rm u} \;=\; -\omega^2\rho_a \mathrm{u} \;-\; \omega^2\,\rho_f \mathrm{w}\,,$$

while the second one (1.8) becomes

$$-\nabla \mathrm{p} + \mathbf{f}_{\rm w} \;=\; -\omega^2\rho_f \mathrm{u} - \omega^2\left(\mathrm{i}\frac{\eta}{\omega\, k(\omega)}\right)\mathrm{w} \quad .$$

Here, $\mathbf{f}_{\rm u}$ and $\mathbf{f}_{\rm w}$ are time-harmonic external volume forces. As in [110, Eq. 77], we introduce the *dynamic density* as

$$\rho_{\rm dyn}(\omega) \;:=\; \mathrm{i}\frac{\eta}{(-\mathfrak{s}\,\omega)\,k(-\mathfrak{s}\,\omega)} \;=\; \mathrm{i}\frac{\eta}{(-\mathfrak{s}\,\omega)\,k_0}\left(\sqrt{1+\mathrm{i}\frac{4}{m}\frac{(-\mathfrak{s}\,\omega)}{\omega_t}} + \mathrm{i}\frac{(-\mathfrak{s}\,\omega)}{\omega_t}\right) . \tag{1.9}$$

The equations of motion in the frequency domain are

$$\boxed{\begin{aligned} \nabla\cdot\boldsymbol{\tau} + \mathbf{f}_{\rm u} \;&=\; -\omega^2\rho_a \mathrm{u} \;-\; \omega^2\,\rho_f \mathrm{w}\,, \\ -\nabla \mathrm{p} + \mathbf{f}_{\rm w} \;&=\; -\omega^2\rho_f \mathrm{u} \;-\; \omega^2\,\rho_{\rm dyn}(\omega)\,\mathrm{w}\,. \end{aligned}} \tag{1.10}$$

1.2.1.3 Formal zero-viscosity limiting for a fixed positive frequency

Below, we write out the form of equation (1.10) when $\eta \to 0$ at a fixed frequency ω and with the other parameters fixed. Note that $\omega_t \to 0$ when $\eta \to 0$, and ω_t is in the denominator of the definition of $\rho_{\rm dyn}$. However, this has a finite limit as $\eta \to 0$. To see this, it suffices to consider the calculation in Convention 1. Using the definition $\omega_t := \frac{\phi}{\mathfrak{t} k_0}\frac{\eta}{\rho_f}$, we write

$$\frac{\eta}{k(\omega)} = \frac{1}{k_0}\left(\sqrt{\eta^2 - \mathrm{i}\,\frac{4}{m}\,\omega\,\eta\,\frac{\eta}{\omega_t}} - \mathrm{i}\frac{\eta}{\omega_t}\omega\right) \;=\; \frac{1}{k_0}\left(\sqrt{\eta^2 - \frac{4\mathrm{i}}{m}\omega\eta\frac{\mathfrak{t} k_0\rho_f}{\phi}} - \mathrm{i}\omega\frac{\mathfrak{t} k_0\rho_f}{\phi}\right).$$

For a fixed $\omega > 0$, we compute the limit of $\frac{\eta}{k(\omega)}$ as $\eta \to 0$ (under the assumption that the quantities $\phi, \mathfrak{t}, k_0, \Gamma, m$ are independent of η), and replace the expression of the dynamic density in (1.9). We obtain similar results for Convention 2. We note by $\rho_{\rm dyn}^{\rm VV}$ the vanishing viscosity limit of $\rho_{\rm dyn}$, i.e.

$$\rho_{\rm dyn}^{\rm VV} := \lim_{\substack{\eta\to 0,\\ \text{fixed } \omega>0}} \rho_{\rm dyn}(\omega) = \frac{\rho_f}{\phi}\,\mathfrak{t}\,. \tag{1.11}$$

We will use this expression in the numerical tests. For material with zero viscosity, we apply the following limiting form of (1.10),

Vanishing Viscosity

$$\begin{aligned} \nabla\cdot\boldsymbol{\tau} + \mathbf{f}_{\rm u} &= -\omega^2\,\rho_a\,{\rm u} - \omega^2\,\rho_f\,{\rm w}\,,\\ -\nabla {\rm p} + \mathbf{f}_{\rm w} &= -\omega^2\rho_f\,{\rm u} - \omega^2\,\rho_{\rm dyn}^{\rm VV}\,{\rm w}\,. \end{aligned}$$

1.2.2 Constitutive laws

The first constitutive law is generalized from that of linear elasticity, where it has been taking into consideration the additional influence of fluid pressure,

$$\boxed{\boldsymbol{\tau} = \mathbf{C}_{\rm fr} : \boldsymbol{\epsilon}_{\rm fr} - \boldsymbol{\alpha}\,{\rm p}\,,} \tag{1.12}$$

where the operation : denotes the tensor scalar product, i.e. for tensors $\boldsymbol{a}$ and $\boldsymbol{b}$, $\boldsymbol{a} : \boldsymbol{b} = \sum_{i,j} a_{ij}\,b_{ij}$. Here, $\mathbf{C}_{\rm fr}$ is the elastic stiffness tensor of the drained frame, and $\boldsymbol{\epsilon}_{\rm fr}$ is the strain tensor of the solid frame,

$$\boldsymbol{\epsilon} = \boldsymbol{\epsilon}_{\rm fr} := \frac{\nabla{\rm u} + (\nabla{\rm u})^T}{2}\,.$$

Under the assumption of isotropy of the material making up the solid frame, the fluid and the frame, (1.12) reduces to

$$\boxed{\begin{aligned} \boldsymbol{\tau} &= \lambda_{\rm fr}\nabla\cdot{\rm u} + 2\mu_{\rm fr}\boldsymbol{\epsilon} - \alpha{\rm p}\\ &= 2\underbrace{\mu_{\rm fr}}_{G}\boldsymbol{\epsilon} + \left(-\tfrac{2}{3}\mu_{\rm fr} + \underbrace{{\rm k}_{\rm fr} + M\alpha^2}_{{\rm k}_G \text{ in } [106]}\right)\nabla\cdot{\rm u}\,\mathbb{I} + \alpha M\nabla\cdot{\rm w}\,\mathbb{I}\\ &= 2\mu_{\rm fr}\boldsymbol{\epsilon} + (\lambda_{\rm fr} + M\alpha^2)\nabla\cdot{\rm u}\,\mathbb{I} + \alpha M\nabla\cdot{\rm w}\,\mathbb{I}\,. \end{aligned}} \tag{1.13}$$

The second constitutive law is

$$\boxed{{\rm p} = -M\,(\nabla\cdot{\rm w} + \mathbf{f}_{\rm p}) - M\,\alpha\nabla\cdot{\rm u}\,.} \tag{1.14}$$

Note that $\mathbf{f}_{\rm p}$ is a time-harmonic external source term. For more meaning on the geophysical meaning of the above equations, we refer to the introduction of [107].

Remark 1.2. Here, the constitutive laws are expressed using the unknowns in the frequency domain. For those in time domain, we only have to replace the unknowns by the corresponding ones in the time domain, including the source in (1.14).

1.2.3 First order formulation

In the first order formulation of the equations of motion, we work with the unknowns

$$\mathbf{u}\quad,\quad \mathbf{w}\quad,\quad \boldsymbol{\tau}\quad,\quad {\rm p}\,, \tag{1.15}$$

where

$$\mathbf{u} = \mathfrak{s}\,{\rm i}\omega\,{\rm u}\quad,\quad \mathbf{w} = \mathfrak{s}\,{\rm i}\omega\,{\rm w}\quad,\quad \boldsymbol{\epsilon} = \frac{\nabla\mathbf{u} + (\nabla\mathbf{u})^T}{2}\,.$$

Here, $\mathbf{u}$ and $\mathbf{w}$ are interpreted as the time-harmonic solid velocity and the relative fluid velocity. They solve the system

$$\begin{cases} \nabla\cdot\boldsymbol{\tau} + \mathbf{f}_u &= \mathfrak{s}\,{\rm i}\omega\,\rho_a\,\mathbf{u} + \mathfrak{s}\,{\rm i}\omega\,\rho_f\,\mathbf{w}\,,\\ -\nabla{\rm p} + \mathbf{f}_{\rm w} &= \mathfrak{s}\,{\rm i}\omega\,\rho_f\mathbf{u} + \mathfrak{s}\,{\rm i}\omega\,\rho_{\rm dyn}\mathbf{w}\,,\\ \mathfrak{s}\,{\rm i}\omega\,\boldsymbol{\tau} &= \mathbf{C}_{\rm fr} : \boldsymbol{\epsilon} - \mathfrak{s}\,{\rm i}\omega\,\boldsymbol{\alpha}\,{\rm p}\,,\\ \mathfrak{s}\,{\rm i}\omega\,({\rm p} + Mf_{\rm p}) &= -M\,\nabla\cdot\mathbf{w} - M\,\boldsymbol{\alpha} : \boldsymbol{\epsilon}\,. \end{cases} \tag{1.16}$$

We obtain this formulation using

$$\mathfrak{s}\,\mathrm{i}\omega\,\mathrm{u} \;=\; \mathbf{u}\,, \quad \text{and } \mathfrak{s}\,\mathrm{i}\omega\,\mathrm{w} \;=\; \mathbf{w}\,,$$

and we next replace the above relations in equations (1.10):

$$\nabla\cdot\boldsymbol{\tau}+\mathbf{f}_{\mathrm{u}}=(\mathfrak{s}\,\mathrm{i}\omega)^2\mathrm{u}\;-\;(\mathfrak{s}\,\mathrm{i}\omega)^2\,\mathrm{w} \quad\Longrightarrow\quad \nabla\cdot\boldsymbol{\tau}\;+\;\mathbf{f}_u \;=\; \mathfrak{s}\,\mathrm{i}\omega\,\rho_a\,\mathbf{u}\;+\;\mathfrak{s}\,\mathrm{i}\omega\,\rho_f\mathbf{w}\,.$$

$$-\nabla\mathrm{p}+\mathbf{f}_{\mathrm{w}} \;=\; (\mathfrak{s}\,\mathrm{i}\omega)^2\,\rho_f\,\mathrm{u}\;+\;(\mathfrak{s}\,\mathrm{i}\omega)^2\rho_{\mathrm{dyn}}\,\mathrm{w} \quad\Longrightarrow\quad -\nabla\mathrm{p}+\mathrm{p}_{\mathrm{w}} \;=\; \mathfrak{s}\,\mathrm{i}\omega\,\rho_f\,\mathbf{u}\;+\;\mathfrak{s}\,\mathrm{i}\omega\,\rho_{\mathrm{dyn}}\,\mathbf{w}\,.$$

$$\boldsymbol{\tau}=\mathbf{C}_{\mathrm{fr}}:\frac{\nabla\mathrm{u}+(\nabla\mathrm{u})^T}{2}-\alpha\mathrm{p} \quad\Longrightarrow\quad \mathfrak{s}\,\mathrm{i}\omega\,\boldsymbol{\tau} \;=\; \mathbf{C}_{\mathrm{fr}}:\boldsymbol{\epsilon}\;-\;\mathfrak{s}\,\mathrm{i}\omega\,\boldsymbol{\alpha}\,\mathrm{p}\,.$$

$$\mathrm{p} \;=\; -\mathrm{m}\nabla\cdot\mathrm{w}\;-\;M f_{\mathrm{p}}\;-\;M\boldsymbol{\alpha}:\frac{\nabla\mathrm{u}+(\nabla\mathrm{u})^T}{2} \quad\Longrightarrow\quad \mathfrak{s}\,\mathrm{i}\omega\,\mathrm{p} \;=\; -M\,\nabla\cdot\mathbf{w}\;-\;\mathfrak{s}\,\mathrm{i}\omega M\,f_{\mathrm{p}}\;-\;M\,\boldsymbol{\alpha}:\boldsymbol{\epsilon}.$$

1.2.4 Second-order formulation

Here, we want to determine the second-order formulation of equation (1.16) in the case of an isotropic medium. We recall the curl operator,

$$\mathbf{curl}\,V \;=\; \begin{pmatrix} \partial_y V_z \;-\; \partial_z V_y \\ \partial_z V_x \;-\; \partial_x V_z \\ \partial_x V_y \;-\; \partial_y V_x \end{pmatrix}. \tag{1.17}$$

and the following properties of the operators:

$$\nabla\cdot\nabla f \;=\Delta f\,, \quad \nabla\cdot(f\mathbb{I})=\nabla f\,, \quad \nabla\cdot\nabla^T V \;=\; \nabla\nabla\cdot V\,,$$

and

$$\Delta V \;=-\,\mathbf{curl}\,\mathbf{curl}\,V\;+\;\nabla\nabla\cdot V\,.$$

Proposition 1.3 (u − w formulation).

- If $(\mathrm{u},\mathrm{w},\boldsymbol{\tau},\mathrm{p})$ is solution of the poroelastic system made up of (1.10), (1.13) and (1.14) in a homogeneous medium, then (u,w) solves the following system

$$\begin{aligned} -\omega^2\rho_a\mathrm{u}\;-\;\rho_f\omega^2\mathrm{w}\;-\;H\,\nabla\nabla\cdot\mathrm{u}\;+\;\mu_{\mathrm{fr}}\,\mathbf{curl}\,\mathbf{curl}\,\mathrm{u}\;-\;\alpha\,M\,\nabla\nabla\cdot\mathrm{w}=\mathbf{f}_{\mathrm{u}}\,,\\ -\omega^2\rho_f\mathrm{u}\;-\;\omega^2\,\rho_{\mathrm{dyn}}(\omega)\,\mathrm{w}-M\,\nabla\nabla\cdot\mathrm{w}\;-\;M\alpha\nabla\nabla\cdot\mathrm{u}=\mathbf{f}_{\mathrm{w}}\;+\;\nabla M\,\mathbf{f}_{\mathrm{p}}\,. \end{aligned} \tag{1.18}$$

- Conversely, if (u,w) solves (1.18), with $\boldsymbol{\tau}$ and p given in terms of u and w by constitutive laws (1.13) and (1.14), then $(\mathrm{u},\mathrm{w},\boldsymbol{\tau},\mathrm{p})$ solves the poroelastic system (1.10).

Proof. We need to express $\nabla\cdot\boldsymbol{\tau}$ and $\nabla\mathrm{p}$ in terms of the divergences and curls of u and w. For $\nabla\mathrm{p}$, we have from (1.14)

$$-\nabla\mathrm{p} \;=\; M\,\nabla\nabla\cdot\mathrm{w}\;+\;M\,\nabla\mathbf{f}_{\mathrm{p}}\;+\;M\,\alpha\,\nabla\nabla\cdot\mathrm{u}\,,$$

and for $\nabla\cdot\boldsymbol{\tau}$, using (1.13), we have

$$\begin{aligned} \boldsymbol{\tau} \;&=\; 2\mu_{\mathrm{fr}}\,\boldsymbol{\epsilon}\;+\;(\lambda_{\mathrm{fr}}\;+\;M\alpha^2)\,\nabla\cdot\mathrm{u}\,\mathbb{I}\;+\;\alpha\,M\,\nabla\cdot\mathrm{w}\,\mathbb{I}\,;\\ \Rightarrow\quad \nabla\cdot\boldsymbol{\tau} \;&=\; \mu_{\mathrm{fr}}\,\nabla\cdot(\nabla+\nabla^T)\mathrm{u}\;+\;(\lambda_{\mathrm{fr}}+M\alpha^2)\nabla\nabla\cdot\mathrm{u}\;+\;\alpha\,M\,\nabla\nabla\cdot\mathrm{w}\\ &=\; \mu_{\mathrm{fr}}\,\Delta\mathrm{u}\;+\;(\mu_{\mathrm{fr}}+\lambda_{\mathrm{fr}}+M\alpha^2)\nabla\nabla\cdot\mathrm{u}\;+\;\alpha\,M\,\nabla\nabla\cdot\mathrm{w}\\ &=\; -\mu_{\mathrm{fr}}\,\mathbf{curl}\,\mathbf{curl}\,\mathrm{u}\;+\;\underbrace{(2\mu_{\mathrm{fr}}\;+\;\lambda_{\mathrm{fr}}\;+\;M\alpha^2)}_{:=H}\nabla\nabla\cdot\mathrm{u}\;+\;\alpha\,M\,\nabla\nabla\cdot\mathrm{w}\,. \end{aligned}$$

Here, we have used the Biot coefficient H defined in (1.5),

$$H \;:=\; 2\mu_{\mathrm{fr}}\;+\;\lambda_{\mathrm{fr}}\;+\;M\,\alpha^2\,.$$

We next substitute these expressions into the equations of motion that have similar expression in both conventions. The first equation

$$\nabla \cdot \boldsymbol{\tau} \ + \ \mathbf{f}_{\mathrm{u}} \ = \ -\omega^2 \, \rho_a \, \mathrm{u} \ - \ \omega^2 \, \rho_f \, \mathrm{w} \, ,$$

gives

$$-\mu_{\mathrm{fr}} \, \mathbf{curl} \, \mathbf{curl} \, \mathrm{u} \ + \ H \, \nabla\nabla \cdot \mathrm{u} \ + \ \alpha M \nabla\nabla \cdot \mathrm{w} + \mathbf{f}_{\mathrm{u}} \ = \ -\omega^2 \, \rho_a \, \mathrm{u} \ - \ \omega^2 \, \rho_f \, \mathrm{w} \, .$$

The second one

$$-\nabla \mathrm{p} \ + \ \mathbf{f}_{\mathrm{w}} \ = \ -\omega^2 \rho_f \mathrm{u} \ - \ \omega^2 \rho_{\mathrm{dyn}}(\omega) \, \mathrm{w} \, ,$$

gives

$$M \nabla\nabla \cdot \mathrm{w} \ + \ M \nabla \mathbf{f}_{\mathrm{p}} \ + \ M \alpha \nabla\nabla \cdot \mathrm{u} \ + \ \mathbf{f}_{\mathrm{w}} \ = \ -\omega^2 \, \rho_a \, \mathrm{u} \ - \ \omega^2 \, \rho_f \, \mathrm{w} \, .$$

The second direction of the equivalence is obtained by rearrangement of the equations. □

Remark 1.4 (Two-dimensional case). In two dimensions, we consider a translation invariance in z direction, see for example [125]. We then introduce the vectorial and scalar rotationals, **curl** and curl. We give the following definitions of the curl for scalar f and vector $\mathbf{V}$:

$$\mathbf{curl} \, f \ = \ \begin{pmatrix} \partial_y f \\ -\partial_x f \end{pmatrix} , \qquad \mathrm{curl} \, \mathbf{V} \ = \ \partial_x V_y \ - \ \partial_y V_x \, . \tag{1.19}$$

In this case, the laplacian of $\mathbf{V}$ is

$$\Delta \, \mathbf{V} \ = - \, \mathbf{curl} \, \mathrm{curl} \, V \ + \ \nabla\nabla \cdot V \, .$$

The second order formulation of the poroelastic equations is

$$-\omega^2 \rho_a \mathrm{u} \ - \ \rho_f \omega^2 \mathrm{w} \ - \ H \, \nabla\nabla \cdot \mathrm{u} \ + \ \mu_{\mathrm{fr}} \, \mathbf{curl} \, \mathrm{curl} \, \mathrm{u} \ - \ \alpha \, M \, \nabla\nabla \cdot \mathrm{w} = \mathbf{f}_{\mathrm{u}} \, ,$$

$$-\omega^2 \rho_f \mathrm{u} \ - \ \omega^2 \, \rho_{\mathrm{dyn}}(\omega) \, \mathrm{w} - M \, \nabla\nabla \cdot \mathrm{w} \ - \ M \alpha \nabla\nabla \cdot \mathrm{u} = \mathbf{f}_{\mathrm{w}} \ + \ \nabla M \, \mathbf{f}_{\mathrm{p}} \, .$$

The proof is similar to the proof in the three-dimensional case.

1.3 Non-dimensionalization of the equations

For numerical implementation, the parameters may have different orders of magnitude. To manipulate numbers with a similar order of amplitude, we write the system (1.16) without source in terms of dimensionless equations. We write $X = X_0 \overline{X}$ for all the terms of the equations with X_0 a characteristic unit of measure and $\overline{X}$ denoting non-dimensional quantities. We assume that the components of $\mathbf{C}$ are written as $C_0 \overline{\mathbf{C}}$, and that the bulk moduli $\mathrm{k}_\bullet$ are written as $\mathrm{k}_\bullet = C_0 \overline{\mathrm{k}_\bullet}$ for $\bullet = \mathrm{s}, \mathrm{f}, \mathrm{fr}$. Hence, $M = C_0 \overline{M}$ and $\alpha_0 = 1$. The porosity $\phi = \frac{V_f}{V_T}$ is considered as a unitless ratio. We assume that ρ_a, ρ_{dyn}, ρ_f and ρ_s have the same characteristic unit ρ_0. The characteristic frequency has the same characteristic unit as ω. The characteristic unity for the lengths is x_0. The system (1.16) with physical parameters becomes:

$$\begin{cases} \mathrm{i} \, \omega_0 \, \overline{\omega} \, \rho_0 \, \overline{\rho_a} \, \mathrm{u}_0 \, \overline{\mathbf{u}} + \mathrm{i} \, \omega_0 \, \overline{\omega} \, \rho_0 \, \overline{\rho_f} \, \mathrm{w}_0 \, \overline{\mathbf{w}} = \ \dfrac{\tau_0}{x_0} \, \nabla \cdot \, \overline{\boldsymbol{\tau}} \, , \\ \mathrm{i} \, \omega_0 \overline{\omega} \, \rho_0 \overline{\rho_f} \mathrm{u}_0 \, \overline{\mathbf{u}} + \mathrm{i} \, \omega_0 \overline{\omega} \, \rho_0 \, \overline{\rho_{\mathrm{dyn}}} \, \mathrm{w}_0 \, \overline{\mathbf{w}} = - \dfrac{\mathrm{p}_0}{x_0} \, \nabla \overline{\mathrm{p}} \, , \\ \mathrm{i} \, \omega_0 \, \overline{\omega} \, \tau_0 \, \overline{\boldsymbol{\tau}} + \mathrm{i} \, \omega_0 \, \overline{\omega} \alpha_0 \, \overline{\boldsymbol{\alpha}} \mathrm{p}_0 \, \overline{\mathrm{p}} \mathbb{I} = \dfrac{C_0 \mathrm{u}_0}{x_0} \, \overline{\mathbf{C}} \, \boldsymbol{\epsilon}(\overline{\mathbf{u}}) \, , \\ \mathrm{i} \, \omega_0 \, \overline{\omega} \, \mathrm{p}_0 \, \overline{\mathrm{p}} = - \dfrac{C_0 \mathrm{w}_0}{x_0} \, \overline{M} \nabla \cdot \overline{\mathbf{w}} - \dfrac{C_0 \alpha_0 \mathrm{u}_0}{x_0} \, \overline{M} \, \overline{\boldsymbol{\alpha}} : \boldsymbol{\epsilon}(\overline{\mathbf{u}}) \, , \\ \rho_0 \, \overline{\rho_{\mathrm{dyn}}} = \dfrac{\eta_0}{\kappa_{0_0} \omega_0} \dfrac{\overline{\eta}}{\overline{k}} \, . \end{cases}$$

The equations are written with dimensionless quantities, and all the constants must be equal. Setting the factors in the coefficients that contain characteristic units, we obtain the following relations:

$$\begin{cases} \omega_0\,\rho_0\,\mathrm{u}_0 \;=\; \omega_0\,\rho_0\,\mathrm{w}_0 \;=\; \dfrac{\tau_0}{x_0}\,, \\ \omega_0\,\rho_0\,\mathrm{u}_0 \;=\; \omega_0\,\rho_0\,\mathrm{w}_0 \;=\; -\dfrac{\mathrm{p}_0}{x_0}\,, \\ \omega_0\,\tau_0 \;=\; \omega_0\,\alpha_0\,\mathrm{p}_0 \;=\; \dfrac{C_0\mathrm{u}_0}{x_0}\,, \\ \omega_0\,\mathrm{p}_0 \;=\; \dfrac{C_0\mathrm{w}_0}{x_0}\;\dfrac{C_0\alpha_0\mathrm{u}_0}{x_0}\,, \\ \rho_0 \;=\; \dfrac{\eta_0}{\kappa_{0_0}\omega_0}\,. \end{cases}$$

Simplifying, we have:

$$\mathrm{u}_0 = \mathrm{w}_0\,, \quad \tau_0 = \mathrm{p}_0 = \omega_0\,\rho_0\,\mathrm{u}_0\,x_0, \quad C_0 u_0 = \omega_0\,\tau_0\,x_0\,, \quad \eta_0 = \rho_0\,\omega_0\,k_{0_0}\,.$$

In many geophysical materials, the magnitude of the bulk modulus and the stiffness tensor is in GPa or MPa, and the magnitude of the densities is in $10^3\mathrm{kg.m}^{-3}$. We hence choose:

$$C_0 = 10^9\mathrm{Pa}\,, \qquad \rho_0 = 10^3\mathrm{kg}\cdot\mathrm{m}^{-3}\,,$$

and it follows that

$$\tau_0 = \mathrm{p}_0 = 10^6\mathrm{Pa}\,, \quad \omega_0 = 10^3\ \mathrm{rad.s}^{-1}\,, \quad x_0 = 1\ \mathrm{m}\,, \quad \mathrm{u}_0 = \mathrm{w}_0 = 1\ \mathrm{m.s}^{-1}\,, \quad \eta_0 = 10^{-3}\ \mathrm{Pa.s}\,, \quad \kappa_{0_0} = 10^{-9}\mathrm{m}^2\,.$$

We note that in other applications using different materials, the magnitude of the physical parameters can differ, and the results presented above may no longer be relevant. In the rest of the text, the overbars denoting the non-dimensionalized quantities are dropped.

1.4 Boundary and interface conditions

We describe the conditions on the boundaries for three different configurations, first a bounded domain, then two interaction problems which include a fluid-solid and a porous-porous interaction.

Bounded domain On the external boundary Γ with outwardly direct unit normal vector $\boldsymbol{n}$, we consider four types of boundary conditions with vector $\boldsymbol{f}_{\mathrm{inc}}$ and scalar g_{inc} denoting the exterior boundary forces,

Type 1 $$\begin{cases} \boldsymbol{\tau}\,\boldsymbol{n} &=& \boldsymbol{f}_{\mathrm{inc}}\,, \\ \mathbf{w}\cdot\boldsymbol{n} &=& g_{\mathrm{inc}}\,, \end{cases} \qquad (1.20a)$$

Type 2 $$\begin{cases} \boldsymbol{\tau}\,\boldsymbol{n} &=& \boldsymbol{f}_{\mathrm{inc}}\,, \\ \mathrm{p} &=& g_{\mathrm{inc}}\,, \end{cases} \qquad (1.20b)$$

Type 3 $$\begin{cases} \mathbf{u} &=& \boldsymbol{f}_{\mathrm{inc}}, \\ \mathrm{p} &=& g_{\mathrm{inc}}\,, \end{cases} \qquad (1.20c)$$

Type 4 $$\begin{cases} \mathbf{u} &=& \boldsymbol{f}_{\mathrm{inc}}\,, \\ \mathbf{w}\cdot\boldsymbol{n} &=& g_{\mathrm{inc}}\,. \end{cases} \qquad (1.20d)$$

It is worth noting that the conditions (1.20b) include the free boundary conditions which are given by

$$\boldsymbol{\tau}\,\boldsymbol{n} = \mathbf{0}\ ,\ \mathrm{p} = 0\,, \qquad \text{Free surface boundary condition}$$

Interaction problems In interaction problems, we will consider the reflection of a solid obstacle immersed in an infinite solid or fluid medium. Denote outer (infinite) medium by $\Omega_{(I)}$ and the solid obstacle by $\Omega_{(II)}$. Transmission conditions are imposed on the interface Γ between these two domains, i.e., on the boundary of the obstacle.

Porous-porous interaction problem When the outer medium is a poroelastic solid, the transmission conditions are (*cf.* Section 2.4):

$$\begin{cases} \mathbf{u}_{(I)} - \mathbf{u}_{(II)} = 0\,, \\ \mathrm{p}_{(I)} - \mathrm{p}_{(II)} = 0\,, \\ (\mathbf{w}_{(I)} - \mathbf{w}_{(II)}) \cdot \boldsymbol{n} = 0\,, \\ (\boldsymbol{\tau}_{(I)} - \boldsymbol{\tau}_{(II)}) \cdot \boldsymbol{n} = 0\,. \end{cases}$$

Fluid-porous interaction problem When the outer medium is a fluid, fluid-poroelastic transmission conditions depend on the value of hydraulic permeability κ_Γ (see Section 2.5). We denote respectively by $\mathrm{p}_{\mathrm{flu}}$ and $\mathbf{u}_{\mathrm{flu}}$ the total pressure and velocity in the fluid. For a finite positive value of κ_Γ, we impose:

$$\begin{cases} (\mathbf{u}_{\mathrm{flu}} - \mathbf{u}) \cdot \boldsymbol{n} \;=\; \mathbf{w} \cdot \boldsymbol{n}\,, \\ \mathrm{p}_{\mathrm{flu}} - \mathrm{p} = \dfrac{1}{\kappa_\Gamma}\, \mathbf{w} \cdot \boldsymbol{n}\,, \\ \boldsymbol{\tau}\, \boldsymbol{n} = \; - \mathrm{p}_{\mathrm{flu}}\, \boldsymbol{n}\,, \end{cases} \tag{1.21}$$

where κ_Γ denotes the hydraulic permeability on the interface. In the fluid,

$$\mathbf{u}_{\mathrm{flu}} = \; - \frac{1}{\rho_{\mathrm{flu}}\, \mathfrak{s}\, \mathrm{i}\, \omega} \nabla\, \mathrm{p}_{\mathrm{flu}}\,.$$

We distinct extreme cases for κ_Γ: When $\kappa_\Gamma \to \infty$, the pores are *opened*, and the second condition becomes $\mathrm{p}_{\mathrm{flu}} - \mathrm{p} = 0$. (1.21) becomes

$$\begin{cases} (\mathbf{u}_{\mathrm{flu}} - \mathbf{u}) \cdot \boldsymbol{n} \;=\; \mathbf{w} \cdot \boldsymbol{n}\,, \\ \mathrm{p}_{\mathrm{flu}} - \mathrm{p} = 0\,, \\ \boldsymbol{\tau}\, \boldsymbol{n} = \; - \mathrm{p}_{\mathrm{flu}}\, \boldsymbol{n}\,. \end{cases}$$

These equations are the ones used in [45]. On the other hand, when $\kappa_\Gamma = 0$, this case is referred to as *sealed pores*, and the second interface condition is modified as $\mathbf{w} \cdot \boldsymbol{n} = 0$. (1.21) becomes

$$\begin{cases} (\mathbf{u}_{\mathrm{flu}} - \mathbf{u}) \cdot \boldsymbol{n} \;=\; \mathbf{w} \cdot \boldsymbol{n}\,, \\ \mathbf{w} \cdot \boldsymbol{n} \;= 0, \\ \boldsymbol{\tau}\, \boldsymbol{n} = \; - \mathrm{p}_{\mathrm{flu}}\, \boldsymbol{n}\,. \end{cases} \qquad \text{or equivalently} \qquad \begin{cases} (\mathbf{u}_{\mathrm{flu}} - \mathbf{u}) \cdot \boldsymbol{n} \;= 0, \\ \mathbf{w} \cdot \boldsymbol{n} \;= 0, \\ \boldsymbol{\tau}\, \boldsymbol{n} = \; - \mathrm{p}_{\mathrm{flu}}\, \boldsymbol{n}\,. \end{cases}$$

Note that the subscript 'flu' indicates the unkwnowns in a fluid, while the subscript f denotes the unknowns and the parameters in the fluid contained in the pores of the poroelastic medium. The first and third equations in the equivalent form represent the perfect transmission in fluid-elastic scattering.[1]

Domain truncation In the above, we have presented boundary conditions for bounded domains. In Chapter 4, we will focus on the development of boundary conditions used for truncating the computational domain.

1.5 Plane wave Analysis

We consider an isotropic poroelastic domain, and we are going to determine which forms of plane wave are admissible solutions of (1.18) without source. The analysis also gives the possible speeds of propagation sustained in a poroelastic medium. Here, we can observe a fast compressional wave and a shear wave as in elastic medium, but also a second slow compressional wave, associated physically to out-of-phase liquid and solid compressional particle motions. With the vectors $\mathbf{k}$ and $\mathbf{d}$, a vectorial time-harmonic plane wave has the form

$$e^{\pm \mathrm{i}\omega t}\, e^{\pm \mathbf{k} \cdot \boldsymbol{X}}\, \mathbf{d}\,.$$

[1] In [6] the transmission condition between fluid and solid are $\boldsymbol{\tau}\, \boldsymbol{n} = \mathrm{p}_{\mathrm{flu}}\, \boldsymbol{n}$, $\omega^2\, \rho_{\mathrm{flu}}\, \mathrm{u} \cdot \boldsymbol{n} = \nabla \mathrm{p}_{\mathrm{flu}} \cdot \boldsymbol{n}$. Here, the condition is in terms of solid displacement u. Since we work with the velocity formulation, using the following identities,

$$\omega^2 = -(\mathfrak{s}\, \mathrm{i}\, \omega)^2\,, \qquad \mathbf{u} = \mathfrak{s}\, \mathrm{i} \omega\, \mathrm{u}\,, \qquad \nabla \mathrm{p}_{\mathrm{flu}} = -\rho_{\mathrm{flu}}\, \mathfrak{s}\, \mathrm{i}\, \omega\, \mathbf{u}_{\mathrm{flu}}\,.$$

we can write the second condition as:

$$-(\mathfrak{s}\, \mathrm{i}\, \omega)\, \rho_{\mathrm{flu}} \mathbf{u} \cdot \boldsymbol{n} = -\rho_{\mathrm{flu}}\, \mathfrak{s}\, \mathrm{i}\, \omega\, \mathbf{u}_{\mathrm{flu}} \cdot \boldsymbol{n} \quad \Rightarrow \quad \mathbf{u} \cdot \boldsymbol{n} = \mathbf{u}_{\mathrm{flu}} \cdot \boldsymbol{n}\,.$$

We will focus on the plane wave that attenuates along its propagation direction in a medium with viscosity. In particular, we consider slowness vector $\mathsf{s} = \mathsf{s}(\omega)$ satisfying

$$(-\mathfrak{s})\,\mathrm{Re}\,\mathsf{s} > 0 \quad , \quad \mathrm{Im}\,\mathsf{s} > 0\,,$$

(this is later defined in (1.43)), and we define the wave vector $\mathbf{k}$ as

$$\mathbf{k} \;=\; \omega\,\mathsf{s}(\omega)\,\widehat{\mathbf{k}} \quad \text{, with } |\widehat{\mathbf{k}}| \;=\; 1\;,$$

The vector $\widehat{\mathbf{k}}$ denotes the direction of propagation. We consider the plane wave with polarization $\widehat{\mathbf{d}}$ with $|\widehat{\mathbf{d}}| = 1$,

$$e^{\mathrm{i}\,\mathfrak{s}\,\omega t}\,e^{\mathrm{i}\,\mathbf{k}\cdot\boldsymbol{X}}\,\mathbf{d}\,.$$

We rewrite the plane wave as

$$e^{\omega\,\mathrm{i}\,\mathfrak{s}\left(\,t\,-\,|\mathrm{Re}\,\mathsf{s}(\omega)|\,\widehat{\mathbf{k}}\cdot\boldsymbol{X}\right)}\,e^{-\,\omega\;\mathrm{Im}\,\mathsf{s}(\omega)\,\widehat{\mathbf{k}}\cdot\boldsymbol{X}} \quad .$$

From this, we define respectively the phase velocity and the attenuation

$$\mathsf{v}(\omega) \;:=\; \frac{1}{|\mathrm{Re}\;\mathsf{s}(\omega)|}\,, \qquad\qquad \mathsf{a}(\omega) \quad :=\; \omega\;\mathrm{Im}\,\mathsf{s}(\omega)\,.$$

We also work with the complex velocity,

$$\mathsf{c}(\omega) \;:=\; \frac{1}{\mathsf{s}(\omega)}\,. \tag{1.22}$$

1.5.1 Admissible plane waves and slowness calculation

Lemma 1.5. We need the following identities.

$$\begin{aligned}
\nabla\nabla\cdot e^{\mathrm{i}\mathbf{k}\cdot\boldsymbol{X}}\,\mathbf{d} \;&=\; -\,(\mathbf{d}\cdot\mathbf{k})\,\mathbf{k}\,e^{\mathrm{i}\,\mathbf{k}\cdot\boldsymbol{X}}\,,\\
\mathbf{curl}\,\mathbf{curl}\;e^{\mathrm{i}\mathbf{k}\cdot\boldsymbol{X}}\mathbf{d} \;&=\; e^{\mathrm{i}\mathbf{k}\cdot\boldsymbol{X}}\Big(\mathbf{k}\times\mathbf{d}\Big)\times\mathbf{k} = e^{\mathrm{i}\mathbf{k}\cdot\boldsymbol{X}}\,\Big(|\mathbf{k}|^2\mathbf{d}\;-\;(\mathbf{k}\cdot\mathbf{d})\,\mathbf{k}\Big)\,.
\end{aligned}$$

Proof.

$$\begin{aligned}
\nabla\cdot\left(e^{\mathrm{i}\mathbf{k}\cdot\boldsymbol{X}}\mathbf{d}\right) \;&=\; e^{\mathrm{i}\mathbf{k}\cdot\boldsymbol{X}}\;\mathbf{d}\cdot\nabla(\mathrm{i}\mathbf{k}\cdot\boldsymbol{X}) \;=\; e^{\mathrm{i}\mathbf{k}\cdot\boldsymbol{X}}\;\mathbf{d}\cdot(\mathrm{i}\,\mathbf{k}) \quad ,\\
\nabla e^{\mathrm{i}\mathbf{k}\cdot\boldsymbol{X}} \;&=\; e^{\mathrm{i}\mathbf{k}\cdot\boldsymbol{X}}\,\nabla(\mathrm{i}\mathbf{k}\cdot\boldsymbol{X}) = e^{\mathrm{i}\mathbf{k}\cdot\boldsymbol{X}}(\mathrm{i}\mathbf{k})\,,\\
\Rightarrow\;\nabla\Big(\nabla\cdot e^{\mathrm{i}\mathbf{k}\cdot\boldsymbol{X}}\,\mathbf{d}\Big) \;&=\; -\,(\mathbf{d}\cdot\mathbf{k})\,\mathbf{k}\,e^{\mathrm{i}\,\mathbf{k}\cdot\boldsymbol{X}}\,.
\end{aligned}$$

We next consider the curl operator. In 3D, we obtain the expression by using:

$$\begin{aligned}
\mathbf{curl}\left(e^{\mathrm{i}\mathbf{k}\cdot\boldsymbol{X}}\,\mathbf{d}\right) \;&=\; -\,\mathrm{i}\,e^{\mathrm{i}\,\mathbf{k}\cdot\boldsymbol{X}}\,(\mathbf{d}\times\mathbf{k})\,,\\
\Rightarrow\mathbf{curl}\,\mathbf{curl}\,e^{\mathrm{i}\mathbf{k}\cdot\boldsymbol{X}}\mathbf{d} \;&=\; \mathbf{curl}\Big(\;-\,\mathrm{i}\,e^{\mathrm{i}\mathbf{k}\cdot\boldsymbol{X}}\,\mathbf{d}\times\mathbf{k}\Big) \;=\; -\,e^{\mathrm{i}\mathbf{k}\cdot\boldsymbol{X}}\Big(\mathbf{d}\times\mathbf{k}\Big)\times\mathbf{k}\\
&=\; e^{\mathrm{i}\mathbf{k}\cdot\boldsymbol{X}}\Big(\mathbf{k}\times\mathbf{d}\Big)\times\mathbf{k} \;=\; e^{\mathrm{i}\mathbf{k}\cdot\boldsymbol{X}}\,\Big(|\mathbf{k}|^2\mathbf{d}\;-\;(\mathbf{k}\cdot\mathbf{d})\,\mathbf{k}\Big)\,.
\end{aligned}$$

In two dimensions, for $\boldsymbol{V} = (V_x, V_y)$, we have the following product rules,

$$\begin{aligned}
\mathrm{curl}(f\,V) \;&=\; \partial_x(f\,V_y)\;-\;\partial_y(f\,V_x) \;=\; (\partial_x f)\,V_y\;-\;(\partial_y f)\,V_x\;+\;f\,(\partial_x V_y\;-\;\partial_y V_x)\\
&=\; -(\mathbf{curl}\,f)\cdot V\;+\;f\,\mathrm{curl}\,V\,,
\end{aligned} \tag{1.23}$$

and for scalars f and g

$$\mathbf{curl}(f\,g) \;=\; \begin{pmatrix}\partial_y(f\,g)\\ -\partial_x(f\,g)\end{pmatrix} \;=\; g\,\begin{pmatrix}\partial_y f\\ -\partial_x f\end{pmatrix}\;+\;f\,\begin{pmatrix}\partial_y g\\ -\partial_x g\end{pmatrix} \;=\; f\,\mathbf{curl}\,g\;+\;g\,\mathbf{curl}\,f\,.$$

By using equation (1.23), we obtain:

$$\begin{aligned}
\operatorname{curl}\left(e^{\mathrm{i}\mathbf{k}\cdot\boldsymbol{X}}\,\mathbf{d}\right) &= -\,(\mathbf{curl}\, e^{\mathrm{i}\mathbf{k}\cdot\boldsymbol{X}})\cdot\mathbf{d} \;=\; -\,\mathrm{i}\,e^{\mathrm{i}\,\mathbf{k}\cdot\boldsymbol{X}}\,(\mathbf{d}\times\mathbf{k})\,,\\
\mathbf{curl}\, e^{\mathrm{i}\mathbf{k}\cdot\boldsymbol{X}} &= \mathrm{i}\,e^{\mathrm{i}\mathbf{k}\cdot\boldsymbol{X}}\,\mathbf{curl}(\mathbf{k}\cdot\boldsymbol{X}) \;=\; \mathrm{i}\,e^{\mathrm{i}\mathbf{k}\cdot\boldsymbol{X}}\begin{pmatrix} k_y\\ -\,k_x\end{pmatrix},\\
\Rightarrow \mathbf{curl}\operatorname{curl}\left(e^{\mathrm{i}\mathbf{k}\cdot\boldsymbol{X}}\mathbf{d}\right) &= \mathbf{curl}\left(\,-\,\mathrm{i}\,e^{\mathrm{i}\mathbf{k}\cdot\boldsymbol{X}}\,\mathbf{d}\times\mathbf{k}\right) \;=\; e^{\mathrm{i}\,\mathbf{k}\cdot\boldsymbol{X}}\Big(|\mathbf{k}|^2\mathbf{d} \;-\; (\mathbf{k}\cdot\mathbf{d})\,\mathbf{k}\Big)\,.
\end{aligned}$$

□

Proposition 1.6 (Plane wave solutions to (1.18)). The three slownesses sustained in a poroelastic medium are

$$\text{S-wave-slowness}\qquad \mathsf{s}_{\mathrm{S}}^2(\omega) \;:=\; \frac{\det A(\omega)}{\mu_{\mathrm{fr}}\,\rho_{\mathrm{dyn}}(\omega)}\,, \tag{1.24a}$$

$$\text{'fast' P-wave-slowness}\qquad 2\,\mathsf{s}_{\mathrm{P}}^2(\omega) \;:=\; \frac{\operatorname{tr} C(\omega)}{\det B} \;-\; \sqrt{\left(\frac{\operatorname{tr} C(\omega)}{\det B}\right)^2 \;-\; 4\frac{\det A(\omega)}{\det B}}\,, \tag{1.24b}$$

$$\text{'slow' P-wave-slowness}\qquad 2\,\mathsf{s}_{\mathrm{B}}^2(\omega) \;:=\; \frac{\operatorname{tr} C(\omega)}{\det B} + \sqrt{\left(\frac{\operatorname{tr} C(\omega)}{\det B}\right)^2 \;-\; 4\frac{\det A(\omega)}{\det B}}\,, \tag{1.24c}$$

where we have defined

$$A(\omega) := \begin{pmatrix}\rho_a & \rho_f\\ \rho_f & \rho_{\mathrm{dyn}}\end{pmatrix}\quad,\quad B := \begin{pmatrix}H & \alpha M\\ \alpha M & M\end{pmatrix}\quad,\quad B^{\mathrm{cof}} = \begin{pmatrix}M & -\alpha M\\ -\alpha M & H\end{pmatrix}\quad,\quad C(\omega) := B^{\mathrm{cof}}\,A(\omega)\,, \tag{1.25}$$

and

$$\begin{aligned}
\operatorname{tr} C(\omega) &= \rho_{\mathrm{dyn}}(\omega)\,H \;-\; 2\alpha\,M\,\rho_f \;+\; \rho_a\,M\,,\\
\det B &= M\,H \;-\; (\alpha\,M)^2 \;=\; M\,(\lambda_{\mathrm{fr}} \;+\; 2\mu_{\mathrm{fr}})\,,\\
\det A(\omega) &= \rho_a\,\rho_{\mathrm{dyn}}(\omega) \;-\; \rho_f^2\,.
\end{aligned} \tag{1.26}$$

For $\bullet \in \{\mathrm{S}\,,\,\mathrm{P}\,,\,\mathrm{B}\}$, if $(\mathrm{u}_\bullet, \mathrm{w}_\bullet)$ is of the form

$$\mathrm{u}_\bullet \;=\; e^{\mathrm{i}\,\mathbf{k}_\bullet\cdot\boldsymbol{X}}\;\widehat{\mathbf{d}}\,,\qquad \mathrm{w}_\bullet \;=\; \mathcal{W}_\bullet\, e^{\mathrm{i}\,\mathbf{k}_\bullet\cdot\boldsymbol{X}}\;\widehat{\mathbf{d}}$$

solving (1.18), then the slowness $\mathsf{s}_\bullet$, the polarization $\widehat{\mathbf{d}}$ and the direction of propagation $\widehat{\mathbf{k}}$ have to satisfy the following constraints.

1. The transverse plane wave (i.e., one with polarization direction orthogonal to the propagation direction) is given by the pair $(\mathrm{u}_{\mathrm{S}}, \mathrm{w}_{\mathrm{S}})$

$$\begin{cases}
\mathbf{k}_{\mathrm{S}} \;=\; \omega\,\mathsf{s}_{\mathrm{S}}(\omega)\,\widehat{\mathbf{k}} \quad;\\
\mathsf{s}_{\mathrm{S}}(\omega) \text{ given by (1.24a)}\,,\\
\widehat{\mathbf{k}} \perp \widehat{\mathbf{d}} \quad,\quad |\widehat{\mathbf{k}}| = |\widehat{\mathbf{d}}| = 1\,,\\
\mathcal{W}_{\mathrm{S}} \;=\; -\,\dfrac{\rho_f}{\rho_{\mathrm{dyn}}(\omega)} \quad \textit{cf.}\,(1.30)\,.
\end{cases}$$

2. There are two types of longitudinal waves (i.e.those with polarization direction parallel to the propagation

direction) given by the pair $(\mathrm{u}_\bullet, \mathrm{w}_\bullet)$ with $\bullet \in \{\mathrm{P}, \mathrm{B}\}$,

$$\begin{cases} \mathbf{k}_\bullet \;=\; \omega\, \mathsf{s}_\bullet(\omega)\, \widehat{\mathbf{d}} \quad , \quad |\widehat{\mathbf{d}}| = 1, \\ \mathsf{s}_\bullet(\omega) \text{ given by (1.24b) or (1.24c)}\,, \\ \mathcal{W}_\bullet \;=\; -\dfrac{H\,\mathsf{s}_\bullet^2(\omega) - \rho_a}{\alpha\, M\, \mathsf{s}_\bullet^2(\omega) \,-\, \rho_f} \quad \textit{cf.}\,(1.33)\,. \end{cases} \tag{1.27}$$

Proof. **Step 1** We write the plane wave solutions as follows:

$$\mathrm{u} \;=\; u_0\, e^{\mathrm{i}\,\mathbf{k}\cdot\boldsymbol{X}}\, \widehat{\mathbf{d}} \quad , \quad \mathrm{w} \;=\; w_0\, e^{\mathrm{i}\,\mathbf{k}\cdot\boldsymbol{X}}\, \widehat{\mathbf{d}}\,,$$

and we replace the expressions of $\nabla\nabla\cdot\,\mathrm{u}$ and $\mathbf{curl}\,\mathbf{curl}\,\mathrm{u}$ into (1.18). We then obtain

$$\begin{aligned} -\omega^2\,\rho_a\,u_0\,\widehat{\mathbf{d}} \;-\; \rho_f\,\omega^2\,w_0\,\widehat{\mathbf{d}} \;+\; H\,u_0\,(\widehat{\mathbf{d}}\cdot\mathbf{k})\,\mathbf{k} + \;\mu_{\mathrm{fr}}\,u_0\,(\mathbf{k}\times\widehat{\mathbf{d}})\,\times\mathbf{k} \;+\; \alpha\,M\,w_0\,(\widehat{\mathbf{d}}\cdot\mathbf{k})\,\mathbf{k} = 0\,, \\ -\omega^2\,\rho_f\,u_0\,\widehat{\mathbf{d}} \;-\; \omega^2\,\rho_{\mathrm{dyn}}\,w_0\,\widehat{\mathbf{d}} \;+\; M\,w_0\,(\widehat{\mathbf{d}}\cdot\mathbf{k})\,\mathbf{k} \;+\; M\alpha u_0\,(\widehat{\mathbf{d}}\cdot\mathbf{k})\,\mathbf{k} = 0\,. \end{aligned} \tag{1.28}$$

Rearranging the terms in (1.28) by using coefficients of u_0 and w_0, we have:

$$\begin{aligned} \Big(H\,u_0 \;+\; \alpha\,M\,w_0\Big)(\widehat{\mathbf{d}}\cdot\mathbf{k})\,\mathbf{k} \;-\; \omega^2\Big(\rho_a\,u_0 \;+\; \rho_f\,w_0\Big)\,\widehat{\mathbf{d}} \;+\; \mu_{\mathrm{fr}}\,u_0\,(\mathbf{k}\times\widehat{\mathbf{d}})\,\times\mathbf{k} \;=\; 0\,, \\ -\omega^2\Big(\rho_f u_0 \;+\; \rho_{\mathrm{dyn}} w_0\Big)\,\widehat{\mathbf{d}} \;+\; M\,\Big(w_0 \;+\; \alpha\,u_0\Big)\,(\widehat{\mathbf{d}}\cdot\mathbf{k})\,\mathbf{k} \;=\; 0\,. \end{aligned} \tag{1.29}$$

Step 2 - Transverse plane waves A S plane wave has the property

$$\mathbf{k}\cdot\widehat{\mathbf{d}} \;=\; 0\,.$$

This means:

$$(\mathbf{k}\times\widehat{\mathbf{d}})\,\times\mathbf{k} \;=\; |\mathbf{k}|^2\,\widehat{\mathbf{d}}\,.$$

Using the above identity and dividing both equalities in (1.29) by $|\mathbf{k}|$, we obtain

$$-\mathsf{c}^2\,\Big(\rho_a\,u_0 \;+\; \rho_f\,w_0\Big)\widehat{\mathbf{d}} + \mu_{\mathrm{fr}}\,u_0\,\widehat{\mathbf{d}} \;=\; 0\,,$$

$$-\mathsf{c}^2(\rho_{\mathrm{f}}\,u_0 \;+\; \rho_{\mathrm{dyn}}\,w_0)\,\widehat{\mathbf{d}} \;=\; 0 \quad .$$

Recall the inverse of the slowness $\mathsf{c} := \dfrac{\omega}{|\mathbf{k}|}$, defined in (1.22). The above system in matrix form is

$$\begin{pmatrix} \mathsf{c}^2\rho_a - \mu_{\mathrm{fr}} & \mathsf{c}^2\rho_f \\ \mathsf{c}^2\rho_f & \mathsf{c}^2\rho_{\mathrm{dyn}} \end{pmatrix} \begin{pmatrix} u_0 \\ w_0 \end{pmatrix} = 0\,.$$

This means, assuming u_0 and w_0 do not vanish, that the above matrix is not invertible and has zero determinant

$$\mathsf{c}^2\rho_{\mathrm{dyn}}\,(\mathsf{c}^2\rho_a - \mu_{\mathrm{fr}}) - \mathsf{c}^4\rho_f^2 \;=\; 0 \quad \Leftrightarrow \quad \mathsf{c}^2\Big[\mathsf{c}^2\,\left(\rho_{\mathrm{dyn}}\,\rho_a - \rho_f^2\right) \;-\; \mu_{\mathrm{fr}}\rho_{\mathrm{dyn}}\Big] \;=\; 0\,.$$

We define the nonzero root to be

$$\mathsf{c}_{\mathrm{S}}(\omega) \;=\; \left(\frac{\mu_{\mathrm{fr}}\,\rho_{\mathrm{dyn}}(\omega)}{\rho_{\mathrm{dyn}}(\omega)\,\rho_a \;-\; \rho_f^2}\right)^{1/2}.$$

The associated shear-wave slowness is then

$$\mathsf{s}_{\mathrm{S}}(\omega) \;=\; \left(\frac{\rho_{\mathrm{dyn}}(\omega)\,\rho_a \;-\; \rho_f^2}{\mu_{\mathrm{fr}}\,\rho_{\mathrm{dyn}}(\omega)}\right)^{1/2}.$$

A corresponding eigenvector is

$$\mathcal{U}_{\mathrm{S}} = 1 \quad , \quad \mathcal{W}_{\mathrm{S}} \;=\; -\,\frac{\rho_f}{\rho_{\mathrm{dyn}}(\omega)}\,. \tag{1.30}$$

Step 3 - Longitudinal plane waves

- A P plane wave has the property

$$\mathbf{k} \times \widehat{\mathbf{d}} \;=\; 0\,.$$

Since $\mathbf{k}$ is parallel to $\widehat{\mathbf{d}}$, we can write

$$\widehat{\mathbf{d}} = a\,\mathbf{k} \quad , \quad \widehat{\mathbf{d}}\cdot\mathbf{k} = a|\mathbf{k}|^2\,, \qquad a\in\mathbb{R}\,,$$

then equation (1.29) becomes

$$\begin{aligned}
\Big(H u_0 + \alpha M w_0\Big)(\widehat{\mathbf{d}}\cdot\mathbf{k})\mathbf{k} - \omega^2\Big(\rho_a\, u_0 + \rho_f\, w_0\Big)\,\widehat{\mathbf{d}} \;&=\; 0\,,\\
-\omega^2(\rho_f\, u_0 \,+\, \rho_{\rm dyn}\, w_0)\,\widehat{\mathbf{d}} + M\Big(w_0 \,+\, \alpha\, u_0\Big)(\widehat{\mathbf{d}}\cdot\mathbf{k})\mathbf{k} \;&=\; 0\,.\\
\Rightarrow \Big(H\, u_0 \,+\, \alpha\, M\, w_0\Big)\, a\,|\mathbf{k}|^2\mathbf{k} - \omega^2\Big(\rho_a\, u_0 \,+\, \rho_f\, w_0\Big)\, a\,\mathbf{k} \;&=\; 0\,,\\
-\omega^2(\rho_f\, u_0 \,+\, \rho_{\rm dyn}\, w_0)\, a\,\mathbf{k} + M\Big(w_0 \,+\, \alpha\, u_0\Big)\, a\,|\mathbf{k}|^2\mathbf{k} \;&=\; 0\,.
\end{aligned} \tag{1.31}$$

Dividing (1.31) by a and $|\mathbf{k}|^2$, gives

$$\begin{aligned}
\Big(H\, u_0 + \,\alpha\, M\, w_0\Big) - \mathsf{c}^2\Big(\rho_a\, u_0 + \rho_f\, w_0\Big) \;&=\; 0\,,\\
-\mathsf{c}^2(\rho_f\, u_0 + \rho_{\rm dyn}\, w_0) + M\Big(w_0 \,+\alpha\, u_0\Big) \;&=\; 0\,.
\end{aligned} \tag{1.32}$$

Written in matrix form, we obtain

$$\begin{pmatrix} H - \mathsf{c}^2\rho_a & \alpha M - \mathsf{c}^2\rho_f \\ -\mathsf{c}^2\rho_f + \alpha M & -\mathsf{c}^2\rho_{\rm dyn} + M \end{pmatrix}\begin{pmatrix} u_0 \\ w_0 \end{pmatrix} = 0\,,$$

or

$$B\begin{pmatrix} u_0 \\ w_0 \end{pmatrix} - \mathsf{c}^2 A\begin{pmatrix} u_0 \\ w_0 \end{pmatrix} = 0 \quad \Rightarrow \quad C\begin{pmatrix} u_0 \\ w_0 \end{pmatrix} - (\det A)\mathsf{c}^2\begin{pmatrix} u_0 \\ w_0 \end{pmatrix} = 0\,,$$

where we have defined

$$B := \begin{pmatrix} H & \alpha M \\ \alpha M & M \end{pmatrix} \quad , \quad A := \begin{pmatrix} \rho_a & \rho_f \\ \rho_f & \rho_{\rm dyn} \end{pmatrix} \quad , A^{\rm cof} = \begin{pmatrix} \rho_{\rm dyn} & -\rho_f \\ -\rho_f & \rho_a \end{pmatrix} \quad ,$$

$$C := A^{\rm cof}B \;=\; \begin{pmatrix} \rho_{\rm dyn} & -\rho_f \\ -\rho_f & \rho_a \end{pmatrix}\begin{pmatrix} H & \alpha M \\ \alpha M & M \end{pmatrix} = \begin{pmatrix} \rho_{\rm dyn}\,H - \alpha M\rho_f & \rho_{\rm dyn}\alpha M - \rho_f M \\ -\rho_f H + \rho_a\alpha M & -\rho_f\alpha M + \rho_a M \end{pmatrix}.$$

This means $(\det A)\,\mathsf{c}^2$ is an eigenvalue of C. Note that both A and B are symmetric, thus diagonalizable.

We next consider the eigenvalues $\tilde{\mathsf{c}}$ of C, which satisfy the quadratic relation

$$\tilde{c}^2 - \tilde{c}\,\mathrm{tr}\,C + \det C \;\;= 0\,,$$

and are thus given by

$$2\tilde{c} := \mathrm{tr}\,C \mp \sqrt{(\mathrm{tr}\,C)^2 \,-\, 4\det C}\,.$$

Here, in presence of viscosity, the argument in the above square root is complex. Without viscosity, we verify in Table 1.2 that the square root is defined for the materials in consideration. This means

$$2\mathsf{c}^2 = \frac{1}{\det A}\left(\mathrm{tr}\,C \mp \sqrt{(\mathrm{tr}\,C)^2 \,-\, 4\det C}\right).$$

Since

$$\det C \;=\; (\det A^{\rm cof})\,\det B = (\det A)\,(\det B) \quad ,$$

we have

$$2\,\mathsf{c}^2 \;=\; \frac{\mathrm{tr}\,C}{\det A} \mp \sqrt{\left(\frac{\mathrm{tr}\,C}{\det A}\right)^2 \,-\, 4\frac{\det B}{\det A}}\,.$$

Longitudinal slowness

- Consider the longitudinal slownesses. Then $(\det B)\mathsf{s}$ is an eigenvalue of $\tilde{C} := B^{\rm cof}A$. We note that

$$\tilde{C} := \begin{pmatrix} M & -\alpha M \\ -\alpha M & H \end{pmatrix} \begin{pmatrix} \rho_a & \rho_f \\ \rho_f & \rho_{\rm dyn} \end{pmatrix} \quad , \quad \Rightarrow \operatorname{tr} \tilde{C} = M\rho_a - 2\alpha M \rho_f + H\rho_{\rm dyn} \;=\; \operatorname{tr} C \,,$$
$$\det \tilde{C} = (\det B)(\det A)\,.$$

As a result,

$$\text{'fast' P-wave-slowness} \quad , \quad 2\,\mathsf{s}_{\rm P}^2 \;:=\; \frac{\operatorname{tr} C}{\det B} - \sqrt{\left(\frac{\operatorname{tr} C}{\det B}\right)^2 - 4\frac{\det A}{\det B}}\,,$$

$$\text{'slow' P-wave-slowness} \quad , \quad 2\,\mathsf{s}_{\rm B}^2 \;:=\; \frac{\operatorname{tr} C}{\det B} + \sqrt{\left(\frac{\operatorname{tr} C}{\det B}\right)^2 - 4\frac{\det A}{\det B}}\,.$$

Here, in presence of viscosity, the argument in the square roots is complex. Without viscosity, we verify in Table 1.2 that the square roots are defined for the materials in consideration. The components of corresponding eigenvectors are read from (1.32):

$$\mathcal{U}_\bullet = 1 \quad , \quad \mathcal{W}_\bullet \;=\; -\frac{H\,\mathsf{s}_\bullet^2 - \rho_a}{\mathsf{s}_\bullet^2\,\alpha\,M - \rho_f}\,, \quad \mathsf{s}_\bullet \in \{\mathsf{s}_{\rm P}\,, \mathsf{s}_{\rm B}\}\,. \tag{1.33}$$

□

Equivalence with Pride notations [107] We compare with the notations used in formula [107, (9.15),(9.19)] for the matrices B and C.

	Pride's notations	Our notation
Undrained bulk modulus	K_U	$\mathsf{k}_{\rm fr} + \alpha^2 M = \lambda_{\rm fr} + \frac{2}{3}\mu_{\rm fr} + \alpha^2 M = H - \frac{4}{3}\mu_{\rm fr}$
Undrained shear modulus	G	$\mu_{\rm fr}$
Biot	C	αM
incompressibilites	M	M
constants[107, (9.18)]	$H = K_U + \frac{4}{3}G$	$\lambda_{\rm fr} + \frac{2}{3}\mu_{\rm fr} + \alpha^2 M + \frac{4}{3}\mu_{\rm fr} \;= \lambda_{\rm fr} + 2\mu_{\rm fr} + \alpha^2 M = H$
	$HM - C^2$	$\det B = MH - (\alpha M)^2 \;= M(\lambda_{\rm fr} + 2\mu_{\rm fr})$
	$\rho_a H + \tilde{\rho} M - 2\rho_f C$	$\operatorname{tr} C = \rho_{\rm dyn} H - 2\alpha M \rho_f + \rho_a M$
[107, (9.20)]	$\gamma = \frac{\rho_a M + \rho_{\rm dyn} H - 2\rho_f C}{HM - C^2}$	$\frac{\operatorname{tr} C}{\det B}$

1.5.2 First order formulation of the corresponding plane wave solution

Using the slowness expresssions from (1.24), the plane wave writes:

1. For the transverse wave (polarization direction perpendicular to the propagation direction):

$$\begin{aligned} \mathbf{u}_{\rm S} \;&=\; e^{\mathrm{i}\,\mathbf{k}_{\rm S}\cdot\boldsymbol{x}}\;(\mathsf{s}\,\mathrm{i}\,\omega)\;\widehat{\mathbf{d}} \quad , \quad \mathbf{w}_{\rm S} \;=\; \mathcal{W}_{\rm S}\,e^{\mathrm{i}\,\mathbf{k}_{\rm S}\cdot\boldsymbol{x}}\;(\mathsf{s}\,\mathrm{i}\,\omega)\;\widehat{\mathbf{d}}\,, \\ \boldsymbol{\tau}_{\rm S} \;&=\; \mathrm{i}\,\omega\,\mathsf{s}_{\rm S}(\omega)\,e^{\mathrm{i}\,\mathbf{k}_{\rm S}\cdot\boldsymbol{x}}\,\mu_{\rm fr}\left(\widehat{\mathbf{k}}\otimes\widehat{\mathbf{d}} + \widehat{\mathbf{d}}\otimes\widehat{\mathbf{k}}\right), \\ \mathrm{p}_{\rm S} \;&=\; 0\,. \end{aligned}$$

with polarization given by

$$\begin{cases} \mathbf{k}_{\rm S} \;=\; \omega\,\mathsf{s}_{\rm S}(\omega)\,\widehat{\mathbf{k}} \quad , \\ \mathsf{s}_{\rm S}(\omega) \text{ given by (1.24a)}\,, \\ \widehat{\mathbf{k}} \perp \widehat{\mathbf{d}} \quad , \quad |\widehat{\mathbf{k}}| = |\widehat{\mathbf{d}}| = 1\,, \\ \mathcal{W}_{\rm S} \;=\; \dfrac{\rho_f}{\rho_{\rm dyn}(\omega)} \quad \textit{cf.}\,(1.30)\,. \end{cases}$$

2. For the two types of longitudinal waves P and B (polarization direction parallel to the propagation direction), which are distinguished by subscript $\bullet \in \{\mathrm{P}, \mathrm{B}\}$:

$$\begin{aligned}
\mathbf{u}_\bullet &= e^{\mathrm{i}\,\mathbf{k}_\bullet\cdot\boldsymbol{x}}\,(\mathfrak{s}\,\mathrm{i}\,\omega)\,\widehat{\mathbf{d}} \quad , \quad \mathbf{w}_\bullet = \mathcal{W}_\bullet\, e^{\mathrm{i}\,\mathbf{k}_\bullet\cdot\boldsymbol{x}}\,(\mathfrak{s}\,\mathrm{i}\,\omega)\,\widehat{\mathbf{d}}\,,\\
\boldsymbol{\tau}_\bullet &= \mathrm{i}\,\omega\,\mathsf{s}_\bullet(\omega)\,e^{\mathrm{i}\mathbf{k}_\bullet\cdot\boldsymbol{x}}\left(2\,\mu_{\mathrm{fr}}\,\widehat{\mathbf{d}}\otimes\widehat{\mathbf{d}} + \Big(\underbrace{-\tfrac{2}{3}\mu_{\mathrm{fr}} + \mathrm{k}_{\mathrm{fr}}}_{\lambda_{\mathrm{fr}}} + M\,\alpha^2 + \mathcal{W}_\bullet\,\alpha\,M\Big)\,\mathbb{I}\right),\\
\mathrm{p}_\bullet &= \mathrm{i}\,\omega\,\mathsf{s}_\bullet(\omega)\,(-M\,\mathcal{W}_\bullet - M\,\alpha)\,e^{\mathrm{i}\mathbf{k}_\bullet\cdot\boldsymbol{x}}\,.
\end{aligned}$$

with polarization given by

$$\begin{cases}
\mathbf{k}_\bullet = \omega\,\mathsf{s}_\bullet(\omega)\,\widehat{\mathbf{d}} \quad , \quad |\widehat{\mathbf{d}}| = 1,\\
\mathsf{s}_\bullet(\omega) \text{ given by (1.24b) or (1.24c)},\\
\mathcal{W}_\bullet = -\dfrac{H\,\mathsf{s}_\bullet^2(\omega) - \rho_a}{\alpha\,M\,\mathsf{s}_\bullet^2(\omega) - \rho_f} \qquad \textit{cf.}\ (1.33)\,.
\end{cases}$$

Proof. The expression of the second order plane wave is of the form:

$$\mathrm{u}_\bullet = e^{\mathrm{i}\,\mathbf{k}_\bullet\cdot\boldsymbol{x}}\,\mathbf{d} \quad , \quad \mathrm{w}_\bullet = \mathcal{W}_\bullet\, e^{\mathrm{i}\,\mathbf{k}_\bullet\cdot\boldsymbol{x}}\,\mathbf{d}\,, \quad \bullet \in \{\mathrm{S}, \mathrm{P}, \mathrm{B}\}\,.$$

The velocities are the time-derivative of the displacement. As a result, we obtain:

$$\mathbf{u}_\bullet = e^{\mathrm{i}\,\mathbf{k}_\bullet\cdot\boldsymbol{x}}\,(\mathfrak{s}\,\mathrm{i}\,\omega)\,\mathbf{d} \quad , \quad \mathbf{w}_\bullet = \mathcal{W}_\bullet\, e^{\mathrm{i}\,\mathbf{k}_\bullet\cdot\boldsymbol{x}}\,(\mathfrak{s}\,\mathrm{i}\,\omega)\,\mathbf{d}\,, \quad \bullet \in \{\mathrm{S}, \mathrm{P}, \mathrm{B}\}\,.$$

The expression of the pressure p is given by (1.14). By using the relation $\nabla\cdot\,(e^{\mathrm{i}\mathbf{k}\cdot\boldsymbol{x}}\mathbf{d}) = \mathrm{i}\,e^{\mathrm{i}\mathbf{k}\cdot\boldsymbol{x}}\mathbf{d}\cdot\mathbf{k}$ and replacing the value of the plane wave, we obtain for p:

$$\begin{aligned}
\mathrm{p}_\bullet &= -M\,\nabla\cdot\mathrm{w} - M\,\alpha\nabla\cdot\mathrm{u}\\
&= \mathrm{i}\,\mathbf{d}\cdot\mathbf{k}\,(-M\,\mathcal{W}_\bullet - M\,\alpha)\,e^{\,\mathrm{i}\mathbf{k}\cdot\boldsymbol{x}}\,.
\end{aligned}$$

The stress tensor $\boldsymbol{\tau}$ is expressed in (1.13). We replace the value of $\nabla\cdot\mathrm{u}$, $\nabla\cdot\mathrm{w}$ and $\boldsymbol{\epsilon}_{\mathrm{fr}} = \mathrm{i}\,e^{\mathrm{i}\mathbf{k}\cdot\boldsymbol{x}}\,\frac{1}{2}\,(\mathbf{d}\otimes\mathbf{k} + \mathbf{k}\otimes\mathbf{d})$, to obtain:

$$\begin{aligned}
\boldsymbol{\tau}_\bullet &= 2\mu_{\mathrm{fr}}\boldsymbol{\epsilon} + \Big(\lambda_{\mathrm{fr}} + M\alpha^2\Big)\,\nabla\cdot\mathrm{u}\,\mathbb{I} + \alpha M\nabla\cdot\mathrm{w}\,\mathbb{I}\\
&= \mathrm{i}\,e^{\mathrm{i}\mathbf{k}\cdot\boldsymbol{x}}\Big(\mu_{\mathrm{fr}}\,(\mathbf{k}\otimes\mathbf{d} + \mathbf{d}\otimes\mathbf{k}) + \big(\lambda_{\mathrm{fr}} + M\alpha^2 + \mathcal{W}_\bullet\,\alpha\,M\big)\,\mathbf{d}\cdot\mathbf{k}\,\mathbb{I}\Big)\,.
\end{aligned}$$

To finish the proof, we only need to symplify the expression of $\boldsymbol{\tau}$ and p by using $\mathbf{k}\cdot\mathbf{d} = 0$ for transverse wave and $\mathbf{k}\times\mathbf{d} = 0$ for longitudinal waves.

□

1.5.3 Expansion of the incident plane wave in Bessel functions in two dimensions

The incident plane wave is expanded to form a right-hand side vector.

For a longitudinal wave Recall the admissible longitudinal plane waves allowed in an isotropic poroelastic medium from (1.35), $\bullet \in \{\mathrm{P}, \mathrm{B}\}$.

$$\begin{aligned}
\mathbf{u}_\bullet^{\mathrm{pw}} &= e^{\mathrm{i}\,\mathbf{k}_\bullet\cdot\boldsymbol{x}}\,(\mathfrak{s}\,\mathrm{i}\,\omega)\,\widehat{\mathbf{d}} = \frac{\mathfrak{s}}{\mathsf{s}_\bullet}\nabla(e^{\mathrm{i}\,\mathbf{k}_\bullet\cdot\boldsymbol{x}}) \quad ,\\
\mathbf{w}_\bullet^{\mathrm{pw}} &= \mathcal{W}_\bullet\, e^{\mathrm{i}\,\mathbf{k}_\bullet\cdot\boldsymbol{x}}\,(\mathfrak{s}\,\mathrm{i}\,\omega)\,\widehat{\mathbf{d}}\,,\\
\boldsymbol{\tau}_\bullet^{\mathrm{pw}} &= \mathrm{i}\,\omega\,\mathsf{s}_\bullet(\omega)\,e^{\mathrm{i}\mathbf{k}_\bullet\cdot\boldsymbol{x}}\left(2\,\mu_{\mathrm{fr}}\,\widehat{\mathbf{d}}\otimes\widehat{\mathbf{d}} + \Big(\underbrace{-\tfrac{2}{3}\mu_{\mathrm{fr}} + \mathrm{k}_{\mathrm{fr}}}_{\lambda_{\mathrm{fr}}} + M\,\alpha^2 + \mathcal{W}_\bullet\,\alpha\,M\Big)\,\mathbb{I}\right),\\
\mathrm{p}_\bullet^{\mathrm{pw}} &= \mathrm{i}\,\omega\,\mathsf{s}_\bullet(\omega)\,(-M\,\mathcal{W}_\bullet - M\,\alpha)\,e^{\mathrm{i}\mathbf{k}_\bullet\cdot\boldsymbol{x}}\,,
\end{aligned} \tag{1.36}$$

with the polarization given by

$$\begin{cases} \mathbf{k}_\bullet \;=\; \omega\, \mathsf{s}_\bullet(\omega)\, \widehat{\mathbf{d}} \quad , \quad \widehat{\mathbf{d}} = (\cos\alpha_{\rm inc}, \sin\alpha_{\rm inc}), \\ \mathsf{s}_\bullet(\omega) \text{ given by (1.24b) or (1.24c)}\,, \\ \mathcal{W}_\bullet \;=\; -\dfrac{H\,\mathsf{s}_\bullet^2(\omega) - \rho_a}{\alpha\, M\, \mathsf{s}_\bullet^2(\omega) - \rho_f} \qquad \textit{cf.}\ (1.33)\,. \end{cases}$$

We have the Jacobi-Anger expansion, see for e.g [91, eqn (2.17)],

$$e^{\mathrm{i}\, t\, \cos\varphi} = \sum_{k=-\infty}^{\infty} \mathrm{i}^k \mathrm{J}_k(t)\, e^{ik\varphi}. \tag{1.37}$$

The multipole expansion relative to the origin $0_{\mathbb{R}^2}$ is given by

$$e^{\mathrm{i}\,\omega\,\mathsf{s}\,\boldsymbol{x}\cdot(\cos\alpha_{\rm inc},\sin\alpha_{\rm inc})} \;=\; e^{\mathrm{i}\,\omega\,\mathsf{s}\,|\boldsymbol{x}|\,\cos(\theta-\alpha_{\rm inc})} \;=\; \sum_{k=-\infty}^{\infty} \mathrm{i}^k\, \mathrm{J}_k(\kappa\,|\boldsymbol{x}|)\; e^{\mathrm{i}\,k(\theta-\alpha_{\rm inc})}\,. \tag{1.38}$$

Thus,

$$e^{\mathrm{i}\,\omega\,\mathsf{s}_\bullet\,\boldsymbol{x}\cdot\widehat{\mathbf{d}}} \;=\; \sum_{k=-\infty}^{\infty} \mathrm{i}^k\, \mathrm{J}_k(\omega\,\mathsf{s}_\bullet\,|\boldsymbol{x}|)\; e^{\mathrm{i}\,k(\theta-\alpha_{\rm inc})}\,.$$

We now work in polar coordinates. We have

$$\mathbf{u}_\bullet^{\rm pw} \;=\; \frac{\mathfrak{s}}{\mathsf{s}_\bullet}\nabla(e^{\mathrm{i}\,\mathbf{k}_\bullet\cdot\boldsymbol{x}})\,,$$

$$\Rightarrow \mathbf{u}_\bullet^{\rm pw} \;=\; \frac{\mathfrak{s}}{\mathsf{s}_\bullet}\nabla\left(\sum_{k=-\infty}^{\infty} \mathrm{i}^k\, \mathrm{J}_k(\omega\,\mathsf{s}_\bullet\, r)\; e^{\mathrm{i}\,k(\theta-\alpha_{\rm inc})}\right).$$

Next, we use ∇ in polar coordinates $\nabla = \partial_r \mathbf{e}_r + \dfrac{1}{r}\partial_\theta \mathbf{e}_\theta$.

$$\mathbf{u}_\bullet^{\rm pw} \;=\; \frac{\mathfrak{s}}{\mathsf{s}_\bullet}\sum_{k=-\infty}^{\infty} \mathrm{i}^k\,\omega\,\mathsf{s}_\bullet\,\mathrm{J}_k'(\omega\,\mathsf{s}_\bullet\, r)\; e^{\mathrm{i}\,k(\theta-\alpha_{\rm inc})}\;\mathbf{e}_r \;+\; \frac{\mathfrak{s}}{\mathsf{s}_\bullet\, r}\sum_{k=-\infty}^{\infty} \mathrm{i}^{k+1}\,k\,\mathrm{J}_k(\omega\,\mathsf{s}_\bullet\, r)\; e^{\mathrm{i}\,k(\theta-\alpha_{\rm inc})}\;\mathbf{e}_\theta\,.$$

We obtain the same thing for $\mathbf{w}$,

$$\mathbf{w}_\bullet^{\rm pw} \;=\; \mathcal{W}_\bullet\, e^{\mathrm{i}\,\mathbf{k}_\bullet\cdot\boldsymbol{x}}\;(\mathfrak{s}\,\mathrm{i}\,\omega)\;\widehat{\mathbf{d}} \;=\; \frac{\mathcal{W}_\bullet}{\mathsf{s}_\bullet}\nabla(e^{\mathrm{i}\,\mathfrak{s}\,\mathbf{k}_\bullet\cdot\boldsymbol{x}})\,,$$

$$\Rightarrow \mathbf{w}_\bullet^{\rm pw} \;=\; \mathfrak{s}\,\frac{\mathcal{W}_\bullet}{\mathsf{s}_\bullet}\nabla\left(\sum_{k=-\infty}^{\infty} \mathrm{i}^k\, \mathrm{J}_k(\omega\,\mathsf{s}_\bullet\, r)\; e^{\mathrm{i}\,k(\theta-\alpha_{\rm inc})}\right).$$

In polar coordinates:

$$\mathbf{w}_\bullet^{\rm pw} \;=\; \mathfrak{s}\,\frac{\mathcal{W}_\bullet}{\mathsf{s}_\bullet}\sum_{k=-\infty}^{\infty} \mathrm{i}^k\,\omega\,\mathsf{s}_\bullet\,\mathrm{J}_k'(\omega\,\mathsf{s}_\bullet\, r)\; e^{\mathrm{i}\,k(\theta-\alpha_{\rm inc})}\,\mathbf{e}_r \;+\; \mathfrak{s}\,\frac{\mathcal{W}_\bullet}{\mathsf{s}_\bullet\, r}\sum_{k=-\infty}^{\infty} \mathrm{i}^{k+1}\,k\,\mathrm{J}_k(\omega\,\mathsf{s}_\bullet\, r)\; e^{\mathrm{i}\,k(\theta-\alpha_{\rm inc})}\,\mathbf{e}_\theta\,.$$

For the stress tensor, (1.36) gives:

$$\boldsymbol{\tau}_\bullet^{\rm pw} \;=\; \frac{2\,\mu_{\rm fr}}{\mathrm{i}\,\omega\,\mathsf{s}_\bullet}\,\nabla^2 e^{\mathrm{i}\mathbf{k}_\bullet\cdot\boldsymbol{x}} \;+\; \Big(\underbrace{-\tfrac{2}{3}\mu_{\rm fr} \;+\; \mathrm{k}_{\rm fr}}_{\lambda_{\rm fr}} + M\,\alpha^2 \;+\; \mathcal{W}_\bullet\,\alpha\,M\Big)\,\mathrm{i}\,\omega\,\mathsf{s}_\bullet\, e^{\mathrm{i}\mathbf{k}_\bullet\cdot\boldsymbol{x}}\,\mathbb{I}\,.$$

As we will be interested by $\boldsymbol{\tau}\,\boldsymbol{n} = \tau_{rr}\,\mathbf{e}_r + \tau_{r\theta}\,\mathbf{e}_\theta$ in circular coordinates, we will only detail the expressions of the components τ_{rr} and $\tau_{r\theta}$:

$$\begin{aligned}
\tau^{\rm pw}_{\bullet,rr} &= \frac{2\,\mu_{\rm fr}}{\mathrm{i}\,\omega\,\mathsf{s}_\bullet}\,\partial_{rr}e^{\mathrm{i}\mathbf{k}_\bullet\cdot\boldsymbol{x}} + \Big(\underbrace{-\tfrac{2}{3}\mu_{\rm fr} + \mathrm{k}_{\rm fr}}_{\lambda_{\rm fr}} + M\,\alpha^2 + \mathcal{W}_\bullet\,\alpha\,M\Big)\,\mathrm{i}\,\omega\,\mathsf{s}_\bullet\,e^{\mathrm{i}\mathbf{k}_\bullet\cdot\boldsymbol{x}}\\
&= \frac{2\,\mu_{\rm fr}}{\mathrm{i}\,\omega\,\mathsf{s}_\bullet}\sum_{k=-\infty}^{\infty}\mathrm{i}^k\omega^2\,\mathsf{s}_\bullet^2\,\mathrm{J}_k''(\omega\,\mathsf{s}_\bullet\,r)\;e^{\mathrm{i}\,k(\theta-\alpha_{\rm inc})}\\
&+ \Big(\underbrace{-\tfrac{2}{3}\mu_{\rm fr} + \mathrm{k}_{\rm fr}}_{\lambda_{\rm fr}} + M\,\alpha^2 + \mathcal{W}_\bullet\,\alpha\,M\Big)\,\mathrm{i}\,\omega\,\mathsf{s}_\bullet\sum_{k=-\infty}^{\infty}\mathrm{i}^k\,\mathrm{J}_k(\omega\,\mathsf{s}_\bullet\,r)\;e^{\mathrm{i}\,k(\theta-\alpha_{\rm inc})}\\
&= 2\,\mu_{\rm fr}\sum_{k=-\infty}^{\infty}\mathrm{i}^{k-1}\,\mathrm{J}_{k+1}(\omega\,\mathsf{s}_\bullet\,r)\;e^{\mathrm{i}\,k(\theta-\alpha_{\rm inc})} - \frac{2\,\mu_{\rm fr}}{\omega\,\mathsf{s}_\bullet}\sum_{k=-\infty}^{\infty}\mathrm{i}^{k-1}\,\mathrm{J}_k(\omega\,\mathsf{s}_\bullet\,r)\;e^{\mathrm{i}\,k(\theta-\alpha_{\rm inc})}\\
&- 2\,\mu_{\rm fr}\sum_{k=-\infty}^{\infty}\mathrm{i}^{k-1}\omega\,\mathsf{s}_\bullet\,\mathrm{J}_k(\omega\,\mathsf{s}_\bullet\,r)\;e^{\mathrm{i}\,k(\theta-\alpha_{\rm inc})} + \frac{2\,\mu_{\rm fr}}{\omega\,\mathsf{s}_\bullet}\sum_{k=-\infty}^{\infty}\mathrm{i}^{k-1}k^2\,\mathrm{J}_k(\omega\,\mathsf{s}_\bullet\,r)\;e^{\mathrm{i}\,k(\theta-\alpha_{\rm inc})}\\
&+ \Big(\underbrace{-\tfrac{2}{3}\mu_{\rm fr} + \mathrm{k}_{\rm fr}}_{\lambda_{\rm fr}} + M\,\alpha^2 + \mathcal{W}_\bullet\,\alpha\,M\Big)\,\mathrm{i}\,\omega\,\mathsf{s}_\bullet\sum_{k=-\infty}^{\infty}\mathrm{i}^k\,\mathrm{J}_k(\omega\,\mathsf{s}_\bullet\,r)\;e^{\mathrm{i}\,k(\theta-\alpha_{\rm inc})}\,,
\end{aligned}$$

$$\begin{aligned}
\tau^{\rm pw}_{\bullet,r\theta} &= \frac{2\,\mu_{\rm fr}}{\mathrm{i}\,\omega\,\mathsf{s}_\bullet}\left(\frac{\partial_\theta r}{r}e^{\mathrm{i}\mathbf{k}_\bullet\cdot\boldsymbol{x}} - \frac{\partial_\theta}{r^2}e^{\mathrm{i}\mathbf{k}_\bullet\cdot\boldsymbol{x}}\right)\\
&= \frac{2\,\mu_{\rm fr}}{\mathrm{i}\,\omega\,\mathsf{s}_\bullet}\left(\frac{1}{r}\sum_{k=-\infty}^{\infty}\omega\,\mathsf{s}_\bullet\,\mathrm{i}^{k+1}\,k\,\mathrm{J}_k'(\omega\,\mathsf{s}_\bullet\,r)\;e^{\mathrm{i}\,k(\theta-\alpha_{\rm inc})} - \frac{1}{r^2}\sum_{k=-\infty}^{\infty}\mathrm{i}^{k+1}\,k\,\mathrm{J}_k(\omega\,\mathsf{s}_\bullet\,r)\;e^{\mathrm{i}\,k(\theta-\alpha_{\rm inc})}\right)\\
&= \sum_{k=-\infty}^{\infty}\frac{2\,\mu_{\rm fr}\,\mathrm{i}^k\,k}{r}\,\mathrm{J}_k'(\omega\,\mathsf{s}_\bullet\,r)\;e^{\mathrm{i}\,k(\theta-\alpha_{\rm inc})} - \sum_{k=-\infty}^{\infty}\frac{2\,\mu_{\rm fr}\mathrm{i}^k\,k}{\omega\,\mathsf{s}_\bullet\,r^2}\,\mathrm{J}_k(\omega\,\mathsf{s}_\bullet\,r)\;e^{\mathrm{i}\,k(\theta-\alpha_{\rm inc})}\,.
\end{aligned}$$

For the pressure, we obtain directly

$$\mathrm{p}^{\rm pw}_\bullet = \mathrm{i}\,\omega\,\mathsf{s}_\bullet\,(-M\,\mathcal{W}_\bullet - M\,\alpha)\sum_{k=-\infty}^{\infty}\mathrm{i}^k\,\mathrm{J}_k(\omega\,\mathsf{s}_\bullet\,r)\;e^{\mathrm{i}\,k(\theta-\alpha_{\rm inc})}\,.$$

For a transverse wave The admissible transverse plane wave allowed in an isotropic poroelastic medium from (1.35) is expressed as:

$$\begin{aligned}
\mathbf{u}^{\rm pw}_{\rm S} &= e^{\mathrm{i}\,\mathbf{k}_{\rm S}\cdot\boldsymbol{x}}\,(\mathfrak{s}\,\mathrm{i}\,\omega)\,\widehat{\mathbf{d}} = -\frac{\mathfrak{s}}{\mathsf{s}_{\rm S}}\mathbf{curl}\left(e^{\mathrm{i}\,\mathfrak{s}\,\mathbf{k}_{\rm S}\cdot\boldsymbol{x}}\right),\\
\mathbf{w}^{\rm pw}_{\rm S} &= \mathcal{W}_{\rm S}\,e^{\mathrm{i}\,\mathbf{k}_{\rm S}\cdot\boldsymbol{x}}\,(\mathfrak{s}\,\mathrm{i}\,\omega)\,\widehat{\mathbf{d}} = -\mathfrak{s}\,\frac{\mathcal{W}_{\rm S}}{\mathsf{s}_{\rm S}}\mathbf{curl}\left(e^{\mathrm{i}\,\mathbf{k}_{\rm S}\cdot\boldsymbol{x}}\right),\\
\boldsymbol{\tau}^{\rm pw}_{\rm S} &= \mathrm{i}\,\omega\,\mathsf{s}_{\rm S}\,e^{\mathrm{i}\,\mathbf{k}_{\rm S}\cdot\boldsymbol{x}}\,\mu_{\rm fr}\left(\widehat{\mathbf{k}}\otimes\widehat{\mathbf{d}} + \widehat{\mathbf{d}}\otimes\widehat{\mathbf{k}}\right),\\
\mathrm{p}^{\rm pw}_{\rm S} &= 0\,,
\end{aligned}\tag{1.39}$$

with the polarization given by

$$\begin{cases}
\mathbf{k}_{\rm S} = \omega\,\mathsf{s}_{\rm S}(\omega)\,\widehat{\mathbf{k}}\quad,\\
\widehat{\mathbf{k}} = (\cos\alpha_{\rm inc},\sin\alpha_{\rm inc})\quad \widehat{\mathbf{d}} = (-\sin\alpha_{\rm inc},\cos\alpha_{\rm inc}),\\
\mathsf{s}_{\rm S}(\omega)\text{ given by (1.24a)}\,,\\
\mathcal{W}_{\rm S} = \dfrac{\rho_f}{\rho_{\rm dyn}(\omega)}\quad \textit{cf.}\,(1.30)\,.
\end{cases}$$

Recall that the multipole expansion relative to the origin $0_{\mathbb{R}^2}$ is given by

$$e^{\mathrm{i}\,\kappa\boldsymbol{x}\cdot(\cos\alpha_{\rm inc},\sin\alpha_{\rm inc})} = \sum_{k=-\infty}^{\infty}\mathrm{i}^k\,\mathrm{J}_k(\kappa\,r)\;e^{\mathrm{i}\,k(\theta-\alpha_{\rm inc})}\,.$$

We have

$$\mathbf{u}_{\mathrm{S}}^{\mathrm{pw}} \;=\; -\,\frac{\mathfrak{s}}{\mathsf{s}_{\mathrm{S}}}\mathbf{curl}(e^{\mathrm{i}\,\mathbf{k}_{\mathrm{S}}\cdot\boldsymbol{x}})\,,$$

$$\Rightarrow \mathbf{u}_{\mathrm{S}}^{\mathrm{pw}} \;=\; -\,\frac{\mathfrak{s}}{\mathsf{s}_{\mathrm{S}}}\mathbf{curl}\left(\sum_{k=-\infty}^{\infty}\mathrm{i}^{k}\,\mathrm{J}_k(\omega\,\mathsf{s}_{\mathrm{S}}\,r)\;e^{\mathrm{i}\,k(\theta-\alpha_{\mathrm{inc}})}\right).$$

Then, we use **curl** in polar coordinates: $\mathbf{curl} = \dfrac{1}{r}\partial_\theta\mathbf{e}_r - \partial_r\mathbf{e}_\theta$

$$\mathbf{u}_{\mathrm{S}}^{\mathrm{pw}} \;=\; -\,\frac{\mathfrak{s}}{\mathsf{s}_{\mathrm{S}}\;r}\sum_{k=-\infty}^{\infty}\mathrm{i}^{k+1}\,k\,\mathrm{J}_k(\omega\,\mathsf{s}_{\mathrm{S}}\,r)\;e^{\mathrm{i}\,k(\theta-\alpha_{\mathrm{inc}})}\;\mathbf{e}_r$$

$$+\,\frac{\mathfrak{s}}{\mathsf{s}_{\mathrm{S}}}\sum_{k=-\infty}^{\infty}\mathrm{i}^{k}\,\omega\,\mathsf{s}_{\mathrm{S}}\,\mathrm{J}_k'(\omega\,\mathsf{s}_{\mathrm{S}}\,r)\;e^{\mathrm{i}\,k(\theta-\alpha_{\mathrm{inc}})}\;\mathbf{e}_\theta\,.$$

Equivalently for $\mathbf{w}$,

$$\mathbf{w}_{\mathrm{S}}^{\mathrm{pw}} \;=\; \mathcal{W}_{\mathrm{S}}\,e^{\mathrm{i}\,\mathbf{k}_{\mathrm{S}}\cdot\boldsymbol{x}}\;(\mathfrak{s}\,\mathrm{i}\,\omega)\;\widehat{\mathbf{d}} \;=\; -\,\mathfrak{s}\,\frac{\mathcal{W}_{\mathrm{S}}}{\mathsf{s}_{\mathrm{S}}}\mathbf{curl}\left(e^{\mathrm{i}\,\mathbf{k}_{\mathrm{S}}\cdot\boldsymbol{x}}\right),$$

$$\Rightarrow \mathbf{w}_{\mathrm{S}}^{\mathrm{pw}} \;=\; -\,\mathfrak{s}\,\frac{\mathcal{W}_{\mathrm{S}}}{\mathsf{s}_{\mathrm{S}}}\mathbf{curl}\left(\sum_{k=-\infty}^{\infty}\mathrm{i}^{k}\,\mathrm{J}_k(\omega\,\mathsf{s}_{\mathrm{S}}\,r)\;e^{\mathrm{i}\,k(\theta-\alpha_{\mathrm{inc}})}\right).$$

$$\mathbf{w}_{\mathrm{S},r}^{\mathrm{pw}} \;=\; -\,\mathfrak{s}\,\frac{\mathcal{W}_{\mathrm{S}}}{\mathsf{s}_{\mathrm{S}}\,r}\sum_{k=-\infty}^{\infty}\mathrm{i}^{k+1}k\;\mathrm{J}_k(\omega\,\mathsf{s}_{\mathrm{S}}\,r)\;e^{\mathrm{i}\,k(\theta-\alpha_{\mathrm{inc}})}\,.$$

For $\boldsymbol{\tau}$, we have from equation (1.39)

$$\begin{aligned}\boldsymbol{\tau}_{\mathrm{S}}^{\mathrm{pw}} \;&=\; \mathrm{i}\,\omega\,\mathsf{s}_{\mathrm{S}}\,e^{\mathrm{i}\,\mathbf{k}_{\mathrm{S}}\cdot\boldsymbol{x}}\,\mu_{\mathrm{fr}}\left(\widehat{\mathbf{k}}\otimes\widehat{\mathbf{d}}\;+\;\widehat{\mathbf{d}}\otimes\widehat{\mathbf{k}}\right)\\ &=\; \mathrm{i}\,\omega\,\mathsf{s}_{\mathrm{S}}\,e^{\mathrm{i}\,\mathbf{k}_{\mathrm{S}}\cdot\boldsymbol{x}}\,\mu_{\mathrm{fr}}\begin{pmatrix}-2\cos\alpha_{\mathrm{inc}}\sin\alpha_{\mathrm{inc}} & \cos\alpha_{\mathrm{inc}}^2-\sin\alpha_{\mathrm{inc}}^2\\ \cos\alpha_{\mathrm{inc}}^2-\sin\alpha_{\mathrm{inc}}^2 & 2\cos\alpha_{\mathrm{inc}}\sin\alpha_{\mathrm{inc}}\end{pmatrix}.\end{aligned}$$

We will consider $\boldsymbol{\tau}\,\boldsymbol{n} \;=\; \tau_{rr}\,\mathbf{e}_r \;+\; \tau_{r\theta}\,\mathbf{e}_\theta$ in polar coordinates, hence, we focus on the components τ_{rr} and $\tau_{r\theta}$:

$$\begin{aligned}\tau_{\mathrm{S},rr}^{\mathrm{pw}} \;&=\; -\,2\frac{\mu_{\mathrm{fr}}}{\mathrm{i}\omega\mathsf{s}_{\mathrm{S}}}\,\frac{\partial_{r\theta}(e^{\mathrm{i}\,\mathbf{k}_{\mathrm{S}}\cdot\boldsymbol{x}})}{r}\\ &=\; \sum_{k=-\infty}^{\infty}-2\frac{\mu_{\mathrm{fr}}}{\mathrm{i}\omega\mathsf{s}_{\mathrm{S}}r}\left(\omega\,\mathsf{s}_{\mathrm{S}}\,\mathrm{i}^{k+1}\,k\,\mathrm{J}_k'(\omega\,\mathsf{s}_{\mathrm{S}}\,r)\;e^{\mathrm{i}\,k(\theta-\alpha_{\mathrm{inc}})}\right)\\ &=\; \sum_{k=-\infty}^{\infty}-2\frac{\mu_{\mathrm{fr}}}{r}\,\mathrm{i}^{k}\,k\,\mathrm{J}_k'(\omega\,\mathsf{s}_{\mathrm{S}}\,r)\;e^{\mathrm{i}\,k(\theta-\alpha_{\mathrm{inc}})}\,,\end{aligned}$$

$$\begin{aligned}\tau_{\mathrm{S},r\theta}^{\mathrm{pw}} \;&=\; -\,\frac{\mu_{\mathrm{fr}}}{\mathrm{i}\omega\mathsf{s}_{\mathrm{S}}}\left(\frac{\partial_{\theta\theta}(e^{\mathrm{i}\,\mathbf{k}_{\mathrm{S}}\cdot\boldsymbol{x}})}{r^2}+\frac{\partial_r(e^{\mathrm{i}\,\mathbf{k}_{\mathrm{S}}\cdot\boldsymbol{x}})}{r}-\partial_{rr}(e^{\mathrm{i}\,\mathbf{k}_{\mathrm{S}}\cdot\boldsymbol{x}})\right)\\ &=\; \sum_{k=-\infty}^{\infty}\frac{\mu_{\mathrm{fr}}}{\mathrm{i}\omega\mathsf{s}_{\mathrm{S}}}\left(\frac{\mathrm{i}^{k}\,k^2}{r^2}\,\mathrm{J}_k(\omega\,\mathsf{s}_{\mathrm{S}}\,r)\;e^{\mathrm{i}\,k(\theta-\alpha_{\mathrm{inc}})}-\frac{\omega\,\mathsf{s}_{\mathrm{S}}\,\mathrm{i}^{k}}{r}\left(\mathrm{J}_k'(\omega\,\mathsf{s}_{\mathrm{S}}\,r)\;e^{\mathrm{i}\,k(\theta-\alpha_{\mathrm{inc}})}\right)\right.\\ &\left.+\omega^2\,\mathsf{s}_{\mathrm{S}}^2\,\mathrm{i}^{k}\,\mathrm{J}_k''(\omega\,\mathsf{s}_{\mathrm{S}}\,r)\;e^{\mathrm{i}\,k(\theta-\alpha_{\mathrm{inc}})}\right)\\ &=\; \sum_{k=-\infty}^{\infty}\frac{\mu_{\mathrm{fr}}\,\mathrm{i}^{k-1}\,k^2}{\omega\mathsf{s}_{\mathrm{S}}\,r^2}\,\mathrm{J}_k(\omega\,\mathsf{s}_{\mathrm{S}}\,r)\;e^{\mathrm{i}\,k(\theta-\alpha_{\mathrm{inc}})}-\sum_{k=-\infty}^{\infty}\frac{\mu_{\mathrm{fr}}\,\mathrm{i}^{k-1}}{r}\,\mathrm{J}_k'(\omega\,\mathsf{s}_{\mathrm{S}}\,r)\;e^{\mathrm{i}\,k(\theta-\alpha_{\mathrm{inc}})}\\ &+\sum_{k=-\infty}^{\infty}\mu_{\mathrm{fr}}\,\mathrm{i}^{k-1}\,\mathrm{J}_{k+1}(\omega\,\mathsf{s}_{\mathrm{S}}\,r)\;e^{\mathrm{i}\,k(\theta-\alpha_{\mathrm{inc}})}\;-\sum_{k=-\infty}^{\infty}\frac{\mu_{\mathrm{fr}}\,k}{\omega\,\mathsf{s}_{\mathrm{S}}}\,\mathrm{i}^{k-1}\,\mathrm{J}_k(\omega\,\mathsf{s}_{\mathrm{S}}\,r)\;e^{\mathrm{i}\,k(\theta-\alpha_{\mathrm{inc}})}\\ &-\sum_{k=-\infty}^{\infty}\mu_{\mathrm{fr}}\,\omega\,\mathsf{s}_{\mathrm{S}}\,\mathrm{i}^{k-1}\,\mathrm{J}_k(\omega\,\mathsf{s}_{\mathrm{S}}\,r)\;e^{\mathrm{i}\,k(\theta-\alpha_{\mathrm{inc}})}\;+\sum_{k=-\infty}^{\infty}\frac{\mu_{\mathrm{fr}}\,k^2}{\omega^2\,\mathsf{s}_{\mathrm{S}}^2}\,\mathrm{i}^{k-1}\,\mathrm{J}_k(\omega\,\mathsf{s}_{\mathrm{S}}\,r)\;e^{\mathrm{i}\,k(\theta-\alpha_{\mathrm{inc}})}\,.\end{aligned}$$

Physical parameters	Sandstone	Sand 1	Shale	Sand 2
Porosity ϕ (%)	0.2	0.3	0.16	0.3
Fluid Density ρ_f $(10^3 kg.m^{-3})$	1.04	1	1.04	1
Solid Density ρ_s $(10^3 kg.m^{-3})$	2.5	2.6	2.21	2.7
Viscosity η $(10^{-3} Pa.s)$	0	1	0	1
Permeability κ_0 $(10^{-9} m^2)$	0.06	0.01	0.01	0.01
Tortuosity $\mathfrak{t}$	2	3	2	3
Solid Bulk Modulus $\mathrm{k_s}$ $(10^9 Pa)$	40	35	7.6	36
Fluid Bulk Modulus $\mathrm{k_f}$ $(10^9 Pa)$	2.5	2.2	2.5	2.2
Frame Bulk Modulus $\mathrm{k_{fr}}$ $(10^9 Pa)$	20	0.4	6.6	7
Frame Shear Modulus μ_{fr} $(10^9 Pa)$	12	0.5	3.96	5
Velocity $(m.s^{-1})$				
v_P	4247	(1860, 4)	2481	(2866, 0.1)
v_B	1021	(82,70)	1127	(190,163)
v_S	2388	(486,1)	1429	(1512, 1)
Transition frequency	—	1kHz	—	1kHz
ρ_{dyn}	10.4	(12.5, -80)	13	(12.5, -80)
$\rho_a + \rho_{\mathrm{dyn}}$	12.6	(14.6, -80)	15	(14.7, -80)
$\mathrm{detA} = \rho_a \rho_{\mathrm{dyn}} - \rho_f^2$	21.88	(25.5 -169)	25.2	(26.4, -174)
$H + M$	50.28	13.74	28.8	24.6
$\mathrm{detB} = H M - \alpha^2 M^2$	411.43	6.83	197.14	90.8
$\mathrm{trC} = \rho_{\mathrm{dyn}} H - 2\alpha M \rho_f + \rho_a M$	417.46	(92.54, -583)	187.2	(228.6, -1432)
$4\dfrac{\mathrm{detA}}{\mathrm{detB}}$	0.212	(14.92, -99)	0.51	(1.16, -7.7)
$\left(\dfrac{\mathrm{trC}}{\mathrm{detB}}\right)^2$	1.03	(-7104, -2311)	0.9	(-242, -7.9)
$\left(\dfrac{\mathrm{trC}}{\mathrm{detB}}\right)^2 - 4\dfrac{\mathrm{detA}}{\mathrm{detB}}$	0.817	(-7119, -2212)	0.39	(-243,-72)
$\sqrt{\left(\dfrac{\mathrm{trC}}{\mathrm{detB}}\right)^2 - 4\dfrac{\mathrm{detA}}{\mathrm{detB}}}$	0.904	(12.96 , -85)	0.624	(2.27, -15.8)
$\dfrac{\mathrm{trC}}{\mathrm{detB}}$	1.015	(13.54, -85)	0.95	(2.51, -15.8)
$\mathsf{s}_{\mathrm{P}}^2$	5.54D-2	(0.29, -1.2D-3)	0.16	(0.12, -8D-5)
s_{P} $(10^{-3}\mathrm{s.m}^{-1})$	0.235	(0.54, -1.1D-3)	0.4	(0.35, -1D-4)
$\mathsf{s}_{\mathrm{B}}^2$	0.96	(13.24, -85)	0.787	(2.39, -15.8)
s_{B} $(10^{-3}\mathrm{s.m}^{-1})$	0.979	(7, -6)	0.89	(3, -2.6)
$\mathsf{s}_{\mathrm{S}}^2$	0.175	(4.24, -2.5D-2)	0.49	(0.44, -2.4D-3)
s_{S} $(10^{-3}\mathrm{s.m}^{-1})$	0.419	(2.06, -6D-3)	0.7	(0.66, -1.8D-3)

Table 1.2: Summary of the physical parameters of media in consideration in this document. The parameters for sand 1 are obtained from [64, Table 1], those for sandstone and shale from [39, Table 5], for sand 2 from [128, Table 1]. Materials velocities and dynamic parameters are calculated for a frequency $f = 200$ Hz, and $\mathfrak{s} = -1$. The definition of slowness follows eq. (1.43).

1.6 Properties of slowness

In this section, we describe the properties of the slowness in a poroelastic medium. These properties are dependent on the convention we use for time-derivative in the frequency domain. Moreover, the value of the viscosity in the domain has an influence on these properties. We distinct two cases for the viscosity: one with vanishing viscosity, using the assumptions of Section 1.2.1.3, and one with a positive viscosity. First, we study the properties of $\mathsf{s}_\bullet^2$, then we propose

a definition of the slownesses.

1.6.1 Properties of slowness square

In Section 1.5.1, we presented the expressions of the slownesses for the three waves, which depend on matrices A, B, C, that we have defined in (1.25). The values of those matrices hence give properties of the slowness. In the case with no viscosity, the matrices are real. Here we present the properties of the slowness square from (1.24).

Zero viscosity From the discussion in Section 1.2.1.3, the dynamic density $\rho_{\rm dyn}(\omega)$ at vanishing viscosity takes the form, cf. (1.11),

$$\lim_{\substack{\eta\to 0,\\ \text{fixed } \omega>0}} \rho_{\rm dyn} \;=\; \rho_{\rm dyn}^{\rm VV} \;=\; \frac{\rho_f}{\phi}\,\mathfrak{t}\,.$$

By its definition (1.1), the porosity ϕ satisfies

$$0 \;\leq \phi \;\leq\; 1\,. \tag{1.40}$$

We can also assume that, considering a porous medium,

$$\mathfrak{t} \;\geq\; 1\,.$$

We also assume that $\mathfrak{t}$ and ϕ are not 1 at the same time, i.e.

$$(1-\mathfrak{t})^2 \;+\; (1-\phi)^2 \;>\; 0\,. \tag{1.41}$$

At zero viscosity, we use $\rho_{\rm dyn}^{\rm VV}$ introduced in (1.11) in the definition of matrices A and C in (1.25) and (1.26). These matrices appear in the definition of the slowness square (1.24). In this case, all the quantities are real.

Proposition 1.7. Under hypothesis (1.40)– (1.41), we have

1. The matrix
$$A_0 \;:=\; \begin{pmatrix} \rho_a & \rho_f \\ \rho_f & \rho_{\rm dyn}^{\rm VV} \end{pmatrix},$$
is symmetric and positive definite.
2. The matrix
$$C_0 \;:=\; B^{\rm cof}\, A_0\,,$$
is diagonalizable with two positive eigenvalues.

Proof. Let us first recall that, from (1.25),

$$B^{\rm cof} \;=\; \begin{pmatrix} M & -\alpha\, M \\ -\alpha M & H \end{pmatrix}.$$

Statement 1 The proof follows [52, Rmk 5.2.1]. We substitute in A_0 the definition of ρ_a given in (1.2) and that of vanishing viscosity density $\rho^{\rm VV}$ in (1.11),

$$\begin{aligned} \det A_0 \;&=\; \rho_a\, \rho_{\rm dyn}^{\rm VV} \;-\; \rho_f^2 \\ &=\; \big((1-\phi)\,\rho_s \;+\; \phi\,\rho_f\big)\,\frac{\rho_f}{\phi}\,\mathfrak{t} \;-\; \rho_f^2 \\ &=\; \big(\mathfrak{t} \;-\; 1\big)\,\rho_f^2 \;+\; \frac{(1-\phi)}{\phi}\,\mathfrak{t}\,\rho_s\,\rho_f\,. \end{aligned}$$

Under hypothesis (1.40)– (1.41), we have

$$\det A_0 \;>\; 0\,, \quad \text{ and } \operatorname{tr} A_0 \;>\; 0\,,$$

since A_0 is symmetric, and thus diagonalizable. With its determinant and trace positive, its two eigenvalues are positive.

Statement 2 The matrix B is always real, symmetric. Due to (1.4)

$$M \;>\; 0 \quad , \quad H \;=\; \lambda_{\rm fr} + 2\mu_{\rm fr} + \alpha^2 M \;>\; 0\,,$$

we have

$$\det B \;=\; M(\lambda_{\rm fr}+2\mu_{\rm fr}) \;>\; 0\,, \qquad \operatorname{tr} B \;=\; M \;+\; H \;>\; 0\,.$$

Since B is symmetric, this means that B is diagonalizable with its eigenvalues positive (and thus positive definite). We can define its square root denoted by $\tilde{B}$,

$$\tilde{B}^2 \;=\; B\,.$$

Since $B = QDQ^T$ with an orthogonal matrix Q i.e. $Q^{-1} = Q^T$, then $\tilde{B} = Q\sqrt{D}Q^T$ and $\tilde{B}^T = \tilde{B}$. We can then note that $\tilde{B}$ is also symmetric and positive definite and so is its inverse $(\tilde{B})^{-1}$. We next show that $B^{-1}A_0$ is similar to the symmetric matrix $\tilde{B}^{-1}A_0\tilde{B}^{-1}$. We first have

$$\tilde{B}\left(B^{-1}\,A_0\right)\tilde{B}^{-1} \;=\; \tilde{B}^{-1}\,A_0\,\tilde{B}^{-1}\,.$$

The latter matrix satisfies,

$$\left(\tilde{B}^{-1}\,A_0\,\tilde{B}^{-1}\right)^T \;=\; \left(\tilde{B}^{-1}\right)^T A_0^T\left(\tilde{B}^{-1}\right)^T,$$

and is thus symmetric since A_0 is symmetric and $\tilde{B}^{-1}$ is symmetric. This means that $\tilde{B}^{-1}A_0\tilde{B}^{-1}$ is diagonalizable. Furthermore, its eigenvalues are positive. This is seen by showing that $\tilde{B}^{-1}A_0\tilde{B}^{-1}$ is positive definite,

$$\left\langle\, \tilde{B}^{-1}\,A_0\,\tilde{B}^{-1}x\;,\; x\,\right\rangle \;=\; \left\langle A_0\,\tilde{B}^{-1}\,x\;,\; (\tilde{B}^{-1})^T\,x\right\rangle \;=\; \left\langle A_0\,\tilde{B}^{-1}\,x\;,\; (\tilde{B}^{-1})\,x\right\rangle \;>\; 0\,.$$

The last inequality is due to the definite positivity of A_0 discussed in statement 1. By similarity, these properties are transferred to matrix $B^{-1}A_0$, and thus C_0. □

Remark 1.8. When $\eta = 0$, all of the concerned quantities are real. A and B are symmetric, hence diagonalizable. The materials in Table 1.2 with zero viscosity (Sandstone and Shale) satisfy the condition guaranteeing the positive definiteness of matrices A and B. For A, this means

$$\rho_a + \rho_{\rm dyn}^{\rm VV} > 0 \quad,\quad \rho_a\rho_{\rm dyn}^{\rm VV} - \rho_f^2 > 0\,.$$

For B, this means

$$H + M > 0 \quad,\quad HM > \alpha^2 M^2\,.$$

△

1.6.2 Definition of slowness

For zero-viscosity, the slowness is real, while in the presence of viscosity we have studied the values of slownesses for the materials listed in table 1.2. For frequencies in the range [1Hz , 1MHz] and viscosity in $[0, 10^{-2}]$ Pa.s, we have verified that the slowness square defined in (1.24) always observes the following:

$$\operatorname{Re}\mathsf{s}_\bullet^2 > 0 \quad,\quad -\mathfrak{s}\,\operatorname{Im}\mathsf{s}_\bullet^2 \;>\; 0 \quad,\quad \text{for } \bullet = \mathrm{P},\mathrm{S},\mathrm{B}\,, \tag{1.42}$$

Definition 1.9. Under the assumption that the slowness square defined in (1.24) satisfies (1.42), we define the slowness to be

$$\mathsf{s}_\bullet \;:=\; -\mathfrak{s}\,\sqrt{\mathsf{s}_\bullet^2}\,. \tag{1.43}$$

Here, the square root uses the principle argument range i.e.the interval $(-\pi, \pi]$.

Under assumption (1.42), the slowness satisfies

$$\operatorname{Im}\mathsf{s}_\bullet \;\geq\; 0 \quad,\quad -\mathfrak{s}\,\operatorname{Re}\mathsf{s}_\bullet \;\geq\; 0\,. \tag{1.44}$$

In addition, in presence of viscosity, the amplitude of the plane wave decreases.

Conclusion

In this chapter, we have first introduced the physical parameters used to describe a poroelastic medium. Then, focusing on the harmonic domain, we have presented the expression of the equations of poroelasticity both in first and second-order formulation. In addition to the equations, we need to express boundary conditions. Here, we have proposed boundary conditions for bounded domain and transmission problems. We have then determined the form of the plane waves sustained in poroelastic materials. We distinguish three plane waves; a fast longitudinal plane wave, called P-wave, a slow longitudinal plane wave, the B-wave, and a transverse plane wave, the S-wave. Associated with the plane wave, we have defined three slownesses. This chapter sets a framework for the rest of the developments given in the following chapters.

Chapter 2

Construction and analysis of analytical solutions in two-dimensions in isotropic media

In this chapter, we focus on the two-dimensional isotropic poroelastic equations presented in Chapter 1. In this configuration, we develop analytical solutions that will be used in order to evaluate the accuracy of the discretization of poroelastic equations by Hybridizable Discontinuous Galerkin method, see Chapter 3. We will consider the homogeneous poroelastic equations on bounded domains, but also the scattering of plane wave by impenetrable and penetrable infinite cylindrical obstacles (thus with circular 2D cross-section), and a fluid-solid interaction problem in circular geometry. This is opposed to horizontally stratified fluid-solid or solid-solid interaction problem, *cf. e.g.* [127, 90, 43, 45, 46]. Finally, we will present a test using point sources.

To obtain analytic solutions, we employ the potential method used by [92] in elasticity, which exploits the very specific form of the poroelastic equations and provides a lighter exposition than the usual approach with Helmholtz decomposition. In addition to the computation of analytic solution for each considered problem, we go further and propose a definition of outgoing solutions cf. Definition 2.3, and investigate numerically the well-posedness for interaction problems among others.

Current works in literature dealing with analytic solutions to the poroelastic equations construct fundamental solutions either for infinite domain, *cf. e.g.* [24], [25], or horizontally stratified domain [45, 46]. For these reasons, they do not directly provide analytic solutions for plane wave scattering in spherical and cylindrical geometries, as were done for the elastic equation, *cf. e.g.* [99]. While the form of generic solutions to the homogeneous equation for infinite domain can be extracted from calculations of the fundamental solution in [24], [25] or in [45, 46], this approach can quickly become complicated, due to the multitude of poroelastic physical parameters whose notations and conventions vary with each work. Additionally, for scattering problems with plane waves, with zero right-hand-side terms, the form of the solution should be much simpler, and an adapted computation for this problem is not quite in the same vein as one employed to compute the fundamental solutions. Lastly, we work with dynamic viscosity [111] which depends on frequency, while [45, 46] work with a low-frequency approximation of the isotropic poroelastic equations and with vanishing viscosity. Our geophysical parameters are based on those in [63, 64, 39, 128].

In the scattering problems, we need to define outgoing solutions. This is not covered in the literature for poroelasticity. Indeed, while the notion of outgoing solution is well-established for elasticity with the Kudrapdze radiation condition [82], the mathematical analysis focus on bounded domains for poroelasticity, see [22].

Similarly, while the well-posedness of the interaction problem for acoustic fluid-elastic solid is covered in *e.g.* [51, 12, 77], this is not yet investigated for isotropic poroelasticity. In particular, the phenomenon of Jones' modes is observed for fluid-elastic scattering. This is characterized by a non-zero solution for a problem without sources. In practice, the scattering problems are written using a transmission matrix, see [51]. To find Jones' modes, we study the invertibility of the transmission matrix, i.e., if, for a fixed frequency, the determinant of the transmission matrix is equal to zero, this frequency is then a Jones' mode. Here, we want to determine the equivalent Jones' modes in fluid-porous and in porous-porous scattering. By extension, we will refer to them as Jones' modes. From our numerical investigations, we do not detect the equivalent of Jones' modes porous-porous interaction problems, see also [22]. For fluid-poroelasticity interaction problems with cylindrical obstacles in the absence of viscosity, we detect the equivalent of Jones' modes, however the modes cease to exist with viscosity. As mentioned above, we work with a frequency-dependent viscosity, and carry out various tests to study the effect of frequency, material parameters and viscosity on the well-posedness of the problem. This study paves the way for theoretical future investigations of questions, such as the well-posedness

of the outgoing solutions and theoretical confirmation of Jones' modes for fluid-poroelasticity.

The chapter is organized as follows. In Section 2.1, we use potential theory to reduce the poroelastic system to a set of Helmholtz equations, and the original poroelastic unknowns are expressed in terms of the potentials which solve the Helmholtz equations. Since these are constant coefficients of the Helmholtz equations, the potential, and thus the poroelastic unknowns, can be expressed in terms of Bessel functions. We apply these results to obtain analytical solutions for the following four settings: bounded domain in Section 2.2, impenetrable obstacles in Section 2.3, penetrable obstacles in Section 2.4, and fluid-solid interaction in Section 2.5. For each case, we study numerically the existence of Jones' modes. We first present detailed expressions of the solutions, which are obtained by solving a linear system, and we then numerically study the invertibility of the coefficient/ transmission matrices (of the aforementioned linear system). Finally, we develop the analytical solution for a point source for poroelasticity in Section 2.6.

2.1 Potential method for isotropic poroelastic equations

In this section, we use the form of the poroelastic equations to find a decomposition of the displacements u and w as functions of scalar unknowns called potentials. Classically, to obtain analytic solutions, fundamental solutions or Green kernels for isotropic elastic or poroelastic equations, one uses the Helmholtz decomposition, the unknowns in this approach are called the Helmholtz potentials. Here, we use a slightly different method without imposing the Helmholtz decomposition on the original unknowns.

2.1.1 Derivation

Notations We recall the following definitions from (1.25).

$$A(\omega) := \begin{pmatrix} \rho_a & \rho_f \\ \rho_f & \rho_{\rm dyn}(\omega) \end{pmatrix} \quad , \quad B := \begin{pmatrix} H & \alpha\, M \\ \alpha M & M \end{pmatrix} \quad , \quad B^{\rm cof} = \begin{pmatrix} M & -\alpha\, M \\ -\alpha M & H \end{pmatrix} \quad , \quad C := B^{\rm cof} A\,.$$

Recall that $\mathrm{s}_{\rm P}^2$ and $\mathrm{s}_{\rm B}^2$ defined in (1.24) are the eigenvalues of $B^{-1}A$, *cf.* (1.25), with corresponding eigenvectors, *cf.* (1.33)

$$\begin{pmatrix} 1 \\ -\dfrac{H\,\mathrm{s}_{\rm P}^2 - \rho_a}{\mathrm{s}_{\rm P}^2\,\alpha\, M \,-\, \rho_f} \end{pmatrix} \quad , \quad \begin{pmatrix} 1 \\ -\dfrac{H\,\mathrm{s}_{\rm B}^2 - \rho_a}{\mathrm{s}_{\rm B}^2\,\alpha\, M \,-\, \rho_f} \end{pmatrix}\,.$$

Here, the change of basis matrix P is,

$$P(\omega) \;:=\; \begin{pmatrix} 1 & 1 \\ \mathcal{W}_{\rm P} & \mathcal{W}_{\rm B} \end{pmatrix} \;=\; \begin{pmatrix} 1 & 1 \\ -\frac{H\,\mathrm{s}_{\rm P}^2-\rho_a}{\mathrm{s}_{\rm P}^2\,\alpha\, M-\rho_f} & -\frac{H\,\mathrm{s}_{\rm B}^2-\rho_a}{\mathrm{s}_{\rm B}^2\,\alpha\, M-\rho_f} \end{pmatrix}\,, \tag{2.1}$$

with $\mathcal{W}_\bullet$ defined in (1.27). Using P, we write

$$B^{-1}A(\omega) \;=\; P(\omega) \begin{pmatrix} \mathrm{s}_{\rm P}^2(\omega) & 0 \\ 0 & \mathrm{s}_{\rm B}^2(\omega) \end{pmatrix} P^{-1}(\omega)\,. \tag{2.2}$$

We also recall the following identities in 2D for a function f and a vector $\mathbf{v}$:

$$\begin{aligned} \nabla\cdot\mathbf{curl} \;&=\; 0 \quad , \quad \mathrm{curl}\,\nabla \;=\; 0\,, \\ \mathrm{curl}\,\mathbf{curl}\, f \;&=\; -\Delta f \quad , \quad \mathbf{curl}\,\mathrm{curl}\,\mathbf{v} \;=\; \nabla\nabla\cdot\mathbf{v} \;-\; \Delta\mathbf{v}\,. \end{aligned}$$

Proposition 2.1. Consider (u,w) a pair of solutions to the poroelastic equations (1.18),

$$-\omega^2\rho_a\mathrm{u} \;-\; \rho_f\omega^2\mathrm{w} - H\nabla\nabla\cdot\mathrm{u} + \mu_{\rm fr}\,\mathbf{curl}\,\mathrm{curl}\,\mathrm{u} - \alpha M\nabla\nabla\cdot\mathrm{w} = \mathbf{f}\,, \tag{2.3a}$$

$$-\omega^2\rho_f\mathrm{u} \;-\; \omega^2\,\rho_{\rm dyn}(\omega)\,\mathrm{w} - M\,\nabla\nabla\cdot\mathrm{w} \;-\; \alpha M\nabla\nabla\cdot\mathrm{u} = \tilde{\mathbf{f}}\,. \tag{2.3b}$$

Then they have to be of the form,

$$\begin{aligned}\omega^2 \mathrm{u} \;&=\; -\mathrm{s}_{\mathrm{P}}^{-2}\,\nabla\chi_{\mathrm{P}} \;-\; \mathrm{s}_{\mathrm{B}}^{-2}\,\nabla\chi_{\mathrm{B}} \;+\; \mathrm{s}_{\mathrm{S}}^{-2}\,\mathbf{curl}\,\chi_{\mathrm{S}} \;-\; \pi_1\left(A^{-1}\begin{pmatrix}\mathbf{f}\\ \tilde{\mathbf{f}}\end{pmatrix}\right),\\ \omega^2 \mathrm{w} \;&=\; -\frac{\mathcal{W}_{\mathrm{P}}}{\mathrm{s}_{\mathrm{P}}^2}\nabla\chi_{\mathrm{P}} \;-\; \frac{\mathcal{W}_{\mathrm{B}}}{\mathrm{s}_{\mathrm{B}}^2}\nabla\chi_{\mathrm{B}} \;-\; \frac{\rho_f\,\mu_{\mathrm{fr}}}{\det A}\mathbf{curl}\,\chi_{\mathrm{S}} \;-\; \pi_2\left(A^{-1}\begin{pmatrix}\mathbf{f}\\ \tilde{\mathbf{f}}\end{pmatrix}\right).\end{aligned} \tag{2.4}$$

Here for $i = 1, 2$, π_i is the projection onto the i-th component of a vector, and the potential $\chi_\bullet$ with $\bullet = \mathrm{P}, \mathrm{S}, \mathrm{B}$ satisfy the Helmholtz equation

$$\begin{aligned}\big(-\Delta \;-\; \omega^2\,\mathrm{s}_{\mathrm{P}}^2\big)\,\chi_{\mathrm{P}} \;&=\; \pi_1\left(P^{-1}\,B^{-1}\begin{pmatrix}\nabla\cdot\mathbf{f}\\ \nabla\cdot\tilde{\mathbf{f}}\end{pmatrix}\right),\\ \big(-\Delta \;-\; \omega^2\,\mathrm{s}_{\mathrm{B}}^2\big)\,\chi_{\mathrm{B}} \;&=\; \pi_2\left(P^{-1}\,B^{-1}\begin{pmatrix}\nabla\cdot\mathbf{f}\\ \nabla\cdot\tilde{\mathbf{f}}\end{pmatrix}\right).\end{aligned}$$

and

$$\big(-\Delta \;-\; \omega^2\,\mathrm{s}_{\mathrm{S}}^2\big)\,\chi_{\mathrm{S}} \;=\; \mathrm{s}_{\mathrm{S}}^2\;\pi_1\left(A^{-1}\begin{pmatrix}\mathrm{curl}\mathbf{f}\\ \mathrm{curl}\tilde{\mathbf{f}}\end{pmatrix}\right). \tag{2.6}$$

Proof. As unknowns, we will work with,

$$\begin{aligned}\varphi \;&:=\; \nabla\cdot\mathrm{u} \quad,\quad \tilde{\varphi} \;:=\; \nabla\cdot\mathrm{w}\,,\\ \psi \;&:=\; \mathrm{curl}\,\mathrm{u} \quad,\quad \tilde{\psi} \;:=\; \mathrm{curl}\,\mathrm{w}\,.\end{aligned}$$

Step 1 We first obtain a system of equations in terms of φ, $\tilde{\varphi}$, ψ and $\tilde{\psi}$. The first two equations are obtained by taking $\nabla\cdot$ of the equations (2.3). Using $\nabla\cdot\mathbf{curl} = 0$, and $\nabla\cdot\nabla = \Delta$, $\nabla\cdot$ of equation (2.3a) gives

$$\begin{aligned}\nabla\cdot\big(-\omega^2\rho_a\mathrm{u} \;-\; \rho_f\omega^2\mathrm{w} - H\nabla\nabla\cdot\mathrm{u} + \mu_{\mathrm{fr}}\,\mathbf{curl}\,\mathrm{curl}\,\mathrm{u} - \alpha M\nabla\nabla\cdot\mathrm{w}\big) \;&=\; \nabla\cdot\mathbf{f}\,,\\ \Rightarrow\quad -\omega^2\rho_a\varphi \;-\; \rho_f\omega^2\tilde{\varphi} - H\Delta\varphi - \alpha M\Delta\tilde{\varphi} \;&=\; \nabla\cdot\mathbf{f}\,,\end{aligned}$$

and the divergence $\nabla\cdot$ of equation (2.3b) leads to

$$\begin{aligned}\nabla\cdot\big(-\omega^2\rho_f\mathrm{u} \;-\; \omega^2\,\rho_{\mathrm{dyn}}(\omega)\,\mathrm{w} - M\,\nabla\nabla\cdot\mathrm{w} \;-\; \alpha\,M\nabla\nabla\cdot\mathrm{u}\big) \;&=\; \nabla\cdot\tilde{\mathbf{f}}\,,\\ \Rightarrow\quad -\omega^2\rho_f\varphi \;-\; \omega^2\,\rho_{\mathrm{dyn}}(\omega)\,\tilde{\varphi} - M\,\Delta\tilde{\varphi} \;-\; \alpha M\Delta\varphi \;&=\; \nabla\cdot\tilde{\mathbf{f}}\,.\end{aligned}$$

The third and fourth equations are obtained by taking the curl of equations (2.3). Using $\mathrm{curl}\,\mathbf{curl} = -\Delta$ and $\mathrm{curl}\nabla = 0$, (2.3a) gives

$$\begin{aligned}\mathrm{curl}\big(-\omega^2\rho_a\mathrm{u} \;-\; \rho_f\omega^2\mathrm{w} \;-\; H\nabla\nabla\cdot\mathrm{u} \;+\; \mu_{\mathrm{fr}}\,\mathbf{curl}\,\mathrm{curl}\,\mathrm{u} \;-\; \alpha\,M\,\nabla\,\nabla\cdot\mathrm{w}\big) \;&=\; \mathrm{curl}\,\mathbf{f}\,,\\ \Rightarrow\quad -\omega^2\,\rho_a\,\psi \;-\; \rho_f\,\omega^2\,\tilde{\psi} \;-\; \mu_{\mathrm{fr}}\,\Delta\psi \;&=\; \mathrm{curl}\,\mathbf{f}\,,\end{aligned}$$

while the second equation (2.3b) gives

$$\begin{aligned}\mathrm{curl}\big(-\omega^2\rho_f\mathrm{u} \;-\; \omega^2\,\rho_{\mathrm{dyn}}(\omega)\,\mathrm{w} - M\,\nabla\nabla\cdot\mathrm{w} \;-\; \alpha M\nabla\nabla\cdot\mathrm{u}\big) \;&=\; \mathrm{curl}\,\tilde{\mathbf{f}}\,,\\ \Rightarrow\quad -\omega^2\,\rho_f\,\psi \;-\; \omega^2\,\rho_{\mathrm{dyn}}(\omega)\,\tilde{\psi} \;&=\; \mathrm{curl}\,\tilde{\mathbf{f}}\,.\end{aligned}$$

We rewrite these four equations in matrix form to obtain,

$$-\omega^2\,A(\omega)\begin{pmatrix}\varphi\\ \tilde{\varphi}\end{pmatrix} \;-\; B\Delta\begin{pmatrix}\varphi\\ \tilde{\varphi}\end{pmatrix} \;=\; \begin{pmatrix}\nabla\cdot\mathbf{f}\\ \nabla\cdot\tilde{\mathbf{f}}\end{pmatrix}, \tag{2.7a}$$

$$\text{and}\quad -\omega^2\,A(\omega)\begin{pmatrix}\psi\\ \tilde{\psi}\end{pmatrix} \;-\; \begin{pmatrix}\mu_{\mathrm{fr}} & 0\\ 0 & 0\end{pmatrix}\Delta\begin{pmatrix}\psi\\ \tilde{\psi}\end{pmatrix} \;=\; \begin{pmatrix}\mathrm{curl}\,\mathbf{f}\\ \mathrm{curl}\,\tilde{\mathbf{f}}\end{pmatrix}. \tag{2.7b}$$

Step 2a Multiply by A^{-1} on both sides, we first rewrite (2.7b) as

$$-\omega^2 \begin{pmatrix} \psi \\ \tilde{\psi} \end{pmatrix} \; - \; A^{-1} \begin{pmatrix} \mu_{\rm fr} & 0 \\ 0 & 0 \end{pmatrix} \Delta \begin{pmatrix} \psi \\ \tilde{\psi} \end{pmatrix} \; = \; A^{-1} \begin{pmatrix} \operatorname{curl} \mathbf{f} \\ \operatorname{curl} \tilde{\mathbf{f}} \end{pmatrix} . \tag{2.8}$$

Using the identity

$$A^{-1} \begin{pmatrix} \mu_{\rm fr} & 0 \\ 0 & 0 \end{pmatrix} = \frac{1}{\det A} \begin{pmatrix} \rho_{\rm dyn} & -\rho_f \\ -\rho_f & \rho_a \end{pmatrix} \begin{pmatrix} \mu_{\rm fr} & 0 \\ 0 & 0 \end{pmatrix} = \frac{1}{\det A} \begin{pmatrix} \rho_{\rm dyn}\, \mu_{\rm fr} & 0 \\ -\rho_f\, \mu_{\rm fr} & 0 \end{pmatrix} , \tag{2.9}$$

the first component of (2.8) gives,

$$-\omega^2 \frac{\det A}{\rho_{\rm dyn}\, \mu_{\rm fr}} \psi - \Delta \psi = \frac{\det A}{\rho_{\rm dyn}\, \mu_{\rm fr}}\, \pi_1 \left(A^{-1} \begin{pmatrix} \mathbf{curl} \mathbf{f} \\ \mathbf{curl} \tilde{\mathbf{f}} \end{pmatrix} \right) .$$

Here π_i for $i = 1, 2$ is the projection onto the i-th component of a vector. Rewriting this in terms of the shear slowness $\mathrm{s_S}$ (1.24a), we obtain that the potential ψ solves the Helmholtz equation (2.6). We define

$$\chi_{\rm S} \; = \; \psi \, .$$

Step 2b Apply B^{-1} to both sides of (2.7a), we obtain

$$-\omega^2\, B^{-1} A(\omega) \begin{pmatrix} \varphi \\ \tilde{\varphi} \end{pmatrix} \; - \; \Delta \begin{pmatrix} \varphi \\ \tilde{\varphi} \end{pmatrix} \; = \; B^{-1} \begin{pmatrix} \nabla \cdot \mathbf{f} \\ \nabla \cdot \tilde{\mathbf{f}} \end{pmatrix} .$$

Next, using the diagonalizing form (2.2) of $B^{-1}A$, the above equation is rewritten as,

$$-\omega^2\, P \begin{pmatrix} \mathrm{s_P^2} & 0 \\ 0 & \mathrm{s_B^2} \end{pmatrix} P^{-1} \begin{pmatrix} \varphi \\ \tilde{\varphi} \end{pmatrix} \; - \; \Delta \begin{pmatrix} \varphi \\ \tilde{\varphi} \end{pmatrix} \; = \; B^{-1} \begin{pmatrix} \nabla \cdot \mathbf{f} \\ \nabla \cdot \tilde{\mathbf{f}} \end{pmatrix} ,$$

$$\Rightarrow -\omega^2 \; \begin{pmatrix} \mathrm{s_P^2} & 0 \\ 0 & \mathrm{s_B^2} \end{pmatrix} P^{-1} \begin{pmatrix} \varphi \\ \tilde{\varphi} \end{pmatrix} \; - \; \Delta P^{-1} \begin{pmatrix} \varphi \\ \tilde{\varphi} \end{pmatrix} \; = \; P^{-1} B^{-1} \begin{pmatrix} \nabla \cdot \mathbf{f} \\ \nabla \cdot \tilde{\mathbf{f}} \end{pmatrix} .$$

Define

$$\begin{pmatrix} \chi_{\rm P} \\ \chi_{\rm B} \end{pmatrix} \; := \; P^{-1} \begin{pmatrix} \varphi \\ \tilde{\varphi} \end{pmatrix} .$$

Then, the potentials $\chi_{\rm P}$ and $\chi_{\rm B}$ satisfy the Helmholtz equations (2.5).

Step 3 We now rewrite u and w in terms of the potential $\chi_\bullet$ which are solutions of the Helmholtz equation (2.5) and (2.6). In particular, from (2.3), we obtain

$$-\omega^2 \begin{pmatrix} \mathrm{u} \\ \mathrm{w} \end{pmatrix} \; - \; A^{-1} B \begin{pmatrix} \nabla \varphi \\ \nabla \tilde{\varphi} \end{pmatrix} \; + \; A^{-1} \begin{pmatrix} \mu_{\rm fr} & 0 \\ 0 & 0 \end{pmatrix} \begin{pmatrix} \mathbf{curl}\, \psi \\ 0 \end{pmatrix} = \; A^{-1} \begin{pmatrix} \mathbf{f} \\ \tilde{\mathbf{f}} \end{pmatrix} .$$

Using the diagonalizing form (2.2) and (2.9), this is further written as,

$$-\omega^2 \begin{pmatrix} \mathrm{u} \\ \mathrm{w} \end{pmatrix} \; - \; P \begin{pmatrix} \mathrm{s_P^{-2}} & 0 \\ 0 & \mathrm{s_B^{-2}} \end{pmatrix} P^{-1} \begin{pmatrix} \nabla \varphi \\ \nabla \tilde{\varphi} \end{pmatrix} \; + \; \frac{1}{\det A} \begin{pmatrix} \rho_{\rm dyn}\, \mu_{\rm fr} & 0 \\ -\rho_f\, \mu_{\rm fr} & 0 \end{pmatrix} \begin{pmatrix} \mathbf{curl}\, \psi \\ 0 \end{pmatrix} = \; A^{-1} \begin{pmatrix} \mathbf{f} \\ \tilde{\mathbf{f}} \end{pmatrix} .$$

Component wise, the above system gives

$$\omega^2 \mathrm{u} \; = \; -\frac{P_{11}}{\mathrm{s_P^2}} \nabla \chi_{\rm P} \; - \; \frac{P_{12}}{\mathrm{s_B^2}} \nabla \chi_{\rm B} \; + \; \frac{1}{\mathrm{s_S^2}}\, \mathbf{curl}\, \chi_{\rm S} \; - \; \pi_1 \left(A^{-1} \begin{pmatrix} \mathbf{f} \\ \tilde{\mathbf{f}} \end{pmatrix} \right) ,$$

$$\omega^2 \mathrm{w} \; = \; -\frac{P_{21}}{\mathrm{s_P^2}} \nabla \chi_{\rm P} \; - \; \frac{P_{22}}{\mathrm{s_B^2}} \nabla \chi_{\rm B} \; - \; \frac{\rho_f\, \mu_{\rm fr}}{\det A} \mathbf{curl}\, \chi_{\rm S} \; - \; \pi_2 \left(A^{-1} \begin{pmatrix} \mathbf{f} \\ \tilde{\mathbf{f}} \end{pmatrix} \right) .$$

This simplifies to give the final form (2.4) of the displacements.

□

Potential form for unknowns (1.15) **in first order formulation** (1.16) We recall that the velocities $\mathbf{u}$ and $\mathbf{w}$ are the time derivatives of the displacements u and w. They are expressed as $\mathbf{u} = \mathfrak{s}\,\mathrm{i}\,\omega\,\mathrm{u}$, and $\mathbf{w} = \mathfrak{s}\,\mathrm{i}\,\omega\,\mathrm{w}$. Since $-\omega^2 = (\mathfrak{s}\mathrm{i}\omega)^2$, we have

$$\boxed{\begin{aligned} \mathfrak{s}\,\mathrm{i}\,\omega\,\mathbf{u} &= \mathrm{s}_{\mathrm{P}}^{-2}\,\nabla\chi_{\mathrm{P}} + \mathrm{s}_{\mathrm{B}}^{-2}\,\nabla\chi_{\mathrm{B}} - \mathrm{s}_{\mathrm{S}}^{-2}\,\mathbf{curl}\,\chi_{\mathrm{S}} + F\,,\\ \mathfrak{s}\,\mathrm{i}\,\omega\,\mathbf{w} &= \frac{\mathcal{W}_{\mathrm{P}}}{\mathrm{s}_{\mathrm{P}}^2}\nabla\chi_{\mathrm{P}} + \frac{\mathcal{W}_{\mathrm{B}}}{\mathrm{s}_{\mathrm{B}}^2}\nabla\chi_{\mathrm{B}} + \frac{\rho_f\,\mu_{\mathrm{fr}}}{\det A}\mathbf{curl}\,\chi_{\mathrm{S}} + \tilde{F}\,. \end{aligned}} \tag{2.10}$$

To obtain the fluid pressure, we use (note that $\nabla\cdot u = \varphi$ and $\nabla\cdot w = \tilde{\varphi}$),

$$\begin{aligned} \mathrm{p} &= -M\,\tilde{\varphi} - M\,\alpha\,\varphi - M\mathbf{f}_{\mathrm{p}}\\ &= -M\,(\mathcal{W}_{\mathrm{P}}\,\chi_{\mathrm{P}} + \mathcal{W}_{\mathrm{B}}\,\chi_{\mathrm{B}}) - M\,\alpha\,(\chi_{\mathrm{P}} + \chi_{\mathrm{B}}) - M\,\mathbf{f}_{\mathrm{p}}\\ &= -M\,(\mathcal{W}_{\mathrm{P}} + \alpha)\chi_{\mathrm{P}} - M\,(\mathcal{W}_{\mathrm{B}} + \alpha)\chi_{\mathrm{B}} - M\,\mathbf{f}_{\mathrm{p}}\,. \end{aligned}$$

Thus

$$\boxed{\mathrm{p} = -M\,(\mathcal{W}_{\mathrm{P}} + \alpha)\chi_{\mathrm{P}} - M\,(\mathcal{W}_{\mathrm{B}} + \alpha)\chi_{\mathrm{B}} - M\,\mathbf{f}_{\mathrm{p}}\,.} \tag{2.11}$$

To find $\boldsymbol{\tau}$ we use

$$\begin{aligned} \boldsymbol{\tau} &= \mu_{\mathrm{fr}}\,(\nabla\mathrm{u} + (\nabla\mathrm{u})^T) + \left(-\tfrac{2}{3}\mu_{\mathrm{fr}} + \mathrm{k}_{\mathrm{fr}} + \alpha^2 M\right)\nabla\cdot\mathrm{u}\,\mathbb{I} + \alpha\,M\,\nabla\cdot\mathrm{w}\,\mathbb{I}\\ \Rightarrow\quad \omega^2\,\boldsymbol{\tau} &= \mu_{\mathrm{fr}}\,(\nabla\omega^2\,\mathrm{u} + (\nabla\omega^2\,\mathrm{u})^T) + \left(-\tfrac{2}{3}\mu_{\mathrm{fr}} + \mathrm{k}_{\mathrm{fr}} + \alpha^2 M\right)\omega^2\nabla\cdot\mathrm{u}\,\mathbb{I} + \alpha\,M\,\omega^2\,\nabla\cdot\mathrm{w}\,\mathbb{I}. \end{aligned}$$

After simplification, we obtain

$$\boxed{\begin{aligned} \omega^2\,\boldsymbol{\tau} &= \mu_{\mathrm{fr}}\left(-\frac{2}{\mathrm{s}_{\mathrm{P}}^2}\nabla^2\chi_{\mathrm{P}} - \frac{2}{\mathrm{s}_{\mathrm{B}}^2}\nabla^2\chi_{\mathrm{B}} + \frac{\nabla\mathbf{curl}\,\chi_{\mathrm{S}} + (\nabla\mathbf{curl}\,\chi_{\mathrm{S}})^T}{\mathrm{s}_{\mathrm{S}}^2} - (\nabla F + (\nabla F)^T)\right)\\ &\quad + \omega^2\left(-\tfrac{2}{3}\mu_{\mathrm{fr}} + \mathrm{k}_{\mathrm{fr}} + \alpha^2 M\right)(\chi_{\mathrm{P}} + \chi_{\mathrm{B}})\,\mathbb{I}\\ &\quad + \omega^2\,\alpha\,M\,(\mathcal{W}_{\mathrm{P}}\,\chi_{\mathrm{P}} + \mathcal{W}_{\mathrm{B}}\,\chi_{\mathrm{B}})\,\mathbb{I}\,. \end{aligned}} \tag{2.12}$$

2.1.2 Expansion of generic solutions to homogeneous equations in terms of Bessel functions

Here, we obtain the form of a general solution in terms of Bessel functions to the homogeneous poroelastic equations in three types of domains: on a disc, in an annulus and outside a disc. When there is no source, i.e., all sources are zero in (2.6) and (2.5), then the potentials $\chi_\bullet$ satisfy the homogeneous Helmholtz equation:

$$\begin{aligned} \left(-\Delta - \omega^2\,\mathsf{s}_{\mathrm{S}}^2\right)\chi_{\mathrm{S}} &= 0\,,\\ \left(-\Delta - \omega^2\,\mathsf{s}_{\mathrm{P}}^2\right)\chi_{\mathrm{P}} &= 0\,,\\ \left(-\Delta - \omega^2\,\mathsf{s}_{\mathrm{B}}^2\right)\chi_{\mathrm{B}} &= 0\,. \end{aligned} \tag{2.13}$$

On each considered domain, $\chi_\bullet$ can be given as an expansion in terms of Bessel functions in polar coordinates.

(a) On a disc $\mathbb{B}_{\mathfrak{a}}$ centered at the origin and of radius $\mathfrak{a}$, a generic solution to the Helmholtz equation is given by:

$$\chi_\bullet(r,\theta) = \sum_{k\in\mathbb{Z}} a_{\bullet,k}\,\mathrm{J}_k(\omega\,\mathsf{s}_\bullet\,r)\,e^{\mathrm{i}\,k\,\theta} \quad,\quad \bullet\in\{\mathrm{S},\mathrm{P},\mathrm{B}\,.\} \tag{2.14}$$

(b) An outgoing solution on $\mathbb{R}^2\setminus\mathbb{B}_{\mathfrak{a}}$ is given by

$$\chi_\bullet(r,\theta) = \sum_{k\in\mathbb{Z}} a_{\bullet,k}\,\mathrm{H}_k^{(1)}(\omega\,\mathsf{s}_\bullet\,r)\,e^{\mathrm{i}\,k\,\theta} \quad,\quad \bullet\in\{\mathrm{S},\mathrm{P},\mathrm{B}\,.\} \tag{2.15}$$

See Remark 2.2 regarding the 'outgoing'-ness of this solution.

(c) On an annulus between inner radius $\mathfrak{a}$ and outer radius $\mathfrak{b}$, a generic solution is given by:

$$\chi_\bullet(r,\theta) = \sum_{k\in\mathbb{Z}} a_{\bullet,k}\,\mathrm{H}_k^{(1)}(\omega\,\mathsf{s}_\bullet\,r)\,e^{\mathrm{i}\,k\,\theta} + \sum_{k\in\mathbb{Z}} \tilde{a}_{\bullet,k}\,\mathrm{H}_k^{(2)}(\omega\,\mathsf{s}_\bullet\,r)\,e^{\mathrm{i}\,k\,\theta} \quad,\quad \bullet\in\{\mathrm{S},\mathrm{P},\mathrm{B}\,.\} \tag{2.16}$$

To obtain the expansion of $\mathbf{u}$, $\mathbf{w}$, $\boldsymbol{\tau}$ and p, depending on the domain, it remains to substitute the expression for $\chi_\bullet$ (2.14), (2.15) or (2.16) into (2.10) - (2.12). We write the expansion for the case (a) (on a disc) and case (b) (outgoing). Denote by Z_k a Bessel function[1].

For case (a), $\mathrm{Z}_k = \mathrm{J}_k$, and for case (b), $\mathrm{Z}_k = \mathrm{H}_k^{(1)}$. Calculations details are given in appendix A.1.

$$
\begin{aligned}
\mathfrak{s}\,\mathrm{i}\,\omega\,\mathbf{u} \;=\; & \sum_{k\in\mathbb{Z}} a_k\ \mathsf{s}_{\mathrm{P}}^{-1}\,\omega\,\mathrm{Z}_k'(\omega\,\mathsf{s}_{\mathrm{P}}\,r)e^{\mathrm{i}k\theta}\mathbf{e}_r \;+\; \sum_{k\in\mathbb{Z}} a_k\ \mathsf{s}_{\mathrm{P}}^{-2}\,\frac{\mathrm{i}k}{r}\mathrm{Z}_k(\omega\,\mathsf{s}_{\mathrm{P}}\,r)e^{\mathrm{i}k\theta}\mathbf{e}_\theta \\
& + \sum_{k\in\mathbb{Z}} b_k\ \mathsf{s}_{\mathrm{B}}^{-1}\,\omega\,\mathrm{Z}_k'(\omega\,\mathsf{s}_{\mathrm{B}}\,r)e^{\mathrm{i}k\theta}\mathbf{e}_r \;+\; \sum_{k\in\mathbb{Z}} b_k\ \mathsf{s}_{\mathrm{B}}^{-2}\,\frac{\mathrm{i}k}{r}\mathrm{Z}_k(\omega\,\mathsf{s}_{\mathrm{B}}\,r)e^{\mathrm{i}k\theta}\mathbf{e}_\theta \\
& - \sum_{k\in\mathbb{Z}} c_k\ \mathsf{s}_{\mathrm{S}}^{-2}\,\frac{\mathrm{i}k}{r}\mathrm{Z}_k(\omega\,\mathsf{s}_{\mathrm{S}}\,r)e^{\mathrm{i}k\theta}\mathbf{e}_r \;+\; \sum_{k\in\mathbb{Z}} c_k\ \mathsf{s}_{\mathrm{S}}^{-1}\,\omega\,\mathrm{Z}_k'(\omega\,\mathsf{s}_{\mathrm{S}}\,r)e^{\mathrm{i}k\theta}\mathbf{e}_\theta\,,
\end{aligned}
\tag{2.17}
$$

$$
\begin{aligned}
\mathfrak{s}\,\mathrm{i}\,\omega\,\mathbf{w} \;=\; & \sum_{k\in\mathbb{Z}} a_k\ \frac{\mathcal{W}_{\mathrm{P}}}{\mathsf{s}_{\mathrm{P}}}\,\omega\,\mathrm{Z}_k'(\omega\,\mathsf{s}_{\mathrm{P}}\,r)e^{\mathrm{i}k\theta}\mathbf{e}_r \;+\; \sum_{k\in\mathbb{Z}} a_k\ \frac{\mathcal{W}_{\mathrm{P}}}{\mathsf{s}_{\mathrm{P}}^2}\,\frac{\mathrm{i}k}{r}\mathrm{Z}_k(\omega\,\mathsf{s}_{\mathrm{P}}\,r)e^{\mathrm{i}k\theta}\mathbf{e}_\theta \\
& + \sum_{k\in\mathbb{Z}} b_k\ \frac{\mathcal{W}_{\mathrm{B}}}{\mathsf{s}_{\mathrm{B}}}\,,\omega\,\mathrm{Z}_k'(\omega\,\mathsf{s}_{\mathrm{B}}\,r)e^{\mathrm{i}k\theta}\mathbf{e}_r \;+\; \sum_{k\in\mathbb{Z}} b_k\ \frac{\mathcal{W}_{\mathrm{B}}}{\mathsf{s}_{\mathrm{B}}^2}\,\frac{\mathrm{i}k}{r}\mathrm{Z}_k(\omega\,\mathsf{s}_{\mathrm{B}}\,r)e^{\mathrm{i}k\theta}\mathbf{e}_\theta \\
& + \sum_{k\in\mathbb{Z}} c_k\ \frac{\rho_f\,\mu_{\mathrm{fr}}}{\det A}\,\frac{\mathrm{i}k}{r}\mathrm{Z}_k(\omega\,\mathsf{s}_{\mathrm{S}}\,r)e^{\mathrm{i}k\theta}\mathbf{e}_r \;-\; \sum_{k\in\mathbb{Z}} c_k\ \frac{\rho_f\,\mu_{\mathrm{fr}}}{\det A}\,\omega\,\mathrm{Z}_k'(\omega\,\mathsf{s}_{\mathrm{S}}\,r)e^{\mathrm{i}k\theta}\mathbf{e}_\theta\,,
\end{aligned}
\tag{2.18}
$$

In the polar basis,

$$
\boldsymbol{\tau} = \boldsymbol{\tau}_{rr}\,\mathbf{e}_r\otimes\mathbf{e}_r + \boldsymbol{\tau}_{r\theta}\,\mathbf{e}_r\otimes\mathbf{e}_\theta + \boldsymbol{\tau}_{\theta r}\,\mathbf{e}_\theta\otimes\mathbf{e}_r + \boldsymbol{\tau}_{\theta\theta}\,\mathbf{e}_\theta\otimes\mathbf{e}_\theta.
$$

We recall that $\boldsymbol{\tau}$ is symmetric, $\boldsymbol{\tau}_{r\theta} = \boldsymbol{\tau}_{\theta r}$. We will use mainly $\boldsymbol{\tau}\,\boldsymbol{n} = \boldsymbol{\tau}_{rr}\,\mathbf{e}_r + \boldsymbol{\tau}_{r\theta}\,\mathbf{e}_\theta$, hence we only list those components:

$$
\begin{aligned}
\omega^2\boldsymbol{\tau}_{rr} = & -\sum_{k\in\mathbb{Z}} \frac{2\,\mu_{\mathrm{fr}}\,\omega}{\mathsf{s}_{\mathrm{P}}\,r}\,a_k\,\mathrm{Z}_{k+1}(\omega\,\mathsf{s}_{\mathrm{P}}\,r)\ e^{\mathrm{i}\,k\,\theta} \;+\sum_{k\in\mathbb{Z}} \frac{2\,\mu_{\mathrm{fr}}\,k}{\mathsf{s}_{\mathrm{P}}^2\,r^2}\,a_k\,\mathrm{Z}_k(\omega\,\mathsf{s}_{\mathrm{P}}\,r)\ e^{\mathrm{i}\,k\,\theta} \\
& + \sum_{k\in\mathbb{Z}} 2\,\mu_{\mathrm{fr}}\,a_k\,\omega^2\,\mathrm{Z}_k(\omega\,\mathsf{s}_{\mathrm{P}}\,r)\ e^{\mathrm{i}\,k\,\theta} \;-\sum_{k\in\mathbb{Z}} \frac{2\,\mu_{\mathrm{fr}}\,k^2}{\mathsf{s}_{\mathrm{P}}^2\,r^2}\,a_k\,\mathrm{Z}_k(\omega\,\mathsf{s}_{\mathrm{P}}\,r)\ e^{\mathrm{i}\,k\,\theta} \\
& - \sum_{k\in\mathbb{Z}} \frac{2\,\mu_{\mathrm{fr}}\,\omega}{\mathsf{s}_{\mathrm{B}}\,r}\,b_k\,\mathrm{Z}_{k+1}(\omega\,\mathsf{s}_{\mathrm{B}}\,r)\ e^{\mathrm{i}\,k\,\theta} \;+\sum_{k\in\mathbb{Z}} \frac{2\,\mu_{\mathrm{fr}}\,k}{\mathsf{s}_{\mathrm{B}}^2\,r^2}\,b_k\,\mathrm{Z}_k(\omega\,\mathsf{s}_{\mathrm{B}}\,r)\ e^{\mathrm{i}\,k\,\theta} \\
& + \sum_{k\in\mathbb{Z}} 2\,\mu_{\mathrm{fr}}\,b_k\,\omega^2\,\mathrm{Z}_k(\omega\,\mathsf{s}_{\mathrm{B}}\,r)\ e^{\mathrm{i}\,k\,\theta} \;-\sum_{k\in\mathbb{Z}} \frac{2\,\mu_{\mathrm{fr}}\,k^2}{\mathsf{s}_{\mathrm{B}}^2\,r^2}\,b_k\,\mathrm{Z}_k(\omega\,\mathsf{s}_{\mathrm{B}}\,r)\ e^{\mathrm{i}\,k\,\theta} \\
& + \sum_{k\in\mathbb{Z}} \frac{2\,\mu_{\mathrm{fr}}}{\mathsf{s}_{\mathrm{S}}\,r}\ c_k\,\omega\,\mathsf{s}_{\mathrm{S}}\,\mathrm{i}k\,\mathrm{Z}_k'(\omega\,r)\ e^{\mathrm{i}\,k\,\theta} \\
& + \sum_{k\in\mathbb{Z}} \omega^2\ \left(-\tfrac{2}{3}\mu_{\mathrm{fr}} \;+\; \mathrm{k}_{\mathrm{fr}} \;+\; \alpha^2 M \;+\; \alpha\,M\mathcal{W}_{\mathrm{P}}\right)\ a_k\,\mathrm{Z}_k(\omega\,\mathsf{s}_{\mathrm{P}}\,r)\ e^{\mathrm{i}\,k\,\theta} \\
& + \sum_{k\in\mathbb{Z}} \omega^2\ \left(-\tfrac{2}{3}\mu_{\mathrm{fr}} \;+\; \mathrm{k}_{\mathrm{fr}} \;+\; \alpha^2 M \;+\; \alpha\,M\mathcal{W}_{\mathrm{B}}\right)\ b_k\,\mathrm{Z}_k(\omega\,\mathsf{s}_{\mathrm{B}}\,r)\ e^{\mathrm{i}\,k\,\theta}\,,
\end{aligned}
\tag{2.19}
$$

---

[1] We recall the definitions of Bessel and Hankel functions.

Bessel functions are solutions of: $z^2\frac{d^2w}{dz^2} + z\frac{dw}{dz} + (z^2-\nu^2)w = 0.$

First-order Bessel function: $J_\nu = (\frac{1}{2}z)^\nu \sum_{k=0}^{\infty}(-1)^k \frac{(\frac{1}{4}z^2)^k}{k!\Gamma(\nu+k+1)}$ with ν the mode and $\Gamma(z) = \int_0^\infty e^{-t}t^{z-1}dt\,.$

Second-order Bessel function:

$$Y_\nu = \frac{J_\nu(z)cos(\nu\pi) - J_{-\nu}(z)}{sin(\nu\pi)}$$

Two kinds of Hankel functions are expressed: $H_\nu^{(1)}(z) = J_\nu(z) + iY_\nu(z)$, and $H_\nu^{(2)}(z) = J_\nu(z) - iY_\nu(z)$.

and

$$\begin{aligned}\omega^2\,\boldsymbol{\tau}_{r\theta} \;=& -\sum_{k\in\mathbb{Z}}\frac{2\,\mu_{\rm fr}\omega\,\mathrm{i}\,k}{r\,\mathsf{s}_{\rm P}}\,a_k\,\mathrm{Z}_k'(\omega\,\mathsf{s}_{\rm P}\,r)\;e^{\mathrm{i}\,k\,\theta}+\sum_{k\in\mathbb{Z}}\frac{2\,\mathrm{i}\,\mu_{\rm fr}\,k}{r^2\,\mathsf{s}_{\rm P}^2}\,a_k\,\mathrm{Z}_k(\omega\,\mathsf{s}_{\rm P}\,r)\;e^{\mathrm{i}\,k\,\theta}\\ &-\sum_{k\in\mathbb{Z}}\frac{2\,\mu_{\rm fr}\omega\,\mathrm{i}\,k}{r\,\mathsf{s}_{\rm B}}\,b_k\,\mathrm{Z}_k'(\omega\,\mathsf{s}_{\rm B}\,r)\;e^{\mathrm{i}\,k\,\theta}+\sum_{k\in\mathbb{Z}}\frac{2\,\mathrm{i}\,\mu_{\rm fr}\,k}{r^2\,\mathsf{s}_{\rm B}^2}\,b_k\,\mathrm{Z}_k(\omega\,\mathsf{s}_{\rm B}\,r)\;e^{\mathrm{i}\,k\,\theta}\\ &-\sum_{k\in\mathbb{Z}}\frac{\mu_{\rm fr}\,k^2}{r^2\,\mathsf{s}_{\rm S}^2}\,c_k\,\mathrm{Z}_k(\omega\,\mathsf{s}_{\rm S}\,r)\;e^{\mathrm{i}\,k\,\theta}+\sum_{k\in\mathbb{Z}}\frac{\mu_{\rm fr}\,\omega}{r\,\mathsf{s}_{\rm S}}\,c_k\,\mathrm{Z}_k'(\omega\,\mathsf{s}_{\rm S}\,r)\;e^{\mathrm{i}\,k\,\theta}\\ &-\sum_{k\in\mathbb{Z}}\mu_{\rm fr}\,\frac{\omega}{\mathsf{s}_{\rm S}\,r}\,c_k\,\mathrm{Z}_{k+1}(\omega\,\mathsf{s}_{\rm S}\,r)\;e^{\mathrm{i}\,k\,\theta}+\sum_{k\in\mathbb{Z}}\mu_{\rm fr}\,\frac{k}{\mathsf{s}_{\rm S}^2\,r^2}c_k\,\mathrm{Z}_k(\omega\,\mathsf{s}_{\rm S}\,r)\;e^{\mathrm{i}\,k\,\theta}\\ &+\sum_{k\in\mathbb{Z}}\mu_{\rm fr}\,\omega^2\,c_k\,\mathrm{Z}_k(\omega\,\mathsf{s}_{\rm S}\,r)\;e^{\mathrm{i}\,k\,\theta}-\sum_{k\in\mathbb{Z}}\mu_{\rm fr}\,\frac{k^2}{\mathsf{s}_{\rm S}^2\,r^2}\,c_k\,\mathrm{Z}_k(\omega\,\mathsf{s}_{\rm S}\,r)\;e^{\mathrm{i}\,k\,\theta}.\end{aligned}\tag{2.20}$$

Finally,

$$\mathrm{p}\;=-\sum_{k\in\mathbb{Z}}a_k\,M\left(\mathcal{W}_{\rm P}\;+\;\alpha\right)\mathrm{Z}_k(\omega\,\mathsf{s}_{\rm P}\,r)\;-\sum_{k\in\mathbb{Z}}b_k\,M\left(\mathcal{W}_{\rm B}\;+\;\alpha\right)\mathrm{Z}_k(\omega\,\mathsf{s}_{\rm P}\,r)\,.\tag{2.21}$$

2.1.3 Notion of outgoing solution

As a corollary of the form of solution given in (2.10) in terms of the potentials which are solutions of the Helmholtz equation, we can formulate a definition of outgoing solution for poroelasticity. This generalizes the Kupradze radiation condition for isotropic elasticity *cf.* [82], see also *e.g.* [93, Eqn 4] in 2D. We recall the form of the solutions given in (2.10), we can write

$$\begin{pmatrix}\mathbf{u}\\ \mathbf{w}\end{pmatrix}=P\,\frac{1}{\mathfrak{s}\mathrm{i}\omega}\begin{pmatrix}\frac{\nabla\chi_P}{\mathsf{s}_{\rm P}^2}\\ \frac{\nabla\chi_B}{\mathsf{s}_{\rm B}^2}\end{pmatrix}+\frac{1}{\mathfrak{s}\mathrm{i}\omega}\,\mathrm{curl}\,\chi_S\begin{pmatrix}-\frac{1}{\mathsf{s}_{\rm S}^2}\\ \frac{\rho_f\,\mu_{\rm fr}}{\det\mathrm{A}}\end{pmatrix},$$

where P is the matrix defined in (2.1) and the potentials $\chi_\bullet$, $\bullet=\mathrm{P},\mathrm{B},\mathrm{S}$ satisfy the Helmholtz equations

$$\begin{aligned}\left(-\Delta\;-\;\omega^2\,\mathsf{s}_{\rm S}^2\right)\chi_{\rm S}\;&=\;0\,,\\ \left(-\Delta\;-\;\omega^2\,\mathsf{s}_{\rm P}^2\right)\chi_{\rm P}\;&=\;0\,,\\ \left(-\Delta\;-\;\omega^2\,\mathsf{s}_{\rm B}^2\right)\chi_{\rm B}\;&=\;0\,.\end{aligned}$$

The notions of outgoing solution $\mathbf{u}$ and $\mathbf{w}$ are based on that imposed on $\chi_\bullet$, i.e.the Sommerfeld radiation condition for the Helmholtz equation. Using the slowness defined in Definition 1.9, we define the wavenumber

$$\mathsf{k}_\bullet=\omega\,\mathsf{s}_\bullet\,.$$

Under the assumption (1.42), from the property of slowness in (1.44), the wavenumber thus has the property

$$\mathrm{Im}\,\mathsf{k}_\bullet\;\geq\;0\quad,\quad-\mathfrak{s}\,\mathrm{Re}\,\mathsf{k}_\bullet\;\geq\;0\,.$$

Remark 2.2. These properties guarantee that when we use $\mathrm{H}_k^{(1)}$ to describe the potentials in (2.15), the resulting solution given by $\mathrm{H}_0^{(1)}$, is outgoing in the case without viscosity. In the presence of viscosity, $\mathrm{Im}\,\mathsf{k}_\bullet\;\geq\;0$, thus $e^{-(\mathrm{Im}\,\mathsf{k}_\bullet)\,r}$ is exponentially decreasing as $r\to\infty$. This hence represents a $L^2(\mathbb{R}^2)$ solution. Here we follow the outgoing convention discussed in Appendix G in [13]. In particular,

$$\mathrm{H}_k^{(1)}(\,\mathsf{k}_\bullet\,r)\;\sim\;e^{\mathrm{i}\mathsf{k}_\bullet\,r}\;=\;e^{\mathrm{i}\,(\mathrm{Re}\,\mathsf{k}_\bullet)\,r}\;e^{-(\mathrm{Im}\,\mathsf{k}_\bullet)\,r}\,.$$

△

For $\bullet=\mathrm{P},\mathrm{B},\mathrm{S}$, $\chi_\bullet$ is called $\mathsf{k}_\bullet$-outgoing if it satisfies the Sommerfeld radiation condition at wave number $\mathsf{k}_\bullet$ uniformly,

$$\lim_{r\to\infty}\sqrt{r}\left(\frac{\partial\varphi_\bullet}{\partial r}\;-\;\mathrm{i}\,\mathsf{k}_\bullet\,\varphi_\bullet\right)\;=\;0\,.\tag{2.22}$$

Using the identity, $\nabla\cdot\mathbf{curl}\;=\;0$ and $\mathrm{curl}\,\nabla\;=\;0$ in equation (2.22), we propose the following definition for the outgoing solution for isotropic poroelastic equations. Note that the strain $\boldsymbol{\tau}$ and the pressure p are uniquely determined by the displacements / velocity. It suffices to impose outgoing criteria for $\mathbf{u}$ and $\mathbf{w}$ (if using the first order formulation) or u and w (if using the original equation).

Definition 2.3 (Outgoing solutions). The fields $\mathbf{u}$ and $\mathbf{w}$ are called outgoing solutions of the poroelastic equations (1.16) if they satisfy the following radiation conditions.

1. Their rotationals $\operatorname{curl}\mathbf{u}$ and $\operatorname{curl}\mathbf{w}$ satisfy the outgoing Sommerfeld radiation condition with wavenumber k_S, *i.e.* for $\chi = \operatorname{curl}\mathbf{u}$ or $\operatorname{curl}\mathbf{w}$, χ satisfies

$$\lim_{r\to\infty} \sqrt{r}\left(\frac{\partial\chi}{\partial r} - \mathrm{i}\,\mathsf{k}_s\,\chi\right) = 0\,,$$

uniformly in all directions.

2. With matrix P defined in (2.1), and for χ_P , χ_B defined as $\begin{pmatrix}\chi_P\\ \chi_B\end{pmatrix} = P^{-1}\begin{pmatrix}\nabla\cdot\mathbf{u}\\ \nabla\cdot\mathbf{w}\end{pmatrix}$, then χ_P and χ_B satisfy the outgoing Sommerfeld radiation condition with wavenumber k_P and k_B respectively:

$$\lim_{r\to\infty} \sqrt{r}\left(\frac{\partial\chi_P}{\partial r} - \mathrm{i}\,\mathsf{k}_P\,\chi_P\right) = 0\,, \quad \text{and} \quad \lim_{r\to\infty} \sqrt{r}\left(\frac{\partial\chi_B}{\partial r} - \mathrm{i}\,\mathsf{k}_B\,\chi_B\right) = 0\,,$$

uniformly in all directions.

Remark 2.4. A similar definition can be proposed to define an outgoing solution if we work with the displacement (u,w), instead of the velocities $\mathbf{u}$ and $\mathbf{w}$. △

2.2 Generic solution to homogeneous equation on bounded domain

We consider the homogeneous poroelastic equations (1.16) on disc $\mathbb{B}_{(0,\mathfrak{a})}$. The solutions $(\mathbf{u},\mathbf{w},\boldsymbol{\tau},\mathrm{p})$ are given by equations (2.10), (2.11) and (2.12), while the potentials are given by (2.13). Hence, in a bounded domain, the potentials satisfy equation (2.14):

$$\begin{aligned}
\chi_{\mathrm{P}}(r,\theta) &= \sum_{k\in\mathbb{Z}} a_k\,\mathrm{J}_k(\omega\,\mathsf{s}_{\mathrm{P}}\,r)\;e^{\mathrm{i}\,k\,\theta}\,,\\
\chi_{\mathrm{B}}(r,\theta) &= \sum_{k\in\mathbb{Z}} b_k\,\mathrm{J}_k(\omega\,\mathsf{s}_{\mathrm{B}}\,r)\;e^{\mathrm{i}\,k\,\theta}\,,\\
\chi_{\mathrm{S}}(r,\theta) &= \sum_{k\in\mathbb{Z}} c_k\,\mathrm{J}_k(\omega\,\mathsf{s}_{\mathrm{S}}\,r)\;e^{\mathrm{i}\,k\,\theta}\,.
\end{aligned}$$

The series coefficients a_k, b_k, c_k are then determined by the boundary conditions imposed on $\partial\mathbb{B}_{(0,\mathfrak{a})}$, which are one of the four types listed in Section 1.4. The boundary conditions of type 2 and 4 are linear combinations of the boundary conditions of type 1 and 3, hence, we only detail the solutions for type 1 and 3 (equations (1.20a) and (1.20c)).

2.2.1 Boundary conditions of type 1

We consider the poroelastic equations (1.16) on the disc $\mathbb{B}_{(0,\mathfrak{a})}$, with boundary conditions:

$$\begin{aligned}
\mathbf{w}\cdot\mathbf{n} &= g \quad , \quad \text{on } \partial\mathbb{B}_{(0,\mathfrak{a})}\,,\\
\boldsymbol{\tau}\,\mathbf{n} &= \boldsymbol{h} \quad , \quad \text{on } \partial\mathbb{B}_{(0,\mathfrak{a})}\,.
\end{aligned}$$

In polar coordinates, $\boldsymbol{n} = \mathbf{e}_r$. Hence, $\mathbf{w}\cdot\boldsymbol{n} = \mathrm{w}_r$, $\boldsymbol{\tau}\,\boldsymbol{n} = \tau_{rr}\,\mathbf{e}_r + \tau_{r\theta}\,\mathbf{e}_\theta$. The boundary conditions are written as:

$$\mathfrak{s}\,\mathrm{i}\,\omega\,\mathrm{w}_r = \mathfrak{s}\,\mathrm{i}\,\omega\,g\,,\quad \omega^2\,\tau_{rr} = \omega^2\,\boldsymbol{h}_r\,,\quad \omega^2\,\tau_{r\theta} = \omega^2\,\boldsymbol{h}_\theta \quad , \quad \partial\mathbb{B}_{(0,\mathfrak{a})}\,. \tag{2.23}$$

Next, we expand the coefficient of each component in Fourier series. For the right hand-side,

$$g = \sum_{k\in\mathbb{Z}} g_k\,e^{\mathrm{i}\,k\,\theta}\,,\quad \boldsymbol{h}_r = \sum_{k\in\mathbb{Z}} \boldsymbol{h}_{r,k}\,e^{\mathrm{i}\,k\,\theta}\,,\quad \boldsymbol{h}_\theta = \sum_{k\in\mathbb{Z}} \boldsymbol{h}_{\theta,k}\,e^{\mathrm{i}\,k\,\theta}\,.$$

For the unknowns:

$$\mathrm{w}_r = \sum_{k\in\mathbb{Z}} \mathrm{w}_{r,k}\,e^{\mathrm{i}\,k\,\theta}\,,\quad \tau_{rr} = \sum_{k\in\mathbb{Z}} \tau_{rr,k}\,e^{\mathrm{i}\,k\,\theta}\,,\quad \tau_{r\theta} = \sum_{k\in\mathbb{Z}} \tau_{r\theta,k}\,e^{\mathrm{i}\,k\,\theta}\,.$$

Using (2.18), (2.19) and (2.20), we have:

$$
\begin{aligned}
\mathfrak{s}\,\mathrm{i}\,\omega\,\mathrm{w}_{r,k} =& a_k\,\frac{\mathcal{W}_\mathrm{P}}{\mathsf{s}_\mathrm{P}}\,\omega\,\mathrm{J}_k'(\omega\,\mathsf{s}_\mathrm{P}\,r)e^{\mathrm{i}k\theta} + b_k\,\frac{\mathcal{W}_\mathrm{B}}{\mathsf{s}_\mathrm{B}}\,\omega\,\mathrm{J}_k'(\omega\,\mathsf{s}_\mathrm{B}\,r)e^{\mathrm{i}k\theta} + c_k\,\frac{\rho_f\,\mu_\mathrm{fr}}{\det A}\,\frac{\mathrm{i}k}{r}\mathrm{J}_k(\omega\,\mathsf{s}_\mathrm{S}\,r)e^{\mathrm{i}k\theta},\\
\omega^2\tau_{rr,k} =& -\frac{2\,\mu_\mathrm{fr}\,\omega}{\mathsf{s}_\mathrm{P}\,r}\,a_k\,\mathrm{J}_{k+1}(\omega\,\mathsf{s}_\mathrm{P}\,r)\;e^{\mathrm{i}\,k\,\theta} + \frac{2\,\mu_\mathrm{fr}\,k}{\mathsf{s}_\mathrm{P}^2\,r^2}\,a_k\,\mathrm{J}_k(\omega\,\mathsf{s}_\mathrm{P}\,r)\;e^{\mathrm{i}\,k\,\theta} + 2\,\mu_\mathrm{fr}\,a_k\,\omega^2\,\mathrm{J}_k(\omega\,\mathsf{s}_\mathrm{P}\,r)\;e^{\mathrm{i}\,k\,\theta}\\
&- \frac{2\,\mu_\mathrm{fr}\,k^2}{\mathsf{s}_\mathrm{P}^2\,r^2}\,a_k\,\mathrm{J}_k(\omega\,\mathsf{s}_\mathrm{P}\,r)\;e^{\mathrm{i}\,k\,\theta} - \frac{2\,\mu_\mathrm{fr}\,\omega}{\mathsf{s}_\mathrm{B}\,r}\,b_k\,\mathrm{J}_{k+1}(\omega\,\mathsf{s}_\mathrm{B}\,r)\;e^{\mathrm{i}\,k\,\theta} + \frac{2\,\mu_\mathrm{fr}\,k}{\mathsf{s}_\mathrm{B}^2\,r^2}\,b_k\,\mathrm{J}_k(\omega\,\mathsf{s}_\mathrm{B}\,r)\;e^{\mathrm{i}\,k\,\theta}\\
&+ 2\,\mu_\mathrm{fr}\,b_k\,\omega^2\,\mathrm{J}_k(\omega\,\mathsf{s}_\mathrm{B}\,r)\;e^{\mathrm{i}\,k\,\theta} - \frac{2\,\mu_\mathrm{fr}\,k^2}{\mathsf{s}_\mathrm{B}^2\,r^2}\,b_k\,\mathrm{J}_k(\omega\,\mathsf{s}_\mathrm{B}\,r)\;e^{\mathrm{i}\,k\,\theta} + \frac{2\,\mu_\mathrm{fr}}{\mathsf{s}_\mathrm{S}^2\,r}\;c_k\,\omega\,\mathsf{s}_\mathrm{S}\,\mathrm{i}k\,\mathrm{J}_k'(\,\omega\,\mathsf{s}_\mathrm{S}\,r)\;e^{\mathrm{i}\,k\,\theta}\\
&+ \omega^2\,\left(-\tfrac{2}{3}\mu_\mathrm{fr} + \mathrm{k}_\mathrm{fr} + M\alpha^2 + \alpha\,M\mathcal{W}_\mathrm{P}\right)\;a_k\,\mathrm{J}_k(\omega\,\mathsf{s}_\mathrm{P}\,r)\;e^{\mathrm{i}\,k\,\theta}\\
&+ \omega^2\,\left(-\tfrac{2}{3}\mu_\mathrm{fr} + \mathrm{k}_\mathrm{fr} + M\alpha^2 + \alpha\,M\mathcal{W}_\mathrm{B}\right)\,b_k\,\mathrm{J}_k(\omega\,\mathsf{s}_\mathrm{B}\,r)\;e^{\mathrm{i}\,k\,\theta},\\
\omega^2\,\tau_{r\theta,k} =& -\frac{2\,\mu_\mathrm{fr}\omega\,\mathrm{i}\,k}{r\,\mathsf{s}_\mathrm{P}}\,a_k\,\mathrm{J}_k'(\omega\,\mathsf{s}_\mathrm{P}\,r)\,e^{\mathrm{i}\,k\,\theta} + \frac{2\,\mathrm{i}\,\mu_\mathrm{fr}\,k}{r^2\,\mathsf{s}_\mathrm{P}^2}\,a_k\,\mathrm{J}_k(\omega\,\mathsf{s}_\mathrm{P}\,r)\,e^{\mathrm{i}\,k\,\theta} - \frac{2\mu_\mathrm{fr}\omega\,\mathrm{i}\,k}{r\,\mathsf{s}_\mathrm{B}}\,b_k\,\mathrm{J}_k'(\omega\,\mathsf{s}_\mathrm{B}\,r)e^{\mathrm{i}\,k\,\theta}\\
&+ \frac{2\,\mathrm{i}\,\mu_\mathrm{fr}\,k}{r^2\,\mathsf{s}_\mathrm{B}^2}\,b_k\,\mathrm{J}_k(\omega\,\mathsf{s}_\mathrm{B}\,r)\;e^{\mathrm{i}\,k\,\theta} - \frac{\mu_\mathrm{fr}\,k^2}{r^2\,\mathsf{s}_\mathrm{S}^2}\,c_k\,\mathrm{J}_k(\omega\,\mathsf{s}_\mathrm{S}\,r)\;e^{\mathrm{i}\,k\,\theta} + \frac{\mu_\mathrm{fr}\,\omega}{r\,\mathsf{s}_\mathrm{S}}\,c_k\,\mathrm{J}_k'(\omega\,\mathsf{s}_\mathrm{S}\,r)\;e^{\mathrm{i}\,k\,\theta}\\
&- \mu_\mathrm{fr}\,\frac{\omega}{\mathsf{s}_\mathrm{S}\,r}\,c_k\,\mathrm{J}_{k+1}(\omega\,\mathsf{s}_\mathrm{S}\,r)\;e^{\mathrm{i}\,k\,\theta} + \mu_\mathrm{fr}\,\frac{k}{\mathsf{s}_\mathrm{S}^2\,r^2}c_k\,\mathrm{J}_k(\omega\,\mathsf{s}_\mathrm{S}\,r)\;e^{\mathrm{i}\,k\,\theta}\\
&+ \omega^2\,c_k\,\mathrm{J}_k(\omega\,\mathsf{s}_\mathrm{S}\,r)\;e^{\mathrm{i}\,k\,\theta} - \mu_\mathrm{fr}\,\frac{k^2}{\mathsf{s}_\mathrm{S}^2\,r^2}\,c_k\,\mathrm{J}_k(\omega\,\mathsf{s}_\mathrm{S}\,r)\;e^{\mathrm{i}\,k\,\theta}.
\end{aligned}
\tag{2.24}
$$

Imposing (2.23), we obtain a linear system satisfied by a_k, b_k, c_k in each mode k.

$$
\mathbb{A}_k^{\mathbf{w},\boldsymbol{\tau}}\begin{pmatrix} a_k\\ b_k\\ c_k\end{pmatrix} = \begin{pmatrix} \mathfrak{s}\,\mathrm{i}\,\omega\,g_k\\ \omega^2\,\boldsymbol{h}_{r,k}\\ \omega^2\,\boldsymbol{h}_{\theta,k}\end{pmatrix},
$$

where the coefficient matrix is defined as:

$$
\mathbb{A}_k^{\mathbf{w},\boldsymbol{\tau}} = \begin{pmatrix} A_{11} & A_{12} & A_{13}\\ A_{21} & A_{22} & A_{23}\\ A_{31} & A_{32} & A_{33}\end{pmatrix}
\tag{2.25}
$$

with

$$
\begin{aligned}
A_{11} =& \frac{WP}{\mathsf{s}_\mathrm{P}}\,\omega\,\mathrm{J}_k'(\omega\,\mathsf{s}_\mathrm{P}\mathfrak{a}), \qquad A_{12} = \frac{\mathcal{W}_\mathrm{B}}{\mathsf{s}_\mathrm{B}}\,\omega\,\mathrm{J}_k'(\omega\,\mathsf{s}_\mathrm{S}\mathfrak{a}), \qquad A_{13} = \frac{\rho_f\,\mu_\mathrm{fr}}{\det A}\,\frac{\mathrm{i}k}{\mathfrak{a}}\mathrm{J}_k(\omega\,\mathsf{s}_\mathrm{S}\mathfrak{a}),\\
A_{21} =& -\frac{2\,\mu_\mathrm{fr}\,\omega}{\mathsf{s}_\mathrm{P}\,\mathfrak{a}}\,\mathrm{J}_{k+1}(\omega\,\mathsf{s}_\mathrm{P}\,\mathfrak{a}) + \frac{2\,\mu_\mathrm{fr}\,k}{\mathsf{s}_\mathrm{P}^2\,\mathfrak{a}^2}\,\mathrm{J}_k(\omega\,\mathsf{s}_\mathrm{P}\,\mathfrak{a}) + 2\,\mu_\mathrm{fr}\,\omega^2\,\mathrm{J}_k(\omega\,\mathsf{s}_\mathrm{P}\,\mathfrak{a})\\
&- \frac{2\,\mu_\mathrm{fr}\,k^2}{\mathsf{s}_\mathrm{P}^2\,\mathfrak{a}^2}\,\mathrm{J}_k(\omega\,\mathsf{s}_\mathrm{P}\,\mathfrak{a}) + \omega^2\,\left(-\tfrac{2}{3}\mu_\mathrm{fr} + \mathrm{k}_\mathrm{fr} + M\alpha^2 + \alpha\,M\mathcal{W}_\mathrm{P}\right)\mathrm{J}_k(\omega\,\mathsf{s}_\mathrm{P}\mathfrak{a}),\\
A_{22} =& -\frac{2\,\mu_\mathrm{fr}\,\omega}{\mathsf{s}_\mathrm{B}\,\mathfrak{a}}\,\mathrm{J}_{k+1}(\omega\,\mathsf{s}_\mathrm{B}\,\mathfrak{a}) + \frac{2\,\mu_\mathrm{fr}\,k}{\mathsf{s}_\mathrm{B}^2\,\mathfrak{a}^2}\,\mathrm{J}_k(\omega\,\mathsf{s}_\mathrm{B}\,\mathfrak{a}) + 2\,\mu_\mathrm{fr}\,\omega^2\,\mathrm{J}_k(\omega\,\mathsf{s}_\mathrm{B}\,\mathfrak{a})\;e^{\mathrm{i}\,k\,\theta}\\
&- \frac{2\,\mu_\mathrm{fr}\,k^2}{\mathsf{s}_\mathrm{B}^2\,\mathfrak{a}^2}\,\mathrm{J}_k(\omega\,\mathsf{s}_\mathrm{B}\,\mathfrak{a})\;e^{\mathrm{i}\,k\,\theta} + \omega^2\,\left(-\tfrac{2}{3}\mu_\mathrm{fr} + \mathrm{k}_\mathrm{fr} + M\alpha^2 + \alpha\,M\mathcal{W}_\mathrm{B}\right)\mathrm{J}_k(\omega\,\mathsf{s}_\mathrm{B}\mathfrak{a}),
\end{aligned}
$$

and

$$A_{23} = \frac{2\mu_{\rm fr}}{\mathsf{s}_{\rm S}\mathfrak{a}}\,\omega\,\mathrm{i}k\,\mathrm{J}_k'(\omega\,\mathsf{s}_{\rm S}\mathfrak{a})\,, \qquad A_{31} = -\frac{2\omega\,\mu_{\rm fr}\mathrm{i}k}{\mathfrak{a}\mathsf{s}_{\rm P}}\mathrm{J}_k'(\omega\,\mathsf{s}_{\rm P}\mathfrak{a}) + \frac{2\,\mu_{\rm fr}\mathrm{i}k}{\mathfrak{a}^2\mathsf{s}_{\rm P}^2}\mathrm{J}_k(\omega\,\mathsf{s}_{\rm P}\mathfrak{a})\,,$$

$$A_{32} = -\frac{2\omega\,\mu_{\rm fr}\mathrm{i}k}{\mathfrak{a}\mathsf{s}_{\rm B}}\mathrm{J}_k'(\omega\,\mathsf{s}_{\rm B}\mathfrak{a}) + \frac{2\mu_{\rm fr}\mathrm{i}k}{\mathfrak{a}^2\mathsf{s}_{\rm B}^2}\mathrm{J}_k(\omega\,\mathsf{s}_{\rm B}\mathfrak{a})\,,$$

$$A_{33} = -\frac{k^2\mu_{\rm fr}}{\mathfrak{a}^2\mathsf{s}_{\rm S}^2}\mathrm{J}_k(\omega\,\mathsf{s}_{\rm S}\,\mathfrak{a}) + \frac{\omega\,\mu_{\rm fr}}{\mathfrak{a}\mathsf{s}_{\rm S}}\mathrm{J}_k'(\omega\,\mathsf{s}_{\rm S}\,\mathfrak{a}) - \frac{\omega}{\mathsf{s}_{\rm S}\,\mathfrak{a}}\,\mathrm{J}_{k+1}(\omega\,\mathsf{s}_{\rm S}\,\mathfrak{a}) + \frac{k}{\mathsf{s}_{\rm S}^2\,\mathfrak{a}^2}\,\mathrm{J}_k(\omega\,\mathsf{s}_{\rm S}\,\mathfrak{a})$$
$$+\,\omega^2\,\mathrm{J}_k(\omega\,\mathsf{s}_{\rm S}\,\mathfrak{a}) - \frac{k^2}{\mathsf{s}_{\rm S}^2\,\mathfrak{a}^2}\,\mathrm{J}_k(\omega\,\mathsf{s}_{\rm S}\,\mathfrak{a})\,.$$

We define the eigenvalues as follows:

Definition 2.5. The pulsation ω is a type 1 boundary conditions eigenvalue if the system of poroelastic equations (1.16) associated with the boundary conditions

$$\begin{aligned}\mathbf{w}\cdot\mathbf{n} &= 0 \quad , \quad \text{on } \partial\mathbb{B}_{(0,\mathfrak{a})}\,,\\ \boldsymbol{\tau}\,\mathbf{n} &= 0 \quad , \quad \text{on } \partial\mathbb{B}_{(0,\mathfrak{a})}\,,\end{aligned}$$

admits a solution $(\mathbf{w}, \boldsymbol{\tau})$ such that $\mathbf{w} \neq 0$, $\boldsymbol{\tau} \neq 0$. This also means that $\det \mathbb{A}_k^{\mathbf{w},\boldsymbol{\tau}}(\omega) = 0$, where $\mathbb{A}_k^{\mathbf{w},\boldsymbol{\tau}}$ is the coefficient matrix defined in equation (2.25).

2.2.2 Boundary conditions of type 3

We consider the poroelastic equations on the disc $\mathbb{B}_{(0,\mathfrak{a})}$, with boundary conditions:

$$\mathbf{u} = \boldsymbol{h}\,, \qquad \mathrm{p} = g \quad , \quad \partial\mathbb{B}_{(0,\mathfrak{a})}\,.$$

We work in polar coordinates, $\boldsymbol{h} = \boldsymbol{h}_r\mathbf{e}_r + \boldsymbol{h}_\theta\,\mathbf{e}_\theta$ and $\mathbf{u} = \mathrm{u}_r\mathbf{e}_r + \mathrm{u}_\theta\,\mathbf{e}_\theta$. The boundary conditions are written as:

$$\mathfrak{s}\,\mathrm{i}\,\omega\,\mathrm{u}_r = \mathfrak{s}\,\mathrm{i}\,\omega\,\boldsymbol{h}_r\,, \quad \mathfrak{s}\,\mathrm{i}\,\omega\,\mathrm{u}_\theta = \mathfrak{s}\,\mathrm{i}\,\omega\,\boldsymbol{h}_\theta\,, \quad \mathrm{p} = g \quad , \quad \partial\mathbb{B}_{(0,\mathfrak{a})}\,. \tag{2.26}$$

Next, we expand the coefficient of each component in Fourier series. For the right hand-side,

$$\boldsymbol{h}_r = \sum_{k\in\mathbb{Z}} \boldsymbol{h}_{r,k}\,e^{\mathrm{i}\,k\,\theta}\,, \quad \boldsymbol{h}_\theta = \sum_{k\in\mathbb{Z}} \boldsymbol{h}_{\theta,k}\,e^{\mathrm{i}\,k\,\theta}\,, \quad g = \sum_{k\in\mathbb{Z}} g_k\,e^{\mathrm{i}\,k\,\theta}\,.$$

For the unknowns:

$$\mathrm{u}_r = \sum_{k\in\mathbb{Z}} \mathrm{u}_{r,k}\,e^{\mathrm{i}\,k\,\theta}\,, \quad \mathrm{u}_\theta = \sum_{k\in\mathbb{Z}} \mathrm{u}_{\theta,k}\,e^{\mathrm{i}\,k\,\theta}\,, \quad \mathrm{p} = \sum_{k\in\mathbb{Z}} \mathrm{p}_k\,e^{\mathrm{i}\,k\,\theta}\,.$$

Using (2.17) and (2.21), we have:

$$\begin{aligned}\mathfrak{s}\,\mathrm{i}\,\omega\,\mathrm{u}_{r,k} &= \sum_{k\in\mathbb{Z}} a_k\;\mathsf{s}_{\rm P}^{-1}\,\omega\,\mathrm{J}_k'(\omega\,\mathsf{s}_{\rm P}\,r)e^{\mathrm{i}k\theta} + \sum_{k\in\mathbb{Z}} b_k\;\mathsf{s}_{\rm B}^{-1}\,\omega\,\mathrm{J}_k'(\omega\,\mathsf{s}_{\rm B}\,r)e^{\mathrm{i}k\theta} - \sum_{k\in\mathbb{Z}} c_k\;\mathsf{s}_{\rm S}^{-2}\,\frac{\mathrm{i}k}{r}\mathrm{J}_k(\omega\,\mathsf{s}_{\rm S}\,r)e^{\mathrm{i}k\theta}\,,\\ \mathfrak{s}\,\mathrm{i}\,\omega\,\mathrm{u}_{\theta,k} &= \sum_{k\in\mathbb{Z}} a_k\;\mathsf{s}_{\rm P}^{-2}\,\frac{\mathrm{i}k}{r}\mathrm{J}_k(\omega\,\mathsf{s}_{\rm P}\,r)e^{\mathrm{i}k\theta} + \sum_{k\in\mathbb{Z}} b_k\;\mathsf{s}_{\rm B}^{-2}\,\frac{\mathrm{i}k}{r}\mathrm{J}_k(\omega\,\mathsf{s}_{\rm B}\,r)e^{\mathrm{i}k\theta} + \sum_{k\in\mathbb{Z}} c_k\;\mathsf{s}_{\rm S}^{-1}\,\omega\,\mathrm{J}_k'(\omega\,\mathsf{s}_{\rm S}\,r)e^{\mathrm{i}k\theta}\,,\\ \mathrm{p}_k &= -\sum_{k\in\mathbb{Z}} a_k\,M\,(\mathcal{W}_{\rm P} + \alpha)\,\mathrm{J}_k(\omega\,\mathsf{s}_{\rm P}\,r)\,e^{\mathrm{i}k\theta} - \sum_{k\in\mathbb{Z}} b_k\,M\,(\mathcal{W}_{\rm B} + \alpha)\,\mathrm{J}_k(\omega\,\mathsf{s}_{\rm B}\,r)\,e^{\mathrm{i}k\theta}\,.\end{aligned} \tag{2.27}$$

Imposing (2.26), we obtain a linear system satisfied by a_k, b_k, c_k in each mode k:

$$\mathbb{A}_k^{\mathbf{u},\mathrm{p}}\begin{pmatrix}a_k\\ b_k\\ c_k\end{pmatrix} = \begin{pmatrix}\mathfrak{s}\,\mathrm{i}\,\omega\,\boldsymbol{h}_{r,k}\\ \mathfrak{s}\,\mathrm{i}\,\omega\,\boldsymbol{h}_{\theta,k}\\ g_k\end{pmatrix}\,, \tag{2.28}$$

where the coefficient matrix $\mathbb{A}_k^{\mathbf{u},\mathrm{p}}$ is defined as:

$$\mathbb{A}_k^{\mathbf{u},\mathrm{p}} = \begin{pmatrix} \mathsf{s}_{\mathrm{P}}^{-1}\,\omega\,\mathrm{J}_k'(\omega\,\mathsf{s}_{\mathrm{P}}\,\mathfrak{a}) & \mathsf{s}_{\mathrm{B}}^{-1}\,\omega\,\mathrm{J}_k'(\omega\,\mathsf{s}_{\mathrm{S}}\,\mathfrak{a}) & -\,\mathsf{s}_{\mathrm{S}}^{-2}\,\dfrac{\mathrm{i}k}{\mathfrak{a}}\mathrm{J}_k(\omega\,\mathsf{s}_{\mathrm{S}}\,\mathfrak{a}) \\ \mathsf{s}_{\mathrm{P}}^{-2}\,\dfrac{\mathrm{i}k}{\mathfrak{a}}\mathrm{J}_k(\omega\,\mathsf{s}_{\mathrm{P}}\,\mathfrak{a}) & \mathsf{s}_{\mathrm{B}}^{-2}\,\dfrac{\mathrm{i}k}{\mathfrak{a}}\mathrm{J}_k(\omega\,\mathsf{s}_{\mathrm{B}}\,\mathfrak{a}) & \mathsf{s}_{\mathrm{S}}^{-1}\,\omega\,\mathrm{J}_k'(\omega\,\mathsf{s}_{\mathrm{S}}\,\mathfrak{a}) \\ -M\left(\mathcal{W}_{\mathrm{P}} + \alpha\right)\mathrm{J}_k(\omega\,\mathsf{s}_{\mathrm{P}}\,\mathfrak{a}) & -M\left(\mathcal{W}_{\mathrm{B}} + \alpha\right)\mathrm{J}_k(\omega\,\mathsf{s}_{\mathrm{B}}\,\mathfrak{a}) & 0 \end{pmatrix}. \tag{2.29}$$

Definition 2.6. The pulsation ω is a type 3 boundary conditions eigenvalue if the system of poroelastic equations (1.16) associated with the boundary conditions

$$\begin{aligned} \mathbf{u} &= 0 \quad , \quad \text{on } \partial\mathbb{B}_{(0,\mathfrak{a})}\,, \\ \mathrm{p} &= 0 \quad , \quad \text{on } \partial\mathbb{B}_{(0,\mathfrak{a})}\,, \end{aligned}$$

admits a solution $(\mathbf{u}, \mathrm{p})$ such that $\mathbf{u} \neq 0$, $\mathrm{p} \neq 0$. This also means that $\det \mathbb{A}_k^{\mathbf{u},\mathrm{p}}(\omega) = 0$, where $\mathbb{A}_k^{\mathbf{u},\mathrm{p}}$ is the coefficient matrix defined in equation (2.28).

2.2.3 Numerical analysis of the coefficient matrix on bounded domain

The objective of the numerical experiments is to determine if we can find eigenvalues, i.e., values of frequency for which the determinant of the coefficient matrices vanishes. Indeed, if the determinant vanishes, we cannot invert the matrix,and the uniqueness of the problem is not guaranteed. We will investigate the invertibility of the coefficient matrices for the first few modes $k = 0, ..., 5$, by looking at the absolute value of their determinant.

We test with sandstone, and vary the value of viscosity of this material, *cf.* Tab. 1.1. For all tests, the cross section radius is $\mathfrak{a} = 1\mathrm{m}$. Recall that we can use four types of boundary conditions (see equations (1.20a), (1.20b), (1.20c) and (1.20d)). Here we only test the boundary conditions of type 1 and 3, which means that we only study the determinant of $\mathbb{A}_k^{\mathbf{w},\boldsymbol{\tau}}$ (2.25) and $\mathbb{A}_k^{\mathbf{u},\mathrm{p}}$ (2.29), as functions of the frequency f. We consider a frequency range between 1Hz and 10MHz to compare with the results in [6] and [51]. Note that the interval ($\omega\mathfrak{a} \leq 1500\mathrm{m.s}^{-1}$) in our plot is more relevant to geophysical experiments[2]. To determine the nature of the peaks, we refine around the peaks in a procedure described in Algorithm 1. This will be used in all the remaining tests of the chapter.

Start Suppose x_{center} is the local minimum on the interval $[a, b]$, with h the current stepsize of the sequence. Say $x_{\text{center}} = N\,h$, and $a = x_{\text{center}} - m\,h$, $b = x_{\text{center}} + m'\,h$, with m, $m' \geq 5$, hence we have at least 5 points before and after x_{center} in the sequence. The interval in consideration always has to satisfy criteria ($\star$), which requires that the function decreases for $x \leq x_{\text{center}}$ and increases for $x \geq x_{\text{center}}$.

Update A new interval $[a, b]$ is chosen, centered around the previous miminum, and thus satisfies the criteria ($\star$). We plot the value of the function on this new interval, with the new step on the frequency equal to $\frac{h}{10}$. In this way, we are on a smaller interval with a finer grid.

Iteration A new center x_{center} is now the new local minimum of the function on this interval. We go back to the start.

Stop criteria The loop is stopped if the size of h is lower than the machine precision or if the minimum value on the interval at the current iteration does not differ from that of the previous one by the threshold ε.

Algorithm 1: Algorithm for detecting the modes of inversibility. There are two behaviours when we refine around a peak: in the case where it is a true zero, the value of the function shown on log scale will decrease until the machine precision on the h interval. If it is not a true zero, the values of the absolute determinant will stabilize to a fixed lower bound. In fact, the threshold ε is implemented qualitatively, i.e., by the observation of the curve. In particular, in the first iterations, we observe a curved down bump, but after a few iterations, we only obtain a horizontal line, which means that the value on the zoomed interval stopped descending.

The results are reported in the following figures:

- Sandstone with no viscosity Figures 2.1 and 2.2.

[2] In [50], and [71], frequencies up to 600Hz are used, on a domain of interest of 10^2m.

- Sandstone with viscosity Figures 2.3 and 2.4.
- Sand 1 with no viscosity, varying the value of μ_{fr} in Figure 2.5.

Observations From these experiments, we obtain the following observations.

- In the geophysical range ($\omega \mathfrak{a} \leq 1500$ rad.m.s^{-1}), generalized eigenvalues are present for non-viscous problems.
- On the initial interval we study, $\omega\, \mathfrak{a}$ in the range $[0, 10^4]$ rad.m.s^{-1}, the curves for material of sandstone with viscosity ressemble those with no viscosity. The curves represent isolated peaks, however, the case with viscosity presents less peaks for the same range of frequencies. After the zoom procedure, their behaviours are different. We applied the zoom procedure to each of the peaks in the graph of absolute determinant of $\mathbb{A}_0^{\mathbf{w},\boldsymbol{\tau}}$ and $\mathbb{A}_0^{\mathbf{u},\mathrm{p}}$. We note that there are differences between those with and without viscosity. There exist generalized eigenvalues for the case without viscosity, manifested by the sharp peaks for both boundary conditions in Figures 2.1 and 2.2.

  Before zooming, the value in the neighbourhood of a peak in consideration is around 10^{-2}. However, after several zooms, the value in this refined neighbourhood drastically drops to 10^{-10} for $\mathbb{A}_0^{\mathbf{w},\boldsymbol{\tau}}$ and 10^{-16} for $\mathbb{A}_0^{\mathbf{u},\mathrm{p}}$. We only show a few examples of this refinement. With finer refinement, the value of the refined neighbourhood will drop to the machine precision. On the contrary, with viscosity, we do not have this behaviour. Although there are apparent peaks before zoom in Figures 2.3 and 2.4, when zoomed around the sharpest peak, the value of the determinant on the refined neighbourhoods stays bounded below, and the sharp peaks become smooth concave up curves. Hence, there are no generalized eigenvalue in this case.
- For sandstone, we have similar pattern of peaks for both boundary conditions, however, the generalized eigenvalues are not the same because the problem on the boundary is different.
- Note that the curves present small peaks, compared to the absence of generalized eigenvalues in the outgoing case (see Section 2.3 Figure 2.8), in which the curves are completely free of peaks .
- The frame shear modulus μ_{fr} has an influence on the peaks. We observe in Figure 2.5 that when the value of the shear frame modulus increases, the number of the peaks, hence of eigenvalues decreases.

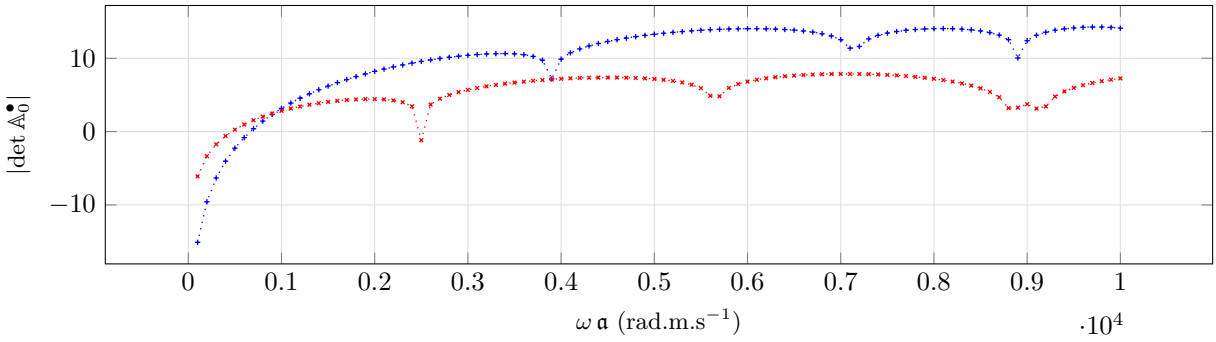

(a) Mode $k = 0$

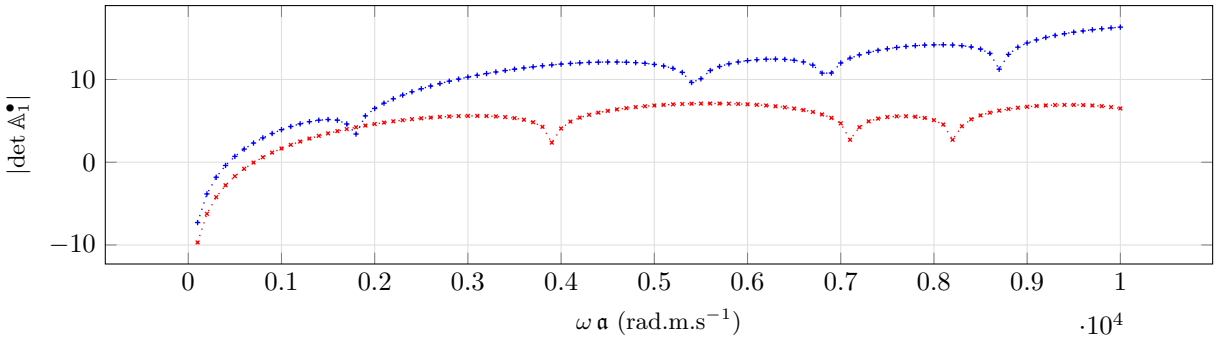

(b) Mode $k = 1$

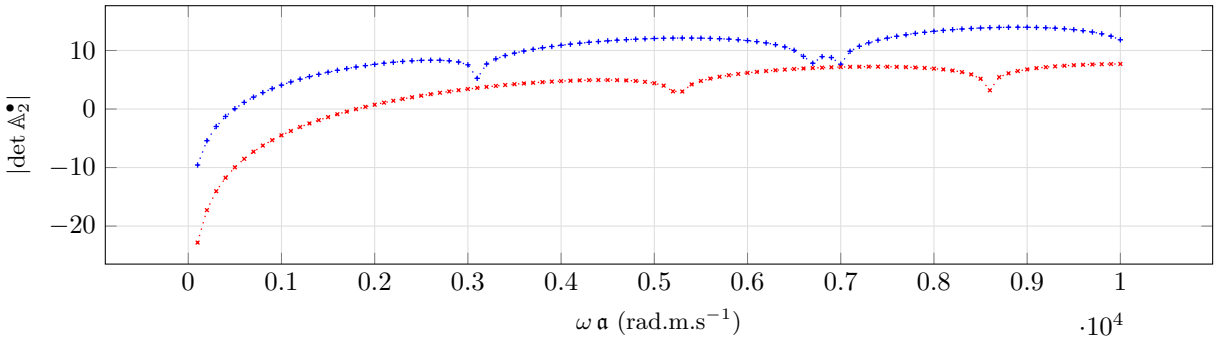

(c) Mode $k = 2$

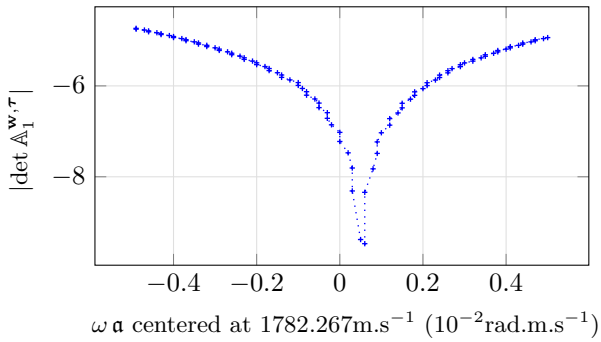

(d) Mode $k = 1$

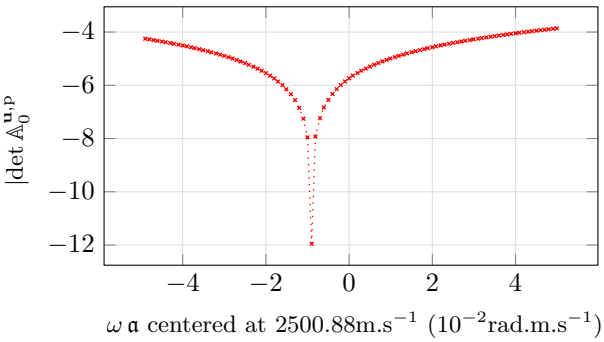

(e) Mode $k = 0$

Figure 2.1: Determinant of the coefficient matrix (log scale) in a bounded domain for k in $0:2$ for sandstone with no viscosity. The matrices corresponding with types of boundary conditions 1 and 3 are considered: $\mathbb{A}_k^{\mathbf{w},\boldsymbol{\tau}}$ (2.25) in blue and $\mathbb{A}_k^{\mathbf{u},\mathrm{p}}$ (2.29) in red .

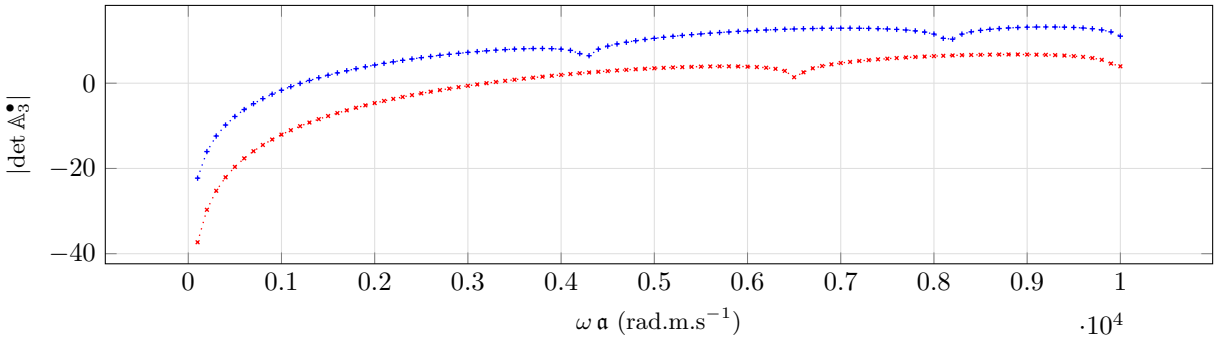

(a) Mode $k = 3$

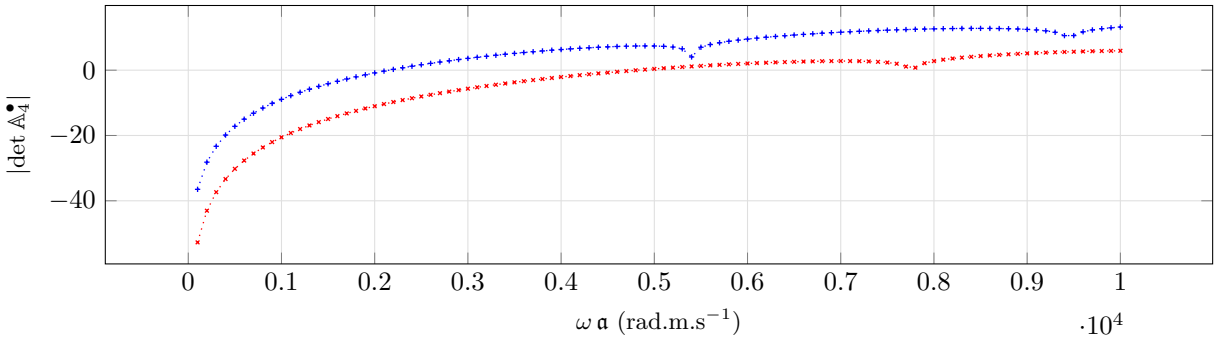

(b) Mode $k = 4$

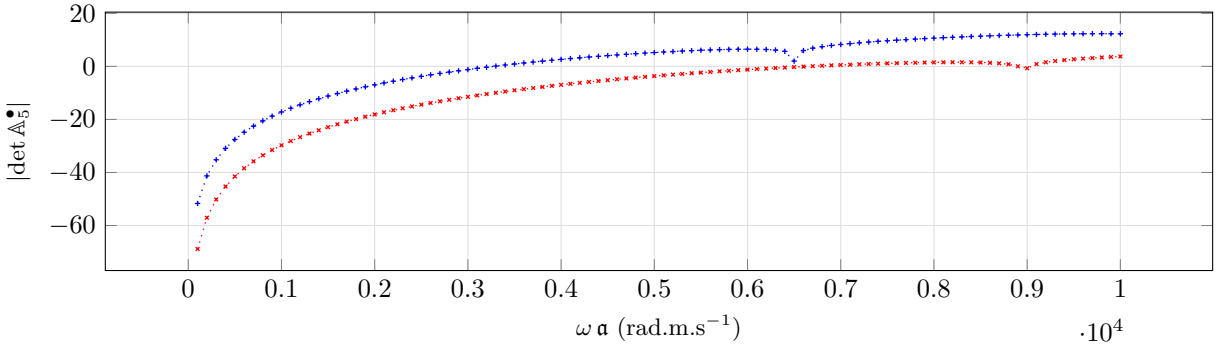

(c) Mode $k = 5$

Figure 2.2: Determinant of the coefficient matrix (log scale) in a bounded domain for k in $3:5$ for sandstone with no viscosity. The matrices corresponding with types of boundary conditions 1 and 3 are considered: $\mathbb{A}_k^{\mathbf{w},\boldsymbol{\tau}}$ (2.25)in blue and $\mathbb{A}_k^{\mathbf{u},\mathrm{p}}$ (2.29) in red .

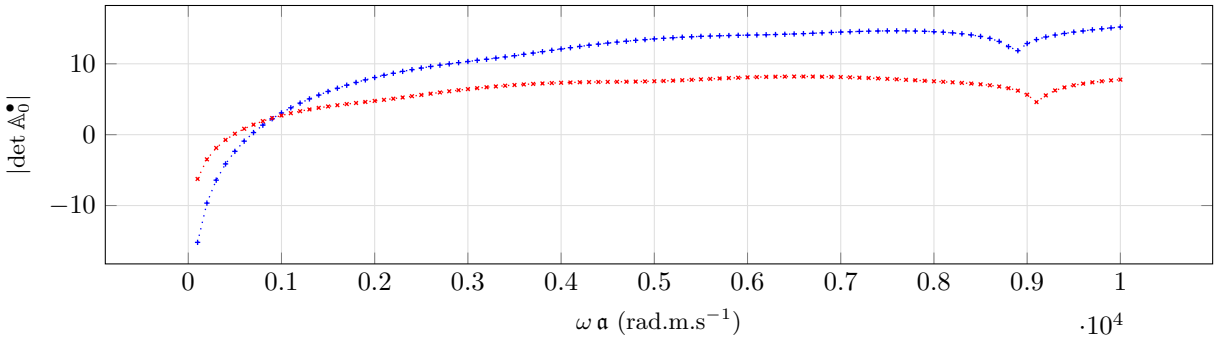

(a) Mode $k = 0$

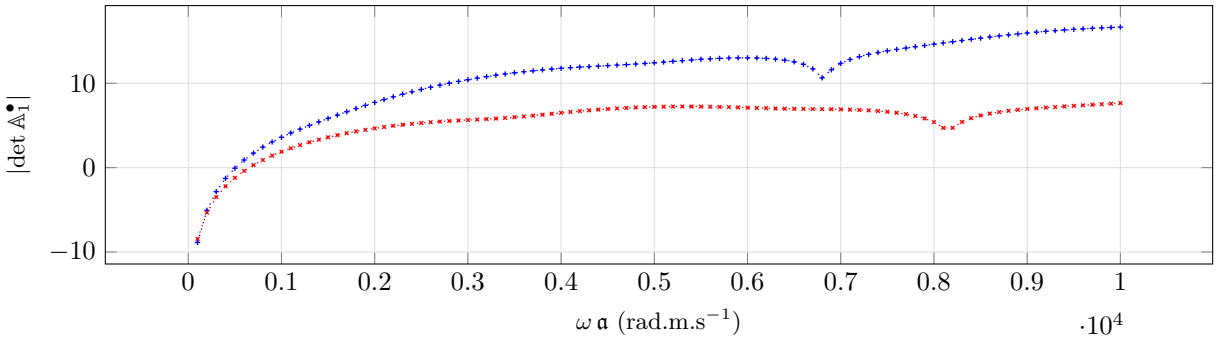

(b) Mode $k = 1$

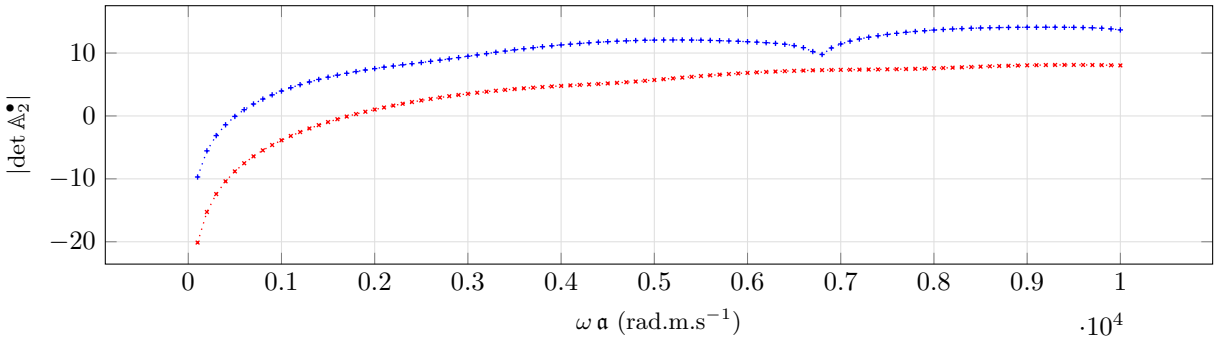

(c) Mode $k = 2$

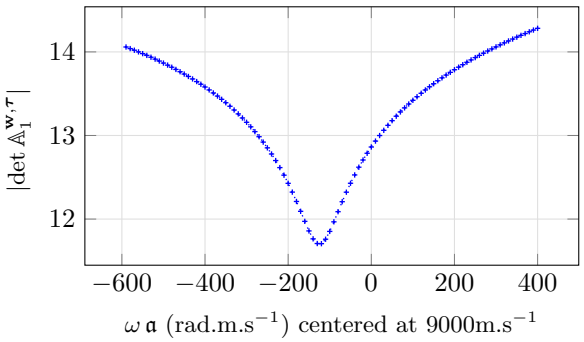

(d) Mode $k = 0$

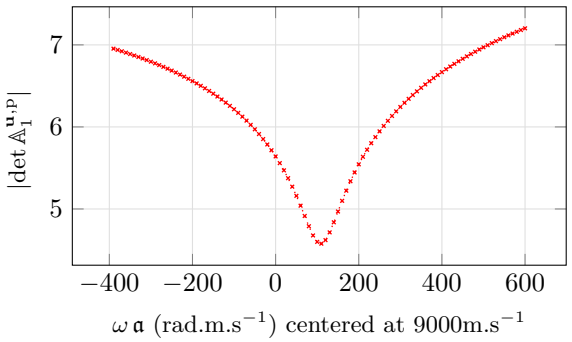

(e) Mode $k = 0$

Figure 2.3: Determinant of the coefficient matrix (log scale) in a bounded domain for k in $0:2$ for a sandstone medium with viscosity $\eta \neq 0$. The matrices corresponding with types of boundary conditions 1 and 3 are considered: $\mathbb{A}_k^{\mathbf{w},\boldsymbol{\tau}}$ (2.25) in blue ···+··· and $\mathbb{A}_k^{\mathbf{u},\mathrm{p}}$ (2.29) in red ···×···.

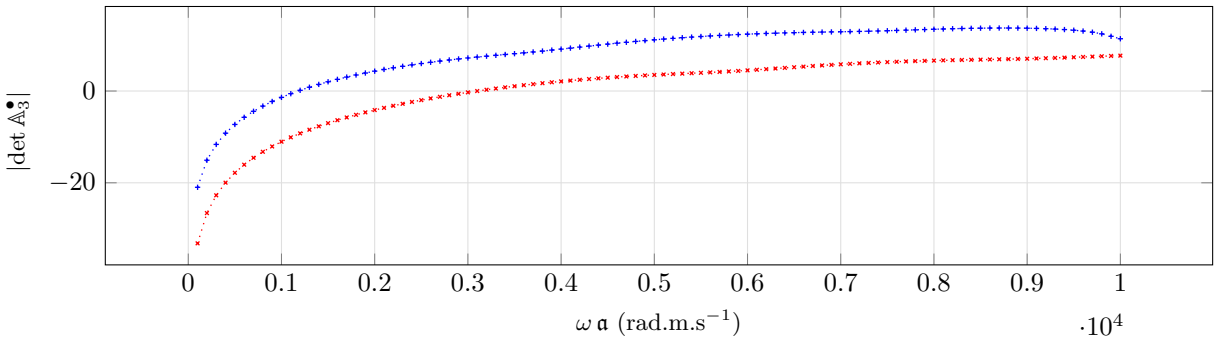

(a) Mode $k = 3$

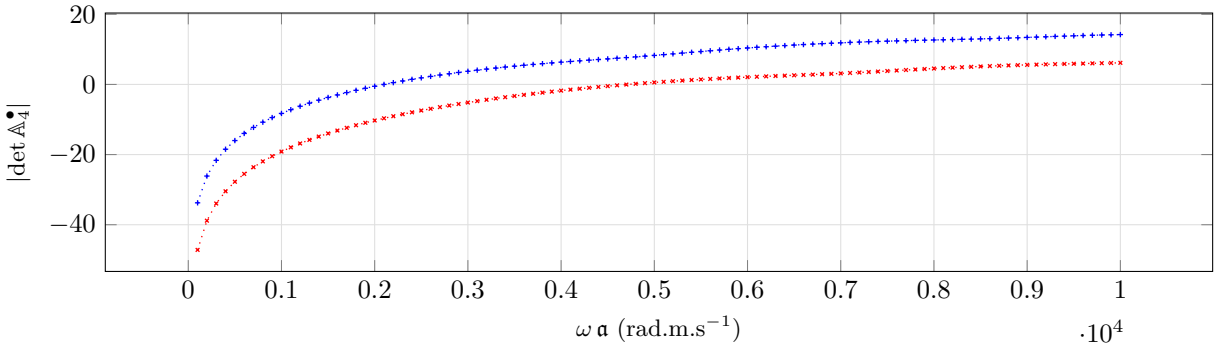

(b) Mode $k = 4$

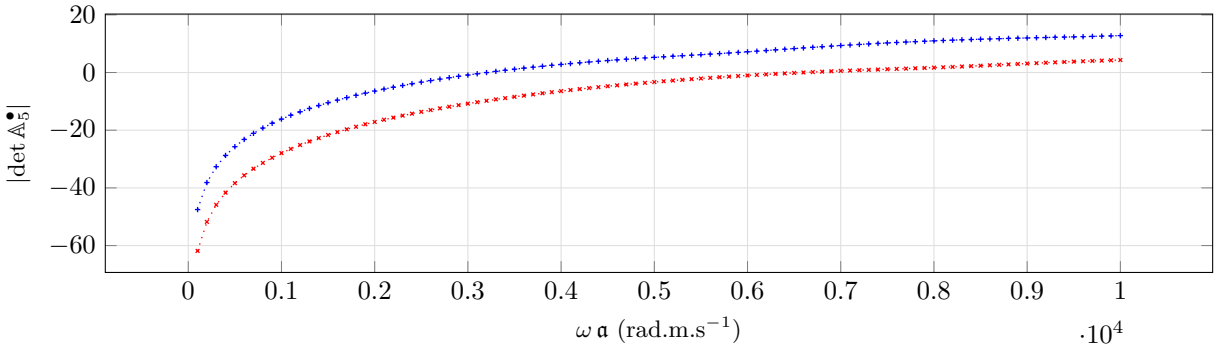

(c) Mode $k = 5$

Figure 2.4: Determinant of the coefficient matrix (log scale) in a bounded domain for k in $3:5$ for a sandstone medium with viscosity $\eta \neq 0$. The matrices corresponding with types of boundary conditions 1 and 3 are considered: $\mathbb{A}_k^{\mathbf{w},\boldsymbol{\tau}}$ (2.25) in blue ····+···· and $\mathbb{A}_k^{\mathbf{u},\mathrm{p}}$ (2.29) in red ····×····.

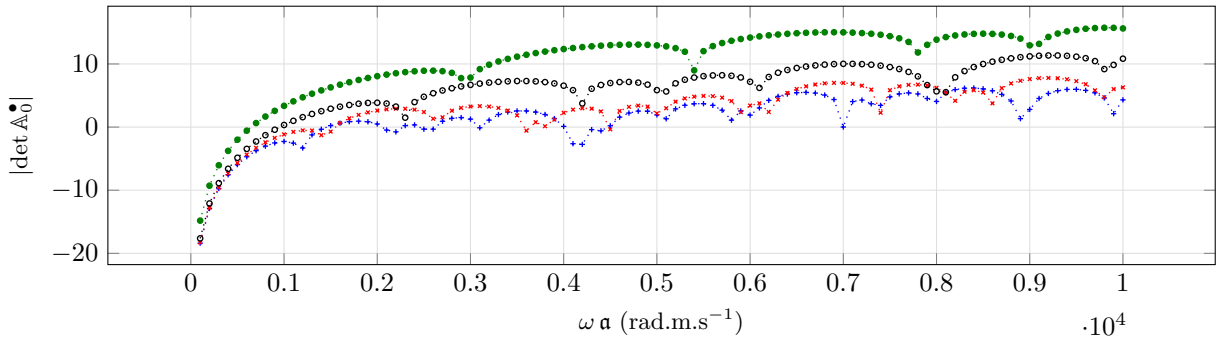

Figure 2.5: Comparison of the determinant of the coefficient matrix (log scale) in a bounded domain for $k = 0$ for different values of μ_{fr} for a medium composed of sand1 with no viscosity. The matrix corresponding with types of boundary conditions 1 is considered: $\mathbb{A}_k^{\mathbf{w},\boldsymbol{\tau}}$. ····+···· represents the case $\mu_{\text{fr}} = 0.5$ GPa, ····×···· represents the case $\mu_{\text{fr}} = 1$ GPa, ····∘···· $\mu_{\text{fr}} = 5$ GPa and ····•···· $\mu_{\text{fr}} = 50$ GPa, .

2.3 Scattering of a plane wave by an impenetrable medium

Consider the scattering of a time-harmonic plane wave by an impenetrable infinite cylinder (see Figure 2.6). The total wave is a superposition of the incident plane wave and the reflected wave with each quantity satisfying poroelastic equations (1.16) in $\mathbb{R}^2 \setminus \mathbb{B}_{(0,\mathfrak{a})}$, also listed below in (2.31) and (2.34), according to the type of boundary conditions. The solutions $(\mathbf{u}, \mathbf{w}, \boldsymbol{\tau}, \mathrm{p})$ are given by equations (2.10), (2.11) and (2.12), while the potentials χ_{P}, χ_{B}, χ_{S} are given by (2.13). The unknown is the reflected wave that is outgoing, this means that it satisfies the Sommerfeld radiation condition (2.22), and is in addition uniquely determined by how the obstacle scatters the plane wave. Hence, the potentials corresponding to the reflected wave are given in equation (2.15):

$$\begin{aligned} \chi_{\mathrm{P}}(r,\theta) &= \sum_{k\in\mathbb{Z}} a_k \, \mathrm{H}_k^{(1)}(\omega \, \mathsf{s}_{\mathrm{P}} \, r) \; e^{\mathrm{i}\, k\, \theta} \,, \\ \chi_{\mathrm{B}}(r,\theta) &= \sum_{k\in\mathbb{Z}} b_k \, \mathrm{H}_k^{(1)}(\omega \, \mathsf{s}_{\mathrm{B}} \, r) \; e^{\mathrm{i}\, k\, \theta} \,, \\ \chi_{\mathrm{S}}(r,\theta) &= \sum_{k\in\mathbb{Z}} c_k \, \mathrm{H}_k^{(1)}(\omega \, \mathsf{s}_{\mathrm{S}} \, r) \; e^{\mathrm{i}\, k\, \theta} \,. \end{aligned} \tag{2.30}$$

The series coefficients a_k, b_k, c_k are then determined by the boundary conditions imposed on the interface Γ. We will consider the boundary conditions of type 1 in Section 2.3.1 and of type 3 in Section 2.3.2.

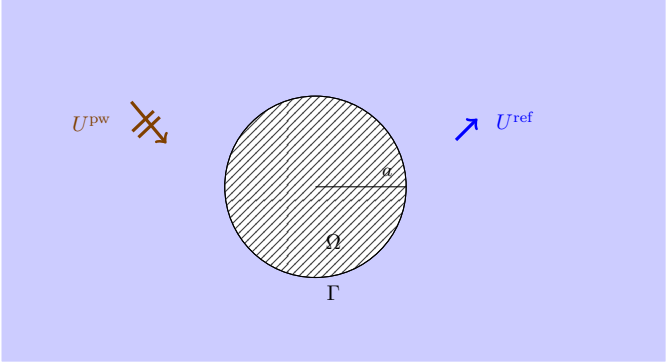

Figure 2.6: Scattering of a plane wave by an impenetrable solid inclusion. The inclusion occupies the domain denoted by Ω. The cross section of the inclusion is a disc of radius denoted by $\mathfrak{a}$. How the obstacle scatters the plane wave is mathematically described by boundary conditions, for example (1.20a) or (1.20c).

2.3.1 Boundary conditions of type 1

For $\bullet$ = total, ref, pw, we denote by

$$U^{\bullet} = \begin{pmatrix} \mathbf{u}^{\bullet} \\ \mathbf{w}^{\bullet} \\ \boldsymbol{\tau}^{\bullet} \\ \mathrm{p}^{\bullet} \end{pmatrix}$$

the total wave, the reflected wave and the incident plane wave correspondingly. The unknown reflected wave solves the poroelastic problem:

$$\begin{cases} U^{\mathrm{ref}} \text{ solves the poroelastic equations (1.16) in } \mathbb{R}^2 \setminus \Omega \,; \\ \\ U^{\mathrm{ref}} \text{ is outgoing by definition (2.22);} \\ \\ \text{Boundary conditions on the interface } \Gamma \\ \quad \mathbf{w}^{\mathrm{pw}} \cdot \mathbf{n} + \mathbf{w}^{\mathrm{ref}} \cdot \mathbf{n} = 0 \quad , \quad \text{on } \partial\mathbb{B}_{(0,\mathfrak{a})} \,; \\ \quad \boldsymbol{\tau}^{\mathrm{pw}} \cdot \mathbf{n} + \boldsymbol{\tau}^{\mathrm{ref}} \cdot \mathbf{n} = 0 \quad , \quad \text{on } \partial\mathbb{B}_{(0,\mathfrak{a})} \,. \end{cases} \tag{2.31}$$

In the current geometry, $\boldsymbol{n} = \mathbf{e}_r$. Hence,

$$\mathbf{w} \cdot \boldsymbol{n} = \mathrm{w}_r \,, \qquad \boldsymbol{\tau}\, \boldsymbol{n} = \tau_{rr}\, \mathbf{e}_r + \tau_{r\theta}\, \mathbf{e}_\theta \,,$$
$$\mathbf{w}^{\mathrm{pw}} \cdot \boldsymbol{n} = \mathbf{w}_r^{\mathrm{pw}} \,, \qquad \boldsymbol{\tau}^{\mathrm{pw}} \cdot \boldsymbol{n} = \boldsymbol{\tau}_{rr}^{\mathrm{pw}}\, \mathbf{e}_r + \boldsymbol{\tau}_{r\theta}^{\mathrm{pw}}\, \mathbf{e}_\theta \,.$$

As we impose $\mathbf{w} \cdot \boldsymbol{n}$ and $\boldsymbol{\tau}\, \boldsymbol{n}$, we do not detail the expressions of w_θ and $\tau_{\theta\theta}$. The boundary conditions are written as:

$$\mathfrak{s}\, \mathrm{i}\, \omega\, \mathrm{w}_r \;=\; -\,\mathfrak{s}\, \mathrm{i}\, \omega\, \mathbf{w}_r^{\mathrm{pw}} \,, \quad \omega^2\, \tau_{rr} \;=\; -\,\omega^2\, \tau_{rr}^{\mathrm{pw}} \,, \quad \omega^2\, \tau_{r\theta} \;=\; -\,\omega^2\, \tau_{r\theta}^{\mathrm{pw}} \quad , \quad \text{on } \partial\mathbb{B}_{(0,\mathfrak{a})} \,. \tag{2.32}$$

Next we expand the coefficients of each component in Fourier series. For the right hand-side,

$$\mathbf{w}_r^{\mathrm{pw}} = \sum_{k\in\mathbb{Z}} \mathbf{w}_{r,k}^{\mathrm{pw}}\, e^{\mathrm{i}\, k\, \theta} \,, \quad \tau_{rr}^{\mathrm{pw}} = \sum_{k\in\mathbb{Z}} \tau_{rr,k}^{\mathrm{pw}}\, e^{\mathrm{i}\, k\, \theta} \,, \quad , \tau_{r\theta}^{\mathrm{pw}} = \sum_{k\in\mathbb{Z}} \tau_{r\theta,k}^{\mathrm{pw}}\, e^{\mathrm{i}\, k\, \theta} \,.$$

For the unknowns:

$$\mathrm{w}_r = \sum_{k\in\mathbb{Z}} \mathrm{w}_{r,k}\, e^{\mathrm{i}\, k\, \theta} \,, \quad \tau_{rr} = \sum_{k\in\mathbb{Z}} \tau_{rr,k}\, e^{\mathrm{i}\, k\, \theta} \,, \quad \tau_{r\theta} = \sum_{k\in\mathbb{Z}} \tau_{r\theta,k}\, e^{\mathrm{i}\, k\, \theta} \,.$$

Using (2.18), (2.19) and (2.20), we have:

$$\begin{aligned}
\mathfrak{s}\, \mathrm{i}\, \omega\, \mathrm{w}_{r,k} =& a_k\, \frac{\mathcal{W}_{\mathrm{P}}}{\mathsf{s}_{\mathrm{P}}}\, \omega\, \mathrm{H}_k^{(1)'}(\omega\, \mathsf{s}_{\mathrm{P}}\, r)\, e^{\mathrm{i}k\theta} \;+\; b_k\, \frac{\mathcal{W}_{\mathrm{B}}}{\mathsf{s}_{\mathrm{B}}}\, \omega\, \mathrm{H}_k^{(1)'}(\omega\, \mathsf{s}_{\mathrm{B}}\, r)\, e^{\mathrm{i}k\theta} \;+\; c_k\, \frac{\rho_f\, \mu_{\mathrm{fr}}}{\det A}\, \frac{\mathrm{i}k}{r} \mathrm{H}_k^{(1)}(\omega\, \mathsf{s}_{\mathrm{S}}\, r)\, e^{\mathrm{i}k\theta} \,, \\
\omega^2 \tau_{rr,k} =& -\,\frac{2\mu_{\mathrm{fr}}\, \omega}{\mathsf{s}_{\mathrm{P}}\, r}\, a_k\, \mathrm{H}_{k+1}^{(1)}(\omega\, \mathsf{s}_{\mathrm{P}}\, r)\, e^{\mathrm{i}\, k\, \theta} \;+\; \frac{2\, \mu_{\mathrm{fr}}\, k}{\mathsf{s}_{\mathrm{P}}^2\, r^2}\, a_k\, \mathrm{H}_k^{(1)}(\omega\, \mathsf{s}_{\mathrm{P}}\, r)\, e^{\mathrm{i}\, k\, \theta} \;+ 2\mu_{\mathrm{fr}}\, a_k\, \omega^2\, \mathrm{H}_k^{(1)}(\omega\, \mathsf{s}_{\mathrm{P}}\, r)\, e^{\mathrm{i}\, k\, \theta} \\
& -\frac{2\, \mu_{\mathrm{fr}}\, k^2}{\mathsf{s}_{\mathrm{P}}^2\, r^2}\, a_k\, \mathrm{H}_k^{(1)}(\omega\, \mathsf{s}_{\mathrm{P}}\, r)\, e^{\mathrm{i}\, k\, \theta} - \frac{2\, \mu_{\mathrm{fr}}\, \omega}{\mathsf{s}_{\mathrm{B}}\, r}\, b_k\, \mathrm{H}_{k+1}^{(1)}(\omega\, \mathsf{s}_{\mathrm{B}}\, r)\, e^{\mathrm{i}\, k\, \theta} \;+\; \frac{2\mu_{\mathrm{fr}}\, k}{\mathsf{s}_{\mathrm{B}}^2\, r^2} b_k\, \mathrm{H}_k^{(1)}(\omega\, \mathsf{s}_{\mathrm{B}}\, r)\, e^{\mathrm{i}\, k\, \theta} \\
& +2\mu_{\mathrm{fr}}\, b_k\, \omega^2\, \mathrm{H}_k^{(1)}(\omega\, \mathsf{s}_{\mathrm{B}}\, r)\, e^{\mathrm{i}\, k\, \theta} \;-\; \frac{2\, \mu_{\mathrm{fr}}\, k^2}{\mathsf{s}_{\mathrm{B}}^2\, r^2} b_k\, \mathrm{H}_k^{(1)}(\omega\, \mathsf{s}_{\mathrm{B}}\, r)\, e^{\mathrm{i}\, k\, \theta} \;+\; \frac{2\, \mu_{\mathrm{fr}}}{\mathsf{s}_{\mathrm{S}}^2 r} c_k\, \omega\, \mathsf{s}_{\mathrm{S}}\, \mathrm{i}k\, \mathrm{H}_k^{(1)'}(\omega\, \mathsf{s}_{\mathrm{S}}\, r)\, e^{\mathrm{i}\, k\, \theta} \\
& +\omega^2\, \left(-\tfrac{2}{3}\mu_{\mathrm{fr}} \;+\; \mathrm{k}_{\mathrm{fr}} \;+\; M\alpha^2 \;+\; \alpha\, M\mathcal{W}_{\mathrm{P}}\right)\; a_k\, \mathrm{H}_k^{(1)}(\omega\, \mathsf{s}_{\mathrm{P}}\, r)\; e^{\mathrm{i}\, k\, \theta} \\
& +\omega^2\, \left(-\tfrac{2}{3}\mu_{\mathrm{fr}} \;+\; \mathrm{k}_{\mathrm{fr}} \;+\; M\alpha^2 \;+\; \alpha\, M\mathcal{W}_{\mathrm{B}}\right)\, b_k\, \mathrm{H}_k^{(1)}(\omega\, \mathsf{s}_{\mathrm{B}}\, r)\; e^{\mathrm{i}\, k\, \theta} \,, \\
\omega^2\, \tau_{r\theta,k} =& -\,\frac{2\mu_{\mathrm{fr}}\omega\, \mathrm{i}k}{r\mathsf{s}_{\mathrm{P}}} a_k \mathrm{H}_k^{(1)'}(\omega\, \mathsf{s}_{\mathrm{P}}\, r)\, e^{\mathrm{i}\, k\, \theta} + \frac{2\mathrm{i}\, \mu_{\mathrm{fr}} k}{r^2\, \mathsf{s}_{\mathrm{P}}^2} a_k \mathrm{H}_k^{(1)}(\omega\, \mathsf{s}_{\mathrm{P}}\, r)\, e^{\mathrm{i}\, k\, \theta} \;-\; \frac{2\mu_{\mathrm{fr}}\omega\, \mathrm{i}\, k}{r\, \mathsf{s}_{\mathrm{B}}} b_k \mathrm{H}_k^{(1)'}(\omega\, \mathsf{s}_{\mathrm{B}}\, r)\, e^{\mathrm{i}\, k\, \theta} \\
& +\frac{2\, \mathrm{i}\, \mu_{\mathrm{fr}}\, k}{r^2 \mathsf{s}_{\mathrm{B}}^2}\, b_k\, \mathrm{H}_k^{(1)}(\omega\, \mathsf{s}_{\mathrm{B}}\, r)\; e^{\mathrm{i}\, k\, \theta} \;-\; \frac{\mu_{\mathrm{fr}}\, k^2}{r^2\, \mathsf{s}_{\mathrm{S}}^2}\, c_k\, \mathrm{H}_k^{(1)}(\omega\, \mathsf{s}_{\mathrm{S}}\, r)\; e^{\mathrm{i}\, k\, \theta} \;+\; \frac{\mu_{\mathrm{fr}}\, \omega}{r\, \mathsf{s}_{\mathrm{S}}}\, c_k\, \mathrm{H}_k^{(1)'}(\omega\, \mathsf{s}_{\mathrm{S}}\, r)\; e^{\mathrm{i}\, k\, \theta} \\
& -\,\mu_{\mathrm{fr}}\, \frac{\omega}{\mathsf{s}_{\mathrm{S}}\, r}\, c_k\, \mathrm{H}_{k+1}^{(1)}(\omega\, \mathsf{s}_{\mathrm{S}}\, r)\; e^{\mathrm{i}\, k\, \theta} \;+\mu_{\mathrm{fr}}\, \frac{k}{\mathsf{s}_{\mathrm{S}}^2\, r^2} c_k\, \mathrm{H}_k^{(1)}(\omega\, \mathsf{s}_{\mathrm{S}}\, r)\; e^{\mathrm{i}\, k\, \theta} \\
& +\omega^2\, c_k\, \mathrm{H}_k^{(1)}(\omega\, \mathsf{s}_{\mathrm{S}}\, r)\; e^{\mathrm{i}\, k\, \theta} \;-\; \mu_{\mathrm{fr}}\, \frac{k^2}{\mathsf{s}_{\mathrm{S}}^2\, r^2}\, c_k\, \mathrm{H}_k^{(1)}(\omega\, \mathsf{s}_{\mathrm{S}}\, r)\; e^{\mathrm{i}\, k\, \theta} .
\end{aligned}$$

Imposing (2.32), we obtain a linear system satisfied by a_k, b_k, c_k in each mode k.

$$\mathbb{A}_k^{\mathbf{w},\boldsymbol{\tau}} \begin{pmatrix} a_k \\ b_k \\ c_k \end{pmatrix} = \begin{pmatrix} -\mathfrak{s}\, \mathrm{i}\, \omega\, \mathrm{w}_r^{\mathrm{pw}} \\ -\omega^2\, \tau_{rr}^{\mathrm{pw}} \\ -\omega^2\, \tau_{r\theta}^{\mathrm{pw}} \end{pmatrix} ,$$

where the coefficient matrix is defined as:

$$\mathbb{A}_k^{\mathbf{w},\boldsymbol{\tau}} = \begin{pmatrix} A_{11} & A_{12} & A_{13} \\ A_{21} & A_{22} & A_{23} \\ A_{31} & A_{32} & A_{33} \end{pmatrix} \tag{2.33}$$

with

$$A_{11} = \frac{\mathcal{W}_{\rm P}}{\mathsf{s}_{\rm P}}\,\omega\,{\rm H}_k^{(1)'}(\omega\,\mathsf{s}_{\rm P}\mathfrak{a})\,, \qquad A_{12} = \frac{\mathcal{W}_{\rm B}}{\mathsf{s}_{\rm B}}\,\omega\,{\rm H}_k^{(1)'}(\omega\,\mathsf{s}_{\rm S}\mathfrak{a}) \qquad A_{13} = \frac{\rho_f\,\mu_{\rm fr}}{\det A}\,\frac{{\rm i}k}{\mathfrak{a}}{\rm H}_k^{(1)}(\omega\,\mathsf{s}_{\rm S}\mathfrak{a})\,,$$

$$A_{21} = -\frac{2\,\mu_{\rm fr}\,\omega}{\mathsf{s}_{\rm P}\,\mathfrak{a}}\,{\rm H}_{k+1}^{(1)}(\omega\,\mathsf{s}_{\rm P}\,\mathfrak{a})\;e^{{\rm i}\,k\,\theta} + \frac{2\,\mu_{\rm fr}\,k}{\mathsf{s}_{\rm P}^2\,\mathfrak{a}^2}\,{\rm H}_k^{(1)}(\omega\,\mathsf{s}_{\rm P}\,\mathfrak{a}) + 2\,\mu_{\rm fr}\,\omega^2\,{\rm H}_k^{(1)}(\omega\,\mathsf{s}_{\rm P}\,\mathfrak{a})$$
$$-\frac{2\,\mu_{\rm fr}\,k^2}{\mathsf{s}_{\rm P}^2\,\mathfrak{a}^2}\,{\rm H}_k^{(1)}(\omega\,\mathsf{s}_{\rm P}\,\mathfrak{a}) + \omega^2\left(-\tfrac{2}{3}\mu_{\rm fr} + {\rm k}_{\rm fr} + M\alpha^2 + \alpha\,M\mathcal{W}_{\rm P}\right){\rm H}_k^{(1)}(\omega\,\mathsf{s}_{\rm P}\mathfrak{a})\,,$$

$$A_{22} = -\frac{2\,\mu_{\rm fr}\,\omega}{\mathsf{s}_{\rm B}\,\mathfrak{a}}\,{\rm H}_{k+1}^{(1)}(\omega\,\mathsf{s}_{\rm B}\,\mathfrak{a}) + \frac{2\,\mu_{\rm fr}\,k}{\mathsf{s}_{\rm B}^2\,\mathfrak{a}^2}\,{\rm H}_k^{(1)}(\omega\,\mathsf{s}_{\rm B}\,\mathfrak{a}) + 2\,\mu_{\rm fr}\,\omega^2\,{\rm H}_k^{(1)}(\omega\,\mathsf{s}_{\rm B}\,\mathfrak{a})$$
$$-\frac{2\,\mu_{\rm fr}\,k^2}{\mathsf{s}_{\rm B}^2\,\mathfrak{a}^2}\,{\rm H}_k^{(1)}(\omega\,\mathsf{s}_{\rm B}\,\mathfrak{a}) + \omega^2\left(-\tfrac{2}{3}\mu_{\rm fr} + {\rm k}_{\rm fr} + M\alpha^2 + \alpha\,M\mathcal{W}_{\rm B}\right){\rm H}_k^{(1)}(\omega\,\mathsf{s}_{\rm B}\mathfrak{a})\,,$$

and

$$A_{23} = \frac{2\mu_{\rm fr}}{\mathsf{s}_{\rm S}\mathfrak{a}}\,\omega\,{\rm i}k\,{\rm H}_k^{(1)'}(\omega\,\mathsf{s}_{\rm S}\mathfrak{a})\,,$$

$$A_{31} = -\frac{2\omega\,\mu_{\rm fr}{\rm i}k}{\mathfrak{a}\mathsf{s}_{\rm P}}{\rm H}_k^{(1)'}(\omega\,\mathsf{s}_{\rm P}\mathfrak{a}) + \frac{2\,\mu_{\rm fr}{\rm i}k}{\mathfrak{a}^2\mathsf{s}_{\rm P}^2}{\rm H}_k^{(1)}(\omega\,\mathsf{s}_{\rm P}\mathfrak{a})\,,$$

$$A_{32} = -\frac{2\omega\,\mu_{\rm fr}{\rm i}k}{\mathfrak{a}\mathsf{s}_{\rm B}}{\rm H}_k^{(1)'}(\omega\,\mathsf{s}_{\rm B}\mathfrak{a}) + \frac{2\mu_{\rm fr}{\rm i}k}{\mathfrak{a}^2\mathsf{s}_{\rm B}^2}{\rm H}_k^{(1)}(\omega\,\mathsf{s}_{\rm B}\mathfrak{a})\,,$$

$$A_{33} = -\frac{k^2\mu_{\rm fr}}{\mathfrak{a}^2\mathsf{s}_{\rm S}^2}{\rm H}_k^{(1)}(\omega\,\mathsf{s}_{\rm S}\,\mathfrak{a}) + \frac{\omega\,\mu_{\rm fr}}{\mathfrak{a}\mathsf{s}_{\rm S}}{\rm H}_k^{(1)'}(\omega\,\mathsf{s}_{\rm S}\,\mathfrak{a}) - \frac{\omega}{\mathsf{s}_{\rm S}\,\mathfrak{a}}\,{\rm H}_{k+1}^{(1)}(\mathsf{s}_{\rm S}\,\mathfrak{a}) + \frac{k}{\mathsf{s}_{\rm S}^2\,\mathfrak{a}^2}\,{\rm H}_k^{(1)}(\omega\,\mathsf{s}_{\rm S}\,\mathfrak{a})\,,$$
$$+\,\omega^2\,{\rm H}_k^{(1)}(\omega\,\mathsf{s}_{\rm S}\,\mathfrak{a})\;e^{{\rm i}\,k\,\theta} - \frac{k^2}{\mathsf{s}_{\rm S}^2\,\mathfrak{a}^2}\,{\rm H}_k^{(1)}(\omega\,\mathsf{s}_{\rm S}\,\mathfrak{a})\,.$$

2.3.2 Boundary conditions of type 3

In this case, the unknown reflected wave solves the following poroelastic problem:

$$\begin{cases} U^{\rm ref} \text{ solves the poroelastic equations (1.16) in } \mathbb{R}^2\setminus\Omega\,; \\ \\ U^{\rm ref} \text{ is outgoing by definition (2.22) ;} \\ \\ \text{Boundary conditions on the interface } \Gamma \\ \quad \mathbf{v}^{\rm pw} + \mathbf{v}^{\rm ref} = 0 \;\text{ on } \Gamma\,, \\ \quad {\rm p}^{\rm pw} + {\rm p}^{\rm ref} = 0 \;\text{ on } \Gamma\,. \end{cases} \tag{2.34}$$

We work in polar coordinates, $\mathbf{u}^{\rm pw} = {\rm u}_r^{\rm pw}\mathbf{e}_r + {\rm u}_\theta^{\rm pw}\,\mathbf{e}_\theta$ and $\mathbf{u} = {\rm u}_r\mathbf{e}_r + {\rm u}_\theta\,\mathbf{e}_\theta$. The boundary conditions are written as:

$$\mathfrak{s}\,{\rm i}\,\omega\,{\rm u}_r \;=\; -\,\mathfrak{s}\,{\rm i}\,\omega\,{\rm u}_r^{\rm pw}\,, \quad \mathfrak{s}\,{\rm i}\,\omega\,{\rm u}_\theta \;=\; -\,\mathfrak{s}\,{\rm i}\,\omega\,{\rm u}_\theta^{\rm pw}\,, \quad {\rm p} \;=\; -\,{\rm p}^{\rm pw} \quad , \quad \partial\mathbb{B}_{(0,\mathfrak{a})}\,. \tag{2.35}$$

We expand the coefficient of each component in Fourier series. For the right hand-side,

$${\rm u}_r^{\rm pw} = \sum_{k\in\mathbb{Z}} {\rm u}_{r,k}^{\rm pw}\,e^{{\rm i}\,k\,\theta}\,, \quad {\rm u}_\theta^{\rm pw} = \sum_{k\in\mathbb{Z}} {\rm u}_{\theta,k}^{\rm pw}\,e^{{\rm i}\,k\,\theta}\,, \quad {\rm p}^{\rm pw} = \sum_{k\in\mathbb{Z}} {\rm p}_k^{\rm pw}\,e^{{\rm i}\,k\,\theta}\,.$$

For the unknowns:

$${\rm u}_r = \sum_{k\in\mathbb{Z}} {\rm u}_{r,k}\,e^{{\rm i}\,k\,\theta}\,, \quad {\rm u}_\theta = \sum_{k\in\mathbb{Z}} {\rm u}_{\theta,k}\,e^{{\rm i}\,k\,\theta}\,, \quad {\rm p}_k = \sum_{k\in\mathbb{Z}} {\rm p}_k\,e^{{\rm i}\,k\,\theta}\,.$$

Using (2.17) and (2.21), we have:

$$
\begin{aligned}
\mathfrak{s}\,\mathrm{i}\,\omega\,\mathrm{u}_{r,k} &= a_k\,\mathsf{s}_{\mathrm{P}}^{-1}\,\omega\,\mathrm{H}_k^{(1)'}(\omega\,\mathsf{s}_{\mathrm{P}}\,r)e^{\mathrm{i}k\theta} + b_k\,\mathsf{s}_{\mathrm{B}}^{-1}\,\omega\,\mathrm{H}_k^{(1)'}(\omega\,\mathsf{s}_{\mathrm{B}}\,r)e^{\mathrm{i}k\theta} - c_k\,\mathsf{s}_{\mathrm{S}}^{-2}\,\frac{\mathrm{i}k}{r}\mathrm{H}_k^{(1)}(\omega\,\mathsf{s}_{\mathrm{S}}\,r)e^{\mathrm{i}k\theta}\,,\\
\mathfrak{s}\,\mathrm{i}\,\omega\,\mathrm{u}_{\theta,k} &= a_k\,\mathsf{s}_{\mathrm{P}}^{-2}\,\frac{\mathrm{i}k}{r}\mathrm{H}_k^{(1)}(\omega\,\mathsf{s}_{\mathrm{P}}\,r)e^{\mathrm{i}k\theta} + b_k\,\mathsf{s}_{\mathrm{B}}^{-2}\,\frac{\mathrm{i}k}{r}\mathrm{H}_k^{(1)}(\omega\,\mathsf{s}_{\mathrm{B}}\,r)e^{\mathrm{i}k\theta} + c_k\,\mathsf{s}_{\mathrm{S}}^{-1}\,\omega\,\mathrm{H}_k^{(1)'}(\omega\,\mathsf{s}_{\mathrm{S}}\,r)e^{\mathrm{i}k\theta}\,,\\
\mathrm{p}_k &= -\,a_k\,M\,(\mathcal{W}_{\mathrm{P}} + \alpha)\,\mathrm{H}_k^{(1)}(\omega\,\mathsf{s}_{\mathrm{P}}\,r)\,e^{\mathrm{i}\,k\,\theta} - b_k\,M\,(\mathcal{W}_{\mathrm{B}} + \alpha)\,\mathrm{H}_k^{(1)}(\omega\,\mathsf{s}_{\mathrm{P}}\,r)\,e^{\mathrm{i}\,k\,\theta}\,.
\end{aligned}
$$

Imposing (2.35), we obtain the following linear system satisfied by a_k, b_k, c_k in each mode k:

$$
\mathbb{A}_k^{\mathbf{u},\mathrm{p}}\begin{pmatrix} a_k\\ b_k\\ c_k\end{pmatrix} = \begin{pmatrix} -\mathfrak{s}\,\mathrm{i}\,\omega\,\mathrm{u}_{r,k}^{\mathrm{pw}}\\ -\mathfrak{s}\,\mathrm{i}\,\omega\,\mathrm{u}_{\theta,k}^{\mathrm{pw}}\\ -\mathrm{p}_k^{\mathrm{pw}}\end{pmatrix}\,,
$$

where the coefficient matrix is defined as:

$$
\mathbb{A}_k^{\mathbf{u},\mathrm{p}} = \begin{pmatrix} \mathsf{s}_{\mathrm{P}}^{-1}\,\omega\,\mathrm{H}_k^{(1)'}(\omega\,\mathsf{s}_{\mathrm{P}}\,\mathfrak{a}) & \mathsf{s}_{\mathrm{B}}^{-1}\,\omega\,\mathrm{H}_k^{(1)'}(\omega\,\mathsf{s}_{\mathrm{B}}\,\mathfrak{a}) & -\,\mathsf{s}_{\mathrm{S}}^{-2}\,\frac{\mathrm{i}k}{\mathfrak{a}}\mathrm{H}_k^{(1)}(\omega\,\mathsf{s}_{\mathrm{S}}\,\mathfrak{a})\\ \mathsf{s}_{\mathrm{P}}^{-2}\,\frac{\mathrm{i}k}{\mathfrak{a}}\mathrm{H}_k^{(1)}(\omega\,\mathsf{s}_{\mathrm{P}}\,\mathfrak{a}) & \mathsf{s}_{\mathrm{B}}^{-2}\,\frac{\mathrm{i}k}{\mathfrak{a}}\mathrm{H}_k^{(1)}(\omega\,\mathsf{s}_{\mathrm{B}}\,\mathfrak{a}) & \mathsf{s}_{\mathrm{S}}^{-1}\,\omega\,\mathrm{H}_k^{(1)'}(\omega\,\mathsf{s}_{\mathrm{S}}\,\mathfrak{a})\\ -M\,(\mathcal{W}_{\mathrm{P}} + \alpha)\,\mathrm{H}_k^{(1)}(\omega\,\mathsf{s}_{\mathrm{P}}\,\mathfrak{a}) & -M\,(\mathcal{W}_{\mathrm{B}} + \alpha)\,\mathrm{H}_k^{(1)}(\omega\,\mathsf{s}_{\mathrm{P}}\,\mathfrak{a}) & 0\end{pmatrix}\,. \tag{2.36}
$$

2.3.3 Numerical tests

In the construction of the analytical solution, the domain is considered as infinite. However, for the representation of the solution, we plot the solutions on an annulus of interior radius equal to 1m and exterior radius equal to 10m. We show the imaginary part of the solid velocity u_x in Figure 2.7. The result is similar to classical figures of scattering problem by a circular obstacle, *cf.* [51]. Here, the scattering mainly creates P waves.

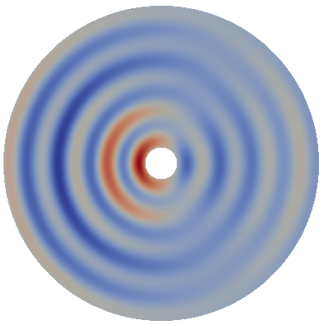

Figure 2.7: Scattering of a P plane wave on an impenetrable solid obstacle. Imaginary part of the solid velocity u_x of the reflected wave for boundary conditions of type 1 in a porous medium composed of inviscid sandstone with $f = 500$ Hz.

As for the previous section, we will investigate the invertibility of the coefficient matrices $\mathbb{A}_k^{\mathbf{w},\boldsymbol{\tau}}$ (2.33) and $\mathbb{A}_k^{\mathbf{u},\mathrm{p}}$ (2.36) for the first modes k. The tests are divided in two parts. First, we consider a medium composed of sandstone with no viscosity, next we run the tests on a medium of sandstone with viscosity *cf.* 1.1. For both tests, the cross section radius is $\mathfrak{a} = 1$m. The results are reported in the following figures:

- Sandstone with no viscosity Figures 2.8 and 2.9.
- Sandstone with viscosity Figures 2.10 and 2.11.

Thanks to the well-posedness of the problem, we expect no generalized eigenvalues in this case, which is clear from the curves of both boundary conditions (see Figures 2.8,2.9, 2.10, and 2.11). Note that the curves here are completely free of peaks, compared to the absence of generalized eigenvalues in the case presented in Figure 2.3, in which the curves present small peaks.

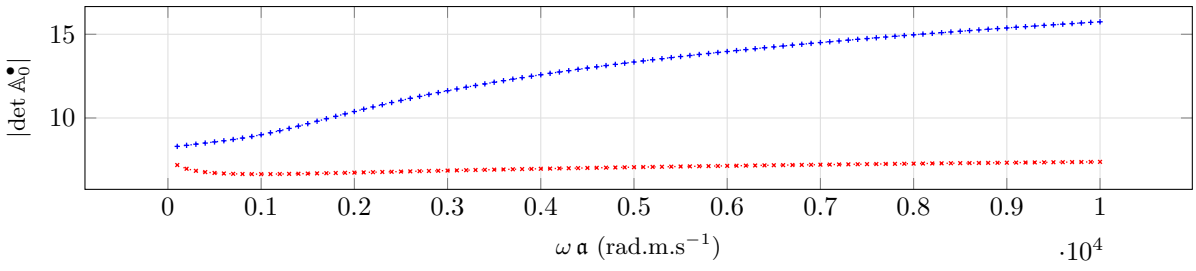

(a) Mode $k = 0$

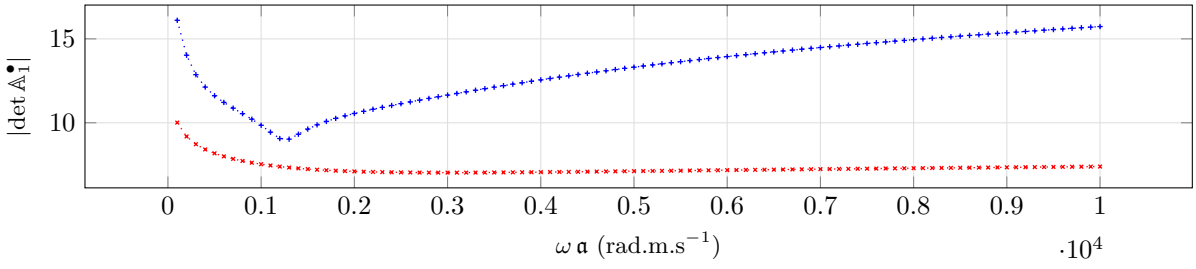

(b) Mode $k = 1$

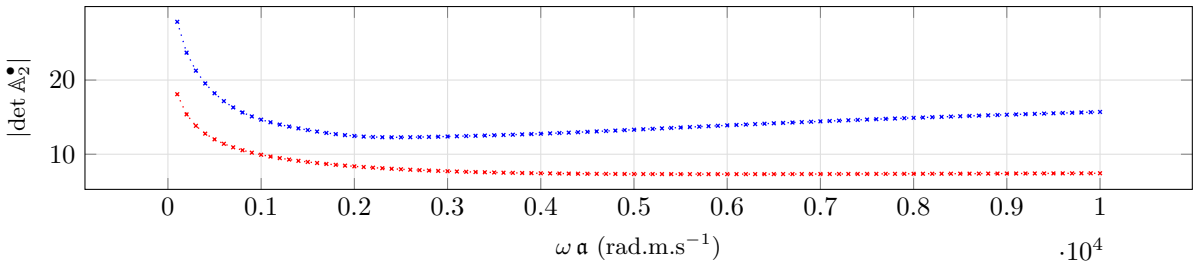

(c) Mode $k = 2$

Figure 2.8: Experiment of a porous infinite medium with an impenetrable solid obstacle. Determinant of the coefficient matrix (log scale) for k in $0:2$ sandstone with no viscosity. The matrices corresponding with types of boundary conditions 1 and 3 are considered: $\mathbb{A}_k^{\mathbf{w},\boldsymbol{\tau}}$ (2.33) in blue and $\mathbb{A}_k^{\mathbf{u},\mathrm{p}}$ (2.36) in red.

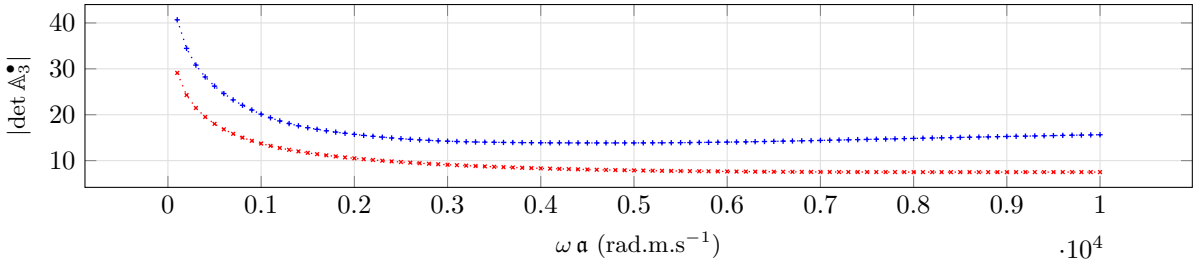

(a) Mode $k = 3$

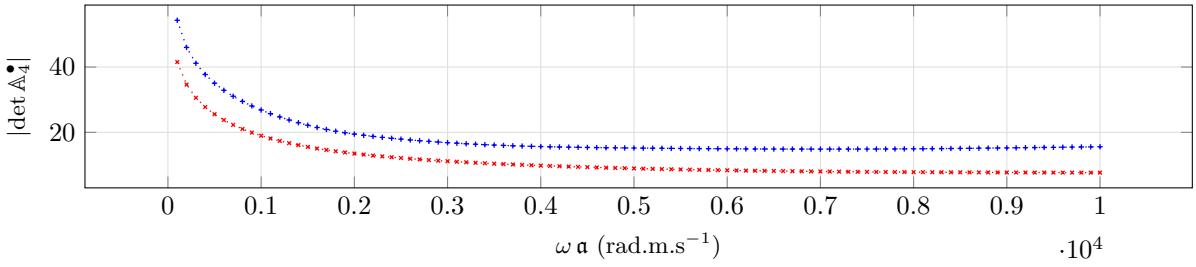

(b) Mode $k = 4$

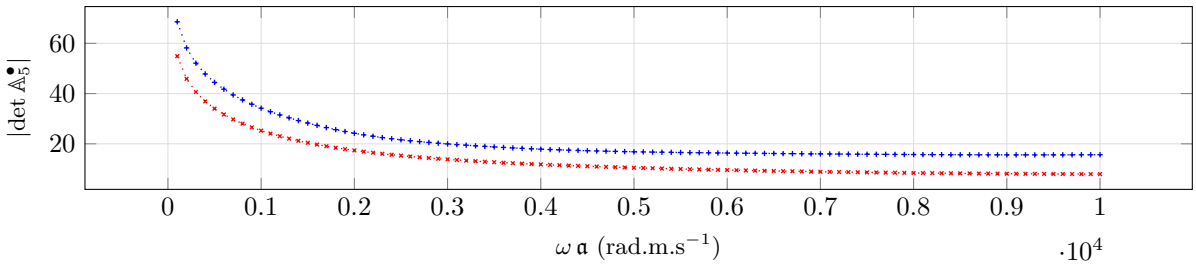

(c) Mode $k = 5$

Figure 2.9: Experiment of a porous infinite medium with an impenetrable solid obstacle. Determinant of the coefficient matrix (log scale) for k in $3:5$ for sandstone with no viscosity. The matrices corresponding with types of boundary conditions 1 and 3 are considered: $\mathbb{A}_k^{\mathbf{w},\boldsymbol{\tau}}$ (2.33) in blue and $\mathbb{A}_k^{\mathbf{u},\mathrm{p}}$ (2.36) in red.

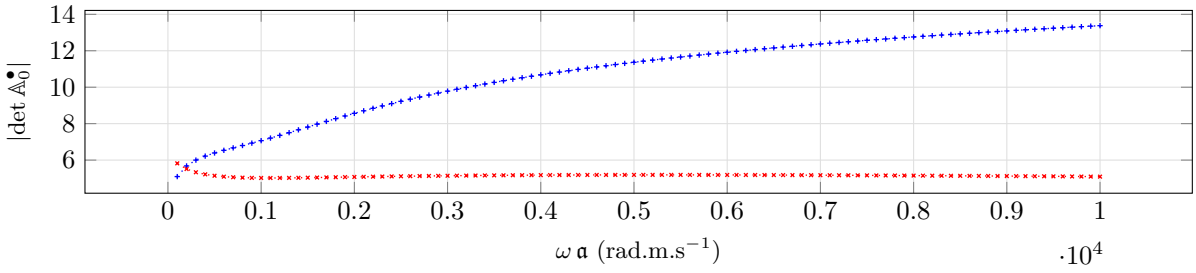

(a) Mode $k = 0$

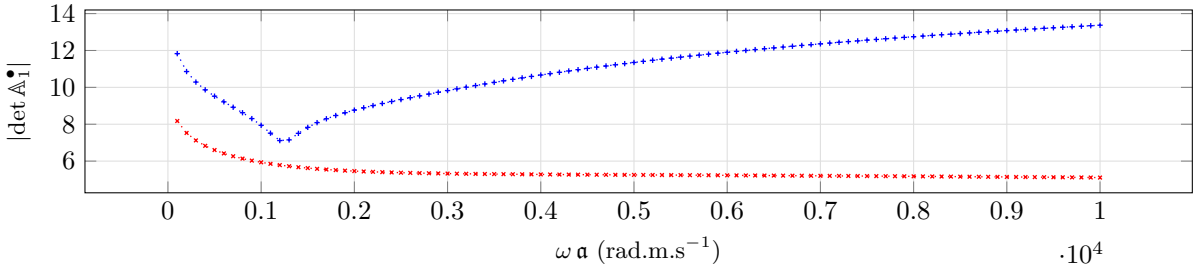

(b) Mode $k = 1$

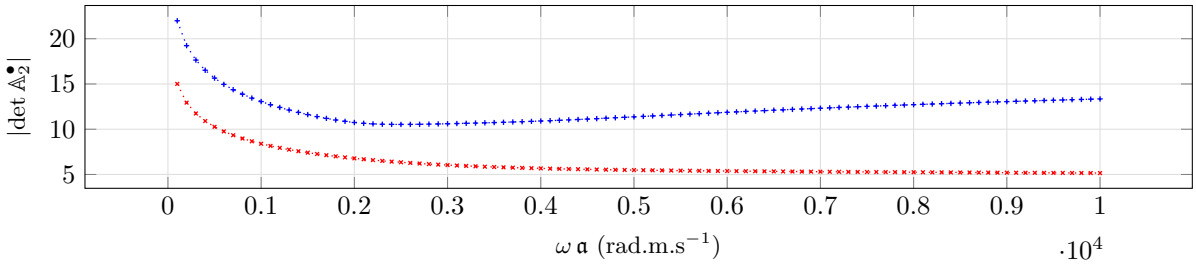

(c) Mode $k = 2$

Figure 2.10: Experiment of a porous infinite medium with an impenetrable solid obstacle. Determinant of the coefficient matrix (log scale) for k in $0:2$ for a sandstone medium with viscosity $\eta \neq 0$. The matrices corresponding with types of boundary conditions 1 and 3 are considered: $\mathbb{A}_k^{\mathbf{w},\boldsymbol{\tau}}$ (2.33) in blue ···•··· and $\mathbb{A}_k^{\mathbf{u},\mathrm{p}}$ (2.36) in red ···×···.

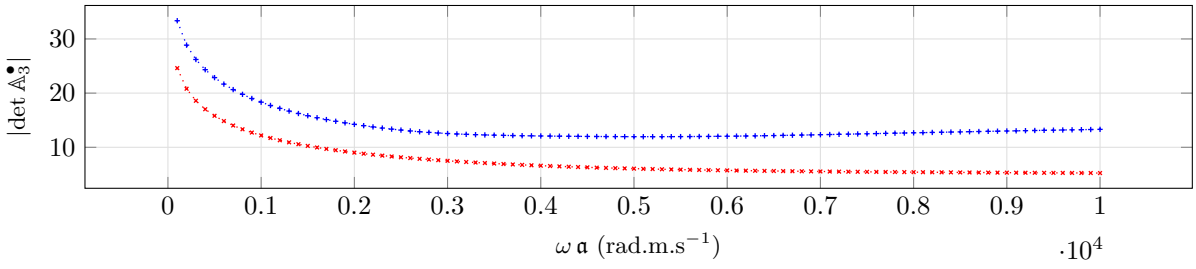

(a) Mode $k = 3$

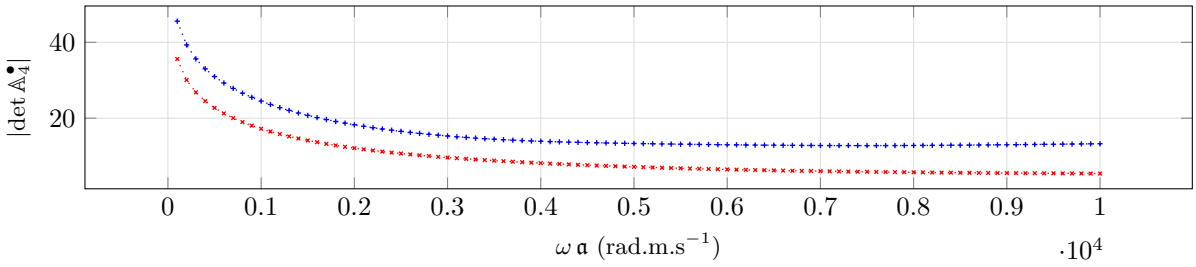

(b) Mode $k = 4$

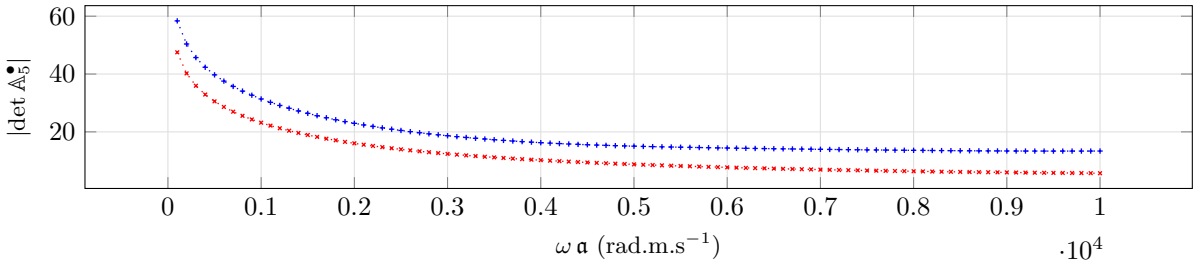

(c) Mode $k = 5$

Figure 2.11: Experiment of a porous infinite medium with an impenetrable solid obstacle. Determinant of the coefficient matrix (log scale) for k in $3:5$ for a sandstone medium with viscosity $\eta \neq 0$. The matrices corresponding with types of boundary conditions 1 and 3 are considered: $\mathbb{A}_k^{\mathbf{w},\boldsymbol{\tau}}$ (2.33) in blue ···•··· and $\mathbb{A}_k^{\mathbf{u},\mathrm{p}}$ (2.36) in red ···×···.

2.4 Scattering of a plane wave by a penetrable porous solid inclusion immersed in a porous medium

Consider the scattering of a time-harmonic plane wave by a penetrable poroelastic infinite cylinder immersed in another poroelastic infinite medium (see figure 2.12). The total wave outside of the cylinder is a superposition of the incident plane wave, and the reflected wave with each quantity satisfying poroelastic equations (1.16) in $\mathbb{R}^2 \setminus \mathbb{B}_{(0,\mathtt{a})}$, while the transmitted wave is described by the displacement inside the cylinder. The unknown is now the reflected wave which is outgoing, and the transmitted wave. They are uniquely determined by transmission conditions imposed on the interface Γ. For $\bullet = \mathrm{pw}, \mathrm{ref}, \mathrm{trans}$, we denote:

$$U^\bullet = \begin{pmatrix} \mathbf{u}^\bullet \\ \mathbf{w}^\bullet \\ \boldsymbol{\tau}^\bullet \\ \mathrm{p}^\bullet \end{pmatrix}.$$

The unknowns U^{ref} and U^{trans} solve the following problem:

$$\begin{cases} U^{\mathrm{ref}} \text{ solves the poroelastic equations (1.16) in } \mathbb{R}^2 \setminus \Omega; \\ \\ U^{\mathrm{trans}} \text{ solves the poroelastic equations (1.16) in } \Omega; \\ \\ U^{\mathrm{ref}} \text{ is outgoing;} \\ \\ \text{Transmission conditions on the interface } \Gamma : \\ \quad \mathbf{u}^{\mathrm{pw}} + \mathbf{u}^{\mathrm{ref}} = \mathbf{u}^{\mathrm{trans}}, \\ \quad \mathrm{p}^{\mathrm{pw}} + \mathrm{p}^{\mathrm{ref}} = \mathrm{p}^{\mathrm{trans}}, \\ \quad \mathbf{w}^{\mathrm{pw}} \cdot \boldsymbol{n} + \mathbf{w}^{\mathrm{ref}} \cdot \boldsymbol{n} = \mathbf{w}^{\mathrm{trans}} \cdot \boldsymbol{n}, \\ \quad \boldsymbol{\tau}^{\mathrm{pw}} \cdot \boldsymbol{n} + \boldsymbol{\tau}^{\mathrm{ref}} \cdot \boldsymbol{n} = \boldsymbol{\tau}^{\mathrm{trans}} \cdot \boldsymbol{n}. \end{cases}$$

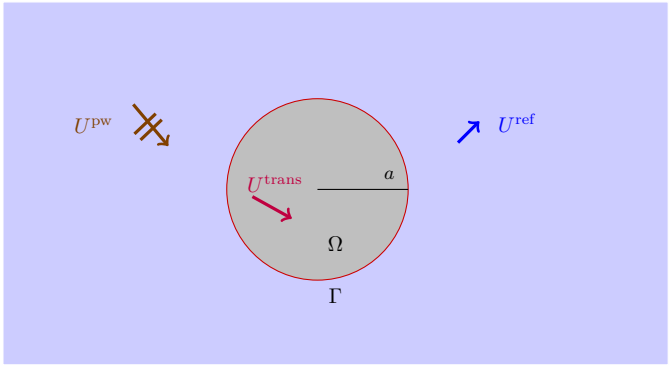

Figure 2.12: Scattering of a plane wave by a penetrable solid inclusion. The inclusion occupies the domain denoted by Ω. The cross section of the inclusion is a disc of radius denoted by a.

2.4.1 Construction of the analytical solution

The medium outside is denoted by medium 1, while the medium inside of the cylinder is denoted by medium 2. The slowness in the medium 1 is denoted by $\mathtt{s}_{\bullet,(I)}$ and in medium 2 by $\mathtt{s}_{\bullet,(II)}$.

The solutions $(\mathbf{u}, \mathbf{w}, \boldsymbol{\tau}, \mathrm{p})$ are given in the two media by equations (2.10), (2.11) and (2.12), while the potentials are given by (2.13). Hence, in medium 1, the potentials corresponding to the outgoing reflected wave satisfy equation

(2.15):

$$\begin{aligned}
\chi_{\mathrm{P,(I)}}(r,\theta) &= \sum_{k\in\mathbb{Z}} a_k\, \mathrm{H}_k^{(1)}(\omega\, \mathsf{s}_{\mathrm{P,(I)}} r)\; e^{\mathrm{i}\, k\, \theta}\,,\\
\chi_{\mathrm{B,(I)}}(r,\theta) &= \sum_{k\in\mathbb{Z}} b_k\, \mathrm{H}_k^{(1)}(\omega\, \mathsf{s}_{\mathrm{B,(I)}} r)\; e^{\mathrm{i}\, k\, \theta}\,,\\
\chi_{\mathrm{S,(I)}}(r,\theta) &= \sum_{k\in\mathbb{Z}} c_k\, \mathrm{H}_k^{(1)}(\omega\, \mathsf{s}_{\mathrm{S,(I)}} r)\; e^{\mathrm{i}\, k\, \theta}\,.
\end{aligned}$$

Similarly, the potentials corresponding to the transmitted wave (*i.e.* in medium 2) are given by (2.14):

$$\begin{aligned}
\chi_{\mathrm{P_{(II)}}}(r,\theta) &= \sum_{k\in\mathbb{Z}} d_k\, \mathrm{J}_k(\omega\, \mathsf{s}_{\mathrm{P,(II)}} r)\; e^{\mathrm{i}\, k\, \theta}\,,\\
\chi_{\mathrm{B_{(II)}}}(r,\theta) &= \sum_{k\in\mathbb{Z}} e_k\, \mathrm{J}_k(\omega\, \mathsf{s}_{\mathrm{B,(II)}} r)\; e^{\mathrm{i}\, k\, \theta}\,,\\
\chi_{\mathrm{S_{(II)}}}(r,\theta) &= \sum_{k\in\mathbb{Z}} f_k\, \mathrm{J}_k(\omega\, \mathsf{s}_{\mathrm{S,(II)}} r)\; e^{\mathrm{i}\, k\, \theta}\,.
\end{aligned}$$

Next, we are going to determine the coefficients a_k, b_k, c_k, d_k, e_k, f_k by imposing the boundary conditions at the interface between the two materials. Hence, they will satisfy the system given in equation (2.38). As previously, using the considered geometry, we express the unknowns in the polar basis:

$$\begin{aligned}
\mathbf{u}^\bullet &= \mathrm{u}_r^\bullet \mathbf{e}_r + \mathrm{u}_\theta^\bullet \mathbf{e}_\theta\,,\\
\mathbf{w}^\bullet \cdot \mathbf{n} &= \mathrm{w}_r^\bullet\,,\\
\boldsymbol{\tau}^\bullet \cdot \boldsymbol{n} &= \tau_{rr}^\bullet\, \mathbf{e}_r + \tau_{r\theta}^\bullet\, \mathbf{e}_\theta\,.
\end{aligned}$$

The boundary conditions are written as:

$$\begin{aligned}
\mathrm{u}_r^{\mathrm{ref}} - \mathrm{u}_r^{\mathrm{trans}} &= -\mathrm{u}_r^{\mathrm{pw}}\,,\\
\mathrm{u}_\theta^{\mathrm{ref}} - \mathrm{u}_\theta^{\mathrm{trans}} &= -\mathrm{u}_\theta^{\mathrm{pw}}\,,\\
\mathrm{p}^{\mathrm{ref}} - \mathrm{p}^{\mathrm{trans}} &= -\mathrm{p}^{\mathrm{pw}}\,,\\
\mathrm{w}_r^{\mathrm{ref}} - \mathrm{w}_r^{\mathrm{trans}} &= -\mathrm{w}_r^{\mathrm{pw}}\,,\\
\tau_{rr}^{\mathrm{ref}} - \tau_{rr}^{\mathrm{trans}} &= -\tau_{rr}^{\mathrm{pw}}\,,\\
\tau_{r\theta}^{\mathrm{ref}} - \tau_{r\theta}^{\mathrm{trans}} &= -\tau_{r\theta}^{\mathrm{pw}}\,.
\end{aligned} \tag{2.37}$$

Here, w_θ and $\tau_{\theta\theta}$ do not appear in the boundary conditions, hence, we do not detail their expressions. The expansion of the coefficient of each component in Fourier series is:

$$\mathrm{u}_r^\bullet = \sum_{k\in\mathbb{Z}} \mathrm{u}_{r,k}^\bullet\, e^{\mathrm{i}\, k\, \theta}\,,\quad \mathrm{u}_\theta^\bullet = \sum_{k\in\mathbb{Z}} \mathrm{u}_{\theta,k}^\bullet\, e^{\mathrm{i}\, k\, \theta}\,,\quad \mathrm{p}^\bullet = \sum_{k\in\mathbb{Z}} \mathrm{p}_k^\bullet\, e^{\mathrm{i}\, k\, \theta}\,,$$

$$\mathrm{w}_r^\bullet = \sum_{k\in\mathbb{Z}} \mathrm{w}_{r,k}^\bullet\, e^{\mathrm{i}\, k\, \theta}\,,\quad \tau_{rr}^\bullet = \sum_{k\in\mathbb{Z}} \tau_{rr,k}^\bullet\, e^{\mathrm{i}\, k\, \theta}\,,\quad \tau_{r\theta}^\bullet = \sum_{k\in\mathbb{Z}} \tau_{r\theta,k}^\bullet\, e^{\mathrm{i}\, k\, \theta}\,.$$

Using equations (2.17),(2.21), (2.18), (2.19) and (2.20), we have for the reflected wave:

$$\mathfrak{s}\,\mathrm{i}\,\omega \mathrm{u}_{r,k}^{\mathrm{ref}} = a_k \frac{\omega}{\mathsf{s}_{\mathrm{P,(I)}}} \mathrm{H}_k^{(1)'}(\omega\, \mathsf{s}_{\mathrm{P,(I)}}\, r) e^{\mathrm{i}k\theta} + b_k \frac{\omega}{\mathsf{s}_{\mathrm{B,(I)}}} \mathrm{H}_k^{(1)'}(\omega\, \mathsf{s}_{\mathrm{B,(I)}}\, r) e^{\mathrm{i}k\theta} - c_k \frac{\mathrm{i}k}{r\mathsf{s}_{\mathrm{S,(I)}}^2} \mathrm{H}_k^{(1)}(\omega\, \mathsf{s}_{\mathrm{S,(I)}}\, r) e^{\mathrm{i}k\theta}\,,$$

$$\mathfrak{s}\,\mathrm{i}\,\omega \mathrm{u}_{\theta,k}^{\mathrm{ref}} = a_k \frac{\mathrm{i}k}{r\,\mathsf{s}_{\mathrm{P,(I)}}^2} \mathrm{H}_k^{(1)}(\omega\, \mathsf{s}_{\mathrm{P,(I)}} r) e^{\mathrm{i}k\theta} + b_k \frac{\mathrm{i}k}{r\,\mathsf{s}_{\mathrm{B,(I)}}^2} \mathrm{H}_k^{(1)}(\omega\, \mathsf{s}_{\mathrm{B,(I)}} r) e^{\mathrm{i}k\theta} + c_k \frac{\omega}{\mathsf{s}_{\mathrm{S,(I)}}} \mathrm{H}_k^{(1)'}(\omega\, \mathsf{s}_{\mathrm{S,(I)}} r) e^{\mathrm{i}k\theta}\,,$$

$$\mathrm{p}_k^{\mathrm{ref}} = -\,a_k\, M_{\mathrm{(I)}} \left(\mathcal{W}_{\mathrm{P,(I)}} + \alpha_{\mathrm{(I)}}\right) \mathrm{H}_k^{(1)}(\omega\, \mathsf{s}_{\mathrm{P,(I)}}\, r)\, e^{\mathrm{i}k\theta} - b_k\, M \left(\mathcal{W}_{\mathrm{B,(I)}} + \alpha_{\mathrm{(I)}}\right) \mathrm{H}_k^{(1)}(\omega\, \mathsf{s}_{\mathrm{B,(I)}}\, r)\, e^{\mathrm{i}k\theta}\,,$$

$$\mathfrak{s}\,\mathrm{i}\,\omega \mathrm{w}_{r,k}^{\mathrm{ref}} = a_k \frac{\mathcal{W}_{\mathrm{P,(I)}}\,\omega}{\mathsf{s}_{\mathrm{P,(I)}}} \mathrm{H}_k^{(1)'}(\omega\, \mathsf{s}_{\mathrm{P,(I)}} r) e^{\mathrm{i}k\theta} + b_k \frac{\mathcal{W}_{\mathrm{B,(I)}}\,\omega}{\mathsf{s}_{\mathrm{B,(I)}}} \mathrm{H}_k^{(1)'}(\omega\, \mathsf{s}_{\mathrm{B,(I)}} r) e^{\mathrm{i}k\theta} + c_k \frac{\rho_{f,\mathrm{(I)}}\,\mu_{\mathrm{fr,(I)}}\,\mathrm{i}k}{\det A_{\mathrm{(I)}} r} \mathrm{H}_k^{(1)}(\omega\, \mathsf{s}_{\mathrm{S,(I)}} r) e^{\mathrm{i}k\theta},$$

and

$$\begin{aligned}
\omega^2\tau^{\mathrm{ref}}_{rr,k} = &-\frac{2\mu_{\mathrm{fr,(I)}}\,\omega}{\mathsf{s}_{\mathrm{P,(I)}}r}a_k\mathrm{H}^{(1)}_{k+1}(\omega\,\mathsf{s}_{\mathrm{P,(I)}}r)e^{\mathrm{i}\,k\,\theta}+\frac{2\mu_{\mathrm{fr,(I)}}\,k}{\mathsf{s}^2_{\mathrm{P,(I)}}\,r^2}a_k\mathrm{H}^{(1)}_{k}(\omega\,\mathsf{s}_{\mathrm{P,(I)}}r)e^{\mathrm{i}\,k\,\theta}+2\mu_{\mathrm{fr,(I)}}\omega^2 a_k\mathrm{H}^{(1)}_{k}(\omega\,\mathsf{s}_{\mathrm{P,(I)}}r)e^{\mathrm{i}\,k\,\theta}\\
&-\frac{2\mu_{\mathrm{fr,(I)}}\,k^2}{\mathsf{s}^2_{\mathrm{P,(I)}}\,r^2}a_k\mathrm{H}^{(1)}_{k}(\omega\,\mathsf{s}_{\mathrm{P,(I)}}\,r)\,e^{\mathrm{i}\,k\,\theta}-\frac{2\mu_{\mathrm{fr,(I)}}\,\omega}{\mathsf{s}_{\mathrm{B,(I)}}r}b_k\,\mathrm{H}^{(1)}_{k+1}(\omega\,\mathsf{s}_{\mathrm{B,(I)}}\,r)\,e^{\mathrm{i}\,k\,\theta}+\frac{2\mu_{\mathrm{fr,(I)}}\,k}{\mathsf{s}^2_{\mathrm{B,(I)}}\,r^2}b_k\,\mathrm{H}^{(1)}_{k}(\omega\,\mathsf{s}_{\mathrm{B,(I)}}\,r)\,e^{\mathrm{i}\,k\,\theta}\\
&+2\mu_{\mathrm{fr,(I)}}\,\omega^2\,b_k\mathrm{H}^{(1)}_{k}(\omega\,\mathsf{s}_{\mathrm{B,(I)}}\,r)\,e^{\mathrm{i}\,k\,\theta}-\frac{2\mu_{\mathrm{fr,(I)}}\,k^2}{\mathsf{s}^2_{\mathrm{B,(I)}}r^2}\,b_k\mathrm{H}^{(1)}_{k}(\omega\,\mathsf{s}_{\mathrm{B,(I)}}\,r)\,e^{\mathrm{i}\,k\,\theta}+\frac{2\mu_{\mathrm{fr,(I)}}\,\omega\,\mathrm{i}\,k}{\mathsf{s}_{\mathrm{S,(I)}}r}\,c_k\mathrm{H}^{(1)'}_{k}(\omega\,\mathsf{s}_{\mathrm{S,(I)}}r)\,e^{\mathrm{i}\,k\,\theta}\\
&+\omega^2\,\left(-\tfrac{2}{3}\mu_{\mathrm{fr,(I)}}\,+\,\mathrm{k}_{\mathrm{fr,(I)}}\,+\,M_{\mathrm{(I)}}\alpha^2_{\mathrm{(I)}}\,+\,\alpha_{\mathrm{(I)}}\,M_{\mathrm{(I)}}\mathcal{W}_{\mathrm{P,(I)}}\right)\;a_k\,\mathrm{H}^{(1)}_{k}(\omega\,\mathsf{s}_{\mathrm{P,(I)}}\,r)\;e^{\mathrm{i}\,k\,\theta}\\
&+\omega^2\,\left(-\tfrac{2}{3}\mu_{\mathrm{fr,(I)}}\,+\,\mathrm{k}_{\mathrm{fr,(I)}}\,+\,M_{\mathrm{(I)}}\alpha^2_{\mathrm{(I)}}\,+\,\alpha_{\mathrm{(I)}}\,M_{\mathrm{(I)}}\mathcal{W}_{\mathrm{P,(I)}}\right)\,b_k\,\mathrm{H}^{(1)}_{k}(\omega\,\mathsf{s}_{\mathrm{B,(I)}}\,r)\;e^{\mathrm{i}\,k\,\theta}\,,\\
\omega^2\,\tau^{\mathrm{ref}}_{r\theta,k}\;=\;&-\frac{2\,\mu_{\mathrm{fr,(I)}}\omega\,\mathrm{i}\,k}{r\,\mathsf{s}_{\mathrm{P,(I)}}}\,a_k\,\mathrm{H}^{(1)'}_{k}(\omega\,\mathsf{s}_{\mathrm{P,(I)}}\,r)\,e^{\mathrm{i}\,k\,\theta}+\frac{2\,\mathrm{i}\,\mu_{\mathrm{fr,(I)}}\,k}{r^2\,\mathsf{s}^2_{\mathrm{P,(I)}}}\,a_k\,\mathrm{H}^{(1)}_{k}(\omega\,\mathsf{s}_{\mathrm{P,(I)}}\,r)\,e^{\mathrm{i}\,k\,\theta}\\
&-\frac{2\,\mu_{\mathrm{fr,(I)}}\omega\,\mathrm{i}\,k}{r\,\mathsf{s}_{\mathrm{B,(I)}}}\,b_k\mathrm{H}^{(1)'}_{k}(\omega\,\mathsf{s}_{\mathrm{B,(I)}}\,r)\,e^{\mathrm{i}\,k\,\theta}+\frac{2\,\mathrm{i}\,\mu_{\mathrm{fr,(I)}}\,k}{r^2\,\mathsf{s}^2_{\mathrm{B,(I)}}}\,b_k\mathrm{H}^{(1)}_{k}(\omega\,\mathsf{s}_{\mathrm{B,(I)}}\,r)\,e^{\mathrm{i}\,k\,\theta}-\frac{\mu_{\mathrm{fr,(I)}}\,k^2}{r^2\,\mathsf{s}^2_{\mathrm{S}}}\,c_k\,\mathrm{H}^{(1)}_{k}(\omega\,\mathsf{s}_{\mathrm{S,(I)}}\,r)\,e^{\mathrm{i}\,k\,\theta}\\
&+\frac{\mu_{\mathrm{fr,(I)}}\,\omega}{r\,\mathsf{s}_{\mathrm{S,(I)}}}\,c_k\,\mathrm{H}^{(1)'}_{k}(\omega\,\mathsf{s}_{\mathrm{S,(I)}}\,r)\;e^{\mathrm{i}\,k\,\theta}\;-\;\mu_{\mathrm{fr,(I)}}\,\frac{\omega}{\mathsf{s}_{\mathrm{S,(I)}}r}\,c_k\,\mathrm{H}^{(1)}_{k+1}(\omega\,\mathsf{s}_{\mathrm{S,(I)}}\,r)\;e^{\mathrm{i}\,k\,\theta}\\
&+\frac{\mu_{\mathrm{fr,(I)}}\,k}{\mathsf{s}^2_{\mathrm{S,(I)}}r^2}c_k\,\mathrm{H}^{(1)}_{k}(\omega\,\mathsf{s}_{\mathrm{S,(I)}}\,r)\;e^{\mathrm{i}\,k\,\theta}\;+\;\omega^2\,c_k\mathrm{H}^{(1)}_{k}(\omega\,\mathsf{s}_{\mathrm{S,(I)}}\,r)\;e^{\mathrm{i}\,k\,\theta}\;-\;\mu_{\mathrm{fr,(I)}}\,\frac{k^2}{\mathsf{s}^2_{\mathrm{S,(I)}}r^2}\,c_k\,\mathrm{H}^{(1)}_{k}(\omega\,\mathsf{s}_{\mathrm{S,(I)}}\,r)\;e^{\mathrm{i}\,k\,\theta},
\end{aligned}$$

and for the transmitted wave:

$$\begin{aligned}
\mathfrak{s}\,\mathrm{i}\,\omega\,\mathrm{u}^{\mathrm{trans}}_{r,k} &= d_k\,\frac{\omega}{\mathsf{s}_{\mathrm{P,(II)}}}\,\mathrm{J}'_k(\omega\,\mathsf{s}_{\mathrm{P,(II)}}r)e^{\mathrm{i}k\theta}+\,e_k\,\frac{\omega}{\mathsf{s}_{\mathrm{B,(II)}}}\,\mathrm{J}'_k(\omega\,\mathsf{s}_{\mathrm{B,(II)}}\,r)e^{\mathrm{i}k\theta}-\,f_k\,\frac{\mathrm{i}k}{r\mathsf{s}^2_{\mathrm{S,(II)}}}\mathrm{J}_k(\omega\,\mathsf{s}_{\mathrm{S,(II)}}r)e^{\mathrm{i}k\theta}\,,\\
\mathfrak{s}\,\mathrm{i}\,\omega\,\mathrm{u}^{\mathrm{trans}}_{\theta,k} &= d_k\frac{\mathrm{i}k}{r\,\mathsf{s}^2_{\mathrm{P,(II)}}}\mathrm{J}_k(\omega\,\mathsf{s}_{\mathrm{P,(II)}}r)e^{\mathrm{i}k\theta}+e_k\,\frac{\mathrm{i}k}{r\,\mathsf{s}^2_{\mathrm{B,(II)}}}\mathrm{J}_k(\omega\,\mathsf{s}_{\mathrm{B,(II)}}r)e^{\mathrm{i}k\theta}+f_k\,\frac{\omega}{\mathsf{s}_{\mathrm{S,(II)}}}\,\mathrm{J}'_k(\omega\,\mathsf{s}_{\mathrm{S,(II)}}r)e^{\mathrm{i}k\theta}\,,\\
\mathrm{p}^{\mathrm{ref}}_k &= -\,d_k\,M_{\mathrm{(II)}}\,\left(\mathcal{W}_{\mathrm{P,(II)}}\,+\,\alpha_{\mathrm{(II)}}\right)\mathrm{J}_k(\omega\,\mathsf{s}_{\mathrm{P,(II)}}\,r)\,e^{\mathrm{i}k\theta}\,-\,e_k\,M_{\mathrm{(II)}}\,\left(\mathcal{W}_{\mathrm{B,(II)}}\,+\,\alpha_{\mathrm{(II)}}\right)\mathrm{J}_k(\omega\,\mathsf{s}_{\mathrm{B,(II)}}\,r)\,e^{\mathrm{i}k\theta}\,,\\
\mathfrak{s}\,\mathrm{i}\,\omega\,\mathrm{w}^{\mathrm{trans}}_{r,k} &= d_k\frac{\mathcal{W}_{\mathrm{P,(II)}}\,\omega}{\mathsf{s}_{\mathrm{P,(II)}}}\mathrm{J}'_k(\omega\,\mathsf{s}_{\mathrm{P,(II)}}r)e^{\mathrm{i}k\theta}+e_k\frac{\mathcal{W}_{\mathrm{B,(II)}}\,\omega}{\mathsf{s}_{\mathrm{B,(II)}}}\mathrm{J}'_k(\omega\,\mathsf{s}_{\mathrm{B,(II)}}r)e^{\mathrm{i}k\theta}+f_k\frac{\rho_{f,(\mathrm{II})}\,\mu_{\mathrm{fr,(II)}}\mathrm{i}k}{\mathrm{detA}_{\mathrm{(II)}}r}\mathrm{J}_k(\omega\,\mathsf{s}_{\mathrm{S,(II)}}r)e^{\mathrm{i}k\theta},
\end{aligned}$$

and

$$\begin{aligned}
\omega^2\tau^{\rm trans}_{rr,k} &= -\frac{2\mu_{\rm fr,(II)}\,\omega}{\mathsf{s}_{\rm P,(II)}r}d_k\mathrm{J}_{k+1}(\omega\,\mathsf{s}_{\rm P,(II)}r)\,e^{\mathrm{i}\,k\,\theta}+\frac{2\mu_{\rm fr,(II)}\,k}{\mathsf{s}^2_{\rm P,(II)}r^2}d_k\mathrm{J}_k(\omega\,\mathsf{s}_{\rm P,(II)}r)\,e^{\mathrm{i}\,k\,\theta}+2\mu_{\rm fr,(II)}\omega^2 d_k\mathrm{J}_k(\omega\,\mathsf{s}_{\rm P,(II)}r)e^{\mathrm{i}\,k\,\theta}\\
&-\frac{2\mu_{\rm fr,(II)}\,k^2}{\mathsf{s}^2_{\rm P,(I)}r^2}d_k\,\mathrm{J}_k(\omega\,\mathsf{s}_{\rm P,(II)}r)\,e^{\mathrm{i}\,k\,\theta}-\frac{2\mu_{\rm fr,(II)}\,\omega}{\mathsf{s}_{\rm B,(II)}r}e_k\mathrm{J}_{k+1}(\omega\,\mathsf{s}_{\rm B,(II)}r)\,e^{\mathrm{i}\,k\,\theta}+\frac{2\mu_{\rm fr,(II)}\,k}{\mathsf{s}^2_{\rm B,(II)}r^2}e_k\mathrm{J}_k(\omega\,\mathsf{s}_{\rm B,(II)}r)\,e^{\mathrm{i}\,k\,\theta}\\
&+2\mu_{\rm fr,(II)}e_k\,\omega^2\mathrm{J}_k(\omega\,\mathsf{s}_{\rm B,(II)}r)\,e^{\mathrm{i}\,k\,\theta}-\frac{2\mu_{\rm fr,(II)}\,k^2}{\mathsf{s}^2_{\rm B,(II)}r^2}\,e_k\mathrm{J}_k(\omega\,\mathsf{s}_{\rm B,(II)}\,r)\,e^{\mathrm{i}\,k\,\theta}+\frac{2\mu_{\rm fr,(II)}\omega\,\mathrm{i}k}{\mathsf{s}_{\rm S,(II)}r}\,f_k\,\mathrm{J}'_k(\omega\,\mathsf{s}_{\rm S,(II)}\,r)\,e^{\mathrm{i}\,k\,\theta}\\
&+\omega^2\left(-\tfrac{2}{3}\mu_{\rm fr,(II)}+\mathrm{k}_{\rm fr,(II)}+M_{\rm (II)}\alpha^2_{\rm (II)}+\alpha_{\rm (II)}\,M_{\rm (II)}\mathcal{W}_{\rm P,(II)}\right)\,d_k\,\mathrm{J}_k(\omega\,\mathsf{s}_{\rm P,(II)}\,r)\,e^{\mathrm{i}\,k\,\theta}\\
&+\omega^2\left(-\tfrac{2}{3}\mu_{\rm fr,(II)}+\mathrm{k}_{\rm fr,(II)}+M_{\rm (II)}\alpha^2_{\rm (II)}+\alpha_{\rm (II)}\,M_{\rm (II)}\mathcal{W}_{\rm B,(II)}\right)\,e_k\,\mathrm{J}_k(\omega\,\mathsf{s}_{\rm B,(II)}\,r)\,e^{\mathrm{i}\,k\,\theta},\\
\omega^2\tau^{\rm trans}_{r\theta,k} &= -\frac{2\mu_{\rm fr,(II)}\,\omega\mathrm{i}\,k}{r\mathsf{s}_{\rm P,(II)}}d_k\mathrm{J}'_k(\omega\mathsf{s}_{\rm P,(II)}r)e^{\mathrm{i}k\theta}+\frac{2\,\mathrm{i}\,k\mu_{\rm fr,(II)}}{r^2\mathsf{s}^2_{\rm P,(II)}}d_k\mathrm{J}_k(\omega\mathsf{s}_{\rm P,(II)}r)e^{\mathrm{i}k\theta}-\frac{2\mu_{\rm fr,(II)}\omega\mathrm{i}k}{r\mathsf{s}_{\rm B,(II)}}e_k\mathrm{J}'_k(\omega\,\mathsf{s}_{\rm B,(II)}r)e^{\mathrm{i}k\theta}\\
&+\frac{2\,\mathrm{i}\,\mu_{\rm fr,(II)}\,k}{r^2\,\mathsf{s}^2_{\rm B,(II)}}e_k\,\mathrm{J}_k(\omega\,\mathsf{s}_{\rm B,(II)}r)\,e^{\mathrm{i}\,k\,\theta}-\frac{\mu_{\rm fr,(II)}\,k^2}{r^2\,\mathsf{s}^2_{\rm S}}f_k\,\mathrm{J}_k(\omega\,\mathsf{s}_{\rm S,(II)}r)\,e^{\mathrm{i}\,k\,\theta}+\frac{\mu_{\rm fr,(II)}\,\omega}{r\,\mathsf{s}_{\rm S,(I)}}f_k\,\mathrm{J}'_k(\omega\,\mathsf{s}_{\rm S,(II)}r)\,e^{\mathrm{i}\,k\,\theta}\\
&-\mu_{\rm fr,(II)}\,\frac{\omega}{\mathsf{s}_{\rm S,(II)}r}\,f_k\,\mathrm{J}_{k+1}(\omega\,\mathsf{s}_{\rm S,(II)}r)\,e^{\mathrm{i}\,k\,\theta}+\mu_{\rm fr,(II)}\,\frac{k}{\mathsf{s}^2_{\rm S,(iI)}r^2}f_k\,\mathrm{J}_k(\omega\,\mathsf{s}_{\rm S,(II)}\,r)\,e^{\mathrm{i}\,k\,\theta}\\
&+\omega^2\,f_k\,\mathrm{J}_k(\omega\,\mathsf{s}_{\rm S,(II)}r)\,e^{\mathrm{i}\,k\,\theta}-\mu_{\rm fr,(II)}\,\frac{k^2}{\mathsf{s}^2_{\rm S,(I)}r^2}\,f_k\,\mathrm{J}_k(\omega\,\mathsf{s}_{\rm S,(II)}r)\,e^{\mathrm{i}\,k\,\theta}.
\end{aligned}$$

Imposing (2.37), we obtain a linear system satisfied by a_k, b_k, c_k, d_k, e_k, f_k in each mode k:

$$\mathbb{A}^{\text{poro-poro}}_k\begin{pmatrix}a_k\\b_k\\c_k\\d_k\\e_k\\f_k\end{pmatrix}=\begin{pmatrix}-\mathfrak{s}\,\mathrm{i}\,\omega\,\mathrm{u}^{\rm pw}_r\\-\mathfrak{s}\,\mathrm{i}\,\omega\,\mathrm{u}^{\rm pw}_\theta\\-\mathrm{p}^{\rm pw}\\-\mathfrak{s}\,\mathrm{i}\,\omega\,\mathrm{w}^{\rm pw}_r\\-\omega^2\,\tau^{\rm pw}_{rr}\\-\omega^2\,\tau^{\rm pw}_{r\theta}\end{pmatrix}\tag{2.38}$$

with

$$\mathbb{A}^{\text{poro-poro}}_k=\begin{pmatrix}A_{11}&A_{12}&A_{13}&A_{14}&A_{15}&A_{16}\\A_{21}&A_{22}&A_{23}&A_{24}&A_{25}&A_{26}\\A_{31}&A_{32}&A_{33}&A_{34}&A_{35}&A_{36}\\A_{41}&A_{42}&A_{43}&A_{44}&A_{45}&A_{46}\\A_{51}&A_{52}&A_{53}&A_{54}&A_{55}&A_{56}\\A_{61}&A_{62}&A_{63}&A_{64}&A_{65}&A_{66}\end{pmatrix}\tag{2.39}$$

$$A_{11}=\frac{\omega}{\mathsf{s}_{\rm P,(I)}}\mathrm{H}^{(1)'}_k(\omega\,\mathsf{s}_{\rm P,(I)}\,\mathfrak{a})\,,\qquad A_{12}=\frac{\omega}{\mathsf{s}_{\rm B,(I)}}\,\mathrm{H}^{(1)'}_k(\omega\,\mathsf{s}_{\rm B,(I)}\,\mathfrak{a})\,,\qquad A_{13}=-\frac{\mathrm{i}k}{\mathfrak{a}\mathsf{s}^2_{\rm S,(I)}}\mathrm{H}^{(1)}_k(\omega\,\mathsf{s}_{\rm S,(I)}\,\mathfrak{a})\,,$$

$$A_{21}=\frac{\mathrm{i}k}{\mathfrak{a}\,\mathsf{s}^2_{\rm P,(I)}}\mathrm{H}^{(1)}_k(\omega\,\mathsf{s}_{\rm P,(I)}\,\mathfrak{a})\,,\qquad A_{22}=\frac{\mathrm{i}k}{\mathfrak{a}\,\mathsf{s}^2_{\rm B,(I)}}\,\mathrm{H}^{(1)}_k(\omega\,\mathsf{s}_{\rm B,(I)}\,\mathfrak{a})\,,\qquad A_{23}=\mathsf{s}^{-1}_{\rm S,(I)}\,\omega\,\mathrm{H}^{(1)'}_k(\omega\,\mathsf{s}_{\rm S,(I)}\,\mathfrak{a})\,,$$

$$A_{31}=-M\left(\mathcal{W}_{\rm P,(I)}+\alpha_{\rm (I)}\right)\mathrm{H}^{(1)}_k(\omega\,\mathsf{s}_{\rm P,(I)}\,\mathfrak{a})\,,\quad A_{32}=-M\left(\mathcal{W}_{\rm B,(I)}+\alpha_{\rm (I)}\right)\mathrm{H}^{(1)}_k(\omega\,\mathsf{s}_{\rm B,(I)}\,\mathfrak{a})\,,\quad A_{33}=0\,,$$

$$A_{14} = -\frac{\omega}{\mathtt{s}_{\mathrm{P},(\mathrm{II})}} \mathrm{J}'_k(\omega\, \mathtt{s}_{\mathrm{P},(\mathrm{II})}\, \mathfrak{a})\,, \qquad A_{15} = -\frac{\omega}{\mathtt{s}_{\mathrm{B},(\mathrm{II})}} \mathrm{J}'_k(\omega\, \mathtt{s}_{\mathrm{B},(\mathrm{II})}\, \mathfrak{a})\,, \qquad A_{16} = \frac{\mathrm{i}k}{\mathfrak{a}\mathtt{s}^2_{\mathrm{S},(\mathrm{II})}} \mathrm{J}_k(\omega\, \mathtt{s}_{\mathrm{S},(\mathrm{II})}\, \mathfrak{a})\,,$$

$$A_{24} = -\frac{\mathrm{i}k}{\mathfrak{a}\, \mathtt{s}^2_{\mathrm{P},(\mathrm{II})}} \mathrm{J}_k(\omega\, \mathtt{s}_{\mathrm{P},(\mathrm{II})}\, \mathfrak{a})\,, \qquad A_{25} = -\frac{\mathrm{i}k}{\mathfrak{a}\, \mathtt{s}^2_{\mathrm{B},(\mathrm{II})}} \mathrm{J}_k(\omega\, \mathtt{s}_{\mathrm{B},(\mathrm{II})}\, \mathfrak{a})\,, \qquad A_{26} = -\mathtt{s}^{-1}_{\mathrm{S},(\mathrm{II})}\, \omega\, \mathrm{J}'_k(\omega\, \mathtt{s}_{\mathrm{S},(\mathrm{II})}\, \mathfrak{a})\,,$$

$$A_{34} = M\left(\mathcal{W}_{\mathrm{P},(\mathrm{II})} \;+\; \alpha_{(\mathrm{II})}\right) \mathrm{J}_k(\omega\, \mathtt{s}_{\mathrm{P},(\mathrm{II})}\, \mathfrak{a})\,, \quad A_{35} = M\left(\mathcal{W}_{\mathrm{B},(\mathrm{II})} \;+\; \alpha_{(\mathrm{II})}\right) \mathrm{J}_k(\omega\, \mathtt{s}_{\mathrm{B},(\mathrm{II})}\, \mathfrak{a})\,, \quad A_{36} = 0\,,$$

$$A_{41} = \frac{\mathcal{W}_{\mathrm{P},(\mathrm{I})}}{\mathtt{s}_{\mathrm{P},(\mathrm{I})}}\, \omega\, \mathrm{H}^{(1)'}_k(\omega\, \mathtt{s}_{\mathrm{P},(\mathrm{I})}\mathfrak{a})\,, \qquad A_{42} = \frac{\mathcal{W}_{\mathrm{B},(\mathrm{I})}}{\mathtt{s}_{\mathrm{B},(\mathrm{I})}}\, \omega\, \mathrm{H}^{(1)'}_k(\omega\, \mathtt{s}_{\mathrm{B},(\mathrm{I})}\mathfrak{a})\,, \qquad A_{43} = \frac{\rho_{f,(\mathrm{I})}\, \mu_{\mathrm{fr},(\mathrm{I})}}{\det A_{(\mathrm{I})}}\, \frac{\mathrm{i}k}{\mathfrak{a}} \mathrm{H}^{(1)}_k(\omega\, \mathtt{s}_{\mathrm{S},(\mathrm{I})}\mathfrak{a})\,,$$

$$A_{51} = -\frac{2\,\mu_{\mathrm{fr},(\mathrm{I})}\,\omega}{\mathtt{s}_{\mathrm{P},(\mathrm{I})}\mathfrak{a}}\, \mathrm{H}^{(1)}_{k+1}(\omega\, \mathtt{s}_{\mathrm{P},(\mathrm{I})}\, \mathfrak{a}) \;+\; \frac{2\,\mu_{\mathrm{fr},(\mathrm{I})}\, k}{\mathtt{s}^2_{\mathrm{P},(\mathrm{I})}\mathfrak{a}^2}\, \mathrm{H}^{(1)}_k(\omega\, \mathtt{s}_{\mathrm{P},(\mathrm{I})}\, \mathfrak{a}) \;+\; 2\,\mu_{\mathrm{fr},(\mathrm{I})}\, \omega^2\, \mathrm{H}^{(1)}_k(\omega\, \mathtt{s}_{\mathrm{P},(\mathrm{I})}\, \mathfrak{a})$$
$$-\; \frac{2\,\mu_{\mathrm{fr}}\, k^2}{\mathtt{s}^2_{\mathrm{P},(\mathrm{I})}\mathfrak{a}^2}\, \mathrm{H}^{(1)}_k(\omega\, \mathtt{s}_{\mathrm{P},(\mathrm{I})}\, \mathfrak{a}) \;+\omega^2 \left(-\tfrac{2}{3}\mu_{\mathrm{fr},(\mathrm{I})} \;+\; \mathrm{k}_{\mathrm{fr},(\mathrm{I})} \;+\; M_{(\mathrm{I})}\alpha^2_{(\mathrm{I})} \;+\; \alpha_{(\mathrm{I})}\, M_{(\mathrm{I})}\mathcal{W}_{\mathrm{P},(\mathrm{I})}\right) \mathrm{H}^{(1)}_k(\omega\, \mathtt{s}_{\mathrm{P},(\mathrm{I})}\mathfrak{a})\,,$$

$$A_{52} = -\frac{2\,\mu_{\mathrm{fr},(\mathrm{I})}\,\omega}{\mathtt{s}_{\mathrm{B},(\mathrm{I})}\mathfrak{a}}\, \mathrm{H}^{(1)}_{k+1}(\omega\, \mathtt{s}_{\mathrm{B},(\mathrm{I})}\, \mathfrak{a}) \;+\; \frac{2\,\mu_{\mathrm{fr},(\mathrm{I})}\, k}{\mathtt{s}^2_{\mathrm{B},(\mathrm{I})}\mathfrak{a}^2}\, \mathrm{H}^{(1)}_k(\omega\, \mathtt{s}_{\mathrm{B},(\mathrm{I})}\, \mathfrak{a}) \;+\; 2\,\mu_{\mathrm{fr},(\mathrm{I})}\, \omega^2\, \mathrm{H}^{(1)}_k(\omega\, \mathtt{s}_{\mathrm{B},(\mathrm{I})}\, \mathfrak{a})$$
$$-\; \frac{2\,\mu_{\mathrm{fr}}\, k^2}{\mathtt{s}^2_{\mathrm{B},(\mathrm{I})}\mathfrak{a}^2}\, \mathrm{H}^{(1)}_k(\omega\, \mathtt{s}_{\mathrm{B},(\mathrm{I})}\, \mathfrak{a}) \;+\omega^2 \left(-\tfrac{2}{3}\mu_{\mathrm{fr},(\mathrm{I})} \;+\; \mathrm{k}_{\mathrm{fr},(\mathrm{I})} \;+\; M_{(\mathrm{I})}\alpha^2_{(\mathrm{I})} \;+\; \alpha_{(\mathrm{I})}\, M_{(\mathrm{I})}\mathcal{W}_{\mathrm{B},(\mathrm{I})}\right) \mathrm{H}^{(1)}_k(\omega\, \mathtt{s}_{\mathrm{B},(\mathrm{I})}\mathfrak{a})\,,$$

$$A_{53} = \frac{2\mu_{\mathrm{fr},(\mathrm{I})}}{\mathtt{s}_{\mathrm{S},(\mathrm{I})}\mathfrak{a}}\, \omega\, \mathrm{i}k\, \mathrm{H}^{(1)'}_k(\omega\, \mathtt{s}_{\mathrm{S}}\mathfrak{a})\,,$$

$$A_{61} = -\frac{2\omega\, \mu_{\mathrm{fr},(\mathrm{I})}\mathrm{i}k}{\mathfrak{a}\, \mathtt{s}_{\mathrm{P},(\mathrm{I})}} \mathrm{H}^{(1)'}_k(\omega\, \mathtt{s}_{\mathrm{P},(\mathrm{I})}\mathfrak{a}) + \frac{2\,\mu_{\mathrm{fr},(\mathrm{I})}\mathrm{i}k}{\mathfrak{a}^2\mathtt{s}^2_{\mathrm{P},(\mathrm{I})}} \mathrm{H}^{(1)}_k(\omega\, \mathtt{s}_{\mathrm{P},(\mathrm{I})}\mathfrak{a})\,,$$

$$A_{62} = -\frac{2\omega\, \mu_{\mathrm{fr},(\mathrm{I})}\mathrm{i}k}{\mathfrak{a}\, \mathtt{s}_{\mathrm{B},(\mathrm{I})}} \mathrm{H}^{(1)'}_k(\omega\, \mathtt{s}_{\mathrm{B},(\mathrm{I})}\mathfrak{a}) + \frac{2\mu_{\mathrm{fr},(\mathrm{I})}\mathrm{i}k}{\mathfrak{a}^2\mathtt{s}^2_{\mathrm{B},(\mathrm{I})}} \mathrm{H}^{(1)}_k(\omega\, \mathtt{s}_{\mathrm{B},(\mathrm{I})}\mathfrak{a})\,,$$

$$A_{63} = -\frac{k^2\mu_{\mathrm{fr},(\mathrm{I})}}{\mathfrak{a}^2\, \mathtt{s}^2_{\mathrm{S},(\mathrm{I})}} \mathrm{H}^{(1)}_k(\omega\, \mathtt{s}_{\mathrm{S},(\mathrm{I})}\, \mathfrak{a}) + \frac{\omega\, \mu_{\mathrm{fr},(\mathrm{I})}}{\mathfrak{a}\, \mathtt{s}_{\mathrm{S},(\mathrm{I})}} \mathrm{H}^{(1)'}_k(\omega\, \mathtt{s}_{\mathrm{S},(\mathrm{I})}\, \mathfrak{a}) \;-\; \frac{\omega}{\mathtt{s}_{\mathrm{S},(\mathrm{I})}\mathfrak{a}}\, \mathrm{H}^{(1)}_{k+1}(\omega\, \mathtt{s}_{\mathrm{S},(\mathrm{I})}\, \mathfrak{a}) \;+\; \frac{k}{\mathtt{s}^2_{\mathrm{S},(\mathrm{I})}\mathfrak{a}^2}\, \mathrm{H}^{(1)}_k(\omega\, \mathtt{s}_{\mathrm{S}}\, \mathfrak{a})\;,$$
$$+\; \omega^2\, \mathrm{H}^{(1)}_k(\omega\, \mathtt{s}_{\mathrm{S},(\mathrm{I})}\, \mathfrak{a})\; e^{\mathrm{i}\,k\,\theta} \;-\; \frac{k^2}{\mathtt{s}^2_{\mathrm{S},(\mathrm{I})}\mathfrak{a}^2}\, \mathrm{H}^{(1)}_k(\omega\, \mathtt{s}_{\mathrm{S},(\mathrm{I})}\, \mathfrak{a})\;,$$

$$A_{44} = -\frac{\mathcal{W}_{\mathrm{P},(\mathrm{II})}}{\mathtt{s}_{\mathrm{P},(\mathrm{II})}}\, \omega\, \mathrm{J}'_k(\omega\, \mathtt{s}_{\mathrm{P},(\mathrm{II})}\mathfrak{a})\,, \qquad A_{45} = -\frac{\mathcal{W}_{\mathrm{B},(\mathrm{II})}}{\mathtt{s}_{\mathrm{B},(\mathrm{II})}}\, \omega\, \mathrm{J}'_k(\omega\, \mathtt{s}_{\mathrm{B},(\mathrm{II})}\mathfrak{a})\,, \qquad A_{46} = -\frac{\rho_{f,(\mathrm{II})}\, \mu_{\mathrm{fr},(\mathrm{II})}}{\det A_{(\mathrm{II})}}\, \frac{\mathrm{i}k}{\mathfrak{a}} \mathrm{J}_k(\omega\, \mathtt{s}_{\mathrm{S},(\mathrm{II})}\mathfrak{a})\,,$$

$$A_{54} = \frac{2\,\mu_{\mathrm{fr},(\mathrm{II})}\,\omega}{\mathtt{s}_{\mathrm{P},(\mathrm{II})}\mathfrak{a}}\, \mathrm{J}_{k+1}(\omega\, \mathtt{s}_{\mathrm{P},(\mathrm{II})}\, \mathfrak{a}) \;-\; \frac{2\,\mu_{\mathrm{fr},(\mathrm{II})}\, k}{\mathtt{s}^2_{\mathrm{P},(\mathrm{I})}\mathfrak{a}^2}\, \mathrm{J}_k(\omega\, \mathtt{s}_{\mathrm{P},(\mathrm{I})}\, \mathfrak{a}) \;-\; 2\,\mu_{\mathrm{fr},(\mathrm{II})}\, \omega^2\, \mathrm{H}^{(1)}_k(\omega\, \mathtt{s}_{\mathrm{P},(\mathrm{II})}\, \mathfrak{a})$$
$$+\; \frac{2\,\mu_{\mathrm{fr},(\mathrm{II})}\, k^2}{\mathtt{s}^2_{\mathrm{P}}\mathfrak{a}^2}\, \mathrm{J}_k(\omega\, \mathtt{s}_{\mathrm{P},(\mathrm{II})}\, \mathfrak{a}) \;-\omega^2 \left(-\tfrac{2}{3}\mu_{\mathrm{fr},(\mathrm{II})} \;+\; \mathrm{k}_{\mathrm{fr},(\mathrm{II})} \;+\; M_{(\mathrm{II})}\alpha^2_{(\mathrm{II})} \;+\; \alpha_{(\mathrm{II})}\, M_{(\mathrm{II})}\mathcal{W}_{\mathrm{P},(\mathrm{II})}\right) \mathrm{J}_k(\omega\, \mathtt{s}_{\mathrm{P},(\mathrm{II})}\mathfrak{a})\,,$$

$$A_{55} = \frac{2\,\mu_{\mathrm{fr},(\mathrm{II})}\,\omega}{\mathtt{s}_{\mathrm{B},(\mathrm{II})}\mathfrak{a}}\, \mathrm{J}_{k+1}(\omega\, \mathtt{s}_{\mathrm{B},(\mathrm{II})}\, \mathfrak{a})\; e^{\mathrm{i}\,k\,\theta} \;-\; \frac{2\,\mu_{\mathrm{fr},(\mathrm{II})}\, k}{\mathtt{s}^2_{\mathrm{B},(\mathrm{I})}\mathfrak{a}^2}\, \mathrm{H}^{(1)}_k(\omega\, \mathtt{s}_{\mathrm{B},(\mathrm{II})}\, \mathfrak{a})\; e^{\mathrm{i}\,k\,\theta} \;-\; 2\,\mu_{\mathrm{fr},(\mathrm{II})}\, \omega^2\, \mathrm{J}_k(\omega\, \mathtt{s}_{\mathrm{B},(\mathrm{II})}\, \mathfrak{a})\; e^{\mathrm{i}\,k\,\theta}$$
$$+\; \frac{2\,\mu_{\mathrm{fr},(\mathrm{II})}\, k^2}{\mathtt{s}^2_{\mathrm{B},(\mathrm{II})}\mathfrak{a}^2}\, \mathrm{J}_k(\omega\, \mathtt{s}_{\mathrm{B},(\mathrm{II})}\, \mathfrak{a})\; e^{\mathrm{i}\,k\,\theta} - \omega^2 \left(-\tfrac{2}{3}\mu_{\mathrm{fr},(\mathrm{II})} \;+\; \mathrm{k}_{\mathrm{fr},(\mathrm{II})} \;+\; M_{(\mathrm{II})}\alpha^2_{(\mathrm{II})} \;+\; \alpha_{(\mathrm{II})}\, M_{(\mathrm{II})}\mathcal{W}_{\mathrm{B},(\mathrm{II})}\right) \mathrm{J}_k(\omega\, \mathtt{s}_{\mathrm{B},(\mathrm{II})}\mathfrak{a})\,,$$

$$A_{56} = -\frac{2\mu_{\mathrm{fr},(\mathrm{II})}}{\mathtt{s}_{\mathrm{S},(\mathrm{II})}\mathfrak{a}}\, \omega\, \mathrm{i}k\, \mathrm{J}'_k(\omega\, \mathtt{s}_{\mathrm{S},(\mathrm{II})}\mathfrak{a})\,,$$

$$A_{64} = \frac{2\omega\,\mu_{\mathrm{fr,(II)}}\mathrm{i}k}{\mathfrak{a}\mathsf{s}_{\mathrm{P,(II)}}}\mathrm{J}_k'(\omega\,\mathsf{s}_{\mathrm{P,(II)}}\mathfrak{a}) - \frac{2\,\mu_{\mathrm{fr,(II)}}\mathrm{i}k}{\mathfrak{a}^2\mathsf{s}^2_{\mathrm{P,(II)}}}\mathrm{J}_k(\omega\,\mathsf{s}_{\mathrm{P,(II)}}\mathfrak{a})\,,$$

$$A_{65} = \frac{2\omega\,\mu_{\mathrm{fr,(II)}}\mathrm{i}k}{\mathfrak{a}\mathsf{s}_{\mathrm{B,(II)}}}\mathrm{J}_k'(\omega\,\mathsf{s}_{\mathrm{B,(II)}}\mathfrak{a}) - \frac{2\mu_{\mathrm{fr,(II)}}\mathrm{i}k}{\mathfrak{a}^2\mathsf{s}^2_{\mathrm{B,(II)}}}\mathrm{J}_k(\omega\,\mathsf{s}_{\mathrm{B,(II)}}\mathfrak{a})\,,$$

$$A_{66} = \frac{k^2\mu_{\mathrm{fr,(II)}}}{\mathfrak{a}^2\mathsf{s}^2_{\mathrm{S,(II)}}}\mathrm{J}_k(\omega\,\mathsf{s}_{\mathrm{S,(II)}}\,\mathfrak{a}) - \frac{\omega\,\mu_{\mathrm{fr,(II)}}}{\mathfrak{a}\mathsf{s}_{\mathrm{S,(II)}}}\mathrm{J}_k'(\omega\,\mathsf{s}_{\mathrm{S,(II)}}\,\mathfrak{a}) + \frac{\omega}{\mathsf{s}_{\mathrm{S}}\mathfrak{a}}\,\mathrm{J}_{k+1}(\omega\,\mathsf{s}_{\mathrm{S,(II)}}\,\mathfrak{a})\;e^{\mathrm{i}\,k\,\theta} - \frac{k}{\mathsf{s}^2_{\mathrm{S,(II)}}\mathfrak{a}^2}\,\mathrm{J}_k(\omega\,\mathsf{s}_{\mathrm{S,(II)}}\,\mathfrak{a})\,,$$
$$- \omega^2\,\mathrm{J}_k(\omega\,\mathsf{s}_{\mathrm{S,(II)}}\,\mathfrak{a})\;e^{\mathrm{i}\,k\,\theta} + \frac{k^2}{\mathsf{s}^2_{\mathrm{S,(II)}}\mathfrak{a}^2}\,\mathrm{J}_k(\omega\,\mathsf{s}_{\mathrm{S,(II)}}\,\mathfrak{a})\,.$$

We define the eigenvalues as follows:

Definition 2.7. ω is porous-porous transmission eigenvalue if $\det \mathbb{A}_k^{\text{poro-poro}}(\omega) = 0$, where $\mathbb{A}_k^{\text{poro-poro}}$ is the coefficient matrix defined in equation (2.39).

2.4.2 Numerical tests

We consider an infinite porous medium denoted as the exterior medium Γ, in which Ω is a porous inclusion (interior medium), see figure 2.12. In the construction of the analytical solution, we consider the exterior medium to be infinite. For the representation of the solution, we only plot the value of the field inside a disc of radius equals to 10m. Considering the total field, we show the imaginary part of the solid velocity u_x in Figure 2.13. The inclusion is located inside with the dashed circle. In the figure, we observe that the scattering generates mainly P-waves for the reflected and transmitted waves.

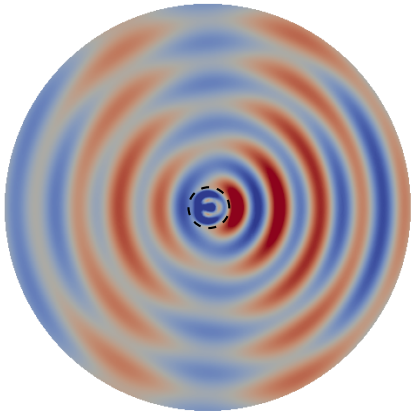

Figure 2.13: Exact solution for the scattering of a P-plane wave by a penetrable solid inclusion, considering the total wave field. We present the imaginary part of the solid velocity u_x for sandstone/shale with no viscosity test with $\omega = 500$ rad.s^{-1}.

To investigate the influence of the material parameters, we consider different cases detailed in the table 2.1. For all of these tests, we study the determinant of the coefficient matrix (2.39) as a function of the pulsation. We first study the influence of the viscosity by varying its value in the interior and exterior medium. Next, we vary the value of the frame shear modulus to observe the differences on the shape of the curves. For all tests, the cross section radius is $\mathfrak{a} = 1$m. We have the following observations:

- As in the case of a bounded domain, the shear frame modulus has an influence on the shape of the curve. When the shear frame modulus of the interior material decreases, we can observe the apparition of smooth peaks. When it is in the exterior material, the general value of the determinant decreases, *cf.* Figure 2.16. This shows that the interior medium has more influence on the determinant of the matrix than the exterior one. This is similar to a result for fluid-elastic scattering (see [51]), where non -zero solutions can appear without any source, as for a bounded domain. On the contrary, the problem in the exterior medium is well-posed.
- For modes 3, 4 and 5, the red curve, which represents the setting in which the interior medium is viscous and the exterior medium has no viscosity, is higher than the other curves for low frequencies, see 2.15. As the modes mainly depend on the characteristics of the interior medium, the viscosity in this medium suppresses the eventual modes.

Exterior medium	Interior medium	Figures
Sandstone ($\eta = 0$ Pa.s and $\mu_{\text{fr}} = 12$GPa)	Shale ($\eta = 0$ Pa.s and $\mu_{\text{fr}} = 3.96$GPa)	2.14, 2.15, 2.16
Sandstone ($\eta = 0$ Pa.s and $\mu_{\text{fr}} = 12$GPa)	Shale ($\eta = 10^{-3}$ Pa.s and $\mu_{\text{fr}} = 3.96$GPa)	2.14, 2.15
Sandstone ($\eta = 10^{-3}$Pa.s and $\mu_{\text{fr}} = 12$GPa)	Shale ($\eta = 0$ Pa.s and $\mu_{\text{fr}} = 3.96$GPa)	2.14, 2.15
Sandstone ($\eta = 10^{-3}$Pa.s and $\mu_{\text{fr}} = 12$GPa)	Shale ($\eta = 10^{-3}$ Pa.s and $\mu_{\text{fr}} = 3.96$GPa)	2.14, 2.15
Sandstone ($\eta = 0$ Pa.s and $\mu_{\text{fr}} = 12$GPa)	Modified Shale ($\eta = 0$ Pa.s and $\mu_{\text{fr}} = 1$GPa)	2.16,
Modified Sandstone ($\eta = 0$ Pa.s and $\mu_{\text{fr}} = 3$GPa)	Shale ($\eta = 0$ Pa.s and $\mu_{\text{fr}} = 3.96$GPa)	2.16
Modified Sandstone ($\eta = 0$ Pa.s and $\mu_{\text{fr}} = 3$GPa)	Modified Shale ($\eta = 0$ Pa.s and $\mu_{\text{fr}} = 1$GPa)	2.16

Table 2.1: List of the tests of porous-porous interaction

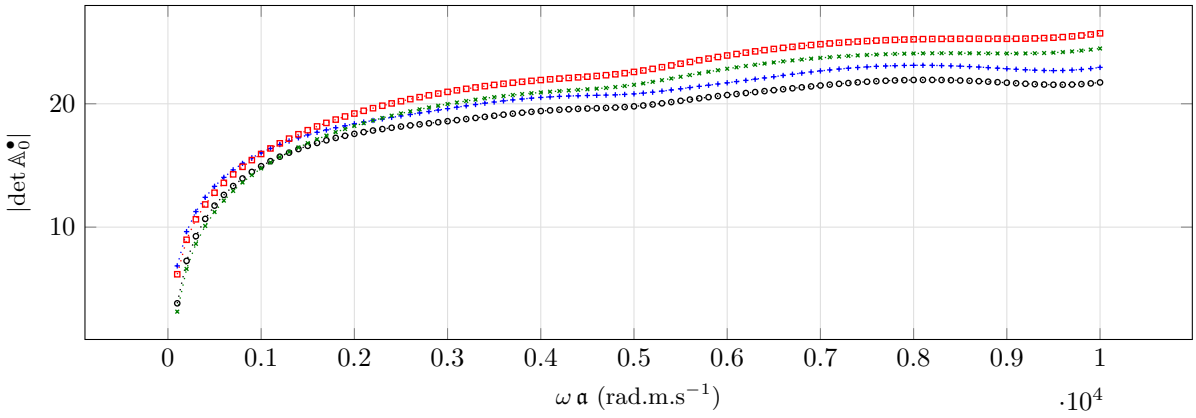

(a) Mode $k = 0$

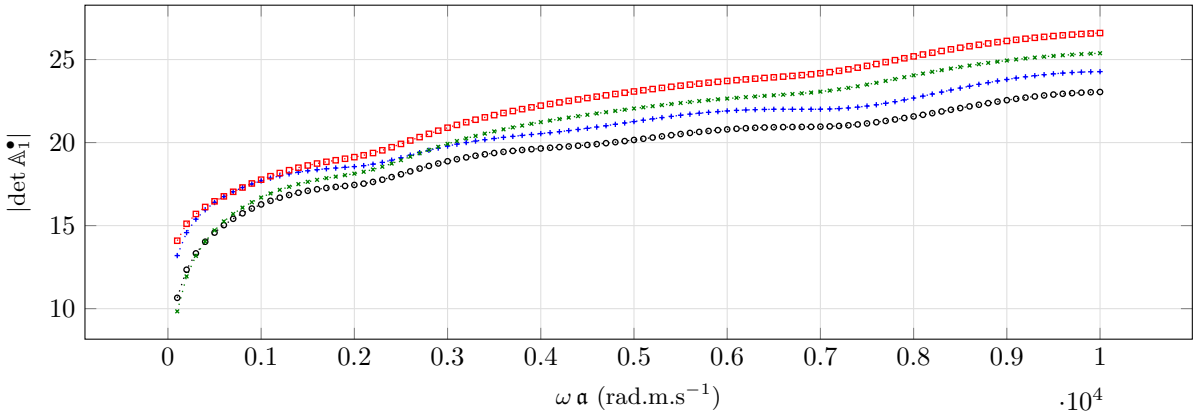

(b) Mode $k = 1$

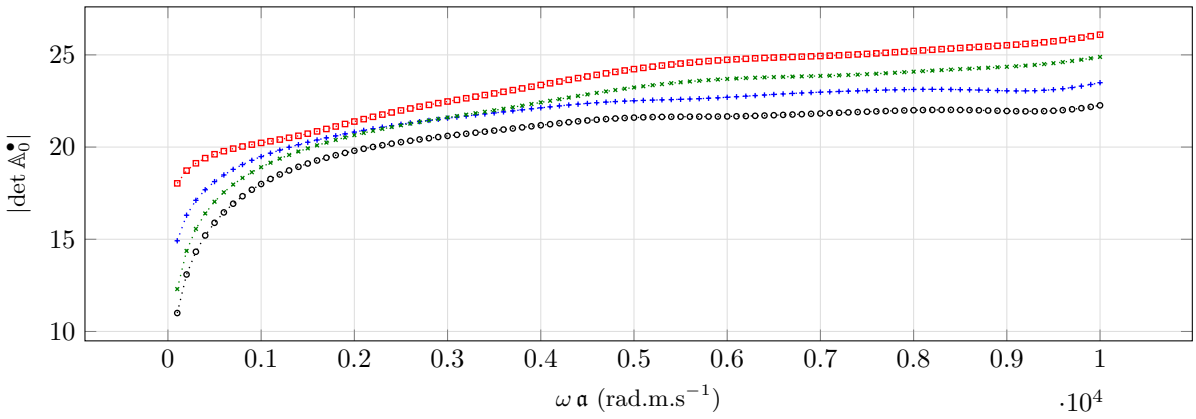

(c) Mode $k = 2$

Figure 2.14: Experiment of a porous-porous interaction: Determinant of the coefficient matrix $\mathbb{A}_k^{\text{poro-poro}}$ (2.39) (log scale) for k in $0:2$ for sandstone/shale with no viscosity in blue ····+····, for inviscid sandstone/ viscous shale in red ····□····, for viscous sandstone/inviscid shale in black ····○···· and for viscous sandstone/viscous shale in green ····×····.

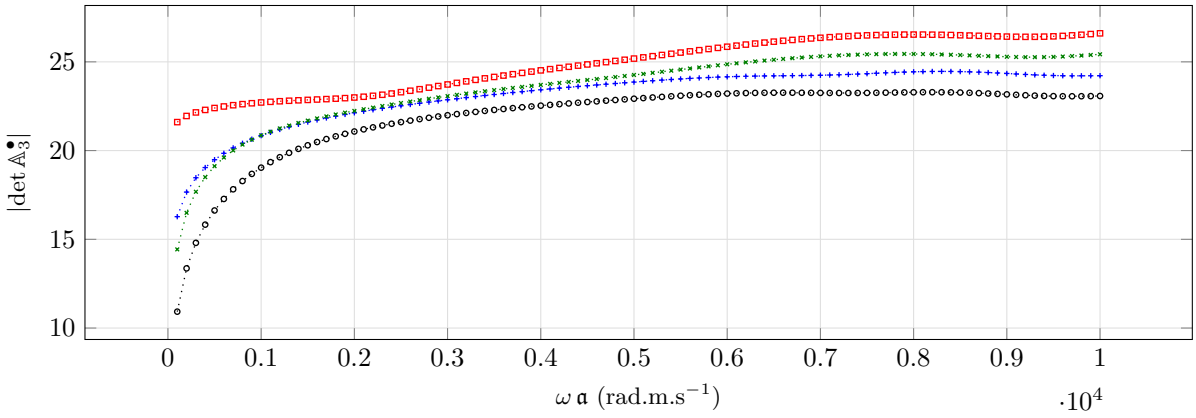

(a) Mode $k = 3$

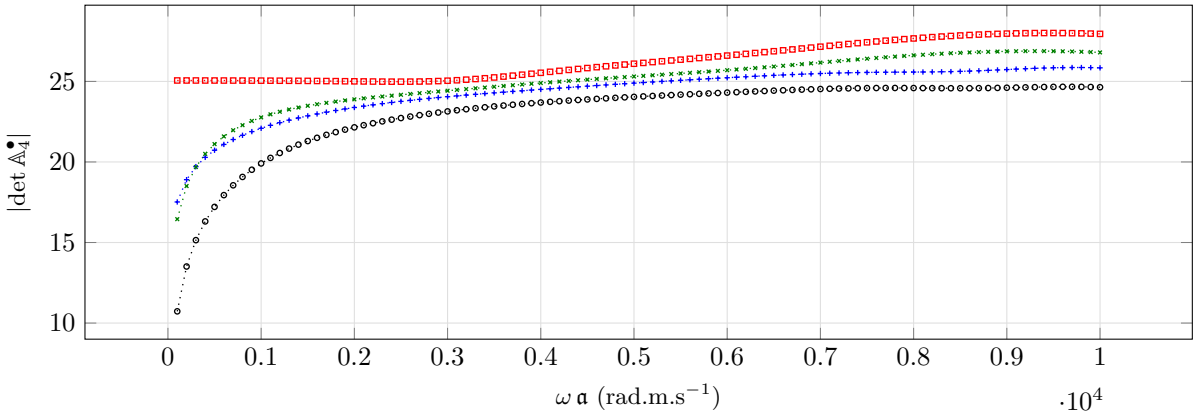

(b) Mode $k = 4$

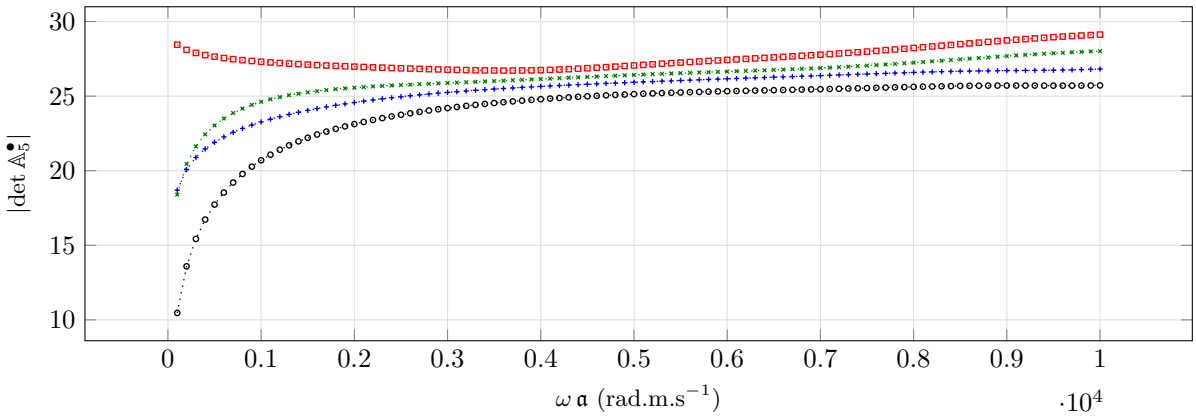

(c) Mode $k = 5$

Figure 2.15: Experiment of a porous-porous interaction: Determinant of the coefficient matrix $\mathbb{A}_k^{\text{poro-poro}}$ (2.39) (log scale) for k in $3:5$ for sandstone/shale with no viscosity in blue ····+····, for inviscid sandstone/ viscous shale in red ····□···· , for viscous sandstone/inviscid shale in black ····○···· and for viscous sandstone/viscous shale in green ····×····.

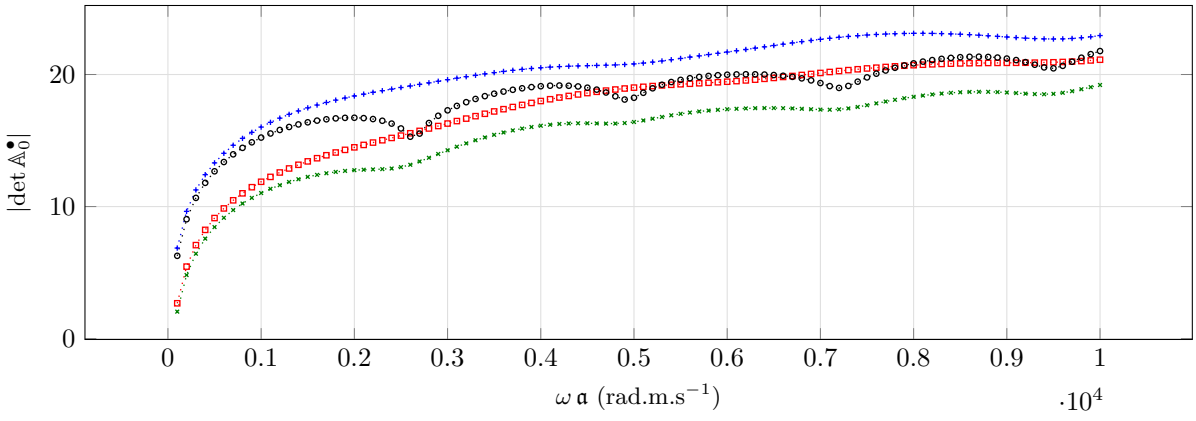

(a) Modes $k = 0$

Figure 2.16: Experiment of a porous-porous interaction: Comparison of the determinant of the coefficient matrix $\mathbb{A}_k^{\text{poro-poro}}$ (2.39) (log scale) for $k = 0$ for sandstone/shale with no viscosity and regular shear frame modulus in blue ····+···. The shear frame modulus of the interior material is divided by four in ····∘····, the one for the exterior material is divided by four in ····□···· and both are divided by four in ····×····.

2.5 Scattering of a plane wave by a poroelastic domain in a fluid medium

We consider the scattering by a plane wave of a poroelastic obstacle in an infinite fluid medium. The total wave outside of the cylinder is a superposition of the incident plane wave and the reflected wave, while the transmitted wave is described by the displacement inside the cylinder. The movement in the fluid region is described by

$$\mathrm{p}_{\mathrm{flu}} = \mathrm{p}^{\mathrm{pw}} + \mathrm{p}^{\mathrm{ref}}, \qquad \mathbf{u}_{\mathrm{flu}} = \mathbf{u}^{\mathrm{pw}} + \mathbf{u}^{\mathrm{ref}}.$$

where $\mathrm{p}_{\mathrm{flu}}$ satisfies the Helmholtz equation,

$$\left(-\Delta - \omega^2\, \mathsf{s}_{\mathrm{flu}}^2\right) \mathrm{p}_{\mathrm{flu}} = 0\,, \tag{2.40}$$

and the velocity in fluid is given by

$$\mathbf{u}_{\mathrm{flu}} = -\frac{1}{\rho_{\mathrm{flu}}\, \mathfrak{s}\, \mathrm{i}\, \omega} \nabla\, \mathrm{p}_{\mathrm{flu}} = \frac{\mathfrak{s}\, \mathrm{i}}{\rho_{\mathrm{flu}}\, \omega} \nabla\, \mathrm{p}_{\mathrm{flu}}\,. \tag{2.41}$$

Here, the slowness of fluid is chosen in the same way as those in the poroelastic interior by Definition (1.43) , i.e.

$$\mathsf{s}_{\mathrm{flu}} = -\mathfrak{s} \sqrt{\mathsf{s}_{\mathrm{flu}}^2}\,.$$

In the interior, the transmitted movements are described by $U^{\mathrm{trans}} = (\mathbf{u}^{\mathrm{trans}}, \mathbf{w}^{\mathrm{trans}}, \boldsymbol{\tau}^{\mathrm{trans}}, \mathrm{p}^{\mathrm{trans}})$ that solves the poroelastic equations (1.16). The interior and exterior quantities are determined by transmission conditions imposed on the interface Γ.

In short, the unknowns of the fluid-solid interaction problem are $(\mathrm{p}_{\mathrm{flu}}, \mathbf{u}_{\mathrm{flu}})$ and U^{trans}, which solve:

$$\begin{cases} (\mathrm{p}_{\mathrm{flu}}, \mathbf{u}_{\mathrm{flu}}) \text{ solves the acoustic equations (2.40) and (2.41) in } \mathbb{R}^2 \setminus \Omega; \\ U^{\mathrm{trans}} \text{ solves the poroelastic equations (1.16) in } \Omega; \\ (\mathrm{p}_{\mathrm{flu}}, \mathbf{u}_{\mathrm{flu}}) \text{ are outgoing in the sense of } \lim\limits_{r\to\infty} \sqrt{r} \left(\dfrac{\partial \mathrm{p}_{\mathrm{flu}}}{\partial r} - \mathrm{i}\, \omega\, \mathsf{s}_{\mathrm{flu}}\, \mathrm{p}_{\mathrm{flu}} \right) = 0\,; \\ \text{Boundary conditions on the interface } \Gamma : (1.21) \\ \quad (\mathbf{u}_{\mathrm{flu}} - \mathbf{u}) \cdot \boldsymbol{n} = \mathbf{w} \cdot \boldsymbol{n}\,, \\ \quad \mathrm{p}_{\mathrm{flu}} - \mathrm{p} = \dfrac{1}{\kappa_\Gamma}\, \mathbf{w} \cdot \boldsymbol{n}\,, \\ \quad \boldsymbol{\tau}\, \boldsymbol{n} = -\mathrm{p}_{\mathrm{flu}} \cdot \boldsymbol{n}\,. \end{cases} \tag{2.42}$$

where κ_Γ denotes the hydraulic permeability on the interface.

We will distinguish three different cases for κ_Γ, we first consider a finite value of κ_Γ in 2.5.1.1. Then when $\kappa_\Gamma \to \infty$, the pores are open, and the second condition in Section (2.42) becomes $\mathrm{p}_{\mathfrak{flu}} - \mathrm{p} = 0$. This case is detailed in Section 2.5.1.2. We finally study the case of sealed pores in Section 2.5.1.3. This means that $\kappa_\Gamma = 0$, and the second interface condition is modified as $\mathbf{w} \cdot \boldsymbol{n} = 0$.

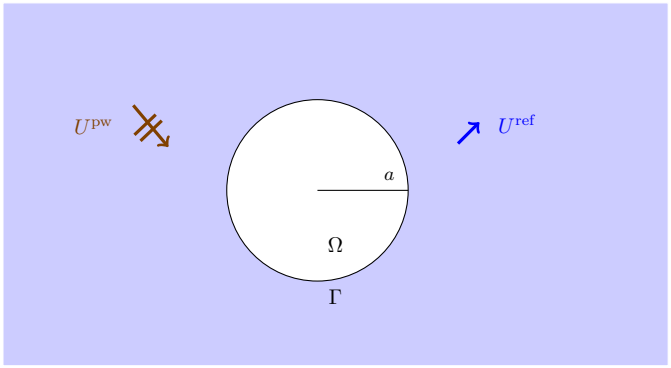

Figure 2.17: Scattering of a fluid plane wave by a poroelastic inclusion. The inclusion occupies the domain denoted by Ω. The cross section of the inclusion is a disc of radius denoted by $\mathfrak{a}$.

2.5.1 Construction of the analytical solution

In the fluid, the pressure and the velocities are expressed as follows:

$$\mathrm{p}_{\mathfrak{flu}} = \mathrm{p}^{\mathrm{pw}} + \mathrm{p}^{\mathrm{ref}}, \qquad \mathbf{u}_{\mathfrak{flu}} = \mathbf{u}^{\mathrm{pw}} + \mathbf{u}^{\mathrm{ref}}.$$

The pressure $\mathrm{p}_{\mathfrak{flu}}$ satisfies the Helmholtz equation. In the fluid,

$$\mathbf{u}_{\mathfrak{flu}} = -\frac{1}{\rho_{\mathfrak{flu}}\,\mathfrak{s}\,\mathrm{i}\,\omega}\nabla\,\mathrm{p}_{\mathfrak{flu}} = \frac{\mathfrak{s}\,\mathrm{i}}{\rho_{\mathfrak{flu}}\,\omega}\nabla\,\mathrm{p}_{\mathfrak{flu}}.$$

The incident plane wave is

$$\mathrm{p}^{\mathrm{pw}}_{\mathfrak{flu}} = \sum_{k=-\infty}^{\infty} \mathrm{i}^k\, J_k(\mathfrak{s}\,\omega\,\mathsf{s}_{\mathfrak{flu}}\,r)\; e^{\mathrm{i}\,k(\theta-\alpha_{\mathrm{inc}})},$$

$$\Rightarrow \mathbf{u}^{\mathrm{pw}}_{\mathfrak{flu}} = \sum_{k=-\infty}^{\infty} \frac{\mathfrak{s}\,\mathrm{i}^{k+1}}{\rho_{\mathfrak{flu}}\,\omega}\nabla\, J_k(\mathfrak{s}\,\omega\,\mathsf{s}_{\mathfrak{flu}}\,r)\; e^{\mathrm{i}\,k(\theta-\alpha_{\mathrm{inc}})}.$$

The reflected wave is written as:

$$\mathrm{p}^{\mathrm{ref}}_{\mathfrak{flu}} = \sum_{k\in\mathbb{Z}} d_k\,\mathrm{H}^{(1)}_k(\omega\,\mathsf{s}_{\mathfrak{flu}}\,r)\; e^{\mathrm{i}\,k\,\theta},$$

$$\Rightarrow \mathbf{u}^{\mathrm{ref}}_{\mathfrak{flu}} = \sum_{k\in\mathbb{Z}} \frac{\mathfrak{s}\,\mathrm{i}}{\rho_{\mathfrak{flu}}\,\omega} d_k\,\nabla\,\mathrm{H}^{(1)}_k(\omega\,\mathsf{s}_{\mathfrak{flu}}\,r)\; e^{\mathrm{i}\,k\,\theta}.$$

In polar coordinates, using $\nabla = \partial_r \mathbf{e}_r + \frac{1}{r}\partial_\theta \mathbf{e}_\theta$, the radial component is:

$$\mathbf{u}^{\mathrm{pw}}_{\mathfrak{flu},r} = \sum_{k\in\mathbb{Z}} \frac{\mathsf{s}_{\mathfrak{flu}}}{\rho_{\mathfrak{flu}}}\,\mathrm{i}^{k+1}\,J'_k(\mathfrak{s}\,\omega\,\mathsf{s}_{\mathfrak{flu}}\,r)\; e^{\mathrm{i}\,k(\theta-\alpha_{\mathrm{inc}})},$$

$$\mathbf{u}^{\mathrm{ref}}_{\mathfrak{flu},r} = \sum_{k\in\mathbb{Z}} \frac{\mathfrak{s}\,\mathsf{s}_{\mathfrak{flu}}}{\rho_{\mathfrak{flu}}}\,\mathrm{i}\,d_k\,\mathrm{H}^{(1)'}_k(\omega\,\mathsf{s}_{\mathfrak{flu}}\,r)\; e^{\mathrm{i}\,k\,\theta}.$$

In the poroelastic domain Ω, the potentials and the expressions of the unknowns are given in Section 2.2 equations (2.24) and (2.27).

2.5.1.1 Finite positive value of hydraulic permeability

On a disc, $\boldsymbol{n} = \mathbf{e}_r$. Imposing the transmission condition (1.21) means that for every mode k:

$$
\begin{aligned}
&\frac{\mathsf{s}_{\text{flu}}}{\rho_{\text{flu}}}\,\mathrm{i}^{k+1}\,J_k'(\omega\,\mathsf{s}_{\text{flu}}\,r)\;e^{-\mathrm{i}\,k\alpha_{\text{inc}}} \;+\; \frac{\mathfrak{s}\,\mathsf{s}_{\text{flu}}}{\rho_{\text{flu}}}\,\mathrm{i}\,d_k\,\mathrm{H}_k^{(1)'}(\omega\,\mathsf{s}_{\text{flu}}\,r)\\
&+\; a_k\,\mathfrak{s}\,\frac{\mathrm{i}}{\mathsf{s}_{\text{P}}}\,\mathrm{J}_k'(\omega\,\mathsf{s}_{\text{P}}\,\mathfrak{a}) \;+\; b_k\,\mathfrak{s}\,\frac{\mathrm{i}}{\mathsf{s}_{\text{B}}}\,\mathrm{J}_k'(\omega\,\mathsf{s}_{\text{B}}\,\mathfrak{a}) \;+\; c_k\,\frac{\mathfrak{s}\,k}{\mathfrak{a}\,\mathsf{s}_{\text{S}}^2\,\omega}\mathrm{J}_k(\omega\,\mathsf{s}_{\text{S}}\,\mathfrak{a})\\
&=-\,a_k\,\mathfrak{s}\,\frac{\mathrm{i}\,\mathcal{W}_{\text{P}}}{\mathsf{s}_{\text{P}}}\,\mathrm{J}_k'(\omega\,\mathsf{s}_{\text{P}}\,\mathfrak{a}) \;-\; b_k\,\mathfrak{s}\,\frac{\mathrm{i}\,\mathcal{W}_{\text{B}}}{\mathsf{s}_{\text{B}}}\,\mathrm{J}_k'(\omega\,\mathsf{s}_{\text{B}}\,\mathfrak{a}) \;+\; c_k\,\frac{\rho_f\,\mu_{\text{fr}}}{\det A}\,\frac{\mathfrak{s}\,k}{\mathfrak{a}\,\omega}\mathrm{J}_k(\omega\,\mathsf{s}_{\text{S}}\,\mathfrak{a})\,,
\end{aligned}
$$

$$
\begin{aligned}
&d_k\,\mathrm{H}_k^{(1)}(\omega\,\mathsf{s}_{\text{flu}}\,\mathfrak{a}) \;+\; \mathrm{i}^k\,J_k(\omega\,\mathsf{s}_{\text{flu}}\,\mathfrak{a})\;e^{-\mathrm{i}\,k\alpha_{\text{inc}}}\\
&+\; a_k\,M\left(\mathcal{W}_{\text{P}} \;+\; \alpha\right)\mathrm{J}_k(\omega\,\mathsf{s}_{\text{P}}\,\mathfrak{a}) \;+\; b_k\,M\left(\mathcal{W}_{\text{B}} \;+\; \alpha\right)\mathrm{J}_k(\omega\,\mathsf{s}_{\text{P}}\,\mathfrak{a})\\
&=-\,a_k\,\mathfrak{s}\,\frac{\mathrm{i}\,\mathcal{W}_{\text{P}}}{\mathsf{s}_{\text{P}}\,\kappa_\Gamma}\,\mathrm{J}_k'(\omega\,\mathsf{s}_{\text{P}}\,\mathfrak{a}) \;-\; b_k\,\mathfrak{s}\,\frac{\mathrm{i}\,\mathcal{W}_{\text{B}}}{\mathsf{s}_{\text{B}}\,\kappa_\Gamma}\,\mathrm{J}_k'(\omega\,\mathsf{s}_{\text{B}}\,\mathfrak{a}) \;+\; c_k\,\frac{\rho_f\,\mu_{\text{fr}}}{\det A}\,\frac{\mathfrak{s}\,k}{\mathfrak{a}\,\omega\,\kappa_\Gamma}\mathrm{J}_k(\omega\,\mathsf{s}_{\text{S}}\,\mathfrak{a})\,,
\end{aligned}
$$

$$
\begin{aligned}
&-\frac{2\,\mu_{\text{fr}}\,\omega}{\mathsf{s}_{\text{P}}\mathfrak{a}}\,a_k\,\mathrm{J}_{k+1}(\omega\,\mathsf{s}_{\text{P}}\,\mathfrak{a}) \;+\; \frac{2\,\mu_{\text{fr}}\,k}{\mathsf{s}_{\text{P}}^2\mathfrak{a}^2}\,a_k\,\mathrm{J}_k(\omega\,\mathsf{s}_{\text{P}}\,\mathfrak{a}) \;+2\,\mu_{\text{fr}}\,a_k\,\omega^2\,\mathrm{J}_k(\omega\,\mathsf{s}_{\text{P}}\,\mathfrak{a})\\
&-\frac{2\,\mu_{\text{fr}}\,k^2}{\mathsf{s}_{\text{P}}^2\mathfrak{a}^2}\,a_k\,\mathrm{J}_k(\omega\,\mathsf{s}_{\text{P}}\,\mathfrak{a}) \;-\; \frac{2\,\mu_{\text{fr}}\,\omega}{\mathsf{s}_{\text{B}}\mathfrak{a}}\,b_k\,\mathrm{J}_{k+1}(\omega\,\mathsf{s}_{\text{B}}\,\mathfrak{a}) \;+\; \frac{2\,\mu_{\text{fr}}\,k}{\mathsf{s}_{\text{B}}^2\mathfrak{a}^2}\,b_k\,\mathrm{J}_k(\omega\,\mathsf{s}_{\text{B}}\,\mathfrak{a})\\
&+2\,\mu_{\text{fr}}\,b_k\,\omega^2\,\mathrm{J}_k(\omega\,\mathsf{s}_{\text{B}}\,\mathfrak{a}) \;-\; \frac{2\,\mu_{\text{fr}}\,k^2}{\mathsf{s}_{\text{B}}^2\mathfrak{a}^2}\,b_k\,\mathrm{J}_k(\omega\,\mathsf{s}_{\text{B}}\,\mathfrak{a}) \;+\; \frac{2\,\mu_{\text{fr}}}{\mathsf{s}_{\text{S}}\mathfrak{a}}\;c_k\,\omega\,\mathrm{i}k\,\mathrm{J}_k'(\omega\,\mathsf{s}_{\text{S}}\,\mathfrak{a})\\
&+\omega^2\left(-\tfrac{2}{3}\mu_{\text{fr}} \;+\mathrm{k}_{\text{fr}} \;+M\alpha^2+\alpha M\mathcal{W}_{\text{P}}\right)\,a_k\mathrm{J}_k(\omega\,\mathsf{s}_{\text{P}}\,\mathfrak{a}) \;+\omega^2\left(-\tfrac{2}{3}\mu_{\text{fr}}+\mathrm{k}_{\text{fr}}+M\alpha^2+\alpha M\mathcal{W}_{\text{B}}\right)\,b_k\mathrm{J}_k(\omega\,\mathsf{s}_{\text{B}}\,\mathfrak{a})\\
&\quad=-\omega^2\,d_k\,\mathrm{H}_k^{(1)}(\omega\,\mathsf{s}_{\text{flu}}\,\mathfrak{a}) \;-\; \omega^2\mathrm{i}^k\,J_k(\omega\,\mathsf{s}_{\text{flu}}\,\mathfrak{a})\;e^{-\mathrm{i}\,k\alpha_{\text{inc}}}\,,
\end{aligned}
$$

$$
\begin{aligned}
&-\frac{2\,\mu_{\text{fr}}\omega\,\mathrm{i}\,k}{\mathfrak{a}\,\mathsf{s}_{\text{P}}}\,a_k\,\mathrm{J}_k'(\omega\,\mathsf{s}_{\text{P}}\,\mathfrak{a}) \;+\; \frac{2\,\mathrm{i}\,\mu_{\text{fr}}\,k}{\mathfrak{a}^2\,\mathsf{s}_{\text{P}}^2}\,a_k\,\mathrm{J}_k(\omega\,\mathsf{s}_{\text{P}}\,\mathfrak{a}) \;-\; \frac{2\,\mu_{\text{fr}}\omega\,\mathrm{i}\,k}{\mathfrak{a}\,\mathsf{s}_{\text{B}}}\,b_k\,\mathrm{J}_k'(\omega\,\mathsf{s}_{\text{B}}\,\mathfrak{a})\\
&\quad+\frac{2\,\mathrm{i}\,\mu_{\text{fr}}\,k}{\mathfrak{a}^2\,\mathsf{s}_{\text{B}}^2}\,b_k\,\mathrm{J}_k(\omega\,\mathsf{s}_{\text{B}}\,\mathfrak{a}) \;-\; \frac{\mu_{\text{fr}}\,k^2}{\mathfrak{a}^2\,\mathsf{s}_{\text{S}}^2}\,c_k\,\mathrm{J}_k(\omega\,\mathsf{s}_{\text{S}}\,\mathfrak{a}) \;+\; \frac{\mu_{\text{fr}}\,\omega}{\mathfrak{a}\,\mathsf{s}_{\text{S}}}\,c_k\,\mathrm{J}_k'(\omega\,\mathsf{s}_{\text{S}}\,\mathfrak{a})\\
&\quad-\;\mu_{\text{fr}}\,\frac{\omega}{\mathsf{s}_{\text{S}}\mathfrak{a}}\,c_k\,\mathrm{J}_{k+1}(\omega\,\mathsf{s}_{\text{S}}\,\mathfrak{a}) \;+\mu_{\text{fr}}\,\frac{k}{\mathsf{s}_{\text{S}}^2\mathfrak{a}^2}c_k\,\mathrm{J}_k(\omega\,\mathsf{s}_{\text{S}}\,\mathfrak{a})\\
&\quad+\;\omega^2\,\mu_{\text{fr}}\,c_k\,\mathrm{J}_k(\omega\,\mathsf{s}_{\text{S}}\,\mathfrak{a}) \;-\; \mu_{\text{fr}}\,\frac{k^2}{\mathsf{s}_{\text{S}}^2\mathfrak{a}^2}\,c_k\,\mathrm{J}_k(\omega\,\mathsf{s}_{\text{S}}\,\mathfrak{a}) \;=0\,.
\end{aligned}
$$

We can build a linear system satisfied by a_k, b_k, c_k, d_k in each mode k.

$$
\mathbb{A}_k^{\text{flu-poro}}\begin{pmatrix} a_k\\ b_k\\ c_k\\ d_k\end{pmatrix} = \begin{pmatrix} -\dfrac{\mathsf{s}_{\text{flu}}}{\rho_{\text{flu}}}\,\mathrm{i}^{k+1}\,J_k'(\omega\,\mathsf{s}_{\text{flu}}\,\mathfrak{a})\;e^{-\mathrm{i}\,k\alpha_{\text{inc}}}\\ -\mathrm{i}^k\,J_k(\omega\,\mathsf{s}_{\text{flu}}\,\mathfrak{a})\;e^{-\mathrm{i}\,k\alpha_{\text{inc}}}\\ -\,\omega^2\,\mathrm{i}^k\,J_k(\omega\,\mathsf{s}_{\text{flu}}\,\mathfrak{a})\;e^{-\mathrm{i}\,k\alpha_{\text{inc}}}\\ 0\end{pmatrix}
$$

with

$$
\mathbb{A}_k^{\text{flu-poro}} = \begin{pmatrix} A_{11} & A_{12} & A_{13} & A_{14}\\ A_{21} & A_{22} & A_{23} & A_{24}\\ A_{31} & A_{32} & A_{33} & A_{34}\\ A_{41} & A_{42} & A_{43} & A_{44}\end{pmatrix} \tag{2.43}
$$

$$A_{11} = \frac{\mathfrak{s}\,\mathrm{i}}{\mathsf{s}_\mathrm{P}}\,\mathrm{J}_k'(\omega\,\mathsf{s}_\mathrm{P}\,\mathfrak{a}) + \frac{\mathcal{W}_\mathrm{P}\,\mathfrak{s}\,\mathrm{i}}{\mathsf{s}_\mathrm{P}}\,\mathrm{J}_k'(\omega\,\mathsf{s}_\mathrm{P}\,\mathfrak{a})\,, \quad A_{12} = \frac{\mathfrak{s}\,\mathrm{i}}{\mathsf{s}_\mathrm{B}}\,\mathrm{J}_k'(\omega\,\mathsf{s}_\mathrm{B}\,\mathfrak{a}) + \frac{\mathcal{W}_\mathrm{B}\,\mathfrak{s}\,\mathrm{i}}{\mathsf{s}_\mathrm{B}}\,\mathrm{J}_k'(\omega\,\mathsf{s}_\mathrm{B}\,\mathfrak{a})\,,$$

$$A_{13} = \frac{\mathfrak{s}\,k}{\omega\,\mathsf{s}_\mathrm{S}^2\,\mathfrak{a}}\mathrm{J}_k(\omega\,\mathsf{s}_\mathrm{S}\,\mathfrak{a}) - \frac{\rho_f\,\mu_\mathrm{fr}\,\mathfrak{s}\,k}{\det A\,\omega\,\mathfrak{a}}\mathrm{J}_k(\omega\,\mathsf{s}_\mathrm{S}\,\mathfrak{a})\,, \quad A_{14} = \frac{\mathfrak{s}\,\mathsf{s}_\mathrm{flu}}{\rho_\mathrm{flu}}\,\mathrm{i}\,\mathrm{H}_k^{(1)'}(\omega\,\mathsf{s}_\mathrm{flu}\,\mathfrak{a})\,,$$

$$A_{21} = M\left(\mathcal{W}_\mathrm{P} + \alpha\right)\mathrm{J}_k(\omega\,\mathsf{s}_\mathrm{P}\,\mathfrak{a}) + \frac{\mathcal{W}_\mathrm{P}\,\mathfrak{s}\,\mathrm{i}}{\kappa_\Gamma\,\mathsf{s}_\mathrm{P}}\,\mathrm{J}_k'(\omega\,\mathsf{s}_\mathrm{P}\,\mathfrak{a})\,, \quad A_{22} = M\left(\mathcal{W}_\mathrm{B} + \alpha\right)\mathrm{J}_k(\omega\,\mathsf{s}_\mathrm{B}\,\mathfrak{a}) + \frac{\mathcal{W}_\mathrm{B}\,\mathfrak{s}\,\mathrm{i}}{\kappa_\Gamma\,\mathsf{s}_\mathrm{B}}\,\mathrm{J}_k'(\omega\,\mathsf{s}_\mathrm{B}\,\mathfrak{a})\,,$$

$$A_{23} = -\frac{\mathfrak{s}\,k\,\rho_f\,\mu_\mathrm{fr}}{\kappa_\Gamma\,\omega\,\det A\,\mathfrak{a}}\mathrm{J}_k(\omega\,\mathsf{s}_\mathrm{S}\,\mathfrak{a})\,, \qquad A_{24} = \mathrm{H}_k^{(1)}(\omega\,\mathsf{s}_\mathrm{flu}\,\mathfrak{a})\,,$$

$$\begin{aligned} A_{31} = &-\frac{2\,\mu_\mathrm{fr}\,\omega}{\mathsf{s}_\mathrm{P}\mathfrak{a}}\,\mathrm{J}_{k+1}(\omega\,\mathsf{s}_\mathrm{P}\,\mathfrak{a}) + \frac{2\,\mu_\mathrm{fr}\,k}{\mathsf{s}_\mathrm{P}^2\mathfrak{a}^2}\,\mathrm{J}_k(\omega\,\mathsf{s}_\mathrm{P}\,\mathfrak{a}) + 2\,\mu_\mathrm{fr}\,\omega^2\,\mathrm{J}_k(\omega\,\mathsf{s}_\mathrm{P}\,\mathfrak{a}) - \frac{2\,\mu_\mathrm{fr}\,k^2}{\mathsf{s}_\mathrm{P}^2\mathfrak{a}^2}\,\mathrm{J}_k(\omega\,\mathsf{s}_\mathrm{P}\,\mathfrak{a}) \\ &+ \omega^2\left(-\tfrac{2}{3}\mu_\mathrm{fr} + \mathrm{k}_\mathrm{fr} + M\alpha^2 + \alpha\,M\mathcal{W}_\mathrm{P}\right)\mathrm{J}_k(\omega\,\mathsf{s}_\mathrm{P}\,\mathfrak{a})\,, \end{aligned}$$

$$\begin{aligned} A_{32} = &-\frac{2\,\mu_\mathrm{fr}\,\omega}{\mathsf{s}_\mathrm{B}\mathfrak{a}}\,\mathrm{J}_{k+1}(\omega\,\mathsf{s}_\mathrm{B}\,\mathfrak{a}) + \frac{2\,\mu_\mathrm{fr}\,k}{\mathsf{s}_\mathrm{B}^2\mathfrak{a}^2}\,\mathrm{J}_k(\omega\,\mathsf{s}_\mathrm{B}\,\mathfrak{a}) + 2\,\mu_\mathrm{fr}\,\omega^2\,\mathrm{J}_k(\omega\,\mathsf{s}_\mathrm{B}\,\mathfrak{a}) - \frac{2\,\mu_\mathrm{fr}\,k^2}{\mathsf{s}_\mathrm{B}^2\mathfrak{a}^2}\,\mathrm{J}_k(\omega\,\mathsf{s}_\mathrm{B}\,\mathfrak{a}) \\ &+ \omega^2\left(-\tfrac{2}{3}\mu_\mathrm{fr} + \mathrm{k}_\mathrm{fr} + M\alpha^2 + \alpha\,M\mathcal{W}_\mathrm{B}\right)\mathrm{J}_k(\omega\,\mathsf{s}_\mathrm{B}\,\mathfrak{a})\,, \end{aligned}$$

$$A_{33} = \frac{2\,\mu_\mathrm{fr}}{\mathsf{s}_\mathrm{S}\mathfrak{a}}\,\omega\,\mathrm{i}k\,\mathrm{J}_k'(\omega\,\mathsf{s}_\mathrm{S}\,\mathfrak{a})\,, \qquad A_{34} = \omega^2\,\mathrm{H}_k^{(1)}(\omega\,\mathsf{s}_\mathrm{flu}\,\mathfrak{a})\,,$$

and

$$A_{41} = -\frac{2\,\mu_\mathrm{fr}\omega\,\mathrm{i}\,k}{\mathfrak{a}\,\mathsf{s}_\mathrm{P}}\,\mathrm{J}_k'(\omega\,\mathsf{s}_\mathrm{P}\,\mathfrak{a}) + \frac{2\,\mathrm{i}\,\mu_\mathrm{fr}\,k}{\mathfrak{a}^2\,\mathsf{s}_\mathrm{P}^2}\,\mathrm{J}_k(\omega\,\mathsf{s}_\mathrm{P}\,\mathfrak{a})\,, \quad A_{42} = -\frac{2\,\mu_\mathrm{fr}\omega\,\mathrm{i}\,k}{\mathfrak{a}\,\mathsf{s}_\mathrm{B}}\,\mathrm{J}_k'(\omega\,\mathsf{s}_\mathrm{B}\,\mathfrak{a}) + \frac{2\,\mathrm{i}\,\mu_\mathrm{fr}\,k}{\mathfrak{a}^2\,\mathsf{s}_\mathrm{B}^2}\,\mathrm{J}_k(\omega\,\mathsf{s}_\mathrm{B}\,\mathfrak{a})\,,$$

$$\begin{aligned} A_{43} = &-\frac{\mu_\mathrm{fr}\,k^2}{\mathfrak{a}^2\,\mathsf{s}_\mathrm{S}^2}\,\mathrm{J}_k(\omega\,\mathsf{s}_\mathrm{S}\,\mathfrak{a}) + \frac{\mu_\mathrm{fr}\,\omega}{\mathfrak{a}\,\mathsf{s}_\mathrm{S}}\,\mathrm{J}_k'(\omega\,\mathsf{s}_\mathrm{S}\,\mathfrak{a}) - \mu_\mathrm{fr}\,\frac{\omega}{\mathsf{s}_\mathrm{S}\mathfrak{a}}\,\mathrm{J}_{k+1}(\omega\,\mathsf{s}_\mathrm{S}\,\mathfrak{a}) + \mu_\mathrm{fr}\,\frac{k}{\mathsf{s}_\mathrm{S}^2\mathfrak{a}^2}\,\mathrm{J}_k(\omega\,\mathsf{s}_\mathrm{S}\,\mathfrak{a}) \\ &+ \omega^2\,\mu_\mathrm{fr}\,\mathrm{J}_k(\omega\,\mathsf{s}_\mathrm{S}\,\mathfrak{a}) - \mu_\mathrm{fr}\,\frac{k^2}{\mathsf{s}_\mathrm{S}^2\mathfrak{a}^2}\,\mathrm{J}_k(\omega\,\mathsf{s}_\mathrm{S}\,\mathfrak{a})\,, \end{aligned}$$

$$A_{44} = 0\,.$$

2.5.1.2 Open pores

If the hydraulic permeability $\kappa_\Gamma \to \infty$, the second equation becomes:

$$\begin{aligned} &d_k\,\mathrm{H}_k^{(1)}(\omega\,\mathsf{s}_\mathrm{flu}\,\mathfrak{a}) + \mathrm{i}^k\,J_k(\omega\,\mathsf{s}_\mathrm{flu}\,\mathfrak{a})\,e^{-\mathrm{i}\,k\alpha_\mathrm{inc}} \\ &-\left(-\,a_k\,M\left(\mathcal{W}_\mathrm{P} + \alpha\right)\mathrm{J}_k(\omega\,\mathsf{s}_\mathrm{P}\,\mathfrak{a}) - b_k\,M\left(\mathcal{W}_\mathrm{B} + \alpha\right)\mathrm{J}_k(\omega\,\mathsf{s}_\mathrm{P}\,\mathfrak{a})\right) = 0\,. \end{aligned}$$

Thus, the system is:

$$\mathbb{A}_k^{\text{flu-poro}}\begin{pmatrix} a_k \\ b_k \\ c_k \\ d_k \end{pmatrix} = \begin{pmatrix} -\dfrac{\mathsf{s}_\mathrm{flu}}{\rho_\mathrm{flu}}\,\mathrm{i}^{k+1}\,J_k'(\omega\,\mathsf{s}_\mathrm{flu}\,\mathfrak{a})\,e^{-\mathrm{i}\,k\alpha_\mathrm{inc}} \\ -\mathrm{i}^k\,J_k(\omega\,\mathsf{s}_\mathrm{flu}\,\mathfrak{a})\,e^{-\mathrm{i}\,k\alpha_\mathrm{inc}} \\ -\,\omega^2\,\mathrm{i}^k\,J_k(\omega\,\mathsf{s}_\mathrm{flu}\,\mathfrak{a})\,e^{-\mathrm{i}\,k\alpha_\mathrm{inc}} \\ 0 \end{pmatrix} \tag{2.44}$$

The second row is modified as:

$$A_{21} = M\left(\mathcal{W}_\mathrm{P} + \alpha\right)\mathrm{J}_k(\omega\,\mathsf{s}_\mathrm{P}\,\mathfrak{a})\,, \quad A_{22} = M\left(\mathcal{W}_\mathrm{B} + \alpha\right)\mathrm{J}_k(\omega\,\mathsf{s}_\mathrm{B}\,\mathfrak{a})\,, \qquad A_{23} = 0,\,, \quad A_{24} = \mathrm{H}_k^{(1)}(\omega\,\mathsf{s}_\mathrm{flu}\,\mathfrak{a})\,.$$

2.5.1.3 Sealed pores

If the hydraulic permeability $\kappa_\Gamma = 0$, the second equation is:

$$a_k\,\frac{\mathcal{W}_\mathrm{P}}{\mathsf{s}_\mathrm{P}}\,\omega\,\mathrm{J}_k'(\omega\,\mathsf{s}_\mathrm{P}\,\mathfrak{a}) + b_k\,\frac{\mathcal{W}_\mathrm{B}}{\mathsf{s}_\mathrm{B}}\,\omega\,\mathrm{J}_k'(\omega\,\mathsf{s}_\mathrm{B}\,\mathfrak{a}) + c_k\,\frac{\rho_f\,\mu_\mathrm{fr}}{\det A}\,\frac{\mathrm{i}k}{\mathfrak{a}}\mathrm{J}_k(\omega\,\mathsf{s}_\mathrm{S}\,\mathfrak{a}) = 0\,.$$

In this case, the system is:

$$\mathbb{A}_k^{\text{flu-poro}} \begin{pmatrix} a_k \\ b_k \\ c_k \\ d_k \end{pmatrix} = \begin{pmatrix} -\frac{\mathsf{s}_{\text{flu}}}{\rho_{\text{flu}}}\, \mathrm{i}^{k+1}\, J_k'(\omega\, \mathsf{s}_{\text{flu}}\, \mathfrak{a})\; e^{-\mathrm{i}\, k \alpha_{\text{inc}}} \\ 0 \\ -\omega^2\, \mathrm{i}^k\, J_k(\omega\, \mathsf{s}_{\text{flu}}\, \mathfrak{a})\; e^{-\mathrm{i}\, k \alpha_{\text{inc}}} \\ 0 \end{pmatrix} \tag{2.45}$$

The second row is modified as:

$$A_{21} = \frac{\mathcal{W}_{\text{P}}\, \omega}{\mathsf{s}_{\text{P}}}\, \mathrm{J}_k'(\omega\, \mathsf{s}_{\text{P}}\, \mathfrak{a})\,, \quad A_{22} = \frac{\mathcal{W}_{\text{B}}\, \omega}{\mathsf{s}_{\text{B}}}\, \mathrm{J}_k'(\omega\, \mathsf{s}_{\text{B}}\, \mathfrak{a})\,, \qquad A_{23} = \frac{\mathrm{i}\, k\, \rho_f\, \mu_{\text{fr}}}{\det A\, \mathfrak{a}} \mathrm{J}_k(\omega\, \mathsf{s}_{\text{S}}\, \mathfrak{a})\,, \quad A_{24} = 0\,.$$

We define the eigenvalues as follows:

Definition 2.8. ω is fluid-porous Jones' mode corresponding to finite, open, sealed pores if $\det \mathbb{A}_k^{\text{flu-poro}}(\omega) = 0$, where $\mathbb{A}_k^{\text{flu-poro}}$ is the coefficient matrix defined in equations (2.43), (2.44) and (2.45) correspondingly.

2.5.2 Numerical tests

In Figure 2.18, we represent the scattering of a fluid plane wave by a poroelastic inclusion. When we build the analytical solution, the exterior fluid domain is considered to be infinite. However,for the representation the solution, we only plot the field on a domain with exterior radius equal to $r = 10$m.

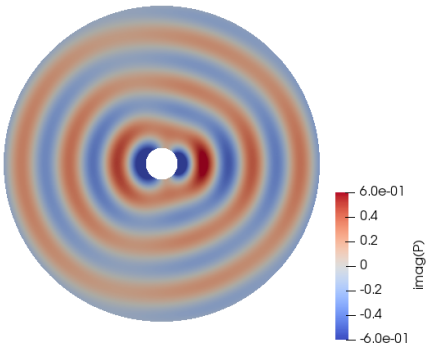

(a) $\kappa_\Gamma = \infty$ (open pores)

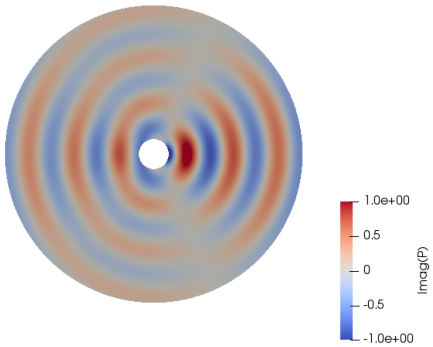

(b) $\kappa_\Gamma = 0$ (sealed pores)

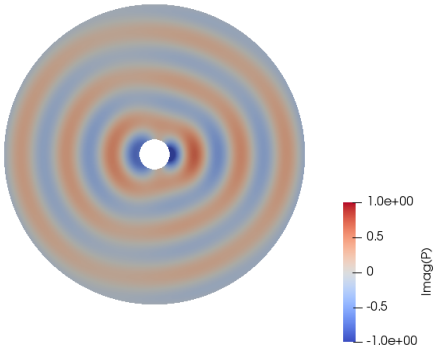

(c) $\kappa_\Gamma = 1$

Figure 2.18: Scattering of a fluid plane wave by a poroelastic inclusion. Reflected solution of the imaginary part of the pressure p for sandstone immersed in water with three values of the hydraulic permeability and no viscosity for $f = 500$ Hz.

We study the trace of the pressure in the fluid using receivers on the radius $r = 8$m for $\omega = 500$ rad.s^{-1} and we sum the modes using $N_{sum} = 50$. Next, we are carrying out six experiments with two types of material configurations: sandstone with and without viscosity. For the three cases, we consider varying hydraulic permeabilities κ_Γ:

- Finite value of κ_Γ. Here we consider $\kappa_\Gamma = 1$.
- $\kappa_\Gamma = 0$, which corresponds to sealed pores.
- $\kappa_\Gamma = \infty$, which corresponds to open pores.

For the first modes k, we will investigate the stability of the coefficient matrices. For all the tests, the cross section radius of the obstacle is $\mathfrak{a} = 1$m. The fluid parameters are given below:

$$\rho_{\text{flu}} = 10^3\, kg\,.\,m^{-3}\,, \quad \mathsf{s}_{\text{flu}} = 1500\, m\,.\,s^{-1}\,.$$

The results are respectively reported as follows:

- The trace of the pressure on a circle of receivers, located on the radius $r = 8$m is presented in figure 2.19, for the three values of hydraulic permeability.
- Water in the exterior medium and sandstone in the inclusion, for $\eta = 0$ in figures 2.21 and 2.22.
- Comparison of water in the exterior medium and sandstone in the inclusion, without viscosity and with viscosity $\eta \neq 0$ in figure 2.24.

We have the following observations:

- In this case we observe the same behaviour for all the experiments with no viscosity. All the curves represent peaks, as in Figures 2.21 and 2.22, but after zooming, some peaks have different behaviours. For most cases, the peaks are bounded from below, hence they do not correspond to generalized eigenvalues. However, few of the peaks correspond to true generalized eigenvalues. To illustrate this, we present in Figure 2.23 six zooms around the peaks for the mode 0. The three figures on the left are the ones corresponding to bounded from below peaks. The three figures on the right are the ones corresponding to true generalized eigenvalues.
- In the case with viscosity, the curves are smoother, we observe less peaks for the same range of frequency, and they are all bounded below after the zoom procedure. Hence as expected, there are no generalized eigenvalues with viscosity.
- For $\kappa_\Gamma = 0$ with viscosity, we tested every peak of $\mathbb{A}_0^{\text{flu-poro}}$, for both media, because it is the closest case to elastic-fluid scattering. All the peaks are bounded below, this means that there is no Jones' mode.
- The effect of the value of κ_Γ is limited. The cases $\kappa_\Gamma = 1$ and ∞ are similar, both for the value of the determinant and the value of the trace of the pressure. This might show that when $\kappa_\Gamma = 1$, the pores are already significantly opened. The results from Figure 2.20 confirm the fact that the value of the hydraulic permeability κ_Γ has a limited impact on the pressure field, because the curves for different values of κ_Γ are similar.
- In Figure 2.19, we study the trace of the pressure in the fluid using receivers on the radius $r = 8$m for the three values of the hydraulic permeability κ_Γ. The viscosity has not a significant impact on the pressure. Moreover, in figure 2.19b, we have added a comparison with a fluid-elastic scattering, by taking the elastic parameters the closest to the considered porous material. The comparison of the fluid-porous interaction with the fluid-elastic interaction highlights the fact that the behaviours are different, even though we took corresponding parameters between elastic and porous materials. This shows the interest of taking into account the porosity of the media.

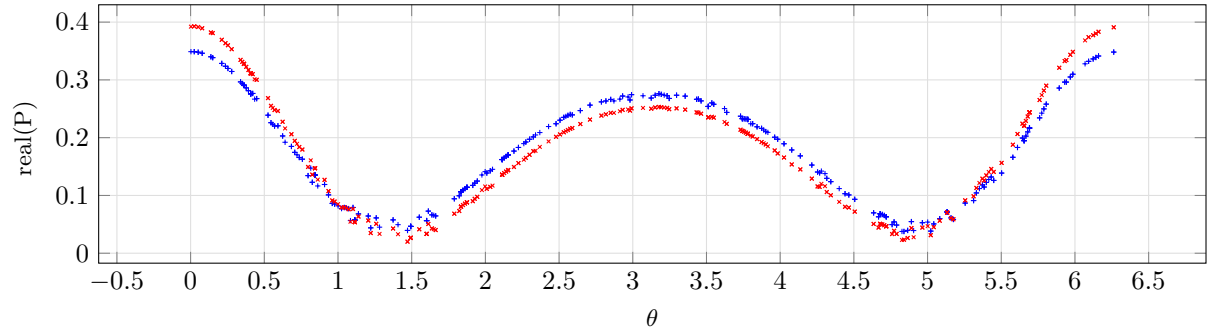

(a) $\kappa_\Gamma = 1$

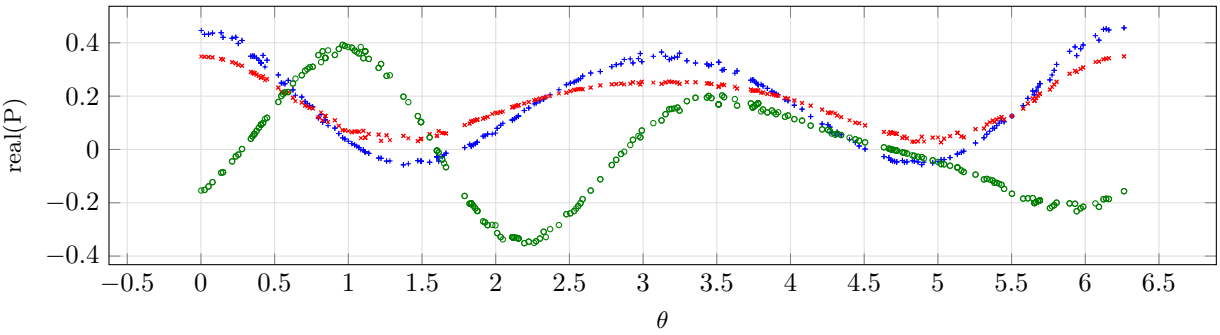

(b) $\kappa_\Gamma = 0$ (sealed pores)

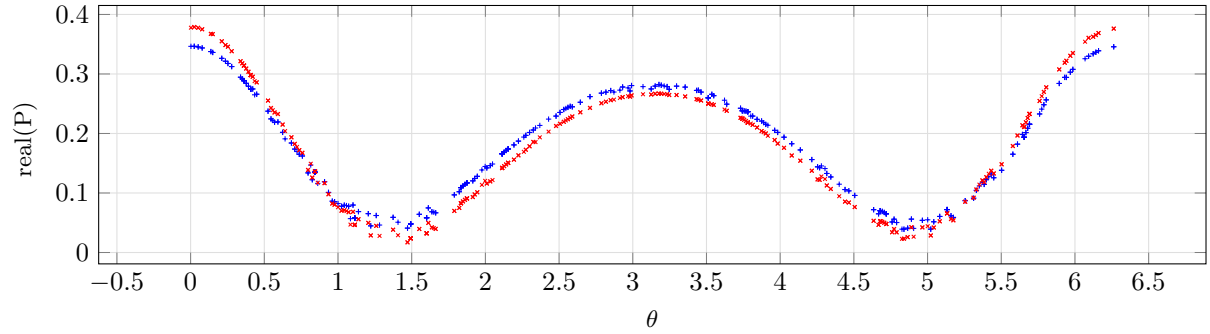

(c) $\kappa_\Gamma = \infty$ (open pores)

Figure 2.19: Experiment of fluid-solid interactions. Comparison of the trace of the pressure for a sandstone solid immersed in water with and without viscosity and for several values of the hydraulic permeability. The test was computed for $f = 500$Hz. The case with no viscosity is represented in blue $+$, while the case with viscosity $\eta = 10^{-3}$Pa.s is represented in red $\times$. The case of an elastic solid is represented in green $\circ$ (only on (b)).

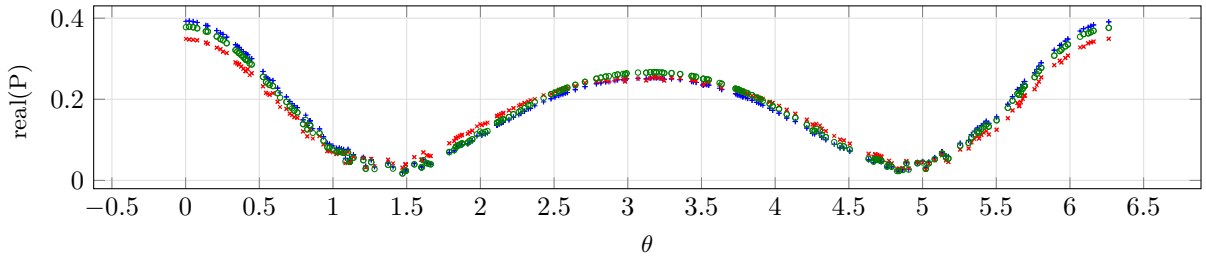

(a) $\eta = 10^{-3}$Pa.s

Figure 2.20: Experiment of a fluid-porous interaction. Comparison of the trace of the pressure for a sandstone solid immersed in water with viscosity $\eta = 10^{-3}$Pa.s for different values of the hydraulic permeability. The case $\kappa_\Gamma = 1$ is represented in blue $+$, the case with sealed pores ($\kappa_\Gamma = 0$) is represented in red $\times$, and the case of open pores ($\kappa_\Gamma = \infty$) is represented in green $\circ$.

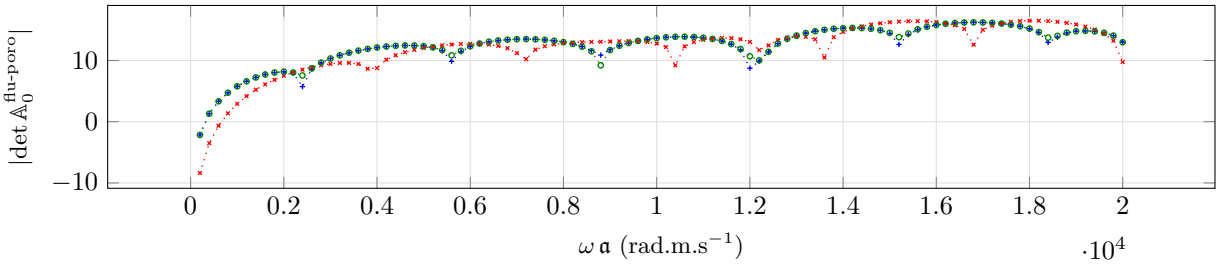

(a) Mode $k = 0$

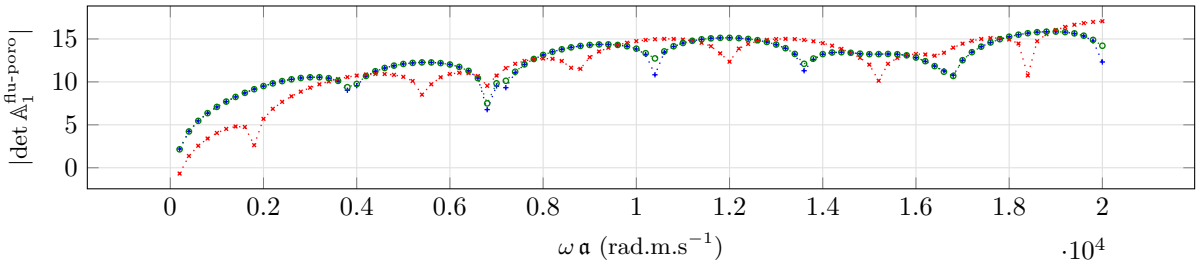

(b) Mode $k = 1$

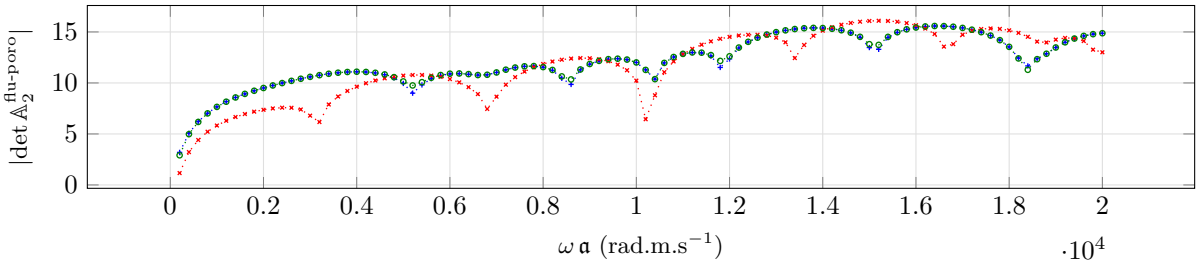

(c) Mode $k = 2$

Figure 2.21: Experiment of a fluid-porous interaction. Determinant of the coefficient matrix $\mathbb{A}_k^{\text{water-sandstone}}$ (2.43) (log scale) for k in $0:2$ for sandstone with no viscosity $\eta = 0$. $\kappa_\Gamma = 1$ is represented in blue $+$, $\kappa_\Gamma = 0$ in red $\times$ and $\kappa_\Gamma = \infty$ in green $\circ$.

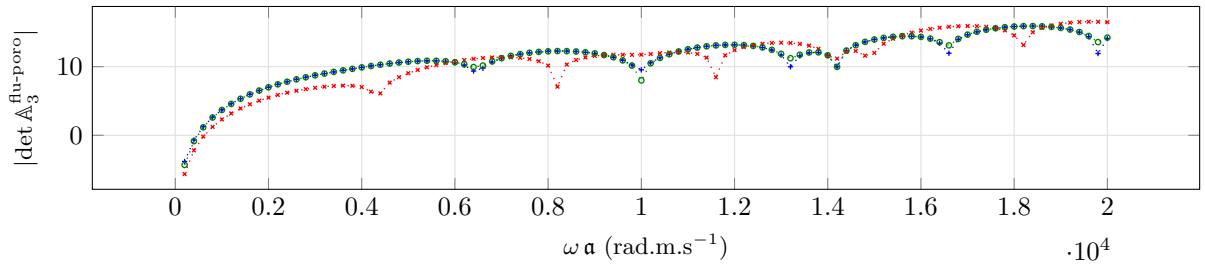

(a) Mode $k = 3$

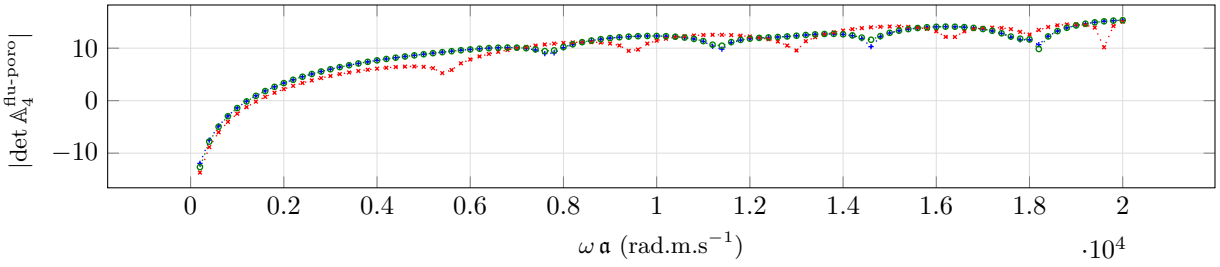

(b) Mode $k = 4$

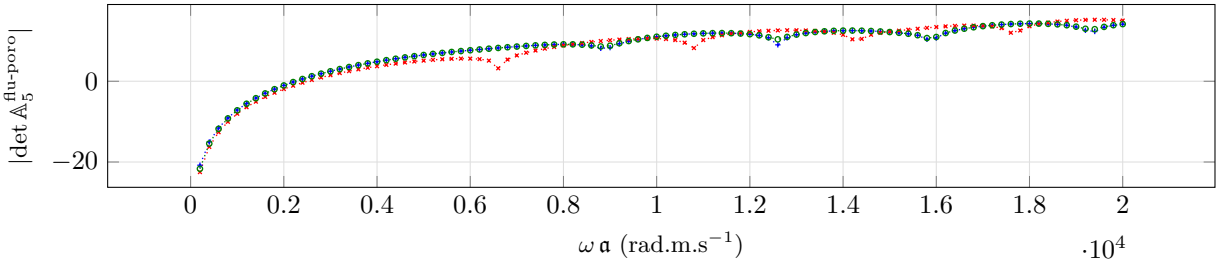

(c) Mode $k = 5$

Figure 2.22: Experiment of a fluid-porous interaction. Determinant of the coefficient matrix $\mathbb{A}_k^{\text{water-sandstone}}$ (2.43) (log scale) for k in $3:5$, for sandstone with no viscosity $\eta = 0$. $\kappa_\Gamma = 1$ is represented in blue ···+···, $\kappa_\Gamma = 0$ in red ···×··· and $\kappa_\Gamma = \infty$ in green ···○···.

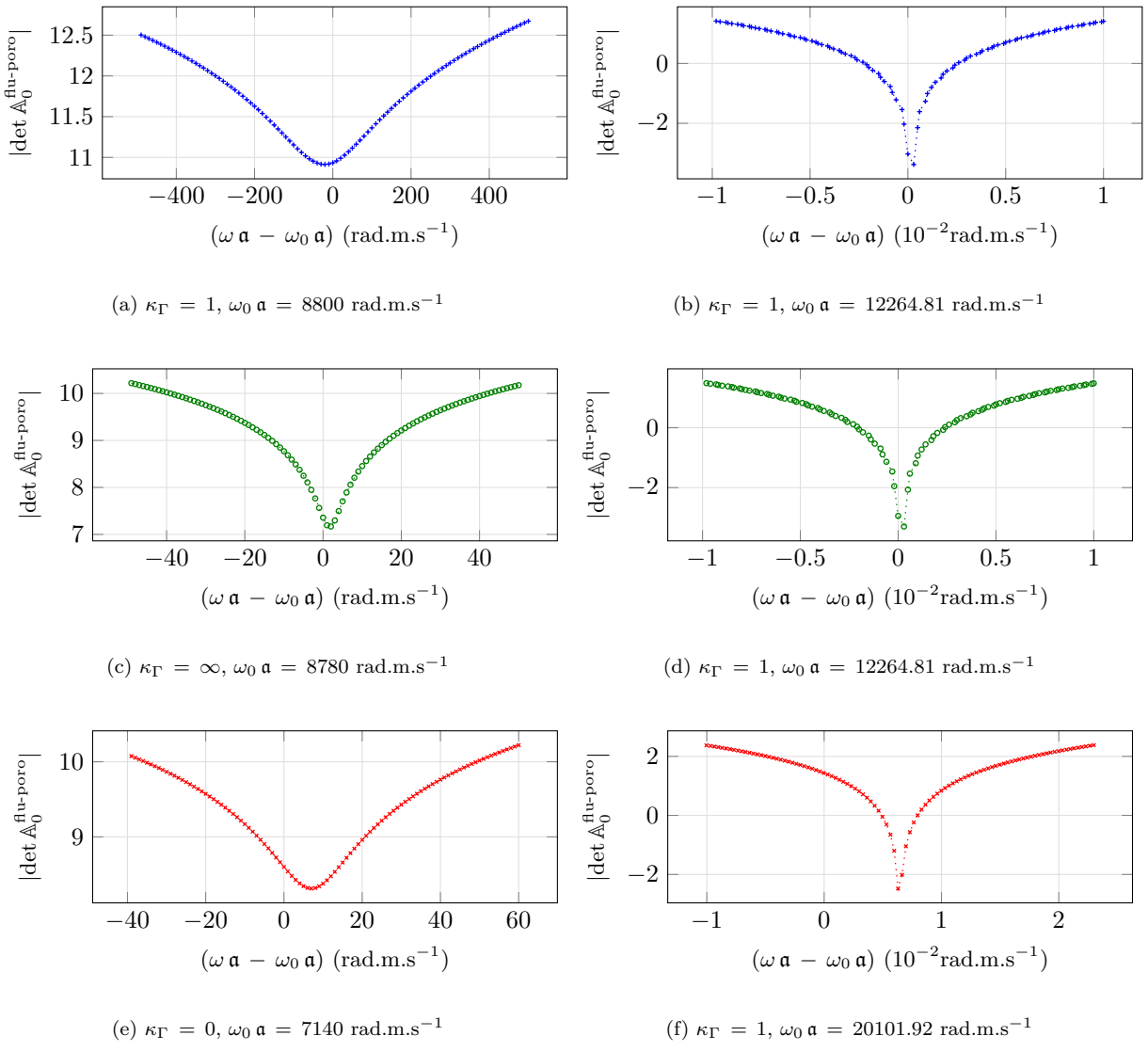

(a) $\kappa_\Gamma = 1$, $\omega_0\,\mathfrak{a} = 8800$ rad.m.s^{-1}

(b) $\kappa_\Gamma = 1$, $\omega_0\,\mathfrak{a} = 12264.81$ rad.m.s^{-1}

(c) $\kappa_\Gamma = \infty$, $\omega_0\,\mathfrak{a} = 8780$ rad.m.s^{-1}

(d) $\kappa_\Gamma = 1$, $\omega_0\,\mathfrak{a} = 12264.81$ rad.m.s^{-1}

(e) $\kappa_\Gamma = 0$, $\omega_0\,\mathfrak{a} = 7140$ rad.m.s^{-1}

(f) $\kappa_\Gamma = 1$, $\omega_0\,\mathfrak{a} = 20101.92$ rad.m.s^{-1}

Figure 2.23: Zoom of the curves of figure 2.21 at several centers denoted $\omega_0\mathfrak{a}$ for mode 0. We present the determinant of the coefficient matrix $\mathbb{A}_k^{\text{water-sandstone}}$ (2.43) (log scale) for sandstone with no viscosity $\eta = 0$. $\kappa_\Gamma = 1$ is represented in blue ····+····, $\kappa_\Gamma = 0$ in red ····×···· and $\kappa_\Gamma = \infty$ in green ····○····.

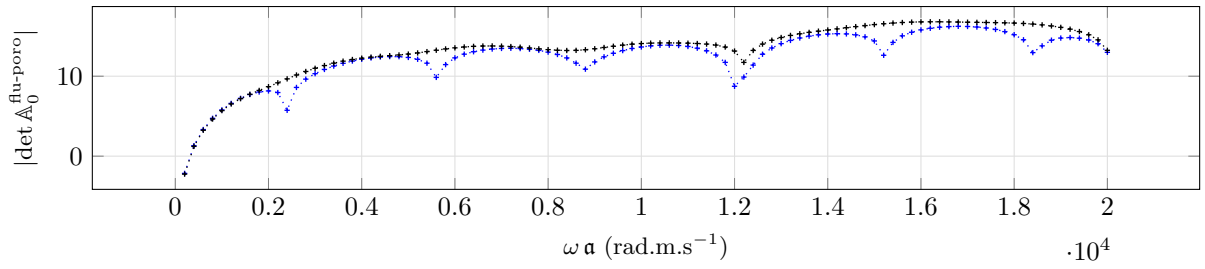

(a) Mode $k = 0$, $\kappa_\Gamma = 1$

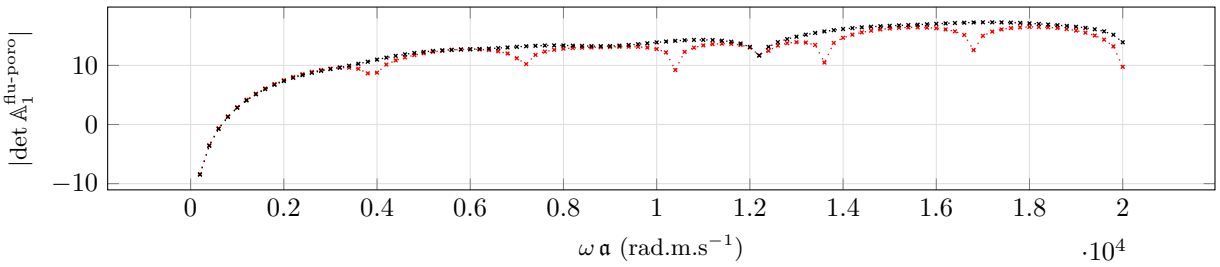

(b) Mode $k = 0$, $\kappa_\Gamma = 0$ (sealed pores)

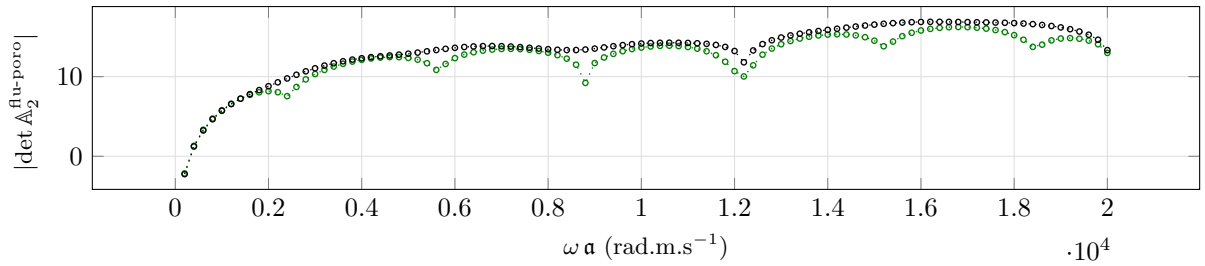

(c) Mode $k = 0$, $\kappa_\Gamma = \infty$ (open pores)

Figure 2.24: Experiment of a fluid-porous interaction. Comparison of the determinant of the coefficient matrix $\mathbb{A}_k^{\text{water-sandstone}}$ (2.43) (log scale) for $k = 0$ for sandstone with and without viscosity for three values of hydraulic permeability. The cases with no viscosity are represented in color and the viscous cases are in black.

2.6 Analytical solution for fundamental solution for poroelasticity

Here, we study analytically the response of an isotropic poroelastic medium to a point source. We consider an isotropic two-dimensional homogeneous poroelastic medium. In terms of potential, the poroelastic equations (1.16) are equivalent to equation (2.4), that we recall below:

$$-\omega^2 \begin{pmatrix} \mathrm{u} \\ \mathrm{w} \end{pmatrix} - P \begin{pmatrix} \mathrm{s_P}^{-2} & 0 \\ 0 & \mathrm{s_B}^{-2} \end{pmatrix} \begin{pmatrix} \nabla \chi_\mathrm{P} \\ \nabla \chi_\mathrm{B} \end{pmatrix} + \frac{1}{\det A} \begin{pmatrix} \rho_{\mathrm{dyn}}\, \mu_{\mathrm{fr}} & 0 \\ -\rho_f\, \mu_{\mathrm{fr}} & 0 \end{pmatrix} \begin{pmatrix} \mathbf{curl}\, \chi_\mathrm{S} \\ 0 \end{pmatrix} = A^{-1} \begin{pmatrix} \mathbf{f} \\ \tilde{\mathbf{f}} \end{pmatrix}, \tag{2.46}$$

with P given in equation (2.1). In addition, the potentials solve the Helmholtz equations:

$$\begin{aligned} \big(-\Delta - \omega^2\, \mathrm{s_P}^2\big)\, \chi_\mathrm{P} &= \pi_1 \left(P^{-1}\, B^{-1} \begin{pmatrix} \nabla \cdot \mathbf{f} \\ \nabla \cdot \tilde{\mathbf{f}} \end{pmatrix} \right), \\ \big(-\Delta - \omega^2\, \mathrm{s_B}^2\big)\, \chi_\mathrm{B} &= \pi_2 \left(P^{-1}\, B^{-1} \begin{pmatrix} \nabla \cdot \mathbf{f} \\ \nabla \cdot \tilde{\mathbf{f}} \end{pmatrix} \right), \\ \big(-\Delta - \omega^2\, \mathrm{s_S}^2\big)\, \chi_\mathrm{S} &= \mathrm{s_S}^2\, \pi_1 \left(A^{-1} \begin{pmatrix} \mathrm{curl}\mathbf{f} \\ \mathrm{curl}\tilde{\mathbf{f}} \end{pmatrix} \right). \end{aligned} \tag{2.47}$$

In the above equations, the matrices A and B are given in equations (1.25). Recall that we can write A and A^{-1} as

$$A = B\, P \begin{pmatrix} \mathrm{s_P}^2 & 0 \\ 0 & \mathrm{s_B}^2 \end{pmatrix} P^{-1} \quad ; \quad A^{-1} = P \begin{pmatrix} \mathrm{s_P}^{-2} & 0 \\ 0 & \mathrm{s_B}^{-2} \end{pmatrix} P^{-1}\, B^{-1}. \tag{2.48}$$

In order to build the analytical solution, we study in a first time a point source causing pressure waves, and secondly a source that produces only transverse waves. A point-source is modeled as a Dirac distribution, denoted by $\delta_\mathbf{Y}$ with $\mathbf{Y}$ the center of the source. We will consider the gradient and Laplacian of the Dirac in the sense of the distributions. We will use the fact that the outgoing Green kernel of

$$(-\Delta - (\omega\, \mathrm{s}_\bullet)^2)\, G(\mathbf{X}) = \delta_\mathbf{Y} \quad \text{is} \quad G_+(\mathbf{X}) = \frac{\mathrm{i}}{4} \mathrm{H}_0^{(1)}(\omega\, \mathrm{s}_\bullet |\mathbf{X} - \mathbf{Y}|), \tag{2.49}$$

with $\mathrm{H}_0^{(1)}$ the Hankel function of first-order. In the following, to simplify the notations, we note the Dirac distribution as δ, and we consider $\mathbf{Y} = 0$. Moreover, in a homogeneous infinite domain, the outgoing solution of

$$(-\Delta - (\omega\, \mathrm{s}_\bullet)^2)\, F(\mathbf{X}) = 0 \quad \text{is} \quad F_+(\mathbf{X}) = 0 \quad \text{in}\, \mathbb{R}^2. \tag{2.50}$$

2.6.1 Source in pressure waves

To model a source producing only pressure waves, we use the fact that $\mathrm{curl}\, \nabla = 0$, which leads to a null value of the transverse potential. We set $\mathbf{f} = \nabla \delta$, $\quad \tilde{\mathbf{f}} = 0$, hence, the Helmholtz equations (2.47) become

$$\begin{aligned} \big(-\Delta - \omega^2\, \mathrm{s_P}^2\big)\, \chi_\mathrm{P} &= [P^{-1}\, B^{-1}]_{11}\, \Delta\, \delta, \\ \big(-\Delta - \omega^2\, \mathrm{s_B}^2\big)\, \chi_\mathrm{B} &= [P^{-1}\, B^{-1}]_{21}\, \Delta \delta; \\ \big(-\Delta - \omega^2\, \mathrm{s_S}^2\big)\, \chi_\mathrm{S} &= 0. \end{aligned}$$

Thus, using equations (2.49) and (2.50), the poroelastic potentials are

$$\begin{aligned} \chi_\mathrm{P} &= [P^{-1}\, B^{-1}]_{11}\, \Delta\, \frac{\mathrm{i}}{4} \mathrm{H}_0^{(1)}(\omega\, \mathrm{s_P} r) = [P^{-1}\, B^{-1}]_{11} \left(-(\omega\, \mathrm{s_P})^2 \frac{\mathrm{i}}{4} \mathrm{H}_0^{(1)}(\omega\, \mathrm{s_P} r) - \delta \right), \\ \chi_\mathrm{B} &= [P^{-1}\, B^{-1}]_{21}\, \Delta\, \mathrm{H}_0^{(1)}(\omega\, \mathrm{s_B} r) = [P^{-1}\, B^{-1}]_{21} \left(-(\omega\, \mathrm{s_B})^2 \frac{\mathrm{i}}{4} \mathrm{H}_0^{(1)}(\omega\, \mathrm{s_B} r) - \delta \right), \\ \chi_\mathrm{S} &= 0. \end{aligned}$$

The expression of the potential gradient is:

$$\begin{aligned} \nabla \chi_\mathrm{P} &= [P^{-1}\, B^{-1}]_{11} \left(-(\omega\, \mathrm{s_P})^2 \frac{\mathrm{i}}{4} \nabla \mathrm{H}_0^{(1)}(\omega\, \mathrm{s_P} r) - \nabla \delta \right) \\ \nabla \chi_\mathrm{B} &= [P^{-1}\, B^{-1}]_{21} \left(-(\omega\, \mathrm{s_B})^2 \frac{\mathrm{i}}{4} \nabla \mathrm{H}_0^{(1)}(\omega\, \mathrm{s_B} r) - \nabla \delta \right). \end{aligned} \tag{2.53}$$

Next, we take into account the fact that $\chi_{\rm S}=0$ in (2.46) and use A^{-1} given by (2.48) to obtain:

$$-\omega^2\begin{pmatrix}\mathrm{u}\\ \mathrm{w}\end{pmatrix} - P\begin{pmatrix}\mathrm{s}_{\rm P}^{-2} & 0\\ 0 & \mathrm{s}_{\rm B}^{-2}\end{pmatrix}\begin{pmatrix}\nabla\chi_{\rm P}\\ \nabla\chi_{\rm B}\end{pmatrix} = P\begin{pmatrix}\mathrm{s}_{\rm P}^{-2} & 0\\ 0 & \mathrm{s}_{\rm B}^{-2}\end{pmatrix}P^{-1}B^{-1}\begin{pmatrix}\nabla\delta\\ 0\end{pmatrix},$$

$$\Rightarrow\quad -\omega^2\begin{pmatrix}\mathrm{u}\\ \mathrm{w}\end{pmatrix} = P\begin{pmatrix}\mathrm{s}_{\rm P}^{-2} & 0\\ 0 & \mathrm{s}_{\rm B}^{-2}\end{pmatrix}\begin{pmatrix}\nabla\chi_{\rm P}+[P^{-1}B^{-1}]_{11}\nabla\delta\\ \nabla\chi_{\rm B}+[P^{-1}B^{-1}]_{21}\nabla\delta\end{pmatrix}.$$

Using equation (2.53), the expression of the displacements u and w in the configuration under consideration is:

$$\boxed{\begin{aligned}\begin{pmatrix}\mathrm{u}\\ \mathrm{w}\end{pmatrix} &= \frac{\mathrm{i}}{4}P\begin{pmatrix}[P^{-1}B^{-1}]_{11}\nabla\mathrm{H}_0^{(1)}(\omega\,\mathrm{s}_{\rm P}r)\\ [P^{-1}B^{-1}]_{21}\nabla\mathrm{H}_0^{(1)}(\omega\,\mathrm{s}_{\rm B}r)\end{pmatrix}\\ &= \frac{\mathrm{i}}{4}\begin{pmatrix}1 & 1\\ \mathcal{W}_{\rm P} & \mathcal{W}_{\rm B}\end{pmatrix}\begin{pmatrix}[P^{-1}B^{-1}]_{11}\nabla\mathrm{H}_0^{(1)}(\omega\,\mathrm{s}_{\rm P}r)\\ [P^{-1}B^{-1}]_{21}\nabla\mathrm{H}_0^{(1)}(\omega\,\mathrm{s}_{\rm B}r)\end{pmatrix}.\end{aligned}}$$

To obtain the final expression of the displacements, we differentiate the Hankel function in polar coordinates:

$$\nabla\mathrm{H}_0^{(1)}(\omega\,\mathrm{s}_\bullet r) = \frac{\partial\mathrm{H}_0^{(1)}(\omega\,\mathrm{s}_\bullet r)}{\partial r}\mathbf{e}_r + \frac{1}{r}\frac{\partial\mathrm{H}_0^{(1)}(\omega\,\mathrm{s}_\bullet r)}{\partial\theta}\mathbf{e}_\theta = \omega\,\mathrm{s}_\bullet\mathrm{H}_0^{(1)'}(\omega\,\mathrm{s}_\bullet r)\mathbf{e}_r\,.$$

For the calculation of $\mathrm{H}_0^{(1)'}(\omega\,\mathrm{s}_\bullet r)$, we use the following connection formula for a Hankel function:

$$\mathrm{H}_k'(z) = -\mathrm{H}_{k+1}(z) + \frac{k}{z}\mathrm{H}_k(z)\,. \tag{2.55}$$

We have for mode 0:

$$\mathrm{H}_0^{(1)'}(\omega\,\mathrm{s}_\bullet r) = -\mathrm{H}_1^{(1)}(\omega\,\mathrm{s}_\bullet r)\,.$$

This gives the following expression of u and w:

$$\begin{aligned}\mathrm{u} &= -\Big(\frac{\mathrm{i}}{4}\,\omega\,\mathrm{s}_{\rm P}\,[P^{-1}B^{-1}]_{11}\mathrm{H}_1^{(1)}(\omega\,\mathrm{s}_{\rm P}r) + \frac{\mathrm{i}}{4}\,\omega\,\mathrm{s}_{\rm B}\,[P^{-1}B^{-1}]_{21}\mathrm{H}_1^{(1)}(\omega\,\mathrm{s}_{\rm B}r)\Big)\mathbf{e}_r\,,\\ \mathrm{w} &= -\Big(\frac{\mathrm{i}\,\mathcal{W}_{\rm P}}{4}\,\omega\,\mathrm{s}_{\rm P}\,[P^{-1}B^{-1}]_{11}\mathrm{H}_1^{(1)}(\omega\,\mathrm{s}_{\rm P}r) + \frac{\mathrm{i}\,\mathcal{W}_{\rm B}}{4}\,\omega\,\mathrm{s}_{\rm B}\,[P^{-1}B^{-1}]_{21}\mathrm{H}_1^{(1)}(\omega\,\mathrm{s}_{\rm B}r)\Big)\mathbf{e}_r\,.\end{aligned} \tag{2.56}$$

Proposition 2.9. The expressions of the first order variables ($\mathbf{u}$, $\mathbf{w}$, $\boldsymbol{\tau}$, p) for a point source in pressure waves are:

$$\begin{aligned}\mathbf{u} &= \Big(\frac{\omega^2}{4}\,\mathrm{s}_{\rm P}\,[P^{-1}B^{-1}]_{11}\mathrm{H}_1^{(1)}(\omega\,\mathrm{s}_{\rm P}r) + \frac{\omega^2}{4}\,\mathrm{s}_{\rm B}\,[P^{-1}B^{-1}]_{21}\mathrm{H}_1^{(1)}(\omega\,\mathrm{s}_{\rm B}r)\Big)\mathbf{e}_r\,,\\ \mathbf{w} &= \Big(\frac{\omega^2\,\mathcal{W}_{\rm P}}{4}\,\mathrm{s}_{\rm P}\,[P^{-1}B^{-1}]_{11}\mathrm{H}_1^{(1)}(\omega\,\mathrm{s}_{\rm P}r) + \frac{\omega^2\,\mathcal{W}_{\rm B}}{4}\,\mathrm{s}_{\rm P}\,[P^{-1}B^{-1}]_{21}\mathrm{H}_1^{(1)}(\omega\,\mathrm{s}_{\rm B}r)\Big)\mathbf{e}_r\,.\end{aligned}$$

The stress tensor is:

$$\boldsymbol{\tau} = \tau_{rr}\mathbf{e}_r\otimes\mathbf{e}_r + \tau_{\theta\theta}\mathbf{e}_\theta\otimes\mathbf{e}_\theta\,,$$

with

$$\begin{aligned}\tau_{rr} &= -(2\mu_{\rm fr}+\lambda_{\rm fr} + M\alpha^2)\Big(\frac{\mathrm{i}}{4}(\omega\,\mathrm{s}_{\rm P})^2\,[P^{-1}B^{-1}]_{11}\mathrm{H}_1^{(1)'}(\omega\,\mathrm{s}_{\rm P}r) + \frac{\mathrm{i}}{4}(\omega\,\mathrm{s}_{\rm B})^2\,[P^{-1}B^{-1}]_{21}\mathrm{H}_1^{(1)'}(\omega\,\mathrm{s}_{\rm B}r)\Big)\\ &\quad - \alpha M\Big(\frac{\mathrm{i}\,\mathcal{W}_{\rm P}}{4}(\omega\,\mathrm{s}_{\rm P})^2\,[P^{-1}B^{-1}]_{11}\mathrm{H}_1^{(1)'}(\omega\,\mathrm{s}_{\rm P}r) + \frac{\mathrm{i}\,\mathcal{W}_{\rm B}}{4}(\omega\,\mathrm{s}_{\rm B})^2\,[P^{-1}B^{-1}]_{21}\mathrm{H}_1^{(1)'}(\omega\,\mathrm{s}_{\rm B}r)\Big)\,,\\ \tau_{\theta\theta} &= -(\lambda_{\rm fr} + M\alpha^2)\Big(\frac{\mathrm{i}}{4}(\omega\,\mathrm{s}_{\rm P})^2\,[P^{-1}B^{-1}]_{11}\mathrm{H}_1^{(1)'}(\omega\,\mathrm{s}_{\rm P}r) + \frac{\mathrm{i}}{4}(\omega\,\mathrm{s}_{\rm B})^2\,[P^{-1}B^{-1}]_{21}\mathrm{H}_1^{(1)'}(\omega\,\mathrm{s}_{\rm B}r)\Big)\\ &\quad - \alpha M\Big(\frac{\mathrm{i}\,\mathcal{W}_{\rm P}}{4}(\omega\,\mathrm{s}_{\rm P})^2\,[P^{-1}B^{-1}]_{11}\mathrm{H}_1^{(1)'}(\omega\,\mathrm{s}_{\rm P}r) + \frac{\mathrm{i}\,\mathcal{W}_{\rm B}}{4}(\omega\,\mathrm{s}_{\rm B})^2\,[P^{-1}B^{-1}]_{21}\mathrm{H}_1^{(1)'}(\omega\,\mathrm{s}_{\rm B}r)\Big)\,,\end{aligned}$$

and

$$\begin{aligned}\mathrm{p} \;=\; & M\left(\frac{\mathrm{i}\,\mathcal{W}_{\mathrm{P}}}{4}\,(\omega\,\mathrm{s}_{\mathrm{P}})^2\,[P^{-1}\,B^{-1}]_{11}\mathrm{H}_1^{(1)'}(\omega\,\mathrm{s}_{\mathrm{P}}r)+\frac{\mathrm{i}\,\mathcal{W}_{\mathrm{B}}}{4}\,(\omega\,\mathrm{s}_{\mathrm{B}})^2\,[P^{-1}\,B^{-1}]_{21}\mathrm{H}_1^{(1)'}(\omega\,\mathrm{s}_{\mathrm{B}}r)\right)\\ & +\; M\,\alpha\left(\frac{\mathrm{i}}{4}\,(\omega\,\mathrm{s}_{\mathrm{P}})^2\,[P^{-1}\,B^{-1}]_{11}\mathrm{H}_1^{(1)'}(\omega\,\mathrm{s}_{\mathrm{P}}r)+\frac{\mathrm{i}}{4}\,(\omega\,\mathrm{s}_{\mathrm{B}})^2\,[P^{-1}\,B^{-1}]_{21}\mathrm{H}_1^{(1)'}(\omega\,\mathrm{s}_{\mathrm{B}}r)\right).\end{aligned}$$

Proof.

- The expression of the velocities $\mathbf{u}$ and $\mathbf{w}$ are obtained by deriving the displacements u and w given in equation (2.56).
- To calculate the stress $\boldsymbol{\tau}$, we use the constitutive laws given in equation (1.10), and the expression of gradient and divergence in polar coordinates:

$$\nabla\cdot\mathrm{u} \;=\; \frac{\partial \mathrm{u}_r}{\partial r}+\frac{1}{r}\frac{\partial \mathrm{u}_\theta}{\partial\theta} \;=\; \frac{\partial \mathrm{u}_r}{\partial r}\,.$$

and

$$\nabla\,\mathrm{u} \;=\; \begin{pmatrix}\dfrac{\partial \mathrm{u}_r}{\partial r} & \dfrac{1}{r}\dfrac{\partial \mathrm{u}_r}{\partial\theta}\\[2mm] \dfrac{\partial \mathrm{u}_\theta}{\partial r} & \dfrac{1}{r}\dfrac{\partial \mathrm{u}_\theta}{\partial\theta}\end{pmatrix} \;=\; \begin{pmatrix}\dfrac{\partial \mathrm{u}_r}{\partial r} & 0\\[2mm] 0 & 0\end{pmatrix},$$

because $\mathrm{u}_\theta = 0$ and u is independant of θ. This means that

$$\begin{aligned}\boldsymbol{\tau} \;&=\; \tau_{rr}\mathbf{e}_r\otimes\mathbf{e}_r+\tau_{\theta\theta}\mathbf{e}_\theta\otimes\mathbf{e}_\theta\\ &=\; \Big(2\mu_{\mathrm{fr}}\frac{\partial \mathrm{u}_r}{\partial r}+(\lambda_{\mathrm{fr}}+M\alpha^2)\frac{\partial \mathrm{u}_r}{\partial r}+\alpha M\frac{\partial \mathrm{w}_r}{\partial r}\Big)\mathbf{e}_r\otimes\mathbf{e}_r+\Big((\lambda_{\mathrm{fr}}+M\alpha^2)\frac{\partial \mathrm{u}_r}{\partial r}+\alpha M\frac{\partial \mathrm{w}_r}{\partial r}\Big)\mathbf{e}_\theta\otimes\mathbf{e}_\theta\,.\end{aligned} \tag{2.58}$$

The radial derivative of $\mathrm{H}_1^{(1)}(\omega\,\mathrm{s}_\bullet r)$ is:

$$\frac{\partial}{\partial r}\mathrm{H}_1^{(1)}(\omega\,\mathrm{s}_\bullet r) \;=\; \omega\,\mathrm{s}_\bullet\mathrm{H}_1^{(1)'}(\omega\,\mathrm{s}_\bullet r) \;=\omega\,\mathrm{s}_\bullet\mathrm{H}_0^{(1)}(\omega\,\mathrm{s}_\bullet r)\;-\;\frac{1}{r}\mathrm{H}_1^{(1)}(\omega\,\mathrm{s}_\bullet r)\,.$$

By injecting this in (2.58), we retrieve the expression of $\boldsymbol{\tau}$.

- For the pressure p, we use the last equation of (1.10) and use the expression of the displacements given in (2.56).

□

This solution will be used for a validation of the code. We give in Figure 2.25 the analytical solution obtained for u_x. The analytical solution has been constructed for an infinite medium. Hence, we do not take into account reflections. However, for the representation of the solution, we restrict the solution to the square domain $[-10m, 10m]\times[-10m, 10m]$. On the figure, we observe mainly the wavefront corresponding to the P wave, because we are studying the solid velocity.

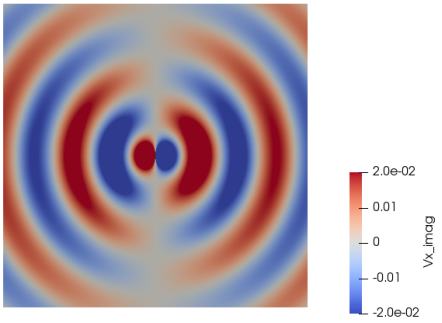

Figure 2.25: Analytical solution for u_x with the sources $\mathbf{f} = \nabla\delta\,,\quad \tilde{\mathbf{f}} = 0\,.$

2.6.2 Source in transverse wave

Now, we want to model a source producing only transverse wave. For this, we use the fact that $\mathbf{curl}\,\nabla\cdot = 0$ and $\operatorname{curl}\mathbf{curl} = -\Delta$. We set $\mathbf{f} = \mathbf{curl}\,\delta\,, \quad \tilde{\mathbf{f}} = 0$ in equation (2.46). The Helmholtz equations (2.47) become

$$\begin{aligned}\left(-\Delta - \omega^2\,\mathsf{s}_{\mathrm{P}}^2\right)\chi_{\mathrm{P}} &= 0\,,\\ \left(-\Delta - \omega^2\,\mathsf{s}_{\mathrm{B}}^2\right)\chi_{\mathrm{B}} &= 0\,,\\ \left(-\Delta - \omega^2\,\mathsf{s}_{\mathrm{S}}^2\right)\chi_{\mathrm{S}} &= -\mathsf{s}_{\mathrm{S}}^2\,[A^{-1}]_{11}\,\Delta\delta\,.\end{aligned}$$

By using the expression of the Green kernel given in equations (2.49) and (2.50), the potentials are

$$\begin{aligned}&\chi_{\mathrm{P}} = 0\,, \qquad\qquad \chi_{\mathrm{B}} = 0\,,\\ &\chi_{\mathrm{S}} = -\mathsf{s}_{\mathrm{S}}^2\,[A^{-1}]_{11}\,\Delta\,\frac{\mathrm{i}}{4}\mathrm{H}_0^{(1)}(\omega\,\mathsf{s}_{\mathrm{S}}r) \;= \mathsf{s}_{\mathrm{S}}^2\;[A^{-1}]_{11}\left((\omega\,\mathsf{s}_{\mathrm{S}})^2\,\frac{\mathrm{i}}{4}\mathrm{H}_0^{(1)}(\omega\,\mathsf{s}_{\mathrm{S}}r) + \delta\right)\,.\end{aligned}$$

Next, we replace the above equation in (2.46).

$$-\omega^2\begin{pmatrix}\mathrm{u}\\ \mathrm{w}\end{pmatrix} + \frac{\mu_{\mathrm{fr}}}{\det A}\begin{pmatrix}\rho_{\mathrm{dyn}} & 0\\ -\rho_f & 0\end{pmatrix}\begin{pmatrix}\mathbf{curl}\,\chi_{\mathrm{S}}\\ 0\end{pmatrix} = A^{-1}\begin{pmatrix}\mathbf{curl}\,\delta\\ 0\end{pmatrix}\,,$$

$$\Rightarrow -\omega^2\begin{pmatrix}\mathrm{u}\\ \mathrm{w}\end{pmatrix} = -\frac{\mu_{\mathrm{fr}}}{\det A}\begin{pmatrix}\rho_{\mathrm{dyn}} & 0\\ -\rho_f & 0\end{pmatrix}\begin{pmatrix}\mathbf{curl}\,\chi_{\mathrm{S}}\\ 0\end{pmatrix} + \frac{1}{\det A}\begin{pmatrix}\rho_{\mathrm{dyn}} & -\rho_f\\ -\rho_f & \rho_a\end{pmatrix}\begin{pmatrix}\mathbf{curl}\,\delta\\ 0\end{pmatrix}\,,$$

$$\Rightarrow -\omega^2\begin{pmatrix}\mathrm{u}\\ \mathrm{w}\end{pmatrix} = -\frac{\mu_{\mathrm{fr}}}{\det A}\begin{pmatrix}\rho_{\mathrm{dyn}} & 0\\ -\rho_f & 0\end{pmatrix}\begin{pmatrix}\mathbf{curl}\,\chi_{\mathrm{S}}\\ 0\end{pmatrix} + \frac{1}{\det A}\begin{pmatrix}\rho_{\mathrm{dyn}} & 0\\ -\rho_f & 0\end{pmatrix}\begin{pmatrix}\mathbf{curl}\,\delta\\ 0\end{pmatrix}\,.$$

Note that

$$\mathsf{s}_{\mathrm{S}}^2\,[A^{-1}]_{11} = \mathsf{s}_{\mathrm{S}}^2\,\frac{\rho_{\mathrm{dyn}}}{\det A} = \frac{\det A}{\mu_{\mathrm{fr}}\,\rho_{\mathrm{dyn}}}\frac{\rho_{\mathrm{dyn}}}{\det A} = \frac{1}{\mu_{\mathrm{fr}}}\,.$$

The curl of the potential χ_{S} is:

$$\mathbf{curl}\,\chi_{\mathrm{S}} = \mathsf{s}_{\mathrm{S}}^2\,[A^{-1}]_{11}\left((\omega\,\mathsf{s}_{\mathrm{S}})^2\,\frac{\mathrm{i}}{4}\mathbf{curl}\,\mathrm{H}_0^{(1)}(\omega\,\mathsf{s}_{\mathrm{S}}r) + \mathbf{curl}\,\delta\right)\,,$$

which gives

$$-\omega^2\begin{pmatrix}\mathrm{u}\\ \mathrm{w}\end{pmatrix} = -\frac{1}{\det A}\begin{pmatrix}\rho_{\mathrm{dyn}} & 0\\ -\rho_f & 0\end{pmatrix}\begin{pmatrix}(\omega\,\mathsf{s}_{\mathrm{S}})^2\,\frac{\mathrm{i}}{4}\mathbf{curl}\,\mathrm{H}_0^{(1)}(\omega\,\mathsf{s}_{\mathrm{S}}r)\\ 0\end{pmatrix}\,,$$

$$\Rightarrow \begin{pmatrix}\mathrm{u}\\ \mathrm{w}\end{pmatrix} = \frac{\mathsf{s}_{\mathrm{S}}^2}{\det A}\frac{\mathrm{i}}{4}\begin{pmatrix}\rho_{\mathrm{dyn}} & 0\\ -\rho_f & 0\end{pmatrix}\begin{pmatrix}\mathbf{curl}\,\mathrm{H}_0^{(1)}(\omega\,\mathsf{s}_{\mathrm{S}}r)\\ 0\end{pmatrix}\,.$$

In polar coordinates, the curl of $\mathrm{H}_0^{(1)}(\omega\,\mathsf{s}_{\mathrm{S}}r)$ is

$$\mathbf{curl}\,\mathrm{H}_0^{(1)}(\omega\,\mathsf{s}_{\mathrm{S}}r) = \begin{pmatrix}\frac{1}{r}\dfrac{\partial\mathrm{H}_0^{(1)}(\omega\,\mathsf{s}_{\mathrm{S}}r)}{\partial\theta}\\ -\dfrac{\partial\mathrm{H}_0^{(1)}(\omega\,\mathsf{s}_{\mathrm{S}}r)}{\partial r}\end{pmatrix} = \begin{pmatrix}0\\ -\omega\,\mathsf{s}_{\mathrm{S}}\mathrm{H}_0^{(1)'}(\omega\,\mathsf{s}_{\mathrm{S}}r)\end{pmatrix} = \begin{pmatrix}0\\ \omega\,\mathsf{s}_{\mathrm{S}}\mathrm{H}_1^{(1)}(\omega\,\mathsf{s}_{\mathrm{S}}r)\end{pmatrix}\,.$$

In the last equality, we have used the connection formula of Hankel functions, given in equation (2.55). This means that the displacements u and w are given by

$$\boxed{\begin{aligned}\mathrm{u} &= \mathrm{u}_\theta\,\mathbf{e}_\theta = \frac{\omega\,\mathsf{s}_{\mathrm{S}}^3\,\rho_{\mathrm{dyn}}}{\det A}\frac{\mathrm{i}}{4}\,\mathrm{H}_1^{(1)}(\omega\,\mathsf{s}_{\mathrm{S}}r)\,\mathbf{e}_\theta\,,\\ \mathrm{w} &= \mathrm{w}_\theta\,\mathbf{e}_\theta = -\frac{\omega\,\mathsf{s}_{\mathrm{S}}^3\,\rho_f}{\det A}\frac{\mathrm{i}}{4}\,\mathrm{H}_1^{(1)}(\omega\,\mathsf{s}_{\mathrm{S}}r)\,\mathbf{e}_\theta\,.\end{aligned}} \tag{2.64}$$

Proposition 2.10. The expressions of the first order variables ($\mathbf{u}$, $\mathbf{w}$, $\boldsymbol{\tau}$, p) for a point source in transverse wave are:

$$\mathbf{u} \,=\, -\,\frac{\mathsf{s}_{\mathrm{S}}^3\,\rho_{\mathrm{dyn}}\,\omega^2}{4\,\det A}\,\mathrm{H}_1^{(1)}(\omega\,\mathrm{s}_{\mathrm{S}}r)\,\mathbf{e}_\theta\,,$$

$$\mathbf{w} \,=\, \frac{\mathsf{s}_{\mathrm{S}}^3\,\rho_f\,\omega^2}{4\,\det A}\,\mathrm{H}_1^{(1)}(\omega\,\mathrm{s}_{\mathrm{S}}r)\,\mathbf{e}_\theta\,.$$

$$\boldsymbol{\tau} \,=\, \tau_{r\theta}\mathbf{e}_r\otimes\mathbf{e}_\theta \,+\tau_{r\theta}\mathbf{e}_\theta\otimes\mathbf{e}_r\,,$$

with

$$\tau_{r\theta} \,=\, \mathrm{i}\,\mu_{\mathrm{fr}}\,\frac{\mathsf{s}_{\mathrm{S}}^3\,\rho_{\mathrm{dyn}}\,\omega}{4\,\det A}\left(\omega\,\mathrm{s}_\bullet\mathrm{H}_0^{(1)}(\omega\,\mathrm{s}_\bullet r)\,-\,\frac{1}{r}\mathrm{H}_1^{(1)}(\omega\,\mathrm{s}_\bullet r)\right),$$

and

$$\mathrm{p}\,=0\,.$$

Proof.

- The expression of the velocities $\mathbf{u}$ and $\mathbf{w}$ are obtained by deriving the displacements u and w given in (2.64).
- For the stress $\boldsymbol{\tau}$, we use (1.10). In polar coordinates, we have

$$\nabla\cdot\mathrm{u} \,=\, \frac{\partial \mathrm{u}_r}{\partial r}\,+\,\frac{1}{r}\frac{\partial \mathrm{u}_\theta}{\partial\theta}\,=\,0\,.$$

and

$$\nabla\,\mathrm{u} \,=\, \begin{pmatrix} \dfrac{\partial \mathrm{u}_r}{\partial r} & \dfrac{1}{r}\dfrac{\partial \mathrm{u}_r}{\partial\theta} \\ \dfrac{\partial \mathrm{u}_\theta}{\partial r} & \dfrac{1}{r}\dfrac{\partial \mathrm{u}_\theta}{\partial\theta}\end{pmatrix} \,=\, \begin{pmatrix} 0 & 0 \\ \dfrac{\partial \mathrm{u}_\theta}{\partial r} & 0\end{pmatrix}.$$

This means that

$$\boldsymbol{\tau} \,=\, \tau_{r\theta}\mathbf{e}_r\otimes\mathbf{e}_\theta \,+\tau_{r\theta}\mathbf{e}_\theta\otimes\mathbf{e}_r\,,$$

with

$$\tau_{r\theta} \,=\, \mu_{\mathrm{fr}}\frac{\partial \mathrm{u}_\theta}{\partial r}\,.$$

The radial derivative of $\mathrm{H}_1^{(1)}(\omega\,\mathrm{s}_\bullet r)$ is:

$$\frac{\partial}{\partial r}\mathrm{H}_1^{(1)}(\omega\,\mathrm{s}_\bullet r) \,=\, \omega\,\mathrm{s}_\bullet\mathrm{H}_1^{(1)'}(\omega\,\mathrm{s}_\bullet r) \,=\omega\,\mathrm{s}_\bullet\mathrm{H}_0^{(1)}(\omega\,\mathrm{s}_\bullet r)\,-\,\frac{1}{r}\mathrm{H}_1^{(1)}(\omega\,\mathrm{s}_\bullet r)\,.$$

Hence

$$\tau_{r\theta} \,=\, \mathrm{i}\,\mu_{\mathrm{fr}}\,\frac{\mathsf{s}_{\mathrm{S}}^3\,\rho_{\mathrm{dyn}}\,\omega}{4\,\det A}\left(\omega\,\mathrm{s}_\bullet\mathrm{H}_0^{(1)}(\omega\,\mathrm{s}_\bullet r)\,-\,\frac{1}{r}\mathrm{H}_1^{(1)}(\omega\,\mathrm{s}_\bullet r)\right).$$

- For the pressure, as the divergence of u and w is null, the pressure is equal to zero.

□

This solution will be used for a validation of the code. We give in Figure 2.26 the analytical solution obtained for u_x. As in the previous section, the analytical solution has been built considering an infinite medium. However, for the representation of the solution, we restrict the solution to the square domain $[-10m, 10m]\times[-10m, 10m]$. Here, we observe only one circular wavefront, corresponding to the transverse wave. The wave propagation is in the vertical direction, i.e., perpendicular to the observed field u_x, because we consider a transverse wave, and it is in the opposed direction to the one in Figure 2.25 where we considered longitudinal waves.

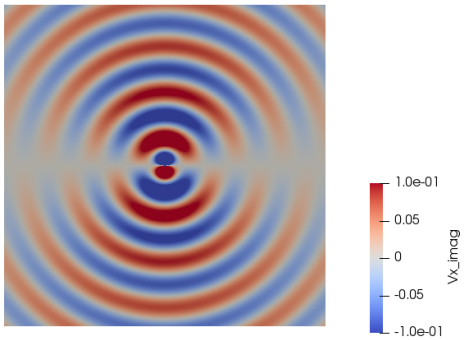

Figure 2.26: Analytical solution for u_x with sources $\mathbf{f} = \mathbf{curl}\,\delta\,, \quad \tilde{\mathbf{f}} = 0\,.$

Conclusion

In this chapter, we have computed analytical solutions in two-dimensions for the following problems: bounded isotropic poroelastic problem, scattering of plane wave in poroelastic medium by penetrable/impenetrable obstacles, fluid-solid interaction problem and response to point-sources in infinite medium. As a first application of these formula, we gave a description of a generic homogeneous solution for isotropic poroelastic equations, which includes outgoing solutions. As a second application, we carried out numerical investigations on the well-posedness of the above problems. From our investigations, the following came out. On bounded domains, the presence of eigenvalues does not come as a surprise when there is no viscosity. However, what is interesting is that there are no eigenvalues with the current model of viscosity. In fluid-elastic interaction problems, the presence of what is equivalent with Jones' modes for poroelastic interior is found without viscosity. However, for the same range of frequency, for a viscous medium, there are no longer eigenvalues. These results are obtained for circular problems, they can be dependent on the considered geometry.

This study paves the way for future theoretical investigations of this question, such as the theoretical confirmation of the absence of equivalent Jones' modes. We used the analytical solutions described in this chapter to perform analytical-numerical comparisons on an HDG method for poroelasticity, see Chapter 3. Moreover, we will make use of the work on outgoing solution to construct low order radiation boundary conditions for isotropic poroelastic equations in Chapter 4.

Chapter 3

HDG method for anisotropic poroelasticity

In the previous chapters, we have presented the phenomenon of poroelasticity and developed some analytical solutions in porous media. In this chapter, we focus on the numerical simulation of the poroelastic equations.[1] In terms of numerical simulation, grid-based numerical methods have long demonstrated a high potential for solving wave equations in complex media that may contain many heterogeneities of widely varying sizes. Works on porous media have employed Finite Volume Method [84], Boundary Element Method [118], Finite Differences [131], continuous Finite Element Method [121], and Spectral-element methods (SEM) [52, 98], a large majority of which being in the time domain. In particular, SEM demonstrated a clear efficiency in the time-domain, when based on hexahedral meshes. However, the representation of geological media is eased by using tetrahedral grids that are capable of more easily reproducing the geometric and constitutive variations of the medium. This is a clear motivation to turn to finite element methods authorizing tetrahedral meshes. Among them, Discontinuous Galerkin (DG) methods [49], initially developed to solve fluid mechanics problems, have also been applied to wave propagation simulations in heterogeneous media, both in time domain [39, 88, 122, 48, 133] and frequency domain [38, 50].

The DG methods have many advantages like good performance on unstructured and irregular meshes thanks to *hp* adaptivity. More importantly, each DG element communicates only with its direct neighbours. On a given mesh, the global matrix has thus a block structure, each block representing the interaction between two elements. This property is also a good point in favor of using high-order approximations since increasing the order does not increase the number of blocks of the matrix and does not modify the connectivity graph between these blocks. In addition, the DG block structure makes the method easily parallelizable. However, using discontinuous basis functions results in a significant increase in the number of degrees of freedom, so that the size of the overall discrete system is much larger than that of the system associated with a continuous finite element method. This is a real disadvantage when working in the frequency domain as one can easily reach the limits of direct solvers available in open-source that are essential to solve the problem.[2]

Hence, given that there is an obvious need in reducing the size of the linear system to be solved, we propose to consider a variant of DG methods which is qualified as hybridizable. They are DG methods amenable to hybridization in the same sense as static condensation [32, 89, 65, 54]. Such methods require applying a local projection at the element level in order to parameterize the solution in terms of numerical traces. Then, transmission conditions are constructed to connect the original solution to numerical traces. The original solution is then reconstructed a posteriori for negligible computational costs, cell by cell by solving local small-sized problems. Hybridizable DG (HDG) methods have been introduced in two seminal papers [35, 124] and successfully developed for many problems, as for example in [37, 101] for acoustics and elastodynamics, in [85, 53] for electromagnetism, in [20, 21, 65, 67] for time-harmonic seismic waves. Note that here, we limit the citations only to wave problems. The HDG solution methodology relies on the possibility of relating local unknowns at the element level to a so-called hybrid variable defined only on the skeleton of the mesh (i.e., the set of edges in 2D and set of faces in 3D) by the mean of transmission conditions. In this way, the HDG solution is obtained by solving a smaller global system for the hybrid variable and the solution is reconstructed thanks to the solution of local systems in parallel.

As far as Biot consolidation model is concerned, the literature contains a lot of work on the finite element approximation of the Biot consolidation model (see e.g., [28, 96, 80, 114] and their references) but very few on the finite element

[1] This chapter is published in a reduced form in [11].

[2] We can mitigate the large size of the linear system by using an iterative solver. However, with an application in iterative inversion in mind, we are more interested in a direct solver due to its multi right-hand-side features.

solution of time-harmonic Biot equations. In two very recent works, Fu [57] and Hungria [76] have implemented the HDG solution of poroelastic wave equations. Fu [57] considered the quasi-static Biot equations using a displacement-pressure formulation. Hungria [76] dealt with both the time-dependent and time-harmonic Biot equations using a displacement-stress-pressure formulation. Herein, we consider a formulation of Biot equations governing the frame velocity, the relative fluid velocity, the pressure field, and the solid stress tensor, written in the frequency domain. Our approach is closer to that of Hungria since we consider time-harmonic equations whereas Fu solved quasi-static equations. It is however worth noting that we do not solve the same formulation as Hungria. As an advantage, the first order formulation gives us access to velocities and stress tensor, which are the actual data displayed by experimental acquisition. This is very important if we want to use the code in an inversion loop for characterizing the propagation in the medium.

In this chapter, following Biot's model [15], we present the development of an HDG method for the anisotropic poroelastic wave equation set in the frequency domain. We consider time-harmonic waves having their time dependency as $e^{\mathrm{i}\omega t}$. In this convention, we set $\partial_t \to \mathrm{i}\omega$, i.e. $\mathfrak{s} = 1$ in (1.16). Let d be the dimension of $\mathcal{D}$ a physical domain in $\mathbb{R}^{\mathrm{d}}$ with boundary Γ. On the domain $\mathcal{D}$, the unknowns $(\mathbf{u}, \mathbf{w}, \boldsymbol{\tau}, \mathrm{p})$ solve the following first-order system with external forces $\mathbf{f}_u$ and $\mathbf{f}_w$

$$\begin{cases} \mathrm{i}\omega\rho_a\mathbf{u} + \mathrm{i}\omega\rho_f\,\mathbf{w} & = \nabla\cdot\boldsymbol{\tau} + \mathbf{f}_u\,, \\ \mathrm{i}\omega\rho_f\mathbf{u} + \mathrm{i}\omega\rho_{\mathrm{dyn}}(\omega)\,\mathbf{w} & = -\nabla\mathrm{p} + \mathbf{f}_w\,, \\ \mathrm{i}\omega\boldsymbol{\tau} + \mathrm{i}\omega\,\boldsymbol{\alpha}\mathrm{p} & = \mathbf{C}_{\mathrm{fr}}\,\boldsymbol{\epsilon}(\mathbf{u})\,, \\ \mathrm{i}\omega\,\mathrm{p} & = -M\nabla\cdot\mathbf{w} - M\boldsymbol{\alpha} : \boldsymbol{\epsilon}(\mathbf{u})\,. \end{cases} \tag{3.1}$$

The first two equations are equations of motion, and the last two ones are constitutive laws. We have written the velocity strain tensor $\boldsymbol{\epsilon} = \frac{\nabla\mathbf{u}+(\nabla\mathbf{u})^T}{2}$, and the operation : denotes the tensor scalar product, i.e., for tensors $\boldsymbol{a}$ and $\boldsymbol{b}$, $\boldsymbol{a} : \boldsymbol{b} = \sum_{i,j} a_{ij}\,b_{ij}$.

On the external boundary Γ with outwardly direct unit normal vector $\boldsymbol{n}$, we consider the boundary conditions with vector $\boldsymbol{f}_{\mathrm{inc}}$ and scalar g_{inc} denoting the exterior boundary forces,

$$\text{Type 1} \qquad \begin{cases} \boldsymbol{\tau}\,\boldsymbol{n} & = & \boldsymbol{f}_{\mathrm{inc}}\,, \\ \mathbf{w}\cdot\boldsymbol{n} & = & g_{\mathrm{inc}}\,, \end{cases} \tag{3.2}$$

To alleviate the notation, we write equation (3.1) with the boundary conditions in (3.2) as

$$\begin{aligned} \mathcal{L}_{\mathrm{poro}}\,\mathfrak{U} &= \big(\boldsymbol{f}_{\mathrm{vol}}, \boldsymbol{g}_{\mathrm{vol}}, \mathbf{0}, 0\big)^T \quad \text{in } \mathcal{D}\,, \\ \mathcal{T}_1\,\mathfrak{U} &= \big(\boldsymbol{f}_{\mathrm{inc}}\,,\, g_{\mathrm{inc}}\big)^T \qquad\quad \text{on } \partial\mathcal{D}\,. \end{aligned}$$

Here, we have introduced the notation of the poroelastic operator $\mathcal{L}_{\mathrm{poro}}$, and boundary operator $\mathcal{T}_1$. In this notation, the unknown is $\mathfrak{U} = \big(\mathbf{u}, \mathbf{w}, \boldsymbol{\tau}, \mathrm{p}\big)^T$, and $\mathbf{0}$ in the volume right-hand-side is the zero (2nd-order) tensor. The right-hand-side in the boundary conditions consists of the vector-valued function $\boldsymbol{f}_{\mathrm{inc}}$ and the scalar function g_{inc}. Note that we present in Appendix B.2 how to handle the presence of the different boundary types 1.20 in the HDG method. In Chapter 4, we will also present the development of boundary conditions used to truncate infinite domains.

In this chapter, we present the HDG formulation in Section 3.1 and the associated discretization in two and three dimensions in Sections 3.2 and 3.3 respectively. The description of the HDG solution methodology is accompanied by a numerical analysis aiming at ensuring that the discrete problem is well-posed in Section 3.5. We carry out the analysis of convergence and the conditioning of the system, see Section 3.5.2.3. We also provide some numerical experiments to validate the method by comparing with analytical solutions developed in Chapter 2.

3.1 Formulation of HDG method

The poroelastic equations are complex and their numerical solution requires a lot of computational power, because of the size of the system. We choose to use HDG method, to get high-order results with computational costs more affordable than when using a standard DG method. As a DG method, the HDG method is usable on unstructured meshes, with discontinuous basis functions. This is also a method on which we can use *hp*-adaptivity and that is easily parallelizable because the calculations can be done elementwise. The main drawback of DG methods is the large number of degrees of freedom compared to finite element methods, which increases the computational cost. In HDG methods, the unknowns are expressed as functions of a hybrid unknown, only defined on the boundaries of the elements [81]. The hybrid unknown is taken as a Lagrange multiplier that satisfies a global system defined from the

surfacic degrees of freedom attached to the boundaries of the elements. This reduces the number of degrees of freedom [20].

3.1.1 Notations

On a domain $\mathcal{D}$ of dimension d, we will work with the following function spaces,

$$\begin{aligned} &L^2(\mathcal{D}),\ \text{the space of square-integrable functions on the domain } \mathcal{D}\,,\\ &V^p(\mathcal{D}),\ \text{the set of polynomials of degree at most } p \text{ on } \mathcal{D}\,,\\ &\boldsymbol{V}^p(\mathcal{D}) = (V^p(\mathcal{D}))^{\mathrm{d}}\,,\\ &\boldsymbol{\Sigma}^p(\mathcal{D}) = \{\boldsymbol{\tau} \in (V^p(\mathcal{D}))^{\mathrm{d}^2} | \boldsymbol{\tau} \text{ symmetric}\}\,. \end{aligned} \tag{3.4}$$

We next consider a triangulation $\mathcal{T}_h$ of the domain $\mathcal{D}$. K denotes an element of the mesh, which is a triangle in 2D and a tetrahedron in 3D. We denote by F a face of the element K, and $\boldsymbol{n}$ stands for the unit normal vector to F. Associated to triangulation $\mathcal{T}_h$, we define the following spaces:

$$\begin{aligned} V_h^p &= \{v \in L^2(\mathcal{D}) : v|_K \in V^p(K)\,,\ \forall K \in \mathcal{T}_h\}\,,\\ \boldsymbol{V}_h^p &= \{\boldsymbol{v} \in (L^2(\mathcal{D}))^{\mathrm{d}} : \boldsymbol{v}|_K \in \boldsymbol{V}^p(K)\,,\ \forall K \in \mathcal{T}_h\}\,,\\ \boldsymbol{\Sigma}_h^p &= \{\boldsymbol{\tau} \in L^2(\mathcal{D})^{\mathrm{d}^2} : \boldsymbol{\tau}|_K \in \boldsymbol{\Sigma}^p(K)\,,\ \forall K \in \mathcal{T}_h\}\,,\\ M_h &= \{\xi \in L^2(\mathcal{F}_h) : \xi|_F \in V^p(F)\,,\ \forall K \in \mathcal{F}_h\}\,,\\ \boldsymbol{M}_h &= \{\eta \in (L^2(\mathcal{F}_h))^{\mathrm{d}} : \eta|_F \in (V^p(F))^{\mathrm{d}}\,,\ \forall K \in \mathcal{F}_h\}\,. \end{aligned} \tag{3.5}$$

Remark 3.1. Note that we strongly impose the symmetry on the stress tensor $\boldsymbol{\tau}$, which prevents the potential loss of half an order described in [34] and [58].

The jumps $[\![\cdot]\!]$ are defined on an interior face $F = \partial K \cap \partial K'$ as

$$[\![\mathbf{w}\cdot\boldsymbol{n}]\!] = \mathbf{w}^K\cdot\boldsymbol{n}^K + \mathbf{w}^{K'}\cdot\boldsymbol{n}^{K'}\,, \qquad [\![\boldsymbol{\tau}\,\boldsymbol{n}]\!] = \boldsymbol{\tau}^K\,\boldsymbol{n}^K + \boldsymbol{\tau}^{K'}\,\boldsymbol{n}^{K'}\,, \tag{3.6}$$

and on a boundary face,

$$[\![\mathbf{w}\cdot\boldsymbol{n}]\!] = \mathbf{w}^K\cdot\boldsymbol{n}^K\,, \qquad [\![\boldsymbol{\tau}\,\boldsymbol{n}]\!] = \boldsymbol{\tau}^K\,\boldsymbol{n}^K\,. \tag{3.7}$$

3.1.2 Local problem

We consider an element K of $\mathcal{T}_h$, and an exact solution of (3.1) on K denoted by $(\mathbf{u}, \mathbf{w}, \boldsymbol{\tau}, \mathrm{p})$. Define the following test functions: $(\tilde{\boldsymbol{u}}, \tilde{\boldsymbol{w}}, \tilde{\boldsymbol{\tau}}, \tilde{\mathrm{p}}) \in (\boldsymbol{V}^p(K) \times \boldsymbol{V}^p(K) \times \boldsymbol{\Sigma}^p(K) \times V^p(K))$. The integration on an element of (3.1) gives:

$$\int_K \mathrm{i}\,\omega\,\rho_a\,\mathbf{u}\cdot\tilde{\boldsymbol{u}} + \int_K \mathrm{i}\,\omega\,\rho_f\,\mathbf{w}\cdot\tilde{\boldsymbol{u}} - \int_K (\nabla\cdot\boldsymbol{\tau})\cdot\tilde{\boldsymbol{u}} = \int_K \boldsymbol{f}_{\mathrm{vol}}\cdot\tilde{\boldsymbol{u}}\,,$$

$$\int_K \mathrm{i}\,\omega\,\rho_f\,\mathbf{u}\cdot\tilde{\boldsymbol{w}} + \int_K \mathrm{i}\,\omega\,\rho_{\mathrm{dyn}}\,\mathbf{w}\cdot\tilde{\boldsymbol{w}} + \int_K (\nabla\,\mathrm{p})\cdot\tilde{\boldsymbol{w}} = \int_K \boldsymbol{g}_{\mathrm{vol}}\cdot\tilde{\boldsymbol{w}}\,,$$

$$\int_K \mathrm{i}\,\omega\,\boldsymbol{\tau} : \tilde{\boldsymbol{\tau}} + \int_K \mathrm{i}\,\omega\,\mathrm{p}\,\boldsymbol{\alpha} : \tilde{\boldsymbol{\tau}} - \int_K (\mathbf{C}_{\mathrm{fr}}\boldsymbol{\epsilon}(\mathbf{u})) : \tilde{\boldsymbol{\tau}} = 0\,,$$

$$\int_K \mathrm{i}\,\omega\,\mathrm{p}\,\tilde{\mathrm{p}} + \int_K M\,\nabla\cdot\mathbf{w}\,\tilde{\mathrm{p}} + \int_K M\,\boldsymbol{\alpha} : \boldsymbol{\epsilon}(\mathbf{u})\,\tilde{\mathrm{p}} = 0\,.$$

By integrating by parts, we have:

$$\int_K \mathrm{i}\,\omega\,\rho_a\,\mathbf{u}\cdot\tilde{\boldsymbol{u}} + \int_K \mathrm{i}\,\omega\,\rho_f\,\mathbf{w}\cdot\tilde{\boldsymbol{u}} + \int_K \boldsymbol{\tau} : \nabla\,\tilde{\boldsymbol{u}} - \int_{\partial K} \hat{\boldsymbol{\tau}}\,\boldsymbol{n}\cdot\tilde{\boldsymbol{u}} = \int_K \boldsymbol{f}_{\mathrm{vol}}\cdot\tilde{\boldsymbol{u}}\,,$$

$$\int_K \mathrm{i}\,\omega\,\rho_f\,\mathbf{u}\cdot\tilde{\boldsymbol{w}} \;+\; \int_K \mathrm{i}\,\omega\,\rho_{\mathrm{dyn}}\,\mathbf{w}\cdot\tilde{\boldsymbol{w}} \;-\; \int_K \mathrm{p}\,\nabla\cdot\tilde{\boldsymbol{w}} \;+\; \int_{\partial K}\hat{\mathrm{p}}\,\boldsymbol{n}\cdot\tilde{\boldsymbol{w}} \;=\; \int_K \boldsymbol{g}_{\mathrm{vol}}\cdot\tilde{\boldsymbol{w}}\,,$$

$$\int_K \mathrm{i}\,\omega\,\boldsymbol{\tau} : \tilde{\boldsymbol{\tau}} \;+\; \int_K \mathrm{i}\,\omega\,\mathrm{p}\,\boldsymbol{\alpha} : \tilde{\boldsymbol{\tau}} \;+\; \int_K \mathbf{u}\cdot(\nabla\cdot(\mathbf{C}_{\mathrm{fr}}\tilde{\boldsymbol{\tau}})) \;-\; \int_{\partial K}\hat{\mathbf{u}}\cdot(\mathbf{C}_{\mathrm{fr}}\,\tilde{\boldsymbol{\tau}}\,\boldsymbol{n}) \;=\; 0\,,$$

$$\int_K \mathrm{i}\,\omega\,\mathrm{p}\,\tilde{\mathrm{p}} \;-\; \int_K M\,\mathbf{w}\cdot\nabla\tilde{\mathrm{p}} \;+\; \int_{\partial K} M\,(\hat{\mathbf{w}}\cdot\boldsymbol{n})\,\tilde{\mathrm{p}} \;-\; \int_K M\,(\boldsymbol{\alpha}\mathbf{u})\cdot\nabla\,\tilde{\mathrm{p}} \;+\; \int_{\partial K} M\,(\boldsymbol{\alpha}\hat{\mathbf{u}})\cdot\boldsymbol{n}\,\tilde{\mathrm{p}} \;=\; 0\,.$$

In the above equation, $\hat{\mathbf{u}}$, $\hat{\mathbf{w}}$, $\hat{\boldsymbol{\tau}}$, $\hat{\mathrm{p}}$ are the numerical traces on the faces of the element K of $\mathbf{u}$, $\mathbf{w}$, $\boldsymbol{\tau}$, p. In addition, $\displaystyle\int_K (\mathbf{C}_{\mathrm{fr}}\boldsymbol{\epsilon}(\mathbf{u}_h)) : \tilde{\boldsymbol{\tau}} = \int_K \boldsymbol{\epsilon}(\mathbf{u}_h) : \mathbf{C}_{\mathrm{fr}}\tilde{\boldsymbol{\tau}}$ because $\mathbf{C}_{\mathrm{fr}}$ is symmetric.

Introduction of the trace variables

The exact solution $(\mathbf{u}, \mathbf{w}, \boldsymbol{\tau}, \mathrm{p})$ on K is approximated by $(\mathbf{u}_h, \mathbf{w}_h, \boldsymbol{\tau}_h, \mathrm{p}_h) \in (\boldsymbol{V}_h^p \times \boldsymbol{V}_h^p \times \boldsymbol{\Sigma}_h^p \times V_h^p)$. Their traces on ∂K are approximated by numerical traces $(\hat{\mathbf{u}}_h, \hat{\mathbf{w}}_h\cdot\boldsymbol{n}, \hat{\boldsymbol{\tau}}_h\boldsymbol{n}, \hat{\mathrm{p}}_h)$. The principle of HDG consists in choosing two traces, one among the "solid" group, $\hat{\boldsymbol{\tau}}_h\boldsymbol{n}$ and $\hat{\mathbf{u}}_h$, and one among the "fluid" group $\hat{\mathbf{w}}_h\cdot\boldsymbol{n}$ and $\hat{\mathrm{p}}_h$, and replacing them by auxiliary unknowns defined only on the edges of the element. This choice should ensure the well-posedness of the local problem when the auxiliary unknowns are used as boundary conditions. We recall that for the acoustic equation, the most common choice is $\hat{\mathrm{p}}_h$ [67], while for the elastic equation, $\hat{\mathbf{u}}_h$ [21] is chosen. For the considered poroelastic equations, there is no particular justification to prefer $\hat{\mathrm{p}}_h$ to $\hat{\mathbf{w}}_h\cdot\boldsymbol{n}$ in the fluid group since both traces are scalar, so that the size of the resulting global system is the same for both choices, and such a choice has no particular impact on the accuracy.

Following the common choice, we have chosen to define the two unknowns $\boldsymbol{\lambda}_1 \in \boldsymbol{M}_h$, $\lambda_2 \in M_h$ to replace the numerical traces $\hat{\mathbf{u}}_h$ and $\hat{\mathrm{p}}_h$:

$$\boldsymbol{\lambda}_1 = \hat{\mathbf{u}}_h, \quad \lambda_2 = \hat{\mathrm{p}}_h, \quad \forall F \in \mathcal{F}_h\,.$$

The traces $\boldsymbol{\lambda}_1$ and λ_2 are the principal unknowns of the problem that we solve. Then, we must define the numerical traces of the 'secondary' unknowns $\hat{\boldsymbol{\tau}}_h\boldsymbol{n}$ and $\hat{\mathbf{w}}_h\cdot\boldsymbol{n}$. These numerical traces are defined as an approximation of the continuous traces with an additional penalization term that guarantees the order of convergence of the method. In acoustics, this penalization term is proportional to $\hat{\mathrm{p}}_h - \lambda$ [67] while in elasticity, it is proportional to $\hat{\mathbf{u}}_h - \boldsymbol{\lambda}$ [21]. Thus, the most natural choice for the considered poroelastic problem should be to penalize the trace of $\hat{\boldsymbol{\tau}}_h\boldsymbol{n}$ by a term proportional to $\hat{\mathbf{u}}_h - \boldsymbol{\lambda}_1$ and the trace of $\hat{\mathbf{w}}_h$ by a term proportional to $\hat{\mathrm{p}}_h - \lambda_2$. However, since all the unknowns are coupled, we propose instead to define $(\hat{\boldsymbol{\tau}}_h\boldsymbol{n}, \hat{\mathbf{w}}_h\cdot\boldsymbol{n})$ as

$$\begin{cases} \hat{\boldsymbol{\tau}}_h\boldsymbol{n} = \boldsymbol{\tau}_h\boldsymbol{n} - \boldsymbol{S}_1(\mathbf{u}_h - \boldsymbol{\lambda}_1) - (\mathrm{p}_h - \lambda_2)\boldsymbol{S}_3\boldsymbol{n}\,, \\ \hat{\mathbf{w}}_h\cdot\boldsymbol{n} = \mathbf{w}_h\cdot\boldsymbol{n} - \big((\mathrm{p}_h - \lambda_2)\boldsymbol{S}_2\boldsymbol{n}\big)\cdot\boldsymbol{n} - \boldsymbol{S}_4\big((\mathbf{u}_h - \boldsymbol{\lambda}_1)\big)\cdot\boldsymbol{n}\,, \end{cases} \tag{3.10}$$

where $\boldsymbol{S}_1$, $\boldsymbol{S}_2$, $\boldsymbol{S}_3$, $\boldsymbol{S}_4$ are called the stabilization matrices, with $\boldsymbol{S}_1$ representing the stabilization on the solid frame, $\boldsymbol{S}_2$ on the fluid, while $\boldsymbol{S}_3$ and $\boldsymbol{S}_4$ are associated with the coupling of these two materials that compose the porous medium.

Remark 3.2. Note that the fact that we use four penalization matrices instead of two, as in the works [57] and [76], does not impact the computational cost of the methods. Indeed, this will only change the value of the coefficients of the global matrix, but not its profile. In Section 3.5.2.2, we will analyze the influence of these four parameters on the accuracy of the scheme and we will show that they are all necessary to guarantee the order of convergence of our formulation.

The numerical traces are replaced by their expressions (3.10) in (3.9) to give:

$$\int_K \mathrm{i}\,\omega\,\rho_a^K\,\mathbf{u}_h\cdot\tilde{\boldsymbol{u}} + \int_K \mathrm{i}\,\omega\,\rho_f^K\,\mathbf{w}_h\cdot\tilde{\boldsymbol{u}} + \int_K \boldsymbol{\tau}_h : \nabla\,\tilde{\boldsymbol{u}} - \int_{\partial K}(\boldsymbol{\tau}_h\,\boldsymbol{n})\cdot\tilde{\boldsymbol{u}}$$
$$+ \int_{\partial K}\boldsymbol{S}_1\,(\mathbf{u}_h - \boldsymbol{\lambda}_1)\cdot\tilde{\boldsymbol{u}} + \int_{\partial K}(\mathrm{p}_h - \lambda_2)\,(\boldsymbol{S}_3\,\boldsymbol{n})\cdot\tilde{\boldsymbol{u}} = \int_K \boldsymbol{f}_{\mathrm{vol}}^K\cdot\tilde{\boldsymbol{u}}\,,$$

$$\int_K \mathrm{i}\omega\,\rho_f^K\,\mathbf{u}_h\cdot\tilde{\boldsymbol{w}} + \int_K \mathrm{i}\omega\,\rho_{\mathrm{dyn}}^K\,\mathbf{w}_h\cdot\tilde{\boldsymbol{w}} - \int_K \mathrm{p}_h\,\nabla\cdot\tilde{\boldsymbol{w}} + \int_{\partial K}\lambda_2\,\boldsymbol{n}\cdot\tilde{\boldsymbol{w}} = \int_K \boldsymbol{g}_{\mathrm{vol}}^K\cdot\tilde{\mathbf{w}}\,,$$

$$\int_K \mathrm{i}\,\omega\,\boldsymbol{\tau}_h : \tilde{\boldsymbol{\tau}} + \int_K \mathrm{i}\,\omega\,\boldsymbol{\alpha}^K \mathrm{p}_h : \tilde{\boldsymbol{\tau}} + \int_K \mathbf{u}_h \cdot \nabla \cdot (\mathbf{C}_{\mathrm{fr}}^K\,\tilde{\boldsymbol{\tau}}) - \int_{\partial K} \boldsymbol{\lambda}_1 \cdot \mathbf{C}_{\mathrm{fr}}^K\,\tilde{\boldsymbol{\tau}}\,\boldsymbol{n} = 0\,,$$

$$\int_K \mathrm{i}\,\omega\,\mathrm{p}_h\,\tilde{\mathrm{p}} - \int_K M\,\mathbf{w}_h \cdot \nabla\tilde{\mathrm{p}} + \int_{\partial K} M^K\,(\mathbf{w}_h \cdot \boldsymbol{n})\,\tilde{\mathrm{p}} - \int_{\partial K} M^K\,(\mathrm{p}_h - \lambda_2)\,(\boldsymbol{S}_2\,\boldsymbol{n}) \cdot \boldsymbol{n}\,\tilde{\mathrm{p}}$$

$$- \int_{\partial K} M^K\,\boldsymbol{S}_4\,(\mathbf{u}_h - \boldsymbol{\lambda}_1) \cdot \boldsymbol{n} \cdot \tilde{\mathrm{p}} - \int_K M^K\,(\boldsymbol{\alpha}^K\,\mathbf{u}_h) \cdot \nabla\,\tilde{\mathrm{p}} + \int_{\partial K} M^K\,(\boldsymbol{\alpha}^K\,\boldsymbol{\lambda}_1) \cdot \boldsymbol{n}\,\tilde{\mathrm{p}} = 0\,.$$

By integrating by parts the first and last equation of the above system, we obtain the local problem:

$$\int_K \mathrm{i}\,\omega\,\rho_a^K\,\mathbf{u}_h \cdot \tilde{\boldsymbol{u}} + \int_K \mathrm{i}\,\omega\,\rho_f^K\,\mathbf{w}_h \cdot \tilde{\boldsymbol{u}} - \int_K (\nabla \cdot \boldsymbol{\tau}_h) \cdot \tilde{\boldsymbol{u}} + \int_{\partial K} \boldsymbol{S}_1\,(\mathbf{u}_h - \boldsymbol{\lambda}_1) \cdot \tilde{\boldsymbol{u}} + \int_{\partial K} (\mathrm{p}_h - \lambda_2)\,(\boldsymbol{S}_3\,\boldsymbol{n}) \cdot \tilde{\boldsymbol{u}} = \int_K \boldsymbol{f}_{\mathrm{vol}}^K \cdot \tilde{\boldsymbol{u}}\,, \tag{3.12a}$$

$$\int_K \mathrm{i}\,\omega\,\rho_f^K\,\mathbf{u}_h \cdot \tilde{\boldsymbol{w}} + \int_K \mathrm{i}\,\omega\,\rho_{\mathrm{dyn}}^K\,\mathbf{w}_h \cdot \tilde{\boldsymbol{w}} - \int_K \mathrm{p}_h \nabla \cdot \tilde{\boldsymbol{w}}\,hathathat + \int_{\partial K} \lambda_2\,\boldsymbol{n} \cdot \tilde{\boldsymbol{w}} = \int_K \boldsymbol{g}_{\mathrm{vol}}^K \cdot \tilde{\boldsymbol{w}}\,, \tag{3.12b}$$

$$\int_K \mathrm{i}\,\omega\,\boldsymbol{\tau}_h : \tilde{\boldsymbol{\tau}} + \int_K \mathrm{i}\,\omega\,\boldsymbol{\alpha}\,\mathrm{p}_h : \tilde{\boldsymbol{\tau}} + \int_K \mathbf{u}_h \cdot \nabla \cdot (\mathbf{C}_{\mathrm{fr}}^K\,\tilde{\boldsymbol{\tau}} - \int_{\partial K} \boldsymbol{\lambda}_1 \cdot (\mathbf{C}_{\mathrm{fr}}^K\,\tilde{\boldsymbol{\tau}}\boldsymbol{n}) = 0\,, \tag{3.12c}$$

$$\int_K \mathrm{i}\,\omega\,\mathrm{p}_h\,\tilde{\mathrm{p}} + \int_K M^K\,\nabla\,\cdot\,\mathbf{w}_h\,\tilde{\mathrm{p}} - \int_{\partial K} M^K\,(\mathrm{p}_h - \lambda_2)\,(\boldsymbol{S}_2\,\boldsymbol{n}) \cdot \boldsymbol{n}\tilde{\mathrm{p}} - \int_{\partial K} M^K\,\boldsymbol{S}_4(\mathbf{u}_h - \boldsymbol{\lambda}_1)\,\cdot \boldsymbol{n}\,\tilde{\mathrm{p}}$$

$$- \int_K M^K\,(\boldsymbol{\alpha} \cdot \mathbf{u}_h) \cdot \nabla\,\tilde{\mathrm{p}} + \int_{\partial K} M^K\,(\boldsymbol{\alpha}\boldsymbol{\lambda}_1) \cdot \boldsymbol{n}\,\tilde{\mathrm{p}} = 0\,. \tag{3.12d}$$

3.1.3 Transmission conditions

The HDG formulation is established by connecting the local problem with two transmission conditions at the interfaces of the mesh. Let $(\boldsymbol{\eta}, \xi) \in \boldsymbol{M}_h \times M_h$ be two test-functions defined on the faces of the element K. The transmission conditions are:

$$\sum_{F \in \mathcal{F}_h} \int_F [\![\hat{\boldsymbol{\tau}}_h\,\boldsymbol{n}]\!] \cdot \boldsymbol{\eta} = \sum_{F \in \mathcal{F}_{\mathrm{ext}}} \int_F \boldsymbol{f}_{\mathrm{inc}} \cdot \boldsymbol{\eta}\,, \qquad \sum_{F \in \mathcal{F}_h} \int_F [\![\hat{\mathbf{w}}_h \cdot \boldsymbol{n}]\!]\,\xi = \sum_{F \in \mathcal{F}_{\mathrm{ext}}} \int_F g_{\mathrm{inc}}\,\xi\,, \tag{3.13}$$

where the jumps have been defined in (3.6) and (3.7).

3.2 Discretization using HDG method in two dimensions

The following section details the two-dimensional discretization of the HDG method in the (x, y) plane. In general formulation of HDG [68, 20, 21, 85], the stabilization matrices $\boldsymbol{S}$ are just required to be positive definite. However, in practice, they are mostly set to be a scalar times the identity matrix. Hence, from now on, we assume that the stabilization matrices in the HDG formulation, cf. (3.10), are diagonal, i.e., $\boldsymbol{S}_i = \gamma_i\,\mathbb{I}$ for $i = 1, 4$. In this way, expression (3.10) simplifies to

$$\begin{cases} \hat{\boldsymbol{\tau}}_h\,\boldsymbol{n} = \boldsymbol{\tau}_h\,\boldsymbol{n} - \gamma_1(\mathbf{u}_h - \boldsymbol{\lambda}_1) - \gamma_3\,(\mathrm{p}_h - \lambda_2)\,\boldsymbol{n}\,, \\ \hat{\mathbf{w}}_h \cdot \boldsymbol{n} = \mathbf{w}_h \cdot \boldsymbol{n} - \gamma_2\,(\mathrm{p}_h - \lambda_2) - \gamma_4\,(\mathbf{u}_h - \boldsymbol{\lambda}_1) \cdot \boldsymbol{n}\,. \end{cases} \tag{3.14}$$

In the formulation, the components of the test functions are decomposed in the basis functions of V_p as φ_i^K for $\tilde{\mathbf{u}}, \tilde{\mathbf{w}}, \tilde{\boldsymbol{\tau}}, \tilde{\mathrm{p}}$ and ψ_j^F for η, ξ. The local solutions are expressed along x and y directions:

$$\mathbf{u}_h = \begin{pmatrix} \mathrm{u}_x^K \\ \mathrm{u}_y^K \end{pmatrix}, \qquad \mathbf{w}_h = \begin{pmatrix} \mathrm{w}_x^K \\ \mathrm{w}_y^K \end{pmatrix}, \qquad \tau_h = \begin{pmatrix} \tau_{xx}^K & \tau_{xy}^K \\ \tau_{xy}^K & \tau_{yy}^K \end{pmatrix}.$$

They are decomposed as:

$$\mathrm{u}_l^K = \sum_{j=1}^{d_i^K} \underline{\mathrm{u}}_{l,j}^K \varphi_j^K\,, \quad \mathrm{w}_l^K = \sum_{j=1}^{d_i^K} \underline{\mathrm{w}}_{l,j}^K \varphi_j^K\,, \quad \tau_{kl}^K = \sum_{j=1}^{d_i^K} \underline{\tau}_{kl,j}^K \varphi_j^K\,, \quad \mathrm{p}_h^K = \sum_{j=1}^{d_i^K} \underline{\mathrm{p}}^K \varphi_j^K\,, \tag{3.15}$$

where d_i^K denotes the number of degrees of freedom of an element, and with $l = x, y$ and $k = x, y$. The local Lagrange unknowns are decomposed as follows:

$$\lambda_{1l}^F = \sum_{j=1}^{d_i^F} \underline{\lambda_{1l}}_j^F \psi_j^F\,, \qquad \lambda_2^F = \sum_{j=1}^{d_i^F} \underline{\lambda_2}_j^F \psi_j^F\,, \qquad \text{with } l = x, y\,, \tag{3.16}$$

where d_i^F denotes the number of degrees of freedom of an edge. In (3.15), each component is considered as a vector of the form $\underline{u}_l^K = (\underline{u}_{l,1}^K, \ldots, \underline{u}_{,d_i^K}^K)^T$ for $l = x, y$. Similarly, every local component of the unknowns in (3.16) is written as: $\underline{\lambda_{1l}}^F = (\underline{\lambda_{1l}}_{l,1}^F, \ldots, \underline{\lambda_{1l}}_{l,d_i^F}^F)^T$, with $l = x, y$. We define the two unknown vectors $\underline{W}^K$ and $\underline{\Lambda}^K$ respectively of size $8\,d_i^K$ and $9\,d_i^F$ as:

$$\underline{W}^K = (\underline{\mathrm{u}}_x^K,\, \underline{\mathrm{u}}_y^K,\, \underline{\mathrm{w}}_x^K,\, \underline{\mathrm{w}}_y^K,\, \underline{\tau}_{xx}^K,\, \underline{\tau}_{yy}^K,\, \underline{\tau}_{xy}^K,\, \underline{\mathrm{p}}^K)^T\,,$$

and

$$\underline{\Lambda}^K = (\underline{\lambda}_{1x}^{\beta(K,1)}, \underline{\lambda}_{1x}^{\beta(K,2)}, \underline{\lambda}_{1x}^{\beta(K,3)}, \underline{\lambda}_{1y}^{\beta(K,1)} \underline{\lambda}_{1y}^{\beta(K,2)}, \underline{\lambda}_{1y}^{\beta(K,3)}, \underline{\lambda}_2^{\beta(K,1)}, \underline{\lambda}_2^{\beta(K,2)}, \underline{\lambda}_2^{\beta(K,3)})^T\,,$$

where $\beta(K, f)$ is the global index of the f-th face of the element K.

We also define the following elementary matrices $\mathbb{M}^K$, $\mathbb{D}_v^K$, $\mathbb{E}^F$, $\mathbb{J}_v^F$ of size $d_i^K \times d_i^K$, $\mathbb{F}^F$, $\mathbb{Q}_v^F$ of size $d_i^K \times d_i^F$, and $\mathbb{G}^F$, $\mathbb{H}_v^F$ of size $d_i^F \times d_i^F$:

$$\begin{aligned}
&\mathbb{M}_{ij}^K = \int_K \varphi_i^K \varphi_j^K\, dX\,, && \mathbb{D}_{vij}^K = \int_K \varphi_j^K \frac{\partial \varphi_i^K}{\partial v} dX\,, \quad \mathbb{E}_{ij}^F = \int_F \varphi_i^K \varphi_j^K\, dS\,, && \mathbb{J}_{vij}^F = \int_F \varphi_i^K \varphi_j^K n_v\, dS\,,\\
&\mathbb{F}_{ij}^F = \int_F \psi_j^F \varphi_i^K dS\,, && \mathbb{Q}_{vij}^F = \int_F \psi_j^F \varphi_i^K n_v\, dS\,, \quad \mathbb{G}_{ij}^F = \int_F \psi_j^F \psi_j^F\, dS\,, && \mathbb{H}_{vij}^F = \int_F \psi_i^F \psi_j^F n_v\, dS\,,
\end{aligned} \tag{3.18}$$

with $v = x, y$. Moreover, we define four elementary source vectors of size d_i^K

$$\big(\mathbb{C}_{1x}^K\big)_i = \int_K f_{\mathrm{vol}\,x}^K\, \varphi_i^K\,, \qquad \big(\mathbb{C}_{1y}^K\big)_i = \int_K f_{\mathrm{vol}\,y}^K\, \varphi_i^K\,, \qquad \big(\mathbb{C}_{2x}^K\big)_i = \int_K g_{\mathrm{vol}\,x}^K\, \varphi_i^K\,, \qquad \big(\mathbb{C}_{2y}^K\big)_i = \int_K g_{\mathrm{vol}\,y}^K\, \varphi_i^K\,.$$

Remark 3.3. In using straight-edge meshes, and Lagrangian polynomials for approximation spaces, the components of the above local matrices are computed by the standard techniques in which they are rewritten in terms of integrals on the reference element or reference edge, (triangle or the line interval $[0, 1]$) with the reference Lagrangian polynomials.

3.2.1 Local problem

Because of the size of the system of equations, we present separately the discretization of each equation of the local problem (3.12). Using the above representation of the local unknowns, each equation is written in terms of the matrices defined in (3.18), (for more details, see [8]).

(a) The equation of motion (3.12a)

Taking $\bullet = x, y$, discretizing equation (3.12a) along the x and y component gives:

$$\begin{aligned}
&\int_K \mathrm{i}\,\omega\,\rho_a^K\, \mathrm{u}_\bullet^K\, \varphi_i^K + \int_K \mathrm{i}\,\omega\,\rho_f^K\, \mathrm{w}_\bullet^K\, \varphi_i^K - \int_K \frac{\partial \tau_{x\bullet}^K}{\partial x}\, \varphi_i^K - \int_K \frac{\partial \tau_{\bullet y}^K}{\partial y}\, \varphi_i^K + \int_{\partial K} \gamma_1\, \mathrm{u}_\bullet^K \varphi_i^K - \int_{\partial K} \gamma_1\, \lambda_{1\bullet} \varphi_i^K\\
&\qquad + \int_{\partial K} \gamma_3\, \mathrm{p}_h^K\, n_\bullet\, \varphi_i^K - \int_{\partial K} \gamma_3\, \lambda_2\, n_\bullet\, \varphi_i^K = \int_K f_{\mathrm{vol}\,\bullet}^K\, \varphi_i^K\,.
\end{aligned}$$

In terms of the local matrices defined in equation (3.18) and the unknown vectors in (3.17), the above equations are

$$\begin{aligned}
&\mathrm{i}\,\omega\,\rho_a^K\, \mathbb{M}^K \underline{\mathrm{u}}_\bullet^K + \mathrm{i}\,\omega\,\rho_f^K\, \mathbb{M}^K \underline{\mathrm{w}}_\bullet^K - (\mathbb{D}_x^K)^T\, \underline{\tau}_{x\bullet}^K - (\mathbb{D}_y^K)^T\, \underline{\tau}_{\bullet y}^K + \sum_{f=1}^{3} \gamma_1\, \mathbb{E}^{\beta(K,f)}\, \underline{\mathrm{u}}_\bullet^K - \sum_{f=1}^{3} \gamma_1\, \mathbb{F}^{\beta(K,f)}\, \underline{\lambda}_{1\bullet}^{\beta(K,f)}\\
&\qquad + \sum_{f=1}^{3} \gamma_3\, \mathbb{J}_\bullet^{\beta(K,f)}\, \underline{\mathrm{p}}^K - \sum_{f=1}^{3} \gamma_3\, \mathbb{Q}_\bullet^{\beta(K,f)}\, \underline{\lambda}_2^{\beta(K,f)} = \mathbb{C}_{1\bullet}^K\,.
\end{aligned}$$

(b) The second equation of motion (3.12b)

Similarly, equation (3.12b) is discretized along x and y direction

$$\int_K \mathrm{i}\,\omega\,\rho_f^K\,\mathrm{u}_\bullet^K\,\varphi_i^K \;+\int_K \mathrm{i}\omega\,\tilde{\rho}^K\,\mathrm{w}_\bullet^K\varphi_i^K \;-\int_K \mathrm{p}_h^K\,\frac{\partial\varphi_i^K}{\partial\bullet} \;+\int_{\partial K}\lambda_2\,n_\bullet\,\varphi_i^K \;=\; \int_K f_{w\bullet}\,\varphi_i^K\,,$$

and gives in terms of the local matrices and the unknown vectors defined respectively in equations (3.18) and (3.17):

$$\mathrm{i}\omega\,\rho_f^K\,\mathbb{M}^K\underline{\mathrm{u}}_\bullet^K \;+\;\mathrm{i}\omega\,\rho_{\mathrm{dyn}}^K\,\mathbb{M}^K\underline{\mathrm{w}}_\bullet^K \;-\mathbb{D}_\bullet^K\,\underline{\mathrm{p}}^K \;-\sum_{f=1}^{3}\mathbb{Q}_\bullet^{\beta(K,f)}\,\underline{\lambda}_2^{\beta(K,f)} \;=\; \mathbb{C}_{2\bullet}^K\,,\quad \text{with } \bullet = x,y\,.$$

(c) The first constitutive law (3.12c)

The constitutive law equation given in (3.12c) is discretized as well and the equations are expressed in terms of local matrices and the unknown vectors defined in equations (3.17) and (3.18):

$$\mathrm{i}\,\omega\,\mathbb{M}^K\,\underline{\tau}_{xx}^K \;+\;\mathrm{i}\,\omega\alpha_{11}^K\mathbb{M}^K\underline{\mathrm{p}}^K \;+C_{11}^K\mathbb{D}_x^K\,\underline{\mathrm{u}}_x^K \;+C_{13}^K\mathbb{D}_y^K\,\underline{\mathrm{u}}_x^K \;+C_{13}^K\mathbb{D}_x^K\,\underline{\mathrm{u}}_y^K \;+C_{12}^K\mathbb{D}_y^K\,\underline{\mathrm{u}}_y^K$$

$$-\sum_{f=1}^{3}\underline{\lambda}_{1x}^{\beta(K,f)}\,(C_{11}^K\mathbb{Q}_x^{\beta(K,f)}+\,C_{13}^K\mathbb{Q}_y^{\beta(K,f)}) - \sum_{f=1}^{3}\underline{\lambda}_{1y}^{\beta(K,f)}\,(C_{13}^K\mathbb{Q}_x^{\beta(K,f)}+\,C_{12}^K\mathbb{Q}_y^{\beta(K,f)}) = \,0\,,$$

$$\mathrm{i}\,\omega\,\mathbb{M}^K\,\underline{\tau}_{yy}^K \;+\;\mathrm{i}\,\omega\,\alpha_{22}^K\,\mathbb{M}^K\,\underline{\mathrm{p}}^K \;+C_{12}^K\mathbb{D}_x^K\,\underline{\mathrm{u}}_x^K \;+C_{23}^K\mathbb{D}_y^K\,\underline{\mathrm{u}}_x^K \;+C_{23}^K\mathbb{D}_x^K\,\underline{\mathrm{u}}_y^K \;+C_{22}^K\mathbb{D}_y^K\,\underline{\mathrm{u}}_y^K$$

$$-\sum_{f=1}^{3}\underline{\lambda}_{1x}^{\beta(K,f)}\,(C_{12}^K\mathbb{Q}_x^{\beta(K,f)}+\,C_{23}\mathbb{Q}_y^{\beta(K,f)}) \;-\sum_{f=1}^{3}\underline{\lambda}_{1y}^{\beta(K,f)}\,(C_{23}\mathbb{Q}_x^{\beta(K,f)}+\,C_{22}\mathbb{Q}_y^{\beta(K,f)}) = \,0\,,$$

and

$$\mathrm{i}\,\omega\,\mathbb{M}^K\,\underline{\tau}_{xy}^K \;+\;\mathrm{i}\,\omega\,\alpha_{12}^K\,\mathbb{M}^K\,\underline{\mathrm{p}}^K \;+C_{13}^K\mathbb{D}_x^K\,\underline{\mathrm{u}}_x^K \;+C_{33}^K\mathbb{D}_y^K\,\underline{\mathrm{u}}_x^K \;+C_{33}^K\mathbb{D}_x^K\,\underline{\mathrm{u}}_y^K \;+C_{23}^K\mathbb{D}_y^K\,\underline{\mathrm{u}}_y^K$$

$$-\sum_{f=1}^{3}\underline{\lambda}_{1x}^{\beta(K,f)}\,(C_{13}^K\mathbb{Q}_x^{\beta(K,f)}+\,C_{33}^K\mathbb{Q}_y^{\beta(K,f)}) \;-\sum_{f=1}^{3}\underline{\lambda}_{1y}^{\beta(K,f)}\,(C_{33}^K\mathbb{Q}_x^{\beta(K,f)}+\,C_{23}^K\mathbb{Q}_y^{\beta(K,f)}) = \,0\,.$$

(d) The second constitutive law (3.12d)

The discretization of equation (3.12d) reads:

$$\int_K \mathrm{i}\,\omega\,\mathrm{p}_h^K\,\varphi_i^K \;+\int_K M^K\,\frac{\partial \mathrm{w}_x^K}{\partial x}\,\varphi_i^K \;+\int_K M^K\,\frac{\partial \mathrm{w}_y^K}{\partial y}\,\varphi_i^K \;-\int_{\partial K} M^K\,\mathrm{p}_h^K\,\gamma_2\,\varphi_i^K + \int_{\partial K} M^K\,\lambda_2\,\gamma_2\,\varphi_i^K \;-\int_{\partial K} M^K\,\gamma_4\mathrm{u}_x^K\,n_x\,\varphi_i^K$$

$$-\int_{\partial K} M^K\,\gamma_4\mathrm{u}_y^K\,n_y\,\varphi_i^K \;+\int_{\partial K} M^K\,\gamma_4\,\lambda_{1x}\,n_x\,\varphi_i^K \;+\int_{\partial K} M^K\,\gamma_4\,\lambda_{1y}\,n_y\varphi_i^K \;-\int_K M^K\,(\alpha_{11}\mathrm{u}_x^K \;+\;\alpha_{12}\mathrm{u}_y^K)\frac{\partial\varphi_i^K}{\partial x}$$

$$-\int_K M^K\,(\alpha_{12}\mathrm{u}_x^K + \alpha_{22}\mathrm{u}_y^K)\frac{\partial\varphi_i^K}{\partial y} \;+\int_K M^K\,(\alpha_{11}\lambda_{1x}+\alpha_{12}\lambda_{1y})n_x\,\varphi_i^K \;+\int_K M^K\,(\alpha_{12}\lambda_{1x}+\alpha_{22}\lambda_{1y})n_y\,\varphi_i^K = 0\,,$$

and writes in terms of the local matrices defined in equation (3.18) and the unknown vectors in (3.17):

$$\begin{aligned}
&\mathrm{i}\,\omega\,\mathbb{M}^K\,\underline{\mathrm{p}}^K + M^K(\mathbb{D}_x^K)^T\,\underline{\mathrm{w}}_x^K + M^K(\mathbb{D}_y^K)^T\,\underline{\mathrm{w}}_y^K - \sum_{f=1}^{3} M^K\,\gamma_2\,\mathbb{E}^{\beta(K,f)}\underline{\mathrm{p}}^K + \sum_{f=1}^{3} M^K\,\gamma_2\,\underline{\lambda}_2^{\beta(K,f)}\mathbb{F}^{\beta(K,f)}\\
&- \sum_{f=1}^{3} M^K\,\gamma_4(\mathbb{J}_x^{\beta(K,f)}\,\underline{\mathrm{u}}_x^K + \mathbb{J}_y^{\beta(K,f)}\,\underline{\mathrm{u}}_y^K) + \sum_{f=1}^{3} M^K\,\gamma_4(\mathbb{Q}_x^{\beta(K,f)}\,\underline{\lambda}_{1x}^{\beta(K,f)} + \mathbb{Q}_y^{\beta(K,f)}\underline{\lambda}_{1y}^{\beta(K,f)})\\
&- M^K\,\alpha_{11}^K\,\mathbb{D}_x^K\,\mathrm{u}_x^K - M^K\,\alpha_{12}^K\mathbb{D}_y^K\,\mathrm{u}_y^K + \sum_{f=1}^{3} M^K(\alpha_{11}\underline{\lambda}_{1x}^{\beta(K,f)} + \alpha_{12}^K\underline{\lambda}_{1y}^{\beta(K,f)})\,\mathbb{Q}_x^{\beta(K,f)}\\
&- M^K\,\alpha_{12}^K\,\mathbb{D}_y^K\,\mathrm{u}_x^K - M^K\,\alpha_{22}^K\,\mathbb{D}_x^K\,\mathrm{u}_y^K + \sum_{f=1}^{3} M^K(\alpha_{12}^K\underline{\lambda}_{1x}^{\beta(K,f)} + \alpha_{22}^K\,\underline{\lambda}_{1y}^{\beta(K,f)})\,\mathbb{Q}_y^{\beta(K,f)} = 0\,.
\end{aligned}$$

Local linear system

The local system obtained from the discretization of (3.12) can be written as:

$$\mathbb{A}^K\underline{W}^K + \mathbb{B}^K\underline{\Lambda}^K = \mathbb{C}^K_{\text{source}}\,,$$

where $\underline{W}^K$ and $\underline{\Lambda}^K$ have been defined in (3.17). In the above equation, $\mathbb{A}^K$ is of dimension $8\,d_i^K \times 8d_i^K$, $\mathbb{B}^K$ of size $8\,d_i^K \times 9d_i^F$, and $\mathbb{C}^K_{\text{source}}$ is the matrix of the external forces of dimension $8\,d_i^K$.

$\underline{W}^K$ is composed of 8 blocks corresponding to different types of unknowns, we hence decompose the elementary matrix $\mathbb{A}^K$ in 8 columns of size $8\,d_i^K \times d_i^K$:

$$\mathbb{A}^K = \begin{pmatrix}\mathbb{A}_1^K & \mathbb{A}_2^K & \mathbb{A}_3^K & \mathbb{A}_4^K & \mathbb{A}_5^K & \mathbb{A}_6^K & \mathbb{A}_7^K & \mathbb{A}_8^K\end{pmatrix}, \quad \text{that are detailed in Appendix B.1.1.}$$

Similarly, based on the structure of the unknown $\underline{\Lambda}^K$ in three times three sub-blocks corresponding to the three Lagrange unknowns decomposed on the three faces of the triangle, we write $\mathbb{B}^K$ in 9 columns of size $8\,d_i^K \times d_i^F$:

$\mathbb{B}^K = \begin{pmatrix}B_{\lambda_{1x},1} & B_{\lambda_{1x},2} & B_{\lambda_{1x},3} & B_{\lambda_{1y},1} & B_{\lambda_{1y},2} & B_{\lambda_{1y},3} & B_{\lambda_2,1} & B_{\lambda_2,2} & B_{\lambda_2,3}\end{pmatrix}$, where $\mathbb{B}^K$ is given in Appendix B.1.1.

Finally the local source vector is:

$$\left(\mathbb{C}^K_{\text{source}}\right)^T = \begin{pmatrix}\mathbb{C}_{1x}^K & \mathbb{C}_{1y}^K & \mathbb{C}_{2x}^K & \mathbb{C}_{2y}^K & 0 & 0 & 0 & 0\end{pmatrix}.$$

3.2.2 Transmission conditions

We recall the transmission conditions given by equation (3.13):

$$\sum_{F\in\mathcal{F}_h}\int_F [\![\hat{\boldsymbol{\tau}}_h\,\boldsymbol{n}]\!]\cdot\eta = \sum_{F\in\mathcal{F}_{\text{ext}}}\int_F \boldsymbol{f}_{\text{inc}}\cdot\eta\,, \qquad \sum_{F\in\mathcal{F}_h}\int_F [\![\hat{\mathbf{w}}_h\cdot\boldsymbol{n}]\!]\,\xi = \sum_{F\in\mathcal{F}_{\text{ext}}}\int_F g_{\text{inc}}\,\xi\,,$$

which are equivalent to

$$\sum_{K\in\mathcal{T}_h}\int_{\partial K}(\hat{\boldsymbol{\tau}}_h\,\boldsymbol{n})\cdot\eta = \sum_{F\in\mathcal{F}_{\text{ext}}}\int_F \boldsymbol{f}_{\text{inc}}\cdot\eta\,, \quad (3.21a) \qquad \sum_{K\in\mathcal{T}_h}\int_{\partial K}\hat{\mathbf{w}}_h\cdot\boldsymbol{n}\,\xi = \sum_{F\in\mathcal{F}_{\text{ext}}}\int_F g_{\text{inc}}\,\xi\,. \quad (3.21b)$$

The above equations are expressed using the definition of the numerical traces on a face in (3.10) and the definition of the jump on an interior face in (3.6). Equation (3.21a) gives:

$$\sum_{K\in\mathcal{T}_h}\int_{\partial K}\boldsymbol{\tau}_h^K\boldsymbol{n}^K\cdot\eta - \sum_{K\in\mathcal{T}_h}\int_{\partial K}\boldsymbol{S}_1(\mathbf{u}_h^K - \boldsymbol{\lambda}_1)\cdot\eta - \sum_{K\in\mathcal{T}_h}\int_{\partial K}(\mathrm{p}_h^K - \lambda_2)\boldsymbol{S}_3\boldsymbol{n}^K\cdot\eta = \sum_{F\in\mathcal{F}_{\text{ext}}}\int_F \boldsymbol{f}_{\text{inc}}\cdot\eta\,, \quad (3.22a)$$

and (3.21b) is expressed as:

$$\sum_{K\in\mathcal{T}_h}\int_{\partial K}\mathbf{w}_h^K\cdot\boldsymbol{n}^K\,\xi-\sum_{K\in\mathcal{T}_h}\int_{\partial K}(\mathrm{p}_h^K-\lambda_2)(\boldsymbol{S}_2\boldsymbol{n}^K)\cdot\boldsymbol{n}^K\,\xi-\sum_{K\in\mathcal{T}_h}\int_{\partial K}\boldsymbol{S}_4(\mathbf{u}_h^K-\boldsymbol{\lambda}_1)\cdot\boldsymbol{n}^K\cdot\xi=\sum_{F\in\mathcal{F}_{\rm ext}}\int_F g_{\rm inc}\,\xi\,. \quad (3.22b)$$

These equations are discretized on (x,y) by decomposing the unknowns using (3.15) and (3.16) and replacing the test functions by the basis functions. They are then expressed in terms of the elementary matrices defined in (3.18).

The first transmission equation (3.22a) The discretization of (3.22a) along x and y direction is, taking $\bullet=x,y$:

$$\sum_{K\in\mathcal{T}_h}\int_{\partial K}\underline{\tau}_{x\bullet}^K\,n_x^K\,\varphi_j^K\,\psi_i^{\beta(K,f)}\,dS+\sum_{K\in\mathcal{T}_h}\int_{\partial K}\underline{\tau}_{\bullet y}^K\,n_y^K\,\varphi_j^K\,\psi_i^{\beta(K,f)}\,dS-\sum_{K\in\mathcal{T}_h}\int_{\partial K}\gamma_1\,\varphi_j^K\,\underline{\mathrm{u}}_\bullet^K\,\psi_i^{\beta(K,f)}\,dS$$

$$+\sum_{K\in\mathcal{T}_h}\int_{\partial K}\gamma_1\,\psi_j^{\beta(K,f)}\underline{\lambda}_{1\bullet}^K\,\psi_i^{\beta(K,f)}\,dS-\sum_{K\in\mathcal{T}_h}\int_{\partial K}\gamma_3 n_\bullet^K\underline{\mathrm{p}}^K\varphi_j^K\psi_i^{\beta(K,f)}dS$$

$$+\sum_{K\in\mathcal{T}_h}\int_{\partial K}\gamma_3 n_\bullet^K\underline{\lambda}_2^K\psi_j^{\beta(K,f)}\psi_i^{\beta(K,f)}dS=\sum_{F\in\mathcal{F}_{\rm ext}}\int_F f_{{\rm inc},\bullet}\,\psi_i^{\beta(K,f)}\,dS\,.$$

This is expressed in terms of the local matrices defined in equation (3.18) and the unknown vectors in (3.17) as:

$$\sum_{K\in\mathcal{T}_h}\Big(\,(\mathbb{Q}_x^{\beta(K,f)})^T\,\underline{\tau}_{x\bullet}^K\,+\,(\mathbb{Q}_y^{\beta(K,f)})^T\,\underline{\tau}_{\bullet y}^K\,-\,\gamma_1\,(\mathbb{F}^{\beta(K,f)})^T\,\underline{\mathrm{u}}_\bullet^K\,+\,\gamma_1\,\mathbb{G}^{\beta(K,f)}\,\underline{\lambda}_{1\bullet}^{\beta(K,f)}$$
$$-\,\gamma_3\,(\mathbb{Q}_\bullet^{\beta(K,f)})^T\,\underline{\mathrm{p}}^K\,+\,\gamma_3\,\mathbb{H}_\bullet^{\beta(K,f)}\,\underline{\lambda}_2^{\beta(K,f)}\Big)\,=\,\sum_{F\in\mathcal{F}_{\rm ext}}\int_F f_{{\rm inc},\bullet}\,\psi_i^{\beta(K,f)}\,dS\,. \quad (3.23)$$

The second transmission condition (3.22b) Similarly, the discretization of equation (3.22b) is

$$\int_F\underline{\mathrm{w}}_x^K\,\varphi_j^K\,n_x^K\,\psi_i^{\beta(K,f)}\,+\int_F\underline{\mathrm{w}}_y^K\,\varphi_j^K\,n_y^K\,\psi_i^{\beta(K,f)}\,-\int_F\underline{\mathrm{p}}^K\,\varphi_j^K\,\gamma_2\,\psi_i^{\beta(K,f)}+\int_F\underline{\lambda}_2^K\,\psi_j^{\beta(K,f)}\,\gamma_2\,\psi_i^{\beta(K,f)}$$

$$-\int_F\underline{\mathrm{u}}_x^K\,\varphi_j^K\,\gamma_4\,n_x^K\,\psi_i^{\beta(K,f)}\,-\int_F\underline{\mathrm{u}}_y^K\,\varphi_j^K\,\gamma_4\,n_y^K\,\psi_i^{\beta(K,f)}\,+\int_F\underline{\lambda}_{1x}^K\,\psi_j^{\beta(K,f)}\,\gamma_4\,n_x^K\,\psi_i^{\beta(K,f)}$$

$$+\int_F\underline{\lambda}_{1y}^K\,\psi_j^{\beta(K,f)}\,\gamma_4\,n_y^K\,\psi_i^{\beta(K,f)}\,=\,0\,,$$

and writes in terms of the local matrices and the unknown vectors defined respectively in equations (3.18) and (3.17):

$$\sum_{K\in\mathcal{T}_h}\Big((\mathbb{Q}_x^{\beta(K,f)})^T\,\underline{\mathrm{w}}_x^K\,+(\mathbb{Q}_y^{\beta(K,f)})^T\,\underline{\mathrm{w}}_y^K\,-(\mathbb{F}^{\beta(K,f)})^T\,\underline{\mathrm{p}}^K\,\gamma_2\,+\mathbb{G}^{\beta(K,f)}\underline{\lambda}_2^K\,\gamma_2-(\mathbb{Q}_x^{\beta(K,f)})^T\underline{\mathrm{u}}_x^K\,\gamma_4$$
$$-(\mathbb{Q}_y^{\beta(K,f)})^T\underline{\mathrm{u}}_y^K\,\gamma_4+\mathbb{H}_x^{\beta(K,f)}\underline{\lambda}_{1x}^K\,\gamma_4+\mathbb{H}_y^{\beta(K,f)}\underline{\lambda}_{1y}^K\,\gamma_4\Big)=\sum_{F\in\mathcal{F}_{\rm ext}}\int_F g_{\rm inc}\,\psi_i^{\beta(K,f)}\,dS\,. \quad (3.24)$$

Global system

Let $N_{\rm face}$ be the number of edges of the mesh. We define the global vector

$$\underline{\Lambda}\,=\,(\underline{\boldsymbol{\lambda}}_1^1,\,\underline{\lambda}_2^1,\,....,\,\underline{\boldsymbol{\lambda}}_1^{N_{\rm face}},\,\underline{\lambda}_2^{N_{\rm face}})\,.$$

Define also the local trace operator $\mathcal{A}_{HDG}$ linking the local degrees of freedom on an element K to the global degrees of freedom of the Lagrange multiplier $\underline{\Lambda}$. This means, for an element K, that

$$\mathcal{A}_{HDG}^K\,\underline{\Lambda}\,=\,\underline{\Lambda}^K\,.$$

The transmission conditions (3.23) and (3.24) are summed on all the faces of each element to give:

$$\sum_{K\in\mathcal{T}_h}(\mathcal{A}_{HDG}^K)^T\left(\mathbb{P}^K\underline{W}^K+\mathbb{T}^K\mathcal{A}_{HDG}^K\underline{\Lambda}\right)=\mathbb{S}_{\rm inc}\,,$$

with $\mathbb{P}^K$ and $\mathbb{T}^K$ two matrices respectively of dimension $9\,d_i^F\times 8\,d_i^K$ and $9\,d_i^F\times 9\,d_i^F$ given in Appendix B.1.1.

3.3 Discretization using HDG method in three dimensions

In this section, we detail the discretization of the HDG method in three dimensions. Similarly as for Section 3.2, we assume that the stabilization matrices in the HDG formulation are diagonal, i.e. $\boldsymbol{S}_i = \gamma_i \mathbb{I}$ for $i = 1, 4$. Hence, the expression of the numerical traces defined in equation (3.10) simplifies to:

$$\begin{cases} \hat{\boldsymbol{\tau}}_h \boldsymbol{n} \;=\; \boldsymbol{\tau}_h \boldsymbol{n} \;-\; \gamma_1(\mathbf{u}_h \,-\, \boldsymbol{\lambda}_1) \;-\; (\mathrm{p}_h \,-\, \lambda_2)\,\gamma_3 \boldsymbol{n}\,, \\ \hat{\mathbf{w}}_h \cdot \boldsymbol{n} \;=\; \mathbf{w}_h \cdot \boldsymbol{n} \;\;-\; \gamma_2\,(\mathrm{p}_h \,-\, \lambda_2) \;\;-\; \gamma_4\,(\mathbf{u}_h \,-\, \boldsymbol{\lambda}_1) \cdot \boldsymbol{n}\,. \end{cases}$$

In the formulation, the components of the test functions are decomposed in the basis functions of V_p as φ_i^K for $\tilde{\mathbf{u}}, \tilde{\mathbf{w}}, \tilde{\boldsymbol{\tau}}, \tilde{\mathrm{p}}$ and ψ_j^F for η, ξ. The local solutions are expressed along x,y and z directions:

$$\mathbf{u}_h \;=\; \begin{pmatrix} \mathrm{u}_x^K \\ \mathrm{u}_y^K \\ \mathrm{u}_z^K \end{pmatrix}, \qquad \mathbf{w}_h \;=\; \begin{pmatrix} \mathrm{w}_x^K \\ \mathrm{w}_y^K \\ \mathrm{w}_z^K \end{pmatrix}, \qquad \tau_h \;=\; \begin{pmatrix} \tau_{xx}^K & \tau_{xy}^K & \tau_{xz}^K \\ \tau_{xy}^K & \tau_{yy}^K & \tau_{yz}^K \\ \tau_{xz}^K & \tau_{yz}^K & \tau_{zz}^K \end{pmatrix},$$

and they are decomposed as:

$$\mathrm{u}_l^K = \sum_{j=1}^{d_i^K} \underline{\mathrm{u}}_{l,j}^K \varphi_j^K\,, \quad \mathrm{w}_l^K = \sum_{j=1}^{d_i^K} \underline{\mathrm{w}}_{l,j}^K \varphi_j^K\,, \quad \tau_{kl}^K = \sum_{j=1}^{d_i^K} \underline{\tau}_{kl,j}^K \varphi_j^K\,, \quad \mathrm{p}_h^K = \sum_{j=1}^{d_i^K} \underline{\mathrm{p}}^K \varphi_j^K\,, \tag{3.25}$$

with d_i^K the number of degrees of freedom of an element, and $l, k = x, y, z$. Similarly, we decompose the local Lagrange unknowns as:

$$\lambda_{1l}^F = \sum_{j=1}^{d_i^F} \underline{\lambda_{1l}}_j^F \psi_j^F\,, \qquad \lambda_2^F = \sum_{j=1}^{d_i^F} \underline{\lambda_2}_j^F \psi_j^F\,, \qquad \text{with } l = x, y, z\,, \tag{3.26}$$

where d_i^F denotes the number of degrees of freedom of an edge. In (3.25), each component is considered as a vector of the form $\underline{u}_l^K = (\underline{u}_{l,1}^K, \ldots, \underline{u}_{,d_i^K}^K)^T$ with $l = x, y, z$, and every local component of the unknowns in (3.26) is written as: $\underline{\lambda_{1l}}^F = (\underline{\lambda_{1l}}_{l,1}^F, \ldots, \underline{\lambda_{1l}}_{l,d_i^F}^F)^T$, for $l = x, y, z$. The unknown vectors $\underline{W}^K$ and $\underline{\Lambda}^K$, respectively of size $13\,d_i^K$ and $16\,d_i^F$, are defined as:

$$\underline{W}^K = (\underline{\mathrm{u}}_x^K, \underline{\mathrm{u}}_y^K, \underline{\mathrm{u}}_z^K, \underline{\mathrm{w}}_x^K, \underline{\mathrm{w}}_y^K, \underline{\mathrm{w}}_z^K, \underline{\tau}_{xx}^K, \underline{\tau}_{yy}^K, \underline{\tau}_{zz}^K, \underline{\tau}_{yz}^K, \underline{\tau}_{xz}^K, \underline{\tau}_{xy}^K, \underline{\mathrm{p}}^K)^T\,,$$

and

$$\underline{\Lambda}^K = \Big(\underline{\lambda}_{1x}^{\beta(K,1)}, \underline{\lambda}_{1x}^{\beta(K,2)}, \underline{\lambda}_{1x}^{\beta(K,3)}, \underline{\lambda}_{1x}^{\beta(K,4)}, \underline{\lambda}_{1y}^{\beta(K,1)} \underline{\lambda}_{1y}^{\beta(K,2)}, \underline{\lambda}_{1y}^{\beta(K,3)}, \underline{\lambda}_{1y}^{\beta(K,4)},$$

$$\underline{\lambda}_{1z}^{\beta(K,1)} \underline{\lambda}_{1z}^{\beta(K,2)}, \underline{\lambda}_{1z}^{\beta(K,3)}, \underline{\lambda}_{1z}^{\beta(K,4)}, \underline{\lambda}_2^{\beta(K,1)}, \underline{\lambda}_2^{\beta(K,2)}, \underline{\lambda}_2^{\beta(K,3)}, \underline{\lambda}_2^{\beta(K,4)}\Big)^T\,,$$

with $\beta(K, f)$ the global index of the f-th face of the element K.

We recall the following elementary matrices defined in equation (3.18) $\mathbb{M}^K$, $\mathbb{D}_v^K$, $\mathbb{E}^F$, $\mathbb{J}_v^F$ of size $d_i^K \times d_i^K$, $\mathbb{F}^F$, $\mathbb{Q}_v^F$ of size $d_i^K \times d_i^F$, and $\mathbb{G}^F$, $\mathbb{H}_v^F$ of size $d_i^F \times d_i^F$, for $v = x, y, z$:

$$\begin{aligned} &\mathbb{M}_{ij}^K = \int_K \varphi_i^K \varphi_j^K dX\,, \qquad \mathbb{D}_{vij}^K = \int_K \varphi_j^K \frac{\partial \varphi_i^K}{\partial v} dX\,, \quad \mathbb{E}_{ij}^F = \int_F \varphi_i^K \varphi_j^K dS\,, \qquad \mathbb{J}_{vij}^F = \int_F \varphi_i^K \varphi_j^K n_v\, dS\,, \\ &\mathbb{F}_{ij}^F = \int_F \psi_j^F \varphi_i^K dS\,, \qquad \mathbb{Q}_{vij}^F = \int_F \psi_j^F \varphi_i^K n_v\, dS\,, \quad \mathbb{G}_{ij}^F = \int_F \psi_j^F \psi_j^F dS\,, \qquad \mathbb{H}_{vij}^F = \int_F \psi_i^F \psi_j^F n_v\, dS\,. \end{aligned} \tag{3.28}$$

Moreover, the six elementary source vectors of size d_i^K are defined as:

$$\begin{aligned} \big(\mathbb{C}_{1x}^K\big)_i \;&=\; \int_K f_{\mathrm{vol}\;x}^K\, \varphi_i^K\,, \qquad \big(\mathbb{C}_{1y}^K\big)_i \;=\; \int_K f_{\mathrm{vol}\;y}^K\, \varphi_i^K\,, \qquad \big(\mathbb{C}_{1z}^K\big)_i \;=\; \int_K f_{\mathrm{vol}\;z}^K\, \varphi_i^K\,, \\ \big(\mathbb{C}_{2x}^K\big)_i \;&=\; \int_K g_{\mathrm{vol}\;x}^K\, \varphi_i^K\,, \qquad \big(\mathbb{C}_{2y}^K\big)_i \;=\; \int_K g_{\mathrm{vol}\;y}^K\, \varphi_i^K\,, \qquad \big(\mathbb{C}_{2z}^K\big)_i \;=\; \int_K g_{\mathrm{vol}\;z}^K\, \varphi_i^K\,. \end{aligned}$$

3.3.1 Local problem

In the following, we present the discretization of each equation of the local problem (3.12). Using the above representation of the local unknowns, each equation is written in terms of the matrices defined in (3.28).

(a) The equation of motion (3.12a)

Taking $\bullet = x, y, z$, the discretization of equation (3.12a) along the x, y and z component is:

$$\int_K \mathrm{i}\,\omega\,\rho_a^K\,\mathrm{u}_\bullet^K\,\varphi_i^K + \int_K \mathrm{i}\,\omega\,\rho_f^K\,\mathrm{w}_\bullet^K\,\varphi_i^K - \int_K \frac{\partial \tau_{x\bullet}^K}{\partial x}\,\varphi_i^K - \int_K \frac{\partial \tau_{\bullet y}^K}{\partial y}\,\varphi_i^K + \int_{\partial K} \gamma_1\,\mathrm{u}_\bullet^K \varphi_i^K - \int_{\partial K} \gamma_1\,\lambda_{1\bullet}\varphi_i^K$$
$$+ \int_{\partial K} \gamma_3\,\mathrm{p}_h^K\,n_\bullet\,\varphi_i^K - \int_{\partial K} \gamma_3\,\lambda_2\,n_\bullet\,\varphi_i^K = \int_K f_{\mathrm{vol}\,\bullet}^K\,\varphi_i^K\,.$$

In terms of the local matrices defined in equation (3.18) and the unknown vectors in (3.17), the above equations read

$$\mathrm{i}\,\omega\,\rho_a^K\,\mathbb{M}^K\underline{\mathrm{u}}_\bullet^K + \mathrm{i}\,\omega\,\rho_f^K\,\mathbb{M}^K\underline{\mathrm{w}}_\bullet^K - (\mathbb{D}_x^K)^T\,\underline{\tau}_{x\bullet}^K - (\mathbb{D}_y^K)^T\,\underline{\tau}_{\bullet y}^K + \sum_{f=1}^{3}\gamma_1\,\mathbb{E}^{\beta(K,f)}\,\underline{\mathrm{u}}_\bullet^K - \sum_{f=1}^{3}\gamma_1\,\mathbb{F}^{\beta(K,f)}\,\underline{\lambda}_{1\bullet}^{\beta(K,f)}$$
$$+ \sum_{f=1}^{3}\gamma_3\,\mathbb{J}_\bullet^{\beta(K,f)}\,\underline{\mathrm{p}}^K - \sum_{f=1}^{3}\gamma_3\,\mathbb{Q}_\bullet^{\beta(K,f)}\,\underline{\lambda}_2^{\beta(K,f)} = \mathbb{C}_{1\bullet}^K\,.$$

(b) The second equation of motion (3.12b)

Similarly, equation (3.12b) is discretized along x, y and z directions

$$\int_K \mathrm{i}\,\omega\,\rho_f^K\,\mathrm{u}_\bullet^K\varphi_i^K + \int_K \mathrm{i}\omega\,\tilde{\rho}^K\,\mathrm{w}_\bullet^K\varphi_i^K - \int_K \mathrm{p}_h^K\,\frac{\partial\varphi_i^K}{\partial\bullet} + \int_{\partial K}\lambda_2\,n_\bullet\,\varphi_i^K = \int_K f_{w\bullet}\,\varphi_i^K\,,$$

and gives in terms of the local matrices and the unknown vectors defined respectively in (3.27) and(3.28):

$$\mathrm{i}\omega\,\rho_f^K\,\mathbb{M}^K\underline{\mathrm{u}}_\bullet^K + \mathrm{i}\omega\,\rho_{\mathrm{dyn}}^K\,\mathbb{M}^K\underline{\mathrm{w}}_\bullet^K - \mathbb{D}_\bullet^K\,\underline{\mathrm{p}}^K - \sum_{f=1}^{3}\mathbb{Q}_\bullet^{\beta(K,f)}\,\underline{\lambda}_2^{\beta(K,f)} = \mathbb{C}_{2\bullet}^K\,,\quad \text{with } \bullet = x, y\,.$$

(c) The first constitutive law (3.12c)

The constitutive law given in (3.12c) is discretized as well. Using the Voigt notation for $\boldsymbol{\tau}$ and $\boldsymbol{\alpha}$, with $\bullet = 1, 6$, we have:

$$\int_K \mathrm{i}\,\omega\,\tau_\bullet\,\varphi_i^K + \int_K \mathrm{i}\,\omega\,\alpha_\bullet\mathrm{p}_h^K\,\varphi_i^K + \int_K \left(C_{\bullet 1}\,\frac{\partial\varphi_i^K}{\partial x} + C_{\bullet 6}\,\frac{\partial\varphi_i^K}{\partial y} + \int_K C_{\bullet 5}\,\frac{\partial\varphi_i^K}{\partial z}\right)\mathrm{u}_x^K$$
$$+ \int_K \left(C_{\bullet 6}\,\frac{\partial\varphi_i^K}{\partial x} + C_{\bullet 2}\,\frac{\partial\varphi_i^K}{\partial y} + C_{\bullet 4}\,\frac{\partial\varphi_i^K}{\partial z}\right)\mathrm{u}_y^K + \int_K \left(C_{\bullet 5}\,\frac{\partial\varphi_i^K}{\partial x} + C_{\bullet 4}\,\frac{\partial\varphi_i^K}{\partial y} + C_{\bullet 3}\,\frac{\partial\varphi_i^K}{\partial z}\right)\mathrm{u}_z^K$$
$$- \int_{\partial K}\left(C_{\bullet 1}\,\varphi_i^K\,n_x + C_{\bullet 6}\,\varphi_i^K\,n_y + C_{\bullet 5}\,\varphi_i^K\,n_z\right)\lambda_{1x} - \int_{\partial K}\left(C_{\bullet 6}\,\varphi_i^K\,n_x + C_{\bullet 2}\,\varphi_i^K\,n_y + C_{\bullet 4}\,\varphi_i^K\,n_z\right)\lambda_{1y}$$
$$- \int_{\partial K}\left(C_{\bullet 5}\,\varphi_i^K\,n_x + C_{\bullet 4}\,\varphi_i^K\,n_y + C_{\bullet 3}\,\varphi_i^K\,n_z\right)\lambda_{1z} = 0\,.$$

Then, the equations are expressed in terms of local matrices and the unknown vectors defined in (3.27) and (3.28):

$$\mathrm{i}\,\omega\,\mathbb{M}^K\,\underline{\tau}_\bullet^K \;+\; \mathrm{i}\,\omega\alpha_\bullet^K\,\mathbb{M}^K\underline{\mathrm{p}}^K \;+\; \big(\,C_{\bullet 1}^K\,\mathbb{D}_x^K \;+\; C_{\bullet 6}^K\mathbb{D}_y^K \;+\; C_{\bullet 5}^K\mathbb{D}_y^K\,\big)\,\underline{\mathrm{u}}_x^K \;+\; \big(C_{\bullet 6}^K\mathbb{D}_x^K \;+\; C_{\bullet 2}^K\mathbb{D}_y^K \;+\; C_{\bullet 4}^K\mathbb{D}_z^K\,\big)\,\underline{\mathrm{u}}_y^K$$

$$+\;\big(C_{\bullet 5}^K\mathbb{D}_x^K \;+\; C_{\bullet 4}^K\mathbb{D}_y^K \;+\; C_{\bullet 3}^K\mathbb{D}_z^K\,\big)\,\underline{\mathrm{u}}_z^K \;-\sum_{f=1}^{4}\Big(C_{\bullet 1}^K\mathbb{Q}_x^{\beta(K,f)} + C_{\bullet 6}^K\mathbb{Q}_y^{\beta(K,f)} \;+\; C_{\bullet 5}^K\mathbb{Q}_z^{\beta(K,f)}\Big)\,\underline{\lambda}_{1x}^{\beta(K,f)}$$

$$-\sum_{f=1}^{4}\Big(C_{\bullet 6}^K\mathbb{Q}_x^{\beta(K,f)} + C_{\bullet 2}^K\mathbb{Q}_y^{\beta(K,f)} \;+\; C_{\bullet 4}^K\mathbb{Q}_z^{\beta(K,f)}\Big)\,\underline{\lambda}_{1y}^{\beta(K,f)}$$

$$-\sum_{f=1}^{4}\Big(C_{\bullet 5}^K\mathbb{Q}_x^{\beta(K,f)} + C_{\bullet 4}^K\mathbb{Q}_y^{\beta(K,f)} \;+\; C_{\bullet 3}^K\mathbb{Q}_z^{\beta(K,f)}\Big)\,\underline{\lambda}_{1z}^{\beta(K,f)} \;=\; 0\,.$$

(d) The second constitutive law (3.12d)

The discretization of equation (3.12d) gives

$$\int_K i\omega\mathrm{p}_h^K\varphi_i^K + \int_K M\frac{\partial \mathrm{w}_x^K}{\partial x}\varphi_i^K + \int_K M\frac{\partial \mathrm{w}_y^K}{\partial y}\varphi_i^K + \int_K M\frac{\partial \mathrm{w}_z^K}{\partial z}\varphi_i^K - \int_{\partial K} M\mathrm{p}_h^K\gamma_2\,\varphi_i^K + \int_{\partial K} M\lambda_2\gamma_2\,\varphi_i^K$$

$$-\int_{\partial K} M\gamma_4\mathrm{u}_x^K\,n_x\varphi_i^K - \int_{\partial K} M\gamma_4\mathrm{u}_y^K\,n_y\varphi_i^K - \int_{\partial K} M\gamma_4\mathrm{u}_z^K\,n_z\varphi_i^K + \int_{\partial K} M\gamma_4\lambda_{1x}\,n_x\varphi_i^K + \int_{\partial K} M\gamma_4\lambda_{1y}\,n_y\varphi_i^K$$

$$+\int_{\partial K} M\gamma_4\lambda_{1z}\,n_z\varphi_i^K - \int_K M(\alpha_{11}\mathrm{u}_x^K + \alpha_{12}\mathrm{u}_y^K + \alpha_{13}\mathrm{u}_z^K)\frac{\partial\varphi_i^K}{\partial x} - \int_K M(\alpha_{12}\mathrm{u}_x^K + \alpha_{22}\mathrm{u}_y^K + \alpha_{23}\mathrm{u}_z^K)\frac{\partial\varphi_i^K}{\partial y}$$

$$-\int_K M(\alpha_{13}\mathrm{u}_x^K + \alpha_{23}\mathrm{u}_y^K + \alpha_{33}\mathrm{u}_z^K)\frac{\partial\varphi_i^K}{\partial z} + \int_K M(\alpha_{11}\lambda_{1x} + \alpha_{12}\lambda_{1y} + \alpha_{13}\lambda_{1z})n_x\varphi_i^K$$

$$+\int_K M(\alpha_{12}\lambda_{1x} + \alpha_{22}\lambda_{1y} + \alpha_{23}\lambda_{1z})n_y\varphi_i^K + \int_K M(\alpha_{13}\lambda_{1x} + \alpha_{23}\lambda_{1y} + \alpha_{33}\lambda_{1z})n_z\varphi_i^K \;=\; 0\,.$$

The above equation is expressed using the local matrices defined in equation (3.28) and the unknown vectors in (3.27) as:

$$\mathrm{i}\,\omega\,\mathbb{M}^K\,\underline{\mathrm{p}}^K \;+ M^K(\mathbb{D}_x^K)^T\,\underline{\mathrm{w}}_x^K \;+ M^K(\mathbb{D}_y^K)^T\,\underline{\mathrm{w}}_y^K \;+ M^K(\mathbb{D}_z^K)^T\,\underline{\mathrm{w}}_z^K \;-\sum_{f=1}^{4} M^K\gamma_2\,\mathbb{E}^{\beta(K,f)}\underline{\mathrm{p}}^K \;+\sum_{f=1}^{4} M^K\gamma_2\,\underline{\lambda}_2^{\beta(K,f)}\mathbb{F}^{\beta(K,f)}$$

$$-\sum_{f=1}^{4} M^K\gamma_4\left(\mathbb{J}_x^{\beta(K,f)}\underline{\mathrm{u}}_x^K + \mathbb{J}_y^{\beta(K,f)}\underline{\mathrm{u}}_y^K + \mathbb{J}_z^{\beta(K,f)}\underline{\mathrm{u}}_z^K\right) + \sum_{f=1}^{4} M^K\gamma_4\left(\mathbb{Q}_x^{\beta(K,f)}\underline{\lambda}_{1x}^{\beta(K,f)} + \mathbb{Q}_y^{\beta(K,f)}\underline{\lambda}_{1y}^{\beta(K,f)} + \mathbb{Q}_z^{\beta(K,f)}\underline{\lambda}_{1z}^{\beta(K,f)}\right)$$

$$-\,M^K\,\mathbb{D}_x^K\left(\alpha_{11}^K\,\underline{\mathrm{u}}_x^K \;+\; \alpha_{12}^K\,\underline{\mathrm{u}}_y^K \;+\; \alpha_{13}^K\,\underline{\mathrm{u}}_z^K\right) + \sum_{f=1}^{4} M^K\left(\alpha_{11}\underline{\lambda}_{1x}^{\beta(K,f)} + \alpha_{12}^K\underline{\lambda}_{1y}^{\beta(K,f)} + \alpha_{13}^K\underline{\lambda}_{1z}^{\beta(K,f)}\right)\mathbb{Q}_x^{\beta(K,f)}$$

$$-\,M^K\,\mathbb{D}_y^K\left(\alpha_{12}^K\,\underline{\mathrm{u}}_x^K \;+\; \alpha_{22}^K\,\underline{\mathrm{u}}_y^K \;+\; \alpha_{23}^K\,\underline{\mathrm{u}}_z^K\right) + \sum_{f=1}^{4} M^K\left(\alpha_{12}^K\underline{\lambda}_{1x}^{\beta(K,f)} + \alpha_{22}^K\,\underline{\lambda}_{1y}^{\beta(K,f)} + \alpha_{23}^K\,\underline{\lambda}_{1z}^{\beta(K,f)}\right)\mathbb{Q}_y^{\beta(K,f)}$$

$$-\,M^K\,\mathbb{D}_y^K\left(\alpha_{13}^K\,\underline{\mathrm{u}}_x^K \;+\; \alpha_{23}^K\,\underline{\mathrm{u}}_y^K \;+\; \alpha_{33}^K\,\underline{\mathrm{u}}_z^K\right) + \sum_{f=1}^{4} M^K\left(\alpha_{13}^K\underline{\lambda}_{1x}^{\beta(K,f)} + \alpha_{23}^K\,\underline{\lambda}_{1y}^{\beta(K,f)} + \alpha_{33}^K\,\underline{\lambda}_{1z}^{\beta(K,f)}\right)\mathbb{Q}_z^{\beta(K,f)} \;=\; 0\,.$$

Local linear system

The local system obtained from the discretization of (3.12) can be written as:

$$\mathbb{A}^K \underline{W}^K + \mathbb{B}^K \underline{\Lambda}^K = \mathbb{C}^K_{\text{source}}\,,$$

where $\underline{W}^K$ and $\underline{\Lambda}^K$ have been defined in (3.27). In the above equation, $\mathbb{A}^K$ is of dimension $13\,d_i^K \times 13 d_i^K$, $\mathbb{B}^K$ of size $13\,d_i^K \times 16 d_i^F$, and $\mathbb{C}^K_{\text{source}}$ is the matrix of the external forces of dimension $13\,d_i^K$.

$\underline{W}^K$ is composed of 13 blocks corresponding to different types of unknowns, we hence decompose the elementary matrix $\mathbb{A}^K$ in 8 columns of size $13\,d_i^K \times d_i^K$, as detailed in Appendix B.1.2:

$$\mathbb{A}^K = \begin{pmatrix} \mathbb{A}^K_1 & \mathbb{A}^K_2 & \mathbb{A}^K_3 & \mathbb{A}^K_4 & \mathbb{A}^K_5 & \mathbb{A}^K_6 & \mathbb{A}^K_7 & \mathbb{A}^K_8 & \mathbb{A}^K_9 & \mathbb{A}^K_{10} & \mathbb{A}^K_{11} & \mathbb{A}^K_{12} & \mathbb{A}^K_{13} \end{pmatrix}.$$

Similarly, based on the structure of the unknown $\underline{\Lambda}^K$ in four times four sub-blocks corresponding to the four scalar Lagrange unknowns decomposed on the four faces of the tetrahedron K, we write $\mathbb{B}^K$ in 16 columns of size $13\,d_i^K \times d_i^F$. $\mathbb{B}^K$ is given in Appendix B.1.2:

$$\mathbb{B}^K = \Bigg(B_{\lambda_{1x},1} \quad B_{\lambda_{1x},2} \quad B_{\lambda_{1x},3} \quad B_{\lambda_{1x},4} \quad B_{\lambda_{1y},1} \quad B_{\lambda_{1y},2} \quad B_{\lambda_{1y},3} \quad B_{\lambda_{1y},4} \quad \ldots$$
$$\ldots \quad B_{\lambda_{1z},1} \quad B_{\lambda_{1z},2} \quad B_{\lambda_{1z},3} \quad B_{\lambda_{1z},4} \quad B_{\lambda_2,1} \quad B_{\lambda_2,2} \quad B_{\lambda_2,3} \quad B_{\lambda_2,4} \Bigg).$$

Finally, the local source vector is expressed as:

$$\left(\mathbb{C}^K_{\text{source}}\right)^T = \begin{pmatrix} \mathbb{C}^K_{1x} & \mathbb{C}^K_{1y} & \mathbb{C}^K_{1z} & \mathbb{C}^K_{2x} & \mathbb{C}^K_{2y} & \mathbb{C}^K_{2z} & 0 & 0 & 0 & 0 & 0 & 0 & 0 \end{pmatrix}.$$

3.3.2 Transmission conditions

The transmission conditions, given by equation (3.22), are expressed using the definition of the numerical traces on a face in equation (3.10). We recall that (3.22a) is:

$$\sum_{K\in\mathcal{T}_h} \int_{\partial K} \boldsymbol{\tau}_h^K \boldsymbol{n}^K \cdot \eta - \sum_{K\in\mathcal{T}_h} \int_{\partial K} \boldsymbol{S}_1(\mathbf{u}_h^K - \boldsymbol{\lambda}_1)\cdot\eta - \sum_{K\in\mathcal{T}_h} \int_{\partial K} (\mathrm{p}_h^K - \lambda_2)\boldsymbol{S}_3\boldsymbol{n}^K\cdot\eta = \sum_{F\in\mathcal{F}_{\text{ext}}} \int_F \boldsymbol{f}_{\text{inc}}\cdot\eta\,,$$

and (3.22b) is expressed as:

$$\sum_{K\in\mathcal{T}_h} \int_{\partial K} \mathbf{w}_h^K \cdot \boldsymbol{n}^K\,\xi - \sum_{K\in\mathcal{T}_h} \int_{\partial K} (\mathrm{p}_h^K - \lambda_2)(\boldsymbol{S}_2\boldsymbol{n}^K)\cdot\boldsymbol{n}^K\,\xi - \sum_{K\in\mathcal{T}_h} \int_{\partial K} \boldsymbol{S}_4(\mathbf{u}_h^K - \boldsymbol{\lambda}_1)\cdot\boldsymbol{n}^K\,\xi = \sum_{F\in\mathcal{F}_{\text{ext}}} \int_F g_{\text{inc}}\,\xi\,.$$

These equations are discretized on (x,y,z) by decomposing the unknowns using (3.25) and (3.26) and replacing the test functions by the basis functions. They are then expressed in terms of the elementary matrices defined in (3.28).

(a) The first transmission equation (3.22a)

The discretization of (3.22a) along x, y and z directions gives, taking $\bullet = x, y, z$:

$$\sum_{K\in\mathcal{T}_h} \int_{\partial K} \underline{\tau}^K_{x\bullet}\, n_x^K\, \varphi_j^K\, \psi_i^{\beta(K,f)}\, dS + \sum_{K\in\mathcal{T}_h} \int_{\partial K} \underline{\tau}^K_{y\bullet}\, n_y^K\, \varphi_j^K\, \psi_i^{\beta(K,f)}\, dS + \sum_{K\in\mathcal{T}_h} \int_{\partial K} \underline{\tau}^K_{z\bullet}\, n_z^K\, \varphi_j^K\, \psi_i^{\beta(K,f)}\, dS$$

$$- \sum_{K\in\mathcal{T}_h} \int_{\partial K} \gamma_1\, \varphi_j^K\, \underline{\mathrm{u}}^K_\bullet\, \psi_i^{\beta(K,f)}\, dS + \sum_{K\in\mathcal{T}_h} \int_{\partial K} \gamma_1\, \psi_j^{\beta(K,f)} \underline{\lambda}^K_{1\bullet}\, \psi_i^{\beta(K,f)}\, dS - \sum_{K\in\mathcal{T}_h} \int_{\partial K} \gamma_3 n^K_\bullet\, \underline{\mathrm{p}}^K \varphi_j^K \psi_i^{\beta(K,f)} dS$$

$$+ \sum_{K\in\mathcal{T}_h} \int_{\partial K} \gamma_3 n^K_\bullet\, \underline{\lambda}^K_2 \psi_j^{\beta(K,f)} \psi_i^{\beta(K,f)} dS = \sum_{F\in\mathcal{F}_{\text{ext}}} \int_F f_{\text{inc},\bullet}\, \psi_i^{\beta(K,f)}\, dS\,.$$

The above equation is expressed in terms of the unknown vectors defined in (3.27) and the local matrices in (3.28) as:

$$\sum_{K\in\mathcal{T}_h} \Big((\mathbb{Q}_x^{\beta(K,f)})^T\, \underline{\tau}^K_{x\bullet} + (\mathbb{Q}_y^{\beta(K,f)})^T\, \underline{\tau}^K_{\bullet y} + (\mathbb{Q}_z^{\beta(K,f)})^T\, \underline{\tau}^K_{\bullet z} - \gamma_1\, (\mathbb{F}^{\beta(K,f)})^T\, \underline{\mathrm{u}}^K_\bullet + \gamma_1\, \mathbb{G}^{\beta(K,f)}\, \underline{\lambda}^{\beta(K,f)}_{1\bullet}$$
$$- \gamma_3\, (\mathbb{Q}_\bullet^{\beta(K,f)})^T\, \underline{\mathrm{p}}^K + \gamma_3\, \mathbb{H}_\bullet^{\beta(K,f)}\, \underline{\lambda}_2^{\beta(K,f)} \Big) = \sum_{F\in\mathcal{F}_{\text{ext}}} \int_F f_{\text{inc},\bullet}\, \psi_i^{\beta(K,f)}\, dS\,. \tag{3.31}$$

(b) The second transmission condition (3.22b)

The equation (3.22b) is also discretized as

$$\sum_{K\in\mathcal{T}_h}\int_{\partial K}\Big(\underline{\mathrm{w}}_x^K\,\varphi_j^K\,n_x^K\psi_i^{\beta(K,f)}+\underline{\mathrm{w}}_y^K\,\varphi_j^K\,n_y^K\psi_i^{\beta(K,f)}+\underline{\mathrm{w}}_z^K\,\varphi_j^K\,n_z^K\psi_i^{\beta(K,f)}-\underline{\mathrm{p}}^K\,\varphi_j^K\,\gamma_2\psi_i^{\beta(K,f)}+\underline{\lambda}_2^K\,\psi_j^{\beta(K,f)}\,\gamma_2\,\psi_i^{\beta(K,f)}$$
$$-\underline{\mathrm{u}}_x^K\,\varphi_j^K\,\gamma_4\,n_x^K\,\psi_i^{\beta(K,f)}-\underline{\mathrm{u}}_y^K\,\varphi_j^K\,\gamma_4\,n_y^K\,\psi_i^{\beta(K,f)}-\underline{\mathrm{u}}_z^K\,\varphi_j^K\,\gamma_4\,n_z^K\,\psi_i^{\beta(K,f)}+\underline{\lambda}_{1x}^K\,\psi_j^{\beta(K,f)}\,\gamma_4\,n_x^K\,\psi_i^{\beta(K,f)}$$
$$+\underline{\lambda}_{1y}^K\,\psi_j^{\beta(K,f)}\,\gamma_4\,n_y^K\,\psi_i^{\beta(K,f)}+\underline{\lambda}_{1z}^K\,\psi_j^{\beta(K,f)}\,\gamma_4\,n_z^K\,\psi_i^{\beta(K,f)}\Big)=\sum_{F\in\mathcal{F}_{\rm ext}}\int_F g_{\rm inc}\,\psi_i^{\beta(K,f)}\,dS\;,$$

and expressed in terms of the local matrices and the unknown vectors defined respectively in (3.28) and (3.27):

$$\sum_{K\in\mathcal{T}_h}\Big((\mathbb{Q}_x^{\beta(K,f)})^T\,\underline{\mathrm{w}}_x^K+(\mathbb{Q}_y^{\beta(K,f)})^T\,\underline{\mathrm{w}}_y^K+(\mathbb{Q}_z^{\beta(K,f)})^T\,\underline{\mathrm{w}}_z^K-(\mathbb{F}^{\beta(K,f)})^T\,\underline{\mathrm{p}}^K\,\gamma_2+\mathbb{G}^{\beta(K,f)}\underline{\lambda}_2^K\,\gamma_2-(\mathbb{Q}_x^{\beta(K,f)})^T\underline{\mathrm{u}}_x^K\,\gamma_4$$
$$-(\mathbb{Q}_y^{\beta(K,f)})^T\underline{\mathrm{u}}_y^K\gamma_4-(\mathbb{Q}_z^{\beta(K,f)})^T\underline{\mathrm{u}}_z^K\gamma_4+\mathbb{H}_x^{\beta(K,f)}\underline{\lambda}_{1x}^K\,\gamma_4+\mathbb{H}_y^{\beta(K,f)}\underline{\lambda}_{1y}^K\gamma_4+\mathbb{H}_z^{\beta(K,f)}\underline{\lambda}_{1z}^K\,\gamma_4\Big)=\sum_{F\in\mathcal{F}_{\rm ext}}\int_F g_{\rm inc}\,\psi_i^{\beta(K,f)}\,dS\,.\tag{3.32}$$

System As for the two-dimensional problem, we define the global vector:

$$\underline{\Lambda}\;=\;(\underline{\boldsymbol{\lambda}}_1^1,\,\underline{\lambda}_2^1,\,....,\,\underline{\boldsymbol{\lambda}}_1^{N_{\rm face}},\,\underline{\lambda}_2^{N_{\rm face}})\,,$$

with $N_{\rm face}$ the number of faces of the mesh. We recall the definition of the local trace operator $\mathcal{A}_{HDG}$ that links the local degrees of freedom on an element K to the global degrees of freedom of the Lagrange multiplier $\underline{\Lambda}$:

$$\mathcal{A}_{HDG}^K\,\underline{\Lambda}\;=\;\underline{\Lambda}^K\,.$$

The transmission conditions (3.31) and (3.32) are summed on all the faces of each element to obtain:

$$\sum_{K\in\mathcal{T}_h}(\mathcal{A}_{HDG}^K)^T\left(\mathbb{P}^K\underline{W}^K+\mathbb{T}^K\mathcal{A}_{HDG}^K\underline{\Lambda}\right)=\mathbb{S}_{\rm inc}\,,$$

with $\mathbb{P}^K$ and $\mathbb{T}^K$ two matrices respectively of dimension $13\,d_i^F\times 16\,d_i^K$ and $16\,d_i^F\times 16\,d_i^F$. The matrices are given in Appendix B.1.2.

3.4 Solution methodology

Now that we have presented the discretization of the method in two and three dimensions, we present the algorithm used for the resolution of the poroelastic equations (3.1) with the HDG method. For an element K, we have built a local system:

$$\mathbb{A}\,\underline{W}^K\;+\;\mathbb{B}\,\underline{\Lambda}^K\;=\;\mathbb{C}_{\rm source}^K\tag{3.33}$$

coupled with the transmission conditions

$$\sum_{K\in\mathcal{T}_h}(\mathcal{A}_{HDG}^K)^T\left(\mathbb{P}^K\underline{W}^K+\mathbb{T}^K\mathcal{A}_{HDG}^K\underline{\Lambda}\right)=\mathbb{S}_{\rm inc}\,.\tag{3.34}$$

Equation (3.33) is written as:

$$\mathbb{A}^K\underline{W}^K=\mathbb{C}_{\rm source}^K-\mathbb{B}^K\mathcal{A}_{HDG}^K\underline{\Lambda}\,.$$

Assuming that $\mathbb{A}^K$ can be inverted for each element, we have:

$$\underline{W}^K=-(\mathbb{A}^K)^{-1}\mathbb{B}^K\mathcal{A}_{HDG}^K\underline{\Lambda}\;+(\mathbb{A}^K)^{-1}\mathbb{C}_{\rm source}^K\,.\tag{3.35}$$

The invertibility of $\mathbb{A}^K$ is numerically investigated in Section 3.5.2.3.

Then, $\underline{W}^K$ is replaced in (3.34) by its expression in (3.35):

$$\sum_{K\in\mathcal{T}_h} (\mathcal{A}^K_{HDG})^T \left(\mathbb{P}^K(\mathbb{A}^K)^{-1}\mathbb{C}^K_{\text{source}} - \mathbb{P}^K(\mathbb{A}^K)^{-1}\mathbb{B}^K\mathcal{A}^K_{HDG}\underline{\Lambda} + \mathbb{T}^K\mathcal{A}^K_{HDG}\underline{\Lambda}\right) = \mathbb{S}_{\text{inc}}\,,$$

which means,

$$\sum_{K\in\mathcal{T}_h} (\mathcal{A}^K_{HDG})^T \left(-\mathbb{P}^K(\mathbb{A}^K)^{-1}\mathbb{B}^K + \mathbb{T}^K\right)\mathcal{A}^K_{HDG}\underline{\Lambda} = -\sum_{K\in\mathcal{T}_h} (\mathcal{A}^K_{HDG})^T\,\mathbb{P}^K(\mathbb{A}^K)^{-1}\,\mathbb{C}^K_{\text{source}} + \mathbb{S}_{\text{inc}}\,.$$

The global problem writes:

$$\mathbb{K}\underline{\Lambda} = \mathbb{S}\,,$$

with $\mathbb{K} = \sum_{K\in\mathcal{T}_h} (\mathcal{A}^K_{HDG})^T \left(-\mathbb{P}^K(\mathbb{A}^K)^{-1}\mathbb{B}^K + \mathbb{T}^K\right)$ and $\mathbb{S} = -\sum_{K\in\mathcal{T}_h} (\mathcal{A}^K_{HDG})^T\,\mathbb{P}^K(\mathbb{A}^K)^{-1}\,\mathbb{C}^K_{\text{source}} + \mathbb{S}_{\text{inc}}$.

The resolution can be divided in four steps, detailed in Algorithm 2. First, we build the global matrix $\mathbb{K}$ and the source matrix $\mathbb{S}$. These calculations can be done element by element. Then the global system is resolved and the solution is constructed. We use the MUMPS direct solver for the resolution of the linear system, and this is the only step that is global. We define N_{elem} the number of elements in the mesh, and N_{fe} the number of faces per element. N_{fe} is equal to 3 in two dimensions, and 4 in three dimensions.

Step 1: Construction of the stiffness matrix
for $K = 1, N_{\text{elem}}$ **do**
  Compute the elementary matrices $\mathbb{M}^K$ and $\mathbb{D}^K_l$, with $l = x, y$ in 2D or $l = x, y, z$ in 3D.
  for $f = 1, N_{\text{fe}}$ **do**
    Compute the elementary matrices $\mathbb{E}^{\beta(K,f)}$, $\mathbb{F}^{\beta(K,f)}$, $\mathbb{G}^{\beta(K,f)}$, $\mathbb{Q}^{\beta(K,f)}_l$, $\mathbb{J}^{\beta(K,f)}_l$, $\mathbb{H}^{\beta(K,f)}_l$, with $l = x, y$ in 2D or $l = x, y, z$ in 3D.
  end for
  Compute the elementary matrices $\mathbb{A}^K$,$(\mathbb{A}^K)^{-1}$, $\mathbb{B}^K$.
  Compute $\mathbb{P}^K$, and $\mathbb{T}^K$ with the corresponding boundary conditions.
  Compute $\mathbb{K}^K = \mathbb{P}^K(\mathbb{A}^K)^{-1}\mathbb{B}^K + \mathbb{T}^K$.
  Use the $\mathcal{A}_{HDG}$ operator to determine the global degrees of freedom of the element and fill the global matrix $\mathbb{K}$.
end for

Step 2: Construction of the source term
Localisation of the point source
for $K = 1, N_{\text{elem}}$ **do**
  Compute the local matrices $\mathbb{C}^K_{\text{source}}$ and $\mathbb{S}^K_{\text{inc}}$.
  Compute $\mathbb{S}^K = \mathbb{P}^K(\mathbb{A}^K)^{-1}\mathbb{C}^K_{\text{source}}$.
  Use the $\mathcal{A}_{HDG}$ operator to determine the global degrees of freedom of the element and fill the global matrix $\mathbb{S}$.
end for

Step 3: Resolution of the global system
Resolution of $\mathbb{K}\underline{\Lambda} = \mathbb{S}$ with MUMPS .

Step 4: Reconstruction of the solution
for $K = 1, N_{\text{elem}}$ **do**
  Compute the solutions $\underline{W}^K$ using the $\mathcal{A}^K_{HDG}$ operator:
  $$\underline{W}^K = -(\mathbb{A}^K)^{-1}\mathbb{B}^K\mathcal{A}^K_{HDG}\underline{\Lambda} + (\mathbb{A}^K)^{-1}\mathbb{C}^K_{\text{source}}.$$
end for

Algorithm 2: Resolution with HDG Method

3.5 Numerical results

The goal of this section is to validate and analyze the performance of our numerical solver described in Section 3.5.2. We will work with the geophysical media listed in Section 3.5.1. In Section 3.5.2, we first validate the code in two dimensions by comparing the HDG numerical solutions with reference ones given in Chapter 2. We then carry out numerical tests to study the effect of stabilization parameters on the numerical error, the order of convergence, and the well-posedness of the problem. We also study the influence of the frequency on the well-posedness of the problem.

3.5.1 Parameterization of the computational domains and quantities of interest

For numerical experiments, we work with sandstone, sand and shale. While sand is filled with a viscous fluid, shale and sandstone materials are filled with brine which is inviscid. We consider the case of isotropic and anisotropic sand whereas sandstone and shale are isotropic. We only specify when it is an anisotropic material. We list in Table 3.1 the physical parameters. Note that the other parameters, *e.g.*, ρ_a, $\boldsymbol{\alpha}$, M, H are obtained with those given in the table, see Section 1.1.

Physical parameters	Sandstone	Shale	Isotropic Sand	Anisotropic Sand
Porosity ϕ	0.2	0.16	0.3	0.3
Fluid Density ρ_f $(10^3 kg.m^{-3})$	1.04	1.04	1	1
Solid Density ρ_s $(10^3 kg.m^{-3})$	2.5	2.21	2.6	2.6
Viscosity η $(mPa.s)$	0	0	1	1
Permeability κ_0 (μm^2)	60	10	60	60
Tortuosity $\mathfrak{t}$	2	2	3	2
Solid Bulk Modulus $\mathrm{k_s}$ (GPa)	40	7.6	35	35
Fluid Bulk Modulus $\mathrm{k_f}$ (GPa)	2.5	2.5	2.2	2.2
Frame Bulk Modulus $\mathrm{k_{fr}}$ (GPa)	20	6.6	0.4	$C_{11} = 1.067\ GPa$
Frame Shear Modulus μ_{fr} (GPa)	12	3.96	0.5	$C_{22} = 2.5\ GPa$
$\mathrm{v_P}$ for $f = 500$Hz $(\mathrm{m.s^{-1}})$	$4.24\,10^3$	$2.48\,10^3$	$(1.88\,10^3,\ 10.4)$	$C_{33} = 0.5\ GPa$
$\mathrm{v_S}$ for $f = 500$Hz $(\mathrm{m.s^{-1}})$	$2.38\,10^3$	$1.43\,10^3$	$(4.93\,10^2,\ 3.76)$	$C_{12} = 0.067\ GPa$
$\mathrm{v_B}$ for $f = 500$Hz $(\mathrm{m.s^{-1}})$	$1.02\,10^3$	$1.13\,10^3$	$(2.57\,10^2,\ 57.9)$	$C_{13} = C_{23} = 0\ GPa$

Table 3.1: Summary of the physical parameters that describe the different media used for the numerical tests. The parameters for sand are obtained from [64, Table 1], those for sandstone and shale from [39, Table 5]. The values given here are the adimensional input values in the program.

Besides the geophysical parameters listed above, we will use the following quantities to assess the accuracy and the efficiency of the HDG numerical method:

- The relative numerical error $e_h(\mathfrak{U})$ is computed from the knowledge of the numerical solution denoted by $\mathfrak{U}_{\mathrm{numeric}}$ and the reference solution $\mathfrak{U}_{\mathrm{reference}}$, following the formula:

$$e_h(\mathfrak{U}) = \frac{||\mathfrak{U}_{\mathrm{numeric}} - \mathfrak{U}_{\mathrm{reference}}||_2}{||\mathfrak{U}_{\mathrm{reference}}||_2}, \quad \text{with} \quad ||\mathfrak{U}||_2 = \left(\sum_{K \in \mathcal{T}_h} \int_K |\mathfrak{U}|^2 \right)^{\frac{1}{2}}.$$

- To study the stability of discretization, we consider the condition number κ, defined, for a matrix $\mathbf{A}$ as $\kappa = \|\mathbf{A}^{-1}\|\,\|\mathbf{A}\|$, with $\|\mathbf{A}\|$ a matrix norm of $\mathbf{A}$. We employ MUMPS [3] or LAPACK [4] to compute κ with the L^∞ norm, defined as $\|\mathbf{A}\|_\infty = \max_i \left(\sum_{j=1}^n |a_{ij}| \right)$, where a_{ij} is a coefficient of $\mathbf{A}$.

3.5.2 Validation of the numerical code and performance analysis in two dimensions

Our numerical analysis in Section 3.5.2 is organized as follows.

1. In Section 3.5.2.1, to evaluate the accuracy of the HDG method, we consider a particular configuration on which the solution is known analytically, and use this to construct a reference solution to be compared with the numerical one.

2. We analyze in Section 3.5.2.2 the impact of the various numerical parameters on the order of convergence of the solution. We first show that the four penalization parameters are necessary in order to guarantee optimal convergence (at the order $p+1$) of all the unknowns. In applying this result, we then set the four penalization parameters to the same value denoted by γ, and show that the higher γ is, the more accurate the solution is.

3. Next, we analyze the well-posedness of the local and global problems for a given choice of penalization parameters in Section 3.5.2.3. We show that a too high value of γ deteriorates the condition number of the global and the local matrices. On the other hand, our numerical experiments show that the frequency does not influence the condition number, provided the mesh is chosen fine enough to guarantee a reasonable accuracy.

The characteristics of the computer used for the numerical experiments are the following: 2 Dodeca-core Haswell Intel®Xeon®E5-2680 v3, at frequency 2.5 GHz, with 128 Go of memory (5.3 Go/core), a OmniPath 100 Gb/s and a Infinipath 40 Gb/s.

3.5.2.1 Validation of the code

(a) Computational domain for problem in Equation (3.38)

(b) Mesh of computational domain with straight-edge triangles

Figure 3.1: Set up for numerical solution $\mathfrak{U}^N_{\rm reference}$ that approximates $\mathfrak{U}_{\rm analytic}$ to machine precision on disc-shaped computation domain $\mathcal{D}_{\mathfrak{b}}$. The latter is the total wave in the scattering problem of a plane wave $\mathfrak{U}_{\rm pw}$ by a penetrable disc-shaped obstacle represented by $\mathcal{D}_{\mathfrak{a}}$, given by equation (3.37) (with the penetrable condition given by Eq. (3.37a) on $r=\mathfrak{a}$).

For the validation of the code, we use a reference solution that we construct as an accurate approximation of an analytic solution. To have an analytic solution, we have to restrict ourselves to a particular configuration. We actually consider the case of a porous disc-shaped solid inclusion of radius $r=\mathfrak{a}$, denoted by $\mathcal{D}_{\mathfrak{a}}$, embedded in an infinite medium ($\mathbb{R}^2 \setminus \mathcal{D}_{\mathfrak{a}}$) made up of a different poroelastic material. We assume that there is a plane wave $\mathfrak{U}_{\rm pw}$ which propagates in the exterior domain and comes across the obstacle $\mathcal{D}_{\mathfrak{a}}$. The following plane wave solutions are, cf. 1,

$$\mathcal{L}_{\rm poro}\,\mathfrak{U}_{\rm pw} \;=\; 0 \text{ in } \mathbb{R}^2 \quad , \quad \text{with } \mathfrak{U}_{\rm pw} = \big(\mathbf{u}_{\rm P}, \mathbf{w}_{\rm P}, \boldsymbol{\tau}_{\rm P}, \mathrm{p}_{\rm P}\big)^T \quad ,$$

where

$$\begin{aligned}
\mathbf{u}_{\rm P} &= e^{\mathrm{i}\,\mathbf{k}_{\rm P}\cdot\boldsymbol{x}}\,(\mathrm{i}\omega)\,\widehat{\mathbf{d}} \quad , \quad \mathbf{w}_{\rm P} \;=\; \mathcal{W}_{\rm P}\,e^{\mathrm{i}\,\mathbf{k}_{\rm P}\cdot\boldsymbol{x}}\,(\mathrm{i}\omega)\,\widehat{\mathbf{d}}\,,\\
\boldsymbol{\tau}_{\rm P} &= \mathrm{i}\omega\,\mathsf{s}_{\rm P}(\omega)\,e^{\mathrm{i}\mathbf{k}_{\rm P}\cdot\boldsymbol{x}}\Big(2\,\mu_{\rm fr}\,\widehat{\mathbf{d}}\otimes\widehat{\mathbf{d}} + \Big(-\tfrac{2}{3}\mu_{\rm fr} + \mathrm{k}_{\rm fr} + M\,\alpha^2 + \mathcal{W}_{\rm P}\,\alpha\,M\Big)\mathbb{I}\Big)\,,\\
\mathrm{p}_{\rm P} &= \mathrm{i}\omega\,\mathsf{s}_{\rm P}(\omega)\,(-M\,\mathcal{W}_{\rm P} \;-\; M\,\alpha)\,e^{\mathrm{i}\mathbf{k}_{\rm P}\cdot\boldsymbol{x}}\,.
\end{aligned}$$

We refer to Section 1.5, equations (1.24a), (1.24b), (1.24c) for the slownesses expressions. We recall that in the above equations, $\mathbf{k}_{\rm P} \;=\; \omega\,\mathsf{s}_{\rm P}(\omega)\,\widehat{\mathbf{d}}$ is the wave number, $\widehat{\mathbf{d}}$ is the polarization with $|\widehat{\mathbf{d}}|=1$. The slowness is given in equation (1.24a) and the amplitude $\mathcal{W}_{\rm P}$ of $\mathbf{w}_{\rm P}$ is read from equation (1.33).

Then, $\mathfrak{U}_{\text{analytic}}$ is the wavefield that arises from scattering of the incident plane wave. It satisfies the following problem:

$$\begin{aligned} \mathcal{L}_{\text{poro}}\,\mathfrak{U}_{\text{analytic}} \;=\; 0 \quad \text{in } \mathbb{R}^2 \quad ; \quad \mathfrak{U}_{\text{analytic}} - \mathfrak{U}_{\text{pw}} \text{ is outgoing}\,, \\ \mathbf{u}^{(I)} - \mathbf{u}^{(II)} = 0\,, \quad \mathrm{p}^{(I)} - \mathrm{p}^{(II)} = 0\,, \quad (\mathbf{w}^{(I)} - \mathbf{w}^{(II)})\cdot\boldsymbol{n} = 0\,, \quad (\boldsymbol{\tau}^{(I)} - \boldsymbol{\tau}^{(II)})\,\boldsymbol{n} = 0 \quad , \quad \text{on } \partial\mathcal{D}_{\mathfrak{a}}. \end{aligned} \tag{3.37a}$$

By 'outgoing', we mean in the sense of Definition 2.3. In the transmission condition (3.37a), the unit normal vector is denoted by $\boldsymbol{n}$, and is outwardly directed to the exterior of the inclusion $\mathcal{D}_{\mathfrak{a}}$. Each condition is expressed in terms of the components of the restriction of the analytic solution, $\mathfrak{U}^{(I)} = \mathfrak{U}_{\text{analytic}}|_{\mathcal{D}_{\mathfrak{a}}}$, and $\mathfrak{U}^{(II)} = \mathfrak{U}_{\text{analytic}}|_{\mathbb{R}^2\setminus\mathcal{D}_{\mathfrak{a}}}$ to the obstacle and the exterior domain respectively. The solution to (3.37) is then given by

$$\mathfrak{U}_{\text{analytic}} \;=\; \mathfrak{U}_{\text{pw}} \,+\, \mathfrak{U}_{\text{scatt}}\ ,\ \text{in } \mathbb{R}^2\setminus\mathcal{D}_{\mathfrak{a}} \quad , \quad \mathfrak{U}_{\text{analytic}} \;=\; \mathfrak{U}_{\text{trans}}\ ,\ \text{in } \mathcal{D}_{\mathfrak{a}}\,,$$

with the scattered field $\mathfrak{U}_{\text{scatt}}$ and transmitted field $\mathfrak{U}_{\text{trans}}$ described explicitly in form of harmonic expansions, *cf.* Section 2.4. These are infinite series whose coefficients are expressed in terms of the Hankel function of the first kind or Bessel J functions. In practice, we only keep the first N terms of the infinite series, with $N \geq 2|\mathbf{k}|\mathfrak{a}+1$ [120]. By this way, we obtain a reference solution denoted by $\mathfrak{U}^N_{\text{reference}}$ and defined by:

$$\mathfrak{U}^N_{\text{reference}} \;=\; \mathfrak{U}_{\text{pw}} \,+\, \mathfrak{U}^N_{\text{scatt}}\ ,\ \text{in } \mathbb{R}^2\setminus\mathcal{D}_{\mathfrak{a}} \quad , \quad \mathfrak{U}^N_{\text{reference}} \;=\; \mathfrak{U}^N_{\text{trans}}\ ,\ \text{in } \mathcal{D}_{\mathfrak{a}}\,,$$

and the exponent indicates that we keep the N first terms in each of the series of the analytic scattered and transmitted fields. In our experiments, $N = 50$, which verifies the above condition, and hence gives a very good approximation of the infinite series. For the HDG-reference comparison, we work with a bounded computational domain, see Figure 3.1(a). We assume that the obstacle is made up of sand, while the surrounding material is sandstone, cf. Table 3.1 for the values of their physical parameters. Here, we work with boundary condition of type 1 defined on a concentric disc of radius $\mathfrak{b}$, denoted by $\mathcal{D}_{\mathfrak{b}}$, which contains the aforementioned sand obstacle, and use the restriction of $\mathfrak{U}^N_{\text{reference}}$ to $\mathcal{D}_{\mathfrak{b}}$ as a reference solution. We introduce the following boundary value problem of type 1

$$\mathcal{L}_{\text{poro}}\,\mathfrak{U} \;=\; 0 \quad \text{in } \mathcal{D}_{\mathfrak{b}} \quad , \quad \mathcal{T}_1\,\mathfrak{U} \;=\; \mathcal{T}_1\,\mathfrak{U}^N_{\text{reference}} \ \text{ on } r=\mathfrak{b}\,, \tag{3.38}$$

set on a disc of radius b, denoted by $\mathcal{D}_b$, which is concentric with and contains the obstacle $\mathcal{D}_{\mathfrak{a}}$. Then the reference solution $\mathfrak{U}^N_{\text{reference}}$ is the unique solution to (3.38) except at eigenvalue frequencies. To construct the numerical solution, we will apply HDG method to (3.38) and compare the obtained numerical solution $\mathfrak{U}_{\text{hdg}}$ to $\mathfrak{U}^N_{\text{reference}}|_{\mathcal{D}_{\mathfrak{b}}}$. In this approach, our HDG unknown in the exterior region is the 'total' wavefield (thus is compared with $\mathfrak{U}_{\text{pw}} + \mathfrak{U}^N_{\text{scatt}}$), and in the interior, it is the 'transmitted' one (thus compared with $\mathfrak{U}^N_{\text{trans}}$). Note that for computing the HDG solution, we use a mesh that is refined near the external boundary and the internal interface to minimize the geometrical errors without using curved elements. In the case of a straight boundary, we have observed that we do not need to refine the mesh.

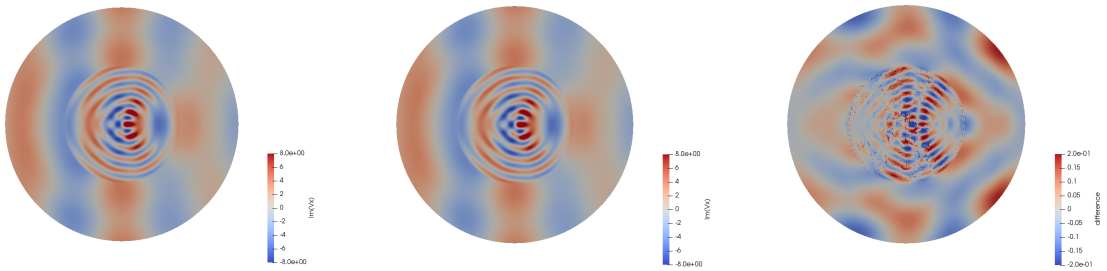

(a) Numerical solution (b) Reference solution (c) Difference

Figure 3.2: Numerical and reference solutions for the scattering of a plane wave by a penetrable poroelastic inclusion at frequency $f = 500$Hz. The result is the imaginary part of the horizontal solid velocity. The resolution of the global system takes 6.52 seconds (CPU time), and it needs 677 MB of memory to solve the global system.

Figure 3.2 shows the reference and numerical solutions for the test-case using the mesh displayed in Figure 3.1(b) and order 3 of discretization. The relative errors between reference and numerical solutions are given in Table 3.2. The stabilization parameters $(\gamma_1, \gamma_2, \gamma_3, \gamma_4)$, cf. (3.14) are equal to 1. We can see that for each component, the error is small.

$e_h(\mathrm{u}_x)$	$e_h(\mathrm{u}_y)$	$e_h(\mathrm{w}_x)$	$e_h(\mathrm{w}_y)$	$e_h(\tau_{xx})$	$e_h(\tau_{yy})$	$e_h(\tau_{xy})$	$e_h(\mathrm{p})$
0.53	0.70	0.53	0.70	0.41	0.44	1.2	1.1

Table 3.2: Relative errors (%) on the components of the unknowns of the HDG method for the experiment shown in Figure 3.2 for an order of interpolation $p = 3$, an incident P wave, at frequency $f = 500$Hz with $\theta = 10°$ and boundary conditions of type 1.

3.5.2.2 Impact of the stabilization parameters on the accuracy of the numerical solution

In the previous section, we have carried out numerical experiments with all the stabilization parameters (γ_1, γ_2, γ_3, γ_4), cf. (3.14), equal to 1. In this section, we want to see the possible effects of various combinations of γ_i on the order of convergence of the method, and then on the numerical error. For that purpose, we consider a homogeneous disc-shaped domain of radius $r = \mathfrak{b}$, where $\mathfrak{b} = 10$m in the numerical tests, using boundary conditions of type 1,

$$\mathcal{L}_{\mathrm{poro}}\,\mathfrak{U} \;=\; 0 \;\text{ in }\; \mathcal{D}_{\mathfrak{b}} \quad , \quad \mathcal{T}_1\,\mathfrak{U} \;=\; \mathcal{T}_1\,\mathfrak{U}_{\mathrm{pw}} \text{ on } r = \mathfrak{b}. \tag{3.39}$$

In this way, the reference (analytic) solution is given by $\mathfrak{U}_{\mathrm{pw}}$ recalled in (3.36). This study will show that if all the parameters are non zero, the relative error is always below 0.15% for $p = 3$.

Order of convergence

First, we want to display the order of convergence of the method in terms of the size of mesh. For that, we use four meshes with straight edges generated by the software Triangle. The refinement of a given mesh consists in dividing each of its cells into four cells. The characteristics of the meshes are summarized in Table 3.3. For the analysis, we introduce the definition of the size of the mesh h, which corresponds to the longest edge of the elements in the mesh. In Table 3.4, we plot the values of the order of convergence for all four unknowns with varying degrees of stabilization.

	Mesh 1	Mesh 2	Mesh 3	Mesh 4
Size of the mesh h (m)	1.514	0.757	0.379	0.189
Number of elements	3270	13080	52320	209280

Table 3.3: Characteristics of the meshes involved in the convergence analysis. The size of the mesh is the longest edge of the elements in the mesh.

We illustrate the convergence curves in the case with full and then zero stabilization, in Figure 3.3(a) and 3.3(b). In these figures, we depict the relative error and thus the convergence order for the x-component u_x as a function of the size of the mesh. We have the following observations.

- In the case of full stabilization with all $\gamma_i = 1$, we observe that the convergence order for u_x is equal to $p + 1$, see also Remark 3.4. We also note that the same order of convergence is obtained for the other components of the numerical solution. The same result is obtained with other (equally set) values of the parameters, for instance when they are all equal to 0.1. This result corroborates the ones obtained in [76] with a different HDG formulation.

- In the case of only partial stabilization (i.e., some or all of the γ_i are set to zero), one obtains a reduced order of convergence, see Figure 3.3(b). It can occur that some components of the numerical solution keep an optimal order of convergence, while it is decreased for others, cf. Table 3.4. The extreme case is when all $\gamma_i = 0$, the loss of convergence is observed for all unknown variables, cf. Figure 3.3(b).

- Additionally, for some combinations of values of the stabilization parameters (not shown in Table 3.4, e.g., when $(\gamma_1, \gamma_2, \gamma_3, \gamma_4) = (1, 1, 0, 0)$), the numerical solution is not accurate with numerical error attaining 200% and not decreasing even with higher degree of approximation and/or mesh refinement. However, we have observed that if the four stabilization parameters are different from zero, the numerical method is accurate with an optimal convergence order.

Remark 3.4. In Cockburn et al [124], it is shown that in the case of linear elasticity, the order of convergence of the displacement can be upgraded to $p + 2$ thanks to an element-per-element post-processing technique. We did not try to apply this idea to the Biot's system. An alternative to the post-processing is to increase the polynomial degree of two unknowns and to use a projection in the variational formulation, see [76].

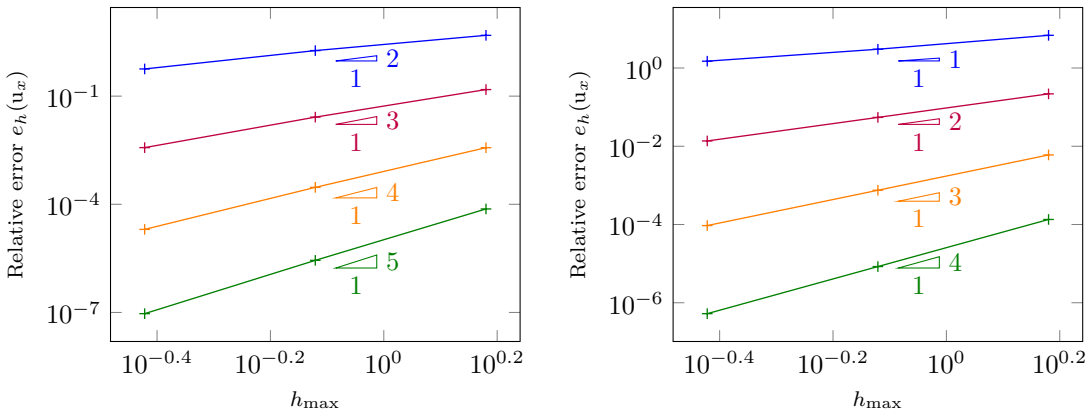

(a) Stabilization parameters set to 1

(b) Stabilization parameters set to 0

Figure 3.3: Convergence curves of HDG method (component u_x) for several orders of interpolation. Results for order 1 are plotted in blue, for order 2 in purple, for order 3 in orange and for order 4 in green Figure 3.3(a) shows the results with the four stabilization parameters set to 1 and figure 3.3(b) with the four stabilization parameters set to 0. As expected, when we use the four stabilization parameters, the convergence is of order $p+1$, while we lose one order of convergence without the stabilization parameters, as for classical DG method without stabilization parameters.

Stabilization parameters (γ_1, γ_2, γ_3, γ_4)	1111	1110	1011	1010	0000	0101	0100	0001
u	$p+1$	$p+1$	$p+1$	$p+1$	p	p	p	p
w	$p+1$	p	$p+1$	$p+1$	p	$p+1$	p	p
$\boldsymbol{\tau}$	$p+1$	$p+1$	p	$p+1$	p	$p+1$	$p+1$	$p+1$
p	$p+1$	$p+1$	p	p	p	$p+1$	$p+1$	p

Table 3.4: Summary of the convergence order of the HDG method depending on the value of the stabilization parameters, defined in (3.14). The four parameters are necessary to obtain the optimal order of convergence on all the unknowns.

Numerical errors

For the rest of the numerical tests, we will set all $\gamma_i = \gamma$. We now study the influence of this value γ on the numerical error. Figure 3.4 shows the relative error as a function of the stabilization parameters, in the case of a polynomial approximation of order 3. The solid velocity **u** behaves in the same way as the elastic solid velocity observed in [20, Fig 3.4.7 p.89]. We also note that the relative fluid velocity **w** and the pressure p seem to behave in a similar way, however of a different pattern from **u**, and which is also different from that of $\boldsymbol{\tau}$. To arrive at a conclusion from these different patterns, we consider the mean value of the relative errors, depicted in Figure 3.5 and defined as,

$$e_h^{\text{mean}} = \frac{\sum_{u\in S} \|u_{\text{numeric}} - u_{\text{reference}}\|_2}{\sum_{u\in S} \|u_{\text{reference}}\|_2} \quad , \quad S = \{\mathrm{u}_x, \mathrm{u}_y, \mathrm{w}_x, \mathrm{w}_y, \tau_{xx}, \tau_{yy}, \tau_{xy}, \mathrm{p}\}\,. \tag{3.40}$$

We observe that the mean error is less than 0.1% when the stabilization parameter is equal to at least 10^3. We also note that the same high level of accuracy is guaranteed when the four stabilization parameters are less than 10^{-3}.

3.5.2.3 Analysis of the well-posedness

In this section, also working with problem (3.39), we continue the numerical study of well-posedness by analyzing the influence of the value of stabilization parameter γ and the frequency on the condition number of the linear system. The latter is an indication of the well-posedness of the problem.

Influence of the stabilization parameters

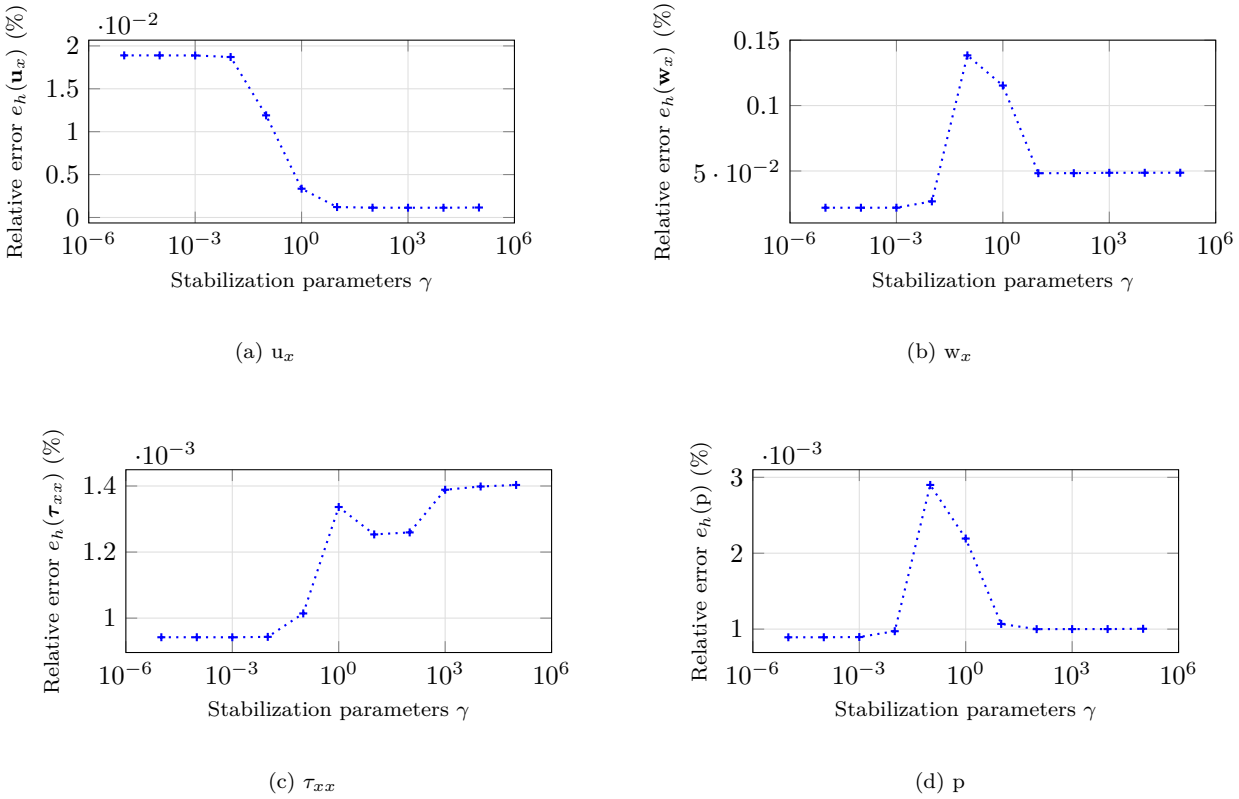

(a) u_x (b) w_x

(c) τ_{xx} (d) p

Figure 3.4: Relative error in L^2-norm of HDG method (%) depending on the stabilization parameters compared with reference solution developed in Section 2.4. The stabilization parameters act differently on each unknown. When it is high, it improves the accuracy on $\mathbf{u}$, while when it is low, it improves the accuracy on τ. It is important to note that the impact is never dramatic : the ratio between the maximal and the minimal error is less than 20.

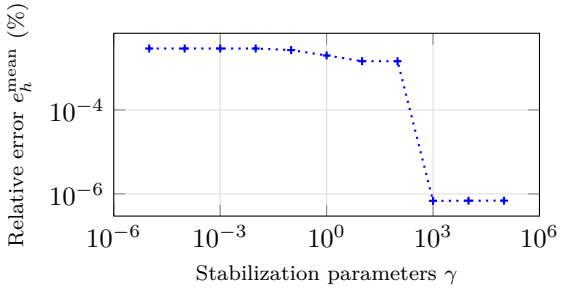

Figure 3.5: Mean relative error (%) of the HDG method, depending on the stabilization parameters in semi-log scale. We defined this mean error (equation (3.40)) in order to identify more precisely the impact of the penalization parameters. This curve indicates that this parameter should be the highest possible

We first consider this question on the local level for the local matrix $\mathbb{A}^K$ and then for the global matrix $\mathbb{K}$.

- For the reconstruction of $\underline{W}^K$, we have to invert the elementary matrix $\mathbb{A}^K$, see equation (3.35). Hence we study the condition number of $\mathbb{A}^K$ to evaluate if the calculation of $(\mathbb{A}^K)^{-1}$ is problematic. If the condition number is too high, the inversion will be less accurate. Since this inversion is performed on every element of the mesh, we consider the maximum value of the condition number, $C_{T_h} = \max_{K \in T_h} \|(A^K)^{-1}\| \|A_K\|$. For three different media and four different interpolation orders, we show the maximal condition number of $\mathbb{A}^K$ for every element of the mesh in infinity norm as a function of the values of the stabilization parameters in Figure 3.6. We observe that for all interpolation orders, the condition number increases with the stabilization parameters. We also note that the variations are similar for the different interpolation orders, also the condition number increases with the

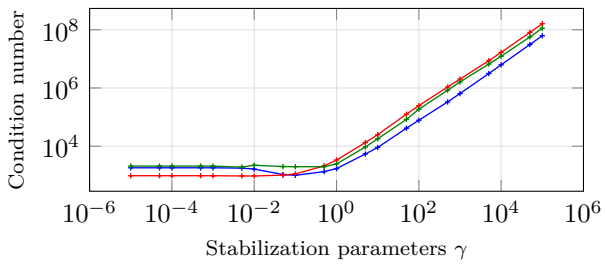

(a) P1

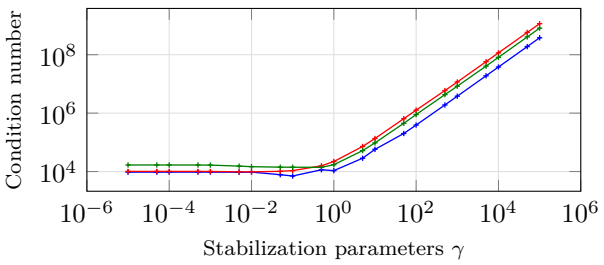

(b) P2

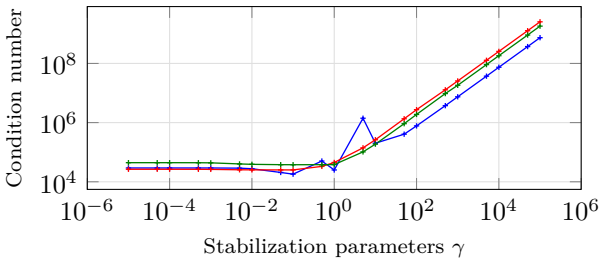

(c) P3

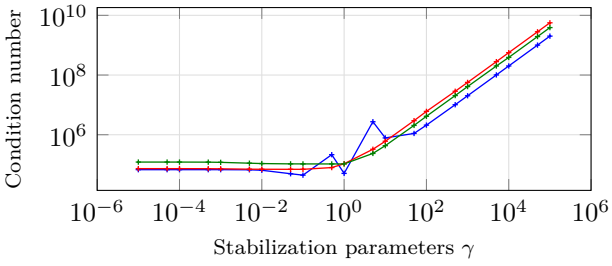

(d) P4

Figure 3.6: Maximal condition number (infinity norm) on all the elementary matrices $\mathbb{A}^K$ as a function of the stabilization parameters, for three materials and four interpolation orders at frequency $f = 500$Hz. The four stabilization parameters are set at the same value. The characteristics of the media are presented in Table 3.1. The results for sand are represented in blue —+—, for shale in red —+— and for sandstone in green —+—. When the stabilization parameter is above 1, the condition number starts to increase. This shows that we should not set it too high.

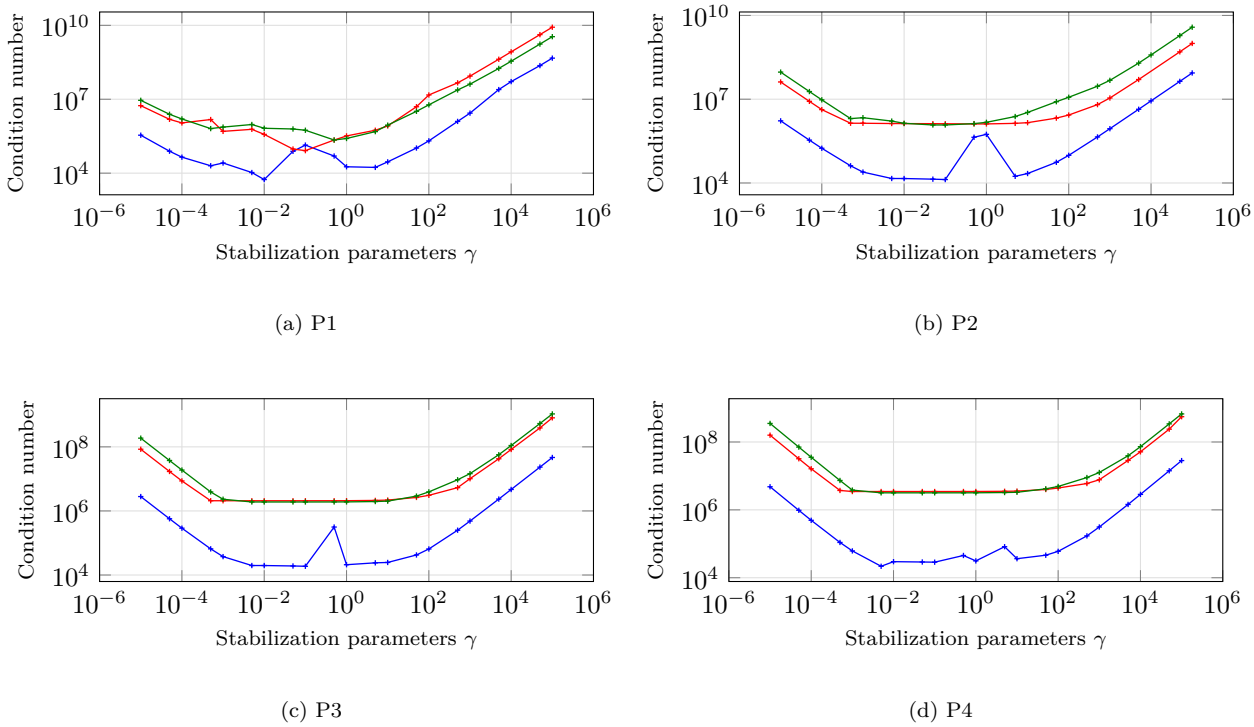

(a) P1

(b) P2

(c) P3

(d) P4

Figure 3.7: Condition number (infinity-norm) of the global matrix $\mathbb{K}$ as a function of the stabilization parameters, for three materials and four interpolation orders at frequency $f = 500$Hz. The four stabilization parameters are set at the same value. The characteristics of the media are presented in Table 3.1. The results for sand are represented in blue —+—, for shale in red —+— and for sandstone in green —+—.

interpolation order, however staying bounded below 10^{10}.

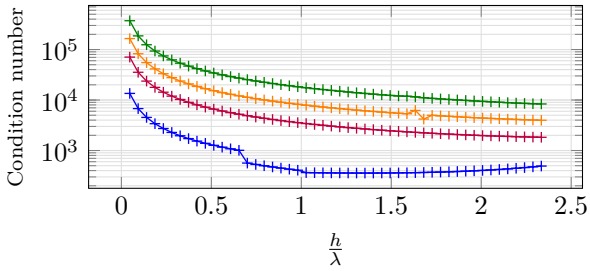

Figure 3.8: Condition number (infinity-norm) of the matrix $\mathbb{A}^K$ for one element function of $\frac{h}{\lambda_B}$, for shale and four interpolation orders. The characteristics of the medium are presented in Table 3.1. The four stabilization parameters are set to 1. Results for order 1 are plotted in blue, for order 2 in purple, for order 3 in orange and for order 4 in green. The condition number is always below 10^8, so that the matrix is easily invertible with a direct solver such as Lapack.

- We now move on to the global system $\mathbb{K}\underline{\Lambda} = \mathbb{S}$. We address the question of well-posedness numerically by computing the condition number of the global matrix $\mathbb{K}$ with the hope it is not too high, which ensures that the matrix can be inverted. As formerly, we consider three different media, which are composed of sand, shale or sandstone (see Table 3.1). The condition number of $\mathbb{K}$ is displayed in Figure 3.7 as a function of the stabilization parameters. The condition number for the test with sand is lower than the one for shale and sandstone. Moreover, the curves have similar trends for every interpolation order. In the interval in consideration for the stabilization parameters, the condition number is stable. This means that the accuracy of the resolution of the global system is not sensitive to the value of the stabilization parameters.

Influence of the frequency

We continue the numerical study of well-posedness by analyzing the influence of the frequency on the condition number of the linear system. Note that the parameters change with frequency. As previously done, we first consider the local system and then the global one.

Remark 3.5. The goal of this experiment is not to analyze precisely the variations of the condition number, but to show that the condition number is lower than 10^8 for each triangle, for the three types of media and for the considered range of frequency, in order to show that all local systems are invertible. Indeed, it is acknowledged that the inversion can be made without difficulties if the condition number is lower than 10^{16}.

- First, for a domain composed of shale, we consider an interior element of the mesh. We denote by h the diameter of the element and by λ_B the wavelength corresponding to the slow wave, and we display the condition number of the elementary matrix $\mathbb{A}^K$ as a function of $\frac{h}{\lambda_B}$, the number of wavelengths in the element. The results are given in Figure 3.8. We observe that the condition number increases with the interpolation orders, but stays however bounded below 10^6. Then, for the three different media described in Table 3.1, we show the maximal condition number of the matrices $\mathbb{A}^K$ on each element as a function of the frequency in Figure 3.9. For sand, the curves are less smooth than for sandstone and shale. We observe here that the condition number can increase without hampering the accuracy.

- Finally, the condition number of the global matrix $\mathbb{K}$ is presented in Figure 3.10 as a function of the frequency. We observe that the condition number of the elementary matrix decreases with the frequency.

As a conclusion, the condition number does not increase with the accuracy (or the number of points per wavelength), and we can obtain both a well conditioned system and an accurate solution.

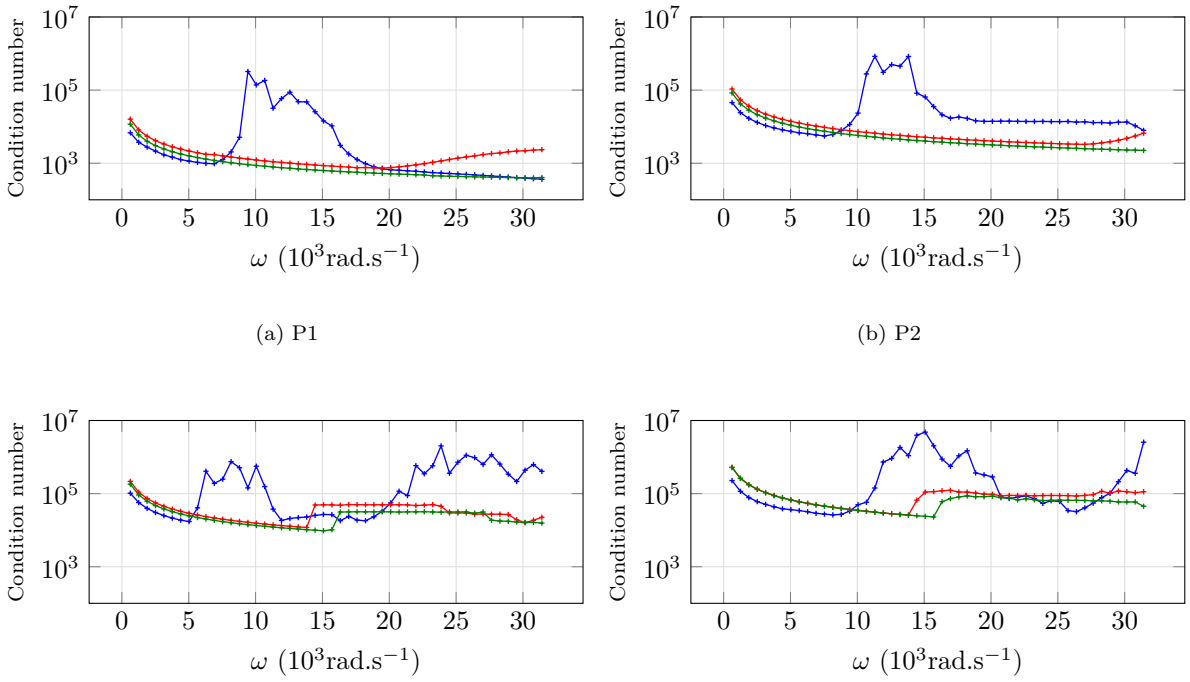

(a) P1

(b) P2

(c) P3

(d) P4

Figure 3.9: Maximal condition number (infinity norm) of the matrix $\mathbb{A}^K$ as a function of the frequency, for three materials and four interpolation orders. The characteristics of the media are presented in Table 3.1. The four stabilization parameters are set to 1. The results for sand are represented in blue —•—, for shale in red —•— and for sandstone in green —•—.

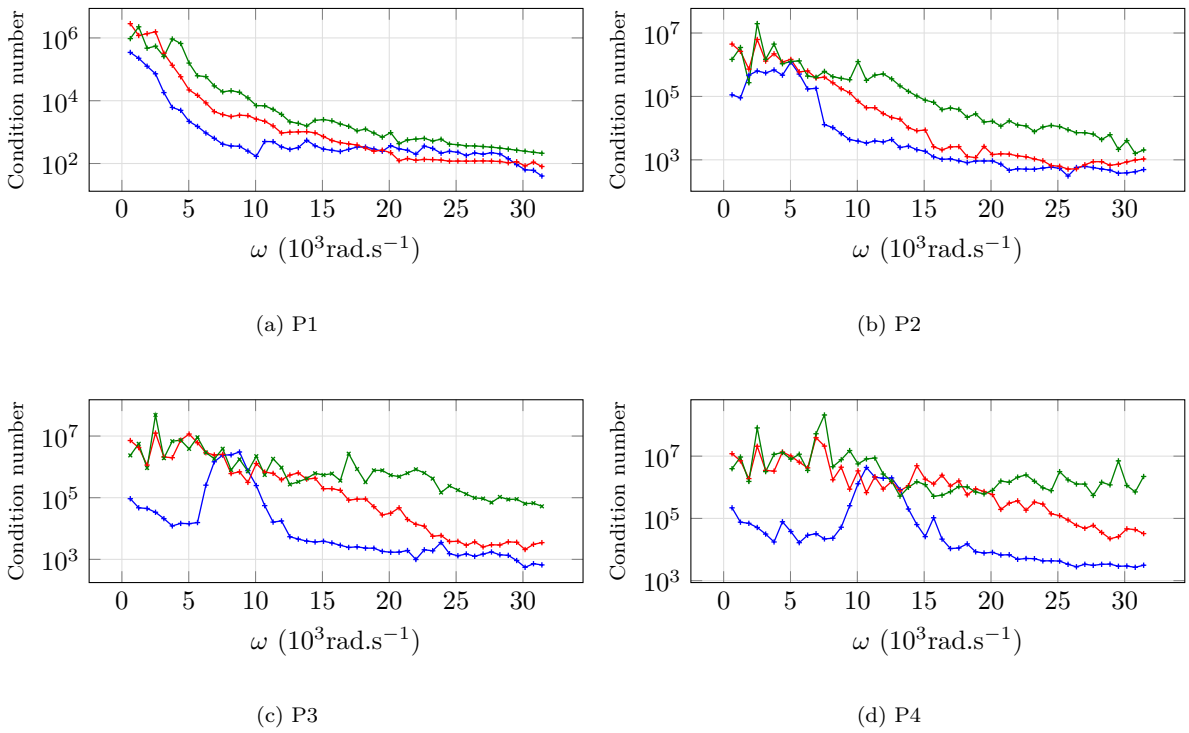

(a) P1 (b) P2

(c) P3 (d) P4

Figure 3.10: Condition number (infinity-norm) of the global matrix $\mathbb{K}$ as a function of the frequency, for three materials and four interpolation orders. The characteristics of the media are presented in Table 3.1. All stabilization parameters are set to 1. The results for sand are represented in blue —+—, for shale in red —+— and for sandstone in green —+—.

3.5.3 Validation of the numerical code in three-dimensions

We now present the results obtained with the HDG method in three dimensions. We consider a poroelastic domain $\mathcal{D}$ of size $[0:10]\times[0:10]\times[0:2]$cm composed of sandstone, see Table 3.1 for the physical parameters. We then consider a triangulation $\mathcal{T}_h$ of the domain $\mathcal{D}$, composed of 1250 elements of degree of interpolation 3. We set $f = 35$kHz, in this case the velocities of the waves are:

$$v_p \;=\; 4247\, m.s^{-1} \quad v_b \;=\; 1021\, m.s^{-1} \quad \text{and } v_s \;=\; 2.388\, m.s^{-1}\,.$$

In this configuration, we study the propagation of a B plane wave, and we impose the exact solution $(\boldsymbol{\tau}_{\text{pw}}\cdot\boldsymbol{n},\, \mathbf{u}_{\text{pw}}\cdot\boldsymbol{n})$ corresponding to the plane wave on the boundaries of the domain. We compare the numerical solution to the exact solution for plane wave propagation, developed in Section 1.5. We plot in Figure 3.11 the horizontal component of the solid velocity $\mathbf{u}$ corresponding to the numerical and exact solutions. In addition, Table 3.5 gives the relative L^2 error on the poroelastic variables. The results of the HDG methos are good, and the error is small, less than 3% on every components.

$e_h(\mathrm{u}_x)$	$e_h(\mathrm{u}_y)$	$e_h(\mathrm{u}_z)$	$e_h(\mathrm{w}_x)$	$e_h(\mathrm{w}_y)$	$e_h(\mathrm{w}_z)$
2.07	1.93	1.69	0.601	0.607	0.511

$e_h(\tau_{xx})$	$e_h(\tau_{yy})$	$e_h(\tau_{zz})$	$e_h(\tau_{yz})$	$e_h(\tau_{xz})$	$e_h(\tau_{xy})$	$e_h(\mathrm{p})$
0.249	0.277	0.370	0.424	0.383	0.516	0.165

Table 3.5: Relative errors (%) on the components of the unknowns of the HDG method for a B plane wave propagating in sandstone, at frequency $f = 35$kHz with boundary conditions of type 1, using an order of discretization 3.

Next, we verify that the HDG method has an optimal order of convergence $p+1$ in three dimensions. We plot the convergence curves for the solid velocity u_x in 3.12 for the first interpolation orders as functions of h, the longest edge

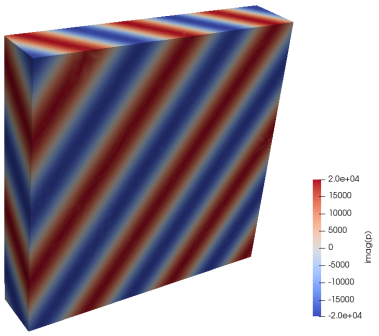

(a) Numerical solution: imaginary part of u_x

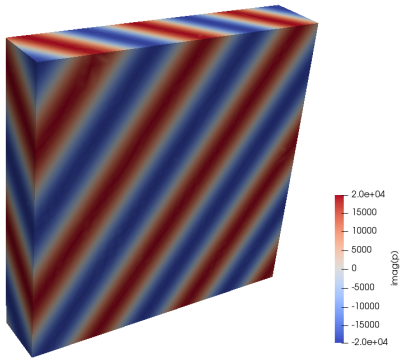

(b) Reference solution: imaginary part of u_x

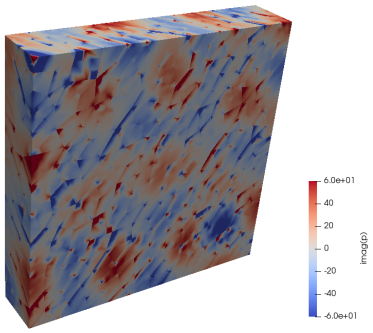

(c) Difference: imaginary part of u_x

Figure 3.11: Numerical and reference solution for the three-dimensional propagation of a B plane wave in sandston. The solid velocity u_x is presented, for $f = 35$kHz and order of interpolation 3.

of the mesh. The curves show that the method keeps an order of convergence $p + 1$ in three dimensions for $\mathbf{u}_x$. This is also the case for the other components of the solid velocity $\mathbf{u}$ and the other unknowns.

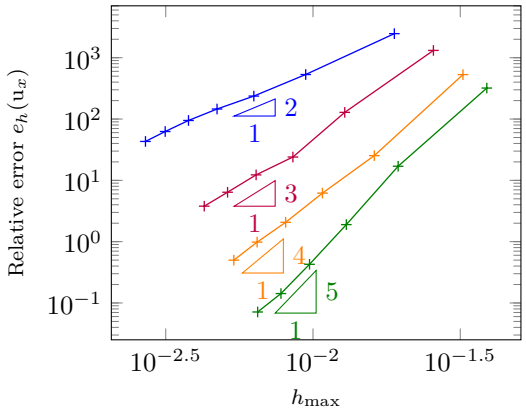

Figure 3.12: Convergence curves of HDG method (component u_x) for several orders of interpolation. Results for order 1 are plotted in blue —+—, for order 2 in purple —+—, for order 3 in orange —+— and for order 4 in green —+—.

Conclusion

In this chapter, we have developed and implemented a HDG method to simulate harmonic wave propagation in anisotropic poroelastic media, governed by Biot's model in two and three dimensions. We have provided a detailed description of the numerical algorithm and the different steps required for its development. Our HDG method was validated by comparing with reference solutions constructed in Chapter 2. In our numerical investigation on the influence of stabilization parameters on the convergence of the method, we have shown that the four stabilization parameters are necessary for the method to keep an optimal order of convergence (p+1). We also note that the symmetry of the strain tensor was imposed strongly, which ensures that we do not lose half an order of convergence. We have also studied numerically the condition number of the global and local problems, and show that they remain in a good range that maintains stability for the geophysical material in consideration. This work lays the foundation for future investigation such as improvement of convergence order to p+2 by using a post-processing method, and construction of absorbing boundary conditions for simulation in infinite domains, see Chapter 4.

Chapter 4

Truncation methods for poroelastic problems

In the previous chapter, we have developed a HDG formulation of time harmonic Biot's equations. In geophysical applications, the source terms that generate the wave propagation are only active in a limited area. This explains that regional simulations are sufficient for reproducing correctly the physical phenomenon performed. The computational domain is thus limited by an external boundary that surrounds the support of the source. Regarding the physical problem, the external boundary is thus artificial and its existence must not interfere with the simulation by creating spurious reflections. For that purpose, one approach consists in applying a boundary condition that models the perfect transmission of a wave from the interior of the computational domain to its exterior. This is what we call a transparent boundary condition (TBC). In practice, TBCs are not easy to implement because they involve pseudo-differential operators, which explains that approximate TBCs are used in general, called Abosrbing Boundary Condition (ABC) in the time domain and Radiation Boundary Condition (RBC) in the frequency domain. In this chapter, we construct an approximate TBC which is obtained from the characterization of outgoing solutions of the 2D isotropic poroelastic equations. The construction is based upon a TBC relating the solid and fluid stress tensors to the velocities of a particular solution that turns out to be an outgoing solution. The TBC is written in a circular domain with radius r and letting r go to infinity, we obtain a condition that approximates the exact condition to the order r^{-1}. The obtained condition is comparable to Lysmer–Kuhlemeyer (LK) absorbing boundary condition for elasticity that has been investigated in [93]. It is worth noting that absorbing boundary conditions for poroelasticity have been given by Degrande [41, 42] and Akiyoshi [1, 2] in the time domain. The methods employed in these reference are different from ours resulting in a different form of ABC. This is in particular for the second reference, whose form of ABC is not given in a compact form conducive for discretization with finite elements. Regarding Degrande's [41, 42] result, it is obtained in a stratified setting, in a form comparable to ours. We have noticed that in [41, 42], the condition is symmetrized while ours is not. Since the condition is obtained as the principal part of an outgoing radiation condition, we call it an outgoing Radiation Boundary Condition (RBC).

Another way to truncate the domain is to use Perfectly Matched Layer (PML). This has been done first for Maxwell's equations by Bérenger in [14]. An absorbing layer is added using attenuation functions that prevent reflections generated by the external boundary. Due to the lack of work on RBC for poroelasticity, most works in the literature *e.g.*, [50], [74] and [136], [134] use PMLs, which are readily available for most partial differential equations (PDEs).

In this chapter, we consider the two truncation methods that are integrated in our HDG method. It is worth noting that the derived RBC can be naturally coupled with HDG, since it resembles the transmission condition of numerical traces. The PML method can also be applied to the local problem of the HDG. This chapter is organized as follows. In Section 4.1, we derive the TBC. Then, by considering the particular case of a circular boundary, we propose a RBC in Section 4.2 as an approximation of the TBC. The performance of this condition is investigated in Section 4.3, by comparison with the outgoing solution that we calculated in Chapter 2. In Section 4.4, the obtained RBC is implemented with Hybridizable discontinuous Galerkin (HDG) method for poroelastic wave equations. Then, in Section 4.5, we consider a second method to truncate the domain by using the Perfectly Matched Layer (PML) also with HDG discretization. Section 4.6 compares the performance of our RBC with that of the PML. Finally, we extend the truncation methods to three-dimensional domains in Section 4.7.

4.1 Derivation of low-order outgoing radiation boundary conditions

In this section, we obtain an outgoing radiation condition at infinity. We consider the scattering of a plane wave by an impenetrable circular obstacle, see Figure 4.1. In this setting, we express the poroelastic unknowns using the potentials $\chi_\bullet$ and we find a condition between the unknowns at infinity. Then, by approximating this condition, we propose a low-order RBC, that will be used to set artificial boundaries on Γ_{abs}. We consider an isotropic porous medium. The

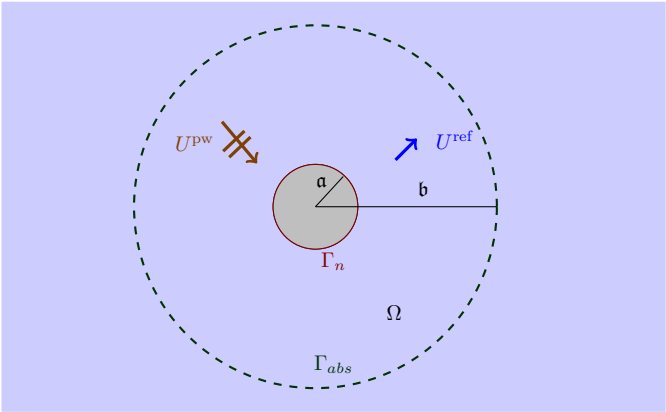

Figure 4.1: Scattering of a plane wave by an impenetrable solid immersed in a porous medium. The cross section of the obstacle is a disc parameterized by $r = \mathfrak{a}$. The artificial boundary is set on $\Gamma_{abs} = \{r = \mathfrak{b}\}$.

vector field ($\mathbf{u}$, $\mathbf{w}$, $\boldsymbol{\tau}$, p) solve the system (*cf.* 1):

$$\left\{\begin{array}{lcl} \nabla\cdot\boldsymbol{\tau} + \mathbf{f}_u &=& \mathrm{i}\,\omega\,\rho_a\,\mathbf{u} \;+\; \mathrm{i}\,\omega\,\rho_f\,\mathbf{w}\,,\\ -\nabla \mathrm{p} + \mathbf{f}_{\mathrm{w}} &=& \mathrm{i}\,\omega\,\rho_f\mathbf{u} \;+\; \mathrm{i}\,\omega\;\rho_{\mathrm{dyn}}\mathbf{w}\,,\\ \mathrm{i}\,\omega\,\boldsymbol{\tau} &=& 2\mu_{\mathrm{fr}}\boldsymbol{\epsilon} \;+\; (\lambda_{\mathrm{fr}} \;+\; M\alpha^2)\nabla\cdot\mathrm{u}\,\mathbb{I} \;+\; \alpha M\nabla\cdot\boldsymbol{w}\,\mathbb{I}\,,\\ \mathrm{i}\,\omega\,\mathrm{p} &=& -M\,\nabla\cdot\mathbf{w} \;-\; M\,\boldsymbol{\alpha}:\boldsymbol{\epsilon}\,. \end{array}\right. \tag{4.1}$$

We recall the expressions of the unknowns ($\mathbf{u}$, $\mathbf{w}$, $\boldsymbol{\tau}$, p) in two dimensions in terms of the potentials $\chi_\bullet$, $\bullet = P, B, S$, as demonstrated in Chapter 2.

$$\begin{aligned} \mathrm{i}\,\omega\,\mathbf{u} &= \mathrm{s}_{\mathrm{P}}^{-2}\,\nabla\chi_{\mathrm{P}} \;+\; \mathrm{s}_{\mathrm{B}}^{-2}\,\nabla\chi_{\mathrm{B}} \;-\; \mathrm{s}_{\mathrm{S}}^{-2}\,\mathbf{curl}\,\chi_{\mathrm{S}}\,,\\ \mathrm{i}\,\omega\,\mathbf{w} &= \frac{\mathcal{W}_{\mathrm{P}}}{\mathrm{s}_{\mathrm{P}}^2}\nabla\chi_{\mathrm{P}} \;+\; \frac{\mathcal{W}_{\mathrm{B}}}{\mathrm{s}_{\mathrm{B}}^2}\nabla\chi_{\mathrm{B}} \;+\; \frac{\rho_f\,\mu_{\mathrm{fr}}}{\det A}\mathbf{curl}\,\chi_{\mathrm{S}}\,,\\ \mathrm{p} &= -M\,(\mathcal{W}_{\mathrm{P}} \;+\; \alpha)\chi_{\mathrm{P}} \;-\; M\,(\mathcal{W}_{\mathrm{B}} \;+\; \alpha)\chi_{\mathrm{B}}\,,\\ \omega^2\,\boldsymbol{\tau} &= \mu_{\mathrm{fr}}\left(-\frac{2}{\mathrm{s}_{\mathrm{P}}^2}\,\nabla^2\chi_{\mathrm{P}} \;-\; \frac{2}{\mathrm{s}_{\mathrm{B}}^2}\,\nabla^2\chi_{\mathrm{B}} \;+\; \frac{\nabla\mathbf{curl}\,\chi_{\mathrm{S}} \;+\; (\nabla\mathbf{curl}\,\chi_{\mathrm{S}})^T}{\mathrm{s}_{\mathrm{S}}^2}\right)\\ &\quad +\; \omega^2\,\left(-\tfrac{2}{3}\mu_{\mathrm{fr}} \;+\; \mathrm{k}_{\mathrm{fr}} \;+\; M\alpha^2\right)\,(\chi_{\mathrm{P}} \;+\; \chi_{\mathrm{B}})\,\mathbb{I} \;+\; \omega^2\,\alpha\,M\,(\mathcal{W}_{\mathrm{P}}\,\chi_{\mathrm{P}} \;+\; \mathcal{W}_{\mathrm{B}}\,\chi_{\mathrm{B}})\,\mathbb{I}\,, \end{aligned} \tag{4.2}$$

with operator **curl** defined in (A.1), ∇^2 in (A.3a), and $\mathbb{I} = \begin{pmatrix} 1 & 0 \\ 0 & 1 \end{pmatrix}$. The potentials $\chi_\bullet$ solve the Helmholtz equation,

$$\left(-\Delta \;-\; \omega^2\,\mathrm{s}_\bullet^2\right)\chi_\bullet \;=\; 0\,.$$

Radiating asymptotic of Hankel functions

Let $\mathrm{H}_k^{(1)}(z)$ be the Hankel function such as $\mathrm{H}_k^{(1)}(z) = \mathrm{J}_k(z) + \mathrm{i}\mathrm{Y}_k(z)$, with J_k and Y_k respectively the first- and second-order Bessel functions. From equations (10.17.2) and (10.17.11) in [103], we have

$$\mathrm{H}_k^{(1)'}(z) \underset{z\to\infty}{\sim} \mathrm{i}\left(\frac{2}{\pi\,z}\right)^{\frac{1}{2}}\,e^{\mathrm{i}\,(z\,-\,\frac{1}{2}\,k\,\pi\,-\,\frac{1}{4}\,\pi)}\left(1 \;+\; \sum_{m=1}^{\infty}(-1)^m\,\frac{b_m(k)}{z^m}\right).$$

Equivalently from equations (10.17.2) and (10.17.5) in [103],

$$\mathrm{H}_k^{(1)}(z) \underset{z\to\infty}{\sim} \left(\frac{2}{\pi\, z}\right)^{\frac{1}{2}} e^{\mathrm{i}\,(z-\frac{1}{2}\,k\,\pi-\frac{1}{4}\,\pi)} \left(1 + \sum_{m=1}^{\infty} \mathrm{i}^m\, \frac{a_m(k)}{z^m}\right).$$

Hence,

$$\mathrm{H}_k^{(1)'}(z) - \mathrm{i}\,\mathrm{H}_k^{(1)}(z) \underset{z\to\infty}{\sim} \left(\frac{2}{\pi\, z}\right)^{\frac{1}{2}} e^{\mathrm{i}\,(z-\frac{1}{2}\,k\,\pi-\frac{1}{4}\,\pi)} \left(\sum_{m=1}^{\infty} \mathrm{i}^m\, \frac{c_m(k)}{z^m}\right).$$

In the end we obtain the radiating asymptotic:

$$\mathrm{H}_k^{(1)'}(z) - \mathrm{i}\,\mathrm{H}_k^{(1)}(z) = O(z^{-\frac{3}{2}}), \quad z\to\infty. \tag{4.3}$$

This will be the main ingredient in the derivation of the radiation boundary conditions.

4.1.1 Outgoing radiation condition at infinity

Considering an infinite domain, as given in Figure 4.1, we recall from (2.30) the potentials $\chi_\bullet$ that define a generic outgoing solution in polar coordinates,

$$\begin{aligned}
\chi_{\mathrm{P}}(r,\theta) &= \sum_{k\in\mathbb{Z}} a_k\, \mathrm{H}_k^{(1)}(\omega\, \mathsf{s}_{\mathrm{P}}\, r)\; e^{\mathrm{i}\,k\,\theta}, \\
\chi_{\mathrm{B}}(r,\theta) &= \sum_{k\in\mathbb{Z}} b_k\, \mathrm{H}_k^{(1)}(\omega\, \mathsf{s}_{\mathrm{B}}\, r)\; e^{\mathrm{i}\,k\,\theta}, \\
\chi_{\mathrm{S}}(r,\theta) &= \sum_{k\in\mathbb{Z}} c_k\, \mathrm{H}_k^{(1)}(\omega\, \mathsf{s}_{\mathrm{S}}\, r)\; e^{\mathrm{i}\,k\,\theta}.
\end{aligned}$$

To obtain the final expression of the poroelastic unknowns, we substitute this form of potentials in equation (4.2). As we study a circular obstacle, we work in polar coordinates. We will use the expression for the action of **curl** ∇ and ∇^2 in polar coordinates presented in Appendix A.1.1. Note that, in the construction of the outgoing solution (see Section 2.3), we only impose conditions on $\mathbf{u}$, $\mathbf{w}\cdot\boldsymbol{n}$, $\boldsymbol{\tau}\,\boldsymbol{n}$ or p, which are in polar coordinates u_r, u_θ, w_r, τ_{rr}, $\tau_{r\theta}$, or p. We obtain the following expressions for the expansion of the unknowns ($\mathbf{u}$, $\mathbf{w}$, $\boldsymbol{\tau}$, p):

$$\begin{aligned}
\mathrm{i}\,\omega\,\mathrm{u}_r &= \sum_{k\in\mathbb{Z}} a_k\, \frac{\omega}{\mathsf{s}_{\mathrm{P}}}\, \mathrm{H}_k^{(1)'}(\omega\, \mathsf{s}_{\mathrm{P}}\, r) e^{\mathrm{i}k\theta} + \sum_{k\in\mathbb{Z}} b_k\, \frac{\omega}{\mathsf{s}_{\mathrm{B}}}\, \mathrm{H}_k^{(1)'}(\omega\, \mathsf{s}_{\mathrm{B}}\, r) e^{\mathrm{i}k\theta} - \sum_{k\in\mathbb{Z}} c_k\, \frac{\mathrm{i}k}{\mathsf{s}_{\mathrm{S}}^2\, r} \mathrm{H}_k^{(1)}(\omega\, \mathsf{s}_{\mathrm{S}}\, r) e^{\mathrm{i}k\theta}, \\
\mathrm{i}\,\omega\,\mathrm{u}_\theta &= \sum_{k\in\mathbb{Z}} a_k\, \frac{\mathrm{i}k}{\mathsf{s}_{\mathrm{P}}^2\, r} \mathrm{H}_k^{(1)}(\omega\, \mathsf{s}_{\mathrm{P}}\, r) e^{\mathrm{i}k\theta} + \sum_{k\in\mathbb{Z}} b_k\, \frac{\mathrm{i}k}{\mathsf{s}_{\mathrm{B}}^2\, r} \mathrm{H}_k^{(1)}(\omega\, \mathsf{s}_{\mathrm{B}}\, r) e^{\mathrm{i}k\theta} + \sum_{k\in\mathbb{Z}} c_k\, \mathsf{s}_{\mathrm{S}}^{-1}\, \omega\, \mathrm{H}_k^{(1)'}(\omega\, \mathsf{s}_{\mathrm{S}}\, r) e^{\mathrm{i}k\theta}, \\
\mathrm{i}\,\omega\,\mathrm{w}_r &= \sum_{k\in\mathbb{Z}} a_k\, \frac{\mathcal{W}_{\mathrm{P}}}{\mathsf{s}_{\mathrm{P}}}\, \omega\, \mathrm{H}_k^{(1)'}(\omega\, \mathsf{s}_{\mathrm{P}}\, r) e^{\mathrm{i}k\theta} + \sum_{k\in\mathbb{Z}} b_k\, \frac{\mathcal{W}_{\mathrm{B}}}{\mathsf{s}_{\mathrm{B}}}\, \omega\, \mathrm{H}_k^{(1)'}(\omega\, \mathsf{s}_{\mathrm{B}}\, r) e^{\mathrm{i}k\theta} + \sum_{k\in\mathbb{Z}} c_k\, \frac{\rho_f\, \mu_{\mathrm{fr}}}{\det A}\, \frac{\mathrm{i}k}{r} \mathrm{H}_k^{(1)}(\omega\, \mathsf{s}_{\mathrm{S}}\, r) e^{\mathrm{i}k\theta}.
\end{aligned}$$

As specified above, we will only be concerned with $\boldsymbol{\tau}\cdot\mathbf{e}_r = \tau_{rr}\mathbf{e}_r + \tau_{r\theta}\mathbf{e}_\theta$,

$$
\begin{aligned}
\omega^2\tau_{rr} = &-\sum_{k\in\mathbb{Z}} \frac{2\,\mu_{\rm fr}\,\omega}{\mathsf{s}_{\rm P}\,r}\,a_k\,\mathrm{H}_{k+1}^{(1)}(\omega\,\mathsf{s}_{\rm P}\,r)\;e^{\mathrm{i}\,k\,\theta} \;+\sum_{k\in\mathbb{Z}} \frac{2\,\mu_{\rm fr}\,k}{\mathsf{s}_{\rm P}^2\,r^2}\,a_k\,\mathrm{H}_{k}^{(1)}(\omega\,\mathsf{s}_{\rm P}\,r)\;e^{\mathrm{i}\,k\,\theta}\\
&+\sum_{k\in\mathbb{Z}} 2\,\mu_{\rm fr}\,a_k\,\omega^2\,\mathrm{H}_{k}^{(1)}(\omega\,\mathsf{s}_{\rm P}\,r)\;e^{\mathrm{i}\,k\,\theta} \;-\sum_{k\in\mathbb{Z}} \frac{2\,\mu_{\rm fr}\,k^2}{\mathsf{s}_{\rm P}^2\,r^2}\,a_k\,\mathrm{H}_{k}^{(1)}(\omega\,\mathsf{s}_{\rm P}\,r)\;e^{\mathrm{i}\,k\,\theta}\\
&-\sum_{k\in\mathbb{Z}} \frac{2\,\mu_{\rm fr}\,\omega}{\mathsf{s}_{\rm B}\,r}\,b_k\,\mathrm{H}_{k+1}^{(1)}(\omega\,\mathsf{s}_{\rm B}\,r)\;e^{\mathrm{i}\,k\,\theta} \;+\sum_{k\in\mathbb{Z}} \frac{2\,\mu_{\rm fr}\,k}{\mathsf{s}_{\rm B}^2\,r^2}\,b_k\,\mathrm{H}_{k}^{(1)}(\omega\,\mathsf{s}_{\rm B}\,r)\;e^{\mathrm{i}\,k\,\theta}\\
&+\sum_{k\in\mathbb{Z}} 2\,\mu_{\rm fr}\,b_k\,\omega^2\,\mathrm{H}_{k}^{(1)}(\omega\,\mathsf{s}_{\rm B}\,r)\;e^{\mathrm{i}\,k\,\theta} \;-\sum_{k\in\mathbb{Z}} \frac{2\,\mu_{\rm fr}\,k^2}{\mathsf{s}_{\rm B}^2\,r^2}\,b_k\,\mathrm{H}_{k}^{(1)}(\omega\,\mathsf{s}_{\rm B}\,r)\;e^{\mathrm{i}\,k\,\theta}\\
&+\sum_{k\in\mathbb{Z}} \frac{2\,\mu_{\rm fr}}{\mathsf{s}_{\rm S}r}\;c_k\,\omega\,\mathrm{i}k\,\mathrm{H}_{k}^{(1)'}(\omega\,\mathsf{s}_{\rm S}\,r)\;e^{\mathrm{i}\,k\,\theta}\\
&+\sum_{k\in\mathbb{Z}} \omega^2\,\left(-\tfrac{2}{3}\mu_{\rm fr}\,+\,\mathrm{k}_{\rm fr}\,+\,M\alpha^2\,+\,\alpha\,M\mathcal{W}_{\rm P}\right)\;a_k\,\mathrm{H}_{k}^{(1)}(\omega\,\mathsf{s}_{\rm P}\,r)\;e^{\mathrm{i}\,k\,\theta}\\
&+\sum_{k\in\mathbb{Z}} \omega^2\,\left(-\tfrac{2}{3}\mu_{\rm fr}\,+\,\mathrm{k}_{\rm fr}\,+\,M\alpha^2\,+\,\alpha\,M\mathcal{W}_{\rm B}\right)\,b_k\,\mathrm{H}_{k}^{(1)}(\omega\,\mathsf{s}_{\rm B}\,r)\;e^{\mathrm{i}\,k\,\theta}\,,
\end{aligned}
$$

$$
\begin{aligned}
\omega^2\,\tau_{r\theta} \;= &-\sum_{k\in\mathbb{Z}} \frac{2\,\mu_{\rm fr}\,\omega\,\mathrm{i}\,k}{r\,\mathsf{s}_{\rm P}}\,a_k\,\mathrm{H}_{k}^{(1)'}(\omega\,\mathsf{s}_{\rm P}\,r)\;e^{\mathrm{i}\,k\,\theta} +\sum_{k\in\mathbb{Z}} \frac{2\,\mathrm{i}\,\mu_{\rm fr}\,k}{r^2\,\mathsf{s}_{\rm P}^2}\,a_k\,\mathrm{H}_{k}^{(1)}(\omega\,\mathsf{s}_{\rm P}\,r)\;e^{\mathrm{i}\,k\,\theta}\\
&-\sum_{k\in\mathbb{Z}} \frac{2\,\mu_{\rm fr}\omega\,\mathrm{i}\,k}{r\,\mathsf{s}_{\rm B}}\,b_k\,\mathrm{H}_{k}^{(1)'}(\omega\,\mathsf{s}_{\rm B}\,r)\;e^{\mathrm{i}\,k\,\theta} +\sum_{k\in\mathbb{Z}} \frac{2\,\mathrm{i}\,\mu_{\rm fr}\,k}{r^2\,\mathsf{s}_{\rm B}^2}\,b_k\,\mathrm{H}_{k}^{(1)}(\omega\,\mathsf{s}_{\rm B}\,r)\;e^{\mathrm{i}\,k\,\theta}\\
&-\sum_{k\in\mathbb{Z}} \frac{\mu_{\rm fr}\,k^2}{r^2\,\mathsf{s}_{\rm S}^2}\,c_k\,\mathrm{H}_{k}^{(1)}(\omega\,\mathsf{s}_{\rm S}\,r)\;e^{\mathrm{i}\,k\,\theta} +\sum_{k\in\mathbb{Z}} \frac{\mu_{\rm fr}\,\omega}{r\,\mathsf{s}_{\rm S}}\,c_k\,\mathrm{H}_{k}^{(1)'}(\omega\,\mathsf{s}_{\rm S}\,r)\;e^{\mathrm{i}\,k\,\theta}\\
&-\sum_{k\in\mathbb{Z}} \mu_{\rm fr}\,\frac{\omega}{\mathsf{s}_{\rm S}\,r}\,c_k\,\mathrm{H}_{k+1}^{(1)}(\omega\,\mathsf{s}_{\rm S}\,r)\;e^{\mathrm{i}\,k\,\theta} +\sum_{k\in\mathbb{Z}} \mu_{\rm fr}\,\frac{k}{\mathsf{s}_{\rm S}^2\,r^2}c_k\,\mathrm{H}_{k}^{(1)}(\omega\,\mathsf{s}_{\rm S}\,r)\;e^{\mathrm{i}\,k\,\theta}\\
&+\sum_{k\in\mathbb{Z}} \mu_{\rm fr}\,\omega^2\,c_k\,\mathrm{H}_{k}^{(1)}(\omega\,\mathsf{s}_{\rm S}\,r)\;e^{\mathrm{i}\,k\,\theta} -\sum_{k\in\mathbb{Z}} \mu_{\rm fr}\,\frac{k^2}{\mathsf{s}_{\rm S}^2\,r^2}\,c_k\,\mathrm{H}_{k}^{(1)}(\omega\,\mathsf{s}_{\rm S}\,r)\;e^{\mathrm{i}\,k\,\theta}\,,\\
\mathrm{p} \;= &-\sum_{k\in\mathbb{Z}} a_k M\left(\mathcal{W}_{\rm P}\;+\;\alpha\right)\mathrm{H}_{k}^{(1)}(\omega\,\mathsf{s}_{\rm P}\,r)\,e^{\mathrm{i}k\theta} \;-\;\sum_{k\in\mathbb{Z}} b_k M\left(\mathcal{W}_{\rm B}\;+\;\alpha\right)\mathrm{H}_{k}^{(1)}(\,\omega\,\mathsf{s}_{\rm B}\,r)\,e^{\mathrm{i}k\theta}\,.
\end{aligned}
$$

We now want to express a relation at infinity between the unknowns $\mathbf{u}$, $\mathbf{w}$, $\boldsymbol{\tau}$, p. We use the fact that $\lim_{r\to\infty}\frac{1}{r}=0$, and we hence choose to approximate the components by truncating at the first order in $\frac{1}{r}$:

$$
\begin{aligned}
\mathrm{u}_r \;&=\; -\sum_{k\in\mathbb{Z}} a_k\,\frac{\mathrm{i}}{\mathsf{s}_{\rm P}}\,\mathrm{H}_{k}^{(1)'}(\omega\,\mathsf{s}_{\rm P}\,r)e^{\mathrm{i}k\theta} \;-\;\sum_{k\in\mathbb{Z}} b_k\,\frac{\mathrm{i}}{\mathsf{s}_{\rm B}}\,\mathrm{H}_{k}^{(1)'}(\omega\,\mathsf{s}_{\rm B}\,r)e^{\mathrm{i}k\theta} \,+\, \mathsf{O}(r^{-\frac{3}{2}})\,,\\
\mathrm{w}_r \;&=\; -\sum_{k\in\mathbb{Z}} a_k\,\frac{\mathrm{i}\,\mathcal{W}_{\rm P}}{\mathsf{s}_{\rm P}}\,\mathrm{H}_{k}^{(1)'}(\omega\,\mathsf{s}_{\rm P}\,r)e^{\mathrm{i}k\theta} \;-\;\sum_{k\in\mathbb{Z}} b_k\,\frac{\mathrm{i}\,\mathcal{W}_{\rm B}}{\mathsf{s}_{\rm B}}\,\mathrm{H}_{k}^{(1)'}(\omega\,\mathsf{s}_{\rm B}\,r)e^{\mathrm{i}k\theta} \,+\, \mathsf{O}(r^{-\frac{3}{2}})\,,\\
\mathrm{u}_\theta \;&=\; -\sum_{k\in\mathbb{Z}} c_k\,\frac{\mathrm{i}}{\mathsf{s}_{\rm S}}\,\mathrm{H}_{k}^{(1)'}(\omega\,\mathsf{s}_{\rm S}\,r) + \,\mathsf{O}(r^{-\frac{3}{2}})\,,
\end{aligned}
\tag{4.5}
$$

and

$$
\begin{aligned}
\tau_{rr} = &\left(\frac{4}{3}\mu_{\rm fr}\,+\,\mathrm{k}_{\rm fr}\,+\,\alpha(M\alpha\,+\,M\mathcal{W}_{\rm P})\right)\sum_{k\in\mathbb{Z}}\;a_k\,\mathrm{H}_{k}^{(1)}(\omega\,\mathsf{s}_{\rm P}\,r)\;e^{\mathrm{i}\,k\,\theta}\\
&+\left(\frac{4}{3}\mu_{\rm fr}\,+\,\mathrm{k}_{\rm fr}\,+\,\alpha(M\alpha\,+\,M\mathcal{W}_{\rm B})\right)\sum_{k\in\mathbb{Z}}\;b_k\,\mathrm{H}_{k}^{(1)}(\omega\,\mathsf{s}_{\rm B}\,r)\;e^{\mathrm{i}\,k\,\theta}\;+\;\mathsf{O}(r^{-\frac{3}{2}})\,,\\
\tau_{r\theta} \;= &\sum_{k\in\mathbb{Z}}\mu_{\rm fr}\,c_k\,\mathrm{H}_{k}^{(1)}(\omega\,\mathsf{s}_{\rm S}\,r)\,e^{\mathrm{i}\,k\,\theta}\;+\;\mathsf{O}(r^{-\frac{3}{2}})\,,\\
\mathrm{p} = &-\sum_{k\in\mathbb{Z}} a_k M\left(\mathcal{W}_{\rm P}\;+\;\alpha\right)\mathrm{H}_{k}^{(1)}(\,\omega\,\mathsf{s}_{\rm P}\,r)\,e^{\mathrm{i}k\theta} \;-\;\sum_{k\in\mathbb{Z}} b_k M\left(\mathcal{W}_{\rm B}\;+\;\alpha\right)\mathrm{H}_{k}^{(1)}(\omega\,\mathsf{s}_{\rm B}\,r)\,e^{\mathrm{i}k\theta}\,.
\end{aligned}
\tag{4.6}
$$

Important identity:
Using the expressions of the radial velocities in (4.5), we can write the system:

$$\begin{pmatrix} \mathrm{i}\,\mathrm{u}_r \\ \mathrm{i}\,\mathrm{w}_r \end{pmatrix} = \begin{pmatrix} \dfrac{1}{\mathsf{s}_\mathrm{P}} & \dfrac{1}{\mathsf{s}_\mathrm{B}} \\ \dfrac{\mathcal{W}_\mathrm{P}}{\mathsf{s}_\mathrm{P}} & \dfrac{\mathcal{W}_\mathrm{B}}{\mathsf{s}_\mathrm{B}} \end{pmatrix} \begin{pmatrix} \displaystyle\sum_{k\in\mathbb{Z}} a_k\ \mathrm{H}_k^{(1)'}(\omega\,\mathsf{s}_\mathrm{P}\,r)e^{\mathrm{i}k\theta} \\ \displaystyle\sum_{k\in\mathbb{Z}} b_k\ \mathrm{H}_k^{(1)'}(\omega\,\mathsf{s}_\mathrm{B}\,r)e^{\mathrm{i}k\theta} \end{pmatrix} + \mathsf{O}(r^{-\frac{3}{2}})\,. \tag{4.7}$$

We can express the inverse of the above matrix:

$$\begin{pmatrix} \frac{1}{\mathsf{s}_\mathrm{P}} & \frac{1}{\mathsf{s}_\mathrm{B}} \\ \frac{\mathcal{W}_\mathrm{P}}{\mathsf{s}_\mathrm{P}} & \frac{\mathcal{W}_\mathrm{B}}{\mathsf{s}_\mathrm{B}} \end{pmatrix}^{-1} = \frac{1}{\mathcal{W}_\mathrm{B}-\mathcal{W}_\mathrm{P}} \begin{pmatrix} \mathcal{W}_\mathrm{B}\,\mathsf{s}_\mathrm{P} & -\mathsf{s}_\mathrm{P} \\ -\mathcal{W}_\mathrm{P}\,\mathsf{s}_\mathrm{B} & \mathsf{s}_\mathrm{B} \end{pmatrix}.$$

Hence, equation (4.7) becomes

$$\boxed{\begin{pmatrix} \displaystyle\sum_{k\in\mathbb{Z}} a_k\ \mathrm{H}_k^{(1)'}(\omega\,\mathsf{s}_\mathrm{P}\,r)e^{\mathrm{i}k\theta} \\ \displaystyle\sum_{k\in\mathbb{Z}} b_k\ \mathrm{H}_k^{(1)'}(\omega\,\mathsf{s}_\mathrm{B}\,r)e^{\mathrm{i}k\theta} \end{pmatrix} = \frac{1}{\mathcal{W}_\mathrm{B}-\mathcal{W}_\mathrm{P}} \begin{pmatrix} \mathsf{s}_\mathrm{P}\,\mathcal{W}_\mathrm{B} & -\mathsf{s}_\mathrm{P} \\ -\mathcal{W}_\mathrm{P}\,\mathsf{s}_\mathrm{B} & \mathsf{s}_\mathrm{B} \end{pmatrix} \begin{pmatrix} \mathrm{i}\,\mathrm{u}_r \\ \mathrm{i}\,\mathrm{w}_r \end{pmatrix} + \mathsf{O}(r^{-\frac{3}{2}})\,.} \tag{4.8}$$

In the following, we express the radial component of the solid stress, the tangential component of the solid stress and the fluid pressure using the velocities **u** and **w**.

(a) Radial component of the solid stress

With the approximate values of τ_{rr} given in equation (4.6), we have:

$$\begin{aligned} \tau_{rr} - \big(\tfrac{4}{3}\mu_\mathrm{fr} + \mathrm{k}_\mathrm{fr} + \alpha(M\alpha + M\mathcal{W}_\mathrm{P})\big) \sum_{k\in\mathbb{Z}} a_k\,\mathrm{H}_k^{(1)}(\omega\,\mathsf{s}_\mathrm{P}\,r)\ e^{\mathrm{i}\,k\,\theta} \\ - \big(\tfrac{4}{3}\mu_\mathrm{fr} + \mathrm{k}_\mathrm{fr} + \alpha(M\alpha + M\mathcal{W}_\mathrm{B})\big) \sum_{k\in\mathbb{Z}} b_k\,\mathrm{H}_k^{(1)}(\omega\,\mathsf{s}_\mathrm{B}\,r)\ e^{\mathrm{i}\,k\,\theta} = \mathsf{O}(r^{-\frac{3}{2}})\,. \end{aligned}$$

Using (4.3), we replace $\mathrm{H}_k^{(1)}(z)$ by

$$\mathrm{H}_k^{(1)}(z) = -\mathrm{i}\,\mathrm{H}_k^{(1)'}(z) + \mathsf{O}(z^{-\frac{3}{2}})\,,$$

to obtain

$$\begin{aligned} \tau_{rr} + \big(\tfrac{4}{3}\mu_\mathrm{fr} + \mathrm{k}_\mathrm{fr} + \alpha(M\alpha + M\mathcal{W}_\mathrm{P})\big) \sum_{k\in\mathbb{Z}} a_k\,\mathrm{i}\,\mathrm{H}_k^{(1)'}(\omega\,\mathsf{s}_\mathrm{P}\,r)\ e^{\mathrm{i}\,k\,\theta} \\ + \big(\tfrac{4}{3}\mu_\mathrm{fr} + \mathrm{k}_\mathrm{fr} + \alpha(M\alpha + M\mathcal{W}_\mathrm{B})\big) \sum_{k\in\mathbb{Z}} b_k\,\mathrm{i}\,\mathrm{H}_k^{(1)'}(\omega\,\mathsf{s}_\mathrm{B}\,r)\ e^{\mathrm{i}\,k\,\theta} = \mathsf{O}(r^{-\frac{3}{2}})\,. \end{aligned}$$

Finally, using (4.8), we obtain a relation between τ_{rr}, u_r and w_r:

$$\begin{aligned} \tau_{rr} - \frac{\frac{4}{3}\mu_\mathrm{fr} + \mathrm{k}_\mathrm{fr} + \alpha(M\alpha + M\mathcal{W}_\mathrm{P})}{\mathcal{W}_\mathrm{B}-\mathcal{W}_\mathrm{P}}\,(\,\mathsf{s}_\mathrm{P}\,\mathcal{W}_\mathrm{B}\,\mathrm{u}_r - \mathsf{s}_\mathrm{P}\mathrm{w}_r) \\ - \frac{\frac{4}{3}\mu_\mathrm{fr} + \mathrm{k}_\mathrm{fr} + \alpha(M\alpha + M\mathcal{W}_\mathrm{B})}{\mathcal{W}_\mathrm{B}-\mathcal{W}_\mathrm{P}}\,(-\mathcal{W}_\mathrm{P}\,\mathsf{s}_\mathrm{B}\,\mathrm{u}_r + \mathsf{s}_\mathrm{B}\mathrm{w}_r) = \mathsf{O}(r^{-\frac{3}{2}})\,. \end{aligned} \tag{4.9}$$

(b) Tangential component of the solid stress

The tangent solid velocity u_θ and $\tau_{r\theta}$ are expressed with equations (4.5) and (4.6). Replace $\mathrm{H}_k^{(1)}$, using the identity (4.3), we obtain:

$$\tau_{r\theta} - \mathsf{s}_\mathrm{S}\,\mu_\mathrm{fr}\,\mathrm{u}_\theta = \mathsf{O}(r^{-\frac{3}{2}})\,. \tag{4.10}$$

(c) Fluid pressure

From the expression of p in (4.6) and the radiating asymptotic (4.3), we have:

$$-\mathrm{p} + M\,(\mathcal{W}_\mathrm{P} + \alpha)\sum_{k\in\mathbb{Z}} a_k \mathrm{i}\mathrm{H}_k^{(1)'}(\,\omega\,\mathsf{s}_\mathrm{P}\,r)\,e^{\mathrm{i}k\theta} + M\,(\mathcal{W}_\mathrm{B} + \alpha)\sum_{k\in\mathbb{Z}} b_k \mathrm{i}\mathrm{H}_k^{(1)'}(\,\omega\,\mathsf{s}_\mathrm{B}\,r)\,e^{\mathrm{i}k\theta} = \mathsf{O}(r^{-\frac{3}{2}})\,.$$

Using equation (4.8), we obtain,

$$-\mathrm{p} - \frac{M\,(\mathcal{W}_\mathrm{P} + \alpha)}{\mathcal{W}_\mathrm{B}-\mathcal{W}_\mathrm{P}}(\mathsf{s}_\mathrm{P}\,\mathcal{W}_\mathrm{B}\,\mathrm{u}_r - \mathsf{s}_\mathrm{P}\mathrm{w}_r) - \frac{M\,(\mathcal{W}_\mathrm{B} + \alpha)}{\mathcal{W}_\mathrm{B}-\mathcal{W}_\mathrm{P}}\,(-\mathsf{s}_\mathrm{B}\,\mathcal{W}_\mathrm{P}\,\mathrm{u}_r + \mathsf{s}_\mathrm{B}\mathrm{w}_r) = \mathsf{O}(r^{-\frac{3}{2}})\,. \tag{4.11}$$

Summary

We have obtained three relations (4.9), (4.10), (4.11) between the poroelastic unknowns at infinity. We denote:

$$\mathbf{X}_1 = -\frac{\frac{4}{3}\mu_{\rm fr} + {\rm k}_{\rm fr} + \alpha(M\alpha + M\mathcal{W}_{\rm P})}{\mathcal{W}_{\rm B} - \mathcal{W}_{\rm P}}\,\mathsf{s}_{\rm P}\,\mathcal{W}_{\rm B} + \frac{\frac{4}{3}\mu_{\rm fr} + {\rm k}_{\rm fr} + \alpha(M\alpha + M\mathcal{W}_{\rm B})}{\mathcal{W}_{\rm B} - \mathcal{W}_{\rm P}}\,\mathcal{W}_{\rm P}\,\mathsf{s}_{\rm B}\,,$$

$$\mathbf{X}_2 = \frac{\frac{4}{3}\mu_{\rm fr} + {\rm k}_{\rm fr} + \alpha(M\alpha + M\mathcal{W}_{\rm P})}{\mathcal{W}_{\rm B} - \mathcal{W}_{\rm P}}\,\mathsf{s}_{\rm P} - \frac{\frac{4}{3}\mu_{\rm fr} + {\rm k}_{\rm fr} + \alpha(M\alpha + M\mathcal{W}_{\rm B})}{\mathcal{W}_{\rm B} - \mathcal{W}_{\rm P}}\,\mathsf{s}_{\rm B}\,,$$

$$\mathbf{X}_3 = -\,\mathsf{s}_{\rm S}\,\mu_{\rm fr}\,,$$

$$\mathbf{X}_4 = \frac{M\left(\mathcal{W}_{\rm P} + \alpha\right)}{\mathcal{W}_{\rm B} - \mathcal{W}_{\rm P}}\mathsf{s}_{\rm P}\,\mathcal{W}_{\rm B} - \frac{M\left(\mathcal{W}_{\rm B} + \alpha\right)}{\mathcal{W}_{\rm B} - \mathcal{W}_{\rm P}}\,\mathsf{s}_{\rm B}\,\mathcal{W}_{\rm P}\,,$$

$$\mathbf{X}_5 = -\frac{M\left(\mathcal{W}_{\rm P} + \alpha\right)}{\mathcal{W}_{\rm B} - \mathcal{W}_{\rm P}}\mathsf{s}_{\rm P} + \frac{M\left(\mathcal{W}_{\rm B} + \alpha\right)}{\mathcal{W}_{\rm B} - \mathcal{W}_{\rm P}}\,\mathsf{s}_{\rm B}\,.$$

Proposition 4.1. For ($\mathbf{u}$, $\mathbf{w}$, $\boldsymbol{\tau}$, p) solution of the poroelasticity equation (4.1), the outgoing radiation condition at infinity is:

$$\begin{cases} \tau_{rr} + \mathbf{X}_1 {\rm u}_r + \mathbf{X}_2 {\rm w}_r &= \mathsf{O}(r^{-\frac{3}{2}})\,, \\ \tau_{r\theta} + \mathbf{X}_3 {\rm u}_\theta &= \mathsf{O}(r^{-\frac{3}{2}})\,, \qquad r \to \infty \\ {\rm p} + \mathbf{X}_4 {\rm u}_r + \mathbf{X}_5 {\rm w}_r &= \mathsf{O}(r^{-\frac{3}{2}})\,. \end{cases} \tag{4.12}$$

4.1.2 Derivation of the radiation boundary condition

Considering the domain described in Figure 4.1, we set artificial boundaries on Γ_{abs}. We work in polar coordinates. In this setting, we have built in the previous section an outgoing radiation condition at infinity for the exact outgoing solutions, given in (4.12). When r tends to infinity, the terms $\mathsf{O}(r^{-\frac{3}{2}})$ can be neglected. We thus approximate equations (4.12) as:

$$\begin{cases} \tau_{rr} + \mathbf{X}_1 {\rm u}_r + \mathbf{X}_2 {\rm w}_r &= 0\,, \\ \tau_{r\theta} + \mathbf{X}_3 {\rm u}_\theta &= 0 \\ {\rm p} + \mathbf{X}_4 {\rm u}_r + \mathbf{X}_5 {\rm w}_r &= 0\,. \end{cases}$$

This is the RBC in polar coordinates. Recall that on a circle, we have:

$${\rm u}_r = \mathbf{u}\cdot\boldsymbol{n}\,, \quad {\rm w}_r = \mathbf{w}\cdot\boldsymbol{n}\,,$$

$${\rm u}_\theta = \mathbf{u}\cdot\mathbf{t}\,, \quad \boldsymbol{\tau}\,\boldsymbol{n} = \tau_{rr}\mathbf{e}_r + \tau_{r\theta}\mathbf{e}_\theta\,,$$

with $\mathbf{t} = \begin{pmatrix} -n_y \\ n_x \end{pmatrix} = \mathbf{e}_\theta$. By replacing the polar unknowns, we obtain the general RBC (4.13).

Conjecture 4.2. For $i = 1, 5$, let $\mathbf{X}_i$ be equal to:

$$\mathbf{X}_1 = -\frac{\frac{4}{3}\mu_{\rm fr} + {\rm k}_{\rm fr} + \alpha(M\alpha + M\mathcal{W}_{\rm P})}{\mathcal{W}_{\rm B} - \mathcal{W}_{\rm P}}\,\mathsf{s}_{\rm P}\,\mathcal{W}_{\rm B} + \frac{\frac{4}{3}\mu_{\rm fr} + {\rm k}_{\rm fr} + \alpha(M\alpha + M\mathcal{W}_{\rm B})}{\mathcal{W}_{\rm B} - \mathcal{W}_{\rm P}}\,\mathcal{W}_{\rm P}\,\mathsf{s}_{\rm B}\,,$$

$$\mathbf{X}_2 = \frac{\frac{4}{3}\mu_{\rm fr} + {\rm k}_{\rm fr} + \alpha(M\alpha + M\mathcal{W}_{\rm P})}{\mathcal{W}_{\rm B} - \mathcal{W}_{\rm P}}\,\mathsf{s}_{\rm P} - \frac{\frac{4}{3}\mu_{\rm fr} + {\rm k}_{\rm fr} + \alpha(M\alpha + M\mathcal{W}_{\rm B})}{\mathcal{W}_{\rm B} - \mathcal{W}_{\rm P}}\,\mathsf{s}_{\rm B}\,,$$

$$\mathbf{X}_3 = -\,\mathsf{s}_{\rm S}\,\mu_{\rm fr}\,,$$

$$\mathbf{X}_4 = \frac{M\left(\mathcal{W}_{\rm P} + \alpha\right)}{\mathcal{W}_{\rm B} - \mathcal{W}_{\rm P}}\mathsf{s}_{\rm P}\,\mathcal{W}_{\rm B} - \frac{M\left(\mathcal{W}_{\rm B} + \alpha\right)}{\mathcal{W}_{\rm B} - \mathcal{W}_{\rm P}}\,\mathsf{s}_{\rm B}\,\mathcal{W}_{\rm P}\,,$$

$$\mathbf{X}_5 = -\frac{M\left(\mathcal{W}_{\rm P} + \alpha\right)}{\mathcal{W}_{\rm B} - \mathcal{W}_{\rm P}}\mathsf{s}_{\rm P} + \frac{M\left(\mathcal{W}_{\rm B} + \alpha\right)}{\mathcal{W}_{\rm B} - \mathcal{W}_{\rm P}}\,\mathsf{s}_{\rm B}\,,$$

we propose the following RBC:

$$\begin{cases} \boldsymbol{\tau}\,\boldsymbol{n} + \big(\mathbf{X}_1(\mathbf{u}\cdot\boldsymbol{n}) + \mathbf{X}_2(\mathbf{w}\cdot\boldsymbol{n})\big)\,\boldsymbol{n} + \mathbf{X}_3(\mathbf{u}\cdot\mathbf{t})\,\mathbf{t} = 0\,, \\ \mathrm{p} + \mathbf{X}_4(\mathbf{u}\cdot\boldsymbol{n}) + \mathbf{X}_5(\mathbf{w}\cdot\boldsymbol{n}) = 0\,. \end{cases} \tag{4.13}$$

Remark 4.3. In [41], the development is done with the displacements instead of the velocities. We cannot compare with our formulations, because they also use different values for $\mathcal{W}_{\mathrm{P}}$, $\mathcal{W}_{\mathrm{B}}$, $\mathcal{W}_{\mathrm{S}}$. They obtain a general form for the boundary condition, which reads:

$$\begin{cases} \tau_{rr} + \tilde{\mathbf{X}}_1 \mathrm{u}_r + \tilde{\mathbf{X}}_2 \mathrm{w}_r = 0\,, \\ \tau_{r\theta} + \tilde{\mathbf{X}}_3 \mathrm{u}_\theta = 0\,, \\ \mathrm{p} + \tilde{\mathbf{X}}_2 \mathrm{u}_r + \tilde{\mathbf{X}}_5 \mathrm{w}_r = 0\,. \end{cases}$$

Remark 4.4. In the elastic case, the form of LK radiation boundary condition is (see [93, 20, 19]):

$$\boldsymbol{\tau}\,\boldsymbol{n} + \mathbf{Y}_1(\mathbf{u}\cdot\boldsymbol{n})\,\boldsymbol{n} + \mathbf{Y}_2(\mathbf{u}\cdot\mathbf{t})\,\mathbf{t} = 0\,.$$

In equation (4.13), without $\mathbf{w}$ and p, we retrieve the same form of the condition.

4.2 Reference solutions for the scattering of an impenetrable obstacle by a plane wave in a bounded domain using RBC

We consider the scattering of a solid circular obstacle immersed in an infinite porous medium by a plane wave, see Figure 4.1. We denote by $\mathbf{D}_{\mathfrak{a}}$ the obstacle whose radius is $\mathfrak{a}$. Its boundary is denoted by $\Gamma_n = \partial\mathbf{D}_{\mathfrak{a}}$. For the RBC solution, we put an artificial boundary at radius $\mathfrak{b}$, denoted by $\Gamma_{abs} = \partial\mathbf{D}_{\mathfrak{b}}$, with $\mathfrak{b} > \mathfrak{a}$, cf. Figure 4.1. We use notation $\mathfrak{U}$ to denote the ordered tuple ($\mathbf{u}$, $\mathbf{w}$, $\boldsymbol{\tau}$, p). We work in polar coordinates, with the variables r and θ.

Definition 4.5 (RBC solution). Considering a domain Ω with $\partial\Omega = \Gamma_{abs} \cup \Gamma_n$, and $\Gamma_{abs} \cap \Gamma_n = 0$. We define the RBC solution of the poroelastic equations on $\Omega_{\mathfrak{ab}}$ as follows:

$\mathfrak{U}$ solves the poroelastic equations (4.1) on Ω, the RBC equation (4.13) on Γ_{abs}, and one of the four boundary conditions from equation (1.20) on Γ_n.

For $i = 1, \ldots, 4$, we will discuss two solutions, an outgoing solution $\mathfrak{U}^{\infty-\mathrm{Ti}}$, that is defined on the whole exterior domain $\mathbb{R}^2 \setminus \mathbf{D}_{\mathfrak{a}}$ and $\mathfrak{U}^{\text{rbc-Ti}}$ the RBC solution (see Definition 4.5) defined on the annulus $\Omega_{\mathfrak{ab}} := \mathbf{D}_{\mathfrak{b}} \setminus \mathbf{D}_{\mathfrak{a}}$. The superscript '$Ti$' denotes the type of boundary condition, given in Section 1.4, equation (1.20), placed on the boundary of the obstacle, to describe its interaction with the incident wave.

The RBC solution $\mathfrak{U}^{\text{rbc-Ti}}$ solves the following problem

$$\begin{cases} \text{the poroelastic equations (4.1) on } \Omega_{\mathfrak{ab}}, \\ \text{boundary condition type i given by (1.20) on } r = \mathfrak{a}\,, \\ \tau_{rr} + \mathbf{X}_1 \mathrm{u}_r + \mathbf{X}_2 \mathrm{w}_r = 0\,, \\ \tau_{r\theta} + \mathbf{X}_3 \mathrm{u}_\theta = 0\,, \qquad\qquad \text{on } r = \mathfrak{b}\,. \\ \mathrm{p} + \mathbf{X}_4 \mathrm{u}_r + \mathbf{X}_5 \mathrm{w}_r = 0\,. \end{cases}$$

The outgoing solution $\mathfrak{U}^{\infty-\mathrm{Ti}}$ solves

$$\begin{cases} \text{the poroelastic equations (4.1) on } \mathbb{R}^2 \setminus \mathbf{D}_{\mathfrak{a}}, \\ \text{boundary condition type i given by (1.20) on } r = \mathfrak{a}\,, \\ \mathfrak{U}^{\infty-\mathrm{Ti}} \text{ is outgoing by Definition 2.3}\,. \end{cases}$$

We write the potentials corresponding to $\mathfrak{U}^{\text{rbc-Ti}}$ and $\mathfrak{U}^{\infty-\mathrm{Ti}}$ as

$$\chi_{\bullet}^{\text{rbc-Ti}} \quad \text{and} \quad \chi_{\bullet}^{\infty-\mathrm{Ti}}, \qquad i = 1, 2, 3, 4\,.$$

The potentials $\chi_\bullet^{\infty-\mathrm{Ti}}$ corresponding to $\mathfrak{U}^{\infty-\mathrm{Ti}}$ are given by

$$\begin{aligned}
\chi_{\mathrm{P}}^{\infty-\mathrm{Ti}}(r,\theta) &= \sum_{k\in\mathbb{Z}} a_k^\infty \,\mathrm{H}_k^{(1)}(\omega\,\mathsf{s}_{\mathrm{P}}\,r)\; e^{\mathrm{i}\,k\,\theta}\,,\\
\chi_{\mathrm{B}}^{\infty-\mathrm{Ti}}(r,\theta) &= \sum_{k\in\mathbb{Z}} b_k^\infty \,\mathrm{H}_k^{(1)}(\omega\,\mathsf{s}_{\mathrm{B}}\,r)\; e^{\mathrm{i}\,k\,\theta}\,,\\
\chi_{\mathrm{S}}^{\infty-\mathrm{Ti}}(r,\theta) &= \sum_{k\in\mathbb{Z}} c_k^\infty \,\mathrm{H}_k^{(1)}(\omega\,\mathsf{s}_{\mathrm{S}}\,r)\; e^{\mathrm{i}\,k\,\theta}\,,
\end{aligned} \tag{4.14}$$

where we have suppressed the dependence on the boundary condition for lighter exposition. The coefficients solve the linear system,

$$\mathbb{A}^{\infty-\mathrm{Ti}}\begin{pmatrix} a_k^\infty\\ b_k^\infty\\ c_k^\infty\end{pmatrix} = \mathfrak{f}_{\mathrm{Ti}}\,. \tag{4.15}$$

The components of $\mathbb{A}^{\infty-\mathrm{Ti}}$ and the right-hand-side $\mathfrak{f}_{\mathrm{Ti}}$ are determined using boundary conditions on $r=\mathfrak{a}$, as done in Section 2.3.

Let $\mathrm{H}_k^{(1)}(z)$ be the Hankel function of the first kind such as $\mathrm{H}_k^{(1)}(z) = \mathrm{J}_k(z) + \mathrm{i}\mathrm{Y}_k(z)$, and $\mathrm{H}_k^{(1)}(z)$ be the Hankel function of the second kind $\mathrm{H}_k^{(2)}(z) = \mathrm{J}_k(z) - \mathrm{i}\mathrm{Y}_k(z)$ with J_k and Y_k the first-order and second-order Bessel functions, see *e.g.* [103]. The function $\mathrm{H}_k^{(2)}$ corresponds to the incoming solution, hence the coefficients associated to $\mathrm{H}_k^{(2)}$ are the coefficients representing the incoming part of the solution. The more those coefficients are small, the more the solution is accurate.

The potentials $\chi_\bullet^{\text{rbc-Ti}}$ are given by

$$\begin{aligned}
\chi_{\mathrm{P}}^{\text{rbc-Ti}}(r,\theta) &= \sum_{k\in\mathbb{Z}} a_k \,\mathrm{H}_k^{(1)}(\omega\,\mathsf{s}_{\mathrm{P}}\,r)\; e^{\mathrm{i}\,k\,\theta} + \sum_{k\in\mathbb{Z}} \tilde{a}_k \,\mathrm{H}_k^{(2)}(\omega\,\mathsf{s}_{\mathrm{P}}\,r)\; e^{\mathrm{i}\,k\,\theta}\,,\\
\chi_{\mathrm{B}}^{\text{rbc-Ti}}(r,\theta) &= \sum_{k\in\mathbb{Z}} b_k \,\mathrm{H}_k^{(1)}(\omega\,\mathsf{s}_{\mathrm{B}}\,r)\; e^{\mathrm{i}\,k\,\theta} + \sum_{k\in\mathbb{Z}} \tilde{b}_k \,\mathrm{H}_k^{(2)}(\omega\,\mathsf{s}_{\mathrm{B}}\,r)\; e^{\mathrm{i}\,k\,\theta}\,,\\
\chi_{\mathrm{S}}^{\text{rbc-Ti}}(r,\theta) &= \sum_{k\in\mathbb{Z}} c_k \,\mathrm{H}_k^{(1)}(\omega\,\mathsf{s}_{\mathrm{S}}\,r)\; e^{\mathrm{i}\,k\,\theta} + \sum_{k\in\mathbb{Z}} \tilde{c}_k \,\mathrm{H}_k^{(2)}(\omega\,\mathsf{s}_{\mathrm{S}}\,r)\; e^{\mathrm{i}\,k\,\theta}\,.
\end{aligned} \tag{4.16}$$

The coefficients a_k, b_k, c_k, $\tilde{a}_k$, $\tilde{b}_k$, $\tilde{c}_k$ solve the linear system

$$\mathbb{A}^{\text{rbc-Ti}}\begin{pmatrix} a_k\\ b_k\\ c_k\\ \tilde{a}_k\\ \tilde{b}_k\\ \tilde{c}_k\end{pmatrix} = \begin{pmatrix} \mathfrak{f}_{\mathrm{Ti}}\\ 0\\ 0\\ 0\end{pmatrix}\,. \tag{4.17}$$

Note that in the above notation for the coefficients, we have suppressed the dependence on the type of boundary condition on Γ_n. The components of $\mathbb{A}^{\text{rbc-Ti}}$ (of size 6×6) and the right-hand-side are determined using boundary conditions on $r=\mathfrak{a}$ and $r=\mathfrak{b}$ as described in the following. In particular, the first three rows of the linear system are determined by one of the boundary condition imposed on Γ_n (the boundary of the obstacle) while the last three rows are determined by the RBC imposed on Γ_{abs} the artificial boundary.

Derivation of $\mathbb{A}^{\text{rbc-T3}}$: As an example, we list below the derivation associated to type 3 boundary condition imposed on the obstacle. Since the derivation of the first three lines are similar to that for $\mathbb{A}^{\infty-\mathrm{T3}}$ (see Section 2.3), we only list the derivation associated to the RBC, i.e., the last three lines. On $r=\mathfrak{b}$, we replace the unknowns using equation (4.2) and we apply condition (4.13) to obtain:

$$\begin{aligned}
&\frac{\mathrm{i}\,\mu_{\mathrm{fr}}}{\omega}\left(-\frac{2}{\mathsf{s}_{\mathrm{P}}^2}\,\partial_{r^2}\chi_{\mathrm{P}} - \frac{2}{\mathsf{s}_{\mathrm{B}}^2}\,\partial_{r^2}\chi_{\mathrm{B}} + \frac{2}{\mathsf{s}_{\mathrm{S}}^2}\left(\frac{1}{\mathfrak{b}}\partial_{r\theta} - \frac{1}{\mathfrak{b}^2}\partial_\theta\right)\chi_{\mathrm{S}}\right) + \mathrm{i}\,\omega\left(-\frac{2}{3}\mu_{\mathrm{fr}} + \mathrm{k}_{\mathrm{fr}} + \alpha^2 M\right)(\chi_{\mathrm{P}} + \chi_{\mathrm{B}}) + \mathrm{i}\,\omega\alpha\, M\mathcal{W}_{\mathrm{P}}\,\chi_{\mathrm{P}}\\
&+ \mathrm{i}\,\omega\alpha\, M\,\mathcal{W}_{\mathrm{B}}\,\chi_{\mathrm{B}} + \mathbf{X}_1\left(\frac{1}{\mathsf{s}_{\mathrm{P}}^2}\,\partial_r\chi_{\mathrm{P}} + \frac{1}{\mathsf{s}_{\mathrm{B}}^2}\,\partial_r\chi_{\mathrm{B}} - \frac{1}{\mathsf{s}_{\mathrm{S}}^2\,\mathfrak{b}}\,\partial_\theta\chi_{\mathrm{S}}\right) + \mathbf{X}_2\left(\frac{\mathcal{W}_{\mathrm{P}}}{\mathsf{s}_{\mathrm{P}}^2}\partial_r\chi_{\mathrm{P}} + \frac{\mathcal{W}_{\mathrm{B}}}{\mathsf{s}_{\mathrm{B}}^2}\partial_r\chi_{\mathrm{B}} + \frac{\rho_f\,\mu_{\mathrm{fr}}}{\det A\,\mathfrak{b}}\partial_\theta\chi_{\mathrm{S}}\right) = 0\,,
\end{aligned}$$

$$\mu_{\rm fr}\left(-\frac{2}{\mathsf{s}_{\rm P}^2}\left(\frac{1}{\mathfrak{b}}\partial_{r\theta}-\frac{1}{\mathfrak{b}^2}\partial_\theta\right)\chi_{\rm P}-\frac{2}{\mathsf{s}_{\rm B}^2}\left(\frac{1}{\mathfrak{b}}\partial_{r\theta}-\frac{1}{\mathfrak{b}^2}\partial_\theta\right)\chi_{\rm B}+\frac{1}{\mathsf{s}_{\rm S}^2}\left(\frac{1}{\mathfrak{b}^2}\partial_{\theta\theta}+\frac{1}{\mathfrak{b}}\partial_r-\partial_{r^2}\right)\chi_{\rm S}\right)$$
$$-\mathbf{X}_3\,\mathrm{i}\,\omega\left(\mathsf{s}_{\rm P}^{-2}\,\frac{1}{\mathfrak{b}}\partial_\theta\chi_{\rm P}+\mathsf{s}_{\rm B}^{-2}\,\frac{1}{\mathfrak{b}}\partial_\theta\chi_{\rm B}+\mathsf{s}_{\rm S}^{-2}\,\partial_r\chi_{\rm S}\right)=0\,,$$

and

$$-\,\mathrm{i}\,\omega\,M\left((\mathcal{W}_{\rm P}\;+\;\alpha)\chi_{\rm P}\;+\;(\mathcal{W}_{\rm B}\;+\;\alpha)\chi_{\rm B}\right)+\mathbf{X}_4\left(\frac{1}{\mathsf{s}_{\rm P}^2}\,\partial_r\chi_{\rm P}\;+\;\frac{1}{\mathsf{s}_{\rm B}^2}\,\partial_r\chi_{\rm B}\;-\;\frac{1}{\mathsf{s}_{\rm S}^2\,\mathfrak{b}}\,\partial_\theta\chi_{\rm S}\right)$$
$$+\,\mathbf{X}_5\left(\frac{\mathcal{W}_{\rm P}}{\mathsf{s}_{\rm P}^2}\partial_r\chi_{\rm P}\;+\;\frac{\mathcal{W}_{\rm B}}{\mathsf{s}_{\rm B}^2}\partial_r\chi_{\rm B}\;+\;\frac{\rho_f\,\mu_{\rm fr}}{\det A\,\mathfrak{b}}\partial_\theta\,\chi_{\rm S}\right)\;=0\,,$$

Below, for clarity, we keep the derivatives of the first and second Hankel functions, they can however be replaced with the identities given in Appendix A.1. The linear system is

$$\mathbb{A}_k^{\text{rbc-T3}}\begin{pmatrix}a_k\\ b_k\\ c_k\\ \tilde{a}_k\\ \tilde{b}_k\\ \tilde{c}_k\end{pmatrix}=\begin{pmatrix}\mathrm{i}\,\omega\,\mathrm{u}_r^{\rm pw}\\ \mathrm{i}\,\omega\,\mathrm{u}_\theta^{\rm pw}\\ \mathrm{p}^{\rm pw}\\ 0\\ 0\\ 0\end{pmatrix},$$

with components A_{ij},

$$A_{11}=\mathsf{s}_{\rm P}^{-1}\,\omega\,\mathrm{H}_k^{(1)'}(\omega\,\mathsf{s}_{\rm P}\,\mathfrak{a})\,,\quad A_{12}=\mathsf{s}_{\rm B}^{-1}\,\omega\,\mathrm{H}_k^{(1)'}(\omega\,\mathsf{s}_{\rm B}\,\mathfrak{a})\,,\quad A_{13}=-\,\mathsf{s}_{\rm S}^{-2}\,\frac{\mathrm{i}k}{\mathfrak{a}}\mathrm{H}_k^{(1)}(\omega\,\mathsf{s}_{\rm S}\,\mathfrak{a})\,,$$
$$A_{14}=\mathsf{s}_{\rm P}^{-1}\,\omega\,\mathrm{H}_k^{(2)'}(\omega\,\mathsf{s}_{\rm P}\,\mathfrak{a})\,,\quad A_{15}=\mathsf{s}_{\rm B}^{-1}\,\omega\,\mathrm{H}_k^{(2)'}(\omega\,\mathsf{s}_{\rm B}\,\mathfrak{a})\,,\quad A_{16}=-\,\mathsf{s}_{\rm S}^{-2}\,\frac{\mathrm{i}k}{\mathfrak{a}}\mathrm{H}_k^{(2)}(\omega\,\mathsf{s}_{\rm S}\,\mathfrak{a})\,,$$

$$A_{21}=\mathsf{s}_{\rm P}^{-2}\,\frac{\mathrm{i}k}{\mathfrak{a}}\mathrm{H}_k^{(1)}(\omega\,\mathsf{s}_{\rm P}\,\mathfrak{a})\,,\quad A_{22}=\mathsf{s}_{\rm B}^{-2}\,\frac{\mathrm{i}k}{\mathfrak{a}}\mathrm{H}_k^{(1)}(\omega\,\mathsf{s}_{\rm B}\,\mathfrak{a})\,,\quad A_{23}=\mathsf{s}_{\rm S}^{-1}\,\omega\,\mathrm{H}_k^{(1)'}(\omega\,\mathsf{s}_{\rm S}\,\mathfrak{a})\,,$$
$$A_{24}=\mathsf{s}_{\rm P}^{-2}\,\frac{\mathrm{i}k}{\mathfrak{a}}\mathrm{H}_k^{(2)}(\omega\,\mathsf{s}_{\rm P}\,\mathfrak{b})\,,\quad A_{25}=\mathsf{s}_{\rm B}^{-2}\,\frac{\mathrm{i}k}{\mathfrak{a}}\mathrm{H}_k^{(2)}(\omega\,\mathsf{s}_{\rm B}\,\mathfrak{a})\,,\quad A_{26}=\mathsf{s}_{\rm S}^{-1}\,\omega\,\mathrm{H}_k^{(2)'}(\omega\,\mathsf{s}_{\rm S}\,\mathfrak{a})\,,$$

$$A_{31}=-M\left(\mathcal{W}_{\rm P}\;+\;\alpha\right)\mathrm{H}_k^{(1)}(\omega\,\mathsf{s}_{\rm P}\,\mathfrak{a})\,,\quad A_{32}=-\,M\left(\mathcal{W}_{\rm B}\;+\;\alpha\right)\mathrm{H}_k^{(1)}(\omega\,\mathsf{s}_{\rm P}\,\mathfrak{a})\,,\quad A_{33}=\,0\,,$$
$$A_{34}=-M\left(\mathcal{W}_{\rm P}\;+\;\alpha\right)\mathrm{H}_k^{(2)}(\omega\,\mathsf{s}_{\rm P}\,\mathfrak{a})\,,\quad A_{35}=-\,M\left(\mathcal{W}_{\rm B}\;+\;\alpha\right)\mathrm{H}_k^{(2)}(\omega\,\mathsf{s}_{\rm P}\,\mathfrak{a})\,,\quad A_{36}=\,0\,,$$

$$A_{41}=\,-\,2\,\mathrm{i}\,\mu_{\rm fr}\,\omega\,\mathrm{H}_k^{(1)''}(\omega\,\mathsf{s}_{\rm P}\,\mathfrak{b})\;+\;\mathrm{i}\omega\left(-\frac{2}{3}\mu_{\rm fr}+\mathrm{k}_{\rm fr}+M\,\alpha(\alpha+\mathcal{W}_{\rm P})\right)\mathrm{H}_k^{(1)}(\omega\,\mathsf{s}_{\rm P}\,\mathfrak{b})$$
$$+\;\frac{\boldsymbol{X}_1\,\omega}{\mathsf{s}_{\rm P}}\mathrm{H}_k^{(1)'}(\omega\,\mathsf{s}_{\rm P}\,\mathfrak{b})+\;\frac{\boldsymbol{X}_2\,\omega\mathcal{W}_{\rm P}}{\mathsf{s}_{\rm P}}\,\mathrm{H}_k^{(1)'}(\omega\,\mathsf{s}_{\rm P}\,\mathfrak{b})\,,$$
$$A_{42}=\,-\,2\,\mathrm{i}\,\mu_{\rm fr}\,\omega\,\mathrm{H}_k^{(1)''}(\omega\,\mathsf{s}_{\rm B}\,\mathfrak{b})\;+\;\mathrm{i}\omega\left(-\frac{2}{3}\mu_{\rm fr}+\mathrm{k}_{\rm fr}+M\,\alpha(\alpha+\mathcal{W}_{\rm B})\right)\mathrm{H}_k^{(1)}(\omega\,\mathsf{s}_{\rm B}\,\mathfrak{b})$$
$$+\;\frac{\boldsymbol{X}_1\,\omega}{\mathsf{s}_{\rm B}}\mathrm{H}_k^{(1)'}(\omega\,\mathsf{s}_{\rm B}\,\mathfrak{b})+\;\frac{\boldsymbol{X}_2\,\omega\mathcal{W}_{\rm B}}{\mathsf{s}_{\rm B}}\,\mathrm{H}_k^{(1)'}(\omega\,\mathsf{s}_{\rm B}\,\mathfrak{b})\,,$$
$$A_{43}=\,-\,\frac{2\,\mu_{\rm fr}\,k}{\mathsf{s}_{\rm S}\,\mathfrak{b}}\,\mathrm{H}_k^{(1)'}(\omega\,\mathsf{s}_{\rm S}\,\mathfrak{b})\;+\;\frac{2\,\mu_{\rm fr}\,k}{\omega\mathsf{s}_{\rm S}^2\,\mathfrak{b}^2}\,\mathrm{H}_k^{(1)}(\omega\,\mathsf{s}_{\rm S}\,\mathfrak{b})\;-\;\frac{\boldsymbol{X}_1\,\mathrm{i}\,k}{\mathsf{s}_{\rm S}^2\,\mathfrak{b}}\,\mathrm{H}_k^{(1)}(\omega\,\mathsf{s}_{\rm S}\,\mathfrak{b})\;+\;\frac{\boldsymbol{X}_2\,\rho_f\,\mu_{\rm fr}\,\mathrm{i}\,k}{\mathrm{detA}\,\mathfrak{b}}\,\mathrm{H}_k^{(1)}(\omega\,\mathsf{s}_{\rm S}\,\mathfrak{b})\,,$$

$$A_{44} = -2\,\mathrm{i}\,\mu_{\rm fr}\,\omega\,\mathrm{H}_k^{(2)''}(\omega\,\mathsf{s}_{\rm P}\,\mathfrak{b}) + \mathrm{i}\omega\left(-\frac{2}{3}\mu_{\rm fr} + \mathrm{k}_{\rm fr} + M\,\alpha(\alpha+\mathcal{W}_{\rm P})\right)\mathrm{H}_k^{(2)}(\omega\,\mathsf{s}_{\rm P}\,\mathfrak{b}) + \frac{\boldsymbol{X}_1\,\omega}{\mathsf{s}_{\rm P}}\mathrm{H}_k^{(2)'}(\omega\,\mathsf{s}_{\rm P}\,\mathfrak{b}) + \frac{\boldsymbol{X}_2\,\omega\mathcal{W}_{\rm P}}{\mathsf{s}_{\rm P}}\,\mathrm{H}_k^{(2)'}(\omega\,\mathsf{s}_{\rm P}\,\mathfrak{b}),$$

$$A_{45} = -2\,\mathrm{i}\,\mu_{\rm fr}\,\omega\,\mathrm{H}_k^{(2)''}(\omega\,\mathsf{s}_{\rm B}\,\mathfrak{b}) + \mathrm{i}\omega\left(-\frac{2}{3}\mu_{\rm fr} + \mathrm{k}_{\rm fr} + M\,\alpha(\alpha+\mathcal{W}_{\rm B})\right)\mathrm{H}_k^{(2)}(\omega\,\mathsf{s}_{\rm B}\,\mathfrak{b}) + \frac{\boldsymbol{X}_1\,\omega}{\mathsf{s}_{\rm B}}\mathrm{H}_k^{(2)'}(\omega\,\mathsf{s}_{\rm B}\,\mathfrak{b}) + \frac{\boldsymbol{X}_2\,\omega\mathcal{W}_{\rm B}}{\mathsf{s}_{\rm B}}\,\mathrm{H}_k^{(2)'}(\omega\,\mathsf{s}_{\rm B}\,\mathfrak{b}),$$

$$A_{46} = -\frac{2\,\mu_{\rm fr}\,k}{\mathsf{s}_{\rm S}\,\mathfrak{b}}\,\mathrm{H}_k^{(2)'}(\omega\,\mathsf{s}_{\rm S}\,\mathfrak{b}) + \frac{2\,\mu_{\rm fr}\,k}{\omega\mathsf{s}_{\rm S}^2\,\mathfrak{b}^2}\,\mathrm{H}_k^{(2)}(\omega\,\mathsf{s}_{\rm S}\,\mathfrak{b}) - \frac{\boldsymbol{X}_1\,\mathrm{i}\,k}{\mathsf{s}_{\rm S}^2\,\mathfrak{b}}\,\mathrm{H}_k^{(2)}(\omega\,\mathsf{s}_{\rm S}\,\mathfrak{b}) + \frac{\boldsymbol{X}_2\,\rho_f\,\mu_{\rm fr}\,\mathrm{i}\,k}{\mathrm{detA}\,\mathfrak{b}}\,\mathrm{H}_k^{(2)}(\omega\,\mathsf{s}_{\rm S}\,\mathfrak{b}),$$

$$A_{51} = -\frac{2\,\mu_{\rm fr}\,\omega\,\mathrm{i}\,k}{\mathsf{s}_{\rm P}\,\mathfrak{b}}\,\mathrm{H}_k^{(1)'}(\omega\,\mathsf{s}_{\rm P}\,\mathfrak{b}) + \frac{2\,\mu_{\rm fr}\,\mathrm{i}\,k}{\mathsf{s}_{\rm P}^2\,\mathfrak{b}^2}\,\mathrm{H}_k^{(1)}(\omega\,\mathsf{s}_{\rm P}\,\mathfrak{b}) + \frac{\boldsymbol{X}_3\,\omega\,k}{\mathsf{s}_{\rm P}^2\mathfrak{b}}\mathrm{H}_k^{(1)}(\omega\,\mathsf{s}_{\rm P}\,\mathfrak{b}),$$

$$A_{52} = -\frac{2\,\mu_{\rm fr}\,\omega\,\mathrm{i}\,k}{\mathsf{s}_{\rm B}\,\mathfrak{b}}\,\mathrm{H}_k^{(1)'}(\omega\,\mathsf{s}_{\rm B}\,\mathfrak{b}) + \frac{2\,\mu_{\rm fr}\,\mathrm{i}\,k}{\mathsf{s}_{\rm B}^2\,\mathfrak{b}^2}\,\mathrm{H}_k^{(1)}(\omega\,\mathsf{s}_{\rm B}\,\mathfrak{b}) + \frac{\boldsymbol{X}_3\,\omega\,k}{\mathsf{s}_{\rm B}^2\mathfrak{b}}\mathrm{H}_k^{(1)}(\omega\,\mathsf{s}_{\rm B}\,\mathfrak{b}),$$

$$A_{53} = -\frac{k^2\,\mu_{\rm fr}}{\mathsf{s}_{\rm S}^2\,\mathfrak{b}^2}\,\mathrm{H}_k^{(1)}(\omega\,\mathsf{s}_{\rm S}\,\mathfrak{b}) + \frac{\omega\,\mu_{\rm fr}}{\mathsf{s}_{\rm S}\,\mathfrak{b}}\,\mathrm{H}_k^{(1)'}(\omega\,\mathsf{s}_{\rm S}\,\mathfrak{b}) - \omega^2\,\mu_{\rm fr}\,\mathrm{H}_k^{(1)''}(\omega\,\mathsf{s}_{\rm S}\,\mathfrak{b}) - \frac{\boldsymbol{X}_3\,\omega^2\,\mathrm{i}}{\mathsf{s}_{\rm S}}\,\mathrm{H}_k^{(1)'}(\omega\,\mathsf{s}_{\rm S}\,\mathfrak{b}),$$

$$A_{54} = -\frac{2\,\mu_{\rm fr}\,\omega\,\mathrm{i}\,k}{\mathsf{s}_{\rm P}\,\mathfrak{b}}\,\mathrm{H}_k^{(2)'}(\omega\,\mathsf{s}_{\rm P}\,\mathfrak{b}) + \frac{2\,\mu_{\rm fr}\,\mathrm{i}\,k}{\mathsf{s}_{\rm P}^2\,\mathfrak{b}^2}\,\mathrm{H}_k^{(2)}(\omega\,\mathsf{s}_{\rm P}\,\mathfrak{b}) + \frac{\boldsymbol{X}_3\,\omega\,k}{\mathsf{s}_{\rm P}^2\mathfrak{b}}\mathrm{H}_k^{(2)}(\omega\,\mathsf{s}_{\rm P}\,\mathfrak{b}),$$

$$A_{55} = -\frac{2\,\mu_{\rm fr}\,\omega\,\mathrm{i}\,k}{\mathsf{s}_{\rm B}\,\mathfrak{b}}\,\mathrm{H}_k^{(2)'}(\omega\,\mathsf{s}_{\rm B}\,\mathfrak{b}) + \frac{2\,\mu_{\rm fr}\,\mathrm{i}\,k}{\mathsf{s}_{\rm B}^2\,\mathfrak{b}^2}\,\mathrm{H}_k^{(2)}(\omega\,\mathsf{s}_{\rm B}\,\mathfrak{b}) + \frac{\boldsymbol{X}_3\,\omega\,k}{\mathsf{s}_{\rm B}^2\mathfrak{b}}\mathrm{H}_k^{(2)}(\omega\,\mathsf{s}_{\rm B}\,\mathfrak{b}),$$

$$A_{56} = -\frac{k^2\,\mu_{\rm fr}}{\mathsf{s}_{\rm S}^2\,\mathfrak{b}^2}\,\mathrm{H}_k^{(2)}(\omega\,\mathsf{s}_{\rm S}\,\mathfrak{b}) + \frac{\omega}{\mathsf{s}_{\rm S}\,\mathfrak{b}}\,\mathrm{H}_k^{(2)'}(\omega\,\mathsf{s}_{\rm S}\,\mathfrak{b}) - \omega^2\,\mu_{\rm fr}\,\mathrm{H}_k^{(2)''}(\omega\,\mathsf{s}_{\rm S}\,\mathfrak{b}) - \frac{\boldsymbol{X}_3\,\omega^2\,\mathrm{i}}{\mathsf{s}_{\rm S}}\,\mathrm{H}_k^{(2)'}(\omega\,\mathsf{s}_{\rm S}\,\mathfrak{b}),$$

and

$$A_{61} = -\mathrm{i}\,\omega\,M\,(\mathcal{W}_{\rm P}+\alpha)\mathrm{H}_k^{(1)}(\omega\,\mathsf{s}_{\rm P}\,\mathfrak{b}) + \frac{\boldsymbol{X}_4\,\omega}{\mathsf{s}_{\rm P}}\mathrm{H}_k^{(1)'}(\omega\,\mathsf{s}_{\rm P}\,\mathfrak{b}) + \frac{\boldsymbol{X}_5\,\omega\,\mathcal{W}_{\rm P}}{\mathsf{s}_{\rm P}}\,\mathrm{H}_k^{(1)'}(\omega\,\mathsf{s}_{\rm P}\,\mathfrak{b}),$$

$$A_{62} = -\mathrm{i}\,\omega\,M\,(\mathcal{W}_{\rm B}+\alpha)\mathrm{H}_k^{(1)}(\omega\,\mathsf{s}_{\rm B}\,\mathfrak{b}) + \frac{\boldsymbol{X}_4\,\omega}{\mathsf{s}_{\rm B}}\mathrm{H}_k^{(1)'}(\omega\,\mathsf{s}_{\rm B}\,\mathfrak{b}) + \frac{\boldsymbol{X}_5\,\omega\,\mathcal{W}_{\rm B}}{\mathsf{s}_{\rm B}}\,\mathrm{H}_k^{(1)'}(\omega\,\mathsf{s}_{\rm B}\,\mathfrak{b}),$$

$$A_{63} = -\frac{\boldsymbol{X}_4\,\mathrm{i}\,k}{\mathsf{s}_{\rm S}^2\,\mathfrak{b}}\,\mathrm{H}_k^{(1)}(\omega\,\mathsf{s}_{\rm S}\,\mathfrak{b}) + \frac{\boldsymbol{X}_5\,\rho_f\,\mu_{\rm fr}\,\mathrm{i}\,k}{\mathrm{detA}\,\mathfrak{b}}\,\mathrm{H}_k^{(1)}(\omega\,\mathsf{s}_{\rm S}\,\mathfrak{b}),$$

$$A_{64} = -\mathrm{i}\,\omega\,M\,(\mathcal{W}_{\rm P}+\alpha)\mathrm{H}_k^{(2)}(\omega\,\mathsf{s}_{\rm P}\,\mathfrak{b}) + \frac{\boldsymbol{X}_4\,\omega}{\mathsf{s}_{\rm P}}\mathrm{H}_k^{(2)'}(\omega\,\mathsf{s}_{\rm P}\,\mathfrak{b}) + \frac{\boldsymbol{X}_5\,\omega\,\mathcal{W}_{\rm P}}{\mathsf{s}_{\rm P}}\,\mathrm{H}_k^{(2)'}(\omega\,\mathsf{s}_{\rm P}\,\mathfrak{b}),$$

$$A_{65} = -\mathrm{i}\,\omega\,M\,(\mathcal{W}_{\rm B}+\alpha)\mathrm{H}_k^{(2)}(\omega\,\mathsf{s}_{\rm B}\,\mathfrak{b}) + \frac{\boldsymbol{X}_4\,\omega}{\mathsf{s}_{\rm B}}\mathrm{H}_k^{(2)'}(\omega\,\mathsf{s}_{\rm B}\,\mathfrak{b}) + \frac{\boldsymbol{X}_5\,\omega\,\mathcal{W}_{\rm B}}{\mathsf{s}_{\rm B}}\,\mathrm{H}_k^{(2)'}(\omega\,\mathsf{s}_{\rm B}\,\mathfrak{b}),$$

$$A_{66} = -\frac{\boldsymbol{X}_4\,\mathrm{i}\,k}{\mathsf{s}_{\rm S}^2\,\mathfrak{b}}\,\mathrm{H}_k^{(2)}(\omega\,\mathsf{s}_{\rm S}\,\mathfrak{b}) + \frac{\boldsymbol{X}_5\,\rho_f\,\mu_{\rm fr}\,\mathrm{i}\,k}{\mathrm{detA}\,\mathfrak{b}}\,\mathrm{H}_k^{(2)}(\omega\,\mathsf{s}_{\rm S}\,\mathfrak{b}).$$

4.3 Performance assessment of the radiation boundary condition in the setting of an obstacle scattering

In the previous section, we have built the reference outgoing solution $\mathfrak{U}^{\infty-\mathrm{Ti}}$ and the RBC solution $\mathfrak{U}^{\text{rbc-Ti}}$ for the scattering of a plane wave by an impenetrable circular obstacle. From now on, we denote by $\mathfrak{U}^{\infty-\mathrm{Ti}}$ the restriction of $\mathfrak{U}^{\infty-\mathrm{Ti}}$ on $\Omega_{\mathfrak{a}\mathfrak{b}}$. In this section, we study the robustness of the RBC by comparing $\mathfrak{U}^{\infty-\mathrm{Ti}}$ with $\mathfrak{U}^{\text{rbc-Ti}}$.

The domain is an annulus described in Figure 4.1 composed of sandstone (see Table 3.1). The boundary of the obstacle $\{r=\mathfrak{a}\}$ is denoted by Γ_n. We set an artificial boundary at radius $\mathfrak{b}$. We will consider the scattering of the

three porous plane waves of type (P,B,S) by the obstacle, for boundary condition of type 1 ("Neumann-like") and 3 ("Dirichlet-like") on $\mathfrak{a}$. In all of our numerical experiments, the radius of the obstacle is kept equal to one meter, i.e., $\mathfrak{a} = 1$m, while the value of the viscosity in the material η, of the frequency f and of the exterior radius $\mathfrak{b}$ will vary.

Recall that the solution $\mathfrak{U}^{\text{rbc-Ti}}$ is represented by the series of coefficients a_k, b_k, c_k, $\tilde{a}_k$, $\tilde{b}_k$, $\tilde{c}_k$, and the solution $\mathfrak{U}^{\infty-\text{Ti}}$ by the coefficients a_k^∞, b_k^∞, c_k^∞ (see equations (4.14)-(4.17)). In the numerical tests, the Hankel functions are infinite series truncated to the first N terms of the series, with $N \geq 2\mathbf{k}\mathfrak{a} + 1$ (cf. [120]), where $\mathbf{k} = \max(k_{\text{P}}, k_{\text{B}}, k_{\text{S}})$.

The comparisons are carried out in terms of the following quantities:

- Comparison mode by mode of a_k^∞, b_k^∞, c_k^∞ with a_k, b_k, c_k. Module of $\tilde{a}_k$, $\tilde{b}_k$, $\tilde{c}_k$. As the function $\text{H}_k^{(2)}$ corresponds to the incoming solution, hence the coefficients $\tilde{a}_k$, $\tilde{b}_k$, $\tilde{c}_k$ represent the incoming part of the solution, that we seek to be small to have an accurate solution.

- Errors on the coefficients:

$$e^2_{\text{coeff}} = \frac{\sum_{k=-N}^{k=N} \left((a_k^\infty - a_k)^2 + (b_k^\infty - b_k)^2 + (c_k^\infty - c_k)^2 + \tilde{a_k}^2 + \tilde{b_k}^2 + \tilde{c_k}^2 \right)}{\sum_{k=-N}^{k=N} (a_k^{\infty 2} + b_k^{\infty 2} + c_k^{\infty 2})}, \qquad e^2_{\text{ref}} = \sum_{k=-N}^{k=N} \left(\tilde{a_k}^2 + \tilde{b_k}^2 + \tilde{c_k}^2 \right). \tag{4.20}$$

- Relative L^2 error of u_x:

$$e_h(\text{u}_x^{\text{rbc -Ti}}) = \frac{||\text{u}_x^{\text{rbc -Ti}} - \text{u}_x^{\infty-\text{Ti}}||_2}{||\text{u}_x^{\infty-\text{Ti}}||_2}. \tag{4.21}$$

  The L^2 norm is theoretically equal to

$$||\text{u}_x^{\text{rbc -Ti}} - \text{u}_x^{\infty-\text{Ti}}||_2 = \left(\int_{\Omega_{\mathfrak{a}\mathfrak{b}}} |\text{u}_x^{\text{rbc -Ti}} - \text{u}_x^{\infty-\text{Ti}}|^2 \right)^{\frac{1}{2}},$$

  In practice, we approximate the above equation by

$$||\text{u}_x^{\text{rbc -Ti}} - \text{u}_x^{\infty-\text{Ti}}||_2 = \left(\sum_{K \in \mathcal{T}_h} \int_K |\text{u}_x^{\text{rbc -Ti}} - \text{u}_x^{\infty-\text{Ti}}|^2 \right)^{\frac{1}{2}},$$

  where we have defined a mesh $\mathcal{T}_h$ of $\Omega_{\mathfrak{a}\mathfrak{b}}$ with N_{elem} elements K which are triangles. We define on each element the 10 Lagrange degrees of freedom corresponding to an interpolation of degree 3 on a triangle, and compute the norm using this interpolation. We focus on the component u_x, but the other components have the same behaviour.

We will study the effect of different factors on the performance of the RBC: the presence of viscosity, the size of the exterior radius $\mathfrak{b}$. the frequency, the type of incident-wave (P,B,S), the type of boundary condition on the interior radius $\mathfrak{a}$. We will focus on type 1 ("Neumann-like") and type 3 ("Dirichlet-like").

In the following, we first present in Section 4.3.1 the modulus of the coefficients for $\mathfrak{b} = 10$m and $f = 1$kHz, for many configurations. Then in Section 4.3.2, we compare the RBC solution with the outgoing solution potential by potential by using a decomposition of the potentials. In Section 4.3.3, we investigate the influence of the size of the domain used for the RBC solution by varying the value of $\mathfrak{b}$. Afterwards, in order to highlight the influence of the viscosity on the performance of the RBC, we compare the RBC solution with the outgoing solution for a material by varying only its viscosity in Section 4.3.4. Finally, in Section 4.3.5 the performance of the RBC is studied for a range of frequencies.

4.3.1 Comparison between the coefficients of outgoing solution and RBC solution

In the following, we display the values of the coefficients series a_k^∞, b_k^∞, c_k^∞ and a_k, b_k c_k, $\tilde{a_k}$, $\tilde{b_k}$, $\tilde{c_k}$ for several configurations:

- Scattering of a P, B, S incident plane wave for sandstone with viscosity $\eta = 10^{-3}$ Pa.s^{-1} and boundary condition of type 1 ("Neumann-like") on $r = \mathfrak{a}$ (*cf.* (1.20a)), respectively in figures 4.2, 4.3, 4.4 for exterior radius $\mathfrak{b} = 10$m.

- Scattering of a P, B, S incident plane wave for sandstone with viscosity $\eta = 10^{-3}$ Pa.s^{-1} and boundary condition of type 3 ("Dirichlet-like") on $r = \mathfrak{a}$ (*cf.* (1.20c)), respectively in figures 4.5, 4.6, 4.7, for exterior radius $\mathfrak{b} = 10$m.
- Scattering of a P, B, S incident plane wave for sandstone with no viscosity $\eta = 0$ Pa.s^{-1} and boundary condition of type 1 ("Neumann-like") on $r = \mathfrak{a}$ (*cf.* (1.20a)), respectively in figures 4.8, 4.9, 4.10 for exterior radius $\mathfrak{b} = 10$m.
- Scattering of a P, B, S incident plane wave for sandstone with no viscosity $\eta = 0$ Pa.s^{-1} and boundary condition of type 3 ("Dirichlet-like") on $r = \mathfrak{a}$ (*cf.* (1.20c)), respectively in figures 4.11, 4.12, 4.13, for exterior radius $\mathfrak{b} = 10$m.

Remark 4.6. Even though the value $\mathfrak{b} = 10$m might seem high compared to the size of $\mathfrak{a}$, we have for the experiments: $k_P\,\mathfrak{b} = 14.76$, $k_B\,\mathfrak{b} = 61.48$, $k_S\,\mathfrak{b} = 26.25$. This means that for the fastest wave, we have $\frac{k_P\,\mathfrak{b}}{2\,\pi} = 2.35$ wavelengths for 10m, which is low. The rule of thumb recommends indeed to set the boundary at least at two wavelengths of the obstacle.

From Figs. 4.2 to 4.13, we observe the following. The coefficients a_k, b_k, c_k, obtained by solving the system with radiation boundaries seem to approximate well the coefficients obtained for the exact solution. For the three incident waves, the coefficients $\tilde{a}_k$ and $\tilde{b}_k$ are close to zero. The coefficients $\tilde{c}_k$ are greater than $\tilde{a}_k$ and $\tilde{b}_k$ in all cases. when the incident plane wave is a B-wave, the values of the coefficients b_k, b_k^∞ are larger than the other coefficients (Figs. 4.3 and 4.6), however, the reflected coefficient $\tilde{b}_k$ remains low. The value of $\tilde{c}_k$ is always at least 10% of the coefficients a_k, b_k, c_k, it can even be of the same order or higher than them (see Figs. 4.10 and 4.13). This means that the reflection of the S-wave has more influence on the error of the radiation boundary condition. For most cases, the behaviour of $\tilde{c}_k$ is related to the one of c_k, *e.g.* Figs. 4.2-4.7, however, in case of an incident B-wave, it seems to be linked to b_k (Figure 4.12). Finally, as in Figures. 4.7, 4.9 and 4.13, the behaviour of $\tilde{c}_k$ seems to be a combination of the behaviour of b_k and c_k. By only studying the coefficients, we cannot observe a significant difference of behaviour with or without viscosity in the material. The errors on the radiation boundary condition is hence mainly due to the conversion of S-wave to S-waves and of B-wave to S-waves.

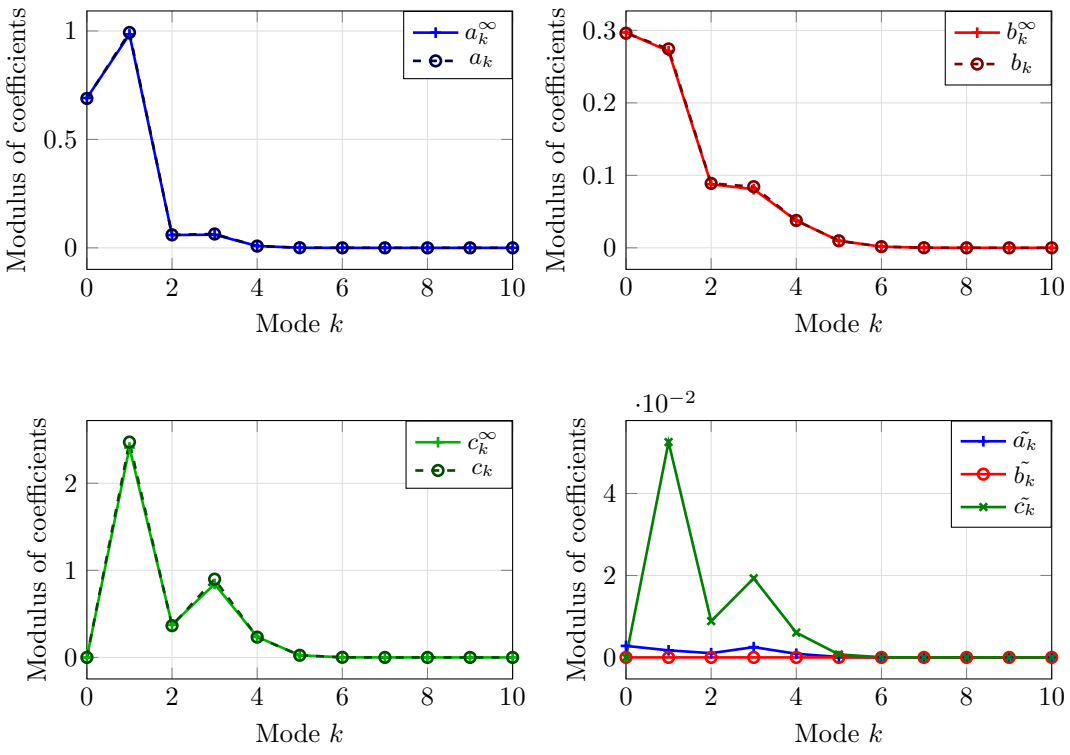

Figure 4.2: Obstacle scattering of an incident plane P-wave type 1 ("Neumann-like" (1.20a)) for the boundary condition on $r = \mathfrak{a}$ at a frequency $f = 1$kHz for a sandstone medium with viscosity $\eta = 10^{-3}$ Pa.s^{-1}. The domain is an annulus with interior radius $\mathfrak{a} = 1$m and exterior radius $\mathfrak{b} = 10$m. The coefficients with ∞ superscript correspond to the exact outgoing solution. a_k^∞ —+—, a_k - -o- -, and $\tilde{a}_k$ —+— are the coefficients corresponding to the potential of the P-wave, b_k^∞ —+—, b_k - -o- -, and $\tilde{b}_k$ —o— the coefficients corresponding to the potential of the B-wave, and c_k^∞ —+—, c_k - -o- -, and $\tilde{c}_k$ —×— the coefficients corresponding to the potential of the S-wave (see (4.16)).

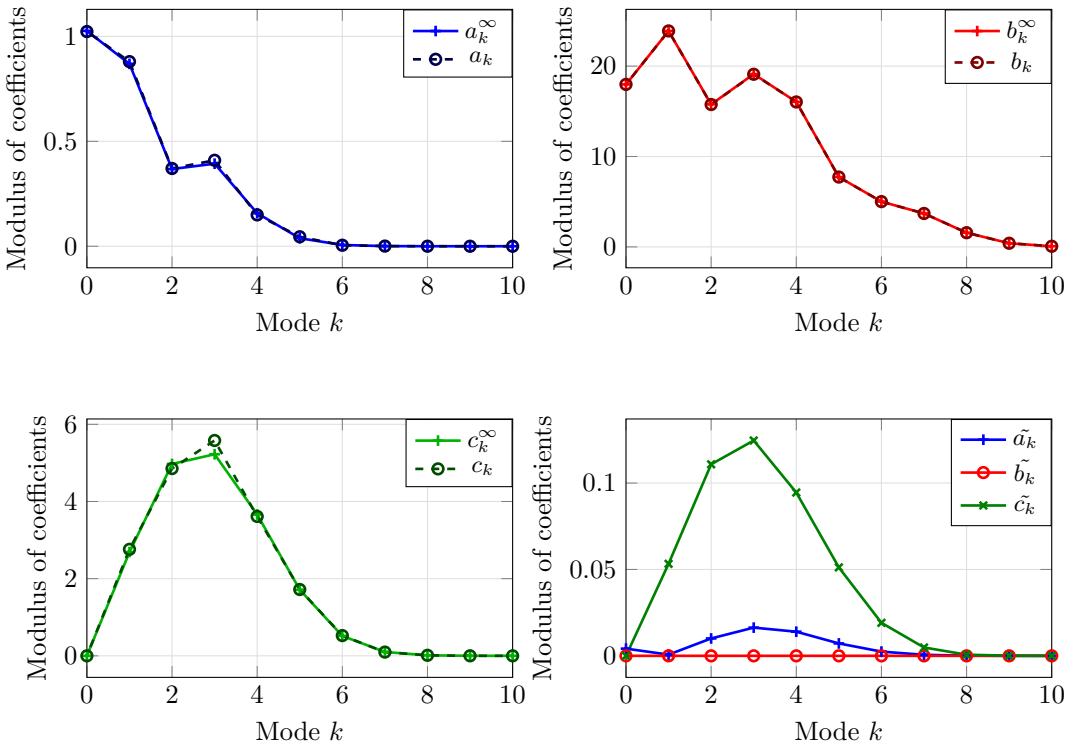

Figure 4.3: Obstacle scattering of an incident plane B-wave with the type 1 ("Neumann-like" (1.20a)) for the boundary condition on $r = \mathfrak{a}$ at a frequency $f = 1\text{kHz}$ for a sandstone medium with viscosity $\eta = 10^{-3}$ Pa.s^{-1}. The domain is an annulus with interior radius $\mathfrak{a} = 1\text{m}$ and exterior radius $\mathfrak{b} = 10\text{m}$. The coefficients with ∞ superscript correspond to the exact outgoing solution. a_k^∞ —, a_k - o -, and $\tilde{a}_k$ — are the coefficients corresponding to the potential of the P-wave, b_k^∞ —, b_k - o -, and $\tilde{b}_k$ — the coefficients corresponding to the potential of the B-wave, and c_k^∞ —, c_k - o -, and $\tilde{c}_k$ — the coefficients corresponding to the potential of the S-wave (see (4.16)).

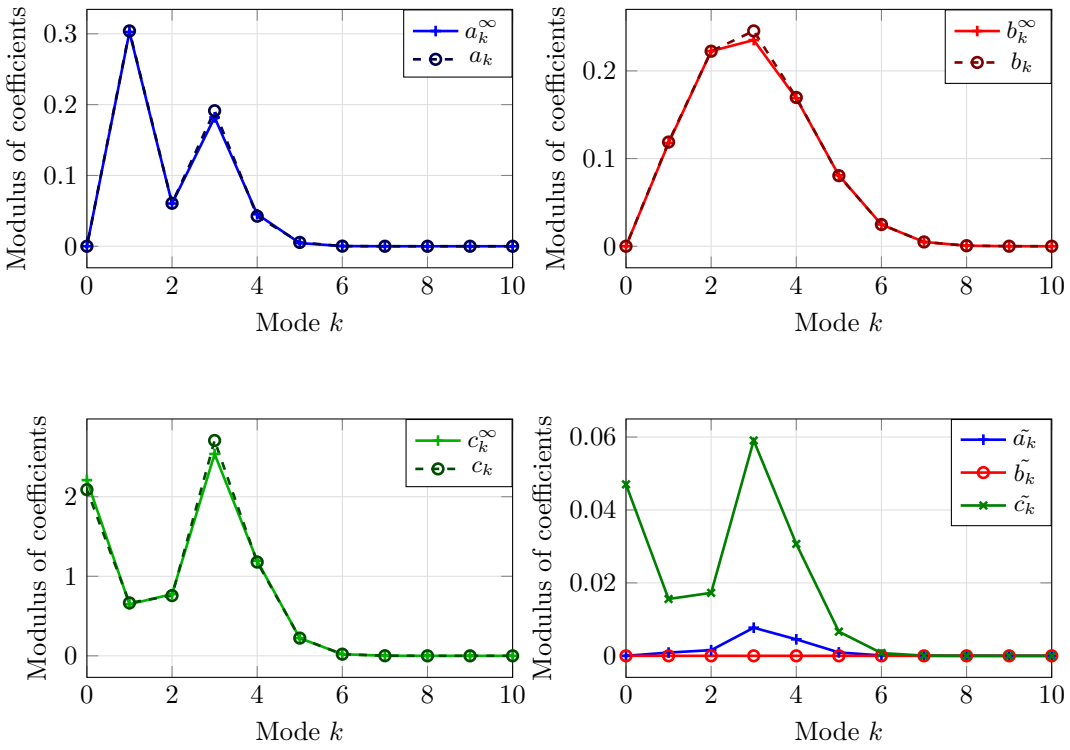

Figure 4.4: Obstacle scattering of an incident plane S-wave with the type 1 ("Neumann-like" (1.20a)) for the boundary condition on $r = \mathfrak{a}$. at a frequency $f = 1$kHz for a sandstone medium with viscosity $\eta = 10^{-3}$ Pa.s^{-1}. The domain is an annulus with interior radius $\mathfrak{a} = 1$m and exterior radius $\mathfrak{b} = 10$m. The coefficients with ∞ superscript correspond to the exact outgoing solution. a_k^∞ —, a_k - ⊙ -, and $\tilde{a}_k$ — are the coefficients corresponding to the potential of the P-wave, b_k^∞ —, b_k - ⊙ -, and $\tilde{b}_k$ — the coefficients corresponding to the potential of the B-wave, and c_k^∞ —, c_k - ⊙ -, and $\tilde{c}_k$ — coefficients corresponding to the potential of the S-wave (see (4.16)).

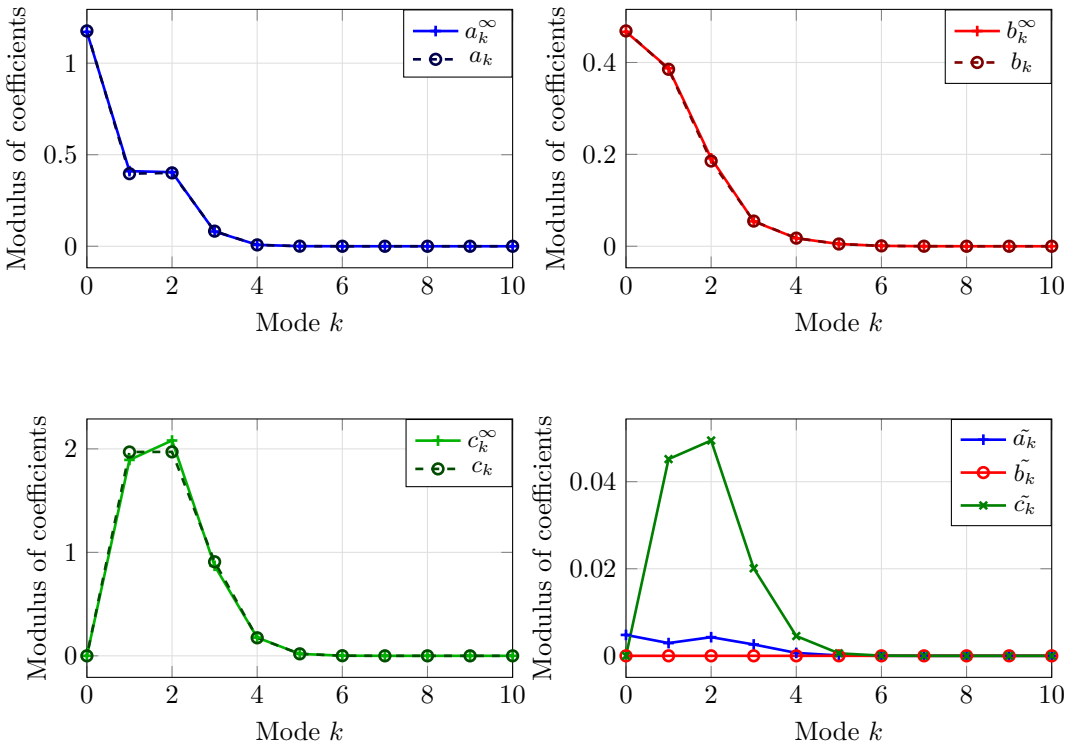

Figure 4.5: Obstacle scattering of an incident plane P-wave type 3 ("Dirichlet-like" (1.20c)) for the boundary condition on $r = \mathfrak{a}$ at a frequency $f = 1$kHz for a sandstone medium with viscosity $\eta = 10^{-3}$ Pa.s^{-1}. The domain is an annulus with interior radius $\mathfrak{a} = 1$m and exterior radius $\mathfrak{b} = 10$m. The coefficients with ∞ superscript correspond to the exact outgoing solution. a_k^∞ —+—, a_k - -o- - , and $\tilde{a}_k$ —+— are the coefficients corresponding to the potential of the P-wave, b_k^∞ —+—, b_k - -o- - , and $\tilde{b}_k$ —o— the coefficients corresponding to the potential of the B-wave, and c_k^∞ —+—, c_k - -o- - , and $\tilde{c}_k$ —x— the coefficients corresponding to the potential of the S-wave (see (4.16)).

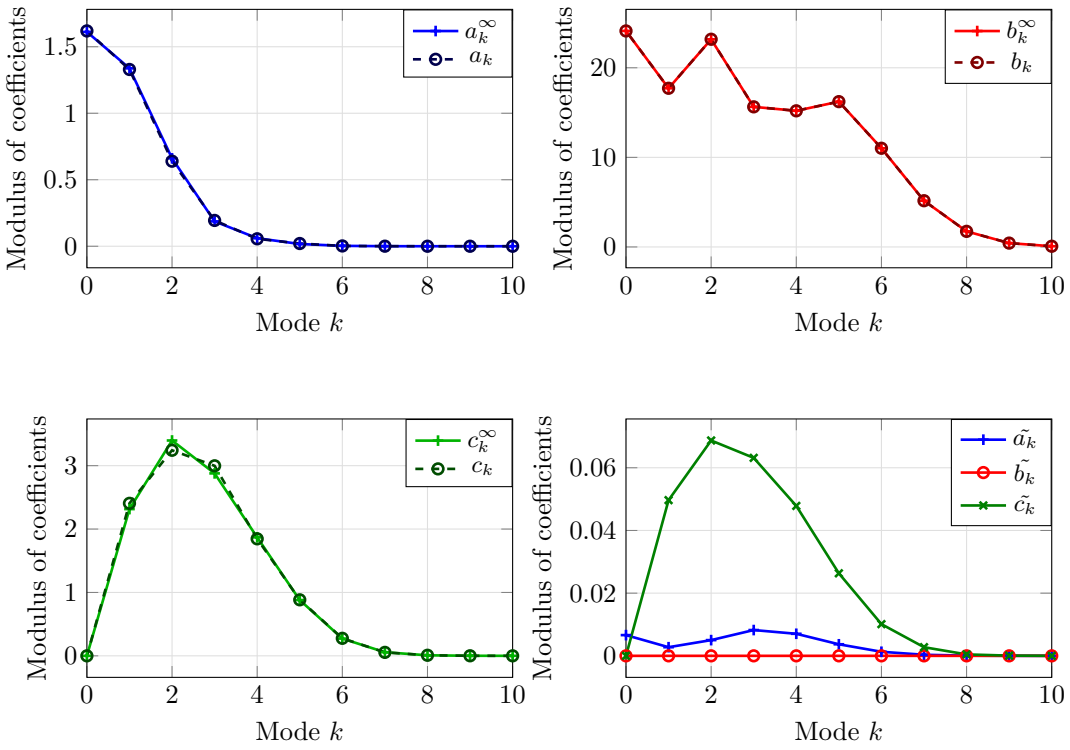

Figure 4.6: Obstacle scattering of an incident plane B-wave with the type 3 ("Dirichlet-like" (1.20c)) for the boundary condition on $r = \mathfrak{a}$ at a frequency $f = 1$kHz for a sandstone medium with viscosity $\eta = 10^{-3}$ Pa.s^{-1}. The domain is an annulus with interior radius $\mathfrak{a} = 1$m and exterior radius $\mathfrak{b} = 10$m. The coefficients with ∞ superscript correspond to the exact outgoing solution. a_k^∞ —, a_k - ⊙ -, and $\tilde{a}_k$ — are the coefficients corresponding to the potential of the P-wave, b_k^∞ —, b_k - ⊙ -, and $\tilde{b}_k$ — the coefficients corresponding to the potential of the B-wave, and c_k^∞ —, c_k - ⊙ -, and $\tilde{c}_k$ — the coefficients corresponding to the potential of the S-wave (see (4.16)).

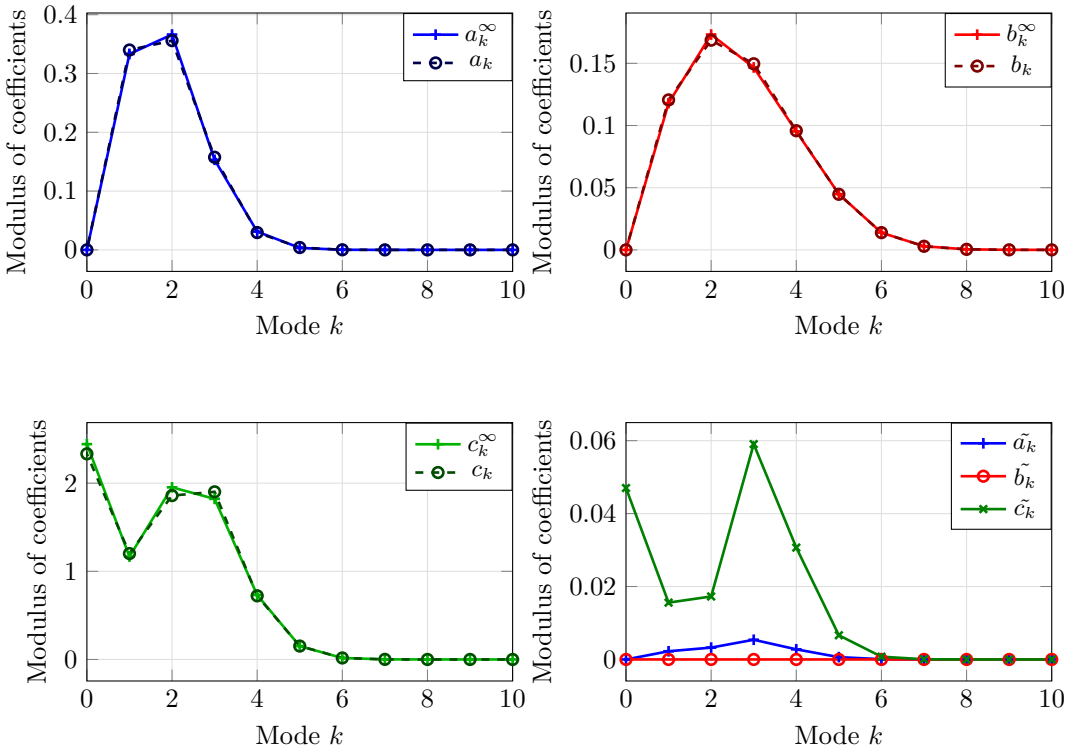

Figure 4.7: Obstacle scattering of an incident plane S-wave with the type 3 ("Dirichlet-like" (1.20c)) for the boundary condition on $r = \mathfrak{a}$ at a frequency $f = 1$kHz for a sandstone medium with viscosity $\eta = 10^{-3}$ Pa.s^{-1}. The domain is an annulus with interior radius $\mathfrak{a} = 1$m and exterior radius $\mathfrak{b} = 10$m. The coefficients with ∞ superscript correspond to the exact outgoing solution. a_k^∞ —, a_k - o -, and $\tilde{a}_k$ — are the coefficients corresponding to the potential of the P-wave, b_k^∞ —, b_k - o -, and $\tilde{b}_k$ — the coefficients corresponding to the potential of the B-wave, and c_k^∞ —, c_k - o -, and $\tilde{c}_k$ — the coefficients corresponding to the potential of the S-wave (see (4.16)).

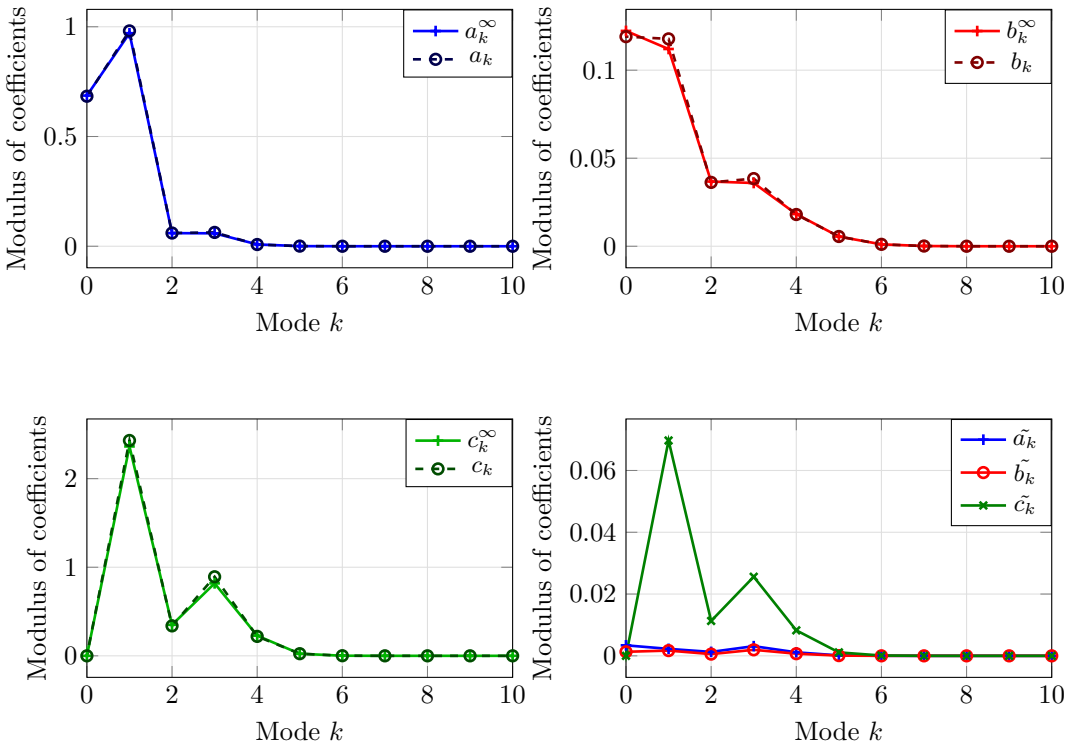

Figure 4.8: Obstacle scattering of an incident plane P-wave type 1 ("Neumann-like" (1.20a)) for the boundary condition on $r = \mathfrak{a}$ at a frequency $f = 1$kHz for a sandstone medium with no viscosity $\eta = 0$ Pa.s^{-1}. The domain is an annulus with interior radius $\mathfrak{a} = 1$m and exterior radius $\mathfrak{b} = 10$m. The coefficients with ∞ superscript correspond to the exact outgoing solution. a_k^∞ —+—, a_k - -o- - , and $\tilde{a}_k$ —+— are the coefficients corresponding to the potential of the P-wave, b_k^∞ —+—, b_k - -o- - , and $\tilde{b}_k$ —o— the coefficients corresponding to the potential of the B-wave, and c_k^∞ —+—, c_k - -o- - , and $\tilde{c}_k$ —x— the coefficients corresponding to the potential of the S-wave (see (4.16)).

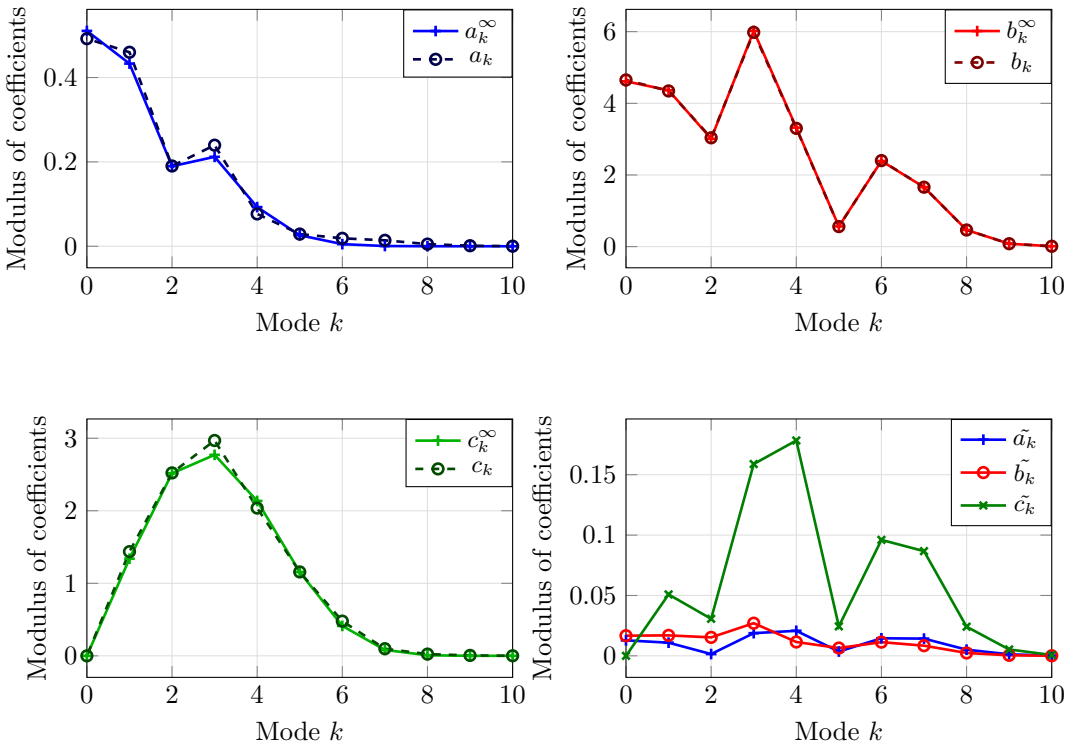

Figure 4.9: Obstacle scattering of an incident plane B-wave with the type 1 ("Neumann-like" (1.20a)) for the boundary condition on $r = \mathfrak{a}$ at a frequency $f = 1$kHz for a sandstone medium with no viscosity $\eta = 0$ Pa.s^{-1}. The domain is an annulus with interior radius $\mathfrak{a} = 1$m and exterior radius $\mathfrak{b} = 10$m. The coefficients with ∞ superscript correspond to the exact outgoing solution. a_k^∞ —, a_k - o -, and $\tilde{a}_k$ — are the coefficients corresponding to the potential of the P-wave, b_k^∞ —, b_k - o -, and $\tilde{b}_k$ — the coefficients corresponding to the potential of the B-wave, and c_k^∞ —, c_k - o -, and $\tilde{c}_k$ — the coefficients corresponding to the potential of the S-wave (see (4.16)).

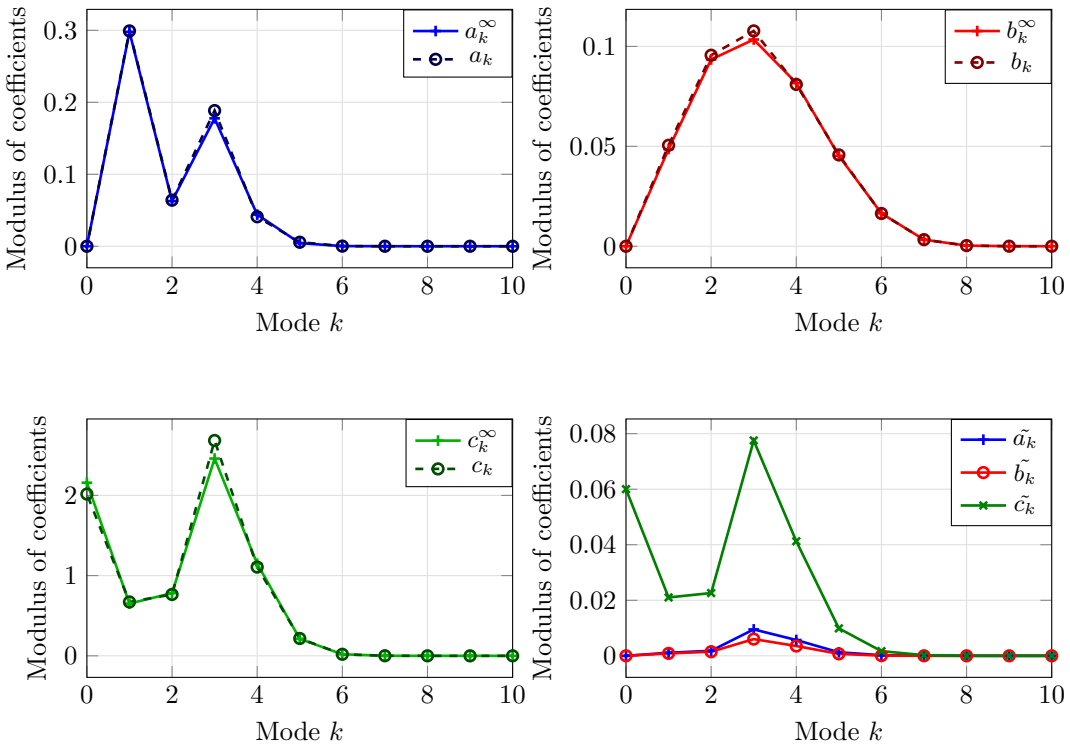

Figure 4.10: Obstacle scattering of an incident plane S-wave with the type 1 ("Neumann-like" (1.20a)) for the boundary condition on $r = \mathfrak{a}$. at a frequency $f = 1$kHz for a sandstone medium with no viscosity $\eta = 0$ Pa.s^{-1}. The domain is an annulus with interior radius $\mathfrak{a} = 1$m and exterior radius $\mathfrak{b} = 10$m. The coefficients with ∞ superscript correspond to the exact outgoing solution. a_k^∞ —, a_k - -, and $\tilde{a}_k$ — are the coefficients corresponding to the potential of the P-wave, b_k^∞ —, b_k - -, and $\tilde{b}_k$ — the coefficients corresponding to the potential of the B-wave, and c_k^∞ —, c_k - -, and $\tilde{c}_k$ — the coefficients corresponding to the potential of the S-wave (see (4.16)).

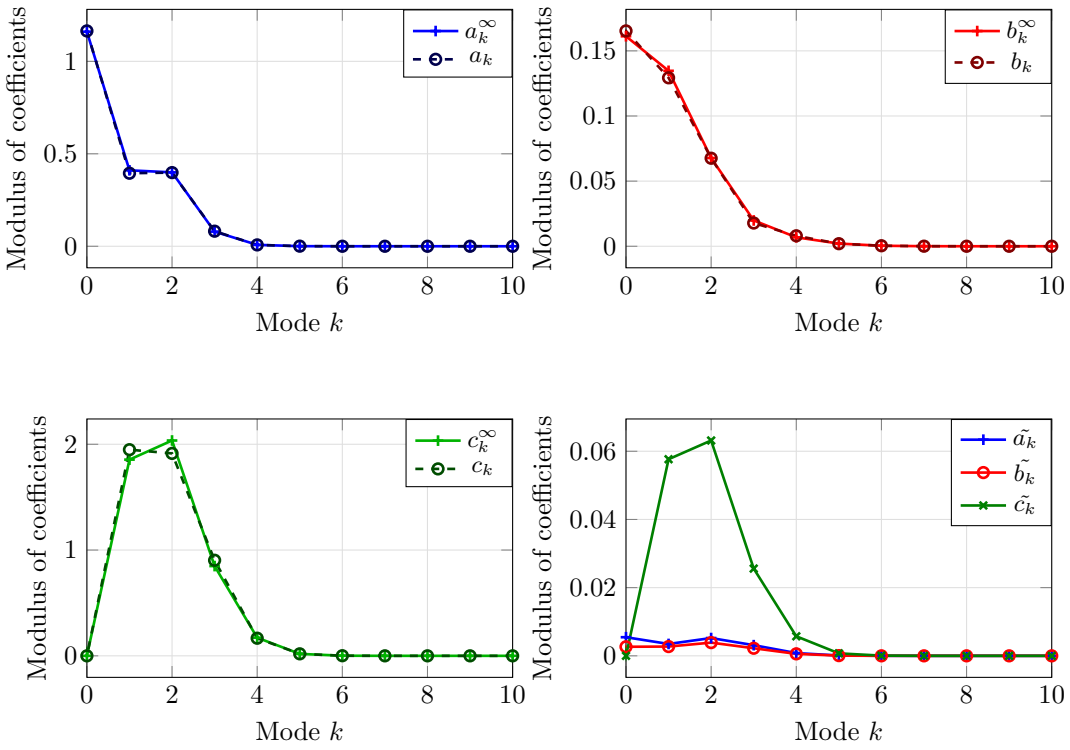

Figure 4.11: Obstacle scattering of an incident plane P-wave type 3 ("Dirichlet-like" (1.20c)) for the boundary condition on $r = \mathfrak{a}$ at a frequency $f = 1$kHz for a sandstone medium with no viscosity $\eta = 0$ Pa.s^{-1}. The domain is an annulus with interior radius $\mathfrak{a} = 1$m and exterior radius $\mathfrak{b} = 10$m. The coefficients with ∞ superscript correspond to the exact outgoing solution. a_k^∞ —+—, a_k - -o- - , and $\tilde{a}_k$ —+— are the coefficients corresponding to the potential of the P-wave, b_k^∞ —+—, b_k - -o- - , and $\tilde{b}_k$ —o— the coefficients corresponding to the potential of the B-wave, and c_k^∞ —+—, c_k - -o- - , and $\tilde{c}_k$ —x— the coefficients corresponding to the potential of the S-wave (see (4.16)).

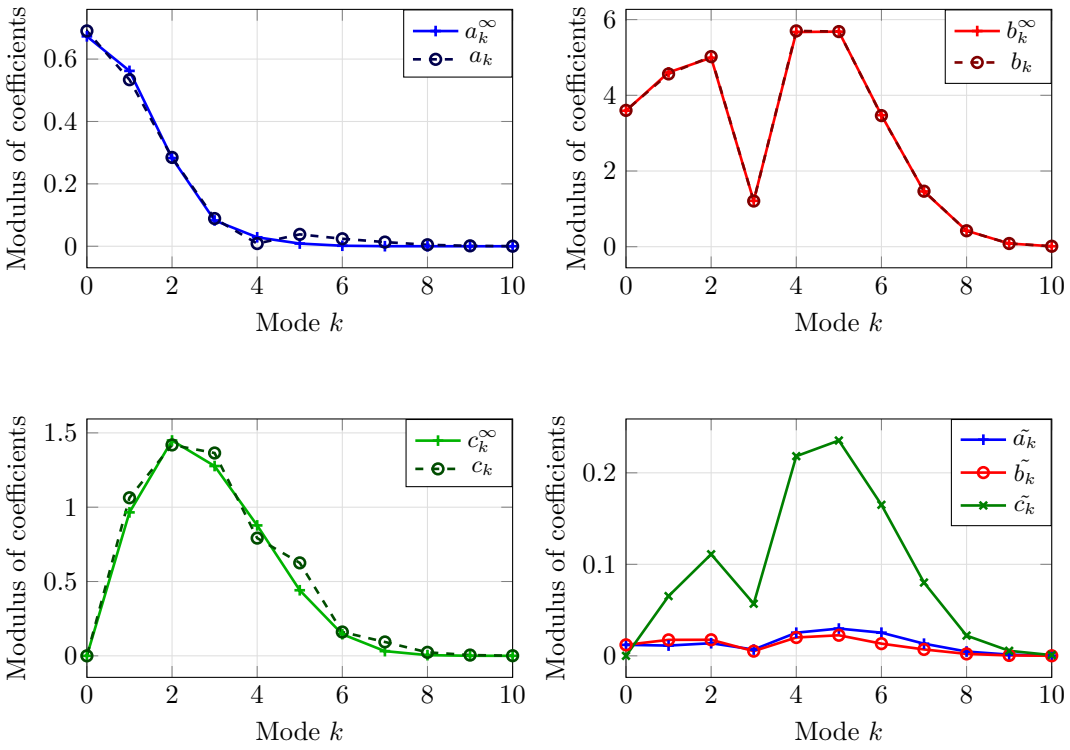

Figure 4.12: Obstacle scattering of an incident plane B-wave with the type 3 ("Dirichlet-like" (1.20c)) for the boundary condition on $r = \mathfrak{a}$ at a frequency $f = 1$kHz for a sandstone medium with no viscosity $\eta = 0$ Pa.s^{-1}. The domain is an annulus with interior radius $\mathfrak{a} = 1$m and exterior radius $\mathfrak{b} = 10$m. The coefficients with ∞ superscript correspond to the exact outgoing solution. a_k^∞ —, a_k - o -, and $\tilde{a}_k$ — are the coefficients corresponding to the potential of the P-wave, b_k^∞ —, b_k - o -, and $\tilde{b}_k$ — the coefficients corresponding to the potential of the B-wave, and c_k^∞ —, c_k - o -, and $\tilde{c}_k$ — the coefficients corresponding to the potential of the S-wave (see (4.16)).

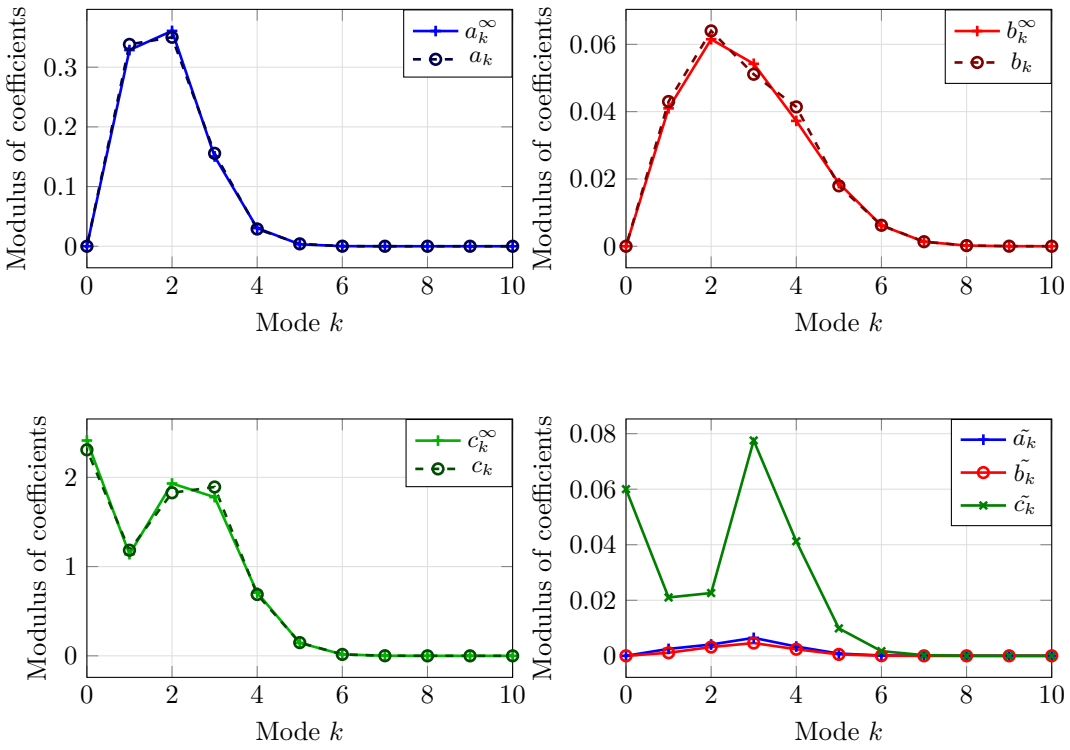

Figure 4.13: Obstacle scattering of an incident plane S-wave with the type 3 ("Dirichlet-like" (1.20c)) for the boundary condition on $r = \mathfrak{a}$ at a frequency $f = 1$kHz for a sandstone medium with no viscosity $\eta = 0$ Pa.s^{-1}. The domain is an annulus with interior radius $\mathfrak{a} = 1$m and exterior radius $\mathfrak{b} = 10$m. The coefficients with ∞ superscript correspond to the exact outgoing solution. a_k^∞ —, a_k - o -, and $\tilde{a}_k$ — are the coefficients corresponding to the potential of the P-wave, b_k^∞ —, b_k - o -, and $\tilde{b}_k$ — the coefficients corresponding to the potential of the B-wave, and c_k^∞ —, c_k - o -, and $\tilde{c}_k$ — the coefficients corresponding to the potential of the S-wave (see equation (4.16)).

4.3.2 Potential decomposition

To illustrate better the effect of the RBC on each of the type of waves, we will use the natural decomposition in potentials given by (4.2). We recall that this equation gives a complete description of the components of the solution $\mathfrak{U}$ in terms of the potentials χ_{P}, χ_{B}, χ_{S}. In this section, we will focus on the velocity $\mathbf{u}$ for type of boundary 1 ("Neumann-like") on $r = \mathfrak{a}$. The wave decomposition for $\mathbf{u}$ of $\mathfrak{U}^{\text{rbc-T1}}$ is given by

$$\mathbf{u}^{\text{rbc-T1}} = \mathbf{u}^{\chi_{\mathrm{P}}^{\text{rbc-T1}}} + \mathbf{u}^{\chi_{\mathrm{B}}^{\text{rbc-T1}}} + \mathbf{u}^{\chi_{\mathrm{S}}^{\text{rbc-T1}}},$$

$$\mathbf{u}^{\chi_{\mathrm{P}}^{\text{rbc-T1}}} = -\frac{\mathrm{i}}{\omega \mathsf{s}_{\mathrm{P}}^2} \nabla \chi_{\mathrm{P}}^{\text{rbc-T1}}, \qquad \mathbf{u}^{\chi_{\mathrm{B}}^{\text{rbc-T1}}} = -\frac{\mathrm{i}}{\omega \mathsf{s}_{\mathrm{B}}^2} \nabla \chi_{\mathrm{B}}^{\text{rbc-T1}}, \qquad \mathbf{u}^{\chi_{\mathrm{S}}^{\text{rbc-T1}}} = \frac{\mathrm{i}}{\omega \mathsf{s}_{\mathrm{S}}^2} \mathbf{curl}\, \chi_{\mathrm{S}}^{\text{rbc-T1}}.$$

Recall that these potentials are represented by the coefficients $(a_k, b_k, c_k, \tilde{a}_k, \tilde{b}_k, \tilde{c}_k)$, cf. (4.16)-(4.17). We will also compare with the decomposition of $\mathbf{u}^{\infty}$ coming from $\mathfrak{U}^{\infty-\text{T1}}$

$$\mathbf{u}^{\infty-\text{T1}} = \mathbf{u}^{\chi_{\mathrm{P}}^{\infty-\text{T1}}} + \mathbf{u}^{\chi_{\mathrm{B}}^{\infty-\text{T1}}} + \mathbf{u}^{\chi_{\mathrm{S}}^{\infty-\text{T1}}},$$

$$\mathbf{u}^{\chi_{\mathrm{P}}^{\infty-\text{T1}}} = -\frac{\mathrm{i}}{\omega \mathsf{s}_{\mathrm{P}}^2} \nabla \chi_{\mathrm{P}}^{\infty-\text{T1}}, \qquad \mathbf{u}^{\chi_{\mathrm{B}}^{\infty-\text{T1}}} = -\frac{\mathrm{i}}{\omega \mathsf{s}_{\mathrm{B}}^2} \nabla \chi_{\mathrm{B}}^{\infty-\text{T1}}, \qquad \mathbf{u}^{\chi_{\mathrm{S}}^{\infty-\text{T1}}} = \frac{\mathrm{i}}{\omega \mathsf{s}_{\mathrm{S}}^2} \mathbf{curl}\, \chi_{\mathrm{S}}^{\infty-\text{T1}}.$$

Recall that these potentials are represented by the coefficients $(a_k^{\infty}, b_k^{\infty}, c_k^{\infty})$, cf. (4.14)-(4.15).

In Figure 4.14, we present the decomposition of the solid velocity in the three potentials.

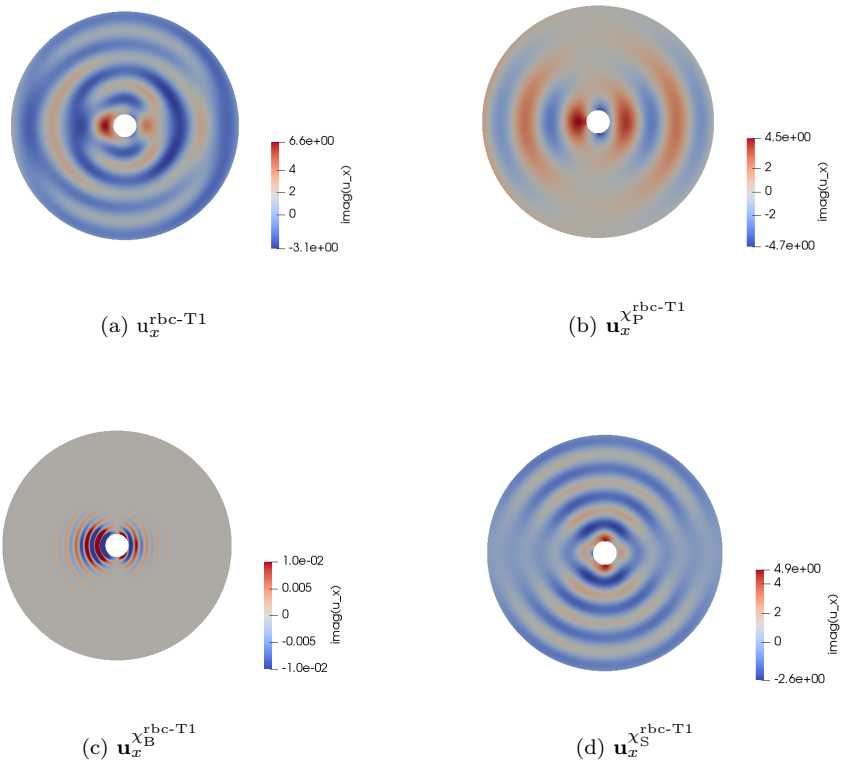

(a) $\mathrm{u}_x^{\text{rbc-T1}}$ (b) $\mathbf{u}_x^{\chi_{\mathrm{P}}^{\text{rbc-T1}}}$

(c) $\mathbf{u}_x^{\chi_{\mathrm{B}}^{\text{rbc-T1}}}$ (d) $\mathbf{u}_x^{\chi_{\mathrm{S}}^{\text{rbc-T1}}}$

Figure 4.14: RBC solution: Decomposition of $\mathbf{u}$ ($\mathrm{m.s}^{-1}$) in the case of the scattering of a P-wave by an impenetrable obstacle with boundary condition of type 1 ("Neumann-like") on $r = \mathfrak{a}$ cf. (1.20a) at a frequency $f = 1\mathrm{kHz}$ for a sandstone medium with viscosity $\eta = 10^{-3}$ $\mathrm{Pa.s}^{-1}$. The radiation boundary condition is set at $\mathfrak{b} = 10\mathrm{m}$.

In Figure 4.14, the weak reflections are barely visible. Comparing to the outgoing solution (Figure 4.15), we cannot see significant differences. This is also confirmed by Table 4.1, where the global error is low and the error on the potentials are included between 1 and 3%. We can also observe the effect of the viscosity on the B-wave, (Figures 4.14(c), 4.16(c)) where the wave is absorbed and the energy is mainly localized around the obstacle when there is viscosity. As expected, this effect is not clearly seen for P and S-waves because there are less sensitive to viscosity.

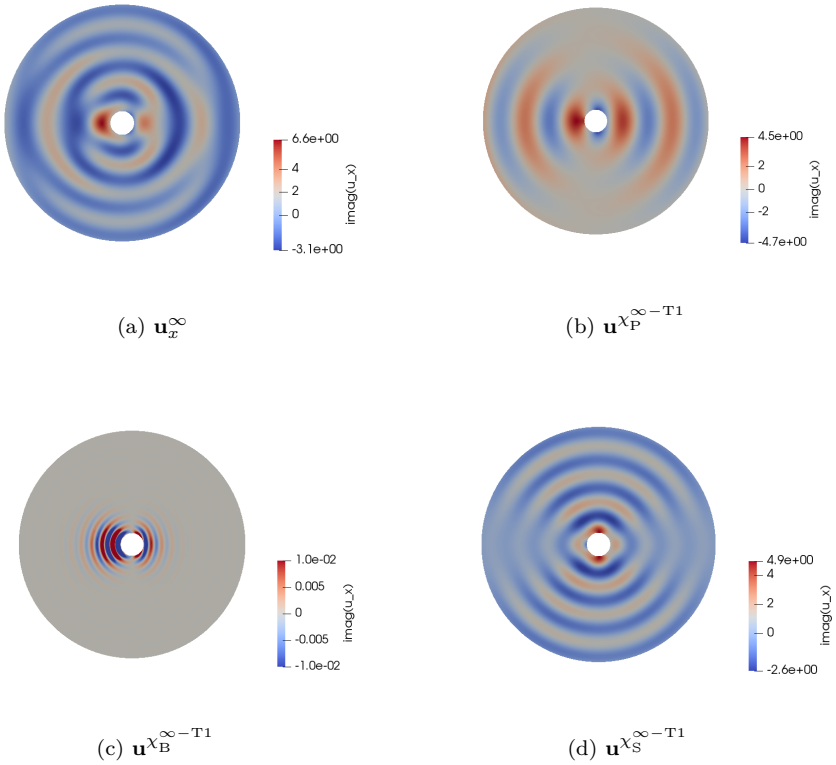

(a) $\mathbf{u}_x^{\infty}$ (b) $\mathbf{u}^{\chi_{\mathrm{P}}\,\infty-\mathrm{T1}}$

(c) $\mathbf{u}^{\chi_{\mathrm{B}}\,\infty-\mathrm{T1}}$ (d) $\mathbf{u}^{\chi_{\mathrm{S}}\,\infty-\mathrm{T1}}$

Figure 4.15: Outgoing solution: Decomposition of $\mathbf{u}$ (m.s^{-1}) in the case of the scattering of a P-wave by an impenetrable obstacle with boundary condition of type 1 ("Neumann-like") on $r = \mathfrak{a}$, cf. (1.20a) at a frequency $f = 1$kHz for a sandstone medium with viscosity $\eta = 10^{-3}$ Pa.s^{-1}.

	$\mathbf{u}$	$\mathbf{u}^{\chi_{\mathrm{P}}}$	$\mathbf{u}^{\chi_{\mathrm{B}}}$	$\mathbf{u}^{\chi_{\mathrm{S}}}$
Relative L^2 error (%)	2.30	2.73	1.22	3.17

Table 4.1: L^2 error (%) on $\mathbf{u}_x$ between the RBC solution and the outgoing solution for the decomposition in potentials.

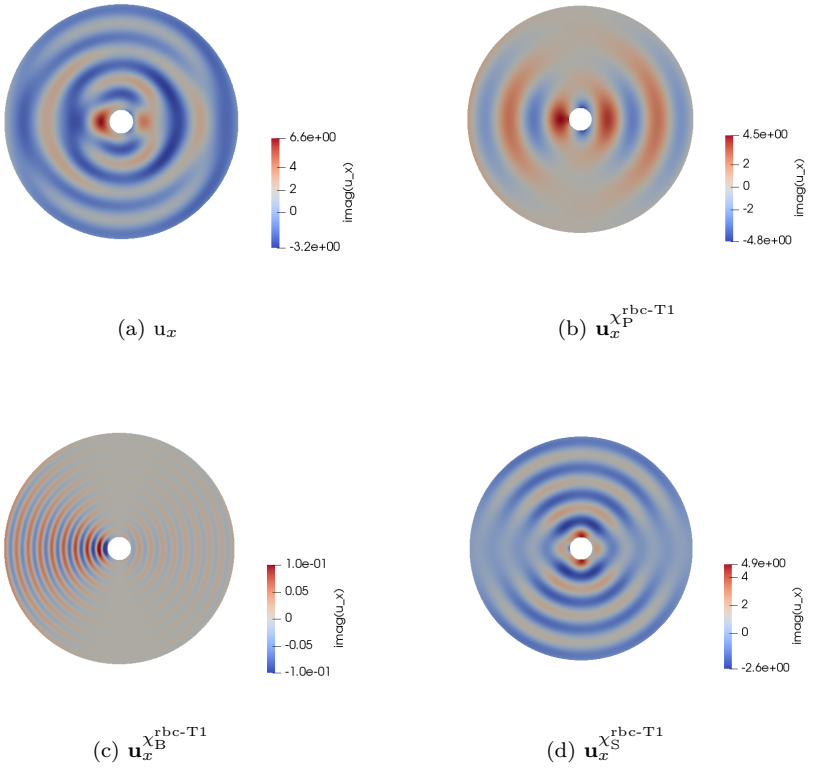

(a) u_x (b) $\mathbf{u}_x^{\chi_{\mathrm{P}}^{\text{rbc-T1}}}$

(c) $\mathbf{u}_x^{\chi_{\mathrm{B}}^{\text{rbc-T1}}}$ (d) $\mathbf{u}_x^{\chi_{\mathrm{S}}^{\text{rbc-T1}}}$

Figure 4.16: RBC solution: Decomposition of $\mathbf{u}$ (m.s^{-1}) in the case of the scattering of a P-wave by an impenetrable obstacle with boundary condition of type 1 ("Neumann-like") on $r = \mathfrak{a}$ cf. (1.20a) at a frequency $f = 1$kHz for a sandstone medium with no viscosity ($\eta = 0$ Pa.s^{-1}). The radiation boundary condition is set at $\mathfrak{b} = 10$m.

4.3.3 Effect of the size of the truncated domain

We have observed previously that the radiation boundary condition has good performance for $\mathfrak{b} = 10$m. In this section, we want to investigate the errors of the condition when the size of the truncated domain varies. Figure 4.17 presents the results of the RBC solution for several sizes of exterior radius. The L^2 error and the errors on the coefficients (e_{coeff}, e_{ref}) defined in equations (4.20) and (4.21), for incident waves P,B,S, are reported in Figs. 4.18 to 4.20. As expected, we observe that when the size of the truncated domain decreases, the error grows. Note that all the unknowns ($\mathbf{u}$, $\mathbf{w}$, $\boldsymbol{\tau}$, p) have the same behavior. The presence of viscosity seems to lower the errors. This will be confirmed by the results of Section 4.3.4. In most cases in our tests, the L^2 error is lower than 5% from $\mathfrak{b} = 10$m. We observe two cases where the error remains high (Figure 4.18) for a B incident wave with no viscosity and for types of boundary condition 1 ("Neumann-like") and 3 ("Dirichlet-like"). This confirms the results from Figs. 4.9 and 4.12 where the values of $\tilde{c}_k$ is high compared to the other coefficients $\tilde{a}_k$ and $\tilde{b}_k$. This shows that the efficiency of the RBC depends also on the kind of incident wave.

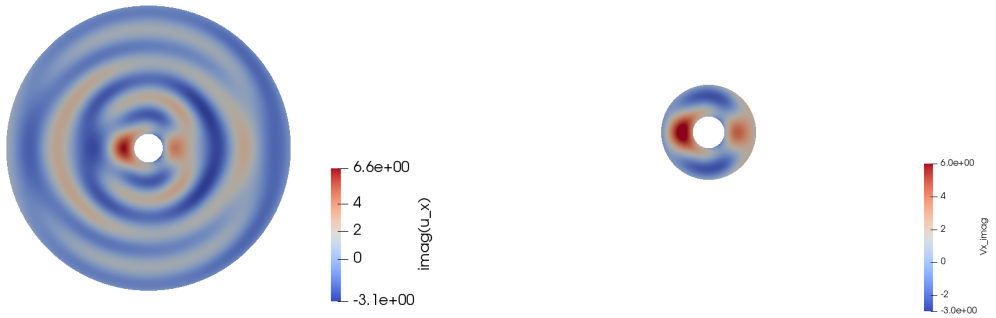

(a) RBC solution with $\mathfrak{b} = 10$m

(b) RBC solution with $\mathfrak{b} = 3$m

Figure 4.17: RBC solution: imaginary part of u_x ($\mathrm{m.s}^{-1}$) for the scattering of a P-wave by a porous obstacle composed of sandstone with viscosity $\eta = 10^{-3}$ $\mathrm{Pa.s}^{-1}$, $f = 1$kHz and boundary condition of type 1 ("Neumann-like") on $\mathfrak{a}$, for different values of $\mathfrak{b}$.

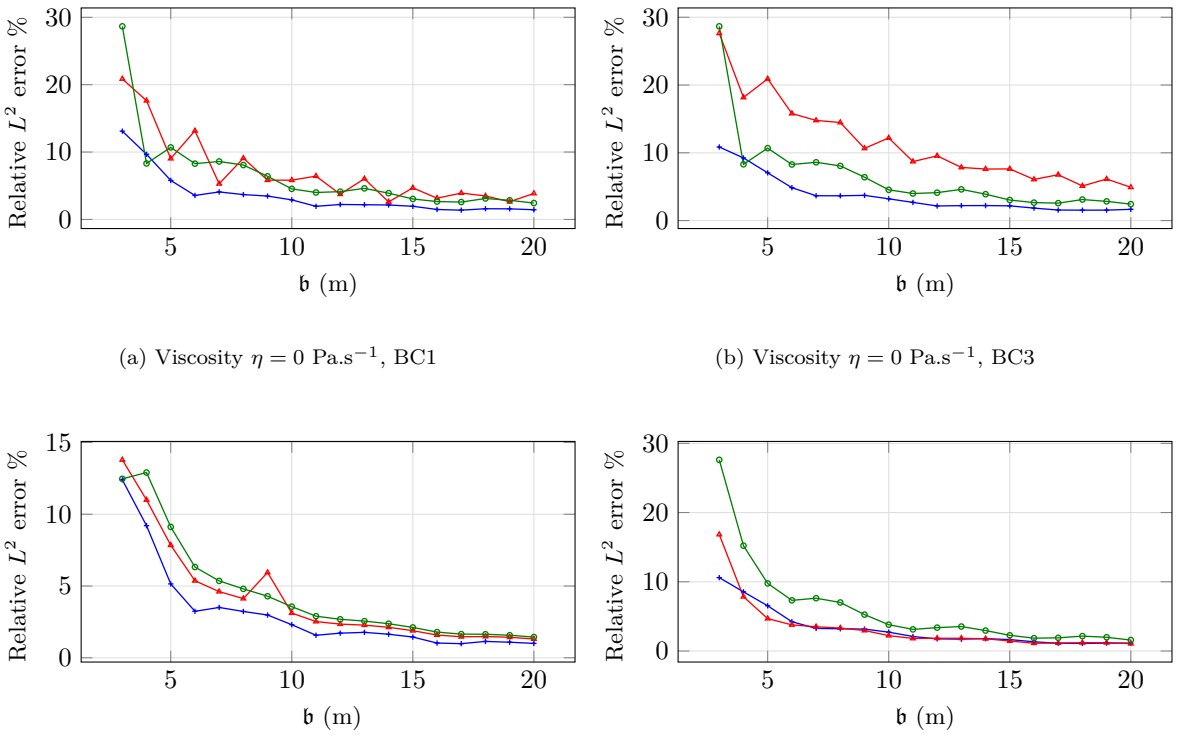

(a) Viscosity $\eta = 0$ Pa.s^{-1}, BC1

(b) Viscosity $\eta = 0$ Pa.s^{-1}, BC3

(c) Viscosity $\eta = 10^{-3}$ Pa.s^{-1}, BC1

(d) Viscosity $\eta = 10^{-3}$ Pa.s^{-1}, BC3

Figure 4.18: Relative L^2 error (%) between the RBC solution and the outgoing solution as a function of the size of the radius $\mathfrak{b}$ for $\eta = 0$ Pa.s^{-1} and $\eta = 10^{-3}$ Pa.s^{-1} for $f = 1$kHz for boundary condition of type 1 ("Neumann-like") and 3 ("Dirichlet-like") on the interior radius. The solutions are represented in blue —+— for the incident P-wave, in red —▲— for the incident B-wave and in green —○— for the incident S-wave.

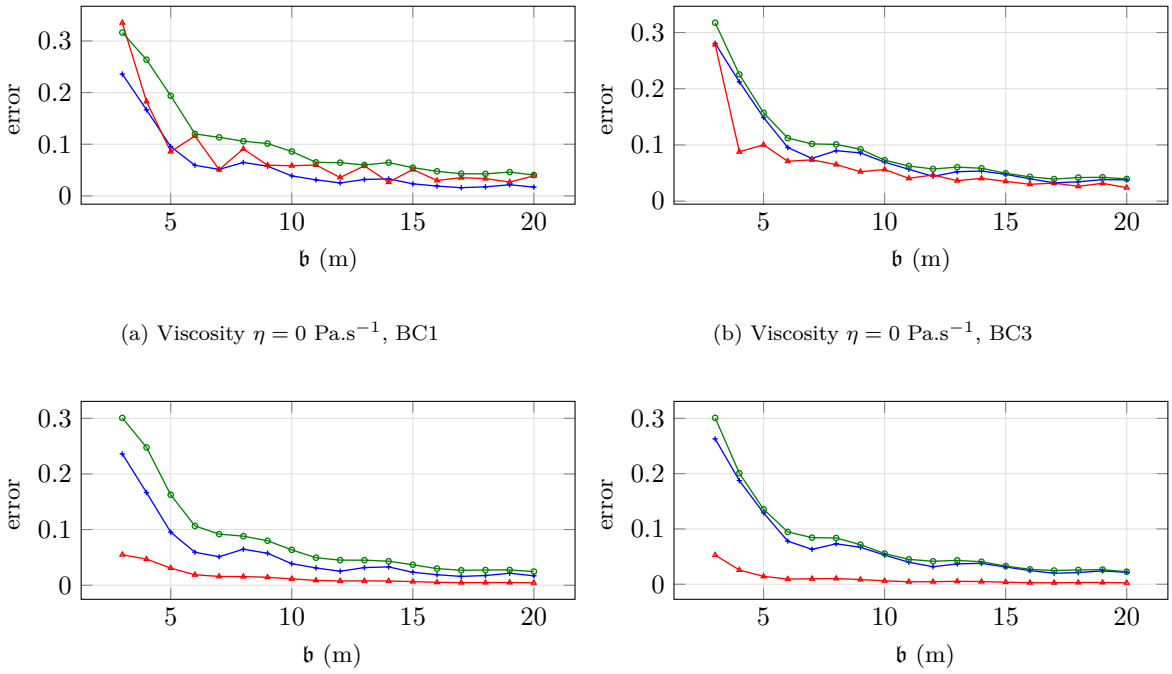

(a) Viscosity $\eta = 0$ Pa.s^{-1}, BC1

(b) Viscosity $\eta = 0$ Pa.s^{-1}, BC3

(c) Viscosity $\eta = 10^{-3}$ Pa.s^{-1}, BC1

(d) Viscosity $\eta = 10^{-3}$ Pa.s^{-1}, BC3

Figure 4.19: Error e_{coeff} function of the size of the radius $\mathfrak{b}$ for $\eta = 0$ Pa.s^{-1} and $\eta = 10^{-3}$ Pa.s^{-1} for $f = 1$kHz for boundary condition of type 1 ("Neumann-like") and 3 ("Dirichlet-like") on the interior radius. The solutions are represented in blue —+— for the incident P-wave, in red —▲— for the incident B-wave and in green —○— for the incident S-wave.

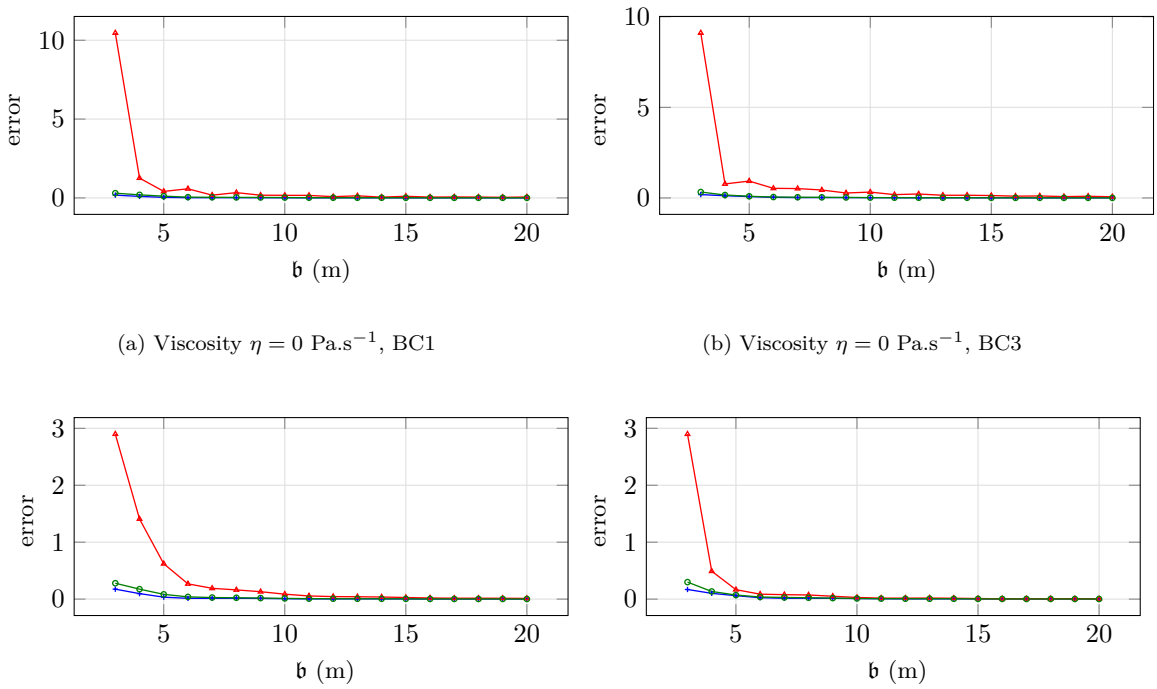

(a) Viscosity $\eta = 0$ Pa.s^{-1}, BC1

(b) Viscosity $\eta = 0$ Pa.s^{-1}, BC3

(c) Viscosity $\eta = 10^{-3}$ Pa.s^{-1}, BC1

(d) Viscosity $\eta = 10^{-3}$ Pa.s^{-1}, BC3

Figure 4.20: Error e_{ref} function of the size of the radius $\mathfrak{b}$ for $\eta = 0$ Pa.s^{-1} and $\eta = 10^{-3}$ Pa.s^{-1} for $f = 1$kHz for boundary condition of type 1 ("Neumann-like") and 3 ("Dirichlet-like") on the interior radius. The solutions are represented in blue —+— for the incident P-wave, in red —▲— for the incident B-wave and in green —○— for the incident S-wave.

For the tests in the following sections, we set $\mathfrak{b} = 10$m, in order to keep the same domain and observe the influence of other parameters. We have observed in the previous figures that this value is sufficient to limit the reflections. Note that this means that for the fastest wave, we have $\frac{k_{\mathrm{P}}\,\mathfrak{b}}{2\,\pi} = 2.35$ wavelengths for 10m for $f = 1$kHz.

4.3.4 Effect of the viscosity

For the domain described in figure 4.1, we consider a medium composed of sandstone (*cf.* Table 3.1) and vary the value of the viscosity in the material. We compare the RBC solution with the outgoing solution for the scattering of the three kinds of plane waves at $f = 1$kHz. The radiation solution is presented in Figure 4.21 for the scattering of a B wave for two values of viscosity. We see that when there is viscosity in the material, the wave is absorbed, and the majority of the energy is localized around the obstacle. As there is less signal near the artificial boundary, we can expect the radiation condition to be more efficient. The presence of the viscosity impacts mainly on the B-wave, as we already observed in Figure 4.14. In Figure 4.22, we show the L^2 error between the RBC solution and the outgoing solution for the scattering of the three plane waves (P,B,S) for a fixed frequency. We observe that the errors decrease when the viscosity grows, as expected. This means that the exterior boundary can be taken closer if the viscosity increases. Moreover, the error is slightly greater for boundary condition of type 3. As mentioned previously, the presence of viscosity has a greater impact on the B-wave than on the other waves, however, as seen in Figure 4.22, the global error decreases, this means that the viscosity causes also absorption on the P and S-waves.

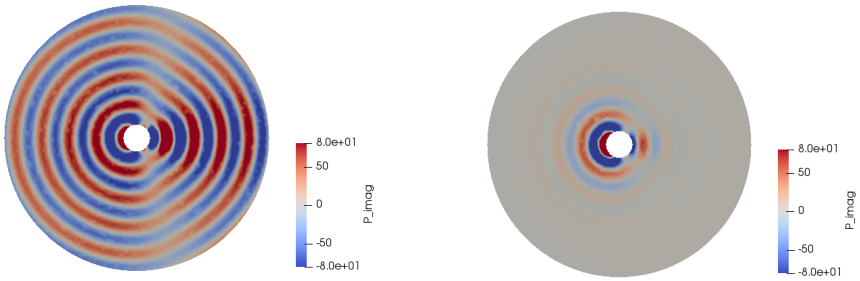

(a) $\eta = 0$Pa.s (b) $\eta = 1.10^{-3}$Pa.s

Figure 4.21: Imaginary part of the pressure p (MPa) of the reflected wave of the scattering by a B plane wave for type of boundary condition 3 ("Dirichlet-like") on the interior radius (*cf.* (1.20c)) with radiation boundary condition on $\mathfrak{b} = 10$m for a porous medium composed of sandstone with two different values of viscosity and with $f = 500$ Hz.

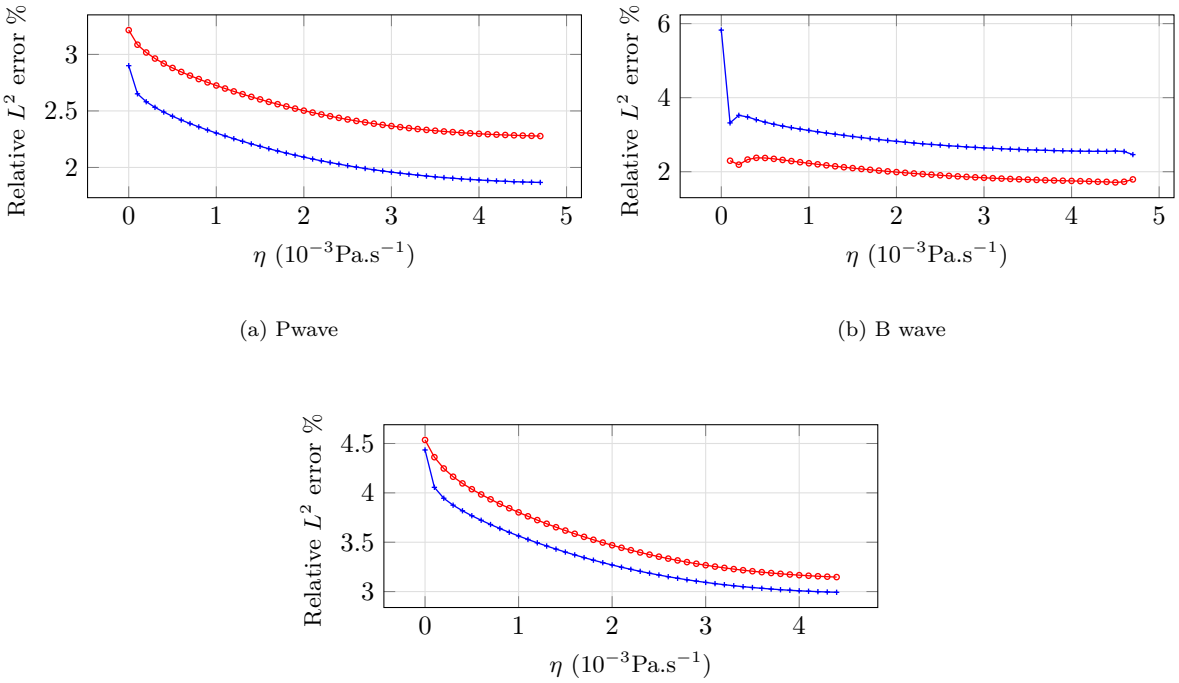

(a) Pwave

(b) B wave

(c) S wave

Figure 4.22: Relative L^2 error (%) between the RBC solution and the outgoing solution with $f = 1$kHz as a function of the viscosity of the medium for the scattering of a plane wave for type of boundary condition 1 ("Neumann-like" eq. (1.20a)) and 3 ("Dirichlet-like" eq. (1.20c)) on $\mathfrak{a}$, respectively represented in blue —+— and in red —○—. The results are given for $\mathfrak{a} = 1$m and $\mathfrak{b} = 10$m.

4.3.5 Effect of the frequency

In this section, we study the influence of the frequency on the performance of the RBC. The results for the scattering of a P-wave are presented in Figure 4.23 for two different frequencies. When the frequency is low, we observe that the RBC solution does not approach the outgoing solution, particularly around the obstacle where the energy explodes. In Figure 4.24, we show the L^2 error between the RBC solution and the outgoing solution for a range of frequency. We display the results for two values of viscosity $\eta = 0$ Pa.s^{-1} and $\eta = 10^{-3}$ Pa.s^{-1}, and for the boundary condition of type 1 ("Neumann-like") and 3 ("Dirichlet-like"). When ω increases, the RBC performs better. In the case of incident B-wave with no viscosity, we observe some oscillations on the errors that are no longer present when the material is viscous. Moreover, for the boundary condition of type 3 ("Dirichlet-like"), the error is around 10%.

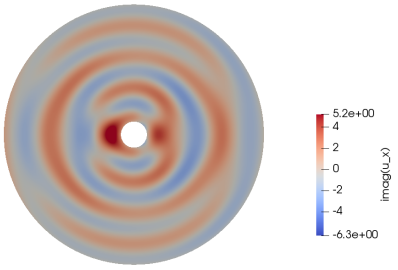

(a) RBC solution at $f = 1$kHz

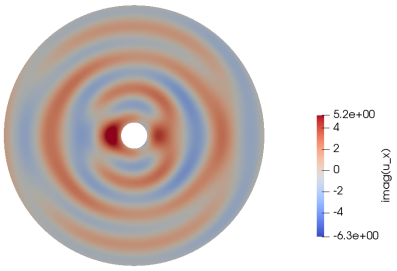

(b) Outgoing solution at $f = 1$kHz

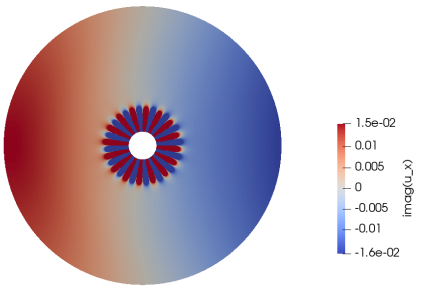

(c) RBC solution at $f = 0.1$kHz

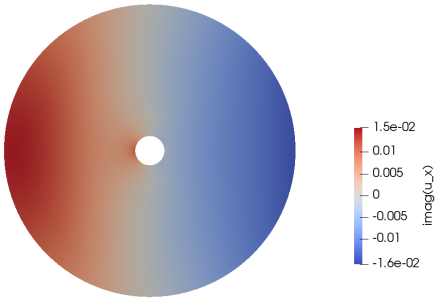

(d) Outgoing solution at $f = 0.1$kHz

Figure 4.23: Scattering of a P plane wave: Imaginary part of the solid velocity u_x (10^3 m.s^{-1}) of RBC solution and outgoing solution for a porous medium composed of inviscid sandstone for type of boundary condition 1 ("Neumann-like") on the interior radius (*cf.* (1.20a)), with $f = 1$kHz and $f = 0.1$ kHz.

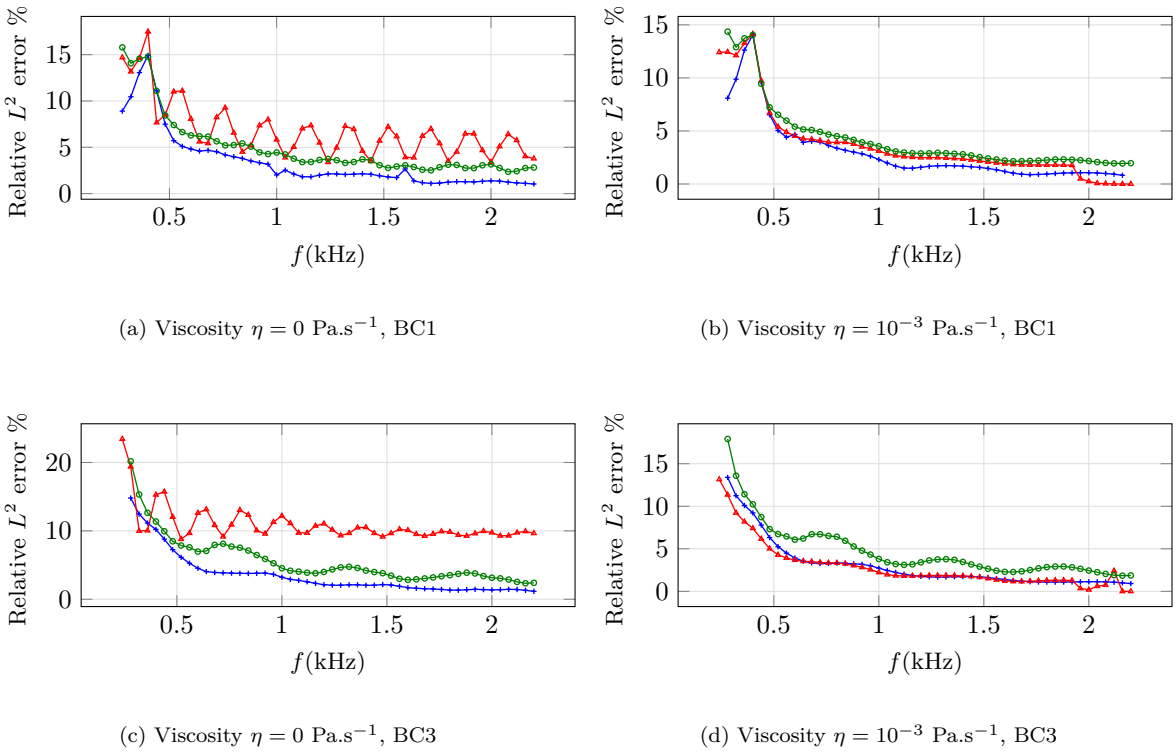

(a) Viscosity $\eta = 0$ Pa.s^{-1}, BC1

(b) Viscosity $\eta = 10^{-3}$ Pa.s^{-1}, BC1

(c) Viscosity $\eta = 0$ Pa.s^{-1}, BC3

(d) Viscosity $\eta = 10^{-3}$ Pa.s^{-1}, BC3

Figure 4.24: Relative L^2 error (%) between the RBC solution and the outgoing solution as a function of the pulsation ω in sandstone for the scattering of a plane wave for boundary condition of type 1 ("Neumann-like" equation (1.20a)), and type 3 ("Dirichlet-like" equation (1.20c)) on $\mathfrak{a}$. The results are given for $\mathfrak{a} = 1$m and $\mathfrak{b} = 10$m for $\eta = 0$ Pa.s^{-1} and $\eta = 10^{-3}$ Pa.s^{-1}. The incident P-wave is represented in blue —+—, the incident B-wave in red —▲— and the incident S-wave in green —○—.

Observations of the tests In the following, we summarize the observations for the tests in Sections 4.3.3, 4.3.4, 4.3.5:

- The radiation condition is efficient if $k_b\, r$ is large enough for the scattering of the three types of plane waves (P, B, S) and the different types of boundary condition on the scattered obstacle. The percentage of the L^2 error is of the same order as for first-order RBC in acoustic or elasticity.
- As expected, we have observed that the error decreases as the number of wavelengths contained in the computational domain increases, that is by using a greater frequency or by setting the artificial boundaries further from the obstacle. This is also the case in acoustic or elasticity.
- The higher the viscosity is, the more the RBC is efficient. This result can lead to another idea to construct RBC: raising artificially the viscosity of the media near the absorbing boundary in order to absorb the incident waves. However, we do not develop this idea here.

4.4 HDG method using Radiation Boundary conditions

This section draws on the HDG discretization for poroelastic equations (4.1), on which we apply the low-order radiation boundary condition derived in Section 4.1. We consider a porous domain Ω with the boundary $\Gamma = \Gamma_n \cup \Gamma_{\text{abs}}$. ($\mathbf{u}$, $\mathbf{w}$, $\boldsymbol{\tau}$, p) solves the poroelastic equations (4.1) on Ω. On Γ_l, we impose one of the four conditions from Section 1.4. From Section 4.1, equation (4.13), on the radiation boundary Γ_{abs}, we impose:

$$\begin{cases} \boldsymbol{\tau}\,\boldsymbol{n} + \big(\mathbf{X}_1(\mathbf{u}\cdot\boldsymbol{n}) + \mathbf{X}_2(\mathbf{w}\cdot\boldsymbol{n})\big)\,\boldsymbol{n} + \mathbf{X}_3(\mathbf{u}\cdot\mathbf{t})\,\mathbf{t} = 0\,, \\ \mathrm{p} + \mathbf{X}_4(\mathbf{u}\cdot\boldsymbol{n}) + \mathbf{X}_5(\mathbf{w}\cdot\boldsymbol{n}) \;= 0\,. \end{cases} \tag{4.22}$$

We consider the triangulation $\mathcal{T}_h$ of the domain Ω of dimension 2. We recall the notations and the function spaces defined in equations (3.4) and (3.5):

$$\begin{aligned} &L^2(\Omega),\ \text{the space of square-integrable functions on the domain } \Omega\,,\\ &V^p(\Omega),\ \text{the set of polynomials of degree at most } p \text{ on } \Omega\,,\\ &\boldsymbol{V}^p(\Omega) = (V^p(\Omega))^2\,,\\ &\boldsymbol{\Sigma}^p(\Omega) = \{\boldsymbol{\tau} \in (V^p(\Omega))^{2^2} | \boldsymbol{\tau} \text{ symmetric}\}\,. \end{aligned}$$

Associated to triangulation $\mathcal{T}_h$, we define the following spaces:

$$\begin{aligned} V_h^p &= \{v \in L^2(\Omega) : v|_K \in V^p(K)\,,\ \forall K \in \mathcal{T}_h\}\,,\\ \boldsymbol{V}_h^p &= \{\boldsymbol{v} \in (L^2(\Omega))^2 : \boldsymbol{v}|_K \in V^p(K)\,,\ \forall K \in \mathcal{T}_h\}\,,\\ \boldsymbol{\Sigma}_h^p &= \{\boldsymbol{\tau} \in L^2(\Omega)^{2^2} : \boldsymbol{\tau}|_K \in \boldsymbol{\Sigma}^p(K)\,,\ \forall K \in \mathcal{T}_h\}\,,\\ M_h &= \{\xi \in L^2(\mathcal{F}_h) : \xi|_F \in V^p(F),\ ,\ \forall K \in \mathcal{F}_h\}\,,\\ \boldsymbol{M}_h &= \{\eta \in (L^2(\mathcal{F}_h))^2 : \eta|_F \in (V^p(F))^2\,,\ \forall K \in \mathcal{F}_h\}\,. \end{aligned}$$

The local unknowns ($\mathbf{u}_h$, $\mathbf{w}_h$, $\boldsymbol{\tau}_h$, p_h) $\in (\boldsymbol{V}_h^p \times \boldsymbol{V}_h^p \times \boldsymbol{\Sigma}_h^p \times V_h^p)$ solve the poroelastic equations (4.1) on $\mathcal{T}_h$. We introduce two unknowns $\boldsymbol{\lambda}_1 \in \boldsymbol{M}_h$, $\lambda_2 \in M_h$ to replace the numerical traces $\hat{\mathbf{u}}_h$ and $\hat{\mathrm{p}}_h$. The other two traces $(\hat{\boldsymbol{\tau}}_h, \hat{\mathbf{w}}_h)$ are expressed in terms of the Lagrange multipliers $\boldsymbol{\lambda}_1$, λ_2. The Lagrange unknowns $\boldsymbol{\lambda}_1$ and λ_2 are dependent of h, however to simplify the expressions, we drop the dependency in h in the notation. The numerical traces of ($\mathbf{u}_h$, $\mathbf{w}_h$, $\boldsymbol{\tau}_h$, p_h) on an edge are defined as:

$$\begin{aligned} \hat{\mathbf{u}}_h &= \boldsymbol{\lambda}_1\,,\\ \hat{\boldsymbol{\tau}}_h &= \boldsymbol{\tau}_h - \boldsymbol{S}_1(\mathbf{u}_h - \boldsymbol{\lambda}_1)\otimes\boldsymbol{n} - (\mathrm{p}_h - \lambda_2)\boldsymbol{S}_3\,,\\ \hat{\mathbf{w}}_h &= \mathbf{w}_h - (\mathrm{p}_h - \lambda_2)\boldsymbol{S}_2\boldsymbol{n} - \boldsymbol{S}_4(\mathbf{u}_h - \boldsymbol{\lambda}_1)\,,\\ \hat{\mathrm{p}}_h &= \lambda_2\,, \end{aligned} \tag{4.23}$$

with $\boldsymbol{S}_1$, $\boldsymbol{S}_3$, $\boldsymbol{S}_2$, $\boldsymbol{S}_4$ the stabilization matrices, that we consider to be of the form $\boldsymbol{S}_i = \gamma_i \mathbb{I}$.

The HDG discretization of the poroelastic equations (4.1), given in details in Section 3.2, is composed of two systems of equations, the local problem on each element, and the transmission conditions connecting the elements using the numerical fluxes. They were given as:

$$\mathbb{A}^K \underline{W}^K + \mathbb{B}^K \underline{\Lambda}^K = \mathbb{C}^K_{\text{source}}, \qquad \text{Local problem,}$$

and

$$\sum_{K\in\mathcal{T}_h} (\mathcal{A}^K_{HDG})^T \left(\mathbb{P}^K \underline{W}^K + \mathbb{T}^K \mathcal{A}^K_{HDG} \underline{\Lambda}\right) = \mathbb{S}_{\text{inc}}, \qquad \text{Transmission conditions,}$$

with

$$\underline{W}^K = (\underline{\mathrm{u}}^K_x, \underline{\mathrm{u}}^K_y, \underline{\mathrm{w}}^K_x, \underline{\mathrm{w}}^K_y, \underline{\tau}^K_{xx}, \underline{\tau}^K_{yy}, \underline{\tau}^K_{xy}, \underline{\mathrm{p}}^K)^T,$$

and

$$\underline{\Lambda}^K = (\underline{\lambda}^{\beta(K,1)}_{1x}, \underline{\lambda}^{\beta(K,2)}_{1x}, \underline{\lambda}^{\beta(K,3)}_{1x}, \underline{\lambda}^{\beta(K,1)}_{1y} \underline{\lambda}^{\beta(K,2)}_{1y}, \underline{\lambda}^{\beta(K,3)}_{1y}, \underline{\lambda}^{\beta(K,1)}_{2}, \underline{\lambda}^{\beta(K,2)}_{2}, \underline{\lambda}^{\beta(K,3)}_{2})^T,$$

with $\beta(K,f)$ the global index of the f-th face of the element K. The local solutions and the local Lagrange unknowns are decomposed as:

$$\mathrm{u}^K_l = \sum_{j=1}^{d_i^K} \underline{\mathrm{u}}^K_{l,j} \varphi^K_j, \ \mathrm{w}^K_l = \sum_{j=1}^{d_i^K} \underline{\mathrm{w}}^K_{l,j} \varphi^K_j, \ \tau^K_{kl} = \sum_{j=1}^{d_i^K} \underline{\tau}^K_{kl,j} \varphi^K_j, \ \mathrm{p}^K = \sum_{j=1}^{d_i^K} \underline{\mathrm{p}}^K \varphi^K_j, \text{ with } k=x,y \text{ and } l=x,y, \tag{4.26a}$$

and

$$\lambda^F_{1l} = \sum_{j=1}^{d_i^F} \underline{\lambda_{1l}}^F_j \psi^F_j, \qquad \lambda^F_2 = \sum_{j=1}^{d_i^F} \underline{\lambda_2}^F_j \psi^F_j \text{ with } l=x,y. \tag{4.26b}$$

Here, d_i^K denotes the number of degrees of freedom of an element, d_i^F the number of degrees of freedom of an edge, and φ^K_j, ψ^F_j are basis functions of the element K and the edge F respectively. The expressions of $\mathbb{A}^K$, $\mathbb{B}^K$, $\mathbb{C}^K_{\text{source}}$, $\mathbb{P}^K$, $\mathbb{T}^K$ are given in Chapter 3 and Appendix B.1 for a bounded domain. The resolution was also given in algorithm 2 in Section 3.4. Here, for the elements on the boundaries of the mesh, the presence of radiation boundary conditions affects the expression of the transmission conditions, while the local problem is not modified. Hence, we do not detail the discretization of the local problem, and we focus on the expression of the transmission conditions on the radiation boundary. On Γ_{abs}, the transmission conditions are replaced by radiation conditions obtained by integrating equation (4.22). This gives:

$$\sum_{F\in\mathcal{F}_{\text{rbc}}} \int_F (\hat{\boldsymbol{\tau}}\,\boldsymbol{n} + (\mathbf{X}_1(\hat{\mathbf{u}}\cdot\boldsymbol{n}) + \mathbf{X}_2(\hat{\mathbf{w}}\cdot\boldsymbol{n}))\,\boldsymbol{n} + \mathbf{X}_3(\hat{\mathbf{u}}\cdot\mathbf{t})\,\mathbf{t})\cdot\boldsymbol{\eta} = 0, \tag{4.27a}$$

$$\sum_{F\in\mathcal{F}_{\text{rbc}}} \int_F (\hat{\mathrm{p}} + \mathbf{X}_4(\hat{\mathbf{u}}\cdot\boldsymbol{n}) + \mathbf{X}_5(\hat{\mathbf{w}}\cdot\boldsymbol{n}))\xi = 0, \tag{4.27b}$$

with $(\boldsymbol{\eta}, \xi) \in \boldsymbol{M}_h \times M_h$ basis-functions on the faces. As we are in two dimensions, equation (4.27) is discretized. We recall the following matrices defined in Chapter 3,

$$\mathbb{F}^F_{ij} = \int_F \varphi^K_i \psi^F_j \, dS, \qquad \mathbb{Q}^F_{kij} = \int_F \varphi^K_i \psi^F_j n_k \, dS, \qquad \mathbb{G}^F_{ij} = \int_F \psi^F_i \psi^F_j \, dS, \qquad \mathbb{H}^F_{kij} = \int_F \psi^F_i \psi^F_j n_k \, dS,$$

and we introduce the matrices (4.28)

$$\mathbb{L}^F_{klij} = \int_F \varphi^K_i \psi^F_j n_k n_l \, dS, \qquad \mathbb{O}^F_{klij} = \int_F \psi^F_i \psi^F_j n_k n_l \, dS, \qquad \text{with } k=x,y, \text{ and } l=x,y.$$

(a) Discretization of the first condition Starting from equation (4.27a):

$$\int_F (\hat{\boldsymbol{\tau}}_h\,\boldsymbol{n} + (\mathbf{X}_1(\hat{\mathbf{u}}_h\cdot\boldsymbol{n}) + \mathbf{X}_2(\hat{\mathbf{w}}_h\cdot\boldsymbol{n}))\,\boldsymbol{n} + \mathbf{X}_3(\hat{\mathbf{u}}_h\cdot\mathbf{t})\,\mathbf{t})\cdot\boldsymbol{\eta} = 0,$$

and replacing the numerical traces $\hat{\boldsymbol{\tau}}_h$, $\hat{\mathbf{w}}_h$ using equation (4.23), we obtain

$$\begin{aligned}
&\int_F (\boldsymbol{\tau}_h\,\boldsymbol{n})\cdot\boldsymbol{\eta} - \int_F \boldsymbol{S}_1(\mathbf{u}_h - \boldsymbol{\lambda}_1)\cdot\boldsymbol{\eta} - \int_F (\mathrm{p}_h - \lambda_2)(\boldsymbol{S}_3\,\boldsymbol{n})\cdot\boldsymbol{\eta} \\
&+ \int_F \Big((\mathbf{X}_1(\boldsymbol{\lambda}_1\cdot\boldsymbol{n})\boldsymbol{n} + \mathbf{X}_2\Big((\mathbf{w}_h\cdot\boldsymbol{n}) - (\mathrm{p}_h - \lambda_2)(\boldsymbol{S}_2\,\boldsymbol{n})\cdot\boldsymbol{n} - \boldsymbol{S}_4(\mathbf{u}_h - \boldsymbol{\lambda}_1)\cdot\boldsymbol{n}\Big)\boldsymbol{n} + \mathbf{X}_3(\boldsymbol{\lambda}_1\cdot\mathbf{t})\,\mathbf{t}\Big)\cdot\boldsymbol{\eta} = 0.
\end{aligned}$$

We replace the test-functions $\boldsymbol{\eta}$, ξ by basis functions, and we decompose the unknowns as given in equations (4.26a) and (4.26b). The discretization of the equation along x axis is written as follows:

$$\begin{aligned}
&\int_F \underline{\tau}_{xx}^K n_x \varphi_j^K \psi_i^{\beta(K,f)} dS + \int_F \underline{\tau}_{xy}^K n_y \varphi_j^K \psi_i^{\beta(K,f)} dS - \int_F \gamma_1 \varphi_j^K \underline{\mathrm{u}}_x^K \psi_i^{\beta(K,f)} dS + \int_F \gamma_1 \psi_j^{\beta(K,f)} \underline{\lambda}_{1x}^{\beta(K,f)} \psi_i^{\beta(K,f)} dS \\
&- \int_F \gamma_3 n_x \underline{\mathrm{p}}^K \varphi_j^K \psi_i^{\beta(K,f)} dS + \int_F \gamma_3 n_x \underline{\lambda}_2^{\beta(K,f)} \psi_j^{\beta(K,f)} \psi_i^{\beta(K,f)} dS + \int_F \mathbf{X}_1 \, \underline{\lambda}_{1x}^{\beta(K,f)} n_x^2 \, \psi_j^{\beta(K,f)} \, \psi_i^{\beta(K,f)} dS \\
&+ \int_F \mathbf{X}_1 \, \underline{\lambda}_{1y}^{\beta(K,f)} n_x n_y \, \psi_j^{\beta(K,f)} \, \psi_i^{\beta(K,f)} dS + \int_F \mathbf{X}_2 \, \underline{\mathrm{w}}_x^K \, n_x^2 \varphi_j^K \, \psi_i^{\beta(K,f)} dS + \int_F \mathbf{X}_2 \, \underline{\mathrm{w}}_y^K \, n_x n_y \varphi_j^K \, \psi_i^{\beta(K,f)} dS \\
&- \int_F \mathbf{X}_2 \, \gamma_2 \underline{\mathrm{p}}^K \, n_x \varphi_j^K \, \psi_i^{\beta(K,f)} dS + \int_F \mathbf{X}_2 \, \gamma_2 \underline{\lambda}_2^{\beta(K,f)} \, n_x \, \psi_j^{\beta(K,f)} \, \psi_i^{\beta(K,f)} dS - \int_F \mathbf{X}_2 \, \gamma_4 \, \underline{\mathrm{u}}_x^K n_x^2 \, \varphi_j^K \, \psi_i^{\beta(K,f)} dS \\
&- \int_F \mathbf{X}_2 \, \gamma_4 \, \underline{\mathrm{u}}_y^K n_x n_y \, \varphi_j^K \, \psi_i^{\beta(K,f)} dS + \int_F \mathbf{X}_2 \, \gamma_4 \, (\underline{\lambda}_{1x}^{\beta(K,f)} n_x + \underline{\lambda}_{1y}^{\beta(K,f)} n_y) n_x \, \psi_j^{\beta(K,f)} \, \psi_i^{\beta(K,f)} dS \\
&+ \int_F \mathbf{X}_3 \, (\underline{\lambda}_{1x}^{\beta(K,f)} n_y^2 - \underline{\lambda}_{1y}^{\beta(K,f)} n_x n_y) \psi_j^{\beta(K,f)} \psi_i^{\beta(K,f)} = 0 \,,
\end{aligned}$$

and along y-axis

$$\begin{aligned}
&\int_F \underline{\tau}_{xy}^K n_x \varphi_j^K \psi_i^{\beta(K,f)} dS + \int_F \underline{\tau}_{yy}^K n_y \varphi_j^K \psi_i^{\beta(K,f)} dS - \int_F \gamma_1 \varphi_j^K \underline{\mathrm{u}}_y^K \psi_i^{\beta(K,f)} dS + \int_F \gamma_1 \varphi_j^K \underline{\lambda}_{1y}^{\beta(K,f)} \psi_i^{\beta(K,f)} dS \\
&- \int_F \gamma_3 n_y \underline{\mathrm{p}}^K \varphi_j^K \psi_i^{\beta(K,f)} dS + \int_F \gamma_3 n_y \underline{\lambda}_2^{\beta(K,f)} \psi_j^{\beta(K,f)} \psi_i^{\beta(K,f)} dS + \int_F \mathbf{X}_1 \, \underline{\lambda}_{1x}^{\beta(K,f)} n_x n_y \, \psi_j^{\beta(K,f)} \, \psi_i^{\beta(K,f)} dS \\
&+ \int_F \mathbf{X}_1 \, \underline{\lambda}_{1y}^{\beta(K,f)} n_y^2 \, \psi_j^{\beta(K,f)} \, \psi_i^{\beta(K,f)} dS + \int_F \mathbf{X}_2 \, \underline{\mathrm{w}}_x^K \, n_x n_y \varphi_j^K \, \psi_i^{\beta(K,f)} dS + \int_F \mathbf{X}_2 \, \underline{\mathrm{w}}_y^K \, n_y^2 \varphi_j^K \, \psi_i^{\beta(K,f)} dS \\
&- \int_F \mathbf{X}_2 \, \gamma_2 \underline{\mathrm{p}}^K \, n_y \varphi_j^K \, \psi_i^{\beta(K,f)} dS + \int_F \mathbf{X}_2 \, \gamma_2 \underline{\lambda}_2^{\beta(K,f)} \, n_y \, \psi_j^{\beta(K,f)} \, \psi_i^{\beta(K,f)} dS - \int_F \mathbf{X}_2 \, \gamma_4 \, \underline{\mathrm{u}}_x^K n_x n_y \, \varphi_j^K \, \psi_i^{\beta(K,f)} dS \\
&- \int_F \mathbf{X}_2 \, \gamma_4 \, \underline{\mathrm{u}}_y^K n_y^2 \, \varphi_j^K \, \psi_i^{\beta(K,f)} dS + \int_F \mathbf{X}_2 \gamma_4 (\underline{\lambda}_{1x}^{\beta(K,f)} n_x + \underline{\lambda}_{1y}^{\beta(K,f)} n_y) n_y \psi_j^{\beta(K,f)} \, \psi_i^{\beta(K,f)} dS \\
&+ \int_F \mathbf{X}_3 (-\underline{\lambda}_{1x}^{\beta(K,f)} n_x n_y + \underline{\lambda}_{1y}^{\beta(K,f)} n_x^2) \psi_j^{\beta(K,f)} \psi_i^{\beta(K,f)} = 0.
\end{aligned}$$

The two above equations can be written using the expressions of the matrices given in (4.28):

$$\begin{aligned}
&(\mathbb{Q}_x^{\beta(K,f)})^T \underline{\tau}_{xx}^K + (\mathbb{Q}_y^{\beta(K,f)})^T \underline{\tau}_{xy}^K - \gamma_1 (\mathbb{F}^{\beta(K,f)})^T \underline{\mathrm{u}}_x^K + \gamma_1 \mathbb{G}^{\beta(K,f)} \underline{\lambda}_{1x}^{\beta(K,f)} - \gamma_3 (\mathbb{Q}_x^{\beta(K,f)})^T \underline{\mathrm{p}}^K + \gamma_3 \mathbb{H}_x^{\beta(K,f)} \underline{\lambda}_2^{\beta(K,f)} \\
&+ \mathbb{O}_{xx}^{\beta(K,f)} \mathbf{X}_1 \, \underline{\lambda}_{1x}^{\beta(K,f)} + \mathbb{O}_{xy}^{\beta(K,f)} \mathbf{X}_1 \underline{\lambda}_{1y}^{\beta(K,f)} + (\mathbb{L}_{xx}^{\beta(K,f)})^T \mathbf{X}_2 \, \underline{\mathrm{w}}_x^K + (\mathbb{L}_{xy}^{\beta(K,f)})^T \mathbf{X}_2 \, \underline{\mathrm{w}}_y^K \\
&- (\mathbb{Q}_x^{\beta(K,f)})^T \mathbf{X}_2 \, \gamma_2 \underline{\mathrm{p}}^K + \mathbb{H}_x^{\beta(K,f)} \mathbf{X}_2 \, \gamma_2 \underline{\lambda}_2^{\beta(K,f)} - (\mathbb{L}_{xx}^{\beta(K,f)})^T \mathbf{X}_2 \, \gamma_4 \, \underline{\mathrm{u}}_x^K - (\mathbb{L}_{xy}^{\beta(K,f)})^T \mathbf{X}_2 \, \gamma_4^{\beta(K,f)} \underline{\mathrm{u}}_y^K \\
&+ \mathbb{O}_{xx}^{\beta(K,f)} \mathbf{X}_2 \, \underline{\lambda}_{1x}^{\beta(K,f)} + \mathbb{O}_{xy}^{\beta(K,f)} \mathbf{X}_2 \underline{\lambda}_{1y}^{\beta(K,f)} + \mathbb{O}_{yy}^{\beta(K,f)} \mathbf{X}_3 \, \underline{\lambda}_{1x}^{\beta(K,f)} - \mathbb{O}_{xy}^{\beta(K,f)} \mathbf{X}_3 \, \underline{\lambda}_{1y}^{\beta(K,f)} = 0 \,,
\end{aligned}$$

and

$$\begin{aligned}
&(\mathbb{Q}_x^{\beta(K,f)})^T \underline{\tau}_{xy}^K + (\mathbb{Q}_y^{\beta(K,f)})^T \underline{\tau}_{yy}^K - \gamma_1 (\mathbb{F}^{\beta(K,f)})^T \underline{\mathrm{u}}_y^K + \gamma_1 \mathbb{G}^{\beta(K,f)} \underline{\lambda}_{1y}^{\beta(K,f)} - \gamma_3 (\mathbb{Q}_y^{\beta(K,f)})^T \underline{\mathrm{p}}^K + \gamma_3 \mathbb{H}_y^{\beta(K,f)} \underline{\lambda}_2^{\beta(K,f)} \\
&+ \mathbb{O}_{xy}^{\beta(K,f)} \mathbf{X}_1 \, \underline{\lambda}_{1x}^{\beta(K,f)} + \mathbb{O}_{yy}^{\beta(K,f)} \mathbf{X}_1 \underline{\lambda}_{1y}^{\beta(K,f)} + (\mathbb{L}_{xy}^{\beta(K,f)})^T \mathbf{X}_2 \, \underline{\mathrm{w}}_x^K + (\mathbb{L}_{yy}^{\beta(K,f)})^T \mathbf{X}_2 \, \underline{\mathrm{w}}_y^K \\
&- (\mathbb{Q}_y^{\beta(K,f)})^T \mathbf{X}_2 \, \gamma_2 \underline{\mathrm{p}}^K + \mathbb{H}_y^K \mathbf{X}_2 \, \gamma_2 \underline{\lambda}_2^{\beta(K,f)} - (\mathbb{L}_{xy}^{\beta(K,f)})^T \mathbf{X}_2 \, \gamma_4 \, \underline{\mathrm{u}}_x^K - (\mathbb{L}_{yy}^{\beta(K,f)})^T \mathbf{X}_2 \, \gamma_4 \underline{\mathrm{u}}_y^K \\
&+ \mathbb{O}_{xy}^{\beta(K,f)} \mathbf{X}_2 \, \underline{\lambda}_{1x}^{\beta(K,f)} + \mathbb{O}_{yy}^{\beta(K,f)} \mathbf{X}_2 \underline{\lambda}_{1y}^{\beta(K,f)} - \mathbb{O}_{xy}^{\beta(K,f)} \mathbf{X}_3 \, \underline{\lambda}_{1x}^{\beta(K,f)} + \mathbb{O}_{xx}^{\beta(K,f)} \mathbf{X}_3 \, \underline{\lambda}_{1y}^{\beta(K,f)} = 0 \,.
\end{aligned}$$

(b) Discretization of the second condition

From equation (4.27b), we have:

$$\int_F (\hat{\mathrm{p}}_h + \mathbf{X}_4 (\hat{\mathbf{u}}_h \cdot \boldsymbol{n}) + \mathbf{X}_5 (\hat{\mathbf{w}}_h \cdot \boldsymbol{n})) \, \xi = 0 \,.$$

Replacing the numerical traces using equation (4.23), we have:

$$\int_F \Big(\lambda_2 + \mathbf{X}_4(\boldsymbol{\lambda}_1 \cdot \boldsymbol{n}) + \mathbf{X}_5\Big((\mathbf{w}_h \cdot \boldsymbol{n}) - (\mathrm{p}_h - \lambda_2)(\boldsymbol{S}_2 \cdot \boldsymbol{n}) \cdot \boldsymbol{n} - \boldsymbol{S}_4(\mathbf{u}_h - \boldsymbol{\lambda}_1) \cdot \boldsymbol{n}\Big)\Big)\, \xi = 0\,.$$

The equation is discretized on (x, y) and the local solutions and Lagrange operators are expressed with (4.26a) and (4.26b).

$$\int_F \underline{\lambda}_2^{\beta(K,f)} \psi_j^{\beta(K,f)} \psi_i^{\beta(K,f)} + \int_F \mathbf{X}_4 (\underline{\lambda}_{1x}^{\beta(K,f)} n_x + \underline{\lambda}_{1y}^{\beta(K,f)} n_y) \psi_j^{\beta(K,f)} \psi_i^{\beta(K,f)} + \int_F \mathbf{X}_5 (\underline{\mathrm{w}}_x^K n_x + \underline{\mathrm{w}}_y^K n_y) \varphi_j^K \psi_i^{\beta(K,f)}$$

$$- \int_F \mathbf{X}_5\, \gamma_2 \underline{\mathrm{p}}^K\, (n_x^2 + n_y^2)\, \varphi_j^K\, \psi_i^{\beta(K,f)} dS + \int_F \mathbf{X}_5\, \gamma_2 \underline{\lambda}_2^{\beta(K,f)}\, (n_x^2 + n_y^2)\, \psi_j^{\beta(K,f)}\, \psi_i^{\beta(K,f)} dS$$

$$- \int_F \mathbf{X}_5\, \gamma_4\, (\underline{\mathrm{u}}_x^K n_x + \underline{\mathrm{u}}_y^K n_y)\, \varphi_j^K\, \psi_i^{\beta(K,f)} dS + \int_F \mathbf{X}_5\, \gamma_4\, (\underline{\lambda}_{1x}^{\beta(K,f)} n_x + \underline{\lambda}_{1y}^{\beta(K,f)} n_y)\, \psi_j^{\beta(K,f)}\, \psi_i^{\beta(K,f)} dS = 0\,.$$

Using the elementary matrices defined in (4.28), we obtain:

$$\mathbb{G}^{\beta(K,f)} \underline{\lambda}_2^{\beta(K,f)} + \mathbb{H}_x^{\beta(K,f)} \mathbf{X}_4 \underline{\lambda}_{1x}^{\beta(K,f)} + \mathbb{H}_y^{\beta(K,f)} \mathbf{X}_4 \underline{\lambda}_{1y}^{\beta(K,f)} + (\mathbb{Q}_x^{\beta(K,f)})^T \mathbf{X}_5 \underline{\mathrm{w}}_x^K$$

$$+ (\mathbb{Q}_y^{\beta(K,f)})^T \mathbf{X}_5 \underline{\mathrm{w}}_y^K - (\mathbb{F}^{\beta(K,f)})^T \mathbf{X}_5\, \gamma_2 \underline{\mathrm{p}}^K + \mathbb{G}^{\beta(K,f)} \mathbf{X}_5\, \gamma_2 \underline{\lambda}_2^{\beta(K,f)} - (\mathbb{Q}_x^{\beta(K,f)})^T \mathbf{X}_5 \gamma_4\, \underline{\mathrm{u}}_x^K$$

$$-(\mathbb{Q}_y^{\beta(K,f)})^T \mathbf{X}_5 \gamma_4\, \underline{\mathrm{u}}_y^K + \mathbb{H}_x^{\beta(K,f)} \mathbf{X}_5 \gamma_4\, \underline{\lambda}_{1x}^{\beta(K,f)} + \mathbb{H}_y^{\beta(K,f)} \mathbf{X}_5 \gamma_4\, \underline{\lambda}_{1y}^{\beta(K,f)} = 0\,.$$

The corresponding elementary matrices $\mathbb{P}^K$ and $\mathbb{T}^K$ are given in Appendix C.1.1.

4.5 HDG method with PML

In this section, we apply a Perfectly Matched Layer (PML) to the discretization of poroelastic equations (1.16) using the HDG method, taking $\mathfrak{s} = 1$. Note that the PML can be applied both for isotropic and anisotropic materials, thus we present the anisotropic poroelastic equations. Generally the PML can be unstable in the anisotropic case, however, in the DG methods, instabilities of the PML can also be observed in the isotropic case. The perfectly matched layer is an artificial absorbing layer on the edges of the computational domain, see Figure 4.25. It prevents the reflections on the artificial boundaries. In the formulation, we use two absorbing functions α and β that represent the attenuation of the wave in the absorbing layer. The attenuation functions α and β are taken equal to zero outside of the absorbing layers. Taking $\partial\Omega$ the interface between the geophysical domain and the PML, the value of the attenuation functions in the PML increases with the distance to $\partial\Omega$. In practice, we replace the derivatives

$$\frac{\partial}{\partial x} \to \frac{i\,\omega}{i\,\omega + \alpha(x)} \frac{\partial}{\partial x}\,, \qquad \text{and} \qquad \frac{\partial}{\partial y} \to \frac{i\,\omega}{i\,\omega + \beta(y)} \frac{\partial}{\partial y}\,.$$

We consider a two-dimensional porous domain Ω with the boundary Γ on the plane (x, y). The fields ($\mathbf{u}$, $\mathbf{w}$, $\boldsymbol{\tau}$, p) solve the poroelastic equations (1.16) in Ω. We consider a triangulation $\mathcal{T}_h$ of Ω, and $\mathcal{F}_h$ the set of all the faces. K is a triangle element of $\mathcal{T}_h$ and F is a face of K. We use the approximation spaces defined in Section 4.4. The local unknowns ($\mathbf{u}_h$, $\mathbf{w}_h$, $\boldsymbol{\tau}_h$, p_h) $\in (\boldsymbol{V}_h^p \times \boldsymbol{V}_h^p \times \boldsymbol{\Sigma}_h^p \times V_h^p)$ solve the poroelastic equations (1.16) on $\mathcal{T}_h$. The HDG discretization of the poroelastic equations (1.16) is modified. However, as the discretization of the equations does not present additional difficulties to the one described in Chapter 3, we detail the rest of the HDG method with PML in Appendix C.1.2. On the boundaries of the mesh, we can set either a condition of type 1 or 3, hence, the boundary conditions are not modified and stay the same as the ones used in HDG method with no PML, see Chapter 3.

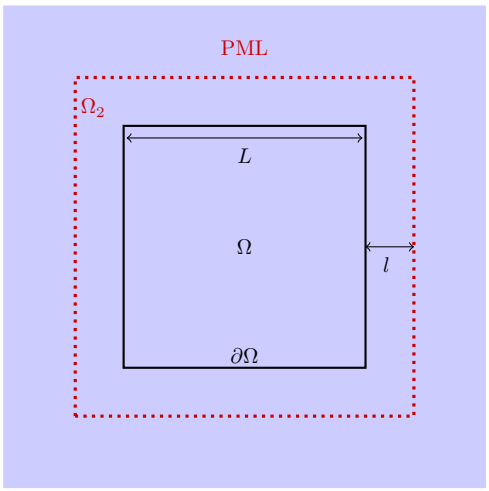

Figure 4.25: Illustration of the PML.

4.6 Numerical tests using HDG discretization

This section aims at evaluating the performance of the HDG discretization of poroelastic equations with radiation boundary conditions or PML, which are detailed in Sections 4.4 and 4.5. We first consider the influence of the geometry of the domain on the result of the numerical solution with radiation boundary conditions in Section 4.6.1. Then, in Section 4.6.2, we compare the two methods, radiation boundary conditions and PML, using reference solutions, for several configurations. Finally, in Section 4.6.3, we illustrate the wave propagation in a stratified porous domain by decomposing the waves. We also consider the configuration of an anisotropic material.

4.6.1 Influence of the geometry of the domain for the RBC

In this section, we test the accuracy of the HDG discretization with radiation boundary conditions. The boundary conditions have been developed for a circular geometry, and we want to test if those radiation boundary conditions remain efficient on a different geometry. We consider an infinite porous medium, in which there is a solid obstacle, and we set artificial boundaries, in one case, circular boundaries, and in the second case square boundaries. We run a test on an annulus described in figure 4.1, and for a square with a hole, see Figure 4.28. The solutions are displayed in Figure 4.27.

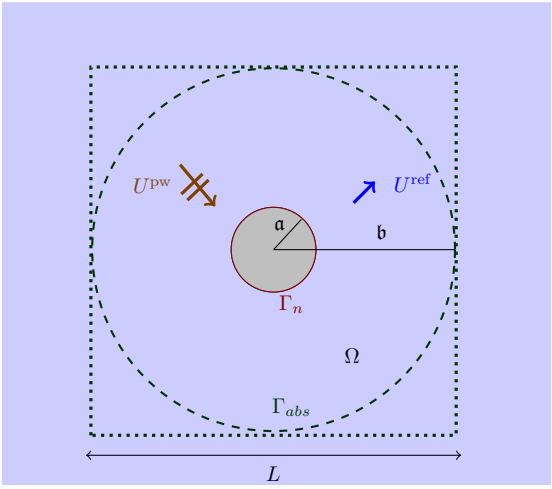

Figure 4.26: Computational domain used for the scattering of a plane wave by an impenetrable solid immersed in a porous medium. The cross section of the inclusion is a disc of radius denoted by $\mathfrak{a}$. The artificial boundaries are imposed either on the circle $r = \mathfrak{b}$ or on the square of length L.

For the numerical tests, we use $\mathfrak{a} = 1$m and $\mathfrak{b} = 10$m, $L = 20$m (see Figure 4.26). For a porous medium composed

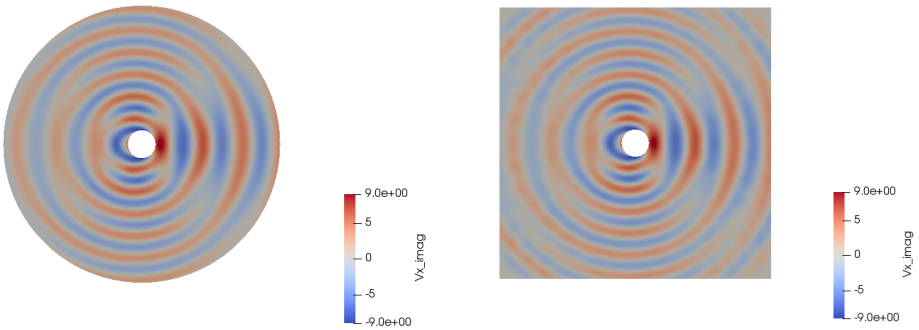

(a) $\mathfrak{b} = 10$m (b) $\mathfrak{b} = 10$m

Figure 4.27: Imaginary part of the solid velocity u_x (m.s^{-1}) of the reflected wave for radiation boundary conditions for a porous medium composed of inviscid sandstone with $f = 1.5$ kHz and boundary conditions 3 for two different domains, with $\mathfrak{a} = 1$m and $\mathfrak{b} = 10$m, $L = 20$m.

of sandstone at $f = 1$kHz, we compare the L^2 error of the solution for an order of discretization 3, for different values of viscosity and for the boundary conditions of type 1 and 3 on Γ_n. We compare the L^2 error between the reference solution and the results with HDG for an annulus, and for a square with a hole, *cf.* Table 4.2.

BC1	Square	Annulus
$\eta = 0$ Pa.s^{-1}	7.70	3.03
$\eta = 10^{-3}$ Pa.s^{-1}	6.09	2.16

BC3	Square	Annulus
$\eta = 0$ Pa.s^{-1}	8.26	4.00
$\eta = 10^{-3}$ Pa.s^{-1}	6.53	2.75

Table 4.2: L^2 relative error (%) on the solid velocity between the reference solution with radiation conditions and the numerical solution with order of discretization 3 for $\eta = 0$ Pa.s^{-1} and $\eta = 10^{-3}$ Pa.s^{-1}. We display the solution for the scattering of a P plane wave for boundary conditions of type 1 and 3, with $\mathfrak{a} = 1$m and $\mathfrak{b} = 10$m, $L = 20$m.

As expected, for a circular geometry, the discretization of radiation boundary conditions is efficient. For a square geometry, the radiation boundaries remain efficient, however, the error is greater than for circular geometry, (see Tab. 4.2). We also observe in the table that the presence of viscosity improves the accuracy of the solution. The error is between 5 and 10%, which is comparable to the results for the LK condition in elasticity ([93, Tabs. 7,8]).

4.6.2 Comparison of HDG methods using RBC or PML

In this section, we compare the two methods of boundary conditions that we have presented in Sections 4.4 and 4.5 : low order RBC and PML applied on the HDG discretization. In the code, we use for the absorption functions (see Section 4.5): $\alpha(x) = \beta_0\, d(x)$ and $\beta(y) = \beta_0\, d(y)$, with d the horizontal or vertical distance between the considered point and the artificial boundary. First, we compare the results on a square domain with an impenetrable obstacle, then we consider a domain composed of two porous layers.

4.6.2.1 Square with a hole

We consider an infinite porous medium, with a solid inclusion Γ, see Figure 4.28. Here, the artificial boundary is a square. For the two different cases, PML or radiation boundary conditions, an incident wave is scattered by the obstacle, and we study the reflected solution. In this case, we can compare the solution with the outgoing solution. Figure 4.29 shows the solution with the two different radiation conditions. In Table 4.3, we present the L^2 error between the solution with radiation boundary conditions and the exact outgoing solution. We denote "RBC" the solution with radiation boundary conditions, "PML" the solution with PML on the boundaries, and "exact" the outgoing solution. Note that the error is calculated only on the part of the domain where the original one is actually solved and which coincides with the domain used for the case with radiation boundary conditions.

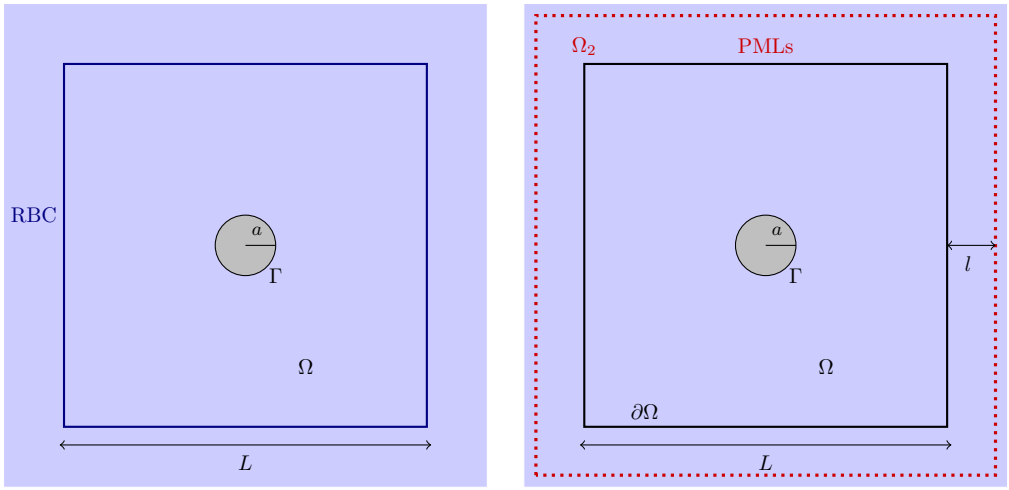

(a) Domain with RBC

(b) Domain with PML

Figure 4.28: Infinite porous domain with a solid obstacle used for the numerical tests, in which we build radiation boundary conditions. In the tests, we take: $a = 1$m, $L = 20$m, $\beta_0 = 6.39$, and $l = 3$m or $l = 6$m. We can use either PML or RBC.

BC1	RBC	PML $l = 3$m	PML $l = 6$m
$\eta = 0$ Pa.s^{-1}	7.70	10.8	3.65
$\eta = 10^{-3}$ Pa.s^{-1}	6.09	9.82	2.8

BC3	RBC	PML $l = 3$m	PML $l = 6$m
$\eta = 0$ Pa.s^{-1}	8.26	9.52	3.81
$\eta = 10^{-3}$ Pa.s^{-1}	6.53	8.72	2.78

Table 4.3: L^2 error (%) on u_x between the reference solution with radiation conditions and the numerical solution for $\eta = 0$ Pa.s^{-1} and $\eta = 10^{-3}$ Pa.s^{-1}. We display the error for the scattering of a P plane wave for boundary conditions of type 1 and 3 on the interior radius.

	RBC	PML $l = 3$m	PML $l = 6$m
Number of edges	10974	17448	25581
Number of dof	43896	69792	102324

Table 4.4: Number of degrees of freedom for the three cases shown in Figure 4.29, with interpolation order equals to 3.

We observe from Table 4.3 that the PML solution with $l = 3$m generates slightly greater errors than radiation boundary conditions and needs more computational time. However, when the size of the layer increases, ($l = 6$m), the error is lower than for the solution with RBC. It also leads to an important increase of the computational time because we need to compute the solution on a larger domain (see Tab. 4.4).

4.6.2.2 Stratified domain

Secondly, we investigate the case of a two-layered stratified plane domain. We consider the configuration detailed in Figure 4.30, with the material parameters given in Table 4.5. A point-source is located in the upper medium of the domain. In Figure 4.30(a), we use radiation boundary conditions on the border of the mesh. In Figure 4.30(b), we add PML on the borders of the domain. Table 4.5 gives the size of the linear system solved by the program. The size of discretization is the same in both meshes. The solutions are presented in Figure 4.31.

Figures 4.31, 4.31(a) and 4.31(b) present similar results in the region outside of the PML. In figure 4.31(b) all the waves are absorbed in the PML region. However, in Figure 4.31(c), with a different value of absorption parameter, the waves are not absorbed in the PML, and we observe many reflections that worsen the accuracy of the solution. Moreover, Figure 4.31(d) shows that for high values of the absorbing coefficients, the energy in the PML explodes. Indeed, the size of the layer and the value of the coefficient of absorption can have an impact on the accuracy of the

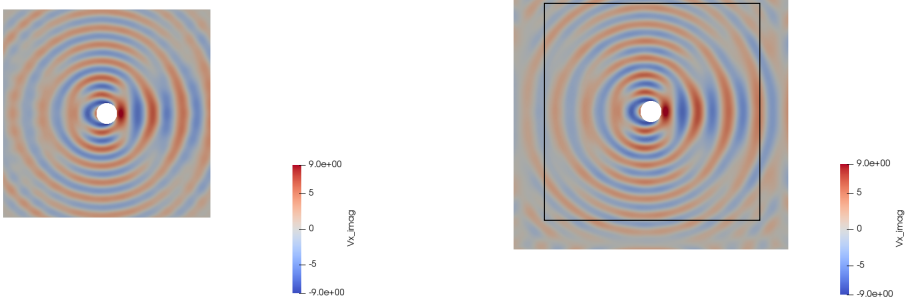

(a) RBC

(b) PML $l = 3$m

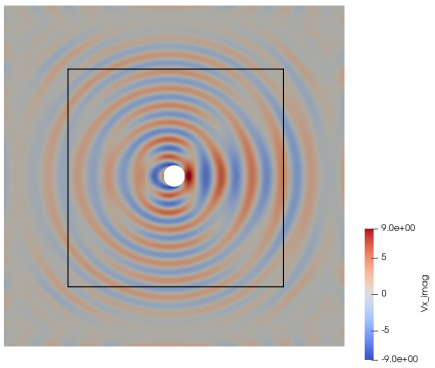

(c) PML $l = 6$m

Figure 4.29: Imaginary part of the solid velocity u_x (m.s^{-1}) of the reflected wave for the scattering of a P-wave on an obstacle with boundary conditions 3 at the interior radius, for a porous medium composed of inviscid sandstone with $f = 1.5$ kHz for a domain with radiation boundary condition and a domain with PML.

	RBC	PML
Number of edges	9380	15949
Number of dof	37520	63796

Table 4.5: Number of degrees of freedom for the cases shown in Fig 4.31, with interpolation order equal to 3.

solution, and the values of these parameters depend on the configuration of the test.

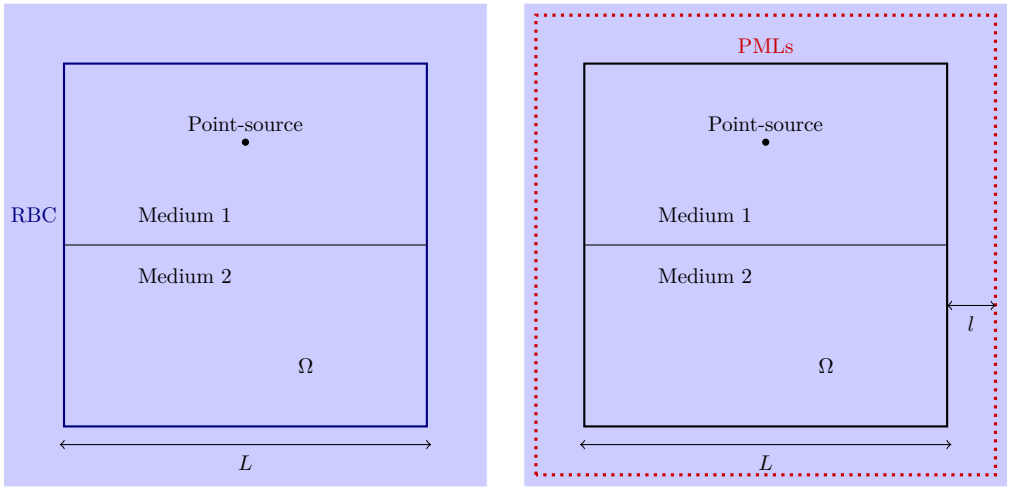

(a) Domain with RBC

(b) Domain with PML

Figure 4.30: Stratified porous domain used for the numerical tests, in which we build radiation boundary conditions. Here, the upper medium is composed of shale while the lower medium is composed of sandstone. The parameters of the media are detailed in Table 3.1. In the tests, we take: $L = 20\text{m}$, $l = 3\text{m}$.

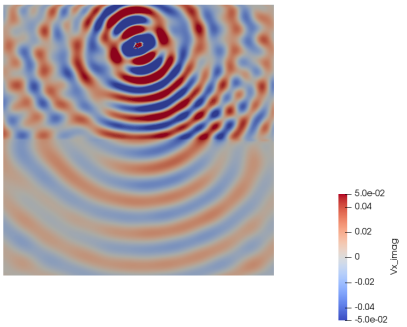

(a) RBC

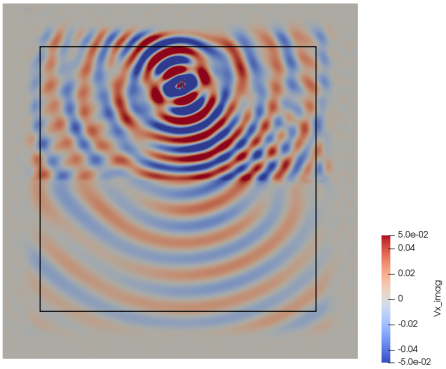

(b) PML with $\beta_0 = 6.4$

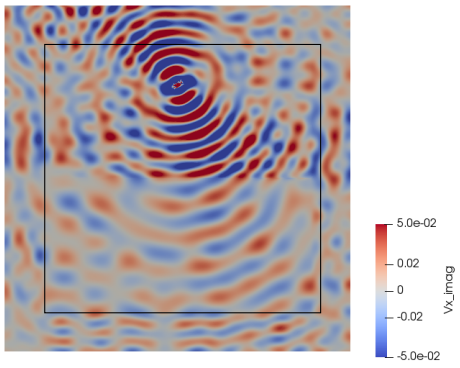

(c) PML with $\beta_0 = 0.1$

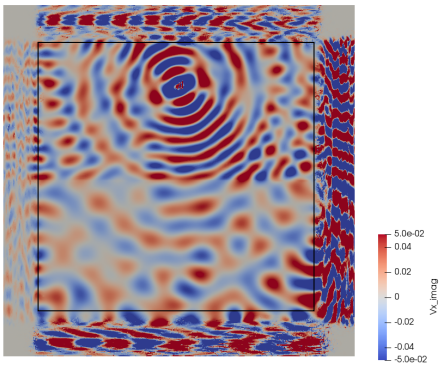

(d) PML with $\beta_0 = 64$

Figure 4.31: Imaginary part of the solid velocity u_x ($m.s^{-1}$) of the reflected wave for a porous medium composed of inviscid sandstone with $f = 1$ kHz for a domain with radiation boundary conditions and for domain with PML with different values of the absorbing coefficient.

4.6.3 Three layered domain

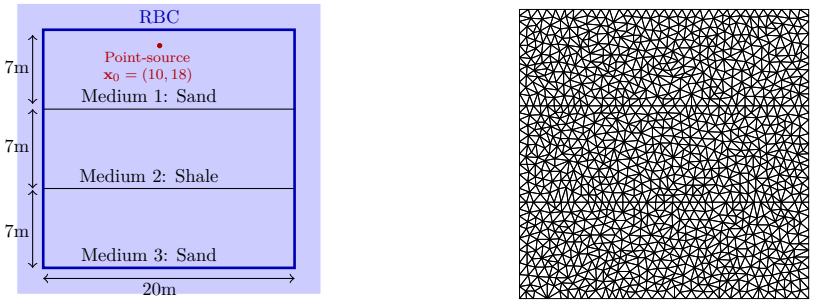

(a) Domain (b) Mesh

Figure 4.32: Domain and mesh used for the three layers test. The parameters of the three media are detailed in Table 3.1.

In this section we apply the HDG method to a stratified geophysical medium composed of three horizontal layers made up of different materials. The domain and the mesh used for this test are shown in Figure 4.32. On the boundary of the domain, we impose the RBC that was constructed in Section 4.1. The velocities and wavelengths $\lambda = \frac{v}{f}$, of the three types of waves in the sand and the shale are given in Table 4.6 for frequency $f = 500$Hz.

Physical parameters	Sand	Shale
$\mathrm{v_P}$ $(\mathrm{m.s^{-1}})$	$(1.88\,10^3,\ 10.4)$	$2.48\,10^3$
$\mathrm{v_S}$ $(\mathrm{m.s^{-1}})$	$(4.93\,10^2,\ 3.76)$	$1.43\,10^3$
$\mathrm{v_B}$ $(\mathrm{m.s^{-1}})$	$(2.57\,10^2,\ 57.9)$	$1.13\,10^3$
λ_P (m)	3.76	4.96
λ_S (m)	0.987	2.86
λ_B (m)	0.562	2.03

Table 4.6: Velocities and wavelengths for $f = 500$Hz in the materials in consideration for the test described in 4.32.

Regarding the external source, we consider a point-source at position $\mathbf{x}_0 \in \mathbb{R}^2$, modeled by Dirac-type distributions $\boldsymbol{\mathcal{E}}'$ acting on smooth vector-valued test functions in $\boldsymbol{\mathcal{E}} := (\mathcal{C}^\infty)^2$. In (1.16), we first consider the problem with $\mathbf{f}_u = \nabla\,\delta_0(\mathbf{x} - \mathbf{x}_0)$, which corresponds to a source in longitudinal waves (P,B). We then consider the problem with $\mathbf{f}_u = \nabla \times \delta(\mathbf{x} - \mathbf{x}_0)$ to have a source in transverse wave S. The actions of these distributions are defined, for $\mathbf{v} = (v_x, v_y)^T \in \boldsymbol{\mathcal{E}}$,

$$\langle \nabla\,\delta(\mathbf{x} - \mathbf{x}_0)\,,\,\mathbf{v}\rangle_{\boldsymbol{\mathcal{E}}',\boldsymbol{\mathcal{E}}} \;=\; -\,(\nabla\cdot\mathbf{v})\,(\mathbf{x}_0) \quad , \quad \langle \nabla\times\,\delta(\mathbf{x} - \mathbf{x}_0)\,,\,\mathbf{v}\rangle_{\boldsymbol{\mathcal{E}}',\boldsymbol{\mathcal{E}}} \;=\; -\,(\partial_x v_y \,-\, \partial_y v_x)\,(\mathbf{x}_0)\,. \tag{4.31}$$

The results due to the point sources in (4.31) using an interpolation order of 6 are given in Figure 4.33. For the case of longitudinal waves, in Figure 4.33(a) and 4.33(b), we observe both B and P waves in the upper layer around the source. On the solid velocity, we observe mainly the P wave in layers 2 and 3, with the B wave mostly absorbed. However, we can observe the presence of the B wave on the relative fluid velocity in the middle layer. For the case with a source in transverse wave in Figure 4.35(b), we mainly observe the S wave in the three layers. From these initial observations, we use the following procedure to separate and highlight the three waves. In order to show the transverse wave, we display in Figure 4.34(c) and 4.35(c) the curl of the solid velocity,

$$\mathsf{W}_\mathrm{S} \;:=\; \mathrm{curl}\,\mathbf{u} \;=\; \partial_x \mathrm{u}_y \,-\, \partial_y \mathrm{u}_x\,. \tag{4.32}$$

Regarding the longitudinal waves, in order to eliminate the B wave and keep the P wave, we compute the quantity

$$\mathsf{W}_\mathrm{P} \;:=\; \nabla\cdot\mathbf{w} \,-\, \beta_\mathrm{B}\,\nabla\cdot\mathbf{u}\,. \tag{4.33}$$

This is shown in Figure 4.34(a) and 4.35(a). Similarly, to keep the B wave and eliminate the P one, in Figure 4.34(b) and 4.35(b), we compute

$$\mathsf{W}_\mathrm{B} \;:=\; \nabla\cdot\mathbf{w} \,-\, \beta_\mathrm{P}\,\nabla\cdot\mathbf{u}\,. \tag{4.34}$$

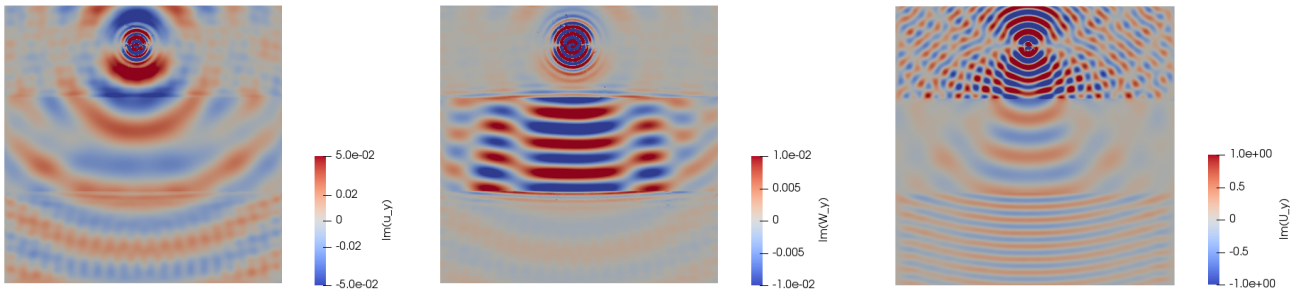

(a) u_y with $\mathbf{f}_u = \nabla(\delta_0(\mathbf{x}-\mathbf{x}_0))$ (b) w_y with $\mathbf{f}_u = \nabla(\delta_0(\mathbf{x}-\mathbf{x}_0))$ (c) u_y with $\mathbf{f}_u = \nabla\times(\delta_0(\mathbf{x}-\mathbf{x}_0))$

Figure 4.33: Vertical component of solid velocity u_y and relative fluid velocity w_y on three layers domain for two types of point source at frequency $f = 500$Hz. For Figures (a) and (b), in the lowest layer, we observe 2 wavelengths in a vertical space of 7 meters, which means that the wavelength λ is approximately 3.5m and agrees with that of P wave, cf. Table 4.6. In Figure (c), the lowest layer contains 7 wavelengths within a depth of 7m, which means that λ is approximately 1m, and thus corresponds to that of S wave, cf. Table 4.6. The resolution of the global system takes 6.90 seconds (CPU time), and it needs 659 MB of memory to solve the global system.

As expected, Figure 4.34(a) illustrates the fact that the longitudinal source generates mostly P and B waves with a

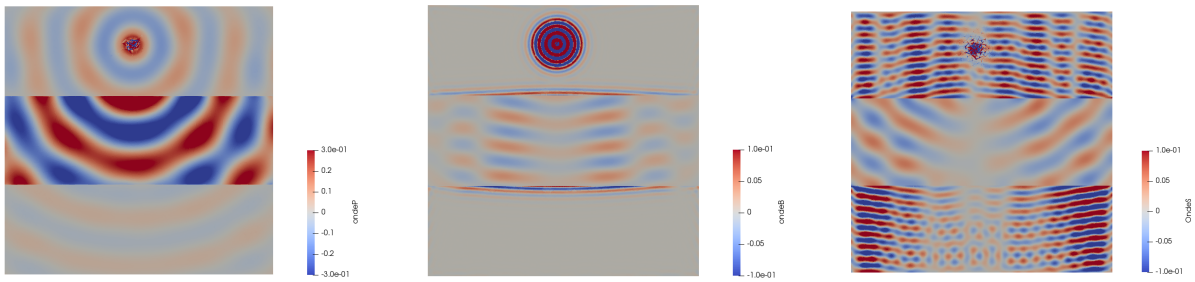

(a) P wave W_{P} defined in (4.33) (b) B wave W_{B} defined in (4.34) (c) S wave W_{S} defined in (4.32)

Figure 4.34: Illustration of the three waves for the source $\mathbf{f}_u = \nabla\,\delta_0(\mathbf{x}-\mathbf{x}_0)$ at frequency $f = 500$Hz. In Figure 4.34(b), B-wave W_{B} is seen around the source and but is mostly absorbed in the first layer. We see its reflection on the interfaces. The B-wave propagates in the second layer because there is no absorption, but is absorbed in the third layer. For the S-wave, we observe an artifact at the position of the source which contains only the longitudinal waves.

small S waves artifact. The attenuation acts mostly on the B wave, which is damped before reaching the first interface. On the contrary, the P wave is not damped and generates transmitted P, B and S waves in the second layer and reflected waves in the first layer. The reflected P wave is barely visible, hidden by the incident P wave, while the reflected B wave is almost immediately damped. Only the reflected S wave is visible. The three transmitted waves propagate without attenuation in the second layer and generate transmitted waves in the third layer. Once again, the transmitted B wave is damped while the S and B waves propagate to the boundary of the domain. Note the efficiency of the radiation boundary conditions for this test case. In Figure 4.35(b), we see that, as expected, the source produces almost only S waves which generate mostly transmitted P and B waves at the interface with the second layer and reflected B waves at the top boundary. These latter decay rapidly, due to the attenuation.

Comparison with anisotropic material: Here, we still consider the stratified geophysical medium composed of three horizontal layers of different materials. However, we modify the composition of the upper layer which is now anisotropic sand, whose characteristic parameters are given in Table 3.1. On the boundary of the computational domain, since the radiation condition in Section 4.1 was obtained under the assumption that the medium is isotropic, we truncate the domain with a PML. The corresponding domain is shown in Figure 4.36(a). The results of this

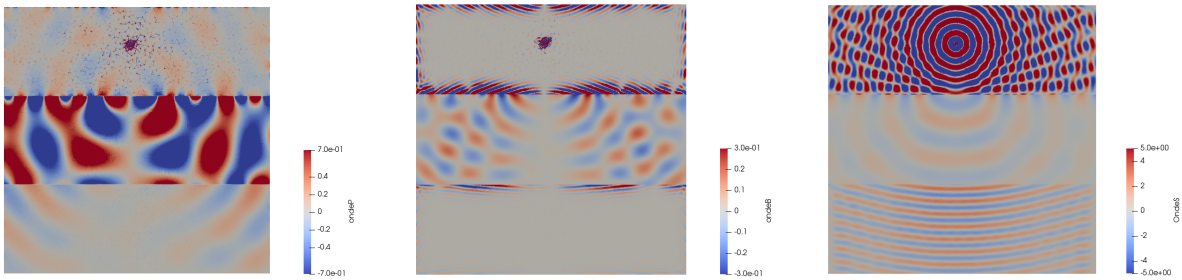

(a) P wave W_{P} defined in (4.33) (b) B wave W_{B} defined in (4.34) (c) S wave W_{S} defined in (4.32)

Figure 4.35: Illustration of the three waves with W_{P}, W_{B}, and W_{S}, defined in (4.33), (4.34), and (4.32) respectively, for the source $\mathbf{f}_u = \nabla \times (\delta(\mathbf{x} - \mathbf{x}_0))$, which corresponds to a source in transverse wave. The solution is given for frequency $f = 500$Hz. As the source is a S-wave, for Figures 4.35(a) and 4.35(b), it should not generate longitudinal waves in the upper layer, however we observe a numerical artifact at the location of the source. However, at the interfaces, with the reflections, P and B-waves appear and propagate in the material. The S-wave is reflected on the boundary of the first layer which is converted into pressure waves. In the second layer, the B-wave propagates and is not absorbed. The S wave propagates correctly around the source and in the three layers.

experiment are given in Figure 4.36(c) and can be compared with Figure 4.36(b) which corresponds to the case where the upper layer is filled with isotropic sand.

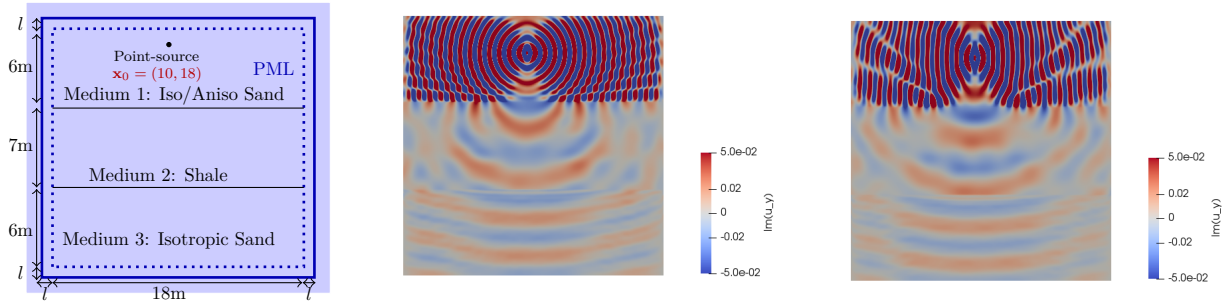

(a) Computational domain with $l = 1$m (b) u_y with isotropic sand (c) u_y with anisotropic sand

Figure 4.36: Vertical component of solid velocity u_y in a three layered domain with a point source $\mathbf{f}_u = (\delta_0(\mathbf{x} - \mathbf{x}_0))\,\mathbf{e}_y$ at frequency $f = 500$Hz, for two different kind of media in the top layer.

In figure 4.36(c), we observe that in the upper layer, the wavefront has an elliptical shape which is characteristic of an anisotropic phenomenon, whereas the wavefront is indeed circular in figure 4.36(b). The shape of the wavefront, more stretched in the vertical direction, indicates that the velocity of the wave is greater in this direction than in the other. This observation is consistent with the fact that the number of wavelengths propagated in the horizontal direction is greater in anisotropic sand than in isotropic sand. This experiment also shows that the simulation remains stable with the introduction of anisotropy. Moreover, the PML does not seem to generate more reflections in the anisotropic medium than in the isotropic medium. It can also be observed that the signal in the deepest layer of Figure 4.36(c) is very close to that of Figure 4.36(b). The difference is more noticeable in the second layer but not very important.

4.7 Extension to three dimensions

We consider a three-dimensional domain $\mathcal{D}$, with $\boldsymbol{n}$ the outgoing unit normal vector and $\mathbf{t}$, $\mathbf{a}$ the unit tangential vectors to the surface. We propose the extension in 3D of the RBC as:

$$\begin{cases} \boldsymbol{\tau}\,\boldsymbol{n} + \big(\mathbf{X}_1(\mathbf{u}\cdot\boldsymbol{n}) + \mathbf{X}_2(\mathbf{w}\cdot\boldsymbol{n})\big)\,\boldsymbol{n} + \mathbf{X}_3(\mathbf{u}\cdot\mathbf{t})\,\mathbf{t} + \mathbf{X}_3(\mathbf{u}\cdot\mathbf{a})\,\mathbf{a} = 0\,, \\ \mathrm{p} + \mathbf{X}_4(\mathbf{u}\cdot\boldsymbol{n}) + \mathbf{X}_5(\mathbf{w}\cdot\boldsymbol{n}) \;= 0\,. \end{cases} \tag{4.35}$$

We present in Appendices C.2.3 and C.3 the HDG method using respectively the RBC and the PML in three dimensions. In the following, we illustrate the HDG method using the absorbing boundary condition and the PML in three dimensions. We consider a domain $\mathcal{D}$ of size $[0:10]\times[0:2]\times[0:10]$m. This domain, described in Figure 4.37, is composed of two horizontal layers of poroelastic materials. The top layer is composed of shale, and the bottom layer of sandstone. The physical parameters of those materials are detailed in Table 3.1.

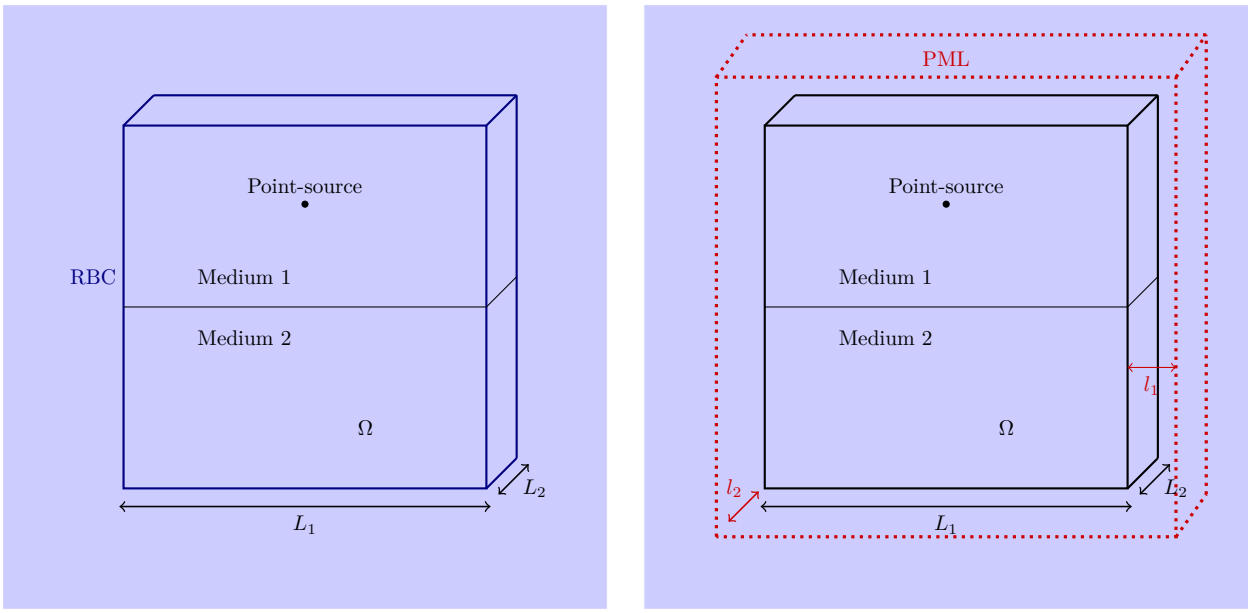

(a) Domain with RBC

(b) Domain with PML

Figure 4.37: Stratified domain used for the numerical tests, in which we set artificial boundaries. Here, the upper medium is composed of shale while the lower medium is composed of sandstone. The parameters of the media are detailed in Table 3.1. In the tests, we set: $L_1 = 10$m, $L_2 = 2$m, $l_1 = 2$m, and $l_2 = 1$m.

On the border of the computational domain, we set artificial boundaries. In a first time, we set absorbing boundary conditions. In this case, the domain $\mathcal{D}$ is discretized in an ustructured mesh composed of 22274 tetrahedra. Secondly, we add PML to the domain, and we use a mesh of 81250 tetrahedra for the computation. Note that this increase of degrees of freedom causes an important increase of memory used for the computation and computational time. For the external source, we consider a point-source at position $\mathbf{x}_0 = (5, 1, 7.5)$m, modeled by Dirac-type distributions. The fields $\mathbf{u}$, $\mathbf{w}$, $\boldsymbol{\tau}$, p solve equations (4.1) in $\mathcal{D}$, with $\mathbf{f}_u = \begin{pmatrix} 0 \\ 0 \\ \delta_0(\mathbf{x}-\mathbf{x}_0) \end{pmatrix}$. The results for the two configurations are given in Figure 4.38, with $f = 2$kHz, and an order of interpolation equal to 3. We observe that the results are similar for the two truncation methods and that the reflections are well-absorbed at the artificial boundaries.

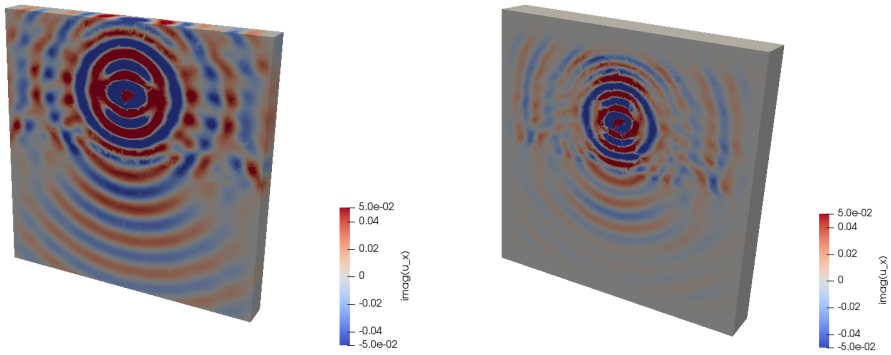

(a) RBC (b) PML

Figure 4.38: Horizontal component of solid velocity u_x on the layered domain for two types of artificial boundaries, for order of interpolation 3 at frequency $f = 2$kHz.

Conclusion

In this chapter, we have built a low-order radiation condition for isotropic poroelastic wave equations in the frequency domain. The performance of this RBC has been evaluated in two groups of numerical investigations. In the first one, in the setting of planewave scattering by circular obstacles, we compare how well the reference solution associated to the RBC approximates the restriction of the true outgoing solution on the truncated domain. We have an overall conclusion that our RBC has comparable robustness to LK for elasticity and to the Sommerfeld condition for the acoustic equation, in the sense that the error is less than 10 % for most cases. In the second investigation, the radiation condition has been implemented in a hybridizable dicontinuous Galerkin (HDG) formulation. We have also applied perfectly matched layers (PML) on the HDG discretization of the poroelastic equations. We then compare the performance of our RBC with the PML technique on different configurations. PML can be an alternative to the radiation condition, but its performance depends on parameters that are specific to each experiment. If the size of the PML is not large enough, the performance is deteriorated. To obtain better results than RBC, the PML can be taken larger but this raises the degrees of freedom and incurs substantial increase of the computational time, while the gain in accuracy is not considerable.

Appendix A

Appendices to Chapter 2

A.1 Detailed calculation for expansion in Bessel functions

A.1.1 Polar coordinates

A point in polar coordinates $(r,\, \theta)$ is defined with the distance of the point from the origin r and an angle θ. The coordinates are linked to Cartesian coordinates by:

$$x \,=\, r\,\cos\theta\,, \qquad \text{and} \quad y \,=\, r\,\sin\theta\,.$$

We define the unit vectors in the polar coordinate system,

$$\mathbf{e}_r \,=\, \begin{pmatrix}\cos\theta\\ \sin\theta\end{pmatrix}\,, \qquad \text{and} \quad \mathbf{e}_\theta \,=\, \begin{pmatrix}-\sin\theta\\ \cos\theta\end{pmatrix}\,.$$

In this system we decompose a vector $\mathbf{a}\in\mathbb{C}^2$ as

$$\mathbf{a} \,=\, \mathbf{a}_r\,\mathbf{e}_r \,+\, \mathbf{e}_\theta\,\mathbf{e}_\theta\,.$$

The tensor product of two vectors in polar coordinates is

$$\mathbf{a}\otimes\mathbf{b} \,=\, \mathbf{a}_r\mathbf{b}_r\;\mathbf{e}_r\otimes\mathbf{e}_r \,+\, \mathbf{a}_r\mathbf{b}_\theta\;\mathbf{e}_r\otimes\mathbf{e}_\theta \,+\, \mathbf{a}_\theta\mathbf{b}_r\;\mathbf{e}_\theta\otimes\mathbf{e}_r \,+\, \mathbf{a}_\theta\mathbf{b}_\theta\;\mathbf{e}_\theta\otimes\mathbf{e}_\theta$$

We also list the action of differential operators in polar coordinates. For a scalar f, we recall the notation of **curl** first in Cartesian coordinates,

$$\mathbf{curl}\, f \;=\; \begin{pmatrix}\partial_y f\\ -\partial_x f\end{pmatrix} \tag{A.1}$$

In polar coordinates, the action of **curl** and gradient ∇ are,

$$\mathbf{curl}\, f = \,\frac{1}{r}\,\partial_\theta f\,\mathbf{e}_r - \partial_r f\,\mathbf{e}_\theta\,, \quad \text{and} \quad \nabla f \,=\partial_r f\,\mathbf{e}_r + \,\frac{\partial_\theta}{r}\,\mathbf{e}_\theta\,. \tag{A.2}$$

We will also need the following second-order operators,

$$\begin{aligned}\nabla^2 f \,:=\, \nabla\,(\nabla f) &= \partial_r^2 f\,\mathbf{e}_r\otimes\mathbf{e}_r + \left(\frac{\partial^2_{r\theta} f}{r} - \frac{\partial_\theta f}{r^2}\right)\,\mathbf{e}_r\otimes\mathbf{e}_\theta + \left(\frac{\partial^2_{r\theta} f}{r} - \frac{\partial_\theta f}{r^2}\right)\,\mathbf{e}_\theta\otimes\mathbf{e}_r + \left(\frac{\partial^2_\theta f}{r} + \frac{\partial_r f}{r}\right)\,\mathbf{e}_\theta\otimes\mathbf{e}_\theta\,,\\ \nabla\,(\mathbf{curl} f) &= \left(\frac{\partial^2_{r\theta} f}{r} - \frac{\partial_\theta f}{r^2}\right)\,\mathbf{e}_r\otimes\mathbf{e}_r + \left(\frac{\partial^2_\theta f}{r^2} + \frac{\partial_r f}{r}\right)\,\mathbf{e}_r\otimes\mathbf{e}_\theta - \partial_r^2 f\,\mathbf{e}_\theta\otimes\mathbf{e}_r + \left(-\frac{\partial^2_{r\theta} f}{r} + \frac{\partial_\theta f}{r^2}\right)\,\mathbf{e}_\theta\otimes\mathbf{e}_\theta.\end{aligned} \tag{A.3a}$$

A.1.2 Calculations for a Bessel function

Denote by Z_k a Bessel function. Using the expressions in equation (A.2) for $\mathbf{u}$ and $\mathbf{w}$, we have:

$$\begin{aligned}\nabla\left(\mathrm{Z}_k(\tilde{\mathfrak{s}}\,\omega\,\mathsf{s}_\bullet\, r)e^{\mathrm{i}k\theta}\right) &= \tilde{\mathfrak{s}}\,\omega\,\mathsf{s}_\bullet \mathrm{Z}_k'(\tilde{\mathfrak{s}}\,\omega\,\mathsf{s}_\bullet\, r)e^{\mathrm{i}k\theta}\mathbf{e}_r + \frac{\mathrm{i}k}{r}\mathrm{Z}_k(\tilde{\mathfrak{s}}\,\omega\,\mathsf{s}_\bullet\, r)e^{\mathrm{i}k\theta}\mathbf{e}_\theta\,,\\ \mathbf{curl}\left(\mathrm{Z}_k(\tilde{\mathfrak{s}}\,\omega\,\mathsf{s}_\bullet\, r)e^{\mathrm{i}k\theta}\right) &= \frac{\mathrm{i}k}{r}\mathrm{Z}_k(\tilde{\mathfrak{s}}\,\omega\,\mathsf{s}_\bullet\, r)e^{\mathrm{i}k\theta}\;\mathbf{e}_r \;-\; \tilde{\mathfrak{s}}\,\omega\,\mathsf{s}_\bullet\;\mathrm{Z}_k'(\tilde{\mathfrak{s}}\,\omega\,\mathsf{s}_\bullet\, r)e^{\mathrm{i}k\theta}\mathbf{e}_\theta.\end{aligned}$$

To express the components of $\boldsymbol{\tau}$, we will need the calculations of $\nabla^2 f$ and $\nabla(\mathrm{curl} f)$, given in equation (A.3a). For $f = \mathrm{Z}_k(\tilde{\mathfrak{s}}\,\omega\,\mathsf{s}_\bullet\, r)\, e^{\mathrm{i}\,k\,\theta}$,

$$\partial_r^2 f \;=\; (\omega\,\mathrm{s}_\bullet)^2\;\mathrm{Z}_k''(\tilde{\mathfrak{s}}\,\omega\,\mathrm{s}_\bullet r)\;e^{\mathrm{i}\,k\,\theta}\,,\quad \partial_{r\theta} f \;=\; \tilde{\mathfrak{s}}\,\omega\,\mathrm{s}_\bullet\,\mathrm{i}\,k\;\mathrm{Z}_k'(\tilde{\mathfrak{s}}\,\omega\,\mathrm{s}_\bullet r)\;e^{\mathrm{i}\,k\,\theta}\,,\quad \partial_\theta^2 f \;=\; -k^2\;\mathrm{Z}_k(\tilde{\mathfrak{s}}\,\omega\,\mathrm{s}_\bullet r)\;e^{\mathrm{i}\,k\,\theta}\,.$$

Next we replace Z'', by using the ODE:

$$z^2\frac{d^2}{dz^2}\mathrm{Z} \;+\; z\frac{d}{dz}\mathrm{Z} \;+\; (z^2 \;-\; k^2)\mathrm{Z} = 0 \quad \Rightarrow \frac{d^2}{dz^2}\mathrm{Z}_k \;=\; -\frac{1}{z}\mathrm{Z}_k' \;-\; (1-\frac{k^2}{z^2})\mathrm{Z}_k\,.$$

Remark A.1. To completely eliminate the derivative, we can use the connection formula

$$\mathrm{Z}_k' = \mathrm{Z}_{k-1}(z) - \frac{k}{z}\mathrm{Z}_k(z) = -\mathrm{Z}_{k+1}(z) + \frac{k}{z}\mathrm{Z}_k(z)\,.$$

Hence, we have:

$$\begin{aligned}\frac{d^2}{dz^2}\mathrm{Z}_k \;&=\; -\frac{1}{z}\left(\mathrm{Z}_{k-1}(z) - \frac{k}{z}\mathrm{Z}_k(z)\right) \;-\; (1-\frac{k^2}{z^2})\mathrm{Z}_k(z)\\ &=\; -\frac{1}{z}\left(-\mathrm{Z}_{k+1}(z) + \frac{k}{z}\mathrm{Z}_k(z)\right) \;-\; (1-\frac{k^2}{z^2})\mathrm{Z}_k(z)\,.\end{aligned}$$

△

Here, we detail the expression of the stress components $\boldsymbol{\tau}_{rr}$ and $\boldsymbol{\tau}_{r\theta}$:

$$\begin{aligned}\omega^2\boldsymbol{\tau}_{rr} =\; & \mu_{\mathrm{fr}}\left(-\frac{2}{\mathsf{s}_{\mathrm{P}}^2}\,\partial_r^2\chi_{\mathrm{P}} \;-\; \frac{2}{\mathsf{s}_{\mathrm{B}}^2}\,\partial_r^2\chi_{\mathrm{B}} \;+2\frac{\partial_{r\theta}\,\chi_{\mathrm{S}}}{\mathsf{s}_{\mathrm{S}}^2 r}\right) + \omega^2\left(-\tfrac{2}{3}\mu_{\mathrm{fr}} \;+\; \mathrm{k}_{\mathrm{fr}} \;+\; M\alpha^2\right)\,(\chi_{\mathrm{P}} + \chi_{\mathrm{B}}) \;+\; \omega^2\alpha M\,(\mathcal{W}_{\mathrm{P}}\,\chi_{\mathrm{P}} + \mathcal{W}_{\mathrm{B}}\,\chi_{\mathrm{B}})\\
=\; & \sum_{k\in\mathbb{Z}}\Bigg[\;\mu_{\mathrm{fr}}\left(-2\,a_k\,\omega^2\,\mathrm{Z}_k''(\tilde{\mathfrak{s}}\,\omega\,\mathsf{s}_{\mathrm{P}}\,r)\;e^{\mathrm{i}\,k\,\theta} \;-\; 2\,b_k\,\omega^2\,\mathrm{Z}_k''(\tilde{\mathfrak{s}}\,\omega\,\mathsf{s}_{\mathrm{B}}\,r)\;e^{\mathrm{i}\,k\,\theta} \;+\; \frac{2}{\mathsf{s}_{\mathrm{S}} r}\,c_k\,\omega\,\tilde{\mathfrak{s}}\,\mathrm{i}k\,\mathrm{Z}_k'(\tilde{\mathfrak{s}}\,\omega\,\mathsf{s}_{\mathrm{S}}\,r)\;e^{\mathrm{i}\,k\,\theta}\right)\\
&\;+\; \omega^2\left(-\tfrac{2}{3}\mu_{\mathrm{fr}} \;+\; \mathrm{k}_{\mathrm{fr}} \;+\; M\alpha^2 \;+\; \alpha\,M\mathcal{W}_{\mathrm{P}}\right)\;\;a_k\,\mathrm{Z}_k(\tilde{\mathfrak{s}}\,\omega\,\mathsf{s}_{\mathrm{P}}\,r)\;e^{\mathrm{i}\,k\,\theta}\\
&\;+\; \omega^2\left(-\tfrac{2}{3}\mu_{\mathrm{fr}} \;+\; \mathrm{k}_{\mathrm{fr}} \;+\; M\alpha^2 \;+\; \alpha\,M\mathcal{W}_{\mathrm{B}}\right)\,b_k\,\mathrm{Z}_k(\tilde{\mathfrak{s}}\,\omega\,\mathsf{s}_{\mathrm{B}}\,r)\;e^{\mathrm{i}\,k\,\theta}\Bigg]\\
=\; & -\sum_{k\in\mathbb{Z}}\frac{2\,\mu_{\mathrm{fr}}\,\omega\,\tilde{\mathfrak{s}}}{\mathsf{s}_{\mathrm{P}}}\,a_k\,\mathrm{Z}_{k+1}(\tilde{\mathfrak{s}}\,\omega\,\mathsf{s}_{\mathrm{P}}\,r)\;e^{\mathrm{i}\,k\,\theta} \;+\sum_{k\in\mathbb{Z}}\frac{2\,\mu_{\mathrm{fr}}\,k}{\mathsf{s}_{\mathrm{P}}^2}\,a_k\,\mathrm{Z}_k(\tilde{\mathfrak{s}}\,\omega\,\mathsf{s}_{\mathrm{P}}\,r)\;e^{\mathrm{i}\,k\,\theta} \;+\sum_{k\in\mathbb{Z}}2\,\mu_{\mathrm{fr}}\,a_k\,\omega^2\,\mathrm{Z}_k(\tilde{\mathfrak{s}}\,\omega\,\mathsf{s}_{\mathrm{P}}\,r)\;e^{\mathrm{i}\,k\,\theta}\\
&-\sum_{k\in\mathbb{Z}}\frac{2\,\mu_{\mathrm{fr}}\,k^2}{\mathsf{s}_{\mathrm{P}}^2}\,a_k\,\mathrm{Z}_k(\tilde{\mathfrak{s}}\,\omega\,\mathsf{s}_{\mathrm{P}}\,r)\;e^{\mathrm{i}\,k\,\theta} - \sum_{k\in\mathbb{Z}}\frac{2\,\mu_{\mathrm{fr}}\,\omega\,\tilde{\mathfrak{s}}}{\mathsf{s}_{\mathrm{B}}}\,b_k\,\mathrm{Z}_{k+1}(\tilde{\mathfrak{s}}\,\omega\,\mathsf{s}_{\mathrm{B}}\,r)\;e^{\mathrm{i}\,k\,\theta} \;+\sum_{k\in\mathbb{Z}}\frac{2\,\mu_{\mathrm{fr}}\,k}{\mathsf{s}_{\mathrm{B}}^2}\,b_k\,\mathrm{Z}_k(\tilde{\mathfrak{s}}\,\omega\,\mathsf{s}_{\mathrm{B}}\,r)\;e^{\mathrm{i}\,k\,\theta}\\
&+\sum_{k\in\mathbb{Z}}2\,\mu_{\mathrm{fr}}\,b_k\,\omega^2\,\mathrm{Z}_k(\tilde{\mathfrak{s}}\,\omega\,\mathsf{s}_{\mathrm{B}}\,r)\;e^{\mathrm{i}\,k\,\theta} - \sum_{k\in\mathbb{Z}}\frac{2\,\mu_{\mathrm{fr}}\,k^2}{\mathsf{s}_{\mathrm{B}}^2}\,b_k\,\mathrm{Z}_k(\tilde{\mathfrak{s}}\,\omega\,\mathsf{s}_{\mathrm{B}}\,r)\;e^{\mathrm{i}\,k\,\theta} \;+\sum_{k\in\mathbb{Z}}\frac{2\,\mu_{\mathrm{fr}}}{\mathsf{s}_{\mathrm{S}}^2 r}\;c_k\,\omega\,\mathsf{s}_{\mathrm{S}}\,\mathrm{i}k\,\mathrm{Z}_k'(\tilde{\mathfrak{s}}\,\omega\,\mathsf{s}_{\mathrm{S}}\,r)\;e^{\mathrm{i}\,k\,\theta}\\
&+\sum_{k\in\mathbb{Z}}\omega^2\left(-\tfrac{2}{3}\mu_{\mathrm{fr}} \;+\; \mathrm{k}_{\mathrm{fr}} \;+\; M\alpha^2 \;+\; \alpha\,M\mathcal{W}_{\mathrm{P}}\right)\;\;a_k\,\mathrm{Z}_k(\tilde{\mathfrak{s}}\,\omega\,\mathsf{s}_{\mathrm{P}}\,r)\;e^{\mathrm{i}\,k\,\theta}\\
&+\sum_{k\in\mathbb{Z}}\omega^2\left(-\tfrac{2}{3}\mu_{\mathrm{fr}} \;+\; \mathrm{k}_{\mathrm{fr}} \;+\; M\alpha^2 \;+\; \alpha\,M\mathcal{W}_{\mathrm{B}}\right)\,b_k\,\mathrm{Z}_k(\tilde{\mathfrak{s}}\,\omega\,\mathsf{s}_{\mathrm{B}}\,r)\;e^{\mathrm{i}\,k\,\theta}\,,\end{aligned}$$

$$
\begin{aligned}
\omega^2\,\boldsymbol{\tau}_{r\theta} &= \mu_{\mathrm{fr}}\left(-\frac{2}{\mathsf{s}_{\mathrm{P}}^2}\left(\frac{\partial_{\theta r}}{r}\chi_{\mathrm{P}}-\frac{\partial_\theta}{r^2}\chi_{\mathrm{P}}\right)\;-\;\frac{2}{\mathsf{s}_{\mathrm{B}}^2}\left(\frac{\partial_{\theta r}}{r}\chi_{\mathrm{B}}-\frac{\partial_\theta}{r^2}\chi_{\mathrm{B}}\right)\;+\;\frac{1}{\mathsf{s}_{\mathrm{S}}^2}\left(\frac{\partial_{\theta\theta}}{r^2}\,\chi_{\mathrm{S}}+\frac{\partial_r}{r}\chi_{\mathrm{S}}\;-\;\partial_{rr}\,\chi_{\mathrm{S}}\right)\right)\\
&= \sum_{k\in\mathbb{Z}}\mu_{\mathrm{fr}}\left[-\frac{2}{\mathsf{s}_{\mathrm{P}}^2}\left(\frac{\omega\,\tilde{\mathfrak{s}}\,\mathsf{s}_{\mathrm{P}}\mathrm{i}\,k}{r}\,a_k\,\mathrm{Z}_k'(\tilde{\mathfrak{s}}\,\omega\,\mathsf{s}_{\mathrm{P}}\,r)\;e^{\mathrm{i}\,k\,\theta}-\frac{\mathrm{i}\,k}{r^2}\,a_k\,\mathrm{Z}_k(\tilde{\mathfrak{s}}\,\omega\,\mathsf{s}_{\mathrm{P}}\,r)\;e^{\mathrm{i}\,k\,\theta}\right)\right.\\
&\quad-\;\frac{2}{\mathsf{s}_{\mathrm{B}}^2}\left(\frac{\omega\,\tilde{\mathfrak{s}}\,\mathsf{s}_{\mathrm{B}}\mathrm{i}\,k}{r}\,b_k\,\mathrm{Z}_k'(\tilde{\mathfrak{s}}\,\omega\,\mathsf{s}_{\mathrm{B}}\,r)\;e^{\mathrm{i}\,k\,\theta}-\frac{\mathrm{i}\,k}{r^2}\,b_k\,\mathrm{Z}_k(\tilde{\mathfrak{s}}\,\omega\,\mathsf{s}_{\mathrm{B}}\,r)\;e^{\mathrm{i}\,k\,\theta}\right)\\
&\quad\left.+\;\frac{1}{\mathsf{s}_{\mathrm{S}}^2}\left(-\frac{k^2}{r^2}\,c_k\,\mathrm{Z}_k(\tilde{\mathfrak{s}}\,\omega\,\mathsf{s}_{\mathrm{S}}\,r)\;e^{\mathrm{i}\,k\,\theta}\;+\frac{\omega\,\tilde{\mathfrak{s}}\,\mathsf{s}_{\mathrm{S}}}{r}\,c_k\,\mathrm{Z}_k'(\tilde{\mathfrak{s}}\,\omega\,\mathsf{s}_{\mathrm{S}}\,r)\;e^{\mathrm{i}\,k\,\theta}\;-\;\omega^2\,\mathsf{s}_{\mathrm{S}}^2\,c_k\,\mathrm{Z}_k''(\tilde{\mathfrak{s}}\,\omega\,\mathsf{s}_{\mathrm{S}}\,r)\;e^{\mathrm{i}\,k\,\theta}\right)\right]\\
&= -\sum_{k\in\mathbb{Z}}\frac{2\,\mu_{\mathrm{fr}}\omega\,\tilde{\mathfrak{s}}\,\mathrm{i}\,k}{r\,\mathsf{s}_{\mathrm{P}}}\,a_k\,\mathrm{Z}_k'(\tilde{\mathfrak{s}}\,\omega\,\mathsf{s}_{\mathrm{P}}\,r)\;e^{\mathrm{i}\,k\,\theta}+\sum_{k\in\mathbb{Z}}\frac{2\,\mathrm{i}\,\mu_{\mathrm{fr}}\,k}{r^2\,\mathsf{s}_{\mathrm{P}}^2}\,a_k\,\mathrm{Z}_k(\tilde{\mathfrak{s}}\,\omega\,\mathsf{s}_{\mathrm{P}}\,r)\;e^{\mathrm{i}\,k\,\theta}\\
&\quad-\sum_{k\in\mathbb{Z}}\frac{2\,\mu_{\mathrm{fr}}\omega\,\tilde{\mathfrak{s}}\,\mathrm{i}\,k}{r\,\mathsf{s}_{\mathrm{B}}}\,b_k\,\mathrm{Z}_k'(\tilde{\mathfrak{s}}\,\omega\,\mathsf{s}_{\mathrm{B}}\,r)\;e^{\mathrm{i}\,k\,\theta}+\sum_{k\in\mathbb{Z}}\frac{2\,\mathrm{i}\,\mu_{\mathrm{fr}}\,k}{r^2\,\mathsf{s}_{\mathrm{B}}^2}\,b_k\,\mathrm{Z}_k(\tilde{\mathfrak{s}}\,\omega\,\mathsf{s}_{\mathrm{B}}\,r)\;e^{\mathrm{i}\,k\,\theta}\\
&\quad-\sum_{k\in\mathbb{Z}}\frac{\mu_{\mathrm{fr}}\,k^2}{r^2\,\mathsf{s}_{\mathrm{S}}^2}\,c_k\,\mathrm{Z}_k(\tilde{\mathfrak{s}}\,\omega\,\mathsf{s}_{\mathrm{S}}\,r)\;e^{\mathrm{i}\,k\,\theta}\;+\sum_{k\in\mathbb{Z}}\frac{\mu_{\mathrm{fr}}\,\omega\,\tilde{\mathfrak{s}}}{r\,\mathsf{s}_{\mathrm{S}}}\,c_k\,\mathrm{Z}_k'(\tilde{\mathfrak{s}}\,\omega\,\mathsf{s}_{\mathrm{S}}\,r)\;e^{\mathrm{i}\,k\,\theta}\\
&\quad-\sum_{k\in\mathbb{Z}}\mu_{\mathrm{fr}}\,\frac{\omega\,\tilde{\mathfrak{s}}}{\mathsf{s}_{\mathrm{S}}}\,c_k\,\mathrm{Z}_{k+1}(\tilde{\mathfrak{s}}\,\omega\,\mathsf{s}_{\mathrm{S}}\,r)\;e^{\mathrm{i}\,k\,\theta}\;+\sum_{k\in\mathbb{Z}}\mu_{\mathrm{fr}}\,\frac{k}{\mathsf{s}_{\mathrm{S}}^2}c_k\,\mathrm{Z}_k(\tilde{\mathfrak{s}}\,\omega\,\mathsf{s}_{\mathrm{S}}\,r)\;e^{\mathrm{i}\,k\,\theta}\\
&\quad+\sum_{k\in\mathbb{Z}}\mu_{\mathrm{fr}}\,\omega^2\,c_k\,\mathrm{Z}_k(\tilde{\mathfrak{s}}\,\omega\,\mathsf{s}_{\mathrm{S}}\,r)\;e^{\mathrm{i}\,k\,\theta}\;-\sum_{k\in\mathbb{Z}}\mu_{\mathrm{fr}}\,\frac{k^2}{\mathsf{s}_{\mathrm{S}}^2}\,c_k\,\mathrm{Z}_k(\tilde{\mathfrak{s}}\,\omega\,\mathsf{s}_{\mathrm{S}}\,r)\;e^{\mathrm{i}\,k\,\theta}\,.
\end{aligned}
$$

Appendix B

Appendices to Chapter 3

B.1 Elementary matrices

In sections 3.2 and 3.3, we have obtained from the discretization of (3.12) the system $\mathbb{A}^K \underline{W}^K + \mathbb{B}^K \underline{\Lambda}^K = \mathbb{C}^K_{\text{source}}$.

B.1.1 In two dimensions

In two dimensions, $\underline{W}^K$ and $\underline{\Lambda}^K$ are defined in (3.17). In the above equation, $\mathbb{A}^K$ is of dimension $8\,d_i^K \times 8d_i^K$, written as:

$$\mathbb{A}^K = \begin{pmatrix} \mathbb{A}_1^K & \mathbb{A}_2^K & \mathbb{A}_3^K & \mathbb{A}_4^K & \mathbb{A}_5^K & \mathbb{A}_6^K & \mathbb{A}_7^K & \mathbb{A}_8^K \end{pmatrix},$$

where

$$\mathbb{A}_1^K = \begin{pmatrix} \mathrm{i}\,\omega\rho_a^K\mathbb{M}^K + \sum_{f=1}^{3}\gamma_1\mathbb{E}^{\beta(K,f)} \\ 0 \\ \mathrm{i}\,\omega\rho_f^K\mathbb{M}^K \\ 0 \\ \left(C_{11}^K\mathbb{D}_x^K + C_{13}^K\mathbb{D}_y^K\right) \\ \left(C_{12}^K\mathbb{D}_x^K + C_{23}^K\mathbb{D}_y^K\right) \\ \left(C_{13}^K\mathbb{D}_x^K + C_{33}^K\mathbb{D}_y^K\right) \\ -M^K\left(\sum_{f=1}^{3}\gamma_4\mathbb{J}_x^{\beta(K,f)} + \alpha_{11}^K\mathbb{D}_x^K + \alpha_{12}^K\mathbb{D}_y^K\right) \end{pmatrix}, \quad \mathbb{A}_2^K = \begin{pmatrix} 0 \\ \mathrm{i}\,\omega\rho_a^K\mathbb{M}^K + \sum_{f=1}^{3}\gamma_1\mathbb{E}^{\beta(K,f)} \\ 0 \\ \mathrm{i}\,\omega\rho_f^K\mathbb{M}^K \\ \left(C_{13}^K\mathbb{D}_x^K + C_{12}^K\mathbb{D}_y^K\right) \\ \left(C_{23}^K\mathbb{D}_x^K + C_{22}^K\mathbb{D}_y^K\right) \\ \left(C_{33}^K\mathbb{D}_x^K + C_{23}^K\mathbb{D}_y^K\right) \\ -M^K\left(\sum_{f=1}^{3}\gamma_4\mathbb{J}_y^{\beta(K,f)} + \alpha_{12}^K\mathbb{D}_x^K + \alpha_{22}^K\mathbb{D}_y^K\right) \end{pmatrix},$$

$$\mathbb{A}_3^K = \begin{pmatrix} \mathrm{i}\,\omega\rho_f^K\mathbb{M}^K \\ 0 \\ \mathrm{i}\,\omega\rho_{\text{dyn}}^K\mathbb{M}^K \\ 0 \\ 0 \\ 0 \\ 0 \\ M^K(\mathbb{D}_x^K)^T \end{pmatrix}, \quad \mathbb{A}_4^K = \begin{pmatrix} 0 \\ \mathrm{i}\,\omega\rho_f^K\mathbb{M}^K \\ 0 \\ \mathrm{i}\,\omega\rho_{\text{dyn}}^K\mathbb{M}^K \\ 0 \\ 0 \\ 0 \\ M^K(\mathbb{D}_y^K)^T \end{pmatrix} \quad \mathbb{A}_5^K = \begin{pmatrix} -(\mathbb{D}_x^K)^T \\ 0 \\ 0 \\ 0 \\ \mathrm{i}\,\omega\,\mathbb{M}^K \\ 0 \\ 0 \\ 0 \end{pmatrix}, \quad \mathbb{A}_6^K = \begin{pmatrix} 0 \\ -(\mathbb{D}_y^K)^T \\ 0 \\ 0 \\ 0 \\ \mathrm{i}\,\omega\,\mathbb{M}^K \\ 0 \\ 0 \end{pmatrix}, \quad \mathbb{A}_7^K = \begin{pmatrix} -(\mathbb{D}_y^K)^T \\ -(\mathbb{D}_x^K)^T \\ 0 \\ 0 \\ 0 \\ 0 \\ \mathrm{i}\,\omega\,\mathbb{M}^K \\ 0 \end{pmatrix},$$

$$\mathbb{A}_8^K = \left(\sum_{f=1}^{3}\gamma_3\mathbb{J}_x^{\beta(K,f)}, \sum_{f=1}^{3}\gamma_3\mathbb{J}_y^{\beta(K,f)}, -\mathbb{D}_x^K, -\mathbb{D}_y^K, \mathrm{i}\,\omega\alpha_{11}^K\mathbb{M}^K, \mathrm{i}\,\omega\alpha_{22}^K\mathbb{M}^K, \mathrm{i}\,\omega\alpha_{12}^K\mathbb{M}^K, \mathrm{i}\,\omega\mathbb{M}^K - \sum_{f=1}^{3}M\gamma_2\mathbb{E}^{\beta(K,f)}\right)^T.$$

Similarly, we write $\mathbb{B}^K$ in 9 columns of size $8\,d_i^K \times d_i^F$:

$$\mathbb{B}^K = \begin{pmatrix} B_{\lambda_{1x},1} & B_{\lambda_{1x},2} & B_{\lambda_{1x},3} & B_{\lambda_{1y},1} & B_{\lambda_{1y},2} & B_{\lambda_{1y},3} & B_{\lambda_2,1} & B_{\lambda_2,2} & B_{\lambda_2,3} \end{pmatrix}$$

with

$$B_{\lambda_{1x},f} = \begin{pmatrix} -\gamma_1\,\mathbb{F}^{\beta(K,f)} \\ 0 \\ 0 \\ 0 \\ (-C_{11}^K\mathbb{Q}_x^{\beta(K,f)} - C_{13}^K\mathbb{Q}_y^{\beta(K,f)}) \\ (-C_{12}^K\mathbb{Q}_x^{\beta(K,f)} - C_{23}^K\mathbb{Q}_y^{\beta(K,f)}) \\ (-C_{13}^K\mathbb{Q}_x^{\beta(K,f)} - C_{33}^K\mathbb{Q}_y^{\beta(K,f)}) \\ M^K\left((\gamma_4+\alpha_{11}^K)\mathbb{Q}_x^{\beta(K,f)} + \alpha_{12}^K\mathbb{Q}_y^{\beta(K,f)}\right) \end{pmatrix}, \quad B_{\lambda_{1y},f} = \begin{pmatrix} 0 \\ -\gamma_1\mathbb{F}^{\beta(K,f)} \\ 0 \\ 0 \\ (-C_{13}^K\mathbb{Q}_x^{\beta(K,f)} - C_{12}^K\mathbb{Q}_y^{\beta(K,f)}) \\ (-C_{23}^K\mathbb{Q}_x^{\beta(K,f)} - C_{22}^K\mathbb{Q}_y^{\beta(K,f)}) \\ (-C_{33}^K\mathbb{Q}_x^{\beta(K,f)} - C_{23}^K\mathbb{Q}_y^{\beta(K,f)}) \\ M^K\left(\alpha_{12}^K\mathbb{Q}_x^{\beta(K,f)} + (\gamma_4+\alpha_{22})\mathbb{Q}_y^{\beta(K,f)}\right) \end{pmatrix},$$

$$B_{\lambda_2,f} = \begin{pmatrix} -\gamma_3\mathbb{Q}_x^{\beta(K,f)} \\ -\gamma_3\mathbb{Q}_y^{\beta(K,f)} \\ \mathbb{Q}_x^{\beta(K,f)} \\ \mathbb{Q}_y^{\beta(K,f)} \\ 0 \\ 0 \\ 0 \\ M^K\gamma_2\,\mathbb{F}^{\beta(K,f)} \end{pmatrix},$$

for $f = 1, 2, 3$.

The matrices $\mathbb{P}^K$ and $\mathbb{T}^K$ are:

$$\mathbb{P}^K = \begin{pmatrix} -\gamma_1\,(\mathbb{F}^{\beta(K,1)})^T & 0 & 0 & 0 & (\mathbb{Q}_x^{\beta(K,1)})^T & 0 & (\mathbb{Q}_y^{\beta(K,1)})^T & -\gamma_3\,(\mathbb{Q}_x^{\beta(K,1)})^T \\ -\gamma_1\,(\mathbb{F}^{\beta(K,2)})^T & 0 & 0 & 0 & (\mathbb{Q}_x^{\beta(K,2)})^T & 0 & (\mathbb{Q}_y^{\beta(K,2)})^T & -\gamma_3\,(\mathbb{Q}_x^{\beta(K,2)})^T \\ -\gamma_1\,(\mathbb{F}^{\beta(K,3)})^T & 0 & 0 & 0 & (\mathbb{Q}_x^{\beta(K,3)})^T & 0 & (\mathbb{Q}_y^{\beta(K,3)})^T & -\gamma_3\,(\mathbb{Q}_x^{\beta(K,3)})^T \\ 0 & -\gamma_1\,(\mathbb{F}^{\beta(K,1)})^T & 0 & 0 & 0 & (\mathbb{Q}_y^{\beta(K,1)})^T & (\mathbb{Q}_x^{\beta(K,1)})^T & -\gamma_3\,(\mathbb{Q}_y^{\beta(K,1)})^T \\ 0 & -\gamma_1\,(\mathbb{F}^{\beta(K,2)})^T & 0 & 0 & 0 & (\mathbb{Q}_y^{\beta(K,2)})^T & (\mathbb{Q}_x^{\beta(K,2)})^T & -\gamma_3\,(\mathbb{Q}_y^{\beta(K,2)})^T \\ 0 & -\gamma_1\,(\mathbb{F}^{\beta(K,3)})^T & 0 & 0 & 0 & (\mathbb{Q}_y^{\beta(K,3)})^T & (\mathbb{Q}_x^{\beta(K,3)})^T & -\gamma_3\,(\mathbb{Q}_y^{\beta(K,3)})^T \\ -\gamma_4\,(\mathbb{Q}_x^{\beta(K,1)})^T & -\gamma_4\,(\mathbb{Q}_y^{\beta(K,1)})^T & (\mathbb{Q}_x^{\beta(K,1)})^T & (\mathbb{Q}_y^{\beta(K,1)})^T & 0 & 0 & 0 & -\gamma_2\,(\mathbb{F}^{\beta(K,1)})^T \\ -\gamma_4\,(\mathbb{Q}_x^{\beta(K,2)})^T & -\gamma_4\,(\mathbb{Q}_y^{\beta(K,2)})^T & (\mathbb{Q}_x^{\beta(K,2)})^T & (\mathbb{Q}_y^{\beta(K,2)})^T & 0 & 0 & 0 & -\gamma_2\,(\mathbb{F}^{\beta(K,2)})^T \\ -\gamma_4\,(\mathbb{Q}_x^{\beta(K,3)})^T & -\gamma_4\,(\mathbb{Q}_y^{\beta(K,3)})^T & (\mathbb{Q}_x^{\beta(K,3)})^T & (\mathbb{Q}_y^{\beta(K,3)})^T & 0 & 0 & 0 & -\gamma_2\,(\mathbb{F}^{\beta(K,3)})^T \end{pmatrix},$$

and

$$\mathbb{T}^K = \begin{pmatrix} \gamma_1\,\mathbb{G}^{\beta(K,1)} & 0 & 0 & 0 & 0 & 0 & \gamma_3\,\mathbb{H}_x^{\beta(K,1)} & 0 & 0 \\ 0 & \gamma_1\,\mathbb{G}^{\beta(K,2)} & 0 & 0 & 0 & 0 & 0 & \gamma_3\,\mathbb{H}_x^{\beta(K,2)} & 0 \\ 0 & 0 & \gamma_1\,\mathbb{G}^{\beta(K,3)} & 0 & 0 & 0 & 0 & 0 & \gamma_3\,\mathbb{H}_x^{\beta(K,3)} \\ 0 & 0 & 0 & \gamma_1\,\mathbb{G}^{\beta(K,1)} & 0 & 0 & \gamma_3\mathbb{H}_y^{\beta(K,1)} & 0 & 0 \\ 0 & 0 & 0 & 0 & \gamma_1\,\mathbb{G}^{\beta(K,2)} & 0 & 0 & \gamma_3\mathbb{H}_y^{\beta(K,2)} & 0 \\ 0 & 0 & 0 & 0 & 0 & \gamma_1\mathbb{G}^{\beta(K,3)} & 0 & 0 & \gamma_3\mathbb{H}_y^{\beta(K,3)} \\ \gamma_4\,\mathbb{H}_x^{\beta(K,1)} & 0 & 0 & \gamma_4\,\mathbb{H}_y^{\beta(K,1)} & 0 & 0 & \gamma_2\,\mathbb{G}^{\beta(K,1)} & 0 & 0 \\ 0 & \gamma_4\,\mathbb{H}_x^{\beta(K,2)} & 0 & 0 & \gamma_4\,\mathbb{H}_y^{\beta(K,2)} & 0 & 0 & \gamma_2\,\mathbb{G}^{\beta(K,2)} & 0 \\ 0 & 0 & \gamma_4\,\mathbb{H}_x^{\beta(K,3)} & 0 & 0 & \gamma_4\,\mathbb{H}_y^{\beta(K,3)} & 0 & 0 & \gamma_2\,\mathbb{G}^{\beta(K,3)}) \end{pmatrix}.$$

B.1.2 In three dimensions

In this case, $\mathbb{A}^K$ is of dimension $13\,d_i^K \times 13 d_i^K$, written as:

$$\mathbb{A}^K = \begin{pmatrix} \mathbb{A}_1^K & \mathbb{A}_2^K & \mathbb{A}_3^K & \mathbb{A}_4^K & \mathbb{A}_5^K & \mathbb{A}_6^K & \mathbb{A}_7^K & \mathbb{A}_8^K & \mathbb{A}_9^K & \mathbb{A}_{10}^K & \mathbb{A}_{11}^K & \mathbb{A}_{12}^K & \mathbb{A}_{13}^K \end{pmatrix},$$

with

$$\mathbb{A}_1^K = \begin{pmatrix} \mathrm{i}\,\omega\rho_a^K\mathbb{M}^K + \sum_{f=1}^{4}\gamma_1\mathbb{E}^{\beta(K,f)} \\ 0 \\ 0 \\ \mathrm{i}\,\omega\rho_f^K\mathbb{M}^K \\ 0 \\ 0 \\ \left(C_{11}^K\mathbb{D}_x^K + C_{16}^K\mathbb{D}_y^K + C_{15}^K\mathbb{D}_z^K\right) \\ \left(C_{21}^K\mathbb{D}_x^K + C_{26}^K\mathbb{D}_y^K + C_{25}^K\mathbb{D}_z^K\right) \\ \left(C_{31}^K\mathbb{D}_x^K + C_{36}^K\mathbb{D}_y^K + C_{35}^K\mathbb{D}_z^K\right) \\ \left(C_{41}^K\mathbb{D}_x^K + C_{46}^K\mathbb{D}_y^K + C_{45}^K\mathbb{D}_z^K\right) \\ \left(C_{51}^K\mathbb{D}_x^K + C_{56}^K\mathbb{D}_y^K + C_{55}^K\mathbb{D}_z^K\right) \\ \left(C_{61}^K\mathbb{D}_x^K + C_{66}^K\mathbb{D}_y^K + C_{65}^K\mathbb{D}_z^K\right) \\ -M^K\left(\sum_{f=1}^{4}\gamma_4\mathbb{J}_x^{\beta(K,f)} + \alpha_{11}^K\mathbb{D}_x^K + \alpha_{12}^K\mathbb{D}_y^K + \alpha_{13}^K\mathbb{D}_z^K\right) \end{pmatrix}, \quad \mathbb{A}_2^K = \begin{pmatrix} 0 \\ \mathrm{i}\,\omega\rho_a^K\mathbb{M}^K + \sum_{f=1}^{4}\gamma_1\mathbb{E}^{\beta(K,f)} \\ 0 \\ 0 \\ \mathrm{i}\,\omega\rho_f^K\mathbb{M}^K \\ 0 \\ \left(C_{16}^K\mathbb{D}_x^K + C_{12}^K\mathbb{D}_y^K + C_{14}^K\mathbb{D}_z^K\right) \\ \left(C_{26}^K\mathbb{D}_x^K + C_{22}^K\mathbb{D}_y^K + C_{24}^K\mathbb{D}_z^K\right) \\ \left(C_{36}^K\mathbb{D}_x^K + C_{32}^K\mathbb{D}_y^K + C_{34}^K\mathbb{D}_z^K\right) \\ \left(C_{46}^K\mathbb{D}_x^K + C_{42}^K\mathbb{D}_y^K + C_{44}^K\mathbb{D}_z^K\right) \\ \left(C_{56}^K\mathbb{D}_x^K + C_{52}^K\mathbb{D}_y^K + C_{54}^K\mathbb{D}_z^K\right) \\ \left(C_{66}^K\mathbb{D}_x^K + C_{62}^K\mathbb{D}_y^K + C_{64}^K\mathbb{D}_z^K\right) \\ -M^K\left(\sum_{f=1}^{4}\gamma_4\mathbb{J}_y^{\beta(K,f)} + \alpha_{12}^K\mathbb{D}_x^K + \alpha_{22}^K\mathbb{D}_y^K + \alpha_{23}^K\mathbb{D}_z^K\right) \end{pmatrix},$$

$$\mathbb{A}_3^K = \begin{pmatrix} 0 \\ 0 \\ \mathrm{i}\,\omega\rho_a^K\mathbb{M}^K + \sum_{f=1}^{4}\gamma_1\mathbb{E}^{\beta(K,f)} \\ 0 \\ 0 \\ \mathrm{i}\,\omega\rho_f^K\mathbb{M}^K \\ \left(C_{15}^K\mathbb{D}_x^K + C_{14}^K\mathbb{D}_y^K + C_{13}^K\mathbb{D}_z^K\right) \\ \left(C_{25}^K\mathbb{D}_x^K + C_{24}^K\mathbb{D}_y^K + C_{23}^K\mathbb{D}_z^K\right) \\ \left(C_{35}^K\mathbb{D}_x^K + C_{34}^K\mathbb{D}_y^K + C_{33}^K\mathbb{D}_z^K\right) \\ \left(C_{45}^K\mathbb{D}_x^K + C_{44}^K\mathbb{D}_y^K + C_{43}^K\mathbb{D}_z^K\right) \\ \left(C_{55}^K\mathbb{D}_x^K + C_{54}^K\mathbb{D}_y^K + C_{53}^K\mathbb{D}_z^K\right) \\ \left(C_{65}^K\mathbb{D}_x^K + C_{64}^K\mathbb{D}_y^K + C_{63}^K\mathbb{D}_z^K\right) \\ -M^K\left(\sum_{f=1}^{4}\gamma_4\mathbb{J}_z^{\beta(K,f)} + \alpha_{13}^K\mathbb{D}_x^K + \alpha_{23}^K\mathbb{D}_y^K + \alpha_{33}^K\mathbb{D}_z^K\right) \end{pmatrix}, \quad \mathbb{A}_4^K = \begin{pmatrix} \mathrm{i}\,\omega\rho_f^K\mathbb{M}^K \\ 0 \\ 0 \\ \mathrm{i}\,\omega\rho_{\mathrm{dyn}}^K\mathbb{M}^K \\ 0 \\ 0 \\ 0 \\ 0 \\ 0 \\ 0 \\ 0 \\ M^K(\mathbb{D}_x^K)^T \end{pmatrix}, \quad \mathbb{A}_5^K = \begin{pmatrix} 0 \\ \mathrm{i}\,\omega\rho_f^K\mathbb{M}^K \\ 0 \\ 0 \\ \mathrm{i}\,\omega\rho_{\mathrm{dyn}}^K\mathbb{M}^K \\ 0 \\ 0 \\ 0 \\ 0 \\ 0 \\ 0 \\ M^K(\mathbb{D}_y^K)^T \end{pmatrix}$$

$$\mathbb{A}_6^K = \begin{pmatrix} 0 \\ 0 \\ \mathrm{i}\,\omega\rho_f^K\mathbb{M}^K \\ 0 \\ \mathrm{i}\,\omega\rho_{\mathrm{dyn}}^K\mathbb{M}^K \\ 0 \\ 0 \\ 0 \\ 0 \\ 0 \\ 0 \\ 0 \\ 0 \\ M^K(\mathbb{D}_z^K)^T \end{pmatrix} \quad \mathbb{A}_7^K = \begin{pmatrix} -(\mathbb{D}_x^K)^T \\ 0 \\ 0 \\ 0 \\ 0 \\ 0 \\ \mathrm{i}\,\omega\,\mathbb{M}^K \\ 0 \\ 0 \\ 0 \\ 0 \\ 0 \\ 0 \\ 0 \end{pmatrix}, \quad \mathbb{A}_8^K = \begin{pmatrix} 0 \\ -(\mathbb{D}_y^K)^T \\ 0 \\ 0 \\ 0 \\ 0 \\ 0 \\ \mathrm{i}\,\omega\,\mathbb{M}^K \\ 0 \\ 0 \\ 0 \\ 0 \\ 0 \\ 0 \end{pmatrix}, \quad \mathbb{A}_9^K = \begin{pmatrix} 0 \\ 0 \\ -(\mathbb{D}_z^K)^T \\ 0 \\ 0 \\ 0 \\ 0 \\ 0 \\ \mathrm{i}\,\omega\,\mathbb{M}^K \\ 0 \\ 0 \\ 0 \\ 0 \\ 0 \end{pmatrix}, \quad \mathbb{A}_{10}^K = \begin{pmatrix} 0 \\ -(\mathbb{D}_z^K)^T \\ -(\mathbb{D}_y^K)^T \\ 0 \\ 0 \\ 0 \\ 0 \\ 0 \\ 0 \\ \mathrm{i}\,\omega\,\mathbb{M}^K \\ 0 \\ 0 \\ 0 \\ 0 \end{pmatrix},$$

$$\mathbb{A}_{11}^K = \begin{pmatrix} -(\mathbb{D}_z^K)^T \\ 0 \\ -(\mathbb{D}_x^K)^T \\ 0 \\ 0 \\ 0 \\ 0 \\ 0 \\ 0 \\ 0 \\ \mathrm{i}\,\omega\,\mathbb{M}^K \\ 0 \\ 0 \end{pmatrix}, \quad \mathbb{A}_{12}^K = \begin{pmatrix} -(\mathbb{D}_y^K)^T \\ -(\mathbb{D}_x^K)^T \\ 0 \\ 0 \\ 0 \\ 0 \\ 0 \\ 0 \\ 0 \\ 0 \\ 0 \\ \mathrm{i}\,\omega\,\mathbb{M}^K \\ 0 \end{pmatrix}, \quad \mathbb{A}_{13}K = \begin{pmatrix} \sum_{f=1}^{4}\gamma_3\mathbb{J}_x^{\beta(K,f)} \\ \sum_{f=1}^{4}\gamma_3\mathbb{J}_y^{\beta(K,f)} \\ \sum_{f=1}^{4}\gamma_3\mathbb{J}_z^{\beta(K,f)} \\ -\mathbb{D}_x^K \\ -\mathbb{D}_y^K \\ -\mathbb{D}_z^K \\ \mathrm{i}\,\omega\alpha_{11}^K\mathbb{M}^K \\ \mathrm{i}\,\omega\alpha_{22}^K\mathbb{M}^K \\ \mathrm{i}\,\omega\alpha_{33}^K\mathbb{M}^K \\ \mathrm{i}\,\omega\alpha_{23}^K\mathbb{M}^K \\ \mathrm{i}\,\omega\alpha_{13}^K\mathbb{M}^K \\ \mathrm{i}\,\omega\alpha_{12}^K\mathbb{M}^K \\ \mathrm{i}\,\omega\mathbb{M}^K - \sum_{f=1}^{4}M\gamma_2\mathbb{E}^{\beta(K,f)} \end{pmatrix}.$$

Based on the structure of the unknown $\underline{\Lambda}^K$, we write $\mathbb{B}^K$ in 16 columns of size $13\,d_i^K \times d_i^F$ as:

$$\mathbb{B}^K = \Big(B_{\lambda_{1x},1} \quad B_{\lambda_{1x},2} \quad B_{\lambda_{1x},3} \quad B_{\lambda_{1x},4} \quad B_{\lambda_{1y},1} \quad B_{\lambda_{1y},2} \quad B_{\lambda_{1y},3} \quad B_{\lambda_{1y},4} \quad \ldots$$
$$\ldots \quad B_{\lambda_{1z},1} \quad B_{\lambda_{1z},2} \quad B_{\lambda_{1z},3} \quad B_{\lambda_{1z},4} \quad B_{\lambda_2,1} \quad B_{\lambda_2,2} \quad B_{\lambda_2,3} \quad B_{\lambda_2,4} \Big),$$

with

$$B_{\lambda_{1x},f} = \begin{pmatrix} -\gamma_1 \, \mathbb{F}^{\beta(K,f)} \\ 0 \\ 0 \\ 0 \\ 0 \\ 0 \\ (-C_{11}^K \mathbb{Q}_x^{\beta(K,f)} - C_{16}^K \mathbb{Q}_y^{\beta(K,f)} - C_{15}^K \mathbb{Q}_z^{\beta(K,f)}) \\ (-C_{21}^K \mathbb{Q}_x^{\beta(K,f)} - C_{26}^K \mathbb{Q}_y^{\beta(K,f)} - C_{25}^K \mathbb{Q}_z^{\beta(K,f)}) \\ (-C_{31}^K \mathbb{Q}_x^{\beta(K,f)} - C_{36}^K \mathbb{Q}_y^{\beta(K,f)} - C_{35}^K \mathbb{Q}_z^{\beta(K,f)}) \\ (-C_{41}^K \mathbb{Q}_x^{\beta(K,f)} - C_{46}^K \mathbb{Q}_y^{\beta(K,f)} - C_{45}^K \mathbb{Q}_z^{\beta(K,f)}) \\ (-C_{51}^K \mathbb{Q}_x^{\beta(K,f)} - C_{56}^K \mathbb{Q}_y^{\beta(K,f)} - C_{55}^K \mathbb{Q}_z^{\beta(K,f)}) \\ (-C_{61}^K \mathbb{Q}_x^{\beta(K,f)} - C_{66}^K \mathbb{Q}_y^{\beta(K,f)} - C_{65}^K \mathbb{Q}_z^{\beta(K,f)}) \\ M^K \left((\gamma_4 + \alpha_{11}^K) \mathbb{Q}_x^{\beta(K,f)} + \alpha_{12}^K \mathbb{Q}_y^{\beta(K,f)} + \alpha_{13}^K \mathbb{Q}_z^{\beta(K,f)} \right) \end{pmatrix}, \quad B_{\lambda_{1y},f} = \begin{pmatrix} 0 \\ -\gamma_1 \, \mathbb{F}^{\beta(K,f)} \\ 0 \\ 0 \\ 0 \\ 0 \\ (-C_{16}^K \mathbb{Q}_x^{\beta(K,f)} - C_{12}^K \mathbb{Q}_y^{\beta(K,f)} - C_{14}^K \mathbb{Q}_z^{\beta(K,f)}) \\ (-C_{26}^K \mathbb{Q}_x^{\beta(K,f)} - C_{22}^K \mathbb{Q}_y^{\beta(K,f)} - C_{24}^K \mathbb{Q}_z^{\beta(K,f)}) \\ (-C_{36}^K \mathbb{Q}_x^{\beta(K,f)} - C_{32}^K \mathbb{Q}_y^{\beta(K,f)} - C_{34}^K \mathbb{Q}_z^{\beta(K,f)}) \\ (-C_{46}^K \mathbb{Q}_x^{\beta(K,f)} - C_{42}^K \mathbb{Q}_y^{\beta(K,f)} - C_{44}^K \mathbb{Q}_z^{\beta(K,f)}) \\ (-C_{56}^K \mathbb{Q}_x^{\beta(K,f)} - C_{52}^K \mathbb{Q}_y^{\beta(K,f)} - C_{54}^K \mathbb{Q}_z^{\beta(K,f)}) \\ (-C_{66}^K \mathbb{Q}_x^{\beta(K,f)} - C_{62}^K \mathbb{Q}_y^{\beta(K,f)} - C_{64}^K \mathbb{Q}_z^{\beta(K,f)}) \\ M^K \left(\alpha_{12}^K \mathbb{Q}_x^{\beta(K,f)} + (\gamma_4 + \alpha_{22}^K) \mathbb{Q}_y^{\beta(K,f)} + \alpha_{23}^K \mathbb{Q}_z^{\beta(K,f)} \right) \end{pmatrix},$$

$$B_{\lambda_{1z},f} = \begin{pmatrix} 0 \\ -\gamma_1 \, \mathbb{F}^{\beta(K,f)} \\ 0 \\ 0 \\ 0 \\ 0 \\ (-C_{15}^K \mathbb{Q}_x^{\beta(K,f)} - C_{14}^K \mathbb{Q}_y^{\beta(K,f)} - C_{13}^K \mathbb{Q}_z^{\beta(K,f)}) \\ (-C_{25}^K \mathbb{Q}_x^{\beta(K,f)} - C_{24}^K \mathbb{Q}_y^{\beta(K,f)} - C_{23}^K \mathbb{Q}_z^{\beta(K,f)}) \\ (-C_{35}^K \mathbb{Q}_x^{\beta(K,f)} - C_{34}^K \mathbb{Q}_y^{\beta(K,f)} - C_{33}^K \mathbb{Q}_z^{\beta(K,f)}) \\ (-C_{45}^K \mathbb{Q}_x^{\beta(K,f)} - C_{44}^K \mathbb{Q}_y^{\beta(K,f)} - C_{43}^K \mathbb{Q}_z^{\beta(K,f)}) \\ (-C_{55}^K \mathbb{Q}_x^{\beta(K,f)} - C_{54}^K \mathbb{Q}_y^{\beta(K,f)} - C_{53}^K \mathbb{Q}_z^{\beta(K,f)}) \\ (-C_{65}^K \mathbb{Q}_x^{\beta(K,f)} - C_{64}^K \mathbb{Q}_y^{\beta(K,f)} - C_{63}^K \mathbb{Q}_z^{\beta(K,f)}) \\ M^K \left(\alpha_{12}^K \mathbb{Q}_x^{\beta(K,f)} + (\gamma_4 + \alpha_{22}^K) \mathbb{Q}_y^{\beta(K,f)} + \alpha_{23}^K \mathbb{Q}_z^{\beta(K,f)} \right) \end{pmatrix}, \qquad B_{\lambda_2,f} = \begin{pmatrix} -\gamma_3 \mathbb{Q}_x^{\beta(K,f)} \\ -\gamma_3 \mathbb{Q}_y^{\beta(K,f)} \\ -\gamma_3 \mathbb{Q}_z^{\beta(K,f)} \\ \mathbb{Q}_x^{\beta(K,f)} \\ \mathbb{Q}_y^{\beta(K,f)} \\ \mathbb{Q}_z^{\beta(K,f)} \\ 0 \\ 0 \\ 0 \\ 0 \\ 0 \\ 0 \\ M^K \gamma_2 \, \mathbb{F}^{\beta(K,f)} \end{pmatrix},$$

for $f = 1, 2, 3, 4$.

The matrices $\mathbb{P}^K$ and $\mathbb{T}^K$ are:

$$\mathbb{P}^K = \begin{pmatrix} -\gamma_1 \, (\mathbb{F}^{\beta(K,1)})^T & 0 & 0 & 0 & 0 & 0 & \dots \\ -\gamma_1 \, (\mathbb{F}^{\beta(K,2)})^T & 0 & 0 & 0 & 0 & 0 & \dots \\ -\gamma_1 \, (\mathbb{F}^{\beta(K,3)})^T & 0 & 0 & 0 & 0 & 0 & \dots \\ -\gamma_1 \, (\mathbb{F}^{\beta(K,4)})^T & 0 & 0 & 0 & 0 & 0 & \dots \\ 0 & -\gamma_1 \, (\mathbb{F}^{\beta(K,1)})^T & 0 & 0 & 0 & 0 & \dots \\ 0 & -\gamma_1 \, (\mathbb{F}^{\beta(K,2)})^T & 0 & 0 & 0 & 0 & \dots \\ 0 & -\gamma_1 \, (\mathbb{F}^{\beta(K,3)})^T & 0 & 0 & 0 & 0 & \dots \\ 0 & -\gamma_1 \, (\mathbb{F}^{\beta(K,4)})^T & 0 & 0 & 0 & 0 & \dots \\ 0 & 0 & -\gamma_1 \, (\mathbb{F}^{\beta(K,1)})^T & 0 & 0 & 0 & \dots \\ 0 & 0 & -\gamma_1 \, (\mathbb{F}^{\beta(K,2)})^T & 0 & 0 & 0 & \dots \\ 0 & 0 & -\gamma_1 \, (\mathbb{F}^{\beta(K,3)})^T & 0 & 0 & 0 & \dots \\ 0 & 0 & -\gamma_1 \, (\mathbb{F}^{\beta(K,4)})^T & 0 & 0 & 0 & \dots \\ -\gamma_4 \, (\mathbb{Q}_x^{\beta(K,1)})^T & -\gamma_4 \, (\mathbb{Q}_y^{\beta(K,1)})^T & -\gamma_4 \, (\mathbb{Q}_z^{\beta(K,1)})^T & (\mathbb{Q}_x^{\beta(K,1)})^T & (\mathbb{Q}_y^{\beta(K,1)})^T & (\mathbb{Q}_z^{\beta(K,1)})^T & \dots \\ \gamma_4 \, (\mathbb{Q}_x^{\beta(K,2)})^T & -\gamma_4 \, (\mathbb{Q}_y^{\beta(K,2)})^T & -\gamma_4 \, (\mathbb{Q}_z^{\beta(K,2)})^T & (\mathbb{Q}_x^{\beta(K,2)})^T & (\mathbb{Q}_y^{\beta(K,2)})^T & (\mathbb{Q}_z^{\beta(K,2)})^T & \dots \\ -\gamma_4 \, (\mathbb{Q}_x^{\beta(K,3)})^T & -\gamma_4 \, (\mathbb{Q}_y^{\beta(K,3)})^T & -\gamma_4 \, (\mathbb{Q}_z^{\beta(K,3)})^T & (\mathbb{Q}_x^{\beta(K,3)})^T & (\mathbb{Q}_y^{\beta(K,3)})^T & (\mathbb{Q}_z^{\beta(K,3)})^T & \dots \\ \gamma_4 \, (\mathbb{Q}_x^{\beta(K,4)})^T & -\gamma_4 \, (\mathbb{Q}_y^{\beta(K,4)})^T & -\gamma_4 \, (\mathbb{Q}_z^{\beta(K,4)})^T & (\mathbb{Q}_x^{\beta(K,4)})^T & (\mathbb{Q}_y^{\beta(K,4)})^T & (\mathbb{Q}_z^{\beta(K,4)})^T & \dots \end{pmatrix},$$

$$
\begin{pmatrix}
\dots & (\mathbb{Q}_x^{\beta(K,1)})^T & 0 & 0 & 0 & (\mathbb{Q}_z^{\beta(K,1)})^T & (\mathbb{Q}_y^{\beta(K,1)})^T & -\gamma_3\,(\mathbb{Q}_x^{\beta(K,1)})^T \\
\dots & (\mathbb{Q}_x^{\beta(K,2)})^T & 0 & 0 & 0 & (\mathbb{Q}_z^{\beta(K,1)})^T & (\mathbb{Q}_y^{\beta(K,2)})^T & -\gamma_3\,(\mathbb{Q}_x^{\beta(K,2)})^T \\
\dots & (\mathbb{Q}_x^{\beta(K,3)})^T & 0 & 0 & 0 & (\mathbb{Q}_z^{\beta(K,1)})^T & (\mathbb{Q}_y^{\beta(K,3)})^T & -\gamma_3\,(\mathbb{Q}_x^{\beta(K,3)})^T \\
\dots & (\mathbb{Q}_x^{\beta(K,4)})^T & 0 & 0 & 0 & (\mathbb{Q}_z^{\beta(K,1)})^T & (\mathbb{Q}_y^{\beta(K,4)})^T & -\gamma_3\,(\mathbb{Q}_x^{\beta(K,4)})^T \\
\dots & 0 & (\mathbb{Q}_y^{\beta(K,1)})^T & 0 & (\mathbb{Q}_z^{\beta(K,1)})^T & 0 & (\mathbb{Q}_x^{\beta(K,1)})^T & -\gamma_3\,(\mathbb{Q}_y^{\beta(K,1)})^T \\
\dots & 0 & (\mathbb{Q}_y^{\beta(K,2)})^T & 0 & (\mathbb{Q}_z^{\beta(K,2)})^T & 0 & (\mathbb{Q}_x^{\beta(K,2)})^T & -\gamma_3\,(\mathbb{Q}_y^{\beta(K,2)})^T \\
\dots & 0 & (\mathbb{Q}_y^{\beta(K,3)})^T & 0 & (\mathbb{Q}_z^{\beta(K,3)})^T & 0 & (\mathbb{Q}_x^{\beta(K,3)})^T & -\gamma_3\,(\mathbb{Q}_y^{\beta(K,3)})^T \\
\dots & 0 & (\mathbb{Q}_y^{\beta(K,4)})^T & 0 & (\mathbb{Q}_z^{\beta(K,4)})^T & 0 & (\mathbb{Q}_x^{\beta(K,4)})^T & -\gamma_3\,(\mathbb{Q}_y^{\beta(K,4)})^T \\
\dots & 0 & 0 & (\mathbb{Q}_z^{\beta(K,1)})^T & (\mathbb{Q}_y^{\beta(K,1)})^T & (\mathbb{Q}_x^{\beta(K,1)})^T & 0 & -\gamma_3\,(\mathbb{Q}_z^{\beta(K,1)})^T \\
\dots & 0 & 0 & (\mathbb{Q}_z^{\beta(K,2)})^T & (\mathbb{Q}_y^{\beta(K,2)})^T & (\mathbb{Q}_x^{\beta(K,2)})^T & 0 & -\gamma_3\,(\mathbb{Q}_z^{\beta(K,2)})^T \\
\dots & 0 & 0 & (\mathbb{Q}_z^{\beta(K,3)})^T & (\mathbb{Q}_y^{\beta(K,3)})^T & (\mathbb{Q}_x^{\beta(K,3)})^T & 0 & -\gamma_3\,(\mathbb{Q}_z^{\beta(K,3)})^T \\
\dots & 0 & 0 & (\mathbb{Q}_z^{\beta(K,4)})^T & (\mathbb{Q}_y^{\beta(K,4)})^T & (\mathbb{Q}_x^{\beta(K,4)})^T & 0 & -\gamma_3\,(\mathbb{Q}_z^{\beta(K,4)})^T \\
\dots & 0 & 0 & 0 & 0 & 0 & 0 & -\gamma_2\,(\mathbb{F}^{\beta(K,1)})^T \\
\dots & 0 & 0 & 0 & 0 & 0 & 0 & -\gamma_2\,(\mathbb{F}^{\beta(K,2)})^T \\
\dots & 0 & 0 & 0 & 0 & 0 & 0 & -\gamma_2\,(\mathbb{F}^{\beta(K,3)})^T \\
\dots & 0 & 0 & 0 & 0 & 0 & 0 & -\gamma_2\,(\mathbb{F}^{\beta(K,4)})^T
\end{pmatrix},
$$

and we write $\mathbb{T}^K$ as

$$
\mathbb{T}^K = \begin{pmatrix} T_1 & 0 & 0 & T_{2x} \\ 0 & T_1 & 0 & T_{2y} \\ 0 & 0 & T_1 & T_{2z} \\ T_{3x} & T_{3y} & T_{3z} & T_4 \end{pmatrix},
$$

with

$$
T_1 = \begin{pmatrix} \gamma_1^{(K,1)}\mathbb{G}^{\beta(K,1)} & 0 & 0 & 0 \\ 0 & \gamma_1^{(K,2)}\mathbb{G}^{\beta(K,2)} & 0 & 0 \\ 0 & 0 & \gamma_1^{(K,3)}\mathbb{G}^{\beta(K,3)} & 0 \\ 0 & 0 & 0 & \gamma_1^{(K,4)}\mathbb{G}^{\beta(K,4)} \end{pmatrix}
$$

$$
T_{2\bullet} = \begin{pmatrix} \gamma_3\mathbb{H}_\bullet^{\beta(K,1)} & 0 & 0 & 0 \\ 0 & \gamma_3\mathbb{H}_\bullet^{\beta(K,2)} & 0 & 0 \\ 0 & 0 & \gamma_3\mathbb{H}_\bullet^{\beta(K,3)} & 0 \\ 0 & 0 & 0 & \gamma_3\mathbb{H}_\bullet^{\beta(K,4)} \end{pmatrix},
$$

$$
T_{3\bullet} = \begin{pmatrix} \gamma_4\mathbb{H}_\bullet^{\beta(K,1)} & 0 & 0 & 0 \\ 0 & \gamma_4\mathbb{H}_\bullet^{\beta(K,2)} & 0 & 0 \\ 0 & 0 & \gamma_4\mathbb{H}_\bullet^{\beta(K,3)} & 0 \\ 0 & 0 & 0 & \gamma_4\mathbb{H}_\bullet^{\beta(K,4)} \end{pmatrix},
$$

and

$$
T_4 = \begin{pmatrix} \gamma_2\mathbb{G}^{\beta(K,1)} & 0 & 0 & 0 \\ 0 & \gamma_2\mathbb{G}^{\beta(K,2)} & 0 & 0 \\ 0 & 0 & \gamma_2\mathbb{G}^{\beta(K,3)} & 0 \\ 0 & 0 & 0 & \gamma_2\mathbb{G}^{\beta(K,4)} \end{pmatrix}.
$$

B.2 Details for the implementation of boundary conditions of type 3

For a face on the boundary of the domain, we can impose four types of boundary conditions, see Section 1.4. In the case of type 1, we impose the continuity of $\boldsymbol{\tau}_h\,\boldsymbol{n}$ and $\mathbf{w}\cdot\boldsymbol{n}$, see equation (3.2). This means that the transmission conditions (3.34) for an interior interface and on the boundary of the mesh are the same. In the following, we detail the expression of the elementary matrices $\mathbb{P}^K$ and $\mathbb{T}^K$ in the case where we impose the continuity of $\mathbf{u}$ and p, as in equation (1.20c). The two other formulations for the boundary conditions are linear combinations of these two formulations. From equation (1.20c), we impose:

$$
\begin{cases} \mathbf{u}_h = f_u, \\ \mathrm{p}_h = f_p\,, \end{cases} \qquad \Rightarrow \qquad \begin{cases} \underline{\boldsymbol{\lambda}}_1 = f_u, \\ \underline{\lambda}_2 = f_p\,, \end{cases}
$$

with f_u and f_p some exterior forces.

Two dimensions Let us consider a two-dimensional element K with the face corresponding to the face 1 in local numbering on the boundary of the domain Ω. In this case, the elementary matrices become:

$$\mathbb{P}^K = \begin{pmatrix} 0 & 0 & 0 & 0 & 0 & 0 & 0 & 0 \\ -\gamma_1 (\mathbb{F}^{\beta(K,2)})^T & 0 & 0 & 0 & (\mathbb{Q}_x^{\beta(K,2)})^T & 0 & (\mathbb{Q}_y^{\beta(K,2)})^T & -\gamma_3 (\mathbb{Q}_x^{\beta(K,2)})^T \\ -\gamma_1 (\mathbb{F}^{\beta(K,3)})^T & 0 & 0 & 0 & (\mathbb{Q}_x^{\beta(K,3)})^T & 0 & (\mathbb{Q}_y^{\beta(K,3)})^T & -\gamma_3 (\mathbb{Q}_x^{\beta(K,3)})^T \\ 0 & 0 & 0 & 0 & 0 & 0 & 0 & 0 \\ 0 & -\gamma_1 (\mathbb{F}^{\beta(K,2)})^T & 0 & 0 & 0 & (\mathbb{Q}_y^{\beta(K,2)})^T & (\mathbb{Q}_x^{\beta(K,2)})^T & -\gamma_3 (\mathbb{Q}_y^{\beta(K,2)})^T \\ 0 & -\gamma_1 (\mathbb{F}^{\beta(K,3)})^T & 0 & 0 & 0 & (\mathbb{Q}_y^{\beta(K,3)})^T & (\mathbb{Q}_x^{\beta(K,3)})^T & -\gamma_3 (\mathbb{Q}_y^{\beta(K,3)})^T \\ 0 & 0 & 0 & 0 & 0 & 0 & 0 & 0 \\ -\gamma_4 (\mathbb{Q}_x^{\beta(K,2)})^T & -\gamma_4 (\mathbb{Q}_y^{\beta(K,2)})^T & (\mathbb{Q}_x^{\beta(K,2)})^T & (\mathbb{Q}_y^{\beta(K,2)})^T & 0 & 0 & 0 & -\gamma_2 (\mathbb{F}^{\beta(K,2)})^T \\ -\gamma_4 (\mathbb{Q}_x^{\beta(K,3)})^T & -\gamma_4 (\mathbb{Q}_y^{\beta(K,3)})^T & (\mathbb{Q}_x^{\beta(K,3)})^T & (\mathbb{Q}_y^{\beta(K,3)})^T & 0 & 0 & 0 & -\gamma_2 (\mathbb{F}^{\beta(K,3)})^T \end{pmatrix},$$

and with $\mathbb{I}$ denoting the identity matrix of size $d_i^F \times d_i^F$,

$$\mathbb{T}^K = \begin{pmatrix} \mathbb{I} & 0 & 0 & 0 & 0 & 0 & 0 & 0 & 0 \\ 0 & \gamma_1 \mathbb{G}^{\beta(K,2)} & 0 & 0 & 0 & 0 & 0 & \gamma_3 \mathbb{H}_x^{\beta(K,2)} & 0 \\ 0 & 0 & \gamma_1 \mathbb{G}^{\beta(K,3)} & 0 & 0 & 0 & 0 & 0 & \gamma_3 \mathbb{H}_x^{\beta(K,3)} \\ 0 & 0 & 0 & \mathbb{I} & 0 & 0 & 0 & 0 & 0 \\ 0 & 0 & 0 & 0 & \gamma_1 \mathbb{G}^{\beta(K,2)} & 0 & 0 & \gamma_3 \mathbb{H}_y^{\beta(K,2)} & 0 \\ 0 & 0 & 0 & 0 & 0 & \gamma_1^{(K,3)} \mathbb{G}^{\beta(K,3)} & 0 & 0 & \gamma_3 \mathbb{H}_y^{\beta(K,3)} \\ 0 & 0 & 0 & 0 & 0 & 0 & \mathbb{I} & 0 & 0 \\ 0 & \gamma_4 \mathbb{H}_x^{\beta(K,2)} & 0 & 0 & \gamma_4 \mathbb{H}_y^{\beta(K,2)} & 0 & 0 & \gamma_2 \mathbb{G}^{\beta(K,2)} & 0 \\ 0 & 0 & \gamma_4 \mathbb{H}_x^{\beta(K,3)} & 0 & 0 & \gamma_4 \mathbb{H}_y^{\beta(K,3)} & 0 & 0 & \gamma_2 \mathbb{G}^{\beta(K,3)}) \end{pmatrix}.$$

Three dimensions In three dimensions, the matrices $\mathbb{P}$ and $\mathbb{T}$ given in Section B.1.2 are modified in order to take into account the boundary conditions of type 3 the same way as in two dimensions. This means that, if the face corresponding to the first face is on the border of the mesh, the lines of $\mathbb{P}$ corresponding to the first face, i.e.the first, fifth, ninth and thirteenth lines of $\mathbb{P}$ will be zeros. Moreover, the lines of $\mathbb{T}$ corresponding to the first face, i.e.the first, fifth, ninth and thirteenth lines of $\mathbb{T}$ will be zeros except for the diagonal terms that will be equal to the identity matrix $\mathbb{I}$.

Appendix C

Appendices to Chapter 4

C.1 Details on the HDG method with RBC and PML

C.1.1 Elementary matrices for HDG method with RBC

Supposing that the first face of the element K is on Γ_{abs}, matrices $\mathbb{P}^K$ and $\mathbb{T}^K$ read then as:

$$\mathbb{P}^K = \begin{pmatrix}
-\gamma_1(\mathbb{F}_1^{\beta(K,1)})^T - \gamma_4\mathbf{X}_2(\mathbb{L}_{xx1}^{\beta(K,1)})^T & -\gamma_4\mathbf{X}_2(\mathbb{L}_{xy1}^{\beta(K,1)})^T & \mathbf{X}_2(\mathbb{L}_{xx1}^{\beta(K,1)})^T & \mathbf{X}_2(\mathbb{L}_{xy1}^{\beta(K,1)})^T & \dots \\
-\gamma_1(\mathbb{F}_2^{\beta(K,2)})^T & 0 & 0 & 0 & \dots \\
-\gamma_1(\mathbb{F}_3^{\beta(K,3)})^T & 0 & 0 & 0 & \dots \\
-\gamma_4\mathbf{X}_2(\mathbb{L}_{xy1}^{\beta(K,1)})^T & -\gamma_1(\mathbb{F}_1^{\beta(K,1)})^T - \gamma_4\mathbf{X}_2(\mathbb{L}_{yy1}^{\beta(K,1)})^T & \mathbf{X}_2(\mathbb{L}_{xy1}^{\beta(K,1)})^T & \mathbf{X}_2(\mathbb{L}_{yy1}^{\beta(K,1)})^T & \dots \\
0 & -\gamma_1(\mathbb{F}_2^{\beta(K,2)})^T & 0 & 0 & \dots \\
0 & -\gamma_1(\mathbb{F}_3^{\beta(K,3)})^T & 0 & 0 & \dots \\
-(\mathbb{Q}_{x1}^{\beta(K,1)})\mathbf{X}_5\,\gamma_4 & -(\mathbb{Q}_{y1}^{\beta(K,1)})^T\mathbf{X}_5\,\gamma_4 & (\mathbb{Q}_{x1}^{\beta(K,1)})^T\mathbf{X}_5 & (\mathbb{Q}_{y1}^{\beta(K,2)})^T\mathbf{X}_5 & \dots \\
-(\mathbb{Q}_x^{\beta(K,2)})^T\gamma_4 & -(\mathbb{Q}_y^{\beta(K,2)})^T\gamma_4 & (\mathbb{Q}_{x2}^{\beta(K,2)})^T & (\mathbb{Q}_{y2}^{\beta(K,2)})^T & \dots \\
-(\mathbb{Q}_x^{\beta(K,3)})^T\gamma_4 & -(\mathbb{Q}_y^{\beta(K,3)})^T\gamma_4 & (\mathbb{Q}_{x3}^{\beta(K,2)})^T & (\mathbb{Q}_{y3}^{\beta(K,2)})^T & \dots
\end{pmatrix}$$

$$\begin{pmatrix}
\dots & (\mathbb{Q}_{x1}^{\beta(K,1)})^T & 0 & (\mathbb{Q}_{y1}^{\beta(K,1)})^T & -\gamma_3(\mathbb{Q}_{x1}^{\beta(K,1)})^T - \gamma_2\mathbf{X}_2(\mathbb{Q}_{x1}^{\beta(K,1)})^T \\
\dots & (\mathbb{Q}_{x2}^{\beta(K,2)})^T & 0 & (\mathbb{Q}_{y2}^{\beta(K,2)})^T & -\gamma_3(\mathbb{Q}_{x2}^{\beta(K,2)})^T \\
\dots & (\mathbb{Q}_{x3}^{\beta(K,3)})^T & 0 & (\mathbb{Q}_{y3}^{\beta(K,3)})^T & -\gamma_3(\mathbb{Q}_{x3}^{\beta(K,3)})^T \\
\dots & 0 & (\mathbb{Q}_{y1}^{\beta(K,1)})^T & (\mathbb{Q}_{x1}^{\beta(K,1)})^T & -\gamma_3(\mathbb{Q}_{y1}^{\beta(K,1)})^T - \gamma_2\mathbf{X}_2(\mathbb{Q}_{y1}^{\beta(K,1)})^T \\
\dots & 0 & (\mathbb{Q}_{y2}^{\beta(K,2)})^T & (\mathbb{Q}_{x2}^{\beta(K,2)})^T & -\gamma_3(\mathbb{Q}_{y2}^{\beta(K,2)})^T \\
\dots & 0 & (\mathbb{Q}_{y3}^{\beta(K,3)})^T & (\mathbb{Q}_{x3}^{\beta(K,3)})^T & -\gamma_3(\mathbb{Q}_{y3}^{\beta(K,3)})^T \\
\dots & 0 & 0 & 0 & -\gamma_2\mathbf{X}_5(\mathbb{F}_1^{\beta(K,1)})^T \\
\dots & 0 & 0 & 0 & -\gamma_2(\mathbb{F}_2^{\beta(K,2)})^T \\
\dots & 0 & 0 & 0 & -\gamma_2(\mathbb{F}_3^{\beta(K,3)})^T
\end{pmatrix},$$

and

$$\mathbb{T}^K = \begin{pmatrix}
\gamma_1\mathbb{G}^{\beta(K,1)} + \mathbb{O}_{xx}^{\beta(K,2)}\gamma_4\mathbf{X}_2 + \mathbb{O}_{xx}^{\beta(K,2)}\mathbf{X}_1 + \mathbb{O}_{yy}^{\beta(K,2)}\mathbf{X}_3 & 0 & 0 & \mathbb{O}_{xy}^{\beta(K,2)}\gamma_4\mathbf{X}_2 + \mathbb{O}_{xy}^{\beta(K,2)}\mathbf{X}_1 - \mathbb{O}_{xy}^{\beta(K,2)}\mathbf{X}_3 & \dots \\
0 & \gamma_1\mathbb{G}^{\beta(K,2)} & 0 & 0 & \dots \\
0 & 0 & \gamma_1\mathbb{G}^{\beta(K,3)} & 0 & \dots \\
\mathbb{O}_{xy}^{\beta(K,2)}\gamma_4\mathbf{X}_2 + \mathbb{O}_{xy}^{\beta(K,2)}\mathbf{X}_1 - \mathbb{O}_{xy}^{\beta(K,2)}\mathbf{X}_3 & 0 & 0 & \gamma_1\mathbb{G}^{\beta(K,1)} + \mathbb{O}_{yy}^{\beta(K,2)}\gamma_4\mathbf{X}_2 + \mathbb{O}_{yy}^{\beta(K,2)}\mathbf{X}_1 + \mathbb{O}_{xx}^{\beta(K,2)}\mathbf{X}_3 & \dots \\
0 & 0 & 0 & 0 & \dots \\
0 & 0 & 0 & 0 & \dots \\
\mathbb{H}_x^{\beta(K,2)}\mathbf{X}_4 + \mathbb{H}_x^{\beta(K,2)}\mathbf{X}_5\gamma_4 & 0 & 0 & \mathbb{H}_y^{\beta(K,2)}\mathbf{X}_4 + \mathbb{H}_y^{\beta(K,2)}\mathbf{X}_5\gamma_4 & \dots \\
0 & \gamma_4\mathbb{H}_x^{\beta(K,2)} & 0 & 0 & \dots \\
0 & 0 & \gamma_4\mathbb{H}_x^{\beta(K,3)} & 0 & \dots
\end{pmatrix}$$

$$
\begin{pmatrix}
\dots & 0 & 0 & \gamma_3\mathbb{H}_x^{\beta(K,1)} + \mathbb{H}_x^{\beta(K,1)}\mathbf{X}_2\ \gamma_2 & 0 & 0 \\
\dots & 0 & 0 & 0 & \gamma_3\mathbb{H}_x^{\beta(K,2)} & 0 \\
\dots & 0 & 0 & 0 & 0 & \gamma_3\mathbb{H}_x^{\beta(K,3)} \\
\dots & 0 & 0 & \gamma_3\mathbb{H}_y^{\beta(K,1)} + \mathbb{H}_y^{\beta(K,2)}\mathbf{X}_2\ \gamma_2 & 0 & 0 \\
\dots & \gamma_1\mathbb{G}^{\beta(K,2)} & 0 & 0 & \gamma_3\mathbb{H}_y^{\beta(K,2)} & 0 \\
\dots & 0 & \gamma_1\mathbb{G}^{\beta(K,3)} & 0 & 0 & \gamma_3\mathbb{H}_y^{\beta(K,3)} \\
\dots & 0 & 0 & \mathbb{G}^{\beta(K,1)}(1+\mathbf{X}_5\gamma_2) & 0 & 0 \\
\dots & \gamma_4\mathbb{H}_y^{\beta(K,2)} & 0 & 0 & \gamma_2\mathbb{G}^{\beta(K,2)} & 0 \\
\dots & 0 & \gamma_4\mathbb{H}_y^{\beta(K,3)} & 0 & 0 & \gamma_2\mathbb{G}^{\beta(K,3)}
\end{pmatrix}.
$$

C.1.2 HDG method with PML

Here, we detail the discretization of equations (1.16) when we use PML. We consider a two-dimensional porous domain Ω with the boundary Γ on the plane (x,y). $(\mathbf{u},\,\mathbf{w},\,\boldsymbol{\tau},\,\mathrm{p})$ solve the poroelastic equations (1.16) on Ω. We consider a triangulation $\mathcal{T}_h$ of Ω, and $\mathcal{F}_h$ the set of all the faces. K is a triangle element of $\mathcal{T}_h$ and F is a face of K. We use the approximation spaces defined in Section 4.4. The local unknowns $(\mathbf{u}_h,\,\mathbf{w}_h,\,\boldsymbol{\tau}_h,\,\mathrm{p}_h) \in (\boldsymbol{V}_h^p \times \boldsymbol{V}_h^p \times \boldsymbol{\Sigma}_h^p \times V_h^p)$ solve the poroelastic equations (1.16) on $\mathcal{T}_h$. We consider an element $K \in \mathcal{T}_h$, $(\tilde{\boldsymbol{u}},\,\tilde{\boldsymbol{w}},\,\tilde{\boldsymbol{\tau}},\,\tilde{\mathrm{p}}) \in (\boldsymbol{V}_h^p \times \boldsymbol{V}_h^p \times \boldsymbol{\Sigma}_h^p \times V_h^p)$ test-functions. We multiply equations (1.16) by the test-functions and integrate on the element K:

$$
\begin{aligned}
&\int_K \mathrm{i}\,\omega\rho_a \mathrm{u}_x^K\tilde{u}_x + \int_K \mathrm{i}\,\omega\rho_a \mathrm{u}_y^K\tilde{u}_y + \int_K \mathrm{i}\,\omega\rho_f \mathrm{w}_x^K\tilde{u}_x + \int_K \mathrm{i}\,\omega\rho_f \mathrm{w}_y^K\tilde{u}_y - \int_K \left(\frac{i\,\omega}{i\,\omega+\alpha(x)}\frac{\partial\tau_{xx}^K}{\partial x} + \frac{i\,\omega}{i\,\omega+\beta(y)}\frac{\partial\tau_{xy}^K}{\partial y}\right)\tilde{u}_x \\
&\quad - \int_K \left(\frac{i\,\omega}{i\,\omega+\alpha(x)}\frac{\partial\tau_{xy}^K}{\partial x} + \frac{i\,\omega}{i\,\omega+\beta(y)}\frac{\partial\tau_{yy}^K}{\partial y}\right)\tilde{u}_y = 0\,, \\
&\int_K \mathrm{i}\omega\rho_f \mathrm{u}_x^K\tilde{w}_x + \int_K \mathrm{i}\omega\rho_f \mathrm{u}_y^K\tilde{w}_y + \int_K \mathrm{i}\omega\tilde{\rho} \mathrm{w}_x^K\tilde{w}_x + \int_K \mathrm{i}\omega\tilde{\rho} \mathrm{w}_y^K\tilde{w}_y + \int_K \frac{i\,\omega}{i\,\omega+\alpha(x)}\frac{\partial \mathrm{p}}{\partial x}\tilde{w}_x + \int_K \frac{i\,\omega}{i\,\omega+\beta(y)}\frac{\partial \mathrm{p}}{\partial y}\tilde{w}_y = 0\,,
\end{aligned}
$$

$$
\begin{aligned}
&\int_K \mathrm{i}\omega\tau_{xx}^K\,\tilde{\tau}_{xx} + \int_K \mathrm{i}\omega\alpha_{11}\mathrm{p}_h\tilde{\tau}_{xx} - \int_K C_{11}\frac{i\,\omega}{i\,\omega+\alpha(x)}\frac{\partial \mathrm{u}_x^K}{\partial x}\tilde{\tau}_{xx} - \int_K C_{12}\frac{i\,\omega}{i\,\omega+\beta(y)}\frac{\partial \mathrm{u}_y^K}{\partial y}\tilde{\tau}_{xx} \\
&\quad - \int_K C_{13}\left(\frac{i\,\omega}{i\,\omega+\alpha(x)}\frac{\partial \mathrm{u}_y^K}{\partial x} + \frac{i\,\omega}{i\,\omega+\beta(y)}\frac{\partial \mathrm{u}_x^K}{\partial y}\right)\tilde{\tau}_{xx} \\
&\quad + \int_K \mathrm{i}\omega\tau_{yy}^K\,\tilde{\tau}_{yy} + \int_K \mathrm{i}\omega\alpha_{22}\mathrm{p}_h\tilde{\tau}_{yy} - \int_K C_{12}\frac{i\,\omega}{i\,\omega+\alpha(x)}\frac{\partial \mathrm{u}_x^K}{\partial x}\tilde{\tau}_{yy} - \int_K C_{22}\frac{i\,\omega}{i\,\omega+\beta(y)}\frac{\partial \mathrm{u}_y^K}{\partial y}\tilde{\tau}_{yy} \\
&\quad - \int_K C_{23}\left(\frac{i\,\omega}{i\,\omega+\alpha(x)}\frac{\partial \mathrm{u}_y^K}{\partial x} + \frac{i\,\omega}{i\,\omega+\beta(y)}\frac{\partial \mathrm{u}_x^K}{\partial y}\right)\tilde{\tau}_{yy} \\
&\quad + \int_K \mathrm{i}\omega\tau_{xy}^K\,\tilde{\tau}_{xy} + \int_K \mathrm{i}\omega\alpha_{12}\mathrm{p}_h\tilde{\tau}_{xy} - \int_K C_{13}\frac{i\,\omega}{i\,\omega+\alpha(x)}\frac{\partial \mathrm{u}_x^K}{\partial x}\tilde{\tau}_{xy} - \int_K C_{23}\frac{i\,\omega}{i\,\omega+\beta(y)}\frac{\partial \mathrm{u}_y^K}{\partial y}\tilde{\tau}_{xy} \\
&\quad - \int_K C_{33}\left(\frac{i\,\omega}{i\,\omega+\alpha(x)}\frac{\partial \mathrm{u}_y^K}{\partial x} + \frac{i\,\omega}{i\,\omega+\beta(y)}\frac{\partial \mathrm{u}_x^K}{\partial y}\right)\tilde{\tau}_{xy} = 0\,,
\end{aligned}
$$

and

$$
\begin{aligned}
&\int_K \mathrm{i}\omega\mathrm{p}_h\tilde{\mathrm{p}} + \int_K M\left(\frac{i\,\omega}{i\,\omega+\alpha(x)}\frac{\partial \mathrm{w}_x^K}{\partial x} + \frac{i\,\omega}{i\,\omega+\beta(y)}\frac{\partial \mathrm{w}_y^K}{\partial y}\right)\tilde{\mathrm{p}} + \int_K M\alpha_{11}\frac{i\,\omega}{i\,\omega+\alpha(x)}\frac{\partial \mathrm{u}_x^K}{\partial x}\tilde{\mathrm{p}} \\
&\quad + \int_K M\alpha_{22}\frac{i\,\omega}{i\,\omega+\beta(y)}\frac{\partial \mathrm{u}_y^K}{\partial y}\tilde{\mathrm{p}} + \int_K M\alpha_{12}\left(\frac{i\,\omega}{i\,\omega+\beta(y)}\frac{\partial \mathrm{u}_x^K}{\partial y} + \frac{i\,\omega}{i\,\omega+\alpha(x)}\frac{\partial \mathrm{u}_y^K}{\partial x}\right)\tilde{\mathrm{p}} = 0\,.
\end{aligned}
$$

By integrating by parts, we obtain:

$$
\begin{aligned}
&\int_K \mathrm{i}\omega\rho_a \mathrm{u}_x^K\tilde{u}_x + \int_K \mathrm{i}\omega\rho_a \mathrm{u}_y^K\tilde{u}_y + \int_K \mathrm{i}\omega\rho_f \mathrm{w}_x^K\tilde{u}_x + \int_K \mathrm{i}\omega\rho_f \mathrm{w}_y^K\tilde{u}_y + \int_K \frac{i\,\omega}{i\,\omega+\alpha(x)}\tau_{xx}^K\frac{\partial\tilde{u}_x}{\partial x} + \int_K \frac{i\,\omega}{i\,\omega+\beta(y)}\tau_{xy}^K\frac{\partial\tilde{u}_x}{\partial y} \\
&\quad - \int_F \frac{i\,\omega}{i\,\omega+\alpha(x)}\hat{\tau}_{xx}^K n_x\tilde{u}_x - \int_F \frac{i\,\omega}{i\,\omega+\beta(y)}\hat{\tau}_{xy}^K n_y\tilde{u}_x + \int_K \frac{i\,\omega}{i\,\omega+\alpha(x)}\tau_{xy}^K\frac{\partial\tilde{u}_y}{\partial x} + \int_K \frac{i\,\omega}{i\,\omega+\beta(y)}\tau_{yy}^K\frac{\partial\tilde{u}_y}{\partial y} \\
&\quad - \int_F \frac{i\,\omega}{i\,\omega+\alpha(x)}\hat{\tau}_{xy}^K n_x\tilde{u}_y - \int_F \frac{i\,\omega}{i\,\omega+\beta(y)}\hat{\tau}_{yy}^K n_y\tilde{u}_y = 0\,,
\end{aligned}
$$

$$\int_K \mathrm{i}\omega\rho_f \mathrm{u}_x^K \tilde{w}_x + \int_K \mathrm{i}\omega\rho_f \mathrm{u}_y^K \tilde{w}_y + \int_K \mathrm{i}\omega\tilde{\rho}\mathrm{w}_x^K \tilde{w}_x + \int_K \mathrm{i}\omega\tilde{\rho}\mathrm{w}_y^K \tilde{w}_y - \int_K \frac{i\,\omega}{i\,\omega+\alpha(x)}\mathrm{p}\frac{\partial \tilde{w}_x}{\partial x} + \int_F \frac{i\,\omega}{i\,\omega+\alpha(x)}\hat{\mathrm{p}} n_x \tilde{w}_x - \int_K \frac{i\,\omega}{i\,\omega+\beta(y)}\mathrm{p}\frac{\partial \tilde{w}_y}{\partial y} + \int_F \frac{i\,\omega}{i\,\omega+\beta(y)}\hat{\mathrm{p}} n_y \tilde{w}_y = 0\,,$$

$$\begin{aligned}
&\int_K \mathrm{i}\omega\tau_{xx}^K \tilde{\tau}_{xx} + \int_K \mathrm{i}\omega\alpha_{11}\mathrm{p}_h\tilde{\tau}_{xx} + \int_K C_{11}\frac{i\,\omega}{i\,\omega+\alpha(x)}\mathrm{u}_x^K\frac{\partial\tilde{\tau}_{xx}}{\partial x} - \int_F C_{11}\frac{i\,\omega}{i\,\omega+\alpha(x)}\hat{\mathrm{u}}_x^K n_x\tilde{\tau}_{xx}\\
&+ \int_K C_{12}\frac{i\,\omega}{i\,\omega+\beta(y)}\mathrm{u}_y^K\frac{\partial\tilde{\tau}_{xx}}{\partial y} - \int_F C_{12}\frac{i\,\omega}{i\,\omega+\beta(y)}\hat{\mathrm{u}}_y^K n_y\tilde{\tau}_{xx} + \int_K C_{13}\frac{i\,\omega}{i\,\omega+\alpha(x)}\mathrm{u}_y^K\frac{\partial\tilde{\tau}_{xx}}{\partial x}\\
&- \int_F C_{13}\frac{i\,\omega}{i\,\omega+\alpha(x)}\hat{\mathrm{u}}_y^K n_x\tilde{\tau}_{xx} + \int_K C_{13}\frac{i\,\omega}{i\,\omega+\beta(y)}\mathrm{u}_x^K\frac{\partial\tilde{\tau}_{xx}}{\partial y} - \int_F C_{13}\frac{i\,\omega}{i\,\omega+\beta(y)}\hat{\mathrm{u}}_x^K n_y\tilde{\tau}_{xx}\\
&+ \int_K \mathrm{i}\omega\tau_{yy}^K \tilde{\tau}_{yy} + \int_K \mathrm{i}\omega\alpha_{22}\mathrm{p}_h\tilde{\tau}_{yy} + \int_K C_{12}\frac{i\,\omega}{i\,\omega+\alpha(x)}\mathrm{u}_x^K\frac{\partial\tilde{\tau}_{yy}}{\partial x} - \int_F C_{12}\frac{i\,\omega}{i\,\omega+\alpha(x)}\hat{\mathrm{u}}_x^K n_x\tilde{\tau}_{yy}\\
&+ \int_K C_{22}\frac{i\,\omega}{i\,\omega+\beta(y)}\mathrm{u}_y^K\frac{\partial\tilde{\tau}_{yy}}{\partial y} - \int_F C_{22}\frac{i\,\omega}{i\,\omega+\beta(y)}\hat{\mathrm{u}}_y^K n_y\tilde{\tau}_{yy} + \int_K C_{23}\frac{i\,\omega}{i\,\omega+\alpha(x)}\mathrm{u}_y^K\frac{\partial\tilde{\tau}_{yy}}{\partial x}\\
&- \int_F C_{23}\frac{i\,\omega}{i\,\omega+\alpha(x)}\hat{\mathrm{u}}_y^K n_x\tilde{\tau}_{yy} + \int_K C_{23}\frac{i\,\omega}{i\,\omega+\beta(y)}\mathrm{u}_x^K\frac{\partial\tilde{\tau}_{yy}}{\partial y} - \int_F C_{23}\frac{i\,\omega}{i\,\omega+\beta(y)}\hat{\mathrm{u}}_x^K n_y\tilde{\tau}_{yy}\\
&+ \int_K \mathrm{i}\omega\tau_{xy}^K \tilde{\tau}_{xy} + \int_K \mathrm{i}\omega\alpha_{12}\mathrm{p}_h\tilde{\tau}_{xy} + \int_K C_{13}\frac{i\,\omega}{i\,\omega+\alpha(x)}\mathrm{u}_x^K\frac{\partial\tilde{\tau}_{xy}}{\partial x} - \int_F C_{13}\frac{i\,\omega}{i\,\omega+\alpha(x)}\hat{\mathrm{u}}_x^K n_x\tilde{\tau}_{xy}\\
&+ \int_K C_{23}\frac{i\,\omega}{i\,\omega+\beta(y)}\mathrm{u}_y^K\frac{\partial\tilde{\tau}_{xy}}{\partial y} - \int_F C_{23}\frac{i\,\omega}{i\,\omega+\beta(y)}\hat{\mathrm{u}}_y^K n_y\tilde{\tau}_{xy} + \int_K C_{33}\frac{i\,\omega}{i\,\omega+\alpha(x)}\mathrm{u}_y^K\frac{\partial\tilde{\tau}_{xy}}{\partial x}\\
&- \int_F C_{33}\frac{i\,\omega}{i\,\omega+\alpha(x)}\hat{\mathrm{u}}_y^K n_x\tilde{\tau}_{xy} + \int_K C_{33}\frac{i\,\omega}{i\,\omega+\beta(y)}\mathrm{u}_x^K\frac{\partial\tilde{\tau}_{xy}}{\partial y} - \int_F C_{33}\frac{i\,\omega}{i\,\omega+\beta(y)}\hat{\mathrm{u}}_x^K n_y\tilde{\tau}_{xy} = 0\,,
\end{aligned}$$

$$\begin{aligned}
&\int_K \mathrm{i}\omega\mathrm{p}_h\tilde{\mathrm{p}} - \int_K M\frac{i\,\omega}{i\,\omega+\alpha(x)}\mathrm{w}_x^K\frac{\partial\tilde{\mathrm{p}}}{\partial x} + \int_F M\frac{i\,\omega}{i\,\omega+\alpha(x)}\hat{\mathrm{w}}_x^K n_x\tilde{\mathrm{p}} - \int_K M\frac{i\,\omega}{i\,\omega+\beta(y)}\mathrm{w}_y^K\frac{\partial\tilde{\mathrm{p}}}{\partial y}\\
&+ \int_F M\frac{i\,\omega}{i\,\omega+\beta(y)}\hat{\mathrm{w}}_y^K n_y\tilde{\mathrm{p}} - \int_K M\alpha_{11}\frac{i\,\omega}{i\,\omega+\alpha(x)}\mathrm{u}_x^K\frac{\partial\tilde{\mathrm{p}}}{\partial x} + \int_F M\alpha_{11}\frac{i\,\omega}{i\,\omega+\alpha(x)}\hat{\mathrm{u}}_x^K n_x\tilde{\mathrm{p}}\\
&- \int_K M\alpha_{22}\frac{i\,\omega}{i\,\omega+\beta(y)}\mathrm{u}_y^K\frac{\partial\tilde{\mathrm{p}}}{\partial y} + \int_F M\alpha_{22}\frac{i\,\omega}{i\,\omega+\beta(y)}\hat{\mathrm{u}}_y^K n_y\tilde{\mathrm{p}} - \int_K M\alpha_{12}\frac{i\,\omega}{i\,\omega+\beta(y)}\mathrm{u}_x^K\frac{\partial\tilde{\mathrm{p}}}{\partial y}\\
&+ \int_F M\alpha_{12}\frac{i\,\omega}{i\,\omega+\beta(y)}\hat{\mathrm{u}}_x^K n_y\tilde{\mathrm{p}} - \int_K M\alpha_{12}\frac{i\,\omega}{i\,\omega+\alpha(x)}\mathrm{u}_y^K\frac{\partial\tilde{\mathrm{p}}}{\partial x} + \int_F M\alpha_{12}\frac{i\,\omega}{i\,\omega+\alpha(x)}\hat{\mathrm{u}}_y^K n_x\tilde{\mathrm{p}} \;=\; 0\,.
\end{aligned}$$

Next we replace the numerical traces $\hat{\mathbf{u}}$, $\hat{\mathbf{w}}$, $\hat{\boldsymbol{\tau}}$ and $\hat{\mathrm{p}}$ by the expressions from equation (4.23):

$$\begin{aligned}
&\int_K \mathrm{i}\omega\rho_a \mathrm{u}_x^K \tilde{u}_x + \int_K \mathrm{i}\omega\rho_a \mathrm{u}_y^K \tilde{u}_y + \int_K \mathrm{i}\omega\rho_f \mathrm{w}_x^K \tilde{u}_x + \int_K \mathrm{i}\omega\rho_f \mathrm{w}_y^K \tilde{u}_y - \int_K \frac{i\,\omega}{i\,\omega+\alpha(x)}\frac{\partial\tau_{xx}^K}{\partial x}\tilde{u}_x\\
&+ \int_F \gamma_1\frac{i\,\omega}{i\,\omega+\alpha(x)}(\mathrm{u}_x^K-\lambda_{1x})n_x^2\tilde{u}_x + \int_F \gamma_3\frac{i\,\omega}{i\,\omega+\alpha(x)}(\mathrm{p}_h-\lambda_2)n_x\tilde{u}_x - \int_K \frac{i\,\omega}{i\,\omega+\beta(y)}\frac{\partial\tau_{xy}^K}{\partial y}\tilde{u}_x\\
&+ \int_F \gamma_1\frac{i\,\omega}{i\,\omega+\beta(y)}(\mathrm{u}_x^K-\lambda_{1x})n_y^2\tilde{u}_x - \int_K \frac{i\,\omega}{i\,\omega+\alpha(x)}\frac{\partial\tau_{xy}^K}{\partial x}\tilde{u}_y + \int_F \gamma_1\frac{i\,\omega}{i\,\omega+\alpha(x)}(\mathrm{u}_y^K-\lambda_{1y})n_x^2\tilde{u}_y\\
&- \int_K \frac{i\,\omega}{i\,\omega+\beta(y)}\frac{\partial\tau_{yy}^K}{\partial y}\tilde{u}_y + \int_F \gamma_1\frac{i\,\omega}{i\,\omega+\beta(y)}(\mathrm{u}_y^K-\lambda_{1y})n_y^2\tilde{u}_y \;+ \int_F \gamma_3\frac{i\,\omega}{i\,\omega+\beta(y)}(\mathrm{p}_h-\lambda_2)n_y\tilde{u}_y \;=\; 0\,,
\end{aligned}$$

$$\begin{aligned}
&\int_K \mathrm{i}\,\omega\rho_f \mathrm{u}_x^K \tilde{w}_x + \int_K \mathrm{i}\,\omega\rho_f \mathrm{u}_y^K \tilde{w}_y + \int_K \mathrm{i}\,\omega\tilde{\rho}\mathrm{w}_x^K \tilde{w}_x + \int_K \mathrm{i}\,\omega\tilde{\rho}\mathrm{w}_y^K \tilde{w}_y - \int_K \frac{i\,\omega}{i\,\omega+\alpha(x)}\mathrm{p}\frac{\partial \tilde{w}_x}{\partial x} + \int_F \frac{i\,\omega}{i\,\omega+\alpha(x)}\lambda_2 n_x \tilde{w}_x\\
&- \int_K \frac{i\,\omega}{i\,\omega+\beta(y)}\mathrm{p}\frac{\partial \tilde{w}_y}{\partial y} + \int_F \frac{i\,\omega}{i\,\omega+\beta(y)}\lambda_2 n_y \tilde{w}_y = 0\,,
\end{aligned}$$

$$
\begin{aligned}
&\int_K \mathrm{i}\omega\tau_{xx}^K\,\tilde\tau_{xx} + \int_K \mathrm{i}\omega\alpha_{11}\mathrm{p}_h\tilde\tau_{xx} + \int_K C_{11}\frac{i\,\omega}{i\,\omega+\alpha(x)}\mathrm{u}_x^K\frac{\partial\tilde\tau_{xx}}{\partial x} - \int_F C_{11}\frac{i\,\omega}{i\,\omega+\alpha(x)}\lambda_{1x}n_x\tilde\tau_{xx}\\
&+\int_K C_{12}\frac{i\,\omega}{i\,\omega+\beta(y)}\mathrm{u}_y^K\frac{\partial\tilde\tau_{xx}}{\partial y} - \int_F C_{12}\frac{i\,\omega}{i\,\omega+\beta(y)}\lambda_{1y}n_y\tilde\tau_{xx} + \int_K C_{13}\frac{i\,\omega}{i\,\omega+\alpha(x)}\mathrm{u}_y^K\frac{\partial\tilde\tau_{xx}}{\partial x}\\
&-\int_F C_{13}\frac{i\,\omega}{i\,\omega+\alpha(x)}\lambda_{1y}n_x\tilde\tau_{xx} + \int_K C_{13}\frac{i\,\omega}{i\,\omega+\beta(y)}\mathrm{u}_x^K\frac{\partial\tilde\tau_{xx}}{\partial y} - \int_F C_{13}\frac{i\,\omega}{i\,\omega+\beta(y)}\lambda_{1x}n_y\tilde\tau_{xx}\\
&+\int_K \mathrm{i}\omega\tau_{yy}^K\,\tilde\tau_{yy} + \int_K \mathrm{i}\omega\alpha_{22}\mathrm{p}_h\tilde\tau_{yy} + \int_K C_{12}\frac{i\,\omega}{i\,\omega+\alpha(x)}\mathrm{u}_x^K\frac{\partial\tilde\tau_{yy}}{\partial x} - \int_F C_{12}\frac{i\,\omega}{i\,\omega+\alpha(x)}\lambda_{1x}n_x\tilde\tau_{yy}\\
&+\int_K C_{22}\frac{i\,\omega}{i\,\omega+\beta(y)}\mathrm{u}_y^K\frac{\partial\tilde\tau_{yy}}{\partial y} - \int_F C_{22}\frac{i\,\omega}{i\,\omega+\beta(y)}\lambda_{1y}n_y\tilde\tau_{yy} + \int_K C_{23}\frac{i\,\omega}{i\,\omega+\alpha(x)}\mathrm{u}_y^K\frac{\partial\tilde\tau_{yy}}{\partial x}\\
&-\int_F C_{23}\frac{i\,\omega}{i\,\omega+\alpha(x)}\lambda_{1y}n_x\tilde\tau_{yy} + \int_K C_{23}\frac{i\,\omega}{i\,\omega+\beta(y)}\mathrm{u}_x^K\frac{\partial\tilde\tau_{yy}}{\partial y} - \int_F C_{23}\frac{i\,\omega}{i\,\omega+\beta(y)}\lambda_{1x}n_y\tilde\tau_{yy}\\
&+\int_K \mathrm{i}\omega\tau_{xy}^K\,\tilde\tau_{xy} + \int_K \mathrm{i}\omega\alpha_{12}\mathrm{p}_h\tilde\tau_{xy} + \int_K C_{13}\frac{i\,\omega}{i\,\omega+\alpha(x)}\mathrm{u}_x^K\frac{\partial\tilde\tau_{xy}}{\partial x} - \int_F C_{13}\frac{i\,\omega}{i\,\omega+\alpha(x)}\lambda_{1x}n_x\tilde\tau_{xy}\\
&+\int_K C_{23}\frac{i\,\omega}{i\,\omega+\beta(y)}\mathrm{u}_y^K\frac{\partial\tilde\tau_{xy}}{\partial y} - \int_F C_{23}\frac{i\,\omega}{i\,\omega+\beta(y)}\lambda_{1y}n_y\tilde\tau_{xy} + \int_K C_{33}\frac{i\,\omega}{i\,\omega+\alpha(x)}\mathrm{u}_y^K\frac{\partial\tilde\tau_{xy}}{\partial x}\\
&-\int_F C_{33}\frac{i\,\omega}{i\,\omega+\alpha(x)}\lambda_{1y}n_x\tilde\tau_{xy} + \int_K C_{33}\frac{i\,\omega}{i\,\omega+\beta(y)}\mathrm{u}_x^K\frac{\partial\tilde\tau_{xy}}{\partial y} - \int_F C_{33}\frac{i\,\omega}{i\,\omega+\beta(y)}\lambda_{1x}n_y\tilde\tau_{xy} = 0\,,\\
&\int_K \mathrm{i}\omega\mathrm{p}_h\tilde{\mathrm{p}} + \int_K M\frac{i\,\omega}{i\,\omega+\alpha(x)}\frac{\partial\mathrm{w}_x^K}{\partial x}\tilde{\mathrm{p}} - \int_F M\gamma_2\frac{i\,\omega}{i\,\omega+\alpha(x)}(\mathrm{p}_h-\lambda_2)n_x^2\tilde{\mathrm{p}} - \int_F M\gamma_4\frac{i\,\omega}{i\,\omega+\alpha(x)}(\mathrm{u}_x^K-\lambda_{1x})n_x\tilde{\mathrm{p}}\\
&+\int_K M\frac{i\,\omega}{i\,\omega+\beta(y)}\frac{\partial\mathrm{w}_y^K}{\partial y}\tilde{\mathrm{p}} - \int_F M\gamma_2\frac{i\,\omega}{i\,\omega+\beta(y)}(\mathrm{p}_h-\lambda_2)n_y^2\tilde{\mathrm{p}} - \int_F M\gamma_4\frac{i\,\omega}{i\,\omega+\beta(y)}(\mathrm{u}_y^K-\lambda_{1y})n_y\tilde{\mathrm{p}}\\
&-\int_K M\alpha_{11}\frac{i\,\omega}{i\,\omega+\alpha(x)}\mathrm{u}_x^K\frac{\partial\tilde{\mathrm{p}}}{\partial x} + \int_F M\alpha_{11}\frac{i\,\omega}{i\,\omega+\alpha(x)}\lambda_{1x}n_x\tilde{\mathrm{p}} - \int_K M\alpha_{22}\frac{i\,\omega}{i\,\omega+\beta(y)}\mathrm{u}_y^K\frac{\partial\tilde{\mathrm{p}}}{\partial y}\\
&+\int_F M\alpha_{22}\frac{i\,\omega}{i\,\omega+\beta(y)}\lambda_{1y}n_y\tilde{\mathrm{p}} - \int_K M\alpha_{12}\frac{i\,\omega}{i\,\omega+\beta(y)}\mathrm{u}_x^K\frac{\partial\tilde{\mathrm{p}}}{\partial y} + \int_F M\alpha_{12}\frac{i\,\omega}{i\,\omega+\beta(y)}\lambda_{1x}n_y\tilde{\mathrm{p}}\\
&-\int_K M\alpha_{12}\frac{i\,\omega}{i\,\omega+\alpha(x)}\mathrm{u}_y^K\frac{\partial\tilde{\mathrm{p}}}{\partial x} + \int_F M\alpha_{12}\frac{i\,\omega}{i\,\omega+\alpha(x)}\lambda_{1y}n_x\tilde{\mathrm{p}} = 0\,.
\end{aligned}
$$

Then, we replace the local unknowns and the local test-functions using equations (4.26a) and (4.26b). We obtain:

$$
\begin{aligned}
&\int_K \mathrm{i}\,\omega\rho_a\underline{\mathrm{u}}_x^K\,\varphi_j^K\varphi_i^K + \int_K \mathrm{i}\,\omega\rho_f\underline{\mathrm{w}}_x^K\,\varphi_j^K\varphi_i^K - \int_K\frac{i\,\omega}{i\,\omega+\alpha(x)}\frac{\partial\underline{\tau}_{xx}^K}{\partial x}\varphi_j^K\varphi_i^K + \int_F\gamma_1\frac{i\,\omega}{i\,\omega+\alpha(x)}(\underline{\mathrm{u}}_x^K\varphi_j^K - \underline{\lambda}_{1x}\psi_j^{\beta(K,f)})n_x^2\varphi_i^K\\
&+\int_F\gamma_3\frac{i\,\omega}{i\,\omega+\alpha(x)}(\underline{\mathrm{p}}^K\varphi_j^K - \underline{\lambda}_2\psi_j^{\beta(K,f)})n_x\varphi_i^K - \int_K\frac{i\,\omega}{i\,\omega+\beta(y)}\frac{\partial\underline{\tau}_{xy}^K}{\partial y}\varphi_j^K\varphi_i^K + \int_F\gamma_1\frac{i\,\omega}{i\,\omega+\beta(y)}(\underline{\mathrm{u}}_x^K\varphi_j^K - \underline{\lambda}_{1x}\psi_j^{\beta(K,f)})n_y^2\varphi_i^K = 0\,,
\end{aligned}
$$

$$
\begin{aligned}
&\int_K \mathrm{i}\omega\rho_a\underline{\mathrm{u}}_y^K\varphi_j^K\varphi_i^K + \int_K \mathrm{i}\omega\rho_f\underline{\mathrm{w}}_y^K\varphi_j^K\varphi_i^K - \int_K\frac{i\,\omega}{i\,\omega+\alpha(x)}\underline{\tau}_{xy}^K\frac{\partial\varphi_j^K}{\partial x}\varphi_i^K + \int_F\gamma_1\frac{i\,\omega}{i\,\omega+\alpha(x)}(\underline{\mathrm{u}}_y^K\varphi_j^K - \underline{\lambda}_{1y}\psi_j^{\beta(K,f)})n_x^2\varphi_i^K\\
&-\int_K\frac{i\,\omega}{i\,\omega+\beta(y)}\frac{\partial\underline{\tau}_{yy}^K}{\partial y}\varphi_j^K\varphi_i^K + \int_F\gamma_1\frac{i\,\omega}{i\,\omega+\beta(y)}(\underline{\mathrm{u}}_y^K\varphi_j^K - \underline{\lambda}_{1y}\psi_j^{\beta(K,f)})n_y^2\varphi_i^K + \int_F\gamma_3\frac{i\,\omega}{i\,\omega+\beta(y)}(\underline{\mathrm{p}}^K\varphi_j^K - \underline{\lambda}_2\psi_j^{\beta(K,f)})n_y\varphi_i^K = 0\,,
\end{aligned}
$$

$$
\begin{aligned}
&\int_K \mathrm{i}\omega\rho_f\underline{\mathrm{u}}_x^K\varphi_j^K\varphi_i^K + \int_K \mathrm{i}\omega\tilde\rho\underline{\mathrm{w}}_x^K\varphi_j^K\varphi_i^K - \int_K\frac{i\,\omega}{i\,\omega+\alpha(x)}\underline{\mathrm{p}}^K\varphi_j^K\frac{\partial\varphi_i^K}{\partial x} + \int_F\frac{i\,\omega}{i\,\omega+\alpha(x)}\underline{\lambda}_2\psi_j^{\beta(K,f)}n_x\varphi_i^K = 0\,,\\
&\int_K \mathrm{i}\omega\rho_f\underline{\mathrm{u}}_y^K\varphi_j^K\varphi_i^K + \int_K \mathrm{i}\omega\tilde\rho\underline{\mathrm{w}}_y^K\varphi_j^K\varphi_i^K - \int_K\frac{i\,\omega}{i\,\omega+\beta(y)}\underline{\mathrm{p}}^K\varphi_j^K\frac{\partial\varphi_i^K}{\partial y} + \int_F\frac{i\,\omega}{i\,\omega+\beta(y)}\underline{\lambda}_2\psi_j^{\beta(K,f)}n_y\varphi_i^K = 0\,,
\end{aligned}
$$

$$\int_K \mathrm{i}\omega \underline{\tau}_{xx}^K \varphi_j^K \varphi_i^K + \int_K \mathrm{i}\omega\alpha_{11}\underline{\mathrm{p}}^K\varphi_j^K\varphi_i^K + \int_K C_{11}\frac{i\,\omega}{i\,\omega+\alpha(x)}\underline{\mathrm{u}}_x^K\varphi_j^K\frac{\partial\varphi_i^K}{\partial x} - \int_F C_{11}\frac{i\,\omega}{i\,\omega+\alpha(x)}\underline{\lambda}_{1x}\psi_j^{\beta(K,f)}n_x\varphi_i^K$$
$$+\int_K C_{12}\frac{i\,\omega}{i\,\omega+\beta(y)}\underline{\mathrm{u}}_y^K\varphi_j^K\frac{\partial\varphi_i^K}{\partial y} - \int_F C_{12}\frac{i\,\omega}{i\,\omega+\beta(y)}\underline{\lambda}_{1y}\psi_j^{\beta(K,f)}n_y\varphi_i^K + \int_K C_{13}\frac{i\,\omega}{i\,\omega+\alpha(x)}\underline{\mathrm{u}}_y^K\varphi_j^K\frac{\partial\varphi_i^K}{\partial x}$$
$$-\int_F C_{13}\frac{i\,\omega}{i\,\omega+\alpha(x)}\underline{\lambda}_{1y}\psi_j^{\beta(K,f)}n_x\varphi_i^K + \int_K C_{13}\frac{i\,\omega}{i\,\omega+\beta(y)}\underline{\mathrm{u}}_x^K\varphi_j^K\frac{\partial\varphi_i^K}{\partial y} - \int_F C_{13}\frac{i\,\omega}{i\,\omega+\beta(y)}\underline{\lambda}_{1x}\psi_j^{\beta(K,f)}n_y\varphi_i^K \;=\; 0\,,$$

$$\int_K \mathrm{i}\omega \underline{\tau}_{yy}^K \varphi_j^K \varphi_i^K + \int_K \mathrm{i}\omega\alpha_{22}\underline{\mathrm{p}}^K\varphi_j^K\varphi_i^K + \int_K C_{12}\frac{i\,\omega}{i\,\omega+\alpha(x)}\underline{\mathrm{u}}_x^K\varphi_j^K\frac{\partial\varphi_i^K}{\partial x} - \int_F C_{12}\frac{i\,\omega}{i\,\omega+\alpha(x)}\underline{\lambda}_{1x}\psi_j^{\beta(K,f)}n_x\varphi_i^K$$
$$+\int_K C_{22}\frac{i\,\omega}{i\,\omega+\beta(y)}\underline{\mathrm{u}}_y^K\varphi_j^K\frac{\partial\varphi_i^K}{\partial y} - \int_F C_{22}\frac{i\,\omega}{i\,\omega+\beta(y)}\underline{\lambda}_{1y}\psi_j^{\beta(K,f)}n_y\varphi_i^K + \int_K C_{23}\frac{i\,\omega}{i\,\omega+\alpha(x)}\underline{\mathrm{u}}_y^K\varphi_j^K\frac{\partial\varphi_i^K}{\partial x}$$
$$-\int_F C_{23}\frac{i\,\omega}{i\,\omega+\alpha(x)}\underline{\lambda}_{1y}\psi_j^{\beta(K,f)}n_x\varphi_i^K + \int_K C_{23}\frac{i\,\omega}{i\,\omega+\beta(y)}\underline{\mathrm{u}}_x^K\varphi_j^K\frac{\partial\varphi_i^K}{\partial y} - \int_F C_{23}\frac{i\,\omega}{i\,\omega+\beta(y)}\underline{\lambda}_{1x}\psi_j^{\beta(K,f)}n_y\varphi_i^K \;=\; 0\,,$$

$$\int_K \mathrm{i}\omega \underline{\tau}_{yy}^K \varphi_j^K \varphi_i^K + \int_K \mathrm{i}\omega\alpha_{22}\mathrm{p}_h\,\varphi_j^K\varphi_i^K + \int_K C_{13}\frac{i\,\omega}{i\,\omega+\alpha(x)}\underline{\mathrm{u}}_x^K\varphi_j^K\frac{\partial\varphi_i^K}{\partial x} - \int_F C_{13}\frac{i\,\omega}{i\,\omega+\alpha(x)}\underline{\lambda}_{1x}\psi_j^{\beta(K,f)}n_x\varphi_i^K$$
$$+\int_K C_{23}\frac{i\,\omega}{i\,\omega+\beta(y)}\underline{\mathrm{u}}_y^K\varphi_j^K\frac{\partial\varphi_i^K}{\partial y} - \int_F C_{23}\frac{i\,\omega}{i\,\omega+\beta(y)}\underline{\lambda}_{1y}\psi_j^{\beta(K,f)}n_y\varphi_i^K + \int_K C_{33}\frac{i\,\omega}{i\,\omega+\alpha(x)}\underline{\mathrm{u}}_y^K\varphi_j^K\frac{\partial\varphi_i^K}{\partial x}$$
$$-\int_F C_{33}\frac{i\,\omega}{i\,\omega+\alpha(x)}\underline{\lambda}_{1y}\psi_j^{\beta(K,f)}n_x\varphi_i^K + \int_K C_{33}\frac{i\,\omega}{i\,\omega+\beta(y)}\underline{\mathrm{u}}_x^K\varphi_j^K\frac{\partial\varphi_i^K}{\partial y} - \int_F C_{33}\frac{i\,\omega}{i\,\omega+\beta(y)}\underline{\lambda}_{1x}\psi_j^{\beta(K,f)}n_y\varphi_i^K = 0\,,$$

and

$$\int_K \mathrm{i}\omega\underline{\mathrm{p}}^K\varphi_j^K\varphi_i^K + \int_K M\frac{i\,\omega}{i\,\omega+\alpha(x)}\underline{\mathrm{w}}_x^K\frac{\partial\varphi_j^K}{\partial x}\varphi_i^K - \int_F M\gamma_2\frac{i\,\omega}{i\,\omega+\alpha(x)}(\underline{\mathrm{p}}^K\varphi_j^K - \underline{\lambda}_2\psi_j^{\beta(K,f)})n_x^2\varphi_i^K$$
$$-\int_F M\gamma_4\frac{i\,\omega}{i\,\omega+\alpha(x)}(\underline{\mathrm{u}}_x^K\varphi_j^K - \underline{\lambda}_{1x}\psi_j^{\beta(K,f)})n_x\varphi_i^K + \int_K M\frac{i\,\omega}{i\,\omega+\beta(y)}\underline{\mathrm{w}}_y^K\frac{\partial\varphi_j^K}{\partial y}\varphi_i^K - \int_F M\gamma_2\frac{i\,\omega}{i\,\omega+\beta(y)}(\underline{\mathrm{p}}^K\varphi_j^K - \underline{\lambda}_2\psi_j^{\beta(K,f)})n_y^2\varphi_i^K$$
$$-\int_F M\gamma_4\frac{i\,\omega}{i\,\omega+\beta(y)}(\underline{\mathrm{u}}_y^K\varphi_j^K - \underline{\lambda}_{1y}\psi_j^{\beta(K,f)})n_y\varphi_i^K - \int_K M\alpha_{11}\frac{i\,\omega}{i\,\omega+\alpha(x)}\underline{\mathrm{u}}_x^K\varphi_j^K\frac{\partial\varphi_i^K}{\partial x} + \int_F M\alpha_{11}\frac{i\,\omega}{i\,\omega+\alpha(x)}\underline{\lambda}_{1x}\psi_j^{\beta(K,f)}n_x\varphi_i^K$$
$$-\int_K M\alpha_{22}\frac{i\,\omega}{i\,\omega+\beta(y)}\underline{\mathrm{u}}_y^K\varphi_j^K\frac{\partial\varphi_i^K}{\partial y} + \int_F M\alpha_{22}\frac{i\,\omega}{i\,\omega+\beta(y)}\underline{\lambda}_{1y}\psi_j^{\beta(K,f)}n_y\varphi_i^K - \int_K M\alpha_{12}\frac{i\,\omega}{i\,\omega+\beta(y)}\underline{\mathrm{u}}_x^K\varphi_j^K\frac{\partial\varphi_i^K}{\partial y}$$
$$+\int_F M\alpha_{12}\frac{i\,\omega}{i\,\omega+\beta(y)}\underline{\lambda}_{1x}\psi_j^{\beta(K,f)}n_y\varphi_i^K - \int_K M\alpha_{12}\frac{i\,\omega}{i\,\omega+\alpha(x)}\underline{\mathrm{u}}_y^K\varphi_j^K\frac{\partial\varphi_i^K}{\partial x} + \int_F M\alpha_{12}\frac{i\,\omega}{i\,\omega+\alpha(x)}\underline{\lambda}_{1y}\psi_j^{\beta(K,f)}n_x\varphi_i^K \;=\; 0\,,$$

We define and recall the following matrices:

$$\mathbb{M}_{ij}^K = \int_K \varphi_i^K\varphi_j^K dX\,, \qquad \mathbb{D}_{vij}^K = \int_K \varphi_j^K\frac{\partial\varphi_i^K}{\partial l}dX\,, \qquad \mathbb{J}_{vij}^F = \int_F \varphi_i^K\varphi_j^K n_v\,dS\,,$$

$$\mathbb{Q}_{vij}^F = \int_F \varphi_i^K\psi_j^F n_u\,dS\,, \qquad \mathbb{L}_{uvij}^F = \int_F \varphi_i^K\psi_j^F n_u n_v dS\,, \qquad \mathbb{N}_{uvij}^F = \int_F \varphi_i^K\varphi_j^K n_u n_v dS\,,$$

with $u = x, y$, $v = x, y$. The elementary matrices $\mathbb{A}^K$ and $\mathbb{B}^K$ are then expressed as follows:

$$\mathbb{A}^K = \begin{pmatrix}\mathbb{A}_1^K & \mathbb{A}_2^K & \mathbb{A}_3^K & \mathbb{A}_4^K & \mathbb{A}_5^K & \mathbb{A}_6^K & \mathbb{A}_7^K & \mathbb{A}_8^K\end{pmatrix},$$

with

$$\mathbb{A}_1^K = \begin{pmatrix} \mathrm{i}\,\omega\rho_a^K\mathbb{M}^K + \sum_{f=1}^{3}\gamma_1\left(\frac{i\,\omega}{i\,\omega+\alpha(x)}\mathbb{N}_{xl}^K + \frac{i\,\omega}{i\,\omega+\beta(y)}\mathbb{N}_{yl}^K\right) \\ 0 \\ \mathrm{i}\,\omega\rho_f^K\mathbb{M}^K \\ 0 \\ \left(C_{11}\frac{i\,\omega}{i\,\omega+\alpha(x)}\mathbb{D}_x^K + C_{13}\frac{i\,\omega}{i\,\omega+\beta(y)}\mathbb{D}_y^K\right) \\ \left(C_{12}\frac{i\,\omega}{i\,\omega+\alpha(x)}\mathbb{D}_x^K + C_{23}\frac{i\,\omega}{i\,\omega+\beta(y)}\mathbb{D}_y^K\right) \\ \left(C_{13}\frac{i\,\omega}{i\,\omega+\alpha(x)}\mathbb{D}_x^K + C_{33}\frac{i\,\omega}{i\,\omega+\beta(y)}\mathbb{D}_y^K\right) \\ -M\left(\sum_{f=1}^{3}\gamma_4\frac{i\,\omega}{i\,\omega+\alpha(x)}\mathbb{J}_x^{\beta(l,f)} + \alpha_{11}\frac{i\,\omega}{i\,\omega+\alpha(x)}\mathbb{D}_x^K + \alpha_{12}\frac{i\,\omega}{i\,\omega+\beta(y)}\mathbb{D}_y^K\right) \end{pmatrix},$$

$$\mathbb{A}_2^K = \begin{pmatrix} 0 \\ \mathrm{i}\,\omega\rho_a^K\mathbb{M}^K + \sum_{f=1}^{3}\gamma_1\left(\frac{i\,\omega}{i\,\omega+\alpha(x)}\mathbb{N}_{xl}^K + \frac{i\,\omega}{i\,\omega+\beta(y)}\mathbb{N}_{yl}^K\right) \\ 0 \\ \mathrm{i}\,\omega\rho_f^K\mathbb{M}^K \\ \left(C_{13}\frac{i\,\omega}{i\,\omega+\alpha(x)}\mathbb{D}_x^K + C_{12}\frac{i\,\omega}{i\,\omega+\beta(y)}\mathbb{D}_y^K\right) \\ \left(C_{23}\frac{i\,\omega}{i\,\omega+\alpha(x)}\mathbb{D}_x^K + C_{22}\frac{i\,\omega}{i\,\omega+\beta(y)}\mathbb{D}_y^K\right) \\ \left(C_{33}\frac{i\,\omega}{i\,\omega+\alpha(x)}\mathbb{D}_x^K + C_{23}\frac{i\,\omega}{i\,\omega+\beta(y)}\mathbb{D}_y^K\right) \\ -M\left(\sum_{f=1}^{3}\gamma_4\frac{i\,\omega}{i\,\omega+\beta(y)}\mathbb{J}_y^{\beta(l,f)} + \alpha_{12}\frac{i\,\omega}{i\,\omega+\alpha(x)}\mathbb{D}_x^K + \alpha_{22}\frac{i\,\omega}{i\,\omega+\beta(y)}\mathbb{D}_y^K\right) \end{pmatrix},$$

$$\mathbb{A}_3^K = \begin{pmatrix} \mathrm{i}\,\omega\rho_f^K\mathbb{M}^K \\ 0 \\ \mathrm{i}\,\omega\tilde{\rho}^K\mathbb{M}^K \\ 0 \\ 0 \\ 0 \\ 0 \\ M\frac{i\,\omega}{i\,\omega+\alpha(x)}(\mathbb{D}_x^K)^T \end{pmatrix}, \qquad \mathbb{A}_4^K = \begin{pmatrix} 0 \\ \mathrm{i}\,\omega\rho_f^K\mathbb{M}^K \\ 0 \\ \mathrm{i}\,\omega\tilde{\rho}^K\mathbb{M}^K \\ 0 \\ 0 \\ 0 \\ M\frac{i\,\omega}{i\,\omega+\beta(y)}(\mathbb{D}_y^K)^T \end{pmatrix},$$

$$\mathbb{A}_5^K = \begin{pmatrix} -\frac{i\,\omega}{i\,\omega+\alpha(x)}(\mathbb{D}_x^K)^T \\ 0 \\ 0 \\ 0 \\ \mathrm{i}\,\omega\mathbb{M}^K \\ 0 \\ 0 \\ 0 \end{pmatrix}, \qquad \mathbb{A}_6^K = \begin{pmatrix} 0 \\ -\frac{i\,\omega}{i\,\omega+\beta(y)}(\mathbb{D}_y^K)^T \\ 0 \\ 0 \\ 0 \\ \mathrm{i}\,\omega\mathbb{M}^K \\ 0 \\ 0 \end{pmatrix}, \qquad \mathbb{A}_7^K = \begin{pmatrix} -\frac{i\,\omega}{i\,\omega+\beta(y)}(\mathbb{D}_y^K)^T \\ -\frac{i\,\omega}{i\,\omega+\alpha(x)}(\mathbb{D}_x^K)^T \\ 0 \\ 0 \\ 0 \\ 0 \\ \mathrm{i}\,\omega\mathbb{M}^K \\ 0 \end{pmatrix},$$

$$\mathbb{A}_8^K = \begin{pmatrix} \sum_{f=1}^{3} \gamma_3 \frac{i\,\omega}{i\,\omega+\alpha(x)} \mathbb{J}_x^{\beta(K,f)} \\ \sum_{f=1}^{3} \gamma_3 \frac{i\,\omega}{i\,\omega+\beta(y)} \mathbb{J}_y^{\beta(K,f)} \\ -\frac{i\,\omega}{i\,\omega+\alpha(x)} \mathbb{D}_x^K \\ -\frac{i\,\omega}{i\,\omega+\beta(y)} \mathbb{D}_y^K \\ \mathrm{i}\omega\alpha_{11}^K \mathbb{M}^K \\ \mathrm{i}\,\omega\alpha_{22}^K \mathbb{M}^K \\ \mathrm{i}\,\omega\alpha_{12}^K \mathbb{M}^K \\ \mathrm{i}\,\omega\mathbb{M}^K - \sum_{f=1}^{3} M\gamma_2 \left(\frac{i\,\omega}{i\,\omega+\alpha(x)} \mathbb{N}_x^{\beta(K,f)} + \frac{i\,\omega}{i\,\omega+\beta(y)} \mathbb{N}_y^{\beta(K,f)} \right) \end{pmatrix},$$

and

$$\mathbb{B}^K = \begin{pmatrix} B_{\lambda_{1x},1} & B_{\lambda_{1x},2} & B_{\lambda_{1x},3} & B_{\lambda_{1y},1} & B_{\lambda_{1y},2} & B_{\lambda_{1y},3} & B_{\lambda_2,1} & B_{\lambda_2,2} & B_{\lambda_2,3} \end{pmatrix}$$

with

$$B_{\lambda_{1x},f} = \begin{pmatrix} -\gamma_1 \left(\frac{i\,\omega}{i\,\omega+\alpha(x)} \mathbb{L}_x^{\beta(K,f)} + \frac{i\,\omega}{i\,\omega+\beta(y)} \mathbb{L}_y^{\beta(K,f)} \right) \\ 0 \\ 0 \\ 0 \\ \left(-C_{11} \frac{i\,\omega}{i\,\omega+\alpha(x)} \mathbb{Q}_x^{\beta(K,f)} - C_{13} \frac{i\,\omega}{i\,\omega+\beta(y)} \mathbb{Q}_y^{\beta(K,f)} \right) \\ \left(-C_{12} \frac{i\,\omega}{i\,\omega+\alpha(x)} \mathbb{Q}_x^{\beta(K,f)} - C_{23} \frac{i\,\omega}{i\,\omega+\beta(y)} \mathbb{Q}_y^{\beta(K,f)} \right) \\ \left(-C_{13} \frac{i\,\omega}{i\,\omega+\alpha(x)} \mathbb{Q}_x^{\beta(K,f)} - C_{33} \frac{i\,\omega}{i\,\omega+\beta(y)} \mathbb{Q}_y^{\beta(K,f)} \right) \\ M \left((\gamma_4+\alpha_{11}) \frac{i\,\omega}{i\,\omega+\alpha(x)} \mathbb{Q}_x^{\beta(K,f)} + \alpha_{12} \frac{i\,\omega}{i\,\omega+\beta(y)} \mathbb{Q}_y^{\beta(K,f)} \right) \end{pmatrix}, \text{ for } f = 1,2,3\,,$$

$$B_{\lambda_{1y},f} = \begin{pmatrix} 0 \\ -\gamma_1 \left(\frac{i\,\omega}{i\,\omega+\alpha(x)} \mathbb{L}_x^{\beta(K,f)} + \frac{i\,\omega}{i\,\omega+\beta(y)} \mathbb{L}_y^{\beta(K,f)} \right) \\ 0 \\ 0 \\ \left(-C_{13} \frac{i\,\omega}{i\,\omega+\alpha(x)} \mathbb{Q}_x^{\beta(K,f)} - C_{12} \frac{i\,\omega}{i\,\omega+\beta(y)} \mathbb{Q}_y^{\beta(K,f)} \right) \\ \left(-C_{23} \frac{i\,\omega}{i\,\omega+\alpha(x)} \mathbb{Q}_x^{\beta(K,f)} - C_{22} \frac{i\,\omega}{i\,\omega+\beta(y)} \mathbb{Q}_y^{\beta(K,f)} \right) \\ \left(-C_{33} \frac{i\,\omega}{i\,\omega+\alpha(x)} \mathbb{Q}_x^{\beta(K,f)} - C_{23} \frac{i\,\omega}{i\,\omega+\beta(y)} \mathbb{Q}_y^{\beta(K,f)} \right) \\ M \left(\alpha_{12} \frac{i\,\omega}{i\,\omega+\alpha(x)} \mathbb{Q}_x^{\beta(K,f)} + (\gamma_4+\alpha_{22}) \frac{i\,\omega}{i\,\omega+\beta(y)} \mathbb{Q}_y^{\beta(K,f)} \right) \end{pmatrix}, \text{ for } f = 1,2,3\,,$$

$$B_{\lambda_2,f} = \begin{pmatrix} -\gamma_3 \frac{i\,\omega}{i\,\omega+\alpha(x)} \mathbb{Q}_x^{\beta(K,f)} \\ -\gamma_3 \frac{i\,\omega}{i\,\omega+\beta(y)} \mathbb{Q}_y^{\beta(K,f)} \\ \frac{i\,\omega}{i\,\omega+\alpha(x)} \mathbb{Q}_x^{\beta(K,f)} \\ \frac{i\,\omega}{i\,\omega+\beta(y)} \mathbb{Q}_y^{\beta(K,f)} \\ 0 \\ 0 \\ 0 \\ M\gamma_2 \left(\frac{i\,\omega}{i\,\omega+\alpha(x)} \mathbb{L}_x^{\beta(K,f)} + \frac{i\,\omega}{i\,\omega+\beta(y)} \mathbb{L}_y^{\beta(K,f)} \right) \end{pmatrix}, \text{ for } f = 1,2,3\,.$$

C.2 HDG method using Absorbing Boundary Conditions

In this section, we present how to take into account the presence of absorbing boundary conditions in the HDG algorithm. Recall that the HDG formulation is obtained by combining the local problem with two transmission conditions at the interfaces of the mesh. The presence of the absorbing boundary has no impact on the local problem. In the previous section, we have obtained the following radiation condition (see (4.35)):

$$\begin{cases} \boldsymbol{\tau}\,\boldsymbol{n} + \Big(\mathbf{X}_1(\mathbf{u}\cdot\boldsymbol{n}) + \mathbf{X}_2(\mathbf{w}\cdot\boldsymbol{n})\Big)\,\boldsymbol{n} + \mathbf{X}_3(\mathbf{u}\cdot\mathbf{t})\,\mathbf{t} + \mathbf{X}_3(\mathbf{u}\cdot\mathbf{a})\,\mathbf{a} = 0\,, \\ \mathrm{p} + \mathbf{X}_4(\mathbf{u}\cdot\boldsymbol{n}) + \mathbf{X}_5(\mathbf{w}\cdot\boldsymbol{n}) \;= 0\,. \end{cases}$$

We consider an element K of a mesh, and $(\boldsymbol{\eta},\,\xi) \in \boldsymbol{M}_h \times M_h$ (spaces defined in (3.5)) two test-functions defined on the faces of the element K. On the absorbing boundary $\mathcal{F}_{\mathrm{rbc}}$, we then impose instead of the transmission conditions:

$$\sum_{F\in\mathcal{F}_{\mathrm{rbc}}} \int_F \left(\hat{\boldsymbol{\tau}}\,\boldsymbol{n} + \Big(\mathbf{X}_1(\hat{\mathbf{u}}\cdot\boldsymbol{n}) + \mathbf{X}_2(\hat{\mathbf{w}}\cdot\boldsymbol{n})\Big)\,\boldsymbol{n} + \mathbf{X}_3(\hat{\mathbf{u}}\cdot\mathbf{t})\,\mathbf{t} + \mathbf{X}_3(\hat{\mathbf{u}}\cdot\mathbf{a})\,\mathbf{a} \right) \cdot \boldsymbol{\eta} = 0\,, \tag{C.2a}$$

$$\sum_{F\in\mathcal{F}_{\mathrm{rbc}}} \int_F (\hat{\mathrm{p}} + \mathbf{X}_4(\hat{\mathbf{u}}\cdot\boldsymbol{n}) + \mathbf{X}_5(\hat{\mathbf{w}}\cdot\boldsymbol{n}))\xi = 0\,. \tag{C.2b}$$

In the following two sections, we consider a face of the mesh F, which is on the absorbing boundary $\mathcal{F}_{\mathrm{rbc}}$, and we present the discretization of the two equations given in (C.2).

C.2.1 Discretization of condition (C.2a)

Starting from equation (C.2a):

$$\int_F \left(\hat{\boldsymbol{\tau}}\,\boldsymbol{n} + \Big(\mathbf{X}_1(\hat{\mathbf{u}}\cdot\boldsymbol{n}) + \mathbf{X}_2(\hat{\mathbf{w}}\cdot\boldsymbol{n})\Big)\,\boldsymbol{n} + \mathbf{X}_3(\hat{\mathbf{u}}\cdot\mathbf{t})\,\mathbf{t} + \mathbf{X}_3(\hat{\mathbf{u}}\cdot\mathbf{a})\,\mathbf{a} \right) \cdot \boldsymbol{\eta} = 0\,,$$

and replacing the numerical traces $\hat{\mathbf{w}}$, $\hat{\boldsymbol{\tau}}$, $\hat{\mathbf{w}}$ by their expressions given respectively in (3.10) and (3.14), we obtain

$$\begin{aligned} &\int_F (\boldsymbol{\tau}_h\,\boldsymbol{n})\cdot\boldsymbol{\eta} - \int_F \gamma_1(\mathbf{u}_h - \boldsymbol{\lambda}_1)\cdot\boldsymbol{\eta} - \int_F \gamma_3(\mathrm{p}_h - \lambda_2)\boldsymbol{n}\cdot\boldsymbol{\eta} + \int_F \Big(\mathbf{X}_1(\boldsymbol{\lambda}_1\cdot\boldsymbol{n})\boldsymbol{n}\Big)\cdot\boldsymbol{\eta} + \int_F \Big(\mathbf{X}_2(\mathbf{w}_h\cdot\boldsymbol{n})\boldsymbol{n}\Big)\cdot\boldsymbol{\eta} \\ &- \int_F \gamma_2\mathbf{X}_2(\mathrm{p}_h - \lambda_2)\boldsymbol{n}\cdot\boldsymbol{\eta} - \int_F \Big(\big(\gamma_4(\mathbf{u}_h - \boldsymbol{\lambda}_1)\cdot\boldsymbol{n}\big)\boldsymbol{n}\Big)\cdot\boldsymbol{\eta} + \int_F \Big(\mathbf{X}_3(\boldsymbol{\lambda}_1\cdot\mathbf{t})\,\mathbf{t}\Big)\cdot\boldsymbol{\eta} + \int_F \Big(\mathbf{X}_3(\boldsymbol{\lambda}_1\cdot\mathbf{a})\,\mathbf{a}\Big)\cdot\boldsymbol{\eta} = 0\,. \end{aligned}$$

The discretization of the equation on (x,y,z) is written for $\bullet = x,y,z$, we replace the test-functions $\eta_\bullet$ by basis functions $\psi_i^{\beta(K,f)}$, and we express the unknowns with their decomposition given in equations (3.26) for the local solutions and equation (3.25) for the local Lagrange unknowns.

$$\begin{aligned} &\int_F \underline{\tau}^K_{x\bullet}\, n_x^K \varphi_j^K \psi_i^{\beta(K,f)} + \int_F \underline{\tau}^K_{y\bullet}\, n_y^K \varphi_j^K \psi_i^{\beta(K,f)} + \int_F \underline{\tau}^K_{z\bullet}\, n_z^K \varphi_j^K \psi_i^{\beta(K,f)} - \int_F \gamma_1 \underline{\mathrm{u}}^K_\bullet \varphi_j^K \psi_i^{\beta(K,f)} dS \\ &+ \int_F \gamma_1 \underline{\lambda}_{1\bullet}^{\beta(K,f)} \psi_j^{\beta(K,f)} \psi_i^{\beta(K,f)} dS - \int_F \gamma_3 n_\bullet^K \underline{\mathrm{p}}^K \varphi_j^K \psi_i^{\beta(K,f)} dS + \int_F \gamma_3 n_\bullet^K \underline{\lambda}_2^K \psi_j^{\beta(K,f)} \psi_i^{\beta(K,f)} dS \\ &+ \int_F \mathbf{X}_1(\underline{\lambda}_{1x}^{\beta(K,f)} n_x + \underline{\lambda}_{1y}^{\beta(K,f)} n_y + \underline{\lambda}_{1z}^{\beta(K,f)} n_z) n_\bullet \psi_j^{\beta(K,f)} \psi_i^{\beta(K,f)} dS + \int_F \mathbf{X}_2(\underline{\mathrm{w}}_x^K n_x + \underline{\mathrm{w}}_y^K n_y + \underline{\mathrm{w}}_z^K n_z) n_\bullet \psi_j^{\beta(K,f)} \psi_i^{\beta(K,f)} dS \\ &- \int_F \mathbf{X}_2 \gamma_2\, \underline{\mathrm{p}}^K n_\bullet \varphi_j^K\, \psi_i^{\beta(K,f)} dS + \int_F \mathbf{X}_2 \gamma_2\, \underline{\lambda}_2^K n_\bullet\, \psi_j^{\beta(K,f)}\, \psi_i^{\beta(K,f)} dS - \int_F \mathbf{X}_2 \gamma_4\, (\underline{\mathrm{u}}_x^K n_x + \underline{\mathrm{u}}_y^K n_y + \underline{\mathrm{u}}_z^K n_z) n_\bullet\, \varphi_j^K\, \psi_i^{\beta(K,f)} dS \\ &+ \int_F \mathbf{X}_2\, \gamma_4\, (\underline{\lambda}_{1x}^{\beta(K,f)} n_x + \underline{\lambda}_{1y}^{\beta(K,f)} n_y + \underline{\lambda}_{1z}^{\beta(K,f)} n_z) n_\bullet\, \psi_j^{\beta(K,f)}\, \psi_i^{\beta(K,f)} dS \\ &+ \int_F \mathbf{X}_3\, (\underline{\lambda}_{1x}^{\beta(K,f)} t_x + \underline{\lambda}_{1y}^{\beta(K,f)} t_y + \underline{\lambda}_{1z}^{\beta(K,f)} t_z) t_\bullet \psi_j^{\beta(K,f)} \psi_i^{\beta(K,f)} dS \\ &+ \int_F \mathbf{X}_3\, (\underline{\lambda}_{1x}^{\beta(K,f)} a_x + \underline{\lambda}_{1y}^{\beta(K,f)} a_y + \underline{\lambda}_{1z}^{\beta(K,f)} a_z) a_\bullet \psi_j^{\beta(K,f)} \psi_i^{\beta(K,f)} dS \;= 0\,, \end{aligned}$$

We write the above equation in terms of the elementary matrices defined in (4.28):

$$(\mathbb{Q}_x^{\beta(K,f)})^T \underline{\tau}_{x\bullet}^K + (\mathbb{Q}_y^{\beta(K,f)})^T \underline{\tau}_{y\bullet}^K + (\mathbb{Q}_z^{\beta(K,f)})^T \underline{\tau}_{z\bullet}^K - \gamma_1 (\mathbb{F}^{\beta(K,f)})^T \underline{\mathrm{u}}_\bullet^K + \gamma_1 \mathbb{G}^{\beta(K,f)} \underline{\lambda}_{1\bullet}^{\beta(K,f)} - \gamma_3 (\mathbb{Q}_\bullet^{\beta(K,f)})^T \underline{\mathrm{p}}^K$$

$$+ \gamma_3 \mathbb{H}_\bullet^{\beta(K,f)} \underline{\lambda}_2^{\beta(K,f)} + \mathbb{O}_{x\bullet}^{\beta(K,f)} \mathbf{X}_1 \underline{\lambda}_{1x}^{\beta(K,f)} + \mathbb{O}_{y\bullet}^{\beta(K,f)} \mathbf{X}_1 \underline{\lambda}_{1y}^{\beta(K,f)} + \mathbb{O}_{z\bullet}^{\beta(K,f)} \mathbf{X}_1 \underline{\lambda}_{1z}^{\beta(K,f)} + (\mathbb{L}_{x\bullet}^{\beta(K,f)})^T \mathbf{X}_2 \underline{\mathrm{w}}_x^K$$

$$+ (\mathbb{L}_{y\bullet}^{\beta(K,f)})^T \mathbf{X}_2 \underline{\mathrm{w}}_y^K + (\mathbb{L}_{z\bullet}^{\beta(K,f)})^T \mathbf{X}_2 \underline{\mathrm{w}}_z^K - (\mathbb{Q}_\bullet^{\beta(K,f)})^T \mathbf{X}_2 \gamma_2 \underline{\mathrm{p}}^K + \mathbb{H}_\bullet^{\beta(K,f)} \mathbf{X}_2 \gamma_2 \underline{\lambda}_2^{\beta(K,f)}$$

$$- (\mathbb{L}_{x\bullet}^{\beta(K,f)})^T \mathbf{X}_2 \gamma_4 \underline{\mathrm{u}}_x^K - (\mathbb{L}_{y\bullet}^{\beta(K,f)})^T \mathbf{X}_2 \gamma_4^{\beta(K,f)} \underline{\mathrm{u}}_y^K - (\mathbb{L}_{z\bullet}^{\beta(K,f)})^T \mathbf{X}_2 \gamma_4^{\beta(K,f)} \underline{\mathrm{u}}_z^K + \mathbb{O}_{x\bullet}^{\beta(K,f)} \mathbf{X}_2 \underline{\lambda}_{1x}^{\beta(K,f)}$$

$$+ \mathbb{O}_{y\bullet}^{\beta(K,f)} \mathbf{X}_2 \underline{\lambda}_{1y}^{\beta(K,f)} + \mathbb{O}_{z\bullet}^{\beta(K,f)} \mathbf{X}_2 \underline{\lambda}_{1z}^{\beta(K,f)} + \mathbb{G}^{\beta(K,f)} t_x t_\bullet \mathbf{X}_3 \underline{\lambda}_{1x}^{\beta(K,f)} + \mathbb{G}_{y\bullet}^{\beta(K,f)} t_y t_\bullet \mathbf{X}_3 \underline{\lambda}_{1y}^{\beta(K,f)}$$

$$+ \mathbb{G}_{z\bullet}^{\beta(K,f)} t_z t_\bullet \mathbf{X}_3 \underline{\lambda}_{1z}^{\beta(K,f)} + \mathbb{G}^{\beta(K,f)} a_x a_\bullet \mathbf{X}_3 \underline{\lambda}_{1x}^{\beta(K,f)} + \mathbb{G}_{y\bullet}^{\beta(K,f)} a_y a_\bullet \mathbf{X}_3 \underline{\lambda}_{1y}^{\beta(K,f)} + \mathbb{G}_{z\bullet}^{\beta(K,f)} a_z a_\bullet \mathbf{X}_3 \underline{\lambda}_{1z}^{\beta(K,f)} = 0\,,$$

C.2.2 Discretization of condition (C.2b)

Considering equation (C.2b) on a face F gives

$$\int_F (\hat{\mathrm{p}} + \mathbf{X}_4(\hat{\mathbf{u}} \cdot \boldsymbol{n}) + \mathbf{X}_5(\hat{\mathbf{w}} \cdot \boldsymbol{n}))\, \xi = 0\,.$$

Using the expressions of the numerical traces $\hat{\mathbf{w}}$ (3.10), $\hat{\mathbf{w}}$ (3.14), we have:

$$\int_F \Big(\lambda_2 + \mathbf{X}_4(\boldsymbol{\lambda}_1 \cdot \boldsymbol{n}) + \mathbf{X}_5 \Big((\mathbf{w}_h - (\mathrm{p}_h - \lambda_2)\, \gamma_2 \, - \gamma_4(\mathbf{u}_h - \boldsymbol{\lambda}_1) \cdot \boldsymbol{n} \Big) \Big)\, \xi = 0\,.$$

The equation is discretized on (x, y, z) and the local solutions and lagrange operators are expressed with the expressions given in (3.26) and (3.25):

$$\int_F \underline{\lambda}_2^K \psi_j^{\beta(K,f)} \psi_i^{\beta(K,f)} dS + \int_F \mathbf{X}_4 (\underline{\lambda}_{1x}^{\beta(K,f)} n_x + \underline{\lambda}_{1y}^{\beta(K,f)} n_y + \underline{\lambda}_{1z}^{\beta(K,f)} n_z) \psi_j^{\beta(K,f)} \psi_i^{\beta(K,f)} dS$$

$$+ \int_F \mathbf{X}_5 (\underline{\mathrm{w}}_x^K n_x + \underline{\mathrm{w}}_y^K n_y + \underline{\mathrm{w}}_z^K n_z) \varphi_j^K \psi_i^{\beta(K,f)} dS - \int_F \mathbf{X}_5\, \gamma_2 \underline{\mathrm{p}}^K\, \varphi_j^K\, \psi_i^{\beta(K,f)} dS + \int_F \mathbf{X}_5\, \gamma_2 \underline{\lambda}_2^K\, \psi_j^{\beta(K,f)}\, \psi_i^{\beta(K,f)} dS$$

$$- \int_F \mathbf{X}_5 \gamma_4 (\underline{\mathrm{u}}_x^K n_x + \underline{\mathrm{u}}_y^K n_y + \underline{\mathrm{u}}_z^K n_z) \varphi_j^K \psi_i^{\beta(K,f)} dS + \int_F \mathbf{X}_5 \gamma_4 (\underline{\lambda}_{1x}^{\beta(K,f)} n_x + \underline{\lambda}_{1y}^{\beta(K,f)} n_y + \underline{\lambda}_{1z}^{\beta(K,f)} n_z) \psi_j^{\beta(K,f)} \psi_i^{\beta(K,f)} dS = 0.$$

Using the elementary matrices, we obtain:

$$\mathbb{G}^{\beta(K,f)} \underline{\lambda}_2^{\beta(K,f)} + \mathbb{H}_x^{\beta(K,f)} \mathbf{X}_4 \underline{\lambda}_{1x}^{\beta(K,f)} + \mathbb{H}_y^{\beta(K,f)} \mathbf{X}_4 \underline{\lambda}_{1y}^{\beta(K,f)} + \mathbb{H}_z^{\beta(K,f)} \mathbf{X}_4 \underline{\lambda}_{1z}^{\beta(K,f)} + (\mathbb{Q}_x^{\beta(K,f)})^T \mathbf{X}_5 \underline{\mathrm{w}}_x^K + (\mathbb{Q}_y^{\beta(K,f)})^T \mathbf{X}_5 \underline{\mathrm{w}}_y^K$$

$$+ (\mathbb{Q}_z^{\beta(K,f)})^T \mathbf{X}_5 \underline{\mathrm{w}}_z^K - \mathbb{F}^{K^T} \mathbf{X}_5\, \gamma_2 \underline{\mathrm{p}}^K + \mathbb{G}^{\beta(K,f)} \mathbf{X}_5\, \gamma_2 \underline{\lambda}_2^K - (\mathbb{Q}_x^{\beta(K,f)})^T \mathbf{X}_5\, \gamma_4\, \underline{\mathrm{u}}_x^K - (\mathbb{Q}_y^{\beta(K,f)})^T \mathbf{X}_5\, \gamma_4\, \underline{\mathrm{u}}_y^K$$

$$- (\mathbb{Q}_z^{\beta(K,f)})^T \mathbf{X}_5\, \gamma_4\, \underline{\mathrm{u}}_z^K + \mathbb{H}_x^{\beta(K,f)} \mathbf{X}_5\, \gamma_4\, \underline{\lambda}_{1x}^{\beta(K,f)} + \mathbb{H}_y^{\beta(K,f)} \mathbf{X}_5\, \gamma_4\, \underline{\lambda}_{1y}^{\beta(K,f)} + \mathbb{H}_z^{\beta(K,f)} \mathbf{X}_5\, \gamma_4\, \underline{\lambda}_{1z}^{\beta(K,f)} = 0\,.$$

With the discretization of the radiation condition, and the transmission condition on the other faces of an element K, we can a build a system of the form

$$\sum_{K \in \mathcal{T}_h} (\mathcal{A}_{HDG}^K)^T \left(\mathbb{P}^K \underline{W}^K + \mathbb{T}^K \mathcal{A}_{HDG}^K \underline{\Lambda} \right) = \mathbb{S}_{\mathrm{inc}}\,,$$

with $\underline{W}^K$ and $\underline{\Lambda}^K$ given in equation (3.27). The expression of the matrices $\mathbb{P}^K$ and $\mathbb{T}^K$ is detailed below. The resolution of the HDG method with absorbing boundary conditions is given in Algorithm 2.

C.2.3 Elementary matrices in three dimensions with RBC

Recall that in the HDG method, the two transmission conditions are used to build a system of the form:

$$\sum_{K \in \mathcal{T}_h} (\mathcal{A}_{HDG}^K)^T \left(\mathbb{P}^K \underline{W}^K + \mathbb{T}^K \mathcal{A}_{HDG}^K \underline{\Lambda} \right) = \mathbb{S}_{\mathrm{inc}}\,.$$

If the four faces of the element K are internal faces, the matrices $\mathbb{P}^K$ and $\mathbb{T}^K$ are given in Appendix B.1.2. Here, we focus on an element with a face on the absorbing boundary. If the face 1 of the element in local numbering is included in $\mathcal{F}_{\text{rbc}}$, the first, fifth, ninth and thirteenth lines of $\mathbb{P}^K$ are modified as follows:

$$\mathbb{P}^K_{1,:} = \Big(-\gamma_1(\mathbb{F}_1^{\beta(K,1)})^T - \gamma_4 \mathbf{X}_2(\mathbb{L}_{xx}^{\beta(K,1)})^T \quad -\gamma_4 \mathbf{X}_2(\mathbb{L}_{xy}^{\beta(K,1)})^T \quad -\gamma_4 \mathbf{X}_2(\mathbb{L}_{xz}^{\beta(K,1)})^T \quad \mathbf{X}_2(\mathbb{L}_{xx}^{\beta(K,1)})^T \quad \mathbf{X}_2(\mathbb{L}_{xy}^{\beta(K,1)})^T \quad ...$$

$$... \quad \mathbf{X}_2(\mathbb{L}_{xz}^{\beta(K,1)})^T \quad (\mathbb{Q}_x^{\beta(K,1)})^T \quad 0 \quad 0 \quad 0 \quad (\mathbb{Q}_z^{\beta(K,1)})^T \quad (\mathbb{Q}_y^{\beta(K,1)})^T \qquad (-\gamma_3 - \gamma_2 \mathbf{X}_2)\,(\mathbb{Q}_x^{\beta(K,1)})^T \Big),$$

$$\mathbb{P}^K_{5,:} = \Big(-\gamma_4 \mathbf{X}_2(\mathbb{L}_{xy}^{\beta(K,1)})^T \quad -\gamma_1(\mathbb{F}_1^{\beta(K,1)})^T - \gamma_4 \mathbf{X}_2(\mathbb{L}_{yy}^{\beta(K,1)})^T \quad -\gamma_4 \mathbf{X}_2(\mathbb{L}_{yz}^{\beta(K,1)})^T \quad \mathbf{X}_2(\mathbb{L}_{xy}^{\beta(K,1)})^T \quad \mathbf{X}_2(\mathbb{L}_{yy}^{\beta(K,1)})^T \quad ...$$

$$... \quad \mathbf{X}_2(\mathbb{L}_{yz}^{\beta(K,1)})^T \quad 0 \quad (\mathbb{Q}_y^{\beta(K,1)})^T \quad 0 \quad (\mathbb{Q}_z^{\beta(K,1)})^T \quad 0 \quad (\mathbb{Q}_y^{\beta(K,1)})^T \qquad (-\gamma_3 - \gamma_2 \mathbf{X}_2)\,(\mathbb{Q}_y^{\beta(K,1)})^T \Big),$$

$$\mathbb{P}^K_{9,:} = \Big(-\gamma_4 \mathbf{X}_2(\mathbb{L}_{xz}^{\beta(K,1)})^T \quad -\gamma_1(\mathbb{F}_1^{\beta(K,1)})^T - \gamma_4 \mathbf{X}_2(\mathbb{L}_{yz}^{\beta(K,1)})^T \quad -\gamma_4 \mathbf{X}_2(\mathbb{L}_{zz}^{\beta(K,1)})^T \quad \mathbf{X}_2(\mathbb{L}_{xz}^{\beta(K,1)})^T \quad \mathbf{X}_2(\mathbb{L}_{yz}^{\beta(K,1)})^T \quad ...$$

$$... \quad \mathbf{X}_2(\mathbb{L}_{zz}^{\beta(K,1)})^T \quad 0 \quad 0 \quad (\mathbb{Q}_z^{\beta(K,1)})^T \quad (\mathbb{Q}_y^{\beta(K,1)})^T \quad (\mathbb{Q}_x^{\beta(K,1)})^T \quad 0 \qquad (-\gamma_3 - \gamma_2 \mathbf{X}_2)\,(\mathbb{Q}_z^{\beta(K,1)})^T \Big),$$

and

$$\mathbb{P}^K_{13,:} = \Big(-\mathbf{X}_5\,\gamma_4(\mathbb{Q}_x^{\beta(K,1)})^T \qquad -\mathbf{X}_5\,\gamma_4(\mathbb{Q}_y^{\beta(K,1)})^T \qquad -\mathbf{X}_5\,\gamma_4(\mathbb{Q}_z^{\beta(K,1)})^T \quad \mathbf{X}_5(\mathbb{Q}_x^{\beta(K,1)})^T \quad \mathbf{X}_5(\mathbb{Q}_y^{\beta(K,1)})^T \quad ...$$

$$... \quad \mathbf{X}_5(\mathbb{Q}_z^{\beta(K,1)})^T \quad 0 \quad 0 \quad 0 \quad 0 \quad 0 \quad 0 \quad -\gamma_2 \mathbf{X}_5(\mathbb{F}^{\beta(K,1)})^T \Big).$$

The first, fifth, ninth and thirteenth lines of $\mathbb{T}^K$ are also modified and are given below:

$$\mathbb{T}^K_{1,:} = \Big(\left(\gamma_1 + \gamma_4 \mathbf{X}_2 n_x^2 + \mathbf{X}_1 n_x^2 + \mathbf{X}_3 t_x^2 + \mathbf{X}_3 a_x^2\right) \mathbb{G}^{\beta(K,1)} \quad 0 \quad 0 \quad 0 \quad (\gamma_4 \mathbf{X}_2 n_x n_y + \mathbf{X}_1 n_x n_y + \mathbf{X}_3 t_x t_y + \mathbf{X}_3 a_x a_y)\,\mathbb{G}^{\beta(K,1)} \quad ...$$

$$... \quad 0 \quad 0 \quad 0 \quad (\gamma_4 \mathbf{X}_2 n_x n_z + \mathbf{X}_1 n_x n_z + \mathbf{X}_3 t_x t_z + \mathbf{X}_3 a_x a_z)\,\mathbb{G}^{\beta(K,1)} \quad 0 \quad 0 \quad 0 \quad (\gamma_3 + \mathbf{X}_2\,\gamma_2)\mathbb{H}_x^{\beta(K,1)} \quad 0 \quad 0 \quad 0 \Big),$$

$$\mathbb{T}^K_{5,:} = \Big((\gamma_1 + \gamma_4 \mathbf{X}_2 n_x n_y + \mathbf{X}_1 n_x n_y + \mathbf{X}_3 t_x t_y + \mathbf{X}_3 a_x a_y)\,\mathbb{G}^{\beta(K,1)} \quad 0 \quad 0 \quad 0 \quad \left(\gamma_4 \mathbf{X}_2 n_y^2 + \mathbf{X}_1 n_y^2 + \mathbf{X}_3 t_y^2 + \mathbf{X}_3 a_y^2\right) \mathbb{G}^{\beta(K,1)} \quad ...$$

$$... \quad 0 \quad 0 \quad 0 \quad (\gamma_4 \mathbf{X}_2 n_y n_z + \mathbf{X}_1 n_y n_z + \mathbf{X}_3 t_y t_z + \mathbf{X}_3 a_y a_z)\,\mathbb{G}^{\beta(K,1)} \quad 0 \quad 0 \quad 0 \quad (\gamma_3 + \mathbf{X}_2\,\gamma_2)\mathbb{H}_y^{\beta(K,1)} \quad 0 \quad 0 \quad 0 \Big),$$

$$\mathbb{T}^K_{9,:} = \Big((\gamma_1 + \gamma_4 \mathbf{X}_2 n_x n_z + \mathbf{X}_1 n_x n_z + \mathbf{X}_3 t_x t_z + \mathbf{X}_3 a_x a_z)\,\mathbb{G}^{\beta(K,1)} \quad 0 \quad 0 \quad 0 \quad (\gamma_4 \mathbf{X}_2 n_y n_z + \mathbf{X}_1 n_y n_z + \mathbf{X}_3 t_y t_z + \mathbf{X}_3 a_y a_z)\,\mathbb{G}^{\beta(K,1)} \quad ...$$

$$... \quad 0 \quad 0 \quad 0 \quad \left(\gamma_4 \mathbf{X}_2 n_z^2 + \mathbf{X}_1 n_z^2 + \mathbf{X}_3 t_z^2 + \mathbf{X}_3 a_z^2\right) \mathbb{G}^{\beta(K,1)} \quad 0 \quad 0 \quad 0 \quad (\gamma_3 + \mathbf{X}_2\,\gamma_2)\mathbb{H}_z^{\beta(K,1)} \quad 0 \quad 0 \quad 0 \Big),$$

and

$$\mathbb{T}^K_{13,:} = \Big((\mathbf{X}_4 + \mathbf{X}_5 \gamma_4)\,\mathbb{H}_x^{\beta(K,1)} \quad 0 \quad 0 \quad 0 \quad (\mathbf{X}_4 + \mathbf{X}_5 \gamma_4)\,\mathbb{H}_y^{\beta(K,1)} \quad 0 \quad 0 \quad 0 \quad ...$$

$$... \quad (\mathbf{X}_4 + \mathbf{X}_5 \gamma_4)\,\mathbb{H}_z^{\beta(K,1)} \quad 0 \quad 0 \quad 0 \quad (1 + \mathbf{X}_5\,\gamma_2)\mathbb{G}^{\beta(K,1)} \quad 0 \quad 0 \quad 0 \Big).$$

C.3 Three-dimensional discretization using PML in the HDG method

Here, we detail the discretization of the poroelastic equations using PML in the HDG method. The PML allow to model an infinite domain. On the borders of our computational domain, we add an artificial absorbing layer, which prevents the reflections by absorbing the outgoing waves. In the formulation, we use three absorbing functions α, β and γ representing the attenuation

of the wave in the absorbing layer. The attenuation functions α, β and γ are taken equal to zero outside of the absorbing layers. Considering $\partial\Omega$ the interface between the geophysical domain and the PML, the value of the attenuation functions in the PML increases with the distance to $\partial\Omega$. In practice the use of PML is taken into account by replacing the spatial derivatives as follows:

$$\partial_x \to \frac{i\,\omega}{i\,\omega+\alpha(x)}\partial_x\,,\quad \partial_y \to \frac{i\,\omega}{i\,\omega+\beta(y)}\partial_y\,,\quad \partial_z \to \frac{i\,\omega}{i\,\omega+\gamma(z)}\partial_z\,.$$

We consider a three-dimensional porous domain Ω with the boundary Γ. The fields ($\mathbf{u}$, $\mathbf{w}$, $\boldsymbol{\tau}$, p) solve the poroelastic equations (1.16) on Ω. We consider a triangulation $\mathcal{T}_h$ of Ω, and $\mathcal{F}_h$ the set of all the faces. K is a triangle element of $\mathcal{T}_h$ and F is a face of K. We use the approximation spaces defined in Section 4.4. The local unknowns ($\mathbf{u}_h$, $\mathbf{w}_h$, $\boldsymbol{\tau}_h$, p_h) $\in (\boldsymbol{V}_h^p \times \boldsymbol{V}_h^p \times \boldsymbol{\Sigma}_h^p \times V_h^p)$ solve the poroelastic equations (1.16) on $\mathcal{T}_h$. The HDG discretization of the poroelastic equations (1.16) is modified. The transmission conditions are not modified and stay the same as the one used in HDG method with no PML, see Chapter 3.

Starting from the poroelastic equations (1.16), we follow the same steps as in Section 3.1 to obtain the local problem. First, we multiply the equations by test-functions and integrate on an element K. Then, we integrate the equation by parts to bring out the numerical traces. Next, the numerical traces $\hat{\mathbf{u}}$, $\hat{\mathbf{w}}$, $\hat{\boldsymbol{\tau}}$ and $\hat{\mathrm{p}}$ are replaced by their expressions given in (3.10).

Once we have obtained the local problem, we discretize the equations as in Section 3.3, by replacing the test-functions by basis functions, and by decomposing the unknowns ($\mathbf{u}$, $\mathbf{w}$, $\boldsymbol{\tau}$, p) and the local Lagrange unknowns $\boldsymbol{\lambda}_1$ and λ_2 as given in equations (3.25) and (3.26). We can then express the obtained system in terms of the elementary matrices defined in (3.28).

We obtain an elementary system expressed as:

$$\mathbb{A}\underline{W}^K + \mathbb{B}\underline{\Lambda}^K = 0\,,$$

with $\underline{W}^K$ and $\underline{\Lambda}^K$ defined in (3.27). The elementary matrices $\mathbb{A}^K$ and $\mathbb{B}^K$ are then expressed as follows:

In this case, $\mathbb{A}^K$ is of dimension $13\,d_i^K \times 13 d_i^K$, written as:

$$\mathbb{A}^K = \begin{pmatrix} \mathbb{A}_1^K & \mathbb{A}_2^K & \mathbb{A}_3^K & \mathbb{A}_4^K & \mathbb{A}_5^K & \mathbb{A}_6^K & \mathbb{A}_7^K & \mathbb{A}_8^K & \mathbb{A}_9^K & \mathbb{A}_{10}^K & \mathbb{A}_{11}^K & \mathbb{A}_{12}^K & \mathbb{A}_{13}^K \end{pmatrix},$$

with

$$\mathbb{A}_1^K = \begin{pmatrix} \mathrm{i}\,\omega\rho_a^K\mathbb{M}^K + \sum_{f=1}^{4}\gamma_1\mathbb{E}^{\beta(K,f)}\left(\frac{i\,\omega}{i\,\omega+\alpha(x)}n_x^2 + \frac{i\,\omega}{i\,\omega+\beta(y)}n_y^2 + \frac{i\,\omega}{i\,\omega+\gamma(z)}n_z^2\right) \\ 0 \\ 0 \\ \mathrm{i}\,\omega\rho_f^K\mathbb{M}^K \\ 0 \\ 0 \\ \left(C_{11}^K\mathbb{D}_x^K\frac{i\,\omega}{i\,\omega+\alpha(x)} + C_{16}^K\mathbb{D}_y^K\frac{i\,\omega}{i\,\omega+\beta(y)} + C_{15}^K\mathbb{D}_z^K\frac{i\,\omega}{i\,\omega+\gamma(z)}\right) \\ \left(C_{21}^K\mathbb{D}_x^K\frac{i\,\omega}{i\,\omega+\alpha(x)} + C_{26}^K\mathbb{D}_y^K\frac{i\,\omega}{i\,\omega+\beta(y)} + C_{25}^K\mathbb{D}_z^K\frac{i\,\omega}{i\,\omega+\gamma(z)}\right) \\ \left(C_{31}^K\mathbb{D}_x^K\frac{i\,\omega}{i\,\omega+\alpha(x)} + C_{36}^K\mathbb{D}_y^K\frac{i\,\omega}{i\,\omega+\beta(y)} + C_{35}^K\mathbb{D}_z^K\frac{i\,\omega}{i\,\omega+\gamma(z)}\right) \\ \left(C_{41}^K\mathbb{D}_x^K\frac{i\,\omega}{i\,\omega+\alpha(x)} + C_{46}^K\mathbb{D}_y^K\frac{i\,\omega}{i\,\omega+\beta(y)} + C_{45}^K\mathbb{D}_z^K\frac{i\,\omega}{i\,\omega+\gamma(z)}\right) \\ \left(C_{51}^K\mathbb{D}_x^K\frac{i\,\omega}{i\,\omega+\alpha(x)} + C_{56}^K\mathbb{D}_y^K\frac{i\,\omega}{i\,\omega+\beta(y)} + C_{55}^K\mathbb{D}_z^K\frac{i\,\omega}{i\,\omega+\gamma(z)}\right) \\ \left(C_{61}^K\mathbb{D}_x^K\frac{i\,\omega}{i\,\omega+\alpha(x)} + C_{66}^K\mathbb{D}_y^K\frac{i\,\omega}{i\,\omega+\beta(y)} + C_{65}^K\mathbb{D}_z^K\frac{i\,\omega}{i\,\omega+\gamma(z)}\right) \\ -M^K\left(\sum_{f=1}^{4}\gamma_4\mathbb{I}_x^{\beta(K,f)}\frac{i\,\omega}{i\,\omega+\alpha(x)} + \alpha_{11}^K\mathbb{D}_x^K\frac{i\,\omega}{i\,\omega+\alpha(x)} + \alpha_{12}^K\mathbb{D}_y^K\frac{i\,\omega}{i\,\omega+\beta(y)} + \alpha_{13}^K\mathbb{D}_z^K\frac{i\,\omega}{i\,\omega+\gamma(z)}\right) \end{pmatrix},$$

$$\mathbb{A}_2^K = \begin{pmatrix} 0 \\ \mathrm{i}\,\omega\rho_a^K\mathbb{M}^K + \sum_{f=1}^{4}\gamma_1\mathbb{E}^{\beta(K,f)}\left(\frac{i\,\omega}{i\,\omega+\alpha(x)}n_x^2 + \frac{i\,\omega}{i\,\omega+\beta(y)}n_y^2 + \frac{i\,\omega}{i\,\omega+\gamma(z)}n_z^2\right) \\ 0 \\ 0 \\ \mathrm{i}\,\omega\rho_f^K\mathbb{M}^K \\ 0 \\ \left(C_{16}^K\mathbb{D}_x^K\frac{i\,\omega}{i\,\omega+\alpha(x)} + C_{12}^K\mathbb{D}_y^K\frac{i\,\omega}{i\,\omega+\beta(y)} + C_{14}^K\mathbb{D}_z^K\frac{i\,\omega}{i\,\omega+\gamma(z)}\right) \\ \left(C_{26}^K\mathbb{D}_x^K\frac{i\,\omega}{i\,\omega+\alpha(x)} + C_{22}^K\mathbb{D}_y^K\frac{i\,\omega}{i\,\omega+\beta(y)} + C_{24}^K\mathbb{D}_z^K\frac{i\,\omega}{i\,\omega+\gamma(z)}\right) \\ \left(C_{36}^K\mathbb{D}_x^K\frac{i\,\omega}{i\,\omega+\alpha(x)} + C_{32}^K\mathbb{D}_y^K\frac{i\,\omega}{i\,\omega+\beta(y)} + C_{34}^K\mathbb{D}_z^K\frac{i\,\omega}{i\,\omega+\gamma(z)}\right) \\ \left(C_{46}^K\mathbb{D}_x^K\frac{i\,\omega}{i\,\omega+\alpha(x)} + C_{42}^K\mathbb{D}_y^K\frac{i\,\omega}{i\,\omega+\beta(y)} + C_{44}^K\mathbb{D}_z^K\frac{i\,\omega}{i\,\omega+\gamma(z)}\right) \\ \left(C_{56}^K\mathbb{D}_x^K\frac{i\,\omega}{i\,\omega+\alpha(x)} + C_{52}^K\mathbb{D}_y^K\frac{i\,\omega}{i\,\omega+\beta(y)} + C_{54}^K\mathbb{D}_z^K\frac{i\,\omega}{i\,\omega+\gamma(z)}\right) \\ \left(C_{66}^K\mathbb{D}_x^K\frac{i\,\omega}{i\,\omega+\alpha(x)} + C_{62}^K\mathbb{D}_y^K\frac{i\,\omega}{i\,\omega+\beta(y)} + C_{64}^K\mathbb{D}_z^K\frac{i\,\omega}{i\,\omega+\gamma(z)}\right) \\ -M^K\left(\sum_{f=1}^{4}\gamma_4\mathbb{J}_y^{\beta(K,f)}\frac{i\,\omega}{i\,\omega+\beta(y)} + \alpha_{12}^K\mathbb{D}_x^K\frac{i\,\omega}{i\,\omega+\alpha(x)} + \alpha_{22}^K\mathbb{D}_y^K\frac{i\,\omega}{i\,\omega+\beta(y)} + \alpha_{23}^K\mathbb{D}_z^K\frac{i\,\omega}{i\,\omega+\gamma(z)}\right) \end{pmatrix},$$

$$\mathbb{A}_3^K = \begin{pmatrix} 0 \\ 0 \\ \mathrm{i}\,\omega\rho_a^K\mathbb{M}^K + \sum_{f=1}^{4}\gamma_1\mathbb{E}^{\beta(K,f)}\left(\frac{i\,\omega}{i\,\omega+\alpha(x)}n_x^2 + \frac{i\,\omega}{i\,\omega+\beta(y)}n_y^2 + \frac{i\,\omega}{i\,\omega+\gamma(z)}n_z^2\right) \\ 0 \\ 0 \\ \mathrm{i}\,\omega\rho_f^K\mathbb{M}^K \\ \left(C_{15}^K\mathbb{D}_x^K\frac{i\,\omega}{i\,\omega+\alpha(x)} + C_{14}^K\mathbb{D}_y^K\frac{i\,\omega}{i\,\omega+\beta(y)} + C_{13}^K\mathbb{D}_z^K\frac{i\,\omega}{i\,\omega+\gamma(z)}\right) \\ \left(C_{25}^K\mathbb{D}_x^K\frac{i\,\omega}{i\,\omega+\alpha(x)} + C_{24}^K\mathbb{D}_y^K\frac{i\,\omega}{i\,\omega+\beta(y)} + C_{23}^K\mathbb{D}_z^K\frac{i\,\omega}{i\,\omega+\gamma(z)}\right) \\ \left(C_{35}^K\mathbb{D}_x^K\frac{i\,\omega}{i\,\omega+\alpha(x)} + C_{34}^K\mathbb{D}_y^K\frac{i\,\omega}{i\,\omega+\beta(y)} + C_{33}^K\mathbb{D}_z^K\frac{i\,\omega}{i\,\omega+\gamma(z)}\right) \\ \left(C_{45}^K\mathbb{D}_x^K\frac{i\,\omega}{i\,\omega+\alpha(x)} + C_{44}^K\mathbb{D}_y^K\frac{i\,\omega}{i\,\omega+\beta(y)} + C_{43}^K\mathbb{D}_z^K\frac{i\,\omega}{i\,\omega+\gamma(z)}\right) \\ \left(C_{55}^K\mathbb{D}_x^K\frac{i\,\omega}{i\,\omega+\alpha(x)} + C_{54}^K\mathbb{D}_y^K\frac{i\,\omega}{i\,\omega+\beta(y)} + C_{53}^K\mathbb{D}_z^K\frac{i\,\omega}{i\,\omega+\gamma(z)}\right) \\ \left(C_{65}^K\mathbb{D}_x^K\frac{i\,\omega}{i\,\omega+\alpha(x)} + C_{64}^K\mathbb{D}_y^K\frac{i\,\omega}{i\,\omega+\beta(y)} + C_{63}^K\mathbb{D}_z^K\frac{i\,\omega}{i\,\omega+\gamma(z)}\right) \\ -M^K\left(\sum_{f=1}^{4}\gamma_4\mathbb{J}_z^{\beta(K,f)}\frac{i\,\omega}{i\,\omega+\gamma(z)} + \alpha_{13}^K\mathbb{D}_x^K\frac{i\,\omega}{i\,\omega+\alpha(x)} + \alpha_{23}^K\mathbb{D}_y^K\frac{i\,\omega}{i\,\omega+\beta(y)} + \alpha_{33}^K\mathbb{D}_z^K\frac{i\,\omega}{i\,\omega+\gamma(z)}\right) \end{pmatrix},$$

$$\mathbb{A}_4^K = \begin{pmatrix} \mathrm{i}\,\omega\rho_f^K\mathbb{M}^K \\ 0 \\ 0 \\ \mathrm{i}\,\omega\rho_{\mathrm{dyn}}^K\mathbb{M}^K \\ 0 \\ 0 \\ 0 \\ 0 \\ 0 \\ 0 \\ 0 \\ 0 \\ M^K(\mathbb{D}_x^K)^T\dfrac{i\,\omega}{i\,\omega+\alpha(x)} \end{pmatrix}, \quad \mathbb{A}_5^K = \begin{pmatrix} 0 \\ \mathrm{i}\,\omega\rho_f^K\mathbb{M}^K \\ 0 \\ 0 \\ \mathrm{i}\,\omega\rho_{\mathrm{dyn}}^K\mathbb{M}^K \\ 0 \\ 0 \\ 0 \\ 0 \\ 0 \\ 0 \\ 0 \\ M^K(\mathbb{D}_y^K)^T\dfrac{i\,\omega}{i\,\omega+\beta(y)} \end{pmatrix} \quad \mathbb{A}_6^K = \begin{pmatrix} 0 \\ 0 \\ \mathrm{i}\,\omega\rho_f^K\mathbb{M}^K \\ 0 \\ \mathrm{i}\,\omega\rho_{\mathrm{dyn}}^K\mathbb{M}^K \\ 0 \\ 0 \\ 0 \\ 0 \\ 0 \\ 0 \\ 0 \\ M^K(\mathbb{D}_z^K)^T\dfrac{i\,\omega}{i\,\omega+\gamma(z)} \end{pmatrix}$$

$$\mathbb{A}_7^K = \begin{pmatrix} -(\mathbb{D}_x^K)^T\dfrac{i\,\omega}{i\,\omega+\alpha(x)} \\ 0 \\ 0 \\ 0 \\ 0 \\ \mathrm{i}\,\omega\,\mathbb{M}^K \\ 0 \\ 0 \\ 0 \\ 0 \\ 0 \\ 0 \end{pmatrix}, \quad \mathbb{A}_8^K = \begin{pmatrix} 0 \\ -(\mathbb{D}_y^K)^T\dfrac{i\,\omega}{i\,\omega+\beta(y)} \\ 0 \\ 0 \\ 0 \\ 0 \\ \mathrm{i}\,\omega\,\mathbb{M}^K \\ 0 \\ 0 \\ 0 \\ 0 \\ 0 \end{pmatrix}, \quad \mathbb{A}_9^K = \begin{pmatrix} 0 \\ 0 \\ -(\mathbb{D}_z^K)^T\dfrac{i\,\omega}{i\,\omega+\gamma(z)} \\ 0 \\ 0 \\ 0 \\ 0 \\ \mathrm{i}\,\omega\,\mathbb{M}^K \\ 0 \\ 0 \\ 0 \\ 0 \end{pmatrix},$$

$$\mathbb{A}_{10}^K = \begin{pmatrix} 0 \\ -(\mathbb{D}_z^K)^T\dfrac{i\,\omega}{i\,\omega+\gamma(z)} \\ -(\mathbb{D}_y^K)^T\dfrac{i\,\omega}{i\,\omega+\beta(y)} \\ 0 \\ 0 \\ 0 \\ 0 \\ 0 \\ 0 \\ \mathrm{i}\,\omega\,\mathbb{M}^K \\ 0 \\ 0 \\ 0 \end{pmatrix}, \quad \mathbb{A}_{11}^K = \begin{pmatrix} -(\mathbb{D}_z^K)^T\dfrac{i\,\omega}{i\,\omega+\gamma(z)} \\ 0 \\ -(\mathbb{D}_x^K)^T\dfrac{i\,\omega}{i\,\omega+\alpha(x)} \\ 0 \\ 0 \\ 0 \\ 0 \\ 0 \\ 0 \\ \mathrm{i}\,\omega\,\mathbb{M}^K \\ 0 \\ 0 \end{pmatrix}, \quad \mathbb{A}_{12}^K = \begin{pmatrix} -(\mathbb{D}_y^K)^T\dfrac{i\,\omega}{i\,\omega+\beta(y)} \\ -(\mathbb{D}_x^K)^T\dfrac{i\,\omega}{i\,\omega+\alpha(x)} \\ 0 \\ 0 \\ 0 \\ 0 \\ 0 \\ 0 \\ 0 \\ 0 \\ \mathrm{i}\,\omega\,\mathbb{M}^K \\ 0 \end{pmatrix},$$

$$\mathbb{A}_{13}^K = \begin{pmatrix} \sum_{f=1}^{4} \gamma_3 \mathbb{J}_x^{\beta(K,f)} \frac{i\,\omega}{i\,\omega + \alpha(x)} \\ \sum_{f=1}^{4} \gamma_3 \mathbb{J}_y^{\beta(K,f)} \frac{i\,\omega}{i\,\omega + \beta(y)} \\ \sum_{f=1}^{4} \gamma_3 \mathbb{J}_z^{\beta(K,f)} \frac{i\,\omega}{i\,\omega + \gamma(z)} \\ -\mathbb{D}_x^K \frac{i\,\omega}{i\,\omega + \alpha(x)} \\ -\mathbb{D}_y^K \frac{i\,\omega}{i\,\omega + \beta(y)} \\ -\mathbb{D}_z^K \frac{i\,\omega}{i\,\omega + \gamma(z)} \\ \mathrm{i}\,\omega \alpha_{11}^K \mathbb{M}^K \\ \mathrm{i}\,\omega \alpha_{22}^K \mathbb{M}^K \\ \mathrm{i}\,\omega \alpha_{33}^K \mathbb{M}^K \\ \mathrm{i}\,\omega \alpha_{23}^K \mathbb{M}^K \\ \mathrm{i}\,\omega \alpha_{13}^K \mathbb{M}^K \\ \mathrm{i}\,\omega \alpha_{12}^K \mathbb{M}^K \\ \mathrm{i}\,\omega \mathbb{M}^K - \sum_{f=1}^{4} M \gamma_2 \mathbb{E}^{\beta(K,f)} \left(\frac{i\,\omega}{i\,\omega + \alpha(x)} n_x^2 + \frac{i\,\omega}{i\,\omega + \beta(y)} n_y^2 + \frac{i\,\omega}{i\,\omega + \gamma(z)} n_z^2 \right) \end{pmatrix}.$$

Based on the structure of the unknown $\underline{\Lambda}^K$, we write $\mathbb{B}^K$ in 16 columns of size $13\,d_i^K \times d_i^F$ as:

$$\mathbb{B}^K = \Big(B_{\lambda_{1x},1} \quad B_{\lambda_{1x},2} \quad B_{\lambda_{1x},3} \quad B_{\lambda_{1x},4} \quad B_{\lambda_{1y},1} \quad B_{\lambda_{1y},2} \quad B_{\lambda_{1y},3} \quad B_{\lambda_{1y},4} \quad \ldots$$
$$\ldots \quad B_{\lambda_{1z},1} \quad B_{\lambda_{1z},2} \quad B_{\lambda_{1z},3} \quad B_{\lambda_{1z},4} \quad B_{\lambda_2,1} \quad B_{\lambda_2,2} \quad B_{\lambda_2,3} \quad B_{\lambda_2,4} \Big),$$

with

$$B_{\lambda_{1x},f} = \begin{pmatrix} -\gamma_1\, \mathbb{F}^{\beta(K,f)} \left(\frac{i\,\omega}{i\,\omega + \alpha(x)} n_x^2 + \frac{i\,\omega}{i\,\omega + \beta(y)} n_y^2 + \frac{i\,\omega}{i\,\omega + \gamma(z)} n_z^2 \right) \\ 0 \\ 0 \\ 0 \\ 0 \\ 0 \\ (-C_{11}^K \mathbb{Q}_x^{\beta(K,f)} \frac{i\,\omega}{i\,\omega + \alpha(x)} - C_{16}^K \mathbb{Q}_y^{\beta(K,f)} \frac{i\,\omega}{i\,\omega + \beta(y)} - C_{15}^K \mathbb{Q}_z^{\beta(K,f)} \frac{i\,\omega}{i\,\omega + \gamma(z)}) \\ (-C_{21}^K \mathbb{Q}_x^{\beta(K,f)} \frac{i\,\omega}{i\,\omega + \alpha(x)} - C_{26}^K \mathbb{Q}_y^{\beta(K,f)} \frac{i\,\omega}{i\,\omega + \beta(y)} - C_{25}^K \mathbb{Q}_z^{\beta(K,f)} \frac{i\,\omega}{i\,\omega + \gamma(z)}) \\ (-C_{31}^K \mathbb{Q}_x^{\beta(K,f)} \frac{i\,\omega}{i\,\omega + \alpha(x)} - C_{36}^K \mathbb{Q}_y^{\beta(K,f)} \frac{i\,\omega}{i\,\omega + \beta(y)} - C_{35}^K \mathbb{Q}_z^{\beta(K,f)} \frac{i\,\omega}{i\,\omega + \gamma(z)}) \\ (-C_{41}^K \mathbb{Q}_x^{\beta(K,f)} \frac{i\,\omega}{i\,\omega + \alpha(x)} - C_{46}^K \mathbb{Q}_y^{\beta(K,f)} \frac{i\,\omega}{i\,\omega + \beta(y)} - C_{45}^K \mathbb{Q}_z^{\beta(K,f)} \frac{i\,\omega}{i\,\omega + \gamma(z)}) \\ (-C_{51}^K \mathbb{Q}_x^{\beta(K,f)} \frac{i\,\omega}{i\,\omega + \alpha(x)} - C_{56}^K \mathbb{Q}_y^{\beta(K,f)} \frac{i\,\omega}{i\,\omega + \beta(y)} - C_{55}^K \mathbb{Q}_z^{\beta(K,f)} \frac{i\,\omega}{i\,\omega + \gamma(z)}) \\ (-C_{61}^K \mathbb{Q}_x^{\beta(K,f)} \frac{i\,\omega}{i\,\omega + \alpha(x)} - C_{66}^K \mathbb{Q}_y^{\beta(K,f)} \frac{i\,\omega}{i\,\omega + \beta(y)} - C_{65}^K \mathbb{Q}_z^{\beta(K,f)} \frac{i\,\omega}{i\,\omega + \gamma(z)}) \\ M^K \left((\gamma_4 + \alpha_{11}^K) \mathbb{Q}_x^{\beta(K,f)} \frac{i\,\omega}{i\,\omega + \alpha(x)} + \alpha_{12}^K \mathbb{Q}_y^{\beta(K,f)} \frac{i\,\omega}{i\,\omega + \beta(y)} + \alpha_{13}^K \mathbb{Q}_z^{\beta(K,f)} \frac{i\,\omega}{i\,\omega + \gamma(z)} \right) \end{pmatrix},$$

$$B_{\lambda_{1y},f} = \begin{pmatrix} 0 \\ -\gamma_1 \mathbb{F}^{\beta(K,f)} \left(\frac{i\omega}{i\omega+\alpha(x)} n_x^2 + \frac{i\omega}{i\omega+\beta(y)} n_y^2 + \frac{i\omega}{i\omega+\gamma(z)} n_z^2 \right) \\ 0 \\ 0 \\ 0 \\ 0 \\ (-C_{16}^K \mathbb{Q}_x^{\beta(K,f)} \frac{i\omega}{i\omega+\alpha(x)} - C_{12}^K \mathbb{Q}_y^{\beta(K,f)} \frac{i\omega}{i\omega+\beta(y)} - C_{14}^K \mathbb{Q}_z^{\beta(K,f)} \frac{i\omega}{i\omega+\gamma(z)}) \\ (-C_{26}^K \mathbb{Q}_x^{\beta(K,f)} \frac{i\omega}{i\omega+\alpha(x)} - C_{22}^K \mathbb{Q}_y^{\beta(K,f)} \frac{i\omega}{i\omega+\beta(y)} - C_{24}^K \mathbb{Q}_z^{\beta(K,f)} \frac{i\omega}{i\omega+\gamma(z)}) \\ (-C_{36}^K \mathbb{Q}_x^{\beta(K,f)} \frac{i\omega}{i\omega+\alpha(x)} - C_{32}^K \mathbb{Q}_y^{\beta(K,f)} \frac{i\omega}{i\omega+\beta(y)} - C_{34}^K \mathbb{Q}_z^{\beta(K,f)} \frac{i\omega}{i\omega+\gamma(z)}) \\ (-C_{46}^K \mathbb{Q}_x^{\beta(K,f)} \frac{i\omega}{i\omega+\alpha(x)} - C_{42}^K \mathbb{Q}_y^{\beta(K,f)} \frac{i\omega}{i\omega+\beta(y)} - C_{44}^K \mathbb{Q}_z^{\beta(K,f)} \frac{i\omega}{i\omega+\gamma(z)}) \\ (-C_{56}^K \mathbb{Q}_x^{\beta(K,f)} \frac{i\omega}{i\omega+\alpha(x)} - C_{52}^K \mathbb{Q}_y^{\beta(K,f)} \frac{i\omega}{i\omega+\beta(y)} - C_{54}^K \mathbb{Q}_z^{\beta(K,f)} \frac{i\omega}{i\omega+\gamma(z)}) \\ (-C_{66}^K \mathbb{Q}_x^{\beta(K,f)} \frac{i\omega}{i\omega+\alpha(x)} - C_{62}^K \mathbb{Q}_y^{\beta(K,f)} \frac{i\omega}{i\omega+\beta(y)} - C_{64}^K \mathbb{Q}_z^{\beta(K,f)} \frac{i\omega}{i\omega+\gamma(z)}) \\ M^K \left(\alpha_{12}^K \mathbb{Q}_x^{\beta(K,f)} \frac{i\omega}{i\omega+\alpha(x)} + (\gamma_4 + \alpha_{22}^K) \mathbb{Q}_y^{\beta(K,f)} \frac{i\omega}{i\omega+\beta(y)} + \alpha_{23}^K \mathbb{Q}_z^{\beta(K,f)} \frac{i\omega}{i\omega+\gamma(z)} \right) \end{pmatrix},$$

$$B_{\lambda_{1z},f} = \begin{pmatrix} 0 \\ -\gamma_1 \mathbb{F}^{\beta(K,f)} \left(\frac{i\omega}{i\omega+\alpha(x)} n_x^2 + \frac{i\omega}{i\omega+\beta(y)} n_y^2 + \frac{i\omega}{i\omega+\gamma(z)} n_z^2 \right) \\ 0 \\ 0 \\ 0 \\ 0 \\ (-C_{15}^K \mathbb{Q}_x^{\beta(K,f)} \frac{i\omega}{i\omega+\alpha(x)} - C_{14}^K \mathbb{Q}_y^{\beta(K,f)} \frac{i\omega}{i\omega+\beta(y)} - C_{13}^K \mathbb{Q}_z^{\beta(K,f)} \frac{i\omega}{i\omega+\gamma(z)}) \\ (-C_{25}^K \mathbb{Q}_x^{\beta(K,f)} \frac{i\omega}{i\omega+\alpha(x)} - C_{24}^K \mathbb{Q}_y^{\beta(K,f)} \frac{i\omega}{i\omega+\beta(y)} - C_{23}^K \mathbb{Q}_z^{\beta(K,f)} \frac{i\omega}{i\omega+\gamma(z)}) \\ (-C_{35}^K \mathbb{Q}_x^{\beta(K,f)} \frac{i\omega}{i\omega+\alpha(x)} - C_{34}^K \mathbb{Q}_y^{\beta(K,f)} \frac{i\omega}{i\omega+\beta(y)} - C_{33}^K \mathbb{Q}_z^{\beta(K,f)} \frac{i\omega}{i\omega+\gamma(z)}) \\ (-C_{45}^K \mathbb{Q}_x^{\beta(K,f)} \frac{i\omega}{i\omega+\alpha(x)} - C_{44}^K \mathbb{Q}_y^{\beta(K,f)} \frac{i\omega}{i\omega+\beta(y)} - C_{43}^K \mathbb{Q}_z^{\beta(K,f)} \frac{i\omega}{i\omega+\gamma(z)}) \\ (-C_{55}^K \mathbb{Q}_x^{\beta(K,f)} \frac{i\omega}{i\omega+\alpha(x)} - C_{54}^K \mathbb{Q}_y^{\beta(K,f)} \frac{i\omega}{i\omega+\beta(y)} - C_{53}^K \mathbb{Q}_z^{\beta(K,f)} \frac{i\omega}{i\omega+\gamma(z)}) \\ (-C_{65}^K \mathbb{Q}_x^{\beta(K,f)} \frac{i\omega}{i\omega+\alpha(x)} - C_{64}^K \mathbb{Q}_y^{\beta(K,f)} \frac{i\omega}{i\omega+\beta(y)} - C_{63}^K \mathbb{Q}_z^{\beta(K,f)} \frac{i\omega}{i\omega+\gamma(z)}) \\ M^K \left(\alpha_{12}^K \mathbb{Q}_x^{\beta(K,f)} \frac{i\omega}{i\omega+\alpha(x)} + (\gamma_4 + \alpha_{22}^K) \mathbb{Q}_y^{\beta(K,f)} \frac{i\omega}{i\omega+\beta(y)} + \alpha_{23}^K \mathbb{Q}_z^{\beta(K,f)} \frac{i\omega}{i\omega+\gamma(z)} \right) \end{pmatrix},$$

$$B_{\lambda_2,f} = \begin{pmatrix} -\gamma_3 \mathbb{Q}_x^{\beta(K,f)} \frac{i\omega}{i\omega+\alpha(x)} \\ -\gamma_3 \mathbb{Q}_y^{\beta(K,f)} \frac{i\omega}{i\omega+\beta(y)} \\ -\gamma_3 \mathbb{Q}_z^{\beta(K,f)} \frac{i\omega}{i\omega+\gamma(z)} \\ \mathbb{Q}_x^{\beta(K,f)} \frac{i\omega}{i\omega+\alpha(x)} \\ \mathbb{Q}_y^{\beta(K,f)} \frac{i\omega}{i\omega+\beta(y)} \\ \mathbb{Q}_z^{\beta(K,f)} \frac{i\omega}{i\omega+\gamma(z)} \\ 0 \\ 0 \\ 0 \\ 0 \\ 0 \\ 0 \\ M^K \gamma_2 \mathbb{F}^{\beta(K,f)} \left(\frac{i\omega}{i\omega+\alpha(x)} n_x^2 + \frac{i\omega}{i\omega+\beta(y)} n_y^2 + \frac{i\omega}{i\omega+\gamma(z)} n_z^2 \right) \end{pmatrix},$$

for $f = 1, 2, 3, 4$.

Part II

Electrokinetics

Chapter 5

The Electrokinetic effects

In this chapter, we present the principles of the electrokinetic, following Pride's theory, [105, 110]. The electrokinetic theory was first introduced by Frenkel [109, 56], then it has been generalized to Pride's model. The conversions have been observed on the field and in laboratory experiments, [23, 117]. In this chapter, we first introduce in Section 5.1 the principles of the electrokinetic and the physical parameters used to describe Pride's equations, that we present in Section 5.2. In order to manipulate quantities with similar amplitudes, we use a non-dimensionalization of the equations, see Section 5.3. Then, we present in Section 5.4 the boundary conditions used for Pride's equations. Finally, in Section 5.5, we obtain by a plane analysis the slownesses of the four waves sustained in conducting poroelastic materials, and the associated solutions.

5.1 Physical parameters

We consider a poroelastic material, composed of a solid frame and pores filled with fluid, or composed of grains immersed in a fluid. In such materials, the wavelengths are significantly larger than the dimensions of the grains or the pores. The geophysical poroelastic materials are neutral media, however, the surface of the solid is usually negatively charged, and the fluid is an electrolyte, with ions in motion in the fluid, attracted by the opposite sign on the solid surface [111, 108, 113]. The charges in the fluid are adsorbed by the negative charges on the surface of the solid, which fixes a part of the positive charges, and forms the Stern layer, see Figure 5.1. In the diffusive layer, the negative charges have an overall displacement that is more important than that of the positive charges, and this relative motion between the charges creates an electric potential [66]. We will consider that the fluid is an ideal electrolyte and that the material is isotropic.

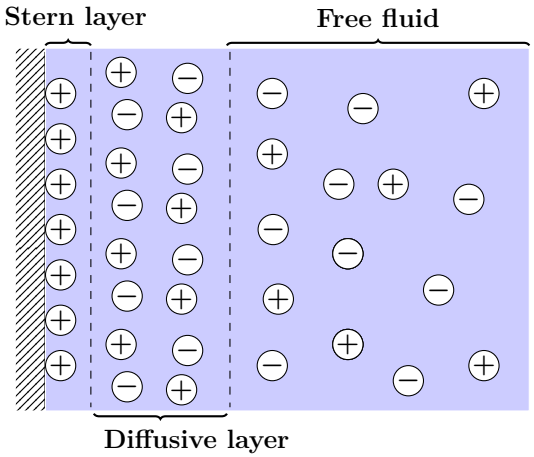

Figure 5.1: Electric double layer

When a seismic wave propagates, the motion of the fluid in the porous media induces an electric current, that creates an electromagnetic signal. This is called the seismoelectric phenomenon [129, 79]. The electromagnetic waves generated with a seismic source are composed of a co-seismic electric or magnetic fields that propagate at the same speed as the produced seismic waves, and the electromagnetic converted wave generated at an interface between two

media with different properties. The converted wave propagates with the electromagnetic wavespeed which is very much higher than the seismic wavespeeds and thus makes the problem multi-scale. We can observe those waves by measuring the electric or magnetic fields. Similarly, an electromagnetic field acting on the layer causes the ions to move in the electrical double layer, which leads to a relative displacement of the fluid and solid frame, and hence seismic waves propagate in the medium. In a conducting poroelastic material, if the source is electromagnetic, we can observed two kinds of waves generated by the electroseismic effects. The first one is a seismic signal accompanying the electromagnetic wave, and the second is a seismic wave created by the reflection of the electromagnetic wave at the interface between two different materials. The two phenomena are called the electrokinetic effects [78]. The converted waves are very interesting because they are heavily sensitive to the medium properties, and have potential applications in the detection of interfaces.

The electrokinetic model is based on the coupling of poroelastic and electromagnetic wave propagation. Thus, the waves propagation in conducting poroelastic materials depend on the poroelastic parameters, electromagnetic parameters and coupling parameters. The poroelastic and electromagnetic quantities have been introduced respectively in Chapter 1 and Appendix G, hence we refer to those chapters for more details. We follow Pride's hypothesis and always assume that the materials are isotropic, which means that the speed of the waves and the attenuation do not depend on the propagation direction.

Poroelastic parameters

We use the same parameters as for poroelasticity in Part I. We summarize the different poroelastic parameters in Table 5.1. The first table gives the input parameters, and the second one gives parameters that are calculated from the values of the first table.

Input parameters	Notation	Unity
Porosity	ϕ	-
Fluid Density	ρ_f	$10^3 kg.m^{-3}$
Solid Density	ρ_s	$10^3 kg.m^{-3}$
Viscosity	η	10^{-3}Pa.s
Permeability zero	κ_0	$10^{-9} m^2$
Tortuosity	$\mathfrak{t}$	-
Solid Bulk Modulus	$\mathrm{k_s}$	GPa
Fluid Bulk Modulus	$\mathrm{k_f}$	GPa
Frame Bulk Modulus	$\mathrm{k_{fr}}$	GPa
Frame Shear Modulus	μ_{fr}	GPa

(a): Input poroelastic parameters

Calculated parameters	Notation	Unity	Formula
Averaged density	ρ_a	$10^3 kg.m^{-3}$	$\rho_a := (1-\phi)\,\rho_s + \phi\,\rho_f\,.$
Dynamic density	ρ_{dyn}	$10^3 kg.m^{-3}$	$\rho_{\mathrm{dyn}}(\omega) = \mathrm{i}\dfrac{\eta}{(-\mathfrak{s}\,\omega)\,k(-\mathfrak{s}\,\omega)}\,.$
Dynamic permeability	k	$10^{-9} m^2$	$\dfrac{1}{k(\omega)} = \dfrac{1}{k_0}\Big(\sqrt{1-\mathrm{i}\dfrac{4}{m}\dfrac{\omega}{\omega_t}} - \mathrm{i}\dfrac{\omega}{\omega_t}\Big)$, with $\omega_t = \dfrac{\phi}{\mathfrak{t}k_0}\dfrac{\eta}{\rho_f}$ and $m = 8$.
Effective stress	$\boldsymbol{\alpha}$	-	$\boldsymbol{\alpha} = \alpha\,\mathbb{I}$, with $\alpha = 1 - \dfrac{\mathrm{k_{fr}}}{\mathrm{k_s}}\,.$
Fluid-solid coupling modulus	M	GPa	$\dfrac{1}{M} = \dfrac{\alpha}{\mathrm{k_s}} + \phi\left(\dfrac{1}{\mathrm{k_f}} - \dfrac{1}{\mathrm{k_s}}\right)\,.$
Biot incompressibilities constant	H	GPa	$\mathrm{k_{fr}} + \dfrac{4}{3}\mu_{\mathrm{fr}} + \alpha^2 M$
Stiffness tensor	$\mathbf{C}$	GPa	given in equations (5.1) in 3D and (5.2) in 2D.

(b): Calculated poroelastic parameters

Table 5.1: Poroelastic parameters.

In isotropic materials, the stiffness tensor $\mathbf{C}_{\mathrm{fr}}$ is expressed in three dimensions as:

$$\mathbf{C} = \begin{pmatrix} \mathrm{k_{fr}} + \frac{4}{3}\mu_{\mathrm{fr}} & \mathrm{k_{fr}} - \frac{2}{3}\mu_{\mathrm{fr}} & \mathrm{k_{fr}} - \frac{2}{3}\mu_{\mathrm{fr}} & 0 & 0 & 0 \\ \mathrm{k_{fr}} - \frac{2}{3}\mu_{\mathrm{fr}} & \mathrm{k_{fr}} + \frac{4}{3}\mu_{\mathrm{fr}} & \mathrm{k_{fr}} - \frac{2}{3}\mu_{\mathrm{fr}} & 0 & 0 & 0 \\ \mathrm{k_{fr}} - \frac{2}{3}\mu_{\mathrm{fr}} & \mathrm{k_{fr}} - \frac{2}{3} & \mathrm{k_{fr}} + \frac{4}{3}\mu_{\mathrm{fr}}\mu_{\mathrm{fr}} & 0 & 0 & 0 \\ 0 & 0 & 0 & \mu_{\mathrm{fr}} & 0 & 0 \\ 0 & 0 & 0 & 0 & \mu_{\mathrm{fr}} & 0 \\ 0 & 0 & 0 & 0 & 0 & \mu_{\mathrm{fr}} \end{pmatrix}, \tag{5.1}$$

which is simplified in two dimensions as:

$$\mathbf{C} = \begin{pmatrix} \mathrm{k_{fr}} + \frac{4}{3}\mu_{\mathrm{fr}} & \mathrm{k_{fr}} - \frac{2}{3}\mu_{\mathrm{fr}} & 0 \\ \mathrm{k_{fr}} - \frac{2}{3}\mu_{\mathrm{fr}} & \mathrm{k_{fr}} + \frac{4}{3}\mu_{\mathrm{fr}} & 0 \\ 0 & 0 & \mu_{\mathrm{fr}} \end{pmatrix}. \tag{5.2}$$

Electromagnetic parameters

We recall the three parameters that describe the electromagnetic wave propagation, see Appendix G:

- μ_0 the permeability (N.A^{-2}),
- ϵ_0 the permittivity (F.m^{-1}),
- σ the conductivity (S.m^{-1}).

Coupling parameters

The coupling is expressed by using the tensor $\mathbf{L}$, dependent on the frequency and as in [110], we write it in the form $\mathbf{L} = \mathrm{L}\,\mathbb{I}$. The coupling parameter is given by [109]:

$$\mathrm{L}(\omega) = \mathrm{L_0}\left(1 - \mathrm{i}\,\frac{\omega}{\omega_t}\right)^{-1/2}, \quad \text{with } \mathrm{L_0} = \frac{\epsilon_0\, k_f\, \zeta}{\eta\, F}.$$

In the above equation, ζ is the electric potential expressed in Volt, and F is a formation factor with no dimension, expressed as $F = \phi^2$, with ϕ the porosity. The viscosity η has a significant role in the coupling tensor, and we always consider materials with viscosity, because otherwise the coupling tensor is not defined.

Finally, in the electrokinetic equations, the second constitutive law of Maxwell's equations is modified and is expressed using the electric factor δ_0 given by:

$$\delta_0 = \epsilon_0\left(\frac{\phi}{\mathfrak{t}}(\kappa_f - \kappa_s) + \kappa_s\right),$$

with κ_f and κ_s the fluid and solid permittivity.

In Table 5.2, we give the input parameters for Sand and Freshwater.

Physical parameters	Sand	Freshwater
Porosity ϕ	0.3	0.15
Fluid Density ρ_f $(10^3 kg.m^{-3})$	1	1
Solid Density ρ_s $(10^3 kg.m^{-3})$	2.7	2.7
Viscosity η $(10^{-3}$Pa.s)	1	1
Permeability κ_0 $(10^{-9} m^2)$	0.01	0.001
Tortuosity $\mathfrak{t}$	3	3
Solid Bulk Modulus k_s (GPa)	36	36
Fluid Bulk Modulus k_f (GPa)	2.2	2.2
Frame Bulk Modulus k_{fr} (GPa)	7	9
Frame Shear Modulus μ_{fr} (GPa)	5	7
Solid permittivity κ_f	4	4
Fluid permittivity κ_s	80	80
Conductivity σ $(10^{-4}$ S.m$^{-1})$	3.88	3.88
Zeta potential ζ (V)	0.1	0.1

Table 5.2: Summary of the physical parameters of media in consideration. The parameters are taken from [71][Table 1].

5.2 Pride's Equations

The electrokinetic equations have been proposed in 1994 by Pride [105]. The derivation of the equations relies on the averaging of the electromagnetic and poroelastic equations on a macroscopic level. The equations have been obtained in the frequency domain. Note that the non-linear dependency on the frequency of the physical parameters, including the coupling tensor $\mathbf{L}$, worsens the difficulties if we work in the time domain. In addition, the difference of wave velocities between the seismic waves and the electromagnetic waves is quite difficult to handle in the time domain. Hence, we choose to work in the harmonic domain, and we consider that the waves have an $e^{\mathfrak{s}\,\mathrm{i}\,\omega\,t}$ dependency. In this framework, the time derivative is $\partial_t \to \mathfrak{s}\,\mathrm{i}\,\omega$. We describe the propagation of waves in conducting poroelastic materials using the following unknowns:

- the frame velocity $\mathbf{u}$,
- the relative fluid velocity $\mathbf{w}$,
- the fluid pressure p,
- the stress tensor $\boldsymbol{\tau}$,
- the electric density field $\boldsymbol{E}$,
- the magnetic intensity field $\boldsymbol{H}$,
- the electric current density $\boldsymbol{J}$.

We will also use the strain tensor, expressed as: $\boldsymbol{\epsilon} = \dfrac{\nabla \mathbf{u} + (\nabla \mathbf{u})^T}{2}$.

In three dimensions, $\mathbf{u}$, $\mathbf{w}$ $\boldsymbol{E}$, $\boldsymbol{H}$, and $\boldsymbol{J}$ are vectors of size 3. The stress $\boldsymbol{\tau}$ is a 6×6 tensor and the pressure p is a scalar. In two dimensions, two configurations can be considered, denoted 'TE' and 'TM' [110]:

- For TM transverse wave, the electric field $\boldsymbol{E}$ has the same polarization as the mechanical velocities and is in the plane (x, y), while the magnetic fields is orthogonal to the plane (x, y) and carried by Oz. In this case, the magnetic field is a scalar denoted by H.
- For TE transverse wave, the polarization of the mechanical velocities and the electric field are orthogonal to the plane (x, y), while the polarization of the magnetic field is in the plane (x, y).

In the following, we always consider the case TM. Hence, in two dimensions, $\mathbf{u}$, $\mathbf{w}$, $\boldsymbol{E}$, and $\boldsymbol{J}$ are vectors of size 2. The stress $\boldsymbol{\tau}$ is a 3×3 tensor, the magnetic field is a scalar that we denote H.

As the electromagnetic wavelengths are very large compared to the other wavelengths, some studies focus on the quasi-static approximation of Maxwell equations. It has been shown in [60] that using this assumption, the electromagnetic and seismic wave equations become uncoupled. The resolution can thus be made separately. In our case, we do not make the quasi-static assumption and we consider the full model.

The first-order harmonic equations are given by:

$$\mathfrak{s}\,\mathrm{i}\,\omega\,\rho_a\mathbf{u} + \mathfrak{s}\,\mathrm{i}\,\omega\,\rho_f\,\mathbf{w} = \nabla\cdot\boldsymbol{\tau} + \mathbf{f}_u\,, \tag{5.3a}$$

$$\mathfrak{s}\,\mathrm{i}\omega\rho_f\mathbf{u} + \mathfrak{s}\,\mathrm{i}\,\omega\,\rho_{\mathrm{dyn}}\,\mathbf{w} = -\nabla\mathrm{p} + \mathfrak{s}\,\mathrm{i}\,\omega\,\rho_{\mathrm{dyn}}\,\mathbf{L}\,\boldsymbol{E} + \mathbf{f}_w\,, \tag{5.3b}$$

$$\mathfrak{s}\,\mathrm{i}\omega\boldsymbol{\tau} + \mathfrak{s}\,\mathrm{i}\omega\,\boldsymbol{\alpha}\mathrm{p} = \mathbf{C} : \boldsymbol{\epsilon}(\mathbf{u})\,, \tag{5.3c}$$

$$\mathfrak{s}\,\mathrm{i}\omega\,\mathrm{p} = -M\nabla\cdot\mathbf{w} - M\boldsymbol{\alpha} : \boldsymbol{\epsilon}(\mathbf{u})\,, \tag{5.3d}$$

$$\mathfrak{s}\,\mathrm{i}\,\omega\,\delta_0\,\boldsymbol{E} = \mathbf{curl}\,\boldsymbol{H} - \boldsymbol{J} + \mathbf{f}_C\,, \tag{5.3e}$$

$$\mathfrak{s}\,\mathrm{i}\,\omega\,\mu_0\boldsymbol{H} = -\,\mathbf{curl}\,\boldsymbol{E}\,, \tag{5.3f}$$

$$\boldsymbol{J} = \sigma\,\boldsymbol{E} + \mathbf{L}(-\nabla\mathrm{p} - \mathfrak{s}\,\mathrm{i}\omega\,\rho_f\,\mathbf{u}\,)\,, \tag{5.3g}$$

with $\mathbf{f}_u$, $\mathbf{f}_w$ and $\mathbf{f}_C$ exterior forces, and the operator : in equations (5.3c) and (5.3d) denoting the tensor scalar product.

As mentioned above, we always consider the materials to be isotropic. This means that equations (5.3c) and (5.3d) can also be written as

$$\begin{aligned}\mathfrak{s}\,\mathrm{i}\omega\boldsymbol{\tau} &= 2\,\mu_{\mathrm{fr}}\,\boldsymbol{\epsilon}(\mathbf{u}) + (\lambda_{\mathrm{fr}} + M\alpha^2)\nabla\cdot\mathbf{u}\,\mathbb{I} + \alpha M\nabla\cdot\mathbf{w}\,\mathbb{I}\,,\\ \mathfrak{s}\,\mathrm{i}\omega\,\mathrm{p} &= -M\,\nabla\cdot\mathbf{w} - \alpha\,M\,\nabla\cdot\mathbf{u}\,.\end{aligned} \tag{5.4}$$

In system (5.3), the four first equations (5.3a), to (5.3d) are the poroelastic equations with a coupling term in equation (5.3b). Similarly, equations (5.3e) to (5.3g) are the electromagnetic equations with a coupling term in equation (5.3g).

Second-order formulation

To manipulate a more compact system of equations, we determine the second-order formulation of Pride's equations (5.3). For this, we introduce the solid and relative fluid displacements u and w, that are defined using the fact that the velocities are the time derivatives of the displacements:

$$\mathbf{u} = \mathfrak{s}\,\mathrm{i}\,\omega\,\mathrm{u}\quad,\quad \mathbf{w} = \mathfrak{s}\,\mathrm{i}\,\omega\,\mathrm{w}\,.$$

In the following, we express the system (5.3) in terms of the solid displacement u, the relative fluid displacement w and the electric field $\boldsymbol{E}$.

Proposition 5.1. Second-order formulation

If $(\mathbf{u},\mathbf{w},\boldsymbol{\tau},\mathrm{p},\boldsymbol{E},\boldsymbol{H},\boldsymbol{J})$ is solution of the electrokinetic system (5.3) in a homogeneous medium, then $(\mathrm{u},\mathrm{w},\boldsymbol{E})$ solves the following system:

$$-\omega^2\rho_a\mathrm{u} - \rho_f\omega^2\mathrm{w} - H\,\nabla\nabla\cdot\mathrm{u} + \mu_{\mathrm{fr}}\,\mathbf{curl}\,\mathbf{curl}\,\mathrm{u} - \alpha\,M\,\nabla\nabla\cdot\mathrm{w} = \mathbf{F_1}\,, \tag{5.5a}$$

$$-\omega^2\rho_f\mathrm{u} - \omega^2\,\rho_{\mathrm{dyn}}\,\mathrm{w} - \frac{\eta}{k}\,\mathbf{L}\,\boldsymbol{E} - M\,\nabla\nabla\cdot\mathrm{w} - M\alpha\nabla\nabla\cdot\mathrm{u} = \mathbf{F_2}\,, \tag{5.5b}$$

$$-\,\omega^2\,\tilde{\boldsymbol{\varepsilon}}\,\mu_0\,\boldsymbol{E} - \mathfrak{s}\,\mathrm{i}\,\omega\,\mu_0\,\mathbf{L}\,\omega^2\,\rho_{\mathrm{dyn}}\,\mathrm{w} + \mathbf{curl}\,\mathbf{curl}\,\boldsymbol{E} = \mathbf{F_3}\,, \tag{5.5c}$$

where we have denoted

$$\tilde{\boldsymbol{\varepsilon}} = \delta_0 - \frac{\mathfrak{s}\,\mathrm{i}}{\omega}\,\sigma + \frac{\mathfrak{s}\,\mathrm{i}}{\omega}\,\frac{\eta}{k}\mathbf{L}^2\,,$$

and with $\mathbf{F_1} = \mathbf{f}_u$, $\mathbf{F_2} = \mathbf{f}_w$ and $\mathbf{F_3} = \mathfrak{s}\,\mathrm{i}\,\omega\,\mu_0\,\mathbf{f}_C$.

Proof. First, we write system (5.3) in terms of the displacements instead of the velocities, using the isotropic notations

(5.4):

$$-\omega^2\,\rho_a \mathrm{u} - \omega^2\,\rho_f\,\mathrm{w} = \nabla\cdot\boldsymbol{\tau} + \mathbf{f}_u\,, \tag{5.6a}$$

$$-\omega^2\,\rho_f \mathrm{u} - \omega^2\,\rho_{\mathrm{dyn}}\,\mathrm{w} = -\nabla \mathrm{p} + \mathfrak{s}\,\mathrm{i}\,\omega\,\rho_{\mathrm{dyn}}\,\mathbf{L}\,\boldsymbol{E} + \mathbf{f}_w\,, \tag{5.6b}$$

$$\boldsymbol{\tau} = 2\,\mu_{\mathrm{fr}}\,\boldsymbol{\epsilon}(\mathrm{u}) + (\lambda_{\mathrm{fr}} + M\alpha^2)\nabla\cdot\mathrm{u}\,\mathbb{I} + \alpha M\nabla\cdot\mathrm{w}\,\mathbb{I}\,, \tag{5.6c}$$

$$\mathrm{p} = -M\,\nabla\cdot\mathrm{w} - \alpha\,M\,\nabla\cdot\mathrm{u}\,, \tag{5.6d}$$

$$\mathfrak{s}\,\mathrm{i}\,\omega\,\delta_0\,\boldsymbol{E} = \mathbf{curl}\,\boldsymbol{H} - \boldsymbol{J} + \mathbf{f}_C\,, \tag{5.6e}$$

$$\mathfrak{s}\,\mathrm{i}\,\omega\,\mu_0\boldsymbol{H} = -\,\mathbf{curl}\,\boldsymbol{E}\,, \tag{5.6f}$$

$$\boldsymbol{J} = \sigma\,\boldsymbol{E} + \mathbf{L}(-\nabla \mathrm{p} + \omega^2\,\rho_f\,\mathrm{u})\,, \tag{5.6g}$$

By using the calculations done for poroelasticity in Section 1.2, we can express the divergence of the stress (equation (5.6c)) and the gradient of the pressure (equation (5.6d)) as:

$$\begin{aligned}\nabla\cdot\boldsymbol{\tau} &= -\mu_{\mathrm{fr}}\,\mathbf{curl}\,\mathbf{curl}\,\mathrm{u} + H\nabla\nabla\cdot\mathrm{u} + \alpha\,M\,\nabla\nabla\cdot\mathrm{w}\,,\\ -\nabla \mathrm{p} &= M\,\nabla\nabla\cdot\mathrm{w} + M\,\nabla\mathbf{f}_{\mathrm{p}} + M\,\alpha\,\nabla\nabla\cdot\mathrm{u}\,.\end{aligned} \tag{5.7}$$

By injecting this form of $\nabla\cdot\boldsymbol{\tau}$ in equation (5.6a), we obtain the first equation of the second-order formulation (5.5a). Then, we inject the form of $\nabla \mathrm{p}$ in (5.6b), and we recall that $\rho_{\mathrm{dyn}} = \dfrac{\mathrm{i}\,\eta}{(-\mathfrak{s}\,\omega)\,k}$, hence $\mathfrak{s}\,\mathrm{i}\,\omega\,\rho_{\mathrm{dyn}} = \dfrac{\eta}{k}$. We then obtain the second equation of the second formulation (5.5b).

For equation (5.5c), we first inject in (5.6e) the magnetic field $\boldsymbol{H}$ given in (5.6f), which gives:

$$\mathbf{curl}\,\mathbf{curl}\,\boldsymbol{E} - \omega^2\,\delta_0\,\mu_0\,\boldsymbol{E} + \mathfrak{s}\,\mathrm{i}\,\omega\,\mu_0\,\boldsymbol{J} = \mathfrak{s}\,\mathrm{i}\,\omega\,\mu_0\,\mathbf{f}_C\,.$$

Then, we inject the expression of $\boldsymbol{J}$ given in (5.6g) in the above equation, and we obtain:

$$\mathbf{curl}\,\mathbf{curl}\,\boldsymbol{E} - \omega^2\,\delta_0\,\mu_0\,\boldsymbol{E} + \mathfrak{s}\,\mathrm{i}\,\omega\,\mu_0\,\sigma\,\boldsymbol{E} + \mathfrak{s}\,\mathrm{i}\,\omega\,\mu_0\,\mathbf{L}(-\nabla \mathrm{p} + \omega^2\rho_f \mathrm{u}) = \mathfrak{s}\,\mathrm{i}\,\omega\,\mu_0\,\mathbf{f}_C\,.$$

We replace the gradient of the pressure $\nabla\,\mathrm{p}$ by its expression given in (5.7). After some simplifications, we have:

$$\mathbf{curl}\,\mathbf{curl}\,\boldsymbol{E} - \omega^2\,\delta_0\,\mu_0\,\boldsymbol{E} + \mathfrak{s}\,\mathrm{i}\,\omega\,\mu_0\,\sigma\,\boldsymbol{E} - \mathfrak{s}\,\mathrm{i}\,\omega\,\mu_0\,\mathbf{L}\,\omega^2\,\rho_{\mathrm{dyn}}\,\mathrm{w} - \mathfrak{s}\,\mathrm{i}\,\omega\,\mu_0\,\frac{\eta}{k}\mathbf{L}^2\,\boldsymbol{E} = \mathfrak{s}\,\mathrm{i}\,\omega\,\mu_0\,\mathbf{f}_C\,.$$

Finally, we introduce

$$\tilde{\boldsymbol{\varepsilon}} = \delta_0 - \frac{\mathfrak{s}\,\mathrm{i}}{\omega}\,\sigma + \frac{\mathfrak{s}\,\mathrm{i}}{\omega}\,\frac{\eta}{k}\mathbf{L}^2\,,$$

and we obtain the last equation of the second-order formulation (5.5c).

□

Remark 5.2. In two dimensions, as mentioned above, the electric field $\boldsymbol{E}$ is in the plane (x, y) and the magnetic field $\boldsymbol{H}$ is a scalar orthogonal to the plane (x, y). We have introduced the vector and scalar rotationals, **curl** and curl in (1.19):

$$\mathbf{curl}\,f = \begin{pmatrix}\partial_y f\\ -\partial_x f\end{pmatrix}\,, \qquad \mathrm{curl}\,\mathbf{V} = \partial_x V_y - \partial_y V_x\,, \qquad \Delta\,\mathbf{V} = -\,\mathbf{curl}\,\mathrm{curl}\,V + \nabla\nabla\cdot V\,.$$

The second order formulation of Pride's equations (5.3) is

$$-\omega^2\rho_a \mathrm{u} - \rho_f\omega^2\mathrm{w} - H\,\nabla\nabla\cdot\mathrm{u} + \mu_{\mathrm{fr}}\,\mathbf{curl}\,\mathrm{curl}\,\mathrm{u} - \alpha\,M\,\nabla\nabla\cdot\mathrm{w} = \mathbf{F_1}\,,$$

$$-\omega^2\rho_f \mathrm{u} - \omega^2\,\rho_{\mathrm{dyn}}\,\mathrm{w} - \frac{\eta}{k}\,\mathbf{L}\,\boldsymbol{E} - M\,\nabla\nabla\cdot\mathrm{w} - M\alpha\nabla\nabla\cdot\mathrm{u} = \mathbf{F_2}\,,$$

$$\mathbf{curl}\,\mathrm{curl}\,\boldsymbol{E} - \omega^2\,\delta_0\,\mu_0\,\boldsymbol{E} + \mathfrak{s}\,\mathrm{i}\,\omega\,\mu_0\,\sigma\,\boldsymbol{E} - \mathfrak{s}\,\mathrm{i}\,\omega\,\mu_0\,\mathbf{L}\,\omega^2\,\rho_{\mathrm{dyn}}\,\mathrm{w} - \mathfrak{s}\,\mathrm{i}\,\omega\,\mu_0\,\frac{\eta}{k}\mathbf{L}^2\,\boldsymbol{E} = \mathbf{F_3}\,.$$

5.3 Non-dimensionalization of the equations

In the equations (5.3) the parameters and quantities have different orders of magnitude. In numerical simulations, this difference can cause numerical errors during the calculations. To prevent this, we write Pride's equations (5.3) in terms of dimensionless equations. We write $X = X_0\overline{X}$ for all the terms of the equations with X_0 a characteristic unit of measure. We assume that all bulk modulus and components of $\mathbf{C}$ are written as $\mathrm{k}_\bullet = C_0\overline{\mathrm{k}_\bullet}$. Hence, $M = C_0\overline{M}$ and $\alpha_0 = 1$. The porosity $\phi = \dfrac{V_f}{V_T}$ is considered as a ratio with no characteristic unit. We assume that ρ_a, ρ_{dyn}, ρ_f and ρ_s have the same characteristic unit ρ_0. The characteristic frequency has the same characteristic unit as ω. The electric factor is expressed as:

$$\delta_0 \;=\; \epsilon_0\left(\frac{\phi}{\alpha}(k_f \;- k_s) + \; k_s\right),$$

with ϕ, α, k_f and k_s with no dimension, which means that δ_0 and ϵ_0 have the same characteristic unit. We have then:

$$\begin{cases} \mathrm{i}\,\omega_0\,\overline{\omega}\,\rho_0\,\overline{\rho_a}\,\mathrm{u}_0\,\overline{\mathbf{u}} + \mathrm{i}\,\omega_0\,\overline{\omega}\,\rho_0\,\overline{\rho_f}\,\mathrm{w}_0\,\overline{\mathbf{w}} = \dfrac{\tau_0}{x_0}\,\nabla\cdot\,\overline{\boldsymbol{\tau}}\,, \\ \mathrm{i}\,\omega_0\overline{\omega}\,\rho_0\overline{\rho_f}\mathrm{u}_0\,\overline{\mathbf{u}} + \mathrm{i}\,\omega_0\overline{\omega}\,\rho_0\,\overline{\rho_{\mathrm{dyn}}}\,\mathrm{w}_0\,\overline{\mathbf{w}} = -\dfrac{\mathrm{p}_0}{x_0}\,\nabla\overline{\mathrm{p}} \;+\; \mathrm{i}\,\omega_0\overline{\omega}\,\rho_0\,\overline{\rho_{\mathrm{dyn}}}\,L_0\,\overline{L}\,\boldsymbol{E}_0\,\overline{\boldsymbol{E}}\,, \\ \mathrm{i}\,\omega_0\,\overline{\omega}\,\tau_0\,\overline{\boldsymbol{\tau}} + \mathrm{i}\,\omega_0\,\overline{\omega}\alpha_0\,\overline{\boldsymbol{\alpha}}\mathrm{p}_0\,\overline{\mathrm{p}} = \dfrac{C_0\mathbf{u}_0}{x_0}\,\overline{\mathbf{C}}\cdot\boldsymbol{\epsilon}(\overline{\mathbf{u}})\,, \\ \mathrm{i}\,\omega_0\,\overline{\omega}\,\mathrm{p}_0\,\overline{\mathrm{p}} = -\dfrac{C_0\mathrm{w}_0}{x_0}\,\overline{M}\nabla\cdot\overline{\mathbf{w}} - \dfrac{C_0\alpha_0\mathrm{u}_0}{x_0}\,\overline{M}\,\overline{\boldsymbol{\alpha}}:\boldsymbol{\epsilon}(\overline{\mathbf{u}})\,, \\ \mathbf{curl}\,\overline{\boldsymbol{E}}\,\dfrac{\boldsymbol{E}_0}{x_0} \;+\mathrm{i}\omega_0\overline{\omega}\,\mu_0\overline{\mu_0}\,\boldsymbol{H}_0\overline{\boldsymbol{H}} \;= 0\,, \\ \mathrm{curl}\,\overline{\boldsymbol{H}}\,\dfrac{\boldsymbol{H}_0}{x_0} \;-\mathrm{i}\omega_0\overline{\omega}\,\delta_0\overline{\delta_0}\,\boldsymbol{E}_0\overline{\boldsymbol{E}} - \sigma_0\overline{\sigma}\boldsymbol{E}_0\overline{\boldsymbol{E}} \;- L_0\,\overline{L}\,\dfrac{\mathrm{p}_0}{x_0}\,\nabla\overline{\mathrm{p}} \;- L_0\,\overline{L}\,\mathrm{i}\,\omega_0\,\overline{\omega}\,\rho_0\,\overline{\rho_f}\,\mathrm{u}_0\,\overline{\mathbf{u}} \;= 0\,. \end{cases} \tag{5.8}$$

In addition, we also write the expression of L_0 and ρ_{dyn} in dimensionless terms:

$$\begin{cases} \rho_0\,\overline{\rho_{\mathrm{dyn}}} = \dfrac{\eta_0}{k_{0_0}\omega_0}\,\dfrac{\overline{\eta}}{\overline{k}}\,, \\ L_0\,\overline{L} \;=\; \dfrac{\epsilon_0\,\overline{\epsilon_0}\,k_f\,\xi_0\,\overline{\xi}}{\eta_0\,\overline{\eta}\,F}\,. \end{cases} \tag{5.9}$$

To keep the equivalence between system (5.8) and Pride's equations (5.3), the characteristic units have to be coherent. We rewrite system (5.8) by isolating the characteristic units and the dimensionless quantities. For example, this gives for the first equation:

$$(\omega_0\,\rho_0\,\mathrm{u}_0)\,\mathrm{i}\,\overline{\omega}\,\overline{\rho_a}\;\overline{\mathbf{u}} + \;(\omega_0\,\rho_0\,\mathrm{w}_0)\,\mathrm{i}\,\overline{\omega}\,\overline{\rho_f}\,\overline{\mathbf{w}} = \left(\frac{\tau_0}{x_0}\right)\,\nabla\cdot\,\overline{\boldsymbol{\tau}}\,.$$

Then, to consider a dimensionless system, the quantities in the parentheses have to be equal:

$$\omega_0\,\rho_0\,\mathrm{u}_0 \;=\; \omega_0\,\rho_0\,\mathrm{w}_0 \;=\; \frac{\tau_0}{x_0}\,.$$

This is done on all the equations of systems (5.8) and (5.9), and after some simplifications, we obtain the following relations:

$$\mathrm{u}_0 = \mathrm{w}_0 \;=\; L_0\,\boldsymbol{E}_0\;, \quad \tau_0 = \mathrm{p}_0 \;=\; \omega_0\,\rho_0\,\mathrm{u}_0\,x_0, \quad \alpha_0 = \;1\,, \quad C_0u_0 = \;\omega_0\,\tau_0\,x_0\,,$$

$$\sigma_0 \;=\omega_0\epsilon_0\;, \qquad \frac{\boldsymbol{E}_0}{x_0} \;=\; \omega_0\mu_0\boldsymbol{H}_0\,, \qquad \frac{\boldsymbol{H}_0}{x_0} \;=\; \omega_0\epsilon_0\boldsymbol{E}_0 \;=\; L_0\,\frac{\mathrm{p}_0}{x_0}\,,$$

$$\text{and} \qquad \rho_0\,\omega_0\,k_{0_0} \;=\; \eta_0\,, \qquad\qquad L_0 \;=\; \frac{\epsilon_0\,\xi_0}{\eta_0}\,.$$

To be consistent with the results in poroelasticity, we choose:

$$\mathrm{u}_0 = \mathrm{w}_0 = 1\ \mathrm{m.s}^{-1}\,, \qquad \tau_0 = \mathrm{p}_0 = 10^6\mathrm{Pa}\,, \qquad \omega_0 = 10^3\ \mathrm{rad.s}^{-1}\,, \qquad x_0 = 1\ \mathrm{m}\,,$$

$$C_0 = 10^9\ \mathrm{Pa}\,, \qquad \rho_0 = 10^3\mathrm{kg}\cdot\mathrm{m}^{-3}\,, \qquad k_{0_0} = 10^{-9}\mathrm{m}^2\,, \qquad \eta_0 = 10^{-3}\ \mathrm{Pa.s}\,.$$

Similarly, we choose for the electromagnetic quantities:

$$\boldsymbol{E}_0 = 10^3\, V.m^{-1} = 10^3\, N.C^{-1} = 10^3\ kg.m.s^{-3}.A^{-1}\,, \qquad \boldsymbol{H}_0 = 10^3\ m^{-1}.A\,,$$
$$\mu_0 = 10^{-3}\, T.m.A^{-1} = 10^{-3}\, kg.m.s^{-2}.A^{-2}\,, \qquad \epsilon_0 = 10^{-3}\, C^2.N^{-1}.m^{-2} = 10^{-3}\, kg^{-1}.m^{-3}.s^4.A^2\,,$$
$$\sigma_0 = 1\, S.m^{-1} = 1\, kg^{-1}.m^{-3}.s^3.A^2\,.$$

Regarding the coupling quantities, this leads to:

$$\mathrm{L}_0 = 10^{-3}\frac{A}{(Pa.m)}\,, \qquad \xi_0 = 10^{-3}\, V\,.$$

5.4 Boundary and interface conditions

In this section, we present the conditions on the boundaries for a bounded domain, and an interaction problem in a conducting poroelastic material.

Bounded domains: On the external boundary Γ with outwardly direct unit normal vector $\boldsymbol{n}$, we consider eight types of boundary conditions with the boundary forces $\boldsymbol{f}_{\text{inc}}$, g_{inc}, h_{inc} .

$$\text{Type 1} \quad \begin{cases} \boldsymbol{\tau}\,\boldsymbol{n} &= \boldsymbol{f}_{\text{inc}}\,, \\ \mathbf{w}\cdot\boldsymbol{n} &= g_{\text{inc}}\,, \\ \boldsymbol{n}\times\boldsymbol{E} &= \boldsymbol{h}_{\text{inc}}\,, \end{cases} \qquad \text{Type 2} \quad \begin{cases} \mathbf{u} &= \boldsymbol{f}_{\text{inc}}\,, \\ \mathbf{w}\cdot\boldsymbol{n} &= g_{\text{inc}}\,, \\ \boldsymbol{n}\times\boldsymbol{E} &= \boldsymbol{h}_{\text{inc}}\,, \end{cases} \tag{5.10a}$$

$$\text{Type 3} \quad \begin{cases} \boldsymbol{\tau}\,\boldsymbol{n} &= \boldsymbol{f}_{\text{inc}}\,, \\ \mathrm{p} &= g_{\text{inc}}\,, \\ \boldsymbol{n}\times\boldsymbol{E} &= \boldsymbol{h}_{\text{inc}}\,, \end{cases} \qquad \text{Type 4} \quad \begin{cases} \mathbf{u} &= \boldsymbol{f}_{\text{inc}}\,, \\ \mathrm{p} &= g_{\text{inc}}\,, \\ \boldsymbol{n}\times\boldsymbol{E} &= \boldsymbol{h}_{\text{inc}}\,, \end{cases}$$

$$\text{Type 5} \quad \begin{cases} \boldsymbol{\tau}\,\boldsymbol{n} &= \boldsymbol{f}_{\text{inc}}\,, \\ \mathbf{w}\cdot\boldsymbol{n} &= g_{\text{inc}}\,, \\ \boldsymbol{n}\times\boldsymbol{H} &= \boldsymbol{h}_{\text{inc}}\,, \end{cases} \qquad \text{Type 6} \quad \begin{cases} \mathbf{u} &= \boldsymbol{f}_{\text{inc}}\,, \\ \mathbf{w}\cdot\boldsymbol{n} &= g_{\text{inc}}\,, \\ \boldsymbol{n}\times\boldsymbol{H} &= \boldsymbol{h}_{\text{inc}}\,, \end{cases}$$

$$\text{Type 7} \quad \begin{cases} \boldsymbol{\tau}\,\boldsymbol{n} &= \boldsymbol{f}_{\text{inc}}\,, \\ \mathrm{p} &= g_{\text{inc}}\,, \\ \boldsymbol{n}\times\boldsymbol{H} &= \boldsymbol{h}_{\text{inc}}\,, \end{cases} \qquad \text{Type 8} \quad \begin{cases} \mathbf{u} &= \boldsymbol{f}_{\text{inc}}\,, \\ \mathrm{p} &= g_{\text{inc}}\,, \\ \boldsymbol{n}\times\boldsymbol{H} &= \boldsymbol{h}_{\text{inc}}\,, \end{cases} \tag{5.10b}$$

We note that the free-surface conditions are given by boundary conditions of type 3 and 7 with $\boldsymbol{f}_{\text{inc}}$ and g_{inc} equal to zero. Similarly, the wall conditions correspond to the conditions of type 2 and 6 with $\boldsymbol{f}_{\text{inc}}$ and g_{inc} equal to zero. In addition, the conditions for a perfect conductor are given by types 1 to 4, with $\boldsymbol{h}_{\text{inc}} = 0$. In two dimensions, the condition $\boldsymbol{n}\times\boldsymbol{H} = \boldsymbol{h}_{\text{inc}}$ is $\mathrm{H} = h_{\text{inc}}$.

Interaction problems: We will consider the reflection of a conducting poroelastic obstacle immersed in an infinite conducting poroelastic solid. We denote the outer infinite medium by $\Omega_{(I)}$ and the obstacle by $\Omega_{(II)}$. On the boundary of the obstacle Γ, we impose the following transmission conditions:

$$\begin{cases} \mathbf{u}_{(I)} - \mathbf{u}_{(II)} &= 0\,, \\ \mathrm{p}_{(I)} - \mathrm{p}_{(II)} &= 0\,, \\ (\mathbf{w}_{(I)} - \mathbf{w}_{(II)})\cdot\boldsymbol{n} &= 0\,, \\ (\boldsymbol{\tau}_{(I)} - \boldsymbol{\tau}_{(II)})\cdot\boldsymbol{n} &= 0\,, \\ \boldsymbol{n}\times(\boldsymbol{E}_{(I)} - \boldsymbol{E}_{(II)}) &= 0\,, \\ \boldsymbol{n}\times\big(\boldsymbol{H}_{(I)} - \boldsymbol{H}_{(II)}\big) &= 0\,. \end{cases}$$

Domain truncation: In the above, we have presented boundary conditions for bounded domains. In Chapter 8, we will present the development of boundary conditions used for truncating the computational domain.

5.5 Plane wave analysis

In this section, we determine the forms of plane waves in conducting poroelastic media solution of (5.3) with no source [107]. In addition, we obtain the values of the plane waves velocities. In conducting poroelastic materials, four kinds of plane waves can propagate:

- "P-wave": the poroelastic fast compression wave,
- "B-wave": the poroelastic slow compression wave (Biot's wave),
- "S-wave": the poroelastic shear wave,
- "EM-wave": the electromagnetic wave.

Considering an isotropic homogeneous conducting poroelastic material, we determine the form of the plane waves and the complex slownesses s, by setting $\mathbf{F_1}$, $\mathbf{F_2}$, $\mathbf{F_3}$ to zero in (5.5):

$$\begin{aligned} -\omega^2\rho_a \mathrm{u} \;-\; \rho_f\omega^2 \mathrm{w} \;-\; H\,\nabla\nabla\cdot \mathrm{u} \;+\; \mu_{\mathrm{fr}}\,\mathbf{curl}\,\mathbf{curl}\,\mathrm{u} \;-\; \alpha\, M\,\nabla\nabla\cdot \mathrm{w} = 0\,,\\ -\omega^2\rho_f \mathrm{u} \;-\; \omega^2\,\rho_{\mathrm{dyn}}\,\mathrm{w} - \frac{\eta}{k}\,\mathbf{L}\,\boldsymbol{E} - M\,\nabla\nabla\cdot \mathrm{w} \;-\; M\alpha\nabla\nabla\cdot \mathrm{u} = 0\,,\\ \mathbf{curl}\,\mathbf{curl}\,\boldsymbol{E} - \omega^2\,\tilde{\boldsymbol{\varepsilon}}\,\mu_0\,\boldsymbol{E} \;-\; \mathfrak{s}\,\mathrm{i}\,\omega\,\mu_0\,\mathbf{L}\,\omega^2\,\rho_{\mathrm{dyn}}\,\mathrm{w} \;=\; 0\,. \end{aligned} \tag{5.11}$$

A vectorial time-harmonic plane wave has the form

$$e^{\mathrm{i}\,\mathfrak{s}\,\omega t}\,e^{\mathrm{i}\,\mathbf{k}\cdot\boldsymbol{X}}\,\mathbf{d}\,,$$

where we have defined the polarization $\widehat{\mathbf{d}}$ with $|\widehat{\mathbf{d}}| = 1$, the wave vector $\mathbf{k} = \omega\,\mathsf{s}(\omega)\,\widehat{\mathbf{k}}$, and the direction of propagation $\widehat{\mathbf{k}}$ with $|\widehat{\mathbf{k}}| = 1$.

Lemma 5.3. We will use the following properties:

$$\begin{aligned} \nabla\nabla\cdot e^{\mathrm{i}\mathbf{k}\cdot\boldsymbol{X}}\,\mathbf{d} \;&=\; -\,(\mathbf{d}\cdot\mathbf{k})\,\mathbf{k}\,e^{\mathrm{i}\,\mathbf{k}\cdot\boldsymbol{X}}\,,\\ \mathbf{curl}\,\mathbf{curl}\;e^{\mathrm{i}\mathbf{k}\cdot\boldsymbol{X}}\mathbf{d} \;&=\; e^{\mathrm{i}\mathbf{k}\cdot\boldsymbol{X}}\Big(\mathbf{k}\times\mathbf{d}\Big)\times\mathbf{k} = e^{\mathrm{i}\mathbf{k}\cdot\boldsymbol{X}}\,\Big(|\mathbf{k}|^2\mathbf{d} \;-\; (\mathbf{k}\cdot\mathbf{d})\,\mathbf{k}\Big)\,. \end{aligned} \tag{5.12}$$

5.5.1 Admissible plane waves and slowness calculation

Proposition 5.4 (Plane wave solutions to (5.11)).

The two longitudinal slownesses sustained in a conducting poroelastic medium are:

$$2\,\mathsf{s}_\bullet^2 \;=\; -\,b \pm \sqrt{b^2 \;-4\,c}\,, \qquad \text{for } \bullet = \mathrm{P}\,\mathrm{B}\,, \tag{5.13}$$

with

$$b \;=\; \frac{-\,\rho_{\mathrm{dyn}}\,H - \;\rho_a\,M \;+\; 2\,\rho_f\,\alpha M + \;\dfrac{H}{\tilde{\boldsymbol{\varepsilon}}}\,\mathbf{L}^2\,\rho_{\mathrm{dyn}}^2}{H\,M \;-\; \alpha^2 M^2},$$

and

$$c \;=\; \frac{\rho_a\,\rho_{\mathrm{dyn}} \;-\rho_f^2 \;-\; \dfrac{\rho_a}{\tilde{\boldsymbol{\varepsilon}}}\,\mathbf{L}^2\,\rho_{\mathrm{dyn}}^2}{H\,M \;-\; \alpha^2 M^2}\,.$$

In (5.13), the $-$ corresponds to the P wave while the $+$ corresponds to the B wave.

The two transverse slownesses sustained in a conducting poroelastic medium are, for $\bullet = \mathrm{S}\,,\mathrm{EM}$:

$$2\,\mathsf{s}_\bullet^2 \;=\; \left(\Big(\frac{\rho_a}{\mu_{\mathrm{fr}}} - \frac{\rho_f^2}{\mu_{\mathrm{fr}}\,\rho_{\mathrm{dyn}}}\Big) + \tilde{\boldsymbol{\varepsilon}}\,\mu_0 + \rho_{\mathrm{dyn}}\,\mathbf{L}^2\,\mu_0\right) \pm \sqrt{\left(\Big(\frac{\rho_a}{\mu_{\mathrm{fr}}} \;-\; \frac{\rho_f^2}{\mu_{\mathrm{fr}}\,\rho_{\mathrm{dyn}}}\Big) \;-\; \tilde{\boldsymbol{\varepsilon}}\,\mu_0 \;-\; \rho_{\mathrm{dyn}}\,\mathbf{L}^2\,\mu_0\right)^2 \;- 4\,\frac{\rho_f^2}{\mu_{\mathrm{fr}}}\,\mathbf{L}^2\,\mu_0}\,. \tag{5.14}$$

The case with the $+$ in front of the square root corresponds to the poroelastic transverse slowness s_{S}, while the case with the $-$ corresponds to the electromagnetic slowness s_{EM}.

For $\bullet \in \{\mathrm{P}\,,\,\mathrm{B}\,,\mathrm{S}\,,\mathrm{EM}\,\}$, if $(\mathrm{u}_\bullet, \mathrm{w}_\bullet, \boldsymbol{E}_\bullet)$ is of the form

$$\mathrm{u}_\bullet \;=\; e^{\mathrm{i}\,\mathbf{k}_\bullet\cdot\boldsymbol{X}}\,\widehat{\mathbf{d}}\,, \qquad \mathrm{w}_\bullet \;=\; \mathcal{W}_\bullet\,e^{\mathrm{i}\,\mathbf{k}_\bullet\cdot\boldsymbol{X}}\,\widehat{\mathbf{d}}\,, \qquad \boldsymbol{E}_\bullet \;=\; \mathcal{E}_\bullet\,e^{\mathrm{i}\,\mathbf{k}_\bullet\cdot\boldsymbol{X}}\,\widehat{\mathbf{d}}\,,$$

solving (5.11), then the slowness $\mathsf{s}_\bullet$, the polarization $\widehat{\mathbf{d}}$ and the direction of propagation $\widehat{\mathbf{k}}$ have the following forms:

1. The two types of longitudinal waves (those with polarization direction parallel to the propagation direction) are given by the pair $(\mathrm{u}_\bullet, \mathrm{w}_\bullet)$ with $\bullet \in \{\mathrm{P}, \mathrm{B}\}$,

$$\begin{cases} \mathbf{k}_\bullet \;=\; \omega\, \mathsf{s}_\bullet(\omega)\, \widehat{\mathbf{d}} \quad , \quad |\widehat{\mathbf{d}}| = 1, \\ \mathsf{s}_\bullet(\omega) \text{ given by (5.13)}, \\ \mathcal{W}_\bullet \;=\; -\,\dfrac{H\,\mathsf{s}_\bullet^2 \,-\, \rho_a}{\mathsf{s}_\bullet^2\,\alpha\, M \,-\, \rho_f}, \\ \mathcal{E}_\bullet \;=\; \dfrac{\mathfrak{s}\,\mathrm{i}\,\omega\,\mathbf{L}\,\rho_{\mathrm{dyn}}}{\tilde{\boldsymbol{\varepsilon}}}\,\dfrac{H\,\mathsf{s}_\bullet^2 \,-\, \rho_a}{\mathsf{s}_\bullet^2\,\alpha\, M \,-\, \rho_f}\,. \end{cases} \tag{5.15}$$

2. The two types of transverse plane waves (those with polarization direction orthogonal to the propagation direction) are given by the pair $(\mathrm{u}_\bullet, \mathrm{w}_\bullet)$ with $\bullet \in \{\mathrm{S}, \mathrm{EM}\}$

$$\begin{cases} \mathbf{k}_{\mathrm{S}} \;=\; \omega\, \mathsf{s}_{\mathrm{S}}(\omega)\, \widehat{\mathbf{k}} \quad ; \\ \mathsf{s}_{\mathrm{S}}(\omega) \text{ given by (5.14)}, \\ \widehat{\mathbf{k}} \perp\, \widehat{\mathbf{d}} \quad , \quad |\widehat{\mathbf{k}}| = |\widehat{\mathbf{d}}| = 1\,, \\ \mathcal{W}_\bullet \;=\; \dfrac{-\,\rho_a \,+\, \mathsf{s}_\bullet^2\,\mu_{\mathrm{fr}}}{\rho_f}, \\ \mathcal{E}_\bullet \;=\; -\dfrac{\mathfrak{s}\,\mathrm{i}\,\omega\,\mu_0\,\rho_{\mathrm{dyn}}\,\mathbf{L}}{\tilde{\boldsymbol{\varepsilon}}\,\mu_0 \,-\, \mathsf{s}_\bullet^2}\,\dfrac{-\,\rho_a \,+\, \mathsf{s}_\bullet^2\,\mu_{\mathrm{fr}}}{\rho_f}\,. \end{cases} \tag{5.16}$$

Proof. We write the plane wave solutions u^{pw}, w^{pw}, $\boldsymbol{E}^{\mathrm{pw}}$ of equation (5.5) as:

$$\mathrm{u}^{\mathrm{pw}} \;=\; u_0\, e^{\mathrm{i}\,\mathbf{k}\cdot\boldsymbol{x}}\,\widehat{\mathbf{d}}\,, \qquad \mathrm{w}^{\mathrm{pw}} \;=\; w_0\, e^{\mathrm{i}\,\mathbf{k}\cdot\boldsymbol{x}}\,\widehat{\mathbf{d}}\,, \qquad \boldsymbol{E}^{\mathrm{pw}} \;=\; E_0\, e^{\mathrm{i}\,\mathbf{k}\cdot\boldsymbol{x}}\,\widehat{\mathbf{d}}\,, \tag{5.17}$$

and we inject those expressions in (5.11). Using equation (5.12) and dividing by $e^{\mathrm{i}\mathbf{k}\cdot\boldsymbol{x}}$, we obtain:

$$\begin{aligned} \Big(-\,\omega^2\,\rho_a\,u_0 \,-\, \omega^2\,\rho_f\,w_0\Big)\,\widehat{\mathbf{d}} + \Big(H\,u_0 \,+\, \alpha\,M\,w_0\Big)(\widehat{\mathbf{d}}\cdot\mathbf{k})\,\mathbf{k} \,+\, \mu_{\mathrm{fr}}\,u_0\,\Big(\widehat{\mathbf{d}}\times\mathbf{k}\Big)\,\mathcal{R}_{-\frac{\pi}{2}} \;&=\; 0\,, \\ \Big(-\,\omega^2\,\rho_f u_0 \,+\, -\omega^2\,\rho_{\mathrm{dyn}} w_0 - \frac{\eta}{k}\,\mathbf{L}\,E_0\Big)\,\widehat{\mathbf{d}} \,+\, M\,\Big(w_0 \,+\, \alpha\,u_0\Big)\,(\widehat{\mathbf{d}}\cdot\mathbf{k})\,\mathbf{k} \;&=\; 0\,, \\ \Big(-\,\omega^2\,\tilde{\boldsymbol{\varepsilon}}\,\mu_0\,E_0 \,-\, \mathfrak{s}\,\mathrm{i}\,\omega\,\mu_0\,\mathbf{L}\,\omega^2\,\rho_{\mathrm{dyn}}\,w_0\Big)\widehat{\mathbf{d}} \,+ E_0\,\Big(\widehat{\mathbf{d}}\times\mathbf{k}\Big)\,\mathcal{R}_{-\frac{\pi}{2}} &= 0\,. \end{aligned} \tag{5.18}$$

- **Transverse waves**

  In the case of a transverse wave, $\mathbf{k}\cdot\widehat{\mathbf{d}} \;=\; 0$. Using this, equation (5.18) gives:

$$\begin{aligned} \Big(-\,\omega^2\,\rho_a\,u_0 \,-\, \omega^2\,\rho_f\,w_0\Big)\,\widehat{\mathbf{d}} \,+\, \mu_{\mathrm{fr}}\,u_0\,\mathbf{k}^2\,\widehat{\mathbf{d}} \;&=\; 0\,, \\ \Big(-\,\omega^2\,\rho_f u_0 \,+\, -\omega^2\,\rho_{\mathrm{dyn}} w_0 - \frac{\eta}{k}\,\mathbf{L}\,\mathcal{E}_\bullet\Big)\,\widehat{\mathbf{d}} \;&=\; 0\,, \\ \Big(-\,\omega^2\,\tilde{\boldsymbol{\varepsilon}}\,\mu_0\,\mathcal{E}_\bullet \,-\, \mathfrak{s}\,\mathrm{i}\,\omega\,\mu_0\,\mathbf{L}\,\omega^2\,\rho_{\mathrm{dyn}}\,w_0\Big)\widehat{\mathbf{d}} \,+ \mathcal{E}_\bullet\,\mathbf{k}^2\,\widehat{\mathbf{d}} \;&=\; 0\,. \end{aligned}$$

  Then, we divide by ω^2 and replace $\mathsf{s} = \dfrac{\mathbf{k}}{\omega}$ to obtain:

$$\begin{aligned} \rho_a\,u_0 \,+\, \rho_f\,w_0 \,-\, \mathsf{s}^2\,\mu_{\mathrm{fr}}\,u_0 \;&=\; 0\,, \\ \rho_f u_0 \,+\, \rho_{\mathrm{dyn}} w_0 + \frac{\eta}{\omega^2\,k}\,\mathbf{L}\,E_0 \;&=\; 0\,, \\ \tilde{\boldsymbol{\varepsilon}}\,\mu_0\,E_0 \,+\, \mathfrak{s}\,\mathrm{i}\,\omega\,\mu_0\,\mathbf{L}\,\rho_{\mathrm{dyn}}\,w_0 \,-\, \mathsf{s}^2\,E_0 \;&=\; 0\,. \end{aligned} \tag{5.19}$$

The above system in matrix form reads as

$$\begin{pmatrix} \rho_a - \mathsf{s}^2\,\mu_{\rm fr} & \rho_f & 0 \\ \rho_f & \rho_{\rm dyn} & \dfrac{\eta}{\omega^2\,k}\,\mathbf{L} \\ 0 & \mathfrak{s}\,\mathrm{i}\,\omega\,\mu_0\,\mathbf{L}\,\rho_{\rm dyn} & \tilde{\varepsilon}\,\mu_0 - \mathsf{s}^2 \end{pmatrix} \begin{pmatrix} u_0 \\ w_0 \\ E_0 \end{pmatrix} = 0\,. \tag{5.20}$$

This means, assuming that u_0, w_0, E_0 do not vanish, that the above matrix is not invertible and has zero determinant. After some calculations detailed in Appendix D.1.1, we obtain two complex roots. We define the two complex slownesses $\mathsf{s}_{\rm S}$ and $\mathsf{s}_{\rm EM}$ as:

$$2\,\mathsf{s}_\bullet^2 = \left(\left(\frac{\rho_a}{\mu_{\rm fr}} - \frac{\rho_f^2}{\mu_{\rm fr}\,\rho_{\rm dyn}} \right) + \tilde{\varepsilon}\,\mu_0 + \rho_{\rm dyn}\,\mathbf{L}^2\,\mu_0 \right) \pm \sqrt{ \left(\left(\frac{\rho_a}{\mu_{\rm fr}} - \frac{\rho_f^2}{\mu_{\rm fr}\,\rho_{\rm dyn}} \right) - \tilde{\varepsilon}\,\mu_0 - \rho_{\rm dyn}\,\mathbf{L}^2\,\mu_0 \right)^2 - 4\,\frac{\rho_f^2}{\mu_{\rm fr}}\,\mathbf{L}^2\,\mu_0 }\,.$$

The case with the $+$ in front of the square root corresponds to the poroelastic transverse slowness $\mathsf{s}_{\rm S}$, while the case with the $-$ corresponds to the electromagnetic slowness $\mathsf{s}_{\rm EM}$. If $\mathbf{L}$ is equal to zero, we retrieve the slownesses of transverse poroelasticity and the electromagnetic slowness. The components of corresponding eigenvectors are obtained from (5.19) for $\bullet = $ S, EM :

$$\mathcal{U}_\bullet = 1 \quad , \quad \mathcal{W}_\bullet = \frac{-\rho_a + \mathsf{s}_\bullet^2\,\mu_{\rm fr}}{\rho_f}\,, \quad \mathcal{E}_\bullet = -\frac{\mathfrak{s}\,\mathrm{i}\,\omega\,\mu_0\,\rho_{\rm dyn}\,\mathbf{L}}{\tilde{\varepsilon}\,\mu_0 - \mathsf{s}_\bullet^2}\,w_0 = -\frac{\mathfrak{s}\,\mathrm{i}\,\omega\,\mu_0\,\rho_{\rm dyn}\,\mathbf{L}}{\tilde{\varepsilon}\,\mu_0 - \mathsf{s}_\bullet^2}\,\frac{-\rho_a + \mathsf{s}_\bullet^2\,\mu_{\rm fr}}{\rho_f}\,.$$

We write system (5.19) as follows:

$$A \begin{pmatrix} u_0 \\ w_0 \\ E_0 \end{pmatrix} - \mathsf{s}^2\,D \begin{pmatrix} u_0 \\ w_0 \\ E_0 \end{pmatrix} = 0\,,$$

where

$$A = \begin{pmatrix} \rho_a & \rho_f & 0 \\ \rho_f & \rho_{\rm dyn} & \dfrac{\eta}{\omega^2\,k}\,\mathbf{L} \\ 0 & \mathfrak{s}\,\mathrm{i}\,\omega\,\mu_0\,\mathbf{L}\,\rho_{\rm dyn} & \tilde{\varepsilon}\,\mu_0 \end{pmatrix} \quad \text{and} \quad D = \begin{pmatrix} \mu_{\rm fr} & 0 & 0 \\ 0 & 0 & 0 \\ 0 & 0 & 1 \end{pmatrix}. \tag{5.21}$$

Supposing A invertible, the system is equivalent to:

$$\mathsf{c}^2 \begin{pmatrix} u_0 \\ w_0 \\ E_0 \end{pmatrix} - A^{-1}\,D \begin{pmatrix} u_0 \\ w_0 \\ E_0 \end{pmatrix} = 0\,, \qquad \text{with } \mathsf{c} = \frac{1}{\mathsf{s}}.$$

This means that $\mathsf{c}_\bullet^2$ are eigenvalues of $A^{-1}D$, and $A^{-1}D$ is diagonalizable. We can write

$$A^{-1}D = P_{\rm trans} \begin{pmatrix} \mathsf{c}_{\rm S}^2 & 0 & 0 \\ 0 & 0 & 0 \\ 0 & 0 & \mathsf{c}_{\rm EM}^2 \end{pmatrix} P_{\rm trans}^{-1}\,, \quad \text{with} \quad P_{\rm trans} = \begin{pmatrix} \mathcal{U}_{\rm S} & 0 & \mathcal{U}_{\rm EM} \\ \mathcal{W}_{\rm S} & 1 & \mathcal{W}_{\rm EM} \\ \mathcal{E}_{\rm S} & 0 & \mathcal{E}_{\rm EM} \end{pmatrix}. \tag{5.22}$$

- **Longitudinal waves**

For a longitudinal wave, $\mathbf{k}$ is parallel to $\widehat{\mathbf{d}}$, $\mathbf{k} \times \widehat{\mathbf{d}} = 0$ and we can write

$$\widehat{\mathbf{d}} = a\,\mathbf{k} \quad , \quad \widehat{\mathbf{d}} \cdot \mathbf{k} = a|\mathbf{k}|^2\,, \qquad a \in \mathbb{R}\,,$$

so that equation (5.18) becomes

$$\begin{aligned} \Big(H\,u_0 + \alpha\,M\,w_0 \Big)\,a\,|\mathbf{k}|^2\mathbf{k} + \Big(-\omega^2\,\rho_a\,u_0 - \omega^2\,\rho_f\,w_0 \Big)\,a\,\mathbf{k} &= 0\,, \\ (-\omega^2\,\rho_f\,u_0 + -\omega^2\,\rho_{\rm dyn}\,w_0 - \frac{\eta}{k}\,\mathbf{L}\,E_0)\,a\,\mathbf{k} + M\Big(w_0 + \alpha\,u_0 \Big)\,a\,|\mathbf{k}|^2\mathbf{k} &= 0\,, \\ \Big(-\omega^2\,\tilde{\varepsilon}\,\mu_0\,E_0 - \mathfrak{s}\,\mathrm{i}\,\omega\,\mu_0\,\mathbf{L}\,\omega^2\,\rho_{\rm dyn}\,w_0 \Big)\,a\,\mathbf{k} &= 0\,. \end{aligned}$$

Dividing by $a\,\mathbf{k}$ and ω^2 gives

$$\begin{aligned} \mathsf{s}^2\left(H\,u_0+\,\alpha\,M\,w_0\right)-\left(\rho_a\,u_0+\rho_f\,w_0\right) &= 0\,,\\ -\left(\rho_f\,u_0+\rho_{\rm dyn}\,w_0\,+\frac{\eta}{\omega^2\,k}\,\mathbf{L}\,E_0\right)+\mathsf{s}^2\,M\left(w_0\,+\alpha\,u_0\right) &= 0\,,\\ -\left(\tilde{\boldsymbol{\varepsilon}}\,\mu_0\,E_0\,+\,\mathfrak{s}\,\mathrm{i}\,\omega\,\mu_0\,\mathbf{L}\,\rho_{\rm dyn}\,w_0\right) &= 0\,. \end{aligned} \tag{5.23}$$

In matrix form, we obtain:

$$\begin{pmatrix} \mathsf{s}^2\,H-\,\rho_a & \mathsf{s}^2\,\alpha M-\,\rho_f & 0\\ -\,\rho_f+\mathsf{s}^2\,\alpha M & -\,\rho_{\rm dyn}+\,\mathsf{s}^2\,M & \dfrac{\eta}{\omega^2\,k}\,\mathbf{L}\\ 0 & \mathfrak{s}\,\mathrm{i}\,\omega\,\mu_0\,\mathbf{L}\,\rho_{\rm dyn} & \tilde{\boldsymbol{\varepsilon}}\,\mu_0 \end{pmatrix}\begin{pmatrix} u_0\\ w_0\\ E_0 \end{pmatrix}=0\,. \tag{5.24}$$

Considering that u_0, w_0, E_0 are non trivial means that the determinant of the matrix is equal to zero. Using the expression of the determinant (see App. D.1.2), we can find two complex slownesses $\mathsf{s}_{\rm P}^2$ and $\mathsf{s}_{\rm B}^2$ that are defined as:

$$2\,\mathsf{s}_\bullet^2\;=\;-\,b\,\pm\sqrt{b^2\,-4\,c}\,,\qquad \bullet=\mathrm{P\,B}\,,$$

with

$$b\;=\;\frac{-\,\rho_{\rm dyn}\,H-\,\rho_a\,M\,+\,2\,\rho_f\,\alpha M+\,\dfrac{H}{\tilde{\boldsymbol{\varepsilon}}}\,\mathbf{L}^2\,\rho_{\rm dyn}^2}{H\,M\,-\,\alpha^2 M^2}\,,$$

and

$$c\;=\;\frac{\rho_a\,\rho_{\rm dyn}\,-\rho_f^2\,-\,\dfrac{\rho_a}{\tilde{\boldsymbol{\varepsilon}}}\,\mathbf{L}^2\,\rho_{\rm dyn}^2}{H\,M\,-\,\alpha^2 M^2}\,.$$

The $-$ corresponds to the P wave while the $+$ corresponds to the B wave. The components of corresponding eigenvectors are read from (5.23) for $\bullet=\mathrm{P},\mathrm{B}$:

$$\mathcal{U}_\bullet\;=\;1\quad,\quad \mathcal{W}_\bullet\;=\;-\,\frac{H\,\mathsf{s}_\bullet^2\,-\,\rho_a}{\mathsf{s}_\bullet^2\,\alpha\,M\,-\,\rho_f}\,,\qquad \mathcal{E}_\bullet\;=\;-\,\frac{\mathfrak{s}\,\mathrm{i}\,\omega\,\mathbf{L}\,\rho_{\rm dyn}}{\tilde{\boldsymbol{\varepsilon}}}\,\mathcal{W}_\bullet\;=\;\frac{\mathfrak{s}\,\mathrm{i}\,\omega\,\mathbf{L}\,\rho_{\rm dyn}}{\tilde{\boldsymbol{\varepsilon}}}\,\frac{H\,\mathsf{s}_\bullet^2\,-\,\rho_a}{\mathsf{s}_\bullet^2\,\alpha\,M\,-\,\rho_f}\,.$$

The system (5.24) is written as

$$A\begin{pmatrix} u_0\\ w_0\\ E_0 \end{pmatrix}\,-\mathsf{s}^2\,B\,\begin{pmatrix} u_0\\ w_0\\ E_0 \end{pmatrix}=0\,,$$

where A is defined in equation (5.21) and

$$B\;=\;\begin{pmatrix} H & \alpha M & 0\\ \alpha M & M & 0\\ 0 & 0 & 0 \end{pmatrix}\,.$$

Supposing A invertible, the above system is then equivalent to:

$$\mathsf{c}^2\begin{pmatrix} u_0\\ w_0\\ E_0 \end{pmatrix}\,-A^{-1}\,B\,\begin{pmatrix} u_0\\ w_0\\ E_0 \end{pmatrix}=0\,,$$

which means that $\mathsf{c}_\bullet^2$ are eigenvalues of $A^{-1}B$, and $A^{-1}B$ is diagonalizable. We can then write:

$$A^{-1}B\;=\;P_{\rm long}\begin{pmatrix} \mathsf{c}_{\rm P}^2 & 0 & 0\\ 0 & \mathsf{c}_{\rm B}^2 & 0\\ 0 & 0 & 0 \end{pmatrix}P_{\rm long}^{-1}\,,\qquad \text{with}\qquad P_{\rm long}\;=\;\begin{pmatrix} \mathcal{U}_{\rm P} & \mathcal{U}_{\rm B} & 0\\ \mathcal{W}_{\rm P} & \mathcal{W}_{\rm B} & 0\\ \mathcal{E}_{\rm P} & \mathcal{E}_{\rm B} & 1 \end{pmatrix}\,. \tag{5.25}$$

□

5.5.2 First order formulation of the plane waves

We detail the plane wave expression of ($\mathbf{u}$, $\mathbf{w}$, $\boldsymbol{\tau}$, p, $\boldsymbol{E}$, $\boldsymbol{H}$, $\boldsymbol{J}$), that we denote ($\mathbf{u}^{\mathrm{pw}}$, $\mathbf{w}^{\mathrm{pw}}$, $\boldsymbol{\tau}^{\mathrm{pw}}$, p^{pw}, $\boldsymbol{E}^{\mathrm{pw}}$, $\boldsymbol{H}^{\mathrm{pw}}$, $\boldsymbol{J}^{\mathrm{pw}}$), for transverse and longitudinal waves.

- For the longitudinal waves P and B, ($\bullet = \mathrm{P}\,,\,\mathrm{B}$), the plane wave is:

$$\begin{aligned}
\mathbf{u}_\bullet^{\mathrm{pw}} &= e^{\mathrm{i}\,\mathbf{k}_\bullet\cdot\boldsymbol{x}}\,(\mathfrak{s}\,\mathrm{i}\,\omega)\,\widehat{\mathbf{d}}\,, & \mathbf{w}_\bullet^{\mathrm{pw}} &= \mathcal{W}_\bullet\, e^{\mathrm{i}\,\mathbf{k}_\bullet\cdot\boldsymbol{x}}\,(\mathfrak{s}\,\mathrm{i}\,\omega)\,\widehat{\mathbf{d}}\,,\\
\boldsymbol{\tau}_\bullet^{\mathrm{pw}} &= \mathrm{i}\,\omega\,\mathsf{s}_\bullet(\omega)\,e^{\mathrm{i}\mathbf{k}_\bullet\cdot\boldsymbol{x}}\left(2\,\mu_{\mathrm{fr}}\,\widehat{\mathbf{d}}\otimes\widehat{\mathbf{d}} + \left(-\frac{2}{3}\mu_{\mathrm{fr}} + \mathrm{k}_{\mathrm{fr}} + M\,\alpha^2 + \mathcal{W}_\bullet\,\alpha\,M\right)\mathbb{I}\right),\\
\mathrm{p}_\bullet^{\mathrm{pw}} &= \mathrm{i}\,\omega\,\mathsf{s}_\bullet(\omega)\,(-M\,\mathcal{W}_\bullet - M\,\alpha)\,e^{\mathrm{i}\mathbf{k}_\bullet\cdot\boldsymbol{x}}, & \boldsymbol{E}_\bullet^{\mathrm{pw}} &= \mathcal{E}_\bullet\, e^{\mathrm{i}\,\mathbf{k}_\bullet\cdot\boldsymbol{x}}\,\widehat{\mathbf{d}}\,,\\
\boldsymbol{H}_\bullet^{\mathrm{pw}} &= 0\,, & \boldsymbol{J}_\bullet^{\mathrm{pw}} &= \left(\sigma\,\mathcal{E}_\bullet + \mathbf{L}\,\omega^2\,\rho_f - \mathbf{L}\,\omega^2\,\mathsf{s}_\bullet^2(\omega)\,M\,(\mathcal{W}_\bullet + \alpha)\right)\,e^{\mathrm{i}\,\mathbf{k}\cdot\boldsymbol{x}}\,\widehat{\mathbf{d}}\,,
\end{aligned} \tag{5.26}$$

  with polarization given by

$$\begin{cases}
\mathbf{k}_\bullet = \omega\,\mathsf{s}_\bullet(\omega)\,\widehat{\mathbf{d}} \quad , \quad |\widehat{\mathbf{d}}| = 1,\\
\mathsf{s}_\bullet(\omega) \text{ given by (5.13)}\,,\\
\mathcal{W}_\bullet \text{ and } \mathcal{E}_\bullet \text{ given by (5.15)}\,.
\end{cases}$$

- The plane wave writes for the two types of transverse waves S and EM ($\bullet = \mathrm{S}\,,\,\mathrm{EM}$):

$$\begin{aligned}
\mathbf{u}_\bullet^{\mathrm{pw}} &= e^{\mathrm{i}\,\mathbf{k}_\bullet\cdot\boldsymbol{x}}\,(\mathfrak{s}\,\mathrm{i}\,\omega)\,\widehat{\mathbf{d}}\,, & \mathbf{w}_\bullet^{\mathrm{pw}} &= \mathcal{W}_\bullet\, e^{\mathrm{i}\,\mathbf{k}_\bullet\cdot\boldsymbol{x}}\,(\mathfrak{s}\,\mathrm{i}\,\omega)\,\widehat{\mathbf{d}}\,,\\
\boldsymbol{\tau}_\bullet^{\mathrm{pw}} &= \mathrm{i}\,\omega\,\mathsf{s}_\bullet(\omega)\,e^{\mathrm{i}\,\mathbf{k}_\bullet\cdot\boldsymbol{x}}\,\mu_{\mathrm{fr}}\left(\widehat{\mathbf{k}}\otimes\widehat{\mathbf{d}} + \widehat{\mathbf{d}}\otimes\widehat{\mathbf{k}}\right), & \mathrm{p}_\bullet^{\mathrm{pw}} &= 0\,,\\
\boldsymbol{E}_\bullet^{\mathrm{pw}} &= \mathcal{E}_\bullet\, e^{\mathrm{i}\,\mathbf{k}_\bullet\cdot\boldsymbol{x}}\,\widehat{\mathbf{d}}\,, & \boldsymbol{H}_\bullet^{\mathrm{pw}} &= -\frac{\mathfrak{s}}{\mu_0}\,\mathsf{s}_\bullet\,\mathcal{E}_\bullet\, e^{\mathrm{i}\,\mathbf{k}\cdot\boldsymbol{x}}\,(\widehat{\mathbf{k}}\times\widehat{\mathbf{d}})\,,\\
\boldsymbol{J}_\bullet^{\mathrm{pw}} &= \left(\sigma\,E_\bullet + \mathbf{L}\,\omega^2\,\rho_f\right)\,e^{\mathrm{i}\,\mathbf{k}\cdot\boldsymbol{x}}\,\widehat{\mathbf{d}}\,,
\end{aligned} \tag{5.27}$$

  with polarization given by

$$\begin{cases}
\mathbf{k}_\bullet = \omega\,\mathsf{s}_\bullet(\omega)\,\widehat{\mathbf{k}}\,, \qquad \widehat{\mathbf{k}}\perp\widehat{\mathbf{d}}\,, \qquad |\widehat{\mathbf{k}}| = |\widehat{\mathbf{d}}| = 1\,,\\
\mathsf{s}_\bullet(\omega) \text{ given by (5.14)}\,,\\
\mathcal{W}_\bullet \text{ and } \mathcal{E}_\bullet \text{ given by (5.16)}\,.
\end{cases}$$

Proof. $\mathbf{u}^{\mathrm{pw}}$, $\mathbf{w}^{\mathrm{pw}}$ are the time derivatives of the displacements given in equation (5.17). The expressions of $\boldsymbol{\tau}^{\mathrm{pw}}$ and p^{pw} are the same as for poroelasticity and their calculations are detailed in Section 1.5.2, page 37. The expression of $\boldsymbol{H}^{\mathrm{pw}}$ is obtained using equation (5.3e):

$$\mathbf{curl}\,\boldsymbol{E} + \mathfrak{s}\,\mathrm{i}\,\omega\,\mu_0\,\boldsymbol{H} = 0\,.$$

We have:

$$\boldsymbol{H}_\bullet^{\mathrm{pw}} = \frac{\mathfrak{s}\,\mathrm{i}}{\omega\,\mu_0}\,\mathrm{curl}\,\boldsymbol{E}_\bullet = \frac{\mathfrak{s}\,\mathrm{i}}{\omega\,\mu_0}\,\mathrm{curl}\left(\mathcal{E}_\bullet\, e^{\mathrm{i}\,\mathbf{k}\cdot\boldsymbol{x}}\,\widehat{\mathbf{d}}\right),$$

with

$$\mathbf{curl}\left(\mathcal{E}_\bullet\, e^{\mathrm{i}\,\mathbf{k}\cdot\boldsymbol{x}}\,\widehat{\mathbf{d}}\right) = \mathcal{E}_\bullet\,\mathrm{i}\,e^{\mathrm{i}\,\mathbf{k}\cdot\boldsymbol{x}}\begin{pmatrix} k_y\,d_z - k_z\,d_y\\ k_z\,d_x - k_x\,d_z\\ k_x\,d_y - k_y\,d_x\end{pmatrix} = \mathcal{E}_\bullet\,\mathrm{i}\,e^{\mathrm{i}\,\mathbf{k}\cdot\boldsymbol{x}}\,(\mathbf{k}\times\widehat{\mathbf{d}})\,.$$

For longitudinal waves, $(\widehat{\mathbf{k}}\times\widehat{\mathbf{d}}) = 0$, hence: $\boldsymbol{H}_\bullet^{\mathrm{pw}} = 0$. For transverse waves, $\mathbf{k} = \omega\,\mathsf{s}_\bullet\,\widehat{\mathbf{k}}$, which gives:

$$\boldsymbol{H}_\bullet^{\mathrm{pw}} = \frac{\mathfrak{s}\,\mathrm{i}}{\omega\,\mu_0}\,\omega\,\mathsf{s}_\bullet\,\mathcal{E}_\bullet\,\mathrm{i}\,e^{\mathrm{i}\,\mathbf{k}\cdot\boldsymbol{x}}\,(\widehat{\mathbf{k}}\times\widehat{\mathbf{d}}) = -\frac{\mathfrak{s}}{\mu_0}\,\mathsf{s}_\bullet\,\mathcal{E}_\bullet\, e^{\mathrm{i}\,\mathbf{k}\cdot\boldsymbol{x}}\,(\widehat{\mathbf{k}}\times\widehat{\mathbf{d}})\,.$$

In two dimensions, $(\widehat{\mathbf{k}} \times \widehat{\mathbf{d}}) = 1$, and the magnetic field is hence

$$\mathrm{H}_\bullet^{\mathrm{pw}} = \frac{\mathfrak{s}\,\mathrm{i}}{\omega\,\mu_0}\,\omega\,\mathsf{s}_\bullet\,\mathcal{E}_\bullet\,\mathrm{i}\,e^{\mathrm{i}\,\mathbf{k}\cdot\boldsymbol{x}}\,.$$

For $\boldsymbol{J}^{\mathrm{pw}}$, from equation (5.3g), we have:

$$\boldsymbol{J}_\bullet^{\mathrm{pw}} = \sigma\,\boldsymbol{E}_\bullet^{\mathrm{pw}} + \mathbf{L}\,(-\nabla\,\mathrm{p}_\bullet^{\mathrm{pw}} + \omega^2\,\rho_f\,\mathrm{u}_\bullet^{\mathrm{pw}})\,.$$

For transverse waves, $\mathrm{p}_\bullet^{\mathrm{pw}} = 0$, which leads to :

$$\boldsymbol{J}_\bullet^{\mathrm{pw}} = \sigma\,\mathcal{E}_\bullet\,e^{\mathrm{i}\,\mathbf{k}\cdot\boldsymbol{x}}\,\widehat{\mathbf{d}} + \mathbf{L}\,\omega^2\,\rho_f\,e^{\mathrm{i}\,\mathbf{k}\cdot\boldsymbol{x}}\,\widehat{\mathbf{d}} = \left(\sigma\,\mathcal{E}_\bullet + \mathbf{L}\,\omega^2\,\rho_f\,\right)\,e^{\mathrm{i}\,\mathbf{k}\cdot\boldsymbol{x}}\,\widehat{\mathbf{d}}\,.$$

For longitudinal waves, we calculate the gradient of p:

$$\mathrm{p}_\bullet^{\mathrm{pw}} = \mathrm{i}\,\omega\,\mathsf{s}_\bullet(\omega)\,(-M\,\mathcal{W}_\bullet - M\,\alpha)\,e^{\mathrm{i}\mathbf{k}_\bullet\cdot\boldsymbol{x}}\,,$$

$$\begin{aligned}\Rightarrow \nabla\,\mathrm{p}_\bullet^{\mathrm{pw}} &= \mathrm{i}\,\omega\,\mathsf{s}_\bullet(\omega)\,(-M\,\mathcal{W}_\bullet - M\,\alpha)\,\nabla\,e^{\mathrm{i}\mathbf{k}_\bullet\cdot\boldsymbol{x}}\\ &= \mathrm{i}\,\omega\,\mathsf{s}_\bullet(\omega)\,(-M\,\mathcal{W}_\bullet - M\,\alpha)\,\mathrm{i}\,\mathbf{k}_\bullet\,e^{\mathrm{i}\mathbf{k}_\bullet\cdot\boldsymbol{x}}\\ &= \omega^2\,\mathsf{s}_\bullet^2(\omega)\,M\,(\mathcal{W}_\bullet + \alpha)\,e^{\mathrm{i}\mathbf{k}_\bullet\cdot\boldsymbol{x}}\,\widehat{\mathbf{d}}\,.\end{aligned}$$

Hence, we obtain

$$\boldsymbol{J}_\bullet^{\mathrm{pw}} = \left(\sigma\,\mathcal{E}_\bullet + \mathbf{L}\,\omega^2\,\rho_f - \mathbf{L}\,\omega^2\,\mathsf{s}_\bullet^2(\omega)\,M\,(\mathcal{W}_\bullet + \alpha)\right)\,e^{\mathrm{i}\,\mathbf{k}\cdot\boldsymbol{x}}\,\widehat{\mathbf{d}}\,.$$

□

5.5.3 Expansion of incident plane waves in Bessel functions in two dimensions

The incident plane waves given in equations (5.27) and (5.26) are expanded in polar coordinates, and expressed with Bessel functions. We choose to work in polar coordinates because we will consider circular geometries in the development of the analytical solutions, see Chapter 6. The Jacobi-Anger expansion, (see for e.g [91, eqn (2.17)]) is

$$e^{\mathrm{i}\,t\,\cos\varphi} = \sum_{k=-\infty}^{\infty}\mathrm{i}^k\mathrm{J}_k(t)\,e^{ik\varphi}\,, \qquad \text{with } \mathrm{J}_k \text{ Bessel function.}$$

When the direction of propagation $\widehat{\mathbf{k}} = \begin{pmatrix}\cos\alpha_{\mathrm{inc}}\\ \sin\alpha_{\mathrm{inc}}\end{pmatrix}$, we have: $e^{\mathrm{i}\,\mathbf{k}\cdot\boldsymbol{x}} = e^{\mathrm{i}\,\omega\,\mathsf{s}\,\widehat{\mathbf{k}}\cdot\boldsymbol{x}} = e^{\mathrm{i}\,\omega\,\mathsf{s}\,(\cos\alpha_{\mathrm{inc}},\sin\alpha_{\mathrm{inc}})\cdot\boldsymbol{x}}$, with s the slowness of the wave. The multipole expansion relative to the origin $0_{\mathbb{R}^2}$ is given by

$$e^{\mathrm{i}\,\omega\,\mathsf{s}\,\boldsymbol{x}\cdot(\cos\alpha_{\mathrm{inc}},\sin\alpha_{\mathrm{inc}})} = e^{\mathrm{i}\,\omega\,\mathsf{s}\,r\,\cos(\theta-\alpha_{\mathrm{inc}})} = \sum_{k=-\infty}^{\infty}\mathrm{i}^k\,\mathrm{J}_k(\omega\,\mathsf{s}\,r)\,e^{\mathrm{i}\,k(\theta-\alpha_{\mathrm{inc}})}\,.$$

Thus,

$$e^{\mathrm{i}\,\omega\,\mathsf{s}_\bullet\,\widehat{\mathbf{k}}\cdot\boldsymbol{x}} = \sum_{k=-\infty}^{\infty}\mathrm{i}^k\,\mathrm{J}_k(\omega\,\mathsf{s}_\bullet\,|\boldsymbol{x}|)\,e^{\mathrm{i}\,k(\theta-\alpha_{\mathrm{inc}})}\,.$$

The above expression will be used to express ($\mathbf{u}^{\mathrm{pw}}$, $\mathbf{w}^{\mathrm{pw}}$, $\boldsymbol{\tau}^{\mathrm{pw}}$, p^{pw}, $\boldsymbol{E}^{\mathrm{pw}}$, H^{pw}, $\boldsymbol{J}^{\mathrm{pw}}$) with series of Bessel functions.

5.5.3.1 Transverse waves

The expansion of the plane wave in equation (5.27) for $\bullet = \mathrm{S}\,,\ \mathrm{EM}$ is given in polar coordinates by:

$$\mathbf{u}_\bullet^{\mathrm{pw}} = -\frac{\mathfrak{s}}{\mathsf{s}_\bullet\,r}\sum_{k=-\infty}^{\infty}\mathrm{i}^{k+1}\,k\,\mathrm{J}_k(\omega\,\mathsf{s}_\bullet\,r)\,e^{\mathrm{i}\,k(\theta-\alpha_{\mathrm{inc}})}\,\mathbf{e}_r + \frac{\mathfrak{s}}{\mathsf{s}_\bullet}\sum_{k=-\infty}^{\infty}\mathrm{i}^k\,\omega\,\mathsf{s}_\bullet\,\mathrm{J}_k'(\omega\,\mathsf{s}_\bullet\,r)\,e^{\mathrm{i}\,k(\theta-\alpha_{\mathrm{inc}})}\,\mathbf{e}_\theta\,,$$

$$\mathbf{w}_\bullet^{\rm pw} \;=\; -\,\frac{\mathfrak{s}\,\mathcal{W}_\bullet}{\mathsf{s}_\bullet\, r}\sum_{k=-\infty}^{\infty} \mathrm{i}^{k+1}\,k\,\mathrm{J}_k(\omega\,\mathsf{s}_\bullet\, r)\; e^{\mathrm{i}\,k(\theta-\alpha_{\rm inc})}\;\mathbf{e}_r \;+\; \frac{\mathfrak{s}\,\mathcal{W}_\bullet}{\mathsf{s}_\bullet}\sum_{k=-\infty}^{\infty} \mathrm{i}^{k}\,\omega\,\mathsf{s}_\bullet\,\mathrm{J}_k'(\omega\,\mathsf{s}_\bullet\, r)\; e^{\mathrm{i}\,k(\theta-\alpha_{\rm inc})}\;\mathbf{e}_\theta\,.$$

In circular geometry, we will use in particular $\boldsymbol{\tau}\,\boldsymbol{n} \;=\; \boldsymbol{\tau}_{rr}\mathbf{e}_r \;+\; \boldsymbol{\tau}_{r\theta}\mathbf{e}_\theta$. Therefore, we detail only the components $\boldsymbol{\tau}_{rr}$ and $\boldsymbol{\tau}_{r\theta}$.

$$\boldsymbol{\tau}_{\bullet,rr}^{\rm pw} \;=\; -\,2\frac{\mu_{\rm fr}}{\mathrm{i}\omega\mathsf{s}_\bullet}\,\frac{\partial_{r\theta}(e^{\mathrm{i}\,\mathbf{k}_\bullet\cdot\boldsymbol{x}})}{r} \;=\; \sum_{k=-\infty}^{\infty} -2\frac{\mu_{\rm fr}}{r}\,\mathrm{i}^{k}\,k\,\mathrm{J}_k'(\omega\,\mathsf{s}_\bullet\, r)\; e^{\mathrm{i}\,k(\theta-\alpha_{\rm inc})}\,,$$

$$\begin{aligned}
\boldsymbol{\tau}_{\bullet,r\theta}^{\rm pw} \;&=\; -\,\frac{\mu_{\rm fr}}{\mathrm{i}\omega\mathsf{s}_\bullet}\left(\frac{\partial_{\theta\theta}(e^{\mathrm{i}\,\mathbf{k}_\bullet\cdot\boldsymbol{x}})}{r^2}+\frac{\partial_r(e^{\mathrm{i}\,\mathbf{k}_\bullet\cdot\boldsymbol{x}})}{r}-\partial_{rr}(e^{\mathrm{i}\,\mathbf{k}_\bullet\cdot\boldsymbol{x}})\right)\\
&=\; \sum_{k=-\infty}^{\infty}\frac{\mu_{\rm fr}\,\mathrm{i}^{k-1}\,k^2}{\omega\mathsf{s}_\bullet\, r^2}\,\mathrm{J}_k(\omega\,\mathsf{s}_\bullet\, r)\; e^{\mathrm{i}\,k(\theta-\alpha_{\rm inc})} - \sum_{k=-\infty}^{\infty}\frac{\mu_{\rm fr}\,\mathrm{i}^{k-1}}{r}\,\mathrm{J}_k'(\omega\,\mathsf{s}_\bullet\, r)\; e^{\mathrm{i}\,k(\theta-\alpha_{\rm inc})}\\
&+\; \sum_{k=-\infty}^{\infty}\mu_{\rm fr}\,\mathrm{i}^{k-1}\,\mathrm{J}_{k+1}(\omega\,\mathsf{s}_\bullet\, r)\; e^{\mathrm{i}\,k(\theta-\alpha_{\rm inc})} - \sum_{k=-\infty}^{\infty}\frac{\mu_{\rm fr}\,k}{\omega\,\mathsf{s}_{\rm S}}\,\mathrm{i}^{k-1}\,\mathrm{J}_k(\omega\,\mathsf{s}_\bullet\, r)\; e^{\mathrm{i}\,k(\theta-\alpha_{\rm inc})}\\
&-\; \sum_{k=-\infty}^{\infty}\mu_{\rm fr}\,\omega\,\mathsf{s}_{\rm S}\,\mathrm{i}^{k-1}\,\mathrm{J}_k(\omega\,\mathsf{s}_\bullet\, r)\; e^{\mathrm{i}\,k(\theta-\alpha_{\rm inc})} + \sum_{k=-\infty}^{\infty}\frac{\mu_{\rm fr}\,k^2}{\omega^2\,\mathsf{s}_\bullet^2}\,\mathrm{i}^{k-1}\,\mathrm{J}_k(\omega\,\mathsf{s}_\bullet\, r)\; e^{\mathrm{i}\,k(\theta-\alpha_{\rm inc})}\,,
\end{aligned}$$

$$\mathrm{p}_\bullet^{\rm pw} \;=\; 0\,,$$

$$\boldsymbol{E}_\bullet^{\rm pw} \;=\; -\,\frac{\mathcal{E}_\bullet}{\omega\,\mathsf{s}_\bullet\, r}\sum_{k=-\infty}^{\infty}\mathrm{i}^{k}\,k\,\mathrm{J}_k(\omega\,\mathsf{s}_\bullet\, r)\,e^{\mathrm{i}\,k(\theta-\alpha_{\rm inc})}\,\mathbf{e}_r \;+\; \frac{\mathcal{E}_\bullet}{\omega\,\mathsf{s}_\bullet}\sum_{k=-\infty}^{\infty}\mathrm{i}^{k-1}\,\omega\,\mathsf{s}_\bullet\,\mathrm{J}_k'(\omega\,\mathsf{s}_\bullet\, r)\,e^{\mathrm{i}\,k(\theta-\alpha_{\rm inc})}\,\mathbf{e}_\theta\,,$$

$$\mathrm{H}_\bullet^{\rm pw} \;=\; -\,\frac{\mathfrak{s}}{\mu_0}\,\mathsf{s}_\bullet\,\mathcal{E}_\bullet\sum_{k=-\infty}^{\infty}\mathrm{i}^{k}\,\mathrm{J}_k(\omega\,\mathsf{s}_\bullet\, r)\; e^{\mathrm{i}\,k(\theta-\alpha_{\rm inc})}\,,$$

and

$$\begin{aligned}
\boldsymbol{J}_\bullet^{\rm pw} \;&=\; -\,\frac{\left(\sigma\;\mathcal{E}_\bullet+\mathbf{L}\,\omega^2\,\rho_f\right)}{\omega\,\mathsf{s}_\bullet\, r}\sum_{k=-\infty}^{\infty}\mathrm{i}^{k}\,k\,\mathrm{J}_k(\omega\,\mathsf{s}_\bullet\, r)\; e^{\mathrm{i}\,k(\theta-\alpha_{\rm inc})}\;\mathbf{e}_r\\
&+\; \frac{\left(\sigma\;\mathcal{E}_\bullet+\mathbf{L}\,\omega^2\,\rho_f\right)}{\omega\,\mathsf{s}_\bullet}\sum_{k=-\infty}^{\infty}\mathrm{i}^{k-1}\,\omega\,\mathsf{s}_\bullet\,\mathrm{J}_k'(\omega\,\mathsf{s}_\bullet\, r)\; e^{\mathrm{i}\,k(\theta-\alpha_{\rm inc})}\;\mathbf{e}_\theta\,.
\end{aligned}$$

Proof. The calculations for the expansion of the poroelastic unknowns $\mathbf{u}^{\rm pw}$, $\mathbf{w}^{\rm pw}$, $\boldsymbol{\tau}^{\rm pw}$, $\mathrm{p}^{\rm pw}$, are given in details in Section 1.5.2, page 37.. We have for $\boldsymbol{E}_\bullet^{\rm pw}$:

$$\boldsymbol{E}_\bullet^{\rm pw} \;=\; \mathcal{E}_\bullet\, e^{\mathrm{i}\,\mathbf{k}_\bullet\cdot\boldsymbol{x}}\;\widehat{\mathbf{d}} \;=\; \frac{\mathcal{E}_\bullet\,\mathrm{i}}{\omega\,\mathsf{s}_\bullet}\mathbf{curl}\left(e^{\mathrm{i}\,\mathbf{k}_\bullet\cdot\boldsymbol{x}}\right)\,.$$

Using $\mathbf{curl}$ in polar coordinates $\mathbf{curl}\, f \;=\; \dfrac{1}{r}\,\partial_\theta f\,\mathbf{e}_r \;-\; \partial_r f\,\mathbf{e}_\theta$, we obtain

$$\boldsymbol{E}_\bullet^{\rm pw} \;=\; -\,\frac{E_\bullet}{\omega\,\mathsf{s}_\bullet\, r}\sum_{k=-\infty}^{\infty}\mathrm{i}^{k}\,k\,\mathrm{J}_k(\omega\,\mathsf{s}_\bullet\, r)\; e^{\mathrm{i}\,k(\theta-\alpha_{\rm inc})}\;\mathbf{e}_r \;+\; \frac{E_\bullet}{\omega\,\mathsf{s}_\bullet}\sum_{k=-\infty}^{\infty}\mathrm{i}^{k-1}\,\omega\,\mathsf{s}_\bullet\,\mathrm{J}_k'(\omega\,\mathsf{s}_\bullet\, r)\; e^{\mathrm{i}\,k(\theta-\alpha_{\rm inc})}\;\mathbf{e}_\theta\,.$$

For $\mathrm{H}_\bullet^{\rm pw}$, we have:

$$\mathrm{H}_\bullet^{\rm pw} \;=\; -\,\frac{\mathfrak{s}}{\mu_0}\,\mathsf{s}_\bullet\,\mathcal{E}_\bullet\, e^{\mathrm{i}\,\mathbf{k}\cdot\boldsymbol{x}} \;=\; -\,\frac{\mathfrak{s}}{\mu_0}\,\mathsf{s}_\bullet\,\mathcal{E}_\bullet\sum_{k=-\infty}^{\infty}\mathrm{i}^{k}\,\mathrm{J}_k(\omega\,\mathsf{s}_\bullet\, r)\; e^{\mathrm{i}\,k(\theta-\alpha_{\rm inc})}\,.$$

Finally,

$$\boldsymbol{J}_\bullet^{\rm pw} \;=\; \left(\sigma\;\mathcal{E}_\bullet+\mathbf{L}\,\omega^2\,\rho_f\right)\, e^{\mathrm{i}\,\mathbf{k}_\bullet\cdot\boldsymbol{x}}\;\widehat{\mathbf{d}} \;=\; \frac{\left(\sigma\;\mathcal{E}_\bullet+\mathbf{L}\,\omega^2\,\rho_f\right)\,\mathrm{i}}{\omega\,\mathsf{s}_\bullet}\mathrm{curl}\left(e^{\mathrm{i}\,\mathbf{k}_\bullet\cdot\boldsymbol{x}}\right)\,.$$

With the expression of **curl** in polar coordinates, we obtain:

$$\boldsymbol{J}_\bullet^{\rm pw} = -\frac{\left(\sigma\,\mathcal{E}_\bullet + \mathbf{L}\,\omega^2\,\rho_f\right)}{\omega\,\mathsf{s}_\bullet\,r}\sum_{k=-\infty}^{\infty}\mathrm{i}^k\,k\,\mathrm{J}_k(\omega\,\mathsf{s}_\bullet\,r)\,e^{\mathrm{i}\,k(\theta-\alpha_{\rm inc})}\,\mathbf{e}_r + \frac{\left(\sigma\,\mathcal{E}_\bullet + \mathbf{L}\,\omega^2\,\rho_f\right)}{\omega\,\mathsf{s}_\bullet}\sum_{k=-\infty}^{\infty}\mathrm{i}^{k-1}\,\omega\,\mathsf{s}_\bullet\,\mathrm{J}_k'(\omega\,\mathsf{s}_\bullet\,r)\,e^{\mathrm{i}\,k(\theta-\alpha_{\rm inc})}\,\mathbf{e}_\theta\,.$$

□

5.5.3.2 Longitudinal waves

The expansions of the unknowns given in equation (5.26) for the longitudinal plane waves ($\bullet = \mathrm{P}\,,\,\mathrm{B}$) are:

$$\mathbf{u}_\bullet^{\rm pw} = \frac{\mathfrak{s}}{\mathsf{s}_\bullet}\sum_{k=-\infty}^{\infty}\mathrm{i}^k\,\omega\,\mathsf{s}_\bullet\,\mathrm{J}_k'(\omega\,\mathsf{s}_\bullet\,r)\,e^{\mathrm{i}\,k(\theta-\alpha_{\rm inc})}\,\mathbf{e}_r + \frac{\mathfrak{s}}{\mathsf{s}_\bullet\,r}\sum_{k=-\infty}^{\infty}\mathrm{i}^{k+1}\,k\,\mathrm{J}_k(\omega\,\mathsf{s}_\bullet\,r)\,e^{\mathrm{i}\,k(\theta-\alpha_{\rm inc})}\,\mathbf{e}_\theta\,,$$

$$\mathbf{w}_\bullet^{\rm pw} = \mathfrak{s}\,\frac{\mathcal{W}_\bullet}{\mathsf{s}_\bullet}\sum_{k=-\infty}^{\infty}\mathrm{i}^k\,\omega\,\mathsf{s}_\bullet\,\mathrm{J}_k'(\omega\,\mathsf{s}_\bullet\,r)\,e^{\mathrm{i}\,k(\theta-\alpha_{\rm inc})}\,\mathbf{e}_r + \mathfrak{s}\,\frac{\mathcal{W}_\bullet}{\mathsf{s}_\bullet\,r}\sum_{k=-\infty}^{\infty}\mathrm{i}^{k+1}\,k\,\mathrm{J}_k(\omega\,\mathsf{s}_\bullet\,r)\,e^{\mathrm{i}\,k(\theta-\alpha_{\rm inc})}\,\mathbf{e}_\theta\,,$$

For the components $\boldsymbol{\tau}_{rr}$ and $\boldsymbol{\tau}_{r\theta}$:

$$\begin{aligned}\boldsymbol{\tau}_{\bullet,rr}^{\rm pw} &= \frac{2\,\mu_{\rm fr}}{\mathrm{i}\,\omega\,\mathsf{s}_\bullet}\,\partial_{rr}e^{\mathrm{i}\mathbf{k}_\bullet\cdot\boldsymbol{x}} + \left(-\tfrac{2}{3}\mu_{\rm fr} + \mathrm{k}_{\rm fr} + M\,\alpha^2 + \mathcal{W}_\bullet\,\alpha\,M\right)\mathrm{i}\,\omega\,\mathsf{s}_\bullet\,e^{\mathrm{i}\mathbf{k}_\bullet\cdot\boldsymbol{x}}\\ &= 2\,\mu_{\rm fr}\sum_{k=-\infty}^{\infty}\mathrm{i}^{k-1}\,\mathrm{J}_{k+1}(\omega\,\mathsf{s}_\bullet\,r)\,e^{\mathrm{i}\,k(\theta-\alpha_{\rm inc})} - \frac{2\,\mu_{\rm fr}}{\omega\,\mathsf{s}_\bullet}\sum_{k=-\infty}^{\infty}\mathrm{i}^{k-1}\,\mathrm{J}_k(\omega\,\mathsf{s}_\bullet\,r)\,e^{\mathrm{i}\,k(\theta-\alpha_{\rm inc})}\\ &\quad - 2\,\mu_{\rm fr}\sum_{k=-\infty}^{\infty}\mathrm{i}^{k-1}\omega\,\mathsf{s}_\bullet\,\mathrm{J}_k(\omega\,\mathsf{s}_\bullet\,r)\,e^{\mathrm{i}\,k(\theta-\alpha_{\rm inc})} + \frac{2\,\mu_{\rm fr}}{\omega\,\mathsf{s}_\bullet}\sum_{k=-\infty}^{\infty}\mathrm{i}^{k-1}k^2\,\mathrm{J}_k(\omega\,\mathsf{s}_\bullet\,r)\,e^{\mathrm{i}\,k(\theta-\alpha_{\rm inc})}\\ &\quad + \left(-\tfrac{2}{3}\mu_{\rm fr} + \mathrm{k}_{\rm fr} + M\,\alpha^2 + \mathcal{W}_\bullet\,\alpha\,M\right)\mathrm{i}\,\omega\,\mathsf{s}_\bullet\sum_{k=-\infty}^{\infty}\mathrm{i}^k\,\mathrm{J}_k(\omega\,\mathsf{s}_\bullet\,r)\,e^{\mathrm{i}\,k(\theta-\alpha_{\rm inc})}\,,\end{aligned}$$

$$\begin{aligned}\boldsymbol{\tau}_{\bullet,r\theta}^{\rm pw} &= \frac{2\,\mu_{\rm fr}}{\mathrm{i}\,\omega\,\mathsf{s}_\bullet}\left(\frac{\partial_\theta r}{r}e^{\mathrm{i}\mathbf{k}_\bullet\cdot\boldsymbol{x}} - \frac{\partial_\theta}{r^2}e^{\mathrm{i}\mathbf{k}_\bullet\cdot\boldsymbol{x}}\right)\\ &= \sum_{k=-\infty}^{\infty}\frac{2\,\mu_{\rm fr}\,\mathrm{i}^k\,k}{r}\,\mathrm{J}_k'(\omega\,\mathsf{s}_\bullet\,r)\,e^{\mathrm{i}\,k(\theta-\alpha_{\rm inc})} - \sum_{k=-\infty}^{\infty}\frac{2\,\mu_{\rm fr}\mathrm{i}^k\,k}{\omega\,\mathsf{s}_\bullet\,r^2}\,\mathrm{J}_k(\omega\,\mathsf{s}_\bullet\,r)\,e^{\mathrm{i}\,k(\theta-\alpha_{\rm inc})}\,.\end{aligned}$$

$$\mathrm{p}_\bullet^{\rm pw} = \mathrm{i}\,\omega\,\mathsf{s}_\bullet\,(-M\,\mathcal{W}_\bullet - M\,\alpha)\sum_{k=-\infty}^{\infty}\mathrm{i}^k\,\mathrm{J}_k(\omega\,\mathsf{s}_\bullet\,r)\,e^{\mathrm{i}\,k(\theta-\alpha_{\rm inc})}\,.$$

$$\boldsymbol{E}_\bullet^{\rm pw} = \frac{\mathcal{E}_\bullet}{\omega\,\mathsf{s}_\bullet}\sum_{k=-\infty}^{\infty}\mathrm{i}^{k-1}\,\omega\,\mathsf{s}_\bullet\,\mathrm{J}_k'(\omega\,\mathsf{s}_\bullet\,r)\,e^{\mathrm{i}\,k(\theta-\alpha_{\rm inc})}\,\mathbf{e}_r + \frac{\mathcal{E}_\bullet}{\omega\,\mathsf{s}_\bullet\,r}\sum_{k=-\infty}^{\infty}\mathrm{i}^k\,k\,\mathrm{J}_k(\omega\,\mathsf{s}_\bullet\,r)\,e^{\mathrm{i}\,k(\theta-\alpha_{\rm inc})}\,\mathbf{e}_\theta\,,$$

$$\mathrm{H}_\bullet^{\rm pw} = 0\,,$$

and

$$\boldsymbol{J}_\bullet^{\rm pw} = \left(\sigma\,\mathcal{E}_\bullet + \mathbf{L}\,\omega^2\,\rho_f - \mathbf{L}\,\omega^2\,\mathsf{s}_\bullet^2(\omega)\,M\,(\mathcal{W}_\bullet + \alpha)\right)\sum_{k=-\infty}^{\infty}\mathrm{i}^{k-1}\,\mathrm{J}_k'(\omega\,\mathsf{s}_\bullet\,r)\,e^{\mathrm{i}\,k(\theta-\alpha_{\rm inc})}\,\mathbf{e}_r + \frac{\left(\sigma\,\mathcal{E}_\bullet + \mathbf{L}\,\omega^2\,\rho_f - \mathbf{L}\,\omega^2\,\mathsf{s}_\bullet^2(\omega)\,M\,(\mathcal{W}_\bullet + \alpha)\right)}{\omega\,\mathsf{s}_\bullet\,r}\sum_{k=-\infty}^{\infty}\mathrm{i}^k\,k\,\mathrm{J}_k(\omega\,\mathsf{s}_\bullet\,r)\,e^{\mathrm{i}\,k(\theta-\alpha_{\rm inc})}\,\mathbf{e}_\theta\,.$$

Proof. For $\mathbf{u}^{\rm pw}$, $\mathbf{w}^{\rm pw}$, $\boldsymbol{\tau}^{\rm pw}$, $\mathrm{p}^{\rm pw}$, the expansion is detailed in 1.5.2, page 37. We have for $\boldsymbol{E}_\bullet^{\rm pw}$:

$$\boldsymbol{E}_\bullet^{\rm pw} = \mathcal{E}_\bullet\,e^{\mathrm{i}\,\mathbf{k}\cdot\boldsymbol{x}}\,\widehat{\mathbf{d}} = -\frac{\mathcal{E}_\bullet\,\mathrm{i}}{\omega\,\mathsf{s}_\bullet}\nabla\left(e^{\mathrm{i}\,\mathbf{k}\cdot\boldsymbol{x}}\right).$$

We use ∇ in polar coordinates $\nabla f = \partial_r f\, \mathbf{e}_r + \frac{1}{r}\partial_\theta f\, \mathbf{e}_\theta$,to obtain

$$\boldsymbol{E}_\bullet^{\mathrm{pw}} = -\frac{\mathcal{E}_\bullet\, \mathrm{i}}{\omega\, \mathsf{s}_\bullet} \sum_{k=-\infty}^{\infty} \mathrm{i}^k\, \omega\, \mathsf{s}_\bullet\, \mathrm{J}_k'(\omega\, \mathsf{s}_\bullet\, r)\; e^{\mathrm{i}\, k(\theta-\alpha_{\mathrm{inc}})}\; \mathbf{e}_r \;-\; \frac{\mathcal{E}_\bullet\, \mathrm{i}}{\omega\, \mathsf{s}_\bullet\, r} \sum_{k=-\infty}^{\infty} \mathrm{i}^{k+1}\, k\, \mathrm{J}_k(\omega\, \mathsf{s}_\bullet\, r)\; e^{\mathrm{i}\, k(\theta-\alpha_{\mathrm{inc}})}\; \mathbf{e}_\theta\,,$$

which leads to

$$\boldsymbol{E}_\bullet^{\mathrm{pw}} = \frac{\mathcal{E}_\bullet}{\omega\, \mathsf{s}_\bullet} \sum_{k=-\infty}^{\infty} \mathrm{i}^{k-1}\, \omega\, \mathsf{s}_\bullet\, \mathrm{J}_k'(\omega\, \mathsf{s}_\bullet\, r)\; e^{\mathrm{i}\, k(\theta-\alpha_{\mathrm{inc}})}\; \mathbf{e}_r \;+\; \frac{\mathcal{E}_\bullet}{\omega\, \mathsf{s}_\bullet\, r} \sum_{k=-\infty}^{\infty} \mathrm{i}^{k}\, k\, \mathrm{J}_k(\omega\, \mathsf{s}_\bullet\, r)\; e^{\mathrm{i}\, k(\theta-\alpha_{\mathrm{inc}})}\; \mathbf{e}_\theta\,,$$

For $\boldsymbol{J}$, we have:

$$\begin{aligned}\boldsymbol{J}_\bullet^{\mathrm{pw}} &= \left(\sigma\, \mathcal{E}_\bullet + \mathbf{L}\, \omega^2\, \rho_f - \mathbf{L}\, \omega^2\, \mathsf{s}_\bullet^2(\omega)\, M\, (\mathcal{W}_\bullet + \alpha)\right) e^{\mathrm{i}\, \mathbf{k}\cdot\boldsymbol{x}}\, \widehat{\mathbf{d}} \\ &= -\left(\sigma\, \mathcal{E}_\bullet + \mathbf{L}\, \omega^2\, \rho_f - \mathbf{L}\, \omega^2\, \mathsf{s}_\bullet^2(\omega)\, M\, (\mathcal{W}_\bullet + \alpha)\right) \frac{\mathrm{i}}{\omega\, \mathsf{s}_\bullet} \nabla\left(e^{\mathrm{i}\, \mathbf{k}\cdot\boldsymbol{x}}\right).\end{aligned}$$

Using the expression of ∇, we finally obtain:

$$\begin{aligned}\boldsymbol{J}_\bullet^{\mathrm{pw}} &= \left(\sigma\, \mathcal{E}_\bullet + \mathbf{L}\, \omega^2\, \rho_f - \mathbf{L}\, \omega^2\, \mathsf{s}_\bullet^2(\omega)\, M\, (\mathcal{W}_\bullet + \alpha)\right) \sum_{k=-\infty}^{\infty} \mathrm{i}^{k-1}\, \mathrm{J}_k'(\omega\, \mathsf{s}_\bullet\, r)\; e^{\mathrm{i}\, k(\theta-\alpha_{\mathrm{inc}})}\; \mathbf{e}_r \\ &+ \frac{\left(\sigma\, \mathcal{E}_\bullet + \mathbf{L}\, \omega^2\, \rho_f - \mathbf{L}\, \omega^2\, \mathsf{s}_\bullet^2(\omega)\, M\, (\mathcal{W}_\bullet + \alpha)\right)}{\omega\, \mathsf{s}_\bullet\, r} \sum_{k=-\infty}^{\infty} \mathrm{i}^{k}\, k\, \mathrm{J}_k(\omega\, \mathsf{s}_\bullet\, r)\; e^{\mathrm{i}\, k(\theta-\alpha_{\mathrm{inc}})}\; \mathbf{e}_\theta\,.\end{aligned}$$

□

Conclusion

In this chapter, we have presented the electrokinetic effects and the conversions appearing in Pride's model. We have introduced the physical parameters used to describe a conducting poroelastic material, then we have presented the expression of Pride's equations in harmonic domain both in first and second-order formulation. We have also proposed boundary conditions for bounded domains and transmission problems. In such materials, we distinguish four kinds of plane waves; a fast longitudinal plane wave, called P-wave, a slow longitudinal plane wave, the B-wave, a shear plane wave, the S-wave and the electromagnetic wave, the EM-wave. We have determined the form of those plane waves and the values of the associated slownesses. For each kind of plane waves, the solid velocity $\mathbf{u}$, the relative fluid velocity $\mathbf{w}$, and the electric field are colinear. In addition, for the longitudinal P- and B-waves, the magnetic field $\boldsymbol{H}$ is zero. For the transverse S- and EM-waves, the fluid pressure p is zero. All the introduced notions will be used in the following chapters.

Chapter 6

Analytical solutions for Pride's equations in two dimensions: construction and analysis

In this chapter, we develop analytical solutions of Pride's equations in two dimensions, presented in Chapter 5. Analytical solutions are of great interest since they allow us to verify the accuracy of the numerical method developed for computing numerical solutions. They are developed for different configurations; an homogeneous bounded domain, the scattering of a plane wave by impenetrable or penetrable obstacles, and the response to a point-source. Following what was formerly done for poroelasticity in Chapter 2, we express the unknowns in terms of potentials.

Concerning the electrokinetic equations, analytical solutions have been developed for point source using the Green functions in homogeneous domain [59, 110, 70, 123] or layered spaces [71, 75]. Analytical solutions in layered materials using the transmission conditions at interfaces have also been developed in many works, *e.g.*, [62, 63, 64, 132]. In [95], analytical solutions have been constructed to consider the response of the vadose zone to a shear source. The decomposition of the waves in potentials has been used in [60], where the authors present the analytical solution for the complete electrokinetic equations and quasi-static EM approximation. This decomposition is also used in [137] for a problem of interaction of fluid and porous medium in the case of a borehole to the complete Pride's equations. Finally, in [116] the authors develop an analytical solution for the fluid/porous interactions in the case of an incident P-wave.

In the chapter, we first express Pride's equations in potentials solving Helmholtz equations, see Section 6.1. The potentials are expressed as series of Bessel functions. Using this, we build analytical solutions for the following configurations: a bounded domain in Section 6.2, the scattering of a plane wave by an impenetrable obstacle in Section 6.3, and by a penetrable obstacle in Section 6.4. For those settings, we investigate numerically the existence of what we denote as corresponding Jones' modes by studying the invertiblity of the analytical system. Finally, we also consider the response of a point-source in an infinite domain in Section 6.5.

6.1 Potential theory

In this section, starting with the second-order formulation of Pride's equations, we find a decomposition of the unknowns as functions of four scalar unknowns called potentials, that satisfy the Helmholtz equation.

6.1.1 Derivation

Recall that we have expressed in Section 5.5 the coefficients $\mathcal{W}_\bullet$ and $\mathcal{E}_\bullet$ for $\bullet =$ P, B, S, EM in equations (5.15) and (5.16). We have also defined the following matrices, using $\mathfrak{s} = \pm 1$:

$$A = \begin{pmatrix} \rho_a & \rho_f & 0 \\ \rho_f & \rho_{\text{dyn}} & \dfrac{\eta}{\omega^2 k}\mathbf{L} \\ 0 & \mathfrak{s}\,\mathrm{i}\omega\mu_0\mathbf{L}\rho_{\text{dyn}} & \tilde{\boldsymbol{\varepsilon}}\mu_0 \end{pmatrix}, \quad B = \begin{pmatrix} H & \alpha M & 0 \\ \alpha M & M & 0 \\ 0 & 0 & 0 \end{pmatrix}, \quad D = \begin{pmatrix} \mu_{\text{fr}} & 0 & 0 \\ 0 & 0 & 0 \\ 0 & 0 & 1 \end{pmatrix}, \tag{6.1}$$

$$P_{\text{trans}} = \begin{pmatrix} \mathcal{U}_{\text{S}} & 0 & \mathcal{U}_{\text{EM}} \\ \mathcal{W}_{\text{S}} & 1 & \mathcal{W}_{\text{EM}} \\ \mathcal{E}_{\text{S}} & 0 & \mathcal{E}_{\text{EM}} \end{pmatrix}, \quad \text{and } P_{\text{long}} = \begin{pmatrix} \mathcal{U}_{\text{P}} & \mathcal{U}_{\text{B}} & 0 \\ \mathcal{W}_{\text{P}} & \mathcal{W}_{\text{B}} & 0 \\ \mathcal{E}_{\text{P}} & \mathcal{E}_{\text{B}} & 1 \end{pmatrix}. \tag{6.2}$$

Proposition 6.1. We consider an infinite medium with perfect outgoing conditions and regular sources. The fields (u, w, $\boldsymbol{E}$) solution of equations

$$-\omega^2\rho_a \mathrm{u} - \rho_f\omega^2 \mathrm{w} - H\,\nabla\nabla\cdot \mathrm{u} + \mu_{\text{fr}}\,\mathbf{curl}\,\mathrm{curl}\,\mathrm{u} - \alpha\, M\,\nabla\nabla\cdot \mathrm{w} = \mathbf{F_1}\,, \tag{6.3a}$$

$$-\omega^2\rho_f \mathrm{u} - \omega^2\,\rho_{\text{dyn}}\,\mathrm{w} - \frac{\eta}{k}\,\mathbf{L}\,\boldsymbol{E} - M\,\nabla\nabla\cdot \mathrm{w} - M\alpha\nabla\nabla\cdot \mathrm{u} = \mathbf{F_2}\,, \tag{6.3b}$$

$$-\omega^2\,\tilde{\boldsymbol{\varepsilon}}\,\mu_0\,\boldsymbol{E} - \mathfrak{s}\,\mathrm{i}\,\omega\,\mu_0\,\mathbf{L}\,\omega^2\,\rho_{\text{dyn}}\,\mathrm{w} + \mathbf{curl}\,\mathrm{curl}\,\boldsymbol{E} = \mathbf{F_3}\,, \tag{6.3c}$$

have the form

$$\begin{aligned} -\omega^2\,\mathrm{u} &= \frac{1}{\mathsf{s}_{\text{P}}^2}\,\nabla\chi_{\text{P}} + \frac{1}{\mathsf{s}_{\text{B}}^2}\,\nabla\chi_{\text{B}} - \frac{1}{\mathsf{s}_{\text{S}}^2}\,\mathbf{curl}\chi_{\text{S}} - \frac{1}{\mathsf{s}_{\text{EM}}^2}\,\mathbf{curl}\chi_{\text{EM}} + \tilde{\mathbf{F}}_{\mathbf{1}}\,, \\ -\omega^2\,\mathrm{w} &= \frac{\mathcal{W}_{\text{P}}}{\mathsf{s}_{\text{P}}^2}\,\nabla\chi_{\text{P}} + \frac{\mathcal{W}_{\text{B}}}{\mathsf{s}_{\text{B}}^2}\,\nabla\chi_{\text{B}} - \frac{\mathcal{W}_{\text{S}}}{\mathsf{s}_{\text{S}}^2}\,\mathbf{curl}\chi_{\text{S}} - \frac{\mathcal{W}_{\text{EM}}}{\mathsf{s}_{\text{EM}}^2}\,\mathbf{curl}\chi_{\text{EM}} + \tilde{\mathbf{F}}_{\mathbf{2}}\,, \\ -\omega^2\,\boldsymbol{E} &= \frac{\mathcal{E}_{\text{P}}}{\mathsf{s}_{\text{P}}^2}\,\nabla\chi_{\text{P}} + \frac{\mathcal{E}_{\text{B}}}{\mathsf{s}_{\text{B}}^2}\,\nabla\chi_{\text{B}} - \frac{\mathcal{E}_{\text{S}}}{\mathsf{s}_{\text{S}}^2}\,\mathsf{s}_{\text{S}}^{-2}\,\mathbf{curl}\chi_{\text{S}} - \frac{\mathcal{E}_{\text{EM}}}{\mathsf{s}_{\text{EM}}^2}\,\mathbf{curl}\chi_{\text{EM}} + \tilde{\mathbf{F}}_{\mathbf{3}}\,, \end{aligned} \tag{6.4}$$

where we have denoted $\tilde{\mathbf{F}}_{\mathbf{i}} = \pi_i\left(A^{-1}\begin{pmatrix}\mathbf{F_1}\\ \mathbf{F_2}\\ \mathbf{F_3}\end{pmatrix}\right)$, π_i is the projection onto the i-th component of a vector. The potentials $\chi_\bullet$ with $\bullet =$ P, B, S, EM are outgoing and satisfy the Helmholtz equations:

$$\begin{aligned} -\omega^2\,\mathsf{s}_{\text{P}}^2\,\chi_{\text{P}} - \Delta\,\chi_{\text{P}} &= \mathsf{s}_{\text{P}}^2\,\pi_1\left(P_{\text{long}}^{-1}\,A^{-1}\begin{pmatrix}\nabla\cdot\mathbf{F_1}\\ \nabla\cdot\mathbf{F_2}\\ \nabla\cdot\mathbf{F_3}\end{pmatrix}\right), \\ -\omega^2\,\mathsf{s}_{\text{B}}^2\,\chi_{\text{B}} - \Delta\,\chi_{\text{B}} &= \mathsf{s}_{\text{B}}^2\,\pi_2\left(P_{\text{long}}^{-1}\,A^{-1}\begin{pmatrix}\nabla\cdot\mathbf{F_1}\\ \nabla\cdot\mathbf{F_2}\\ \nabla\cdot\mathbf{F_3}\end{pmatrix}\right), \\ -\omega^2\,\mathsf{s}_{\text{S}}^2\,\chi_{\text{S}} - \Delta\,\chi_{\text{S}} &= \mathsf{s}_{\text{S}}^2\,\pi_1\left(P_{\text{trans}}^{-1}\,A^{-1}\begin{pmatrix}\mathrm{curl}\,\mathbf{F_1}\\ \mathrm{curl}\,\mathbf{F_2}\\ \mathrm{curl}\,\mathbf{F_3}\end{pmatrix}\right), \\ -\omega^2\,\mathsf{s}_{\text{EM}}^2\,\chi_{\text{EM}} - \Delta\,\chi_{\text{EM}} &= \mathsf{s}_{\text{EM}}^2\,\pi_3\left(P_{\text{trans}}^{-1}\,A^{-1}\begin{pmatrix}\mathrm{curl}\,\mathbf{F_1}\\ \mathrm{curl}\,\mathbf{F_2}\\ \mathrm{curl}\,\mathbf{F_3}\end{pmatrix}\right). \end{aligned} \tag{6.5}$$

Proof. We work with the following unknowns:

$$\begin{aligned} \varphi &:= \nabla\cdot\mathrm{u}\quad, \quad \tilde{\varphi} := \nabla\cdot\mathrm{w}\,, \qquad \overline{\varphi} := \nabla\cdot\boldsymbol{E}\,, \\ \psi &:= \mathrm{curl}\,\mathrm{u}\quad, \quad \tilde{\psi} := \mathrm{curl}\,\mathrm{w}\,, \qquad \overline{\psi} := \mathrm{curl}\,\boldsymbol{E}\,. \end{aligned} \tag{6.6}$$

Step1 We first build a system of equations in terms of the unknowns defined in equation (6.6). We take the divergence $\nabla\cdot$ of equations (6.3a), and use the fact that $\nabla\cdot\mathbf{curl} = 0$, and $\nabla\cdot\nabla = \Delta$, to obtain

$$\begin{aligned} \nabla\cdot\left(-\omega^2\rho_a\mathrm{u} - \rho_f\omega^2\mathrm{w} - H\nabla\nabla\cdot\mathrm{u} + \mu_{\text{fr}}\,\mathbf{curl}\,\mathrm{curl}\,\mathrm{u} - \alpha M\nabla\nabla\cdot\mathrm{w}\right) &= \nabla\cdot\mathbf{F_1}\,, \\ \Rightarrow \quad -\omega^2\rho_a\varphi - \rho_f\omega^2\tilde{\varphi} - H\Delta\varphi - \alpha M\Delta\tilde{\varphi} &= \nabla\cdot\mathbf{F_1}\,. \end{aligned}$$

The divergence of equation (6.3b) leads to

$$\begin{aligned} \nabla\cdot\left(-\omega^2\rho_f\mathrm{u} - \omega^2\,\rho_{\text{dyn}}(\omega)\,\mathrm{w} - \frac{\eta}{k}\,\mathbf{L}\,\boldsymbol{E} - M\,\nabla\nabla\cdot\mathrm{w} - M\alpha\nabla\nabla\cdot\mathrm{u}\right) &= \nabla\mathbf{F_3}\,, \\ \Rightarrow \quad -\omega^2\rho_f\varphi - \omega^2\,\rho_{\text{dyn}}\,\tilde{\varphi} - \frac{\eta}{k}\,\mathbf{L}\,\overline{\varphi} - M\,\Delta\tilde{\varphi} - M\alpha\Delta\varphi &= \nabla\cdot\mathbf{F_3}\,. \end{aligned}$$

Finally, applying the divergence to equation (6.3c) gives

$$\nabla\cdot(\mathbf{curl}\,\mathrm{curl}\,\boldsymbol{E} - \omega^2\,\tilde{\boldsymbol{\varepsilon}}\,\mu_0\,\boldsymbol{E} - \mathfrak{s}\,\mathrm{i}\,\omega\,\mu_0\,\mathbf{L}\,\omega^2\,\rho_{\mathrm{dyn}}\,\mathrm{w}) = \nabla\cdot\mathbf{F_3}\,,$$

$$\Rightarrow\quad -\omega^2\,\tilde{\boldsymbol{\varepsilon}}\,\mu_0\,\overline{\varphi} - \mathfrak{s}\,\mathrm{i}\,\omega\,\mu_0\,\mathbf{L}\,\omega^2\,\rho_{\mathrm{dyn}}\,\tilde{\varphi} = \nabla\cdot\mathbf{F_3}\,.$$

The three next equations are obtained by taking curl of equations (6.3). Using $\mathrm{curl}\,\mathbf{curl} = -\Delta$ and $\mathrm{curl}\,\nabla = 0$, we have

$$\mathrm{curl}\,\big(-\omega^2\rho_a\mathrm{u} - \rho_f\omega^2\mathrm{w} - H\nabla\nabla\cdot\mathrm{u} + \mu_{\mathrm{fr}}\,\mathbf{curl}\,\mathrm{curl}\,\mathrm{u} - \alpha\,M\,\nabla\nabla\cdot\mathrm{w}\big) = \mathrm{curl}\,\mathbf{f}\,,$$

$$\Rightarrow\quad -\omega^2\,\rho_a\,\psi - \rho_f\,\omega^2\,\tilde{\psi} - \mu_{\mathrm{fr}}\,\Delta\psi = \mathrm{curl}\,\mathbf{f}\,,$$

while the second equation (6.3b) gives

$$\mathrm{curl}\,\big(-\omega^2\rho_f\mathrm{u} - \omega^2\,\rho_{\mathrm{dyn}}\,\mathrm{w} - \frac{\eta}{k}\,\mathbf{L}\,\boldsymbol{E} - M\,\nabla\nabla\cdot\mathrm{w} - M\alpha\nabla\nabla\cdot\mathrm{u}\big) = \mathrm{curl}\,\tilde{\mathbf{f}}\,,$$

$$\Rightarrow\quad -\omega^2\,\rho_f\,\psi - \omega^2\,\rho_{\mathrm{dyn}}\,\tilde{\psi} - \frac{\eta}{k}\,\mathbf{L}\,\overline{\psi} = \mathrm{curl}\,\tilde{\mathbf{f}}\,,$$

and the third equation (6.3c) becomes

$$\mathrm{curl}\,\big(\mathbf{curl}\,\mathrm{curl}\,\boldsymbol{E} - \omega^2\,\tilde{\boldsymbol{\varepsilon}}\,\mu_0\,\boldsymbol{E} - \mathfrak{s}\,\mathrm{i}\,\omega\,\mu_0\,\mathbf{L}\,\omega^2\,\rho_{\mathrm{dyn}}\,\mathrm{w}\big) = \mathrm{curl}\,\mathbf{F_3}\,,$$

$$\Rightarrow\quad -\Delta\overline{\psi} - \omega^2\,\tilde{\boldsymbol{\varepsilon}}\,\mu_0\,\overline{\psi} - \mathfrak{s}\,\mathrm{i}\,\omega\,\mu_0\,\mathbf{L}\,\omega^2\,\rho_{\mathrm{dyn}}\,\tilde{\psi} = \mathrm{curl}\,\mathbf{F_3}\,.$$

We rewrite these six equations in matrix form to obtain

$$-\omega^2\,A\begin{pmatrix}\varphi\\ \tilde{\varphi}\\ \overline{\varphi}\end{pmatrix} - B\Delta\begin{pmatrix}\varphi\\ \tilde{\varphi}\\ \overline{\varphi}\end{pmatrix} = \begin{pmatrix}\nabla\cdot\mathbf{F_1}\\ \nabla\cdot\mathbf{F_2}\\ \nabla\cdot\mathbf{F_3}\end{pmatrix}, \tag{6.7a}$$

$$\text{and}\quad -\omega^2\,A\begin{pmatrix}\psi\\ \tilde{\psi}\\ \overline{\psi}\end{pmatrix} - D\Delta\begin{pmatrix}\psi\\ \tilde{\psi}\\ \overline{\psi}\end{pmatrix} = \begin{pmatrix}\mathrm{curl}\,\mathbf{F_1}\\ \mathrm{curl}\,\mathbf{F_2}\\ \mathrm{curl}\,\mathbf{F_3}\end{pmatrix}, \tag{6.7b}$$

with the matrices defined in Section 5.5 and recalled in equation (6.1). We have also used the following notation for the Laplacian: $\Delta\begin{pmatrix}\psi\\ \tilde{\psi}\\ \overline{\psi}\end{pmatrix} := \begin{pmatrix}\Delta\psi\\ \Delta\tilde{\psi}\\ \Delta\overline{\psi}\end{pmatrix}$.

Step 2a: Transverse waves Supposing that A can be inverted, we multiply equation (6.7b) by A^{-1}, to obtain:

$$-\omega^2\begin{pmatrix}\psi\\ \tilde{\psi}\\ \overline{\psi}\end{pmatrix} - A^{-1}\,D\Delta\begin{pmatrix}\psi\\ \tilde{\psi}\\ \overline{\psi}\end{pmatrix} = A^{-1}\begin{pmatrix}\mathrm{curl}\,\mathbf{F_1}\\ \mathrm{curl}\,\mathbf{F_2}\\ \mathrm{curl}\,\mathbf{F_3}\end{pmatrix}. \tag{6.8}$$

We have seen in Section 5.5 that $A^{-1}D$ can be diagonalized, and expressed as (see eq. (5.22)):

$$A^{-1}D = P_{\mathrm{trans}}\begin{pmatrix}\mathsf{c}_{\mathsf{S}}^2 & 0 & 0\\ 0 & 0 & 0\\ 0 & 0 & \mathsf{c}_{\mathsf{EM}}^2\end{pmatrix}P_{\mathrm{trans}}^{-1}\,,\qquad P_{\mathrm{trans}} = \begin{pmatrix}\mathcal{U}_{\mathrm{S}} & 0 & \mathcal{U}_{\mathrm{EM}}\\ \mathcal{W}_{\mathrm{S}} & 1 & \mathcal{W}_{\mathrm{EM}}\\ \mathcal{E}_{\mathrm{S}} & 0 & \mathcal{E}_{\mathrm{EM}}\end{pmatrix}.$$

Equation (6.8) can hence be written as:

$$-\omega^2\begin{pmatrix}\psi\\ \tilde{\psi}\\ \overline{\psi}\end{pmatrix} - P_{\mathrm{trans}}\begin{pmatrix}\mathsf{c}_{\mathsf{S}}^2 & 0 & 0\\ 0 & 0 & 0\\ 0 & 0 & \mathsf{c}_{\mathsf{EM}}^2\end{pmatrix}P_{\mathrm{trans}}^{-1}\Delta\begin{pmatrix}\psi\\ \tilde{\psi}\\ \overline{\psi}\end{pmatrix} = A^{-1}\begin{pmatrix}\mathrm{curl}\,\mathbf{F_1}\\ \mathrm{curl}\,\mathbf{F_2}\\ \mathrm{curl}\,\mathbf{F_3}\end{pmatrix},$$

Multiplying by P_{trans}^{-1}, we have

$$-\omega^2\,P_{\mathrm{trans}}^{-1}\begin{pmatrix}\psi\\ \tilde{\psi}\\ \overline{\psi}\end{pmatrix} - \begin{pmatrix}\mathsf{c}_{\mathsf{S}}^2 & 0 & 0\\ 0 & 0 & 0\\ 0 & 0 & \mathsf{c}_{\mathsf{EM}}^2\end{pmatrix}P_{\mathrm{trans}}^{-1}\Delta\begin{pmatrix}\psi\\ \tilde{\psi}\\ \overline{\psi}\end{pmatrix} = P_{\mathrm{trans}}^{-1}\,A^{-1}\begin{pmatrix}\mathrm{curl}\,\mathbf{F_1}\\ \mathrm{curl}\,\mathbf{F_2}\\ \mathrm{curl}\,\mathbf{F_3}\end{pmatrix},$$

which leads to

$$-\omega^2 P_{\text{trans}}^{-1} \begin{pmatrix} \psi \\ \tilde{\psi} \\ \overline{\psi} \end{pmatrix} - \begin{pmatrix} \mathsf{c}_{\mathsf{S}}^2 & 0 & 0 \\ 0 & 0 & 0 \\ 0 & 0 & \mathsf{c}_{\mathsf{EM}}^2 \end{pmatrix} \Delta \left(P_{\text{trans}}^{-1} \begin{pmatrix} \psi \\ \tilde{\psi} \\ \overline{\psi} \end{pmatrix} \right) = P_{\text{trans}}^{-1} A^{-1} \begin{pmatrix} \operatorname{curl} \mathbf{F_1} \\ \operatorname{curl} \mathbf{F_2} \\ \operatorname{curl} \mathbf{F_3} \end{pmatrix}.$$

We define the potentials

$$\begin{pmatrix} \chi_{\text{S}} \\ \chi_0 \\ \chi_{\text{EM}} \end{pmatrix} := P_{\text{trans}}^{-1} \begin{pmatrix} \psi \\ \tilde{\psi} \\ \overline{\psi} \end{pmatrix}. \tag{6.9}$$

We have then:

$$-\omega^2 \begin{pmatrix} \chi_{\text{S}} \\ \chi_0 \\ \chi_{\text{EM}} \end{pmatrix} - \begin{pmatrix} \mathsf{c}_{\mathsf{S}}^2 & 0 & 0 \\ 0 & 0 & 0 \\ 0 & 0 & \mathsf{c}_{\mathsf{EM}}^2 \end{pmatrix} \Delta \begin{pmatrix} \chi_{\text{S}} \\ \chi_0 \\ \chi_{\text{EM}} \end{pmatrix} = P_{\text{trans}}^{-1} A^{-1} \begin{pmatrix} \operatorname{curl} \mathbf{F_1} \\ \operatorname{curl} \mathbf{F_2} \\ \operatorname{curl} \mathbf{F_3} \end{pmatrix}. \tag{6.10}$$

If we take first component of the above equation, we have:

$$-\omega^2 \chi_{\text{S}} - \mathsf{c}_{\mathsf{S}}^2 \Delta \chi_{\text{S}} = \pi_1 \left(P_{\text{trans}}^{-1} A^{-1} \begin{pmatrix} \operatorname{curl} \mathbf{F_1} \\ \operatorname{curl} \mathbf{F_2} \\ \operatorname{curl} \mathbf{F_3} \end{pmatrix} \right),$$

which means that:

$$-\omega^2 \mathsf{s}_{\text{S}}^2 \chi_{\text{S}} - \Delta \chi_{\text{S}} = \mathsf{s}_{\text{S}}^2 \pi_1 \left(P_{\text{trans}}^{-1} A^{-1} \begin{pmatrix} \operatorname{curl} \mathbf{F_1} \\ \operatorname{curl} \mathbf{F_2} \\ \operatorname{curl} \mathbf{F_3} \end{pmatrix} \right).$$

The same calculation for the third component of (6.10) gives:

$$-\omega^2 \mathsf{s}_{\text{EM}}^2 \chi_{\text{EM}} - \Delta \chi_{\text{EM}} = \mathsf{s}_{\text{EM}}^2 \pi_3 \left(P_{\text{trans}}^{-1} A^{-1} \begin{pmatrix} \operatorname{curl} \mathbf{F_1} \\ \operatorname{curl} \mathbf{F_2} \\ \operatorname{curl} \mathbf{F_3} \end{pmatrix} \right).$$

Steb 2b: Longitudinal waves Multiplying equation (6.7a) by A^{-1}, we obtain:

$$-\omega^2 \begin{pmatrix} \varphi \\ \tilde{\varphi} \\ \overline{\varphi} \end{pmatrix} - A^{-1} B \Delta \begin{pmatrix} \varphi \\ \tilde{\varphi} \\ \overline{\varphi} \end{pmatrix} = A^{-1} \begin{pmatrix} \nabla \cdot \mathbf{F_1} \\ \nabla \cdot \mathbf{F_2} \\ \nabla \cdot \mathbf{F_3} \end{pmatrix}, \tag{6.11}$$

Recall that $A^{-1}B$ can be diagonalized (see eq. (5.22)), we write

$$A^{-1}B = P_{\text{long}} \begin{pmatrix} \mathsf{c}_{\mathsf{P}}^2 & 0 & 0 \\ 0 & \mathsf{c}_{\mathsf{B}}^2 & 0 \\ 0 & 0 & 0 \end{pmatrix} P_{\text{long}}^{-1}, \qquad \text{and} \qquad P_{\text{trans}} = \begin{pmatrix} \mathcal{U}_{\text{P}} & \mathcal{U}_{\text{B}} & 0 \\ \mathcal{W}_{\text{P}} & \mathcal{W}_{\text{B}} & 0 \\ \mathcal{E}_{\text{P}} & \mathcal{E}_{\text{B}} & 1 \end{pmatrix}.$$

Equation (6.11) is hence written as:

$$-\omega^2 \begin{pmatrix} \varphi \\ \tilde{\varphi} \\ \overline{\varphi} \end{pmatrix} - P_{\text{long}} \begin{pmatrix} \mathsf{c}_{\mathsf{P}}^2 & 0 & 0 \\ 0 & \mathsf{c}_{\mathsf{B}}^2 & 0 \\ 0 & 0 & 0 \end{pmatrix} P_{\text{long}}^{-1} \Delta \begin{pmatrix} \varphi \\ \tilde{\varphi} \\ \overline{\varphi} \end{pmatrix} = A^{-1} \begin{pmatrix} \nabla \cdot \mathbf{F_1} \\ \nabla \cdot \mathbf{F_2} \\ \nabla \cdot \mathbf{F_3} \end{pmatrix}.$$

Multiplying the above equation by P_{long}^{-1} gives

$$-\omega^2 P_{\text{long}}^{-1} \begin{pmatrix} \varphi \\ \tilde{\varphi} \\ \overline{\varphi} \end{pmatrix} - \begin{pmatrix} \mathsf{c}_{\mathsf{P}}^2 & 0 & 0 \\ 0 & \mathsf{c}_{\mathsf{B}}^2 & 0 \\ 0 & 0 & 0 \end{pmatrix} P_{\text{long}}^{-1} \Delta \begin{pmatrix} \varphi \\ \tilde{\varphi} \\ \overline{\varphi} \end{pmatrix} = P_{\text{long}}^{-1} A^{-1} \begin{pmatrix} \nabla \cdot \mathbf{F_1} \\ \nabla \cdot \mathbf{F_2} \\ \nabla \cdot \mathbf{F_3} \end{pmatrix}.$$

We define the potentials:

$$\begin{pmatrix} \chi_{\text{P}} \\ \chi_{\text{B}} \\ \chi_{0l} \end{pmatrix} := P_{\text{long}}^{-1} \begin{pmatrix} \varphi \\ \tilde{\varphi} \\ \overline{\varphi} \end{pmatrix}, \tag{6.12}$$

and obtain

$$-\omega^2 \begin{pmatrix} \chi_{\rm P} \\ \chi_{\rm B} \\ \chi_{0l} \end{pmatrix} - \begin{pmatrix} \mathsf{c}_{\mathsf{P}}^2 & 0 & 0 \\ 0 & \mathsf{c}_{\mathsf{B}}^2 & 0 \\ 0 & 0 & 0 \end{pmatrix} \Delta \begin{pmatrix} \chi_{\rm P} \\ \chi_{\rm B} \\ \chi_{0l} \end{pmatrix} = P_{\rm long}^{-1} A^{-1} \begin{pmatrix} \nabla \cdot \mathbf{F_1} \\ \nabla \cdot \mathbf{F_2} \\ \nabla \cdot \mathbf{F_3} \end{pmatrix} . \tag{6.13}$$

If we take first component of the above equation, we have:

$$-\omega^2 \chi_{\rm P} - \mathsf{c}_{\mathsf{P}}^2 \Delta \chi_{\rm P} = \pi_1 P_{\rm long}^{-1} A^{-1} \begin{pmatrix} \nabla \cdot \mathbf{F_1} \\ \nabla \cdot \mathbf{F_2} \\ \nabla \cdot \mathbf{F_3} \end{pmatrix} ,$$

which means that

$$-\omega^2 \mathsf{s}_{\rm P}^2 \chi_{\rm P} - \Delta \chi_{\rm P} = \mathsf{s}_{\rm P}^2 \pi_1 \left(P_{\rm long}^{-1} A^{-1} \begin{pmatrix} \nabla \cdot \mathbf{F_1} \\ \nabla \cdot \mathbf{F_2} \\ \nabla \cdot \mathbf{F_3} \end{pmatrix} \right) .$$

From the second component of equation (6.13), we obtain:

$$-\omega^2 \mathsf{s}_{\rm B}^2 \chi_{\rm P} - \chi_{\rm P} = \mathsf{s}_{\rm B}^2 \pi_2 \left(P_{\rm long}^{-1} A^{-1} \begin{pmatrix} \nabla \cdot \mathbf{F_1} \\ \nabla \cdot \mathbf{F_2} \\ \nabla \cdot \mathbf{F_3} \end{pmatrix} \right) .$$

Step 3: Expression of the unknowns u, w, $\boldsymbol{E}$ in terms of the potentials $\chi_\bullet$.
From the second-order formulation of Pride's equations (6.3), and the definition of φ and ψ, we have:

$$-\omega^2 A \begin{pmatrix} \mathrm{u} \\ \mathrm{w} \\ \boldsymbol{E} \end{pmatrix} - B \begin{pmatrix} \nabla\varphi \\ \nabla\tilde{\varphi} \\ \nabla\overline{\varphi} \end{pmatrix} + D \begin{pmatrix} \mathbf{curl}\psi \\ \mathbf{curl}\tilde{\psi} \\ \mathbf{curl}\overline{\psi} \end{pmatrix} = \begin{pmatrix} \mathbf{F_1} \\ \mathbf{F_2} \\ \mathbf{F_3} \end{pmatrix} .$$

We multiply the above equation by A^{-1},

$$-\omega^2 \begin{pmatrix} \mathrm{u} \\ \mathrm{w} \\ \boldsymbol{E} \end{pmatrix} - A^{-1} B \begin{pmatrix} \nabla\varphi \\ \nabla\tilde{\varphi} \\ \nabla\overline{\varphi} \end{pmatrix} + A^{-1} D \begin{pmatrix} \mathbf{curl}\psi \\ \mathbf{curl}\tilde{\psi} \\ \mathbf{curl}\overline{\psi} \end{pmatrix} = A^{-1} \begin{pmatrix} \mathbf{F_1} \\ \mathbf{F_2} \\ \mathbf{F_3} \end{pmatrix} ,$$

and we use the diagonalized forms of the matrices (eqs. (5.22) and (5.25)) to obtain:

$$-\omega^2 \begin{pmatrix} \mathrm{u} \\ \mathrm{w} \\ \boldsymbol{E} \end{pmatrix} - P_{\rm long} \begin{pmatrix} \mathsf{c}_{\mathsf{P}}^2 & 0 & 0 \\ 0 & \mathsf{c}_{\mathsf{B}}^2 & 0 \\ 0 & 0 & 0 \end{pmatrix} P_{\rm long}^{-1} \begin{pmatrix} \nabla\varphi \\ \nabla\tilde{\varphi} \\ \nabla\overline{\varphi} \end{pmatrix} + P_{\rm trans} \begin{pmatrix} \mathsf{c}_{\mathsf{S}}^2 & 0 & 0 \\ 0 & 0 & 0 \\ 0 & 0 & \mathsf{c}_{\mathsf{EM}}^2 \end{pmatrix} P_{\rm trans}^{-1} \begin{pmatrix} \mathbf{curl}\psi \\ \mathbf{curl}\tilde{\psi} \\ \mathbf{curl}\overline{\psi} \end{pmatrix} = A^{-1} \begin{pmatrix} \mathbf{F_1} \\ \mathbf{F_2} \\ \mathbf{F_3} \end{pmatrix} .$$

This can be expressed in terms of the potentials defined in equations (6.9) and (6.12) as follows:

$$-\omega^2 \begin{pmatrix} \mathrm{u} \\ \mathrm{w} \\ \boldsymbol{E} \end{pmatrix} - P_{\rm long} \begin{pmatrix} \mathsf{c}_{\mathsf{P}}^2 & 0 & 0 \\ 0 & \mathsf{c}_{\mathsf{B}}^2 & 0 \\ 0 & 0 & 0 \end{pmatrix} \begin{pmatrix} \nabla\chi_{\rm P} \\ \nabla\chi_{\rm B} \\ \nabla\chi_{0l} \end{pmatrix} + P_{\rm trans} \begin{pmatrix} \mathsf{c}_{\mathsf{S}}^2 & 0 & 0 \\ 0 & 0 & 0 \\ 0 & 0 & \mathsf{c}_{\mathsf{EM}}^2 \end{pmatrix} \begin{pmatrix} \mathbf{curl}\chi_{\rm S} \\ \mathbf{curl}\chi_0 \\ \mathbf{curl}\chi_{\rm EM} \end{pmatrix} = A^{-1} \begin{pmatrix} \mathbf{F_1} \\ \mathbf{F_2} \\ \mathbf{F_3} \end{pmatrix} .$$

We obtain for the displacements and electric field respectively:

$$\begin{aligned} -\omega^2 \mathrm{u} &= P_{\rm long_{11}} \mathsf{c}_{\mathsf{P}}^2 \nabla\chi_{\rm P} + P_{\rm long_{12}} \mathsf{c}_{\mathsf{B}}^2 \nabla\chi_{\rm B} - P_{\rm trans_{11}} \mathsf{c}_{\mathsf{S}}^2 \mathbf{curl}\chi_{\rm S} - P_{\rm trans_{13}} \mathsf{c}_{\mathsf{EM}}^2 \mathbf{curl}\chi_{\rm EM} + \tilde{\mathbf{F}}_{\mathbf{1}} , \\ -\omega^2 \mathrm{w} &= P_{\rm long_{21}} \mathsf{c}_{\mathsf{P}}^2 \nabla\chi_{\rm P} + P_{\rm long_{22}} \mathsf{c}_{\mathsf{B}}^2 \nabla\chi_{\rm B} - P_{\rm trans_{21}} \mathsf{c}_{\mathsf{S}}^2 \mathbf{curl}\chi_{\rm S} - P_{\rm trans_{23}} \mathsf{c}_{\mathsf{EM}}^2 \mathbf{curl}\chi_{\rm EM} + \tilde{\mathbf{F}}_{\mathbf{2}} , \\ -\omega^2 \boldsymbol{E} &= P_{\rm long_{31}} \mathsf{c}_{\mathsf{P}}^2 \nabla\chi_{\rm P} + P_{\rm long_{32}} \mathsf{c}_{\mathsf{B}}^2 \nabla\chi_{\rm B} - P_{\rm trans_{31}} \mathsf{c}_{\mathsf{S}}^2 \mathbf{curl}\chi_{\rm S} - P_{\rm trans_{33}} \mathsf{c}_{\mathsf{EM}}^2 \mathbf{curl}\chi_{\rm EM} + \tilde{\mathbf{F}}_{\mathbf{3}} . \end{aligned}$$

Expressing the values of $P_{\rm trans}$ and $P_{\rm long}$ from equation (6.2) in the above system leads to equation (6.4).

□

6.1.2 Potential form of the unknowns in first order formulation

The unknowns ($\mathbf{u}$, $\mathbf{w}$, $\boldsymbol{\tau}$, p, $\boldsymbol{E}$, H, $\boldsymbol{J}$) are expressed with the potentials as:

$$
\begin{aligned}
\mathfrak{s}\,\mathrm{i}\omega\,\mathbf{u} &= \frac{1}{\mathsf{s}_{\mathrm{P}}^2}\nabla\chi_{\mathrm{P}} + \frac{1}{\mathsf{s}_{\mathrm{B}}^2}\nabla\chi_{\mathrm{B}} - \frac{1}{\mathsf{s}_{\mathrm{S}}^2}\mathbf{curl}\chi_{\mathrm{S}} - \frac{1}{\mathsf{s}_{\mathrm{EM}}^2}\mathbf{curl}\chi_{\mathrm{EM}} + \tilde{\mathbf{F}}_{\mathbf{1}}\,,\\
\mathfrak{s}\,\mathrm{i}\omega\,\mathbf{w} &= \frac{\mathcal{W}_{\mathrm{P}}}{\mathsf{s}_{\mathrm{P}}^2}\nabla\chi_{\mathrm{P}} + \frac{\mathcal{W}_{\mathrm{B}}}{\mathsf{s}_{\mathrm{B}}^2}\nabla\chi_{\mathrm{B}} - \frac{\mathcal{W}_{\mathrm{S}}}{\mathsf{s}_{\mathrm{S}}^2}\mathbf{curl}\chi_{\mathrm{S}} - \frac{\mathcal{W}_{\mathrm{EM}}}{\mathsf{s}_{\mathrm{EM}}^2}\mathbf{curl}\chi_{\mathrm{EM}} + \tilde{\mathbf{F}}_{\mathbf{2}}\,,\\
\mathrm{p} &= -M\left(\mathcal{W}_{\mathrm{P}} + \alpha\right)\chi_{\mathrm{P}} - M\left(\mathcal{W}_{\mathrm{B}} + \alpha\right)\chi_{\mathrm{B}} - M\,\mathbf{f}_{\mathrm{p}}\,, \qquad (6.14a)\\
\boldsymbol{\tau} &= \frac{\mu_{\mathrm{fr}}}{\omega^2}\left(-\frac{2}{\mathsf{s}_{\mathrm{P}}^2}\nabla^2\chi_{\mathrm{P}} - \frac{2}{\mathsf{s}_{\mathrm{B}}^2}\nabla^2\chi_{\mathrm{B}} + \frac{\nabla\mathbf{curl}\,\chi_{\mathrm{S}} + \nabla^T\mathbf{curl}\,\chi_{\mathrm{S}}}{\mathsf{s}_{\mathrm{S}}^2} + \frac{\nabla\mathbf{curl}\,\chi_{\mathrm{EM}} + \nabla^T\mathbf{curl}\,\chi_{\mathrm{EM}}}{\mathsf{s}_{\mathrm{EM}}^2}\right)\\
&\quad + \left(-\tfrac{2}{3}\mu_{\mathrm{fr}} + \mathrm{k}_{\mathrm{fr}} + M\alpha^2 + \alpha\,M\,\mathcal{W}_{\mathrm{P}}\right)\chi_{\mathrm{P}}\,\mathbb{I}\\
&\quad + \left(-\tfrac{2}{3}\mu_{\mathrm{fr}} + \mathrm{k}_{\mathrm{fr}} + M\alpha^2 + \alpha\,M\,\mathcal{W}_{\mathrm{B}}\right)\chi_{\mathrm{B}}\,\mathbb{I} - \frac{\mu_{\mathrm{fr}}}{\omega^2}\left(\nabla\tilde{\mathbf{F}}_{\mathbf{1}} + \nabla^T\tilde{\mathbf{F}}_{\mathbf{1}}\right),\\
-\omega^2\,\boldsymbol{\mathcal{E}} &= \frac{\mathcal{E}_{\mathrm{P}}}{\mathsf{s}_{\mathrm{P}}^2}\nabla\chi_{\mathrm{P}} + \frac{\mathcal{E}_{\mathrm{B}}}{\mathsf{s}_{\mathrm{B}}^2}\nabla\chi_{\mathrm{B}} - \frac{\mathcal{E}_{\mathrm{S}}}{\mathsf{s}_{\mathrm{S}}^2}\mathbf{curl}\chi_{\mathrm{S}} - \frac{\mathcal{E}_{\mathrm{EM}}}{\mathsf{s}_{\mathrm{EM}}^2}\mathbf{curl}\chi_{\mathrm{EM}} + \tilde{\mathbf{F}}_{\mathbf{3}}\,,\\
\mathrm{H} &= \frac{\mathfrak{s}\,\mathrm{i}}{\omega\,\mu_0}\left(\mathcal{E}_{\mathrm{S}}\,\chi_{\mathrm{S}} + \mathcal{E}_{\mathrm{EM}}\,\chi_{\mathrm{EM}}\right),
\end{aligned}
$$

and

$$
\begin{aligned}
\boldsymbol{J} &= \left(-\frac{\sigma}{\omega^2}\mathcal{E}_{\mathrm{P}}\,\mathsf{s}_{\mathrm{P}}^{-2} + \mathbf{L}\,M\left(\mathcal{W}_{\mathrm{P}} + \alpha\right) - \mathbf{L}\,\rho_f\,\mathsf{s}_{\mathrm{P}}^{-2}\right)\nabla\chi_{\mathrm{P}} + \left(-\frac{\sigma}{\omega^2}\mathcal{E}_{\mathrm{B}}\,\mathsf{s}_{\mathrm{B}}^{-2} + \mathbf{L}\,M\left(\mathcal{W}_{\mathrm{B}} + \alpha\right) - \mathbf{L}\,\rho_f\,\mathsf{s}_{\mathrm{B}}^{-2}\right)\nabla\chi_{\mathrm{B}}\\
&\quad + \left(\frac{\sigma}{\omega^2}\mathcal{E}_{\mathrm{S}}\,\mathsf{s}_{\mathrm{S}}^{-2} + \mathbf{L}\,\rho_f\,\mathsf{s}_{\mathrm{S}}^{-2}\right)\mathbf{curl}\chi_{\mathrm{S}} + \left(\frac{\sigma}{\omega^2}\mathcal{E}_{\mathrm{EM}}\,\mathsf{s}_{\mathrm{S}}^{-2} + \mathbf{L}\,\rho_f\,\mathsf{s}_{\mathrm{EM}}^{-2}\right)\mathbf{curl}\chi_{\mathrm{EM}} + F\,.
\end{aligned}
\qquad (6.14b)
$$

Proof. The velocities $\mathbf{u}$ and $\mathbf{w}$ are the time-derivatives of u and w defined in terms of potentials in equation (6.4). The electric field $\boldsymbol{E}$ was also expressed with the potentials in this equation. The calculations for the poroelastic unknowns ($\boldsymbol{\tau}$, p) are similar to the ones detailed in Chapter 2, Section 2.1. We only detail in the following the calculations for H and $\boldsymbol{J}$. The magnetic field is given by equation (5.3e):

$$
\mathrm{H} = -\frac{1}{\mathfrak{s}\,\mathrm{i}\,\omega\,\mu_0}\,\mathrm{curl}\,\boldsymbol{E} = \frac{\mathfrak{s}\,\mathrm{i}}{\omega\,\mu_0}\,\mathrm{curl}\,\boldsymbol{E} = \frac{\mathfrak{s}\,\mathrm{i}}{\omega\,\mu_0}\,\overline{\psi}\,.
$$

Using (6.9), we have

$$
\overline{\psi} = \mathcal{E}_{\mathrm{S}}\,\chi_{\mathrm{S}} + \mathcal{E}_{\mathrm{EM}}\,\chi_{\mathrm{EM}}\,.
$$

Hence,

$$
\mathrm{H} = \frac{\mathfrak{s}\,\mathrm{i}}{\omega\,\mu_0}\left(\mathcal{E}_{\mathrm{S}}\,\chi_{\mathrm{S}} + \mathcal{E}_{\mathrm{EM}}\,\chi_{\mathrm{EM}}\right).
$$

The current density is expressed using equation (5.3g)

$$
\boldsymbol{J} = \sigma\boldsymbol{E} + \mathbf{L}(-\nabla\mathrm{p} + \omega^2\rho_f\mathrm{u})\,.
$$

Using equations (6.4) and (6.14a), we have:

$$
\begin{aligned}
\boldsymbol{J} &= -\frac{\sigma}{\omega^2}\left(\mathcal{E}_{\mathrm{P}}\,\mathsf{s}_{\mathrm{P}}^{-2}\nabla\chi_{\mathrm{P}} + \mathcal{E}_{\mathrm{B}}\,\mathsf{s}_{\mathrm{B}}^{-2}\nabla\chi_{\mathrm{B}} - \mathcal{E}_{\mathrm{S}}\,\mathsf{s}_{\mathrm{S}}^{-2}\mathbf{curl}\chi_{\mathrm{S}} - \mathcal{E}_{\mathrm{EM}}\,\mathsf{s}_{\mathrm{EM}}^{-2}\mathbf{curl}\chi_{\mathrm{EM}} + \tilde{\mathbf{F}}_{\mathbf{3}}\right)\\
&\quad + \mathbf{L}\left(M\left(\mathcal{W}_{\mathrm{P}} + \alpha\right)\nabla\chi_{\mathrm{P}} + M\left(\mathcal{W}_{\mathrm{B}} + \alpha\right)\nabla\chi_{\mathrm{B}} + M\,\nabla\mathbf{f}_{\mathrm{p}}\right)\\
&\quad - \mathbf{L}\,\rho_f\left(\mathsf{s}_{\mathrm{P}}^{-2}\nabla\chi_{\mathrm{P}} + \mathsf{s}_{\mathrm{B}}^{-2}\nabla\chi_{\mathrm{B}} - \mathsf{s}_{\mathrm{S}}^{-2}\mathbf{curl}\chi_{\mathrm{S}} - \mathsf{s}_{\mathrm{EM}}^{-2}\mathbf{curl}\chi_{\mathrm{EM}} + \tilde{\mathbf{F}}_{\mathbf{1}}\right),
\end{aligned}
$$

Reorganizing the terms gives equation (6.14b), where

$$
F = -\frac{\sigma}{\omega^2}\tilde{\mathbf{F}}_{\mathbf{3}} + \mathbf{L}\,M\,\nabla\mathbf{f}_{\mathrm{p}} - \mathbf{L}\,\rho_f\,\tilde{\mathbf{F}}_{\mathbf{1}}\,.
$$

□

6.1.3 Expansion of generic solutions in terms of Bessel functions

We consider system (6.5) with no sources. In this case, the potentials $\chi_\bullet$ satisfy the homogeneous Helmholtz equation:

$$\begin{aligned}\big(-\Delta \;-\; \omega^2\,\mathsf{s}_{\mathrm{P}}^2\big)\,\chi_{\mathrm{P}} &= 0\,,\\ \big(-\Delta \;-\; \omega^2\,\mathsf{s}_{\mathrm{B}}^2\big)\,\chi_{\mathrm{B}} &= 0\,,\\ \big(-\Delta \;-\; \omega^2\,\mathsf{s}_{\mathrm{S}}^2\big)\,\chi_{\mathrm{S}} &= 0\,,\\ \big(-\Delta \;-\; \omega^2\,\mathsf{s}_{\mathrm{EM}}^2\big)\,\chi_{\mathrm{EM}} &= 0\,.\end{aligned} \tag{6.15}$$

We can obtain the form of the general solution of equations (5.3) in terms of Bessel functions for the following types of domains: inside a disc, in an annulus and outside of a disc. On each considered domain, the potentials $\chi_\bullet$ can be given as an expansion in terms of Bessel functions in polar coordinates.

(a) Inside a disc $\mathbb{B}_{\mathfrak{a}}$ centered at the origin and of radius $\mathfrak{a}$, a generic solution is given by:

$$\chi_\bullet(r,\theta) \;=\; \sum_{k\in\mathbb{Z}} a_{\bullet,k}\,\mathrm{J}_k(\,\omega\,\mathsf{s}_\bullet\,r)\;e^{\mathrm{i}\,k\,\theta} \quad,\quad \bullet\in\{\mathrm{P},\mathrm{B},\mathrm{S},\mathrm{EM}\,.\} \tag{6.16}$$

(b) An outgoing solution on $\mathbb{R}^2\setminus\mathbb{B}_{\mathfrak{a}}$ is given by

$$\chi_\bullet(r,\theta) \;=\; \sum_{k\in\mathbb{Z}} a_{\bullet,k}\,\mathrm{H}_k^{(1)}(\,\omega\,\mathsf{s}_\bullet\,r)\;e^{\mathrm{i}\,k\,\theta} \quad,\quad \bullet\in\{\mathrm{P},\mathrm{B},\mathrm{S},\mathrm{EM}\,.\} \tag{6.17}$$

Regarding the 'outgoing'-ness of this solution, we refer to Remark 2.2, and Definition 2.3, see Chapter 2.

(c) On an annulus between inner radius $\mathfrak{a}$ and outer radius $\mathfrak{b}$, a generic solution is given by:

$$\chi_\bullet(r,\theta) \;=\; \sum_{k\in\mathbb{Z}} a_{\bullet,k}\,\mathrm{H}_k^{(1)}(\omega\,\mathsf{s}_\bullet\,r)\;e^{\mathrm{i}\,k\,\theta} + \sum_{k\in\mathbb{Z}} \tilde{a}_{\bullet,k}\,\mathrm{H}_k^{(2)}(\omega\,\mathsf{s}_\bullet\,r)\;e^{\mathrm{i}\,k\,\theta} \quad,\quad \bullet\in\{\mathrm{P},\mathrm{B},\mathrm{S},\mathrm{EM}\,.\} \tag{6.18}$$

The expansion of $\mathbf{u}$, $\mathbf{w}$, $\boldsymbol{\tau}$, p, $\boldsymbol{E}$, H, $\boldsymbol{J}$, is obtained by substituting the expression of the potentials $\chi_\bullet$ (6.16), (6.17) or (6.18) into (6.14). We also use the expression of **curl** ∇ and ∇^2 in polar coordinates presented in Section A.1.1,. Case (a) is covered in Section 6.2, and case (b) in Section 6.3.

6.2 Generic solution to homogeneous equation on bounded domain

We consider Pride's equations (5.3) inside the disc $\mathbb{B}_{(0,\mathfrak{a})}$ with boundary conditions of type 1 and 8. Equation (6.14) gives ($\mathbf{u}$, $\mathbf{w}$, $\boldsymbol{\tau}$, p, $\boldsymbol{E}$, H, $\boldsymbol{J}$), while the potentials are given by (6.15). Hence, in a bounded domain, the potentials satisfy equation (6.16) and have the form:

$$\begin{aligned}\chi_{\mathrm{P}}(r,\theta) &= \sum_{k\in\mathbb{Z}} a_k\,\mathrm{J}_k(\omega\,\mathsf{s}_{\mathrm{P}}\,r)\;e^{\mathrm{i}\,k\,\theta}\,,\\ \chi_{\mathrm{B}}(r,\theta) &= \sum_{k\in\mathbb{Z}} b_k\,\mathrm{J}_k(\omega\,\mathsf{s}_{\mathrm{B}}\,r)\;e^{\mathrm{i}\,k\,\theta}\,,\\ \chi_{\mathrm{S}}(r,\theta) &= \sum_{k\in\mathbb{Z}} c_k\,\mathrm{J}_k(\omega\,\mathsf{s}_{\mathrm{S}}\,r)\;e^{\mathrm{i}\,k\,\theta}\,,\\ \chi_{\mathrm{EM}}(r,\theta) &= \sum_{k\in\mathbb{Z}} d_k\,\mathrm{J}_k(\omega\,\mathsf{s}_{\mathrm{EM}}\,r)\;e^{\mathrm{i}\,k\,\theta}\,.\end{aligned}$$

The series coefficients a_k, b_k, c_k, d_k are then determined by the boundary conditions imposed on $\partial\mathbb{B}_{(0,\mathfrak{a})}$, which are one of the 8 types given in Section 5.4. Here we only detail the solutions for type 1 and 8, the others types are combinations of the two presented.

6.2.1 Boundary conditions of type 1

We consider equation (5.3) on the disc $\mathbb{B}_{(0,\mathfrak{a})}$ with the following boundary conditions

$$\begin{aligned} \mathbf{w}\cdot\boldsymbol{n} &= f \quad , \quad \text{on } \partial\mathbb{B}_{(0,\mathfrak{a})}\,, \\ \boldsymbol{\tau}\,\boldsymbol{n} &= \boldsymbol{g} \quad , \quad \text{on } \partial\mathbb{B}_{(0,\mathfrak{a})}\,, \\ \boldsymbol{n}\times\boldsymbol{E} &= h \quad , \quad \text{on } \partial\mathbb{B}_{(0,\mathfrak{a})}\,. \end{aligned}$$

In polar coordinates, we have $\boldsymbol{n}=\mathbf{e}_r$, which means that $\mathbf{w}\cdot\boldsymbol{n}=\mathrm{w}_r$, $\boldsymbol{\tau}\,\boldsymbol{n}=\tau_{rr}\,\mathbf{e}_r+\tau_{r\theta}\,\mathbf{e}_\theta$, and $\boldsymbol{n}\times\boldsymbol{E}=E_\theta$. Hence, in the following, we do not detail all the components of the vectors $\mathbf{w}$, $\boldsymbol{E}$ and the tensor $\boldsymbol{\tau}$, and we focus on the expressions of w_r, E_θ, τ_{rr} and $\tau_{r\theta}$. For convenience, the boundary conditions are written as:

$$\mathfrak{s}\,\mathrm{i}\,\omega\,\mathrm{w}_r = \mathfrak{s}\,\mathrm{i}\,\omega\,f\,, \quad \omega^2\,\tau_{rr} = \omega^2\,g_r\,, \quad \omega^2\,\tau_{r\theta} = \omega^2\,g_\theta \quad \omega^2\,E_\theta = \omega^2\,h\,, \quad \text{on } \partial\mathbb{B}_{(0,\mathfrak{a})}\,. \tag{6.19}$$

Next, we expand the coefficients of each component in Fourier series. This gives for the right hand-side

$$f=\sum_{k\in\mathbb{Z}} f_k\,e^{\mathrm{i}\,k\,\theta}\,, \quad g_r=\sum_{k\in\mathbb{Z}} g_{r,k}\,e^{\mathrm{i}\,k\,\theta}\,, \quad g_\theta=\sum_{k\in\mathbb{Z}} g_{\theta,k}\,e^{\mathrm{i}\,k\,\theta} \quad h_\theta=\sum_{k\in\mathbb{Z}} h_{\theta,k}\,e^{\mathrm{i}\,k\,\theta}\,,$$

and for the unknowns:

$$\mathrm{w}_r=\sum_{k\in\mathbb{Z}} \mathrm{w}_{r,k}\,e^{\mathrm{i}\,k\,\theta}\,, \quad \tau_{rr}=\sum_{k\in\mathbb{Z}} \tau_{rr,k}\,e^{\mathrm{i}\,k\,\theta}\,, \quad \tau_{r\theta}=\sum_{k\in\mathbb{Z}} \tau_{r\theta,k}\,e^{\mathrm{i}\,k\,\theta}\,, \quad E_\theta=\sum_{k\in\mathbb{Z}} E_{\theta,k}\,e^{\mathrm{i}\,k\,\theta}\,.$$

Using the expression of the unknowns in terms of potential (6.14) we have:

$$
\begin{aligned}
\mathfrak{s}\,\mathrm{i}\,\omega\,\mathrm{w}_{r,k} =& a_k\,\frac{\mathcal{W}_\mathrm{P}}{\mathsf{s}_\mathrm{P}}\,\omega\,\mathrm{J}_k'(\omega\,\mathsf{s}_\mathrm{P}\,r)e^{\mathrm{i}k\theta} + b_k\,\frac{\mathcal{W}_\mathrm{B}}{\mathsf{s}_\mathrm{B}}\,\omega\,\mathrm{J}_k'(\omega\,\mathsf{s}_\mathrm{B}\,r)e^{\mathrm{i}k\theta}\\
&- c_k\,\frac{\mathcal{W}_\mathrm{S}}{\mathsf{s}_\mathrm{S}^2}\,\frac{\mathrm{i}k}{r}\mathrm{J}_k(\omega\,\mathsf{s}_\mathrm{S}\,r)e^{\mathrm{i}k\theta} - d_k\,\frac{\mathcal{W}_\mathrm{EM}}{\mathsf{s}_\mathrm{EM}^2}\,\frac{\mathrm{i}k}{r}\mathrm{J}_k(\omega\,\mathsf{s}_\mathrm{EM}\,r)e^{\mathrm{i}k\theta}\,,\\
\omega^2\tau_{rr,k} =& -\frac{2\,\mu_\mathrm{fr}\,\omega}{\mathsf{s}_\mathrm{P}\,r}\,a_k\,\mathrm{J}_{k+1}(\omega\,\mathsf{s}_\mathrm{P}\,r)\;e^{\mathrm{i}\,k\,\theta} + \frac{2\,\mu_\mathrm{fr}\,k}{\mathsf{s}_\mathrm{P}^2\,r^2}\,a_k\,\mathrm{J}_k(\omega\,\mathsf{s}_\mathrm{P}\,r)\;e^{\mathrm{i}\,k\,\theta} + 2\,\mu_\mathrm{fr}\,a_k\,\omega^2\,\mathrm{J}_k(\omega\,\mathsf{s}_\mathrm{P}\,r)\;e^{\mathrm{i}\,k\,\theta}\\
&- \frac{2\,\mu_\mathrm{fr}\,k^2}{\mathsf{s}_\mathrm{P}^2\,r^2}\,a_k\,\mathrm{J}_k(\omega\,\mathsf{s}_\mathrm{P}\,r)\;e^{\mathrm{i}\,k\,\theta} - \frac{2\,\mu_\mathrm{fr}\,\omega}{\mathsf{s}_\mathrm{B}\,r}\,b_k\,\mathrm{J}_{k+1}(\omega\,\mathsf{s}_\mathrm{B}\,r)\;e^{\mathrm{i}\,k\,\theta} + \frac{2\,\mu_\mathrm{fr}\,k}{\mathsf{s}_\mathrm{B}^2\,r^2}\,b_k\,\mathrm{J}_k(\omega\,\mathsf{s}_\mathrm{B}\,r)\;e^{\mathrm{i}\,k\,\theta}\\
&+ 2\,\mu_\mathrm{fr}\,b_k\,\omega^2\,\mathrm{J}_k(\omega\,\mathsf{s}_\mathrm{B}\,r)\;e^{\mathrm{i}\,k\,\theta} - \frac{2\,\mu_\mathrm{fr}\,k^2}{\mathsf{s}_\mathrm{B}^2\,r^2}\,b_k\,\mathrm{J}_k(\omega\,\mathsf{s}_\mathrm{B}\,r)\;e^{\mathrm{i}\,k\,\theta} + \frac{2\,\mu_\mathrm{fr}}{\mathsf{s}_\mathrm{S}^2\,r}\,c_k\,\omega\,\mathsf{s}_\mathrm{S}\,\mathrm{i}k\,\mathrm{J}_k'(\omega\,\mathsf{s}_\mathrm{S}\,r)\;e^{\mathrm{i}\,k\,\theta}\\
&+ \frac{2\,\mu_\mathrm{fr}}{\mathsf{s}_\mathrm{EM}^2\,r}\,d_k\,\omega\,\mathsf{s}_\mathrm{EM}\,\mathrm{i}k\,\mathrm{J}_k'(\omega\,\mathsf{s}_\mathrm{EM}\,r)\;e^{\mathrm{i}\,k\,\theta} + \omega^2\left(-\frac{2}{3}\mu_\mathrm{fr} + \mathrm{k}_\mathrm{fr} + M\alpha^2 + \alpha\,M\mathcal{W}_\mathrm{P}\right)\;a_k\,\mathrm{J}_k(\omega\,\mathsf{s}_\mathrm{P}\,r)\;e^{\mathrm{i}\,k\,\theta}\\
&+ \omega^2\left(-\frac{2}{3}\mu_\mathrm{fr} + \mathrm{k}_\mathrm{fr} + M\alpha^2 + \alpha\,M\mathcal{W}_\mathrm{B}\right)\;b_k\,\mathrm{J}_k(\omega\,\mathsf{s}_\mathrm{B}\,r)\;e^{\mathrm{i}\,k\,\theta}\,,\\
\omega^2\,\tau_{r\theta,k} =& -\frac{2\,\mu_\mathrm{fr}\omega\,\mathrm{i}\,k}{r\,\mathsf{s}_\mathrm{P}}\,a_k\,\mathrm{J}_k'(\omega\,\mathsf{s}_\mathrm{P}\,r)\,e^{\mathrm{i}\,k\,\theta} + \frac{2\,\mathrm{i}\,\mu_\mathrm{fr}\,k}{r^2\,\mathsf{s}_\mathrm{P}^2}\,a_k\,\mathrm{J}_k(\omega\,\mathsf{s}_\mathrm{P}\,r)\,e^{\mathrm{i}\,k\,\theta} - \frac{2\mu_\mathrm{fr}\omega\,\mathrm{i}\,k}{r\,\mathsf{s}_\mathrm{B}}\,b_k\,\mathrm{J}_k'(\omega\,\mathsf{s}_\mathrm{B}\,r)e^{\mathrm{i}\,k\,\theta}\\
&+ \frac{2\,\mathrm{i}\,\mu_\mathrm{fr}\,k}{r^2\,\mathsf{s}_\mathrm{B}^2}\,b_k\,\mathrm{J}_k(\omega\,\mathsf{s}_\mathrm{B}\,r)\;e^{\mathrm{i}\,k\,\theta} - \frac{\mu_\mathrm{fr}\,k^2}{r^2\,\mathsf{s}_\mathrm{S}^2}\,c_k\,\mathrm{J}_k(\omega\,\mathsf{s}_\mathrm{S}\,r)\;e^{\mathrm{i}\,k\,\theta} + \frac{\mu_\mathrm{fr}\,\omega}{r\,\mathsf{s}_\mathrm{S}}\,c_k\,\mathrm{J}_k'(\omega\,\mathsf{s}_\mathrm{S}\,r)\;e^{\mathrm{i}\,k\,\theta}\\
&- \mu_\mathrm{fr}\,\frac{\omega}{\mathsf{s}_\mathrm{S}\,r}\,c_k\,\mathrm{J}_{k+1}(\omega\,\mathsf{s}_\mathrm{S}\,r)\;e^{\mathrm{i}\,k\,\theta} + \mu_\mathrm{fr}\,\frac{k}{\mathsf{s}_\mathrm{S}^2\,r^2}c_k\,\mathrm{J}_k(\omega\,\mathsf{s}_\mathrm{S}\,r)\;e^{\mathrm{i}\,k\,\theta}\\
&+ \omega^2\,c_k\,\mathrm{J}_k(\omega\,\mathsf{s}_\mathrm{S}\,r)\;e^{\mathrm{i}\,k\,\theta} - \mu_\mathrm{fr}\,\frac{k^2}{\mathsf{s}_\mathrm{S}^2\,r^2}\,c_k\,\mathrm{J}_k(\omega\,\mathsf{s}_\mathrm{S}\,r)\;e^{\mathrm{i}\,k\,\theta}\\
&- \frac{\mu_\mathrm{fr}\,k^2}{r^2\,\mathsf{s}_\mathrm{EM}^2}\,d_k\,\mathrm{J}_k(\omega\,\mathsf{s}_\mathrm{EM}\,r)\;e^{\mathrm{i}\,k\,\theta} + \frac{\mu_\mathrm{fr}\,\omega}{r\,\mathsf{s}_\mathrm{EM}}\,d_k\,\mathrm{J}_k'(\omega\,\mathsf{s}_\mathrm{EM}\,r)\;e^{\mathrm{i}\,k\,\theta}\\
&- \mu_\mathrm{fr}\,\frac{\omega}{\mathsf{s}_\mathrm{EM}\,r}\,d_k\,\mathrm{J}_{k+1}(\omega\,\mathsf{s}_\mathrm{EM}\,r)\;e^{\mathrm{i}\,k\,\theta} + \mu_\mathrm{fr}\,\frac{k}{\mathsf{s}_\mathrm{EM}^2\,r^2}d_k\,\mathrm{J}_k(\omega\,\mathsf{s}_\mathrm{EM}\,r)\;e^{\mathrm{i}\,k\,\theta}\\
&+ \omega^2\,d_k\,\mathrm{J}_k(\omega\,\mathsf{s}_\mathrm{EM}\,r)\;e^{\mathrm{i}\,k\,\theta} - \mu_\mathrm{fr}\,\frac{k^2}{\mathsf{s}_\mathrm{EM}^2\,r^2}\,d_k\,\mathrm{J}_k(\omega\,\mathsf{s}_\mathrm{EM}\,r)\;e^{\mathrm{i}\,k\,\theta}\,,\\
-\omega^2\,E_{\theta,k} =& \sum_{k\in\mathbb{Z}} a_k\,\mathcal{E}_\mathrm{P}\,\mathsf{s}_\mathrm{P}^{-2}\,\frac{\mathrm{i}k}{r}\mathrm{J}_k(\omega\,\mathsf{s}_\mathrm{P}\,r)e^{\mathrm{i}k\theta} + \sum_{k\in\mathbb{Z}} b_k\,\mathcal{E}_\mathrm{B}\,\mathsf{s}_\mathrm{B}^{-2}\,\frac{\mathrm{i}k}{r}\mathrm{J}_k(\omega\,\mathsf{s}_\mathrm{B}\,r)e^{\mathrm{i}k\theta}\\
&+ \sum_{k\in\mathbb{Z}} c_k\,\mathcal{E}_\mathrm{S}\,\mathsf{s}_\mathrm{S}^{-1}\,\omega\,\mathrm{J}_k'(\omega\,\mathsf{s}_\mathrm{S}\,r)e^{\mathrm{i}k\theta} + \sum_{k\in\mathbb{Z}} d_k\,\mathcal{E}_\mathrm{EM}\,\mathsf{s}_\mathrm{EM}^{-1}\,\omega\,\mathrm{J}_k'(\omega\,\mathsf{s}_\mathrm{EM}\,r)e^{\mathrm{i}k\theta}\,.
\end{aligned}
$$

Imposing (6.19), we obtain a linear system satisfied by a_k, b_k, c_k, d_k in each mode k

$$
\mathbb{A}_k^{\mathbf{w},\boldsymbol{\tau},\boldsymbol{E}}\begin{pmatrix} a_k\\ b_k\\ c_k\\ d_k\end{pmatrix} = \begin{pmatrix} \mathfrak{s}\,\mathrm{i}\,\omega\,f_k\\ \omega^2\,g_{r,k}\\ \omega^2\,g_{\theta,k}\\ -\omega^2\,h_{\theta,k}\end{pmatrix}\,,
$$

where the coefficient matrix is defined as:

$$
\mathbb{A}_k^{\mathbf{w},\boldsymbol{\tau},\boldsymbol{E}} = \begin{pmatrix} A_{11} & A_{12} & A_{13} & A_{14}\\ A_{21} & A_{22} & A_{23} & A_{24}\\ A_{31} & A_{32} & A_{33} & A_{34}\\ A_{41} & A_{42} & A_{43} & A_{44}\end{pmatrix} \tag{6.20}
$$

with

$$A_{11} = \frac{\mathcal{W}_{\mathrm{P}}}{\mathsf{s}_{\mathrm{P}}}\,\omega\,\mathrm{J}'_k(\omega\,\mathsf{s}_{\mathrm{P}}\mathfrak{a})\,,\quad A_{12} = \frac{\mathcal{W}_{\mathrm{B}}}{\mathsf{s}_{\mathrm{B}}}\,\omega\,\mathrm{J}'_k(\omega\,\mathsf{s}_{\mathrm{S}}\mathfrak{a})\,,\qquad A_{13} = -\frac{\mathcal{W}_{\mathrm{S}}}{\mathsf{s}_{\mathrm{S}}^2}\,\frac{\mathrm{i}k}{r}\,\mathrm{J}_k(\omega\,\mathsf{s}_{\mathrm{S}}\mathfrak{a})\,,\quad A_{14} = -\frac{\mathcal{W}_{\mathrm{EM}}}{\mathsf{s}_{\mathrm{EM}}^2}\,\frac{\mathrm{i}k}{r}\,\mathrm{J}_k(\omega\,\mathsf{s}_{\mathrm{EM}}\mathfrak{a})\,,$$

$$\begin{aligned}A_{21} = &-\frac{2\,\mu_{\mathrm{fr}}\,\omega}{\mathsf{s}_{\mathrm{P}}\,\mathfrak{a}}\,\mathrm{J}_{k+1}(\omega\,\mathsf{s}_{\mathrm{P}}\,\mathfrak{a}) + \frac{2\,\mu_{\mathrm{fr}}\,k}{\mathsf{s}_{\mathrm{P}}^2\,\mathfrak{a}^2}\,\mathrm{J}_k(\omega\,\mathsf{s}_{\mathrm{P}}\,\mathfrak{a}) + 2\,\mu_{\mathrm{fr}}\,\omega^2\,\mathrm{J}_k(\omega\,\mathsf{s}_{\mathrm{P}}\,\mathfrak{a})\\ &-\frac{2\,\mu_{\mathrm{fr}}\,k^2}{\mathsf{s}_{\mathrm{P}}^2\,\mathfrak{a}^2}\,\mathrm{J}_k(\omega\,\mathsf{s}_{\mathrm{P}}\,\mathfrak{a}) + \omega^2\left(-\frac{2}{3}\mu_{\mathrm{fr}} + \mathrm{k}_{\mathrm{fr}} + M\alpha^2 + \alpha\,M\mathcal{W}_{\mathrm{P}}\right)\mathrm{J}_k(\omega\,\mathsf{s}_{\mathrm{P}}\mathfrak{a})\,,\end{aligned}$$

$$\begin{aligned}A_{22} = &-\frac{2\,\mu_{\mathrm{fr}}\,\omega}{\mathsf{s}_{\mathrm{B}}\,\mathfrak{a}}\,\mathrm{J}_{k+1}(\omega\,\mathsf{s}_{\mathrm{B}}\,\mathfrak{a}) + \frac{2\,\mu_{\mathrm{fr}}\,k}{\mathsf{s}_{\mathrm{B}}^2\,\mathfrak{a}^2}\,\mathrm{J}_k(\omega\,\mathsf{s}_{\mathrm{B}}\,\mathfrak{a}) + 2\,\mu_{\mathrm{fr}}\,\omega^2\,\mathrm{J}_k(\omega\,\mathsf{s}_{\mathrm{B}}\,\mathfrak{a})\,e^{\mathrm{i}\,k\,\theta}\\ &-\frac{2\,\mu_{\mathrm{fr}}\,k^2}{\mathsf{s}_{\mathrm{B}}^2\,\mathfrak{a}^2}\,\mathrm{J}_k(\omega\,\mathsf{s}_{\mathrm{B}}\,\mathfrak{a})\,e^{\mathrm{i}\,k\,\theta} + \omega^2\left(-\frac{2}{3}\mu_{\mathrm{fr}} + \mathrm{k}_{\mathrm{fr}} + M\alpha^2 + \alpha\,M\mathcal{W}_{\mathrm{B}}\right)\mathrm{J}_k(\omega\,\mathsf{s}_{\mathrm{B}}\mathfrak{a})\,,\end{aligned}$$

$$A_{23} = \frac{2\mu_{\mathrm{fr}}}{\mathsf{s}_{\mathrm{S}}\mathfrak{a}}\,\omega\,\mathrm{i}k\,\mathrm{J}'_k(\omega\,\mathsf{s}_{\mathrm{S}}\mathfrak{a})\,,\qquad A_{24} = \frac{2\mu_{\mathrm{fr}}}{\mathsf{s}_{\mathrm{EM}}\mathfrak{a}}\,\omega\,\mathrm{i}k\,\mathrm{J}'_k(\omega\,\mathsf{s}_{\mathrm{EM}}\mathfrak{a})\,,\qquad A_{31} = -\frac{2\omega\,\mu_{\mathrm{fr}}\mathrm{i}k}{\mathfrak{a}\mathsf{s}_{\mathrm{P}}}\mathrm{J}'_k(\omega\,\mathsf{s}_{\mathrm{P}}\mathfrak{a}) + \frac{2\,\mu_{\mathrm{fr}}\mathrm{i}k}{\mathfrak{a}^2\mathsf{s}_{\mathrm{P}}^2}\mathrm{J}_k(\omega\,\mathsf{s}_{\mathrm{P}}\mathfrak{a})\,,$$

$$A_{32} = -\frac{2\omega\,\mu_{\mathrm{fr}}\mathrm{i}k}{\mathfrak{a}\mathsf{s}_{\mathrm{B}}}\mathrm{J}'_k(\omega\,\mathsf{s}_{\mathrm{B}}\mathfrak{a}) + \frac{2\mu_{\mathrm{fr}}\mathrm{i}k}{\mathfrak{a}^2\mathsf{s}_{\mathrm{B}}^2}\mathrm{J}_k(\omega\,\mathsf{s}_{\mathrm{B}}\mathfrak{a})\,,$$

$$\begin{aligned}A_{33} = &-\frac{k^2\mu_{\mathrm{fr}}}{\mathfrak{a}^2\mathsf{s}_{\mathrm{S}}^2}\mathrm{J}_k(\omega\,\mathsf{s}_{\mathrm{S}}\,\mathfrak{a}) + \frac{\omega\,\mu_{\mathrm{fr}}}{\mathfrak{a}\mathsf{s}_{\mathrm{S}}}\mathrm{J}'_k(\omega\,\mathsf{s}_{\mathrm{S}}\,\mathfrak{a}) - \frac{\mu_{\mathrm{fr}}\,\omega}{\mathsf{s}_{\mathrm{S}}\,\mathfrak{a}}\,\mathrm{J}_{k+1}(\omega\,\mathsf{s}_{\mathrm{S}}\,\mathfrak{a}) + \frac{\mu_{\mathrm{fr}}\,k}{\mathsf{s}_{\mathrm{S}}^2\,\mathfrak{a}^2}\,\mathrm{J}_k(\omega\,\mathsf{s}_{\mathrm{S}}\,\mathfrak{a})\\ &+\mu_{\mathrm{fr}}\,\omega^2\,\mathrm{J}_k(\omega\,\mathsf{s}_{\mathrm{S}}\,\mathfrak{a}) - \frac{\mu_{\mathrm{fr}}\,k^2}{\mathsf{s}_{\mathrm{S}}^2\,\mathfrak{a}^2}\,\mathrm{J}_k(\omega\,\mathsf{s}_{\mathrm{S}}\,\mathfrak{a})\,,\end{aligned}$$

$$\begin{aligned}A_{34} = &-\frac{k^2\mu_{\mathrm{fr}}}{\mathfrak{a}^2\mathsf{s}_{\mathrm{EM}}^2}\mathrm{J}_k(\omega\,\mathsf{s}_{\mathrm{EM}}\,\mathfrak{a}) + \frac{\omega\,\mu_{\mathrm{fr}}}{\mathfrak{a}\mathsf{s}_{\mathrm{EM}}}\mathrm{J}'_k(\omega\,\mathsf{s}_{\mathrm{EM}}\,\mathfrak{a}) - \frac{\mu_{\mathrm{fr}}\,\omega}{\mathsf{s}_{\mathrm{EM}}\,\mathfrak{a}}\,\mathrm{J}_{k+1}(\omega\,\mathsf{s}_{\mathrm{EM}}\,\mathfrak{a}) + \frac{\mu_{\mathrm{fr}}\,k}{\mathsf{s}_{\mathrm{EM}}^2\,\mathfrak{a}^2}\,\mathrm{J}_k(\omega\,\mathsf{s}_{\mathrm{EM}}\,\mathfrak{a})\\ &+\mu_{\mathrm{fr}}\,\omega^2\,\mathrm{J}_k(\omega\,\mathsf{s}_{\mathrm{EM}}\,\mathfrak{a}) - \frac{\mu_{\mathrm{fr}}\,k^2}{\mathsf{s}_{\mathrm{EM}}^2\,\mathfrak{a}^2}\,\mathrm{J}_k(\omega\,\mathsf{s}_{\mathrm{EM}}\,\mathfrak{a})\,,\end{aligned}$$

and

$$\begin{aligned}A_{41} &= \mathcal{E}_{\mathrm{P}}\,\mathsf{s}_{\mathrm{P}}^{-2}\,\frac{\mathrm{i}k}{\mathfrak{a}}\mathrm{J}_k(\omega\,\mathsf{s}_{\mathrm{P}}\,\mathfrak{a})\,,\qquad & A_{42} &= \mathcal{E}_{\mathrm{B}}\,\mathsf{s}_{\mathrm{B}}^{-2}\,\frac{\mathrm{i}k}{\mathfrak{a}}\mathrm{J}_k(\omega\,\mathsf{s}_{\mathrm{B}}\,\mathfrak{a})\,,\\ A_{43} &= \mathcal{E}_{\mathrm{S}}\,\mathsf{s}_{\mathrm{S}}^{-1}\,\omega\,\mathrm{J}'_k(\omega\,\mathsf{s}_{\mathrm{S}}\,\mathfrak{a})\,,\qquad & A_{44} &= \mathcal{E}_{\mathrm{EM}}\,\mathsf{s}_{\mathrm{EM}}^{-1}\,\omega\,\mathrm{J}'_k(\omega\,\mathsf{s}_{\mathrm{EM}}\,\mathfrak{a})\,.\end{aligned}$$

The uniqueness of the problem is characterized by the invertibility of the matrix $\mathbb{A}_k^{\mathbf{w},\boldsymbol{\tau},\boldsymbol{E}}$. If $\mathbb{A}_k^{\mathbf{w},\boldsymbol{\tau},\boldsymbol{E}}$ can be inverted, i.e.the determinant of $\mathbb{A}_k^{\mathbf{w},\boldsymbol{\tau},\boldsymbol{E}}$ does not vanish, the uniqueness of the problem is guaranteed. Hence, we study the eigenvalues of $\mathbb{A}_k^{\mathbf{w},\boldsymbol{\tau},\boldsymbol{E}}$. In the numerical experiments (Section 6.2.3), we investigate the value of the determinant of $\mathbb{A}_k^{\mathbf{w},\boldsymbol{\tau},\boldsymbol{E}}$ for the first modes k on a large range of frequency.

Definition 6.2. The pulsation ω is a type 1 boundary conditions eigenvalue if the system of equations (5.3) associated with the boundary conditions

$$\begin{aligned}\mathbf{w}\cdot\boldsymbol{n} &= 0 \quad , \quad \text{on } \partial\mathbb{B}_{(0,\mathfrak{a})}\,,\\ \boldsymbol{\tau}\,\boldsymbol{n} &= 0 \quad , \quad \text{on } \partial\mathbb{B}_{(0,\mathfrak{a})}\,,\\ \boldsymbol{n}\times\boldsymbol{E} &= 0 \quad , \quad \text{on } \partial\mathbb{B}_{(0,\mathfrak{a})}\end{aligned}$$

admits a solution ($\mathbf{w}$, $\boldsymbol{\tau}$, $\boldsymbol{E}$) such that $\mathbf{w}\neq 0$, $\boldsymbol{\tau}\neq 0$, $\boldsymbol{E}\neq 0$. This also means that $\det\mathbb{A}_k^{\mathbf{w},\boldsymbol{\tau},\boldsymbol{E}}(\omega) = 0$, where $\mathbb{A}_k^{\mathbf{w},\boldsymbol{\tau},\boldsymbol{E}}$ is the coefficient matrix defined in equation (6.20).

6.2.2 Boundary conditions of type 8

We consider equations (5.3) on the disc $\mathbb{B}_{(0,\mathfrak{a})}$, with boundary conditions:

$$\mathbf{u} \;=\; \boldsymbol{f}\,, \qquad \mathrm{p} \;=\; g\,, \qquad \mathrm{H} \;=\; h\,, \quad \text{ on } \partial\mathbb{B}_{(0,\mathfrak{a})}\,.$$

We work in polar coordinates, $\boldsymbol{f} = f_r\mathbf{e}_r + f_\theta\,\mathbf{e}_\theta$ and $\mathbf{u} = \mathrm{u}_r\mathbf{e}_r + \mathrm{u}_\theta\,\mathbf{e}_\theta$. For clarity, the boundary conditions are written as:

$$\mathfrak{s}\,\mathrm{i}\,\omega\,\mathrm{u}_r \;=\; \mathfrak{s}\,\mathrm{i}\,\omega\,h_r\,, \quad \mathfrak{s}\,\mathrm{i}\,\omega\,\mathrm{u}_\theta \;=\; \mathfrak{s}\,\mathrm{i}\,\omega\,h_\theta\,, \quad \mathrm{p} \;=\; g\,, \quad \mathrm{H} \;=\; h\,, \quad \text{ on } \partial\mathbb{B}_{(0,\mathfrak{a})}\,. \tag{6.21}$$

The coefficients of each component are then expanded in Fourier series. We have for the right hand-side

$$f_r = \sum_{k\in\mathbb{Z}} f_{r,k}\,e^{\mathrm{i}\,k\,\theta}\,, \quad f_\theta = \sum_{k\in\mathbb{Z}} f_{\theta,k}\,e^{\mathrm{i}\,k\,\theta}\,, \quad g = \sum_{k\in\mathbb{Z}} g_k\,e^{\mathrm{i}\,k\,\theta}\,, \quad h = \sum_{k\in\mathbb{Z}} h_k\,e^{\mathrm{i}\,k\,\theta}\,,$$

and for the unknowns:

$$\mathrm{u}_r = \sum_{k\in\mathbb{Z}} \mathbf{u}_{r,k}\,e^{\mathrm{i}\,k\,\theta}\,, \quad \mathrm{u}_\theta = \sum_{k\in\mathbb{Z}} \mathbf{u}_{\theta,k}\,e^{\mathrm{i}\,k\,\theta}\,, \quad \mathrm{p} = \sum_{k\in\mathbb{Z}} \mathrm{p}_k\,e^{\mathrm{i}\,k\,\theta}\,, \quad \mathrm{H} = \sum_{k\in\mathbb{Z}} H_k\,e^{\mathrm{i}\,k\,\theta}\,.$$

Using the expression of the unknowns given in equations (6.14), we have:

$$\begin{aligned}
\mathfrak{s}\,\mathrm{i}\,\omega\,\mathrm{u}_{r,k} \;&=\; \sum_{k\in\mathbb{Z}} a_k\;\mathsf{s}_{\mathrm{P}}^{-1}\,\omega\,\mathrm{J}_k'(\omega\,\mathsf{s}_{\mathrm{P}}\,r)e^{\mathrm{i}k\theta} \;+\; \sum_{k\in\mathbb{Z}} b_k\;\mathsf{s}_{\mathrm{B}}^{-1}\,\omega\,\mathrm{J}_k'(\omega\,\mathsf{s}_{\mathrm{B}}\,r)e^{\mathrm{i}k\theta} \\
&\quad - \sum_{k\in\mathbb{Z}} c_k\;\mathsf{s}_{\mathrm{S}}^{-2}\,\frac{\mathrm{i}k}{r}\mathrm{J}_k(\omega\,\mathsf{s}_{\mathrm{S}}\,r)e^{\mathrm{i}k\theta} \;-\; \sum_{k\in\mathbb{Z}} d_k\;\mathsf{s}_{\mathrm{EM}}^{-2}\,\frac{\mathrm{i}k}{r}\mathrm{J}_k(\omega\,\mathsf{s}_{\mathrm{EM}}\,r)e^{\mathrm{i}k\theta}\,, \\
\mathfrak{s}\,\mathrm{i}\,\omega\,\mathrm{u}_{\theta,k} \;&=\; \sum_{k\in\mathbb{Z}} a_k\;\mathsf{s}_{\mathrm{P}}^{-2}\,\frac{\mathrm{i}k}{r}\mathrm{J}_k(\omega\,\mathsf{s}_{\mathrm{P}}\,r)e^{\mathrm{i}k\theta} \;+\; \sum_{k\in\mathbb{Z}} b_k\;\mathsf{s}_{\mathrm{B}}^{-2}\,\frac{\mathrm{i}k}{r}\mathrm{J}_k(\omega\,\mathsf{s}_{\mathrm{B}}\,r)e^{\mathrm{i}k\theta} \\
&\quad + \sum_{k\in\mathbb{Z}} c_k\;\mathsf{s}_{\mathrm{S}}^{-1}\,\omega\,\mathrm{J}_k'(\omega\,\mathsf{s}_{\mathrm{S}}\,r)e^{\mathrm{i}k\theta} \;+\; \sum_{k\in\mathbb{Z}} d_k\;\mathsf{s}_{\mathrm{EM}}^{-1}\,\omega\,\mathrm{J}_k'(\omega\,\mathsf{s}_{\mathrm{EM}}\,r)e^{\mathrm{i}k\theta}\,, \\
\mathrm{p}_k \;&=\; -\sum_{k\in\mathbb{Z}} a_k\,M\left(WP \;+\; \alpha\right)\mathrm{J}_k(\omega\,\mathsf{s}_{\mathrm{P}}\,r)\,e^{\mathrm{i}k\theta} \;-\; \sum_{k\in\mathbb{Z}} b_k\,M\left(\mathcal{W}_{\mathrm{B}} \;+\; \alpha\right)\mathrm{J}_k(\omega\,\mathsf{s}_{\mathrm{B}}\,r)\,e^{\mathrm{i}k\theta}\,, \\
H_k \;&=\; \sum_{k\in\mathbb{Z}} c_k\,\frac{\mathfrak{s}\,\mathrm{i}}{\omega\,\mu_0}\,\mathcal{E}_{\mathrm{S}}\,\mathrm{J}_k(\omega\,\mathsf{s}_{\mathrm{S}}\,r)\;e^{\mathrm{i}\,k\,\theta} \;+\; \sum_{k\in\mathbb{Z}} d_k\,\frac{\mathfrak{s}\,\mathrm{i}}{\omega\,\mu_0}\,\mathcal{E}_{\mathrm{EM}}\,\mathrm{J}_k(\omega\,\mathsf{s}_{\mathrm{EM}}\,r)\,e^{\mathrm{i}\,k\,\theta}\,.
\end{aligned}$$

Imposing (6.21), we obtain a linear system satisfied by a_k, b_k, c_k, d_k in each mode k:

$$\mathbb{A}_k^{\mathbf{u},\mathrm{p},\mathrm{H}}\begin{pmatrix} a_k \\ b_k \\ c_k \\ d_k \end{pmatrix} = \begin{pmatrix} \mathfrak{s}\,\mathrm{i}\,\omega\,h_{r,k} \\ \mathfrak{s}\,\mathrm{i}\,\omega\,h_{\theta,k} \\ g_k \\ f_k \end{pmatrix}\,,$$

where the coefficient matrix $\mathbb{A}_k^{\mathbf{u},\mathrm{p},\mathrm{H}}$ is defined as:

$$\mathbb{A}_k^{\mathbf{u},\mathrm{p},\mathrm{H}} = \begin{pmatrix}
\mathsf{s}_{\mathrm{P}}^{-1}\,\omega\,\mathrm{J}_k'(\omega\,\mathsf{s}_{\mathrm{P}}\,\mathfrak{a}) & \mathsf{s}_{\mathrm{B}}^{-1}\,\omega\,\mathrm{J}_k'(\omega\,\mathsf{s}_{\mathrm{S}}\,\mathfrak{a}) & -\,\mathsf{s}_{\mathrm{S}}^{-2}\,\dfrac{\mathrm{i}k}{\mathfrak{a}}\mathrm{J}_k(\omega\,\mathsf{s}_{\mathrm{S}}\,\mathfrak{a}) & -\,\mathsf{s}_{\mathrm{EM}}^{-2}\,\dfrac{\mathrm{i}k}{\mathfrak{a}}\mathrm{J}_k(\omega\,\mathsf{s}_{\mathrm{EM}}\,\mathfrak{a}) \\
\mathsf{s}_{\mathrm{P}}^{-2}\,\dfrac{\mathrm{i}k}{\mathfrak{a}}\mathrm{J}_k(\omega\,\mathsf{s}_{\mathrm{P}}\,\mathfrak{a}) & \mathsf{s}_{\mathrm{B}}^{-2}\,\dfrac{\mathrm{i}k}{\mathfrak{a}}\mathrm{J}_k(\omega\,\mathsf{s}_{\mathrm{B}}\,\mathfrak{a}) & \mathsf{s}_{\mathrm{S}}^{-1}\,\omega\,\mathrm{J}_k'(\omega\,\mathsf{s}_{\mathrm{S}}\,\mathfrak{a}) & \mathsf{s}_{\mathrm{EM}}^{-1}\,\omega\,\mathrm{J}_k'(\omega\,\mathsf{s}_{\mathrm{EM}}\,\mathfrak{a}) \\
-M\left(\mathcal{W}_{\mathrm{P}} \;+\; \alpha\right)\mathrm{J}_k(\omega\,\mathsf{s}_{\mathrm{P}}\,\mathfrak{a}) & -M\left(\mathcal{W}_{\mathrm{B}} \;+\; \alpha\right)\mathrm{J}_k(\omega\,\mathsf{s}_{\mathrm{B}}\,\mathfrak{a}) & 0 & 0 \\
0 & 0 & \dfrac{\mathfrak{s}\,\mathrm{i}}{\omega\,\mu_0}\,\mathcal{E}_{\mathrm{S}}\,\mathrm{J}_k(\omega\,\mathsf{s}_{\mathrm{S}}\,\mathfrak{a}) & \dfrac{\mathfrak{s}\,\mathrm{i}}{\omega\,\mu_0}\,\mathcal{E}_{\mathrm{EM}}\,\mathrm{J}_k(\omega\,\mathsf{s}_{\mathrm{EM}}\,\mathfrak{a})
\end{pmatrix}. \tag{6.22}$$

As before, the uniqueness of the problem is characterized by the value of the determinant of $\mathbb{A}_k^{\mathbf{u},\mathrm{p},\mathrm{H}}$. There is uniqueness of the problem if the matrix $\mathbb{A}_k^{\mathbf{u},\mathrm{p},\mathrm{H}}$ can be inverted, i.e.the determinant of $\mathbb{A}_k^{\mathbf{w},\boldsymbol{\tau},\boldsymbol{E}}$ does not vanish. In the numerical experiments (Section 6.2.3), we investigate the value of the determinant of $\mathbb{A}_k^{\mathbf{u},\mathrm{p},\mathrm{H}}$ for the first modes k on a large range of frequency.

Definition 6.3. We define the pulsation ω as a type 8 boundary conditions eigenvalue if the system of equations (5.3) associated with the boundary conditions

$$\begin{aligned} \mathbf{u} &= 0 \quad , \quad \text{on } \partial\mathbb{B}_{(0,\mathfrak{a})} \, , \\ \mathrm{p} &= 0 \quad , \quad \text{on } \partial\mathbb{B}_{(0,\mathfrak{a})} \, , \\ \mathrm{H} &= 0 \quad , \quad \text{on } \partial\mathbb{B}_{(0,\mathfrak{a})} \, , \end{aligned}$$

admits a solution ($\mathbf{u}$, p, H) such that $\mathbf{u} \neq 0$, $\mathrm{p} \neq 0$, $\mathrm{H} \neq 0$. This also means that $\det \mathbb{A}_k^{\mathbf{u},\mathrm{p},\mathrm{H}}(\omega) = 0$, where $\mathbb{A}_k^{\mathbf{u},\mathrm{p},\mathrm{H}}$ is the coefficient matrix defined in equation (6.22).

6.2.3 Numerical tests on bounded domain

The objective of this section is to determine if the uniqueness of the problem is guaranteed. For that purpose, we study the value of the determinant of the coefficient matrices. If the determinant is equal to zero, we cannot invert the matrix, and this means that the frequency is a eigenvalue. We will investigate the invertibility of the coefficient matrices $\mathbb{A}_k^{\mathbf{u},\mathrm{p},\mathrm{H}}$ and $\mathbb{A}_k^{\mathbf{w},\boldsymbol{\tau},\boldsymbol{E}}$ for the first modes $k = 0, ..., 5$, by looking at the absolute value of their determinant. For the test, we consider the disc $\mathbb{B}_{(0,\mathfrak{a})}$ with $\mathfrak{a} = 1\mathrm{m}$. From Section (5.4), we have seen that we can use 8 types of boundary conditions. Here we only present tests for types 1 and 8. The corresponding coefficient matrices are given in equations (6.22) and (6.20). We will consider a range $[0, 10^4]$ m.s^{-1} for $\omega\mathfrak{a}$. We run the tests for a material composed of sand. The characteristics of the materials are given in Table 5.2. From Figures 6.1 and 6.2, we do not observe the presence of generalized eigenvalues in geophysical range 10^4 m.s^{-1}, for both boundary conditions of type 1 and 8. The global trend of the curves is growing, with small oscillations. Here, no problem of invertibility of the matrix has been identified in the considered range of frequency.

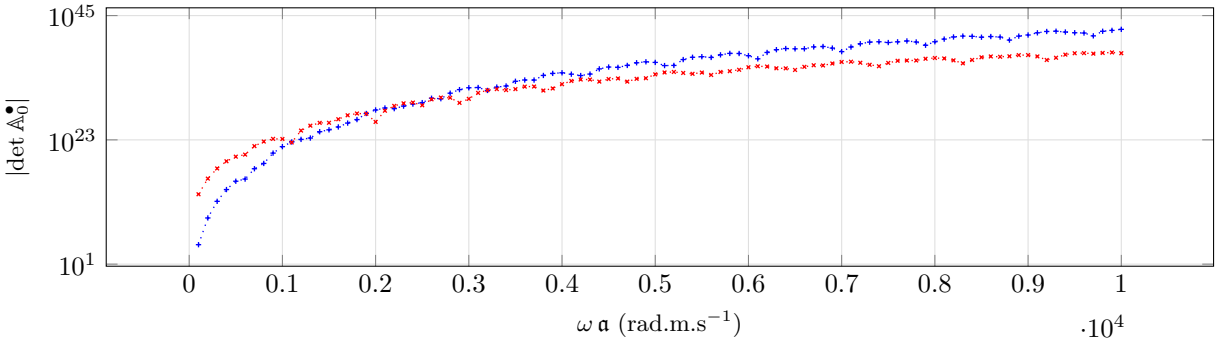

(a) Mode $k = 0$

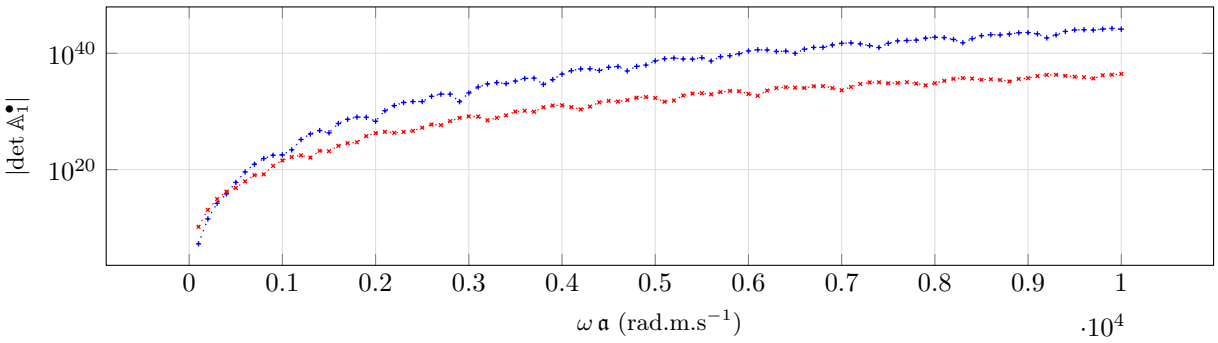

(b) Mode $k = 1$

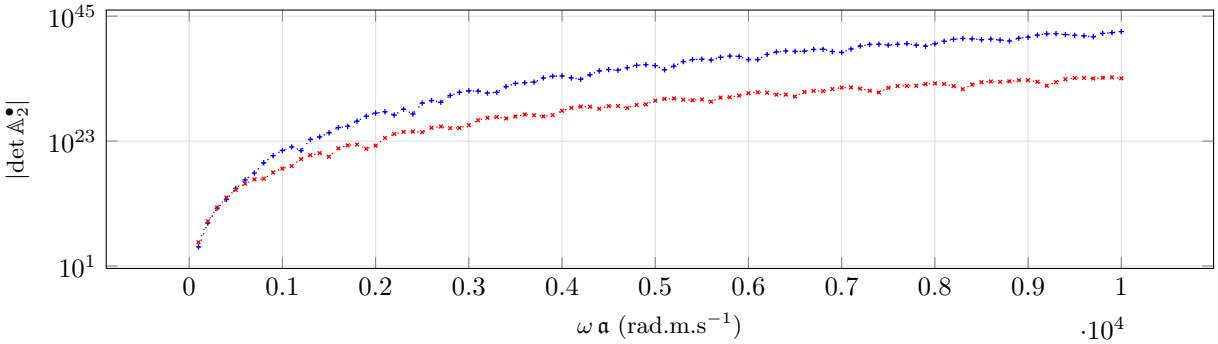

(c) Mode $k = 2$

Figure 6.1: Module of determinant of the coefficient matrix (log scale) in a bounded domain for modes 0 to 2 for sand. The matrices corresponding with boundary conditions 1 and 8: $\mathbb{A}_k^{\mathbf{w},\boldsymbol{\tau},\boldsymbol{E}}$ (6.20) in blue ···+··· and $\mathbb{A}_k^{\mathbf{u},\mathrm{p},\mathrm{H}}$ (6.22) in red ···×···.

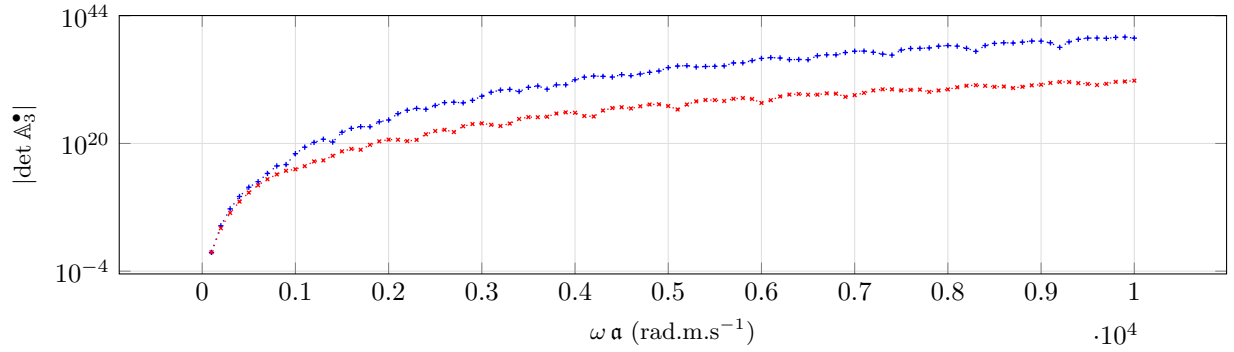

(a) Mode $k = 3$

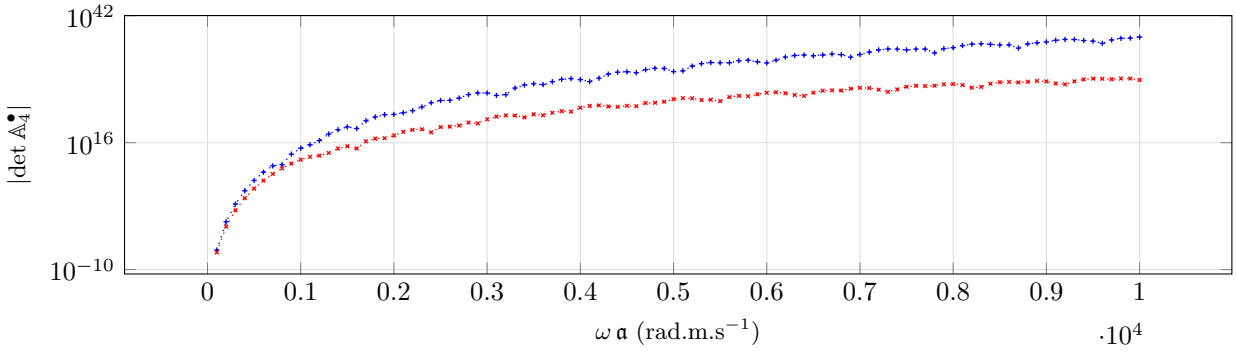

(b) Mode $k = 4$

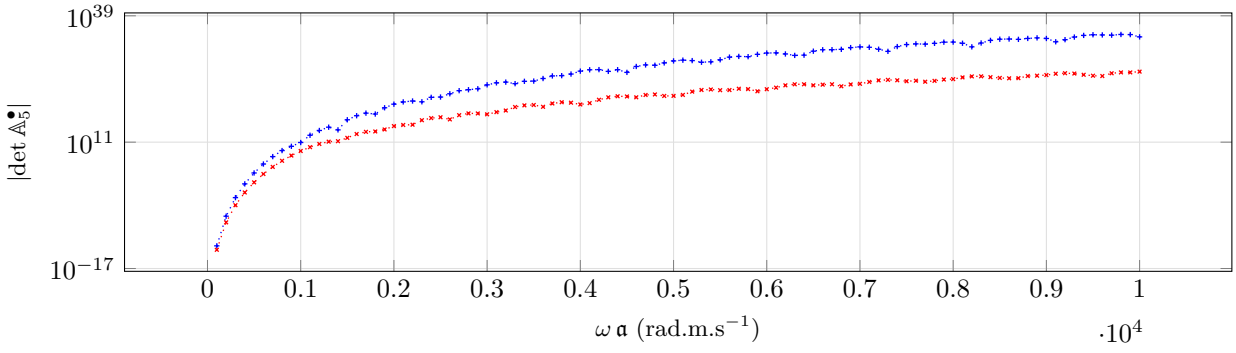

(c) Mode $k = 5$

Figure 6.2: Module of determinant of the coefficient matrix (log scale) in a bounded domain for k in $3:5$ for sand. The matrices corresponding with boundary conditions 1 and 8: $\mathbb{A}_k^{\mathbf{w},\boldsymbol{\tau},\boldsymbol{E}}$ (6.20)in blue ···+··· and $\mathbb{A}_k^{\mathbf{u},\mathrm{p},\mathrm{H}}$ (6.22) in red ···×···.

6.3 Scattering of an impenetrable obstacle by a plane wave

We consider the scattering of a plane-wave by an impenetrable circular obstacle, as described in Figure 6.3. The total wave is a superposition of the incident plane wave and the reflected wave. We define $\mathfrak{U}^\bullet = (\mathbf{u}, \mathbf{w}, \boldsymbol{\tau}, \mathrm{p}, \boldsymbol{E}, \mathrm{H}, \boldsymbol{J})$ for $\bullet = \mathrm{pw}, \mathrm{ref}$. Both $\mathfrak{U}^{\mathrm{pw}}$ and $\mathfrak{U}^{\mathrm{ref}}$ satisfy Pride equations (5.3) in $\mathbb{R}^2 \setminus \mathbb{B}_{(0,\mathfrak{a})}$. The potentials satisfy Helmholtz equation (6.15) and the unknowns $\mathbf{u}$, $\mathbf{w}$, $\boldsymbol{\tau}$, p, $\boldsymbol{E}$, H, $\boldsymbol{J}$ are given by equation (6.14). The unknown is the scattered wave that is outgoing, this means that it satisfies the outgoing Sommerfeld radiation condition (2.22), and is in addition uniquely determined by how the obstacle scatters the plane wave. In this configuration, the potentials corresponding to the reflected wave are given in equation (6.17):

$$\begin{aligned}
\chi_{\mathrm{P}}(r,\theta) &= \sum_{k\in\mathbb{Z}} a_k \, \mathrm{H}_k^{(1)}(\omega\, \mathsf{s}_{\mathrm{P}}\, r)\; e^{\mathrm{i}\, k\, \theta}\,, \\
\chi_{\mathrm{B}}(r,\theta) &= \sum_{k\in\mathbb{Z}} b_k \, \mathrm{H}_k^{(1)}(\omega\, \mathsf{s}_{\mathrm{B}}\, r)\; e^{\mathrm{i}\, k\, \theta}\,, \\
\chi_{\mathrm{S}}(r,\theta) &= \sum_{k\in\mathbb{Z}} c_k \, \mathrm{H}_k^{(1)}(\omega\, \mathsf{s}_{\mathrm{S}}\, r)\; e^{\mathrm{i}\, k\, \theta}\,, \\
\chi_{\mathrm{EM}}(r,\theta) &= \sum_{k\in\mathbb{Z}} d_k \, \mathrm{H}_k^{(1)}(\omega\, \mathsf{s}_{\mathrm{EM}}\, r)\; e^{\mathrm{i}\, k\, \theta}\,.
\end{aligned}$$

The series coefficients a_k, b_k, c_k, d_k are then determined by the boundary conditions imposed on $\partial\mathbb{B}_{(0,\mathfrak{a})}$, which are one of the 8 conditions given in Section 5.4. Here we only detail the solutions for boundary conditions of type 1 and 8. The others are combinations of the two presented.

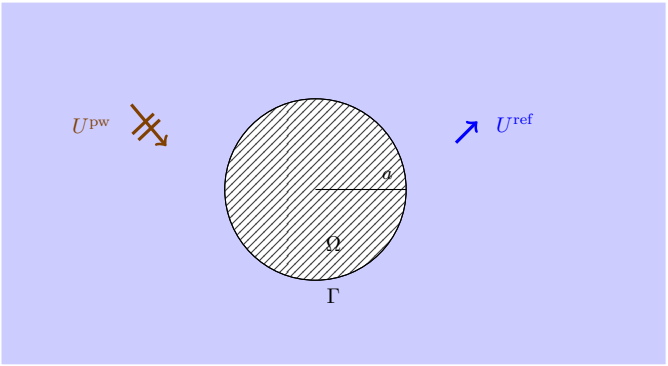

Figure 6.3: Scattering of a plane wave by an impenetrable solid inclusion. The inclusion occupies the domain denoted by Ω. The cross section of the inclusion is a disc of radius $\mathfrak{a}$. How the obstacle scatters the plane wave is mathematically described by boundary conditions, for example (5.10a) or (5.10b).

6.3.1 Boundary conditions of type 1

With boundary conditions of type 1, the unknowns solve the poroelastic problem:

$$\begin{cases}
\mathfrak{U}^{\mathrm{ref}} \text{ solves Pride equations (5.3) in } \mathbb{R}^2 \setminus \Omega\,; \\
\mathfrak{U}^{\mathrm{ref}} \text{ is outgoing by definition (2.22);} \\
\text{Boundary conditions} \\
\quad \mathbf{w}^{\mathrm{pw}} \cdot \mathbf{n} + \mathbf{w}^{\mathrm{ref}} \cdot \mathbf{n} = 0\,, \quad \text{on } \partial\mathbb{B}_{(0,\mathfrak{a})}\,, \\
\quad \boldsymbol{\tau}^{\mathrm{pw}} \cdot \mathbf{n} + \boldsymbol{\tau}^{\mathrm{ref}} \cdot \mathbf{n} = 0\,, \quad \text{on } \partial\mathbb{B}_{(0,\mathfrak{a})}\,, \\
\quad \boldsymbol{n} \times \boldsymbol{E}^{\mathrm{pw}} + \boldsymbol{n} \times \boldsymbol{E}^{\mathrm{ref}} = 0\,, \quad \text{on } \partial\mathbb{B}_{(0,\mathfrak{a})}\,.
\end{cases}$$

In circular geometry, $\boldsymbol{n} = \mathbf{e}_r$, which means,

$$\mathbf{w} \cdot \boldsymbol{n} = \mathrm{w}_r\,, \qquad \boldsymbol{\tau}\, \boldsymbol{n} = \tau_{rr}\, \mathbf{e}_r + \tau_{r\theta}\, \mathbf{e}_\theta\,, \qquad \boldsymbol{n} \times \boldsymbol{E} = E_\theta\,.$$

Hence, in the following, we do not detail all the components of the vectors $\mathbf{w}$, $\boldsymbol{E}$ and the tensor $\boldsymbol{\tau}$, and we focus on the expressions of w_r, E_θ, τ_{rr} and $\tau_{r\theta}$. For convenience, the boundary conditions are written as:

$$\mathfrak{s}\,\mathrm{i}\,\omega\,\mathrm{w}_r^{\mathrm{ref}} = -\,\mathfrak{s}\,\mathrm{i}\,\omega\,\mathbf{w}_r^{\mathrm{pw}}\,,\quad \omega^2\,\tau_{rr}^{\mathrm{ref}} = -\,\omega^2\,\tau_{rr}^{\mathrm{pw}}\,,\quad \omega^2\,\tau_{r\theta} = \omega^2\,\tau_{r\theta}^{\mathrm{pw}}\,,\quad \omega^2\,\boldsymbol{E}_\theta^{\mathrm{ref}} = -\,\omega^2\,\boldsymbol{E}_\theta^{\mathrm{pw}}\,,\quad \text{on } \partial\mathbb{B}_{(0,\mathfrak{a})}\,.$$

Next we expand the coefficients of each component in Fourier series. We have for the right hand-side,

$$\mathbf{w}_r^{\mathrm{pw}} = \sum_{k\in\mathbb{Z}} \mathbf{w}_{r,k}^{\mathrm{pw}}\,e^{\mathrm{i}\,k\,\theta}\,,\quad \tau_{rr}^{\mathrm{pw}} = \sum_{k\in\mathbb{Z}} \tau_{rr,k}^{\mathrm{pw}}\,e^{\mathrm{i}\,k\,\theta}\,,\quad \tau_{r\theta}^{\mathrm{pw}} = \sum_{k\in\mathbb{Z}} \tau_{r\theta,k}^{\mathrm{pw}}\,e^{\mathrm{i}\,k\,\theta}\,,\quad E_\theta^{\mathrm{pw}} = \sum_{k\in\mathbb{Z}} E_{\theta,k}^{\mathrm{pw}}\,e^{\mathrm{i}\,k\,\theta}\,,$$

and for the unknowns:

$$\mathrm{w}_r^{\mathrm{ref}} = \sum_{k\in\mathbb{Z}} \mathrm{w}_{r,k}^{\mathrm{ref}}\,e^{\mathrm{i}\,k\,\theta}\,,\quad \tau_{rr}^{\mathrm{ref}} = \sum_{k\in\mathbb{Z}} \tau_{rr,k}^{\mathrm{ref}}\,e^{\mathrm{i}\,k\,\theta}\,,\quad \tau_{r\theta}^{\mathrm{ref}} = \sum_{k\in\mathbb{Z}} \tau_{r\theta,k}^{\mathrm{ref}}\,e^{\mathrm{i}\,k\,\theta}\,,\quad E_\theta^{\mathrm{ref}} = \sum_{k\in\mathbb{Z}} E_{\theta,k}^{\mathrm{ref}}\,e^{\mathrm{i}\,k\,\theta}\,.$$

Using the expansion of the unknowns in terms of potentials (6.14), we have for mode $k\in\mathbb{Z}$:

$$\begin{aligned}
\mathfrak{s}\,\mathrm{i}\,\omega\,\mathrm{w}_{r,k} =& a_k\,\frac{\mathcal{W}_{\mathrm{P}}}{\mathsf{s}_{\mathrm{P}}}\,\omega\,\mathrm{H}_k^{(1)'}(\omega\,\mathsf{s}_{\mathrm{P}}\,r)\,e^{\mathrm{i}k\theta} + b_k\,\frac{\mathcal{W}_{\mathrm{B}}}{\mathsf{s}_{\mathrm{B}}}\,\omega\,\mathrm{H}_k^{(1)'}(\omega\,\mathsf{s}_{\mathrm{B}}\,r)\,e^{\mathrm{i}k\theta}\\
&- c_k\,\frac{\mathcal{W}_{\mathrm{S}}}{\mathsf{s}_{\mathrm{S}}^2}\,\frac{\mathrm{i}k}{r}\mathrm{H}_k^{(1)}(\omega\,\mathsf{s}_{\mathrm{S}}\,r)\,e^{\mathrm{i}k\theta} - d_k\,\frac{\mathcal{W}_{\mathrm{EM}}}{\mathsf{s}_{\mathrm{EM}}^2}\,\frac{\mathrm{i}k}{r}\mathrm{H}_k^{(1)}(\omega\,\mathsf{s}_{\mathrm{EM}}\,r)\,e^{\mathrm{i}k\theta}\,,\\
\omega^2\tau_{rr,k} =& -\frac{2\mu_{\mathrm{fr}}\,\omega}{\mathsf{s}_{\mathrm{P}}\,r}\,a_k\,\mathrm{H}_{k+1}^{(1)}(\omega\,\mathsf{s}_{\mathrm{P}}\,r)\,e^{\mathrm{i}\,k\,\theta} + \frac{2\,\mu_{\mathrm{fr}}\,k}{\mathsf{s}_{\mathrm{P}}^2\,r^2}\,a_k\,\mathrm{H}_k^{(1)}(\omega\,\mathsf{s}_{\mathrm{P}}\,r)\,e^{\mathrm{i}\,k\,\theta} + 2\mu_{\mathrm{fr}}\,a_k\,\omega^2\,\mathrm{H}_k^{(1)}(\omega\,\mathsf{s}_{\mathrm{P}}\,r)\,e^{\mathrm{i}\,k\,\theta}\\
&-\frac{2\,\mu_{\mathrm{fr}}\,k^2}{\mathsf{s}_{\mathrm{P}}^2\,r^2}\,a_k\,\mathrm{H}_k^{(1)}(\omega\,\mathsf{s}_{\mathrm{P}}\,r)\,e^{\mathrm{i}\,k\,\theta} - \frac{2\,\mu_{\mathrm{fr}}\,\omega}{\mathsf{s}_{\mathrm{B}}\,r}\,b_k\,\mathrm{H}_{k+1}^{(1)}(\omega\,\mathsf{s}_{\mathrm{B}}\,r)\,e^{\mathrm{i}\,k\,\theta} + \frac{2\mu_{\mathrm{fr}}\,k}{\mathsf{s}_{\mathrm{B}}^2\,r^2}b_k\,\mathrm{H}_k^{(1)}(\omega\,\mathsf{s}_{\mathrm{B}}\,r)\,e^{\mathrm{i}\,k\,\theta}\\
&+2\mu_{\mathrm{fr}}\,b_k\,\omega^2\,\mathrm{H}_k^{(1)}(\omega\,\mathsf{s}_{\mathrm{B}}\,r)\,e^{\mathrm{i}\,k\,\theta} - \frac{2\,\mu_{\mathrm{fr}}\,k^2}{\mathsf{s}_{\mathrm{B}}^2\,r^2}b_k\,\mathrm{H}_k^{(1)}(\omega\,\mathsf{s}_{\mathrm{B}}\,r)\,e^{\mathrm{i}\,k\,\theta} + \frac{2\,\mu_{\mathrm{fr}}}{\mathsf{s}_{\mathrm{S}}^2 r}c_k\,\omega\,\mathsf{s}_{\mathrm{S}}\,\mathrm{i}k\,\mathrm{H}_k^{(1)'}(\omega\,\mathsf{s}_{\mathrm{S}}\,r)\,e^{\mathrm{i}\,k\,\theta}\\
&+\frac{2\,\mu_{\mathrm{fr}}}{\mathsf{s}_{\mathrm{EM}}^2\,r}\,d_k\,\omega\,\mathsf{s}_{\mathrm{EM}}\,\mathrm{i}k\,\mathrm{H}_k^{(1)'}(\,\omega\,\mathsf{s}_{\mathrm{EM}}\,r)\,e^{\mathrm{i}\,k\,\theta} + \omega^2\,\left(-\frac{2}{3}\mu_{\mathrm{fr}} + \mathrm{k}_{\mathrm{fr}} + M\alpha^2 + \alpha\,M\mathcal{W}_{\mathrm{P}}\right)\,a_k\,\mathrm{H}_k^{(1)}(\omega\,\mathsf{s}_{\mathrm{P}}\,r)\,e^{\mathrm{i}\,k\,\theta}\\
&+\omega^2\,\left(-\frac{2}{3}\mu_{\mathrm{fr}} + \mathrm{k}_{\mathrm{fr}} + M\alpha^2 + \alpha\,M\mathcal{W}_{\mathrm{B}}\right)\,b_k\,\mathrm{H}_k^{(1)}(\omega\,\mathsf{s}_{\mathrm{B}}\,r)\,e^{\mathrm{i}\,k\,\theta}\,,\\
\omega^2\,\tau_{r\theta,k} =& -\frac{2\mu_{\mathrm{fr}}\omega\,\mathrm{i}k}{r\mathsf{s}_{\mathrm{P}}}a_k\mathrm{H}_k^{(1)'}(\omega\,\mathsf{s}_{\mathrm{P}}r)\,e^{\mathrm{i}\,k\,\theta} + \frac{2\mathrm{i}\,\mu_{\mathrm{fr}}k}{r^2\,\mathsf{s}_{\mathrm{P}}^2}a_k\mathrm{H}_k^{(1)}(\omega\,\mathsf{s}_{\mathrm{P}}\,r)\,e^{\mathrm{i}\,k\,\theta} - \frac{2\mu_{\mathrm{fr}}\omega\,\mathrm{i}\,k}{r\,\mathsf{s}_{\mathrm{B}}}b_k\mathrm{H}_k^{(1)'}(\omega\,\mathsf{s}_{\mathrm{B}}r)\,e^{\mathrm{i}\,k\,\theta}\\
&+\frac{2\,\mathrm{i}\,\mu_{\mathrm{fr}}\,k}{r^2\mathsf{s}_{\mathrm{B}}^2}\,b_k\,\mathrm{H}_k^{(1)}(\omega\,\mathsf{s}_{\mathrm{B}}r)\,e^{\mathrm{i}\,k\,\theta} - \frac{\mu_{\mathrm{fr}}\,k^2}{r^2\,\mathsf{s}_{\mathrm{S}}^2}\,c_k\,\mathrm{H}_k^{(1)}(\omega\,\mathsf{s}_{\mathrm{S}}\,r)\,e^{\mathrm{i}\,k\,\theta} + \frac{\mu_{\mathrm{fr}}\,\omega}{r\,\mathsf{s}_{\mathrm{S}}}\,c_k\,\mathrm{H}_k^{(1)'}(\omega\,\mathsf{s}_{\mathrm{S}}\,r)\,e^{\mathrm{i}\,k\,\theta}\\
&-\mu_{\mathrm{fr}}\,\frac{\omega}{\mathsf{s}_{\mathrm{S}}\,r}\,c_k\,\mathrm{H}_{k+1}^{(1)}(\omega\,\mathsf{s}_{\mathrm{S}}\,r)\,e^{\mathrm{i}\,k\,\theta} + \mu_{\mathrm{fr}}\,\frac{k}{\mathsf{s}_{\mathrm{S}}^2\,r^2}c_k\,\mathrm{H}_k^{(1)}(\omega\,\mathsf{s}_{\mathrm{S}}\,r)\,e^{\mathrm{i}\,k\,\theta}\\
&+\omega^2\,c_k\,\mathrm{H}_k^{(1)}(\omega\,\mathsf{s}_{\mathrm{S}}\,r)\,e^{\mathrm{i}\,k\,\theta} - \mu_{\mathrm{fr}}\,\frac{k^2}{\mathsf{s}_{\mathrm{S}}^2\,r^2}\,c_k\,\mathrm{H}_k^{(1)}(\omega\,\mathsf{s}_{\mathrm{S}}\,r)\,e^{\mathrm{i}\,k\,\theta}\\
&-\frac{\mu_{\mathrm{fr}}\,k^2}{r^2\,\mathsf{s}_{\mathrm{EM}}^2}\,d_k\,\mathrm{H}_k^{(1)}(\omega\,\mathsf{s}_{\mathrm{EM}}\,r)\,e^{\mathrm{i}\,k\,\theta} + \frac{\mu_{\mathrm{fr}}\,\omega}{r\,\mathsf{s}_{\mathrm{EM}}}\,d_k\,\mathrm{H}_k^{(1)'}(\omega\,\mathsf{s}_{\mathrm{EM}}\,r)\,e^{\mathrm{i}\,k\,\theta}\\
&-\mu_{\mathrm{fr}}\,\frac{\omega}{\mathsf{s}_{\mathrm{EM}}\,r}\,d_k\,\mathrm{H}_{k+1}^{(1)}(\omega\,\mathsf{s}_{\mathrm{EM}}\,r)\,e^{\mathrm{i}\,k\,\theta} + \mu_{\mathrm{fr}}\,\frac{k}{\mathsf{s}_{\mathrm{EM}}^2\,r^2}d_k\,\mathrm{H}_k^{(1)}(\omega\,\mathsf{s}_{\mathrm{EM}}\,r)\,e^{\mathrm{i}\,k\,\theta}\\
&+\omega^2\,d_k\,\mathrm{H}_k^{(1)}(\omega\,\mathsf{s}_{\mathrm{EM}}\,r)\,e^{\mathrm{i}\,k\,\theta} - \mu_{\mathrm{fr}}\,\frac{k^2}{\mathsf{s}_{\mathrm{EM}}^2\,r^2}\,d_k\,\mathrm{H}_k^{(1)}(\omega\,\mathsf{s}_{\mathrm{EM}}\,r)\,e^{\mathrm{i}\,k\,\theta}\,,\\
-\omega^2\,E_{\theta,k} =& a_k\,\mathcal{E}_{\mathrm{P}}\,\mathsf{s}_{\mathrm{P}}^{-2}\,\frac{\mathrm{i}k}{r}\mathrm{H}_k^{(1)}(\omega\,\mathsf{s}_{\mathrm{P}}\,r)e^{\mathrm{i}k\theta} + b_k\,\mathcal{E}_{\mathrm{B}}\,\mathsf{s}_{\mathrm{B}}^{-2}\,\frac{\mathrm{i}k}{r}\mathrm{H}_k^{(1)}(\omega\,\mathsf{s}_{\mathrm{B}}\,r)e^{\mathrm{i}k\theta}\\
&+ c_k\,\mathcal{E}_{\mathrm{S}}\,\mathsf{s}_{\mathrm{S}}^{-1}\,\omega\,\mathrm{H}_k^{(1)'}(\omega\,\mathsf{s}_{\mathrm{S}}\,r)e^{\mathrm{i}k\theta} + d_k\,\mathcal{E}_{\mathrm{EM}}\,\mathsf{s}_{\mathrm{EM}}^{-1}\,\omega\,\mathrm{H}_k^{(1)'}(\omega\,\mathsf{s}_{\mathrm{EM}}\,r)e^{\mathrm{i}k\theta}\,.
\end{aligned}$$

Imposing the boundary condition, we obtain a linear system satisfied by a_k, b_k, c_k, d_k in each mode k.

$$\mathbb{A}_k^{\mathbf{w},\boldsymbol{\tau},\boldsymbol{E}} \begin{pmatrix} a_k \\ b_k \\ c_k \\ d_k \end{pmatrix} = \begin{pmatrix} -\mathfrak{s}\,\mathrm{i}\,\omega\,\mathrm{w}_{r,k}^{\mathrm{pw}} \\ -\omega^2\,\tau_{rr,k}^{\mathrm{pw}} \\ -\omega^2\,\tau_{r\theta,k}^{\mathrm{pw}} \\ \omega^2\,E_{\theta,k}^{\mathrm{pw}} \end{pmatrix},$$

where the coefficients matrix is defined as:

$$\mathbb{A}_k^{\mathbf{w},\boldsymbol{\tau}} = \begin{pmatrix} A_{11} & A_{12} & A_{13} & A_{14} \\ A_{21} & A_{22} & A_{23} & A_{24} \\ A_{31} & A_{32} & A_{33} & A_{34} \\ A_{41} & A_{42} & A_{43} & A_{44} \end{pmatrix} \tag{6.23}$$

with

$$A_{11} = \frac{\mathcal{W}_{\mathrm{P}}}{\mathsf{s}_{\mathrm{P}}}\,\omega\,\mathrm{H}_k^{(1)'}(\omega\,\mathsf{s}_{\mathrm{P}}\mathfrak{a}),\ A_{12} = \frac{\mathcal{W}_{\mathrm{B}}}{\mathsf{s}_{\mathrm{B}}}\,\omega\,\mathrm{H}_k^{(1)'}(\omega\,\mathsf{s}_{\mathrm{S}}\mathfrak{a}),\quad A_{13} = -\frac{\mathcal{W}_{\mathrm{S}}}{\mathsf{s}_{\mathrm{S}}^2}\frac{\mathrm{i}k}{r}\,\mathrm{H}_k^{(1)}(\omega\,\mathsf{s}_{\mathrm{S}}\mathfrak{a}),\ A_{14} = -\frac{\mathcal{W}_{\mathrm{EM}}}{\mathsf{s}_{\mathrm{EM}}^2}\frac{\mathrm{i}k}{r}\,\mathrm{H}_k^{(1)}(\omega\,\mathsf{s}_{\mathrm{EM}}\mathfrak{a}),$$

$$\begin{aligned} A_{21} = &-\frac{2\,\mu_{\mathrm{fr}}\,\omega}{\mathsf{s}_{\mathrm{P}}\,\mathfrak{a}}\,\mathrm{H}_{k+1}^{(1)}(\omega\,\mathsf{s}_{\mathrm{P}}\,\mathfrak{a})\,e^{\mathrm{i}\,k\,\theta} + \frac{2\,\mu_{\mathrm{fr}}\,k}{\mathsf{s}_{\mathrm{P}}^2\,\mathfrak{a}^2}\,\mathrm{H}_k^{(1)}(\omega\,\mathsf{s}_{\mathrm{P}}\,\mathfrak{a}) + 2\,\mu_{\mathrm{fr}}\,\omega^2\,\mathrm{H}_k^{(1)}(\omega\,\mathsf{s}_{\mathrm{P}}\,\mathfrak{a}) \\ &- \frac{2\,\mu_{\mathrm{fr}}\,k^2}{\mathsf{s}_{\mathrm{P}}^2\,\mathfrak{a}^2}\,\mathrm{H}_k^{(1)}(\omega\,\mathsf{s}_{\mathrm{P}}\,\mathfrak{a}) + \omega^2\left(-\frac{2}{3}\mu_{\mathrm{fr}} + \mathrm{k}_{\mathrm{fr}} + M\alpha^2 + \alpha\,M\mathcal{W}_{\mathrm{P}}\right)\mathrm{H}_k^{(1)}(\omega\,\mathsf{s}_{\mathrm{P}}\mathfrak{a}), \end{aligned}$$

$$\begin{aligned} A_{22} = &-\frac{2\,\mu_{\mathrm{fr}}\,\omega}{\mathsf{s}_{\mathrm{B}}\,\mathfrak{a}}\,\mathrm{H}_{k+1}^{(1)}(\omega\,\mathsf{s}_{\mathrm{B}}\,\mathfrak{a}) + \frac{2\,\mu_{\mathrm{fr}}\,k}{\mathsf{s}_{\mathrm{B}}^2\,\mathfrak{a}^2}\,\mathrm{H}_k^{(1)}(\omega\,\mathsf{s}_{\mathrm{B}}\,\mathfrak{a}) + 2\,\mu_{\mathrm{fr}}\,\omega^2\,\mathrm{H}_k^{(1)}(\omega\,\mathsf{s}_{\mathrm{B}}\,\mathfrak{a}) \\ &- \frac{2\,\mu_{\mathrm{fr}}\,k^2}{\mathsf{s}_{\mathrm{B}}^2\,\mathfrak{a}^2}\,\mathrm{H}_k^{(1)}(\omega\,\mathsf{s}_{\mathrm{B}}\,\mathfrak{a}) + \omega^2\left(-\frac{2}{3}\mu_{\mathrm{fr}} + \mathrm{k}_{\mathrm{fr}} + M\alpha^2 + \alpha\,M\mathcal{W}_{\mathrm{B}}\right)\mathrm{H}_k^{(1)}(\omega\,\mathsf{s}_{\mathrm{B}}\mathfrak{a}), \end{aligned}$$

and

$$A_{23} = \frac{2\mu_{\mathrm{fr}}}{\mathsf{s}_{\mathrm{S}}\mathfrak{a}}\,\omega\,\mathrm{i}k\,\mathrm{H}_k^{(1)'}(\omega\,\mathsf{s}_{\mathrm{S}}\mathfrak{a}),\quad A_{24} = \frac{2\mu_{\mathrm{fr}}}{\mathsf{s}_{\mathrm{EM}}\mathfrak{a}}\,\omega\,\mathrm{i}k\,\mathrm{H}_k^{(1)'}(\omega\,\mathsf{s}_{\mathrm{EM}}\mathfrak{a}),\quad A_{31} = -\frac{2\omega\,\mu_{\mathrm{fr}}\mathrm{i}k}{\mathfrak{a}\mathsf{s}_{\mathrm{P}}}\mathrm{H}_k^{(1)'}(\omega\,\mathsf{s}_{\mathrm{P}}\mathfrak{a}) + \frac{2\,\mu_{\mathrm{fr}}\mathrm{i}k}{\mathfrak{a}^2\mathsf{s}_{\mathrm{P}}^2}\mathrm{H}_k^{(1)}(\omega\,\mathsf{s}_{\mathrm{P}}\mathfrak{a}),$$

$$A_{32} = -\frac{2\omega\,\mu_{\mathrm{fr}}\mathrm{i}k}{\mathfrak{a}\mathsf{s}_{\mathrm{B}}}\mathrm{H}_k^{(1)'}(\omega\,\mathsf{s}_{\mathrm{B}}\mathfrak{a}) + \frac{2\mu_{\mathrm{fr}}\mathrm{i}k}{\mathfrak{a}^2\mathsf{s}_{\mathrm{B}}^2}\mathrm{H}_k^{(1)}(\omega\,\mathsf{s}_{\mathrm{B}}\mathfrak{a}),$$

$$\begin{aligned} A_{33} = &-\frac{k^2\mu_{\mathrm{fr}}}{\mathfrak{a}^2\mathsf{s}_{\mathrm{S}}^2}\mathrm{H}_k^{(1)}(\omega\,\mathsf{s}_{\mathrm{S}}\,\mathfrak{a}) + \frac{\omega\,\mu_{\mathrm{fr}}}{\mathfrak{a}\mathsf{s}_{\mathrm{S}}}\mathrm{H}_k^{(1)'}(\omega\,\mathsf{s}_{\mathrm{S}}\,\mathfrak{a}) - \frac{\omega}{\mathsf{s}_{\mathrm{S}}\,\mathfrak{a}}\,\mathrm{H}_{k+1}^{(1)}(\mathsf{s}_{\mathrm{S}}\,\mathfrak{a}) + \frac{k}{\mathsf{s}_{\mathrm{S}}^2\,\mathfrak{a}^2}\,\mathrm{H}_k^{(1)}(\omega\,\mathsf{s}_{\mathrm{S}}\,\mathfrak{a}), \\ &+ \omega^2\,\mathrm{H}_k^{(1)}(\omega\,\mathsf{s}_{\mathrm{S}}\,\mathfrak{a})\,e^{\mathrm{i}\,k\,\theta} - \frac{k^2}{\mathsf{s}_{\mathrm{S}}^2\,\mathfrak{a}^2}\,\mathrm{H}_k^{(1)}(\omega\,\mathsf{s}_{\mathrm{S}}\,\mathfrak{a}), \end{aligned}$$

$$\begin{aligned} A_{34} = &-\frac{k^2\mu_{\mathrm{fr}}}{\mathfrak{a}^2\mathsf{s}_{\mathrm{EM}}^2}\mathrm{H}_k^{(1)}(\omega\,\mathsf{s}_{\mathrm{EM}}\,\mathfrak{a}) + \frac{\omega\,\mu_{\mathrm{fr}}}{\mathfrak{a}\mathsf{s}_{\mathrm{EM}}}\mathrm{H}_k^{(1)'}(\omega\,\mathsf{s}_{\mathrm{EM}}\,\mathfrak{a}) - \frac{\omega}{\mathsf{s}_{\mathrm{EM}}\,\mathfrak{a}}\,\mathrm{H}_{k+1}^{(1)}(\mathsf{s}_{\mathrm{EM}}\,\mathfrak{a}) + \frac{k}{\mathsf{s}_{\mathrm{EM}}^2\,\mathfrak{a}^2}\,\mathrm{H}_k^{(1)}(\omega\,\mathsf{s}_{\mathrm{EM}}\,\mathfrak{a}), \\ &+ \omega^2\,\mathrm{H}_k^{(1)}(\omega\,\mathsf{s}_{\mathrm{EM}}\,\mathfrak{a})\,e^{\mathrm{i}\,k\,\theta} - \frac{k^2}{\mathsf{s}_{\mathrm{S}}^2\,\mathfrak{a}^2}\,\mathrm{H}_k^{(1)}(\omega\,\mathsf{s}_{\mathrm{EM}}\,\mathfrak{a}). \end{aligned}$$

6.3.2 Boundary conditions of type 8

With boundary conditions of type 8, the scattered wave solves the following system:

$$\begin{cases} \mathfrak{U}^{\mathrm{ref}} \text{ solves Pride equations (5.3) in } \mathbb{R}^2 \setminus \Omega\,; \\ \\ \mathfrak{U}^{\mathrm{ref}} \text{ is outgoing by definition (2.22) ;} \\ \\ \text{Boundary conditions} \\ \quad \mathbf{v}^{\mathrm{pw}} + \mathbf{v}^{\mathrm{ref}} = 0 \ \text{ on } \partial\mathbb{B}_{(0,\mathfrak{a})}\,, \\ \quad \mathrm{p}^{\mathrm{pw}} + \mathrm{p}^{\mathrm{ref}} = 0 \ \text{ on } \partial\mathbb{B}_{(0,\mathfrak{a})}\,, \\ \quad \mathrm{H}^{\mathrm{pw}} + \mathrm{H}^{\mathrm{ref}} = 0 \quad \text{on } \partial\mathbb{B}_{(0,\mathfrak{a})}\,. \end{cases}$$

In polar coordinates, we have $\mathbf{u}^{\mathrm{pw}} = \mathrm{u}_r^{\mathrm{pw}}\mathbf{e}_r + \mathrm{u}_\theta^{\mathrm{pw}}\,\mathbf{e}_\theta$ and $\mathbf{u}^{\mathrm{ref}} = \mathbf{u}_r^{\mathrm{ref}}\mathbf{e}_r + \mathbf{u}_\theta^{\mathrm{ref}}\,\mathbf{e}_\theta$. For convenience, the boundary conditions are written as:

$$\mathfrak{s}\,\mathrm{i}\,\omega\,\mathrm{u}_r^{\mathrm{ref}} = -\,\mathfrak{s}\,\mathrm{i}\,\omega\,\mathrm{u}_r^{\mathrm{pw}}\,, \quad \mathfrak{s}\,\mathrm{i}\,\omega\,\mathrm{u}_\theta^{\mathrm{ref}} = -\,\mathfrak{s}\,\mathrm{i}\,\omega\,\mathrm{u}_\theta^{\mathrm{pw}}\,, \quad \mathrm{p}^{\mathrm{ref}} = -\,\mathrm{p}^{\mathrm{pw}}\,, \quad \mathrm{H}^{\mathrm{ref}} = -\,\mathrm{H}^{\mathrm{pw}} \quad , \quad \partial\mathbb{B}_{(0,\mathfrak{a})}\,. \tag{6.24}$$

We expand the coefficient of each component in Fourier series. For the right hand-side we have,

$$\mathrm{u}_r^{\mathrm{pw}} = \sum_{k\in\mathbb{Z}} \mathrm{u}_{r,k}^{\mathrm{pw}}\, e^{\mathrm{i}\,k\,\theta}\,, \quad \mathrm{u}_\theta^{\mathrm{pw}} = \sum_{k\in\mathbb{Z}} \mathrm{u}_{\theta,k}^{\mathrm{pw}}\, e^{\mathrm{i}\,k\,\theta}\,, \quad \mathrm{p}^{\mathrm{pw}} = \sum_{k\in\mathbb{Z}} \mathrm{p}_k^{\mathrm{pw}}\, e^{\mathrm{i}\,k\,\theta}\,, \quad \mathrm{H}^{\mathrm{pw}} = \sum_{k\in\mathbb{Z}} \boldsymbol{H}_k^{\mathrm{pw}}\, e^{\mathrm{i}\,k\,\theta}\,,$$

and for the unknowns:

$$\mathrm{u}_r^{\mathrm{ref}} = \sum_{k\in\mathbb{Z}} \mathrm{u}_{r,k}^{\mathrm{ref}}\, e^{\mathrm{i}\,k\,\theta}\,, \quad \mathrm{u}_\theta^{\mathrm{ref}} = \sum_{k\in\mathbb{Z}} \mathrm{u}_{\theta,k}^{\mathrm{ref}}\, e^{\mathrm{i}\,k\,\theta}\,, \quad \mathrm{p}_k^{\mathrm{ref}} = \sum_{k\in\mathbb{Z}} \mathrm{p}_k^{\mathrm{ref}}\, e^{\mathrm{i}\,k\,\theta}\,, \quad \mathrm{H}_k^{\mathrm{ref}} = \sum_{k\in\mathbb{Z}} \mathrm{H}_k^{\mathrm{ref}}\, e^{\mathrm{i}\,k\,\theta}\,.$$

Using the expansions of the unknowns given in equation (6.14), we have:

$$\begin{aligned}
\mathfrak{s}\,\mathrm{i}\,\omega\,\mathrm{u}_{r,k} &= a_k\,\mathrm{s}_{\mathrm{P}}^{-1}\,\omega\,\mathrm{H}_k^{(1)'}(\omega\,\mathrm{s}_{\mathrm{P}}\,r)e^{\mathrm{i}k\theta} + b_k\,\mathrm{s}_{\mathrm{B}}^{-1}\,\omega\,\mathrm{H}_k^{(1)'}(\omega\,\mathrm{s}_{\mathrm{B}}\,r)e^{\mathrm{i}k\theta} - c_k\,\mathrm{s}_{\mathrm{S}}^{-2}\,\frac{\mathrm{i}k}{r}\mathrm{H}_k^{(1)}(\omega\,\mathrm{s}_{\mathrm{S}}\,r)e^{\mathrm{i}k\theta} \\
&\quad - d_k\,\mathrm{s}_{\mathrm{EM}}^{-2}\,\frac{\mathrm{i}k}{r}\mathrm{H}_k^{(1)}(\omega\,\mathrm{s}_{\mathrm{EM}}\,r)e^{\mathrm{i}k\theta}\,, \\
\mathfrak{s}\,\mathrm{i}\,\omega\,\mathrm{u}_{\theta,k} &= a_k\,\mathrm{s}_{\mathrm{P}}^{-2}\,\frac{\mathrm{i}k}{r}\mathrm{H}_k^{(1)}(\omega\,\mathrm{s}_{\mathrm{P}}\,r)e^{\mathrm{i}k\theta} + b_k\,\mathrm{s}_{\mathrm{B}}^{-2}\,\frac{\mathrm{i}k}{r}\mathrm{H}_k^{(1)}(\omega\,\mathrm{s}_{\mathrm{B}}\,r)e^{\mathrm{i}k\theta} + c_k\,\mathrm{s}_{\mathrm{S}}^{-1}\,\omega\,\mathrm{H}_k^{(1)'}(\omega\,\mathrm{s}_{\mathrm{S}}\,r)e^{\mathrm{i}k\theta} \\
&\quad + d_k\,\mathrm{s}_{\mathrm{EM}}^{-1}\,\omega\,\mathrm{H}_k^{(1)'}(\omega\,\mathrm{s}_{\mathrm{EM}}\,r)e^{\mathrm{i}k\theta}\,, \\
\mathrm{p}_k &= -\,a_k\,M\,\big(\mathcal{W}_{\mathrm{P}} + \alpha\big)\,\mathrm{H}_k^{(1)}(\omega\,\mathrm{s}_{\mathrm{P}}\,r)\,e^{\mathrm{i}\,k\,\theta} - b_k\,M\,\big(\mathcal{W}_{\mathrm{B}} + \alpha\big)\,\mathrm{H}_k^{(1)}(\omega\,\mathrm{s}_{\mathrm{P}}\,r)\,e^{\mathrm{i}\,k\,\theta}\,, \\
\mathrm{H}_k &= c_k\,\frac{\mathfrak{s}\,\mathrm{i}}{\omega\,\mu_0}\,\mathcal{E}_{\mathrm{S}}\,\mathrm{H}_k^{(1)}(\omega\,\mathrm{s}_{\mathrm{S}}\,r)\;e^{\mathrm{i}\,k\,\theta} + d_k\,\frac{\mathfrak{s}\,\mathrm{i}}{\omega\,\mu_0}\,\mathcal{E}_{\mathrm{EM}}\,\mathrm{H}_k^{(1)}(\omega\,\mathrm{s}_{\mathrm{EM}}\,r)\,e^{\mathrm{i}\,k\,\theta}\,.
\end{aligned}$$

Imposing (6.24), we obtain the following linear system satisfied by a_k, b_k, c_k in each mode k:

$$\mathbb{A}_k^{\mathbf{u},\mathrm{p},\mathrm{H}} \begin{pmatrix} a_k \\ b_k \\ c_k \\ d_k \end{pmatrix} = \begin{pmatrix} -\mathfrak{s}\,\mathrm{i}\,\omega\,\mathrm{u}_{r,k}^{\mathrm{pw}} \\ -\mathfrak{s}\,\mathrm{i}\,\omega\,\mathrm{u}_{\theta,k}^{\mathrm{pw}} \\ -\mathrm{p}_k^{\mathrm{pw}} \\ -\mathrm{H}_k^{\mathrm{pw}} \end{pmatrix},$$

where the coefficients matrix is defined as:

$$\mathbb{A}_k^{\mathbf{u},\mathrm{p},\mathrm{H}} = \begin{pmatrix} \mathrm{s}_{\mathrm{P}}^{-1}\,\omega\,\mathrm{H}_k^{(1)'}(\omega\,\mathrm{s}_{\mathrm{P}}\,\mathfrak{a}) & \mathrm{s}_{\mathrm{B}}^{-1}\,\omega\,\mathrm{H}_k^{(1)'}(\omega\,\mathrm{s}_{\mathrm{B}}\,\mathfrak{a}) & -\,\mathrm{s}_{\mathrm{S}}^{-2}\,\frac{\mathrm{i}k}{\mathfrak{a}}\mathrm{H}_k^{(1)}(\omega\,\mathrm{s}_{\mathrm{S}}\,\mathfrak{a}) & -\,\mathrm{s}_{\mathrm{EM}}^{-2}\,\frac{\mathrm{i}k}{\mathfrak{a}}\mathrm{H}_k^{(1)}(\omega\,\mathrm{s}_{\mathrm{EM}}\,\mathfrak{a}) \\ \mathrm{s}_{\mathrm{P}}^{-2}\,\frac{\mathrm{i}k}{\mathfrak{a}}\mathrm{H}_k^{(1)}(\omega\,\mathrm{s}_{\mathrm{P}}\,\mathfrak{a}) & \mathrm{s}_{\mathrm{B}}^{-2}\,\frac{\mathrm{i}k}{\mathfrak{a}}\mathrm{H}_k^{(1)}(\omega\,\mathrm{s}_{\mathrm{B}}\,\mathfrak{a}) & \mathrm{s}_{\mathrm{S}}^{-1}\,\omega\,\mathrm{H}_k^{(1)'}(\omega\,\mathrm{s}_{\mathrm{S}}\,\mathfrak{a}) & \mathrm{s}_{\mathrm{EM}}^{-1}\,\omega\,\mathrm{H}_k^{(1)'}(\omega\,\mathrm{s}_{\mathrm{EM}}\,\mathfrak{a}) \\ -M\big(\mathcal{W}_{\mathrm{P}} + \alpha\big)\mathrm{H}_k^{(1)}(\omega\,\mathrm{s}_{\mathrm{P}}\,\mathfrak{a}) & -M\big(\mathcal{W}_{\mathrm{B}} + \alpha\big)\mathrm{H}_k^{(1)}(\omega\,\mathrm{s}_{\mathrm{B}}\,\mathfrak{a}) & 0 & 0 \\ 0 & 0 & \frac{\mathfrak{s}\,\mathrm{i}}{\omega\,\mu_0}\,\mathcal{E}_{\mathrm{S}}\,\mathrm{H}_k^{(1)}(\omega\,\mathrm{s}_{\mathrm{S}}\,\mathfrak{a}) & \frac{\mathfrak{s}\,\mathrm{i}}{\omega\,\mu_0}\,\mathcal{E}_{\mathrm{EM}}\,\mathrm{H}_k^{(1)}(\omega\,\mathrm{s}_{\mathrm{EM}}\,\mathfrak{a}) \end{pmatrix}. \tag{6.25}$$

6.3.3 Numerical tests

In Figure 6.4, we present the solution of the scattering of an incident P plane wave by a circular obstacle with radius $\mathfrak{a} = 1$m for two types of conditions, 1 and 8. In the development of the solution, we have considered an infinite domain. However, for the representation of the solution, we only show the solution on an annulus with exterior radius equal to 10m. The figure is similar to classical scattering figures. As for bounded domain, we study the invertibility of the coefficient matrices $\mathbb{A}_k^{\mathbf{w},\boldsymbol{\tau},\boldsymbol{E}}$ (6.23) and $\mathbb{A}_k^{\mathbf{u},\mathrm{p},\mathrm{H}}$ (6.25) for $k = 0, ...5$ by computing the determinant of these matrices, in order to determine if we can detect values of frequency for which the determinant of the coefficient matrices vanishes. Here, we expect no generalized eigenvalues because the problem is well-posed for outgoing solutions. This is confirmed by the curves shown in Figures 6.5 and 6.6, which are free of peaks for each mode. We also observe that the determinant for boundary conditions of type 1 is higher than the one for type 8.

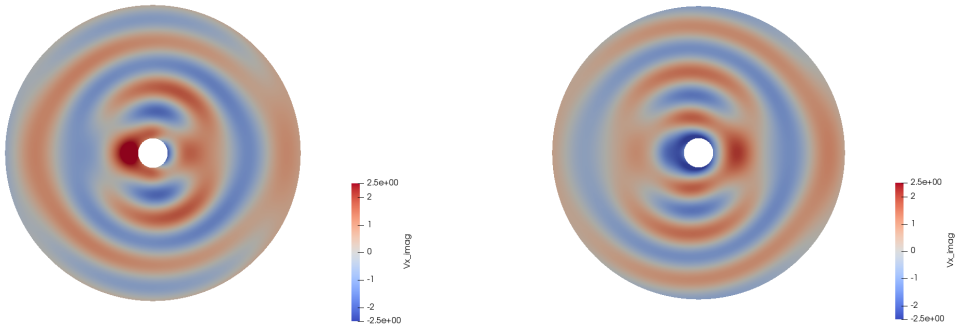

(a) BC 1 (b) BC 8

Figure 6.4: Scattering of a P plane wave: Imaginary part of the solid velocity u_x (10^3 m.s^{-1}) for a medium composed of sand for type of boundary condition 1 and 8, with $f = 500$Hz.

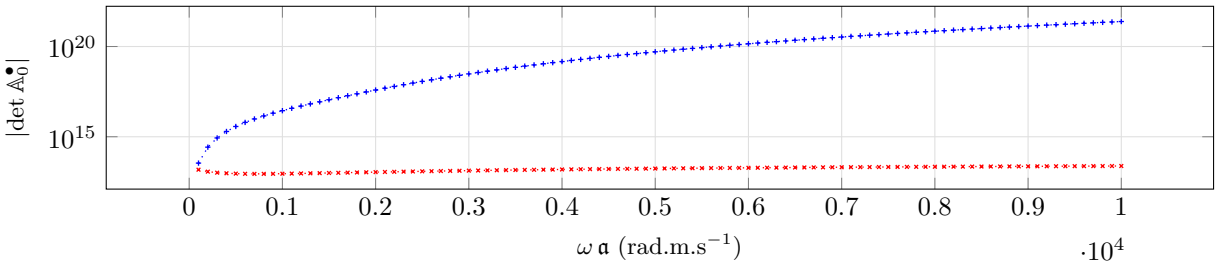

(a) Mode $k = 0$

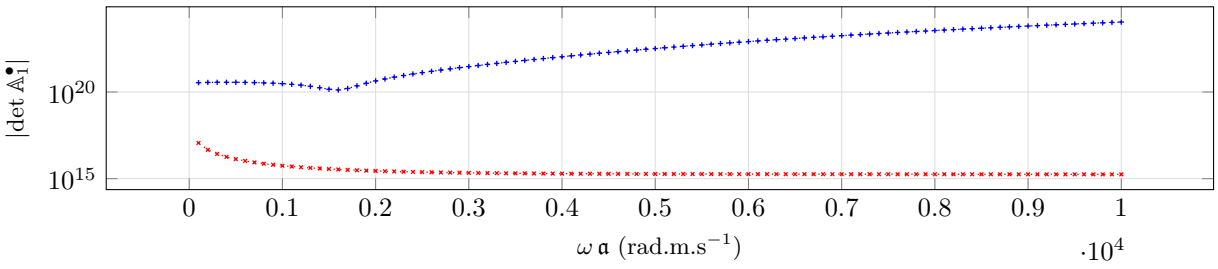

(b) Mode $k = 1$

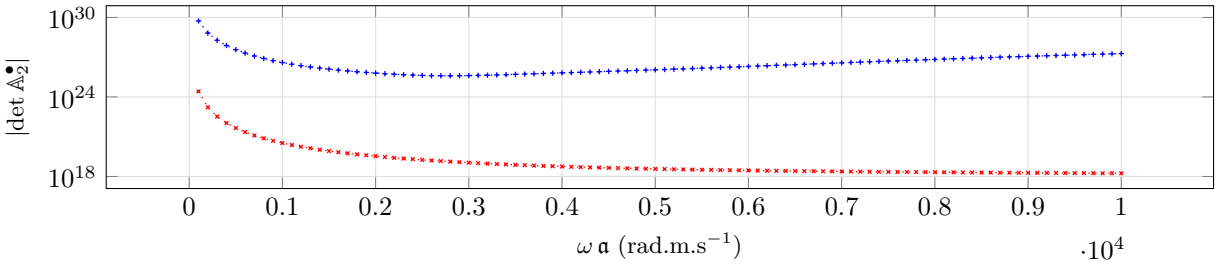

(c) Mode $k = 2$

Figure 6.5: Module of determinant of the coefficients matrix (log scale) for modes 0 to 2 for sand. The matrices corresponding with boundary conditions 1 and 8: $\mathbb{A}_k^{\mathbf{w},\boldsymbol{\tau},\boldsymbol{E}}$ (6.20) in blue and $\mathbb{A}_k^{\mathbf{u},\mathrm{p},\mathrm{H}}$ (6.22) in red.

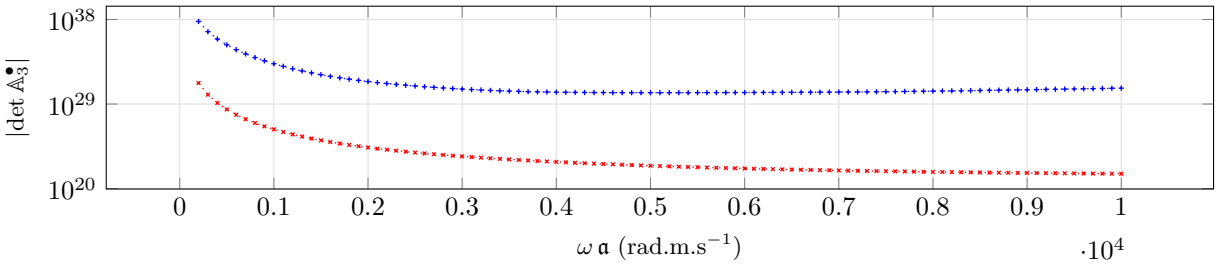

(a) Mode $k = 3$

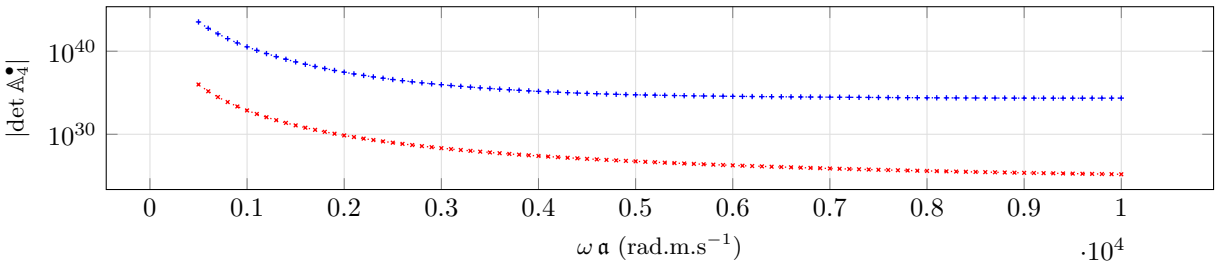

(b) Mode $k = 4$

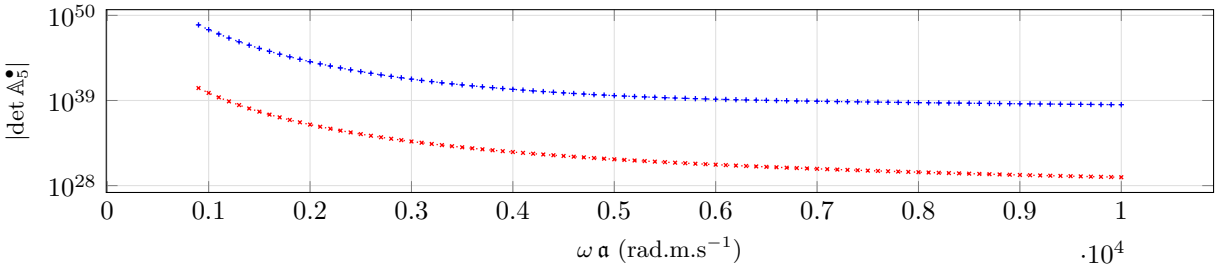

(c) Mode $k = 5$

Figure 6.6: Module of determinant of the coefficients matrix (log scale) for k in 3 : 5 for sand. The matrices corresponding with oundary conditions 1 and 8: $\mathbb{A}_k^{\mathbf{w},\boldsymbol{\tau},\boldsymbol{E}}$ (6.20) in blue ····+···· and $\mathbb{A}_k^{\mathbf{u},\mathrm{p},\mathrm{H}}$ (6.22) in red ····×····.

6.4 Scattering of a penetrable obstacle by a plane wave

Consider the scattering of a time-harmonic plane wave by a penetrable circular obstacle immersed in an infinite medium (see figure 6.7). The total wave outside the obstacle is a superposition of the incident plane wave, and the reflected wave with each quantity satisfying Pride's equations (5.3) in $\mathbb{R}^2 \setminus \mathbb{B}_{(0,\mathfrak{a})}$, while the transmitted wave is described by the displacement inside the cylinder. The unknowns are now the reflected wave which is outgoing, and the transmitted wave. They are uniquely determined by transmission conditions imposed on the interface Γ. For $\bullet = \text{pw, ref, trans}$, we denote: $\mathfrak{U}^\bullet = (\mathbf{u}^\bullet, \mathbf{w}^\bullet, \boldsymbol{\tau}^\bullet, \mathrm{p}^\bullet, \boldsymbol{E}^\bullet, \mathrm{H}^\bullet, \boldsymbol{J}^\bullet)$. The unknowns $\mathfrak{U}^{\mathrm{ref}}$ and $\mathfrak{U}^{\mathrm{trans}}$ solve the following problem:

$$
\begin{cases}
\mathfrak{U}^{\mathrm{ref}} \text{ solves Pride equations (5.3) in } \mathbb{R}^2 \setminus \Omega; \\
\mathfrak{U}^{\mathrm{trans}} \text{ solves Pride equations (5.3) in } \Omega; \\
\mathfrak{U}^{\mathrm{ref}} \text{ is outgoing;} \\
\text{Transmission conditions on the interface } \Gamma : \\
\quad \mathbf{u}^{\mathrm{pw}} + \mathbf{u}^{\mathrm{ref}} = \mathbf{u}^{\mathrm{trans}}, \\
\quad \mathrm{p}^{\mathrm{pw}} + \mathrm{p}^{\mathrm{ref}} = \mathrm{p}^{\mathrm{trans}}, \\
\quad \mathbf{w}^{\mathrm{pw}} \cdot \boldsymbol{n} + \mathbf{w}^{\mathrm{ref}} \cdot \boldsymbol{n} = \mathbf{w}^{\mathrm{trans}} \cdot \boldsymbol{n}, \\
\quad \boldsymbol{\tau}^{\mathrm{pw}} \cdot \boldsymbol{n} + \boldsymbol{\tau}^{\mathrm{ref}} \cdot \boldsymbol{n} = \boldsymbol{\tau}^{\mathrm{trans}} \cdot \boldsymbol{n}, \\
\quad \boldsymbol{n} \times \boldsymbol{E}^{\mathrm{pw}} + \boldsymbol{n} \times \boldsymbol{E}^{\mathrm{ref}} = \boldsymbol{n} \times \boldsymbol{E}^{\mathrm{trans}}, \\
\quad \mathrm{H}^{\mathrm{pw}} + \mathrm{H}^{\mathrm{ref}} = \mathrm{H}^{\mathrm{trans}}.
\end{cases}
\tag{6.26}
$$

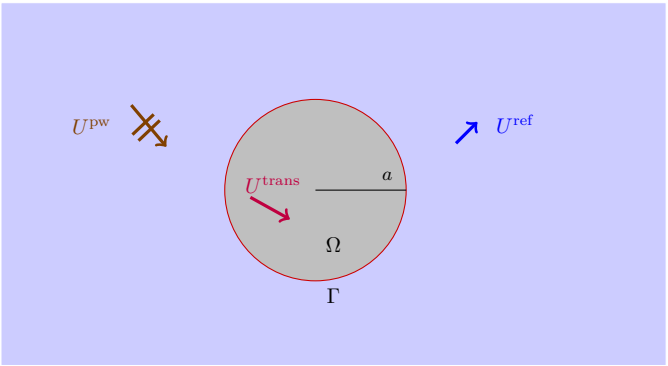

Figure 6.7: Scattering of a plane wave by a penetrable inclusion. The inclusion occupies the domain denoted by Ω. The cross section of the inclusion is a disc of radius denoted by $\mathfrak{a}$.

6.4.1 Construction of the analytical solution

The medium outside of the inclusion is denoted by medium 1, while the medium inside of the obstacle is denoted by medium 2. We denote the slowness in the medium 1 by $\mathsf{s}_{\bullet,(I)}$ and in medium 2 by $\mathsf{s}_{\bullet,(II)}$. The unknown $\mathfrak{U}^\bullet$ is given in the two media by equation (6.14). In medium 1, the potentials corresponding to the outgoing reflected wave satisfy equation (6.17):

$$
\begin{aligned}
\chi_{\mathrm{P,(I)}}(r,\theta) &= \sum_{k\in\mathbb{Z}} a_k \, \mathrm{H}_k^{(1)}(\omega \, \mathsf{s}_{\mathrm{P,(I)}} r) \; e^{\mathrm{i}\, k\, \theta}, \\
\chi_{\mathrm{B,(I)}}(r,\theta) &= \sum_{k\in\mathbb{Z}} b_k \, \mathrm{H}_k^{(1)}(\omega \, \mathsf{s}_{\mathrm{B,(I)}} r) \; e^{\mathrm{i}\, k\, \theta}, \\
\chi_{\mathrm{S,(I)}}(r,\theta) &= \sum_{k\in\mathbb{Z}} c_k \, \mathrm{H}_k^{(1)}(\omega \, \mathsf{s}_{\mathrm{S,(I)}} r) \; e^{\mathrm{i}\, k\, \theta}, \\
\chi_{\mathrm{EM,(I)}}(r,\theta) &= \sum_{k\in\mathbb{Z}} d_k \, \mathrm{H}_k^{(1)}(\omega \, \mathsf{s}_{\mathrm{EM,(I)}} r) \; e^{\mathrm{i}\, k\, \theta}.
\end{aligned}
$$

In medium 2, the potentials associated with the transmitted wave are given by equation (6.16):

$$\begin{aligned}
\chi_{\mathrm{P}_{(\mathrm{II})}}(r,\theta) &= \sum_{k\in\mathbb{Z}} e_k\, \mathrm{J}_k(\omega\, \mathsf{s}_{\mathrm{P},(\mathrm{II})} r)\; e^{\mathrm{i}\, k\, \theta}\,,\\
\chi_{\mathrm{B}_{(\mathrm{II})}}(r,\theta) &= \sum_{k\in\mathbb{Z}} f_k\, \mathrm{J}_k(\omega\, \mathsf{s}_{\mathrm{B},(\mathrm{II})} r)\; e^{\mathrm{i}\, k\, \theta}\,,\\
\chi_{\mathrm{S}_{(\mathrm{II})}}(r,\theta) &= \sum_{k\in\mathbb{Z}} g_k\, \mathrm{J}_k(\omega\, \mathsf{s}_{\mathrm{S},(\mathrm{II})} r)\; e^{\mathrm{i}\, k\, \theta}\,,\\
\chi_{\mathrm{EM}_{(\mathrm{II})}}(r,\theta) &= \sum_{k\in\mathbb{Z}} h_k\, \mathrm{J}_k(\omega\, \mathsf{s}_{\mathrm{EM},(\mathrm{II})} r)\; e^{\mathrm{i}\, k\, \theta}\,.
\end{aligned}$$

We next determine the coefficients a_k, b_k, c_k, d_k, e_k, f_k by imposing the boundary conditions (6.26) at the interface between the two materials. On Γ, we have in the polar basis:

$$\begin{aligned}
\mathbf{u}^\bullet = \mathbf{u}^\bullet_r \mathbf{e}_r + \mathbf{u}^\bullet_\theta \mathbf{e}_\theta\,, \qquad & \mathbf{w}^\bullet \cdot \mathbf{n} = \mathbf{w}^\bullet_r\,,\\
\boldsymbol{\tau}^\bullet \cdot \boldsymbol{n} = \tau^\bullet_{rr}\, \mathbf{e}_r + \tau^\bullet_{r\theta}\, \mathbf{e}_\theta\,, \qquad & \boldsymbol{n} \times \boldsymbol{E}^\bullet = \boldsymbol{E}^\bullet_\theta\,,
\end{aligned}$$

which leads to the following eight transmission conditions:

$$\begin{aligned}
\mathbf{u}^{\mathrm{ref}}_r - \mathbf{u}^{\mathrm{trans}}_r &= -\mathbf{u}^{\mathrm{pw}}_r\,,\\
\mathbf{u}^{\mathrm{ref}}_\theta - \mathbf{u}^{\mathrm{trans}}_\theta &= -\mathbf{u}^{\mathrm{pw}}_\theta\,,\\
\mathrm{p}^{\mathrm{ref}} - \mathrm{p}^{\mathrm{trans}} &= -\mathrm{p}^{\mathrm{pw}}\,,\\
\mathbf{w}^{\mathrm{ref}}_r - \mathbf{w}^{\mathrm{trans}}_r &= -\mathbf{w}^{\mathrm{pw}}_r\,,\\
\boldsymbol{\tau}^{\mathrm{ref}}_{rr} - \boldsymbol{\tau}^{\mathrm{trans}}_{rr} &= -\boldsymbol{\tau}^{\mathrm{pw}}_{rr}\,,\\
\boldsymbol{\tau}^{\mathrm{ref}}_{r\theta} - \boldsymbol{\tau}^{\mathrm{trans}}_{r\theta} &= -\boldsymbol{\tau}^{\mathrm{pw}}_{r\theta}\,,\\
\boldsymbol{E}^{\mathrm{ref}}_\theta - \boldsymbol{E}^{\mathrm{trans}}_\theta &= -\boldsymbol{E}^{\mathrm{pw}}_\theta\,,\\
\mathrm{H}^{\mathrm{ref}}_z - \mathrm{H}^{\mathrm{trans}}_z &= -\mathrm{H}^{\mathrm{pw}}_z\,.
\end{aligned} \tag{6.27}$$

The expansion of the components in Fourier series is:

$$\mathrm{u}^\bullet_r = \sum_{k\in\mathbb{Z}} \mathrm{u}^\bullet_{r,k}\, e^{\mathrm{i}\, k\, \theta}\,, \quad \mathrm{u}^\bullet_\theta = \sum_{k\in\mathbb{Z}} \mathrm{u}^\bullet_{\theta,k}\, e^{\mathrm{i}\, k\, \theta}\,, \quad \mathrm{p}^\bullet = \sum_{k\in\mathbb{Z}} \mathrm{p}^\bullet_k\, e^{\mathrm{i}\, k\, \theta}\,, \quad \boldsymbol{E}^\bullet_\theta = \sum_{k\in\mathbb{Z}} E^\bullet_k\, e^{\mathrm{i}\, k\, \theta}\,,$$

$$\mathrm{w}^\bullet_r = \sum_{k\in\mathbb{Z}} \mathrm{w}^\bullet_{r,k}\, e^{\mathrm{i}\, k\, \theta}\,, \quad \tau^\bullet_{rr} = \sum_{k\in\mathbb{Z}} \tau^\bullet_{rr,k}\, e^{\mathrm{i}\, k\, \theta}\,, \quad \tau^\bullet_{r\theta} = \sum_{k\in\mathbb{Z}} \tau^\bullet_{r\theta,k}\, e^{\mathrm{i}\, k\, \theta}\,, \quad \mathrm{H}^\bullet = \sum_{k\in\mathbb{Z}} \mathrm{p}^\bullet_k\, e^{\mathrm{i}\, k\, \theta}\,, \quad .$$

We have for the reflected wave:

$$\begin{aligned}
\mathfrak{s}\, \mathrm{i}\, \omega \mathrm{u}^{\mathrm{ref}}_{r,k} &= a_k \frac{\omega}{\mathsf{s}_{\mathrm{P},(\mathrm{I})}} \mathrm{H}^{(1)'}_k(\omega\, \mathsf{s}_{\mathrm{P},(\mathrm{I})}\, r) e^{\mathrm{i}k\theta} + b_k \frac{\omega}{\mathsf{s}_{\mathrm{B},(\mathrm{I})}} \mathrm{H}^{(1)'}_k(\omega\, \mathsf{s}_{\mathrm{B},(\mathrm{I})}\, r) e^{\mathrm{i}k\theta}\\
&\quad - c_k \frac{\mathrm{i}k}{r \mathsf{s}^2_{\mathrm{S},(\mathrm{I})}} \mathrm{H}^{(1)}_k(\omega\, \mathsf{s}_{\mathrm{S},(\mathrm{I})}\, r) e^{\mathrm{i}k\theta} - d_k \frac{\mathrm{i}k}{r \mathsf{s}^2_{\mathrm{EM},(\mathrm{I})}} \mathrm{H}^{(1)}_k(\omega\, \mathsf{s}_{\mathrm{EM},(\mathrm{I})}\, r) e^{\mathrm{i}k\theta}\,,\\
\mathfrak{s}\, \mathrm{i}\, \omega \mathrm{u}^{\mathrm{ref}}_{\theta,k} &= a_k \frac{\mathrm{i}k}{r\, \mathsf{s}^2_{\mathrm{P},(\mathrm{I})}} \mathrm{H}^{(1)}_k(\omega\, \mathsf{s}_{\mathrm{P},(\mathrm{I})} r) e^{\mathrm{i}k\theta} + b_k \frac{\mathrm{i}k}{r\, \mathsf{s}^2_{\mathrm{B},(\mathrm{I})}} \mathrm{H}^{(1)}_k(\omega\, \mathsf{s}_{\mathrm{B},(\mathrm{I})} r) e^{\mathrm{i}k\theta}\\
&\quad + c_k \frac{\omega}{\mathsf{s}_{\mathrm{S},(\mathrm{I})}} \mathrm{H}^{(1)'}_k(\omega\, \mathsf{s}_{\mathrm{S},(\mathrm{I})} r) e^{\mathrm{i}k\theta} + d_k \frac{\omega}{\mathsf{s}_{\mathrm{EM},(\mathrm{I})}} \mathrm{H}^{(1)'}_k(\omega\, \mathsf{s}_{\mathrm{EM},(\mathrm{I})} r) e^{\mathrm{i}k\theta}\,,\\
\mathrm{p}^{\mathrm{ref}}_k &= -a_k\, M\, (w_{\mathrm{P},(\mathrm{I})} + \alpha)\, \mathrm{H}^{(1)}_k(\omega\, \mathsf{s}_{\mathrm{P},(\mathrm{I})}\, r)\, e^{\mathrm{i}k\theta} - b_k\, M\, (w_{\mathrm{B},(\mathrm{I})} + \alpha)\, \mathrm{H}^{(1)}_k(\omega\, \mathsf{s}_{\mathrm{B},(\mathrm{I})}\, r)\, e^{\mathrm{i}k\theta}\,,\\
\mathfrak{s}\, \mathrm{i}\, \omega\, \mathrm{w}^{\mathrm{ref}}_{r,k} &= a_k \frac{w_{\mathrm{P},(\mathrm{I})}\, \omega}{\mathsf{s}_{\mathrm{P},(\mathrm{I})}} \mathrm{H}^{(1)'}_k(\omega\, \mathsf{s}_{\mathrm{P},(\mathrm{I})} r) e^{\mathrm{i}k\theta} + b_k \frac{w_{\mathrm{B},(\mathrm{I})}\, \omega}{\mathsf{s}_{\mathrm{B},(\mathrm{I})}} \mathrm{H}^{(1)'}_k(\omega\, \mathsf{s}_{\mathrm{B},(\mathrm{I})} r) e^{\mathrm{i}k\theta}\\
&\quad - c_k \frac{w_{\mathrm{S},(\mathrm{I})}}{\mathsf{s}^2_{\mathrm{S},(\mathrm{I})}} \frac{\mathrm{i}k}{r} \mathrm{H}^{(1)}_k(\omega\, \mathsf{s}_{\mathrm{S},(\mathrm{I})} r) e^{\mathrm{i}k\theta} - d_k \frac{w_{\mathrm{EM},(\mathrm{I})}}{\mathsf{s}^2_{\mathrm{EM},(\mathrm{I})}} \frac{\mathrm{i}k}{r} \mathrm{H}^{(1)}_k(\omega\, \mathsf{s}_{\mathrm{EM},(\mathrm{I})} r) e^{\mathrm{i}k\theta}\,,
\end{aligned}$$

$$\omega^2\tau^{\text{ref}}_{rr,k} = -\frac{2\mu_{\text{fr}}\,\omega}{\mathsf{s}_{\text{P,(I)}}\,r}a_k\,\text{H}^{(1)}_{k+1}(\omega\,\mathsf{s}_{\text{P,(I)}}r)e^{\text{i}\,k\,\theta} + \frac{2\mu_{\text{fr}}\,k}{\mathsf{s}^2_{\text{P,(I)}}\,r^2}a_k\,\text{H}^{(1)}_{k}(\omega\,\mathsf{s}_{\text{P,(I)}}r)e^{\text{i}\,k\,\theta} + 2\mu_{\text{fr}}\,\omega^2 a_k\,\text{H}^{(1)}_{k}(\omega\,\mathsf{s}_{\text{P,(I)}}r)e^{\text{i}\,k\,\theta}$$
$$-\frac{2\mu_{\text{fr}}\,k^2}{\mathsf{s}^2_{\text{P,(I)}}\,r^2}a_k\,\text{H}^{(1)}_{k}(\omega\,\mathsf{s}_{\text{P,(I)}}\,r)\,e^{\text{i}\,k\,\theta} - \frac{2\mu_{\text{fr}}\,\omega}{\mathsf{s}_{\text{B,(I)}}\,r}b_k\,\text{H}^{(1)}_{k+1}(\omega\,\mathsf{s}_{\text{B,(I)}}\,r)\,e^{\text{i}\,k\,\theta} + \frac{2\mu_{\text{fr}}\,k}{\mathsf{s}^2_{\text{B,(I)}}\,r^2}b_k\,\text{H}^{(1)}_{k}(\omega\,\mathsf{s}_{\text{B,(I)}}\,r)\,e^{\text{i}\,k\,\theta}$$
$$+2\mu_{\text{fr}}\,\omega^2\,b_k\text{H}^{(1)}_{k}(\omega\,\mathsf{s}_{\text{B,(I)}}\,r)\,e^{\text{i}\,k\,\theta} - \frac{2\mu_{\text{fr}}\,k^2}{\mathsf{s}^2_{\text{B,(I)}}\,r^2}\,b_k\,\text{H}^{(1)}_{k}(\omega\,\mathsf{s}_{\text{B,(I)}}\,r)\,e^{\text{i}\,k\,\theta} + \frac{2\mu_{\text{fr}}\,\omega\text{i}k}{\mathsf{s}_{\text{S,(I)}}r}\,c_k\,\text{H}^{(1)'}_{k}(\omega\,\mathsf{s}_{\text{S,(I)}}r)\,e^{\text{i}\,k\,\theta}$$
$$+\frac{2\mu_{\text{fr}}\,\omega\text{i}k}{\mathsf{s}_{\text{EM,(I)}}r}\,d_k\,\text{H}^{(1)'}_{k}(\omega\,\mathsf{s}_{\text{EM,(I)}}r)\,e^{\text{i}\,k\,\theta} + \omega^2\left(-\frac{2}{3}\mu_{\text{fr}} + \text{k}_{\text{fr}} + M\alpha^2 + \alpha\,M w_{\text{P,(I)}}\right)\,a_k\,\text{H}^{(1)}_{k}(\omega\,\mathsf{s}_{\text{P,(I)}}\,r)\,e^{\text{i}\,k\,\theta}$$
$$+\omega^2\left(-\frac{2}{3}\mu_{\text{fr}} + \text{k}_{\text{fr}} + M\alpha^2 + \alpha\,M w_{\text{B,(I)}}\right)\,b_k\,\text{H}^{(1)}_{k}(\omega\,\mathsf{s}_{\text{B,(I)}}\,r)\,e^{\text{i}\,k\,\theta},$$

$$\omega^2\,\tau^{\text{ref}}_{r\theta,k} = -\frac{2\,\mu_{\text{fr}}\omega\,\text{i}\,k}{r\,\mathsf{s}_{\text{P,(I)}}}\,a_k\,\text{H}^{(1)'}_{k}(\omega\,\mathsf{s}_{\text{P,(I)}}\,r)\,e^{\text{i}\,k\,\theta} + \frac{2\,\text{i}\,\mu_{\text{fr}}\,k}{r^2\,\mathsf{s}^2_{\text{P,(I)}}}\,a_k\,\text{H}^{(1)}_{k}(\omega\,\mathsf{s}_{\text{P,(I)}}\,r)\,e^{\text{i}\,k\,\theta}$$
$$-\frac{2\,\mu_{\text{fr}}\omega\,\text{i}\,k}{r\,\mathsf{s}_{\text{B,(I)}}}\,b_k\,\text{H}^{(1)'}_{k}(\omega\,\mathsf{s}_{\text{B,(I)}}\,r)\,e^{\text{i}\,k\,\theta} + \frac{2\,\text{i}\,\mu_{\text{fr}}\,k}{r^2\,\mathsf{s}^2_{\text{B,(I)}}}\,b_k\,\text{H}^{(1)}_{k}(\omega\,\mathsf{s}_{\text{B,(I)}}\,r)\,e^{\text{i}\,k\,\theta} - \frac{\mu_{\text{fr}}\,k^2}{r^2\,\mathsf{s}^2_{\text{S,(I)}}}\,c_k\,\text{H}^{(1)}_{k}(\omega\,\mathsf{s}_{\text{S,(I)}}\,r)\,e^{\text{i}\,k\,\theta}$$
$$+\frac{\mu_{\text{fr}}\,\omega}{r\,\mathsf{s}_{\text{S,(I)}}}\,c_k\,\text{H}^{(1)'}_{k}(\omega\,\mathsf{s}_{\text{S,(I)}}\,r)\,e^{\text{i}\,k\,\theta} - \mu_{\text{fr}}\,\frac{\omega}{\mathsf{s}_{\text{S,(I)}}r}\,c_k\,\text{H}^{(1)}_{k+1}(\omega\,\mathsf{s}_{\text{S,(I)}}\,r)\,e^{\text{i}\,k\,\theta}$$
$$+\mu_{\text{fr}}\,\frac{k}{\mathsf{s}^2_{\text{S,(I)}}r^2}c_k\,\text{H}^{(1)}_{k}(\omega\,\mathsf{s}_{\text{S,(I)}}\,r)\,e^{\text{i}\,k\,\theta} + \omega^2\,c_k\,\text{H}^{(1)}_{k}(\omega\,\mathsf{s}_{\text{S,(I)}}\,r)\,e^{\text{i}\,k\,\theta} - \mu_{\text{fr}}\,\frac{k^2}{\mathsf{s}^2_{\text{S,(I)}}r^2}\,c_k\,\text{H}^{(1)}_{k}(\omega\,\mathsf{s}_{\text{S,(I)}}\,r)\,e^{\text{i}\,k\,\theta}$$
$$-\frac{\mu_{\text{fr}}\,k^2}{r^2\,\mathsf{s}^2_{\text{EM,(I)}}}\,d_k\,\text{H}^{(1)}_{k}(\omega\,\mathsf{s}_{\text{EM,(I)}}\,r)\,e^{\text{i}\,k\,\theta} + \frac{\mu_{\text{fr}}\,\omega}{r\,\mathsf{s}_{\text{EM,(I)}}}\,d_k\,\text{H}^{(1)'}_{k}(\omega\,\mathsf{s}_{\text{EM,(I)}}\,r)\,e^{\text{i}\,k\,\theta}$$
$$-\mu_{\text{fr}}\,\frac{\omega}{\mathsf{s}_{\text{EM,(I)}}r}\,d_k\,\text{H}^{(1)}_{k+1}(\omega\,\mathsf{s}_{\text{EM,(I)}}\,r)\,e^{\text{i}\,k\,\theta} + \mu_{\text{fr}}\,\frac{k}{\mathsf{s}^2_{\text{EM,(I)}}r^2}d_k\,\text{H}^{(1)}_{k}(\omega\,\mathsf{s}_{\text{EM,(I)}}\,r)\,e^{\text{i}\,k\,\theta}$$
$$+\omega^2\,d_k\,\text{H}^{(1)}_{k}(\omega\,\mathsf{s}_{\text{EM,(I)}}\,r)\,e^{\text{i}\,k\,\theta} - \mu_{\text{fr}}\,\frac{k^2}{\mathsf{s}^2_{\text{EM,(I)}}r^2}\,d_k\,\text{H}^{(1)}_{k}(\omega\,\mathsf{s}_{\text{EM,(I)}}\,r)\,e^{\text{i}\,k\,\theta},$$

and

$$-\omega^2\,E_{\theta,k} = a_k\,\frac{\text{i}k}{r\,\mathsf{s}^2_{\text{P,(I)}}}E_{\text{P,(I)}}\text{H}^{(1)}_{k}(\omega\,\mathsf{s}_{\text{P,(I)}}r)e^{\text{i}k\theta} + b_k\,\frac{\text{i}k}{r\,\mathsf{s}^2_{\text{B,(I)}}}E_{\text{B,(I)}}\text{H}^{(1)}_{k}(\omega\,\mathsf{s}_{\text{B,(I)}}r)e^{\text{i}k\theta}$$
$$+c_k\,\frac{\omega}{\mathsf{s}_{\text{S,(I)}}}\,E_{\text{S,(I)}}\text{H}^{(1)'}_{k}(\omega\,\mathsf{s}_{\text{S,(I)}}r)e^{\text{i}k\theta} + d_k\,\frac{\omega}{\mathsf{s}_{\text{EM,(I)}}}\,E_{\text{EM,(I)}}\text{H}^{(1)'}_{k}(\omega\,\mathsf{s}_{\text{EM,(I)}}r)e^{\text{i}k\theta},$$

$$H_{z,k} = c_k\,\frac{\mathfrak{s}\,\text{i}}{\omega\,\mu_0}\,E_{\text{S,(I)}}\,\text{H}^{(1)}_{k}(\omega\,\mathsf{s}_{\text{S,(I)}}\,r)\,e^{\text{i}\,k\,\theta} + d_k\,\frac{\mathfrak{s}\,\text{i}}{\omega\,\mu_0}\,E_{\text{EM,(I)}}\,\text{H}^{(1)}_{k}(\omega\,\mathsf{s}_{\text{EM,(I)}}\,r)\,e^{\text{i}\,k\,\theta}.$$

The expression of the transmitted wave is given below:

$$\mathfrak{s}\,\text{i}\,\omega\,\text{u}^{\text{trans}}_{r,k} = e_k\,\frac{\omega}{\mathsf{s}_{\text{P,(II)}}}\,\text{J}'_k(\omega\,\mathsf{s}_{\text{P,(II)}}r)e^{\text{i}k\theta} + f_k\,\frac{\omega}{\mathsf{s}_{\text{B,(II)}}}\,\text{J}'_k(\omega\,\mathsf{s}_{\text{B,(II)}}\,r)e^{\text{i}k\theta} - g_k\,\frac{\text{i}k}{r\mathsf{s}^2_{\text{S,(II)}}}\text{J}_k(\omega\,\mathsf{s}_{\text{S,(II)}}r)e^{\text{i}k\theta}$$
$$-h_k\,\frac{\text{i}k}{r\mathsf{s}^2_{\text{EM,(II)}}}\text{J}_k(\omega\,\mathsf{s}_{\text{EM,(II)}}\,r)e^{\text{i}k\theta},$$

$$\mathfrak{s}\,\text{i}\,\omega\,\text{u}^{\text{trans}}_{\theta,k} = e_k\,\frac{\text{i}k}{r\,\mathsf{s}^2_{\text{P,(II)}}}\text{J}_k(\omega\,\mathsf{s}_{\text{P,(II)}}r)e^{\text{i}k\theta} + f_k\,\frac{\text{i}k}{r\,\mathsf{s}^2_{\text{B,(II)}}}\text{J}_k(\omega\,\mathsf{s}_{\text{B,(II)}}r)e^{\text{i}k\theta} + g_k\,\frac{\omega}{\mathsf{s}_{\text{S,(II)}}}\,\text{J}'_k(\omega\,\mathsf{s}_{\text{S,(II)}}r)e^{\text{i}k\theta}$$
$$+h_k\,\frac{\omega}{\mathsf{s}_{\text{EM,(II)}}}\,\text{J}'_k(\omega\,\mathsf{s}_{\text{EM,(II)}}r)e^{\text{i}k\theta},$$

$$\text{p}^{\text{ref}}_k = -a_k\,M\,(w_{\text{P}} + \alpha)\,\text{J}_k(\omega\,\mathsf{s}_{\text{P,(II)}}\,r)\,e^{\text{i}k\theta} - b_k\,M\,(w_{\text{B}} + \alpha)\,\text{J}_k(\omega\,\mathsf{s}_{\text{B,(II)}}\,r)\,e^{\text{i}k\theta},$$

$$\mathfrak{s}\,\text{i}\,\omega\,\text{w}^{\text{trans}}_{r,k} = e_k\,\frac{w_{\text{P,(II)}}\,\omega}{\mathsf{s}_{\text{P,(II)}}}\text{J}'_k(\omega\,\mathsf{s}_{\text{P,(II)}}r)e^{\text{i}k\theta} + f_k\,\frac{w_{\text{P,(II)}}\,\omega}{\mathsf{s}_{\text{B,(II)}}}\text{J}'_k(\omega\,\mathsf{s}_{\text{B,(II)}}r)e^{\text{i}k\theta} - g_k\,\frac{w_{\text{S,(II)}}}{\mathsf{s}^2_{\text{S,(II)}}}\,\frac{\text{i}k}{r}\,\text{J}_k(\omega\,\mathsf{s}_{\text{S,(II)}}r)e^{\text{i}k\theta}$$
$$-h_k\,\frac{w_{\text{EM,(II)}}}{\mathsf{s}^2_{\text{EM,(II)}}}\,\frac{\text{i}k}{r}\,\text{J}_k(\omega\,\mathsf{s}_{\text{EM,(II)}}r)e^{\text{i}k\theta},$$

$$\begin{aligned}
\omega^2\tau^{\text{trans}}_{rr,k} &= -\frac{2\mu_{\text{fr}}\,\omega}{\mathsf{s}_{\text{P},(\text{II})}r}e_k\mathrm{J}_{k+1}(\omega\,\mathsf{s}_{\text{P},(\text{II})}r)\,e^{\mathrm{i}\,k\,\theta}+\frac{2\mu_{\text{fr}}\,k}{\mathsf{s}^2_{\text{P},(\text{II})}r^2}e_k\mathrm{J}_k(\omega\,\mathsf{s}_{\text{P},(\text{II})}r)\,e^{\mathrm{i}\,k\,\theta}+2\mu_{\text{fr}}\,\omega^2\,e_k\mathrm{J}_k(\omega\,\mathsf{s}_{\text{P},(\text{II})}r)\,e^{\mathrm{i}\,k\,\theta}\\
&-\frac{2\mu_{\text{fr}}\,k^2}{\mathsf{s}^2_{\text{P},(\text{I})}r^2}e_k\,\mathrm{J}_k(\omega\,\mathsf{s}_{\text{P},(\text{II})}r)\,e^{\mathrm{i}\,k\,\theta}-\frac{2\mu_{\text{fr}}\,\omega}{\mathsf{s}_{\text{B},(\text{II})}r}f_k\,\mathrm{J}_{k+1}(\omega\,\mathsf{s}_{\text{B},(\text{II})}r)\,e^{\mathrm{i}\,k\,\theta}+\frac{2\mu_{\text{fr}}\,k}{\mathsf{s}^2_{\text{B},(\text{II})}r^2}f_k\,\mathrm{J}_k(\omega\,\mathsf{s}_{\text{B},(\text{II})}r)\,e^{\mathrm{i}\,k\,\theta}\\
&+2\mu_{\text{fr}}\,f_k\,\omega^2\,\mathrm{J}_k(\omega\,\mathsf{s}_{\text{B},(\text{II})}r)\,e^{\mathrm{i}\,k\,\theta}-\frac{2\mu_{\text{fr}}\,k^2}{\mathsf{s}^2_{\text{B},(\text{II})}r^2}\,f_k\,\mathrm{J}_k(\omega\,\mathsf{s}_{\text{B},(\text{II})}\,r)\,e^{\mathrm{i}\,k\,\theta}+\frac{2\mu_{\text{fr}}\omega\,\mathrm{i}k}{\mathsf{s}_{\text{S},(\text{II})}r}\,g_k\,\mathrm{J}'_k(\omega\,\mathsf{s}_{\text{S},(\text{II})}\,r)\,e^{\mathrm{i}\,k\,\theta}\\
&+\frac{2\mu_{\text{fr}}\omega\,\mathrm{i}k}{\mathsf{s}_{\text{EM},(\text{II})}r}\,h_k\,\mathrm{J}'_k(\omega\,\mathsf{s}_{\text{EM},(\text{II})}\,r)\,e^{\mathrm{i}\,k\,\theta}+\omega^2\left(-\frac{2}{3}\mu_{\text{fr}}+\mathrm{k}_{\text{fr}}+M\alpha^2+\alpha\,M w_{\text{P}}\right)\,e_k\,\mathrm{J}_k(\omega\,\mathsf{s}_{\text{P},(\text{II})}\,r)\,e^{\mathrm{i}\,k\,\theta}\\
&+\omega^2\left(-\frac{2}{3}\mu_{\text{fr}}+\mathrm{k}_{\text{fr}}+M\alpha^2+\alpha\,M w_{\text{B}}\right)\,f_k\,\mathrm{J}_k(\omega\,\mathsf{s}_{\text{B},(\text{II})}\,r)\,e^{\mathrm{i}\,k\,\theta},
\end{aligned}$$

$$\begin{aligned}
\omega^2\tau^{\text{trans}}_{r\theta,k} &= -\frac{2\mu_{\text{fr}}\omega\mathrm{i}k}{r\mathsf{s}_{\text{P},(\text{II})}}e_k\mathrm{J}'_k(\omega\mathsf{s}_{\text{P},(\text{II})}r)e^{\mathrm{i}k\theta}+\frac{2\,\mathrm{i}\,\mu_{\text{fr}}k}{r^2\mathsf{s}^2_{\text{P},(\text{II})}}e_k\mathrm{J}_k(\omega\mathsf{s}_{\text{P},(\text{II})}r)e^{\mathrm{i}k\theta}-\frac{2\mu_{\text{fr}}\omega\mathrm{i}k}{r\mathsf{s}_{\text{B},(\text{II})}}f_k\mathrm{J}'_k(\omega\,\mathsf{s}_{\text{B},(\text{II})}r)e^{\mathrm{i}k\theta}\\
&+\frac{2\,\mathrm{i}\,\mu_{\text{fr}}\,k}{r^2\,\mathsf{s}^2_{\text{B},(\text{II})}}f_k\,\mathrm{J}_k(\omega\,\mathsf{s}_{\text{B},(\text{II})}r)\,e^{\mathrm{i}\,k\,\theta}-\frac{\mu_{\text{fr}}\,k^2}{r^2\,\mathsf{s}^2_{\text{S},(\text{II})}}g_k\,\mathrm{J}_k(\omega\,\mathsf{s}_{\text{S},(\text{II})}r)\,e^{\mathrm{i}\,k\,\theta}+\frac{\mu_{\text{fr}}\,\omega}{r\,\mathsf{s}_{\text{S},(\text{II})}}g_k\,\mathrm{J}'_k(\omega\,\mathsf{s}_{\text{S},(\text{II})}r)\,e^{\mathrm{i}\,k\,\theta}\\
&-\mu_{\text{fr}}\,\frac{\omega}{\mathsf{s}_{\text{S},(\text{II})}r}\,g_k\,\mathrm{J}_{k+1}(\omega\,\mathsf{s}_{\text{S},(\text{II})}r)\,e^{\mathrm{i}\,k\,\theta}+\mu_{\text{fr}}\,\frac{k}{\mathsf{s}^2_{\text{S},(\text{II})}r^2}g_k\,\mathrm{J}_k(\omega\,\mathsf{s}_{\text{S},(\text{II})}\,r)\,e^{\mathrm{i}\,k\,\theta}\\
&+\omega^2\,g_k\,\mathrm{J}_k(\omega\,\mathsf{s}_{\text{S},(\text{II})}r)\,e^{\mathrm{i}\,k\,\theta}-\mu_{\text{fr}}\,\frac{k^2}{\mathsf{s}^2_{\text{S},(\text{II})}r^2}\,g_k\,\mathrm{J}_k(\omega\,\mathsf{s}_{\text{S},(\text{II})}r)\,e^{\mathrm{i}\,k\,\theta}\\
&-\frac{\mu_{\text{fr}}\,k^2}{r^2\,\mathsf{s}^2_{\text{EM},(\text{II})}}h_k\,\mathrm{J}_k(\omega\,\mathsf{s}_{\text{EM},(\text{II})}r)\,e^{\mathrm{i}\,k\,\theta}+\frac{\mu_{\text{fr}}\,\omega}{r\,\mathsf{s}_{\text{EM},(\text{II})}}h_k\,\mathrm{J}'_k(\omega\,\mathsf{s}_{\text{EM},(\text{II})}r)\,e^{\mathrm{i}\,k\,\theta}\\
&-\mu_{\text{fr}}\,\frac{\omega}{\mathsf{s}_{\text{EM},(\text{II})}r}\,h_k\,\mathrm{J}_{k+1}(\omega\,\mathsf{s}_{\text{EM},(\text{II})}r)\,e^{\mathrm{i}\,k\,\theta}+\mu_{\text{fr}}\,\frac{k}{\mathsf{s}^2_{\text{EM},(\text{II})}r^2}h_k\,\mathrm{J}_k(\omega\,\mathsf{s}_{\text{EM},(\text{II})}\,r)\,e^{\mathrm{i}\,k\,\theta}\\
&+\omega^2\,h_k\,\mathrm{J}_k(\omega\,\mathsf{s}_{\text{EM},(\text{II})}r)\,e^{\mathrm{i}\,k\,\theta}-\mu_{\text{fr}}\,\frac{k^2}{\mathsf{s}^2_{\text{EM},(\text{II})}r^2}\,h_k\,\mathrm{J}_k(\omega\,\mathsf{s}_{\text{EM},(\text{II})}r)\,e^{\mathrm{i}\,k\,\theta},
\end{aligned}$$

and

$$\begin{aligned}
-\omega^2\,E_{\theta,k} &= e_k\,\frac{\mathrm{i}k}{r\,\mathsf{s}^2_{\text{P},(\text{II})}}E_{\text{P},(\text{II})}\mathrm{J}_k(\omega\,\mathsf{s}_{\text{P},(\text{II})}r)e^{\mathrm{i}k\theta}+f_k\,\frac{\mathrm{i}k}{r\,\mathsf{s}^2_{\text{B},(\text{II})}}E_{\text{B},(\text{II})}\mathrm{J}_k(\omega\,\mathsf{s}_{\text{B},(\text{II})}r)e^{\mathrm{i}k\theta}\\
&+g_k\,\frac{\omega}{\mathsf{s}_{\text{S},(\text{II})}}\,E_{\text{S},(\text{II})}\mathrm{J}'_k(\omega\,\mathsf{s}_{\text{S},(\text{II})}r)e^{\mathrm{i}k\theta}+h_k\,\frac{\omega}{\mathsf{s}_{\text{EM},(\text{II})}}\,E_{\text{EM},(\text{II})}\mathrm{J}'_k(\omega\,\mathsf{s}_{\text{EM},(\text{II})}r)e^{\mathrm{i}k\theta},\\
\mathrm{H}_k &= g_k\,\frac{\mathfrak{s}\,\mathrm{i}}{\omega\,\mu_0}\,E_{\text{S},(\text{II})}\,\mathrm{J}_k(\omega\,\mathsf{s}_{\text{S},(\text{II})}\,r)\,e^{\mathrm{i}\,k\,\theta}+h_k\,\frac{\mathfrak{s}\,\mathrm{i}}{\omega\,\mu_0}\,E_{\text{EM},(\text{II})}\,\mathrm{J}_k(\omega\,\mathsf{s}_{\text{EM},(\text{II})}\,r)\,e^{\mathrm{i}\,k\,\theta}.
\end{aligned}$$

Imposing (6.27), we obtain a linear system satisfied by a_k, b_k, c_k, d_k, e_k, f_k, g_k, h_k in each mode k:

$$\mathbb{A}_k\begin{pmatrix}a_k\\b_k\\c_k\\d_k\\e_k\\f_k\\g_k\\h_k\end{pmatrix}=\begin{pmatrix}-\mathfrak{s}\,\mathrm{i}\,\omega\,\mathrm{u}^{\text{pw}}_{r,k}\\-\mathfrak{s}\,\mathrm{i}\,\omega\,\mathrm{u}^{\text{pw}}_{\theta,k}\\-\mathrm{p}^{\text{pw}}\\-\mathfrak{s}\,\mathrm{i}\,\omega\,\mathrm{w}^{\text{pw}}_{r,k}\\-\omega^2\,\tau^{\text{pw}}_{rr,k}\\-\omega^2\,\tau^{\text{pw}}_{r\theta,k}\\\omega^2\,E^{\text{pw}}_{\theta,k}\\-\mathrm{H}^{\text{pw}}_k\end{pmatrix},$$

with

$$\mathbb{A}_k^{\text{2media}} = \begin{pmatrix} A_{11} & A_{12} & A_{13} & A_{14} & A_{15} & A_{16} & A_{17} & A_{18} \\ A_{21} & A_{22} & A_{23} & A_{24} & A_{25} & A_{26} & A_{27} & A_{28} \\ A_{31} & A_{32} & A_{33} & A_{34} & A_{35} & A_{36} & A_{37} & A_{38} \\ A_{41} & A_{42} & A_{43} & A_{44} & A_{45} & A_{46} & A_{47} & A_{48} \\ A_{51} & A_{52} & A_{53} & A_{54} & A_{55} & A_{56} & A_{57} & A_{58} \\ A_{61} & A_{62} & A_{63} & A_{64} & A_{65} & A_{66} & A_{67} & A_{68} \\ A_{71} & A_{72} & A_{73} & A_{74} & A_{75} & A_{76} & A_{77} & A_{78} \\ A_{81} & A_{82} & A_{83} & A_{84} & A_{85} & A_{86} & A_{87} & A_{88} \end{pmatrix}, \tag{6.28}$$

$$A_{11} = \frac{\omega}{\mathsf{s}_{\mathrm{P},(\mathrm{I})}} \mathrm{H}_k^{(1)'}(\omega\, \mathsf{s}_{\mathrm{P},(\mathrm{I})}\, \mathfrak{a}), \qquad A_{12} = \frac{\omega}{\mathsf{s}_{\mathrm{B},(\mathrm{I})}} \mathrm{H}_k^{(1)'}(\omega\, \mathsf{s}_{\mathrm{B},(\mathrm{I})}\, \mathfrak{a}),$$

$$A_{13} = -\frac{\mathrm{i}k}{\mathfrak{a}\mathsf{s}^2_{\mathrm{S},(\mathrm{I})}} \mathrm{H}_k^{(1)}(\omega\, \mathsf{s}_{\mathrm{S},(\mathrm{I})}\, \mathfrak{a}), \qquad A_{14} = -\frac{\mathrm{i}k}{\mathfrak{a}\mathsf{s}^2_{\mathrm{EM},(\mathrm{I})}} \mathrm{H}_k^{(1)}(\omega\, \mathsf{s}_{\mathrm{EM},(\mathrm{I})}\, \mathfrak{a}),$$

$$A_{15} = -\frac{\omega}{\mathsf{s}_{\mathrm{P},(\mathrm{II})}} \mathrm{J}_k'(\omega\, \mathsf{s}_{\mathrm{P},(\mathrm{II})}\, \mathfrak{a}), \qquad A_{16} = -\frac{\omega}{\mathsf{s}_{\mathrm{B},(\mathrm{II})}} \mathrm{J}_k'(\omega\, \mathsf{s}_{\mathrm{B},(\mathrm{II})}\, \mathfrak{a}),$$

$$A_{17} = \frac{\mathrm{i}k}{\mathfrak{a}\mathsf{s}^2_{\mathrm{S},(\mathrm{II})}} \mathrm{J}_k(\omega\, \mathsf{s}_{\mathrm{S},(\mathrm{II})}\, \mathfrak{a}), \qquad A_{18} = \frac{\mathrm{i}k}{\mathfrak{a}\mathsf{s}^2_{\mathrm{EM},(\mathrm{II})}} \mathrm{J}_k(\omega\, \mathsf{s}_{\mathrm{EM},(\mathrm{II})}\, \mathfrak{a}),$$

$$A_{21} = \frac{\mathrm{i}k}{\mathfrak{a}\, \mathsf{s}^2_{\mathrm{P},(\mathrm{I})}} \mathrm{H}_k^{(1)}(\omega\, \mathsf{s}_{\mathrm{P},(\mathrm{I})}\, \mathfrak{a}), \qquad A_{22} = \frac{\mathrm{i}k}{\mathfrak{a}\, \mathsf{s}^2_{\mathrm{B},(\mathrm{I})}} \mathrm{H}_k^{(1)}(\omega\, \mathsf{s}_{\mathrm{B},(\mathrm{I})}\, \mathfrak{a}),$$

$$A_{23} = \mathsf{s}^{-1}_{\mathrm{S},(\mathrm{I})}\, \omega\, \mathrm{H}_k^{(1)'}(\omega\, \mathsf{s}_{\mathrm{S},(\mathrm{I})}\, \mathfrak{a}), \qquad A_{24} = \mathsf{s}^{-1}_{\mathrm{EM},(\mathrm{I})}\, \omega\, \mathrm{H}_k^{(1)'}(\omega\, \mathsf{s}_{\mathrm{EM},(\mathrm{I})}\, \mathfrak{a}),$$

$$A_{25} = -\frac{\mathrm{i}k}{\mathfrak{a}\, \mathsf{s}^2_{\mathrm{P},(\mathrm{II})}} \mathrm{J}_k(\omega\, \mathsf{s}_{\mathrm{P},(\mathrm{II})}\, \mathfrak{a}), \qquad A_{26} = -\frac{\mathrm{i}k}{\mathfrak{a}\, \mathsf{s}^2_{\mathrm{B},(\mathrm{II})}} \mathrm{J}_k(\omega\, \mathsf{s}_{\mathrm{B},(\mathrm{II})}\, \mathfrak{a}),$$

$$A_{27} = -\mathsf{s}^{-1}_{\mathrm{S},(\mathrm{II})}\, \omega\, \mathrm{J}_k'(\omega\, \mathsf{s}_{\mathrm{S},(\mathrm{II})}\, \mathfrak{a}), \qquad A_{28} = -\mathsf{s}^{-1}_{\mathrm{EM},(\mathrm{II})}\, \omega\, \mathrm{J}_k'(\omega\, \mathsf{s}_{\mathrm{EM},(\mathrm{II})}\, \mathfrak{a}),$$

$$A_{31} = -M\left(w_{\mathrm{P},(\mathrm{I})} + \alpha\right) \mathrm{H}_k^{(1)}(\omega\, \mathsf{s}_{\mathrm{P},(\mathrm{I})}\, \mathfrak{a}), \quad A_{32} = -M\left(w_{\mathrm{B},(\mathrm{I})} + \alpha\right) \mathrm{H}_k^{(1)}(\omega\, \mathsf{s}_{\mathrm{B},(\mathrm{I})}\, \mathfrak{a}), \quad A_{33} = 0, \quad A_{34} = 0,$$

$$A_{35} = M\left(w_{\mathrm{P},(\mathrm{II})} + \alpha\right) \mathrm{J}_k(\omega\, \mathsf{s}_{\mathrm{P},(\mathrm{II})}\, \mathfrak{a}), \qquad A_{36} = M\left(w_{\mathrm{B},(\mathrm{II})} + \alpha\right) \mathrm{J}_k(\omega\, \mathsf{s}_{\mathrm{B},(\mathrm{II})}\, \mathfrak{a}), \qquad A_{37} = 0, \quad A_{38} = 0,$$

$$A_{41} = \frac{w_{\mathrm{P},(\mathrm{I})}}{\mathsf{s}_{\mathrm{P},(\mathrm{I})}}\, \omega\, \mathrm{H}_k^{(1)'}(\omega\, \mathsf{s}_{\mathrm{P},(\mathrm{I})}\mathfrak{a}), \qquad A_{42} = \frac{w_{\mathrm{B},(\mathrm{I})}}{\mathsf{s}_{\mathrm{B},(\mathrm{I})}}\, \omega\, \mathrm{H}_k^{(1)'}(\omega\, \mathsf{s}_{\mathrm{B},(\mathrm{I})}\mathfrak{a}),$$

$$A_{43} = -\frac{w_{\mathrm{S},(\mathrm{I})}}{\mathsf{s}^2_{\mathrm{S},(\mathrm{I})}}\, \frac{\mathrm{i}k}{\mathfrak{a}} \mathrm{H}_k^{(1)}(\omega\, \mathsf{s}_{\mathrm{S},(\mathrm{I})}\mathfrak{a}), \qquad A_{44} = -\frac{w_{\mathrm{EM},(\mathrm{I})}}{\mathsf{s}^2_{\mathrm{EM},(\mathrm{I})}}\, \frac{\mathrm{i}k}{\mathfrak{a}} \mathrm{H}_k^{(1)}(\omega\, \mathsf{s}_{\mathrm{EM},(\mathrm{I})}\mathfrak{a}),$$

$$A_{45} = -\frac{w_{\mathrm{P},(\mathrm{II})}}{\mathsf{s}_{\mathrm{P},(\mathrm{II})}}\, \omega\, \mathrm{J}_k'(\omega\, \mathsf{s}_{\mathrm{P},(\mathrm{II})}\mathfrak{a}), \qquad A_{46} = -\frac{w_{\mathrm{B},(\mathrm{II})}}{\mathsf{s}_{\mathrm{B},(\mathrm{II})}}\, \omega\, \mathrm{J}_k'(\omega\, \mathsf{s}_{\mathrm{B},(\mathrm{II})}\mathfrak{a}),$$

$$A_{47} = \frac{w_{\mathrm{S},(\mathrm{II})}}{\mathsf{s}^2_{\mathrm{S},(\mathrm{II})}}\, \frac{\mathrm{i}k}{\mathfrak{a}} \mathrm{J}_k(\omega\, \mathsf{s}_{\mathrm{S},(\mathrm{II})}\mathfrak{a}), \qquad A_{48} = \frac{w_{\mathrm{EM},(\mathrm{II})}}{\mathsf{s}^2_{\mathrm{EM},(\mathrm{II})}}\, \frac{\mathrm{i}k}{\mathfrak{a}} \mathrm{J}_k(\omega\, \mathsf{s}_{\mathrm{EM},(\mathrm{II})}\mathfrak{a}),$$

$$A_{51} = -\frac{2\,\mu_{\rm fr}\,\omega}{\mathsf{s}_{\rm P,(I)}\mathfrak{a}}\,{\rm H}^{(1)}_{k+1}(\omega\,\mathsf{s}_{\rm P,(I)}\,\mathfrak{a}) \;+\; \frac{2\,\mu_{\rm fr}\,k}{\mathsf{s}^2_{\rm P,(I)}\mathfrak{a}^2}\,{\rm H}^{(1)}_{k}(\omega\,\mathsf{s}_{\rm P,(I)}\,\mathfrak{a}) \;+\; 2\,\mu_{\rm fr}\,\omega^2\,{\rm H}^{(1)}_{k}(\omega\,\mathsf{s}_{\rm P,(I)}\,\mathfrak{a})$$
$$-\;\frac{2\,\mu_{\rm fr}\,k^2}{\mathsf{s}^2_{\rm P,(I)}\mathfrak{a}^2}\,{\rm H}^{(1)}_{k}(\omega\,\mathsf{s}_{\rm P,(I)}\,\mathfrak{a}) \;+\omega^2\,\left(-\frac{2}{3}\mu_{\rm fr}\;+\;{\rm k}_{\rm fr}\;+\;M\alpha^2\;+\;\alpha\,M w_{\rm P,(I)}\right){\rm H}^{(1)}_{k}(\omega\,\mathsf{s}_{\rm P,(I)}\mathfrak{a})\,,$$

$$A_{52} = -\frac{2\,\mu_{\rm fr}\,\omega}{\mathsf{s}_{\rm B,(I)}\mathfrak{a}}\,{\rm H}^{(1)}_{k+1}(\omega\,\mathsf{s}_{\rm B,(I)}\,\mathfrak{a}) \;+\; \frac{2\,\mu_{\rm fr}\,k}{\mathsf{s}^2_{\rm B,(I)}\mathfrak{a}^2}\,{\rm H}^{(1)}_{k}(\omega\,\mathsf{s}_{\rm B,(I)}\,\mathfrak{a}) \;+\; 2\,\mu_{\rm fr}\,\omega^2\,{\rm H}^{(1)}_{k}(\omega\,\mathsf{s}_{\rm B,(I)}\,\mathfrak{a})$$
$$-\;\frac{2\,\mu_{\rm fr}\,k^2}{\mathsf{s}^2_{\rm B,(I)}\mathfrak{a}^2}\,{\rm H}^{(1)}_{k}(\omega\,\mathsf{s}_{\rm B,(I)}\,\mathfrak{a}) \;+\omega^2\,\left(-\frac{2}{3}\mu_{\rm fr}\;+\;{\rm k}_{\rm fr}\;+\;M\alpha^2\;+\;\alpha\,M w_{\rm B,(I)}\right){\rm H}^{(1)}_{k}(\omega\,\mathsf{s}_{\rm B,(I)}\mathfrak{a})\,,$$

$$A_{53} = \frac{2\mu_{\rm fr}}{\mathsf{s}_{\rm S,(I)}\mathfrak{a}}\,\omega\,{\rm i}k\,{\rm H}^{(1)'}_{k}(\omega\,\mathsf{s}_{\rm S,(I)}\mathfrak{a})\,, \qquad A_{54} = \frac{2\mu_{\rm fr}}{\mathsf{s}_{\rm EM,(I)}\mathfrak{a}}\,\omega\,{\rm i}k\,{\rm H}^{(1)'}_{k}(\omega\,\mathsf{s}_{\rm S,(I)}\mathfrak{a})\,,$$

$$A_{55} = \frac{2\,\mu_{\rm fr}\,\omega}{\mathsf{s}_{\rm P,(II)}\mathfrak{a}}\,{\rm J}_{k+1}(\omega\,\mathsf{s}_{\rm P,(II)}\,\mathfrak{a}) \;-\; \frac{2\,\mu_{\rm fr}\,k}{\mathsf{s}^2_{\rm P,(I)}\mathfrak{a}^2}\,{\rm J}_{k}(\omega\,\mathsf{s}_{\rm P,(I)}\,\mathfrak{a}) \;-\; 2\,\mu_{\rm fr}\,\omega^2\,{\rm H}^{(1)}_{k}(\omega\,\mathsf{s}_{\rm P,(II)}\,\mathfrak{a})$$
$$+\;\frac{2\,\mu_{\rm fr}\,k^2}{\mathsf{s}^2_{\rm P}\mathfrak{a}^2}\,{\rm J}_{k}(\omega\,\mathsf{s}_{\rm P,(II)}\,\mathfrak{a}) \;-\omega^2\,\left(-\frac{2}{3}\mu_{\rm fr}\;+\;{\rm k}_{\rm fr}\;+\;M\alpha^2\;+\;\alpha\,M w_{\rm P,(II)}\right){\rm J}_{k}(\omega\,\mathsf{s}_{\rm P,(II)}\mathfrak{a})\,,$$

$$A_{56} = \frac{2\,\mu_{\rm fr}\,\omega}{\mathsf{s}_{\rm B,(II)}\mathfrak{a}}\,{\rm J}_{k+1}(\omega\,\mathsf{s}_{\rm B,(II)}\,\mathfrak{a}) \;-\; \frac{2\,\mu_{\rm fr}\,k}{\mathsf{s}^2_{\rm B,(I)}\mathfrak{a}^2}\,{\rm H}^{(1)}_{k}(\omega\,\mathsf{s}_{\rm B,(II)}\,\mathfrak{a}) \;-\; 2\,\mu_{\rm fr}\,\omega^2\,{\rm J}_{k}(\omega\,\mathsf{s}_{\rm B,(II)}\,\mathfrak{a})$$
$$+\;\frac{2\,\mu_{\rm fr}\,k^2}{\mathsf{s}^2_{\rm B,(II)}\mathfrak{a}^2}\,{\rm J}_{k}(\omega\,\mathsf{s}_{\rm B,(II)}\,\mathfrak{a})\;e^{{\rm i}\,k\,\theta} - \omega^2\,\left(-\frac{2}{3}\mu_{\rm fr}\;+\;{\rm k}_{\rm fr}\;+\;M\alpha^2\;+\;\alpha\,M w_{\rm B,(II)}\right){\rm J}_{k}(\omega\,\mathsf{s}_{\rm B,(II)}\mathfrak{a})\,,$$

$$A_{57} = -\frac{2\mu_{\rm fr}}{\mathsf{s}_{\rm S,(II)}\mathfrak{a}}\,\omega\,{\rm i}k\,{\rm J}^{'}_{k}(\omega\,\mathsf{s}_{\rm S,(II)}\mathfrak{a})\,, \qquad A_{58} = -\frac{2\mu_{\rm fr}}{\mathsf{s}_{\rm EM,(II)}\mathfrak{a}}\,\omega\,{\rm i}k\,{\rm J}^{'}_{k}(\omega\,\mathsf{s}_{\rm EM,(II)}\mathfrak{a})\,,$$

$$A_{61} = -\frac{2\omega\,\mu_{\rm fr}{\rm i}k}{\mathfrak{a}\mathsf{s}_{\rm P,(I)}}{\rm H}^{(1)'}_{k}(\omega\,\mathsf{s}_{\rm P,(I)}\mathfrak{a}) + \frac{2\,\mu_{\rm fr}{\rm i}k}{\mathfrak{a}^2\mathsf{s}^2_{\rm P,(I)}}{\rm H}^{(1)}_{k}(\omega\,\mathsf{s}_{\rm P,(I)}\mathfrak{a})\,,$$

$$A_{62} = -\frac{2\omega\,\mu_{\rm fr}{\rm i}k}{\mathfrak{a}\mathsf{s}_{\rm B,(I)}}{\rm H}^{(1)'}_{k}(\omega\,\mathsf{s}_{\rm B,(I)}\mathfrak{a}) + \frac{2\mu_{\rm fr}{\rm i}k}{\mathfrak{a}^2\mathsf{s}^2_{\rm B,(I)}}{\rm H}^{(1)}_{k}(\omega\,\mathsf{s}_{\rm B,(I)}\mathfrak{a})\,,$$

$$A_{63} = -\frac{k^2\mu_{\rm fr}}{\mathfrak{a}^2\mathsf{s}^2_{\rm S,(I)}}{\rm H}^{(1)}_{k}(\omega\,\mathsf{s}_{\rm S,(I)}\,\mathfrak{a}) + \frac{\omega\,\mu_{\rm fr}}{\mathfrak{a}\mathsf{s}_{\rm S,(I)}}{\rm H}^{(1)'}_{k}(\omega\,\mathsf{s}_{\rm S,(I)}\,\mathfrak{a}) \;-\; \frac{\omega}{\mathsf{s}_{\rm S,(I)}\mathfrak{a}}\,{\rm H}^{(1)}_{k+1}(\omega\,\mathsf{s}_{\rm S,(I)}\,\mathfrak{a})$$
$$+\;\frac{k}{\mathsf{s}^2_{\rm S,(I)}\mathfrak{a}^2}\,{\rm H}^{(1)}_{k}(\omega\,\mathsf{s}^2_{\rm S,(I)}\,\mathfrak{a}) \;+\;\omega^2\,{\rm H}^{(1)}_{k}(\omega\,\mathsf{s}_{\rm S,(I)}\,\mathfrak{a})\;e^{{\rm i}\,k\,\theta} \;-\; \frac{k^2}{\mathsf{s}^2_{\rm S,(I)}\mathfrak{a}^2}\,{\rm H}^{(1)}_{k}(\omega\,\mathsf{s}_{\rm S,(I)}\,\mathfrak{a})\;,$$

$$A_{64} = -\frac{k^2\mu_{\rm fr}}{\mathfrak{a}^2\mathsf{s}^2_{\rm EM,(I)}}{\rm H}^{(1)}_{k}(\omega\,\mathsf{s}_{\rm EM,(I)}\,\mathfrak{a}) + \frac{\omega\,\mu_{\rm fr}}{\mathfrak{a}\mathsf{s}_{\rm EM,(I)}}{\rm H}^{(1)'}_{k}(\omega\,\mathsf{s}_{\rm EM,(I)}\,\mathfrak{a}) \;-\; \frac{\omega}{\mathsf{s}_{\rm EM,(I)}\mathfrak{a}}\,{\rm H}^{(1)}_{k+1}(\omega\,\mathsf{s}_{\rm EM,(I)}\,\mathfrak{a})$$
$$+\;\frac{k}{\mathsf{s}^2_{\rm EM,(I)}\mathfrak{a}^2}\,{\rm H}^{(1)}_{k}(\omega\,\mathsf{s}^2_{\rm EM,(I)}\,\mathfrak{a}) \;+\;\omega^2\,{\rm H}^{(1)}_{k}(\omega\,\mathsf{s}_{\rm EM,(I)}\,\mathfrak{a})\;e^{{\rm i}\,k\,\theta} \;-\; \frac{k^2}{\mathsf{s}^2_{\rm EM,(I)}\mathfrak{a}^2}\,{\rm H}^{(1)}_{k}(\omega\,\mathsf{s}_{\rm EM,(I)}\,\mathfrak{a})\;,$$

$$A_{65} = \frac{2\omega\,\mu_{\mathrm{fr}}\mathrm{i}k}{\mathfrak{a}\mathsf{s}_{\mathrm{P},(\mathrm{II})}}\mathrm{J}_k'(\omega\,\mathsf{s}_{\mathrm{P},(\mathrm{II})}\mathfrak{a}) - \frac{2\,\mu_{\mathrm{fr}}\mathrm{i}k}{\mathfrak{a}^2\mathsf{s}^2_{\mathrm{P},(\mathrm{II})}}\mathrm{J}_k(\omega\,\mathsf{s}_{\mathrm{P},(\mathrm{II})}\mathfrak{a})\,,$$

$$A_{66} = \frac{2\omega\,\mu_{\mathrm{fr}}\mathrm{i}k}{\mathfrak{a}\mathsf{s}_{\mathrm{B},(\mathrm{II})}}\mathrm{J}_k'(\omega\,\mathsf{s}_{\mathrm{B},(\mathrm{II})}\mathfrak{a}) - \frac{2\mu_{\mathrm{fr}}\mathrm{i}k}{\mathfrak{a}^2\mathsf{s}^2_{\mathrm{B},(\mathrm{II})}}\mathrm{J}_k(\omega\,\mathsf{s}_{\mathrm{B},(\mathrm{II})}\mathfrak{a})\,,$$

$$A_{67} = \frac{k^2\mu_{\mathrm{fr}}}{\mathfrak{a}^2\mathsf{s}^2_{\mathrm{S},(\mathrm{II})}}\mathrm{J}_k(\omega\,\mathsf{s}_{\mathrm{S},(\mathrm{II})}\,\mathfrak{a}) - \frac{\omega\,\mu_{\mathrm{fr}}}{\mathfrak{a}\mathsf{s}_{\mathrm{S},(\mathrm{II})}}\mathrm{J}_k'(\omega\,\mathsf{s}_{\mathrm{S},(\mathrm{II})}\,\mathfrak{a}) + \frac{\omega}{\mathsf{s}_{\mathrm{S},(\mathrm{II})}\mathfrak{a}}\,\mathrm{J}_{k+1}(\omega\,\mathsf{s}_{\mathrm{S},(\mathrm{II})}\,\mathfrak{a})$$
$$- \frac{k}{\mathsf{s}^2_{\mathrm{S},(\mathrm{II})}\mathfrak{a}^2}\,\mathrm{J}_k(\omega\,\mathsf{s}_{\mathrm{S},(\mathrm{II})}\,\mathfrak{a}) - \omega^2\,\mathrm{J}_k(\omega\,\mathsf{s}_{\mathrm{S},(\mathrm{II})}\,\mathfrak{a})\,e^{\mathrm{i}\,k\,\theta} + \frac{k^2}{\mathsf{s}^2_{\mathrm{S},(\mathrm{II})}\mathfrak{a}^2}\,\mathrm{J}_k(\omega\,\mathsf{s}_{\mathrm{S},(\mathrm{II})}\,\mathfrak{a})\,,$$

$$A_{68} = \frac{k^2\mu_{\mathrm{fr}}}{\mathfrak{a}^2\mathsf{s}^2_{\mathrm{EM},(\mathrm{II})}}\mathrm{J}_k(\omega\,\mathsf{s}_{\mathrm{EM},(\mathrm{II})}\,\mathfrak{a}) - \frac{\omega\,\mu_{\mathrm{fr}}}{\mathfrak{a}\mathsf{s}_{\mathrm{EM},(\mathrm{II})}}\mathrm{J}_k'(\omega\,\mathsf{s}_{\mathrm{EM},(\mathrm{II})}\,\mathfrak{a}) + \frac{\omega}{\mathsf{s}_{\mathrm{EM},(\mathrm{II})}\mathfrak{a}}\,\mathrm{J}_{k+1}(\omega\,\mathsf{s}_{\mathrm{EM},(\mathrm{II})}\,\mathfrak{a})$$
$$- \frac{k}{\mathsf{s}^2_{\mathrm{EM},(\mathrm{II})}\mathfrak{a}^2}\,\mathrm{J}_k(\omega\,\mathsf{s}_{\mathrm{EM},(\mathrm{II})}\,\mathfrak{a}) - \omega^2\,\mathrm{J}_k(\omega\,\mathsf{s}_{\mathrm{EM},(\mathrm{II})}\,\mathfrak{a}) + \frac{k^2}{\mathsf{s}^2_{\mathrm{EM},(\mathrm{II})}\mathfrak{a}^2}\,\mathrm{J}_k(\omega\,\mathsf{s}_{\mathrm{EM},(\mathrm{II})}\,\mathfrak{a})\,.$$

$$A_{71} = \frac{\mathrm{i}k}{\mathfrak{a}\,\mathsf{s}^2_{\mathrm{P},(\mathrm{I})}}E_{\mathrm{P},(\mathrm{I})}\mathrm{H}_k^{(1)}(\omega\,\mathsf{s}_{\mathrm{P},(\mathrm{I})}\,\mathfrak{a})\,, \qquad A_{72} = \frac{\mathrm{i}k}{\mathfrak{a}\,\mathsf{s}^2_{\mathrm{B},(\mathrm{I})}}\,E_{\mathrm{B},(\mathrm{I})}\mathrm{H}_k^{(1)}(\omega\,\mathsf{s}_{\mathrm{B},(\mathrm{I})}\,\mathfrak{a})\,,$$

$$A_{73} = \mathsf{s}^{-1}_{\mathrm{S},(\mathrm{I})}\,\omega\,E_{\mathrm{S},(\mathrm{I})}\mathrm{H}_k^{(1)'}(\omega\,\mathsf{s}_{\mathrm{S},(\mathrm{I})}\,\mathfrak{a})\,, \qquad A_{74} = \mathsf{s}^{-1}_{\mathrm{EM},(\mathrm{I})}\,\omega\,E_{\mathrm{EM},(\mathrm{I})}\mathrm{H}_k^{(1)'}(\omega\,\mathsf{s}_{\mathrm{EM},(\mathrm{I})}\,\mathfrak{a})\,,$$

$$A_{75} = -\frac{\mathrm{i}k}{\mathfrak{a}\,\mathsf{s}^2_{\mathrm{P},(\mathrm{II})}}E_{\mathrm{P},(\mathrm{II})}\mathrm{J}_k(\omega\,\mathsf{s}_{\mathrm{P},(\mathrm{II})}\,\mathfrak{a})\,, \qquad A_{76} = -\frac{\mathrm{i}k}{\mathfrak{a}\,\mathsf{s}^2_{\mathrm{B},(\mathrm{II})}}E_{\mathrm{B},(\mathrm{II})}\mathrm{J}_k(\omega\,\mathsf{s}_{\mathrm{B},(\mathrm{II})}\,\mathfrak{a})\,,$$

$$A_{77} = -\mathsf{s}^{-1}_{\mathrm{S},(\mathrm{II})}\,\omega\,E_{\mathrm{S},(\mathrm{II})}\mathrm{J}_k'(\omega\,\mathsf{s}_{\mathrm{S},(\mathrm{II})}\,\mathfrak{a})\,, \qquad A_{78} = -\mathsf{s}^{-1}_{\mathrm{EM},(\mathrm{II})}\,\omega\,E_{\mathrm{EM},(\mathrm{II})}\mathrm{J}_k'(\omega\,\mathsf{s}_{\mathrm{EM},(\mathrm{II})}\,\mathfrak{a})\,,$$

$$A_{81} = 0\,, \qquad A_{82} = 0\,, \qquad A_{83} = \frac{\mathfrak{s}\,\mathrm{i}}{\omega\,\mu_0}\,E_{\mathrm{S},(\mathrm{I})}\mathrm{H}_k^{(1)}(\omega\,\mathsf{s}_{\mathrm{S},(\mathrm{I})}\,\mathfrak{a})\,, \qquad A_{84} = \frac{\mathfrak{s}\,\mathrm{i}}{\omega\,\mu_0}\,E_{\mathrm{EM},(\mathrm{I})}\mathrm{H}_k^{(1)}(\omega\,\mathsf{s}_{\mathrm{EM},(\mathrm{I})}\,\mathfrak{a})\,,$$

$$A_{85} = 0\,, \qquad A_{86} = 0\,, \qquad A_{87} = -\frac{\mathfrak{s}\,\mathrm{i}}{\omega\,\mu_0}\,E_{\mathrm{S},(\mathrm{II})}\mathrm{J}_k(\omega\,\mathsf{s}_{\mathrm{S},(\mathrm{II})}\,\mathfrak{a})\,, \qquad A_{88} = -\frac{\mathfrak{s}\,\mathrm{i}}{\omega\,\mu_0}\,E_{\mathrm{EM},(\mathrm{II})}\mathrm{J}_k(\omega\,\mathsf{s}_{\mathrm{EM},(\mathrm{II})}\,\mathfrak{a})\,,$$

6.4.2 Numerical tests

We consider an infinite medium denoted as the exterior medium, in which Ω is a circular inclusion (interior medium) with radius $\mathfrak{a} = 5$m, see Figure 6.7, and we study the scattering of a P-plane wave by the inclusion. The solution is plotted on the disc of radius $r = 10$m in Figure 6.8 for the exterior medium composed of freshwater and the interior medium composed of sand (see Table 5.2). The total wave is presented, we can observe the bands of the incident plane wave, which are a little distorted due to the reflections on the inclusion. Here, we want to determine if we can find values of frequency for which the determinant of the coefficient matrices vanishes, which are the equivalent of electrokinetic Jones' modes. Hence, we study the determinant of the coefficients matrix (6.28) as a function of ω for the first modes $k = 0, ..., 5$. From Figures 6.9 and 6.10, we can observe that there is no peaks on the curves, which means that there is no eigenvalues in the problem for the considered frequency range.

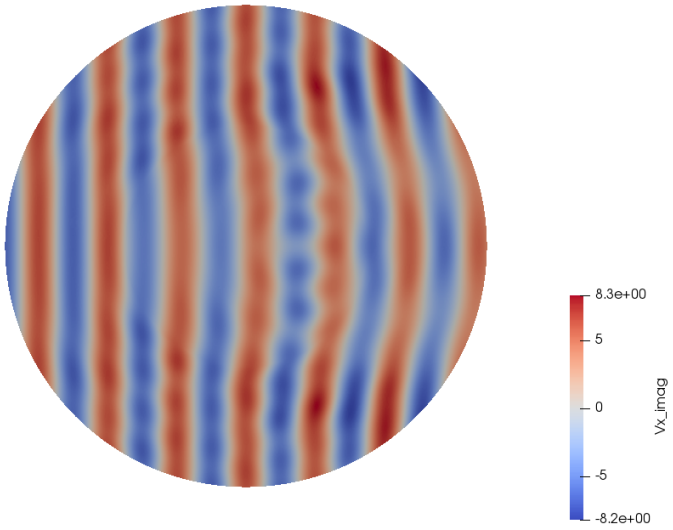

Figure 6.8: Scattering of a P plane wave by a penetrable solid inclusion. Total solution of the imaginary part of the solid velocity u_x for freshwater/sand test with $f = 1$kHz.

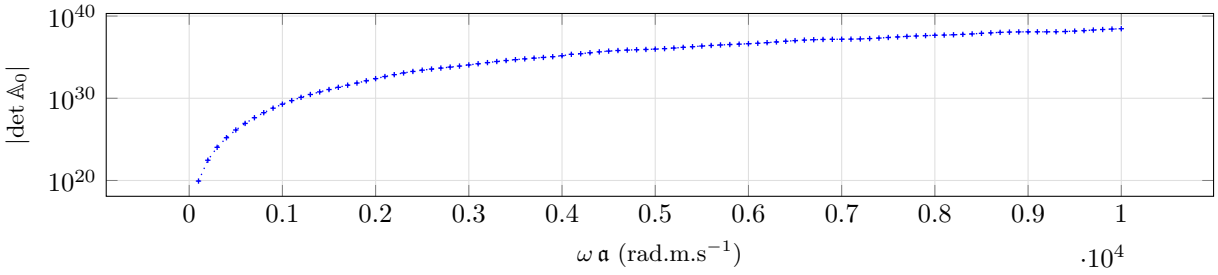

(a) Mode $k = 0$

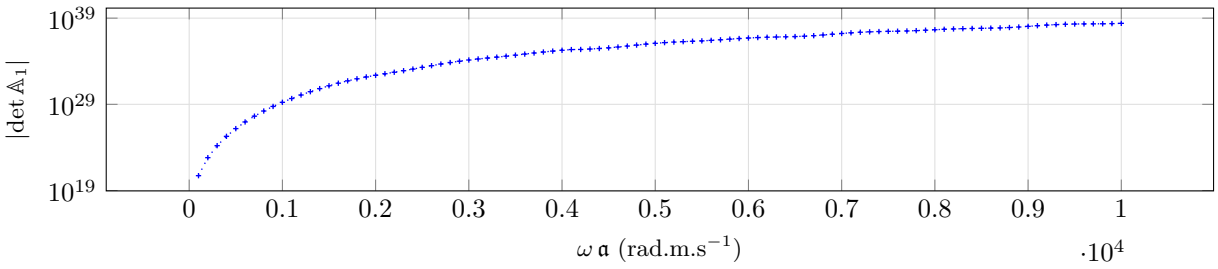

(b) Mode $k = 1$

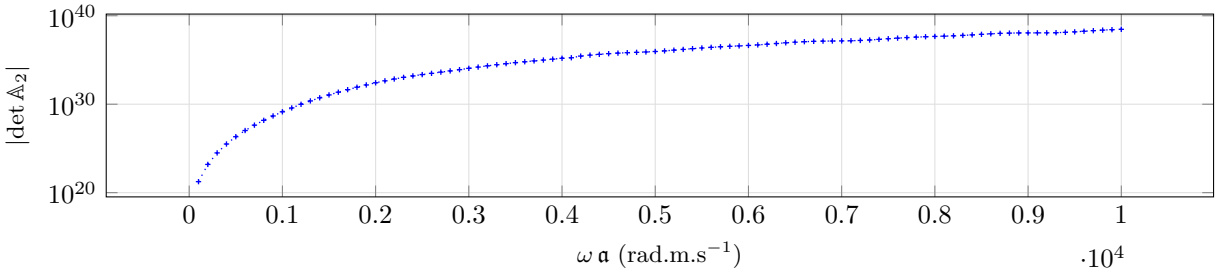

(c) Mode $k = 2$

Figure 6.9: Module of determinant of the coefficients matrix $\mathbb{A}_k$ (log scale) for modes 0 to 2 for for the exterior medium composed of freshwater and the interior medium of sand.

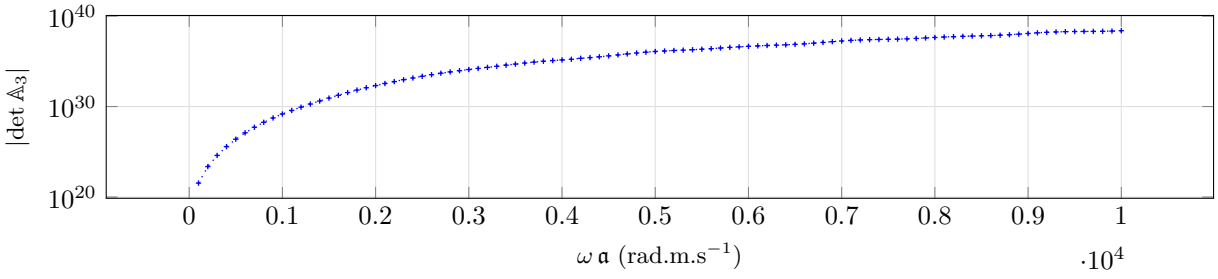

(a) Mode $k = 3$

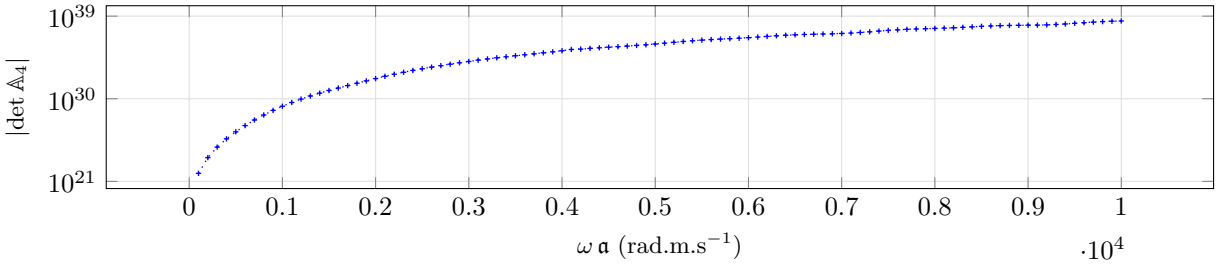

(b) Mode $k = 4$

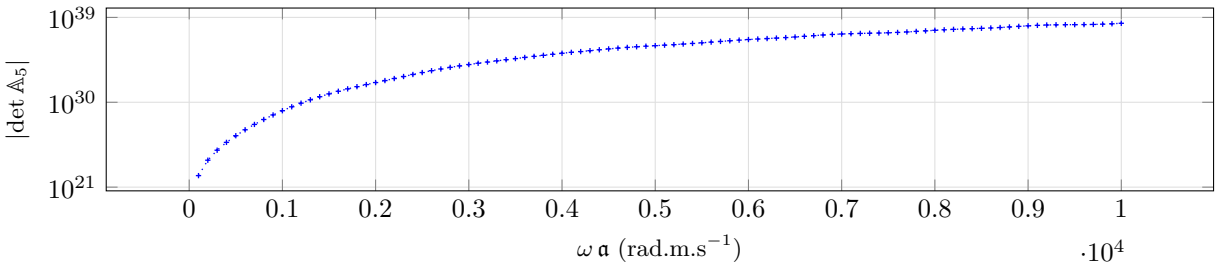

(c) Mode $k = 5$

Figure 6.10: Module of determinant of the coefficients matrix $\mathbb{A}_k$ (log scale) for modes 3 to 5 for the exterior medium composed of freshwater and the interior medium of sand.

6.5 Analytical solution for fundamental solution for Pride's equations

In this section, we consider a two-dimensional homogeneous medium, and we build the analytical solution corresponding with the response to a point source. Starting with the second-order formulation of Pride's equations (5.5), we have expressed in (6.4) the unknowns u, w, $\boldsymbol{E}$ in terms of the potentials as:

$$-\omega^2 \begin{pmatrix} \mathrm{u} \\ \mathrm{w} \\ \boldsymbol{E} \end{pmatrix} - P_{\mathrm{long}} \begin{pmatrix} \mathsf{s}_{\mathrm{P}}^{-2} & 0 & 0 \\ 0 & \mathsf{s}_{\mathrm{B}}^{-2} & 0 \\ 0 & 0 & 0 \end{pmatrix} \begin{pmatrix} \nabla\chi_{\mathrm{P}} \\ \nabla\chi_{\mathrm{B}} \\ 0 \end{pmatrix} - P_{\mathrm{trans}} \begin{pmatrix} \mathsf{s}_{\mathrm{S}}^{-2} & 0 & 0 \\ 0 & 0 & 0 \\ 0 & 0 & \mathsf{s}_{\mathrm{EM}}^{-2} \end{pmatrix} \begin{pmatrix} \mathbf{curl}\chi_{\mathrm{S}} \\ 0 \\ \mathbf{curl}\chi_{\mathrm{EM}} \end{pmatrix} = A^{-1} \begin{pmatrix} \mathbf{f}_{\mathrm{u}} \\ \mathbf{f}_{\mathrm{w}} + \nabla M \mathbf{f}_{\mathrm{p}} \\ -\mathfrak{s}\,\mathrm{i}\,\omega\,\mu_0\,\mathbf{f}_C \end{pmatrix}, \quad (6.29)$$

where the matrices A, P_{long} and P_{trans} have been given in (6.1) and (6.2). In addition, the potentials $\chi_\bullet$ solve Helmholtz equations

$$\begin{aligned} -\omega^2\,\mathsf{s}_{\mathrm{P}}^2\,\chi_{\mathrm{P}} - \Delta\,\chi_{\mathrm{P}} &= \mathsf{s}_{\mathrm{P}}^2\,\pi_1 \left(P_{\mathrm{long}}^{-1}\,A^{-1} \begin{pmatrix} \nabla\cdot\mathbf{F_1} \\ \nabla\cdot\mathbf{F_2} \\ \nabla\cdot\mathbf{F_3} \end{pmatrix} \right), \\ -\omega^2\,\mathsf{s}_{\mathrm{B}}^2\,\chi_{\mathrm{B}} - \Delta\,\chi_{\mathrm{B}} &= \mathsf{s}_{\mathrm{B}}^2\,\pi_2 \left(P_{\mathrm{long}}^{-1}\,A^{-1} \begin{pmatrix} \nabla\cdot\mathbf{F_1} \\ \nabla\cdot\mathbf{F_2} \\ \nabla\cdot\mathbf{F_3} \end{pmatrix} \right), \\ -\omega^2\,\mathsf{s}_{\mathrm{S}}^2\,\chi_{\mathrm{S}} - \Delta\,\chi_{\mathrm{S}} &= \mathsf{s}_{\mathrm{S}}^2\,\pi_1 \left(P_{\mathrm{trans}}^{-1}\,A^{-1} \begin{pmatrix} \mathrm{curl}\,\mathbf{F_1} \\ \mathrm{curl}\,\mathbf{F_2} \\ \mathrm{curl}\,\mathbf{F_3} \end{pmatrix} \right), \\ -\omega^2\,\mathsf{s}_{\mathrm{EM}}^2\,\chi_{\mathrm{EM}} - \Delta\,\chi_{\mathrm{EM}} &= \mathsf{s}_{\mathrm{EM}}^2\,\pi_3 \left(P_{\mathrm{trans}}^{-1}\,A^{-1} \begin{pmatrix} \mathrm{curl}\,\mathbf{F_1} \\ \mathrm{curl}\,\mathbf{F_2} \\ \mathrm{curl}\,\mathbf{F_3} \end{pmatrix} \right). \end{aligned} \quad (6.30)$$

with

$$\mathbf{F_1} = \mathbf{f}_{\mathrm{u}}\,, \quad \mathbf{F_2} = \mathbf{f}_{\mathrm{w}} + \nabla M\,\mathbf{f}_{\mathrm{p}}\,, \quad \mathbf{F_3} = -\mathfrak{s}\,\mathrm{i}\,\omega\,\mu_0\,\mathbf{f}_C\,.$$

In the following, we first study a point source generating pressure waves, and secondly a source that produces only transverse waves, and we build an analytical solution for each case. Recall that a point-source is modeled as a Dirac distribution, denoted by $\delta_{\mathbf{Y}}$ with $\mathbf{Y}$ the center of the source. We will use the fact that the outgoing Green kernel of

$$(-\Delta - (\omega\,\mathsf{s}_\bullet)^2)G(\mathbf{X}) = \delta_{\mathbf{Y}} \quad \text{is} \quad G_+(\mathbf{X}) = \frac{\mathrm{i}}{4}\mathrm{H}_0^{(1)}(\omega\,\mathsf{s}_\bullet|\mathbf{X}-\mathbf{Y}|)\,, \quad (6.31)$$

with $\mathrm{H}_0^{(1)}$ the Hankel function of first-order. In the following, to simplify the notations, we denote the Dirac distribution by δ, and we consider $\mathbf{Y} = 0$. Moreover, in a homogeneous infinite domain, the outgoing solution of

$$(-\Delta - (\omega\,\mathsf{s}_\bullet)^2)\,G(\mathbf{X}) = 0 \quad \text{is} \quad G_+(\mathbf{X}) = 0 \quad \text{in}\,\mathbb{R}^2\,. \quad (6.32)$$

6.5.1 Source generating pressure waves

To model a source generating only pressure waves, we use the fact that $\mathrm{curl}\,\nabla = 0$, which leads to a null value of the transverse potential. We set $\mathbf{f}_{\mathrm{u}} = \nabla\delta\,, \quad \mathbf{f}_{\mathrm{w}} = 0\,, \quad \mathbf{f}_{\mathrm{p}} = 0\,, \quad \mathbf{f}_C = 0\,,$ which means that $\mathbf{F_1} = \nabla\delta\,, \quad \mathbf{F_2} = 0\,, \quad \mathbf{F_3} = 0\,.$ Since $\mathrm{curl}\,\nabla = 0$, the Helmholtz equations (6.30) become

$$\begin{aligned} \left(-\Delta - \omega^2\,\mathsf{s}_{\mathrm{P}}^2\right)\chi_{\mathrm{P}} &= \mathsf{s}_{\mathrm{P}}^2\,[P_{\mathrm{long}}^{-1}\,A^{-1}]_{11}\,\Delta\,\delta\,, \\ \left(-\Delta - \omega^2\,\mathsf{s}_{\mathrm{B}}^2\right)\chi_{\mathrm{B}} &= \mathsf{s}_{\mathrm{B}}^2\,[P_{\mathrm{long}}^{-1}\,A^{-1}]_{21}\,\Delta\delta\,, \\ \left(-\Delta - \omega^2\,\mathsf{s}_{\mathrm{S}}^2\right)\chi_{\mathrm{S}} &= 0\,, \\ \left(-\Delta - \omega^2\,\mathsf{s}_{\mathrm{EM}}^2\right)\chi_{\mathrm{EM}} &= 0\,, \end{aligned}$$

with the matrices P_{long} and A defined in (5.21) and (5.25). Using the relations given in (6.31) and (6.32), the potentials read as:

$$\begin{aligned} \chi_{\mathrm{P}} &= \mathsf{s}_{\mathrm{P}}^2\,[P_{\mathrm{long}}^{-1}\,A^{-1}]_{11}\,\Delta\,\frac{\mathrm{i}}{4}\mathrm{H}_0^{(1)}(\omega\,\mathsf{s}_{\mathrm{P}}r) = \mathsf{s}_{\mathrm{P}}^2\,[P_{\mathrm{long}}^{-1}\,A^{-1}]_{11}\left(-(\omega\,\mathsf{s}_{\mathrm{P}})^2\frac{\mathrm{i}}{4}\mathrm{H}_0^{(1)}(\omega\,\mathsf{s}_{\mathrm{P}}r) - \delta\right), \\ \chi_{\mathrm{B}} &= \mathsf{s}_{\mathrm{B}}^2\,[P_{\mathrm{long}}^{-1}\,A^{-1}]_{21}\,\Delta\,\mathrm{H}_0^{(1)}(\omega\,\mathsf{s}_{\mathrm{B}}r) = \mathsf{s}_{\mathrm{B}}^2\,[P_{\mathrm{long}}^{-1}\,A^{-1}]_{21}\left(-(\omega\,\mathsf{s}_{\mathrm{B}})^2\frac{\mathrm{i}}{4}\mathrm{H}_0^{(1)}(\omega\,\mathsf{s}_{\mathrm{B}}r) - \delta\right), \\ \chi_{\mathrm{S}} &= 0\,, \quad \chi_{\mathrm{EM}} = 0\,. \end{aligned}$$

The gradients of the longitudinal potentials are:

$$\nabla\chi_{\mathrm{P}} = \mathsf{s}_{\mathrm{P}}^2\,[P_{\mathrm{long}}^{-1}\,A^{-1}]_{11}\left(-(\omega\,\mathsf{s}_{\mathrm{P}})^2\frac{\mathrm{i}}{4}\nabla\mathrm{H}_0^{(1)}(\omega\,\mathsf{s}_{\mathrm{P}}r)-\nabla\delta\right),$$
$$\nabla\chi_{\mathrm{B}} = \mathsf{s}_{\mathrm{B}}^2\,[P_{\mathrm{long}}^{-1}\,A^{-1}]_{21}\left(-(\omega\,\mathsf{s}_{\mathrm{B}})^2\frac{\mathrm{i}}{4}\nabla\mathrm{H}_0^{(1)}(\omega\,\mathsf{s}_{\mathrm{B}}r)-\nabla\delta\right).$$

Then, we write equation (6.29) by using the above expression and the expression of A given in equation (6.1):

$$-\omega^2\begin{pmatrix}\mathrm{u}\\ \mathrm{w}\\ \boldsymbol{E}\end{pmatrix} - P_{\mathrm{long}}\begin{pmatrix}[P_{\mathrm{long}}^{-1}\,A^{-1}]_{11}\left(-(\omega\,\mathsf{s}_{\mathrm{P}})^2\frac{\mathrm{i}}{4}\nabla\mathrm{H}_0^{(1)}(\omega\,\mathsf{s}_{\mathrm{P}}r)-\nabla\delta\right)\\ [P_{\mathrm{long}}^{-1}\,A^{-1}]_{21}\left(-(\omega\,\mathsf{s}_{\mathrm{B}})^2\frac{\mathrm{i}}{4}\nabla\mathrm{H}_0^{(1)}(\omega\,\mathsf{s}_{\mathrm{B}}r)-\nabla\delta\right)\\ 0\end{pmatrix} = A^{-1}\begin{pmatrix}\nabla\delta\\ 0\\ 0\end{pmatrix}.$$

Note that here, $\nabla\delta$ is the gradient of the Dirac in the sense of the distributions. Multiplying the above equation by P_{long}^{-1}, we obtain:

$$-\omega^2\,P_{\mathrm{long}}^{-1}\begin{pmatrix}\mathrm{u}\\ \mathrm{w}\\ \boldsymbol{E}\end{pmatrix} - \begin{pmatrix}[P_{\mathrm{long}}^{-1}\,A^{-1}]_{11}\left(-(\omega\,\mathsf{s}_{\mathrm{P}})^2\frac{\mathrm{i}}{4}\nabla\mathrm{H}_0^{(1)}(\omega\,\mathsf{s}_{\mathrm{P}}r)-\nabla\delta\right)\\ [P_{\mathrm{long}}^{-1}\,A^{-1}]_{21}\left(-(\omega\,\mathsf{s}_{\mathrm{B}})^2\frac{\mathrm{i}}{4}\nabla\mathrm{H}_0^{(1)}(\omega\,\mathsf{s}_{\mathrm{B}}r)-\nabla\delta\right)\\ 0\end{pmatrix} = \begin{pmatrix}[P_{\mathrm{long}}^{-1}\,A^{-1}]_{11}\,\nabla\delta\\ [P_{\mathrm{long}}^{-1}\,A^{-1}]_{21}\,\nabla\delta\\ 0\end{pmatrix}.$$

In the above equation, we simplify the gradient of Dirac in the second term and in the right-hand side. Then, we multiply the system by $-\omega^{-2}\,P_{\mathrm{long}}$, to obtain the expressions of the displacements u, w, and the electric field $\boldsymbol{E}$:

$$\begin{pmatrix}\mathrm{u}\\ \mathrm{w}\\ \boldsymbol{E}\end{pmatrix} = P_{\mathrm{long}}\begin{pmatrix}[P_{\mathrm{long}}^{-1}\,A^{-1}]_{11}\left(\mathsf{s}_{\mathrm{P}}^2\frac{\mathrm{i}}{4}\nabla\mathrm{H}_0^{(1)}(\omega\,\mathsf{s}_{\mathrm{P}}r)\right)\\ [P_{\mathrm{long}}^{-1}\,A^{-1}]_{21}\left(\mathsf{s}_{\mathrm{B}}^2\frac{\mathrm{i}}{4}\nabla\mathrm{H}_0^{(1)}(\omega\,\mathsf{s}_{\mathrm{B}}r)\right)\\ 0\end{pmatrix}.$$

Recall that in polar coordinates

$$\nabla\mathrm{H}_0^{(1)}(\omega\,\mathsf{s}_\bullet r) = \omega\,\mathsf{s}_\bullet\mathrm{H}_0^{(1)'}(\omega\,\mathsf{s}_\bullet r)\mathbf{e}_r\,,\qquad\text{and}\qquad \mathrm{H}_0^{(1)'}(\omega\,\mathsf{s}_\bullet r) = -\mathrm{H}_1^{(1)}(\omega\,\mathsf{s}_\bullet r)\,.$$

Hence

$$\mathrm{u} = \left(-\,[P_{\mathrm{long}}^{-1}\,A^{-1}]_{11}\,\omega\,\mathsf{s}_{\mathrm{P}}^3\,\frac{\mathrm{i}}{4}\mathrm{H}_1^{(1)}(\omega\,\mathsf{s}_{\mathrm{P}}r) - [P_{\mathrm{long}}^{-1}\,A^{-1}]_{21}\,\omega\,\mathsf{s}_{\mathrm{B}}^3\,\frac{\mathrm{i}}{4}\mathrm{H}_1^{(1)}(\omega\,\mathsf{s}_{\mathrm{B}}r)\right)\mathrm{e}_r\,,$$
$$\mathrm{w} = \left(-\,\mathcal{W}_{\mathrm{P}}\,[P_{\mathrm{long}}^{-1}\,A^{-1}]_{11}\,\omega\,\mathsf{s}_{\mathrm{P}}^3\,\frac{\mathrm{i}}{4}\mathrm{H}_1^{(1)}(\omega\,\mathsf{s}_{\mathrm{P}}r) - \mathcal{W}_{\mathrm{B}}\,[P_{\mathrm{long}}^{-1}\,A^{-1}]_{21}\,\omega\,\mathsf{s}_{\mathrm{B}}^3\,\frac{\mathrm{i}}{4}\mathrm{H}_1^{(1)}(\omega\,\mathsf{s}_{\mathrm{B}}r)\right)\mathrm{e}_r\,,$$
$$\boldsymbol{E} = \left(-\,\mathcal{E}_{\mathrm{P}}\,[P_{\mathrm{long}}^{-1}\,A^{-1}]_{11}\,\omega\,\mathsf{s}_{\mathrm{P}}^3\,\frac{\mathrm{i}}{4}\mathrm{H}_1^{(1)}(\omega\,\mathsf{s}_{\mathrm{P}}r) - \mathcal{E}_{\mathrm{B}}\,[P_{\mathrm{long}}^{-1}\,A^{-1}]_{21}\,\omega\,\mathsf{s}_{\mathrm{B}}^3\,\frac{\mathrm{i}}{4}\mathrm{H}_1^{(1)}(\omega\,\mathsf{s}_{\mathrm{B}}r)\right)\mathrm{e}_r\,.$$

Proposition 6.4. The first-order variables for a point source in pressure waves are for the velocities:

$$\mathbf{u} = \left([P_{\mathrm{long}}^{-1}\,A^{-1}]_{11}\,\frac{\omega^2\,\mathsf{s}_{\mathrm{P}}^3}{4}\mathrm{H}_1^{(1)}(\omega\,\mathsf{s}_{\mathrm{P}}r) + [P_{\mathrm{long}}^{-1}\,A^{-1}]_{21}\,\frac{\omega^2\,\mathsf{s}_{\mathrm{B}}^3}{4}\mathrm{H}_1^{(1)}(\omega\,\mathsf{s}_{\mathrm{B}}r)\right)\mathrm{e}_r\,,$$
$$\mathbf{w} = \left(\mathcal{W}_{\mathrm{P}}\,[P_{\mathrm{long}}^{-1}\,A^{-1}]_{11}\,\frac{\omega^2\,\mathsf{s}_{\mathrm{P}}^3}{4}\mathrm{H}_1^{(1)}(\omega\,\mathsf{s}_{\mathrm{P}}r) + \mathcal{W}_{\mathrm{B}}\,[P_{\mathrm{long}}^{-1}\,A^{-1}]_{21}\,\frac{\omega^2\,\mathsf{s}_{\mathrm{B}}^3}{4}\mathrm{H}_1^{(1)}(\omega\,\mathsf{s}_{\mathrm{B}}r)\right)\mathrm{e}_r\,.$$

The stress tensor is:

$$\boldsymbol{\tau} = \tau_{rr}\mathbf{e}_r\otimes\mathbf{e}_r + \tau_{\theta\theta}\mathbf{e}_\theta\otimes\mathbf{e}_\theta\,,$$

with

$$\begin{aligned}
\tau_{rr} &= -(2\mu_{\rm fr} + \lambda_{\rm fr} + M\alpha^2)\Big(\frac{\mathrm{i}}{4}\omega^2\,\mathsf{s}_{\rm P}^4\,[P_{\rm long}^{-1}A^{-1}]_{11}\mathrm{H}_1^{(1)'}(\omega\,\mathrm{s}_{\rm P}r) + \frac{\mathrm{i}}{4}\omega^2\,\mathsf{s}_{\rm B}^4\,[P_{\rm long}^{-1}A^{-1}]_{21}\mathrm{H}_1^{(1)'}(\omega\,\mathrm{s}_{\rm B}r)\Big)\\
&\quad - \alpha M\Big(\frac{\mathrm{i}\,\mathcal{W}_{\rm P}}{4}\omega^2\,\mathsf{s}_{\rm P}^4\,[P_{\rm long}^{-1}A^{-1}]_{11}\mathrm{H}_1^{(1)'}(\omega\,\mathrm{s}_{\rm P}r) + \frac{\mathrm{i}\,\mathcal{W}_{\rm B}}{4}\omega^2\,\mathsf{s}_{\rm B}^4\,[P_{\rm long}^{-1}A^{-1}]_{21}\mathrm{H}_1^{(1)'}(\omega\,\mathrm{s}_{\rm B}r)\Big),\\
\tau_{\theta\theta} &= -(\lambda_{\rm fr} + M\alpha^2)\Big(\frac{\mathrm{i}}{4}\omega^2\,\mathsf{s}_{\rm P}^4\,[P_{\rm long}^{-1}A^{-1}]_{11}\mathrm{H}_1^{(1)'}(\omega\,\mathrm{s}_{\rm P}r) + \frac{\mathrm{i}}{4}\omega^2\,\mathsf{s}_{\rm B}^4\,[P_{\rm long}^{-1}A^{-1}]_{21}\mathrm{H}_1^{(1)'}(\omega\,\mathrm{s}_{\rm B}r)\Big)\\
&\quad - \alpha M\Big(\frac{\mathrm{i}\,\mathcal{W}_{\rm P}}{4}\omega^2\,\mathsf{s}_{\rm P}^4\,[P_{\rm long}^{-1}A^{-1}]_{11}\mathrm{H}_1^{(1)'}(\omega\,\mathrm{s}_{\rm P}r) + \frac{\mathrm{i}\,\mathcal{W}_{\rm B}}{4}\omega^2\,\mathsf{s}_{\rm B}^4\,[P_{\rm long}^{-1}A^{-1}]_{21}\mathrm{H}_1^{(1)'}(\omega\,\mathrm{s}_{\rm B}r)\Big).
\end{aligned}$$

The pressure is given as:

$$\begin{aligned}
\mathrm{p} &= M\Big(\frac{\mathrm{i}\,\mathcal{W}_{\rm P}}{4}\omega^2\,\mathsf{s}_{\rm P}^4\,[P_{\rm long}^{-1}A^{-1}]_{11}\mathrm{H}_1^{(1)'}(\omega\,\mathrm{s}_{\rm P}r) + \frac{\mathrm{i}\,\mathcal{W}_{\rm B}}{4}\omega^2\,\mathsf{s}_{\rm B}^4\,[P_{\rm long}^{-1}A^{-1}]_{21}\mathrm{H}_1^{(1)'}(\omega\,\mathrm{s}_{\rm B}r)\Big)\\
&\quad + M\,\alpha\Big(\frac{\mathrm{i}}{4}\omega^2\,\mathsf{s}_{\rm P}^4\,[P_{\rm long}^{-1}A^{-1}]_{11}\mathrm{H}_1^{(1)'}(\omega\,\mathrm{s}_{\rm P}r) + \frac{\mathrm{i}}{4}\omega^2\,\mathsf{s}_{\rm B}^4\,[P_{\rm long}^{-1}A^{-1}]_{21}\mathrm{H}_1^{(1)'}(\omega\,\mathrm{s}_{\rm B}r)\Big).
\end{aligned}$$

The electromagnetic variables are

$$\begin{aligned}
\boldsymbol{E} &= \Big(-\mathcal{E}_{\rm P}\,[P_{\rm long}^{-1}A^{-1}]_{11}\,\omega\,\mathsf{s}_{\rm P}^3\,\frac{\mathrm{i}}{4}\mathrm{H}_1^{(1)}(\omega\,\mathrm{s}_{\rm P}r) - \mathcal{E}_{\rm B}\,[P_{\rm long}^{-1}A^{-1}]_{21}\,\omega\,\mathsf{s}_{\rm B}^3\,\frac{\mathrm{i}}{4}\mathrm{H}_1^{(1)}(\omega\,\mathrm{s}_{\rm B}r)\Big)\,\mathrm{e}_r\,,\\
\mathrm{H} &= 0\,,\\
\boldsymbol{J} &= -\mathsf{s}\,\mathrm{i}\,\omega\,\delta_0\,\Big(-\mathcal{E}_{\rm P}\,[P_{\rm long}^{-1}A^{-1}]_{11}\,\omega\,\mathsf{s}_{\rm P}^3\,\frac{\mathrm{i}}{4}\mathrm{H}_1^{(1)}(\omega\,\mathrm{s}_{\rm P}r) - \mathcal{E}_{\rm B}\,[P_{\rm long}^{-1}A^{-1}]_{21}\,\omega\,\mathsf{s}_{\rm B}^3\,\frac{\mathrm{i}}{4}\mathrm{H}_1^{(1)}(\omega\,\mathrm{s}_{\rm B}r)\Big)\,\mathbf{e}_r\,.
\end{aligned}$$

Proof.

- The velocities $\mathbf{u}$ and $\mathbf{w}$ are calculated by taking the time derivative of the displacements u and w.
- From the calculation of $\boldsymbol{\tau}$ in Section 2.6 for poroelasticity, we have

$$\begin{aligned}
\boldsymbol{\tau} &= \Big(2\mu_{\rm fr}\frac{\partial \mathrm{u}_r}{\partial r} + (\lambda_{\rm fr} + M\alpha^2)\frac{\partial \mathrm{u}_r}{\partial r} + \alpha M\frac{\partial \mathrm{w}_r}{\partial r}\Big)\mathbf{e}_r\otimes\mathbf{e}_r\\
&\quad + \Big((\lambda_{\rm fr} + M\alpha^2)\frac{\partial \mathrm{u}_r}{\partial r} + \alpha M\frac{\partial \mathrm{w}_r}{\partial r}\Big)\mathbf{e}_\theta\otimes\mathbf{e}_\theta\,,
\end{aligned}$$

  and the radial derivative of $\mathrm{H}_1^{(1)}(\omega\,\mathrm{s}_\bullet r)$ is:

$$\frac{\partial}{\partial r}\mathrm{H}_1^{(1)}(\omega\,\mathrm{s}_\bullet r) = \omega\,\mathrm{s}_\bullet\mathrm{H}_1^{(1)'}(\omega\,\mathrm{s}_\bullet r) = \omega\,\mathrm{s}_\bullet\mathrm{H}_0^{(1)}(\omega\,\mathrm{s}_\bullet r) - \frac{1}{r}\mathrm{H}_1^{(1)}(\omega\,\mathrm{s}_\bullet r)\,.$$

  With those two expressions, we obtain the expression of $\boldsymbol{\tau}$.
- For the calculation of p, we use the constitutive law (5.3d) and the expressions of the displacements u and w.
- Concerning the expression of the magnetic field H, we use equation (5.3e):

$$\mathrm{H} = \frac{\mathsf{s}\,\mathrm{i}}{\omega\,\mu_0}\,\mathrm{curl}\,\boldsymbol{E}\,,$$

  and the curl of the electric field is:

$$\mathrm{curl}\,\boldsymbol{E} = \partial_r\boldsymbol{E}_\theta - \frac{1}{r}\,\partial_\theta\boldsymbol{E}_r = 0\,,$$

  because $\boldsymbol{E}_\theta = 0$, and $\boldsymbol{E}_r$ is independent of θ. Hence, the magnetic field is equal to zero.
- Finally, for the calculation of $\boldsymbol{J}$, equation (5.3g) gives:

$$\boldsymbol{J} = \mathbf{curl}\,\mathrm{H} - \mathsf{s}\,\mathrm{i}\,\omega\,\delta_0\,\boldsymbol{E} = -\mathsf{s}\,\mathrm{i}\,\omega\,\delta_0\,E_r\,\mathbf{e}_r\,,$$

  because the magnetic field H is equal to zero.

□

This analytical solution will be used to verify the numerical solution obtained with the HDG method (see Chapter 7). The solutions in terms of solid velocity $\mathbf{u}$ and electric field $\boldsymbol{E}$ are given respectively in Figures 6.11 and 6.12. On the left, we present the total solution. Then, in figures (b), we only plot the contribution of the P-wave to the fields. Similarly, in figures (c), we only show the contribution of the B-wave. By this way, we can identify clearly the two kinds of longitudinal waves propagating in the medium. We observe that for $\mathbf{u}$, the magnitude of contributions of the P- and B-waves are close (see Figure 6.11). However, for $\boldsymbol{E}$, the contribution of the B-wave has a greater amplitude than the P-wave (*cf.* Figure 6.12). It shows that in this case, the conversion from seismic source to electromagnetic signal is mostly carried by the B-wave.

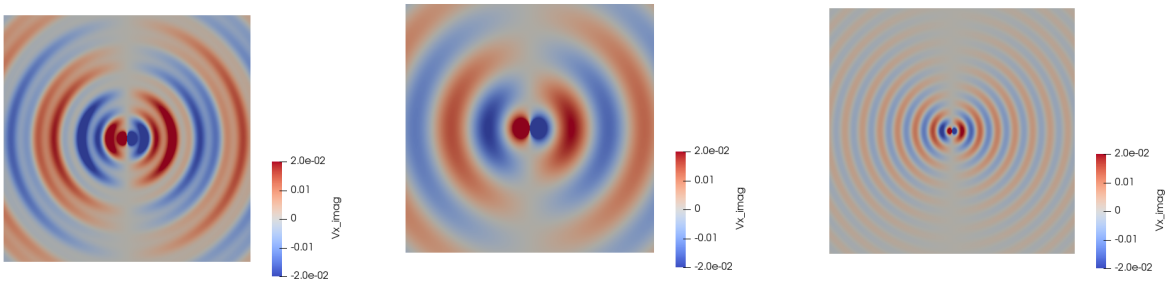

(a) Total wave $\mathbf{u}$ (b) P-wave $\mathbf{u}$ (c) B-wave $\mathbf{u}$

Figure 6.11: Decomposition of the analytical solution of $\mathbf{u}$ in longitudinal waves.

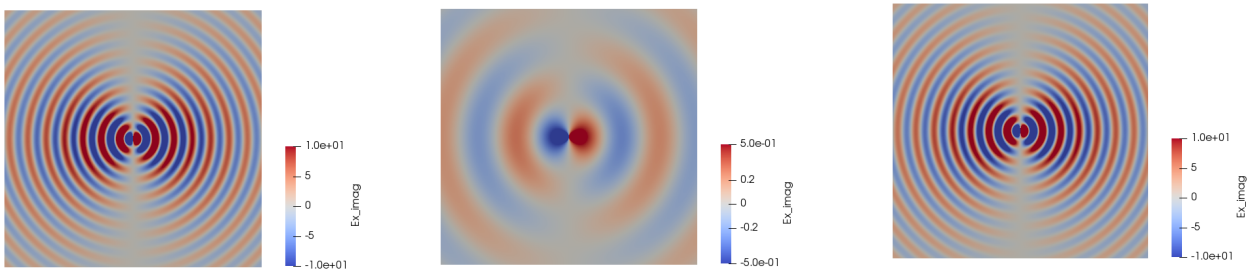

(a) Total wave $\boldsymbol{E}$ (b) P-wave $\boldsymbol{E}$ (c) B-wave $\boldsymbol{E}$

Figure 6.12: Decomposition of the analytical solution of $\boldsymbol{E}$ in longitudinal waves.

6.5.2 Source generating transverse waves

Here, we want to have a point-source producing only transverse waves. For that, we set the forces to $\mathbf{f}_{\mathrm{u}} = \mathbf{curl}\,\delta$, $\mathbf{f}_{\mathrm{w}} = 0$, $\mathbf{f}_{\mathrm{p}} = 0$, and $\mathbf{f}_C = 0$, which means that $\mathbf{F_1} = \mathbf{curl}\,\delta$, $\mathbf{F_2} = 0$, and $\mathbf{F_3} = 0$. Since $\operatorname{curl}\nabla = 0$, the Helmholtz equations (6.30) become

$$
\begin{aligned}
\left(-\Delta - \omega^2\,\mathsf{s}_{\mathrm{P}}^2\right)\chi_{\mathrm{P}} &= 0\,,\\
\left(-\Delta - \omega^2\,\mathsf{s}_{\mathrm{B}}^2\right)\chi_{\mathrm{B}} &= 0\,,\\
\left(-\Delta - \omega^2\,\mathsf{s}_{\mathrm{S}}^2\right)\chi_{\mathrm{S}} &= -\mathsf{s}_{\mathrm{S}}^2\,[P_{\mathrm{trans}}^{-1}\,A^{-1}]_{11}\,\Delta\,\delta\,,\\
\left(-\Delta - \omega^2\,\mathsf{s}_{\mathrm{EM}}^2\right)\chi_{\mathrm{EM}} &= -\mathsf{s}_{\mathrm{EM}}^2\,[P_{\mathrm{trans}}^{-1}\,A^{-1}]_{31}\,\Delta\,\delta\,.
\end{aligned}
$$

Hence, using the expression (6.31) and (6.32) the potentials are:

$$\chi_{\rm P} = 0\,, \quad \chi_{\rm B} = 0\,,$$

$$\chi_{\rm S} = -\,\mathsf{s}_{\rm S}^2\,[P_{\rm trans}^{-1}\,A^{-1}]_{11}\,\Delta\,\frac{\mathrm{i}}{4}\mathrm{H}_0^{(1)}(\omega\,\mathsf{s}_{\rm S} r) \;=\; \mathsf{s}_{\rm S}^2\,[P_{\rm trans}^{-1}\,A^{-1}]_{11}\left((\omega\,\mathsf{s}_{\rm S})^2\,\frac{\mathrm{i}}{4}\mathrm{H}_0^{(1)}(\omega\,\mathsf{s}_{\rm S} r) + \delta\right)\,,$$

$$\chi_{\rm EM} = -\,\mathsf{s}_{\rm EM}^2\,[P_{\rm trans}^{-1}\,A^{-1}]_{31}\,\Delta\,\mathrm{H}_0^{(1)}(\omega\,\mathsf{s}_{\rm EM} r) \;=\; \mathsf{s}_{\rm EM}^2\,[P_{\rm trans}^{-1}\,A^{-1}]_{31}\left((\omega\,\mathsf{s}_{\rm EM})^2\,\frac{\mathrm{i}}{4}\mathrm{H}_0^{(1)}(\omega\,\mathsf{s}_{\rm EM} r) + \delta\right)\,.$$

The curls of the transverse potentials $\chi_{\rm S}$ and $\chi_{\rm EM}$ are

$$\mathbf{curl}\,\chi_{\rm S} = \mathsf{s}_{\rm S}^2\,[P_{\rm trans}^{-1}\,A^{-1}]_{11}\left((\omega\,\mathsf{s}_{\rm S})^2\,\frac{\mathrm{i}}{4}\mathbf{curl}\,\mathrm{H}_0^{(1)}(\omega\,\mathsf{s}_{\rm S} r) + \mathbf{curl}\,\delta\right)\,,$$

$$\mathbf{curl}\,\chi_{\rm EM} = \mathsf{s}_{\rm EM}^2\,[P_{\rm trans}^{-1}\,A^{-1}]_{31}\left((\omega\,\mathsf{s}_{\rm EM})^2\,\frac{\mathrm{i}}{4}\mathbf{curl}\,\mathrm{H}_0^{(1)}(\omega\,\mathsf{s}_{\rm EM} r) + \mathbf{curl}\,\delta\right)\,.$$

We inject the above expression in equation (6.29):

$$-\omega^2\begin{pmatrix}\mathrm{u}\\ \mathrm{w}\\ \boldsymbol{E}\end{pmatrix} - P_{\rm trans}\begin{pmatrix}[P_{\rm trans}^{-1}\,A^{-1}]_{11}\left((\omega\,\mathsf{s}_{\rm S})^2\,\frac{\mathrm{i}}{4}\mathbf{curl}\,\mathrm{H}_0^{(1)}(\omega\,\mathsf{s}_{\rm S} r) + \mathbf{curl}\,\delta\right)\\ 0\\ [P_{\rm trans}^{-1}\,A^{-1}]_{31}\left((\omega\,\mathsf{s}_{\rm EM})^2\,\frac{\mathrm{i}}{4}\mathbf{curl}\,\mathrm{H}_0^{(1)}(\omega\,\mathsf{s}_{\rm EM} r) + \mathbf{curl}\,\delta\right)\end{pmatrix} = A^{-1}\begin{pmatrix}\mathbf{curl}\delta\\ 0\\ 0\end{pmatrix}\,.$$

Then, we multiply the system by $P_{\rm trans}^{-1}$, which gives:

$$-\omega^2\,P_{\rm trans}^{-1}\begin{pmatrix}\mathrm{u}\\ \mathrm{w}\\ \boldsymbol{E}\end{pmatrix} - \begin{pmatrix}[P_{\rm trans}^{-1}\,A^{-1}]_{11}\left((\omega\,\mathsf{s}_{\rm S})^2\,\frac{\mathrm{i}}{4}\mathbf{curl}\,\mathrm{H}_0^{(1)}(\omega\,\mathsf{s}_{\rm S} r) + \mathbf{curl}\,\delta\right)\\ 0\\ [P_{\rm trans}^{-1}\,A^{-1}]_{31}\left((\omega\,\mathsf{s}_{\rm EM})^2\,\frac{\mathrm{i}}{4}\mathbf{curl}\,\mathrm{H}_0^{(1)}(\omega\,\mathsf{s}_{\rm EM} r) + \mathbf{curl}\,\delta\right)\end{pmatrix} = \begin{pmatrix}[P_{\rm trans}^{-1}\,A^{-1}]_{11}\mathbf{curl}\delta\\ 0\\ [P_{\rm trans}^{-1}\,A^{-1}]_{31}\mathbf{curl}\delta\end{pmatrix}\,.$$

The curls of the Dirac distribution in right-hand side and in the second term are simplified, and we finally multiply the system by $-\omega^{-2}\,P_{\rm trans}$ to obtain the expression of the displacements u, w, and $\boldsymbol{E}$:

$$\begin{pmatrix}\mathrm{u}\\ \mathrm{w}\\ \boldsymbol{E}\end{pmatrix} = P_{\rm trans}\begin{pmatrix}[P_{\rm trans}^{-1}\,A^{-1}]_{11}\,\mathsf{s}_{\rm S}^2\,\frac{\mathrm{i}}{4}\mathbf{curl}\,\mathrm{H}_0^{(1)}(\omega\,\mathsf{s}_{\rm S} r)\\ 0\\ [P_{\rm trans}^{-1}\,A^{-1}]_{31}\,\mathsf{s}_{\rm EM}^2\,\frac{\mathrm{i}}{4}\mathbf{curl}\,\mathrm{H}_0^{(1)}(\omega\,\mathsf{s}_{\rm EM} r)\end{pmatrix}\,.$$

Recall that in polar coordinates, the curl of $\mathrm{H}_0^{(1)}(\omega\,\mathsf{s}_{\rm S} r)$ is

$$\mathbf{curl}\,\mathrm{H}_0^{(1)}(\omega\,\mathsf{s}_\bullet r) \;=\; -\,\omega\,\mathsf{s}_\bullet \mathrm{H}_0^{(1)'}(\omega\,\mathsf{s}_\bullet r)\mathbf{e}_\theta\,, \qquad \text{and} \qquad \text{and } \mathrm{H}_0^{(1)'}(\omega\,\mathsf{s}_\bullet r) \;= -\mathrm{H}_1^{(1)}(\omega\,\mathsf{s}_\bullet r)\,.$$

Hence,

$$\mathrm{u} \;=\; \left([P_{\rm trans}^{-1}\,A^{-1}]_{11}\,\omega\,\mathsf{s}_{\rm S}^3\,\frac{\mathrm{i}}{4}\mathrm{H}_1^{(1)}(\omega\,\mathsf{s}_{\rm S} r) \;+\; [P_{\rm trans}^{-1}\,A^{-1}]_{31}\,\omega\,\mathsf{s}_{\rm EM}^3\,\frac{\mathrm{i}}{4}\mathrm{H}_1^{(1)}(\omega\,\mathsf{s}_{\rm EM} r)\right)\,\mathrm{e}_\theta\,,$$

$$\mathrm{w} \;=\; \left(\mathcal{W}_{\rm S}\,[P_{\rm trans}^{-1}\,A^{-1}]_{11}\,\omega\,\mathsf{s}_{\rm S}^3\,\frac{\mathrm{i}}{4}\mathrm{H}_1^{(1)}(\omega\,\mathsf{s}_{\rm S} r) \;+\; \mathcal{W}_{\rm EM}\,[P_{\rm trans}^{-1}\,A^{-1}]_{31}\,\omega\,\mathsf{s}_{\rm EM}^3\,\frac{\mathrm{i}}{4}\mathrm{H}_1^{(1)}(\omega\,\mathsf{s}_{\rm EM} r)\right)\,\mathrm{e}_\theta\,,$$

$$\boldsymbol{E} \;=\; \left(\mathcal{E}_{\rm S}\,[P_{\rm trans}^{-1}\,A^{-1}]_{11}\,\omega\,\mathsf{s}_{\rm S}^3\,\frac{\mathrm{i}}{4}\mathrm{H}_1^{(1)}(\omega\,\mathsf{s}_{\rm S} r) \;+\; \mathcal{E}_{\rm EM}\,[P_{\rm trans}^{-1}\,A^{-1}]_{31}\,\omega\,\mathsf{s}_{\rm EM}^3\,\frac{\mathrm{i}}{4}\mathrm{H}_1^{(1)}(\omega\,\mathsf{s}_{\rm EM} r)\right)\,\mathrm{e}_\theta\,.$$

Proposition 6.5. The first-order variables for a point source in transverse waves are expressed as:

$$\mathbf{u} \;=\; -\left([P_{\rm trans}^{-1}\,A^{-1}]_{11}\,\frac{\omega^2\,\mathsf{s}_{\rm S}^3}{4}\mathrm{H}_1^{(1)}(\omega\,\mathsf{s}_{\rm S} r) \;+\; [P_{\rm trans}^{-1}\,A^{-1}]_{31}\,\frac{\omega^2\,\mathsf{s}_{\rm EM}^3}{4}\mathrm{H}_1^{(1)}(\omega\,\mathsf{s}_{\rm EM} r)\right)\,\mathrm{e}_\theta\,,$$

$$\mathbf{w} \;=\; -\left(\mathcal{W}_{\rm S}\,[P_{\rm trans}^{-1}\,A^{-1}]_{11}\,\frac{\omega^2\,\mathsf{s}_{\rm S}^3}{4}\mathrm{H}_1^{(1)}(\omega\,\mathsf{s}_{\rm S} r) \;+\; \mathcal{W}_{\rm EM}\,[P_{\rm trans}^{-1}\,A^{-1}]_{31}\,\frac{\omega^2\,\mathsf{s}_{\rm EM}^3}{4}\mathrm{H}_1^{(1)}(\omega\,\mathsf{s}_{\rm EM} r)\right)\,\mathrm{e}_\theta\,,$$

for the velocities, the stress tensor is

$$\boldsymbol{\tau} \;=\; \tau_{r\theta}\mathbf{e}_r \otimes \mathbf{e}_\theta \;+ \tau_{r\theta}\mathbf{e}_\theta \otimes \mathbf{e}_r \,,$$

with

$$\tau_{r\theta} \;=\; \mu_{\rm fr}\left([P^{-1}_{\rm trans}\, A^{-1}]_{11}\, \omega^2\, \mathsf{s}_{\rm S}^4\, \frac{\mathrm{i}}{4}\mathrm{H}_1^{(1)'}(\omega\, \mathsf{s}_{\rm S} r) \;+\; [P^{-1}_{\rm trans}\, A^{-1}]_{31}\, \omega^2\, \mathsf{s}_{\rm EM}^4\, \frac{\mathrm{i}}{4}\mathrm{H}_1^{(1)'}(\omega\, \mathsf{s}_{\rm EM} r)\right) .$$

The pressure is equal to zero

$$\mathrm{p} \;=\; 0\,,$$

and the electromagnetic variables are:

$$\boldsymbol{E} \;=\; \left(\mathcal{E}_{\rm S}\, [P^{-1}_{\rm trans}\, A^{-1}]_{11}\, \omega\, \mathsf{s}_{\rm S}^3\, \frac{\mathrm{i}}{4}\mathrm{H}_1^{(1)}(\omega\, \mathsf{s}_{\rm S} r) \;+\; \mathcal{E}_{\rm EM}\, [P^{-1}_{\rm trans}\, A^{-1}]_{31}\, \omega\, \mathsf{s}_{\rm EM}^3\, \frac{\mathrm{i}}{4}\mathrm{H}_1^{(1)}(\omega\, \mathsf{s}_{\rm EM} r)\right) \mathrm{e}_\theta \,,$$

$$\mathrm{H} \;=\; \frac{\mathfrak{s}\,\mathrm{i}}{\omega\, \mu_0} \left(\mathcal{E}_{\rm S}\, [P^{-1}_{\rm trans}\, A^{-1}]_{11}\, \omega^2\, \mathsf{s}_{\rm S}^4\, \frac{\mathrm{i}}{4}\mathrm{H}_1^{(1)'}(\omega\, \mathsf{s}_{\rm S} r) \;+\; \mathcal{E}_{\rm EM}\, [P^{-1}_{\rm trans}\, A^{-1}]_{31}\, \omega^2\, \mathsf{s}_{\rm EM}^4\, \frac{\mathrm{i}}{4}\mathrm{H}_1^{(1)'}(\omega\, \mathsf{s}_{\rm EM} r)\right) .$$

Proof.

- The velocities $\mathbf{u}$ and $\mathbf{w}$ are calculated by taking the time-derivative of the displacements u and w.

$$\mathbf{u} \;=\; -\left([P^{-1}_{\rm trans}\, A^{-1}]_{11}\, \frac{\omega^2\, \mathsf{s}_{\rm S}^3}{4}\mathrm{H}_1^{(1)}(\omega\, \mathsf{s}_{\rm S} r) \;+\; [P^{-1}_{\rm trans}\, A^{-1}]_{31}\, \frac{\omega^2\, \mathsf{s}_{\rm EM}^3}{4}\mathrm{H}_1^{(1)}(\omega\, \mathsf{s}_{\rm EM} r)\right) \mathrm{e}_\theta \,,$$

$$\mathbf{w} \;=\; -\left(\mathcal{W}_{\rm S}\, [P^{-1}_{\rm trans}\, A^{-1}]_{11}\, \frac{\omega^2\, \mathsf{s}_{\rm S}^3}{4}\mathrm{H}_1^{(1)}(\omega\, \mathsf{s}_{\rm S} r) \;+\; \mathcal{W}_{\rm EM}\, [P^{-1}_{\rm trans}\, A^{-1}]_{31}\, \frac{\omega^2\, \mathsf{s}_{\rm EM}^3}{4}\mathrm{H}_1^{(1)}(\omega\, \mathsf{s}_{\rm EM} r)\right) \mathrm{e}_\theta \,.$$

- From the calculation of $\boldsymbol{\tau}$ in Section 2.6 for poroelasticity, we have

$$\boldsymbol{\tau} \;=\; \tau_{r\theta}\, \mathbf{e}_r \otimes \mathbf{e}_\theta \;+ \tau_{r\theta}\, \mathbf{e}_\theta \otimes \mathbf{e}_r \,, \qquad \text{with } \tau_{r\theta} \;=\; \mu_{\rm fr} \frac{\partial \mathrm{u}_\theta}{\partial r} \,.$$

  By using the expression of the radial derivative of $\mathrm{H}_1^{(1)}(\omega\, \mathrm{s}_\bullet r)$,

$$\frac{\partial}{\partial r}\mathrm{H}_1^{(1)}(\omega\, \mathrm{s}_\bullet r) \;=\; \omega\, \mathrm{s}_\bullet \mathrm{H}_1^{(1)'}(\omega\, \mathrm{s}_\bullet r) \;= \omega\, \mathrm{s}_\bullet \mathrm{H}_0^{(1)}(\omega\, \mathrm{s}_\bullet r) \;-\; \frac{1}{r}\mathrm{H}_1^{(1)}(\omega\, \mathrm{s}_\bullet r) \,,$$

  we find the value of $\tau_{r\theta}$.

- For the calculation of p, we use the constitutive law (5.3d) and the expressions of the displacements u and w.

- Concerning the expression of the magnetic field H, we use equation (5.3e):

$$\mathrm{H} = \frac{\mathfrak{s}\,\mathrm{i}}{\omega\, \mu_0} \operatorname{curl} \boldsymbol{E} \,,$$

  and the curl of the electric field is:

$$\operatorname{curl} \boldsymbol{E} \;=\; \partial_r \boldsymbol{E}_\theta \;-\; \frac{1}{r}\, \partial_\theta \boldsymbol{E}_r \;=\; \partial_r \boldsymbol{E}_\theta \,,$$

  because $\boldsymbol{E}_r = 0$. Hence, we find the expression of the magnetic field.

- Finally, for the calculation of $\boldsymbol{J}$, equation (5.3g) gives:

$$\boldsymbol{J} \;= \mathbf{curl}\, \mathrm{H} \;-\; \mathfrak{s}\, \mathrm{i}\, \omega\, \delta_0\, \boldsymbol{E} \;=\; (-\,\partial_r\, \mathrm{H} \;-\; \mathfrak{s}\, \mathrm{i}\, \omega\, \delta_0\, E_\theta)\; \mathbf{e}_\theta \,,$$

  because the magnetic field H is independent of θ.

  We have

$$\partial_r\, \mathrm{H} \;=\; -\,\frac{\mathfrak{s}\,\mathrm{i}}{\omega\, \mu_0} \left(\mathcal{E}_{\rm S}\, [P^{-1}_{\rm trans}\, A^{-1}]_{11}\, \omega^3\, \mathsf{s}_{\rm S}^5\, \frac{\mathrm{i}}{4}\mathrm{H}_1^{(1)''}(\omega\, \mathsf{s}_{\rm S} r) \;+\; \mathcal{E}_{\rm EM}\, [P^{-1}_{\rm trans}\, A^{-1}]_{31}\, \omega^3\, \mathsf{s}_{\rm EM}^5\, \frac{\mathrm{i}}{4}\mathrm{H}_1^{(1)''}(\omega\, \mathsf{s}_{\rm EM} r)\right) .$$

  Using the fact that the Hankel functions solve the following equation:

$$\frac{d^2}{dz^2}\mathrm{H}_k^{(1)} \;=\; -\frac{1}{z}\mathrm{H}_k^{(1)'} \;-\; (1 - \frac{k^2}{z^2})\mathrm{H}_k^{(1)} \,,$$

  we can determine $\partial_r\, \mathrm{H}$ and hence $\boldsymbol{J}$.

□

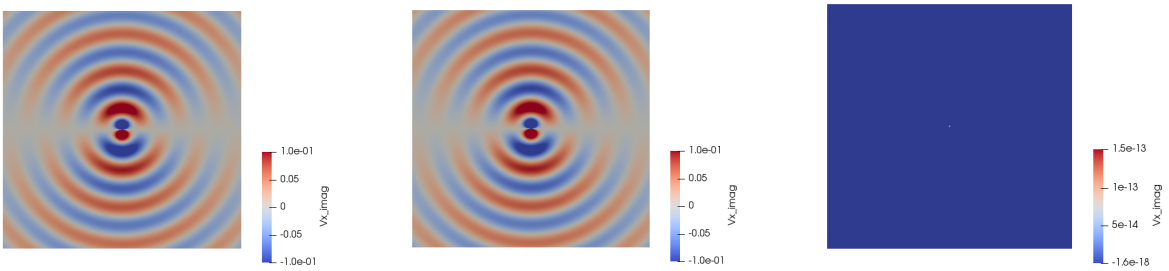

(a) Total wave $\mathbf{u}$ (b) S-wave $\mathbf{u}$ (c) EM-wave $\mathbf{u}$

Figure 6.13: Decomposition for $\mathbf{u}$.

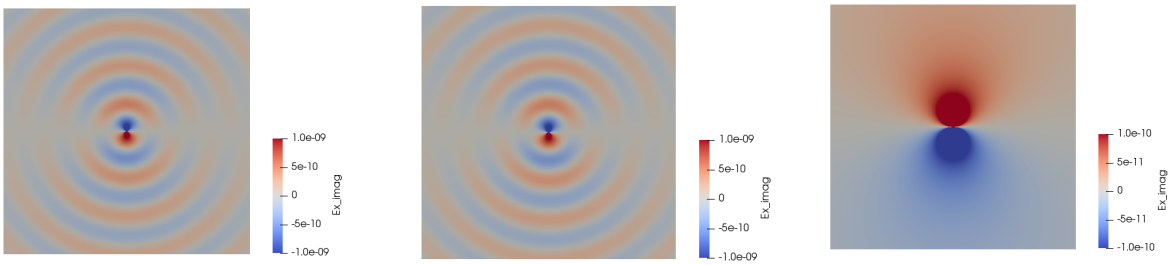

(a) Total wave $\boldsymbol{E}$ (b) S-wave $\boldsymbol{E}$ (c) EM-wave $\boldsymbol{E}$

Figure 6.14: Decomposition for $\boldsymbol{E}$.

We will use this analytical solution to verify the numerical solution obtained with the HDG method (see Chapter 7). The solutions are given in Figure 6.13 for the solid velocity $\mathbf{u}$ and in Figure 6.14 for the electric field $\boldsymbol{E}$. We show the total solution on the left. Then, in figures (b), we remove the contribution of the EM-wave to the fields, in order to isolate the EM-wave. Similarly, in figures (c), we remove the contribution of the S-wave to the fields. By this way, we can identify clearly the two kinds of transverse waves propagating in the medium. For $\mathbf{u}$, the wave is entirely a S-wave, as we can see Figure 6.13c, there is no contribution of the EM-wave. For the electric field $\boldsymbol{E}$, we observe that the amplitude of the solution is very small. Moreover, the decomposition shows that the solution is mainly due to contribution of the S-wave, however, we also observe the EM-wave, but with a smaller amplitude.

Conclusion

In this chapter, using the expression of the variables as functions of four potentials, we have built analytical solutions in two-dimensions for different configurations: a bounded isotropic problem, the scattering of a plane wave penetrable or impenetrable obstacles, and the response to a point-sources in infinite medium. We have performed numerical investigations on the stability of the above problems. We did not observe corresponding Jones' modes for any cases. This is certainly due to the presence of viscosity in the equations. Indeed, in the poroelastic case (Chapter 2), we have observed Jone's modes when the material is inviscid, however, in the presence of viscosity, we did not observe mode. The results of this chapter will play a crucial role in the two following chapters where we validate a HDG formulation for solving Pride's equations in harmonic regime (Chapter 7) and we construct a low-order radiation boundary conditions for performing regional computations in bounded domains (Chapter 8).

Chapter 7

HDG method for Pride's equations

The aim of this chapter is to develop a HDG method to solve Pride's equations in the harmonic domain. We base the proposed method on what has been developed for poroelasticity in Chapter 3 and for Maxwell's equations in Appendix G. Concerning the numerical simulations of electrokinetics, different methods have been developed. In the time domain, due to the large difference of the seismic and electromagnetic wavespeeds, it is necessary to make approximations of Pride's model in order to decouple the electromagnetic fields from the poroelastic variables. For example, Haines and Pride [72] consider a low frequency approximation, which leads to a reduced model, Wei [130], Tohti [126] and Pain [104] makes the assumption that the electromagnetic problem is quasi-static Han & Wang [73] and Zyserman [139], only consider the rotational shear wave. In harmonic domain, as we do not need time schemes, we can consider the full model. However, in the literature, the authors consider approximations of Pride's model, for example Gao [61], Santos [115], Zyserman [138] only focus on the shear wave, and Revil [113] consider a quasi-static problem. A different approach is to use a quasi-analytical method in layered domains [71, 62, 64, 132, 112, 83]. The authors follow the Ursin or Kennett methods and perform a Fourier transform in time and space domain. This results in an algebric system corresponding to the reflection-transmission matrix. More details on this method can be found in [132].

As previously, we choose to develop a HDG method to solve the full Pride's model. To the best of our knowledge, the resolution of Pride's equations has not been done using high-order DG methods. These methods present the significant advantages to be robust to numerical pollution, to have good performance on unstructured meshes and to have the major parts of the calculations done element-wise. As we have detailed before, the DG methods classically need to duplicate the degrees of freedom. This is prevented in the HDG methods, where we introduce hybrid variables to express the numerical traces on the skeleton of the mesh. This also allows to have access to the first-order formulation unknowns by computing a system of the size of the second-order unknowns. We refer to Chapter 3 for additional details and references on DG and HDG methods.

In this chapter, based on what we have done in Chapter 3 for poroelasticity and Appendix G for Maxwell's equations, we develop an HDG method for Pride's equation in frequency domain. We consider that the time-harmonic waves have their time dependency as $e^{\mathrm{i}\omega t}$. This means that we have $\partial_t \to \mathrm{i}\omega$, which corresponds to setting $\mathfrak{s} = 1$ in (5.3). We first present in Section 7.1 the formulation of the HDG method. Then, we detail the associated discretization in two dimensions in Section 7.2, and we provide validations of the numerical simulations in Section 7.4. We also investigate numerically the well-posedness of the problem, and the formulation of the HDG method, especially the values of the stabilization parameters used to express the numerical traces. In Section 7.5, we describe the discretization of the proposed method in three dimensions, and we perform numerical tests for the verification of the method in Section 7.6.

7.1 HDG formulation of Pride's equations

In this section, we develop a HDG formulation for Pride's equations (5.3), taking $\mathfrak{s} = 1$, and using boundary conditions of type 1, see (5.10a). We first introduce useful notations, then describe how we obtain both the local problem and the transmission conditions that are used to solve the equations.

7.1.1 Notations

On a domain $\mathcal{D}$, we recall the following function spaces,

$$L^2(\mathcal{D}),\ \text{the space of square-integrable functions on the domain } \mathcal{D}\,,$$

$$V^p(\mathcal{D}),\ \text{the set of polynomials of degree at most } p \text{ on } \mathcal{D}\,,$$

$$\boldsymbol{V}^p(\mathcal{D}) = (V^p(\mathcal{D}))^{\mathrm{d}}\,,$$

$$\boldsymbol{\Sigma}^p(\mathcal{D}) = \{\boldsymbol{\tau} \in (V^p(\mathcal{D}))^{\mathrm{d}\times\mathrm{d}} |\ \boldsymbol{\tau} \text{ symmetric}\}\,.$$

We next consider a triangulation $\mathcal{T}_h$ of the domain $\mathcal{D}$ of dimension d. Note that we impose strongly the symmetry on the stress tensor. We denote by K an element of the mesh, which in 2D is a triangle and in 3D a tetrahedron. We also denote by F a face of the element K, and by $\boldsymbol{n}$ the outgoing unit normal vector to F. For a given triangulation $\mathcal{T}_h$, we define the following spaces:

$$V_h^p = \{v \in L^2(\mathcal{D}) : v|_K \in V^p(K)\,,\ \forall K \in \mathcal{T}_h\}\,,$$

$$\boldsymbol{V}_h^p = \{\boldsymbol{v} \in (L^2(\mathcal{D}))^{\mathrm{d}} : \boldsymbol{v}|_K \in V^p(K)\,,\ \forall K \in \mathcal{T}_h\}\,,$$

$$\boldsymbol{\Sigma}_h^p = \{\boldsymbol{\tau} \in L^2(\mathcal{D})^{\mathrm{d}^2} : \boldsymbol{\tau}|_K \in \boldsymbol{\Sigma}^p(K)\,,\ \forall K \in \mathcal{T}_h\}\,,$$

$$M_h = \{\xi \in L^2(\mathcal{F}_h) : \xi|_F \in V^p(F),\ ,\ \forall K \in \mathcal{F}_h\}\,,$$

$$\boldsymbol{M}_h = \{\eta \in (L^2(\mathcal{F}_h))^{\mathrm{d}} : \eta|_F \in (V^p(F))^{\mathrm{d}}\,,\ \forall K \in \mathcal{F}_h\}\,.$$

The jumps $[\![\cdot]\!]$ are defined as follows:

- On an interior face $F = \partial K \cap \partial K'$:

$$[\![\mathbf{w}\cdot\boldsymbol{n}]\!] = \mathbf{w}^K\cdot\boldsymbol{n}^K + \mathbf{w}^{K'}\cdot\boldsymbol{n}^{K'}\,,\qquad [\![\boldsymbol{\tau}\,\boldsymbol{n}]\!] = \boldsymbol{\tau}^K\boldsymbol{n}^K + \boldsymbol{\tau}^{K'}\boldsymbol{n}^{K'}\,,\qquad [\![\boldsymbol{E}\times\boldsymbol{n}]\!] = \boldsymbol{E}^K\times\boldsymbol{n}^K + \boldsymbol{E}^{K'}\times\boldsymbol{n}^{K'}\,,$$

- On an external boundary face:

$$[\![\mathbf{w}\cdot\boldsymbol{n}]\!] = \mathbf{w}^K\cdot\boldsymbol{n}^K\,,\qquad [\![\boldsymbol{\tau}\,\boldsymbol{n}]\!] = \boldsymbol{\tau}^K\boldsymbol{n}^K\,,\qquad [\![\boldsymbol{E}\times\boldsymbol{n}]\!] = \boldsymbol{E}^K\times\boldsymbol{n}^K\,.$$

7.1.2 Local problem

We consider an element K of $\mathcal{T}_h$, and a solution to Pride's equations (5.3) on an element K denoted by $(\mathbf{u}, \mathbf{w}, \boldsymbol{\tau}, \mathrm{p}, \boldsymbol{E}, \boldsymbol{H}, \boldsymbol{J})$. We then define the following test functions:

$$(\tilde{\boldsymbol{u}}, \tilde{\boldsymbol{w}}, \tilde{\boldsymbol{\tau}}, \tilde{\mathrm{p}}, \tilde{\boldsymbol{e}}, \tilde{h}, \tilde{\boldsymbol{j}}) \in (\boldsymbol{V}^p(K)\times\boldsymbol{V}^p(K)\times\boldsymbol{\Sigma}^p(K)\times V^p(K)\times\boldsymbol{V}^p(K)\times V^p(K)\times\boldsymbol{V}^p(K))\,.$$

The integration on an element of (5.3) gives:

$$\int_K \mathrm{i}\,\omega\,\rho_a\,\mathbf{u}\cdot\tilde{\boldsymbol{u}} + \int_K \mathrm{i}\,\omega\,\rho_f\,\mathbf{w}\cdot\tilde{\boldsymbol{u}} - \int_K(\nabla\cdot\boldsymbol{\tau})\cdot\tilde{\boldsymbol{u}} = \int_K \mathbf{f}_u\cdot\tilde{\boldsymbol{u}}\,,$$

$$\int_K \mathrm{i}\,\omega\,\rho_f\,\mathbf{u}\cdot\tilde{\boldsymbol{w}} + \int_K \mathrm{i}\,\omega\,\rho_{\mathrm{dyn}}\,\mathbf{w}\cdot\tilde{\boldsymbol{w}} + \int_K(\nabla\,\mathrm{p})\cdot\tilde{\boldsymbol{w}} - \int_K \mathrm{i}\,\omega\,\rho_{\mathrm{dyn}}\,(\mathbf{L}\,\boldsymbol{E})\cdot\tilde{\boldsymbol{w}} = \int_K \mathbf{f}_w\cdot\tilde{\boldsymbol{w}}\,,$$

$$\int_K \mathrm{i}\,\omega\,\boldsymbol{\tau} : \tilde{\boldsymbol{\tau}} + \int_K \mathrm{i}\,\omega\,\boldsymbol{\alpha}\,\mathrm{p} : \tilde{\boldsymbol{\tau}} - \int_K(\mathbf{C}\boldsymbol{\epsilon}(\mathbf{u})) : \tilde{\boldsymbol{\tau}} = 0\,,$$

$$\int_K \mathrm{i}\,\omega\,\mathrm{p}\,\tilde{\mathrm{p}} + \int_K M\,\nabla\cdot\mathbf{w}\,\tilde{\mathrm{p}} + \int_K M\,\boldsymbol{\alpha} : \boldsymbol{\epsilon}(\mathbf{u})\,\tilde{\mathrm{p}} = 0\,,$$

$$\int_K \mathrm{i}\,\omega\,\delta_0\,\boldsymbol{E}\cdot\tilde{\boldsymbol{e}} - \int_K \mathbf{curl}\,\boldsymbol{H}\cdot\tilde{\boldsymbol{e}} + \int_K \boldsymbol{J}\cdot\tilde{\boldsymbol{e}} = \int_K \mathbf{f}_C\cdot\tilde{\boldsymbol{e}}\,,$$

$$\int_K \mathrm{i}\,\omega\,\mu_0\boldsymbol{H}\,\tilde{h} + \int_K \mathrm{curl}\,\boldsymbol{E}\,\tilde{h} = 0\,,$$

$$\int_K \boldsymbol{J}\cdot\tilde{\boldsymbol{j}} - \int_K \sigma\,\boldsymbol{E}\cdot\tilde{\boldsymbol{j}} + \int_K(\mathbf{L}\,\nabla\mathrm{p})\cdot\tilde{\boldsymbol{j}} + \int_K \mathrm{i}\omega\,\rho_f\,(\mathbf{L}\,\mathbf{u})\cdot\tilde{\boldsymbol{j}} = \int_K(\mathbf{L}\,\mathbf{f}_w)\cdot\tilde{\boldsymbol{j}}\,.$$

By integrating by parts, we have:

$$\int_K \mathrm{i}\,\omega\,\rho_a\,\mathbf{u}\cdot\tilde{\boldsymbol{u}} + \int_K \mathrm{i}\,\omega\,\rho_f\,\mathbf{w}\cdot\tilde{\boldsymbol{u}} + \int_K \boldsymbol{\tau} : \nabla\tilde{\boldsymbol{u}} - \int_{\partial K}\hat{\boldsymbol{\tau}}\boldsymbol{n}\cdot\tilde{\boldsymbol{u}} = \int_K \mathbf{f}_u\cdot\tilde{\boldsymbol{u}}\,,$$

$$\int_K \mathrm{i}\,\omega\,\rho_f\,\mathbf{u}\cdot\tilde{\boldsymbol{w}} + \int_K \mathrm{i}\,\omega\,\rho_{\mathrm{dyn}}\,\mathbf{w}\cdot\tilde{\boldsymbol{w}} - \int_K \mathrm{p}\,\nabla\cdot\tilde{\boldsymbol{w}} + \int_{\partial K}\hat{\mathrm{p}}\,\boldsymbol{n}\cdot\tilde{\boldsymbol{w}} - \int_K \mathrm{i}\,\omega\,\rho_{\mathrm{dyn}}\,(\mathbf{L}\,\boldsymbol{E})\cdot\tilde{\boldsymbol{w}} = \int_K \mathbf{f}_w\cdot\tilde{\boldsymbol{w}}\,,$$

$$\int_K \mathrm{i}\,\omega\boldsymbol{\tau} : \tilde{\boldsymbol{\tau}} + \int_K \mathrm{i}\,\omega\boldsymbol{\alpha}\mathrm{p} : \tilde{\boldsymbol{\tau}} + \int_K \mathbf{u}\cdot\big(\nabla\cdot(\mathbf{C}\tilde{\boldsymbol{\tau}})\big) - \int_{\partial K}(\hat{\mathbf{u}}\cdot\mathbf{C}\tilde{\boldsymbol{\tau}})\boldsymbol{n} = 0\,,$$

$$\int_K \mathrm{i}\,\omega\,\mathrm{p}\,\tilde{\mathrm{p}} - \int_K M\,\mathbf{w}\cdot\nabla\tilde{\mathrm{p}} + \int_{\partial K} M\,(\hat{\mathbf{w}}\cdot\boldsymbol{n})\,\tilde{\mathrm{p}} - \int_K M\,(\boldsymbol{\alpha}\mathbf{u})\cdot\nabla\tilde{\mathrm{p}} + \int_{\partial K} M\,(\boldsymbol{\alpha}\hat{\mathbf{u}})\cdot\boldsymbol{n}\,\tilde{\mathrm{p}} = 0\,,$$

$$\int_K \mathrm{i}\,\omega\,\delta_0\,\boldsymbol{E}\cdot\tilde{\boldsymbol{e}} - \int_K \boldsymbol{H}\,\mathrm{curl}\,\tilde{\boldsymbol{e}} + \int_{\partial K}(\boldsymbol{n}\times\tilde{\boldsymbol{e}})\,\hat{\boldsymbol{H}} + \int_K \boldsymbol{J}\cdot\tilde{\boldsymbol{e}} = \int_K \mathbf{f}_C\cdot\tilde{\boldsymbol{e}}\,,$$

$$\int_K \mathrm{i}\,\omega\,\mu_0\boldsymbol{H}\,\tilde{h} + \int_K \boldsymbol{E}\cdot\mathbf{curl}\,\tilde{h} + \int_{\partial K}(\boldsymbol{n}\times\hat{\boldsymbol{E}})\,\tilde{h} = 0\,,$$

$$\int_K \boldsymbol{J}\cdot\tilde{\boldsymbol{j}} - \int_K \sigma\,\boldsymbol{E}\cdot\tilde{\boldsymbol{j}} - \int_K \mathrm{p}\,\mathbf{L} : \nabla\tilde{\boldsymbol{j}} + \int_{\partial K}\hat{\mathrm{p}}\,(\mathbf{L}\,\boldsymbol{n})\cdot\tilde{\boldsymbol{j}} + \int_K \mathrm{i}\omega\,\rho_f\,(\mathbf{L}\,\mathbf{u})\cdot\tilde{\boldsymbol{j}} = \int_K (\mathbf{L}\,\mathbf{f}_w)\cdot\tilde{\boldsymbol{j}}\,.$$

Note that in the above equation, $\displaystyle\int_K (\mathbf{C}\boldsymbol{\epsilon}(\mathbf{u}_h)) : \tilde{\boldsymbol{\tau}} = \int_K \boldsymbol{\epsilon}(\mathbf{u}_h) : \mathbf{C}\tilde{\boldsymbol{\tau}}$ because $\mathbf{C}$ is symmetric.

Introduction of the trace variables: We approximate the exact solution ($\mathbf{u}$, $\mathbf{w}$, $\boldsymbol{\tau}$, p, $\boldsymbol{E}$, $\boldsymbol{H}$, $\boldsymbol{J}$) on K by ($\mathbf{u}_h$, $\mathbf{w}_h$, $\boldsymbol{\tau}_h$, p_h, $\boldsymbol{E}_h$, $\boldsymbol{H}_h$, $\boldsymbol{J}_h$) $\in (\boldsymbol{V}^p(K)\times\boldsymbol{V}^p(K)\times\boldsymbol{\Sigma}^p(K)\times V^p(K)\times\boldsymbol{V}^p(K)\times V^p(K)\times\boldsymbol{V}^p(K))$. The traces on ∂K are approximated by numerical traces ($\hat{\mathbf{u}}_h$, $\hat{\mathbf{w}}_h$, $\hat{\boldsymbol{\tau}}_h$, $\hat{\mathrm{p}}_h$, $\hat{\boldsymbol{E}}_h$, $\hat{\boldsymbol{H}}_h$). Following what we have done in Chapter 3 for poroelasticity and Appendix G for Maxwell's equations, we define three hybrid unknowns $\boldsymbol{\lambda}_1\in\boldsymbol{M}_h$, $\lambda_2\in M_h$, $\boldsymbol{\lambda}_3\in\boldsymbol{M}_h$ to replace the numerical traces $\hat{\mathbf{u}}_h$, $\hat{\mathrm{p}}_h$ and $\hat{\boldsymbol{E}}_h$, which are the the principal unknowns of the system. Note that $\boldsymbol{\lambda}_1$, λ_2, and $\boldsymbol{\lambda}_3$ are mesh-dependent and depend on h. However, for lighter notations, we drop the dependency in h.

$$\boldsymbol{\lambda}_1 = \hat{\mathbf{u}}_h, \qquad \lambda_2 = \hat{\mathrm{p}}_h, \qquad \boldsymbol{\lambda}_3 = \hat{\boldsymbol{H}}_h^t, \quad \forall F\in\mathcal{F}_h. \tag{7.3}$$

We consider that the physical parameters are constant per element. We express the other traces ($\hat{\boldsymbol{\tau}}_h$, $\hat{\mathbf{w}}_h$, $\hat{\boldsymbol{E}}_h$) in terms of the hybrid unknowns $\boldsymbol{\lambda}_1$, λ_2, $\boldsymbol{\lambda}_3$ as follows:

$$\begin{cases} \hat{\boldsymbol{\tau}}_h\,\boldsymbol{n} = \boldsymbol{\tau}_h\,\boldsymbol{n} - \boldsymbol{S}_1(\mathbf{u}_h-\boldsymbol{\lambda}_1) - (\mathrm{p}_h-\lambda_2)\boldsymbol{S}_3\,\boldsymbol{n}\,, \\ \hat{\mathbf{w}}_h\cdot\boldsymbol{n} = \mathbf{w}_h\cdot\boldsymbol{n} - \big((\mathrm{p}_h-\lambda_2)\boldsymbol{S}_2\boldsymbol{n}\big)\cdot\boldsymbol{n} - \big(\boldsymbol{S}_4(\mathbf{u}_h-\boldsymbol{\lambda}_1)\big)\cdot\boldsymbol{n}\,, \\ \boldsymbol{n}\times\hat{\boldsymbol{E}}_h = \boldsymbol{n}\times\boldsymbol{E}_h - \boldsymbol{n}\times\Big(\boldsymbol{S}_5\big(\,(\boldsymbol{H}_h^t-\boldsymbol{\lambda}_3)\times\boldsymbol{n}\big)\Big)\,. \end{cases} \tag{7.4}$$

where $\boldsymbol{S}_i$, $i=1,5$ are the stabilization matrices. In particular, the two first equations of (7.4) are the transmission conditions of poroelasticity (*cf.* Chapter 3 and [9]), and the last equation is the transmission condition for electromagnetic wave equations, as in Appendix G and [85]. The solution is approximated and the numerical traces are replaced

by their expressions (7.3) and (7.4) in (7.2) to give:

$$\int_K \mathrm{i}\,\omega\,\rho_a\,\mathbf{u}_h\cdot\tilde{\boldsymbol{u}} + \int_K \mathrm{i}\,\omega\,\rho_f\,\mathbf{w}_h\cdot\tilde{\boldsymbol{u}} + \int_K \boldsymbol{\tau}_h : \nabla\,\tilde{\boldsymbol{u}} - \int_{\partial K}\boldsymbol{\tau}_h\boldsymbol{n}\cdot\tilde{\boldsymbol{u}} + \int_{\partial K}\boldsymbol{S}_1\,(\mathbf{u}_h-\boldsymbol{\lambda}_1)\cdot\tilde{\boldsymbol{u}}$$
$$+\int_{\partial K}(\mathrm{p}_h-\lambda_2)\,(\boldsymbol{S}_3\,\boldsymbol{n})\cdot\tilde{\boldsymbol{u}} = \int_K \mathbf{f}_u\cdot\tilde{\boldsymbol{u}}\,,$$

$$\int_K \mathrm{i}\,\omega\,\rho_f\,\mathbf{u}_h\cdot\tilde{\boldsymbol{w}} + \int_K \mathrm{i}\,\omega\,\rho_{\mathrm{dyn}}\,\mathbf{w}_h\cdot\tilde{\boldsymbol{w}} - \int_K \mathrm{p}_h\,\nabla\cdot\tilde{\boldsymbol{w}} + \int_{\partial K}\lambda_2\,\boldsymbol{n}\cdot\tilde{\boldsymbol{w}} - \int_K \mathrm{i}\,\omega\,\rho_{\mathrm{dyn}}\,(\mathbf{L}\,\boldsymbol{E}_h)\cdot\tilde{\boldsymbol{w}} = \int_K \mathbf{f}_w\cdot\tilde{\boldsymbol{w}},$$

$$\int_K \mathrm{i}\,\omega\boldsymbol{\tau}_h : \tilde{\boldsymbol{\tau}} + \int_K \mathrm{i}\,\omega\boldsymbol{\alpha}\,\mathrm{p}_h : \tilde{\boldsymbol{\tau}} + \int_K \mathbf{u}_h\cdot\big(\nabla\cdot(\mathbf{C}\tilde{\boldsymbol{\tau}})\big) - \int_{\partial K}(\boldsymbol{\lambda}_1\cdot\mathbf{C}\tilde{\boldsymbol{\tau}})\,\boldsymbol{n} = 0\,,$$

$$\int_K \mathrm{i}\,\omega\,\mathrm{p}_h\,\tilde{\mathrm{p}} - \int_K M\,\mathbf{w}_h\cdot\nabla\tilde{\mathrm{p}} + \int_{\partial K} M\,(\mathbf{w}_h\cdot\boldsymbol{n})\,\tilde{\mathrm{p}} - \int_{\partial K} M\,(\mathrm{p}_h-\lambda_2)\,(\boldsymbol{S}_2\,\boldsymbol{n})\cdot\boldsymbol{n}\tilde{\mathrm{p}} - \int_{\partial K} M\,\boldsymbol{S}_4(\mathbf{u}_h-\boldsymbol{\lambda}_1)\cdot\boldsymbol{n}\,\tilde{\mathrm{p}}$$
$$-\int_K M\,(\boldsymbol{\alpha}\,\mathbf{u}_h)\cdot\nabla\,\tilde{\mathrm{p}} + \int_{\partial K} M\,(\boldsymbol{\alpha}\,\boldsymbol{\lambda}_1)\cdot\boldsymbol{n}\,\tilde{\mathrm{p}} = 0\,,$$

$$\int_K \mathrm{i}\,\omega\,\delta_0\,\boldsymbol{E}_h\cdot\tilde{\boldsymbol{e}} - \int_K \boldsymbol{H}_h\,\mathrm{curl}\,\tilde{\boldsymbol{e}} + \int_{\partial K}(\boldsymbol{n}\times\tilde{\boldsymbol{e}})\,\boldsymbol{\lambda}_3 + \int_K \boldsymbol{J}_h\cdot\tilde{\boldsymbol{e}} = \int_K \mathbf{f}_C\cdot\tilde{\boldsymbol{e}}\,,$$

$$\int_K \mathrm{i}\,\omega\,\mu_0\boldsymbol{H}_h\,\tilde{h} + \int_K \boldsymbol{E}_h\cdot\mathbf{curl}\,\tilde{h} + \int_{\partial K}(\boldsymbol{n}\times\boldsymbol{E}_h)\,\tilde{h} - \int_{\partial K}\boldsymbol{n}\times\Big(\boldsymbol{S}_5\big((\boldsymbol{H}_h-\boldsymbol{\lambda}_3)\times\boldsymbol{n}\big)\Big)\,\tilde{h} = 0\,,$$

$$\int_K \boldsymbol{J}_h\cdot\tilde{\boldsymbol{j}} - \int_K \sigma\,\boldsymbol{E}_h\cdot\tilde{\boldsymbol{j}} - \int_K \mathrm{p}_h\,\mathbf{L} : \nabla\tilde{\boldsymbol{j}} + \int_{\partial K}\lambda_2\,(\mathbf{L}\,\boldsymbol{n})\cdot\tilde{\boldsymbol{j}} + \int_K \mathrm{i}\,\omega\,\rho_f\,(\mathbf{L}\,\mathbf{u}_h)\cdot\tilde{\boldsymbol{j}} = \int_K (\mathbf{L}\,\mathbf{f}_w)\cdot\tilde{\boldsymbol{j}}\,.$$

By integrating by parts, we obtain the local problem:

$$\int_K \mathrm{i}\,\omega\,\rho_a\,\mathbf{u}_h\cdot\tilde{\boldsymbol{u}} + \int_K \mathrm{i}\,\omega\,\rho_f\,\mathbf{w}_h\cdot\tilde{\boldsymbol{u}} - \int_K (\nabla\cdot\boldsymbol{\tau}_h)\cdot\tilde{\boldsymbol{u}} + \int_{\partial K}\boldsymbol{S}_1\,(\mathbf{u}_h-\boldsymbol{\lambda}_1)\cdot\tilde{\boldsymbol{u}}$$
$$+\int_{\partial K}(\mathrm{p}_h-\lambda_2)\,(\boldsymbol{S}_3\,\boldsymbol{n})\cdot\tilde{\boldsymbol{u}} = \int_K \mathbf{f}_u\cdot\tilde{\boldsymbol{u}}\,, \tag{7.6a}$$

$$\int_K \mathrm{i}\,\omega\,\rho_f\,\mathbf{u}_h\cdot\tilde{\boldsymbol{w}} + \int_K \mathrm{i}\,\omega\,\rho_{\mathrm{dyn}}\,\mathbf{w}_h\cdot\tilde{\boldsymbol{w}} - \int_K \mathrm{p}_h\,\nabla\cdot\tilde{\boldsymbol{w}} + \int_{\partial K}\lambda_2\,\boldsymbol{n}\cdot\tilde{\boldsymbol{w}} - \int_K \mathrm{i}\,\omega\,\rho_{\mathrm{dyn}}\,(\mathbf{L}\,\boldsymbol{E}_h)\cdot\tilde{\boldsymbol{w}} = \int_K \mathbf{f}_w\cdot\tilde{\boldsymbol{w}}, \tag{7.6b}$$

$$\int_K \mathrm{i}\,\omega\boldsymbol{\tau}_h : \tilde{\boldsymbol{\tau}} + \int_K \mathrm{i}\,\omega\boldsymbol{\alpha}\,\mathrm{p}_h : \tilde{\boldsymbol{\tau}} + \int_K \mathbf{u}_h\cdot\big(\nabla\cdot(\mathbf{C}\tilde{\boldsymbol{\tau}})\big) - \int_{\partial K}(\boldsymbol{\lambda}_1\cdot\mathbf{C}\tilde{\boldsymbol{\tau}})\,\boldsymbol{n} = 0\,, \tag{7.6c}$$

$$\int_K \mathrm{i}\,\omega\,\mathrm{p}_h\,\tilde{\mathrm{p}} + \int_K M\nabla\cdot\,\mathbf{w}_h\,\tilde{\mathrm{p}} - \int_{\partial K} M\,(\mathrm{p}_h-\lambda_2)\,(\boldsymbol{S}_2\,\boldsymbol{n})\cdot\boldsymbol{n}\tilde{\mathrm{p}} - \int_{\partial K} M\,\boldsymbol{S}_4(\mathbf{u}_h-\boldsymbol{\lambda}_1)\cdot\boldsymbol{n}\,\tilde{\mathrm{p}}$$
$$-\int_K M\,(\boldsymbol{\alpha}\,\mathbf{u}_h)\cdot\nabla\,\tilde{\mathrm{p}} + \int_{\partial K} M\,(\boldsymbol{\alpha}\,\boldsymbol{\lambda}_1)\cdot\boldsymbol{n}\,\tilde{\mathrm{p}} = 0\,, \tag{7.6d}$$

$$\int_K \mathrm{i}\,\omega\,\delta_0\,\boldsymbol{E}_h\cdot\tilde{\boldsymbol{e}} - \int_K \boldsymbol{H}_h\,\mathrm{curl}\,\tilde{\boldsymbol{e}} + \int_{\partial K}(\boldsymbol{n}\times\tilde{\boldsymbol{e}})\,\boldsymbol{\lambda}_3 + \int_K \boldsymbol{J}_h\cdot\tilde{\boldsymbol{e}} = \int_K \mathbf{f}_C\cdot\tilde{\boldsymbol{e}}\,, \tag{7.6e}$$

$$\int_K \mathrm{i}\,\omega\,\mu_0\boldsymbol{H}_h\,\tilde{h} + \int_K \mathrm{curl}\,\boldsymbol{E}_h\,\tilde{h} - \int_{\partial K}\boldsymbol{n}\times\Big(\boldsymbol{S}_5\big((\boldsymbol{H}_h-\boldsymbol{\lambda}_3)\times\boldsymbol{n}\big)\Big)\,\tilde{h} = 0\,, \tag{7.6f}$$

$$\int_K \boldsymbol{J}_h\cdot\tilde{\boldsymbol{j}} - \int_K \sigma\,\boldsymbol{E}_h\cdot\tilde{\boldsymbol{j}} - \int_K \mathrm{p}_h\,\mathbf{L} : \nabla\tilde{\boldsymbol{j}} + \int_{\partial K}\lambda_2\,(\mathbf{L}\,\boldsymbol{n})\cdot\tilde{\boldsymbol{j}} + \int_K \mathrm{i}\,\omega\,\rho_f\,(\mathbf{L}\,\mathbf{u}_h)\cdot\tilde{\boldsymbol{j}} = \int_K (\mathbf{L}\,\mathbf{f}_w)\cdot\tilde{\boldsymbol{j}}\,. \tag{7.6g}$$

7.1.3 Transmission conditions

We determine the HDG formulation by associating the local problem with transmission conditions at the interfaces of the mesh. To construct the global HDG formulation, local problems have to be connected thanks to transmission conditions that are set on the interfaces between elements. We define $(\boldsymbol{\eta},\,\xi,\nu)\in\boldsymbol{M}_h\times M_h\times M_h$ three test-functions defined on the faces of the element K. We impose the following transmission conditions between the elements:

$$\sum_{F\in\mathcal{F}_h}\int_F[\![\hat{\boldsymbol{\tau}}_h\,\boldsymbol{n}]\!]\cdot\boldsymbol{\eta} = \sum_{F\in\mathcal{F}_{\mathrm{ext}}}\int_F \boldsymbol{f}_{\mathrm{inc}}\cdot\boldsymbol{\eta}\,,\quad \sum_{F\in\mathcal{F}_h}\int_F[\![\hat{\mathbf{w}}_h\cdot\boldsymbol{n}]\!]\,\xi = \sum_{F\in\mathcal{F}_{\mathrm{ext}}}\int_F g_{\mathrm{inc}}\,\xi\,,\quad \sum_{F\in\mathcal{F}_h}\int_F[\![\boldsymbol{n}\times\hat{\boldsymbol{E}}_h]\!]\cdot\boldsymbol{\nu} = \sum_{F\in\mathcal{F}_{\mathrm{ext}}}\int_F h_{\mathrm{inc}}\cdot\boldsymbol{\nu}\,,$$

which are equivalent to

$$\sum_{K\in\mathcal{T}_h}\int_{\partial K}(\hat{\boldsymbol{\tau}}_h\,\boldsymbol{n})\cdot\boldsymbol{\eta}=\sum_{F\in\mathcal{F}_{\text{ext}}}\int_F \boldsymbol{f}_{\text{inc}}\cdot\boldsymbol{\eta}\,,\quad \sum_{K\in\mathcal{T}_h}\int_{\partial K}(\hat{\mathbf{w}}_h\cdot\boldsymbol{n})\,\xi=\sum_{F\in\mathcal{F}_{\text{ext}}}\int_F g_{\text{inc}}\,\xi\,,\quad \sum_{K\in\mathcal{T}_h}\int_{\partial K}(\boldsymbol{n}\times\hat{\boldsymbol{E}}_h)\cdot\boldsymbol{\nu}=\sum_{F\in\mathcal{F}_{\text{ext}}}\int_F h_{\text{inc}}\cdot\boldsymbol{\nu}\,.$$

(7.7a) (7.7b) (7.7c)

7.2 Discretization of the HDG formulation in two dimensions

In this section, we detail the two-dimensional discretization of the HDG method in the (x, y) plane. In two dimensions, the magnetic field $\boldsymbol{H}_h$ and the Lagrange unknown $\boldsymbol{\lambda}_3$ are scalars, denoted respectively by H_h and λ_3. We consider the stabilization matrices defined in (7.4), to be diagonal, i.e., $\boldsymbol{S}_i=\gamma_i\,\mathbb{I}$ for $i=1,5$. In this way, the expression (7.4) simplifies to

$$\begin{cases}\hat{\boldsymbol{\tau}}_h\,\boldsymbol{n} \;=\; \boldsymbol{\tau}_h\,\boldsymbol{n}-\gamma_1(\mathbf{u}_h-\boldsymbol{\lambda}_1)-(\mathrm{p}_h-\lambda_2)\gamma_3\,\boldsymbol{n}\,,\\ \hat{\mathbf{w}}_h\cdot\boldsymbol{n} \;=\; \mathbf{w}_h\cdot\boldsymbol{n}-\gamma_2(\mathrm{p}_h-\lambda_2)-\gamma_4(\mathbf{u}_h-\boldsymbol{\lambda}_1)\cdot\boldsymbol{n}\,,\\ \boldsymbol{n}\times\hat{\boldsymbol{E}}_h \;=\; \boldsymbol{n}\times\boldsymbol{E}_h-\gamma_5\,(\mathrm{H}_h-\lambda_3)\,,\end{cases}$$

As seen previsouly in Chapter 5, the coupling tensor matrix $\mathbf{L}$ is diagonal and reads as $\mathbf{L}=\mathrm{L}\,\mathbb{I}$. The local solutions are expressed along the x and y directions as:

$$\mathbf{u}_h=\begin{pmatrix}\mathrm{u}_x^K\\ \mathrm{u}_y^K\end{pmatrix},\qquad \mathbf{w}_h=\begin{pmatrix}\mathrm{w}_x^K\\ \mathrm{w}_y^K\end{pmatrix},\qquad \boldsymbol{\tau}_h=\begin{pmatrix}\tau_{xx}^K & \tau_{xy}^K\\ \tau_{xy}^K & \tau_{yy}^K\end{pmatrix},\qquad \boldsymbol{E}_h=\begin{pmatrix}E_x^K\\ E_y^K\end{pmatrix}.$$

Then, each component is written in terms of basis functions as follows:

$$\begin{aligned}&\mathrm{u}_l^K=\sum_{j=1}^{d_i^K}\underline{\mathrm{u}}_{l,j}^K\varphi_j^K\,,\qquad \mathrm{w}_l^K=\sum_{j=1}^{d_i^K}\underline{\mathrm{w}}_{l,j}^K\varphi_j^K\,,\quad \tau_{kl}^K=\sum_{j=1}^{d_i^K}\underline{\tau}_{kl,j}^K\varphi_j^K\,,\quad \mathrm{p}_h^K=\sum_{j=1}^{d_i^K}\underline{\mathrm{p}}^K\varphi_j^K\,,\\ &E_l^K=\sum_{j=1}^{d_i^K}\underline{E}_{l,j}^K\varphi_j^K\,,\quad \mathrm{H}_h^K=\sum_{j=1}^{d_i^K}\underline{H}^K\varphi_j^K\,,\quad J_l^K=\sum_{j=1}^{d_i^K}\underline{J}_{l,j}^K\varphi_j^K\,,\ \text{with } l=x,y \text{ and } k=x,y\,,\end{aligned}\tag{7.8}$$

where φ_j^K denotes a basis function of V_h^p and d_i^K denotes the number of degrees of freedom of an element. The local hybrid unknowns are also decomposed as follows:

$$\lambda_{1l}^F=\sum_{j=1}^{d_i^F}\underline{\lambda_{1l}}_j^F\psi_j^F\,,\qquad \lambda_2^F=\sum_{j=1}^{d_i^F}\underline{\lambda_2}_j^F\psi_j^F\qquad \lambda_3^F=\sum_{j=1}^{d_i^F}\underline{\lambda_3}_j^F\psi_j^F\,,\qquad \text{with } l=x,y\,,\tag{7.9}$$

where ψ_i^F denotes a basis function of M_h and d_i^F the number of degrees of freedom of an edge. In (3.15), each component is considered as a vector of the form $\underline{\mathrm{u}}_l^K=(\underline{\mathrm{u}}_{l,1}^K,\dots,\underline{\mathrm{u}}_{l,d_i^K}^K)^T$ for $l=x,y$. Similarly, every local component of the unknowns in (7.9) is written as: $\underline{\lambda_{1l}}^F=(\underline{\lambda_{1l}}_1^F,\dots,\underline{\lambda_{1l}}_{d_i^F}^F)^T$, with $l=x,y$. We then define two vectors of unknowns $\underline{W}^K$ and $\underline{\Lambda}^K$ respectively of size $13\,d_i^K$ and $12\,d_i^F$ as:

$$\underline{W}^K=(\underline{\mathrm{u}}_x^K,\,\underline{\mathrm{u}}_y^K,\,\underline{\mathrm{w}}_x^K,\,\underline{\mathrm{w}}_y^K,\,\underline{\tau}_{xx}^K,\,\underline{\tau}_{yy}^K,\,\underline{\tau}_{xy}^K,\,\underline{\mathrm{p}}^K,\,\underline{E}_x^K,\,\underline{E}_y^K,\,\underline{H}^K,\,\underline{J}_x^K,\,\underline{J}_y^K)^T\,,$$

and

$$\underline{\Lambda}^K=(\underline{\lambda}_{1x}^{\beta(K,1)},\underline{\lambda}_{1x}^{\beta(K,2)},\underline{\lambda}_{1x}^{\beta(K,3)},\underline{\lambda}_{1y}^{\beta(K,1)}\underline{\lambda}_{1y}^{\beta(K,2)},\underline{\lambda}_{1y}^{\beta(K,3)},\underline{\lambda}_2^{\beta(K,1)},\underline{\lambda}_2^{\beta(K,2)},\underline{\lambda}_2^{\beta(K,3)},\underline{\lambda_3}^{\beta(K,1)},\underline{\lambda_3}^{\beta(K,2)},\underline{\lambda_3}^{\beta(K,3)})^T\,,$$

where $\beta(K,f)$ is the index in the global numbering of the f-th face of the element K. We also define the following elementary matrices $\mathbb{M}^K$, $\mathbb{D}^K$, $\mathbb{E}^K$, $\mathbb{J}^K$ of size $d_i^K\times d_i^K$, and $\mathbb{F}^K$, $\mathbb{Q}^K$ of size $d_i^F\times d_i^F$:

$$\begin{aligned}&\mathbb{M}_{ij}^K=\int_K\varphi_i^K\varphi_j^K\,dX\,,\qquad \mathbb{D}_{lij}^K=\int_K\varphi_j^K\frac{\partial\varphi_i^K}{\partial l}dX\,,\quad \mathbb{E}_{ij}^F=\int_F\varphi_i^K\varphi_j^K\,dS\,,\qquad \mathbb{J}_{lij}^F=\int_F\varphi_i^K\varphi_j^K n_l\,dS\,,\\ &\mathbb{F}_{ij}^F=\int_F\psi_j^F\varphi_i^K dS\,,\qquad \mathbb{Q}_{lij}^F=\int_F\psi_j^F\varphi_i^K n_l\,dS\,,\quad \mathbb{G}_{ij}^F=\int_F\psi_j^F\psi_j^F\,dS\,,\qquad \mathbb{H}_{lij}^F=\int_F\psi_i^F\psi_j^F n_l\,dS\,,\end{aligned}\tag{7.11}$$

with $l = x, y$. Finally, we define six elementary source matrices of size d_i^K

$$\left(\mathbb{C}_{1x}^K\right)_i = \int_K f_{ux}^K \varphi_i^K, \quad \left(\mathbb{C}_{1y}^K\right)_i = \int_K f_{uy}^K \varphi_i^K, \quad \left(\mathbb{C}_{2x}^K\right)_i = \int_K f_{wx}^K \varphi_i^K,$$
$$\left(\mathbb{C}_{2y}^K\right)_i = \int_K f_{wy}^K \varphi_i^K, \quad \left(\mathbb{C}_{3x}^K\right)_i = \int_K f_{Cx}^K \varphi_i^K, \quad \left(\mathbb{C}_{3y}^K\right)_i = \int_K f_{Cy}^K \varphi_i^K.$$

7.2.1 Local problem

We discretize the seven equations of the local problem (7.6). We use the representations of the local unknowns given above, and we write each equation in terms of the matrices defined in (7.11).

(a) Discretization of equation (7.6a)

Discretizing equation (7.6a) along the $x-$ and $y-$ component gives, taking $\bullet = x, y$:

$$\int_K \mathrm{i}\,\omega\,\rho_a^K\,\mathrm{u}_\bullet^K\,\varphi_i^K + \int_K \mathrm{i}\,\omega\,\rho_f^K\,\mathrm{w}_\bullet^K\,\varphi_i^K - \int_K \frac{\partial \tau_{x\bullet}^K}{\partial x}\,\varphi_i^K - \int_K \frac{\partial \tau_{y\bullet}^K}{\partial y}\,\varphi_i^K + \int_{\partial K} \gamma_1\,\mathrm{u}_\bullet^K \varphi_i^K - \int_{\partial K} \gamma_1\,\lambda_{1\bullet}\,\varphi_i^K$$
$$+ \int_{\partial K} \gamma_3\,\mathrm{p}_h^K\,n_\bullet\,\varphi_i^K - \int_{\partial K} \gamma_3\,\lambda_2\,n_\bullet\,\varphi_i^K = \int_K f_{u\bullet}\,\varphi_i^K.$$

This can be rewritten as matrix-vector products between the local matrices and the unknown vectors defined respectively in equations (7.11) and (7.10):

$$\mathrm{i}\,\omega\,\rho_a^K\,\mathbb{M}^K\underline{\mathrm{u}}_\bullet^K + \mathrm{i}\,\omega\,\rho_f^K\,\mathbb{M}^K\underline{\mathrm{w}}_\bullet^K - (\mathbb{D}_x^K)^T\,\underline{\tau}_{x\bullet}^K - (\mathbb{D}_y^K)^T\,\underline{\tau}_{y\bullet}^K + \sum_{f=1}^{3}\gamma_1\,\mathbb{E}^{\beta(K,f)}\,\underline{\mathrm{u}}_\bullet^K - \sum_{f=1}^{3}\gamma_1\,\mathbb{F}^{\beta(K,f)}\,\underline{\lambda}_{1\bullet}^{\beta(K,f)}$$
$$+ \sum_{f=1}^{3}\gamma_3\,\mathbb{J}_\bullet^{\beta(K,f)}\,\underline{\mathrm{p}}^K - \sum_{f=1}^{3}\gamma_3\,\mathbb{Q}_\bullet^{\beta(K,f)}\,\underline{\lambda}_2^{\beta(K,f)} = \mathbb{C}_{1\bullet}^K.$$

(b) Discretization of equation (7.6b)

Taking $\bullet = x, y$, the discretization of (7.6b) along x and y directions is:

$$\int_K \mathrm{i}\,\omega\,\rho_f^K\,\mathrm{u}_\bullet^K\,\varphi_i^K + \int_K \mathrm{i}\,\omega\,\rho_{\mathrm{dyn}}^K\,\mathrm{w}_\bullet^K\,\varphi_i^K - \int_K \mathrm{p}_h^K\,\frac{\partial \varphi_i^K}{\partial \bullet} + \int_{\partial K}\lambda_2\,n_\bullet\,\varphi_i^K - \int_K \mathrm{i}\,\omega\,\rho_{\mathrm{dyn}}^K\,\mathrm{L}\,E_\bullet^K\,\varphi_i^K = \int_K f_{w\bullet}\,\varphi_i^K.$$

In terms of the local matrices in (7.11) and the unknown vectors in (7.10), the above equation reads:

$$\mathrm{i}\,\omega\,\rho_f^K\,\mathbb{M}^K\underline{\mathrm{u}}_\bullet^K + \mathrm{i}\,\omega\,\rho_{\mathrm{dyn}}^K\,\mathbb{M}^K\underline{\mathrm{w}}_\bullet^K - \mathbb{D}_\bullet^K\,\underline{\mathrm{p}}^K - \sum_{f=1}^{3}\mathbb{Q}_\bullet^{\beta(K,f)}\,\underline{\lambda}_2^{\beta(K,f)} - \mathrm{i}\,\omega\,\rho_{\mathrm{dyn}}^K\,\mathrm{L}\,\mathbb{M}^K\underline{E}_\bullet^K = \mathbb{C}_{2\bullet}^K.$$

(c) Discretization of equation (7.6c)

The constitutive law expressed in (7.6c) is discretized in three equations corresponding to the three values of the test function $\tilde{\boldsymbol{\tau}}$. We have for the discretization on xx:

$$\int_K \mathrm{i}\,\omega\,\tau_{xx}^K\,\varphi_i^K + \int_K \mathrm{i}\,\omega\,\alpha_{11}\,\mathrm{p}_h^K\,\varphi_i^K + \int_K C_{11}\,\mathrm{u}_x^K\,\frac{\partial \varphi_i^K}{\partial x} + \int_K C_{13}\,\mathrm{u}_x^K\,\frac{\partial \varphi_i^K}{\partial y} + \int_K C_{13}\,\mathrm{u}_y^K\,\frac{\partial \varphi_i^K}{\partial x}$$
$$+ \int_K C_{12}\,\mathrm{u}_y^K\,\frac{\partial \varphi_i^K}{\partial y} - \int_{\partial K}\lambda_{1x}\,(C_{11}\varphi_i^K n_x + C_{13}\varphi_i^K n_y) - \int_{\partial K}\lambda_{1y}\,(C_{13}\varphi_i^K n_x + C_{12}\varphi_i^K n_y) = 0,$$

then on yy:

$$\int_K \mathrm{i}\,\omega\,\tau_{yy}^K\,\varphi_i^K + \int_K \mathrm{i}\,\omega\,\alpha_{22}\,\mathrm{p}_h^K\,\varphi_i^K + \int_K C_{12}\,\mathrm{u}_x^K\,\frac{\partial \varphi_i^K}{\partial x} + \int_K C_{23}\,\mathrm{u}_x^K\,\frac{\partial \varphi_i^K}{\partial y} + \int_K C_{23}\,\mathrm{u}_y^K\,\frac{\partial \varphi_i^K}{\partial x}$$
$$+ \int_K C_{22}\,\mathrm{u}_y^K\,\frac{\partial \varphi_i^K}{\partial y} - \int_{\partial K}\lambda_{1x}\,(C_{12}\varphi_i^K n_x + C_{23}\varphi_i^K n_y) - \int_{\partial K}\lambda_{1y}\,(C_{23}\varphi_i^K n_x + C_{22}\varphi_i^K n_y) = 0,$$

while the equation on xy gives:

$$\int_K \mathrm{i}\,\omega\,\tau_{xy}^K\,\varphi_i^K \;+\int_K \mathrm{i}\,\omega\,\alpha_{12}\,\mathrm{p}_h^K\,\varphi_i^K \;+\int_K C_{13}\,\mathrm{u}_x^K\,\frac{\partial\varphi_i^K}{\partial x} \;+\int_K C_{33}\,\mathrm{u}_x^K\,\frac{\partial\varphi_i^K}{\partial y} \;+\int_K C_{33}\,\mathrm{u}_y^K\,\frac{\partial\varphi_i^K}{\partial x}$$

$$+\int_K C_{23}\,\mathrm{u}_y^K\,\frac{\partial\varphi_i^K}{\partial y} \;-\int_{\partial K}\lambda_{1x}\,(C_{13}\varphi_i^K n_x+\,C_{33}\varphi_i^K n_y) \;-\int_{\partial K}\lambda_{1y}\,(C_{33}\varphi_i^K n_x+\,C_{23}\varphi_i^K n_y)=\,0.$$

Then, we express the above equations in terms of local matrices and the unknown vectors defined in equations (7.11) and (7.10):

$$\mathrm{i}\,\omega\,\mathbb{M}^K\,\underline{\tau}_{xx}^K \;+\,\mathrm{i}\,\omega\alpha_{11}\mathbb{M}^K\underline{\mathrm{p}}^K \;+C_{11}\mathbb{D}_x^K\,\underline{\mathrm{u}}_x^K \;+C_{13}\mathbb{D}_y^K\,\underline{\mathrm{u}}_x^K \;+C_{13}\mathbb{D}_x^K\,\underline{\mathrm{u}}_y^K \;+C_{12}\mathbb{D}_y^K\,\underline{\mathrm{u}}_y^K$$

$$-\sum_{f=1}^{3}\underline{\lambda}_{1x}^{\beta(K,f)}\,(C_{11}\mathbb{Q}_{xf}^K+\,C_{13}\mathbb{Q}_{yf}^K)-\sum_{f=1}^{3}\underline{\lambda}_{1y}^{\beta(K,f)}\,(C_{13}\mathbb{Q}_{xf}^K+\,C_{12}\mathbb{Q}_{yf}^K)=\,0\,,$$

$$\mathrm{i}\,\omega\,\mathbb{M}^K\,\underline{\tau}_{yy}^K \;+\,\mathrm{i}\,\omega\,\alpha_{22}\,\mathbb{M}^K\,\underline{\mathrm{p}}^K \;+C_{12}\mathbb{D}_x^K\,\underline{\mathrm{u}}_x^K \;+C_{23}\mathbb{D}_y^K\,\underline{\mathrm{u}}_x^K \;+C_{23}\mathbb{D}_x^K\,\underline{\mathrm{u}}_y^K \;+C_{22}\mathbb{D}_y^K\,\underline{\mathrm{u}}_y^K$$

$$-\sum_{f=1}^{3}\underline{\lambda}_{1x}^{\beta(K,f)}\,(C_{12}\mathbb{Q}_{xf}^K+\,C_{23}\mathbb{Q}_{yf}^K) \;-\sum_{f=1}^{3}\underline{\lambda}_{1y}^{\beta(K,f)}\,(C_{23}\mathbb{Q}_{xf}^K+\,C_{22}\mathbb{Q}_{yf}^K)=\,0\,,$$

and

$$\mathrm{i}\,\omega\,\mathbb{M}^K\,\underline{\tau}_{xy}^K \;+\,\mathrm{i}\,\omega\,\alpha_{12}\,\mathbb{M}^K\,\underline{\mathrm{p}}^K \;+C_{13}\mathbb{D}_x^K\,\underline{\mathrm{u}}_x^K \;+C_{33}\mathbb{D}_y^K\,\underline{\mathrm{u}}_x^K \;+C_{33}\mathbb{D}_x^K\,\underline{\mathrm{u}}_y^K \;+C_{23}\mathbb{D}_y^K\,\underline{\mathrm{u}}_y^K$$

$$-\sum_{f=1}^{3}\underline{\lambda}_{1x}^{\beta(K,f)}\,(C_{13}\mathbb{Q}_{xf}^K+\,C_{33}\mathbb{Q}_{yf}^K) \;-\sum_{f=1}^{3}\underline{\lambda}_{1y}^{\beta(K,f)}\,(C_{33}\mathbb{Q}_{xf}^K+\,C_{23}\mathbb{Q}_{yf}^K)=\,0\,.$$

(d) Discretization of equation (7.6d)

The discretization of equation (7.6d) gives:

$$\int_K \mathrm{i}\,\omega\,\mathrm{p}_h^K\,\varphi_i^K \;+\int_K M\,\frac{\partial \mathrm{w}_x^K}{\partial x}\,\varphi_i^K \;+\int_K M\,\frac{\partial \mathrm{w}_y^K}{\partial y}\,\varphi_i^K \;-\int_{\partial K} M\,\mathrm{p}_h^K\,\gamma_2\,\varphi_i^K \;+\int_{\partial K} M\,\lambda_2\,\gamma_2\,\varphi_i^K$$

$$-\int_{\partial K} M\,\gamma_4\mathrm{u}_x^K\,n_x\,\varphi_i^K \;-\int_{\partial K} M\,\gamma_4\mathrm{u}_y^K\,n_y\,\varphi_i^K+\int_{\partial K} M\,\gamma_4\,\lambda_{1x}\,n_x\,\varphi_i^K \;+\int_{\partial K} M\,\gamma_4\,\lambda_{1y}\,n_y\varphi_i^K$$

$$-\int_K M\,(\alpha_{11}\mathrm{u}_x^K+\,\alpha_{12}\mathrm{u}_y^K)\frac{\partial\varphi_i^K}{\partial x}-\int_K M\,(\alpha_{12}\mathrm{u}_x^K+\,\alpha_{22}\mathrm{u}_y^K)\frac{\partial\varphi_i^K}{\partial y}$$

$$+\int_K M\,(\alpha_{11}\lambda_{1x}+\,\alpha_{12}\lambda_{1y})n_x\,\varphi_i^K+\int_K M\,(\alpha_{12}\lambda_{1x}+\,\alpha_{22}\lambda_{1y})n_y\,\varphi_i^K=\,0\,.$$

In terms of the local matrices in (7.11) and the unknown vectors in (7.10), the above equations are

$$\mathrm{i}\,\omega\,\mathbb{M}^K\,\underline{\mathrm{p}}^K \;+M(\mathbb{D}_x^K)^T\,\underline{\mathrm{w}}_x^K \;+M(\mathbb{D}_y^K)^T\,\underline{\mathrm{w}}_y^K \;-\sum_{f=1}^{3}M\,\gamma_2\,\mathbb{E}^{\beta(K,f)}\underline{\mathrm{p}}^K+\sum_{f=1}^{3}M\,\gamma_2\,\mathbb{F}^{\beta(K,f)}\,\underline{\lambda}_2^{\beta(K,f)}$$

$$-\sum_{f=1}^{3}M\,\gamma_4(\mathbb{J}_x^{\beta(K,f)}\,\underline{\mathrm{u}}_x^K+\,\mathbb{J}_y^{\beta(K,f)}\,\underline{\mathrm{u}}_y^K)+\sum_{f=1}^{3}M\,\gamma_4(\mathbb{Q}_x^{\beta(K,f)}\,\underline{\lambda}_{1x}^{\beta(K,f)}+\,\mathbb{Q}_y^{\beta(K,f)}\underline{\lambda}_{1y}^{\beta(K,f)})$$

$$-M\,\alpha_{11}\,\mathbb{D}_x^K\,\mathrm{u}_x^K-M\,\alpha_{12}\mathbb{D}_y^K\,\mathrm{u}_y^K+\sum_{f=1}^{3}M(\alpha_{11}\underline{\lambda}_{1x}^{\beta(K,f)}+\,\alpha_{12}\underline{\lambda}_{1y}^{\beta(K,f)})\mathbb{Q}_x^{\beta(K,f)}$$

$$-M\,\alpha_{12}\,\mathbb{D}_y^K\,\mathrm{u}_x^K-M\,\alpha_{22}\,\mathbb{D}_x^K\,\mathrm{u}_y^K+\sum_{f=1}^{3}M(\alpha_{12}\underline{\lambda}_{1x}^{\beta(K,f)}+\,\alpha_{22}\,\underline{\lambda}_{1y}^{\beta(K,f)})\,\mathbb{Q}_y^{\beta(K,f)}=\,0\,.$$

(e) Discretization of equation (7.6e)

Equation (7.6e) is discretized along $x-$ component:

$$\int_K \mathrm{i}\,\omega\,\delta_0^K\,E_x^K\,\varphi_i^K\;+\int_K \mathrm{H}_h\,\frac{\partial\varphi_i^K}{\partial y}\;-\int_{\partial K}\lambda_3 n_y\,\varphi_i^K\;+\int_K J_x^K\,\varphi_i^K\;=\int_K f_{Cx}\,\varphi_i^K\,,$$

and along $y-$ component:

$$\int_K \mathrm{i}\,\omega\,\delta_0^K\,E_y^K\,\varphi_i^K\;-\int_K \mathrm{H}_h\,\frac{\partial\varphi_i^K}{\partial x}\;+\int_{\partial K}\lambda_3 n_x\,\varphi_i^K\;+\int_K J_y^K\,\varphi_i^K\;=\int_K f_{Cy}\,\varphi_i^K\,.$$

This is expressed in terms of local matrices (equation (7.11)) and the unknown vectors ((7.10)):

$$\mathbb{M}^K\,\mathrm{i}\,\omega\,\delta_0^K\,\underline{E}_x^K\;+\mathbb{D}_y^K\,\underline{H}^K-\sum_{f=1}^{3}\mathbb{Q}_y^{\beta(K,f)}\underline{\lambda_3}+\mathbb{M}^K\,\underline{J}_x^K\;=\mathbb{C}_5^K\,,$$

and

$$\mathbb{M}^K\,\mathrm{i}\,\omega\,\delta_0^K\,\underline{E}_y^K\;-\mathbb{D}_x^K\,\underline{H}^K+\sum_{f=1}^{3}\mathbb{Q}_x^{\beta(K,f)}\underline{\lambda_3}+\mathbb{M}^K\,\underline{J}_y^K\;=\mathbb{C}_6^K\,.$$

(f) Discretization of equation (7.6f)

The discretization of equation (7.6f) is:

$$\int_K \mathrm{i}\,\omega\,\mu_0^K\,\mathrm{H}_h\,\varphi_i^K\;+\int_K\left(\frac{\partial E_y^K}{\partial x}-\frac{\partial E_x^K}{\partial y}\right)\varphi_i^K\;-\int_{\partial K}\gamma_5\,(\mathrm{H}_h-\lambda_3)\,\varphi_i^K\;=0\,.$$

This is expressed with the local matrices and local unknowns that have been defined in equations (7.11) and (7.10).

$$\mathbb{M}^K\,\mathrm{i}\,\omega\,\mu_0^K\,\underline{H}^K\;+(\mathbb{D}_x^K)^T\,\underline{E}_y^K\;-(\mathbb{D}_y^K)^T\,\underline{E}_x^K\;-\sum_{f=1}^{3}\mathbb{E}^K\,\gamma_5\,\underline{H}^K\;+\sum_{f=1}^{3}\mathbb{F}_f^K\,\gamma_5\,\underline{\lambda_3}\;=0\,.$$

(g) Discretization of equation (7.6g)

We discretize the last equation of the local problem (7.6g) on x and y direction. Taking $\bullet=x,y$, we have:

$$\int_K J_\bullet^K\,\varphi_i^K\;-\int_K\sigma^K\,E_\bullet^K\,\varphi_i^K\;-\int_K \mathrm{p}_h^K\,\mathrm{L}\,\frac{\partial\varphi_i^K}{\partial\bullet}\;+\int_{\partial K}\mathrm{L}\,n_\bullet\,\lambda_2\,\varphi_i^K\;+\int_K \mathrm{i}\,\omega\,\rho_f^K\,\mathrm{L}\,\mathrm{u}_\bullet^K\,\varphi_i^K\;=\mathrm{L}\int_K f_{w\bullet}\,\varphi_i^K\,,$$

which is written in terms of local matrices and unknowns from equations (7.11) and (7.10) as

$$\mathbb{M}^K\,\underline{J}_\bullet^K\;-\mathbb{M}^K\sigma^K\,\underline{E}_\bullet^K\;-\mathbb{D}_\bullet^K\,\mathrm{L}\,\underline{\mathrm{p}}^K\;+\sum_{f=1}^{3}\mathbb{Q}_{\bullet f}^K\,\mathrm{L}\,\underline{\lambda}_2\;+\mathbb{M}^K\,\mathrm{i}\,\omega\,\rho_f^K\,\mathrm{L}\,\underline{\mathrm{u}}_\bullet^K\;=\mathrm{L}\,\mathbb{C}_{2\bullet}^K\,.$$

Local system

The discretization of the local problem (7.6) detailed above can be written as a linear system of the form:

$$\mathbb{A}^K\underline{W}^K+\mathbb{B}^K\underline{\Lambda}^K=\mathbb{C}_{\text{source}}^K\,,$$

where $\underline{W}^K$ and $\underline{\Lambda}^K$ have been defined in (7.10). The matrix $\mathbb{A}^K$ is of dimension $13\,d_i^K\times 13d_i^K$, $\mathbb{B}^K$ of size $13\,d_i^K\times 12d_i^F$, and $\mathbb{C}_{\text{source}}^K$ is the matrix of the external forces of dimension $13\,d_i^K$. The elementary matrix $\mathbb{A}^K$ is written as:

$$\mathbb{A}^K\;=\;\begin{pmatrix}\mathbb{A}_{\mathbf{poro}}^K & \mathbb{A}_{\substack{\text{coupling}\\ \text{EM}\to\text{poro}}}^K\\ \mathbb{A}_{\substack{\text{coupling}\\ \text{poro}\to\text{EM}}}^K & \mathbb{A}_{\mathbf{EM}}^K\end{pmatrix}.$$

The expression of $\mathbb{A}_{\mathbf{poro}}^K$ (of dimension $8\,d_i^K\times 8d_i^K$) corresponds to the matrix for poroelasticity with no electrokinetic coupling (see [7]). Similarly, the expression $\mathbb{A}_{\mathbf{EM}}^K$ (of dimension $5\,d_i^K\times 5d_i^K$) corresponds to the matrix for Maxwell's

equations. Matrices $\mathbb{A}^K_{\substack{\text{coupling}\\ \text{EM}\to\text{poro}}}$ (of dimension $8\,d_i^K \times 5d_i^K$) and $\mathbb{A}^K_{\substack{\text{coupling}\\ \text{poro}\to\text{EM}}}$ (of dimension $5\,d_i^K \times 8d_i^K$) represent the electrokinetic coupling. The matrix $\mathbb{A}^K_{\mathbf{poro}}$ is the same as for poroelasticity, and is given in Appendix B.1.1. The electromagnetic matrix $\mathbb{A}^K_{\mathbf{EM}}$ is given in equation (G.24), taking $\delta_0 = \epsilon_0$. Then, the coupling matrices $\mathbb{A}^K_{\substack{\text{coupling}\\ \text{EM}\to\text{poro}}}$ and $\mathbb{A}^K_{\substack{\text{coupling}\\ \text{poro}\to\text{EM}}}$ are expressed as:

$$\mathbb{A}^K_{\substack{\text{coupling}\\ \text{EM}\to\text{poro}}} = \begin{pmatrix} 0 & 0 & 0 & 0 & 0 \\ 0 & 0 & 0 & 0 & 0 \\ -\mathrm{i}\,\omega\rho_{\text{dyn}}\mathbb{M}^K\mathrm{L} & 0 & 0 & 0 & 0 \\ 0 & -\mathrm{i}\,\omega\rho_{\text{dyn}}\mathbb{M}^K\mathrm{L} & 0 & 0 & 0 \\ 0 & 0 & 0 & 0 & 0 \\ 0 & 0 & 0 & 0 & 0 \\ 0 & 0 & 0 & 0 & 0 \\ 0 & 0 & 0 & 0 & 0 \end{pmatrix},$$

and

$$\mathbb{A}^K_{\substack{\text{coupling}\\ \text{poro}\to\text{EM}}} = \begin{pmatrix} 0 & 0 & 0 & 0 & 0 & 0 & 0 & 0 \\ 0 & 0 & 0 & 0 & 0 & 0 & 0 & 0 \\ 0 & 0 & 0 & 0 & 0 & 0 & 0 & 0 \\ \mathbb{M}^K\,\mathrm{i}\,\omega\rho_f\mathrm{L} & 0 & 0 & 0 & 0 & 0 & 0 & -\mathbb{D}_x^K\mathrm{L} \\ 0 & \mathbb{M}^K\,\mathrm{i}\,\omega\rho_f\mathrm{L} & 0 & 0 & 0 & 0 & 0 & -\mathbb{D}_y^K\mathrm{L} \end{pmatrix}.$$

The unknown $\underline{\Lambda}^K$ is composed of 4 times 3 subblocks corresponding to the four Lagrange unknowns (three poroelastic variables and one electromagnetic variable) decomposed on the three faces of the triangle. Hence, $\mathbb{B}^K$ has the form:

$$\mathbb{B}^K = \begin{pmatrix} \mathbb{B}^K_{\mathbf{poro}} & \mathbb{B}^K_{\substack{\text{coupling}\\ \text{EM}\to\text{poro}}} \\ \mathbb{B}^K_{\substack{\text{coupling}\\ \text{poro}\to\text{EM}}} & \mathbb{B}^K_{\mathbf{EM}} \end{pmatrix}.$$

$\mathbb{B}^K_{\mathbf{poro}}$ corresponds to the matrix for poroelasticity and is given in Appendix B.1.1. The matrix $\mathbb{B}^K_{\mathbf{EM}}$ is given in equation (G.25). $\mathbb{B}^K_{\substack{\text{coupling}\\ \text{EM}\to\text{poro}}}$ is written as

$$\mathbb{B}^K_{\substack{\text{coupling}\\ \text{EM}\to\text{poro}}} = \begin{pmatrix} B^{\lambda_3,1}_{\substack{\text{coupling}\\ \text{EM}\to\text{poro}}} & B^{\lambda_3,2}_{\substack{\text{coupling}\\ \text{EM}\to\text{poro}}} & B^{\lambda_3 3}_{\substack{\text{coupling}\\ \text{EM}\to\text{poro}}} \end{pmatrix}, \quad \text{with } B^{\lambda_3,f}_{\substack{\text{coupling}\\ \text{EM}\to\text{poro}}} = 0, \quad \text{for } f = 1,2,3.$$

Similarly, the block $\mathbb{B}^K_{\substack{\text{coupling}\\ \text{poro}\to\text{EM}}}$ is decomposed as:

$$\mathbb{B}^K_{\substack{\text{coupling}\\ \text{poro}\to\text{EM}}} = \begin{pmatrix} B^{\lambda_{1x},1}_{\substack{\text{coupling}\\ \text{poro}\to\text{EM}}} & B^{\lambda_{1x},2}_{\substack{\text{coupling}\\ \text{poro}\to\text{EM}}} & B^{\lambda_{1x},3}_{\substack{\text{coupling}\\ \text{poro}\to\text{EM}}} & B^{\lambda_{1y},1}_{\substack{\text{coupling}\\ \text{poro}\to\text{EM}}} & B^{\lambda_{1y},2}_{\substack{\text{coupling}\\ \text{poro}\to\text{EM}}} & B^{\lambda_{1y},3}_{\substack{\text{coupling}\\ \text{poro}\to\text{EM}}} & B^{\lambda_2,1}_{\substack{\text{coupling}\\ \text{poro}\to\text{EM}}} & B^{\lambda_2,2}_{\substack{\text{coupling}\\ \text{poro}\to\text{EM}}} & B^{\lambda_2,3}_{\substack{\text{coupling}\\ \text{poro}\to\text{EM}}} \end{pmatrix},$$

with

$$B^{\lambda_{1x},f}_{\substack{\text{coupling}\\ \text{poro}\to\text{EM}}} = 0, \quad B^{\lambda_{1y},f}_{\substack{\text{coupling}\\ \text{poro}\to\text{EM}}} = 0, \quad B^{\lambda_2,f}_{\substack{\text{coupling}\\ \text{poro}\to\text{EM}}} = \begin{pmatrix} 0 \\ 0 \\ 0 \\ \mathrm{L}\,\mathbb{Q}^{\beta(K,f)}_{xf} \\ \mathrm{L}\,\mathbb{Q}^{\beta(K,f)}_{yf} \end{pmatrix}, \quad \text{for } f = 1,2,3.$$

Finally the local source vector is:

$$\mathbb{C}^K_{\text{source}} = \begin{pmatrix} \mathbb{C}^K_1 & \mathbb{C}^K_2 & \mathbb{C}^K_3 & \mathbb{C}^K_4 & 0 & 0 & 0 & 0 & \mathbb{C}^K_5 & \mathbb{C}^K_6 & 0 & 0 & 0 \end{pmatrix}^T.$$

Now that we have constructed the elementary problems on every cell, we connect them thanks to the physical transmission conditions.

7.2.2 Transmission conditions

We consider an interior face F of the triangulation $\mathcal{T}_h$ such as $F = \partial K \cap \partial K'$ which means that $\beta(K,f) = \beta(K',g)$. This means that the global index of the f-th face of K is the same as g-th face of K'. We define $\boldsymbol{n}$ the unit normal vector of the face F outwardly directed to element K. Using the decomposition of the test functions $\boldsymbol{\eta}$, ξ and ν, in basis functions ψ_i^F we discretize the transmission conditions (7.7) for this face, and write them with the elementary matrices and local unknowns defined in equations (7.11) and (7.10).

(a) Discretization of equation (7.7a)

The first transmission equation (7.7a) is expressed as:

$$\sum_{K\in\mathcal{T}_h}\int_{\partial K}\Big((\boldsymbol{\tau}_h^K\,\boldsymbol{n})\cdot\boldsymbol{\eta}-\gamma_1(\mathbf{u}_h^K-\boldsymbol{\lambda}_1)\cdot\boldsymbol{\eta}-\gamma_3\,(\mathrm{p}_h^K-\lambda_2)\,\boldsymbol{n}\cdot\boldsymbol{\eta}\;=\;\sum_{F\in\mathcal{F}_{\rm ext}}\int_F\boldsymbol{f}_{\rm inc}\cdot\boldsymbol{\eta}\,,$$

The discretization of the above equation along x and y direction gives, with $\bullet = x, y$:

$$\sum_{K\in\mathcal{T}_h}\int_{\partial K}\Big(\underline{\tau}_{x\bullet}^K\,n_x\,\varphi_j^K\,\psi_i^F\,dS\;+\underline{\tau}_{y\bullet}^K\,n_y\,\varphi_j^K\,\psi_i^F\,dS\;-\gamma_1\,\varphi_j^K\,\underline{\mathrm{u}}_\bullet^K\,\psi_i^F\,dS\;+\gamma_1\,\psi_j^F\,\underline{\lambda}_{1\bullet}\,\psi_i^F\,dS$$

$$-\gamma_3\,n_\bullet\,\underline{\mathrm{p}}^K\varphi_j^K\psi_i^F\,dS\;+\gamma_3\,n_\bullet\,\underline{\lambda}_2\,\psi_j^F\psi_i^F\,dS\Big)=\sum_{F\in\mathcal{F}_{\rm ext}}\int_F f_{{\rm inc},\bullet}\psi_i^F\,dS\,.$$

Next, we write these equations in terms of the elementary matrices defined in equation (7.11). We have:

$$\sum_{K\in\mathcal{T}_h}\Big((\mathbb{Q}_x^{\beta(K,f)})^T\,\underline{\tau}_{x\bullet}^K+(\mathbb{Q}_y^{\beta(K,f)})^T\,\underline{\tau}_{y\bullet}^K-\gamma_1\,(\mathbb{F}^{\beta(K,f)})^T\,\underline{\mathrm{u}}_\bullet^K+\gamma_1\,\mathbb{G}^{\beta(K,f)}\,\underline{\lambda}_{1\bullet}$$

$$-\gamma_3\,(\mathbb{Q}_\bullet^{\beta(K,f)})^T\,\underline{\mathrm{p}}^K+\gamma_3\,\mathbb{H}_\bullet^{\beta(K,f)}\,\underline{\lambda}_2\Big)\;=\;\sum_{F\in\mathcal{F}_{\rm ext}}\int_F f_{{\rm inc},\bullet}\,\psi_i^F\,dS\,. \tag{7.22}$$

(b) Discretization of equation (7.7b)

The second transmission equation is:

$$\sum_{K\in\mathcal{T}_h}\int_{\partial K}\Big((\mathbf{w}_h^K\cdot\boldsymbol{n})\,\xi-\gamma_2\,(\mathrm{p}_h^K-\lambda_2)\,\xi-\gamma_4\,(\mathbf{u}_h^K-\boldsymbol{\lambda}_1)\cdot\boldsymbol{n}\,\xi\Big)\;=\;\sum_{F\in\mathcal{F}_{\rm ext}}\int_F g_{\rm inc}\,\xi\,,$$

which is discretized by replacing the test-functions by the basis functions and by introducing the local unknowns defined in (7.10) to give:

$$\sum_{K\in\mathcal{T}_h}\int_{\partial K}\Big(\underline{\mathrm{w}}_x^K\,\varphi_j^K\,n_x^K\,\psi_i^F\,dS+\underline{\mathrm{w}}_y^K\,\varphi_j^K\,n_y^K\,\psi_i^F\,dS-\underline{\mathrm{p}}^K\,\varphi_j^K\,\gamma_2\,\psi_i^F\,dS+\underline{\lambda}_2\,\psi_j^F\,\gamma_2\,\psi_i^F\,dS-\underline{\mathrm{u}}_x^K\,\varphi_j^K\,\gamma_4\,n_x^K\,\psi_i^F\,dS$$

$$-\underline{\mathrm{u}}_y^K\,\varphi_j^K\,\gamma_4\,n_y^K\,\psi_i^F\,dS+\underline{\lambda}_{1x}^K\,\psi_j^F\,\gamma_4\,n_x^K\,\psi_i^F\,dS+\underline{\lambda}_{1y}^K\,\psi_j^F\,\gamma_4\,n_y^K\,\psi_i^F\,dS\Big)\;=\;\sum_{F\in\mathcal{F}_{\rm ext}}\int_F g_{\rm inc}\,\psi_i^F\,.$$

This can be expressed in terms of the matrices defined in equation (7.11):

$$\sum_{K\in\mathcal{T}_h}\int_{\partial K}\Big((\mathbb{Q}_x^{\beta(K,f)})^T\,\underline{\mathrm{w}}_x^K+(\mathbb{Q}_y^{\beta(K,f)})^T\,\underline{\mathrm{w}}_y^K-(\mathbb{F}^{\beta(K,f)})^T\,\underline{\mathrm{p}}^K\,\gamma_2+\mathbb{G}^{\beta(K,f)}\,\underline{\lambda}_2\,\gamma_2-(\mathbb{Q}_x^{\beta(K,f)})^T\,\underline{\mathrm{u}}_x^K\,\gamma_4$$

$$-(\mathbb{Q}_y^{\beta(K,f)})^T\,\underline{\mathrm{u}}_y^K\,\gamma_4+\mathbb{H}_x^{\beta(K,f)}\,\underline{\lambda}_{1x}\,\gamma_4+\mathbb{H}_y^{\beta(K,f)}\,\underline{\lambda}_{1y}\,\gamma_4\Big)\;=\;\sum_{F\in\mathcal{F}_{\rm ext}}\int_F g_{\rm inc}\,\psi_i^F\,. \tag{7.23}$$

(c) Discretization of equation (7.7c)

The third transmission equation is expressed as:

$$\sum_{K\in\mathcal{T}_h}\int_{\partial K}\Big((\boldsymbol{n}\times\boldsymbol{E}_h^K)\,\nu-\gamma_5\big(\mathrm{H}_h^K-\lambda_3\big)\,\nu\Big)=\sum_{F\in\mathcal{F}_{\text{ext}}}\int_F h_{\text{inc}}\,\nu\,.$$

The above expression can be rewritten in terms of the basis functions and the local unknowns defined in (7.10):

$$\sum_{K\in\mathcal{T}_h}\int_{\partial K}\Big(\big(n_x^K\,\underline{E}_y^K-n_y^K\,\underline{E}_x^K\big)\;\varphi_j^K\,\psi_i^F dS-\gamma_5\;\big(\underline{H}^K\varphi_j^K-\underline{\lambda_3}\psi_j^F\big)\;\psi_i^F\,dS\Big)=\sum_{F\in\mathcal{F}_{\text{ext}}}\int_F h_{\text{inc}}\,\psi_i^F\,,$$

which can be rewritten using the elementary matrices given in (7.11):

$$\sum_{K\in\mathcal{T}_h}\Big((\mathbb{Q}_x^{\beta(K,f)})^T\underline{E}_y^K\;-(\mathbb{Q}_y^{\beta(K,f)})^T\underline{E}_x^K\;-(\mathbb{F}^{\beta(K,f)})^T\underline{H}^K\,\gamma_5\;+\mathbb{G}^{\beta(K,f)}\underline{\lambda_3}\,\gamma_5\Big)=\sum_{F\in\mathcal{F}_{\text{ext}}}\int_F h_{\text{inc}}\,\psi_i^F\,.\tag{7.24}$$

Local system

The transmission conditions, equations (7.22), (7.23), (7.24) form the following system:

$$\sum_{K\in\mathcal{T}_h}(\mathcal{A}_{HDG}^K)^T\left(\mathbb{P}^K\underline{W}^K+\mathbb{T}^K\mathcal{A}_{HDG}^K\underline{\Lambda}\right)=\mathbb{S}_{\text{inc}}\,,$$

where $\mathbb{S}_{\text{inc}}$ represents the matrices of the incident forces. Similarly to $\mathbb{A}^K$ and $\mathbb{B}^K$, the elementary matrix $\mathbb{P}^K$ has the form:

$$\mathbb{P}^K\;=\;\begin{pmatrix}\mathbb{P}^K_{\mathbf{poro}} & 0\\ 0 & \mathbb{P}^K_{\mathbf{EM}}\end{pmatrix},$$

where $\mathbb{P}^K_{\mathbf{poro}}$, corresponds to the matrix for poroelasticity, given in Appendix B.1.1, and $\mathbb{P}^K_{\mathbf{EM}}$ to the electromagnetic matrix given in equation (G.26).

Similarly, $\mathbb{T}^K$ has the form:

$$\mathbb{T}^K\;=\;\begin{pmatrix}\mathbb{T}^K_{\mathbf{poro}} & 0\\ 0 & \mathbb{T}^K_{\mathbf{EM}}\end{pmatrix},$$

where the poroelastic matrix $\mathbb{T}^K_{\mathbf{poro}}$ is given in Appendix B.1.1, and the electromagnetic matrix $\mathbb{T}^K_{\mathbf{EM}}$ is given in (G.26).

Remark 7.1. For a face on the boundary of the domain, we can impose one of the eight types of boundary conditions, see Section 5.4. For type 1, we impose the continuity of $\hat{\boldsymbol{\tau}}\,\boldsymbol{n}$, $\hat{\mathbf{w}}\cdot\boldsymbol{n}$ and $\boldsymbol{n}\times\hat{\boldsymbol{E}}$. This means that the boundary conditions for an external face are treated the same way as the transmission conditions (7.7) for an interior interface. However, if we choose to impose a different boundary condition, the expression of the elementary matrices $\mathbb{P}^K$ and $\mathbb{T}^K$ is modified. Here, we detail the boundary condition of type 8, as in equation (5.10b). The other formulations can be easily deduced from these two formulations. This is similar to what has been done for poroelasticity. For the boundary condition of type 8, we impose the condition in the strong way in the linear system, which means that we impose the value of $\hat{\mathbf{u}}$, $\hat{\mathrm{p}}$, and $\hat{\boldsymbol{H}}$. From equation (5.10b), we impose:

$$\boldsymbol{\lambda}_1=\mathbf{f}_{\text{inc}}\,,\qquad\lambda_2=g_{\text{inc}}\,,\qquad\lambda_3=h_{\text{inc}}\,.$$

We consider an element with the first local face on the boundary of the mesh. In this case, the matrices $\mathbb{P}^K_{\mathbf{poro}}$ and $\mathbb{T}^K_{\mathbf{poro}}$ are given in Appendix B.2, $\mathbb{P}^K_{\mathbf{EM}}$ and $\mathbb{P}^K_{\mathbf{EM}}$ in (G.27). The corresponding lines of $\mathbb{P}^K_{\substack{\text{coupling}\\ \text{poro}\to\text{EM}}}$, and $\mathbb{T}^K_{\substack{\text{coupling}\\ \text{poro}\to\text{EM}}}$, i.e., lines 1, 4 and 7 are equal to zero, and the first line of $\mathbb{P}^K_{\substack{\text{coupling}\\ \text{EM}\to\text{poro}}}$ and $\mathbb{T}^K_{\substack{\text{coupling}\\ \text{EM}\to\text{poro}}}$ are zero.

7.3 Resolution using HDG method

Here, we detail the algorithm for the resolution of Pride's equations using the proposed HDG method. This is very similar to what is done for poroelasticity, however since there are coupling terms to handle with, we detail the method in the following. For an element K, we have the local system:

$$\mathbb{A}\,\underline{W}^K\;+\;\mathbb{B}\,\underline{\Lambda}^K\;=\;\mathbb{C}^K_{\text{source}}\tag{7.25}$$

and the global system

$$\sum_{K\in\mathcal{T}_h} (\mathcal{A}_{HDG}^K)^T \left(\mathbb{P}^K \underline{W}^K + \mathbb{T}^K \mathcal{A}_{HDG}^K \underline{\Lambda}\right) = \mathbb{S}_{\text{inc}}\,. \tag{7.26}$$

If K is an interior element, $\mathbb{S}_{\text{inc}}^K = 0$. Let N_{face} be the number of edges of the mesh in two dimensions and number of faces in three dimensions. We define the global vector:

$$\underline{\Lambda} = (\underline{\boldsymbol{\lambda}}_1^1, \underline{\lambda}_2^1, \underline{\lambda_3}^1, ..., \underline{\boldsymbol{\lambda}}_1^{N_{face}}, \underline{\lambda}_2^{N_{face}}, \underline{\lambda_3}^{N_{face}})\,.$$

We also define the local trace operator $\mathcal{A}_{HDG}$ that links the local degrees of freedom of an element K to the global degrees of freedom of the Lagrange multiplier $\underline{\Lambda}$. This means that, for an element K,

$$\mathcal{A}_{HDG}^K \underline{\Lambda} = \underline{\Lambda}^K\,.$$

Equation (7.25) is written as:

$$\mathbb{A}^K \underline{W}^K = \mathbb{C}_{\text{source}}^K - \mathbb{B}^K \mathcal{A}_{HDG}^K \underline{\Lambda}\,.$$

Assuming that $\mathbb{A}^K$ can be inverted for each element, we have:

$$\underline{W}^K = -(\mathbb{A}^K)^{-1}\mathbb{B}^K \mathcal{A}_{HDG}^K \underline{\Lambda} + (\mathbb{A}^K)^{-1}\mathbb{C}_{\text{source}}^K\,. \tag{7.27}$$

Then $\underline{W}^K$ is replaced in (7.26) by its expression in (7.27):

$$\sum_{K\in\mathcal{T}_h} (\mathcal{A}_{HDG}^K)^T \left(\mathbb{P}^K(\mathbb{A}^K)^{-1}\mathbb{C}_{\text{source}}^K - \mathbb{P}^K(\mathbb{A}^K)^{-1}\mathbb{B}^K \mathcal{A}_{HDG}^K \underline{\Lambda} + \mathbb{T}^K \mathcal{A}_{HDG}^K \underline{\Lambda}\right) = \mathbb{S}_{\text{inc}}\,,$$

which means,

$$\sum_{K\in\mathcal{T}_h} (\mathcal{A}_{HDG}^K)^T \left(-\mathbb{P}^K(\mathbb{A}^K)^{-1}\mathbb{B}^K + \mathbb{T}^K\right) \mathcal{A}_{HDG}^K \underline{\Lambda} = -\sum_{K\in\mathcal{T}_h} (\mathcal{A}_{HDG}^K)^T\, \mathbb{P}^K(\mathbb{A}^K)^{-1}\, \mathbb{C}_{\text{source}}^K + \mathbb{S}_{\text{inc}}\,.$$

The global problem reads as:

$$\mathbb{K}\underline{\Lambda} = \mathbb{S}\,,$$

with $\mathbb{K} = \sum_{K\in\mathcal{T}_h} (\mathcal{A}_{HDG}^K)^T \left(-\mathbb{P}^K(\mathbb{A}^K)^{-1}\mathbb{B}^K + \mathbb{T}^K\right)$ and $\mathbb{S} = -\sum_{K\in\mathcal{T}_h} (\mathcal{A}_{HDG}^K)^T\, \mathbb{P}^K(\mathbb{A}^K)^{-1}\, \mathbb{C}_{\text{source}}^K + \mathbb{S}_{\text{inc}}$.

The resolution can be divided in four steps, detailed in the following algorithm. First, we build the stiffness matrix $\mathbb{K}$ and the source matrix $\mathbb{S}$. These calculations can be done element by element. Then, the global system is resolved and the solution is constructed. We use the MUMPS direct solver [3] for the resolution of the linear system, and this is the only step that is global.

Step 1: Construction of the stiffness matrix
for $K = 1, N_{\text{elem}}$ **do**
Compute the matrices $\mathbb{M}^K$ and $\mathbb{D}_v^K$, with $v = x, y$.
for $f = 1, 3$ **do**
Compute the matrices $\mathbb{E}^{\beta(K,f)}$, $\mathbb{F}^{\beta(K,f)}$, $\mathbb{G}_v^{\beta(K,f)}$, $\mathbb{Q}_v^{\beta(K,f)}$, $\mathbb{J}_v^{\beta(K,f)}$, $\mathbb{H}_v^{\beta(K,f)}$, with $v = x, y$.
end for
Compute the matrices $\mathbb{A}^K$,$(\mathbb{A}^K)^{-1}$, $\mathbb{B}^K$.
Compute $(\mathbb{A}^K)^{-1}\mathbb{B}$.
Compute $\mathbb{P}^K$, and $\mathbb{T}^K$ with the corresponding boundary conditions.
Compute $\mathbb{K}^K = \mathbb{P}^K(\mathbb{A}^K)^{-1}\mathbb{B}^K + \mathbb{T}^K$.
Use the $\mathcal{A}_{HDG}$ operator to determine the global degrees of freedom of the element and fill the global matrix $\mathbb{K}$.
end for

Step 2: Construction of the source term
Localisation of the point source
for $K = 1, N_{\text{elem}}$ **do**
Compute the local matrices $\mathbb{C}^K_{\text{source}}$ and $\mathbb{S}^K_{\text{inc}}$.
Compute $\mathbb{P}^K(\mathbb{A}^K)^{-1}\mathbb{C}^K_{\text{source}}$.
Use the $\mathcal{A}_{HDG}$ operator to determine the global degrees of freedom of the element and fill the global matrix $\mathbb{S}$.
end for

Step 3: Resolution of the global system
Resolution of $\mathbb{K}\underline{\Lambda} = \mathbb{S}$ with MUMPS .

Step 4: Reconstruction of the solution
for $K = 1, N_{\text{elem}}$ **do**
Compute the solutions $\underline{W}^K$ using the $\mathcal{A}^K_{HDG}$ operator:
$\underline{W}^K = -(\mathbb{A}^K)^{-1}\mathbb{B}^K\mathcal{A}^K_{HDG}\underline{\Lambda}$.
end for

Algorithm 3: Resolution with HDG Method

7.4 Numerical results in two dimensions

In this section, we validate the HDG method detailed in Section 7.1, and analyze the performance of our numerical solver. First, we introduce the geophysical media considered in the numerical tests, and the quantities used to assess the solver. Then, in Section 7.4.2, we validate the code in two dimensions by comparing the HDG numerical solutions with reference ones. We carry out numerical tests to study the effect of stabilization parameters introduced in the method on the numerical error, and the order of convergence. We show numerically that the presence of some of the stabilization parameters leads to important errors, and prevents from obtaining an optimal order of convergence. Finally, in Section 7.4.3, we study numerically the influence of the values of the stabilization parameters and the frequency on the well-posedness of the problem.

7.4.1 Parameterization of the computational domains and quantities of interest

In the numerical experiments, we work with three different materials: two kinds of sand and freshwater. The corresponding input physical parameters are listed in Table 7.1. The other parameters are deduced using the relations given in Section 5.1.

To assess the accuracy and the efficiency of the HDG numerical method, we will use the following quantities:

- The relative numerical error $e_h(\mathfrak{U})$ is computed from the knowledge of the numerical solution denoted by $\mathfrak{U}_{\text{numeric}}$ and the reference solution $\mathfrak{U}_{\text{reference}}$, following the formula:

$$e_h(\mathfrak{U}) = \frac{||\mathfrak{U}_{\text{numeric}} - \mathfrak{U}_{\text{reference}}||_2}{||\mathfrak{U}_{\text{reference}}||_2}, \quad \text{with} \quad ||\mathfrak{U}||_2 = \left(\sum_{K\in\mathcal{T}_h}\int_K |\mathfrak{U}|^2\right)^{\frac{1}{2}}. \tag{7.28}$$

- To study the stability of the discretization, we consider the condition number κ, defined, for a matrix $\mathbf{A}$ as $\kappa = \|\mathbf{A}^{-1}\|\,\|\mathbf{A}\|$, where $\|\mathbf{A}\|$ stands for a matrix norm of $\mathbf{A}$. We employ MUMPS [3] or LAPACK [4] to compute κ with the L^∞ norm, $\|\mathbf{A}\|_\infty = \max_i\left(\sum_{j=1}^n |a_{ij}|\right)$, where a_{ij} are the coefficients of $\mathbf{A}$.

Physical parameters	Sand1	Freshwater	Sand2
Porosity ϕ	0.3	0.15	0.4
Fluid Density ρ_f $(10^3 kg.m^{-3})$	1	1	0.998
Solid Density ρ_s $(10^3 kg.m^{-3})$	2.7	2.7	2.5
Viscosity η $(10^{-3}$Pa.s)	1	1	1
Permeability κ_0 $(10^{-9} m^2)$	0.01	0.001	0.00102
Tortuosity $\mathfrak{t}$	3	3	1.75
Solid Bulk Modulus $\mathrm{k_s}$ (GPa)	36	36	36
Fluid Bulk Modulus $\mathrm{k_f}$ (GPa)	2.2	2.2	2.5
Frame Bulk Modulus $\mathrm{k_{fr}}$ (GPa)	7	9	13.16e-3
Frame Shear Modulus μ_{fr} (GPa)	5	7	7.9e-3
Solid permittivity κ_{f}	4	4	4
Fluid permittivity κ_{s}	80	80	80
Conductivity σ $(10^{-4}$ S.m$^{-1})$	3.88	3.88	86.871
Zeta potential ζ (V)	0.1	0.1	

Table 7.1: Summary of the physical parameters of media in consideration. The parameters for Sand1 and Freshwater are taken from [71][Table 1].

7.4.2 Impact of the stabilization parameters on the accuracy of the numerical solution

In Section 7.1, we have expressed the numerical traces $\hat{\boldsymbol{\tau}}_h$, $\hat{\mathbf{w}}_h$, $\hat{\boldsymbol{E}}_h$ in the most general way, because we have written the three traces as functions of $(\mathbf{u}_h - \boldsymbol{\lambda}_1)$, $(\mathrm{p}_h - \lambda_2)$, and $(\mathrm{H}_h - \lambda_3)$, see (7.4). For that, we have used five stabilization parameters, denoted γ_i, for $i = 1, 5$. We recall the expression of the numerical traces below:

$$\begin{cases} \hat{\boldsymbol{\tau}}_h \boldsymbol{n} \,=\, \boldsymbol{\tau}_h \boldsymbol{n} - \gamma_1(\mathbf{u}_h - \boldsymbol{\lambda}_1) - (\mathrm{p}_h - \lambda_2)\gamma_3 \boldsymbol{n}\,, \\ \hat{\mathbf{w}}_h \cdot \boldsymbol{n} \,=\, \mathbf{w}_h \cdot \boldsymbol{n} - \gamma_2(\mathrm{p}_h - \lambda_2) - \gamma_4(\mathbf{u}_h - \boldsymbol{\lambda}_1)\cdot \boldsymbol{n}\,, \\ \boldsymbol{n} \times \hat{\boldsymbol{E}}_h \,=\, \boldsymbol{n} \times \boldsymbol{E}_h - \gamma_5\,(\mathrm{H}_h - \lambda_3)\,, \end{cases} \tag{7.29}$$

In the following, we are going to determine if, in (7.29), all the stabilization parameters are necessary. For poroelasticity, we have observed that we need the four parameters γ_1, γ_2, γ_3 and γ_4 to be different from zero to obtain the optimal order $(p+1)$ of convergence of the HDG method. In addition, if the four parameters are zero, we obtain an order of convergence p. From now on, for simplicity, we consider that the four poroelastic stabilization parameters γ_1, γ_2, γ_3 and γ_4 are taken equal. For the electromagnetic wave equation, the presence of γ_5 is necessary to obtain an optimal convergence order of the method, see Appendix G.

We consider the propagation of an incident plane wave in a bounded domain of size $\mathcal{D} = [0:20] \times [0:20]$m composed of homogeneous sand. The physical parameters of the material are given in Table 7.1. The domain $\mathcal{D}$ is discretized by an unstructured mesh composed of 1239 triangles. On the edges of the mesh, we impose the exact solution of the plane wave, which has been obtained in Section 5.5. We consider $\gamma_i = 1$, for $i = 1, 5$. We will work with the four kinds of incident plane waves (P, B, S, EM). We present in Figure 7.1 the solution on the solid velocity u_x for the four kinds of plane waves. For the Biot incident wave, we observe the attenuation of the wave. For the EM wave, we consider a significantly greater frequency than for the seismic waves, because the velocity of the EM wave has an order of magnitude much greater than the others. In Tables 7.2 to 7.5, we show the relative error (defined in (7.28)) of the numerical fields, for different kinds of incident waves.

$e_h(\mathrm{u}_x)$	$e_h(\mathrm{u}_y)$	$e_h(\mathrm{w}_x)$	$e_h(\mathrm{w}_y)$	$e_h(\tau_{xx})$	$e_h(\tau_{yy})$	$e_h(\tau_{xy})$	$e_h(\mathrm{p})$
4.09e-3	4.46e-3	3.15e-2	4.29e-2	1.92e-3	1.98e-3	3.59e-3	2.29e-3

$e_h(E_x)$	$e_h(E_y)$	$e_h(\mathrm{H})$	$e_h(J_y)$	$e_h(J_x)$
2.62e-2	3.26e-2	inf	69	106

Table 7.2: Relative errors (%) on the components of the unknowns of the HDG method for an incident P-wave, at frequency $f = 500$Hz with $\theta = 0.58$ rad and boundary conditions of type 1, using an order of discretization 4.

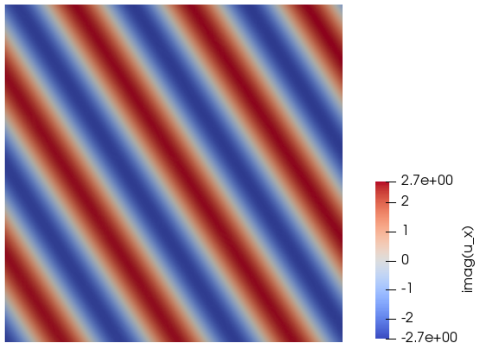

(a) Incident P-wave: solid velocity u_x, with $f =$ 500Hz.

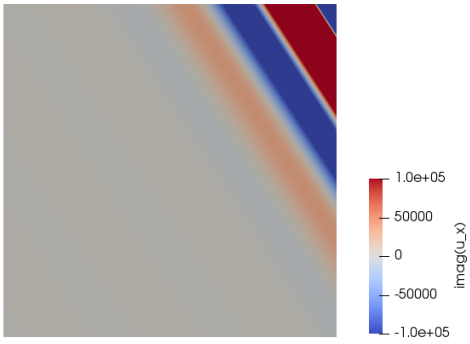

(b) Incident B-wave: solid velocity u_x, with $f =$ 100Hz.

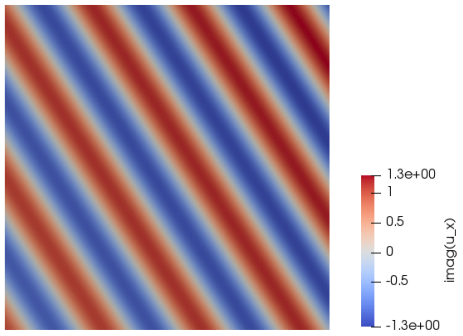

(c) Incident S-wave: solid velocity u_x, with $f =$ 300Hz.

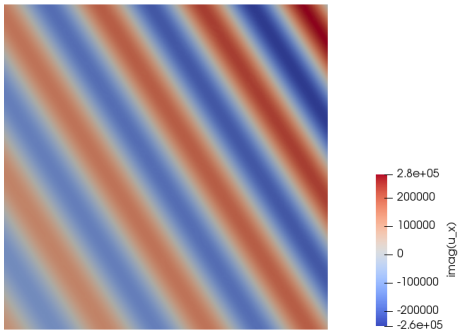

(d) Incident EM-wave: solid velocity u_x, with $f =$ 30MHz.

Figure 7.1: Plane waves in homogeneous sand: imaginary part of the horizontal solid velocity u_x for the four kinds of plane waves.

For the incident P-wave, *cf.* Table 7.2, the poroelastic variables and the electric field are well simulated and the relative error is small (less than $10^{-2}\%$). Note that the error on the magnetic field H is infinite because in the case of compression waves, the exact magnetic field is zero, hence the relative error is infinite. The relative error on the current density $\boldsymbol{J}$ is also non-negligible because the norm of the exact solution is very small (10^{10}), hence the numerical method cannot attain this precision. For the incident B-wave, we retrieve the same results as for an incident P-wave,

$e_h(u_x)$	$e_h(u_y)$	$e_h(w_x)$	$e_h(w_y)$	$e_h(\tau_{xx})$	$e_h(\tau_{yy})$	$e_h(\tau_{xy})$	$e_h(p)$
3.30e-2	3.59e-2	1.61e-2	1.97e-2	9.19e-3	4.71e-3	4.54e-3	2.33e-3

$e_h(E_x)$	$e_h(E_y)$	$e_h(H)$	$e_h(J_y)$	$e_h(J_x)$
1.36e-2	1.63e-2	inf	157	238

Table 7.3: Relative errors (%) on the components of the unknowns of the HDG method for an incident B-wave, at frequency $f = 100$Hz with $\theta = 0.58$ rad and boundary conditions of type 1, using an order of discretization 4.

see Table 7.3. As before, the relative error on the current density $\boldsymbol{J}$ remains however non-negligible because the norm of the exact solution is very small.

For the incident S-wave, *cf.* Table 7.4, the relative error for the poroelastic variables is small (less than $10^{-2}\%$). For the pressure, as we are now studying a transverse shear wave, the exact solution is equal to zero, hence the numerical relative error is infinite. For the electromagnetic fields, the magnetic field H and the current density $\boldsymbol{J}$ are well simulated. For the electric field $\boldsymbol{E}$, the relative error remains non-negligible, because the norm of the exact

$e_h(\mathrm{u}_x)$	$e_h(\mathrm{u}_y)$	$e_h(\mathrm{w}_x)$	$e_h(\mathrm{w}_y)$	$e_h(\tau_{xx})$	$e_h(\tau_{yy})$	$e_h(\tau_{xy})$	$e_h(\mathrm{p})$
3.63e-3	3.41e-3	3.03e-2	2.02e-2	3.45e-3	3.69e-3	3.87e-3	inf

$e_h(E_x)$	$e_h(E_y)$	$e_h(\mathrm{H})$	$e_h(J_y)$	$e_h(J_x)$
3.32e4	2.10e4	2.74e-3	2.35e-2	1.48e-2

Table 7.4: Relative errors (%) on the components of the unknowns of the HDG method for an incident S-wave, at frequency $f = 300$Hz with $\theta = 0.58$ rad and boundary conditions of type 1, using an order of discretization 4.

solution is very small (10^{-10}), hence the numerical method cannot attain this precision and the numerical error can not compensate it. For the incident EM-wave, see Table 7.5, the approximation of the electromagnetic variables and

$e_h(\mathrm{u}_x)$	$e_h(\mathrm{u}_y)$	$e_h(\mathrm{w}_x)$	$e_h(\mathrm{w}_y)$	$e_h(\tau_{xx})$	$e_h(\tau_{yy})$	$e_h(\tau_{xy})$	$e_h(\mathrm{p})$
2.42e-3	2.28e-3	2.42e-3	2.28e-3	9.35	13.9	4.11e-2	inf

$e_h(E_x)$	$e_h(E_y)$	$e_h(\mathrm{H})$	$e_h(J_y)$	$e_h(J_x)$
2.42e-3	2.28e-3	2.00e-3	2.42e-3	2.27e-3

Table 7.5: Relative errors (%) on the components of the unknowns of the HDG method for an incident EM-wave, at frequency $f = 300$MHz with $\theta = 0.58$ rad and boundary conditions of type 1, using an order of discretization 4.

the velocities $\mathbf{u}$ and $\mathbf{w}$ is accurate, with a relative error smaller than $10^{-2}\%$. The incident wave is a transverse wave, which means the exact pressure p is equal to zero, hence the numerical relative error is infinite. The error on the solid stress $\boldsymbol{\tau}$ is non-negligible, because the norm of the exact solution is very small.

We are now studying the order $(p+1)$ of convergence of the method, to make sure that we obtain the optimal order of convergence of the HDG method. We present the order of convergence of the method in terms of the size of mesh. For that, we use four meshes with straight edges generated by the software Triangle. The refinement of a given mesh consists in dividing each of its cells into four cells. We denote by h the size of the mesh, which corresponds to the longest edge of the elements in the mesh. We present the convergence curves for the case $\gamma_{1\to5} = 1$ in Figure 7.2,

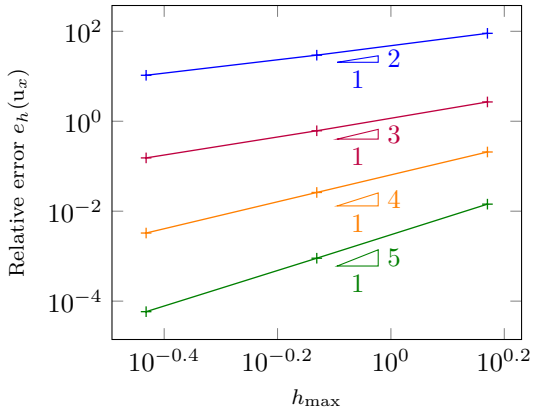

Figure 7.2: Convergence curves of HDG method (component u_x) for several orders of interpolation. Results for order 1 are plotted in blue, for order 2 in purple, for order 3 in orange and for order 4 in green.

where we display the relative error and thus the convergence order for the x-component u_x as a function of the size of the mesh. We observe that the solid velocity has a $p+1$ order of convergence. In Table 7.6, we give the results of the order of convergence for all the fields, depending on the values of the stabilization parameters. These results show that the presence of poroelastic stabilization parameters $\gamma_{1\to4}$ and the electromagnetic stabilization parameter γ_5 is necessary to have the optimal order of convergence.

In the following, we consider that the stabilization parametrs γ_1, γ_2, γ_3, γ_4 and γ_5 are equal. We denote $\gamma_i = \gamma$, for $i = 1, 5$.

Stabilization parameters	$\mathbf{u}$	$\mathbf{w}$	$\boldsymbol{\tau}$	p	$\boldsymbol{E}$	H	$\boldsymbol{J}$
1111 1	$p+1$	$p+1$	$p+1$	$p+1$	$p+1$	$p+1$	$p+1$
1111 0	$p+1$	$p+1$	$p+1$	$p+1$	p	p	$p+1$
0000 1	p	p	p	p	$p+1$	$p+1$	p

Table 7.6: Convergence order of the HDG method depending on the value of the stabilization parameters.

7.4.3 Numerical analysis of the well-posedness

In this section, we study numerically the well-posedness of the problem by analyzing the influence of the value of stabilization parameter γ and the frequency on the condition number of the linear system. We consider the propagation of a P plane wave in the domain $\mathcal{D}$, in three different materials, sand1, freshwater, and sand2. The materials are described in Table 7.1.

Influence of the stabilization parameters

We first consider the question of well-posedness at the local level for the local matrix $\mathbb{A}^K$, and secondly for the global matrix $\mathbb{K}$.

- For the reconstruction of $\underline{W}^K$, we have to invert the elementary matrix $\mathbb{A}^K$, see equation (7.27). Hence we study the condition number of $\mathbb{A}^K$ to evaluate if the calculation of $(\mathbb{A}^K)^{-1}$ can be problematic. If the condition number is too high, the inversion will be less accurate. Since this inversion is performed on every element of the mesh, we consider the maximum value of the condition number, $C_{T_h} = \max_{K\in T_h} \|(A^K)^{-1}\| \|A_K\|$. For three different media and four different interpolation orders, we show the maximal condition number of $\mathbb{A}^K$ for every element of the mesh in infinity norm as a function of the values of the stabilization parameters in Figure 7.3. We observe that for all interpolation orders for the three materials, the condition number increases with the stabilization parameters. For orders 2,3 and 4, the value of the condition number is close to 10^{16} for the stabilization parameter γ greater than 10^4. This value of the condition number can start to be problematic for the inversion of $\mathbb{A}^K$. Moreover, if the stabilization parameter γ is lower than 10^2, the condition number will be smaller than 10^{10}. Hence, we suggest to keep a value of γ smaller than 10^2 to have the smallest condition number possible.

- Next, we focus on the global system $\mathbb{K}\underline{\Lambda} = \mathbb{S}$. We study numerically the question of the well-posedness by computing the condition number of the global matrix $\mathbb{K}$. If it is not too high, it ensures that the matrix can be inverted. As formerly, we consider three different media (see Table 7.1). The condition number of $\mathbb{K}$ is presented in Figure 7.4 as a function of the stabilization parameter γ. We observe that the curves have similar trends for the three materials and every interpolation order. For γ between 10^{-6} and 1, the condition number decreases, while for γ greater than 1, the condition number increases. For the three materials in consideration and the four interpolation orders, the condition number stays below 10^8, which means that the inversion of the global system will be obtained with a good accuracy. However, in order to attain the best precision, we suggest to choose γ between 10^{-2} and 10^2.

Influence of the frequency

We continue the numerical study of the well-posedness by analyzing the influence of the frequency on the condition number of the linear system. Note that, due to their dependency on the frequency, the parameters change with frequency in the experiments. As previously done, we first consider the local system and then the global one. We set $\gamma_{1\to5} = 1$ and $\gamma_{6\to9} = 0$.

- For the three different media described in Table 7.1, we show the maximal condition number of the matrices $\mathbb{A}^K$ on each element as a function of the frequency in Figure 7.5. For the three materials, and for the considered frequencies, the condition number stays stable for the four orders of interpolation, and below 10^{-10}. This means that the elementary matrices $\mathbb{A}^K$ can be inverted.

- Finally, the condition number of the global matrix $\mathbb{K}$ is presented in Figure 7.6 as a function of the frequency. We observe that, overall, the condition number of the elementary matrix decreases with the frequency, and stays below 10^7, which means that the inversion of the global system will be obtained with good accuracy.

As a conclusion, the condition number does not increase with the accuracy (or the number of points per wavelength), and we can obtain both a well conditioned system and an accurate solution.

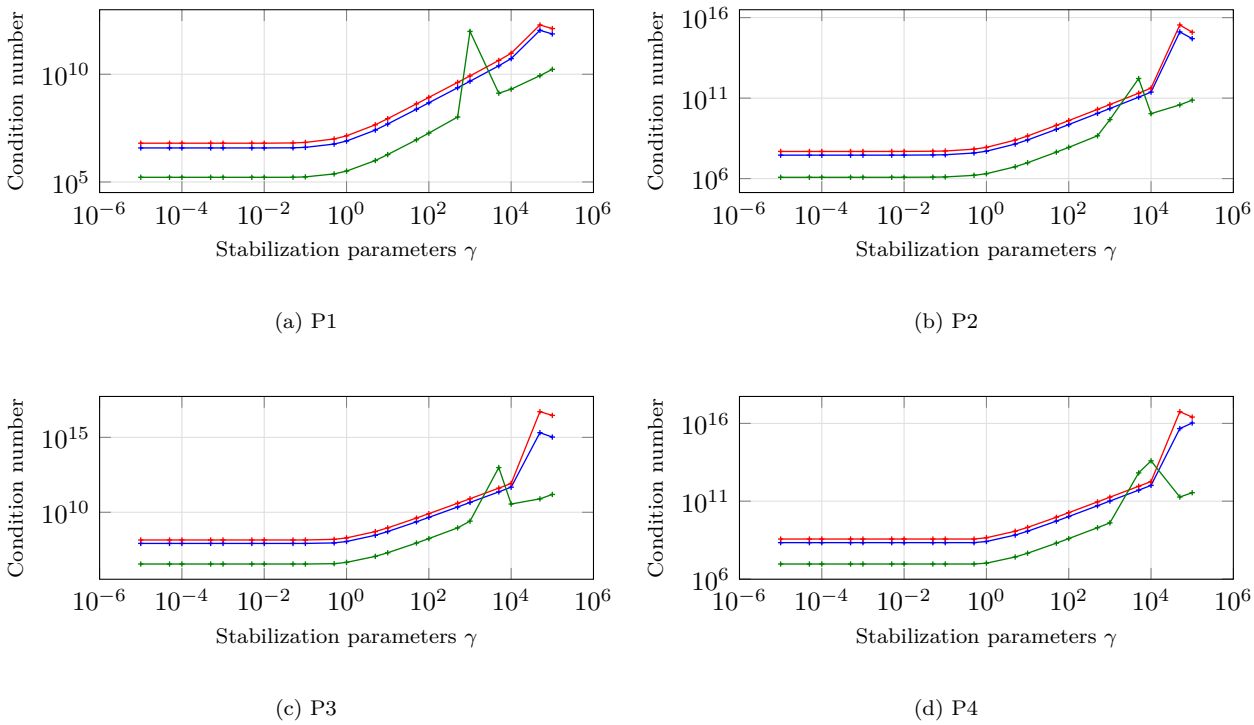

(a) P1

(b) P2

(c) P3

(d) P4

Figure 7.3: Maximal condition number (infinity norm) on all the elementary matrices $\mathbb{A}^K$ as a function of the stabilization parameters, for three materials and three interpolation orders at frequency $f = 1$kHz. The stabilization parameters $\gamma_{1\to5}$ are set at the same value γ, and $\gamma_{6\to9} = 0$. The characteristics of the media are presented in Table 7.1. The results for sand1 are represented in blue —+—, for freshwater in red —+— and for sand2 in green —+—.

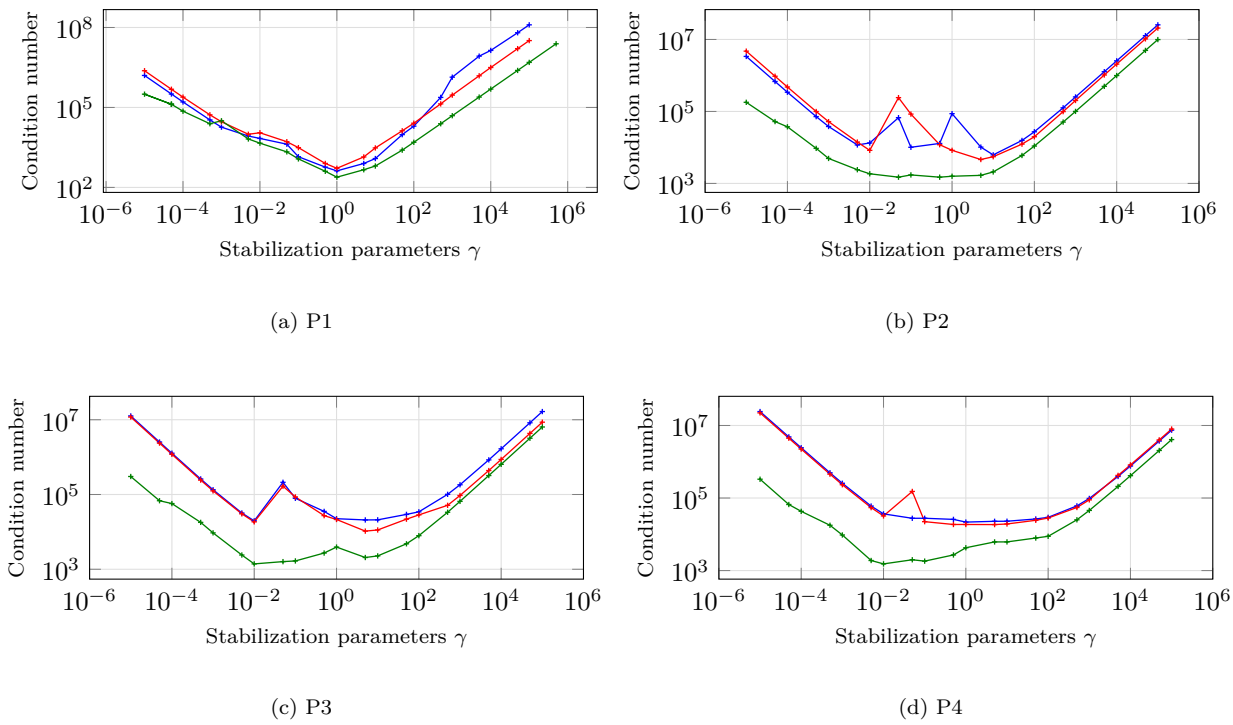

Figure 7.4: Condition number (infinity-norm) of the global matrix $\mathbb{K}$ as a function of the stabilization parameters, for three materials and three interpolation orders at frequency $f = 1$kHz. The stabilization parameters $\gamma_{1\to5}$ are set at the same value γ, and $\gamma_{6\to9} = 0$. The characteristics of the media are presented in Table 7.1. The results for sand1 are represented in blue —+—, for freshwater in red —+— and for sand2 in green —+—.

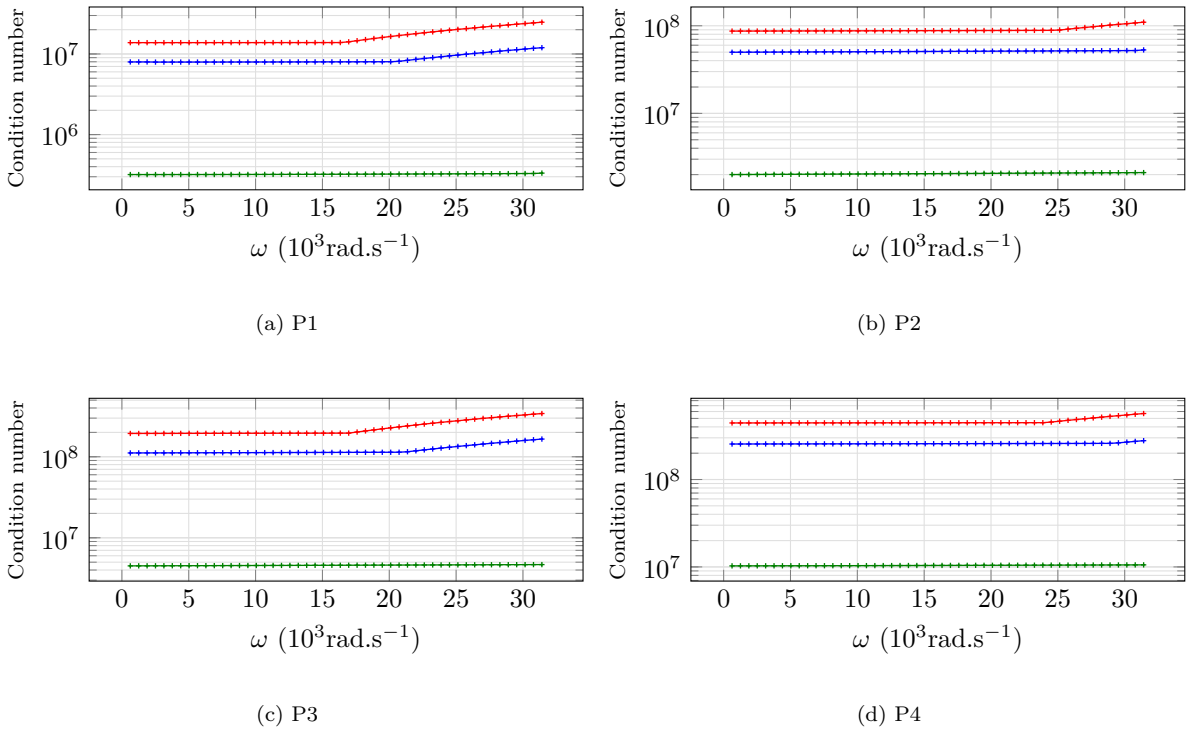

(a) P1 (b) P2

(c) P3 (d) P4

Figure 7.5: Maximal condition number (infinity norm) of the matrix $\mathbb{A}^K$ as a function of the frequency, for three materials and four interpolation orders. The characteristics of the media are presented in Table 7.1. The stabilization parameters are $\gamma_{1\to5} = 1$ and $\gamma_{6\to9} = 0$. The results for sand1 are represented in blue —+—, for freshwater in red —+— and for sand2 in green —+—.

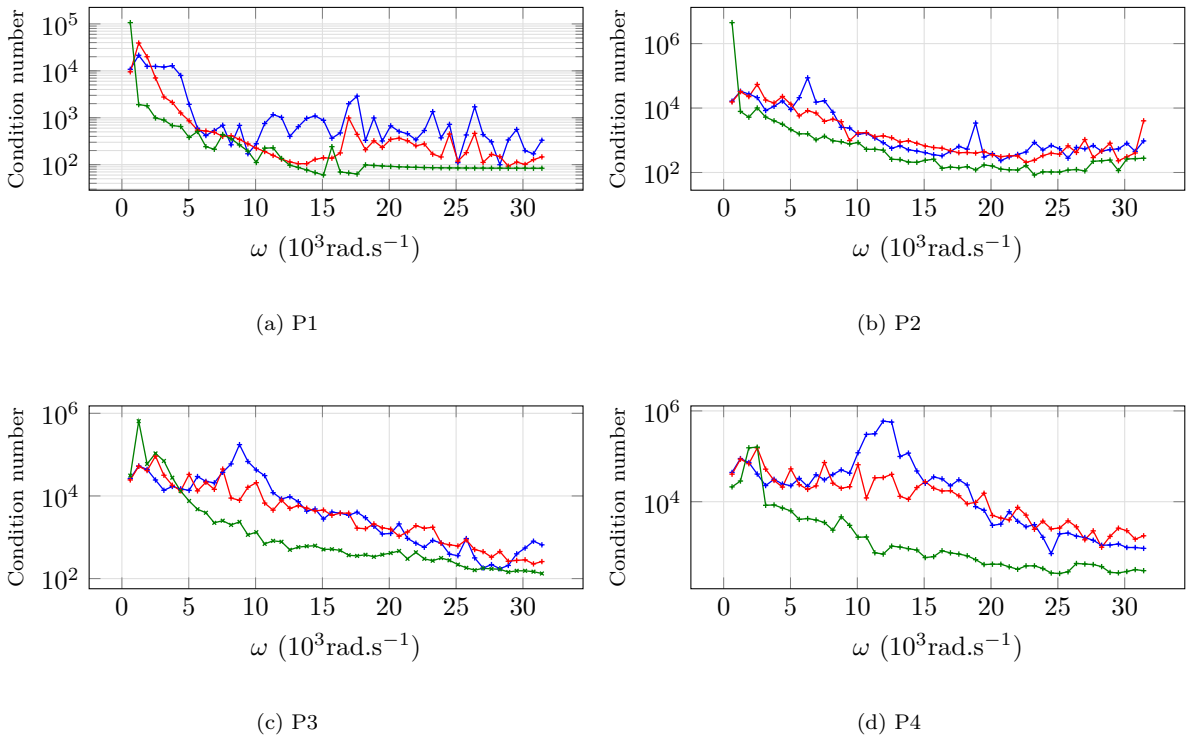

(a) P1 (b) P2

(c) P3 (d) P4

Figure 7.6: Condition number (infinity-norm) of the global matrix $\mathbb{K}$ as a function of the frequency, for three materials and three interpolation orders. The characteristics of the media are presented in Table 7.1. The stabilization parameters are $\gamma_{1\to5} = 1$ and $\gamma_{6\to9} = 0$. The results for sand1 are represented in blue —+—, for freshwater in red —+— and for sand2 in green —+—.

7.5 Discretization of the HDG formulation in three-dimensions

We consider the stabilization matrices defined in (7.4), to be diagonal, i.e. $\boldsymbol{S}_i = \gamma_i \mathbb{I}$ for $i = 1, 5$. As for Maxwell's equations, we also consider that we only penalize the tangential component of the magnetic field $\boldsymbol{H}_h$, see Appendix G.4. In addition, we have seen in Section 7.4, that the coupling stabilization parameters $\gamma_{6\to 9}$ should be taken as zero. In this way, the expression (7.4) simplifies to

$$\begin{cases} \hat{\boldsymbol{\tau}}_h \boldsymbol{n} & = \boldsymbol{\tau}_h \boldsymbol{n} - \gamma_1(\mathbf{u}_h - \boldsymbol{\lambda}_1) - (\mathrm{p}_h - \lambda_2)\gamma_3 \boldsymbol{n}\,, \\ \hat{\mathbf{w}}_h \cdot \boldsymbol{n} & = \mathbf{w}_h \cdot \boldsymbol{n} - \gamma_2(\mathrm{p}_h - \lambda_2) - \gamma_4(\mathbf{u}_h - \boldsymbol{\lambda}_1)\cdot \boldsymbol{n}\,, \\ \boldsymbol{n} \times \hat{\boldsymbol{E}}_h & = \boldsymbol{n} \times \boldsymbol{E}_h - \gamma_5 \left(\boldsymbol{H}_h^t - \boldsymbol{\lambda}_3\right)\,. \end{cases}$$

The coupling tensor matrix $\mathbf{L}$ has the form $\mathbf{L} = \mathrm{L}\,\mathbb{I}$. In the formulation, the test functions are decomposed in the basis functions of V_p as φ_i^K for $\tilde{\boldsymbol{u}}$, $\tilde{\boldsymbol{w}}$, $\tilde{\boldsymbol{\tau}}$, $\tilde{\mathrm{p}}$, $\tilde{\boldsymbol{e}}$, $\tilde{h}$, $\tilde{\boldsymbol{j}}$ and as ψ_i^F for $\boldsymbol{\eta}$, ξ and $\boldsymbol{\nu}$. We define two unknown vectors $\underline{W}^K$ and $\underline{\Lambda}^K$ respectively of size $22\,d_i^K$ and $26\,d_i^F$ as:

$$\underline{W}^K = (\underline{\mathrm{u}}_x^K, \underline{\mathrm{u}}_y^K, \underline{\mathrm{u}}_z^K, \underline{\mathrm{w}}_x^K, \underline{\mathrm{w}}_y^K, \underline{\mathrm{w}}_z^K, \underline{\tau}_{xx}^K, \underline{\tau}_{yy}^K, \underline{\tau}_{zz}^K, \underline{\tau}_{yz}^K, \underline{\tau}_{xz}^K, \underline{\tau}_{xy}^K, \underline{\mathrm{p}}^K, \underline{E}_x^K, \underline{E}_y^K, \underline{E}_z^K, \underline{H}_x^K, \underline{H}_y^K, \underline{H}_z^K, \underline{J}_x^K, \underline{J}_y^K, \underline{J}_z^K)^T\,, \tag{7.30a}$$

and

$$\begin{aligned} \underline{\Lambda}^K = & (\underline{\lambda}_{1x}^{\beta(K,1)}, \underline{\lambda}_{1x}^{\beta(K,2)}, \underline{\lambda}_{1x}^{\beta(K,3)}, \underline{\lambda}_{1x}^{\beta(K,4)}, \underline{\lambda}_{1y}^{\beta(K,1)} \underline{\lambda}_{1y}^{\beta(K,2)}, \underline{\lambda}_{1y}^{\beta(K,3)}, \underline{\lambda}_{1y}^{\beta(K,4)}, \underline{\lambda}_{1z}^{\beta(K,1)} \underline{\lambda}_{1z}^{\beta(K,2)}, \underline{\lambda}_{1z}^{\beta(K,3)}, \underline{\lambda}_{1z}^{\beta(K,4)}, \\ & \underline{\lambda}_{2}^{\beta(K,1)}, \underline{\lambda}_{2}^{\beta(K,2)}, \underline{\lambda}_{2}^{\beta(K,3)}, \underline{\lambda}_{2}^{\beta(K,4)}, \underline{\lambda}_{3x}^{\beta(K,1)}, \underline{\lambda}_{3x}^{\beta(K,2)}, \underline{\lambda}_{3x}^{\beta(K,3)}, \underline{\lambda}_{3x}^{\beta(K,4)}, \\ & \underline{\lambda}_{3y}^{\beta(K,1)}, \underline{\lambda}_{3y}^{\beta(K,2)}, \underline{\lambda}_{3y}^{\beta(K,3)}, \underline{\lambda}_{3y}^{\beta(K,4)}, \underline{\lambda}_{3z}^{\beta(K,1)}, \underline{\lambda}_{3z}^{\beta(K,2)}, \underline{\lambda}_{3z}^{\beta(K,3)}, \underline{\lambda}_{3z}^{\beta(K,4)})^T\,, \end{aligned} \tag{7.30b}$$

where $\beta(K, f)$ is the global index of the f-th face of the element K. We also define the following elementary matrices $\mathbb{M}^K$, $\mathbb{D}^K$, $\mathbb{E}^K$, $\mathbb{J}^K$ of size $d_i^K \times d_i^K$, $\mathbb{F}^K$, $\mathbb{Q}^K$ of size $d_i^K \times d_i^F$, and $\mathbb{F}^K$, $\mathbb{Q}^K$ of size $d_i^F \times d_i^F$:

$$\begin{aligned} &\mathbb{M}_{ij}^K = \int_K \varphi_i^K \varphi_j^K\, dX\,, \qquad \mathbb{D}_{vij}^K = \int_K \varphi_j^K \frac{\partial \varphi_i^K}{\partial v} dX\,, \quad \mathbb{E}_{ij}^F = \int_F \varphi_i^K \varphi_j^K\, dS\,, \qquad \mathbb{J}_{vij}^F = \int_F \varphi_i^K \varphi_j^K n_v\, dS\,, \\ &\mathbb{F}_{ij}^F = \int_F \psi_j^F \varphi_i^K dS\,, \qquad \mathbb{Q}_{vij}^F = \int_F \psi_j^F \varphi_i^K n_v\, dS\,, \quad \mathbb{G}_{ij}^F = \int_F \psi_j^F \psi_j^F\, dS\,, \qquad \mathbb{H}_{vij}^F = \int_F \psi_i^F \psi_j^F n_v\, dS\,, \end{aligned} \tag{7.31}$$

with $v = x, y, z$. Finally, we define the elementary source matrices of size d_i^K

$$\begin{aligned} \left(\mathbb{C}_{1x}^K\right)_i &= \int_K f_{ux}^K\, \varphi_i^K\,, \quad \left(\mathbb{C}_{1y}^K\right)_i = \int_K f_{uy}^K\, \varphi_i^K\,, \quad \left(\mathbb{C}_{1z}^K\right)_i = \int_K f_{uz}^K\, \varphi_i^K\,, \\ \left(\mathbb{C}_{2x}^K\right)_i &= \int_K f_{wx}^K\, \varphi_i^K\,, \quad \left(\mathbb{C}_{2y}^K\right)_i = \int_K f_{wy}^K\, \varphi_i^K\,, \quad \left(\mathbb{C}_{2z}^K\right)_i = \int_K f_{wz}^K\, \varphi_i^K\,, \\ \left(\mathbb{C}_{3x}^K\right)_i &= \int_K f_{Cx}^K\, \varphi_i^K\,, \quad \left(\mathbb{C}_{3y}^K\right)_i = \int_K f_{Cy}^K\, \varphi_i^K\,, \quad \left(\mathbb{C}_{3z}^K\right)_i = \int_K f_{Cz}^K\, \varphi_i^K\,. \end{aligned}$$

7.5.1 Local problem

(a) Discretization of equation (7.6a)

Discretizing equation (7.6a) along the $x-$ $y-$ and $z-$ component gives, for $\bullet = x, y, z$:

$$\int_K \mathrm{i}\,\omega\,\rho_a\,\mathrm{u}_\bullet\,\varphi_i^K + \int_K \mathrm{i}\,\omega\,\rho_f\,\mathrm{w}_\bullet\,\varphi_i^K - \int_K \frac{\partial \tau_{x\bullet}}{\partial x}\,\varphi_i^K - \int_K \frac{\partial \tau_{y\bullet}}{\partial y}\,\varphi_i^K - \int_K \frac{\partial \tau_{z\bullet}}{\partial z}\,\varphi_i^K + \int_{\partial K} \gamma_1\,\mathrm{u}_\bullet \varphi_i^K - \int_{\partial K} \gamma_1\,\lambda_{1\bullet}\,\varphi_i^K$$

$$+ \int_{\partial K} \gamma_3\,\mathrm{p}_h^K\,n_\bullet\,\varphi_i^K - \int_{\partial K} \gamma_3\,\lambda_2\,n_\bullet\,\varphi_i^K = \int_K f_{u\bullet}\,\varphi_i^K\,.$$

This gives in terms of the local matrices and the unknown vectors defined respectively in equations (7.31) and (7.30a), for $\bullet = x, y, z$:

$$\mathrm{i}\,\omega\,\rho_a\,\mathbb{M}^K \underline{\mathrm{u}}_\bullet^K + \mathrm{i}\,\omega\,\rho_f\,\mathbb{M}^K \underline{\mathrm{w}}_\bullet^K - (\mathbb{D}_x^K)^T\,\underline{\tau}_{x\bullet}^K - (\mathbb{D}_y^K)^T\,\underline{\tau}_{y\bullet}^K - (\mathbb{D}_z^K)^T\,\underline{\tau}_{z\bullet}^K + \sum_{f=1}^4 \gamma_1\,\mathbb{E}^{\beta(K,f)}\,\underline{\mathrm{u}}_\bullet^K - \sum_{f=1}^4 \gamma_1\,\mathbb{F}^{\beta(K,f)}\,\underline{\lambda}_{1\bullet}^{\beta(K,f)}$$

$$+ \sum_{f=1}^4 \gamma_3\,\mathbb{J}_\bullet^{\beta(K,f)}\,\underline{\mathrm{p}}^K - \sum_{f=1}^4 \gamma_3\,\mathbb{Q}_\bullet^{\beta(K,f)}\,\underline{\lambda}_2^{\beta(K,f)} = \mathbb{C}_{1\bullet}^K\,.$$

(b) Discretization of equation (7.6b)

The discretization of (7.6b) along x, y, and z direction is, for $\bullet = x, y, z$:

$$\int_K \mathrm{i}\,\omega\,\rho_f\,\mathrm{u}_\bullet^K\,\varphi_i^K \;+\; \int_K \mathrm{i}\,\omega\,\rho_{\mathrm{dyn}}\,\mathrm{w}_\bullet^K\,\varphi_i^K \;-\; \int_K \mathrm{p}_h^K\,\frac{\partial\varphi_i^K}{\partial\bullet} \;+\; \int_{\partial K} \lambda_2\,n_\bullet\,\varphi_i^K \;-\; \int_K \mathrm{i}\,\omega\,\rho_{\mathrm{dyn}}\,\mathrm{L}\,E_\bullet^K\,\varphi_i^K \;=\; \int_K f_{w\bullet}\,\varphi_i^K\,.$$

In terms of the local matrices defined in equation (7.31) and the unknown vectors in (7.30a), the above equations read as, for $\bullet = x, y, z$:

$$\mathrm{i}\,\omega\,\rho_f\,\mathbb{M}^K\underline{\mathrm{u}}_\bullet^K \;+\; \mathrm{i}\,\omega\,\rho_{\mathrm{dyn}}\,\mathbb{M}^K\underline{\mathrm{w}}_\bullet^K \;-\; \mathbb{D}_x^K\,\underline{\mathrm{p}}^K \;-\; \sum_{f=1}^{3}\mathbb{Q}_\bullet^{\beta(K,f)}\,\underline{\lambda}_2^{\beta(K,f)} \;-\; \mathrm{i}\,\omega\,\rho_{\mathrm{dyn}}\,\mathrm{L}\,\mathbb{M}^K\underline{E}_\bullet^K \;=\; \mathbb{C}_{2\bullet}^K\,.$$

(c) Discretization of equation (7.6c)

The constitutive law expressed in (7.6c) is discretized in six equations corresponding to the six values of the test function $\tilde{\boldsymbol{\tau}}$. Using the Voigt notation for $\boldsymbol{\tau}$, $\boldsymbol{\alpha}$ and $\mathbf{C}$, with $\bullet = 1, 6$, we have:

$$\begin{aligned}
&\int_K \mathrm{i}\,\omega\,\tau_\bullet\,\varphi_i^K \;+\; \int_K \mathrm{i}\,\omega\,\alpha_\bullet \mathrm{p}_h^K\,\varphi_i^K \;+\; \int_K \left(C_{\bullet 1}\,\frac{\partial\varphi_i^K}{\partial x} \;+\; C_{\bullet 6}\,\frac{\partial\varphi_i^K}{\partial y} + \int_K C_{\bullet 5}\,\frac{\partial\varphi_i^K}{\partial z}\right)\mathrm{u}_x^K \\
&+\; \int_K \left(C_{\bullet 6}\,\frac{\partial\varphi_i^K}{\partial x} \;+\; C_{\bullet 2}\,\frac{\partial\varphi_i^K}{\partial y} + C_{\bullet 4}\,\frac{\partial\varphi_i^K}{\partial z}\right)\mathrm{u}_y^K \;+\; \int_K \left(C_{\bullet 5}\,\frac{\partial\varphi_i^K}{\partial x} + C_{\bullet 4}\,\frac{\partial\varphi_i^K}{\partial y} + C_{\bullet 3}\,\frac{\partial\varphi_i^K}{\partial z}\right)\mathrm{u}_z^K \\
&-\; \int_{\partial K} \left(C_{\bullet 1}\,\varphi_i^K\,n_x \;+\; C_{\bullet 6}\,\varphi_i^K\,n_y \;+\; C_{\bullet 5}\,\varphi_i^K\,n_z\right)\lambda_{1x} - \int_{\partial K} \left(C_{\bullet 6}\,\varphi_i^K\,n_x \;+\; C_{\bullet 2}\,\varphi_i^K\,n_y \;+\; C_{\bullet 4}\,\varphi_i^K\,n_z\right)\lambda_{1y} \\
&-\; \int_{\partial K} (C_{\bullet 5}\,\varphi_i^K\,n_x \;+\; C_{\bullet 4}\,\varphi_i^K\,n_y \;+\; C_{\bullet 3}\,\varphi_i^K\,n_z)\,\lambda_{1z} \;=0\,.
\end{aligned}$$

Then, the equations are expressed in terms of local matrices and the unknown vectors defined in (7.30a) and (7.31):

$$\begin{aligned}
&\mathrm{i}\,\omega\,\mathbb{M}^K\,\underline{\tau}_\bullet^K \;+\; \mathrm{i}\omega\alpha_\bullet^K\,\mathbb{M}^K\underline{\mathrm{p}}^K \;+\; \left(C_{\bullet 1}^K\,\mathbb{D}_x^K \;+\; C_{\bullet 6}^K\mathbb{D}_y^K \;+\; C_{\bullet 5}^K\mathbb{D}_y^K\right)\underline{\mathrm{u}}_x^K \;+\; \left(C_{\bullet 6}^K\mathbb{D}_x^K \;+\; C_{\bullet 2}^K\mathbb{D}_y^K \;+\; C_{\bullet 4}^K\mathbb{D}_z^K\right)\underline{\mathrm{u}}_y^K \\
&+\; \left(C_{\bullet 5}^K\mathbb{D}_x^K \;+\; C_{\bullet 4}^K\mathbb{D}_y^K \;+\; C_{\bullet 3}^K\mathbb{D}_z^K\right)\underline{\mathrm{u}}_z^K \;-\; \sum_{f=1}^{4}\left(C_{\bullet 1}^K\mathbb{Q}_x^{\beta(K,f)} + C_{\bullet 6}^K\mathbb{Q}_y^{\beta(K,f)} \;+\; C_{\bullet 5}^K\mathbb{Q}_z^{\beta(K,f)}\right)\underline{\lambda}_{1x}^{\beta(K,f)} \\
&-\; \sum_{f=1}^{4}\left(C_{\bullet 6}^K\mathbb{Q}_x^{\beta(K,f)} + C_{\bullet 2}^K\mathbb{Q}_y^{\beta(K,f)} \;+\; C_{\bullet 4}^K\mathbb{Q}_z^{\beta(K,f)}\right)\underline{\lambda}_{1y}^{\beta(K,f)} \\
&-\; \sum_{f=1}^{4}\left(C_{\bullet 5}^K\mathbb{Q}_x^{\beta(K,f)} + C_{\bullet 4}^K\mathbb{Q}_y^{\beta(K,f)} \;+\; C_{\bullet 3}^K\mathbb{Q}_z^{\beta(K,f)}\right)\underline{\lambda}_{1z}^{\beta(K,f)} \;=\; 0\,.
\end{aligned}$$

(d) Discretization of equation (7.6d)

The discretization of equation (7.6d) gives:

$$\begin{aligned}
&\int_K i\omega\mathrm{p}_h^K\varphi_i^K + \int_K M\frac{\partial\mathrm{w}_x^K}{\partial x}\varphi_i^K + \int_K M\frac{\partial\mathrm{w}_y^K}{\partial y}\varphi_i^K + \int_K M\frac{\partial\mathrm{w}_z^K}{\partial z}\varphi_i^K - \int_{\partial K} M\mathrm{p}_h^K\gamma_2\,\varphi_i^K \;+\; \int_{\partial K} M\lambda_2\gamma_2\,\varphi_i^K \\
&-\; \int_{\partial K} M\gamma_4\mathrm{u}_x^K\,n_x\varphi_i^K - \int_{\partial K} M\gamma_4\mathrm{u}_y^K\,n_y\varphi_i^K - \int_{\partial K} M\gamma_4\mathrm{u}_z^K\,n_z\varphi_i^K + \int_{\partial K} M\gamma_4\lambda_{1x}\,n_x\varphi_i^K + \int_{\partial K} M\gamma_4\lambda_{1y}\,n_y\varphi_i^K \\
&+\; \int_{\partial K} M\gamma_4\lambda_{1z}\,n_z\varphi_i^K - \int_K M(\alpha_{11}\mathrm{u}_x^K + \alpha_{12}\mathrm{u}_y^K + \alpha_{13}\mathrm{u}_z^K)\frac{\partial\varphi_i^K}{\partial x} - \int_K M(\alpha_{12}\mathrm{u}_x^K + \alpha_{22}\mathrm{u}_y^K + \alpha_{23}\mathrm{u}_z^K)\frac{\partial\varphi_i^K}{\partial y} \\
&-\; \int_K M(\alpha_{13}\mathrm{u}_x^K + \alpha_{23}\mathrm{u}_y^K + \alpha_{33}\mathrm{u}_z^K)\frac{\partial\varphi_i^K}{\partial z} + \int_K M(\alpha_{11}\lambda_{1x} + \alpha_{12}\lambda_{1y} + \alpha_{13}\lambda_{1z})n_x\varphi_i^K \\
&+\; \int_K M(\alpha_{12}\lambda_{1x} + \alpha_{22}\lambda_{1y} + \alpha_{23}\lambda_{1z})n_y\varphi_i^K + \int_K M(\alpha_{13}\lambda_{1x} + \alpha_{23}\lambda_{1y} + \alpha_{33}\lambda_{1z})n_z\varphi_i^K \;=\; 0\,.
\end{aligned}$$

In terms of the local matrices defined in equation (7.31) and the unknown vectors in (7.30a), the above equations are written as

$$\mathrm{i}\,\omega\,\mathbb{M}^K\,\underline{\mathrm{p}}^K + M^K(\mathbb{D}_x^K)^T\,\underline{\mathrm{w}}_x^K + M^K(\mathbb{D}_y^K)^T\,\underline{\mathrm{w}}_y^K + M^K(\mathbb{D}_z^K)^T\,\underline{\mathrm{w}}_z^K - \sum_{f=1}^{4} M^K\gamma_2\,\mathbb{E}^{\beta(K,f)}\underline{\mathrm{p}}^K + \sum_{f=1}^{4} M^K\gamma_2\,\underline{\lambda}_2^{\beta(K,f)}\mathbb{F}^{\beta(K,f)}$$

$$-\sum_{f=1}^{4} M^K\gamma_4\left(\mathbb{J}_x^{\beta(K,f)}\underline{\mathrm{u}}_x^K + \mathbb{J}_y^{\beta(K,f)}\underline{\mathrm{u}}_y^K + \mathbb{J}_z^{\beta(K,f)}\underline{\mathrm{u}}_z^K\right) + \sum_{f=1}^{4} M^K\gamma_4\left(\mathbb{Q}_x^{\beta(K,f)}\underline{\lambda}_{1x}^{\beta(K,f)} + \mathbb{Q}_y^{\beta(K,f)}\underline{\lambda}_{1y}^{\beta(K,f)} + \mathbb{Q}_z^{\beta(K,f)}\underline{\lambda}_{1z}^{\beta(K,f)}\right)$$

$$- M^K\,\mathbb{D}_x^K\left(\alpha_{11}^K\,\underline{\mathrm{u}}_x^K + \alpha_{12}^K\,\underline{\mathrm{u}}_y^K + \alpha_{13}^K\,\underline{\mathrm{u}}_z^K\right) + \sum_{f=1}^{4} M^K\left(\alpha_{11}\underline{\lambda}_{1x}^{\beta(K,f)} + \alpha_{12}^K\underline{\lambda}_{1y}^{\beta(K,f)} + \alpha_{13}^K\underline{\lambda}_{1z}^{\beta(K,f)}\right)\mathbb{Q}_x^{\beta(K,f)}$$

$$- M^K\,\mathbb{D}_y^K\left(\alpha_{12}^K\,\underline{\mathrm{u}}_x^K + \alpha_{22}^K\,\underline{\mathrm{u}}_y^K + \alpha_{23}^K\,\underline{\mathrm{u}}_z^K\right) + \sum_{f=1}^{4} M^K\left(\alpha_{12}^K\underline{\lambda}_{1x}^{\beta(K,f)} + \alpha_{22}^K\,\underline{\lambda}_{1y}^{\beta(K,f)} + \alpha_{23}^K\,\underline{\lambda}_{1z}^{\beta(K,f)}\right)\mathbb{Q}_y^{\beta(K,f)}$$

$$- M^K\,\mathbb{D}_y^K\left(\alpha_{13}^K\,\underline{\mathrm{u}}_x^K + \alpha_{23}^K\,\underline{\mathrm{u}}_y^K + \alpha_{33}^K\,\underline{\mathrm{u}}_z^K\right) + \sum_{f=1}^{4} M^K\left(\alpha_{13}^K\underline{\lambda}_{1x}^{\beta(K,f)} + \alpha_{23}^K\,\underline{\lambda}_{1y}^{\beta(K,f)} + \alpha_{33}^K\,\underline{\lambda}_{1z}^{\beta(K,f)}\right)\mathbb{Q}_z^{\beta(K,f)} = 0\,.$$

(e) Discretization of equation (7.6e)

Equation (7.6e) is discretized along $x-$ component to give:

$$\int_K \mathrm{i}\,\omega\,\delta_0\,E_x^K\,\varphi_i^K + \int_K H_y^K\,\frac{\partial\varphi_i^K}{\partial z} - \int_K H_z^K\,\frac{\partial\varphi_i^K}{\partial y} - \int_{\partial K}\lambda_{3y}n_z\,\varphi_i^K + \int_{\partial K}\lambda_{3z}n_y\,\varphi_i^K + \int_K J_x^K\,\varphi_i^K = \int_K \mathbf{f}_{Cx}\,\tilde{\boldsymbol{e}}_x\,,$$

along $y-$ component:

$$\int_K \mathrm{i}\,\omega\,\delta_0\,E_y^K\,\varphi_i^K - \int_K H_x^K\,\frac{\partial\varphi_i^K}{\partial z} + \int_K H_z^K\,\frac{\partial\varphi_i^K}{\partial x} + \int_{\partial K}\lambda_{3x}n_z\,\varphi_i^K - \int_{\partial K}\lambda_{3z}n_x\,\varphi_i^K + \int_K J_y^K\,\varphi_i^K = \int_K \mathbf{f}_{Cy}\,\tilde{\boldsymbol{e}}_y\,,$$

and along $z-$ component:

$$\int_K \mathrm{i}\,\omega\,\delta_0\,E_z^K\,\varphi_i^K + \int_K H_x^K\,\frac{\partial\varphi_i^K}{\partial y} - \int_K H_y^K\,\frac{\partial\varphi_i^K}{\partial x} - \int_{\partial K}\lambda_{3x}n_y\,\varphi_i^K + \int_{\partial K}\lambda_{3y}n_x\,\varphi_i^K + \int_K J_z^K\,\varphi_i^K = \int_K \mathbf{f}_{Cz}\,\tilde{\boldsymbol{e}}_z\,.$$

This is expressed in terms of local matrices (equation (7.31)) and the unknown vectors ((7.30a)):

$$\mathbb{M}^K\,\mathrm{i}\,\omega\,\delta_0\,\underline{E}_x^K + \mathbb{D}_z^K\,\underline{H}_y^K - \mathbb{D}_y^K\,\underline{H}_z^K - \sum_{f=1}^{4}\mathbb{Q}_{zl}^K\,\underline{\lambda}_{3y}^{\beta(K,f)} + \sum_{f=1}^{4}\mathbb{Q}_{yl}^K\,\underline{\lambda}_{3z}^{\beta(K,f)} + \mathbb{M}^K\,\underline{J}_x^K = \mathbb{C}_5^K\,,$$

$$\mathbb{M}^K\,\mathrm{i}\,\omega\,\delta_0\,\underline{E}_y^K - \mathbb{D}_z^K\,\underline{H}_x^K + \mathbb{D}_x^K\,\underline{H}_z^K + \sum_{f=1}^{4}\mathbb{Q}_{zl}^K\,\underline{\lambda}_{3x}^{\beta(K,f)} - \sum_{f=1}^{4}\mathbb{Q}_{xl}^K\,\underline{\lambda}_{3z}^{\beta(K,f)} + \mathbb{M}^K\,\underline{J}_y^K = \mathbb{C}_6^K\,,$$

and

$$\mathbb{M}^K\,\mathrm{i}\,\omega\,\delta_0\,\underline{E}_z^K + \mathbb{D}_y^K\,\underline{H}_x^K - \mathbb{D}_x^K\,\underline{H}_y^K - \sum_{f=1}^{4}\mathbb{Q}_{yl}^K\,\underline{\lambda}_{3x}^{\beta(K,f)} + \sum_{f=1}^{4}\mathbb{Q}_{xl}^K\,\underline{\lambda}_{3y}^{\beta(K,f)} + \mathbb{M}^K\,\underline{J}_y^K = \mathbb{C}_{6z}^K\,.$$

(f) Discretization of equation (7.6f)

The discretization of equation (7.6f) is:

$$\int_K \mathrm{i}\,\omega\,\mu_0\,H_x^K\,\varphi_i^K + \int_K\left(\frac{\partial E_z^K}{\partial y} - \frac{\partial E_y^K}{\partial z}\right)\varphi_i^K - \int_{\partial K}\gamma_5\,\left(H_x^t - \lambda_{3x}\right)\,\varphi_i^K = 0\,,$$

$$\int_K \mathrm{i}\,\omega\,\mu_0\,H_y^K\,\varphi_i^K + \int_K\left(\frac{\partial E_x^K}{\partial z} - \frac{\partial E_z^K}{\partial x}\right)\varphi_i^K - \int_{\partial K}\gamma_5\,\left(H_y^t - \lambda_{3y}\right)\,\varphi_i^K = 0\,,$$

$$\int_K \mathrm{i}\,\omega\,\mu_0\,H_z^K\,\varphi_i^K + \int_K\left(\frac{\partial E_y^K}{\partial x} - \frac{\partial E_x^K}{\partial y}\right)\varphi_i^K - \int_{\partial K}\gamma_5\,\left(H_z^t - \lambda_{3z}\right)\,\varphi_i^K = 0\,.$$

This is expressed with the local matrices and local unknowns that have been defined in equations (7.31) and (7.30a).

$$\mathbb{M}^K \,\mathrm{i}\,\omega\,\mu_0\,\underline{H}_x^K + (\mathbb{D}_y^K)^T\,\underline{E}_z^K - (\mathbb{D}_z^K)^T\,\underline{E}_y^K - \sum_{f=1}^{4}\mathbb{E}^{\beta(K,f)}\,\gamma_5\,\underline{H}_x^t + \sum_{f=1}^{4}\mathbb{F}^{\beta(K,f)}\,\gamma_5\,\underline{\lambda}_{3x}^{\beta(K,f)} = 0\,,$$

$$\mathbb{M}^K \,\mathrm{i}\,\omega\,\mu_0\,\underline{H}_y^K + (\mathbb{D}_z^K)^T\,\underline{E}_x^K - (\mathbb{D}_x^K)^T\,\underline{E}_z^K - \sum_{f=1}^{4}\mathbb{E}^{\beta(K,f)}\,\underline{H}_y^t + \sum_{f=1}^{4}\mathbb{F}^{\beta(K,f)}\,\gamma_5\,\underline{\lambda}_{3y}^{\beta(K,f)} = 0\,,$$

$$\mathbb{M}^K \,\mathrm{i}\,\omega\,\mu_0\,\underline{H}_z^K + (\mathbb{D}_x^K)^T\,\underline{E}_y^K - (\mathbb{D}_y^K)^T\,\underline{E}_x^K - \sum_{f=1}^{4}\mathbb{E}^{\beta(K,f)}\,\underline{H}_z^t + \sum_{f=1}^{4}\mathbb{F}^{\beta(K,f)}\,\gamma_5\,\underline{\lambda}_{3z}^{\beta(K,f)} = 0\,.$$

(g) Discretization of equation (7.6g)

We discretize the last equation of the local problem (7.6g) on x, y and z direction. We have for $\bullet = x, y, z$:

$$\int_K J_\bullet^K\,\varphi_i^K - \int_K \sigma\,E_\bullet^K\,\varphi_i^K - \int_K \mathrm{p}_h^K\,\mathrm{L}\,\frac{\partial\varphi_i^K}{\partial\bullet} + \int_{\partial K}\mathrm{L}\,n_\bullet\,\lambda_2\,\varphi_i^K + \int_K \mathrm{i}\,\omega\,\rho_f\,\mathrm{L}\,\mathrm{u}_\bullet^K\,\varphi_i^K = \mathrm{L}\int_K f_{w\bullet}\,\varphi_i^K\,,$$

which is written in terms of local matrices and unknowns from equations (7.31) and (7.30a) as

$$\mathbb{M}^K\underline{J}_\bullet^K - \mathbb{M}^K\sigma\,\underline{E}_\bullet^K - \mathbb{D}_\bullet^K\mathrm{L}\,\underline{\mathrm{p}}^K + \sum_{f=1}^{3}\mathbb{Q}_\bullet^{\beta(K,f)}\,\mathrm{L}\,\underline{\lambda}_2 + \mathbb{M}^K\,\mathrm{i}\,\omega\,\rho_f\,\mathrm{L}\,\underline{\mathrm{u}}_\bullet^K = \mathrm{L}\,\mathbb{C}_{2\bullet}^K\,.$$

Local system The discretization of the local problem (7.6) detailed above can be written as a system of the form:

$$\mathbb{A}^K\underline{W}^K + \mathbb{B}^K\underline{\Lambda}^K = \mathbb{C}_{\text{source}}^K\,,$$

where $\underline{W}^K$ and $\underline{\Lambda}^K$ have been defined in (7.30a). The matrix $\mathbb{A}^K$ is of dimension $22\,d_i^K \times 22d_i^K$, $\mathbb{B}^K$ of size $22\,d_i^K \times 26d_i^F$, and $\mathbb{C}_{\text{source}}^K$ is the matrix of the external forces of dimension $22\,d_i^K$. The elementary matrix $\mathbb{A}^K$ is written as:

$$\mathbb{A}^K = \begin{pmatrix} \mathbb{A}_{\mathbf{poro}}^K & \mathbb{A}^K_{\substack{\text{coupling}\\ \text{EM}\to\text{poro}}} \\ \mathbb{A}^K_{\substack{\text{coupling}\\ \text{poro}\to\text{EM}}} & \mathbb{A}_{\mathbf{EM}}^K \end{pmatrix}.$$

The expression of $\mathbb{A}_{\mathbf{poro}}^K$ (of dimension $13\,d_i^K \times 13d_i^K$) corresponds to the matrix obtained for poroelasticity with no electrokinetic coupling, given in Appendix B.1.2. Similarly, the matrix $\mathbb{A}_{\mathbf{EM}}^K$ (of dimension $9\,d_i^K \times 9d_i^K$) corresponds to the matrix obtained for Maxwell's equations, see (G.33). Matrices $\mathbb{A}^K_{\substack{\text{coupling}\\ \text{EM}\to\text{poro}}}$ (of dimension $13\,d_i^K \times 9d_i^K$) and $\mathbb{A}^K_{\substack{\text{coupling}\\ \text{poro}\to\text{EM}}}$ (of dimension $9\,d_i^K \times 13d_i^K$) represent the electrokinetic coupling. The coupling matrices $\mathbb{A}^K$ are given by:

$$\mathbb{A}^K_{\substack{\text{coupling}\\ \text{EM}\to\text{poro}}} = \begin{pmatrix}
0 & 0 & 0 & 0&0&0&0&0&0\\
0 & 0 & 0 & 0&0&0&0&0&0\\
0 & 0 & 0 & 0&0&0&0&0&0\\
-\,\mathrm{i}\,\omega\rho_{\text{dyn}}\mathbb{M}^K\mathrm{L} & 0 & 0 & 0&0&0&0&0&0\\
0 & -\,\mathrm{i}\,\omega\rho_{\text{dyn}}\mathbb{M}^K\mathrm{L} & 0 & 0&0&0&0&0&0\\
0 & 0 & -\,\mathrm{i}\,\omega\rho_{\text{dyn}}\mathbb{M}^K\mathrm{L} & 0&0&0&0&0&0\\
0 & 0 & 0 & 0&0&0&0&0&0\\
0 & 0 & 0 & 0&0&0&0&0&0\\
0 & 0 & 0 & 0&0&0&0&0&0\\
0 & 0 & 0 & 0&0&0&0&0&0\\
0 & 0 & 0 & 0&0&0&0&0&0\\
0 & 0 & 0 & 0&0&0&0&0&0\\
0 & 0 & 0 & 0&0&0&0&0&0
\end{pmatrix},$$

and

$$\mathbb{A}^K_{\substack{\text{coupling}\\ \text{poro}\to\text{EM}}} = \begin{pmatrix} 0 & 0 & 0 & 0&0&0&0&0&0&0&0&0 & 0 \\ 0 & 0 & 0 & 0&0&0&0&0&0&0&0&0 & 0 \\ 0 & 0 & 0 & 0&0&0&0&0&0&0&0&0 & 0 \\ 0 & 0 & 0 & 0&0&0&0&0&0&0&0&0 & 0 \\ 0 & 0 & 0 & 0&0&0&0&0&0&0&0&0 & 0 \\ 0 & 0 & 0 & 0&0&0&0&0&0&0&0&0 & 0 \\ \mathbb{M}^K\,\mathrm{i}\,\omega\rho_f \mathrm{L} & 0 & 0 & 0&0&0&0&0&0&0&0&0 & -\mathbb{D}_x^K \mathrm{L} \\ 0 & \mathbb{M}^K\,\mathrm{i}\,\omega\rho_f \mathrm{L} & 0 & 0&0&0&0&0&0&0&0&0 & -\mathbb{D}_y^K \mathrm{L} \\ 0 & 0 & \mathbb{M}^K\,\mathrm{i}\,\omega\rho_f \mathrm{L} & 0&0&0&0&0&0&0&0&0 & -\mathbb{D}_z^K \mathrm{L} \end{pmatrix}.$$

The unknown $\underline{\Lambda}^K$ is composed of 7 times 4 columns corresponding to the four Lagrange unknowns (four poroelastic variables and three electromagnetic variables) decomposed on the four faces of the element. Hence, $\mathbb{B}^K$ has the form:

$$\mathbb{B}^K = \begin{pmatrix} \mathbb{B}^K_{\mathbf{poro}} & \mathbb{B}^K_{\substack{\text{coupling}\\ \text{EM}\to\text{poro}}} \\ \mathbb{B}^K_{\substack{\text{coupling}\\ \text{poro}\to\text{EM}}} & \mathbb{B}^K_{\mathbf{EM}} \end{pmatrix}.$$

$\mathbb{B}^K_{\mathbf{poro}}$ corresponds to the matrix for poroelasticity, see Appendix B.1.2. $\mathbb{B}^K_{\mathbf{EM}}$ is the electromagnetic matrix given in (G.34). The coupling matrix $\mathbb{B}^K_{\substack{\text{coupling}\\ \text{EM}\to\text{poro}}}$ is written in 12 columns corresponding to the Lagrange unknown $\boldsymbol{\lambda}_3$. We have:

$$\mathbb{B}^K_{\substack{\text{coupling}\\ \text{EM}\to\text{poro}}} = 0\,.$$

The block $\mathbb{B}^K_{\substack{\text{coupling}\\ \text{poro}\to\text{EM}}}$ is decomposed as:

$$\mathbb{B}^K_{\substack{\text{coupling}\\ \text{poro}\to\text{EM}}} = \Big(B^{\lambda_{1x},1}_{\substack{\text{coupling}\\ \text{poro}\to\text{EM}}}, B^{\lambda_{1x},2}_{\substack{\text{coupling}\\ \text{poro}\to\text{EM}}}, B^{\lambda_{1x},3}_{\substack{\text{coupling}\\ \text{poro}\to\text{EM}}}, B^{\lambda_{1x},4}_{\substack{\text{coupling}\\ \text{poro}\to\text{EM}}}, B^{\lambda_{1y},1}_{\substack{\text{coupling}\\ \text{poro}\to\text{EM}}}, B^{\lambda_{1y},2}_{\substack{\text{coupling}\\ \text{poro}\to\text{EM}}}, B^{\lambda_{1y},3}_{\substack{\text{coupling}\\ \text{poro}\to\text{EM}}}, B^{\lambda_{1y},4}_{\substack{\text{coupling}\\ \text{poro}\to\text{EM}}},$$
$$B^{\lambda_{1z},1}_{\substack{\text{coupling}\\ \text{poro}\to\text{EM}}}, B^{\lambda_{1z},2}_{\substack{\text{coupling}\\ \text{poro}\to\text{EM}}}, B^{\lambda_{1z},3}_{\substack{\text{coupling}\\ \text{poro}\to\text{EM}}}, B^{\lambda_{1z},4}_{\substack{\text{coupling}\\ \text{poro}\to\text{EM}}}, B^{\lambda_{2},1}_{\substack{\text{coupling}\\ \text{poro}\to\text{EM}}}, B^{\lambda_{2},2}_{\substack{\text{coupling}\\ \text{poro}\to\text{EM}}}, B^{\lambda_{2},3}_{\substack{\text{coupling}\\ \text{poro}\to\text{EM}}}, B^{\lambda_{2},4}_{\substack{\text{coupling}\\ \text{poro}\to\text{EM}}} \Big),$$

with

$$B^{\lambda_{1\bullet},f}_{\substack{\text{coupling}\\ \text{poro}\to\text{EM}}} = 0\,, \quad \text{for } \bullet = x,y,z \text{ and } f = 1,4,$$

and

$$B_{\lambda_2,f} = \begin{pmatrix} 0 \\ 0 \\ 0 \\ 0 \\ 0 \\ 0 \\ \mathrm{L}\,\mathbb{Q}_{xf}^{\beta(K,f)} \\ \mathrm{L}\,\mathbb{Q}_{yf}^{\beta(K,f)} \\ \mathrm{L}\,\mathbb{Q}_{zf}^{\beta(K,f)} \end{pmatrix}, \quad \text{for } f = 1,4.$$

Finally, the local source vector is:

$$\mathbb{C}^K_{\text{source}} = \big(\mathbb{C}^K_{1x}\ \ \mathbb{C}^K_{1y}\ \ \mathbb{C}^K_{1z}\ \ \mathbb{C}^K_{2x}\ \ \mathbb{C}^K_{2y}\ \ \mathbb{C}^K_{2z}\ \ 0\ 0\ 0\ 0\ 0\ 0\ 0\ \mathbb{C}^K_{3x}\ \ \mathbb{C}^K_{3y}\ \ \mathbb{C}^K_{3z}\ \ 0\ 0\ 0\ \ \mathrm{L}\,\mathbb{C}^K_{2x}\ \ \mathrm{L}\,\mathbb{C}^K_{2y}\ \ \mathrm{L}\,\mathbb{C}^K_{2z}\big)^T.$$

7.5.2 Transmission conditions

The transmission conditions, given by equation (7.7), are expressed using the definition of the numerical traces in equations (7.3) and (7.4). The equations are discretized on (x,y,z) by decomposing the unknowns using (7.30a) and (7.30b) and replacing the test functions by the basis functions. They are then expressed in terms of the elementary matrices defined in (7.31).

(a) The first transmission equation (7.7a)

Equation (7.7a) is expressed as:

$$\sum_{K\in\mathcal{T}_h}\int_{\partial K}\boldsymbol{\tau}_h^K\boldsymbol{n}^K\cdot\eta-\sum_{K\in\mathcal{T}_h}\int_{\partial K}\gamma_1\left(\mathbf{u}_h^K-\boldsymbol{\lambda}_1\right)\cdot\eta-\sum_{K\in\mathcal{T}_h}\int_{\partial K}\gamma_3\left(\mathrm{p}_h^K-\lambda_2\right)\boldsymbol{n}^K\cdot\eta=\sum_{F\in\mathcal{F}_{\text{ext}}}\int_F\boldsymbol{f}_{\text{inc}}\cdot\eta\,, \tag{7.37}$$

The discretization of (7.37) along x, y and z directions gives, taking $\bullet=x,y,z$:

$$\begin{aligned}&\sum_{K\in\mathcal{T}_h}\int_{\partial K}\underline{\tau}_{x\bullet}^K\,n_x^K\,\varphi_j^K\,\psi_i^{\beta(K,f)}\,dS+\sum_{K\in\mathcal{T}_h}\int_{\partial K}\underline{\tau}_{y\bullet}^K\,n_y^K\,\varphi_j^K\,\psi_i^{\beta(K,f)}\,dS+\sum_{K\in\mathcal{T}_h}\int_{\partial K}\underline{\tau}_{z\bullet}^K\,n_z^K\,\varphi_j^K\,\psi_i^{\beta(K,f)}\,dS\\&-\sum_{K\in\mathcal{T}_h}\int_{\partial K}\gamma_1\,\varphi_j^K\,\underline{\mathrm{u}}_\bullet^K\,\psi_i^{\beta(K,f)}\,dS+\sum_{K\in\mathcal{T}_h}\int_{\partial K}\gamma_1\,\psi_j^{\beta(K,f)}\underline{\lambda}_{1\bullet}^K\,\psi_i^{\beta(K,f)}\,dS-\sum_{K\in\mathcal{T}_h}\int_{\partial K}\gamma_3 n_\bullet^K\underline{\mathrm{p}}^K\varphi_j^K\psi_i^{\beta(K,f)}dS\\&+\sum_{K\in\mathcal{T}_h}\int_{\partial K}\gamma_3 n_\bullet^K\underline{\lambda}_2^K\psi_j^{\beta(K,f)}\psi_i^{\beta(K,f)}dS=\sum_{F\in\mathcal{F}_{\text{ext}}}\int_F f_{\text{inc},\bullet}\,\psi_i^{\beta(K,f)}\,dS\,.\end{aligned}$$

The above equation is expressed in terms of the unknown vectors defined in (7.30a) and the local matrices in (7.31) as:

$$\begin{aligned}\sum_{K\in\mathcal{T}_h}\Big(&(\mathbb{Q}_x^{\beta(K,f)})^T\,\underline{\tau}_{x\bullet}^K+(\mathbb{Q}_y^{\beta(K,f)})^T\,\underline{\tau}_{\bullet y}^K+(\mathbb{Q}_z^{\beta(K,f)})^T\,\underline{\tau}_{\bullet z}^K-\gamma_1\,(\mathbb{F}^{\beta(K,f)})^T\,\underline{\mathrm{u}}_\bullet^K+\gamma_1\,\mathbb{G}^{\beta(K,f)}\,\underline{\lambda}_{1\bullet}^{\beta(K,f)}\\&-\gamma_3\,(\mathbb{Q}_\bullet^{\beta(K,f)})^T\,\underline{\mathrm{p}}^K+\gamma_3\,\mathbb{H}_\bullet^{\beta(K,f)}\,\underline{\lambda}_2^{\beta(K,f)}\Big)=\sum_{F\in\mathcal{F}_{\text{ext}}}\int_F f_{\text{inc},\bullet}\,\psi_i^{\beta(K,f)}\,dS\,.\end{aligned} \tag{7.38}$$

(b) The second transmission condition (7.7b)

Equation (7.7b) is expressed as:

$$\sum_{K\in\mathcal{T}_h}\int_{\partial K}\mathbf{w}_h^K\cdot\boldsymbol{n}^K\,\xi-\sum_{K\in\mathcal{T}_h}\gamma_2\int_{\partial K}(\mathrm{p}_h^K-\lambda_2)\,\xi-\sum_{K\in\mathcal{T}_h}\int_{\partial K}\gamma_4\left(\mathbf{u}_h^K-\boldsymbol{\lambda}_1\right)\cdot\boldsymbol{n}^K\,\xi=\sum_{F\in\mathcal{F}_{\text{ext}}}\int_F g_{\text{inc}}\,\xi\,. \tag{7.39}$$

The equation (7.39) is also discretized as

$$\begin{aligned}&\sum_{K\in\mathcal{T}_h}\int_{\partial K}\Big(\underline{\mathrm{w}}_x^K\,\varphi_j^K\,n_x^K\psi_i^{\beta(K,f)}+\underline{\mathrm{w}}_y^K\,\varphi_j^K\,n_y^K\psi_i^{\beta(K,f)}+\underline{\mathrm{w}}_z^K\,\varphi_j^K\,n_z^K\psi_i^{\beta(K,f)}-\underline{\mathrm{p}}^K\,\varphi_j^K\,\gamma_2\psi_i^{\beta(K,f)}+\underline{\lambda}_2^K\,\psi_j^{\beta(K,f)}\,\gamma_2\,\psi_i^{\beta(K,f)}\\&-\underline{\mathrm{u}}_x^K\,\varphi_j^K\,\gamma_4\,n_x^K\,\psi_i^{\beta(K,f)}-\underline{\mathrm{u}}_y^K\,\varphi_j^K\,\gamma_4\,n_y^K\,\psi_i^{\beta(K,f)}-\underline{\mathrm{u}}_z^K\,\varphi_j^K\,\gamma_4\,n_z^K\,\psi_i^{\beta(K,f)}+\underline{\lambda}_{1x}^K\,\psi_j^{\beta(K,f)}\,\gamma_4\,n_x^K\,\psi_i^{\beta(K,f)}\\&+\underline{\lambda}_{1y}^K\,\psi_j^{\beta(K,f)}\,\gamma_4\,n_y^K\,\psi_i^{\beta(K,f)}+\underline{\lambda}_{1z}^K\,\psi_j^{\beta(K,f)}\,\gamma_4\,n_z^K\,\psi_i^{\beta(K,f)}\Big)=\sum_{F\in\mathcal{F}_{\text{ext}}}\int_F g_{\text{inc}}\,\psi_i^{\beta(K,f)}\,dS\,,\end{aligned}$$

and expressed in terms of the local matrices and the unknown vectors defined respectively in (7.31) and (7.30a):

$$\begin{aligned}\sum_{K\in\mathcal{T}_h}\Big(&(\mathbb{Q}_x^{\beta(K,f)})^T\,\underline{\mathrm{w}}_x^K+(\mathbb{Q}_y^{\beta(K,f)})^T\,\underline{\mathrm{w}}_y^K+(\mathbb{Q}_z^{\beta(K,f)})^T\,\underline{\mathrm{w}}_z^K-(\mathbb{F}^{\beta(K,f)})^T\,\underline{\mathrm{p}}^K\,\gamma_2+\mathbb{G}^{\beta(K,f)}\underline{\lambda}_2^K\,\gamma_2-(\mathbb{Q}_x^{\beta(K,f)})^T\underline{\mathrm{u}}_x^K\,\gamma_4\\&-(\mathbb{Q}_y^{\beta(K,f)})^T\underline{\mathrm{u}}_y^K\gamma_4-(\mathbb{Q}_z^{\beta(K,f)})^T\underline{\mathrm{u}}_z^K\gamma_4+\mathbb{H}_x^{\beta(K,f)}\underline{\lambda}_{1x}^K\,\gamma_4+\mathbb{H}_y^{\beta(K,f)}\underline{\lambda}_{1y}^K\gamma_4+\mathbb{H}_z^{\beta(K,f)}\underline{\lambda}_{1z}^K\,\gamma_4\Big)=\sum_{F\in\mathcal{F}_{\text{ext}}}\int_F g_{\text{inc}}\,\psi_i^{\beta(K,f)}\,dS\,.\end{aligned} \tag{7.40}$$

(c) Discretization of the third transmission equation (7.7c)

Equation (7.7c) is expressed as:

$$\sum_{K\in\mathcal{T}_h}\int_{\partial K}(\boldsymbol{n}^K\times\boldsymbol{E}_h^K)\cdot\boldsymbol{\nu}-\sum_{K\in\mathcal{T}_h}\int_{\partial K}\gamma_5\big(\boldsymbol{H}_h^t-\boldsymbol{\lambda}_3\big)\cdot\boldsymbol{\nu}=\sum_{F\in\mathcal{F}_{\text{ext}}}\int_F\boldsymbol{h}_{\text{inc}}\,\xi\,.$$

We write the above expression in terms of the basis functions and the local unknowns defined in (7.30a):

$$\int_F (n_y^K \underline{E}_z^K - n_z^K \underline{E}_y^K)\, \varphi_j^K\, \psi_i^F - \int_F \gamma_5 \left(\underline{H}_x^t \varphi_j^K - \underline{\lambda}_{3x} \psi_j^F\right) \psi_i^F \,,$$
$$\int_F (n_z^K \underline{E}_x^K - n_x^K \underline{E}_z^K)\, \varphi_j^K\, \psi_i^F - \int_F \gamma_5 \left(\underline{H}_y^t \varphi_j^K - \underline{\lambda}_{3y} \psi_j^F\right) \psi_i^F \,,$$
$$\int_F (n_x^K \underline{E}_y^K - n_y^K \underline{E}_x^K)\, \varphi_j^K\, \psi_i^F - \int_F \gamma_5 \left(\underline{H}_z^t \varphi_j^K - \underline{\lambda}_{3z} \psi_j^F\right) \psi_i^F \,.$$

which reads in terms of elementary matrices (7.31):

$$\begin{aligned}
&(\mathbb{Q}_y^F)^T \underline{E}_z^K - (\mathbb{Q}_z^F)^T \underline{E}_y^K - (\mathbb{F}^F)^T \underline{H}_x^t\, \gamma_5 + \mathbb{G}^F \underline{\lambda}_{3x}\, \gamma_5 \,, \\
&(\mathbb{Q}_z^F)^T \underline{E}_x^K - (\mathbb{Q}_x^F)^T \underline{E}_z^K - (\mathbb{F}^F)^T \underline{H}_y^t\, \gamma_5 + \mathbb{G}^F \underline{\lambda}_{3y}\, \gamma_5 \,, \\
&(\mathbb{Q}_x^F)^T \underline{E}_y^K - (\mathbb{Q}_y^F)^T \underline{E}_x^K - (\mathbb{F}^F)^T \underline{H}_z^t\, \gamma_5 + \mathbb{G}^F \underline{\lambda}_{3z}\, \gamma_5 \,.
\end{aligned} \tag{7.41}$$

Local system The transmission conditions, equations (7.38), (7.40), (7.41) form the following system:

$$\sum_{K \in \mathcal{T}_h} (\mathcal{A}_{HDG}^K)^T \left(\mathbb{P}^K \underline{W}^K + \mathbb{T}^K \mathcal{A}_{HDG}^K \underline{\Lambda}\right) = \mathbb{S}_{\text{inc}} \,,$$

where $\mathbb{S}_{\text{inc}}$ represents the matrices of the incident forces. Similarly to $\mathbb{A}^K$ and $\mathbb{B}^K$, the elementary matrix $\mathbb{P}^K$ has the form:

$$\mathbb{P}^K = \begin{pmatrix} \mathbb{P}^K_{\mathbf{poro}} & 0 \\ 0 & \mathbb{P}^K_{\mathbf{EM}} \end{pmatrix},$$

where $\mathbb{P}^K_{\mathbf{poro}}$ corresponds to the matrix for poroelasticity, see Appendix B.1.2, and $\mathbb{P}^K_{\mathbf{EM}}$ to the electromagnetic matrix given in (G.35).

$\mathbb{T}^K$ has the same form:

$$\mathbb{T}^K = \begin{pmatrix} \mathbb{T}^K_{\mathbf{poro}} & 0 \\ 0 & \mathbb{T}^K_{\mathbf{EM}} \end{pmatrix},$$

where the poroelastic matrix $\mathbb{T}^K_{\mathbf{poro}}$ is given in Appendix B.1.2, and the electromagnetic matrix $\mathbb{T}^K_{\mathbf{EM}}$ is given in (G.36).

Remark 7.2. For a face on the boundary of the domain, we can impose one of the eight types of boundary conditions, see Section 5.4. For type 1, we impose the continuity of $\boldsymbol{\tau}\, \boldsymbol{n}$, $\mathbf{w} \cdot \boldsymbol{n}$ and $\boldsymbol{n} \times \hat{\boldsymbol{E}}$. This means that the transmission conditions (7.7) for an interior interface and on the boundary of the mesh are the same. However, if we choose to impose a different boundary condition, the expression of the elementary matrices $\mathbb{P}^K$ and $\mathbb{T}^K$ are modified. Here, we detail the boundary condition of type 8 as in equation (5.10b). The other formulations can be easily deduced from these two formulations. This is similar to what has been done for poroelasticity. For the boundary condition of type 8, we impose the condition in the strong way in the linear system, which means that we impose the value of $\hat{\mathbf{u}}$, $\hat{\mathrm{p}}$, and $\hat{\boldsymbol{H}}$. From equation (5.10b), we impose:

$$\boldsymbol{\lambda}_1 = \mathbf{f}_{\text{inc}} \,, \qquad \lambda_2 = g_{\text{inc}} \,, \qquad \boldsymbol{\lambda}_3 = \mathbf{h}_{\text{inc}} \,.$$

We consider an element with the first local face on the boundary of the mesh. In this case, the matrices $\mathbb{P}^K_{\mathbf{poro}}$ and $\mathbb{T}^K_{\mathbf{poro}}$ are given in Appendix B.2, $\mathbb{P}^K_{\mathbf{EM}}$ and $\mathbb{P}^K_{\mathbf{EM}}$ in (G.37). The coupling matrices $\mathbb{P}^K_{\substack{\text{coupling} \\ \text{poro}\to\text{EM}}}$, $\mathbb{T}^K_{\substack{\text{coupling} \\ \text{poro}\to\text{EM}}}$, $\mathbb{P}^K_{\substack{\text{coupling} \\ \text{EM}\to\text{poro}}}$ and $\mathbb{T}^K_{\substack{\text{coupling} \\ \text{EM}\to\text{poro}}}$ remain equal to zero.

7.6 Numerical results in three dimensions

In this section, we present the results obtained with the HDG method in three dimensions. We use the geophysical materials, the relative numerical error and the condition numbers introduced in Section 7.4. We also use the results obtained in two dimensions for the stabilization parameters, i.e., $\gamma_i = 1$ for $i = 1, 5$. We consider a porous domain $\mathcal{D}$ of size $[0:10] \times [0:10] \times [0:2]$cm composed of sand1, given in Table 7.1 page 274. The domain is discretized in

a mesh composed of 8164 elements (tetrahedra). A plane wave propagates in the material, and we impose the exact solution $(\boldsymbol{\tau}_{\text{pw}} \cdot \boldsymbol{n},\ \mathbf{u}_{\text{pw}} \cdot \boldsymbol{n},\ \boldsymbol{n} \times \boldsymbol{E}_{\text{pw}})$ corresponding to the plane wave on the boundaries of the mesh. To validate the code, we compare the numerical solution to the exact solution for plane wave, see Chapter 5. In Figure 7.7, we present the numerical and exact solutions of the propagation of an incident B plane wave in sand1, for a frequency $f = 1.7$kHz, and order of interpolation 3. We also give in Table 7.7 the relative L^2 error on the variables. We observe that the results are good, and the error is small, less than 1% on every component. We have also tested for the other kinds of incident waves (P,S,EM). The results have a similar accuracy.

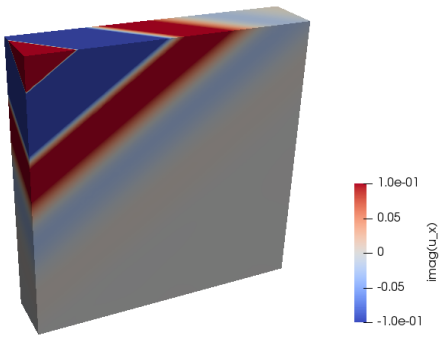

(a) Numerical solution: imaginary part of u_x

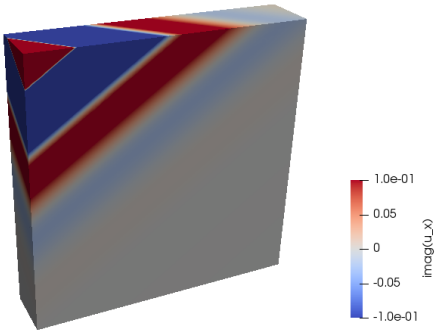

(b) Reference solution: imaginary part of u_x

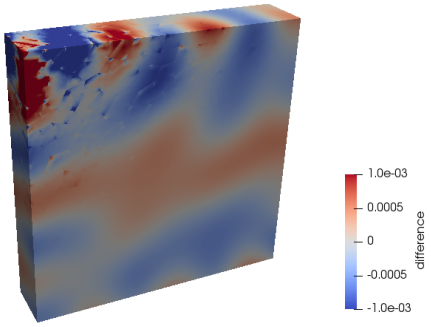

(c) Difference: imaginary part of u_x

Figure 7.7: Numerical and reference solution for the three-dimensional propagation of an incident B plane wave in sand1. The solid velocity u_x is presented, for $f = 400$Hz and order of interpolation 3.

$e_h(\mathrm{u}_x)$	$e_h(\mathrm{u}_y)$	$e_h(\mathrm{u}_z)$	$e_h(\mathrm{w}_x)$	$e_h(\mathrm{w}_y)$	$e_h(\mathrm{w}_z)$	$e_h(\tau_{xx})$	$e_h(\tau_{yy})$	$e_h(\tau_{zz})$
0.16	0.22	0.19	7.1e-2	7.6e-2	6.9e-2	9.2e-2	0.10	0.20

$e_h(\tau_{yz})$	$e_h(\tau_{xz})$	$e_h(\tau_{xy})$	$e_h(\mathrm{p})$	$e_h(E_x)$	$e_h(E_y)$	$e_h(E_z)$	$e_h(H_x)$	$e_h(H_y)$	$e_h(H_z)$
0.17	0.13	0.17	6.1e-2	0.12	0.13	9.8e-2	inf	inf	inf

Table 7.7: Relative errors (%) on the components of the unknowns of the HDG method for an incident B plane wave propagating in sand, at frequency $f = 400$Hz with boundary conditions of type 1, using an order of discretization 3. The error for $\boldsymbol{H}$ is infinite because the exact solution is equal to zero, hence the relative error on $\boldsymbol{H}$ is not defined.

We now verify that the HDG method keeps an optimal order of convergence $p + 1$ in three dimensions. The convergence curves are plotted for the solid velocity u_x in 7.8 for the first interpolation orders as functions of h, the

longest edge of the mesh. We observe on the curves that the method has an order of convergence $p+1$ for $\mathbf{u}_x$. This is also the case for the other components of the solid velocity $\mathbf{u}$ and the other unknowns.

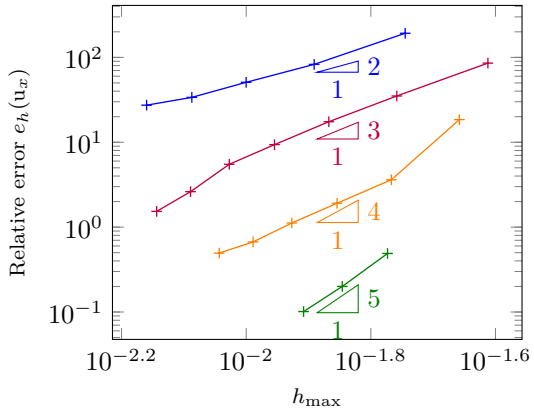

Figure 7.8: Convergence curves of HDG method (component u_x) for several orders of interpolation. Results for order 1 are plotted in blue, for order 2 in purple, for order 3 in orange and for order 4 in green.

Conclusion

In this chapter, we have proposed a HDG method to solve Pride's equations in harmonic domain. We have detailed and implemented this method in two and three dimensions. The method has been validated using the comparison with reference solutions and we have shown numerically that the method attains the optimal order of convergence. In two dimensions, we have provided a detailed investigation on the influence of the stabilization parameters on the accuracy and convergence of the method. In addition, we have numerically studied the condition number of the global and local problems, and observed that its value remains in a good range to have stability and accuracy of the method for the considered geophysical materials. Then, using the results on the stabilization parameters in two dimensions, we have validated the method in three dimensions using plane wave propagation and verified that the method keeps an optimal order of convergence. In the next chapter, we will detail this HDG method when we use two truncation methods (ABC and PML) to simulate infinite domains.

Chapter 8

Truncation methods in two dimensions for Pride's equations

In this chapter, we address the same problem as in Chapter 4 for Pride's equations. To our best knowledge, it does not exist any radiation boundary condition (RBC) for Pride's model. Contrary to the RBC, PMLs have been applied to Pride's equations, see [69, 61]. Gao [61] highlights the difficulty for the PML to absorb both the seismic and electromagnetic waves. This comes from the fact that the wavelengths of the seismic and electromagnetic waves have very different sizes. To prevent this, the authors propose to absorb only the seismic waves with the PML and to extend widely the domain outside of the PML to prevent the reflections. This leads to a dramatic increase of computational time.

In the following, we derive in Section 8.1 a low order RBC for Pride's equations. For this, we first obtain an outgoing radiation condition at infinity by using the expression of the unknowns in potentials and the expansions of outgoing solutions given in Chapter 6. Then, when written in circular geometry, this exact condition is approximated to obtain the RBC, assuming the radius of the circular boundary is large enough. The resulting condition consists of the expression of the solid stress tensor $\boldsymbol{\tau}$, the fluid pressure p and the magnetic field H as functions of the solid velocity $\mathbf{u}$, the relative fluid velocity $\mathbf{w}$ and the electric field $\boldsymbol{E}$. The relation is comparable to the relation obtained for poroelasticity in Chapter 4. We then develop in Section 8.2 a reference solution associated with the radiation condition on an annulus, which will be used to study the performance of the RBC. We investigate the performance of the condition in Section 8.3, by comparison with the outgoing solution that we obtained in Chapter 6. We implement in Section 8.4 the radiation condition in the HDG method presented in Chapter 7. In addition, we consider Perfectly Matched Layer (PML) to prevent the reflections on the artificial boundaries of the domain. We also apply PML to the HDG discretization in Section 8.5. Finally, we perform numerical tests to evaluate and compare the accuracy of the HDG method using the RBC and PML in Section 8.6. We study in particular if the PML can absorb all kinds of waves.

8.1 Derivation of low-order outgoing boundary radiation condition

In this section, we build a radiation boundary condition for Pride's equations. For this purpose, we derive the outgoing radiation conditions at infinity to find a relation between the stresses and the magnetic field ($\boldsymbol{\tau}$, p, H), and the velocities and the electric field ($\mathbf{u}$, $\mathbf{w}$, $\boldsymbol{E}$). We consider the scattering of a solid circular obstacle immersed in an infinite porous medium by a plane wave, see Figure 8.1. First, we recall the expressions of the fields ($\mathbf{u}$, $\mathbf{w}$, $\boldsymbol{\tau}$, p, $\boldsymbol{E}$, H, $\boldsymbol{J}$) in terms of the potentials $\chi_\bullet$ (6.4):

$$
\begin{aligned}
\mathrm{i}\,\omega\,\mathbf{u} &= \frac{1}{\mathsf{s}_{\mathrm{P}}^2}\,\nabla\chi_{\mathrm{P}} + \frac{1}{\mathsf{s}_{\mathrm{B}}^2}\,\nabla\chi_{\mathrm{B}} - \frac{1}{\mathsf{s}_{\mathrm{S}}^2}\,\mathbf{curl}\chi_{\mathrm{S}} - \frac{1}{\mathsf{s}_{\mathrm{EM}}^2}\,\mathbf{curl}\chi_{\mathrm{EM}} + \tilde{\mathbf{F}}_{\mathbf{1}}\,,\\
\mathrm{i}\,\omega\,\mathbf{w} &= \frac{\mathcal{W}_{\mathrm{P}}}{\mathsf{s}_{\mathrm{P}}^2}\,\nabla\chi_{\mathrm{P}} + \frac{\mathcal{W}_{\mathrm{B}}}{\mathsf{s}_{\mathrm{B}}^2}\,\nabla\chi_{\mathrm{B}} - \frac{\mathcal{W}_{\mathrm{S}}}{\mathsf{s}_{\mathrm{S}}^2}\,\mathbf{curl}\chi_{\mathrm{S}} - \frac{\mathcal{W}_{\mathrm{EM}}}{\mathsf{s}_{\mathrm{EM}}^2}\,\mathbf{curl}\chi_{\mathrm{EM}} + \tilde{\mathbf{F}}_{\mathbf{2}}\,,\\
\mathrm{p} &= -M\,(\mathcal{W}_{\mathrm{P}} + \alpha)\chi_{\mathrm{P}} - M\,(\mathcal{W}_{\mathrm{B}} + \alpha)\chi_{\mathrm{B}} - M\,\mathbf{f}_{\mathrm{p}}\,,
\end{aligned}
$$

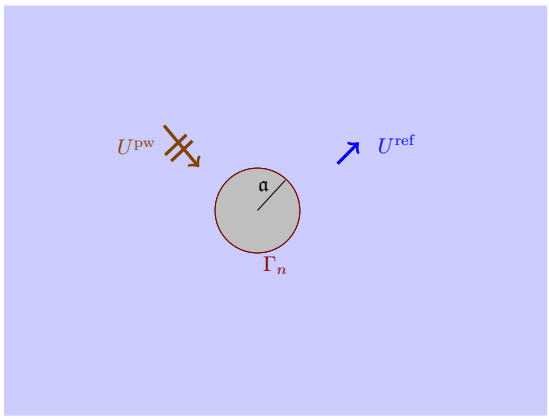

Figure 8.1: Scattering of a plane wave by an impenetrable solid immersed in a porous medium. The cross section of the obstacle is a disc parameterized by $r = \mathfrak{a}$.

$$
\begin{aligned}
\boldsymbol{\tau} \;=\; & \frac{\mu_{\rm fr}}{\omega^2}\left(-\frac{2}{\mathsf{s}_{\rm P}^2}\,\nabla^2\chi_{\rm P} \;-\; \frac{2}{\mathsf{s}_{\rm B}^2}\,\nabla^2\chi_{\rm B} \;+\; \frac{\nabla\mathbf{curl}\,\chi_{\rm S} \;+\; (\nabla\mathbf{curl}\,\chi_{\rm S})^T}{\mathsf{s}_{\rm S}^2} \;+\; \frac{\nabla\mathbf{curl}\,\chi_{\rm EM} \;+\; (\nabla\mathbf{curl}\,\chi_{\rm EM})^T}{\mathsf{s}_{\rm EM}^2}\right)\\
& +\left(-\frac{2}{3}\mu_{\rm fr} \;+\; \mathrm{k}_{\rm fr} \;+\; M\alpha^2 \;+\; \alpha\, M\,\mathcal{W}_{\rm P}\right)\chi_{\rm P}\,\mathbb{I}\\
& +\left(-\frac{2}{3}\mu_{\rm fr} \;+\; \mathrm{k}_{\rm fr} \;+\; M\alpha^2 \;+\; \alpha\, M\,\mathcal{W}_{\rm B}\right)\chi_{\rm B}\,\mathbb{I} - \;\frac{\mu_{\rm fr}}{\omega^2}\left(\nabla\tilde{\mathbf{F}}_{\mathbf{1}} + (\nabla\tilde{\mathbf{F}}_{\mathbf{1}})^T\right),\\
-\omega^2\,\boldsymbol{E} \;=\; & \frac{\mathcal{E}_{\rm P}}{\mathsf{s}_{\rm P}^2}\,\nabla\chi_{\rm P} \;+\; \frac{\mathcal{E}_{\rm B}}{\mathsf{s}_{\rm B}^2}\,\nabla\chi_{\rm B} - \;\frac{\mathcal{E}_{\rm S}}{\mathsf{s}_{\rm S}^2}\,\mathbf{curl}\chi_{\rm S} \;-\; \frac{\mathcal{E}_{\rm EM}}{\mathsf{s}_{\rm EM}^2}\,\mathbf{curl}\chi_{\rm EM} \;+\; \tilde{\mathbf{F}}_{\mathbf{3}}\,,\\
\mathrm{H} \;=\; & \frac{\mathrm{i}}{\omega\,\mu_0}\left(\mathcal{E}_{\rm S}\,\chi_{\rm S} \;+\; \mathcal{E}_{\rm EM}\,\chi_{\rm EM}\right),
\end{aligned}
$$

and

$$
\begin{aligned}
\boldsymbol{J} \;=\; & \left(-\frac{\sigma}{\omega^2}\,\mathcal{E}_{\rm P}\,\mathsf{s}_{\rm P}^{-2} + \mathbf{L}\,M\,(\mathcal{W}_{\rm P} \;+\; \alpha) - \mathbf{L}\,\rho_f\;\mathsf{s}_{\rm P}^{-2}\right)\nabla\chi_{\rm P} \;+\; \left(-\frac{\sigma}{\omega^2}\,\mathcal{E}_{\rm B}\,\mathsf{s}_{\rm B}^{-2} + \mathbf{L}\,M\,(\mathcal{W}_{\rm B} \;+\; \alpha) - \mathbf{L}\,\rho_f\;\mathsf{s}_{\rm B}^{-2}\right)\nabla\chi_{\rm B}\\
& +\left(\frac{\sigma}{\omega^2}\,\mathcal{E}_{\rm S}\,\mathsf{s}_{\rm S}^{-2} \;+\; \mathbf{L}\,\rho_f\,\mathsf{s}_{\rm S}^{-2}\right)\mathbf{curl}\chi_{\rm S} \;+\; \left(\frac{\sigma}{\omega^2}\,\mathcal{E}_{\rm EM}\,\mathsf{s}_{\rm S}^{-2} \;+\; \mathbf{L}\,\rho_f\,\mathsf{s}_{\rm EM}^{-2}\right)\mathbf{curl}\chi_{\rm EM} \;+F\,.
\end{aligned}
$$

The potentials $\chi_\bullet$ solve the Helmholtz equation,

$$
\left(-\Delta \;-\; \omega^2\,\mathsf{s}_\bullet^2\right)\chi_\bullet \;=\; 0\,,
$$

and they can be expanded in terms of Bessel functions, as we describe in the next section.

8.1.1 Outgoing radiation condition at infinity

In polar coordinates, the potentials $\chi_\bullet$ that define a generic outgoing solution only contains $\mathrm{H}_k^{(1)}$ Bessel functions and are expressed as (eq. (6.17)).

$$
\begin{aligned}
\chi_{\rm P}(r,\theta) \;&=\; \sum_{k\in\mathbb{Z}} a_k\,\mathrm{H}_k^{(1)}(\omega\,\mathsf{s}_{\rm P}\,r)\;e^{\mathrm{i}\,k\,\theta}\,,\\
\chi_{\rm B}(r,\theta) \;&=\; \sum_{k\in\mathbb{Z}} b_k\,\mathrm{H}_k^{(1)}(\omega\,\mathsf{s}_{\rm B}\,r)\;e^{\mathrm{i}\,k\,\theta}\,,\\
\chi_{\rm S}(r,\theta) \;&=\; \sum_{k\in\mathbb{Z}} c_k\,\mathrm{H}_k^{(1)}(\omega\,\mathsf{s}_{\rm S}\,r)\;e^{\mathrm{i}\,k\,\theta}\,,\\
\chi_{\rm EM}(r,\theta) \;&=\; \sum_{k\in\mathbb{Z}} d_k\,\mathrm{H}_k^{(1)}(\omega\,\mathsf{s}_{\rm EM}\,r)\;e^{\mathrm{i}\,k\,\theta}\,.
\end{aligned}
$$

The expressions for the expansion of the unknowns ($\mathbf{u}$, $\mathbf{w}$, $\boldsymbol{\tau}$, p, $\boldsymbol{E}$, H) are obtained by substituting this form of potential in equation (8.1) and use the expression of $\mathbf{curl}\,\nabla$ and ∇^2 in polar coordinates presented in Appendix A.1.1.

We obtain the following expressions for the velocities:

$$
\begin{aligned}
\mathrm{i}\,\omega\,\mathrm{u}_r \;=\; & \sum_{k\in\mathbb{Z}} a_k\,\frac{\omega}{\mathsf{s}_\mathrm{P}}\,\mathrm{H}_k^{(1)'}(\omega\,\mathsf{s}_\mathrm{P}\,r)e^{\mathrm{i}k\theta} \;+\; \sum_{k\in\mathbb{Z}} b_k\,\frac{\omega}{\mathsf{s}_\mathrm{B}}\,\mathrm{H}_k^{(1)'}(\omega\,\mathsf{s}_\mathrm{B}\,r)e^{\mathrm{i}k\theta} \\
& - \sum_{k\in\mathbb{Z}} c_k\,\frac{\mathrm{i}k}{\mathsf{s}_\mathrm{S}^2\,r}\mathrm{H}_k^{(1)}(\omega\,\mathsf{s}_\mathrm{S}\,r)e^{\mathrm{i}k\theta} \;-\; \sum_{k\in\mathbb{Z}} d_k\,\frac{\mathrm{i}k}{\mathsf{s}_\mathrm{EM}^2\,r}\mathrm{H}_k^{(1)}(\omega\,\mathsf{s}_\mathrm{EM}\,r)e^{\mathrm{i}k\theta}\,, \\
\mathrm{i}\,\omega\,\mathrm{u}_\theta \;=\; & \sum_{k\in\mathbb{Z}} a_k\,\frac{\mathrm{i}k}{\mathsf{s}_\mathrm{P}^2\,r}\mathrm{H}_k^{(1)}(\omega\,\mathsf{s}_\mathrm{P}\,r)e^{\mathrm{i}k\theta} \;+\; \sum_{k\in\mathbb{Z}} b_k\,\frac{\mathrm{i}k}{\mathsf{s}_\mathrm{B}^2\,r}\mathrm{H}_k^{(1)}(\omega\,\mathsf{s}_\mathrm{B}\,r)e^{\mathrm{i}k\theta} \\
& + \sum_{k\in\mathbb{Z}} c_k\,\frac{\omega}{\mathsf{s}_\mathrm{S}}\,\mathrm{H}_k^{(1)'}(\omega\,\mathsf{s}_\mathrm{S}\,r)e^{\mathrm{i}k\theta} \;+\; \sum_{k\in\mathbb{Z}} d_k\,\frac{\omega}{\mathsf{s}_\mathrm{EM}}\,\mathrm{H}_k^{(1)'}(\omega\,\mathsf{s}_\mathrm{S}\,r)e^{\mathrm{i}k\theta}\,,
\end{aligned}
$$

$$
\begin{aligned}
\mathrm{i}\,\omega\,\mathrm{w}_r \;=\; & \sum_{k\in\mathbb{Z}} a_k\,\frac{\mathcal{W}_\mathrm{P}}{\mathsf{s}_\mathrm{P}}\,\omega\,\mathrm{H}_k^{(1)'}(\omega\,\mathsf{s}_\mathrm{P}\,r)e^{\mathrm{i}k\theta} \;+\; \sum_{k\in\mathbb{Z}} b_k\,\frac{\mathcal{W}_\mathrm{B}}{\mathsf{s}_\mathrm{B}}\,\omega\,\mathrm{H}_k^{(1)'}(\omega\,\mathsf{s}_\mathrm{B}\,r)e^{\mathrm{i}k\theta} \\
& - \sum_{k\in\mathbb{Z}} c_k\,\mathrm{i}k\,\frac{\mathcal{W}_\mathrm{S}}{\mathsf{s}_\mathrm{S}^2\,r}\mathrm{H}_k^{(1)}(\omega\,\mathsf{s}_\mathrm{S}\,r)e^{\mathrm{i}k\theta} \;-\; \sum_{k\in\mathbb{Z}} d_k\,\mathrm{i}k\,\frac{\mathcal{W}_\mathrm{EM}}{\mathsf{s}_\mathrm{EM}^2\,r}\mathrm{H}_k^{(1)}(\omega\,\mathsf{s}_\mathrm{EM}\,r)e^{\mathrm{i}k\theta}\,.
\end{aligned}
$$

For the stress $\boldsymbol{\tau}$, we have:

$$
\begin{aligned}
\omega^2\tau_{rr} = & -\sum_{k\in\mathbb{Z}} \frac{2\,\mu_\mathrm{fr}\,\omega}{\mathsf{s}_\mathrm{P}\,r}\,a_k\,\mathrm{H}_{k+1}^{(1)}(\omega\,\mathsf{s}_\mathrm{P}\,r)\;e^{\mathrm{i}\,k\,\theta} \;+\sum_{k\in\mathbb{Z}} \frac{2\,\mu_\mathrm{fr}\,k}{\mathsf{s}_\mathrm{P}^2\,r^2}\,a_k\,\mathrm{H}_k^{(1)}(\omega\,\mathsf{s}_\mathrm{P}\,r)\;e^{\mathrm{i}\,k\,\theta} \\
& + \sum_{k\in\mathbb{Z}} 2\,\mu_\mathrm{fr}\,a_k\,\omega^2\,\mathrm{H}_k^{(1)}(\omega\,\mathsf{s}_\mathrm{P}\,r)\;e^{\mathrm{i}\,k\,\theta} - \sum_{k\in\mathbb{Z}} \frac{2\,\mu_\mathrm{fr}\,k^2}{\mathsf{s}_\mathrm{P}^2\,r^2}\,a_k\,\mathrm{H}_k^{(1)}(\omega\,\mathsf{s}_\mathrm{P}\,r)\;e^{\mathrm{i}\,k\,\theta} \\
& - \sum_{k\in\mathbb{Z}} \frac{2\,\mu_\mathrm{fr}\,\omega}{\mathsf{s}_\mathrm{B}\,r}\,b_k\,\mathrm{H}_{k+1}^{(1)}(\omega\,\mathsf{s}_\mathrm{B}\,r)\;e^{\mathrm{i}\,k\,\theta} \;+\sum_{k\in\mathbb{Z}} \frac{2\,\mu_\mathrm{fr}\,k}{\mathsf{s}_\mathrm{B}^2\,r^2}\,b_k\,\mathrm{H}_k^{(1)}(\omega\,\mathsf{s}_\mathrm{B}\,r)\;e^{\mathrm{i}\,k\,\theta} \\
& + \sum_{k\in\mathbb{Z}} 2\,\mu_\mathrm{fr}\,b_k\,\omega^2\,\mathrm{H}_k^{(1)}(\omega\,\mathsf{s}_\mathrm{B}\,r)\;e^{\mathrm{i}\,k\,\theta} - \sum_{k\in\mathbb{Z}} \frac{2\,\mu_\mathrm{fr}\,k^2}{\mathsf{s}_\mathrm{B}^2\,r^2}\,b_k\,\mathrm{H}_k^{(1)}(\omega\,\mathsf{s}_\mathrm{B}\,r)\;e^{\mathrm{i}\,k\,\theta} \\
& + \sum_{k\in\mathbb{Z}} \frac{2\,\mu_\mathrm{fr}}{\mathsf{s}_\mathrm{S} r}\;c_k\,\omega\,\mathrm{i}k\,\mathrm{H}_k^{(1)'}(\omega\,\mathsf{s}_\mathrm{S}\,r)\;e^{\mathrm{i}\,k\,\theta} + \sum_{k\in\mathbb{Z}} \frac{2\,\mu_\mathrm{fr}}{\mathsf{s}_\mathrm{EM} r}\;d_k\,\omega\,\mathrm{i}k\,\mathrm{H}_k^{(1)'}(\omega\,\mathsf{s}_\mathrm{EM}\,r)\;e^{\mathrm{i}\,k\,\theta} \\
& + \sum_{k\in\mathbb{Z}} \omega^2\,\left(-\frac{2}{3}\mu_\mathrm{fr} \;+\; \mathrm{k}_\mathrm{fr} \;+\; M\alpha^2 \;+\; \alpha\,M\mathcal{W}_\mathrm{P}\right)\;a_k\,\mathrm{H}_k^{(1)}(\omega\,\mathsf{s}_\mathrm{P}\,r)\;e^{\mathrm{i}\,k\,\theta} \\
& + \sum_{k\in\mathbb{Z}} \omega^2\,\left(-\frac{2}{3}\mu_\mathrm{fr} \;+\; \mathrm{k}_\mathrm{fr} \;+\; M\alpha^2 \;+\; \alpha\,M\mathcal{W}_\mathrm{B}\right)\;b_k\,\mathrm{H}_k^{(1)}(\omega\,\mathsf{s}_\mathrm{B}\,r)\;e^{\mathrm{i}\,k\,\theta}\,,
\end{aligned}
$$

$$
\begin{aligned}
\omega^2\,\tau_{r\theta} \;=& -\sum_{k\in\mathbb{Z}} \frac{2\,\mu_{\rm fr}\,\omega\,{\rm i}\,k}{r\,{\rm s_P}}\,a_k\,{\rm H}_k^{(1)'}(\omega\,{\rm s_P}\,r)\;e^{{\rm i}\,k\,\theta} + \sum_{k\in\mathbb{Z}} \frac{2\,{\rm i}\,\mu_{\rm fr}\,k}{r^2\,{\rm s_P^2}}\,a_k\,{\rm H}_k^{(1)}(\omega\,{\rm s_P}\,r)\;e^{{\rm i}\,k\,\theta}\\
&- \sum_{k\in\mathbb{Z}} \frac{2\,\mu_{\rm fr}\omega\,{\rm i}\,k}{r\,{\rm s_B}}\,b_k\,{\rm H}_k^{(1)'}(\omega\,{\rm s_B}\,r)\;e^{{\rm i}\,k\,\theta} + \sum_{k\in\mathbb{Z}} \frac{2\,{\rm i}\,\mu_{\rm fr}\,k}{r^2\,{\rm s_B^2}}\,b_k\,{\rm H}_k^{(1)}(\omega\,{\rm s_B}\,r)\;e^{{\rm i}\,k\,\theta}\\
&- \sum_{k\in\mathbb{Z}} \frac{\mu_{\rm fr}\,k^2}{r^2\,{\rm s_S^2}}\,c_k\,{\rm H}_k^{(1)}(\omega\,{\rm s_S}\,r)\;e^{{\rm i}\,k\,\theta} + \sum_{k\in\mathbb{Z}} \frac{\mu_{\rm fr}\,\omega}{r\,{\rm s_S}}\,c_k\,{\rm H}_k^{(1)'}(\omega\,{\rm s_S}\,r)\;e^{{\rm i}\,k\,\theta}\\
&- \sum_{k\in\mathbb{Z}} \mu_{\rm fr}\,\frac{\omega}{{\rm s_S}\,r}\,c_k\,{\rm H}_{k+1}^{(1)}(\omega\,{\rm s_S}\,r)\;e^{{\rm i}\,k\,\theta} + \sum_{k\in\mathbb{Z}} \mu_{\rm fr}\,\frac{k}{{\rm s_S^2}\,r^2}c_k\,{\rm H}_k^{(1)}(\omega\,{\rm s_S}\,r)\;e^{{\rm i}\,k\,\theta}\\
&+ \sum_{k\in\mathbb{Z}} \mu_{\rm fr}\,\omega^2\,c_k\,{\rm H}_k^{(1)}(\omega\,{\rm s_S}\,r)\;e^{{\rm i}\,k\,\theta} - \sum_{k\in\mathbb{Z}} \mu_{\rm fr}\,\frac{k^2}{{\rm s_S^2}\,r^2}\,c_k\,{\rm H}_k^{(1)}(\omega\,{\rm s_S}\,r)\;e^{{\rm i}\,k\,\theta}\\
&- \sum_{k\in\mathbb{Z}} \frac{\mu_{\rm fr}\,k^2}{r^2\,{\rm s_{EM}^2}}\,d_k\,{\rm H}_k^{(1)}(\omega\,{\rm s_{EM}}\,r)\;e^{{\rm i}\,k\,\theta} + \sum_{k\in\mathbb{Z}} \frac{\mu_{\rm fr}\,\omega}{r\,{\rm s_{EM}}}\,d_k\,{\rm H}_k^{(1)'}(\omega\,{\rm s_{EM}}\,r)\;e^{{\rm i}\,k\,\theta}\\
&- \sum_{k\in\mathbb{Z}} \mu_{\rm fr}\,\frac{\omega}{{\rm s_{EM}}\,r}\,d_k\,{\rm H}_{k+1}^{(1)}(\omega\,{\rm s_{EM}}\,r)\;e^{{\rm i}\,k\,\theta} + \sum_{k\in\mathbb{Z}} \mu_{\rm fr}\,\frac{k}{{\rm s_{EM}^2}\,r^2}d_k\,{\rm H}_k^{(1)}(\omega\,{\rm s_{EM}}\,r)\;e^{{\rm i}\,k\,\theta}\\
&+ \sum_{k\in\mathbb{Z}} \mu_{\rm fr}\,\omega^2\,d_k\,{\rm H}_k^{(1)}(\omega\,{\rm s_{EM}}\,r)\;e^{{\rm i}\,k\,\theta} - \sum_{k\in\mathbb{Z}} \mu_{\rm fr}\,\frac{k^2}{{\rm s_{EM}^2}\,r^2}\,d_k\,{\rm H}_k^{(1)}(\omega\,{\rm s_{EM}}\,r)\;e^{{\rm i}\,k\,\theta}\,,\\
{\rm p} \;=& -\sum_{k\in\mathbb{Z}} a_k\,M\,\big(\mathcal{W}_{\rm P} \;+\; \alpha){\rm H}_k^{(1)}(\omega\,{\rm s_P}\,r)\,e^{{\rm i}k\theta} \;-\; \sum_{k\in\mathbb{Z}} b_k\,M\,\big(\mathcal{W}_{\rm B} \;+\; \alpha){\rm H}_k^{(1)}(\,\omega\,{\rm s_B}\,r)\,e^{{\rm i}k\theta}\,.
\end{aligned}
$$

The tangential component of the electric field is

$$
\begin{aligned}
-\,\omega^2\,E_\theta \;=& \sum_{k\in\mathbb{Z}} a_k\,\mathcal{E}_{\rm P}\,\frac{{\rm i}k}{{\rm s_P^2}r}{\rm H}_k^{(1)}(\omega\,{\rm s_P}\,r)e^{{\rm i}k\theta} \;+\; \sum_{k\in\mathbb{Z}} b_k\,\mathcal{E}_{\rm B}\,\frac{{\rm i}k}{{\rm s_B^2}r}{\rm H}_k^{(1)}(\omega\,{\rm s_B}\,r)e^{{\rm i}k\theta}\\
&+ \sum_{k\in\mathbb{Z}} c_k\,\frac{\mathcal{E}_{\rm S}}{{\rm s_S}}\,\omega\,{\rm H}_k^{(1)'}(\omega\,{\rm s_S}\,r)e^{{\rm i}k\theta} \;+\; \sum_{k\in\mathbb{Z}} d_k\,\frac{\mathcal{E}_{\rm EM}}{{\rm s_{EM}}}\,\omega\,{\rm H}_k^{(1)'}(\omega\,{\rm s_{EM}}\,r)e^{{\rm i}k\theta}\,,
\end{aligned}
$$

and the magnetic field is expressed as

$$
{\rm H} \;=\; c_k\,\frac{\rm i}{\omega\,\mu_0}\,\mathcal{E}_{\rm S}\,{\rm H}_k^{(1)}(\omega\,{\rm s_S}\,r)\;e^{{\rm i}\,k\,\theta} \;+\; d_k\,\frac{\rm i}{\omega\,\mu_0}\,\mathcal{E}_{\rm EM}\,{\rm H}_k^{(1)}(\omega\,{\rm s_{EM}}\,r)\,e^{{\rm i}\,k\,\theta}\,.
$$

In order to find a relation between the unknowns $\boldsymbol{\tau}$, p, H and $\mathbf{u}$, $\mathbf{w}$, $\boldsymbol{E}$, we choose to approximate the components by truncating at the first order in $\frac{1}{r}$. We obtain for the poroelastic variables:

$$
\begin{aligned}
{\rm u}_r \;&=\; -\sum_{k\in\mathbb{Z}} a_k\,\frac{\rm i}{\rm s_P}\,{\rm H}_k^{(1)'}(\omega\,{\rm s_P}\,r)e^{{\rm i}k\theta} \;-\; \sum_{k\in\mathbb{Z}} b_k\,\frac{\rm i}{\rm s_B}\,{\rm H}_k^{(1)'}(\omega\,{\rm s_B}\,r)e^{{\rm i}k\theta} \;+\; {\rm O}(r^{-\frac{3}{2}})\,,\\
{\rm w}_r \;&=\; -\sum_{k\in\mathbb{Z}} a_k\,\frac{{\rm i}\,\mathcal{W}_{\rm P}}{\rm s_P}\,{\rm H}_k^{(1)'}(\omega\,{\rm s_P}\,r)e^{{\rm i}k\theta} \;-\; \sum_{k\in\mathbb{Z}} b_k\,\frac{{\rm i}\,\mathcal{W}_{\rm B}}{\rm s_B}\,{\rm H}_k^{(1)'}(\omega\,{\rm s_B}\,r)e^{{\rm i}k\theta} \;+\; {\rm O}(r^{-\frac{3}{2}})\,,\\
{\rm u}_\theta \;&=\; -\sum_{k\in\mathbb{Z}} c_k\,\frac{\rm i}{\rm s_S}\,{\rm H}_k^{(1)'}(\omega\,{\rm s_S}\,r) + {\rm O}(r^{-\frac{3}{2}}) \;-\; \sum_{k\in\mathbb{Z}} d_k\,\frac{\rm i}{\rm s_{EM}}\,{\rm H}_k^{(1)'}(\omega\,{\rm s_{EM}}\,r) + {\rm O}(r^{-\frac{3}{2}})\,,
\end{aligned}
\tag{8.3}
$$

and

$$
\begin{aligned}
\tau_{rr} =& \left(\frac{4}{3}\mu_{\rm fr} \;+\; {\rm k_{fr}} \;+\; \alpha(M\alpha \;+\; M\mathcal{W}_{\rm P})\right) \sum_{k\in\mathbb{Z}} \;a_k\,{\rm H}_k^{(1)}(\omega\,{\rm s_P}\,r)\;e^{{\rm i}\,k\,\theta}\\
&+ \left(\frac{4}{3}\mu_{\rm fr} \;+\; {\rm k_{fr}} \;+\; \alpha(M\alpha \;+\; M\mathcal{W}_{\rm B})\right) \sum_{k\in\mathbb{Z}} \;b_k\,{\rm H}_k^{(1)}(\omega\,{\rm s_B}\,r)\;e^{{\rm i}\,k\,\theta} \;+\; {\rm O}(r^{-\frac{3}{2}})\,,\\
\tau_{r\theta} \;=& \sum_{k\in\mathbb{Z}} \mu_{\rm fr}\,c_k\,{\rm H}_k^{(1)}(\omega\,{\rm s_S}\,r)\,e^{{\rm i}\,k\,\theta} \;+\sum_{k\in\mathbb{Z}} \mu_{\rm fr}\,d_k\,{\rm H}_k^{(1)}(\omega\,{\rm s_{EM}}\,r)\,e^{{\rm i}\,k\,\theta} \;+\; {\rm O}(r^{-\frac{3}{2}})\,,\\
{\rm p} =& -\sum_{k\in\mathbb{Z}} a_k\,M\,\big(\mathcal{W}_{\rm P} \;+\; \alpha){\rm H}_k^{(1)}(\,\omega\,{\rm s_P}\,r)\,e^{{\rm i}k\theta} \;-\; \sum_{k\in\mathbb{Z}} b_k\,M\,\big(\mathcal{W}_{\rm B} \;+\; \alpha){\rm H}_k^{(1)}(\omega\,{\rm s_B}\,r)\,e^{{\rm i}k\theta}\,.
\end{aligned}
\tag{8.4}
$$

Note that these truncated expressions are the same as the ones obtained for the poroelasticity, (see Section 4.1) except for the expressions of u_θ and $\tau_{r\theta}$. The electromagnetic variables are approwimated as follows:

$$\begin{aligned} E_\theta &= -\sum_{k\in\mathbb{Z}} c_k \frac{E_{\mathrm{S}}}{\omega\, \mathsf{s}_{\mathrm{S}}} \mathrm{H}_k^{(1)'}(\omega\, \mathsf{s}_{\mathrm{S}}\, r) e^{\mathrm{i}k\theta} - \sum_{k\in\mathbb{Z}} d_k \frac{E_{\mathrm{EM}}}{\omega\, \mathsf{s}_{\mathrm{EM}}} \mathrm{H}_k^{(1)'}(\omega\, \mathsf{s}_{\mathrm{EM}}\, r) e^{\mathrm{i}k\theta} + \mathsf{O}(r^{-\frac{3}{2}}), \\ \mathrm{H} &= \sum_{k\in\mathbb{Z}} c_k \frac{\mathrm{i}}{\omega\, \mu_0} E_S\, \mathrm{H}_k^{(1)}(\omega\, \mathsf{s}_{\mathrm{S}}\, r)\, e^{\mathrm{i}\,k\,\theta} + \sum_{k\in\mathbb{Z}} d_k \frac{\mathrm{i}}{\omega\, \mu_0} E_{EM}\, \mathrm{H}_k^{(1)}(\omega\, \mathsf{s}_{\mathrm{EM}}\, r)\, e^{\mathrm{i}\,k\,\theta} + \mathsf{O}(r^{-\frac{3}{2}}). \end{aligned} \tag{8.5}$$

Important identities We recall the following asymptotic of Hankel functions, see equation (4.3).

$$H_k^{(1)'}(z) - \mathrm{i}\, H_k^{(1)}(z) = O(z^{-\frac{3}{2}}), \quad z \to \infty. \tag{8.6}$$

- Since the expressions of the radial velocities are the same as the ones obtained for poroelasticity, we can use once again the relation obtained in Section 4.1:

$$\begin{pmatrix} \sum\limits_{k\in\mathbb{Z}} a_k\, \mathrm{H}_k^{(1)'}(\omega\, \mathsf{s}_{\mathrm{P}}\, r) e^{\mathrm{i}k\theta} \\ \sum\limits_{k\in\mathbb{Z}} b_k\, \mathrm{H}_k^{(1)'}(\omega\, \mathsf{s}_{\mathrm{B}}\, r) e^{\mathrm{i}k\theta} \end{pmatrix} = \frac{1}{\mathcal{W}_{\mathrm{B}} - \mathcal{W}_{\mathrm{P}}} \begin{pmatrix} \mathsf{s}_{\mathrm{P}}\, \mathcal{W}_{\mathrm{B}} & -\mathsf{s}_{\mathrm{P}} \\ -\mathcal{W}_{\mathrm{P}}\, \mathsf{s}_{\mathrm{B}} & \mathsf{s}_{\mathrm{B}} \end{pmatrix} \begin{pmatrix} \mathrm{i}\, \mathrm{u}_r \\ \mathrm{i}\, \mathrm{w}_r \end{pmatrix} + \mathsf{O}(r^{-\frac{3}{2}}). \tag{8.7}$$

- Using equations (8.3) and (8.5), we can write the system:

$$\begin{pmatrix} \mathbf{u}_\theta \\ E_\theta \end{pmatrix} = \begin{pmatrix} -\dfrac{\mathrm{i}}{\mathsf{s}_{\mathrm{S}}} & -\dfrac{\mathrm{i}}{\mathsf{s}_{\mathrm{EM}}} \\ \dfrac{E_{\mathrm{S}}}{\omega\, \mathsf{s}_{\mathrm{S}}} & \dfrac{E_{\mathrm{EM}}}{\omega\, \mathsf{s}_{\mathrm{EM}}} \end{pmatrix} \begin{pmatrix} \sum\limits_{k\in\mathbb{Z}} c_k\, \mathrm{H}_k^{(1)'}(\omega\, \mathsf{s}_{\mathrm{S}}\, r) e^{\mathrm{i}k\theta} \\ \sum\limits_{k\in\mathbb{Z}} d_k\, \mathrm{H}_k^{(1)'}(\omega\, \mathsf{s}_{\mathrm{EM}}\, r) e^{\mathrm{i}k\theta} \end{pmatrix} + \mathsf{O}(r^{-\frac{3}{2}}). \tag{8.8}$$

  We can invert the above matrix:

$$\begin{pmatrix} -\dfrac{\mathrm{i}}{\mathsf{s}_{\mathrm{S}}} & -\dfrac{\mathrm{i}}{\mathsf{s}_{\mathrm{EM}}} \\ \dfrac{E_{\mathrm{S}}}{\omega\, \mathsf{s}_{\mathrm{S}}} & \dfrac{E_{\mathrm{EM}}}{\omega\, \mathsf{s}_{\mathrm{EM}}} \end{pmatrix}^{-1} = \frac{1}{E_{\mathrm{EM}} - E_{\mathrm{S}}} \begin{pmatrix} \mathrm{i}\, \mathsf{s}_{\mathrm{S}}\, E_{\mathrm{EM}} & -\omega\, \mathsf{s}_{\mathrm{S}} \\ -\mathrm{i}\, \mathsf{s}_{\mathrm{EM}}\, E_{\mathrm{S}} & \omega\, \mathsf{s}_{\mathrm{EM}} \end{pmatrix}.$$

  Hence, equation (8.8) becomes

$$\begin{pmatrix} \sum_{k\in\mathbb{Z}} c_k\, \mathrm{H}_k^{(1)'}(\omega\, \mathsf{s}_{\mathrm{S}}\, r) e^{\mathrm{i}k\theta} \\ \sum_{k\in\mathbb{Z}} d_k\, \mathrm{H}_k^{(1)'}(\omega\, \mathsf{s}_{\mathrm{EM}}\, r) e^{\mathrm{i}k\theta} \end{pmatrix} = \frac{1}{E_{\mathrm{EM}} - E_{\mathrm{S}}} \begin{pmatrix} \mathrm{i}\, \mathsf{s}_{\mathrm{S}}\, E_{\mathrm{EM}} & -\omega\, \mathsf{s}_{\mathrm{S}} \\ -\mathrm{i}\, \mathsf{s}_{\mathrm{EM}}\, E_{\mathrm{S}} & \omega\, \mathsf{s}_{\mathrm{EM}} \end{pmatrix} \begin{pmatrix} \mathrm{u}_\theta \\ E_\theta \end{pmatrix} + \mathsf{O}(r^{-\frac{3}{2}}). \tag{8.9}$$

In the following, we express the solid stress $\boldsymbol{\tau}$, the fluid pressure p and the magnetic field H as functions of the velocities $\mathbf{u}$, $\mathbf{w}$ and the electrical field $\boldsymbol{E}$.

(a) Radial component of the solid stress

Since the fields τ_{rr}, u_r and w_r have the same expression as for poroelasticity, they are linked by the same relation, given in Section 4.1:

$$\tau_{rr} + \mathbf{X}_1 \mathrm{u}_r + \mathbf{X}_2 \mathrm{w}_r = \mathsf{O}(r^{-\frac{3}{2}}),$$

with

$$\begin{aligned} \mathbf{X}_1 &= -\frac{\frac{4}{3}\mu_{\mathrm{fr}} + \mathrm{k}_{\mathrm{fr}} + \alpha(M\alpha + M\mathcal{W}_{\mathrm{P}})}{\mathcal{W}_{\mathrm{B}} - \mathcal{W}_{\mathrm{P}}} \mathsf{s}_{\mathrm{P}}\, \mathcal{W}_{\mathrm{B}} + \frac{\frac{4}{3}\mu_{\mathrm{fr}} + \mathrm{k}_{\mathrm{fr}} + \alpha(M\alpha + M\mathcal{W}_{\mathrm{B}})}{\mathcal{W}_{\mathrm{B}} - \mathcal{W}_{\mathrm{P}}} \mathcal{W}_{\mathrm{P}}\, \mathsf{s}_{\mathrm{B}}, \\ \mathbf{X}_2 &= \frac{\frac{4}{3}\mu_{\mathrm{fr}} + \mathrm{k}_{\mathrm{fr}} + \alpha(M\alpha + M\mathcal{W}_{\mathrm{P}})}{\mathcal{W}_{\mathrm{B}} - \mathcal{W}_{\mathrm{P}}} \mathsf{s}_{\mathrm{P}} - \frac{\frac{4}{3}\mu_{\mathrm{fr}} + \mathrm{k}_{\mathrm{fr}} + \alpha(M\alpha + M\mathcal{W}_{\mathrm{B}})}{\mathcal{W}_{\mathrm{B}} - \mathcal{W}_{\mathrm{P}}} \mathsf{s}_{\mathrm{B}}. \end{aligned}$$

(b) Tangential component of the solid stress

The tangential stress $\tau_{r\theta}$ is expressed with equation (8.4). Using the identity (8.6), we have

$$\tau_{r\theta} \,+\, \mu_{\rm fr}\,{\rm i}\sum_{k\in\mathbb{Z}} c_k\,{\rm H}_k^{(1)'}(\omega\,{\rm s}_{\rm S}\,r)\,e^{{\rm i}\,k\,\theta} \,+\, \mu_{\rm fr}\,{\rm i}\sum_{k\in\mathbb{Z}} d_k\,{\rm H}_k^{(1)'}(\omega\,{\rm s}_{\rm EM}\,r)\,e^{{\rm i}\,k\,\theta} \,=\, \mathsf{O}(r^{-\frac{3}{2}})\,.$$

We relate this expression with u_θ and E_θ by using the system (8.9), and we obtain:

$$\tau_{r\theta} \,+\, \frac{\mu_{\rm fr}\,{\rm i}}{E_{\rm EM}-E_{\rm S}}\,({\rm i}\,{\rm s}_{\rm S}\,E_{\rm EM}\,{\rm u}_\theta-\omega\,{\rm s}_{\rm S}E_\theta) \,+\, \frac{\mu_{\rm fr}\,{\rm i}}{E_{\rm EM}-E_{\rm S}}\,(-\,{\rm i}\,{\rm s}_{\rm EM}\,E_{\rm S}\,{\rm u}_\theta+\omega\,{\rm s}_{\rm EM}\,E_\theta) \,=\, \mathsf{O}(r^{-\frac{3}{2}})\,.$$

Reorganizing the terms gives:

$$\tau_{r\theta} \,+\, \frac{\mu_{\rm fr}}{E_{\rm EM}-E_{\rm S}}\,({\rm s}_{\rm EM}\,E_{\rm S}\,-\,{\rm s}_{\rm S}\,E_{\rm EM}\,)\,{\rm u}_\theta \,+\, \frac{\mu_{\rm fr}\,{\rm i}\,\omega}{E_{\rm EM}-E_{\rm S}}\,({\rm s}_{\rm EM}-{\rm s}_{\rm S}\,)\,E_\theta \,=\, \mathsf{O}(r^{-\frac{3}{2}})\,.$$

We write then:

$$\tau_{r\theta}+\mathbf{X}_3{\rm u}_\theta\,+\mathbf{X}_4E_\theta=\mathsf{O}(r^{-\frac{3}{2}})\,,$$

with

$$\mathbf{X}_3 \,=\, \frac{\mu_{\rm fr}}{E_{\rm EM}-E_{\rm S}}\,({\rm s}_{\rm EM}\,E_{\rm S}\,-\,{\rm s}_{\rm S}\,E_{\rm EM}\,)\,,\quad\text{ and }\quad \mathbf{X}_4 \,=\, \frac{\mu_{\rm fr}\,{\rm i}\,\omega}{E_{\rm EM}-E_{\rm S}}\,({\rm s}_{\rm EM}-{\rm s}_{\rm S}\,)\,.$$

(c) Fluid pressure

The truncated expression of p is the same as for poroelasticity, *cf.* Section 4.1, hence, using equation (8.4), the radiating asymptotic (8.6) and the relation (8.7), we have:

$$\mathrm{p}+\mathbf{X}_5{\rm u}_r+\mathbf{X}_6{\rm w}_r=\,\mathsf{O}(r^{-\frac{3}{2}})\,,$$

with

$$\mathbf{X}_5=\frac{M\,(\mathcal{W}_{\rm P}\,+\,\alpha)}{\mathcal{W}_{\rm B}-\mathcal{W}_{\rm P}}{\rm s}_{\rm P}\,\mathcal{W}_{\rm B}\,-\,\frac{M\,(\mathcal{W}_{\rm B}\,+\,\alpha)}{\mathcal{W}_{\rm B}-\mathcal{W}_{\rm P}}\,{\rm s}_{\rm B}\,\mathcal{W}_{\rm P}\,,\quad\text{ and }\quad \mathbf{X}_6=-\frac{M\,(\mathcal{W}_{\rm P}\,+\,\alpha)}{\mathcal{W}_{\rm B}-\mathcal{W}_{\rm P}}{\rm s}_{\rm P}+\frac{M\,(\mathcal{W}_{\rm B}\,+\,\alpha)}{\mathcal{W}_{\rm B}-\mathcal{W}_{\rm P}}\,{\rm s}_{\rm B}\,.$$

(d) Magnetic field

The magnetic field H given in equation (8.5) is expressed with relation (8.6):

$$\mathrm{H}\,-\sum_{k\in\mathbb{Z}}c_k\,\frac{}{\omega\,\mu_0}\,E_S\,{\rm H}_k^{(1)'}(\omega\,{\rm s}_{\rm S}\,r)\;e^{{\rm i}\,k\,\theta}\,-\sum_{k\in\mathbb{Z}}d_k\,\frac{1}{\omega\,\mu_0}\,E_{EM}\,{\rm H}_k^{(1)'}(\omega\,{\rm s}_{\rm EM}\,r)\,e^{{\rm i}\,k\,\theta}\,=\mathsf{O}(r^{-\frac{3}{2}})\,.$$

Using equation (8.9), we have:

$$\mathrm{H}\,-\frac{1}{\omega\,\mu_0}\,\frac{E_S}{E_{\rm EM}-E_{\rm S}}\,({\rm i}\,{\rm s}_{\rm S}\,E_{\rm EM}\,{\rm u}_\theta-\omega\,{\rm s}_{\rm S}E_\theta)\,-\,\frac{1}{\omega\,\mu_0}\,\frac{E_{EM}}{E_{\rm EM}-E_{\rm S}}\,(-\,{\rm i}\,{\rm s}_{\rm EM}\,E_{\rm S}\,{\rm u}_\theta+\omega\,{\rm s}_{\rm EM}\,E_\theta)=\mathsf{O}(r^{-\frac{3}{2}})\,.$$

We reorganize the terms to obtain:

$$\mathrm{H}\,+\frac{\rm i}{\omega\,\mu_0}\,\frac{E_{\rm S}\,E_{\rm EM}}{E_{\rm EM}-E_{\rm S}}\,(\,{\rm s}_{\rm EM}\,-\,{\rm s}_{\rm S}\,)\,{\rm u}_\theta\,+\,\frac{1}{\mu_0}\,\frac{1}{E_{\rm EM}-E_{\rm S}}\,(\,{\rm s}_{\rm S}\,E_{\rm S}\,-\,{\rm s}_{\rm EM}\,E_{\rm EM})\,E_\theta=\mathsf{O}(r^{-\frac{3}{2}})\,.$$

We have:

$$\mathrm{H}+\mathbf{X}_7\,{\rm u}_\theta\,+\mathbf{X}_8\,E_\theta=\mathsf{O}(r^{-\frac{3}{2}})\,,$$

with

$$\mathbf{X}_7 \,=\, \frac{\rm i}{\omega\,\mu_0}\,\frac{E_{\rm S}\,E_{\rm EM}}{E_{\rm EM}-E_{\rm S}}\,(\,{\rm s}_{\rm EM}\,-\,{\rm s}_{\rm S}\,)\,,\quad\text{ and }\quad \mathbf{X}_8 \,=\, \frac{1}{\mu_0}\,\frac{1}{E_{\rm EM}-E_{\rm S}}\,(\,{\rm s}_{\rm S}\,E_{\rm S}\,-\,{\rm s}_{\rm EM}\,E_{\rm EM})\,.$$

Proposition 8.1. **Outgoing radiation condition at infinity.** In circular geometry, if ($\mathbf{u}$, $\mathbf{w}$, $\boldsymbol{\tau}$, p, $\boldsymbol{E}$, H,) are outgoing solutions of Pride's equation (5.3), then they are solution to the outgoing radiation condition at infinity:

$$\left\{\begin{array}{rcl}\tau_{rr}+\mathbf{X}_1{\rm u}_r+\mathbf{X}_2{\rm w}_r &=& \mathsf{O}(r^{-\frac{3}{2}})\,,\\ \tau_{r\theta}+\mathbf{X}_3{\rm u}_\theta+\mathbf{X}_4E_\theta &=& \mathsf{O}(r^{-\frac{3}{2}})\,,\\ \mathrm{p}\;+\mathbf{X}_5{\rm u}_r+\mathbf{X}_6{\rm w}_r &=& \mathsf{O}(r^{-\frac{3}{2}}),\\ \mathrm{H}+\mathbf{X}_7{\rm u}_\theta\,+\,\mathbf{X}_8\,E_\theta &=& \mathsf{O}(r^{-\frac{3}{2}})\,.\end{array}\right. \tag{8.10}$$

8.1.2 Derivation of the radiation boundary condition

In the following, we propose the general radiation boundary condition.

Considering the domain described in Figure 8.2, we set artificial boundaries on Γ_{abs}, and we work in polar coordinates. We have constructed in the previous section an outgoing radiation condition at infinity for the exact outgoing solutions, see (8.10). When r tends to infinity, the terms $\mathsf{O}(r^{-\frac{3}{2}})$ can be neglected. Hence, if we consider r large enough, we can approximate equations (8.10) to obtain the RBC in polar coordinates:

$$\begin{cases} \tau_{rr} + \mathbf{X}_1 \mathrm{u}_r + \mathbf{X}_2 \mathrm{w}_r &= 0\,, \\ \tau_{r\theta} + \mathbf{X}_3 \mathrm{u}_\theta + \mathbf{X}_4 E_\theta &= 0\,, \\ \mathrm{p} + \mathbf{X}_5 \mathrm{u}_r + \mathbf{X}_6 \mathrm{w}_r &= 0, \\ \mathrm{H} + \mathbf{X}_7 \mathrm{u}_\theta + \mathbf{X}_8\, E_\theta &= 0\,. \end{cases} \tag{8.11}$$

Recall that on a circle, we have:

$$\mathrm{u}_r = \mathbf{u}\cdot\boldsymbol{n}\,, \quad \mathrm{w}_r = \mathbf{w}\cdot\boldsymbol{n}\,, \quad \mathrm{u}_\theta = \mathbf{u}\cdot\mathbf{t} = \boldsymbol{n}\times\mathbf{u}\,,$$
$$\boldsymbol{\tau}\,\boldsymbol{n} = \tau_{rr}\mathbf{e}_r + \tau_{r\theta}\mathbf{e}_\theta\,, \quad \text{and} \quad E_\theta = \boldsymbol{E}\cdot\mathbf{t} = \boldsymbol{n}\times\boldsymbol{E}\,, \quad \text{with} \quad \mathbf{t} = \begin{pmatrix} -n_y \\ n_x \end{pmatrix} = \mathbf{e}_\theta\,.$$

By replacing the polar unknowns, we obtain the generalized RBC given below.

Conjecture 8.2. A low-order radiation boundary condition is given by:

$$\begin{cases} \boldsymbol{\tau}\,\boldsymbol{n} + \big(\mathbf{X}_1(\mathbf{u}\cdot\boldsymbol{n}) + \mathbf{X}_2(\mathbf{w}\cdot\boldsymbol{n})\big)\,\boldsymbol{n} + \mathbf{X}_3(\boldsymbol{n}\times\mathbf{u})\,\mathbf{t} + \mathbf{X}_4(\boldsymbol{n}\times\boldsymbol{E})\,\mathbf{t} = 0\,, \\ \mathrm{p} + \mathbf{X}_5(\mathbf{u}\cdot\boldsymbol{n}) + \mathbf{X}_6(\mathbf{w}\cdot\boldsymbol{n}) = 0\,, \\ \mathrm{H} + \mathbf{X}_7(\boldsymbol{n}\times\mathbf{u}) + \mathbf{X}_8\,(\boldsymbol{n}\times\boldsymbol{E}) = 0\,, \end{cases} \tag{8.12}$$

with

$$\mathbf{X}_1 = -\frac{\frac{4}{3}\mu_{\mathrm{fr}} + \mathrm{k}_{\mathrm{fr}} + \alpha(M\alpha + M\mathcal{W}_{\mathrm{P}})}{\mathcal{W}_{\mathrm{B}} - \mathcal{W}_{\mathrm{P}}}\,\mathsf{s}_{\mathrm{P}}\,\mathcal{W}_{\mathrm{B}} + \frac{\frac{4}{3}\mu_{\mathrm{fr}} + \mathrm{k}_{\mathrm{fr}} + \alpha(M\alpha + M\mathcal{W}_{\mathrm{B}})}{\mathcal{W}_{\mathrm{B}} - \mathcal{W}_{\mathrm{P}}}\,\mathcal{W}_{\mathrm{P}}\,\mathsf{s}_{\mathrm{B}}\,,$$

$$\mathbf{X}_2 = \frac{\frac{4}{3}\mu_{\mathrm{fr}} + \mathrm{k}_{\mathrm{fr}} + \alpha(M\alpha + M\mathcal{W}_{\mathrm{P}})}{\mathcal{W}_{\mathrm{B}} - \mathcal{W}_{\mathrm{P}}}\,\mathsf{s}_{\mathrm{P}} - \frac{\frac{4}{3}\mu_{\mathrm{fr}} + \mathrm{k}_{\mathrm{fr}} + \alpha(M\alpha + M\mathcal{W}_{\mathrm{B}})}{\mathcal{W}_{\mathrm{B}} - \mathcal{W}_{\mathrm{P}}}\,\mathsf{s}_{\mathrm{B}}\,,$$

$$\mathbf{X}_3 = \frac{\mu_{\mathrm{fr}}}{E_{\mathrm{EM}} - E_{\mathrm{S}}}\,(\mathsf{s}_{\mathrm{EM}}\,E_{\mathrm{S}} - \mathsf{s}_{\mathrm{S}}\,E_{\mathrm{EM}})\,, \qquad \mathbf{X}_4 = \frac{\mu_{\mathrm{fr}}\,\mathrm{i}\,\omega}{E_{\mathrm{EM}} - E_{\mathrm{S}}}\,(\mathsf{s}_{\mathrm{EM}} - \mathsf{s}_{\mathrm{S}})\,,$$

$$\mathbf{X}_5 = \frac{M\,(\mathcal{W}_{\mathrm{P}} + \alpha)}{\mathcal{W}_{\mathrm{B}} - \mathcal{W}_{\mathrm{P}}}\mathsf{s}_{\mathrm{P}}\,\mathcal{W}_{\mathrm{B}} - \frac{M\,(\mathcal{W}_{\mathrm{B}} + \alpha)}{\mathcal{W}_{\mathrm{B}} - \mathcal{W}_{\mathrm{P}}}\,\mathsf{s}_{\mathrm{B}}\,\mathcal{W}_{\mathrm{P}}\,, \quad \mathbf{X}_6 = -\frac{M\,(\mathcal{W}_{\mathrm{P}} + \alpha)}{\mathcal{W}_{\mathrm{B}} - \mathcal{W}_{\mathrm{P}}}\mathsf{s}_{\mathrm{P}} + \frac{M\,(\mathcal{W}_{\mathrm{B}} + \alpha)}{\mathcal{W}_{\mathrm{B}} - \mathcal{W}_{\mathrm{P}}}\,\mathsf{s}_{\mathrm{B}}\,,$$

$$\mathbf{X}_7 = \frac{\mathrm{i}}{\omega\,\mu_0}\,\frac{E_{\mathrm{S}}\,E_{\mathrm{EM}}}{E_{\mathrm{EM}} - E_{\mathrm{S}}}\,(\mathsf{s}_{\mathrm{EM}} - \mathsf{s}_{\mathrm{S}})\,, \qquad \text{and} \qquad \mathbf{X}_8 = \frac{1}{\mu_0}\,\frac{1}{E_{\mathrm{EM}} - E_{\mathrm{S}}}\,(\mathsf{s}_{\mathrm{S}}\,E_{\mathrm{S}} - \mathsf{s}_{\mathrm{EM}}\,E_{\mathrm{EM}})\,.$$

The two first equations of the condition are comparable to the one obtain for poroelasticity (see Chapter 4), without the electric field. The last equation also resembles the RBC solution for Maxwell's equations (see Appendix G) without the solid velocity.

8.2 Reference RBC solution for the scattering of an impenetrable obstacle by a plane wave

We consider the scattering of a solid circular obstacle immersed in an infinite porous medium by a plane wave. We denote by $\mathbf{D}_{\mathfrak{a}}$ the obstacle whose radius is $\mathfrak{a}$. Its boundary is denoted by $\Gamma_n = \partial\mathbf{D}_{\mathfrak{a}}$, see Figure 8.2.

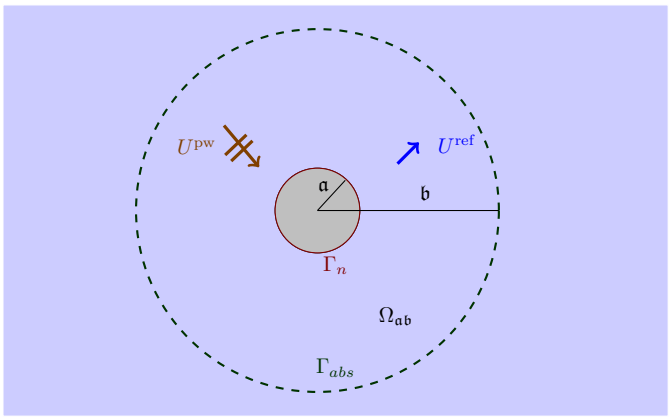

Figure 8.2: Scattering of a plane wave by an impenetrable solid immersed in a porous medium. The cross section of the obstacle is a disc parameterized by $r = \mathfrak{a}$. The artificial boundary is set on $\Gamma_{abs} = \{r = \mathfrak{b}\}$.

For the RBC solution, we set an artificial boundary at radius $\mathfrak{b}$, denoted by $\Gamma_{abs} = \partial\mathbf{D}_{\mathfrak{b}}$, with $\mathfrak{b} > \mathfrak{a}$, cf. Figure 8.2. The RBC solution is then defined on the annulus $\Omega_{\mathfrak{a}\mathfrak{b}} := \mathbf{D}_{\mathfrak{b}} \setminus \mathbf{D}_{\mathfrak{a}}$.

Definition 8.3 (RBC solution). Considering a domain Ω with $\partial\Omega = \Gamma_{abs} \cup \Gamma_n$, and $\Gamma_{abs} \cap \Gamma_n = 0$. We define the RBC solution of Pride equations (5.3) on Ω as follows:
($\mathbf{u}$, $\mathbf{w}$, $\boldsymbol{\tau}$, p, $\boldsymbol{E}$, H) solves Pride equations (5.3) on Ω, the RBC (8.12) on Γ_{abs}, and one of the eight boundary conditions from equation (5.4) on Γ_n.

We use notation $\mathfrak{U}$ to denote the ordered tuple ($\mathbf{u}$, $\mathbf{w}$, $\boldsymbol{\tau}$, p, $\boldsymbol{E}$, H, $\boldsymbol{J}$). The RBC solution $\mathfrak{U}^{\text{rbc -Ti}}$ solves the following problem

$$\begin{cases} \text{Pride equations (5.3) on } \Omega_{\mathfrak{a}\mathfrak{b}}, \\ \text{Boundary condition Type i given in equation (5.4) on } r = \mathfrak{a}\,, \\ \boldsymbol{\tau}\,\boldsymbol{n} + \big(\mathbf{X}_1(\mathbf{u}\cdot\boldsymbol{n}) + \mathbf{X}_2(\mathbf{w}\cdot\boldsymbol{n})\big)\,\boldsymbol{n} + \mathbf{X}_3(\boldsymbol{n}\times\mathbf{u})\,\mathbf{t} + \mathbf{X}_4(\boldsymbol{n}\times\boldsymbol{E})\,\mathbf{t} = 0\,, \\ \mathrm{p} + \mathbf{X}_5(\mathbf{u}\cdot\boldsymbol{n}) + \mathbf{X}_6(\mathbf{w}\cdot\boldsymbol{n}) = 0\,, \qquad \text{on } r = \mathfrak{b}, \\ \mathrm{H} + \mathbf{X}_7(\boldsymbol{n}\times\mathbf{u}) + \mathbf{X}_8\,(\boldsymbol{n}\times\boldsymbol{E}) = 0\,. \end{cases}$$

We recall that the solution $\mathfrak{U}$ is completely determined by the potentials $\chi_\bullet$, cf. (8.1), which are given by (6.18) in the case of an annulus:

$$\begin{aligned} \chi_{\mathrm{P}}(r,\theta) &= \sum_{k\in\mathbb{Z}} a_k\,\mathrm{H}_k^{(1)}(\omega\,\mathsf{s}_P\,r)\;e^{\mathrm{i}\,k\,\theta} + \sum_{k\in\mathbb{Z}} \tilde{a}_k\,\mathrm{H}_k^{(2)}(\omega\,\mathsf{s}_{\mathrm{P}}\,r)\;e^{\mathrm{i}\,k\,\theta}\,, \\ \chi_{\mathrm{B}}(r,\theta) &= \sum_{k\in\mathbb{Z}} b_k\,\mathrm{H}_k^{(1)}(\omega\,\mathsf{s}_{\mathrm{B}}\,r)\;e^{\mathrm{i}\,k\,\theta} + \sum_{k\in\mathbb{Z}} \tilde{b}_k\,\mathrm{H}_k^{(2)}(\omega\,\mathsf{s}_{\mathrm{B}}\,r)\;e^{\mathrm{i}\,k\,\theta}\,, \\ \chi_{\mathrm{S}}(r,\theta) &= \sum_{k\in\mathbb{Z}} c_k\,\mathrm{H}_k^{(1)}(\omega\,\mathsf{s}_{\mathrm{S}}\,r)\;e^{\mathrm{i}\,k\,\theta} + \sum_{k\in\mathbb{Z}} \tilde{c}_k\,\mathrm{H}_k^{(2)}(\omega\,\mathsf{s}_{\mathrm{S}}\,r)\;e^{\mathrm{i}\,k\,\theta}\,, \\ \chi_{\mathrm{EM}}(r,\theta) &= \sum_{k\in\mathbb{Z}} d_k\,\mathrm{H}_k^{(1)}(\omega\,\mathsf{s}_{\mathrm{EM}}\,r)\;e^{\mathrm{i}\,k\,\theta} + \sum_{k\in\mathbb{Z}} \tilde{d}_k\,\mathrm{H}_k^{(2)}(\omega\,\mathsf{s}_{\mathrm{EM}}\,r)\;e^{\mathrm{i}\,k\,\theta}\,, \end{aligned} \tag{8.13}$$

with the Hankel functions $\mathrm{H}_k^{(1)}(z) = \mathrm{J}_k(z) + \mathrm{Y}_k(z)$ and $\mathrm{H}_k^{(2)}(z) = \mathrm{J}_k(z) - \mathrm{Y}_k(z)$. The solution $\mathfrak{U}$ is now represented

by the coefficients a_k, b_k, c_k, d_k, $\tilde{a}_k$, $\tilde{b}_k$, $\tilde{c}_k$, $\tilde{d}_k$. We build a linear system solved by these coefficients of the form:

$$\mathbb{A}^{\text{rbc-Ti}} \begin{pmatrix} a_k \\ b_k \\ c_k \\ d_k \\ \tilde{a}_k \\ \tilde{b}_k \\ \tilde{c}_k \\ \tilde{d}_k \end{pmatrix} = \begin{pmatrix} \mathfrak{f}_{\text{Ti}}^{\text{rbc}} \\ 0 \\ 0 \\ 0 \\ 0 \end{pmatrix},$$

where $\mathbb{A}^{\text{rbc-Ti}}$ is a 8×8 matrix and the right-hand-sides $\mathfrak{f}_{\text{Ti}}^{\text{rbc}}$ are determined using boundary conditions on $r = \mathfrak{a}$. The first four rows of the linear system are determined by the boundary condition imposed on Γ_n (the boundary of the obstacle) while the last four rows are determined by the RBC imposed on Γ_{abs} the artificial boundary. The derivation of the four first lines is similar to the ones given in Sections 6.2, 6.3 or 6.4.Therefore, we only detail here the derivation associated to the RBC in order to obtain the last four lines of $\mathbb{A}^{\text{rbc-Ti}}$. On $r = \mathfrak{b}$, we apply condition (8.11) and we replace the unknowns using equation (6.14):

- $\tau_{rr} + \mathbf{X}_1 \mathrm{u}_r + \mathbf{X}_2 \mathrm{w}_r = 0$ gives:

$$\begin{aligned} &\frac{\mathrm{i}\,\mu_{\text{fr}}}{\omega}\left(-\frac{2}{\mathsf{s}_{\text{P}}^2}\,\partial_{r^2}\chi_{\text{P}} \;-\; \frac{2}{\mathsf{s}_{\text{B}}^2}\,\partial_{r^2}\chi_{\text{B}} \;+\; \frac{2}{\mathsf{s}_{\text{S}}^2}\left(\frac{1}{\mathfrak{b}}\partial_{r\theta} - \frac{1}{\mathfrak{b}^2}\partial_\theta\right)\chi_{\text{S}} \;+\; \frac{2}{\mathsf{s}_{\text{EM}}^2}\left(\frac{1}{\mathfrak{b}}\partial_{r\theta} - \frac{1}{\mathfrak{b}^2}\partial_\theta\right)\chi_{\text{EM}}\right) \\ &\quad + \mathrm{i}\,\omega\left(-\frac{2}{3}\mu_{\text{fr}} + \mathrm{k}_{\text{fr}} + M\alpha^2\right)(\chi_{\text{P}} + \chi_{\text{B}}) \quad + \mathrm{i}\,\omega\alpha\, M\,(w_{\text{P}}\,\chi_{\text{P}} + w_{\text{B}}\,\chi_{\text{B}}) \\ &+ \mathbf{X}_1\left(\frac{1}{\mathsf{s}_{\text{P}}^2}\,\partial_r\chi_{\text{P}} + \frac{1}{\mathsf{s}_{\text{B}}^2}\,\partial_r\chi_{\text{B}} - \frac{1}{\mathsf{s}_{\text{S}}^2\,\mathfrak{b}}\,\partial_\theta\chi_{\text{S}} - \frac{1}{\mathsf{s}_{\text{EM}}^2\,\mathfrak{b}}\,\partial_\theta\chi_{\text{EM}}\right) \\ &+ \mathbf{X}_2\left(\frac{w_{\text{P}}}{\mathsf{s}_{\text{P}}^2}\partial_r\chi_{\text{P}} + \frac{w_{\text{B}}}{\mathsf{s}_{\text{B}}^2}\partial_r\chi_{\text{B}} - \frac{w_{\text{S}}}{\mathsf{s}_{\text{S}}^2\,\mathfrak{b}}\,\partial_\theta\chi_{\text{S}} - \frac{w_{\text{EM}}}{\mathsf{s}_{\text{EM}}^2\,\mathfrak{b}}\,\partial_\theta\chi_{\text{EM}}\right) = 0\,. \end{aligned}$$

- $\tau_{r\theta} + \mathbf{X}_3 \mathrm{u}_\theta + \mathbf{X}_4 \boldsymbol{E}_\theta = 0$ is expressed as

$$\begin{aligned} &-\frac{2\,\mu_{\text{fr}}}{\mathsf{s}_{\text{P}}^2}\left(\frac{1}{\mathfrak{b}}\partial_{r\theta} - \frac{1}{\mathfrak{b}^2}\partial_\theta\right)\chi_{\text{P}} \;-\; \frac{2\,\mu_{\text{fr}}}{\mathsf{s}_{\text{B}}^2}\left(\frac{1}{\mathfrak{b}}\partial_{r\theta} - \frac{1}{\mathfrak{b}^2}\partial_\theta\right)\chi_{\text{B}} \;+\; \frac{1}{\mathsf{s}_{\text{S}}^2}\left(\frac{\mu_{\text{fr}}}{\mathfrak{b}^2}\partial_{\theta\theta} + \frac{1}{\mathfrak{b}}\partial_r - \partial_{r^2}\right)\chi_{\text{S}} \\ &+ \frac{\mu_{\text{fr}}}{\mathsf{s}_{\text{EM}}^2}\left(\frac{1}{\mathfrak{b}^2}\partial_{\theta\theta} + \frac{1}{\mathfrak{b}}\partial_r - \partial_{r^2}\right)\chi_{\text{EM}} - \mathbf{X}_3\,\mathrm{i}\,\omega\left(\mathsf{s}_{\text{P}}^{-2}\,\frac{1}{\mathfrak{b}}\partial_\theta\chi_{\text{P}} + \mathsf{s}_{\text{B}}^{-2}\,\frac{1}{\mathfrak{b}}\partial_\theta\chi_{\text{B}} + \mathsf{s}_{\text{S}}^{-2}\,\partial_r\chi_{\text{S}} + \mathsf{s}_{\text{EM}}^{-2}\,\partial_r\chi_{\text{EM}}\right) \\ &- \mathbf{X}_4\left(\mathcal{E}_{\text{P}}\mathsf{s}_{\text{P}}^{-2}\,\frac{1}{\mathfrak{b}}\partial_\theta\chi_{\text{P}} + \mathcal{E}_{\text{B}}\mathsf{s}_{\text{B}}^{-2}\,\frac{1}{\mathfrak{b}}\partial_\theta\chi_{\text{B}} + \mathcal{E}_{\text{S}}\mathsf{s}_{\text{S}}^{-2}\,\partial_r\chi_{\text{S}} + \mathcal{E}_{\text{EM}}\mathsf{s}_{\text{EM}}^{-2}\,\partial_r\chi_{\text{EM}}\right) = 0\,. \end{aligned}$$

- Next, we write $\mathrm{p} + \mathbf{X}_5 \mathrm{u}_r + \mathbf{X}_6 \mathrm{w}_r = 0$ as

$$\begin{aligned} &-\mathrm{i}\,\omega\, M\,(w_{\text{P}} + \alpha)\chi_{\text{P}} - \mathrm{i}\,\omega\, M\,(w_{\text{B}} + \alpha)\chi_{\text{B}} + \mathbf{X}_5\left(\frac{1}{\mathsf{s}_{\text{P}}^2}\,\partial_r\chi_{\text{P}} + \frac{1}{\mathsf{s}_{\text{B}}^2}\,\partial_r\chi_{\text{B}} - \frac{1}{\mathsf{s}_{\text{S}}^2\,\mathfrak{b}}\,\partial_\theta\chi_{\text{S}} - \frac{1}{\mathsf{s}_{\text{EM}}^2\,\mathfrak{b}}\,\partial_\theta\chi_{\text{EM}}\right) \\ &+ \mathbf{X}_6\left(\frac{w_{\text{P}}}{\mathsf{s}_{\text{P}}^2}\partial_r\chi_{\text{P}} + \frac{w_{\text{B}}}{\mathsf{s}_{\text{B}}^2}\partial_r\chi_{\text{B}} - \frac{w_{\text{S}}}{\mathsf{s}_{\text{S}}^2\,\mathfrak{b}}\partial_\theta\,\chi_{\text{S}} - \frac{w_{\text{EM}}}{\mathsf{s}_{\text{EM}}^2\,\mathfrak{b}}\partial_\theta\,\chi_{\text{EM}}\right) = 0\,. \end{aligned}$$

- Finally, the expression of $\mathrm{H} + \mathbf{X}_7 \mathrm{u}_\theta + \mathbf{X}_8\, E_\theta = 0$ is

$$\begin{aligned} &\frac{\mathrm{i}}{\omega\,\mu_0}\left(\mathcal{E}_{\text{S}}\,\chi_{\text{S}} + \mathcal{E}_{\text{EM}}\,\chi_{\text{EM}}\right) + \frac{\mathbf{X}_7}{\mathrm{i}\,\omega}\left(\mathsf{s}_{\text{P}}^{-2}\,\frac{1}{\mathfrak{b}}\partial_\theta\chi_{\text{P}} + \mathsf{s}_{\text{B}}^{-2}\,\frac{1}{\mathfrak{b}}\partial_\theta\chi_{\text{B}} + \mathsf{s}_{\text{S}}^{-2}\,\partial_r\chi_{\text{S}} + \mathsf{s}_{\text{EM}}^{-2}\,\partial_r\chi_{\text{EM}}\right) \\ &- \frac{\mathbf{X}_8}{\omega^2}\left(\mathcal{E}_{\text{P}}\mathsf{s}_{\text{P}}^{-2}\,\frac{1}{\mathfrak{b}}\partial_\theta\chi_{\text{P}} + \mathcal{E}_{\text{B}}\mathsf{s}_{\text{B}}^{-2}\,\frac{1}{\mathfrak{b}}\partial_\theta\chi_{\text{B}} + \mathcal{E}_{\text{S}}\mathsf{s}_{\text{S}}^{-2}\,\partial_r\chi_{\text{S}} + \mathcal{E}_{\text{EM}}\mathsf{s}_{\text{EM}}^{-2}\,\partial_r\chi_{\text{EM}}\right) = 0\,. \end{aligned}$$

The matrix components corresponding to the RBC are given by:

$$
\begin{aligned}
A_{51} =& -2\,\mathrm{i}\,\mu_{\mathrm{fr}}\,\omega\,\mathrm{H}_k^{(1)''}(\omega\,\mathsf{s}_{\mathrm{P}}\,\mathfrak{b}) + \mathrm{i}\omega(-\frac{2}{3}\mu_{\mathrm{fr}} + \mathrm{k}_{\mathrm{fr}} + M\,\alpha(\alpha + w_{\mathrm{P}}))\,\mathrm{H}_k^{(1)}(\omega\,\mathsf{s}_{\mathrm{P}}\,\mathfrak{b}) \\
&+ \frac{\boldsymbol{X}_1\,\omega}{\mathsf{s}_{\mathrm{P}}}\mathrm{H}_k^{(1)'}(\omega\,\mathsf{s}_{\mathrm{P}}\,\mathfrak{b}) + \frac{\boldsymbol{X}_2\,\omega\,w_{\mathrm{P}}}{\mathsf{s}_{\mathrm{P}}}\,\mathrm{H}_k^{(1)'}(\omega\,\mathsf{s}_{\mathrm{P}}\,\mathfrak{b}),
\end{aligned}
$$

$$
\begin{aligned}
A_{52} =& -2\,\mathrm{i}\,\mu_{\mathrm{fr}}\,\omega\,\mathrm{H}_k^{(1)''}(\omega\,\mathsf{s}_{\mathrm{B}}\,\mathfrak{b}) + \mathrm{i}\omega(-\frac{2}{3}\mu_{\mathrm{fr}} + \mathrm{k}_{\mathrm{fr}} + M\,\alpha(\alpha + w_{\mathrm{B}}))\,\mathrm{H}_k^{(1)}(\omega\,\mathsf{s}_{\mathrm{B}}\,\mathfrak{b}) \\
&+ \frac{\boldsymbol{X}_1\,\omega}{\mathsf{s}_{\mathrm{B}}}\mathrm{H}_k^{(1)'}(\omega\,\mathsf{s}_{\mathrm{B}}\,\mathfrak{b}) + \frac{\boldsymbol{X}_2\,\omega\,w_{\mathrm{B}}}{\mathsf{s}_{\mathrm{B}}}\,\mathrm{H}_k^{(1)'}(\omega\,\mathsf{s}_{\mathrm{B}}\,\mathfrak{b}),
\end{aligned}
$$

$$
A_{53} = -\frac{2\,\mu_{\mathrm{fr}}\,k}{\mathsf{s}_{\mathrm{S}}\,\mathfrak{b}}\,\mathrm{H}_k^{(1)'}(\omega\,\mathsf{s}_{\mathrm{S}}\,\mathfrak{b}) + \frac{2\,\mu_{\mathrm{fr}}\,k}{\omega\mathsf{s}_{\mathrm{S}}^2\,\mathfrak{b}^2}\,\mathrm{H}_k^{(1)}(\omega\,\mathsf{s}_{\mathrm{S}}\,\mathfrak{b}) - \frac{\boldsymbol{X}_1\,\mathrm{i}\,k}{\mathsf{s}_{\mathrm{S}}^2\,\mathfrak{b}}\,\mathrm{H}_k^{(1)}(\omega\,\mathsf{s}_{\mathrm{S}}\,\mathfrak{b}) - \frac{\boldsymbol{X}_2\,w_{\mathrm{S}}\,\mathrm{i}\,k}{\mathsf{s}_{\mathrm{S}}^2\,\mathfrak{b}}\,\mathrm{H}_k^{(1)}(\omega\,\mathsf{s}_{\mathrm{S}}\,\mathfrak{b}),
$$

$$
A_{54} = -\frac{2\,\mu_{\mathrm{fr}}\,k}{\mathsf{s}_{\mathrm{EM}}\,\mathfrak{b}}\,\mathrm{H}_k^{(1)'}(\omega\,\mathsf{s}_{\mathrm{EM}}\,\mathfrak{b}) + \frac{2\,\mu_{\mathrm{fr}}\,k}{\omega\mathsf{s}_{\mathrm{EM}}^2\,\mathfrak{b}^2}\,\mathrm{H}_k^{(1)}(\omega\,\mathsf{s}_{\mathrm{EM}}\,\mathfrak{b}) - \frac{\boldsymbol{X}_1\,\mathrm{i}\,k}{\mathsf{s}_{\mathrm{EM}}^2\,\mathfrak{b}}\,\mathrm{H}_k^{(1)}(\omega\,\mathsf{s}_{\mathrm{EM}}\,\mathfrak{b}) - \frac{\boldsymbol{X}_2\,w_{\mathrm{EM}}\,\mathrm{i}\,k}{\mathsf{s}_{\mathrm{EM}}^2\,\mathfrak{b}}\,\mathrm{H}_k^{(1)}(\omega\,\mathsf{s}_{\mathrm{EM}}\,\mathfrak{b}),
$$

$$
\begin{aligned}
A_{55} =& -2\,\mathrm{i}\,\mu_{\mathrm{fr}}\,\omega\,\mathrm{H}_k^{(2)''}(\omega\,\mathsf{s}_{\mathrm{P}}\,\mathfrak{b}) + \mathrm{i}\omega(-\frac{2}{3}\mu_{\mathrm{fr}} + \mathrm{k}_{\mathrm{fr}} + M\,\alpha(\alpha + w_{\mathrm{P}}))\mathrm{H}_k^{(2)}(\omega\,\mathsf{s}_{\mathrm{P}}\,\mathfrak{b}) \\
&+ \frac{\boldsymbol{X}_1\,\omega}{\mathsf{s}_{\mathrm{P}}}\mathrm{H}_k^{(2)'}(\omega\,\mathsf{s}_{\mathrm{P}}\,\mathfrak{b}) + \frac{\boldsymbol{X}_2\,\omega w_{\mathrm{P}}}{\mathsf{s}_{\mathrm{P}}}\,\mathrm{H}_k^{(2)'}(\omega\,\mathsf{s}_{\mathrm{P}}\,\mathfrak{b}),
\end{aligned}
$$

$$
\begin{aligned}
A_{56} =& -2\,\mathrm{i}\,\mu_{\mathrm{fr}}\,\omega\,\mathrm{H}_k^{(2)''}(\omega\,\mathsf{s}_{\mathrm{B}}\,\mathfrak{b}) + \mathrm{i}\omega(-\frac{2}{3}\mu_{\mathrm{fr}} + \mathrm{k}_{\mathrm{fr}} + M\,\alpha(\alpha + w_{\mathrm{B}}))\mathrm{H}_k^{(2)}(\omega\,\mathsf{s}_{\mathrm{B}}\,\mathfrak{b}) \\
&+ \frac{\boldsymbol{X}_1\,\omega}{\mathsf{s}_{\mathrm{B}}}\mathrm{H}_k^{(2)'}(\omega\,\mathsf{s}_{\mathrm{B}}\,\mathfrak{b}) + \frac{\boldsymbol{X}_2\,\omega w_{\mathrm{B}}}{\mathsf{s}_{\mathrm{B}}}\,\mathrm{H}_k^{(2)'}(\omega\,\mathsf{s}_{\mathrm{B}}\,\mathfrak{b}),
\end{aligned}
$$

$$
A_{57} = -\frac{2\,\mu_{\mathrm{fr}}\,k}{\mathsf{s}_{\mathrm{S}}\,\mathfrak{b}}\,\mathrm{H}_k^{(2)'}(\omega\,\mathsf{s}_{\mathrm{S}}\,\mathfrak{b}) + \frac{2\,\mu_{\mathrm{fr}}\,k}{\omega\mathsf{s}_{\mathrm{S}}^2\,\mathfrak{b}^2}\,\mathrm{H}_k^{(2)}(\omega\,\mathsf{s}_{\mathrm{S}}\,\mathfrak{b}) - \frac{\boldsymbol{X}_1\,\mathrm{i}\,k}{\mathsf{s}_{\mathrm{S}}^2\,\mathfrak{b}}\,\mathrm{H}_k^{(2)}(\omega\,\mathsf{s}_{\mathrm{S}}\,\mathfrak{b}) - \frac{\boldsymbol{X}_2\,w_{\mathrm{S}}\,\mathrm{i}\,k}{\mathsf{s}_{\mathrm{S}}^2\,\mathfrak{b}}\,\mathrm{H}_k^{(1)}(\omega\,\mathsf{s}_{\mathrm{S}}\,\mathfrak{b}),
$$

$$
A_{58} = -\frac{2\,\mu_{\mathrm{fr}}\,k}{\mathsf{s}_{\mathrm{EM}}\,\mathfrak{b}}\,\mathrm{H}_k^{(2)'}(\omega\,\mathsf{s}_{\mathrm{EM}}\,\mathfrak{b}) + \frac{2\,\mu_{\mathrm{fr}}\,k}{\omega\mathsf{s}_{\mathrm{EM}}^2\,\mathfrak{b}^2}\,\mathrm{H}_k^{(2)}(\omega\,\mathsf{s}_{\mathrm{EM}}\,\mathfrak{b}) - \frac{\boldsymbol{X}_1\,\mathrm{i}\,k}{\mathsf{s}_{\mathrm{EM}}^2\,\mathfrak{b}}\,\mathrm{H}_k^{(2)}(\omega\,\mathsf{s}_{\mathrm{EM}}\,\mathfrak{b}) - \frac{\boldsymbol{X}_2\,w_{\mathrm{EM}}\,\mathrm{i}\,k}{\mathsf{s}_{\mathrm{EM}}^2\,\mathfrak{b}}\,\mathrm{H}_k^{(1)}(\omega\,\mathsf{s}_{\mathrm{EM}}\,\mathfrak{b}),
$$

$$
A_{61} = -\frac{2\,\mu_{\mathrm{fr}}\,\omega\,\mathrm{i}\,k}{\mathsf{s}_{\mathrm{P}}\,\mathfrak{b}}\,\mathrm{H}_k^{(1)'}(\omega\,\mathsf{s}_{\mathrm{P}}\,\mathfrak{b}) + \frac{2\,\mu_{\mathrm{fr}}\,\mathrm{i}\,k}{\mathsf{s}_{\mathrm{P}}^2\,\mathfrak{b}^2}\,\mathrm{H}_k^{(1)}(\omega\,\mathsf{s}_{\mathrm{P}}\,\mathfrak{b}) + \frac{\boldsymbol{X}_3\,\omega\,k}{\mathsf{s}_{\mathrm{P}}^2\mathfrak{b}}\mathrm{H}_k^{(1)}(\omega\,\mathsf{s}_{\mathrm{P}}\,\mathfrak{b}) - \frac{\boldsymbol{X}_4\,\mathcal{E}_{\mathrm{P}}\,\mathrm{i}\,k}{\mathsf{s}_{\mathrm{P}}^2\mathfrak{b}}\mathrm{H}_k^{(1)}(\omega\,\mathsf{s}_{\mathrm{P}}\,\mathfrak{b}),
$$

$$
A_{62} = -\frac{2\,\mu_{\mathrm{fr}}\,\omega\,\mathrm{i}\,k}{\mathsf{s}_{\mathrm{B}}\,\mathfrak{b}}\,\mathrm{H}_k^{(1)'}(\omega\,\mathsf{s}_{\mathrm{B}}\,\mathfrak{b}) + \frac{2\,\mu_{\mathrm{fr}}\,\mathrm{i}\,k}{\mathsf{s}_{\mathrm{B}}^2\,\mathfrak{b}^2}\,\mathrm{H}_k^{(1)}(\omega\,\mathsf{s}_{\mathrm{B}}\,\mathfrak{b}) + \frac{\boldsymbol{X}_3\,\omega\,k}{\mathsf{s}_{\mathrm{B}}^2\mathfrak{b}}\mathrm{H}_k^{(1)}(\omega\,\mathsf{s}_{\mathrm{B}}\,\mathfrak{b}) - \frac{\boldsymbol{X}_4\mathcal{E}_{\mathrm{B}}\,\mathrm{i}\,k}{\mathsf{s}_{\mathrm{B}}^2\mathfrak{b}}\mathrm{H}_k^{(1)}(\omega\,\mathsf{s}_{\mathrm{B}}\,\mathfrak{b}),
$$

$$
\begin{aligned}
A_{63} =& -\frac{k^2\,\mu_{\mathrm{fr}}}{\mathsf{s}_{\mathrm{S}}^2\,\mathfrak{b}^2}\,\mathrm{H}_k^{(1)}(\omega\,\mathsf{s}_{\mathrm{S}}\,\mathfrak{b}) + \frac{\omega\,\mu_{\mathrm{fr}}}{\mathsf{s}_{\mathrm{S}}\,\mathfrak{b}}\,\mathrm{H}_k^{(1)'}(\omega\,\mathsf{s}_{\mathrm{S}}\,\mathfrak{b}) - \omega^2\,\mu_{\mathrm{fr}}\,\mathrm{H}_k^{(1)''}(\omega\,\mathsf{s}_{\mathrm{S}}\,\mathfrak{b}) \\
&- \frac{\boldsymbol{X}_3\,\omega^2\,\mathrm{i}}{\mathsf{s}_{\mathrm{S}}}\,\mathrm{H}_k^{(1)'}(\omega\,\mathsf{s}_{\mathrm{S}}\,\mathfrak{b}) - \frac{\boldsymbol{X}_4\,\mathcal{E}_{\mathrm{S}}\omega}{\mathsf{s}_{\mathrm{S}}}\,\mathrm{H}_k^{(1)'}(\omega\,\mathsf{s}_{\mathrm{S}}\,\mathfrak{b}),
\end{aligned}
$$

$$
\begin{aligned}
A_{64} =& -\frac{k^2\,\mu_{\mathrm{fr}}}{\mathsf{s}_{\mathrm{EM}}^2\,\mathfrak{b}^2}\,\mathrm{H}_k^{(1)}(\omega\,\mathsf{s}_{\mathrm{EM}}\,\mathfrak{b}) + \frac{\omega\,\mu_{\mathrm{fr}}}{\mathsf{s}_{\mathrm{EM}}\,\mathfrak{b}}\,\mathrm{H}_k^{(1)'}(\omega\,\mathsf{s}_{\mathrm{EM}}\,\mathfrak{b}) - \omega^2\,\mu_{\mathrm{fr}}\,\mathrm{H}_k^{(1)''}(\omega\,\mathsf{s}_{\mathrm{EM}}\,\mathfrak{b}) \\
&- \frac{\boldsymbol{X}_3\,\omega^2\,\mathrm{i}}{\mathsf{s}_{\mathrm{EM}}}\,\mathrm{H}_k^{(1)'}(\omega\,\mathsf{s}_{\mathrm{EM}}\,\mathfrak{b}) - \frac{\boldsymbol{X}_4\,\mathcal{E}_{\mathrm{EM}}\omega}{\mathsf{s}_{\mathrm{EM}}}\,\mathrm{H}_k^{(1)'}(\omega\,\mathsf{s}_{\mathrm{EM}}\,\mathfrak{b}),
\end{aligned}
$$

$$A_{65} = -\frac{2\,\mu_{\rm fr}\,\omega\,{\rm i}\,k}{{\sf s}_{\rm P}\,\mathfrak{b}}\,{\rm H}_k^{(2)'}(\omega\,{\sf s}_{\rm P}\,\mathfrak{b}) + \frac{2\,\mu_{\rm fr}\,{\rm i}\,k}{{\sf s}_{\rm P}^2\,\mathfrak{b}^2}\,{\rm H}_k^{(2)}(\omega\,{\sf s}_{\rm P}\,\mathfrak{b}) + \frac{\boldsymbol{X}_3\,\omega\,k}{{\sf s}_{\rm P}^2\mathfrak{b}}{\rm H}_k^{(1)}(\omega\,{\sf s}_{\rm P}\,\mathfrak{b}),$$

$$A_{66} = -\frac{2\,\mu_{\rm fr}\,\omega\,{\rm i}\,k}{{\sf s}_{\rm B}\,\mathfrak{b}}\,{\rm H}_k^{(2)'}(\omega\,{\sf s}_{\rm B}\,\mathfrak{b}) + \frac{2\,\mu_{\rm fr}\,{\rm i}\,k}{{\sf s}_{\rm B}^2\,\mathfrak{b}^2}\,{\rm H}_k^{(2)}(\omega\,{\sf s}_{\rm B}\,\mathfrak{b}) + \frac{\boldsymbol{X}_3\,\omega\,k}{{\sf s}_{\rm B}^2\mathfrak{b}}{\rm H}_k^{(2)}(\omega\,{\sf s}_{\rm B}\,\mathfrak{b}) - \frac{\boldsymbol{X}_4\mathcal{E}_{\rm B}\,{\rm i}\,k}{{\sf s}_{\rm B}^2\mathfrak{b}}{\rm H}_k^{(2)}(\omega\,{\sf s}_{\rm B}\,\mathfrak{b}),$$

$$A_{67} = -\frac{k^2\,\mu_{\rm fr}}{{\sf s}_{\rm S}^2\,\mathfrak{b}^2}\,{\rm H}_k^{(2)}(\omega\,{\sf s}_{\rm S}\,\mathfrak{b}) + \frac{\omega}{{\sf s}_{\rm S}\,\mathfrak{b}}\,{\rm H}_k^{(2)'}(\omega\,{\sf s}_{\rm S}\,\mathfrak{b}) - \omega^2\,\mu_{\rm fr}\,{\rm H}_k^{(2)''}(\omega\,{\sf s}_{\rm S}\,\mathfrak{b})$$
$$- \frac{\boldsymbol{X}_3\,\omega^2\,{\rm i}}{{\sf s}_{\rm S}}\,{\rm H}_k^{(2)'}(\omega\,{\sf s}_{\rm S}\,\mathfrak{b}) - \frac{\boldsymbol{X}_4\,\mathcal{E}_{\rm S}\omega}{{\sf s}_{\rm S}}\,{\rm H}_k^{(2)'}(\omega\,{\sf s}_{\rm S}\,\mathfrak{b}),$$

$$A_{68} = -\frac{k^2\,\mu_{\rm fr}}{{\sf s}_{\rm EM}^2\,\mathfrak{b}^2}\,{\rm H}_k^{(2)}(\omega\,{\sf s}_{\rm EM}\,\mathfrak{b}) + \frac{\omega\,\mu_{\rm fr}}{{\sf s}_{\rm EM}\,\mathfrak{b}}\,{\rm H}_k^{(2)'}(\omega\,{\sf s}_{\rm EM}\,\mathfrak{b}) - \omega^2\,\mu_{\rm fr}\,{\rm H}_k^{(1)''}(\omega\,{\sf s}_{\rm EM}\,\mathfrak{b})$$
$$- \frac{\boldsymbol{X}_3\,\omega^2\,{\rm i}}{{\sf s}_{\rm EM}}\,{\rm H}_k^{(2)'}(\omega\,{\sf s}_{\rm EM}\,\mathfrak{b}) - \frac{\boldsymbol{X}_4\,\mathcal{E}_{\rm EM}\omega}{{\sf s}_{\rm EM}}\,{\rm H}_k^{(2)'}(\omega\,{\sf s}_{\rm EM}\,\mathfrak{b}),$$

$$A_{71} = -{\rm i}\,\omega\,M\,(w_{\rm P}+\alpha){\rm H}_k^{(1)}(\omega\,{\sf s}_{\rm P}\,\mathfrak{b}) + \frac{\boldsymbol{X}_5\,\omega}{{\sf s}_{\rm P}}{\rm H}_k^{(1)'}(\omega\,{\sf s}_{\rm P}\,\mathfrak{b}) + \frac{\boldsymbol{X}_6\,\omega\,w_{\rm P}}{{\sf s}_{\rm P}}\,{\rm H}_k^{(1)'}(\omega\,{\sf s}_{\rm P}\,\mathfrak{b}),$$

$$A_{72} = -{\rm i}\,\omega\,M\,(w_{\rm B}+\alpha){\rm H}_k^{(1)}(\omega\,{\sf s}_{\rm B}\,\mathfrak{b}) + \frac{\boldsymbol{X}_5\,\omega}{{\sf s}_{\rm B}}{\rm H}_k^{(1)'}(\omega\,{\sf s}_{\rm B}\,\mathfrak{b}) + \frac{\boldsymbol{X}_6\,\omega\,w_{\rm B}}{{\sf s}_{\rm B}}\,{\rm H}_k^{(1)'}(\omega\,{\sf s}_{\rm B}\,\mathfrak{b}),$$

$$A_{73} = -\frac{\boldsymbol{X}_5\,{\rm i}\,k}{{\sf s}_{\rm S}^2\,\mathfrak{b}}\,{\rm H}_k^{(1)}(\omega\,{\sf s}_{\rm S}\,\mathfrak{b}) - \frac{\boldsymbol{X}_6\,w_{\rm S}\,{\rm i}\,k}{{\sf s}_{\rm S}^2}\,{\rm H}_k^{(1)}(\omega\,{\sf s}_{\rm S}\,\mathfrak{b}),$$

$$A_{74} = -\frac{\boldsymbol{X}_5\,{\rm i}\,k}{{\sf s}_{\rm EM}^2\,\mathfrak{b}}\,{\rm H}_k^{(1)}(\omega\,{\sf s}_{\rm EM}\,\mathfrak{b}) - \frac{\boldsymbol{X}_6\,w_{\rm EM}\,{\rm i}\,k}{{\sf s}_{\rm S}^2}\,{\rm H}_k^{(1)}(\omega\,{\sf s}_{\rm EM}\,\mathfrak{b}),$$

$$A_{75} = -{\rm i}\,\omega\,M\,(w_{\rm P}+\alpha){\rm H}_k^{(2)}(\omega\,{\sf s}_{\rm P}\,\mathfrak{b}) + \frac{\boldsymbol{X}_5\,\omega}{{\sf s}_{\rm P}}{\rm H}_k^{(2)'}(\omega\,{\sf s}_{\rm P}\,\mathfrak{b}) + \frac{\boldsymbol{X}_6\,\omega\,w_{\rm P}}{{\sf s}_{\rm P}}\,{\rm H}_k^{(2)'}(\omega\,{\sf s}_{\rm P}\,\mathfrak{b}),$$

$$A_{76} = -{\rm i}\,\omega\,M\,(w_{\rm B}+\alpha){\rm H}_k^{(2)}(\omega\,{\sf s}_{\rm B}\,\mathfrak{b}) + \frac{\boldsymbol{X}_5\,\omega}{{\sf s}_{\rm B}}{\rm H}_k^{(2)'}(\omega\,{\sf s}_{\rm B}\,\mathfrak{b}) + \frac{\boldsymbol{X}_6\,\omega\,w_{\rm B}}{{\sf s}_{\rm B}}\,{\rm H}_k^{(2)'}(\omega\,{\sf s}_{\rm B}\,\mathfrak{b}),$$

$$A_{77} = -\frac{\boldsymbol{X}_5\,{\rm i}\,k}{{\sf s}_{\rm S}^2\,\mathfrak{b}}\,{\rm H}_k^{(2)}(\omega\,{\sf s}_{\rm S}\,\mathfrak{b}) - \frac{\boldsymbol{X}_6\,w_{\rm S}\,{\rm i}\,k}{{\sf s}_{\rm S}^2}\,{\rm H}_k^{(2)}(\omega\,{\sf s}_{\rm S}\,\mathfrak{b}),$$

$$A_{78} = -\frac{\boldsymbol{X}_5\,{\rm i}\,k}{{\sf s}_{\rm EM}^2\,\mathfrak{b}}\,{\rm H}_k^{(2)}(\omega\,{\sf s}_{\rm EM}\,\mathfrak{b}) - \frac{\boldsymbol{X}_6\,w_{\rm EM}\,{\rm i}\,k}{{\sf s}_{\rm S}^2}\,{\rm H}_k^{(2)}(\omega\,{\sf s}_{\rm EM}\,\mathfrak{b}),$$

$$A_{81} = \frac{\boldsymbol{X}_7\,k}{{\sf s}_{\rm P}^2\,\omega\,\mathfrak{b}}{\rm H}_k^{(1)}(\omega\,{\sf s}_{\rm P}\,\mathfrak{b}) - \frac{\boldsymbol{X}_8\,\mathcal{E}_{\rm P}\,{\rm i}\,k}{{\sf s}_{\rm P}^2\,\omega^2\,\mathfrak{b}}{\rm H}_k^{(1)}(\omega\,{\sf s}_{\rm P}\,\mathfrak{b}),$$

$$A_{82} = \frac{\boldsymbol{X}_7\,k}{{\sf s}_{\rm B}^2\,\omega\,\mathfrak{b}}{\rm H}_k^{(1)}(\omega\,{\sf s}_{\rm B}\,\mathfrak{b}) - \frac{\boldsymbol{X}_8\mathcal{E}_{\rm B}\,{\rm i}\,k}{{\sf s}_{\rm B}^2\,\omega^2\,\mathfrak{b}}{\rm H}_k^{(1)}(\omega\,{\sf s}_{\rm B}\,\mathfrak{b}),$$

$$A_{83} = \mathcal{E}_{\rm S}\,\frac{\rm i}{\omega\,\mu_0}\,{\rm H}_k^{(1)}(\omega\,{\sf s}_{\rm S}\,\mathfrak{b}) - \frac{\boldsymbol{X}_7\,{\rm i}}{{\sf s}_{\rm S}}\,{\rm H}_k^{(1)'}(\omega\,{\sf s}_{\rm S}\,\mathfrak{b}) - \frac{\boldsymbol{X}_8\,\mathcal{E}_{\rm S}}{\omega\,{\sf s}_{\rm S}}\,{\rm H}_k^{(1)'}(\omega\,{\sf s}_{\rm S}\,\mathfrak{b}),$$

$$A_{84} = \mathcal{E}_{\rm EM}\,\frac{\rm i}{\omega\,\mu_0}\,{\rm H}_k^{(1)}(\omega\,{\sf s}_{\rm EM}\,\mathfrak{b}) - \frac{\boldsymbol{X}_7\,{\rm i}}{{\sf s}_{\rm EM}}\,{\rm H}_k^{(1)'}(\omega\,{\sf s}_{\rm EM}\,\mathfrak{b}) - \frac{\boldsymbol{X}_8\,\mathcal{E}_{\rm EM}}{\omega\,{\sf s}_{\rm EM}}\,{\rm H}_k^{(1)'}(\omega\,{\sf s}_{\rm EM}\,\mathfrak{b}),$$

$$A_{85} = \frac{\boldsymbol{X}_7\, k}{\mathsf{s}_{\mathrm{P}}^2\, \omega\, \mathfrak{b}} \mathrm{H}_k^{(2)}(\omega\, \mathsf{s}_{\mathrm{P}}\, \mathfrak{b}) \; - \; \frac{\boldsymbol{X}_8\, \mathcal{E}_{\mathrm{P}}\, \mathrm{i}\, k}{\mathsf{s}_{\mathrm{P}}^2\, \omega^2\, \mathfrak{b}} \mathrm{H}_k^{(2)}(\omega\, \mathsf{s}_{\mathrm{P}}\, \mathfrak{b})\,,$$

$$A_{86} = \frac{\boldsymbol{X}_7\, k}{\mathsf{s}_{\mathrm{B}}^2\, \omega\, \mathfrak{b}} \mathrm{H}_k^{(2)}(\omega\, \mathsf{s}_{\mathrm{B}}\, \mathfrak{b}) - \frac{\boldsymbol{X}_8 \mathcal{E}_{\mathrm{B}}\, \mathrm{i}\, k}{\mathsf{s}_{\mathrm{B}}^2\, \omega^2\, \mathfrak{b}} \mathrm{H}_k^{(2)}(\omega\, \mathsf{s}_{\mathrm{B}}\, \mathfrak{b})\,,$$

$$A_{87} = \mathcal{E}_{\mathrm{S}}\, \frac{\mathrm{i}}{\omega\, \mu_0}\, \mathrm{H}_k^{(2)}(\omega\, \mathsf{s}_{\mathrm{S}}\, \mathfrak{b}) \; - \; \frac{\boldsymbol{X}_7\, \mathrm{i}}{\mathsf{s}_{\mathrm{S}}}\, \mathrm{H}_k^{(2)'}(\omega\, \mathsf{s}_{\mathrm{S}}\, \mathfrak{b}) - \; \frac{\boldsymbol{X}_8\, \mathcal{E}_{\mathrm{S}}}{\omega\, \mathsf{s}_{\mathrm{S}}}\, \mathrm{H}_k^{(2)'}(\omega\, \mathsf{s}_{\mathrm{S}}\, \mathfrak{b})\,,$$

$$A_{88} = \mathcal{E}_{\mathrm{EM}}\, \frac{\mathrm{i}}{\omega\, \mu_0}\, \mathrm{H}_k^{(2)}(\omega\, \mathsf{s}_{\mathrm{EM}}\, \mathfrak{b}) \; - \; \frac{\boldsymbol{X}_7\, \mathrm{i}}{\mathsf{s}_{\mathrm{EM}}}\, \mathrm{H}_k^{(2)'}(\omega\, \mathsf{s}_{\mathrm{EM}}\, \mathfrak{b}) - \; \frac{\boldsymbol{X}_8\, \mathcal{E}_{\mathrm{EM}}}{\omega\, \mathsf{s}_{\mathrm{EM}}}\, \mathrm{H}_k^{(2)'}(\omega\, \mathsf{s}_{\mathrm{EM}}\, \mathfrak{b})\,.$$

By inverting matrix $\mathbb{A}^{\text{rbc-Ti}}$ for every mode k, we obtained the series of coefficients. Then, we can obtain the value of the potentials $\chi_\bullet$ and the solution $\mathfrak{U}$. Now that we have obtained a reference solution, we are going to analyze the performance of the RBC using this solution.

8.3 Performance assessment of the RBC

We have constructed the analytical outgoing solution $\mathfrak{U}^{\infty-\mathrm{Ti}}$ and the RBC solution $\mathfrak{U}^{\text{rbc-Ti}}$ for the scattering of a plane wave by an impenetrable circular obstacle respectively in Sections 6.3 and 8.2. We consider the domain $\Omega_{\mathfrak{a}\mathfrak{b}}$ presented in Figure 8.2, and we denote by $\mathfrak{U}^{\infty-\mathrm{Ti}}$ the restriction of $\mathfrak{U}^{\infty-\mathrm{Ti}}$ to $\Omega_{\mathfrak{a}\mathfrak{b}}$. The boundary of the obstacle $\{r = \mathfrak{a}\}$ is denoted by Γ_1, and we set an artificial boundary at radius $\mathfrak{b}$. In the following, we investigate the performance of the RBC by comparing $\mathfrak{U}^{\infty-\mathrm{Ti}}$ to $\mathfrak{U}^{\text{rbc-Ti}}$. We focus on the boundary condition of type 1 ("Neumann-like") on $\mathfrak{a}$, see Section 5.4. We simplify the notations $\mathfrak{U}^{\infty-\mathrm{T1}}$ and $\mathfrak{U}^{\text{rbc-T1}}$ to $\mathfrak{U}^{\infty}$ and $\mathfrak{U}^{\text{rbc}}$. We study a material composed of sand1 (see Table 5.2), and we consider the scattering of the four plane waves of type (P, B, S, EM) by the obstacle. For all the numerical experiments, we set $\mathfrak{a} = 1\text{m}$, while the value of the frequency f and of the exterior radius $\mathfrak{b}$ will vary.

The outgoing solution $\mathfrak{U}^{\infty}$ is represented by the coefficients a_k^∞, b_k^∞, c_k^∞, d_k^∞, and the corresponding potentials $\chi_\bullet^\infty$ are given by

$$\chi_{\mathrm{P}}^\infty(r,\theta) \;=\; \sum_{k\in\mathbb{Z}} a_k^\infty\, \mathrm{H}_k^{(1)}(\omega\, \mathsf{s}_{\mathrm{P}}\, r)\; e^{\mathrm{i}\, k\, \theta}\,,$$

$$\chi_{\mathrm{B}}^\infty(r,\theta) \;=\; \sum_{k\in\mathbb{Z}} b_k^\infty\, \mathrm{H}_k^{(1)}(\omega\, \mathsf{s}_{\mathrm{B}}\, r)\; e^{\mathrm{i}\, k\, \theta}\,,$$

$$\chi_{\mathrm{S}}^\infty(r,\theta) \;=\; \sum_{k\in\mathbb{Z}} c_k^\infty\, \mathrm{H}_k^{(1)}(\omega\, \mathsf{s}_{\mathrm{S}}\, r)\; e^{\mathrm{i}\, k\, \theta}\,,$$

$$\chi_{\mathrm{EM}}^\infty(r,\theta) \;=\; \sum_{k\in\mathbb{Z}} d_k^\infty\, \mathrm{H}_k^{(1)}(\omega\, \mathsf{s}_{\mathrm{EM}}\, r)\; e^{\mathrm{i}\, k\, \theta}\,.$$

Similarly, the RBC solution $\mathfrak{U}^{\text{rbc}}$ is represented by the series of coefficients a_k, b_k, c_k, d_k, $\tilde{a}_k$, $\tilde{b}_k$, $\tilde{c}_k$, $\tilde{d}_k$, and the corresponding potentials $\chi_\bullet^{\text{rbc}}$ are given by

$$\chi_{\mathrm{P}}^{\text{rbc}}(r,\theta) \;=\; \sum_{k\in\mathbb{Z}} a_k\, \mathrm{H}_k^{(1)}(\omega\, \mathsf{s}_{\mathrm{P}}\, r)\; e^{\mathrm{i}\, k\, \theta} + \sum_{k\in\mathbb{Z}} \tilde{a}_k\, \mathrm{H}_k^{(2)}(\omega\, \mathsf{s}_{\mathrm{P}}\, r)\; e^{\mathrm{i}\, k\, \theta}\,,$$

$$\chi_{\mathrm{B}}^{\text{rbc}}(r,\theta) \;=\; \sum_{k\in\mathbb{Z}} b_k\, \mathrm{H}_k^{(1)}(\omega\, \mathsf{s}_{\mathrm{B}}\, r)\; e^{\mathrm{i}\, k\, \theta} + \sum_{k\in\mathbb{Z}} \tilde{b}_k\, \mathrm{H}_k^{(2)}(\omega\, \mathsf{s}_{\mathrm{B}}\, r)\; e^{\mathrm{i}\, k\, \theta}\,,$$

$$\chi_{\mathrm{S}}^{\text{rbc}}(r,\theta) \;=\; \sum_{k\in\mathbb{Z}} c_k\, \mathrm{H}_k^{(1)}(\omega\, \mathsf{s}_{\mathrm{S}}\, r)\; e^{\mathrm{i}\, k\, \theta} + \sum_{k\in\mathbb{Z}} \tilde{c}_k\, \mathrm{H}_k^{(2)}(\omega\, \mathsf{s}_{\mathrm{S}}\, r)\; e^{\mathrm{i}\, k\, \theta}\,,$$

$$\chi_{\mathrm{EM}}^{\text{rbc}}(r,\theta) \;=\; \sum_{k\in\mathbb{Z}} d_k\, \mathrm{H}_k^{(1)}(\omega\, \mathsf{s}_{\mathrm{EM}}\, r)\; e^{\mathrm{i}\, k\, \theta} + \sum_{k\in\mathbb{Z}} \tilde{d}_k\, \mathrm{H}_k^{(2)}(\omega\, \mathsf{s}_{\mathrm{EM}}\, r)\; e^{\mathrm{i}\, k\, \theta}\,.$$

The function $\mathrm{H}_k^{(2)}$ corresponds to the incoming solution, hence the coefficients associated to $\mathrm{H}_k^{(2)}$ are the coefficients representing the incoming part of the solution. For the solution to be accurate, we hence expect the coefficients $\tilde{a}_k$, $\tilde{b}_k$, $\tilde{c}_k$, $\tilde{d}_k$ to be small. In the numerical tests, the Hankel functions are infinite series truncated to the first N terms of the series, with $N \geq 2\mathbf{k}\mathfrak{a} + 1$ (see. [120]), where $\mathbf{k} = \max(k_{\mathrm{P}}, k_{\mathrm{B}}, k_{\mathrm{S}}, k_{\mathrm{EM}})$. We compare the outgoing and RBC solution using the following quantities:

- Comparison mode by mode of a_k^∞, b_k^∞, c_k^∞, d_k^∞ with a_k, b_k, c_k, d_k. Module of $\tilde{a}_k$, $\tilde{b}_k$, $\tilde{c}_k$, $\tilde{d}_k$.

- Relative L^2 error of u_x:

$$e_h(\mathrm{u}_x^{\mathrm{rbc}}) \;=\; \frac{||\mathrm{u}_x^{\mathrm{rbc}} - \mathrm{u}_x^{\infty}||_2}{||\mathrm{u}_x^{\infty}||_2}\,. \tag{8.15}$$

  The L^2 norm is theoretically equal to

$$||\mathrm{u}_x^{\mathrm{rbc}} - \mathrm{u}_x^{\infty}||_2 \;=\; \left(\int_{\Omega_{\mathfrak{a}\mathfrak{b}}} |\mathrm{u}_x^{\mathrm{rbc}} - \mathrm{u}_x^{\infty}|^2\right)^{\frac{1}{2}}\,,$$

  In practice, we approximate the above equation by

$$||\mathrm{u}_x^{\mathrm{rbc}} - \mathrm{u}_x^{\infty}||_2 \;=\; \left(\sum_{K\in\mathcal{T}_h}\int_K |\mathrm{u}_x^{\mathrm{rbc}} - \mathrm{u}_x^{\infty}|^2\right)^{\frac{1}{2}}\,,$$

  where we have defined a mesh $\mathcal{T}_h$ of Ω with N_{elem} elements K which are triangles. We define on each element the 10 Lagrange degrees of freedom corresponding with an interpolation of degree 3 on a triangle, and compute the norm using this interpolation. We focus on the component u_x, but the other components have the same behaviour.

We will study the effect of different factors on the performance of the RBC:

- size of the exterior radius $\mathfrak{b}$.
- frequency,
- type of incident-wave (P,B,S,EM),

In the following, we first present in Section 8.3.1 the modules of the coefficients for $\mathfrak{b} = 10$m and $f = 500$Hz, for various configurations. Then, in Section 8.3.2, we compare the RBC solution with the outgoing solution by using a decomposition of the solution in potentials. In Section 8.3.3, we investigate the influence of the size of the domain used for the RBC solution by varying the value of $\mathfrak{b}$. Afterwards, in Section 8.3.4 the performance of the RBC is studied for a range of frequencies.

8.3.1 Comparison of the coefficients of outgoing and truncated solution

We consider the domain $\Omega_{\mathfrak{a}\mathfrak{b}}$ composed of sand1 (see Table 5.2), with $\mathfrak{a} = 1$m and $\mathfrak{b} = 10$m. We plot for frequency $f = 500$Hz the values of the first terms of the coefficients series a_k^{∞}, b_k^{∞}, c_k^{∞}, d_k^{∞} and a_k, b_k, c_k, d_k, $\tilde{a_k}$, $\tilde{b_k}$, $\tilde{c_k}$, $\tilde{d_k}$ for the scattering of a P, B, S, EM incident plane wave for sand1 with boundary condition of type 1 ("Neumann-like") on $r = \mathfrak{a}$ (*cf.* (5.10a)), respectively in figures 8.3, 8.4, 8.5, 8.6.

From Figures 8.3 to 8.6, we can observe the following. The coefficients a_k, b_k, c_k, d_k representing the RBC solution seem to approximate well the coefficients obtained for the outgoing solution. The coefficients $\tilde{c}_k$ are greater than $\tilde{a}_k$ and $\tilde{b}_k$ in every case. In addition, $\tilde{c}_k$ seems to follow the same pattern as c_k and c_k^{∞}. When the incident plane wave is a P-wave, the coefficients a_k and b_k are very close to the corresponding outgoing coefficients. We observe a bigger difference for c_k.We also note a difference for the coefficient d_k but this is small because the amplitude of d_k^{∞} is small (10^{-11}). When the incident plane wave is a B-wave, we observe a slightly larger difference for a_k, but the other observations remain the same. For the four cases, the amplitude of d_k is much smaller than the amplitudes of a_k, b_k and c_k.

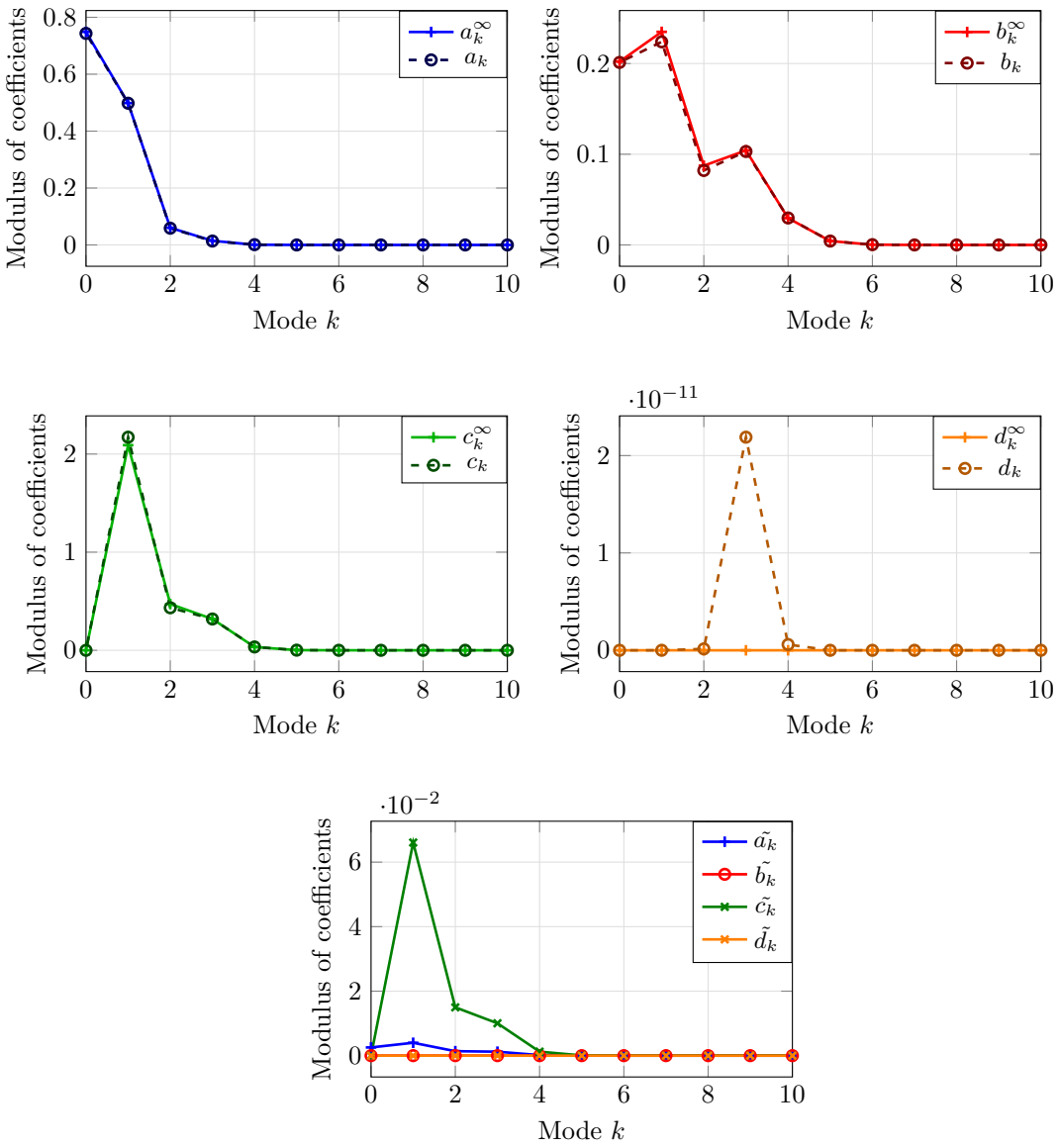

Figure 8.3: Obstacle scattering of an incident plane P-wave for the boundary condition of type 1 ("Neumann-like" (5.10a)) on $r = \mathfrak{a}$ at a frequency $f = 500$Hz for sandstone. The domain is an annulus with interior radius $\mathfrak{a} = 1$m and exterior radius $\mathfrak{b} = 10$m. The coefficients with ∞ superscript correspond to the exact outgoing solution. a_k^∞ —, a_k - ⊙ -, and $\tilde{a}_k$ —| are the coefficients corresponding to the potential of the P-wave, b_k^∞ —, b_k - ⊙ -, and $\tilde{b}_k$ —⊙— the coefficients corresponding to the potential of the B-wave, c_k^∞ —, c_k - ⊙ -, and $\tilde{c}_k$ —× — the coefficients corresponding to the potential of the S-wave, and d_k^∞ —, d_k - ⊙ -, and $\tilde{d}_k$ —× — the coefficients corresponding to the potential of the EM-wave (see (8.13)).

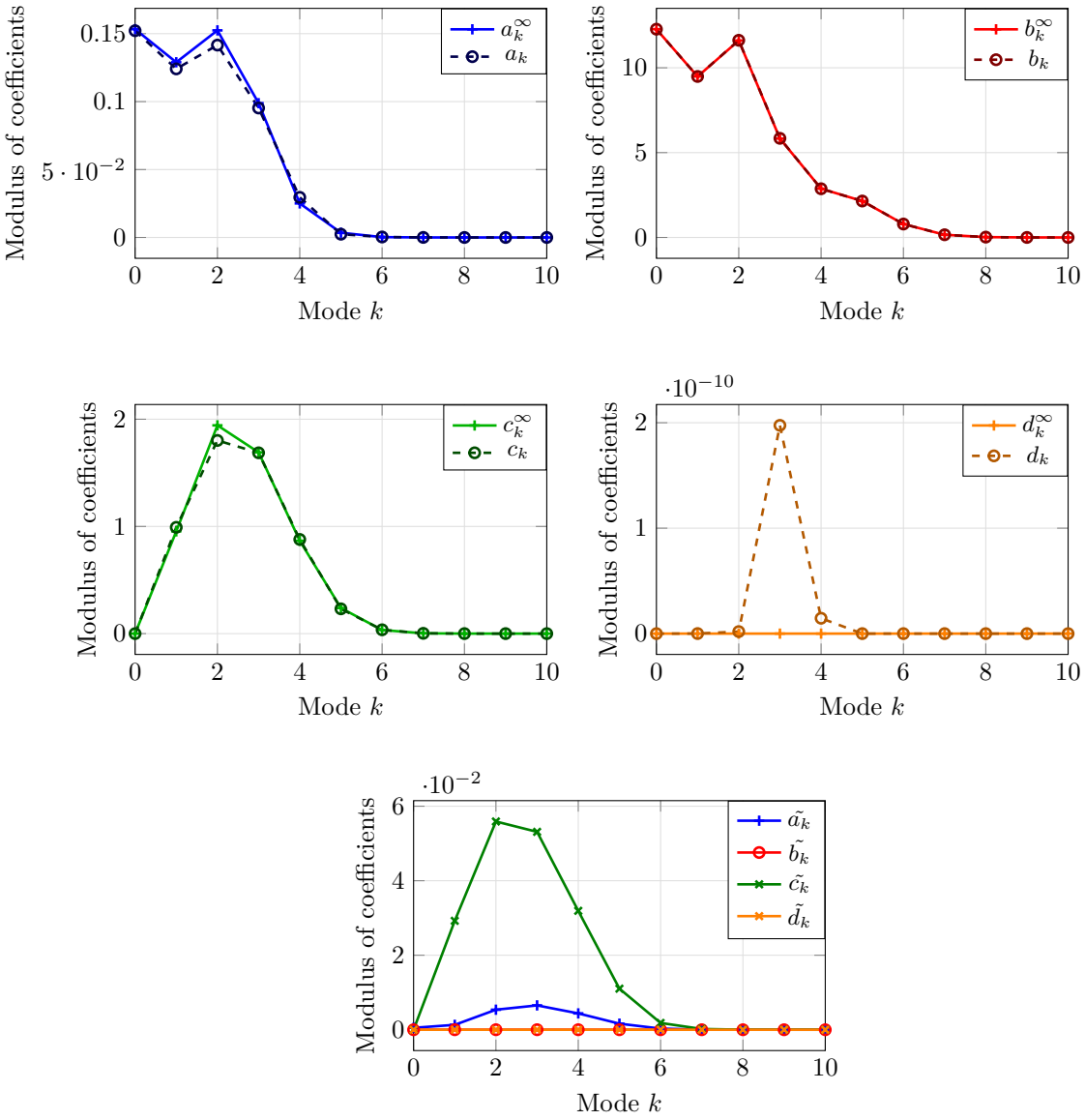

Figure 8.4: Obstacle scattering of an incident plane B-wave for the boundary condition of type 1 ("Neumann-like" (5.10a)) on $r = \mathfrak{a}$ at a frequency $f = 500$Hz for sandstone. The domain is an annulus with interior radius $\mathfrak{a} = 1$m and exterior radius $\mathfrak{b} = 10$m. The coefficients with ∞ superscript correspond to the exact outgoing solution. a_k^∞ —, a_k - ⊙ -, and $\tilde{a}_k$ — are the coefficients corresponding to the potential of the P-wave, b_k^∞ —, b_k - ⊙ -, and $\tilde{b}_k$ — the coefficients corresponding to the potential of the B-wave, c_k^∞ —, c_k - ⊙ -, and $\tilde{c}_k$ — the coefficients corresponding to the potential of the S-wave, and d_k^∞ —, d_k - ⊙ -, and $\tilde{d}_k$ — the coefficients corresponding to the potential of the EM-wave (see (8.13)).

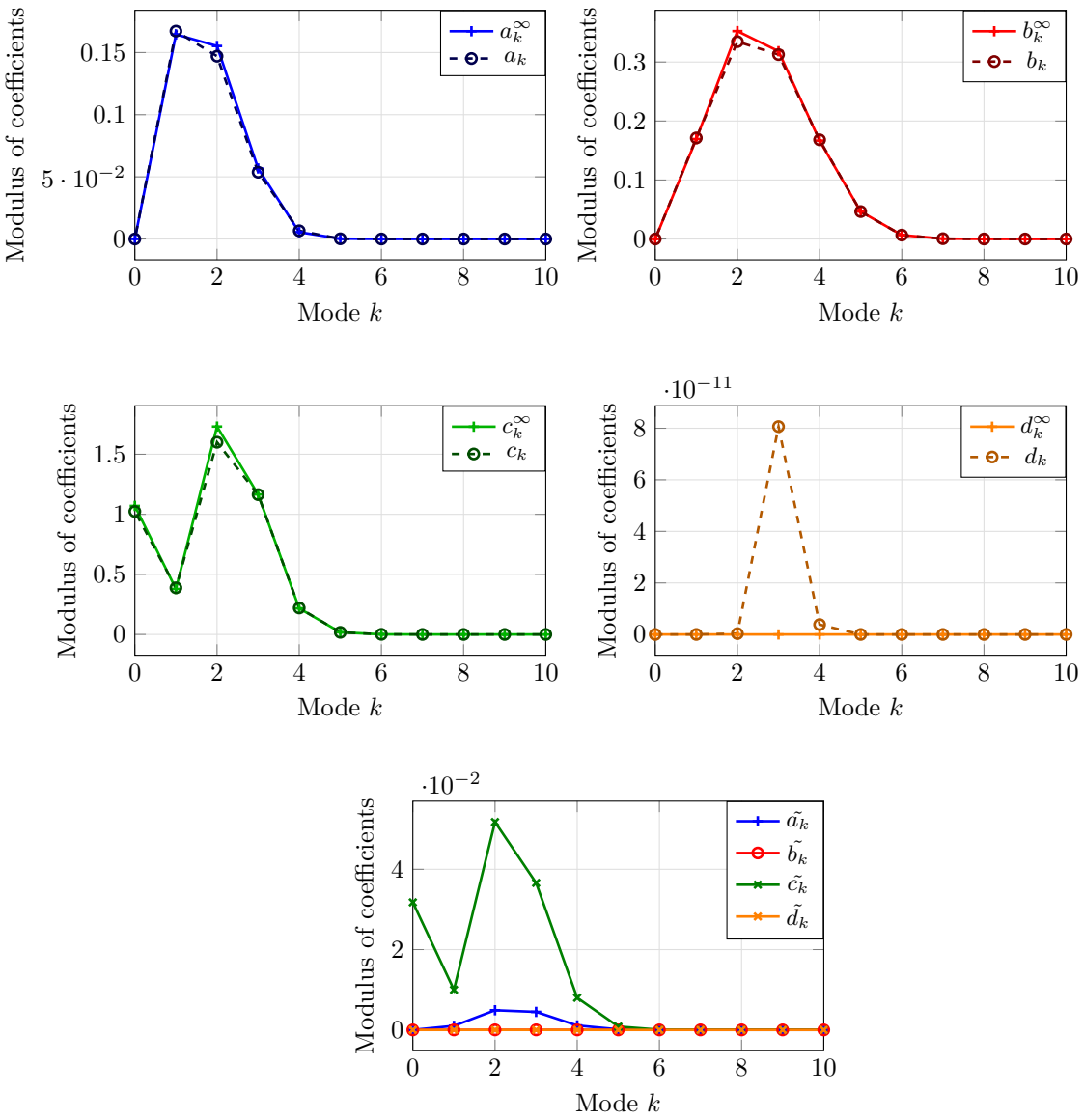

Figure 8.5: Obstacle scattering of an incident plane S-wave for the boundary condition of type 1 ("Neumann-like" (5.10a)) on $r = \mathfrak{a}$ at a frequency $f = 500$Hz for sandstone. The domain is an annulus with interior radius $\mathfrak{a} = 1$m and exterior radius $\mathfrak{b} = 10$m. The coefficients with ∞ superscript correspond to the exact outgoing solution. a_k^∞ —, a_k - ⊙ -, and $\tilde{a}_k$ — are the coefficients corresponding to the potential of the P-wave, b_k^∞ —, b_k - ⊙ -, and $\tilde{b}_k$ — the coefficients corresponding to the potential of the B-wave, c_k^∞ —, c_k - ⊙ -, and $\tilde{c}_k$ — the coefficients corresponding to the potential of the S-wave, and d_k^∞ —, d_k - ⊙ -, and $\tilde{d}_k$ — the coefficients corresponding to the potential of the EM-wave (see (8.13)).

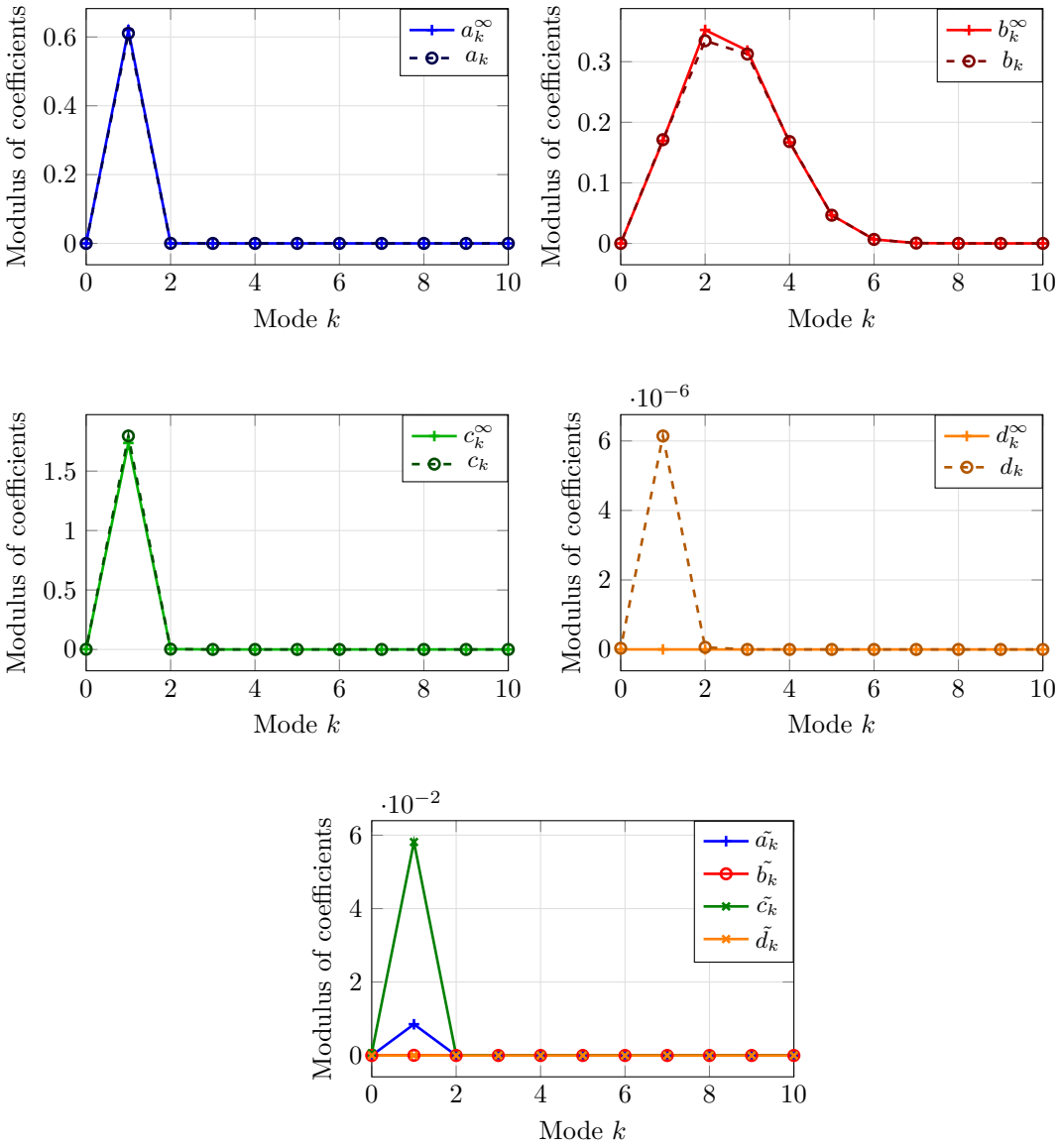

Figure 8.6: Obstacle scattering of an incident plane EM-wave for the boundary condition of type 1 ("Neumann-like" (5.10a)) on $r = \mathfrak{a}$ at a frequency $f = 500$Hz for sandstone. The domain is an annulus with interior radius $\mathfrak{a} = 1$m and exterior radius $\mathfrak{b} = 10$m. The coefficients with ∞ superscript correspond to the exact outgoing solution. a_k^∞ —, a_k - ⊙ -, and $\tilde{a}_k$ — are the coefficients corresponding to the potential of the P-wave, b_k^∞ —, b_k - ⊙ -, and $\tilde{b}_k$ — the coefficients corresponding to the potential of the B-wave, c_k^∞ —, c_k - ⊙ -, and $\tilde{c}_k$ — the coefficients corresponding to the potential of the S-wave, and d_k^∞ —, d_k - ⊙ -, and $\tilde{d}_k$ — the coefficients corresponding to the potential of the EM-wave (see (8.13)).

8.3.2 Potential decomposition

In this section, we want to study more precisely the effect of the RBC on the four kinds of incident waves. For this, we use the decomposition of the solution in potentials χ_{P}, χ_{B}, χ_{S}, χ_{EM} given in (6.14). We focus on the value of the velocity $\mathbf{u}$ and boundary condition of type 1 ("Neumann-like") on $r = \mathfrak{a}$. The wave decomposition of $\mathbf{u}$ for the truncated solution is given by

$$\mathbf{u}^{\text{abc-T1}} = \mathbf{u}^{\chi_{\mathrm{P}}^{\text{abc-T1}}} + \mathbf{u}^{\chi_{\mathrm{P}}^{\text{abc-T1}}} + \mathbf{u}^{\chi_{\mathrm{P}}^{\text{abc-T1}}},$$

with

$$\mathbf{u}^{\chi_{\mathrm{P}}^{\text{abc-T1}}} = -\frac{\mathrm{i}}{\omega \mathsf{s}_{\mathrm{P}}^2} \nabla \chi_{\mathrm{P}}^{\text{abc-T1}}, \quad \mathbf{u}^{\chi_{\mathrm{B}}^{\text{abc-T1}}} = -\frac{\mathrm{i}}{\omega \mathsf{s}_{\mathrm{B}}^2} \nabla \chi_{\mathrm{B}}^{\text{abc-T1}},$$

$$\mathbf{u}^{\chi_{\mathrm{S}}^{\text{abc-T1}}} = \frac{\mathrm{i}}{\omega \mathsf{s}_{\mathrm{S}}^2} \mathbf{curl}\, \chi_{\mathrm{S}}^{\text{abc-T1}}, \quad \mathbf{u}^{\chi_{\mathrm{EM}}^{\text{abc-T1}}} = \frac{\mathrm{i}}{\omega \mathsf{s}_{\mathrm{EM}}^2} \mathbf{curl}\, \chi_{\mathrm{EM}}^{\text{abc-T1}}.$$

The potentials $\chi_{\bullet}^{\text{abc-T1}}$ are given in 8.3 and are represented by the coefficients $(a_k, b_k, c_k, d_k, \tilde{a}_k, \tilde{b}_k, \tilde{c}_k, \tilde{d}_k)$. Concerning the outgoing solution, the velocity $\mathbf{u}^{\infty}$ is decomposed as:

$$\mathbf{u}^{\infty-\text{T1}} = \mathbf{u}^{\chi_{\mathrm{P}}^{\infty-\text{T1}}} + \mathbf{u}^{\chi_{\mathrm{B}}^{\infty-\text{T1}}} + \mathbf{u}^{\chi_{\mathrm{S}}^{\infty-\text{T1}}},$$

with

$$\mathbf{u}^{\chi_{\mathrm{P}}^{\infty-\text{T1}}} = -\frac{\mathrm{i}}{\omega \mathsf{s}_{\mathrm{P}}^2} \nabla \chi_{\mathrm{P}}^{\infty-\text{T1}}, \quad \mathbf{u}^{\chi_{\mathrm{B}}^{\infty-\text{T1}}} = -\frac{\mathrm{i}}{\omega \mathsf{s}_{\mathrm{B}}^2} \nabla \chi_{\mathrm{B}}^{\infty-\text{T1}},$$

$$\mathbf{u}^{\chi_{\mathrm{S}}^{\infty-\text{T1}}} = \frac{\mathrm{i}}{\omega \mathsf{s}_{\mathrm{S}}^2} \mathbf{curl}\, \chi_{\mathrm{S}}^{\infty-\text{T1}}, \quad \mathbf{u}^{\chi_{\mathrm{EM}}^{\infty-\text{T1}}} = \frac{\mathrm{i}}{\omega \mathsf{s}_{\mathrm{EM}}^2} \mathbf{curl}\, \chi_{\mathrm{EM}}^{\infty-\text{T1}},$$

with the potentials represented by the coefficients $(a_k^{\infty}, b_k^{\infty}, c_k^{\infty}, d_k^{\infty})$.

We plot in Figures 8.7 and 8.8 the decomposition of the horizontal component of the solid velocity in the four potentials for the truncated solution and the outgoing solution respectively.

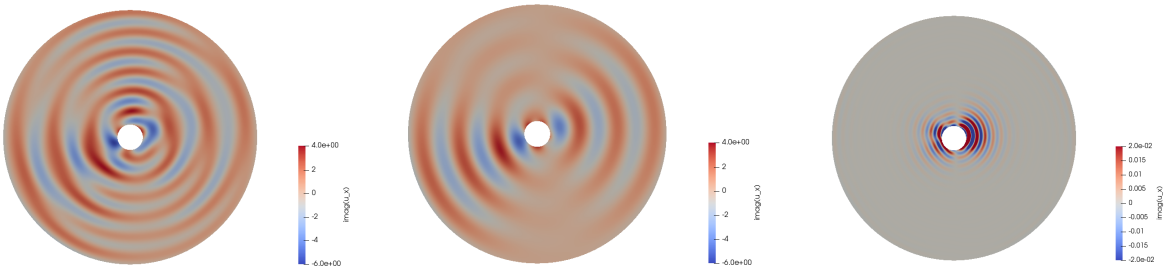

(a) $\mathrm{u}_x^{\text{abc-T1}}$ (b) $\mathbf{u}_x^{\chi_{\mathrm{P}}^{\text{abc-T1}}}$ (c) $\mathbf{u}_x^{\chi_{\mathrm{B}}^{\text{abc-T1}}}$

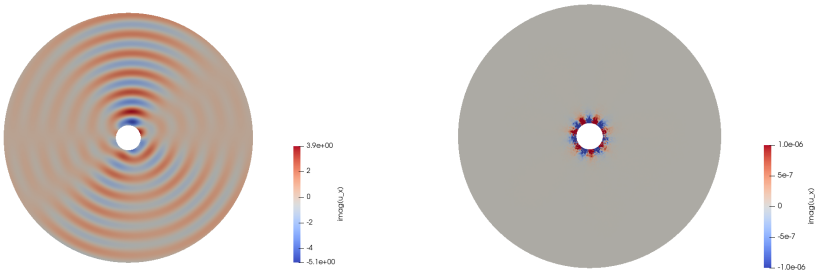

(d) $\mathbf{u}_x^{\chi_{\mathrm{S}}^{\text{abc-T1}}}$ (e) $\mathbf{u}_x^{\chi_{\mathrm{EM}}^{\text{abc-T1}}}$

Figure 8.7: Truncated solution: Decomposition of $\mathbf{u}$ ($\mathrm{m.s}^{-1}$) in the case of the scattering of a P-wave by an impenetrable obstacle with boundary condition of type 1 ("Neumann-like") on $r = \mathfrak{a}$ cf. (1.20a) at a frequency $f = 1\mathrm{kHz}$ for sand1. The radiation boundary condition is set at $\mathfrak{b} = 10\mathrm{m}$.

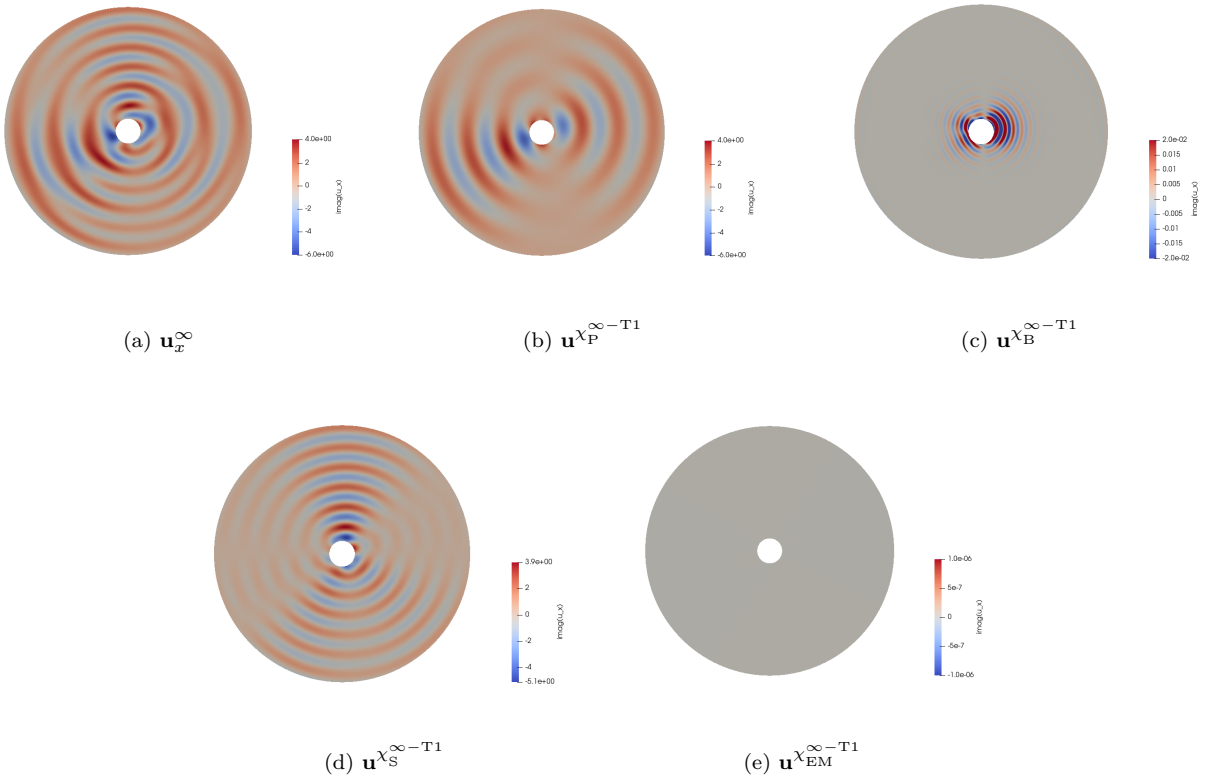

(a) $\mathbf{u}_x^{\infty}$ (b) $\mathbf{u}^{\chi_{\mathrm{P}}^{\infty-\mathrm{T1}}}$ (c) $\mathbf{u}^{\chi_{\mathrm{B}}^{\infty-\mathrm{T1}}}$

(d) $\mathbf{u}^{\chi_{\mathrm{S}}^{\infty-\mathrm{T1}}}$ (e) $\mathbf{u}^{\chi_{\mathrm{EM}}^{\infty-\mathrm{T1}}}$

Figure 8.8: Outgoing solution: Decomposition of $\mathbf{u}$ ($\mathrm{m.s}^{-1}$) in the case of the scattering of a P-wave by an impenetrable obstacle with boundary condition of type 1 ("Neumann-like") on $r = \mathfrak{a}$, cf. (1.20a) at a frequency $f = 1\mathrm{kHz}$ for sand1.

	u_x	$\mathrm{u}_x^{\chi_{\mathrm{P}}}$	$\mathrm{u}_x^{\chi_{\mathrm{B}}}$	$\mathrm{u}_x^{\chi_{\mathrm{S}}}$	$\mathrm{u}_x^{\chi_{\mathrm{EM}}}$
Relative L^2 error (%)	1.19	0.65	5.85	1.82	7.86e5

Table 8.1: Relative L^2 error (%) on u_x between the truncated solution and the outgoing solution for the decomposition in potentials.

We compare the outgoing solution plotted in Figure 8.7 to the outgoing solution given in Figure 8.8. We do not observe reflections on the RBC solution for the total wave and the potentials P, B, and S, but there can be weak reflections that are not visible. For the EM potential, we observe a numerical artifact near the obstacle, that remains small. Hence, this artifact does not affect much the total wave. The relative errors given Table 8.1, confirm that the global error is low. This is also the case for potentials P,B and S. For the EM potential, the error is important. This is also because the field associated to the EM potential is very small.

8.3.3 Influence of the size of the truncated domain

In the previous sections, we set the artificial boundaries at $\mathfrak{b} = 10$m. For this value, we have observed good performance of the RBC. We study now the errors of the RBC when the size of the truncated domain varies. We show in Figure 4.17 the RBC solution for two sizes of exterior radius. In addition, we plot the L^2 error defined in equation (8.15), for incident waves P, B, S, EM in Figure 8.10. As expected, when the size of the truncated domain decreases, the error grows. Note that all the unknowns have the same behavior. For the incident B-wave, the error is greater than for the P or S incident wave for $\mathfrak{b} = 9$m and $\mathfrak{b} = 14$m, see Figure 8.10.

For the four kinds of incident waves, the L^2 error is lower than 5% from $\mathfrak{b} = 10$m. Hence, in the following tests, we set $\mathfrak{b} = 10$m, in order to keep the same domain and observe the influence of other parameters. We have observed in the previous section that this value is sufficient to limit the reflections.

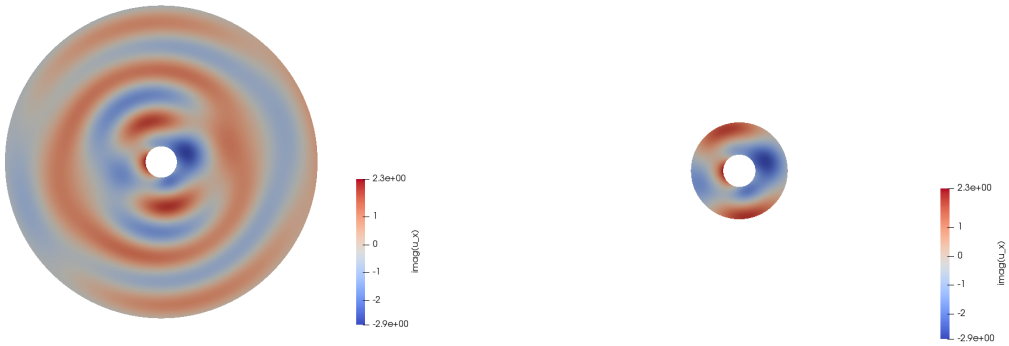

(a) RBC solution with $\mathfrak{b} = 10$m

(b) RBC solution with $\mathfrak{b} = 3$m

Figure 8.9: RBC solution: imaginary part of u_x (m.s^{-1}) for the scattering of a P-wave by a porous obstacle composed of sand1 with boundary condition of type 1 ("Neumann-like") on $\mathfrak{a}$, for different values of $\mathfrak{b}$.

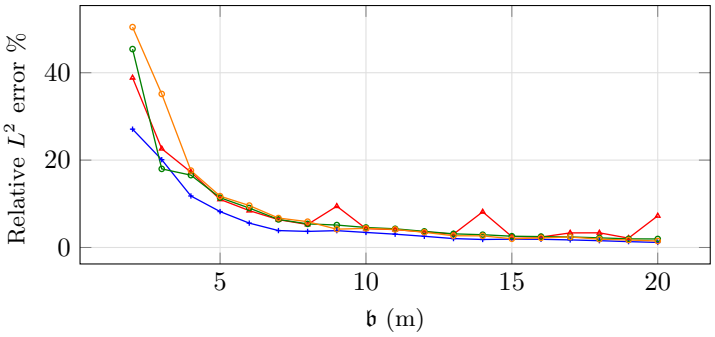

Figure 8.10: Relative L^2 error (%) between the RBC solution and the outgoing solution as a function of the size of the radius $\mathfrak{b}$ for $f = 500$Hz and for boundary condition of type 1 ("Neumann-like") on the interior radius. The solutions are represented in blue for the incident P-wave, in red for the incident B-wave in green for the incident S-wave and in orange for the incident EM-wave.

8.3.4 Effect of the frequency

We now investigate the influence of the frequency on the accuracy of the RBC. We present two figures of scattering of a P-wave for two different frequencies in Figure 8.11. In addition, we plot the L^2 error between the truncated and outgoing solution for a range of frequency $[0.2 : 2.65]$kHz in Figure 8.12.

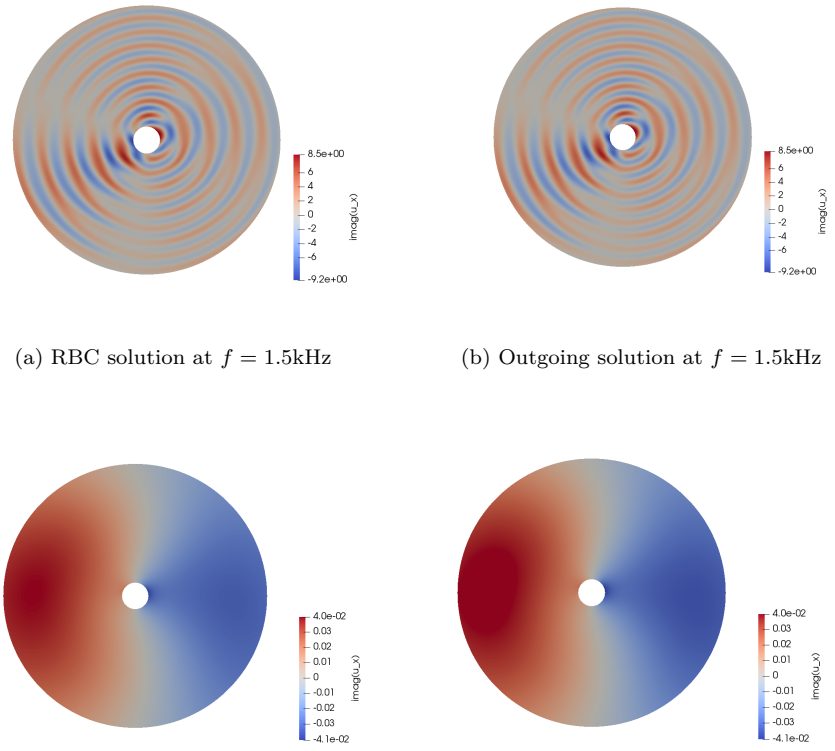

(a) RBC solution at $f = 1.5$kHz

(b) Outgoing solution at $f = 1.5$kHz

(c) RBC solution at $f = 0.2$kHz

(d) Outgoing solution at $f = 0.2$kHz

Figure 8.11: Scattering of a P plane wave: Imaginary part of the solid velocity u_x (10^3 m.s^{-1}) of RBC solution for a porous medium composed of inviscid sandstone for type of boundary condition 1 ("Neumann-like") on the interior radius, for $f = 1.5$kHz and $f = 0.2$ kHz.

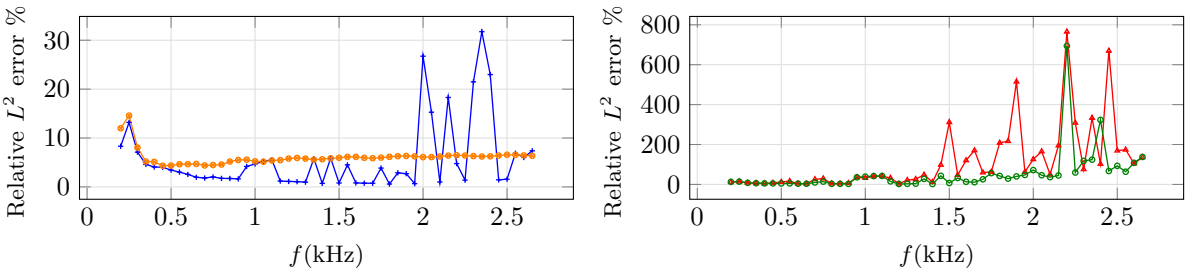

Figure 8.12: Relative L^2 error (%) between the RBC solution and the outgoing solution as a function of the frequency f in sand1 for the scattering of a plane wave for boundary condition of type 1 ("Neumann-like") on $\mathfrak{a}$. The results are given for $\mathfrak{a} = 1$m and $\mathfrak{b} = 10$m. The result for the incident P-wave is represented in blue —+—, for the incident B-wave in red —▲—, for the incident S-wave in green —○— and for the incident EM-wave in orange —●—.

For most of the frequencies, the error of the RBC solution is less than 10%. However, for some frequencies, the

error is very high, and the solution is not good. This is due to the inversion of the matrix $\mathbb{A}^{\text{abc-T1}}$, see Section 8.2. The Hankel function for the complex slowness s_{EM} can indeed be very high (it can reach 10^{50}). Hence, when we need to invert $\mathbb{A}^{\text{abc-T1}}$, for some frequencies, the condition number of the matrix is very high and the determinant can be close to zero. This leads to a lack of precision during the numerical inversion, and the RBC solution cannot be computed correctly.

We have hence studied the performance of the RBC when varying several parameters. As expected, the error of the RBC decreases when we consider more wavelengths in the domain. The performance of the RBC has a similar order as the RBC constructed for poroelasticity in Chapter 4.

8.4 HDG method using Radiation Boundary conditions

In this section, we apply the HDG method for Pride's equation with the low-order radiation boundary condition derived in Section 8.1. We consider a two-dimensional domain Ω with the boundary $\Gamma = \Gamma_l \cup \Gamma_{\text{abs}}$. The fields ($\mathbf{u}$, $\mathbf{w}$, $\boldsymbol{\tau}$, $\mathrm{p}\,\boldsymbol{E}$, H, $\boldsymbol{J}$) solve Pride's equations (5.3) on Ω. On Γ_l, we impose one of the eight conditions given in Section 5.4. From Section 8.1, equation (8.12), we impose on the absorbing boundary Γ_{abs}:

$$\begin{aligned}
&\boldsymbol{\tau}\,\boldsymbol{n} + \big(\mathbf{X}_1(\mathbf{u}\cdot\boldsymbol{n}) + \mathbf{X}_2(\mathbf{w}\cdot\boldsymbol{n})\big)\,\boldsymbol{n} + \mathbf{X}_3(\boldsymbol{n}\times\mathbf{u})\,\mathbf{t} + \mathbf{X}_4(\boldsymbol{n}\times\boldsymbol{E})\,\mathbf{t} = 0\,,\\
&\mathrm{p} + \mathbf{X}_5(\mathbf{u}\cdot\boldsymbol{n}) + \mathbf{X}_6(\mathbf{w}\cdot\boldsymbol{n}) = 0\,,\\
&\mathrm{H} + \mathbf{X}_7(\boldsymbol{n}\times\mathbf{u}) + \mathbf{X}_8\,(\boldsymbol{n}\times\boldsymbol{E}) = 0\,.
\end{aligned} \tag{8.16}$$

We consider a triangulation $\mathcal{T}_h$ of the domain Ω of dimension 2, and we denote by F an edge of the element K, and $\boldsymbol{n}$ the unit normal vector to F. We will use the function spaces defined in Section 7.1. The approximate fields ($\mathbf{u}_h$, $\mathbf{w}_h$, $\boldsymbol{\tau}_h$, p_h, $\boldsymbol{E}_h$, H_h, $\boldsymbol{J}_h$) $\in$ ($\boldsymbol{V}^p(K)\times\boldsymbol{V}^p(K)\times\boldsymbol{\Sigma}^p(K)\times V^p(K)\times\boldsymbol{V}^p(K)\times V^p(K)\times\boldsymbol{V}^p(K)$) solve Pride's equations (5.3) on $\mathcal{T}_h$. The local problem given in Section 7.2 is not modified. The transmission conditions on the interior faces and on Γ_l are also the ones given in Section 7.2. However, on the faces Γ_{abs}, the transmission conditions are replaced by the radiation conditions by integrating equation (8.16), which gives:

$$\sum_{F\in\mathcal{F}_{\text{abc}}}\int_F \Big(\hat{\boldsymbol{\tau}}_h\,\boldsymbol{n} + (\mathbf{X}_1(\hat{\mathbf{u}}_h\cdot\boldsymbol{n}) + \mathbf{X}_2(\hat{\mathbf{w}}_h\cdot\boldsymbol{n}))\,\boldsymbol{n} + \mathbf{X}_3(\boldsymbol{n}\times\hat{\mathbf{u}}_h)\,\mathbf{t} + \mathbf{X}_4(\boldsymbol{n}\times\hat{\boldsymbol{E}}_h)\,\mathbf{t}\Big)\cdot\boldsymbol{\eta} = 0\,, \tag{8.17a}$$

$$\sum_{F\in\mathcal{F}_{\text{abc}}}\int_F \Big(\hat{\mathrm{p}}_h + \mathbf{X}_5(\hat{\mathbf{u}}_h\cdot\boldsymbol{n}) + \mathbf{X}_6(\hat{\mathbf{w}}_h\cdot\boldsymbol{n})\Big)\,\xi = 0\,, \tag{8.17b}$$

$$\sum_{F\in\mathcal{F}_{\text{abc}}}\int_F \Big(\hat{\boldsymbol{H}}_h + \mathbf{X}_7(\boldsymbol{n}\times\hat{\mathbf{u}}_h) + \mathbf{X}_8\,(\boldsymbol{n}\times\hat{\boldsymbol{E}}_h)\Big)\,\nu = 0\,, \tag{8.17c}$$

with ($\boldsymbol{\eta}$, ξ, ν) $\in$ ($\boldsymbol{M}_h\times M_h\times M_h$) basis-functions on the faces. Then, we replace the numerical traces by their values, *cf.* equations (7.3) and (7.4).

(a) Discretization of condition (8.17a)

We consider a face F in Γ_{abs}, and we replace the numerical traces in equation (8.17a). The fields $\hat{\boldsymbol{\tau}}_h$, $\hat{\mathbf{w}}_h$ and $\hat{\boldsymbol{E}}_h$ are expressed using equation (7.4), and $\hat{\mathbf{u}}_h$ is replaced by $\boldsymbol{\lambda}_1$, as given in equation (7.3). We obtain

$$\begin{aligned}
&\int_F(\boldsymbol{\tau}_h\,\boldsymbol{n})\cdot\boldsymbol{\eta} - \int_F\gamma_1\,(\mathbf{u}_h-\boldsymbol{\lambda}_1)\cdot\boldsymbol{\eta} - \int_F\gamma_3\,(\mathrm{p}_h-\lambda_2)\,\boldsymbol{n}\cdot\boldsymbol{\eta} + \int_F\Big(\mathbf{X}_1(\boldsymbol{\lambda}_1\cdot\boldsymbol{n})\boldsymbol{n}\Big)\cdot\boldsymbol{\eta}\\
&+\int_F\mathbf{X}_2\Big((\mathbf{w}_h\cdot\boldsymbol{n}) - \gamma_2\,(\mathrm{p}_h-\lambda_2) - \gamma_4(\mathbf{u}_h-\boldsymbol{\lambda}_1)\cdot\boldsymbol{n}\Big)\cdot\boldsymbol{\eta} + \int_F\Big(\mathbf{X}_3(\boldsymbol{\lambda}_1\cdot\mathbf{t})\,\mathbf{t}\Big)\cdot\boldsymbol{\eta}\\
&+\int_F\Big(\mathbf{X}_4\big(\boldsymbol{E}_h\cdot\mathbf{t} - \gamma_5\,(\mathrm{H}_h-\lambda_3)\big)\Big)\cdot\boldsymbol{\eta} = 0\,.
\end{aligned}$$

We replace the test-function $\boldsymbol{\eta}$ by the basis function ψ_i^F, and we decompose the unknowns using equations (7.8) and

(7.9). The discretization of the equation on (x, y) is written as follows:

$$\int_F \underline{\tau}_{xx}^K n_x \varphi_j^K \psi_i^F dS + \int_F \underline{\tau}_{xy}^K n_y \varphi_j^K \psi_i^F dS - \int_F \gamma_1 \varphi_j^K \underline{\mathrm{u}}_x^K \psi_i^F dS + \int_F \gamma_1 \psi_j^F \underline{\lambda}_{1x}^{\beta(K,f)} \psi_i^F dS - \int_F \gamma_3 n_x \underline{\mathrm{p}}^K \varphi_j^K \psi_i^F dS$$
$$+ \int_F \gamma_3 n_x \underline{\lambda}_2^{\beta(K,f)} \psi_j^F \psi_i^F dS + \int_F \mathbf{X}_1 \, (\underline{\lambda}_{1x}^{\beta(K,f)} n_x + \underline{\lambda}_{1y}^{\beta(K,f)} n_y) n_x \, \psi_j^F \, \psi_i^F dS + \int_F \mathbf{X}_2 \, \underline{\mathrm{w}}_x^K \, n_x^2 \varphi_j^K \, \psi_i^F dS$$
$$+ \int_F \mathbf{X}_2 \, \underline{\mathrm{w}}_y^K \, n_x n_y \varphi_j^K \, \psi_i^F dS - \int_F \mathbf{X}_2 \, \gamma_2 \underline{\mathrm{p}}^K \, n_x \varphi_j^K \, \psi_i^F dS + \int_F \mathbf{X}_2 \, \gamma_2 \underline{\lambda}_2^{\beta(K,f)} \, n_x \, \psi_j^F \, \psi_i^F dS - \int_F \mathbf{X}_2 \, \gamma_4 \, \underline{\mathrm{u}}_x^K n_x^2 \, \varphi_j^K \, \psi_i^F dS$$
$$- \int_F \mathbf{X}_2 \, \gamma_4 \, \underline{\mathrm{u}}_y^K n_x n_y \, \varphi_j^K \, \psi_i^F dS + \int_F \mathbf{X}_2 \, \gamma_4 \, (\underline{\lambda}_{1x}^{\beta(K,f)} n_x + \underline{\lambda}_{1y}^{\beta(K,f)} n_y) n_x \, \psi_j^F \, \psi_i^F dS$$
$$+ \int_F \mathbf{X}_3 \, (\underline{\lambda}_{1x}^{\beta(K,f)} n_y^2 - \underline{\lambda}_{1y}^{\beta(K,f)} n_x n_y) \psi_j^F \psi_i^F + \int_F \mathbf{X}_4 \, (\underline{E}_x^K n_y^2 - \underline{E}_y^K n_x n_y) \varphi_j^K \psi_i^F$$
$$+ \int_F \mathbf{X}_4 \, \gamma_5 \underline{H}^K \, n_y \varphi_j^K \, \psi_i^F dS - \int_F \mathbf{X}_4 \, \gamma_5 \underline{\lambda_3}^{\beta(K,f)} \, n_y \, \psi_j^F \, \psi_i^F dS = 0 \,,$$

and

$$\int_F \underline{\tau}_{xy}^K n_x \varphi_j^K \psi_i^F dS + \int_F \underline{\tau}_{yy}^K n_y \varphi_j^K \psi_i^F dS - \int_F \gamma_1 \varphi_j^K \underline{\mathrm{u}}_y^K \psi_i^F dS + \int_F \gamma_1 \varphi_j^K \underline{\lambda}_{1y}^{\beta(K,f)} \psi_i^F dS - \int_F \gamma_3 n_y \underline{\mathrm{p}}^K \varphi_j^K \psi_i^F dS$$
$$+ \int_F \gamma_3 n_y \underline{\lambda}_2^{\beta(K,f)} \psi_j^F \psi_i^F dS + \int_F \mathbf{X}_1 \, (\underline{\lambda}_{1x}^{\beta(K,f)} n_x + \underline{\lambda}_{1y}^{\beta(K,f)} n_y) n_y \, \psi_j^F \, \psi_i^F dS + \int_F \mathbf{X}_2 \, \underline{\mathrm{w}}_x^K \, n_x n_y \varphi_j^K \, \psi_i^F dS$$
$$+ \int_F \mathbf{X}_2 \, \underline{\mathrm{w}}_y^K \, n_y^2 \varphi_j^K \, \psi_i^F dS - \int_F \mathbf{X}_2 \, \gamma_2 \underline{\mathrm{p}}^K \, n_y \varphi_j^K \, \psi_i^F dS + \int_F \mathbf{X}_2 \, \gamma_2 \underline{\lambda}_2^{\beta(K,f)} \, n_y \, \psi_j^F \, \psi_i^F dS - \int_F \mathbf{X}_2 \, \gamma_4 \, \underline{\mathrm{u}}_x^K n_x n_y \, \varphi_j^K \, \psi_i^F dS$$
$$- \int_F \mathbf{X}_2 \, \gamma_4 \, \underline{\mathrm{u}}_y^K n_y^2 \, \varphi_j^K \, \psi_i^F dS + \int_F \mathbf{X}_2 \, \gamma_4 \, (\underline{\lambda}_{1x}^{\beta(K,f)} n_x + \underline{\lambda}_{1y}^{\beta(K,f)} n_y) n_y \, \psi_j^F \, \psi_i^F dS$$
$$+ \int_F \mathbf{X}_3 \, (-\underline{\lambda}_{1x}^{\beta(K,f)} n_x n_y + \underline{\lambda}_{1y}^{\beta(K,f)} n_x^2) \psi_j^F \psi_i^F dS + \int_F \mathbf{X}_4 \, (-\underline{E}_x^K n_x n_y + \underline{E}_y^K n_x^2) \psi_j^F \psi_i^F dS$$
$$- \int_F \mathbf{X}_4 \, \gamma_5 \underline{H}^K \, n_x \varphi_j^K \, \psi_i^F dS + \int_F \mathbf{X}_4 \, \gamma_5 \underline{\lambda_3}^{\beta(K,f)} \, n_x \, \psi_j^F \, \psi_i^F dS = 0 \,.$$

In section 7.2, we have defined the following matrices:

$$\begin{aligned} \mathbb{F}_{ij}^F &= \int_F \varphi_i^K \psi_j^F dS \,, \qquad (\mathbb{Q}_k^F)_{ij} = \int_F \varphi_i^K \psi_j^F n_k \, dS \,, \qquad (\mathbb{L}_{kl}^F)_{ij} = \int_F \varphi_i^K \psi_j^F n_k \, n_l \, dS \,, \\ \mathbb{G}_{ij}^F &= \int_F \psi_i^F \psi_j^F dS \,, \qquad (\mathbb{H}_k^F)_{ij} = \int_F \psi_i^F \psi_j^F n_k \, dS \,, \qquad (\mathbb{O}_{kl}^F)_{ij} = \int_F \psi_i^F \psi_j^F n_k \, n_l \, dS \,, \end{aligned} \tag{8.18}$$

with $k = x, y$, and $l = x, y$.

Using these notations, the two above equations are written as:

$$(\mathbb{Q}_x^{\beta(K,f)})^T \underline{\tau}_{xx}^K + (\mathbb{Q}_y^{\beta(K,f)})^T \underline{\tau}_{xy}^K - \gamma_1 (\mathbb{F}^{\beta(K,f)})^T \underline{\mathrm{u}}_x^K + \gamma_1 \mathbb{G}^{\beta(K,f)} \underline{\lambda}_{1x}^{\beta(K,f)} - \gamma_3 (\mathbb{Q}_x^{\beta(K,f)})^T \underline{\mathrm{p}}^K + \gamma_3 \mathbb{H}_x^j \underline{\lambda}_2^{\beta(K,f)}$$
$$+ \mathbb{O}_{xx}^{\beta(K,f)} \mathbf{X}_1 \, \underline{\lambda}_{1\bullet}^{\beta(K,f)} + \mathbb{O}_{xy}^{\beta(K,f)} \mathbf{X}_1 \underline{\lambda}_{1y}^{\beta(K,f)} + (\mathbb{L}_{xx}^{\beta(K,f)})^T \mathbf{X}_2 \, \underline{\mathrm{w}}_x^K + (\mathbb{L}_{xyl}^{\beta(K,f)})^T \mathbf{X}_2 \, \underline{\mathrm{w}}_y^K - (\mathbb{Q}_x^{\beta(K,f)})^T \mathbf{X}_2 \, \gamma_2 \underline{\mathrm{p}}^K$$
$$+ \mathbb{H}_x^{\beta(K,f)} \mathbf{X}_2 \, \gamma_2 \underline{\lambda}_2^{\beta(K,f)} - (\mathbb{L}_{xx}^{\beta(K,f)})^T \mathbf{X}_2 \, \gamma_4 \, \underline{\mathrm{u}}_x^K - (\mathbb{L}_{xy}^{\beta(K,f)})^T \mathbf{X}_2 \, \gamma_4 \underline{\mathrm{u}}_y^K + \mathbb{O}_{xx}^{\beta(K,f)} \mathbf{X}_2 \, \gamma_4 \underline{\lambda}_{1x}^{\beta(K,f)} + \mathbb{O}_{xy}^{\beta(K,f)} \mathbf{X}_2 \gamma_4 \underline{\lambda}_{1y}^{\beta(K,f)}$$
$$+ \mathbb{O}_{yy}^{\beta(K,f)} \mathbf{X}_3 \, \underline{\lambda}_{1x}^{\beta(K,f)} - \mathbb{O}_{xy}^{\beta(K,f)} \mathbf{X}_3 \, \underline{\lambda}_{1y}^{\beta(K,f)} + (\mathbb{L}_{yy}^{\beta(K,f)})^T \mathbf{X}_4 \, \underline{E}_x^K - (\mathbb{L}_{xy}^{\beta(K,f)})^T \mathbf{X}_4 \, \underline{E}_y^K$$
$$+ (\mathbb{Q}_{yl}^{\beta(K,f)})^T \mathbf{X}_4 \, \gamma_5 \underline{H}^K - \mathbb{H}_y^{\beta(K,f)} \mathbf{X}_4 \, \gamma_5 \underline{\lambda_3}^{\beta(K,f)} + \mathbb{O}_{yy}^{\beta(K,f)} \mathbf{X}_4 \, \underline{\lambda}_{1x}^{\beta(K,f)} - \mathbb{O}_{xy}^{\beta(K,f)} \mathbf{X}_4 \underline{\lambda}_{1y}^{\beta(K,f)} = 0 \,,$$

and

$$(\mathbb{Q}_x^{\beta(K,f)})^T \underline{\tau}_{xy}^K + (\mathbb{Q}_y^{\beta(K,f)})^T \underline{\tau}_{yy}^K - \gamma_1 (\mathbb{F}^{\beta(K,f)})^T \underline{\mathrm{u}}_y^K + \gamma_1 \mathbb{G}^{\beta(K,f)} \underline{\lambda}_{1y}^{\beta(K,f)} - \gamma_3 (\mathbb{Q}_y^{\beta(K,f)})^T \underline{\mathrm{p}}^K + \gamma_3 \mathbb{H}_y^{\beta(K,f)} \underline{\lambda}_2^{\beta(K,f)}$$

$$+ \mathbb{O}_{xy}^{\beta(K,f)} \mathbf{X}_1 \underline{\lambda}_{1x}^{\beta(K,f)} + \mathbb{O}_{yy}^{\beta(K,f)} \mathbf{X}_1 \underline{\lambda}_{1y}^{\beta(K,f)} + (\mathbb{L}_{xy}^{\beta(K,f)})^T \mathbf{X}_2 \underline{\mathrm{w}}_x^K + (\mathbb{L}_{yy}^{\beta(K,f)})^T \mathbf{X}_2 \underline{\mathrm{w}}_y^K - (\mathbb{Q}_y^{\beta(K,f)})^T \mathbf{X}_2 \gamma_2 \underline{\mathrm{p}}^K$$

$$+ \mathbb{H}_y^{\beta(K,f)} \mathbf{X}_2 \gamma_2 \underline{\lambda}_2^{\beta(K,f)} - (\mathbb{L}_{xy}^{\beta(K,f)})^T \mathbf{X}_2 \gamma_4 \underline{\mathrm{u}}_x^K - (\mathbb{L}_{yy}^{\beta(K,f)})^T \mathbf{X}_2 \gamma_4 \underline{\mathrm{u}}_y^K + \mathbb{O}_{xy}^{\beta(K,f)} \mathbf{X}_2 \gamma_4 \underline{\lambda}_{1x}^{\beta(K,f)} + \mathbb{O}_{yy}^{\beta(K,f)} \mathbf{X}_2 \gamma_4 \underline{\lambda}_{1y}^{\beta(K,f)}$$

$$- \mathbb{O}_{xy}^{\beta(K,f)} \mathbf{X}_3 \underline{\lambda}_{1x}^{\beta(K,f)} + \mathbb{O}_{xx}^{\beta(K,f)} \mathbf{X}_3 \underline{\lambda}_{1y}^{\beta(K,f)} - (\mathbb{L}_{xy}^{\beta(K,f)})^T \mathbf{X}_4 \underline{E}_x^K + (\mathbb{L}_{xx}^{\beta(K,f)})^T \mathbf{X}_4 \underline{E}_y^K$$

$$- (\mathbb{Q}_x^{\beta(K,f)})^T \mathbf{X}_4 \gamma_5 \underline{H}^K + \mathbb{H}_x^{\beta(K,f)} \mathbf{X}_4 \gamma_5 \underline{\lambda_3}^{\beta(K,f)} - \mathbb{O}_{xy}^{\beta(K,f)} \mathbf{X}_4 \underline{\lambda}_{1x}^{\beta(K,f)} + \mathbb{O}_{xx}^{\beta(K,f)} \mathbf{X}_4 \underline{\lambda}_{1y}^{\beta(K,f)} = 0\,.$$

(b) Discretization of condition (8.17b)

Considering a face F in Γ_{abs}, we replace in equation (8.17b) the numerical traces $\hat{\mathbf{w}}_h$ by using equation (7.4), and $\hat{\mathbf{u}}_h$ is replaced by $\boldsymbol{\lambda}_1$, as given in equation (7.3), which gives:

$$\int_F \Big(\lambda_2 + \mathbf{X}_5 (\boldsymbol{\lambda}_1 \cdot \boldsymbol{n}) + \mathbf{X}_6 \Big((\mathbf{w}_h \cdot \boldsymbol{n}) - \gamma_2 (\mathrm{p}_h - \lambda_2) - \boldsymbol{S}_4 (\mathbf{u}_h - \boldsymbol{\lambda}_1) \cdot \boldsymbol{n} \Big) \Big) \xi = 0\,.$$

The test-function ξ is replaced by the basis function ψ_i^F, and we decompose the unknowns using equations (7.8) and (7.9). We have:

$$\int_F \underline{\lambda}_2^{\beta(K,f)} \psi_j^F \psi_i^F dS + \int_F \mathbf{X}_5 (\underline{\lambda}_{1x}^{\beta(K,f)} n_x + \underline{\lambda}_{1y}^{\beta(K,f)} n_y) \psi_j^F \psi_i^F dS + \int_F \mathbf{X}_6 (\underline{\mathrm{w}}_x^K n_x + \underline{\mathrm{w}}_y^K n_y) \varphi_j^K \psi_i^F dS$$

$$- \int_F \mathbf{X}_6 \gamma_2 \underline{\mathrm{p}}^K \varphi_j^K \psi_i^F dS + \int_F \mathbf{X}_6 \gamma_2 \underline{\lambda}_2^{\beta(K,f)} \psi_j^F \psi_i^F dS - \int_F \mathbf{X}_6 \gamma_4 (\underline{\mathrm{u}}_x^K n_x + \underline{\mathrm{u}}_y^K n_y) \varphi_j^K \psi_i^F dS$$

$$+ \int_F \mathbf{X}_6 \gamma_4 (\underline{\lambda}_{1x}^{\beta(K,f)} n_x + \underline{\lambda}_{1y}^{\beta(K,f)} n_y) \psi_j^F \psi_i^F dS = 0\,.$$

Using the elementary matrices defined in equation (8.18), we obtain:

$$\mathbb{G}^{\beta(K,f)} \underline{\lambda}_2^{\beta(K,f)} + \mathbb{H}_x^{\beta(K,f)} \mathbf{X}_5 \underline{\lambda}_{1x}^{\beta(K,f)} + \mathbb{H}_y^{\beta(K,f)} \mathbf{X}_5 \underline{\lambda}_{1y}^{\beta(K,f)} + (\mathbb{Q}_x^{\beta(K,f)})^T \mathbf{X}_6 \underline{\mathrm{w}}_x^K$$

$$+ (\mathbb{Q}_y^{\beta(K,f)})^T \mathbf{X}_6 \underline{\mathrm{w}}_y^K - (\mathbb{F}^{\beta(K,f)})^T \mathbf{X}_6 \gamma_2 \underline{\mathrm{p}}^K + \mathbb{G}^{\beta(K,f)} \mathbf{X}_6 \gamma_2 \underline{\lambda}_2^{\beta(K,f)} - (\mathbb{Q}_{xl}^{\beta(K,f)})^T \mathbf{X}_6 \gamma_4 \underline{\mathrm{u}}_x^K$$

$$- (\mathbb{Q}_{yl}^{\beta(K,f)})^T \mathbf{X}_6 \gamma_4 \underline{\mathrm{u}}_y^K + \mathbb{H}_x^{\beta(K,f)} \mathbf{X}_6 \gamma_4 \underline{\lambda}_{1x}^{\beta(K,f)} + \mathbb{H}_y^{\beta(K,f)} \mathbf{X}_6 \gamma_4 \underline{\lambda}_{1y}^{\beta(K,f)} = 0\,.$$

(c) Discretization of condition (8.17c)

We consider a face F in Γ_{abs}, and we replace in equation (8.17c) the numerical trace $\hat{\boldsymbol{E}}_h$ by using equation (7.4).We have:

$$\int_F \boldsymbol{\lambda}_3 \nu + \int_F \mathbf{X}_7 (\boldsymbol{\lambda}_1 \cdot \mathbf{t}) \nu + \int_F \mathbf{X}_8 \Big(\boldsymbol{E}_h \cdot \mathbf{t} - \gamma_5 (\mathrm{H}_h - \lambda_3) \Big) \nu = 0\,.$$

We replace ν by the basis function ψ_i^F, and the unknowns are decomposed using equations (7.8) and (7.9):

$$\int_F \underline{\lambda_3}^{\beta(K,f)} \psi_j^F \psi_i^F dS + \int_F \mathbf{X}_7 (-\underline{\lambda}_{1x}^{\beta(K,f)} n_y + \underline{\lambda}_{1y}^{\beta(K,f)} n_x) \psi_j^F \psi_i^F dS + \int_F \mathbf{X}_8 (-\underline{E}_x^K n_y + \underline{E}_y^K n_x) \varphi_j^K \psi_i^F dS$$

$$- \int_F \mathbf{X}_8 \gamma_5 \underline{H}^K \varphi_j^K \psi_i^F dS + \int_F \mathbf{X}_8 \gamma_5 \underline{\lambda_3}^{\beta(K,f)} \psi_j^F \psi_i^F dS = 0\,.$$

Finally, we express the above equation by using the notations introduced in equation (8.18):

$$\mathbb{G}^{\beta(K,f)} \underline{\lambda_3}^{\beta(K,f)} - \mathbb{H}_y^{\beta(K,f)} \mathbf{X}_7 \underline{\lambda}_{1x}^{\beta(K,f)} + \mathbb{H}_x^{\beta(K,f)} \mathbf{X}_7 \underline{\lambda}_{1y}^{\beta(K,f)} - (\mathbb{Q}_y^{\beta(K,f)})^T \mathbf{X}_8 \underline{E}_x^K + (\mathbb{Q}_x^{\beta(K,f)})^T \mathbf{X}_8 \underline{E}_y^K$$

$$- (\mathbb{F}^{\beta(K,f)})^T \mathbf{X}_8 \gamma_5 \underline{H}^K + \mathbb{G}^{\beta(K,f)} \mathbf{X}_8 \gamma_5 \underline{\lambda_3}^K = 0\,.$$

The expression of the elementary matrices $\mathbb{P}^K$ and $\mathbb{T}^K$ for an element with a face on the absorbing border Γ_{abs} is detailed in Appendix E.1.1.

8.5 Local problem with PML

In this section, we apply a Perfectly Matched Layer (PML) to the discretization of Pride equations (5.3) using HDG method. The perfectly matched layer is an artificial absorbing layer on the edges of the computational domain. It absorbs the outgoing waves and prevents reflections. In the formulation, we use two damping functions α and β that cause the attenuation of the wave in the absorbing layer. The absorption functions α and β are taken equal to zero outside the absorbing layers, and the further the considered points in the layers are from the part with no attenuation, the more their values grow. In practice, we replace the derivatives

$$\frac{\partial}{\partial x} \to \frac{i\,\omega}{i\,\omega + \alpha(x)} \frac{\partial}{\partial x}, \qquad \text{and} \qquad \frac{\partial}{\partial y} \to \frac{i\,\omega}{i\,\omega + \beta(y)} \frac{\partial}{\partial y}.$$

The application of the PML only changes the local problem, but does not modify the transmission conditions or the boundary conditions. We give in Appendix E.1.2 the discretization of the local problem of Pride's equations (5.3) with PML.

8.6 Numerical results using HDG discretization

In this section, we study the HDG discretization of poroelastic equations with radiation boundary conditions or PML, detailed in Sections 8.4 and 8.5. For several configurations, we evaluate the performance of two truncation methods, by comparing the numerical solutions with reference solutions. In the code, for the PML, we use for the absorption functions (see Section 8.5): $\alpha(x) = \beta_0\, d(x)$ and $\beta(y) = \beta_0\, d(y)$, with d the horizontal or vertical distance between the considered point and the beginning of the PML.

8.6.1 Square with a hole

We consider an infinite porous medium composed of sand1 (see Table 7.1), with a solid impenetrable inclusion Γ, see Figure 8.13. We set artificial boundaries using either PML or RBC. In the first case, we impose the low-order RBC developed in Section 8.1 as described in Section 8.4 on the square $\partial\Omega$. Secondly, we consider additional layers Γ_2 on

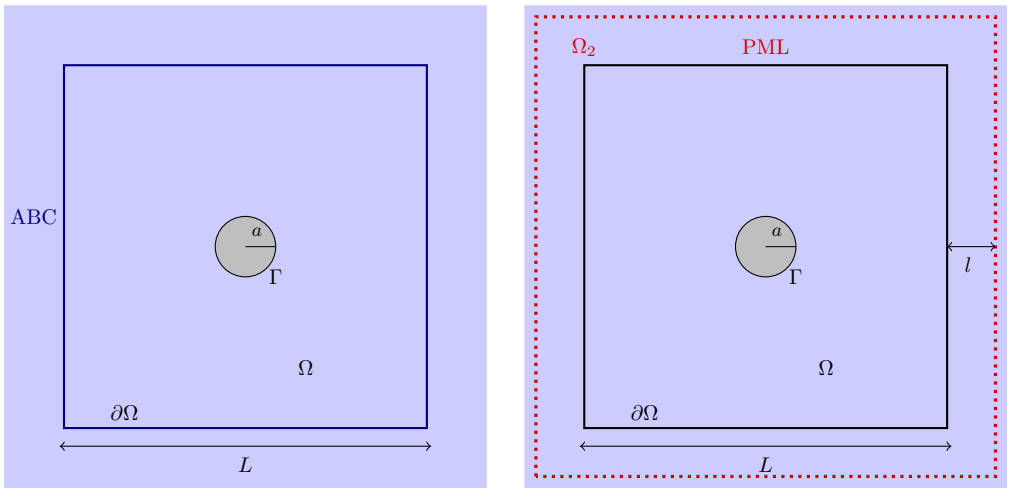

(a) Domain with RBC

(b) Domain with PML

Figure 8.13: Infinite porous domain with a solid obstacle, in which we build radiation boundary conditions. In the tests, we take: $a = 1$m, $L = 20$m, $\beta_0 = 6.39$, and $l = 5$m. We can use either PML or RBC.

the borders of Ω of length $l = 5$m, that we take as PML. We denote by "RBC" the solution with radiation boundary conditions, "PML" the solution with PML, and "exact" the reference solution. For the numerical tests, we use $\mathfrak{a} = 1$m and $L = 20$m. On Γ, we set boundary conditions of type 1, see equation (5.10a). We can compare the solutions with the reference solution developed in Section 8.2. We plot in Figure 8.14 the solution obtained on the horizontal solid velocity u_x for the two kinds of artificial boundaries. In the case of the RBC, the computational domain is discretized

with 7116 elements. For the case with PML, as we need to discretize also the additional layers, the computational mesh is composed of 14851 elements, which increases the time of the simulation. Note that the error is calculated only

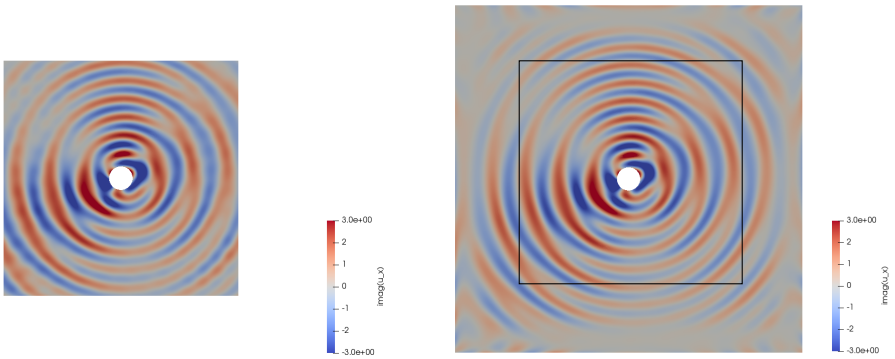

(a) RBC

(b) PML

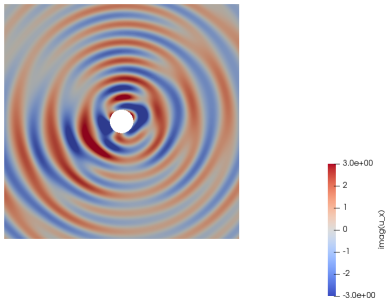

(c) Reference solution

Figure 8.14: Imaginary part of the solid velocity u_x ($\mathrm{m.s}^{-1}$) of the reflected wave for the scattering of a P-wave on an obstacle with boundary conditions 1 at the interior radius, for a medium composed of sand1 with $f = 1$ kHz for a domain with radiation boundary condition and a domain with PML.

on the part of the domain where the original problem is actually solved and which coincides with the domain used for the case with radiation boundary conditions. We obtain for the L^2 relative errors:

$$e_h(\mathrm{u}_x) = 5.34\% \quad \text{for RBC and } e_h(\mathrm{u}_x) = 3.35\% \quad \text{for PML.}$$

The order of magnitude for the errors is the same for the two truncation methods. They seem to both perform well.

8.6.2 Source in electromagnetic waves

We now want to study if the truncation methods are efficient to absorb the electromagnetic waves. In the previous example, the amplitude of the electromagnetic wave was small, and the truncation methods had a good performance. As the electromagnetic waves have a velocity way larger than the other velocities, it can be problematic for the artificial conditions to prevent reflections. To observe the fast electromagnetic waves, we take a source as $\mathbf{f}_C = \delta\, \mathrm{e}_x$, with δ a Dirac distribution. We consider an homogeneous domain composed of sand1. For the numerical simulations, we set artificial boundaries, first using RBC then PML. For the case with the RBC, we truncate the domain to the square $\mathcal{D} = [0, 20] \times [0, 20]\mathrm{m}$. For the PML, we use the domain $\mathcal{D}$ and we add absorbing layers. The total computational domain is $\mathcal{D}_{\mathrm{pml}} = [-4, 24] \times [-4, 24]\mathrm{m}$. The point source is taken at $(x, y) = (10, 10)$. We plot the results for the solid velocity u_x and the electric field E_x in Figure 8.15 for RBC and PML. Concerning the solid velocity u_x, we observe mainly the S wave, that seems to be well absorbed. We do not observe significant reflections. On the electric field E_x,

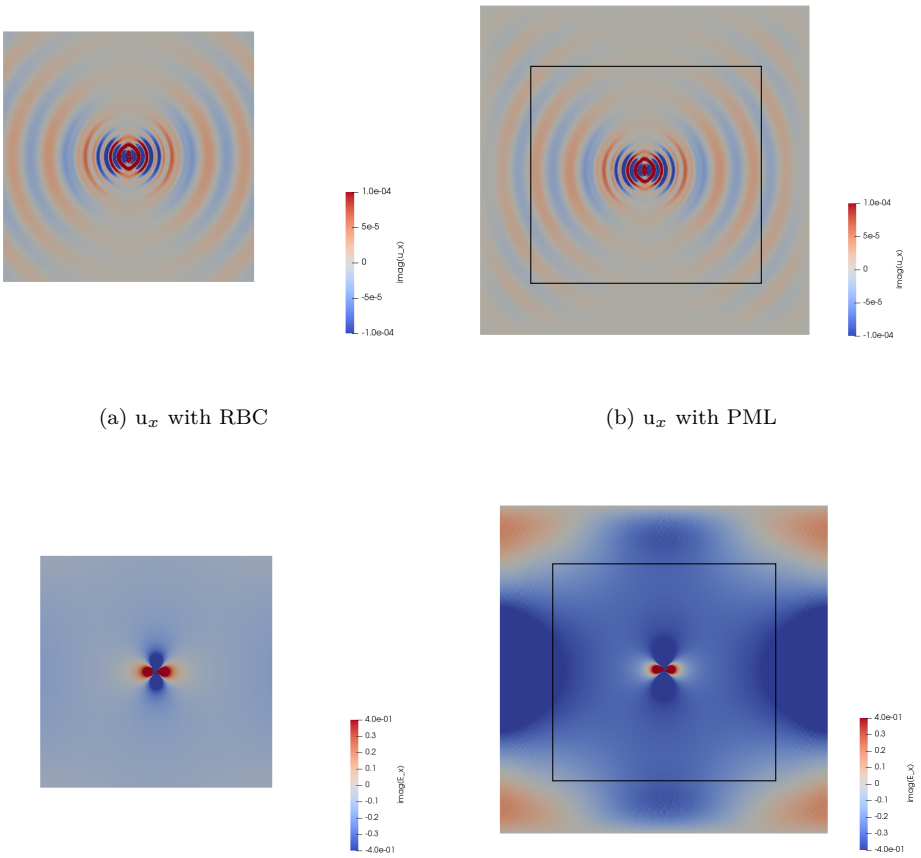

(a) u_x with RBC

(b) u_x with PML

(c) E_x with RBC

(d) E_x with PML

Figure 8.15: Imaginary part of the solid velocity u_x ($m.s^{-1}$) and imaginary part of the electric field E_x ($V.m^{-1}$) for a porous medium composed of sand1 with $f = 1$ kHz for a domain with radiation boundary condition and a domain with PML.

we can see the EM wave. For the method with RBC, we can observe the point source and no reflections are clearly visible. However, for the PML, the solution is not as good as for the RBC. In the PML, we observe a strong reflected wave. In this case, the RBC seems to be better than PML, but this can be different for other configurations. The problem of the PML comes from the fact that the EM wave has a very large wavelength. In general, the size of the PML is taken of the same order of one wavelength. However, for the EM wave, this would lead to a very large PML and a drastic increase of computational time. This is the problem that also appears in [61].

Conclusion

In this chapter, starting from the potential formulation of the unknowns, we have built a low-order radiation condition for Pride's equations in two dimensions in harmonic domain. We have built an analytical solution associated to the RBC in the setting of plane scattering by circular obstacles. We have used this analytical solution to assess the performance of the RBC by comparing the RBC solution to the outgoing solution. The RBC has good accuracy, but the inversion of the matrix for the computation of the reference RBC solution can be difficult, due to the large size of the Hankel functions, which causes the condition number of the matrix to be very large. This problem only appears in the reference RBC solution, which uses the Hankel functions, but not in HDG method, because we do not use those functions. Then, we have implemented the radiation condition in a hybridizable dicontinuous Galerkin (HDG) formulation. In addition, perfectly matched layers (PML) have also been included in the HDG discretization. We have performed numerical tests to compare the performance of RBC and PML on several configurations. The HDG method with RBC or PML performs well, regarding the simulation of the seismic waves (P, B, S). However, for the fast EM

wave, we have observed a configuration where the PML does not prevent reflections, and deteriorates the solution.

Chapter 9

Towards comparison with geophysical experiments

In the previous chapters, we have constructed a HDG method to solve the electrokinetic equations in the harmonic domain. We have validated the method by using analytical solutions. The objective of this chapter is to perform numerical experiments as a first step in the comparison between synthetic data and real data obtained in the laboratory. For that purpose, we have to check the efficiency of the code snapshots as laboratory experiments deliver time-dependent data . We focus on the simulation of converted waves as they have been recently measured in the laboratory by Victor Martins Gomez, as part of his thesis in the CHICkPEA project. We consider two types of conversions: the first one is the converted seismic wave obtained at an interface with an electromagnetic source. The second is the converted electromagnetic wave that appears at the interface when a coseismic wave is reflected. For that, a first step is to obtain the results in the time domain. The method to obtain the results in the time domain is detailed in Section 9.1. We present in Section 9.2 the investigation of the electroseismic conversion. Then, in Section 9.3, we study the seismoelectric conversion.

9.1 Time domain transformation

In the previous chapters, we have worked at a fixed frequency. In this section, we present how to obtain the results in the time domain from results in the frequency domain. The method is verified by comparing the results with a reference solution.

9.1.1 Frequency to time transformation method

Let us consider a Ricker function in the time domain, of the form:

$$s_{\text{time}} = -2\,\alpha\,(1 + 2\,\alpha\,t_1^2)\,e^{\alpha\,t_1^2}, \quad \text{with } t_1 = t - t_0\,, \quad t_0 = 1.2/f_0\,, \quad \alpha = \pi^2\,f_0^2\,, \text{ and } f_0 = 25\,\text{kHz}.$$

The source is studied for a time range of $[0\,,\,t_{\max}]$, and the signal is discretized in N_{time} points with a time step dt, with $t_{\max} = dt\,N_{\text{time}}$, as given in Figure 9.1.

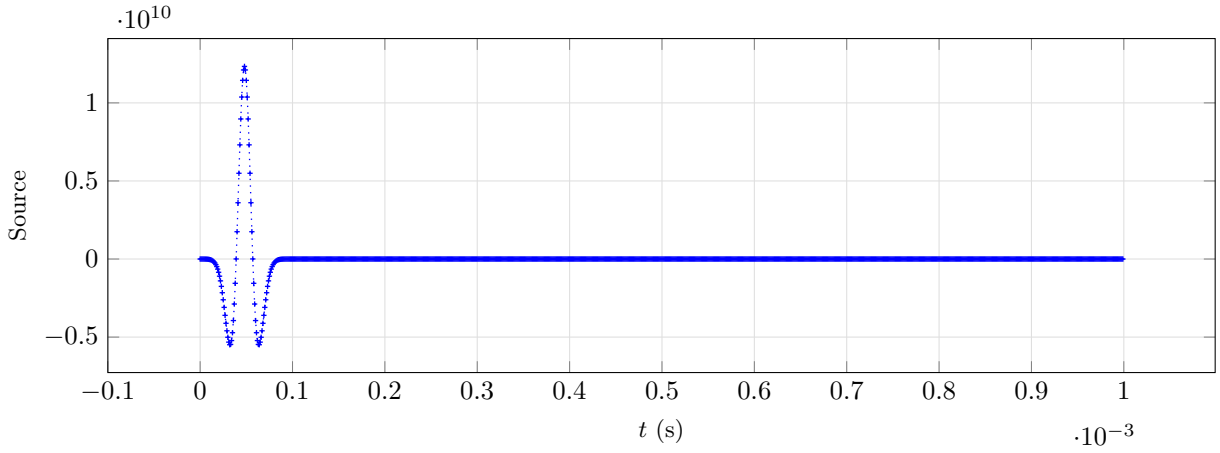

Figure 9.1: Source in the time domain, with $t_{\max} = 2\,\text{ms}$ and $dt = 1\,\mu\text{s}$.

To obtain the source in frequency domain, we apply a Fast Fourier Transform (FFT) to the signal. For this, we use the function *fft* of the software Octave. The time interval is sampled as follows: if $t_{\max} = dt\, N_{\text{time}}$ and $t_n = n\, dt$, n is an integer between 0 and N_{time}, the frequencies are given in the following order:

$$f = \frac{1}{t_{\max}} \left[0, 1, ..., \frac{N_{\text{time}}}{2} - 1, -\frac{N_{\text{time}}}{2}, ..., -1\right] \text{ if } N_{\text{time}} \text{ is even}\,,$$
$$f = \frac{1}{t_{\max}} \left[0, 1, ..., \frac{N_{\text{time}} - 1}{2}, -\frac{N_{\text{time}} - 1}{2}, ..., -1\right] \text{ if } N_{\text{time}} \text{ is odd}\,.$$

We then use the function *fftshift* of the software Octave to obtain the signal in the right order, and we only keep the positive frequencies. The negative frequencies will be taken into account when we do the inverse Fourier transform (IFT) by using the conjugate of the positive frequencies. For $f = 0\text{Hz}$, we consider the signal to be zero. The signal of the source used is given in Figure 9.2.

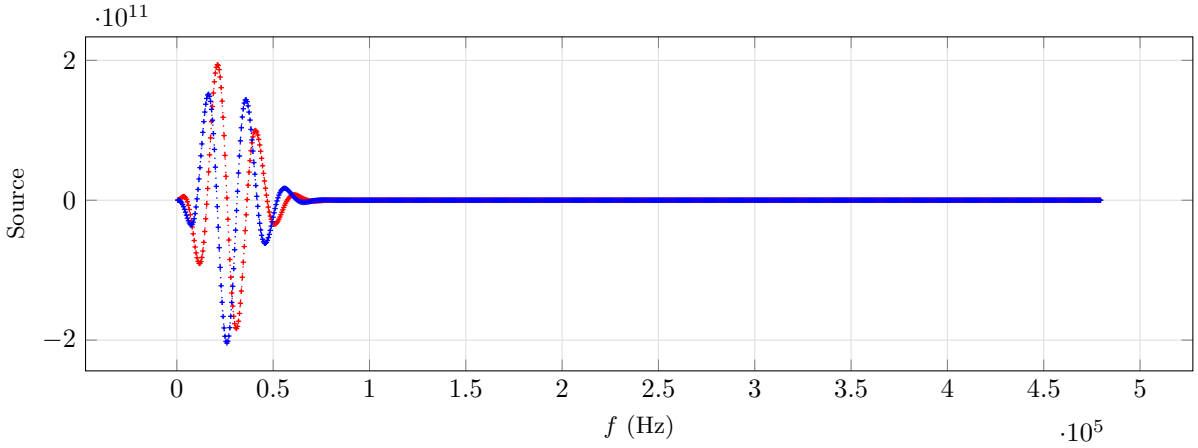

Figure 9.2: FFT of the source given in Figure 9.1, in the frequency domain, with $f_{\max} = 500\,\text{kHz}$ and $df = 500\,\text{Hz}$. The real part of the source is given in red ····+····, and the imaginary part of the source in blue ····+····.

We have now a list of frequencies between df and $f_{\max}$, with $f_{\max} = \dfrac{1}{2\,dt}$ and $df = \dfrac{1}{t_{\max}}$, and a corresponding signal. We run the code for all the frequencies, with the given source. Because of the linearity of the problem, we can either multiply the source at a fixed frequency by the signal given in Figure 9.2 in the code, or use the same source for each frequency, and multiply afterwards the result by the corresponding amplitude given in Figure 9.2. Finally, we perform an IFT on the obtained results to compute the signals in the time domain, by using the function *ifftreal*.

9.1.2 Verification of the time transformation

We now verify that our algorithm for the time transformation is correct. For this, we compare our results with a reference solution, developed in the software Gar6more [45]. The reference solution is developed in the time domain,

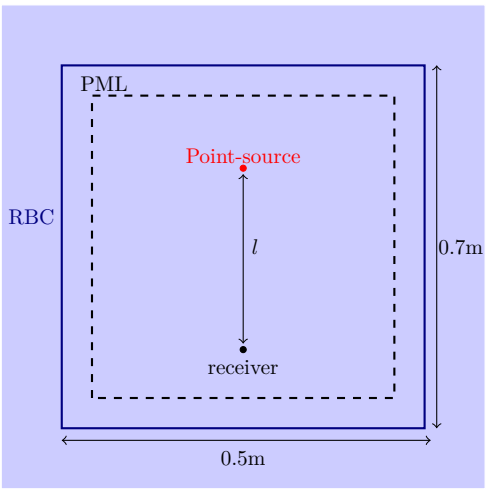

Figure 9.3: Computational domain

however with necessary assumptions: the viscosity and the conductivity of the material are supposed to be equal to zero, and the coupling tensor has a fixed value. In this case, we need to define limits for some parameters.

First, for k, we have:

$$\frac{\eta}{k(\omega)} = \frac{1}{k_0}\left(\sqrt{\eta^2 - \mathrm{i}\,\frac{4}{m}\,\omega\,\eta\,\frac{\eta}{\omega_t}} - \mathrm{i}\frac{\eta}{\omega_t}\omega\right) = \frac{1}{k_0}\left(\sqrt{\eta^2 - \frac{4\mathrm{i}}{m}\omega\eta\frac{\mathsf{t}k_0\rho_f}{\phi}} - \mathrm{i}\omega\frac{\mathsf{t}k_0\rho_f}{\phi}\right),$$

which leads to

$$\lim_{\eta\to 0,}\ \frac{\eta}{k(\omega)} = -\,\mathrm{i}\omega\frac{\mathsf{t}\,\rho_f}{\phi}\,.$$

For a fixed $\mathbf{L}$, and a zero conductivity σ we will use the following expression of $\tilde{\boldsymbol{\varepsilon}}$:

$$\tilde{\boldsymbol{\varepsilon}} = \delta_0 + \frac{\mathsf{t}\,\rho_f}{\phi}\,\mathbf{L}^2\,.$$

We consider a homogenous domain composed of sand2, see Table 7.1. On the boundary of the computational domain, we use ABC and PML (see Chapter 8). We set $\mathrm{L} = 1e-9$ A.Pa^{-1}.m^{-1}.

The analytical solution is computed with Gar6more. In Chapter 6, equation (6.14), we have obtained the following expression of the electric field $\boldsymbol{E}$:

$$-\omega^2\,\boldsymbol{E} = \frac{\mathcal{E}_{\mathrm{P}}}{\mathsf{s}_{\mathrm{P}}^2}\,\nabla\chi_{\mathrm{P}} + \frac{\mathcal{E}_{\mathrm{B}}}{\mathsf{s}_{\mathrm{B}}^2}\,\nabla\chi_{\mathrm{B}} - \frac{\mathcal{E}_{\mathrm{S}}}{\mathsf{s}_{\mathrm{S}}^2}\,\mathbf{curl}\chi_{\mathrm{S}} - \frac{\mathcal{E}_{\mathrm{EM}}}{\mathsf{s}_{\mathrm{EM}}^2}\,\mathbf{curl}\chi_{\mathrm{EM}} + \tilde{\mathbf{F}}_{\mathbf{3}}\,, \tag{9.1}$$

with the potentials $\chi_\bullet$ with $\bullet =$ P, B, S, EM solutions of the Helmholtz equation. We assume that $\tilde{\mathbf{F}}_{\mathbf{3}} = 0$, that the potentials $\chi_{\mathrm{B}} = \chi_{\mathrm{S}} = \chi_{\mathrm{EM}} = 0$, and

$$-\,\omega^2\,\mathsf{s}_{\mathrm{P}}^2\,\chi_{\mathrm{P}} - \Delta\,\chi_{\mathrm{P}} = -\,\omega^2\,\delta f(\omega)\,, \tag{9.2}$$

with δ a Dirac distribution in spatial domain and f the function plotted in Figure 9.2. By doing an inverse Fourier transform, equation (9.2) is expressed in the time domain as:

$$\left(\frac{\partial^2}{\partial t^2} - \mathsf{c}_{\mathrm{P}}^2\,\Delta\right)\hat{\chi}_{\mathrm{P}} = \delta\,\hat{f}''(t)\,,$$

with $\hat{f}$ the transform function of f in the time domain, $\mathsf{c}_{\mathrm{P}} = \mathsf{s}_{\mathrm{P}}^{-1}$ the velocity of the P-wave, and $f''(t)$ the Ricker function plotted in Figure 9.1, where we consider that $f''(0) = f'(0) = 0$. Hence,

$$\hat{\chi}_{\mathrm{P}} = G(x,y,t) * f''(t)\,,$$

with G the Green function in the time domain in an acoustic infinite media with velocity c_{P} (see *e.g.* [44]). Hence, using expression (9.1), the electric field satisfies:

$$\frac{\partial^2}{\partial t^2}\,\boldsymbol{E}(x,y,t) = \mathcal{E}_{\mathrm{P}}\,\mathsf{c}_{\mathrm{P}}^2\,\nabla\,G(x,y,t) * f''(t)\,,$$

which means that

$$\boldsymbol{E}(x,y,t) \;=\; \mathcal{E}_{\mathrm{P}}\,\mathsf{c}_{\mathrm{P}}^2\,\nabla\, G(x,y,t) * f(t)\,.$$

The expression $\nabla\, G(x,y,t) * f(t)$ is the same as for acoustics and can be computed with Gar6more. Hence, we can obtain the value of the electric field $\boldsymbol{E}$. We can also obtain the other unknowns of the electrokinetic equations in the same way.

Concerning the source in the HDG code, we set a source that only generates P-waves. For this, we take the source as a point-source of the form:

$$\mathbf{f}_u \;=\; \frac{(\rho_a \,+\rho_f\,\mathcal{W}_{\mathrm{P}})}{\omega^2\,\mathsf{s}_{\mathrm{P}}^4}\,\nabla\,\delta\,,\qquad \mathbf{f}_w \;=\; \frac{(\rho_f \;+\; \rho_{\mathrm{dyn}}\,\mathcal{W}_{\mathrm{P}} \,-\, \mathrm{i}\,\dfrac{\mathsf{t}\,\rho_f}{\omega\,\phi}\,\mathbf{L}\,\mathcal{E}_{\mathrm{P}})}{\omega^2\,\mathsf{s}_{\mathrm{P}}^4}\nabla\,\delta\,,\qquad \mathbf{f}_C \;=\; \frac{\Big(\mathbf{L}\,\rho_{\mathrm{dyn}}\mathcal{W}_{\mathrm{P}} \,-\, \dfrac{\mathfrak{s}\mathrm{i}\,\tilde{\boldsymbol{\varepsilon}}}{\omega}\,\mathcal{E}_{\mathrm{P}}\Big)}{\omega^2\,\mathsf{s}_{\mathrm{P}}^4}\nabla\,\delta\,,$$

with $\mathbf{f}_u$, $\mathbf{f}_w$, $\mathbf{f}_C$ the exterior forces of Pride's equation (5.3). The calculations to obtain a source generating only P-waves are given in Appendix F.1. We use a receiver at a distance of the source $l = 0.222$m. The results are plotted in Figure 9.4. We observe that the two results are similar, however we observe oscillations in the numerical solution after $t = 250\mu$s due to the spurious reflections on the boundary of the computational domain. The small difference between the analytical and the numerical solution is due to the numerical error of the HDG method.

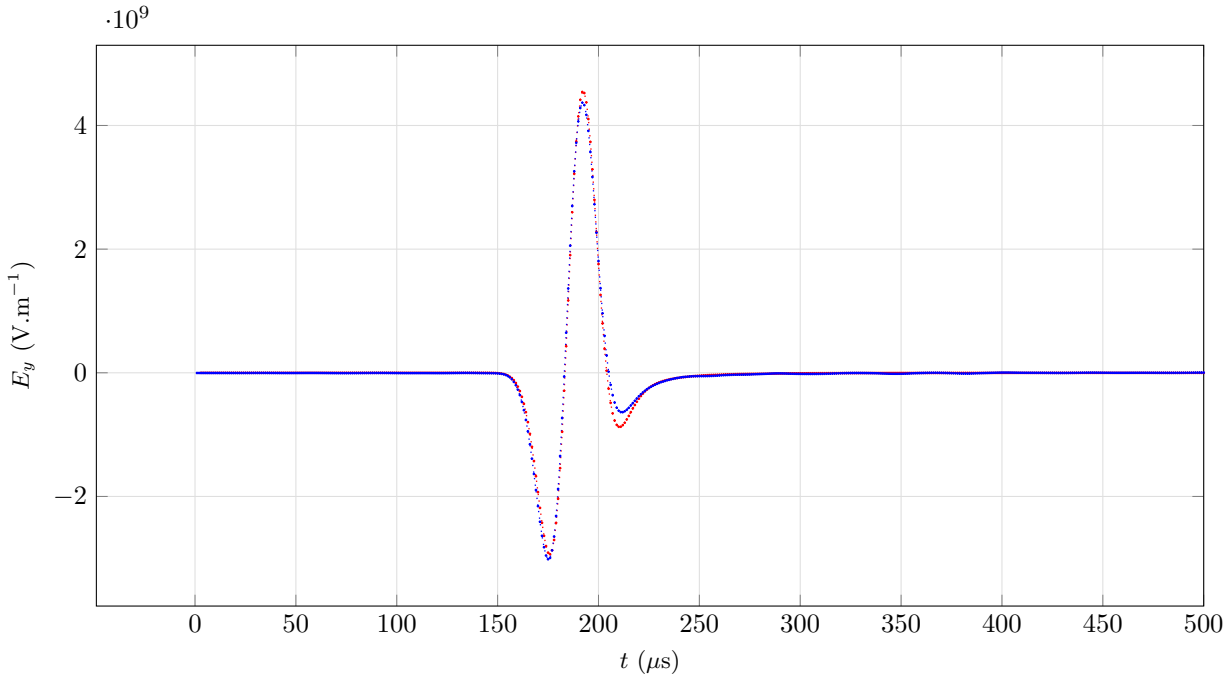

Figure 9.4: Comparison of the seismogram on E_y. The result obtained numerically is represented in blue ····· and the reference solution is in red ·····.

9.2 Electroseismic conversion

In this section, we want to detect the electroseismic conversion. When an electromagnetic wave propagates in a conducting poroelastic material and impinges an interface, a converted wave is generated. We consider an infinite domain composed of sand2 (see Table 7.1). On the edges of the computational domain, we set artificial boundaries using the RBC developed in Chapter 8. The computational domain is presented in Figure 9.5. In the upper medium (medium 1), we consider that the coupling tensor $\mathbf{L}$ is a hundred times larger than in medium 2, by setting the zeta potential $\zeta = 0.1$ V in medium 1 and $\zeta = 10$ V in medium 2. The interface between the two media is plane and horizontal.

The source in space is a point source at the coordinates $(500, 800)$. A point source is modeled as a Dirac distribution, denoted by δ. We consider the problem (5.3) with

$$\mathbf{f}_u \;=\; 0\,,\qquad \mathbf{f}_w \;=\; 0\,,\qquad \mathbf{f}_C \;=\; \delta\,\mathbf{e}_y\,.$$

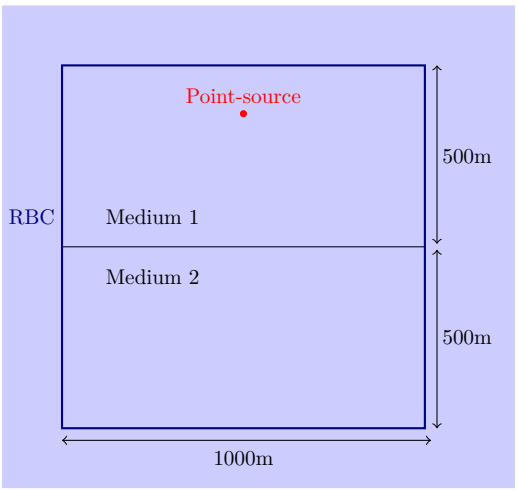

Figure 9.5: Computational domain for the electroseismic conversion

In time, we consider the amplitude of the source as a Gaussian function, given by:

$$I(t) = \frac{1}{\sigma_g \sqrt{2\,\pi}}\, e^{-\frac{(t-t_0)^2}{2\,\sigma_g^2}},$$

with $t_0 = 2.5 \cdot 10^{-2}$s and $\sigma_g = \frac{t_0}{2}$. We discretize this function for $t_n = dt\,, 2\,dt\,, \ldots t_{\max}$, with $dt = 5 \cdot 10^{-3}$s and $t_{\max} = 0.5$s. The Fourier transform of this function is:

$$\tilde{I}(f) = e^{-2\,\pi^2\,f^2\,\sigma_g^2}\, e^{\mathrm{i}\,2\,\pi\,f\,t_0}.$$

We use this source for $f = df\,, 2\,df\,, \ldots f_{\max}$, with $df = \frac{1}{t_{\max}} = 1$ Hz and $f_{\max} = \frac{1}{2\,dt} = 100$Hz, see Figure 9.6.

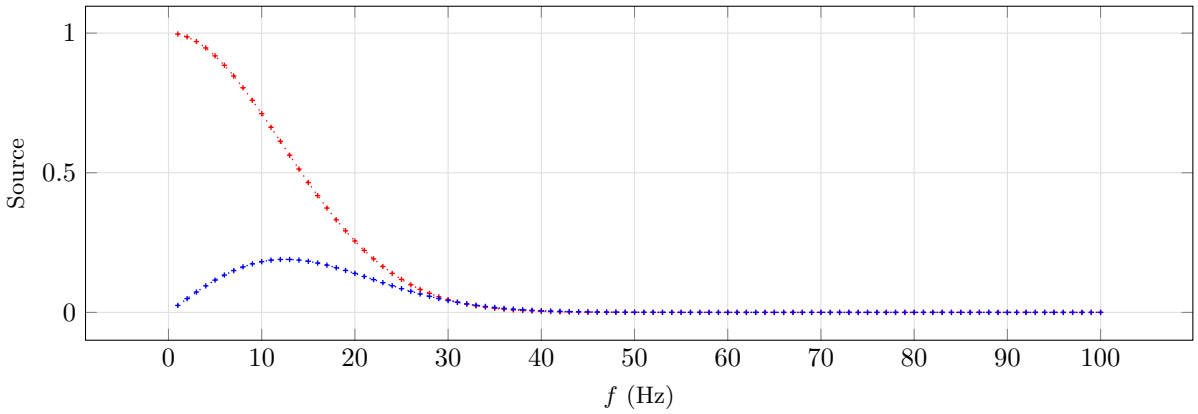

Figure 9.6: Source in frequency domain, with $f_{\max} = 100\,\mathrm{Hz}$ and $df = 0.2\,\mathrm{Hz}$. The real part of the source is given in red ····+····, and the imaginary part of the source in blue ····+····.

We run the code for the corresponding frequencies, and transform the result to time domain. We present in Figure 9.7 (respectively Figure 9.8) the electric field (respectively the velocity) at times $t = 5, 50, 200, 600$ms (respectively $t = 5, 50, 100, 150, 200, 250, 300, 350$ms).

On the electric field (Figure 9.7), we observe mainly the EM wave generated by the point-source. This wave propagates in the material very fast and has a large wavelength. As soon as the source is generated, the electromagnetic waves propagate and impinges the interface. When this happens, it creates a seismic plane wave at the interface. The electric field is not disturbed by the interface because the difference between the two materials is only in the coupling tensor. On the velocity (Figure 9.8), we can observe both the wave generated by the point-source and the converted

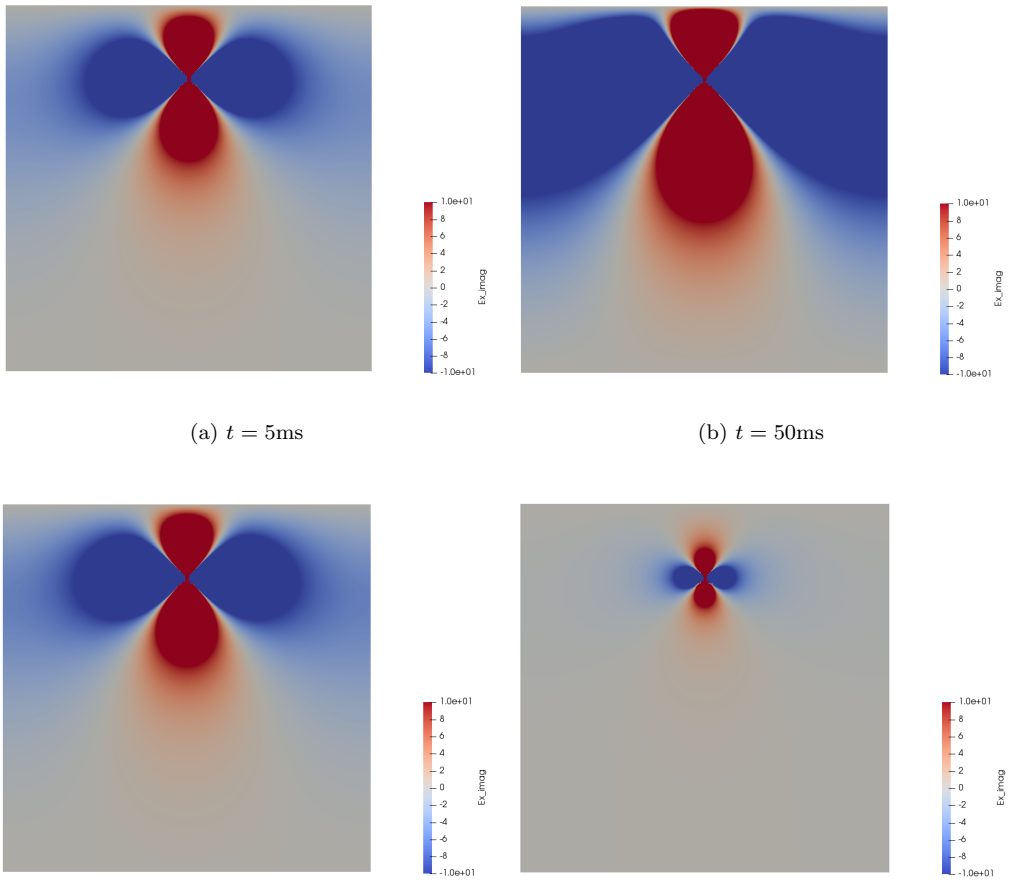

(a) $t = 5$ms

(b) $t = 50$ms

(c) $t = 200$ms

(d) $t = 600$ms

Figure 9.7: Electric field E_x at $t = 5, 50, 200, 600$ms.

plane wave generated at the interface. The first wave propagates from the source point. The converted waves is generated at the plane interface, as soon as the electromagnetic impinges the interface, and propagates vertically in the material.

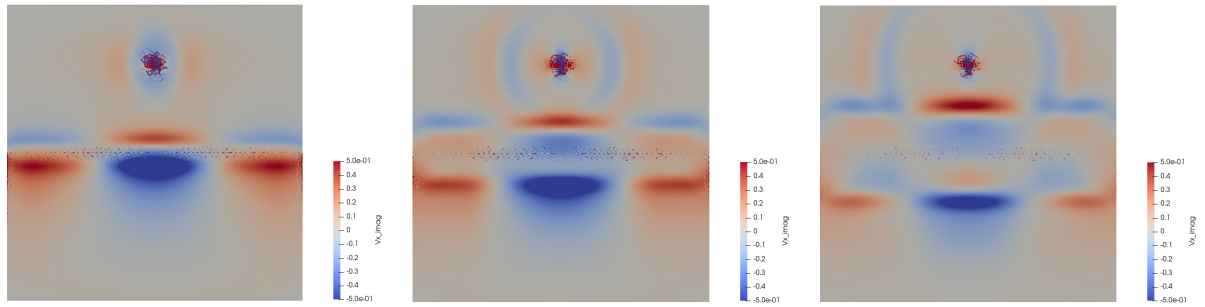

(a) $t = 5$ms (b) $t = 50$ms (c) $t = 100$ms

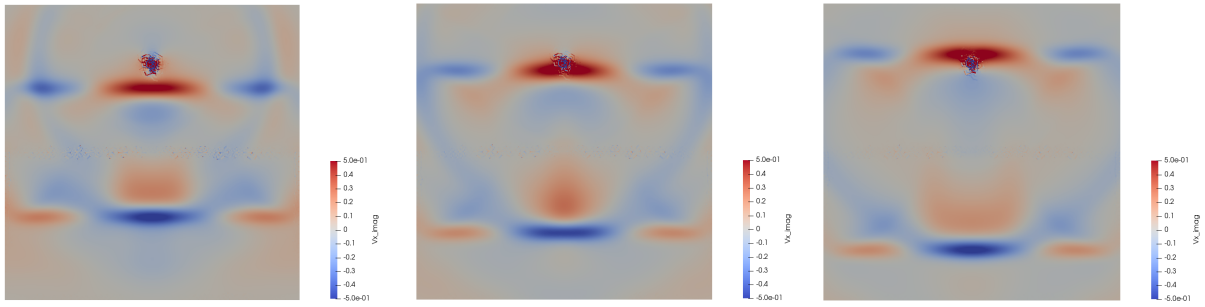

(d) $t = 150$ms (e) $t = 200$ms (f) $t = 250$ms

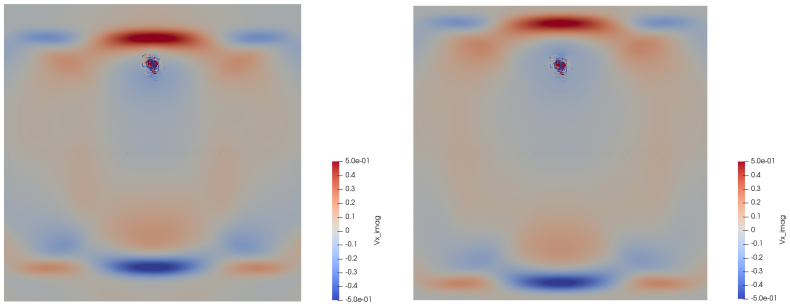

(g) $t = 300$ms (h) $t = 350$ms

Figure 9.8: Solid velocity u_x at $t = 5, 50, 100, 150, 200, 250, 300, 350$ms.

9.3 Seismoelectric conversion

In this section, we study the seismoelectric converted wave, *e.g.*, a seismic wave generated by a seismic wave impinging an interface and propagating at the electromagnetic wavespeed. We consider an infinite layered domain composed of sand2 and sandstone. The corresponding physical parameters are given in Table 7.1. We set artificial boundaries using the RBC developed in Chapter 8. The computational domain is presented in Figure 9.9. The interface between the two media is plane and vertical. The source is a point source modeled as:

$$\mathbf{f}_u = \delta\, \mathbf{e}_x\,, \qquad \mathbf{f}_w = 0\,, \qquad \mathbf{f}_C = 0\,.$$

We use the source given in Figure 9.2.

We record the signals by using a line of 200 receivers, see Figure 9.9. We present in Figure 9.10 the horizontal solid velocity u_x and the horizontal electric field E_x. On the velocity u_x, we mainly observe the propagation of the P-wave. On the electric field E_x, we observe a wave propagating at the same time as the P-wave on the velocity. This is the coseismic wave. In addition, we observe another signal propagating at a very large speed when the P-wave is reflected

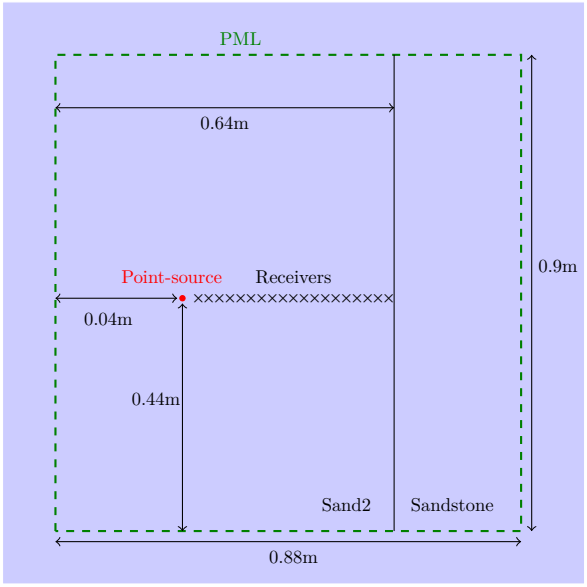

Figure 9.9: Computational domain for the seismoelectric conversion

on the interface between the sand2 and the sandstone, and this is the converted wave. The amplitude of this wave is smaller than the coseismic wave, and we can observe it only if saturating the picture. We also observe a much slower wave corresponding to the S-wave.

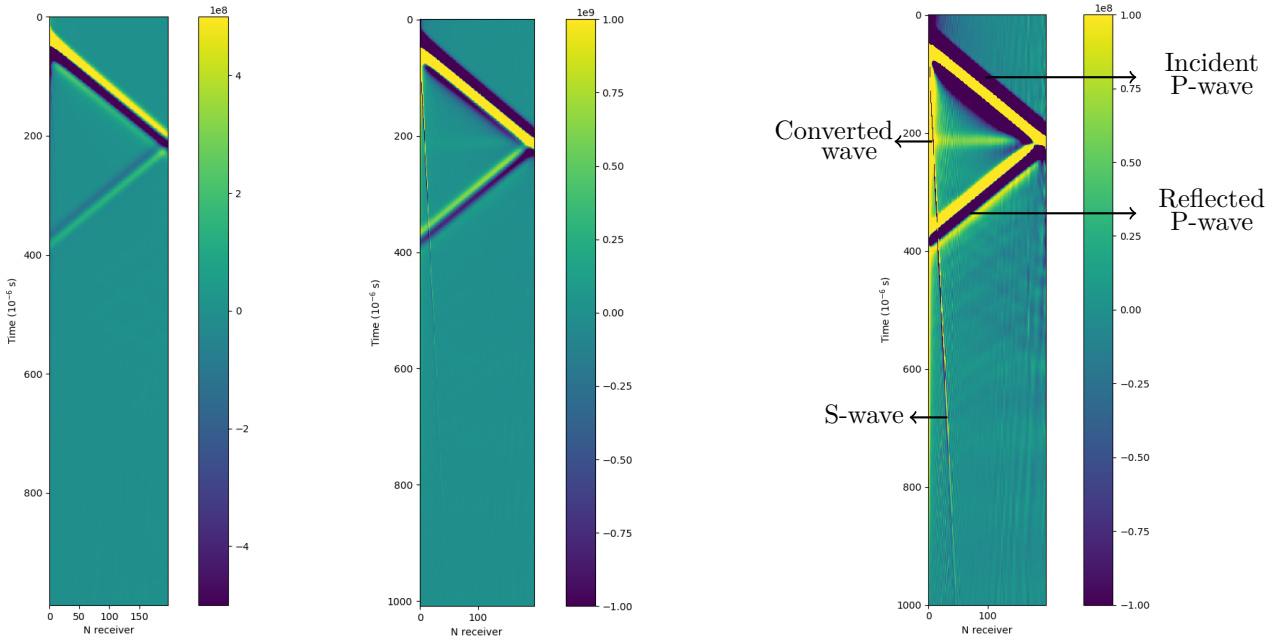

(a) Solid velocity u_x (b) Electric field E_x (c) Electric field E_x with higher saturation

Figure 9.10: Solid velocity u_x and electric field E_x.

Conclusion

In this chapter, we have succeeded in numerically reproducing the converted waves associated with an electroseismic case and a seismoelectric case. Those phenomena, in particular the seismo-electric one, are however hard to simulate,

because their amplitudes are smaller than the amplitude of the other waves. The converted waves can also be hidden by the other waves or the reflections on the border of the computational domain. We have presented the results for two-dimensional cases. This can be extended to three dimensions, however this is quite difficult, due to the large size of the global system that we need to inverse for each frequency. The main problem is that we use a direct solver for the inversion of the matrix, which needs a very large amount of memory, hence we need to have access to large computational resources. However, the use of a direct solver is essential, in particular for fields experiments, where there are several thousands of sources and where we want to use the multi right-hand side functionality of the solver MUMPS. To improve the performance of the solver in three dimensions, we will study the block analysis of the solver and the Block-Low-Range (BLR) functionality, which allows to decrease the memory needed for the inversion of the system.

Appendix D

Appendices to Chapter 5

D.1 Calculation details on the determinant of the plane wave matrix

D.1.1 Transverse wave

From equation (5.20), we want to calculate the determinant of the matrix

$$\begin{pmatrix} \rho_a - \mathsf{s}^2\,\mu_{\mathrm{fr}} & \rho_f & 0 \\ \rho_f & \rho_{\mathrm{dyn}} & \dfrac{\eta}{\omega^2\,k}\,\mathbf{L} \\ 0 & \mathfrak{s}\,\mathrm{i}\,\omega\,\mu_0\,\mathbf{L}\,\rho_{\mathrm{dyn}} & \tilde{\varepsilon}\,\mu_0 - \mathsf{s}^2 \end{pmatrix},$$

which is equals to zero. The determinant is:

$$\left(\tilde{\varepsilon}\,\mu_0 - \mathsf{s}^2\right)\left(\left(\rho_a - \mathsf{s}^2\,\mu_{\mathrm{fr}}\right)\rho_{\mathrm{dyn}} - \rho_f^2\right) - \frac{\eta}{\omega^2\,k}\,\mathbf{L}\,\mathfrak{s}\,\mathrm{i}\,\omega\,\mu_0\,\mathbf{L}\,\rho_{\mathrm{dyn}}\left(\rho_a - \mathsf{s}^2\,\mu_{\mathrm{fr}}\right) = 0\,,$$

Using

$$\frac{\eta}{\omega^2\,k}\,\mathbf{L} = \frac{\mathfrak{s}\,\mathrm{i}\,\rho_{\mathrm{dyn}}}{\omega}\,\mathbf{L}\,,$$

we have

$$\left(\tilde{\varepsilon}\,\mu_0 - \mathsf{s}^2\right)\left(\left(\rho_a - \mathsf{s}^2\,\mu_{\mathrm{fr}}\right)\rho_{\mathrm{dyn}} - \rho_f^2\right) - \frac{\mathfrak{s}\,\mathrm{i}\,\rho_{\mathrm{dyn}}}{\omega}\,\mathbf{L}\,\mathfrak{s}\,\mathrm{i}\,\omega\,\mu_0\,\mathbf{L}\,\rho_{\mathrm{dyn}}\left(\rho_a - \mathsf{s}^2\,\mu_{\mathrm{fr}}\right) = 0\,,$$

$$\Rightarrow \left(\tilde{\varepsilon}\,\mu_0 - \mathsf{s}^2\right)\left(\left(\rho_a - \mathsf{s}^2\,\mu_{\mathrm{fr}}\right)\rho_{\mathrm{dyn}} - \rho_f^2\right) + \rho_{\mathrm{dyn}}^2\,\mathbf{L}^2\,\mu_0\left(\rho_a - \mathsf{s}^2\,\mu_{\mathrm{fr}}\right) = 0\,,$$

We develop the above expression

$$\left(\tilde{\varepsilon}\,\mu_0 - \mathsf{s}^2\right)\left(\rho_a - \mathsf{s}^2\,\mu_{\mathrm{fr}}\right)\rho_{\mathrm{dyn}} - \left(\tilde{\varepsilon}\,\mu_0 - \mathsf{s}^2\right)\rho_f^2 + \rho_{\mathrm{dyn}}^2\,\mathbf{L}^2\,\mu_0\,\rho_a - \rho_{\mathrm{dyn}}^2\,\mathbf{L}^2\,\mu_0\,\mathsf{s}^2\,\mu_{\mathrm{fr}} = 0\,,$$

$$\left(\tilde{\varepsilon}\,\mu_0 - \mathsf{s}^2\right)\rho_a\,\rho_{\mathrm{dyn}} - \left(\tilde{\varepsilon}\,\mu_0 - \mathsf{s}^2\right)\mathsf{s}^2\,\mu_{\mathrm{fr}}\,\rho_{\mathrm{dyn}} - \left(\tilde{\varepsilon}\,\mu_0 - \mathsf{s}^2\right)\rho_f^2 + \rho_{\mathrm{dyn}}^2\,\mathbf{L}^2\,\mu_0\,\rho_a - \rho_{\mathrm{dyn}}^2\,\mathbf{L}^2\,\mu_0\,\mathsf{s}^2\,\mu_{\mathrm{fr}} = 0\,,$$

$$\tilde{\varepsilon}\,\mu_0\,\rho_a\,\rho_{\mathrm{dyn}} - \mathsf{s}^2\,\rho_a\,\rho_{\mathrm{dyn}} - \tilde{\varepsilon}\,\mu_0\,\mathsf{s}^2\,\mu_{\mathrm{fr}}\,\rho_{\mathrm{dyn}} + \mathsf{s}^2\,\mathsf{s}^2\,\mu_{\mathrm{fr}}\,\rho_{\mathrm{dyn}} - \tilde{\varepsilon}\,\mu_0\,\rho_f^2 + \mathsf{s}^2\,\rho_f^2 + \rho_{\mathrm{dyn}}^2\,\mathbf{L}^2\,\mu_0\,\rho_a - \rho_{\mathrm{dyn}}^2\,\mathbf{L}^2\,\mu_0\,\mathsf{s}^2\,\mu_{\mathrm{fr}} = 0\,,$$

and obtain:

$$\mathsf{s}^4\,\mu_{\mathrm{fr}}\,\rho_{\mathrm{dyn}} - \mathsf{s}^2\left(\left(\rho_a\,\rho_{\mathrm{dyn}} - \rho_f^2\right) + \tilde{\varepsilon}\,\mu_0\,\mu_{\mathrm{fr}}\,\rho_{\mathrm{dyn}} + \rho_{\mathrm{dyn}}^2\,\mathbf{L}^2\,\mu_0\,\mu_{\mathrm{fr}}\right) + \left(\tilde{\varepsilon}\,\mu_0\left(\rho_a\,\rho_{\mathrm{dyn}} - \rho_f^2\right) + \rho_{\mathrm{dyn}}^2\,\mathbf{L}^2\,\mu_0\,\rho_a\right) = 0\,. \quad \text{(D.1)}$$

This is a quadratic equation in s^2. The discriminant Δ is:

$$\begin{aligned}
\Delta &= \big((\,\rho_a\,\rho_{\rm dyn} - \rho_f^2\,) + \tilde{\varepsilon}\,\mu_0\,\mu_{\rm fr}\,\rho_{\rm dyn} + \rho_{\rm dyn}^2\,\mathbf{L}^2\,\mu_0\,\mu_{\rm fr}\big)^2 - 4\,\mu_{\rm fr}\,\rho_{\rm dyn}\,(\,\tilde{\varepsilon}\,\mu_0\,(\,\rho_a\,\rho_{\rm dyn} - \rho_f^2) + \rho_{\rm dyn}^2\,\mathbf{L}^2\,\mu_0\,\rho_a\,)\,,\\
&= (\,\rho_a\,\rho_{\rm dyn} - \rho_f^2\,)^2 + \big(\tilde{\varepsilon}\,\mu_0\,\mu_{\rm fr}\,\rho_{\rm dyn} + \rho_{\rm dyn}^2\,\mathbf{L}^2\,\mu_0\,\mu_{\rm fr}\big)^2 + 2\,(\,\rho_a\,\rho_{\rm dyn} - \rho_f^2\,)\,\big(\tilde{\varepsilon}\,\mu_0\,\mu_{\rm fr}\,\rho_{\rm dyn} + \rho_{\rm dyn}^2\,\mathbf{L}^2\,\mu_0\,\mu_{\rm fr}\big)\\
&\quad - 4\,\mu_{\rm fr}\,\rho_{\rm dyn}\,(\,\tilde{\varepsilon}\,\mu_0\,(\,\rho_a\,\rho_{\rm dyn} - \rho_f^2) + \rho_{\rm dyn}^2\,\mathbf{L}^2\,\mu_0\,\rho_a\,)\,,\\
&= (\,\rho_a\,\rho_{\rm dyn} - \rho_f^2\,)^2 + \big(\tilde{\varepsilon}\,\mu_0\,\mu_{\rm fr}\,\rho_{\rm dyn} + \rho_{\rm dyn}^2\,\mathbf{L}^2\,\mu_0\,\mu_{\rm fr}\big)^2\\
&\quad + 2\,(\,\rho_a\,\rho_{\rm dyn} - \rho_f^2\,)\,\tilde{\varepsilon}\,\mu_0\,\mu_{\rm fr}\,\rho_{\rm dyn} + 2\,\rho_a\,\rho_{\rm dyn}^3\,\mathbf{L}^2\,\mu_0\,\mu_{\rm fr} - 2\,\rho_f^2\,\rho_{\rm dyn}^2\,\mathbf{L}^2\,\mu_0\,\mu_{\rm fr}\\
&\quad - 4\,(\,\rho_a\,\rho_{\rm dyn} - \rho_f^2)\,\tilde{\varepsilon}\,\mu_0\,\mu_{\rm fr}\,\rho_{\rm dyn} - 4\,\rho_a\,\rho_{\rm dyn}^3\,\mathbf{L}^2\,\mu_0\,\mu_{\rm fr}\,,\\
&= (\,\rho_a\,\rho_{\rm dyn} - \rho_f^2\,)^2 + \big(\tilde{\varepsilon}\,\mu_0\,\mu_{\rm fr}\,\rho_{\rm dyn} + \rho_{\rm dyn}^2\,\mathbf{L}^2\,\mu_0\,\mu_{\rm fr}\big)^2\\
&\quad - 2\,(\,\rho_a\,\rho_{\rm dyn} - \rho_f^2)\,\tilde{\varepsilon}\,\mu_0\,\mu_{\rm fr}\,\rho_{\rm dyn} - 2\,\rho_a\,\rho_{\rm dyn}^3\,\mathbf{L}^2\,\mu_0\,\mu_{\rm fr} - 2\,\rho_f^2\,\rho_{\rm dyn}^2\,\mathbf{L}^2\,\mu_0\,\mu_{\rm fr}\,,
\end{aligned}$$

$$\Rightarrow \Delta = \big((\,\rho_a\,\rho_{\rm dyn} - \rho_f^2\,) - \tilde{\varepsilon}\,\mu_0\,\mu_{\rm fr}\,\rho_{\rm dyn} - \rho_{\rm dyn}^2\,\mathbf{L}^2\,\mu_0\,\mu_{\rm fr}\big)^2 - 4\,\rho_f^2\,\rho_{\rm dyn}^2\,\mathbf{L}^2\,\mu_0\,\mu_{\rm fr}\,.$$

The two roots of equation (D.1) are:

$$2\,\mathsf{s}_\bullet^2 = \frac{-\big((\,\rho_a\,\rho_{\rm dyn} - \rho_f^2\,) + \tilde{\varepsilon}\,\mu_0\,\mu_{\rm fr}\,\rho_{\rm dyn} + \rho_{\rm dyn}^2\,\mathbf{L}^2\,\mu_0\,\mu_{\rm fr}\big) \pm \sqrt{\Delta}}{\mu_{\rm fr}\,\rho_{\rm dyn}}\,,$$

using,

$$\frac{\Delta}{(\mu_{\rm fr}\,\rho_{\rm dyn})^2} = \big((\,\frac{\rho_a}{\mu_{\rm fr}} - \frac{\rho_f^2}{\mu_{\rm fr}\,\rho_{\rm dyn}}\,) - \tilde{\varepsilon}\,\mu_0 - \rho_{\rm dyn}\,\mathbf{L}^2\,\mu_0\big)^2 - 4\,\frac{\rho_f^2}{\mu_{\rm fr}}\,\mathbf{L}^2\,\mu_0\,,$$

we have

$$2\,\mathsf{s}_\bullet^2 = \left((\,\frac{\rho_a}{\mu_{\rm fr}} - \frac{\rho_f^2}{\mu_{\rm fr}\,\rho_{\rm dyn}}\,) + \tilde{\varepsilon}\,\mu_0 + \rho_{\rm dyn}\,\mathbf{L}^2\,\mu_0\right) \pm \sqrt{\left((\,\frac{\rho_a}{\mu_{\rm fr}} - \frac{\rho_f^2}{\mu_{\rm fr}\,\rho_{\rm dyn}}\,) - \tilde{\varepsilon}\,\mu_0 - \rho_{\rm dyn}\,\mathbf{L}^2\,\mu_0\right)^2 - 4\,\frac{\rho_f^2}{\mu_{\rm fr}}\,\mathbf{L}^2\,\mu_0}\,.$$

D.1.2 Longitudinal waves

We want to calculate the determinant of the following matrix (see equation (5.24)).

$$\begin{pmatrix}
\mathsf{s}^2\,H - \rho_a & \mathsf{s}^2\,\alpha M - \rho_f & 0\\
-\,\rho_f + \mathsf{s}^2\,\alpha M & -\,\rho_{\rm dyn} + \mathsf{s}^2\,M & \dfrac{\eta}{\omega^2\,k}\,\mathbf{L}\\
0 & \mathfrak{s}\,\mathrm{i}\,\omega\,\mu_0\,\mathbf{L}\,\rho_{\rm dyn} & \tilde{\varepsilon}\,\mu_0
\end{pmatrix}.$$

The determinant is zero:

$$\tilde{\varepsilon}\,\mu_0\left((\mathsf{s}^2\,H - \rho_a)\,(-\,\rho_{\rm dyn} + \mathsf{s}^2\,M) - (-\,\rho_f + \mathsf{s}^2\,\alpha M)^2\right) - \frac{\eta}{\omega^2\,k}\,\mathbf{L}\,(\mathsf{s}^2\,H - \rho_a)\,\mathfrak{s}\,\mathrm{i}\,\omega\,\mu_0\,\mathbf{L}\,\rho_{\rm dyn} = 0\,.$$

Using $\dfrac{\eta}{\omega^2\,k}\,\mathbf{L} = \dfrac{\mathfrak{s}\,\mathrm{i}\,\rho_{\rm dyn}}{\omega}\,\mathbf{L}$, we have

$$\tilde{\varepsilon}\,\mu_0\left((\mathsf{s}^2\,H - \rho_a)\,(-\,\rho_{\rm dyn} + \mathsf{s}^2\,M) - (-\,\rho_f + \mathsf{s}^2\,\alpha M)^2\right) - \frac{\mathfrak{s}\,\mathrm{i}\,\rho_{\rm dyn}}{\omega}\,\mathbf{L}(\mathsf{s}^2\,H - \rho_a)\,\mathfrak{s}\,\mathrm{i}\,\omega\,\mu_0\,\mathbf{L}\,\rho_{\rm dyn} = 0\,,$$

which gives

$$(\mathsf{s}^2\,H - \rho_a)\,(-\,\rho_{\rm dyn} + \mathsf{s}^2\,M) - (-\,\rho_f + \mathsf{s}^2\,\alpha M)^2 + \frac{(\mathsf{s}^2\,H - \rho_a)}{\tilde{\varepsilon}}\,\mathbf{L}^2\,\rho_{\rm dyn}^2 = 0\,.$$

We develop the above expression and obtain

$$-\,\rho_{\rm dyn}\,\mathsf{s}^2\,H + \rho_a\,\rho_{\rm dyn} + \mathsf{s}^4\,H\,M - \mathsf{s}^2\,\rho_a\,M\,\frac{\eta}{\omega^2\,k}\,\mathbf{L} - \rho_f^2 - \mathsf{s}^4\,\alpha^2 M^2 + 2\,\rho_f\,\mathsf{s}^2\,\alpha M + \frac{(\mathsf{s}^2\,H - \rho_a)}{\tilde{\varepsilon}}\,\mathbf{L}^2\,\rho_{\rm dyn}^2 = 0\,.$$

The quadratic equation in $\mathsf{s}_\bullet^2$ is:

$$\mathsf{s}^4 \left(H\,M \,-\, \alpha^2 M^2 \right) + \mathsf{s}^2 \left(\,-\, \rho_{\text{dyn}}\, H - \,\rho_a\, M\, \frac{\eta}{\omega^2\, k}\, \mathbf{L} \,+\, 2\,\rho_f\, \alpha M + \,\frac{H}{\tilde{\boldsymbol{\varepsilon}}}\, \mathbf{L}^2\, \rho_{\text{dyn}}^2 \right) + \left(\rho_a\, \rho_{\text{dyn}} \,-\, \rho_f^2 \,-\, \frac{\rho_a}{\tilde{\boldsymbol{\varepsilon}}}\, \mathbf{L}^2\, \rho_{\text{dyn}}^2 \right) = 0\,,$$

and we can define the roots as:

$$2\,\mathsf{s}_\bullet^2 \,=\, -\,b \,\pm\, \sqrt{b^2 \,-\, 4\,c}\,,$$

with

$$b \,=\, \frac{-\,\rho_{\text{dyn}}\, H - \,\rho_a\, M \,+\, 2\,\rho_f\, \alpha M + \,\dfrac{H}{\tilde{\boldsymbol{\varepsilon}}}\, \mathbf{L}^2\, \rho_{\text{dyn}}^2}{H\,M \,-\, \alpha^2 M^2}\,,$$

and

$$c \,=\, \frac{\rho_a\, \rho_{\text{dyn}} \,-\, \rho_f^2 \,-\, \dfrac{\rho_a}{\tilde{\boldsymbol{\varepsilon}}}\, \mathbf{L}^2\, \rho_{\text{dyn}}^2}{H\,M \,-\, \alpha^2 M^2}\,.$$

Appendix E

Appendices to Chapter 8

E.1 Details on the HDG method with RBC and PML

E.1.1 Elementary matrices for HDG method with RBC

The elementary matrices $\mathbb{P}^K$ and $\mathbb{T}^K$ are modified for the rows corresponding to the faces on Γ_{abs}. We suppose that the first face of the element K is on Γ_{abs} Then, the matrix $\mathbb{P}^K$ has the following structure,

$$\mathbb{P}^K = \begin{pmatrix} \mathbb{P}^K_{\mathbf{poro}} & \mathbb{P}^K_{\substack{\text{coupling} \\ \text{EM}\to\text{poro}}} \\ \mathbb{P}^K_{\substack{\text{coupling} \\ \text{poro}\to\text{EM}}} & \mathbb{P}^K_{\mathbf{EM}} \end{pmatrix},$$

with

$$\mathbb{P}^K_{\mathbf{poro}} = \begin{pmatrix} -\gamma_1(\mathbb{F}^{\beta(K,1)})^T - \gamma_4\mathbf{X}_2(\mathbb{L}^{\beta(K,1)}_{xx})^T & -\gamma_4\mathbf{X}_2(\mathbb{L}^{\beta(K,1)}_{xy})^T & \mathbf{X}_2(\mathbb{L}^{\beta(K,1)}_{xx})^T & \dots \\ -\gamma_1(\mathbb{F}^{\beta(K,2)})^T & 0 & 0 & \dots \\ -\gamma_1(\mathbb{F}^{\beta(K,3)})^T & 0 & 0 & \dots \\ -\gamma_4\mathbf{X}_2(\mathbb{L}^{\beta(K,1)}_{xy})^T & -\gamma_1(\mathbb{F}^{\beta(K,1)})^T - \gamma_4\mathbf{X}_2(\mathbb{L}^{\beta(K,1)}_{yy})^T & \mathbf{X}_2(\mathbb{L}^{\beta(K,1)}_{xy})^T & \dots \\ 0 & -\gamma_1(\mathbb{F}^{\beta(K,2)})^T & 0 & \dots \\ 0 & -\gamma_1(\mathbb{F}^{\beta(K,3)})^T & 0 & \dots \\ -\mathbf{X}_6\gamma_4(\mathbb{Q}^{\beta(K,1)}_x) & -\mathbf{X}_6\gamma_4(\mathbb{Q}^{\beta(K,1)}_y)^T & \mathbf{X}_6(\mathbb{Q}^{\beta(K,1)}_x)^T & \dots \\ -(\mathbb{Q}^{\beta(K,2)}_x)^T\gamma_4 & -(\mathbb{Q}^{\beta(K,2)}_y)^T\gamma_4 & (\mathbb{Q}^{\beta(K,2)}_x)^T & \dots \\ -(\mathbb{Q}^{\beta(K,3)}_x)^T\gamma_4 & -(\mathbb{Q}^{\beta(K,3)}_y)^T\gamma_4 & (\mathbb{Q}^{\beta(K,3)}_x)^T & \dots \end{pmatrix}$$

$$\begin{pmatrix} \dots & \mathbf{X}_2(\mathbb{L}^{\beta(K,1)}_{xy})^T & (\mathbb{Q}^{\beta(K,1)}_x)^T & 0 & (\mathbb{Q}^{\beta(K,1)}_y)^T & (-\gamma_3-\gamma_2\mathbf{X}_2)(\mathbb{Q}^{\beta(K,1)}_{x1})^T \\ \dots & 0 & (\mathbb{Q}^{\beta(K,2)}_x)^T & 0 & (\mathbb{Q}^{\beta(K,2)}_y)^T & -\gamma_3(\mathbb{Q}^{\beta(K,2)}_x)^T \\ \dots & 0 & (\mathbb{Q}^{\beta(K,3)}_x)^T & 0 & (\mathbb{Q}^{\beta(K,3)}_y)^T & -\gamma_3(\mathbb{Q}^{\beta(K,3)}_x)^T \\ \dots & \mathbf{X}_2(\mathbb{L}^{\beta(K,1)}_{yy})^T & 0 & (\mathbb{Q}^{\beta(K,1)}_y)^T & (\mathbb{Q}^{\beta(K,1)}_x)^T & (-\gamma_3-\gamma_2\mathbf{X}_2)(\mathbb{Q}^{\beta(K,1)}_y)^T \\ \dots & 0 & 0 & (\mathbb{Q}^{\beta(K,2)}_y)^T & (\mathbb{Q}^{\beta(K,2)}_x)^T & -\gamma_3(\mathbb{Q}^{\beta(K,2)}_y)^T \\ \dots & 0 & 0 & (\mathbb{Q}^{\beta(K,3)}_y)^T & (\mathbb{Q}^{\beta(K,3)}_x)^T & -\gamma_3(\mathbb{Q}^{\beta(K,3)}_y)^T \\ \dots & \mathbf{X}_6(\mathbb{Q}^{\beta(K,1)}_y)^T & 0 & 0 & 0 & -\gamma_2\mathbf{X}_6(\mathbb{F}^{\beta(K,1)})^T \\ \dots & (\mathbb{Q}^{\beta(K,2)}_y)^T & 0 & 0 & 0 & -\gamma_2(\mathbb{F}^{\beta(K,2)})^T \\ \dots & (\mathbb{Q}^{\beta(K,3)}_y)^T & 0 & 0 & 0 & -\gamma_2(\mathbb{F}^{\beta(K,3)})^T \end{pmatrix},$$

$$\mathbb{P}^K_{\substack{\text{coupling}\\ \text{poro}\to\text{EM}}} = \begin{pmatrix} \mathbf{X}_4(\mathbb{L}^{\beta(K,1)}_{yy})^T & -\mathbf{X}_4(\mathbb{L}^{\beta(K,1)}_{xy})^T & \mathbf{X}_4\,\gamma_5(\mathbb{Q}^{\beta(K,1)}_{y})^T & 0 & 0 \\ 0 & 0 & 0 & 0 & 0 \\ 0 & 0 & 0 & 0 & 0 \\ -\mathbf{X}_4(\mathbb{L}^{\beta(K,1)}_{xy})^T & \mathbf{X}_4(\mathbb{L}^{\beta(K,1)}_{xx})^T & -\mathbf{X}_4\,\gamma_5(\mathbb{Q}^{\beta(K,1)}_{x})^T & 0 & 0 \\ 0 & 0 & 0 & 0 & 0 \\ 0 & 0 & 0 & 0 & 0 \\ 0 & 0 & 0 & 0 & 0 \\ 0 & 0 & 0 & 0 & 0 \\ 0 & 0 & 0 & 0 & 0 \end{pmatrix},$$

$$\mathbb{P}^K_{\mathbf{EM}} = \begin{pmatrix} -\mathbf{X}_8(\mathbb{Q}^{\beta(K,1)}_{y})^T & \mathbf{X}_8(\mathbb{Q}^{\beta(K,1)}_{x})^T & -\mathbf{X}_8\,\gamma_5(\mathbb{F}^{\beta(K,1)})^T & 0 & 0 \\ -(\mathbb{Q}^{\beta(K,2)}_{y})^T & (\mathbb{Q}^{\beta(K,2)}_{x})^T & -\gamma_5(\mathbb{F}^{\beta(K,2)})^T & 0 & 0 \\ -(\mathbb{Q}^{\beta(K,3)}_{y})^T & (\mathbb{Q}^{\beta(K,3)}_{x})^T & -\gamma_5(\mathbb{F}^{\beta(K,3)})^T & 0 & 0 \end{pmatrix}, \quad \text{and } \mathbb{P}^K_{\substack{\text{coupling}\\ \text{EM}\to\text{poro}}} = 0\,.$$

Then, $\mathbb{T}^K$ has the form:

$$\mathbb{T}^K = \begin{pmatrix} \mathbb{T}^K_{\mathbf{poro}} & \mathbb{T}^K_{\substack{\text{coupling}\\ \text{EM}\to\text{poro}}} \\ \mathbb{T}^K_{\substack{\text{coupling}\\ \text{poro}\to\text{EM}}} & \mathbb{T}^K_{\mathbf{EM}} \end{pmatrix},$$

with the matrices

$$\mathbb{T}^K_{\mathbf{poro}} = \begin{pmatrix} \gamma_1\mathbb{G}^{\beta(K,1)} + (\gamma_4\mathbf{X}_2 + \mathbf{X}_1)\mathbb{O}^{\beta(K,1)}_{xx} + (\mathbf{X}_3 + \mathbf{X}_4)\mathbb{O}^{\beta(K,1)}_{yy} & 0 & 0 & (\gamma_4\mathbf{X}_2 + \mathbf{X}_1 - \mathbf{X}_3 - \mathbf{X}_4)\mathbb{O}^{\beta(K,1)}_{xy} & \dots \\ 0 & \gamma_1\mathbb{G}^{\beta(K,2)} & 0 & 0 & \dots \\ 0 & 0 & \gamma_1\mathbb{G}^{\beta(K,3)} & 0 & \dots \\ (\gamma_4\mathbf{X}_2 + \mathbf{X}_1 - \mathbf{X}_3 - \mathbf{X}_4)\mathbb{O}^{\beta(K,1)}_{xy} & 0 & 0 & \gamma_1\mathbb{G}^{\beta(K,1)} + (\gamma_4\mathbf{X}_2 + \mathbf{X}_1)\mathbb{O}^{\beta(K,1)}_{yy} + (\mathbf{X}_3 + \mathbf{X}_4)\mathbb{O}^{\beta(K,1)}_{xx} & \dots \\ 0 & 0 & 0 & 0 & \dots \\ 0 & 0 & 0 & 0 & \dots \\ (\mathbf{X}_5 + \mathbf{X}_6\gamma_4)\mathbb{H}^{\beta(K,1)}_{x} & 0 & 0 & (\mathbf{X}_5 + \mathbf{X}_6\gamma_4)\mathbb{H}^{\beta(K,1)}_{y} & \dots \\ 0 & \gamma_4\mathbb{H}^{\beta(K,2)}_{x} & 0 & 0 & \dots \\ 0 & 0 & \gamma_4\mathbb{H}^{\beta(K,3)}_{x} & 0 & \dots \end{pmatrix}$$

$$\begin{pmatrix} \dots & 0 & 0 & (\gamma_3 + \mathbf{X}_2\gamma_2)\mathbb{H}^{\beta(K,1)}_{x} & 0 & 0 \\ \dots & 0 & 0 & 0 & \gamma_3\mathbb{H}^{\beta(K,2)}_{x} & 0 \\ \dots & 0 & 0 & 0 & 0 & \gamma_3\mathbb{H}^{\beta(K,3)}_{x} \\ \dots & 0 & 0 & (\gamma_3 + \mathbf{X}_2\gamma_2)\mathbb{H}^{\beta(K,1)}_{y} & 0 & 0 \\ \dots & \gamma_1\mathbb{G}^{\beta(K,2)} & 0 & 0 & \gamma_3\mathbb{H}^{\beta(K,2)}_{y} & 0 \\ \dots & 0 & \gamma_1\mathbb{G}^{\beta(K,3)} & 0 & 0 & \gamma_3\mathbb{H}^{\beta(K,3)}_{y} \\ \dots & 0 & 0 & (1 + \mathbf{X}_6\gamma_2)\mathbb{G}^{\beta(K,1)} & 0 & 0 \\ \dots & \gamma_4\mathbb{H}^{\beta(K,2)}_{y} & 0 & 0 & \gamma_2\mathbb{G}^{\beta(K,2)} & 0 \\ \dots & 0 & \gamma_4\mathbb{H}^{\beta(K,3)}_{y} & 0 & 0 & \gamma_2\mathbb{G}^{\beta(K,3)} \end{pmatrix},$$

$$\mathbb{T}^K_{\substack{\text{coupling}\\ \text{poro}\to\text{EM}}} = \begin{pmatrix} -\mathbf{X}_4\gamma_5\mathbb{H}_y^{\beta(K,1)} & 0 & 0 \\ 0 & 0 & 0 \\ 0 & 0 & 0 \\ \mathbf{X}_4\gamma_5\mathbb{H}_x^{\beta(K,1)} & 0 & 0 \\ 0 & 0 & 0 \\ 0 & 0 & 0 \\ 0 & 0 & 0 \\ 0 & 0 & 0 \\ 0 & 0 & 0 \end{pmatrix}, \qquad \mathbb{T}^K_{\mathbf{EM}} = \begin{pmatrix} (1+\mathbf{X}_8\gamma_5)\mathbb{G}^{\beta(K,1)} & 0 & 0 \\ 0 & \gamma_5\mathbb{G}^{\beta(K,2)} & 0 \\ 0 & 0 & \gamma_5\mathbb{G}^{\beta(K,3)} \end{pmatrix},$$

and

$$\mathbb{T}^K_{\substack{\text{coupling}\\ \text{EM}\to\text{poro}}} = \begin{pmatrix} -\mathbf{X}_7\mathbb{H}_y^{\beta(K,1)} & 0 & 0 & \mathbf{X}_7\mathbb{H}_x^{\beta(K,1)} & 0 & 0 & 0 & 0 & 0 \\ 0 & 0 & 0 & 0 & 0 & 0 & 0 & 0 & 0 \\ 0 & 0 & 0 & 0 & 0 & 0 & 0 & 0 & 0 \end{pmatrix}.$$

E.1.2 HDG method with PML

Here, we write the discretization of the local problem with Pride's equations (5.3) and PML. The transmission conditions are not modified and stay the same as the one used in HDG method with no PML, see Section 3.1. We consider a two-dimensional domain Ω with the boundary Γ on the plane (x, y). ($\mathbf{u}$, $\mathbf{w}$, $\boldsymbol{\tau}$, p $\boldsymbol{E}$, H, $\boldsymbol{J}$) solve Pride's equations (5.3) on Ω. We consider a triangulation $\mathcal{T}_h$ of Ω, and $\mathcal{F}_h$ the set of all the faces. K is a triangular element of $\mathcal{T}_h$ and F is an edge of K. We approximate the exact solution ($\mathbf{u}$, $\mathbf{w}$, $\boldsymbol{\tau}$, p, $\boldsymbol{E}$, H, $\boldsymbol{J}$) on K by ($\mathbf{u}_h$, $\mathbf{w}_h$, $\boldsymbol{\tau}_h$, p_h, $\boldsymbol{E}_h$, H_h, $\boldsymbol{J}_h$) $\in (\boldsymbol{V}^p(K)\times\boldsymbol{V}^p(K)\times\boldsymbol{\Sigma}^p(K)\times V^p(K)\times\boldsymbol{V}^p(K)\times V^p(K)\times\boldsymbol{V}^p(K))$. The local unknowns solve Pride's equations (5.3)on $\mathcal{T}_h$.

We define the following test functions:

$$(\tilde{\boldsymbol{u}}, \tilde{\boldsymbol{w}}, \tilde{\boldsymbol{\tau}}, \tilde{\mathrm{p}}, \tilde{\boldsymbol{e}}, \tilde{h}, \tilde{\boldsymbol{j}}) \in (\boldsymbol{V}^p(K) \times \boldsymbol{V}^p(K) \times \boldsymbol{\Sigma}^p(K) \times V^p(K) \times \boldsymbol{V}^p(K) \times V^p(K) \times \boldsymbol{V}^p(K)).$$

We present the discretization equation by equation.

Discretization of equation (5.3a) We multiply equations (5.3a) with zero sources by the test-functions and integrate on the element K:

$$\begin{aligned}\int_K \mathrm{i}\,\omega\rho_a \mathrm{u}_x^K\tilde{u}_x + \int_K \mathrm{i}\,\omega\rho_a \mathrm{u}_y^K\tilde{u}_y + \int_K \mathrm{i}\,\omega\rho_f \mathrm{w}_x^K\tilde{u}_x + \int_K \mathrm{i}\,\omega\rho_f \mathrm{w}_y^K\tilde{u}_y - \int_K \left(\frac{i\,\omega}{i\,\omega+\alpha(x)}\frac{\partial\tau_{xx}^K}{\partial x} + \frac{i\,\omega}{i\,\omega+\beta(y)}\frac{\partial\tau_{xy}^K}{\partial y}\right)\tilde{u}_x \\ - \int_K \left(\frac{i\,\omega}{i\,\omega+\alpha(x)}\frac{\partial\tau_{xy}^K}{\partial x} + \frac{i\,\omega}{i\,\omega+\beta(y)}\frac{\partial\tau_{yy}^K}{\partial y}\right)\tilde{u}_y = 0\,.\end{aligned}$$

By integrating by parts, we obtain:

$$\begin{aligned}\int_K \mathrm{i}\,\omega\rho_a \mathrm{u}_x^K\tilde{u}_x + \int_K \mathrm{i}\,\omega\rho_a \mathrm{u}_y^K\tilde{u}_y + \int_K \mathrm{i}\,\omega\rho_f \mathrm{w}_x^K\tilde{u}_x + \int_K \mathrm{i}\,\omega\rho_f \mathrm{w}_y^K\tilde{u}_y + \int_K \frac{i\,\omega}{i\,\omega+\alpha(x)}\tau_{xx}^K\frac{\partial\tilde{u}_x}{\partial x} + \int_K \frac{i\,\omega}{i\,\omega+\beta(y)}\tau_{xy}^K\frac{\partial\tilde{u}_x}{\partial y} \\ - \int_F \frac{i\,\omega}{i\,\omega+\alpha(x)}\hat{\tau}_{xx}^K n_x\tilde{u}_x - \int_F \frac{i\,\omega}{i\,\omega+\beta(y)}\hat{\tau}_{xy}^K n_y\tilde{u}_x + \int_K \frac{i\,\omega}{i\,\omega+\alpha(x)}\tau_{xy}^K\frac{\partial\tilde{u}_y}{\partial x} + \int_K \frac{i\,\omega}{i\,\omega+\beta(y)}\tau_{yy}^K\frac{\partial\tilde{u}_y}{\partial y} \\ - \int_F \frac{i\,\omega}{i\,\omega+\alpha(x)}\hat{\tau}_{xy}^K n_x\tilde{u}_y - \int_F \frac{i\,\omega}{i\,\omega+\beta(y)}\hat{\tau}_{yy}^K n_y\tilde{u}_y = 0\,,\end{aligned}$$

Then we replace the numerical trace $\hat{\boldsymbol{\tau}}_h$ by the expressions from equation (7.4) and integrate by parts the space derivatives of $\boldsymbol{\tau}$:

$$\begin{aligned}
&\int_K \mathrm{i}\omega\rho_a \mathrm{u}_x^K \tilde{u}_x + \int_K \mathrm{i}\omega\rho_a \mathrm{u}_y^K \tilde{u}_y + \int_K \mathrm{i}\omega\rho_f \mathrm{w}_x^K \tilde{u}_x + \int_K \mathrm{i}\omega\rho_f \mathrm{w}_y^K \tilde{u}_y - \int_K \frac{i\,\omega}{i\,\omega+\alpha(x)} \frac{\partial \tau_{xx}^K}{\partial x} \tilde{u}_x \\
&+ \int_F \gamma_1 \frac{i\,\omega}{i\,\omega+\alpha(x)} (\mathrm{u}_x^K - \lambda_{1x}) n_x^2 \tilde{u}_x + \int_F \gamma_3 \frac{i\,\omega}{i\,\omega+\alpha(x)} (\mathrm{p}_h - \lambda_2) n_x \tilde{u}_x \\
&- \int_K \frac{i\,\omega}{i\,\omega+\beta(y)} \frac{\partial \tau_{xy}^K}{\partial y} \tilde{u}_x + \int_F \gamma_1 \frac{i\,\omega}{i\,\omega+\beta(y)} (\mathrm{u}_x^K - \lambda_{1x}) n_y^2 \tilde{u}_x - \int_K \frac{i\,\omega}{i\,\omega+\alpha(x)} \frac{\partial \tau_{xy}^K}{\partial x} \tilde{u}_y + \int_F \gamma_1 \frac{i\,\omega}{i\,\omega+\alpha(x)} (\mathrm{u}_y^K - \lambda_{1y}) n_x^2 \tilde{u}_y \\
&- \int_K \frac{i\,\omega}{i\,\omega+\beta(y)} \frac{\partial \tau_{yy}^K}{\partial y} \tilde{u}_y + \int_F \gamma_1 \frac{i\,\omega}{i\,\omega+\beta(y)} (\mathrm{u}_y^K - \lambda_{1y}) n_y^2 \tilde{u}_y + \int_F \gamma_3 \frac{i\,\omega}{i\,\omega+\beta(y)} (\mathrm{p}_h - \lambda_2) n_y \tilde{u}_y = 0\,.
\end{aligned}$$

Finally, we replace the local unknowns and the local test-functions using equations (3.15) and (3.16). We obtain on x:

$$\begin{aligned}
&\int_K \mathrm{i}\omega\rho_a \underline{\mathrm{u}}_x^K \varphi_j^K \varphi_i^K + \int_K \mathrm{i}\omega\rho_f \underline{\mathrm{w}}_x^K \varphi_j^K \varphi_i^K - \int_K \frac{i\,\omega}{i\,\omega+\alpha(x)} \underline{\tau}_{xx}^K \frac{\partial \varphi_j^K}{\partial x} \varphi_i^K + \int_{\partial K} \gamma_1 \frac{i\,\omega}{i\,\omega+\alpha(x)} (\underline{\mathrm{u}}_x^K \varphi_j^K - \underline{\lambda}_{1x} \psi_j^F) n_x^2 \varphi_i^K \\
&+ \int_{\partial K} \gamma_3 \frac{i\,\omega}{i\,\omega+\alpha(x)} (\underline{\mathrm{p}}^K \varphi_j^K - \underline{\lambda}_2 \psi_j^F) n_x \varphi_i^K - \int_K \frac{i\,\omega}{i\,\omega+\beta(y)} \underline{\tau}_{xy}^K \frac{\partial \varphi_j^K}{\partial y} \varphi_i^K \\
&+ \int_{\partial K} \gamma_1 \frac{i\,\omega}{i\,\omega+\beta(y)} (\underline{\mathrm{u}}_x^K \varphi_j^K - \underline{\lambda}_{1x} \psi_j^F) n_y^2 \varphi_i^K = 0\,,
\end{aligned}$$

and on y :

$$\begin{aligned}
&\int_K \mathrm{i}\omega\rho_a \underline{\mathrm{u}}_y^K \varphi_j^K \varphi_i^K + \int_K \mathrm{i}\omega\rho_f \underline{\mathrm{w}}_y^K \varphi_j^K \varphi_i^K - \int_K \frac{i\,\omega}{i\,\omega+\alpha(x)} \underline{\tau}_{xy}^K \frac{\partial \varphi_j^K}{\partial x} \varphi_i^K + \int_{\partial K} \gamma_1 \frac{i\,\omega}{i\,\omega+\alpha(x)} (\underline{\mathrm{u}}_y^K \varphi_j^K - \underline{\lambda}_{1y} \psi_j^F) n_x^2 \varphi_i^K \\
&- \int_K \frac{i\,\omega}{i\,\omega+\beta(y)} \underline{\tau}_{yy}^K \frac{\partial \varphi_j^K}{\partial y} \varphi_i^K + \int_{\partial K} \gamma_1 \frac{i\,\omega}{i\,\omega+\beta(y)} (\underline{\mathrm{u}}_y^K \varphi_j^K - \underline{\lambda}_{1y} \psi_j^F) n_y^2 \varphi_i^K + \int_{\partial K} \gamma_3 \frac{i\,\omega}{i\,\omega+\beta(y)} (\underline{\mathrm{p}}^K \varphi_j^K - \underline{\lambda}_2 \psi_j^F) n_y \varphi_i^K = 0\,.
\end{aligned}$$

Discretization of equation (5.3b) The integration of (5.3b) with zero sources on the element K gives:

$$\begin{aligned}
&\int_K \mathrm{i}\omega\rho_f \mathrm{u}_x^K \tilde{w}_x + \int_K \mathrm{i}\omega\rho_f \mathrm{u}_y^K \tilde{w}_y + \int_K \mathrm{i}\omega\rho_{\mathrm{dyn}} \mathrm{w}_x^K \tilde{w}_x + \int_K \mathrm{i}\omega\rho_{\mathrm{dyn}} \mathrm{w}_y^K \tilde{w}_y + \int_K \frac{i\,\omega}{i\,\omega+\alpha(x)} \frac{\partial \mathrm{p}}{\partial x} \tilde{w}_x + \int_K \frac{i\,\omega}{i\,\omega+\beta(y)} \frac{\partial \mathrm{p}}{\partial y} \tilde{w}_y \\
&\qquad + \int_K \mathrm{i}\omega\,\rho_{\mathrm{dyn}}\,\mathrm{L}\,E_x^K\,\tilde{w}_x + \int_K \mathrm{i}\omega\,\rho_{\mathrm{dyn}}\,\mathrm{L}\,E_y^K\,\tilde{w}_y = 0\,.
\end{aligned}$$

Next we integrate by parts:

$$\begin{aligned}
&\int_K \mathrm{i}\omega\rho_f \mathrm{u}_x^K \tilde{w}_x + \int_K \mathrm{i}\omega\rho_f \mathrm{u}_y^K \tilde{w}_y + \int_K \mathrm{i}\omega\rho_{\mathrm{dyn}} \mathrm{w}_x^K \tilde{w}_x + \int_K \mathrm{i}\omega\rho_{\mathrm{dyn}} \mathrm{w}_y^K \tilde{w}_y - \int_K \frac{i\,\omega}{i\,\omega+\alpha(x)} \mathrm{p} \frac{\partial \tilde{w}_x}{\partial x} + \int_F \frac{i\,\omega}{i\,\omega+\alpha(x)} \hat{\mathrm{p}}_h\, n_x \tilde{w}_x \\
&\qquad - \int_K \frac{i\,\omega}{i\,\omega+\beta(y)} \mathrm{p} \frac{\partial \tilde{w}_y}{\partial y} + \int_F \frac{i\,\omega}{i\,\omega+\beta(y)} \hat{\mathrm{p}}_h\, n_y \tilde{w}_y + \int_K \mathrm{i}\omega\,\rho_{\mathrm{dyn}}\,\mathrm{L}\,E_x^K\,\tilde{w}_x + \int_K \mathrm{i}\omega\,\rho_{\mathrm{dyn}}\,\mathrm{L}\,E_y^K\,\tilde{w}_y = 0\,.
\end{aligned}$$

Then we replace the numerical trace $\hat{\mathrm{p}}_h$ by λ_2 as given in equation (7.3) to obtain:

$$\begin{aligned}
&\int_K \mathrm{i}\omega\rho_f \mathrm{u}_x^K \tilde{w}_x + \int_K \mathrm{i}\omega\rho_f \mathrm{u}_y^K \tilde{w}_y + \int_K \mathrm{i}\omega\rho_{\mathrm{dyn}} \mathrm{w}_x^K \tilde{w}_x + \int_K \mathrm{i}\omega\rho_{\mathrm{dyn}} \mathrm{w}_y^K \tilde{w}_y - \int_K \frac{i\,\omega}{i\,\omega+\alpha(x)} \mathrm{p} \frac{\partial \tilde{w}_x}{\partial x} + \int_F \frac{i\,\omega}{i\,\omega+\alpha(x)} \lambda_2 n_x \tilde{w}_x \\
&- \int_K \frac{i\,\omega}{i\,\omega+\beta(y)} \mathrm{p} \frac{\partial \tilde{w}_y}{\partial y} + \int_F \frac{i\,\omega}{i\,\omega+\beta(y)} \lambda_2 n_y \tilde{w}_y + \int_K \mathrm{i}\omega\,\rho_{\mathrm{dyn}}\,\mathrm{L}\,E_x^K\,\tilde{w}_x + \int_K \mathrm{i}\omega\,\rho_{\mathrm{dyn}}\,\mathrm{L}\,E_y^K\,\tilde{w}_y = 0\,.
\end{aligned}$$

Finally, we replace the local unknowns and the local test-functions using equations (3.15) and (3.16). This gives on x-direction:

$$\int_K \mathrm{i}\omega\rho_f \underline{\mathrm{u}}_x^K \varphi_j^K \varphi_i^K + \int_K \mathrm{i}\omega\rho_{\mathrm{dyn}}\, \underline{\mathrm{w}}_x^K \varphi_j^K \varphi_i^K - \int_K \frac{i\,\omega}{i\,\omega+\alpha(x)} \underline{\mathrm{p}}^K \varphi_j^K \frac{\partial \varphi_i^K}{\partial x} + \int_F \frac{i\,\omega}{i\,\omega+\alpha(x)} \underline{\lambda}_2 \psi_j^F n_x \varphi_i^K + \int_K \mathrm{i}\omega\rho_{\mathrm{dyn}} \mathrm{L} E_x^K \varphi_i^K = 0\,,$$

and on y-direction:

$$\int_K \mathrm{i}\omega\rho_f \underline{\mathrm{u}}_y^K \varphi_j^K \varphi_i^K + \int_K \mathrm{i}\omega\rho_{\mathrm{dyn}}\, \underline{\mathrm{w}}_y^K \varphi_j^K \varphi_i^K - \int_K \frac{i\,\omega}{i\,\omega+\beta(y)} \underline{\mathrm{p}}^K \varphi_j^K \frac{\partial \varphi_i^K}{\partial y} + \int_F \frac{i\,\omega}{i\,\omega+\beta(y)} \underline{\lambda}_2 \psi_j^F n_y \varphi_i^K + \int_K \mathrm{i}\omega\rho_{\mathrm{dyn}} \mathrm{L} E_y^K \varphi_i^K = 0\,.$$

Discretization of equation (5.3c) The variational formulation of equations (5.3c) is:

$$\begin{aligned}
&\int_K \mathrm{i}\omega\tau_{xx}^K\,\tilde\tau_{xx} + \int_K \mathrm{i}\omega\alpha_{11}\mathrm{p}_h\tilde\tau_{xx} - \int_K C_{11}\frac{i\,\omega}{i\,\omega+\alpha(x)}\frac{\partial \mathrm{u}_x^K}{\partial x}\tilde\tau_{xx} - \int_K C_{12}\frac{i\,\omega}{i\,\omega+\beta(y)}\frac{\partial \mathrm{u}_y^K}{\partial y}\tilde\tau_{xx}\\
&\quad - \int_K C_{13}\left(\frac{i\,\omega}{i\,\omega+\alpha(x)}\frac{\partial \mathrm{u}_y^K}{\partial x} + \frac{i\,\omega}{i\,\omega+\beta(y)}\frac{\partial \mathrm{u}_x^K}{\partial y}\right)\tilde\tau_{xx}\\
&\quad + \int_K \mathrm{i}\omega\tau_{yy}^K\,\tilde\tau_{yy} + \int_K \mathrm{i}\omega\alpha_{22}\mathrm{p}_h\tilde\tau_{yy} - \int_K C_{12}\frac{i\,\omega}{i\,\omega+\alpha(x)}\frac{\partial \mathrm{u}_x^K}{\partial x}\tilde\tau_{yy} - \int_K C_{22}\frac{i\,\omega}{i\,\omega+\beta(y)}\frac{\partial \mathrm{u}_y^K}{\partial y}\tilde\tau_{yy}\\
&\quad - \int_K C_{23}\left(\frac{i\,\omega}{i\,\omega+\alpha(x)}\frac{\partial \mathrm{u}_y^K}{\partial x} + \frac{i\,\omega}{i\,\omega+\beta(y)}\frac{\partial \mathrm{u}_x^K}{\partial y}\right)\tilde\tau_{yy}\\
&\quad + \int_K \mathrm{i}\omega\tau_{xy}^K\,\tilde\tau_{xy} + \int_K \mathrm{i}\omega\alpha_{12}\mathrm{p}_h\tilde\tau_{xy} - \int_K C_{13}\frac{i\,\omega}{i\,\omega+\alpha(x)}\frac{\partial \mathrm{u}_x^K}{\partial x}\tilde\tau_{xy} - \int_K C_{23}\frac{i\,\omega}{i\,\omega+\beta(y)}\frac{\partial \mathrm{u}_y^K}{\partial y}\tilde\tau_{xy}\\
&\quad - \int_K C_{33}\left(\frac{i\,\omega}{i\,\omega+\alpha(x)}\frac{\partial \mathrm{u}_y^K}{\partial x} + \frac{i\,\omega}{i\,\omega+\beta(y)}\frac{\partial \mathrm{u}_x^K}{\partial y}\right)\tilde\tau_{xy} = 0\,.
\end{aligned}$$

By integrating by parts, we have:

$$\begin{aligned}
&\int_K \mathrm{i}\omega\tau_{xx}^K\,\tilde\tau_{xx} + \int_K \mathrm{i}\omega\alpha_{11}\mathrm{p}_h\tilde\tau_{xx} + \int_K C_{11}\frac{i\,\omega}{i\,\omega+\alpha(x)}\mathrm{u}_x^K\frac{\partial\tilde\tau_{xx}}{\partial x} - \int_F C_{11}\frac{i\,\omega}{i\,\omega+\alpha(x)}\hat{\mathrm{u}}_x^K n_x\tilde\tau_{xx}\\
&+ \int_K C_{12}\frac{i\,\omega}{i\,\omega+\beta(y)}\mathrm{u}_y^K\frac{\partial\tilde\tau_{xx}}{\partial y} - \int_F C_{12}\frac{i\,\omega}{i\,\omega+\beta(y)}\hat{\mathrm{u}}_y^K n_y\tilde\tau_{xx} + \int_K C_{13}\frac{i\,\omega}{i\,\omega+\alpha(x)}\mathrm{u}_y^K\frac{\partial\tilde\tau_{xx}}{\partial x}\\
&- \int_F C_{13}\frac{i\,\omega}{i\,\omega+\alpha(x)}\hat{\mathrm{u}}_y^K n_x\tilde\tau_{xx} + \int_K C_{13}\frac{i\,\omega}{i\,\omega+\beta(y)}\mathrm{u}_x^K\frac{\partial\tilde\tau_{xx}}{\partial y} - \int_F C_{13}\frac{i\,\omega}{i\,\omega+\beta(y)}\hat{\mathrm{u}}_x^K n_y\tilde\tau_{xx}\\
&+ \int_K \mathrm{i}\omega\tau_{yy}^K\,\tilde\tau_{yy} + \int_K \mathrm{i}\omega\alpha_{22}\mathrm{p}_h\tilde\tau_{yy} + \int_K C_{12}\frac{i\,\omega}{i\,\omega+\alpha(x)}\mathrm{u}_x^K\frac{\partial\tilde\tau_{yy}}{\partial x} - \int_F C_{12}\frac{i\,\omega}{i\,\omega+\alpha(x)}\hat{\mathrm{u}}_x^K n_x\tilde\tau_{yy}\\
&+ \int_K C_{22}\frac{i\,\omega}{i\,\omega+\beta(y)}\mathrm{u}_y^K\frac{\partial\tilde\tau_{yy}}{\partial y} - \int_F C_{22}\frac{i\,\omega}{i\,\omega+\beta(y)}\hat{\mathrm{u}}_y^K n_y\tilde\tau_{yy} + \int_K C_{23}\frac{i\,\omega}{i\,\omega+\alpha(x)}\mathrm{u}_y^K\frac{\partial\tilde\tau_{yy}}{\partial x}\\
&- \int_F C_{23}\frac{i\,\omega}{i\,\omega+\alpha(x)}\hat{\mathrm{u}}_y^K n_x\tilde\tau_{yy} + \int_K C_{23}\frac{i\,\omega}{i\,\omega+\beta(y)}\mathrm{u}_x^K\frac{\partial\tilde\tau_{yy}}{\partial y} - \int_F C_{23}\frac{i\,\omega}{i\,\omega+\beta(y)}\hat{\mathrm{u}}_x^K n_y\tilde\tau_{yy}\\
&+ \int_K \mathrm{i}\omega\tau_{xy}^K\,\tilde\tau_{xy} + \int_K \mathrm{i}\omega\alpha_{12}\mathrm{p}_h\tilde\tau_{xy} + \int_K C_{13}\frac{i\,\omega}{i\,\omega+\alpha(x)}\mathrm{u}_x^K\frac{\partial\tilde\tau_{xy}}{\partial x} - \int_F C_{13}\frac{i\,\omega}{i\,\omega+\alpha(x)}\hat{\mathrm{u}}_x^K n_x\tilde\tau_{xy}\\
&+ \int_K C_{23}\frac{i\,\omega}{i\,\omega+\beta(y)}\mathrm{u}_y^K\frac{\partial\tilde\tau_{xy}}{\partial y} - \int_F C_{23}\frac{i\,\omega}{i\,\omega+\beta(y)}\hat{\mathrm{u}}_y^K n_y\tilde\tau_{xy} + \int_K C_{33}\frac{i\,\omega}{i\,\omega+\alpha(x)}\mathrm{u}_y^K\frac{\partial\tilde\tau_{xy}}{\partial x}\\
&- \int_F C_{33}\frac{i\,\omega}{i\,\omega+\alpha(x)}\hat{\mathrm{u}}_y^K n_x\tilde\tau_{xy} + \int_K C_{33}\frac{i\,\omega}{i\,\omega+\beta(y)}\mathrm{u}_x^K\frac{\partial\tilde\tau_{xy}}{\partial y} - \int_F C_{33}\frac{i\,\omega}{i\,\omega+\beta(y)}\hat{\mathrm{u}}_x^K n_y\tilde\tau_{xy} = 0\,.
\end{aligned}$$

Then we replace the numerical trace $\hat{\mathbf{u}}_h$ by $\boldsymbol{\lambda}_1$ from equation (7.3):

$$\begin{aligned}
&\int_K \mathrm{i}\omega\tau_{xx}^K\,\tilde{\tau}_{xx} + \int_K \mathrm{i}\omega\alpha_{11}\mathrm{p}_h\tilde{\tau}_{xx} + \int_K C_{11}\frac{i\,\omega}{i\,\omega+\alpha(x)}\mathrm{u}_x^K\frac{\partial\tilde{\tau}_{xx}}{\partial x} - \int_F C_{11}\frac{i\,\omega}{i\,\omega+\alpha(x)}\lambda_{1x}n_x\tilde{\tau}_{xx}\\
&+\int_K C_{12}\frac{i\,\omega}{i\,\omega+\beta(y)}\mathrm{u}_y^K\frac{\partial\tilde{\tau}_{xx}}{\partial y} - \int_F C_{12}\frac{i\,\omega}{i\,\omega+\beta(y)}\lambda_{1y}n_y\tilde{\tau}_{xx} + \int_K C_{13}\frac{i\,\omega}{i\,\omega+\alpha(x)}\mathrm{u}_y^K\frac{\partial\tilde{\tau}_{xx}}{\partial x}\\
&-\int_F C_{13}\frac{i\,\omega}{i\,\omega+\alpha(x)}\lambda_{1y}n_x\tilde{\tau}_{xx} + \int_K C_{13}\frac{i\,\omega}{i\,\omega+\beta(y)}\mathrm{u}_x^K\frac{\partial\tilde{\tau}_{xx}}{\partial y} - \int_F C_{13}\frac{i\,\omega}{i\,\omega+\beta(y)}\lambda_{1x}n_y\tilde{\tau}_{xx}\\
&+\int_K \mathrm{i}\omega\tau_{yy}^K\,\tilde{\tau}_{yy} + \int_K \mathrm{i}\omega\alpha_{22}\mathrm{p}_h\tilde{\tau}_{yy} + \int_K C_{12}\frac{i\,\omega}{i\,\omega+\alpha(x)}\mathrm{u}_x^K\frac{\partial\tilde{\tau}_{yy}}{\partial x} - \int_F C_{12}\frac{i\,\omega}{i\,\omega+\alpha(x)}\lambda_{1x}n_x\tilde{\tau}_{yy}\\
&+\int_K C_{22}\frac{i\,\omega}{i\,\omega+\beta(y)}\mathrm{u}_y^K\frac{\partial\tilde{\tau}_{yy}}{\partial y} - \int_F C_{22}\frac{i\,\omega}{i\,\omega+\beta(y)}\lambda_{1y}n_y\tilde{\tau}_{yy} + \int_K C_{23}\frac{i\,\omega}{i\,\omega+\alpha(x)}\mathrm{u}_y^K\frac{\partial\tilde{\tau}_{yy}}{\partial x}\\
&-\int_F C_{23}\frac{i\,\omega}{i\,\omega+\alpha(x)}\lambda_{1y}n_x\tilde{\tau}_{yy} + \int_K C_{23}\frac{i\,\omega}{i\,\omega+\beta(y)}\mathrm{u}_x^K\frac{\partial\tilde{\tau}_{yy}}{\partial y} - \int_F C_{23}\frac{i\,\omega}{i\,\omega+\beta(y)}\lambda_{1x}n_y\tilde{\tau}_{yy}\\
&+\int_K \mathrm{i}\omega\tau_{xy}^K\,\tilde{\tau}_{xy} + \int_K \mathrm{i}\omega\alpha_{12}\mathrm{p}_h\tilde{\tau}_{xy} + \int_K C_{13}\frac{i\,\omega}{i\,\omega+\alpha(x)}\mathrm{u}_x^K\frac{\partial\tilde{\tau}_{xy}}{\partial x} - \int_F C_{13}\frac{i\,\omega}{i\,\omega+\alpha(x)}\lambda_{1x}n_x\tilde{\tau}_{xy}\\
&+\int_K C_{23}\frac{i\,\omega}{i\,\omega+\beta(y)}\mathrm{u}_y^K\frac{\partial\tilde{\tau}_{xy}}{\partial y} - \int_F C_{23}\frac{i\,\omega}{i\,\omega+\beta(y)}\lambda_{1y}n_y\tilde{\tau}_{xy} + \int_K C_{33}\frac{i\,\omega}{i\,\omega+\alpha(x)}\mathrm{u}_y^K\frac{\partial\tilde{\tau}_{xy}}{\partial x}\\
&-\int_F C_{33}\frac{i\,\omega}{i\,\omega+\alpha(x)}\lambda_{1y}n_x\tilde{\tau}_{xy} + \int_K C_{33}\frac{i\,\omega}{i\,\omega+\beta(y)}\mathrm{u}_x^K\frac{\partial\tilde{\tau}_{xy}}{\partial y} - \int_F C_{33}\frac{i\,\omega}{i\,\omega+\beta(y)}\lambda_{1x}n_y\tilde{\tau}_{xy} = 0\,.
\end{aligned}$$

Finally, we replace the local unknowns and the local test-functions using equations (3.15) and (3.16). This gives the three following equations:

$$\begin{aligned}
&\int_K \mathrm{i}\omega\underline{\tau}_{xx}^K\,\varphi_j^K\varphi_i^K + \int_K \mathrm{i}\omega\alpha_{11}\underline{\mathrm{p}}^K\varphi_j^K\varphi_i^K + \int_K C_{11}\frac{i\,\omega}{i\,\omega+\alpha(x)}\underline{\mathrm{u}}_x^K\varphi_j^K\frac{\partial\varphi_i^K}{\partial x} - \int_F C_{11}\frac{i\,\omega}{i\,\omega+\alpha(x)}\underline{\lambda}_{1x}\psi_j^F n_x\varphi_i^K\\
&+\int_K C_{12}\frac{i\,\omega}{i\,\omega+\beta(y)}\underline{\mathrm{u}}_y^K\varphi_j^K\frac{\partial\varphi_i^K}{\partial y} - \int_F C_{12}\frac{i\,\omega}{i\,\omega+\beta(y)}\underline{\lambda}_{1y}\psi_j^F n_y\varphi_i^K + \int_K C_{13}\frac{i\,\omega}{i\,\omega+\alpha(x)}\underline{\mathrm{u}}_y^K\varphi_j^K\frac{\partial\varphi_i^K}{\partial x}\\
&-\int_F C_{13}\frac{i\,\omega}{i\,\omega+\alpha(x)}\underline{\lambda}_{1y}\psi_j^F n_x\varphi_i^K + \int_K C_{13}\frac{i\,\omega}{i\,\omega+\beta(y)}\underline{\mathrm{u}}_x^K\varphi_j^K\frac{\partial\varphi_i^K}{\partial y} - \int_F C_{13}\frac{i\,\omega}{i\,\omega+\beta(y)}\underline{\lambda}_{1x}\psi_j^F n_y\varphi_i^K \;=\; 0\,,
\end{aligned}$$

$$\begin{aligned}
&\int_K \mathrm{i}\omega\underline{\tau}_{yy}^K\varphi_j^K\,\varphi_i^K + \int_K \mathrm{i}\omega\alpha_{22}\underline{\mathrm{p}}^K\varphi_j^K\varphi_i^K + \int_K C_{12}\frac{i\,\omega}{i\,\omega+\alpha(x)}\underline{\mathrm{u}}_x^K\varphi_j^K\frac{\partial\varphi_i^K}{\partial x} - \int_F C_{12}\frac{i\,\omega}{i\,\omega+\alpha(x)}\underline{\lambda}_{1x}\psi_j^F n_x\varphi_i^K\\
&+\int_K C_{22}\frac{i\,\omega}{i\,\omega+\beta(y)}\underline{\mathrm{u}}_y^K\varphi_j^K\frac{\partial\varphi_i^K}{\partial y} - \int_F C_{22}\frac{i\,\omega}{i\,\omega+\beta(y)}\underline{\lambda}_{1y}\psi_j^F n_y\varphi_i^K + \int_K C_{23}\frac{i\,\omega}{i\,\omega+\alpha(x)}\underline{\mathrm{u}}_y^K\varphi_j^K\frac{\partial\varphi_i^K}{\partial x}\\
&-\int_F C_{23}\frac{i\,\omega}{i\,\omega+\alpha(x)}\underline{\lambda}_{1y}\psi_j^F n_x\varphi_i^K + \int_K C_{23}\frac{i\,\omega}{i\,\omega+\beta(y)}\underline{\mathrm{u}}_x^K\varphi_j^K\frac{\partial\varphi_i^K}{\partial y} - \int_F C_{23}\frac{i\,\omega}{i\,\omega+\beta(y)}\underline{\lambda}_{1x}\psi_j^F n_y\varphi_i^K \;=\; 0\,,
\end{aligned}$$

and

$$\begin{aligned}
&\int_K \mathrm{i}\omega\underline{\tau}_{yy}^K\,\varphi_j^K\varphi_i^K + \int_K \mathrm{i}\omega\alpha_{22}\mathrm{p}_h\,\varphi_j^K\varphi_i^K + \int_K C_{13}\frac{i\,\omega}{i\,\omega+\alpha(x)}\underline{\mathrm{u}}_x^K\varphi_j^K\frac{\partial\varphi_i^K}{\partial x} - \int_F C_{13}\frac{i\,\omega}{i\,\omega+\alpha(x)}\underline{\lambda}_{1x}\psi_j^F n_x\varphi_i^K\\
&+\int_K C_{23}\frac{i\,\omega}{i\,\omega+\beta(y)}\underline{\mathrm{u}}_y^K\varphi_j^K\frac{\partial\varphi_i^K}{\partial y} - \int_F C_{23}\frac{i\,\omega}{i\,\omega+\beta(y)}\underline{\lambda}_{1y}\psi_j^F n_y\varphi_i^K + \int_K C_{33}\frac{i\,\omega}{i\,\omega+\alpha(x)}\underline{\mathrm{u}}_y^K\varphi_j^K\frac{\partial\varphi_i^K}{\partial x}\\
&-\int_F C_{33}\frac{i\,\omega}{i\,\omega+\alpha(x)}\underline{\lambda}_{1y}\psi_j^F n_x\varphi_i^K + \int_K C_{33}\frac{i\,\omega}{i\,\omega+\beta(y)}\underline{\mathrm{u}}_x^K\varphi_j^K\frac{\partial\varphi_i^K}{\partial y} - \int_F C_{33}\frac{i\,\omega}{i\,\omega+\beta(y)}\underline{\lambda}_{1x}\psi_j^F n_y\varphi_i^K = 0\,.
\end{aligned}$$

Discretization of equation (5.3d) We multiply equations (5.3d) by the test-functions and integrate on the element K to obtain:

$$\begin{aligned}
&\int_K \mathrm{i}\omega\mathrm{p}_h\tilde{\mathrm{p}} + \int_K M\left(\frac{i\,\omega}{i\,\omega+\alpha(x)}\frac{\partial\mathrm{w}_x^K}{\partial x} + \frac{i\,\omega}{i\,\omega+\beta(y)}\frac{\partial\mathrm{w}_y^K}{\partial y}\right)\tilde{\mathrm{p}} + \int_K M\alpha_{11}\frac{i\,\omega}{i\,\omega+\alpha(x)}\frac{\partial\mathrm{u}_x^K}{\partial x}\tilde{\mathrm{p}}\\
&\qquad+\int_K M\alpha_{22}\frac{i\,\omega}{i\,\omega+\beta(y)}\frac{\partial\mathrm{u}_y^K}{\partial y}\tilde{\mathrm{p}} + \int_K M\alpha_{12}\left(\frac{i\,\omega}{i\,\omega+\beta(y)}\frac{\partial\mathrm{u}_x^K}{\partial y} + \frac{i\,\omega}{i\,\omega+\alpha(x)}\frac{\partial\mathrm{u}_y^K}{\partial x}\right)\tilde{\mathrm{p}} = 0\,.
\end{aligned}$$

The integration by parts of the space derivatives of $\mathbf{u}$ and $\mathbf{w}$ gives:

$$\begin{aligned}
&\int_K \mathrm{i}\omega \mathrm{p}_h\tilde{\mathrm{p}} - \int_K M\frac{i\,\omega}{i\,\omega+\alpha(x)}\mathrm{w}_x^K\frac{\partial\tilde{\mathrm{p}}}{\partial x} + \int_F M\frac{i\,\omega}{i\,\omega+\alpha(x)}\hat{\mathrm{w}}_x^K n_x\tilde{\mathrm{p}} - \int_K M\frac{i\,\omega}{i\,\omega+\beta(y)}\mathrm{w}_y^K\frac{\partial\tilde{\mathrm{p}}}{\partial y}\\
&+\int_F M\frac{i\,\omega}{i\,\omega+\beta(y)}\hat{\mathrm{w}}_y^K n_y\tilde{\mathrm{p}} - \int_K M\alpha_{11}\frac{i\,\omega}{i\,\omega+\alpha(x)}\mathrm{u}_x^K\frac{\partial\tilde{\mathrm{p}}}{\partial x} + \int_F M\alpha_{11}\frac{i\,\omega}{i\,\omega+\alpha(x)}\hat{\mathrm{u}}_x^K n_x\tilde{\mathrm{p}}\\
&-\int_K M\alpha_{22}\frac{i\,\omega}{i\,\omega+\beta(y)}\mathrm{u}_y^K\frac{\partial\tilde{\mathrm{p}}}{\partial y} + \int_F M\alpha_{22}\frac{i\,\omega}{i\,\omega+\beta(y)}\hat{\mathrm{u}}_y^K n_y\tilde{\mathrm{p}} - \int_K M\alpha_{12}\frac{i\,\omega}{i\,\omega+\beta(y)}\mathrm{u}_x^K\frac{\partial\tilde{\mathrm{p}}}{\partial y}\\
&+\int_F M\alpha_{12}\frac{i\,\omega}{i\,\omega+\beta(y)}\hat{\mathrm{u}}_x^K n_y\tilde{\mathrm{p}} - \int_K M\alpha_{12}\frac{i\,\omega}{i\,\omega+\alpha(x)}\mathrm{u}_y^K\frac{\partial\tilde{\mathrm{p}}}{\partial x} + \int_F M\alpha_{12}\frac{i\,\omega}{i\,\omega+\alpha(x)}\hat{\mathrm{u}}_y^K n_x\tilde{\mathrm{p}} \;=\; 0\,.
\end{aligned}$$

Next we replace the numerical traces $\hat{\mathbf{u}}_h$ and $\hat{\mathbf{w}}_h$ by their expression given in equations (7.3) and (7.4):

$$\begin{aligned}
&\int_K \mathrm{i}\omega \mathrm{p}_h\tilde{\mathrm{p}} + \int_K M\frac{i\,\omega}{i\,\omega+\alpha(x)}\frac{\partial\mathrm{w}_x^K}{\partial x}\tilde{\mathrm{p}} - \int_F M\gamma_2\frac{i\,\omega}{i\,\omega+\alpha(x)}(\mathrm{p}_h-\lambda_2)n_x^2\tilde{\mathrm{p}} - \int_F M\gamma_4\frac{i\,\omega}{i\,\omega+\alpha(x)}(\mathrm{u}_x^K-\lambda_{1x})n_x\tilde{\mathrm{p}}\\
&+\int_K M\frac{i\,\omega}{i\,\omega+\beta(y)}\frac{\partial\mathrm{w}_y^K}{\partial y}\tilde{\mathrm{p}} - \int_F M\gamma_2\frac{i\,\omega}{i\,\omega+\beta(y)}(\mathrm{p}_h-\lambda_2)n_y^2\tilde{\mathrm{p}} - \int_F M\gamma_4\frac{i\,\omega}{i\,\omega+\beta(y)}(\mathrm{u}_y^K-\lambda_{1y})n_y\tilde{\mathrm{p}}\\
&-\int_K M\alpha_{11}\frac{i\,\omega}{i\,\omega+\alpha(x)}\mathrm{u}_x^K\frac{\partial\tilde{\mathrm{p}}}{\partial x} + \int_F M\alpha_{11}\frac{i\,\omega}{i\,\omega+\alpha(x)}\lambda_{1x}n_x\tilde{\mathrm{p}} - \int_K M\alpha_{22}\frac{i\,\omega}{i\,\omega+\beta(y)}\mathrm{u}_y^K\frac{\partial\tilde{\mathrm{p}}}{\partial y}\\
&+\int_F M\alpha_{22}\frac{i\,\omega}{i\,\omega+\beta(y)}\lambda_{1y}n_y\tilde{\mathrm{p}} - \int_K M\alpha_{12}\frac{i\,\omega}{i\,\omega+\beta(y)}\mathrm{u}_x^K\frac{\partial\tilde{\mathrm{p}}}{\partial y} + \int_F M\alpha_{12}\frac{i\,\omega}{i\,\omega+\beta(y)}\lambda_{1x}n_y\tilde{\mathrm{p}}\\
&-\int_K M\alpha_{12}\frac{i\,\omega}{i\,\omega+\alpha(x)}\mathrm{u}_y^K\frac{\partial\tilde{\mathrm{p}}}{\partial x} + \int_F M\alpha_{12}\frac{i\,\omega}{i\,\omega+\alpha(x)}\lambda_{1y}n_x\tilde{\mathrm{p}} \;=\; 0\,.
\end{aligned}$$

Finally, the local unknowns and the local test-functions are replaced using equations (3.15) and (3.16):

$$\begin{aligned}
&\int_K \mathrm{i}\omega\underline{\mathrm{p}}^K\varphi_j^K\varphi_i^K + \int_K M\frac{i\,\omega}{i\,\omega+\alpha(x)}\underline{\mathrm{w}}_x^K\frac{\partial\varphi_j^K}{\partial x}\varphi_i^K - \int_F M\gamma_2\frac{i\,\omega}{i\,\omega+\alpha(x)}(\underline{\mathrm{p}}^K\varphi_j^K-\underline{\lambda}_2\psi_j^F)n_x^2\varphi_i^K\\
&-\int_F M\gamma_4\frac{i\,\omega}{i\,\omega+\alpha(x)}(\underline{\mathrm{u}}_x^K\varphi_j^K-\underline{\lambda}_{1x}\psi_j^F)n_x\varphi_i^K + \int_K M\frac{i\,\omega}{i\,\omega+\beta(y)}\underline{\mathrm{w}}_y^K\frac{\partial\varphi_j^K}{\partial y}\varphi_i^K - \int_F M\gamma_2\frac{i\,\omega}{i\,\omega+\beta(y)}(\underline{\mathrm{p}}^K\varphi_j^K-\underline{\lambda}_2\psi_j^F)n_y^2\varphi_i^K\\
&-\int_F M\gamma_4\frac{i\,\omega}{i\,\omega+\beta(y)}(\underline{\mathrm{u}}_y^K\varphi_j^K-\underline{\lambda}_{1y}\psi_j^F)n_y\varphi_i^K - \int_K M\alpha_{11}\frac{i\,\omega}{i\,\omega+\alpha(x)}\underline{\mathrm{u}}_x^K\varphi_j^K\frac{\partial\varphi_i^K}{\partial x} + \int_F M\alpha_{11}\frac{i\,\omega}{i\,\omega+\alpha(x)}\underline{\lambda}_{1x}\psi_j^F n_x\varphi_i^K\\
&-\int_K M\alpha_{22}\frac{i\,\omega}{i\,\omega+\beta(y)}\underline{\mathrm{u}}_y^K\varphi_j^K\frac{\partial\varphi_i^K}{\partial y} + \int_F M\alpha_{22}\frac{i\,\omega}{i\,\omega+\beta(y)}\underline{\lambda}_{1y}\psi_j^F n_y\varphi_i^K - \int_K M\alpha_{12}\frac{i\,\omega}{i\,\omega+\beta(y)}\underline{\mathrm{u}}_x^K\varphi_j^K\frac{\partial\varphi_i^K}{\partial y}\\
&+\int_F M\alpha_{12}\frac{i\,\omega}{i\,\omega+\beta(y)}\underline{\lambda}_{1x}\psi_j^F n_y\varphi_i^K - \int_K M\alpha_{12}\frac{i\,\omega}{i\,\omega+\alpha(x)}\underline{\mathrm{u}}_y^K\varphi_j^K\frac{\partial\varphi_i^K}{\partial x} + \int_F M\alpha_{12}\frac{i\,\omega}{i\,\omega+\alpha(x)}\underline{\lambda}_{1y}\psi_j^F n_x\varphi_i^K \;=\; 0\,.
\end{aligned}$$

Discretization of equation (5.3e) The integration on an element of (5.3e) with zero sources gives:

$$\int_K \mathrm{i}\,\omega\,\delta_0\,E_x^K\tilde{e}_x \;+\int_K \mathrm{i}\,\omega\,\delta_0\,E_y^K\tilde{e}_y \;-\int_K\frac{i\,\omega}{i\,\omega+\beta(y)}\frac{\partial H_z^K}{\partial y}\,\tilde{e}_x \;+\int_K\frac{i\,\omega}{i\,\omega+\alpha(x)}\frac{\partial H_z^K}{\partial x}\,\tilde{e}_y \;+\int_K J_x^K\tilde{e}_x \;+\int_K J_y^K\tilde{e}_y \;=0\,.$$

By integrating the space derivatives of H_z^K, we have:

$$\begin{aligned}
&\int_K \mathrm{i}\,\omega\,\delta_0\,E_x^K\tilde{e}_x \;+\int_K \mathrm{i}\,\omega\,\delta_0\,E_y^K\tilde{e}_y \;+\int_K\frac{i\,\omega}{i\,\omega+\beta(y)}H_z^K\frac{\partial\tilde{e}_x}{\partial y} \;-\int_{\partial K}\frac{i\,\omega}{i\,\omega+\beta(y)}\hat{\boldsymbol{H}}_h n_y\tilde{e}_x\\
&-\int_K\frac{i\,\omega}{i\,\omega+\alpha(x)}H_z^K\frac{\partial\tilde{e}_y}{\partial x} \;+\int_{\partial K}\frac{i\,\omega}{i\,\omega+\alpha(x)}\hat{\boldsymbol{H}}_h n_x\tilde{e}_y \;+\int_K J_x^K\tilde{e}_x \;+\int_K J_y^K\tilde{e}_y \;=0\,.
\end{aligned}$$

Then we replace the numerical trace $\hat{\boldsymbol{H}}_h$ by $\boldsymbol{\lambda}_3$ as given in equation (7.3):

$$\begin{aligned}
&\int_K \mathrm{i}\,\omega\,\delta_0\,E_x^K\tilde{e}_x \;+\int_K \mathrm{i}\,\omega\,\delta_0\,E_y^K\tilde{e}_y \;+\int_K\frac{i\,\omega}{i\,\omega+\beta(y)}H_z^K\frac{\partial\tilde{e}_x}{\partial y} \;-\int_{\partial K}\frac{i\,\omega}{i\,\omega+\beta(y)}\boldsymbol{\lambda}_3 n_y\tilde{e}_x\\
&-\int_K\frac{i\,\omega}{i\,\omega+\alpha(x)}H_z^K\frac{\partial\tilde{e}_y}{\partial x} \;+\int_{\partial K}\frac{i\,\omega}{i\,\omega+\alpha(x)}\boldsymbol{\lambda}_3 n_x\tilde{e}_y \;+\int_K J_x^K\tilde{e}_x \;+\int_K J_y^K\tilde{e}_y \;=0\,.
\end{aligned}$$

Next, the local unknowns and the local test-functions are replaced with the expressions given in equations (3.15) and (3.16): The discretization along $x-$ component gives:

$$\int_K \mathrm{i}\,\omega\,\delta_0\,\underline{E}_x^K\,\varphi_i^K\,\varphi_j^K \;+\int_K \frac{i\,\omega}{i\,\omega+\beta(y)}\underline{H}^K\,\frac{\partial\varphi_i^K}{\partial y}\,\varphi_j^K \;-\int_{\partial K}\frac{i\,\omega}{i\,\omega+\beta(y)}\underline{\lambda_3}n_y\,\varphi_i^K\,\varphi_j^K \;+\int_K \underline{J}_x^K\,\varphi_i^K\,\varphi_j^K \;=0\,,$$

and along $y-$ component:

$$\int_K \mathrm{i}\,\omega\,\delta_0\,\underline{E}_y^K\,\varphi_i^K\,\varphi_j^K \;-\int_K \frac{i\,\omega}{i\,\omega+\alpha(x)}\underline{H}^K\,\frac{\partial\varphi_i^K}{\partial x}\,\varphi_j^K \;+\int_{\partial K}\frac{i\,\omega}{i\,\omega+\alpha(x)}\underline{\lambda_3}n_x\,\varphi_i^K\,\varphi_j^K \;+\int_K \underline{J}_y^K\,\varphi_i^K\,\varphi_j^K \;=0\,.$$

Discretization of equation (5.3f) The multiplication of equations (5.3f) by the test-functions and integration on the element K is:

$$\int_K \mathrm{i}\,\omega\,\mu_0 H_z^K\,\tilde{h} \;+\int_K \frac{i\,\omega}{i\,\omega+\alpha(x)}\frac{\partial E_y^K}{\partial x}\;\tilde{h} \;-\int_K \frac{i\,\omega}{i\,\omega+\beta(y)}\frac{\partial E_x^K}{\partial y}\;\tilde{h} \;=\;0\,.$$

By integrating by parts, we have:

$$\int_K \mathrm{i}\,\omega\,\mu_0 H_z^K\,\tilde{h} - \int_K \frac{i\,\omega}{i\,\omega+\alpha(x)}E_y^K\frac{\partial\tilde{h}}{\partial x} + \int_{\partial K}\frac{i\,\omega}{i\,\omega+\alpha(x)}\hat{\mathrm{E}}_y^K\,n_x\,\tilde{h} + \int_K \frac{i\,\omega}{i\,\omega+\beta(y)}E_x^K\frac{\partial\tilde{h}}{\partial y} - \int_{\partial K}\frac{i\,\omega}{i\,\omega+\beta(y)}\hat{\mathrm{E}}_x^K\,n_y\,\tilde{h} \;=\;0\,.$$

Next, we replace the numerical trace $\hat{\boldsymbol{E}}$ by the expression given in equation (7.4) and integrate by parts the space derivatives of $\boldsymbol{E}$: :

$$\begin{aligned}&\int_K \mathrm{i}\,\omega\,\mu_0 H_z^K\,\tilde{h} \;+\int_K \frac{i\,\omega}{i\,\omega+\alpha(x)}\frac{\partial E_y^K}{\partial x}\;\tilde{h} \;-\int_K \frac{i\,\omega}{i\,\omega+\beta(y)}\frac{\partial E_x^K}{\partial y}\;\tilde{h} \;-\int_{\partial K}\gamma_5\frac{i\,\omega}{i\,\omega+\alpha(x)}H_z^K\,n_x^2\,\tilde{h}\\ &+\int_{\partial K}\gamma_5\frac{i\,\omega}{i\,\omega+\alpha(x)}\lambda_3\,n_x^2\,\tilde{h} \;-\int_{\partial K}\gamma_5\frac{i\,\omega}{i\,\omega+\beta(y)}H_z^K\,n_y^2\,\tilde{h} \;+\int_{\partial K}\gamma_5\frac{i\,\omega}{i\,\omega+\beta(y)}\lambda_3\,n_y^2\,\tilde{h} \;=\;0\,.\end{aligned}$$

Then we replace the local unknowns and the local test-functions using equations (3.15) and (3.16):

$$\begin{aligned}&\int_K \mathrm{i}\,\omega\,\mu_0\underline{H}^K\,\varphi_i^K\varphi_j^K + \int_K \frac{i\,\omega}{i\,\omega+\alpha(x)}\underline{E}_y^K\frac{\partial\varphi_j^K}{\partial x}\varphi_i^K - \int_K \frac{i\,\omega}{i\,\omega+\beta(y)}\underline{E}_x^K\frac{\partial\varphi_j^K}{\partial y}\varphi_i^K - \int_{\partial K}\gamma_5\frac{i\,\omega}{i\,\omega+\alpha(x)}\underline{H}^K n_x^2\varphi_i^K\varphi_j^K\\ &+\int_{\partial K}\gamma_5\frac{i\,\omega}{i\,\omega+\alpha(x)}\underline{\lambda_3}n_x^2\varphi_i^K\varphi_j^K - \int_{\partial K}\gamma_5\frac{i\,\omega}{i\,\omega+\beta(y)}\underline{H}^K n_y^2\varphi_i^K\varphi_j^K + \int_{\partial K}\gamma_5\frac{i\,\omega}{i\,\omega+\beta(y)}\underline{\lambda_3}n_y^2\,\varphi_i^K\varphi_j^K \;=\;0\,.\end{aligned}$$

Discretization of equation (5.3g) Finally, the variational formulation of equation (5.3g) on K with zero source is:

$$\begin{aligned}&\int_K J_x^K\,\tilde{e}_x \;+\int_K J_y^K\,\tilde{e}_y \;-\int_K \sigma\,E_x^K\,\tilde{e}_x \;-\int_K \sigma\,E_y^K\,\tilde{e}_y \;+\int_K \mathrm{L}\,\frac{i\,\omega}{i\,\omega+\alpha(x)}\frac{\partial \mathrm{p}}{\partial x}\,\tilde{e}_x \;+\int_K \mathrm{L}\,\frac{i\,\omega}{i\,\omega+\beta(y)}\frac{\partial \mathrm{p}}{\partial y}\,\tilde{e}_y\\ &+\int_K \mathrm{i}\omega\,\rho_f\,\mathrm{L}\,\mathrm{u}_x^K\,\tilde{e}_x \;+\int_K \mathrm{i}\omega\,\rho_f\,\mathrm{L}\,\mathrm{u}_y^K\,\tilde{e}_y \;=0\,.\end{aligned}$$

By integrating by parts the space derivatives of p, we have:

$$\begin{aligned}&\int_K J_x^K\,\tilde{e}_x \;+\int_K J_y^K\,\tilde{e}_y \;-\int_K \sigma\,E_x^K\,\tilde{e}_x \;-\int_K \sigma\,E_y^K\,\tilde{e}_y \;-\int_K \mathrm{L}\,\frac{i\,\omega}{i\,\omega+\alpha(x)}\mathrm{p}\frac{\partial\tilde{e}_x}{\partial x} \;+\int_{\partial K}\mathrm{L}\,\frac{i\,\omega}{i\,\omega+\alpha(x)}\hat{\mathrm{p}}\,n_x\,\tilde{e}_x\\ &+\int_K \mathrm{L}\,\frac{i\,\omega}{i\,\omega+\beta(y)}\mathrm{p}\frac{\partial\tilde{e}_y}{\partial y} \;-\int_{\partial K}\mathrm{L}\,\frac{i\,\omega}{i\,\omega+\beta(y)}\hat{\mathrm{p}}\,n_y\,\tilde{e}_y \;+\int_K \mathrm{i}\omega\,\rho_f\,\mathrm{L}\,\mathrm{u}_x^K\,\tilde{e}_x \;+\int_K \mathrm{i}\omega\,\rho_f\,\mathrm{L}\,\mathrm{u}_y^K\,\tilde{e}_y \;=0\,.\end{aligned}$$

Next, the numerical trace $\hat{\mathrm{p}}$ is replaced by λ_2 as given in equation (7.3). This gives:

$$\begin{aligned}&\int_K J_x^K\,\tilde{e}_x \;+\int_K J_y^K\,\tilde{e}_y \;-\int_K \sigma\,E_x^K\,\tilde{e}_x \;-\int_K \sigma\,E_y^K\,\tilde{e}_y \;-\int_K \mathrm{L}\,\frac{i\,\omega}{i\,\omega+\alpha(x)}\mathrm{p}\frac{\partial\tilde{e}_x}{\partial x} \;+\int_{\partial K}\mathrm{L}\,\frac{i\,\omega}{i\,\omega+\alpha(x)}\lambda_2\,n_x\,\tilde{e}_x\\ &+\int_K \mathrm{L}\,\frac{i\,\omega}{i\,\omega+\beta(y)}\mathrm{p}\frac{\partial\tilde{e}_y}{\partial y} \;-\int_{\partial K}\mathrm{L}\,\frac{i\,\omega}{i\,\omega+\beta(y)}\lambda_2\,n_y\,\tilde{e}_y \;+\int_K \mathrm{i}\omega\,\rho_f\,\mathrm{L}\,\mathrm{u}_x^K\,\tilde{e}_x \;+\int_K \mathrm{i}\omega\,\rho_f\,\mathrm{L}\,\mathrm{u}_y^K\,\tilde{e}_y \;=0\,.\end{aligned}$$

Finally, we replace the local unknowns and the local test-functions using equations (3.15) and (3.16). This gives on x-direction:

$$\int_K \underline{J}_x^K \varphi_i^K \varphi_j^K - \int_K \sigma \underline{E}_x^K \varphi_i^K \varphi_j^K - \int_K \underline{\mathrm{p}}^K \mathrm{L} \frac{i\,\omega}{i\,\omega + \alpha(x)} \frac{\partial \varphi_i^K}{\partial x} \varphi_j^K + \int_{\partial K} \mathrm{L} \frac{i\,\omega}{i\,\omega + \alpha(x)} n_x \underline{\lambda}_2 \varphi_i^K \varphi_j^K + \int_K \mathrm{i}\omega\rho_f \mathrm{L} \underline{\mathrm{u}}_x^K \varphi_i^K \varphi_j^K = 0\,,$$

and on y-direction:

$$\int_K \underline{J}_y^K \varphi_i^K \varphi_j^K - \int_K \sigma \underline{E}_y^K \varphi_i^K \varphi_j^K - \int_K \underline{\mathrm{p}}^K \mathrm{L} \frac{i\,\omega}{i\,\omega + \beta(y)} \frac{\partial \varphi_i^K}{\partial y} \varphi_j^K + \int_{\partial K} \mathrm{L} \frac{i\,\omega}{i\,\omega + \beta(y)} n_y \underline{\lambda}_2 \varphi_i^K \varphi_j^K + \int_K \mathrm{i}\omega\rho_f \mathrm{L} \underline{\mathrm{u}}_y^K \varphi_i^K \varphi_j^K = 0\,.$$

Local system As in Section 7.2, the discretization of the seven equations composing the local problem detailed above can be written as a system of the form:

$$\mathbb{A}^K \underline{W}^K + \mathbb{B}^K \underline{\Lambda}^K = \mathbb{C}^K_{\text{source}}\,,$$

where $\underline{W}^K$ and $\underline{\Lambda}^K$ have been defined in (3.17).

We now define the following matrices:

$$\mathbb{M}^K_{ij} = \int_K \varphi_i^K \varphi_j^K dX\,, \qquad \mathbb{D}^K_{xij} = \int_K \frac{i\,\omega}{i\,\omega + \alpha(x)} \varphi_j^K \frac{\partial \varphi_i^K}{\partial x} dX\,, \qquad \mathbb{D}^K_{yij} = \int_K \frac{i\,\omega}{i\,\omega + \beta(y)} \varphi_j^K \frac{\partial \varphi_i^K}{\partial y} dX\,,$$

$$\mathbb{J}^F_{xij} = \int_F \frac{i\,\omega}{i\,\omega + \alpha(x)} \varphi_i^K \varphi_j^K n_y\, dS\,, \qquad \mathbb{J}^F_{yij} = \int_F \frac{i\,\omega}{i\,\omega + \beta(y)} \varphi_i^K \varphi_j^K n_y\, dS\,,$$

$$\mathbb{Q}^F_{xij} = \int_F \frac{i\,\omega}{i\,\omega + \alpha(x)} \varphi_i^K \psi_j^F n_x\, dS\,, \qquad \mathbb{Q}^F_{yij} = \int_F \frac{i\,\omega}{i\,\omega + \beta(y)} \varphi_i^K \psi_j^F n_y\, dS\,,$$

$$\mathbb{E}^F_{ij} = \int_F \frac{i\,\omega}{i\,\omega + \alpha(x)} \varphi_i^K \varphi_j^K n_x^2 dS + \int_F \frac{i\,\omega}{i\,\omega + \beta(y)} \varphi_i^K \varphi_j^K n_y^2 dS\,,$$

$$\mathbb{F}^F_{ij} = \int_F \frac{i\,\omega}{i\,\omega + \alpha(x)} \varphi_i^K \psi_j^F n_x^2 dS + \int_F \frac{i\,\omega}{i\,\omega + \beta(y)} \varphi_i^K \psi_j^F n_y^2 dS\,.$$

With this notation, the matrices $\mathbb{A}^K$ and $\mathbb{B}^K$ are the ones given in Section 7.2.

Appendix F

Appendices to Chapter 9

F.1 Calculation for the point-source in P-wave

In this section, we determine which source needs to be taken in order to generate only P-wave. We start from Pride's equations of the second-order with no sources:

$$\begin{aligned} -\omega^2\rho_a \mathrm{u} \;-\; \rho_f\omega^2 \mathrm{w} \;-\; H\,\nabla\nabla\cdot \mathrm{u} \;+\; \mu_{\mathrm{fr}}\,\mathbf{curl}\,\mathrm{curl}\,\mathrm{u} \;-\; \alpha\, M\,\nabla\nabla\cdot \mathrm{w} &= 0\,,\\ -\omega^2\rho_f \mathrm{u} \;-\; \omega^2\,\rho_{\mathrm{dyn}}\,\mathrm{w} - \frac{\eta}{k}\,\mathbf{L}\,\boldsymbol{E} \;-\; M\,\nabla\nabla\cdot \mathrm{w} \;-\; M\alpha\nabla\nabla\cdot \mathrm{u} &= 0\,,\\ \mathbf{curl}\,\mathrm{curl}\,\boldsymbol{E} - \omega^2\,\tilde{\boldsymbol{\varepsilon}}\,\mu_0\,\boldsymbol{E} \;-\; \mathfrak{s}\,\mathrm{i}\,\omega\,\mu_0\,\mathbf{L}\,\omega^2\,\rho_{\mathrm{dyn}}\,\mathrm{w} &= 0\,, \end{aligned} \tag{F.1}$$

and we express u, w and $\boldsymbol{E}$ as:

$$\mathrm{u} = \tilde{\mathrm{u}} + \mathrm{u}_{\mathrm{src}}\,, \qquad \mathrm{w} = \tilde{\mathrm{w}} + \mathrm{w}_{\mathrm{src}}\,, \qquad \boldsymbol{E} = \tilde{\boldsymbol{E}} + \boldsymbol{E}_{\mathrm{src}}\,.$$

The displacements $\mathrm{u}_{\mathrm{src}}$, $\mathrm{w}_{\mathrm{src}}$, and the electric field $\boldsymbol{E}_{\mathrm{src}}$ are the fields generated by the point source, in an homogeneous domain, and those terms are used as a right-hand side. This is injected in equation (F.1):

$$\begin{aligned} -\omega^2\rho_a \tilde{\mathrm{u}} \;-\; \rho_f\omega^2 \tilde{\mathrm{w}} \;-\; H\,\nabla\nabla\cdot \tilde{\mathrm{u}} \;+\; \mu_{\mathrm{fr}}\,\mathbf{curl}\,\mathrm{curl}\,\tilde{\mathrm{u}} \;-\; \alpha\, M\,\nabla\nabla\cdot \tilde{\mathrm{w}} &= \boldsymbol{rhs}_1\,,\\ -\omega^2\rho_f \tilde{\mathrm{u}} \;-\; \omega^2\,\rho_{\mathrm{dyn}}\,\tilde{\mathrm{w}} - \frac{\eta}{k}\,\mathbf{L}\,\tilde{\boldsymbol{E}} \;-\; M\,\nabla\nabla\cdot \tilde{\mathrm{w}} \;-\; M\alpha\nabla\nabla\cdot \tilde{\mathrm{u}} &= \boldsymbol{rhs}_2\,,\\ \mathbf{curl}\,\mathrm{curl}\,\tilde{\boldsymbol{E}} - \omega^2\,\tilde{\boldsymbol{\varepsilon}}\,\mu_0\,\tilde{\boldsymbol{E}} \;-\; \mathfrak{s}\,\mathrm{i}\,\omega\,\mu_0\,\mathbf{L}\,\omega^2\,\rho_{\mathrm{dyn}}\,\tilde{\mathrm{w}} &= \boldsymbol{rhs}_3\,, \end{aligned}$$

with

$$\begin{aligned} \boldsymbol{rhs}_1 &= \omega^2\rho_a \mathrm{u}_{\mathrm{src}} \;+\; \rho_f\omega^2 \mathrm{w}_{\mathrm{src}} \;+\; H\,\nabla\nabla\cdot \mathrm{u}_{\mathrm{src}} \;-\; \mu_{\mathrm{fr}}\,\mathbf{curl}\,\mathrm{curl}\,\mathrm{u}_{\mathrm{src}} \;+\; \alpha\, M\,\nabla\nabla\cdot \mathrm{w}_{\mathrm{src}}\,,\\ \boldsymbol{rhs}_2 &= \omega^2\rho_f \mathrm{u}_{\mathrm{src}} \;+\; \omega^2\,\rho_{\mathrm{dyn}}\,\mathrm{w}_{\mathrm{src}} + \frac{\eta}{k}\,\mathbf{L}\,\boldsymbol{E}_{\mathrm{src}} + M\,\nabla\nabla\cdot \mathrm{w}_{\mathrm{src}} + M\alpha\nabla\nabla\cdot \mathrm{u}_{\mathrm{src}}\,,\\ \boldsymbol{rhs}_3 &= -\,\mathbf{curl}\,\mathrm{curl}\,\boldsymbol{E}_{\mathrm{src}} + \omega^2\,\tilde{\boldsymbol{\varepsilon}}\,\mu_0\,\boldsymbol{E}_{\mathrm{src}} \;+\; \mathfrak{s}\,\mathrm{i}\,\omega\,\mu_0\,\mathbf{L}\,\omega^2\,\rho_{\mathrm{dyn}}\,\mathrm{w}_{\mathrm{src}}\,. \end{aligned} \tag{F.3}$$

We express $\mathrm{u}_{\mathrm{src}}$, $\mathrm{w}_{\mathrm{src}}$ and $\boldsymbol{E}_{\mathrm{src}}$ using the potential decomposition, with $\chi_{\mathrm{B}} = \chi_{\mathrm{S}} = \chi_{\mathrm{EM}} = 0$. We have:

$$\mathrm{u}_{\mathrm{src}} = -\frac{1}{\omega^2\,\mathsf{s}_{\mathrm{P}}^2}\,\nabla\chi_{\mathrm{P}}\,, \qquad \mathrm{w}_{\mathrm{src}} = -\frac{\mathcal{W}_{\mathrm{P}}}{\omega^2\,\mathsf{s}_{\mathrm{P}}^2}\,\nabla\chi_{\mathrm{P}}\,, \qquad \boldsymbol{E}_{\mathrm{src}} = -\frac{\mathcal{E}_{\mathrm{P}}}{\omega^2\,\mathsf{s}_{\mathrm{P}}^2}\,\nabla\chi_{\mathrm{P}}\,,$$

with the potential χ_{P} solution of the Helmholtz equation:

$$-\,\omega^2\,\mathsf{s}_{\mathrm{P}}^2\,\chi_{\mathrm{P}} \;-\; \Delta\,\chi_{\mathrm{P}} = \delta\,.$$

We inject the expressions in equation (F.3). We use the fact that:

$$\mathrm{curl}\,(\nabla\,\chi_{\mathrm{P}}) = 0\,, \qquad \nabla\nabla\cdot\,(\nabla\,\chi_{\mathrm{P}}) = \Delta(\nabla\,\chi_{\mathrm{P}})\,.$$

We obtain:

$$\boldsymbol{rhs} = -\frac{1}{\mathsf{s}_{\mathrm{P}}^2}\,A\begin{pmatrix}\nabla\chi_{\mathrm{P}}\\ \mathcal{W}_{\mathrm{P}}\,\nabla\chi_{\mathrm{P}}\\ \mathcal{E}_{\mathrm{P}}\,\nabla\chi_{\mathrm{P}}\end{pmatrix} \;-\; \frac{1}{\omega^2\,\mathsf{s}_{\mathrm{P}}^2}\,B\Delta\begin{pmatrix}\nabla\chi_{\mathrm{P}}\\ \mathcal{W}_{\mathrm{P}}\,\nabla\chi_{\mathrm{P}}\\ \mathcal{E}_{\mathrm{P}}\,\nabla\chi_{\mathrm{P}}\end{pmatrix}\,,$$

that we write

$$\omega^2\,\mathsf{s}_\mathrm{P}^2\,\boldsymbol{rhs} \;=\; -\,\omega^2\,A\begin{pmatrix}\nabla\chi_\mathrm{P}\\ \mathcal{W}_\mathrm{P}\,\nabla\chi_\mathrm{P}\\ \mathcal{E}_\mathrm{P}\,\nabla\chi_\mathrm{P}\end{pmatrix} \;-\; B\Delta\begin{pmatrix}\nabla\chi_\mathrm{P}\\ \mathcal{W}_\mathrm{P}\,\nabla\chi_\mathrm{P}\\ \mathcal{E}_\mathrm{P}\,\nabla\chi_\mathrm{P}\end{pmatrix},$$

with the matrices

$$A \;=\; \begin{pmatrix}\rho_a & \rho_f & 0\\ \rho_f & \rho_\mathrm{dyn} & \dfrac{\eta}{\omega^2\,k}\,\mathbf{L}\\ 0 & \mathfrak{s}\,\mathrm{i}\,\omega\,\mu_0\,\mathbf{L}\,\rho_\mathrm{dyn} & \tilde{\boldsymbol{\varepsilon}}\,\mu_0\end{pmatrix}, \quad B \;=\; \begin{pmatrix}H & \alpha M & 0\\ \alpha M & M & 0\\ 0 & 0 & 0\end{pmatrix},$$

Multiplying by A^{-1}, we have:

$$A^{-1}\,\omega^2\,\mathsf{s}_\mathrm{P}^2\,\boldsymbol{rhs} \;=\; -\,\omega^2\begin{pmatrix}\nabla\chi_\mathrm{P}\\ \mathcal{W}_\mathrm{P}\,\nabla\chi_\mathrm{P}\\ \mathcal{E}_\mathrm{P}\,\nabla\chi_\mathrm{P}\end{pmatrix} \;-\; A^{-1}\,B\Delta\begin{pmatrix}\nabla\chi_\mathrm{P}\\ \mathcal{W}_\mathrm{P}\,\nabla\chi_\mathrm{P}\\ \mathcal{E}_\mathrm{P}\,\nabla\chi_\mathrm{P}\end{pmatrix},$$

Recall that $A^{-1}B$ can be diagonalized, and is equal to

$$A^{-1}B \;=\; P_\mathrm{long}\begin{pmatrix}\mathsf{c}_\mathsf{P}^2 & 0 & 0\\ 0 & \mathsf{c}_\mathsf{B}^2 & 0\\ 0 & 0 & 0\end{pmatrix}P_\mathrm{long}^{-1}, \qquad \text{and} \qquad P_\mathrm{long} \;=\; \begin{pmatrix}1 & 1 & 0\\ \mathcal{W}_\mathrm{P} & \mathcal{W}_\mathrm{B} & 0\\ \mathcal{E}_\mathrm{P} & \mathcal{E}_\mathrm{B} & 1\end{pmatrix}.$$

This leads to:

$$A^{-1}\,\omega^2\,\mathsf{s}_\mathrm{P}^2\,\boldsymbol{rhs} \;=\; -\,\omega^2\begin{pmatrix}\nabla\chi_\mathrm{P}\\ \mathcal{W}_\mathrm{P}\,\nabla\chi_\mathrm{P}\\ \mathcal{E}_\mathrm{P}\,\nabla\chi_\mathrm{P}\end{pmatrix} \;-\; P_\mathrm{long}\begin{pmatrix}\mathsf{c}_\mathsf{P}^2 & 0 & 0\\ 0 & \mathsf{c}_\mathsf{B}^2 & 0\\ 0 & 0 & 0\end{pmatrix}P_\mathrm{long}^{-1}\Delta\begin{pmatrix}\nabla\chi_\mathrm{P}\\ \mathcal{W}_\mathrm{P}\,\nabla\chi_\mathrm{P}\\ \mathcal{E}_\mathrm{P}\,\nabla\chi_\mathrm{P}\end{pmatrix}.$$

Multiplying the above equation by P_long^{-1} gives

$$P_\mathrm{long}^{-1}\,A^{-1}\,\omega^2\,\mathsf{s}_\mathrm{P}^2\,\boldsymbol{rhs} \;=\; -\,\omega^2\,P_\mathrm{long}^{-1}\begin{pmatrix}\nabla\chi_\mathrm{P}\\ \mathcal{W}_\mathrm{P}\,\nabla\chi_\mathrm{P}\\ \mathcal{E}_\mathrm{P}\,\nabla\chi_\mathrm{P}\end{pmatrix} \;-\; \begin{pmatrix}\mathsf{c}_\mathsf{P}^2 & 0 & 0\\ 0 & \mathsf{c}_\mathsf{B}^2 & 0\\ 0 & 0 & 0\end{pmatrix}P_\mathrm{long}^{-1}\Delta\begin{pmatrix}\nabla\chi_\mathrm{P}\\ \mathcal{W}_\mathrm{P}\,\nabla\chi_\mathrm{P}\\ \mathcal{E}_\mathrm{P}\,\nabla\chi_\mathrm{P}\end{pmatrix}. \tag{F.4}$$

The inverse of P_long is,

$$P_\mathrm{long}^{-1} \;=\; \frac{1}{\mathcal{W}_\mathrm{B}-\mathcal{W}_\mathrm{P}}\begin{pmatrix}\mathcal{W}_\mathrm{B} & -1 & 0\\ -\mathcal{W}_\mathrm{P} & 1 & 0\\ \mathcal{E}_\mathrm{B}\mathcal{W}_\mathrm{P}-\mathcal{E}_\mathrm{P}\mathcal{W}_\mathrm{B} & \mathcal{E}_\mathrm{P}-\mathcal{E}_\mathrm{B} & \mathcal{W}_\mathrm{B}-\mathcal{W}_\mathrm{P}\end{pmatrix},$$

and we have:

$$P_\mathrm{long}^{-1}\begin{pmatrix}\nabla\chi_\mathrm{P}\\ \mathcal{W}_\mathrm{P}\,\nabla\chi_\mathrm{P}\\ \mathcal{E}_\mathrm{P}\,\nabla\chi_\mathrm{P}\end{pmatrix} \;=\; \begin{pmatrix}\nabla\chi_\mathrm{P}\\ 0\\ 0\end{pmatrix}$$

We replace this in (F.4):

$$P_\mathrm{long}^{-1}\,A^{-1}\,\omega^2\,\mathsf{s}_\mathrm{P}^2\,\boldsymbol{rhs} \;=\; -\,\omega^2\begin{pmatrix}\nabla\chi_\mathrm{P}\\ 0\\ 0\end{pmatrix} \;-\; \begin{pmatrix}\mathsf{c}_\mathsf{P}^2 & 0 & 0\\ 0 & \mathsf{c}_\mathsf{B}^2 & 0\\ 0 & 0 & 0\end{pmatrix}\Delta\begin{pmatrix}\nabla\chi_\mathrm{P}\\ 0\\ 0\end{pmatrix},$$

which gives

$$P_\mathrm{long}^{-1}\,A^{-1}\,\omega^2\,\mathsf{s}_\mathrm{P}^4\,\boldsymbol{rhs} \;=\; \begin{pmatrix}-\,\omega^2\,\mathsf{s}_\mathrm{P}^2\,\nabla\chi_\mathrm{P} \;-\; \Delta\Big(\nabla\chi_\mathrm{P}\Big)\\ 0\\ 0\end{pmatrix} \;=\; \begin{pmatrix}\nabla\,\delta\\ 0\\ 0\end{pmatrix}.$$

Hence the right-hand side is,

$$\boldsymbol{rhs} \;=\; \frac{1}{\omega^2\,\mathsf{s}_\mathrm{P}^4}\,A\,P_\mathrm{long}\begin{pmatrix}\nabla\,\delta\\ 0\\ 0\end{pmatrix} \;=\; \frac{1}{\omega^2\,\mathsf{s}_\mathrm{P}^4}\begin{pmatrix}(A\,P_\mathrm{long})_{11}\,\nabla\,\delta\\ (A\,P_\mathrm{long})_{21}\,\nabla\,\delta\\ (A\,P_\mathrm{long})_{31}\,\nabla\,\delta\end{pmatrix} \;=\; \frac{1}{\omega^2\,\mathsf{s}_\mathrm{P}^4}\begin{pmatrix}(\rho_a \;+\; \rho_f\,\mathcal{W}_\mathrm{P})\,\nabla\,\delta\\ (\rho_f \;+\; \tilde{\rho}\,\mathcal{W}_\mathrm{P} \;+\; \dfrac{\eta}{\omega^2\,k}\,\mathbf{L}\,\mathcal{E}_\mathrm{P})\,\nabla\,\delta\\ (\mathfrak{s}\,\mathrm{i}\,\omega\,\mu_0\,\mathbf{L}\,\rho_\mathrm{dyn}\,\mathcal{W}_\mathrm{P} + \tilde{\boldsymbol{\varepsilon}}\,\mu_0\,\mathcal{E}_\mathrm{P})\,\nabla\,\delta\end{pmatrix}.$$

We now need to express the exterior forces from equation (5.3). We recall that (see Proposition 5.1):

$$rhs_1 \,=\, \mathbf{f}_u\,, \qquad rhs_2 \,=\, \mathbf{f}_w\,, \qquad rhs_3 \,=\, \mathfrak{s}\,\mathrm{i}\,\omega\,\mu_0\,\mathbf{f}_C\,.$$

Hence, we have:

$$\mathbf{f}_u \,=\, \frac{(\rho_a \,+\, \rho_f\,\mathcal{W}_{\mathrm{P}})}{\omega^2\,\mathsf{s}_{\mathrm{P}}^4}\,\nabla\,\delta\,, \quad \mathbf{f}_w \,=\, \frac{(\rho_f \,+\, \rho_{\mathrm{dyn}}\,\mathcal{W}_{\mathrm{P}} \,+\, \dfrac{\eta}{\omega^2\,k}\,\mathbf{L}\,\mathcal{E}_{\mathrm{P}})}{\omega^2\,\mathsf{s}_{\mathrm{P}}^4}\,\nabla\,\delta\,, \quad \mathbf{f}_C \,=\, \frac{1}{\omega^2\,\mathsf{s}_{\mathrm{P}}^4}\,\Big(\mathbf{L}\,\rho_{\mathrm{dyn}}\,\mathcal{W}_{\mathrm{P}} \,-\, \frac{\mathfrak{s}\,\mathrm{i}\,\tilde{\boldsymbol{\varepsilon}}}{\omega}\,\mathcal{E}_{\mathrm{P}}\Big)\,\nabla\,\delta\,.$$

Appendix G

Propagation of electromagnetic waves

In this appendix, we introduce a computational framework based upon a HDG solution methodology for solving Maxwell's equations set in the timer-harmonic regime. It is worth mentioning that this does not contain new ideas. It adopts the approach developed in [85] and [102]. However we have chosen to present this work in detail since it is an important step forward in the development of a piece of software dedicated to electrokinetics which is actually targeted in this thesis.

The modeling of electromagnetic (EM) waves has been introduced by Maxwell [94] and these equations are still extensively studied in time and harmonic domain as they are involved in many applications. Several numerical methods have been applied to solve the electromagnetic equations, as Finite Difference, Finite Volume [135] or Finite Element *e.g.*, [5] in the time domain and [119] in frequency domain. Discontinuous Galerkin (DG) methods have also been used to obtain a solution of Maxwell's equations [36, 55, 47]. More recently, HDG methods for electromagnetism have been proposed in time domain [100, 31] and harmonic domain [85, 102, 87, 86, 53].

In the following, we first present in Section G.1 the electromagnetic equations and plane wave solutions. Then, we construct in Section G.2 analytical solutions in circular geometry. We develop in Sections G.3 and G.4 a HDG method for Maxwell's equations in two and three dimensions. We extend the method to the modeling of infinite domains by applying a Radiation Boundary Condition (RBC) to the HDG discretization in Section G.5 and PML in Section G.6. Finally, we present some numerical tests and results to valivate the HDG method in Section G.7.

G.1 Electromagnetic equations

The equations of propagation of electromagnetic waves have been proposed by Maxwell [94], and are represented by the following quantities:

- the electric density $\boldsymbol{E}$ (V.m^{-1}),
- the magnetic intensity $\boldsymbol{H}$ (A.m^{-1}),
- the current density $\boldsymbol{J}$ (A.m^{-2}),
- the electric induction $\boldsymbol{D}$ (C.m^{-2}),
- the magnetic induction $\boldsymbol{B}$ (T).

The equations of electromagnetic wave propagation depend on the following parameters:

- the electromagnetic vacuum permeability μ_0, expressed in (N/A^2), that is a magnetic constant in vacuum, equal to $12.566\,10^{-7}$ N/A^2.
- the electromagnetic vacuum permittivity ϵ_0, equal to $8.8595\,10^{-12}$ F.m^{-1}.
- the conductivity σ (S.m^{-1}).

Remark G.1. In two dimensions, we can consider two kinds of configurations corresponding to polarized waves:

- For a Transverse Magnetic wave, the magnetic field is supported by an axis $\mathbf{d}$ while the electric field is in the plane orthogonal to $\mathbf{d}$.

- For a Transverse Electric field, the electric field is supported by an axis **d** while the magnetic field lies in the plane orthogonal to **d**.

In this chapter, when we will only consider the case Transverse Magnetic (TM) electromagnetic fields . This is also the configuration used for the electrokinetic equations in two dimensions.

The electromagnetic constitutive laws are expressed as:

$$\begin{aligned} \boldsymbol{B} &= \mu_0 \boldsymbol{H}\,, \\ \boldsymbol{D} &= \epsilon_0 \boldsymbol{E}\,, \\ \boldsymbol{J} &= \sigma \boldsymbol{E}\,. \end{aligned}$$

The electromagnetic waves are governed by Maxwell's equations::

$$\begin{aligned} \mathbf{curl}\boldsymbol{E} + \mu_0 \frac{\partial \boldsymbol{B}}{\partial_t} &= 0\,, \\ \mathbf{curl}\boldsymbol{H} - \epsilon_0 \frac{\partial \boldsymbol{D}}{\partial_t} - \boldsymbol{J} &= \mathbf{f}_C\,. \end{aligned}$$

with the operator **curl** defined in (1.17) in three dimensions, and $\mathbf{f}_C$ an exterior force.

For the boundary conditions, we impose for a bounded domain of boundary Γ:

$$\boldsymbol{E} \times \boldsymbol{n} = \boldsymbol{n} \times \mathbf{e}^{\text{inc}}\,, \quad \text{or} \quad \boldsymbol{H} \times \boldsymbol{n} = \boldsymbol{h}_{\text{inc}} \times \boldsymbol{n} \quad \text{on } \Gamma\,, \tag{G.1}$$

where $\boldsymbol{f}_{\text{inc}}$ and $\boldsymbol{h}_{\text{inc}}$ are incident forces. In two dimensions, the boundary condition for the magnetic field is:

$$\boldsymbol{E} \times \boldsymbol{n} = \boldsymbol{n} \times \mathbf{e}^{\text{inc}}\,, \quad \text{or} \quad \mathrm{H} = h_{\text{inc}} \quad \text{on } \Gamma\,. \tag{G.2}$$

Harmonic equations: Assuming that the electromagnetic fields are $e^{i\omega t}\boldsymbol{E}(x)$ and $e^{i\omega t}\boldsymbol{H}(x)$, the pair ($\boldsymbol{E}$,$\boldsymbol{H}$) satisfies the time-harmonic Maxwell's equations: We study the electromagnetic equation in the following form, by considering a time derivative $\mathrm{i}\,\omega$:

$$\begin{aligned} &\mathbf{curl}\,\boldsymbol{E} + \mathrm{i}\,\omega\,\mu_0 \boldsymbol{H} = 0\,, \\ &\mathbf{curl}\,\boldsymbol{H} - \mathrm{i}\,\omega\,\epsilon_0 \boldsymbol{E} - \boldsymbol{J} = \mathbf{f}_C\,, \\ &\boldsymbol{J} = \sigma\,\boldsymbol{E}\,. \end{aligned} \tag{G.3}$$

As we have said above, in two dimensions, we consider the case of transverse electric, which means that $\boldsymbol{E} = (E_x\,,\, E_y)$ and $\mathrm{H} = H_z$. In this case, we write Maxwell's equation (G.3) as:

$$\begin{aligned} &\mathrm{curl}\,\boldsymbol{E} + \mathrm{i}\,\omega\,\mu_0 \mathrm{H} = 0\,, \\ &\mathbf{curl}\,\mathrm{H} - \mathrm{i}\,\omega\,\epsilon_0 \boldsymbol{E} - \boldsymbol{J} = \mathbf{f}_C\,, \\ &\boldsymbol{J} = \sigma\,\boldsymbol{E}\,, \end{aligned} \tag{G.4}$$

with the operators curl and **curl** defined in equation (1.19) in two dimensions.

G.1.1 Plane wave analysis

In two dimensions First, we write Maxwell's equation (G.3) without sources as:

$$\begin{aligned} &\mathrm{curl}\,\boldsymbol{E} + \mathrm{i}\,\omega\,\mu_0 \mathrm{H} = 0\,, \\ &\mathbf{curl}\,\mathrm{H} - \mathrm{i}\,\omega \left(\epsilon_0 - \frac{\mathrm{i}\,\sigma}{\omega}\right) \boldsymbol{E} = 0\,. \end{aligned} \tag{G.5}$$

The plane wave solutions of the above equations can be written as :

$$\mathrm{H} = \mathcal{H}\, e^{\mathrm{i}\mathbf{k}\cdot\boldsymbol{X}}\,, \qquad \boldsymbol{E} = \mathcal{E}\, e^{\mathrm{i}\mathbf{k}\cdot\boldsymbol{X}}\, \widehat{\mathbf{d}}\,, \tag{G.6}$$

with $\widehat{\mathbf{d}}$ the wave polarization and $\mathbf{k}$ the wave vector, equal to $\mathbf{k} = \omega\,\mathsf{s}\,\widehat{\mathbf{k}}$, with s the wave slowness, $|\mathbf{k}|$ the wavenumber and $\widehat{\mathbf{k}}$ the direction of propagation. Then, we replace those expressions in (G.5) and divide by $e^{\mathrm{i}\mathbf{k}\cdot X}$. Using the expression of the rotational in two dimensions (1.19), we have:

$$\begin{aligned} \mathrm{i}\,|\boldsymbol{k}|\,\hat{k}_x\,\mathcal{E}\,\hat{d}_y - \mathrm{i}\,|\boldsymbol{k}|\,\hat{k}_y\,\mathcal{E}\hat{d}_x + \mathrm{i}\,\omega\,\mu_0\mathcal{H} &= 0\,, \\ \mathrm{i}\,\mathcal{H}\,|\boldsymbol{k}|\,\hat{k}_y - \mathrm{i}\omega \left(\epsilon_0 - \frac{\mathrm{i}\sigma}{\omega}\right) \mathcal{E}\,\hat{d}_x &= 0\,, \\ -\mathrm{i}\,\mathcal{H}\,|\boldsymbol{k}|\,\hat{k}_x - \mathrm{i}\,\omega \left(\epsilon_0 - \frac{\mathrm{i}\sigma}{\omega}\right) \mathcal{E}\,\hat{d}_y &= 0\,. \end{aligned} \tag{G.7}$$

As the polarization of the wave is transverse, we have $\boldsymbol{k}\cdot\boldsymbol{d}=0$, and $\widehat{\mathbf{d}}$ reads as $\widehat{\mathbf{d}}=\begin{pmatrix}-\hat{k}_y\\ \hat{k}_x\end{pmatrix}$. This means that, using $|\widehat{\mathbf{k}}|=1$, system (G.7) simplifies to:

$$\begin{aligned}\mathrm{i}\,\mathcal{E}\,|\boldsymbol{k}|+\mathrm{i}\omega\,\mu_0\,\mathcal{H}&=0\,,\\ \mathrm{i}\,\mathcal{H}\,|\boldsymbol{k}|+\mathrm{i}\omega\left(\epsilon_0-\frac{\mathrm{i}\sigma}{\omega}\right)\mathcal{E}&=0\,.\end{aligned}$$

Then, we divide by i and $|\mathbf{k}|$, and we replace $\dfrac{\omega}{|\mathbf{k}|}$ by c to obtain:

$$\begin{aligned}\mathcal{E}+c\,\mu_0\,\mathcal{H}&=0\,,\\ \mathcal{H}+c\left(\epsilon_0-\frac{\mathrm{i}\sigma}{\omega}\right)\mathcal{E}&=0\,.\end{aligned}$$

This system, expressed in matrix form is equal to:

$$\begin{pmatrix}c\,\mu_0 & 1\\ 1 & c\left(\epsilon_0-\dfrac{\mathrm{i}\sigma}{\omega}\right)\end{pmatrix}\begin{pmatrix}\mathcal{H}\\ \mathcal{E}\end{pmatrix}=0\,. \tag{G.8}$$

This system admits non trivial solutions if the determinant of the above matrix is zero.

$$c^2\left(\epsilon_0-\frac{\mathrm{i}\sigma}{\omega}\right)\mu_0-1=0\,,$$

which leads to:

$$c=\frac{1}{\sqrt{\left(\epsilon_0-\dfrac{\mathrm{i}\sigma}{\omega}\right)\mu_0}}\,.$$

A solution of system (G.8) is:

$$\mathcal{H}=1,\quad \mathcal{E}=-\,c\,\mu_0=-\frac{\mu_0}{\mathsf{s}_{\mathrm{EM}}}\,,\qquad \text{with } \mathsf{s}_{\mathrm{EM}}=\sqrt{\left(\epsilon_0-\frac{\mathrm{i}\sigma}{\omega}\right)\mu_0}\,. \tag{G.9}$$

In three dimensions First, we write Maxwell's equation (G.3) as:

$$\begin{aligned}\mathbf{curl}\,\boldsymbol{E}+\mathrm{i}\,\omega\,\mu_0\boldsymbol{H}&=0\,,\\ \mathbf{curl}\,\boldsymbol{H}-\mathrm{i}\,\omega\left(\epsilon_0-\frac{\mathrm{i}\,\sigma}{\omega}\right)\boldsymbol{E}&=0\,.\end{aligned}$$

The plane wave solution is expressed as:

$$\boldsymbol{E}=\mathcal{E}\,e^{i\mathbf{k}\cdot\boldsymbol{X}}\,\widehat{\mathbf{d}}\,,\qquad\qquad \boldsymbol{H}=\mathcal{H}\,e^{\mathrm{i}\mathbf{k}\cdot\boldsymbol{X}}\,\widehat{\mathbf{k}}\times\widehat{\mathbf{d}}\,.$$

Using the definition of rotational in three dimensions (1.17), the electromagnetic equations are written as:

$$\begin{aligned}
&\mathrm{i}\,|\boldsymbol{k}|\,\hat{k}_y\,\mathcal{E}\,d_z-\mathrm{i}\,|\boldsymbol{k}|\,\hat{k}_z\,\mathcal{E}\,d_y+\mathrm{i}\omega\mu_0\mathcal{H}\,(\,\hat{k}_y\,d_z-\hat{k}_z\,d_y\,)=0\,,\\
&\mathrm{i}\,|\boldsymbol{k}|\,\hat{k}_z\,\mathcal{E}\,d_x-\mathrm{i}\,|\boldsymbol{k}|\,\hat{k}_x\,\mathcal{E}\,d_z+\mathrm{i}\omega\mu_0\mathcal{H}\,(\,\hat{k}_z\,d_x-\hat{k}_x\,d_z\,)=0\,,\\
&\mathrm{i}\,|\boldsymbol{k}|\,\hat{k}_x\,\mathcal{E}\,d_y-\mathrm{i}\,|\boldsymbol{k}|\,\hat{k}_y\,\mathcal{E}\,d_x+\mathrm{i}\omega\mu_0\mathcal{H}\,(\,\hat{k}_x\,d_y-\hat{k}_y\,d_x\,)=0\,,\\
&\mathrm{i}\,|\boldsymbol{k}|\,\hat{k}_y\,\mathcal{H}\,(\,\hat{k}_x\,d_y-\hat{k}_y\,d_x\,)-\mathrm{i}\,|\boldsymbol{k}|\,\hat{k}_z\,\mathcal{H}\,(\,\hat{k}_z\,d_x-\hat{k}_x\,d_z\,)-\mathrm{i}\omega\left(\epsilon_0-\frac{\mathrm{i}\,\sigma}{\omega}\right)\mathcal{E}\,d_x=0\,,\\
&\mathrm{i}\,|\boldsymbol{k}|\,\hat{k}_z\,\mathcal{H}\,(\,\hat{k}_y\,d_z-\hat{k}_z\,d_y\,)-\mathrm{i}\,|\boldsymbol{k}|\,\hat{k}_x\,\mathcal{H}\,(\,\hat{k}_x\,d_y-\hat{k}_y\,d_x\,)-\mathrm{i}\omega\left(\epsilon_0-\frac{\mathrm{i}\,\sigma}{\omega}\right)\mathcal{E}\,d_y=0\,,\\
&\mathrm{i}\,|\boldsymbol{k}|\,\hat{k}_x\,\mathcal{H}\,(\,\hat{k}_z\,d_x-\hat{k}_x\,d_z\,)-\mathrm{i}\,|\boldsymbol{k}|\,\hat{k}_y\,\mathcal{H}\,(\,\hat{k}_y\,d_z-\hat{k}_z\,d_y\,)-\mathrm{i}\omega\left(\epsilon_0-\frac{\mathrm{i}\,\sigma}{\omega}\right)\mathcal{E}\,d_z=0\,.
\end{aligned} \tag{G.10}$$

The wave is transverse, hence $\boldsymbol{k}\cdot\boldsymbol{d}=0$. After some calculations, system (G.10) simplifies to:

$$\begin{aligned}(\mathrm{i}\,|\boldsymbol{k}|\,\mathcal{E}\,+\,\mathrm{i}\,\omega\,\mu_0\mathcal{H}\,)\,\widehat{\mathbf{d}}\,&=\,0\,,\\(-\,\mathrm{i}\,|\boldsymbol{k}|\,\mathcal{H}\,-\,\mathrm{i}\omega\epsilon_0\,\mathcal{E}\,)\,\widehat{\mathbf{d}}\,&=0\,.\end{aligned}$$

Dividing by i, $\widehat{\mathbf{d}}$ and $|\boldsymbol{k}|$, we obtain:

$$\begin{aligned}\mathcal{E}+\,c\mu_0\mathcal{H}\,&=0\,,\\\mathcal{H}+\,c\,\epsilon_0\mathcal{E}\,&=\,0\,,\end{aligned}$$

with $c\,=\,\dfrac{\omega}{|\mathbf{k}|}$, which gives in matrix form:

$$\begin{pmatrix}c\mu_0 & 1\\ 1 & c\,\epsilon_0\end{pmatrix}\begin{pmatrix}\mathcal{H}\\ \mathcal{E}\end{pmatrix}=0\,.$$

We assume that $\mathcal{E}$ and $\mathcal{H}$ do not vanish, which means that the above matrix has zero determinant:

$$c^2\,\epsilon_0\,\mu_0-1=0\,,$$

which gives:

$$c=\frac{1}{\sqrt{\left(\epsilon_0\,-\,\dfrac{\mathrm{i}\sigma}{\omega}\right)\,\mu_0}}\,.$$

A solution of system G.1.1 is :

$$\mathcal{H}=1,\quad \mathcal{E}\,=\,-\,c\,\mu_0\,=\,-\,\frac{\mu_0}{\mathsf{s}_{\mathrm{EM}}}\,,$$

with s_{EM} the slowness defined in equation (G.9).

G.1.2 Expansion of plane waves in Bessel functions in two dimensions

The propagation of a plane wave can be expressed using series of Bessel functions. This will be used to build the right-hand side at each mode for analytical solutions, see Section G.2. We will consider circular geometry, hence we work in polar coordinates. First, we express the plane wave solutions (G.6), using the results from the previous section:

$$\mathrm{H}^{\mathrm{pw}}\,=\,e^{\mathrm{i}\mathbf{k}\cdot\boldsymbol{X}}\,,\qquad \boldsymbol{E}^{\mathrm{pw}}\,=\,-\frac{\mu_0}{\mathsf{s}_{\mathrm{EM}}}\,e^{\mathrm{i}\mathbf{k}\cdot\boldsymbol{X}}\,\mathbf{d}\,=\,-\frac{\mu_0}{\mathsf{s}_{\mathrm{EM}}}\,\frac{1}{\mathrm{i}\,\omega\,\mathsf{s}_{\mathrm{EM}}}\,\mathbf{curl}\left(e^{\mathrm{i}\mathbf{k}\cdot\boldsymbol{X}}\right)\,. \tag{G.11}$$

Using the Jacobi-Anger and the multipole expansions given in (1.37), and (1.38), we have the following equality:

$$e^{\mathrm{i}\,\omega\,\mathsf{s}_{\mathrm{EM}}\,\hat{\mathbf{k}}\cdot\boldsymbol{X}}\;=\;\sum_{k\in\mathbb{Z}}\mathrm{i}^k\,J_k(\,\omega\,\mathsf{s}_{\mathrm{EM}}\,|\boldsymbol{X}|)\;e^{\mathrm{i}\,k(\theta-\alpha_{\mathrm{inc}})}\,.$$

By replacing the above expression in the plane wave solution (G.11), the electric and magnetic fields are expressed in polar coordinates as:

$$\begin{aligned}\boldsymbol{E}^{\mathrm{pw}}\,&=\,-\,\frac{\mu_0}{\mathrm{i}\,\omega\,\mathsf{s}_{\mathrm{EM}}^2}\,\mathbf{curl}\left(\sum_{k\in\mathbb{Z}}\mathrm{i}^k\,J_k(\omega\,\mathsf{s}_{\mathrm{EM}}\,r)\;e^{\mathrm{i}\,k(\theta-\alpha_{\mathrm{inc}})}\right)\,,\\\mathrm{H}^{\mathrm{pw}}\,&=\,\sum_{k\in\mathbb{Z}}\mathrm{i}^k\,J_k(\omega\,\mathsf{s}_{\mathrm{EM}}\,r)\;e^{\mathrm{i}\,k(\theta-\alpha_{\mathrm{inc}})}\,.\end{aligned}$$

The components in polar coordinates of the electric field are given below:

$$\begin{aligned}E_r^{\mathrm{pw}}\,&=\,-\,\frac{\mu_0}{\mathrm{i}\,\omega\,\mathsf{s}_{\mathrm{EM}}^2}\,\frac{1}{r}\,\partial_\theta\left(\sum_{k\in\mathbb{Z}}\mathrm{i}^k\,J_k(\omega\,\mathsf{s}_{\mathrm{EM}}\,r)\;e^{\mathrm{i}\,k(\theta-\alpha_{\mathrm{inc}})}\right)\,=\,-\sum_{k\in\mathbb{Z}}\frac{\mu_0\,\mathrm{i}^k\,k}{r\,\omega\,\mathsf{s}_{\mathrm{EM}}^2}\,J_k(\omega\,\mathsf{s}_{\mathrm{EM}}\,r)\;e^{\mathrm{i}\,k(\theta-\alpha_{\mathrm{inc}})}\,,\\E_\theta^{\mathrm{pw}}\,&=\,\frac{\mu_0}{\mathrm{i}\,\omega\,\mathsf{s}_{\mathrm{EM}}^2}\,\partial_r\left(\sum_{k\in\mathbb{Z}}\mathrm{i}^k\,J_k(\omega\,\mathsf{s}_{\mathrm{EM}}\,r)\;e^{\mathrm{i}\,k(\theta-\alpha_{\mathrm{inc}})}\right)\;=\,-\sum_{k\in\mathbb{Z}}\frac{\mu_0}{\mathsf{s}_{\mathrm{EM}}}\,\mathrm{i}^{k+1}\,J_k'(\omega\,\mathsf{s}_{\mathrm{EM}}\,r)\;e^{\mathrm{i}\,k(\theta-\alpha_{\mathrm{inc}})}\,.\end{aligned}$$

G.2 Construction of analytical solutions in two dimensions

In this section, we build two analytical solutions for the two-dimensional electromagnetic equations. First, we express the electromagnetic fields $\boldsymbol{E}$ and H in terms of a potential χ. For circular problems, this potential can be expressed using series of Bessel functions. We use this form of potential to build the analytical solution on a bounded circular domain, and for the scattering of a plane wave by a circular obstacle. Those solutions will be used as reference solutions to verify the HDG method developed in Section G.3.

G.2.1 Expression of the electromagnetic variables in terms of potential

First, we write the second-order formulation of Maxwell's equations (G.4) with no sources, by eliminating $\boldsymbol{E}$ and $\boldsymbol{J}$:

$$\operatorname{curl} \frac{1}{\mathrm{i}\omega\epsilon_0 + \sigma} \mathbf{curl}\, \mathrm{H} + \mathrm{i}\omega\,\mu_0\, \mathrm{H} = 0\,.$$

Using $\operatorname{curl}\mathbf{curl} = \Delta$, the above expression leads to

$$-\Delta\, \mathrm{H} - \omega^2\, \mathsf{s}_{\mathrm{EM}}^2\, \boldsymbol{H} = 0\,,$$

with s_{EM} defined in (G.9). Hence, $\boldsymbol{H}$ verifies the homogeneous Helmholtz equation:

$$\Delta\, \mathrm{H} + k^2 \mathrm{H} = 0\,,$$

with $k = \omega\, \mathsf{s}_{\mathrm{EM}}$ the wave number. Hence we have the following result:

If the electromagnetic fields $\boldsymbol{E}$ and H are solution of equation (G.4), then H is solution of

$$\operatorname{curl} \frac{1}{\mathrm{i}\omega\epsilon_0 + \sigma} \mathbf{curl}\, \mathrm{H} + \mathrm{i}\omega\,\mu_0\, \mathrm{H} = 0\,,$$

and the electric field $\boldsymbol{E}$ reads:

$$\boldsymbol{E} = \frac{1}{\mathrm{i}\,\omega \left(\epsilon_0 - \dfrac{\mathrm{i}\,\sigma}{\omega}\right)} \mathbf{curl}\, \chi\,, \tag{G.12}$$

with $\mathrm{H} = \chi$, and where the potential χ is a solution of the homogeneous Helmholtz equation:

$$\Delta\, \chi + k^2 \chi = 0\,. \tag{G.13}$$

In the following, we will study two configurations, for which H admits a particular representation has a specific expression:

a) On a disc $\mathbb{B}_{\mathfrak{a}}$ centered at the origin and of radius $\mathfrak{a}$, a generic solution is given by:

$$\chi(x) = \sum_{k\in\mathbb{Z}} a_{\bullet,k}\, \mathrm{J}_k(n\,\omega\,\mathsf{s}_{\mathrm{EM}}\, r)\; e^{\mathrm{i}\,k\,\theta}\,.$$

b) An outgoing solution on $\mathbb{R}^2 \setminus \mathbb{B}_{\mathfrak{a}}$ is given by

$$\chi(x) = \sum_{k\in\mathbb{Z}} a_{\bullet,k}\, \mathrm{H}_k^{(1)}(\,\omega\,\mathsf{s}_{\mathrm{EM}}\, r)\; e^{\mathrm{i}\,k\,\theta}\,.$$

G.2.2 Generic solution to homogeneous equation on bounded domain

Here, we consider the homogeneous two-dimensional electromagnetic equations (G.4) on a disc $\mathbb{B}_{\mathfrak{a}}$ of radius $\mathfrak{a}$. The unknowns $\boldsymbol{E}$ and H are given by equation (G.12), while the potential verifies equation (G.13), and is expressed as:

$$\chi = \sum_{k\in\mathbb{Z}} a_k\, \mathrm{J}_k(\omega\,\mathsf{s}_{\mathrm{EM}}\, r)\; e^{\mathrm{i}\,k\,\theta}\,.$$

This means that $\boldsymbol{E}$ and H are given by:

$$\begin{aligned}
\mathrm{H}(x) &= \sum_{k\in\mathbb{Z}} a_k\, \mathrm{J}_k(\,\omega\, \mathsf{s}_{\mathrm{EM}}\, r)\; e^{\mathrm{i}\,k\,\theta}\,,\\
\boldsymbol{E}_r(x) &= \sum_{k\in\mathbb{Z}} \frac{\mathrm{i}\,k}{(\mathrm{i}\,\omega\epsilon_0+\sigma)r} a_k\, \mathrm{J}_k(\omega\, \mathsf{s}_{\mathrm{EM}}\, r)\; e^{\mathrm{i}\,k\,\theta}\,,\\
\boldsymbol{E}_\theta(x) &= -\sum_{k\in\mathbb{Z}} \frac{\omega\, \mathsf{s}_{\mathrm{EM}}}{(\mathrm{i}\,\omega\,\epsilon_0\,+\,\sigma)}\; a_k\, \mathrm{J}_k'(\omega\, \mathsf{s}_{\mathrm{EM}}\, r)\; e^{\mathrm{i}\,k\,\theta}\,.
\end{aligned}$$

In order to find the value of a_k, we impose a condition on the boundary of the disc, i.e., for $r = \mathfrak{a}$. We can impose the following condition,

$$\mathrm{H} \,=\, \mathrm{H}^{\mathrm{pw}}\,, \qquad \text{or} \qquad \boldsymbol{n}\times\boldsymbol{E} \,=\, \boldsymbol{n}\times\boldsymbol{E}^{\mathrm{pw}}\,,$$

with H^{pw} and $\boldsymbol{E}^{\mathrm{pw}}$ given in G.1.2.

Condition imposed on H: We impose $\mathrm{H} = \mathrm{H}^{\mathrm{pw}}$ for $r = \mathfrak{a}$, which gives

$$\sum_{k\in\mathbb{Z}} a_k\, \mathrm{J}_k(\,\omega\, \mathsf{s}_{\mathrm{EM}}\, \mathfrak{a})\; e^{\mathrm{i}\,k\,\theta} = \sum_{k\in\mathbb{Z}} \mathrm{i}^k\, J_k(\,\omega\, \mathsf{s}_{\mathrm{EM}}\, \mathfrak{a})\; e^{\mathrm{i}\,k(\theta-\alpha_{\mathrm{inc}})}\,.$$

This means that for each mode k:

$$a_k = \mathrm{i}^k\, e^{-\mathrm{i}\,k\alpha_{\mathrm{inc}}}\,, \quad \text{for} \quad k\in\mathbb{Z}\,.$$

Condition imposed on $\boldsymbol{E}$: We impose $\boldsymbol{n}\times\boldsymbol{E} = \boldsymbol{n}\times\boldsymbol{E}^{\mathrm{pw}}$. On a disc, $\boldsymbol{n} = \mathbf{e}_r$, hence $\boldsymbol{n}\times\boldsymbol{E} = \boldsymbol{E}_\theta$. Then, the condition becomes:

$$-\sum_{k\in\mathbb{Z}} \frac{\omega\, \mathsf{s}_{\mathrm{EM}}}{(\mathrm{i}\,\omega\,\epsilon_0+\sigma)}\; a_k\, \mathrm{J}_k'(\,\omega\, \mathsf{s}_{\mathrm{EM}}\, \mathfrak{a})\; e^{\mathrm{i}\,k\,\theta} = -\sum_{k\in\mathbb{Z}} \frac{\mu_0}{\mathsf{s}_{\mathrm{EM}}}\, \mathrm{i}^{k+1}\, J_k'(\,\omega\, \mathsf{s}_{\mathrm{EM}}\, \mathfrak{a})\; e^{\mathrm{i}\,k(\theta-\alpha_{\mathrm{inc}})}\,.$$

This means that, for each mode $k\in\mathbb{Z}$:

$$a_k \,=\, \mathrm{i}^k\, e^{-\mathrm{i}\,k\alpha_{\mathrm{inc}}}\,.$$

G.2.3 Scattering of a plane wave by an impenetrable medium

We now consider a circular obstacle of radius $\mathfrak{a}$ in an infinite medium, and we study the electromagnetic equations on $\mathbb{R}^2\setminus\mathbb{B}_{\mathfrak{a}}$. The unknowns $\boldsymbol{E}$ and H are given by equation (G.12), while the potential verifies equation (G.13). Hence, the potential is expressed as:

$$\chi = \sum_{k\in\mathbb{Z}} a_k\, \mathrm{H}_k^{(1)}(\omega\, \mathsf{s}_{\mathrm{EM}}\, r)\; e^{\mathrm{i}\,k\,\theta}\,.$$

To express completely $\boldsymbol{E}$ and H, we need to impose a condition on the boundary of the obstacle that leads to determine the coefficients a_k.

Condition imposed on H: We impose $\mathrm{H} = \mathrm{H}^{\mathrm{pw}}$ for $r = \mathfrak{a}$, which gives

$$a_k = -\,\mathrm{i}^k\, \frac{\mathrm{J}_k(\omega\, \mathsf{s}_{\mathrm{EM}}\, \mathfrak{a})}{\mathrm{H}_k^{(1)}(\,\omega\, \mathsf{s}_{\mathrm{EM}}\, \mathfrak{a})} e^{-\mathrm{i}\,k\alpha_{\mathrm{inc}}}\,, \quad \text{for} \quad k\in\mathbb{Z}\,.$$

Condition imposed on $\boldsymbol{E}$: We impose $\boldsymbol{n}\times\boldsymbol{E} = \boldsymbol{n}\times\boldsymbol{E}^{\mathrm{pw}}$. On a disc, $\boldsymbol{n} = \mathbf{e}_r$, hence $\boldsymbol{n}\times\boldsymbol{E} = \boldsymbol{E}_\theta$. Then, the condition is:

$$-\sum_{k\in\mathbb{Z}} \frac{\omega \mathsf{s}_{\mathrm{EM}}}{(\mathrm{i}\omega\epsilon_0+\sigma)}\; a_k\, \mathrm{H}_k^{(1)'}(\omega\, \mathsf{s}_{\mathrm{EM}}\, r)\; e^{\mathrm{i}\,k\,\theta} = -\sum_{k\in\mathbb{Z}} \frac{\mu_0}{\mathsf{s}_{\mathrm{EM}}}\, \mathrm{i}^{k+1}\, J_k'(\omega\, \mathsf{s}_{\mathrm{EM}}\, r)\; e^{\mathrm{i}\,k(\theta-\alpha_{\mathrm{inc}})}\,.$$

This condition can be written equivalently for each mode k:

$$a_k \,=\, -\,\mathrm{i}^{k+1}\, \mu_0\, \frac{\mathrm{J}_k'(\omega\, \mathsf{s}_{\mathrm{EM}}\, \mathfrak{a})}{\mathrm{H}_k^{(1)'}(\,\omega\, \mathsf{s}_{\mathrm{EM}}\, \mathfrak{a})} e^{-\mathrm{i}\,k\alpha_{\mathrm{inc}}}\,, \quad \text{for} \quad k\in\mathbb{Z}\,.$$

We consider the electromagnetic equations on the domain $\mathbb{R}^2\setminus\mathbb{B}_{\mathfrak{a}}$, with $a = 10\mathrm{m}$, $\mu_0 = 12.566\,10^{-7}$ N/A^2, $\epsilon_0 = 8.8595\,10^{-12}$ F.m-1, and $\sigma = 10^{-9}$ S.m^{-1} at frequency $f = 150\mathrm{kHz}$. In the construction of the analytical solution, the domain is considered as infinite, but the representation of the solution is plotted only on an annulus of interior radius equal to 1m and exterior radius equal to 10m. We present the result in Figure G.1.

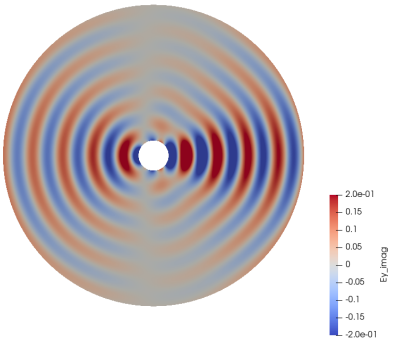

Figure G.1: Scattering of an EM plane wave on an impenetrable solid obstacle. Imaginary part of the electric field E_y.

G.3 HDG method in two dimensions

In this section, we consider two-dimensional domain in the (x, y) plane. We work in the transverse electric setting, which means that we consider $\boldsymbol{E} = (E_x, E_y)$, $\boldsymbol{J} = (J_x, J_y)$ and $\mathrm{H} = H_z$. We base our development on the HDG method described in [85]. However, in this paper, the authors consider the transverse magnetic configuration, which justifies that we need to detail the development.

G.3.1 Formulation of the HDG method

We consider a two-dimensional domain $\mathcal{D}$, and we will use the notations introduced in Section 3.1.1:

$$\begin{aligned} &L^2(\mathcal{D}), \text{ the space of square-integrable functions on the domain } \mathcal{D}\,,\\ &V^p(\mathcal{D}), \text{ the set of polynomials of degree at most } p \text{ on } \mathcal{D}\,,\\ &\boldsymbol{V}^p(\mathcal{D}) = (V^p(\mathcal{D}))^{\mathrm{d}}\,, \end{aligned} \tag{G.14}$$

with d the dimension of the domain $\mathcal{D}$. We consider a triangulation $\mathcal{T}_h$ of the domain $\mathcal{D}$, where K denotes an element of the mesh, F a face of the element K, and $\boldsymbol{n}$ the outgoing unit normal vector to F. We consider here meshes composed of triangles. Associated to triangulation $\mathcal{T}_h$, we introduce the following spaces:

$$\begin{aligned} V_h^p &= \{v \in L^2(\mathcal{D}) : v|_K \in V^p(K)\,, \forall K \in \mathcal{T}_h\}\,,\\ \boldsymbol{V}_h^p &= \{\boldsymbol{v} \in (L^2(\mathcal{D}))^{\mathrm{d}} : \boldsymbol{v}|_K \in V^p(K)\,, \forall K \in \mathcal{T}_h\}\,,\\ M_h &= \{\xi \in L^2(\mathcal{F}_h) : \xi|_F \in V^p(F),\,, \forall K \in \mathcal{F}_h\}\,,\\ \boldsymbol{M}_h &= \{\eta \in (L^2(\mathcal{F}_h))^2 : \eta|_F \in (V^p(F))^{\mathrm{d}}\,, \forall K \in \mathcal{F}_h\}\,. \end{aligned} \tag{G.15}$$

First, we consider equations (G.4) on an element K of $\mathcal{T}_h$. We multiply the equation by test functions $(\tilde{e}, \tilde{\boldsymbol{h}}, \tilde{\boldsymbol{j}}) \in (V^p(K) \times \boldsymbol{V}^p(K) \times \boldsymbol{V}^p(K))$ and integrate on the element K:

$$\begin{aligned} &\int_K \operatorname{curl} \boldsymbol{E}\, \tilde{e} + \int_K \mathrm{i}\,\omega\,\mu_0\,\mathrm{H}\,\tilde{e} \;= 0\,,\\ &\int_K \mathbf{curl}\,\mathrm{H}\cdot\tilde{\boldsymbol{h}} - \int_K \mathrm{i}\,\omega\,\epsilon_0\,\boldsymbol{E}\cdot\tilde{\boldsymbol{h}} - \int_K \boldsymbol{J}\cdot\tilde{\boldsymbol{h}} = \int_K \mathbf{f}_C\cdot\tilde{\boldsymbol{h}}\,,\\ &\int_K \boldsymbol{J}\cdot\tilde{\boldsymbol{j}} - \int_K \sigma\,\boldsymbol{E}\cdot\tilde{\boldsymbol{j}} \;= 0\,. \end{aligned}$$

By integrating by parts, we obtain

$$\begin{aligned} &\int_K \boldsymbol{E}\cdot\mathbf{curl}\,\tilde{e} - \int_{\partial K} (\boldsymbol{n}\times\hat{\boldsymbol{E}})\,\tilde{e} + \int_K \mathrm{i}\,\omega\,\mu_0\,\mathrm{H}\,\tilde{e} \;= 0\,,\\ &\int_K \mathrm{H}\operatorname{curl}\tilde{\boldsymbol{h}} + \int_{\partial K} (\boldsymbol{n}\times\tilde{\boldsymbol{h}})\,\hat{\mathrm{H}} - \int_K \mathrm{i}\,\omega\,\epsilon_0\,\boldsymbol{E}\cdot\tilde{\boldsymbol{h}} - \int_K \boldsymbol{J}\cdot\tilde{\boldsymbol{h}} = \int_K \mathbf{f}_C\cdot\tilde{\boldsymbol{h}}\,,\\ &\int_K \boldsymbol{J}\,\tilde{\boldsymbol{j}} - \int_K \sigma\,\boldsymbol{E}\cdot\tilde{\boldsymbol{j}} = 0\,. \end{aligned} \tag{G.16}$$

Introduction of the trace variables: The exact solution ($\boldsymbol{E}$, H, $\boldsymbol{J}$) is approximated by ($\boldsymbol{E}_h$, H_h, $\boldsymbol{J}_h$) $\in$ ($\boldsymbol{V}_h^p \times V_h^p \times \boldsymbol{V}_h^p \times V_h^p$). The traces on ∂K are approximated by numerical traces ($\hat{\boldsymbol{E}}_h, \hat{\boldsymbol{H}}_h$), that we choose as follows:

$$\hat{\mathrm{H}}_h = \lambda_3\,, \qquad \hat{\boldsymbol{E}}_h \,=\, \boldsymbol{E}_h - \gamma_5\,(\mathrm{H}_h - \lambda_3)\times \boldsymbol{n}\,, \tag{G.17}$$

with γ_5 a stabilization parameter.[1] We replace the traces in equation (G.16) by their expressions (G.17), and integrate by parts the first equation of (G.16), to obtain the following local problem.

$$\begin{aligned}
&\int_K \operatorname{curl}\boldsymbol{E}_h\,\tilde{e} + \int_{\partial K}\gamma_5\,(\mathrm{H}_h-\lambda_3)\,\tilde{e} + \int_K \mathrm{i}\omega\mu_0\mathrm{H}_h\,\tilde{e} \,=0\,,\\
&\int_K \mathrm{H}_h \operatorname{curl}\tilde{\boldsymbol{h}} + \int_{\partial K}(\boldsymbol{n}\times\tilde{\boldsymbol{h}})\,\lambda_3 - \int_K \mathrm{i}\omega\epsilon_0\boldsymbol{E}_h\cdot\tilde{\boldsymbol{h}} - \int_K \boldsymbol{J}_h\cdot\tilde{\boldsymbol{h}} \,=\, \int_K \mathbf{f}_C\,\cdot\,\tilde{\boldsymbol{h}}\,,\\
&\int_K \boldsymbol{J}_h\cdot\tilde{\boldsymbol{j}} - \int_K \sigma\boldsymbol{E}_h\cdot\tilde{\boldsymbol{j}} = 0\,.
\end{aligned} \tag{G.18}$$

To obtain the HDG method formulation, we need to associate the above local problem on the elements with a transmission condition between the elements. We use the physical condition given in (G.2). The transmission condition is, using a test-function $\nu \in M_h$:

$$\sum_{F\in\mathcal{F}_h}\int_F [\![\boldsymbol{n}\times\hat{\boldsymbol{E}}_h]\!]\,\nu = \sum_{F\in\mathcal{F}_{\mathrm{ext}}}\int_F h_{\mathrm{inc}}\,\nu\,,$$

or equivalently

$$\sum_{K\in\mathcal{T}_h}\int_{\partial K}(\boldsymbol{n}\times\hat{\boldsymbol{E}}_h)\,\nu = \sum_{F\in\mathcal{F}_{\mathrm{ext}}}\int_F h_{\mathrm{inc}}\,\nu\,. \tag{G.19}$$

G.3.2 Discretization of the HDG method

In this section, we detail the two-dimensional discretization of the HDG method in the (x, y) plane. In the formulation, the test functions are decomposed with the basis functions of V_p as φ_i^K for $\tilde{e}, \tilde{\boldsymbol{h}}, \tilde{\boldsymbol{j}}$ and ψ_j^F for ν. The local solutions are expressed along x and y directions:

$$\boldsymbol{E}_h^K \,=\begin{pmatrix} E_x^K \\ E_y^K\end{pmatrix}, \qquad \boldsymbol{J}_h^K \,=\begin{pmatrix} J_x^K \\ J_y^K\end{pmatrix}.$$

They are decomposed as:

$$E_l^K = \sum_{j=1}^{d_i^K}\underline{E}_{l,j}^K\varphi_j^K\,, \quad H^K = \sum_{j=1}^{d_i^K}\underline{H}_j^K\varphi_j^K\,, \quad \text{and } J_l^K = \sum_{j=1}^{d_i^K}\underline{J}_{l,j}^K\varphi_j^K\,, \tag{G.20}$$

where d_i^K denotes the number of degrees of freedom of an element, and with $l = x, y$. The local Lagrange unknowns are also decomposed as:

$$\lambda_3^F \,=\sum_{j=1}^{d_i^F}\underline{\lambda_3}_j^F\psi_j^F\,, \tag{G.21}$$

where d_i^F denotes the number of degrees of freedom of an edge. In (G.20), each component is considered as a vector of the form $\underline{E}_l^K = (\underline{E}_{l,1}^K, \ldots, \underline{E}_{,d_i^K}^K)^T$ for $l = x, y$. We define the two unknown vectors $\underline{W}^K$ and $\underline{\Lambda}^K$ respectively of size $5\,d_i^K$ and $3\,d_i^F$ as:

$$\underline{W}^K = (\underline{\mathrm{E}}_x^K\,,\,\underline{\mathrm{E}}_y^K\,,\,\underline{\mathrm{H}}^K,\,\underline{J}_x^K\,,\,\underline{J}_y^K)^T\,, \quad \text{and} \quad \underline{\Lambda}^K = (\underline{\lambda}_3^{\beta(K,1)}, \underline{\lambda}_3^{\beta(K,2)}, \underline{\lambda}_3^{\beta(K,3)})^T\,, \tag{G.22}$$

where $\beta(K, f)$ is the global index of the f-th face of the element K. Moreover, we also recall the following elementary matrices (*cf.* (3.18)): $\mathbb{M}^K$, $\mathbb{D}_v^K$, $\mathbb{E}^F$, $\mathbb{J}_v^F$ of size $d_i^K \times d_i^K$, $\mathbb{F}^F$, $\mathbb{Q}_v^F$ of size $d_i^K \times d_i^F$, and $\mathbb{G}^F$, $\mathbb{H}_v^F$ of size $d_i^F \times d_i^F$:

$$\begin{aligned}
&\mathbb{M}_{ij}^K = \int_K \varphi_i^K\varphi_j^K dX\,, \qquad \mathbb{D}_{vij}^K = \int_K \varphi_j^K\frac{\partial\varphi_i^K}{\partial v}dX\,, \quad \mathbb{E}_{ij}^F = \int_F \varphi_i^K\varphi_j^K dS\,, \qquad \mathbb{J}_{vij}^F = \int_F \varphi_i^K\varphi_j^K n_v\,dS\,,\\
&\mathbb{F}_{ij}^F = \int_F \psi_j^F\varphi_i^K dS\,, \qquad \mathbb{Q}_{vij}^F = \int_F \psi_j^F\varphi_i^K n_v\,dS\,, \quad \mathbb{G}_{ij}^F = \int_F \psi_j^F\psi_j^F dS\,, \qquad \mathbb{H}_{vij}^F = \int_F \psi_i^F\psi_j^F n_v\,dS\,,
\end{aligned} \tag{G.23}$$

[1] Here, we number the stabilization parameter γ_5 after the poroelastic parameters.

with $v = x, y$. Finally, we define the elementary source vectors of size d_i^K

$$\left(\mathbb{C}_{1x}^K\right)_i = \int_K f_{C,x}^K \varphi_i^K\,, \qquad \left(\mathbb{C}_{1y}^K\right)_i = \int_K f_{C,y}^K \varphi_i^K\,.$$

Local problem The discretization of the local problem (G.18) gives:

$$\begin{aligned}
&\int_K \left(\frac{\partial E_y^K}{\partial x} - \frac{\partial E_x^K}{\partial y}\right) \varphi_i^K - \int_{\partial K} \gamma_5 \left(H_h^K - \lambda_3\right) \varphi_i^K + \int_K \mathrm{i}\,\omega\,\mu_0\, H_h^K\, \varphi_i^K = 0\,,\\
&-\int_K H_h^K \frac{\partial \varphi_i^K}{\partial y} - \int_{\partial K} \lambda_3\, n_y \varphi_i^K - \int_K \mathrm{i}\,\omega\,\epsilon_0\, E_x^K\, \varphi_i^K - \int_K J_x^K\, \varphi_i^K = \int_K f_{C,x}^K\, \varphi_i^K\,,\\
&\int_K H_h^K \frac{\partial \varphi_i^K}{\partial x} + \int_{\partial K} \lambda_3\, n_x \varphi_i^K - \int_K \mathrm{i}\,\omega\,\epsilon_0\, E_y^K\, \varphi_i^K - \int_K J_y^K\, \varphi_i^K = \int_K f_{C,y}^K\, \varphi_i^K\,,\\
&\int_K J_x^K\, \varphi_i^K - \int_K \sigma E_x^K\, \varphi_i^K = 0\,,\\
&\int_K J_y^K\, \varphi_i^K - \int_K \sigma E_y^K\, \varphi_i^K = 0\,.
\end{aligned}$$

We express the above system in terms of local unknowns and elementary matrices defined respectively in (G.22) and (G.23):

$$\begin{aligned}
&(\mathbb{D}_x^K)^T\, \underline{E}_y^K - (\mathbb{D}_y^K)^T\, \underline{E}_x^K - \sum_{f=1}^3 \mathbb{E}^{\beta(K,f)} K\, \gamma_5\, \underline{\mathrm{H}}^K + \sum_{f=1}^3 \mathbb{F}^{\beta(K,f)} \gamma_5\, \underline{\lambda}_3 + \mathbb{M}^K \mathrm{i}\,\omega\,\mu_0\, \underline{\mathrm{H}}^K = 0\,,\\
&-\mathbb{D}_y^K\, \underline{\mathrm{H}}^K - \sum_{f=1}^3 \mathbb{Q}_y^{\beta(K,f-)}\, \underline{\lambda}_3 - \mathbb{M}^K\, \mathrm{i}\,\omega\,\epsilon_0\, \underline{E}_x^K - \mathbb{M}^K\, \underline{J}_x^K = \mathbb{C}_x^K\,,\\
&\mathbb{D}_x^K\, \underline{\mathrm{H}}^K + \sum_{f=1}^3 \mathbb{Q}_x^{\beta(K,f)}\, \underline{\lambda}_3 - \mathbb{M}^K\, \mathrm{i}\,\omega\,\epsilon_0\, \underline{E}_y^K - \mathbb{M}^K\, \underline{J}_y^K = \mathbb{C}_y^K\,,\\
&\mathbb{M}^K \underline{J}_x^K - \mathbb{M}^K\, \sigma\, \underline{E}_x^K = 0\,,\\
&\mathbb{M}^K \underline{J}_y^K - \mathbb{M}^K\, \sigma\, \underline{E}_y^K = 0\,.
\end{aligned}$$

The above equations are written as the following system:

$$\mathbb{A}\, \underline{W}^K + \mathbb{B}\, \underline{\Lambda}^K = \mathbb{C}_{\text{source}}^K\,,$$

where $\underline{W}^K$ and $\underline{\Lambda}^K$ have been defined in (G.22). The matrices $\mathbb{A}^K$ and $\mathbb{B}^K$ are:

$$\mathbb{A}^K = \begin{pmatrix}
-\mathbb{M}^K \mathrm{i}\omega\epsilon_0 & 0 & -\mathbb{D}_y^K & -\mathbb{M}^K & 0\\
0 & -\mathbb{M}^K \mathrm{i}\omega\epsilon_0 & \mathbb{D}_x^K & 0 & -\mathbb{M}^K\\
-(\mathbb{D}_y^K)^T & (\mathbb{D}_x^K)^T & \mathbb{M}^K \mathrm{i}\,\omega\,\mu_0 - \displaystyle\sum_{f=1}^3 \gamma_5\, \mathbb{E}^{\beta(K,f)} & 0 & 0\\
-\mathbb{M}^K\, \sigma & 0 & 0 & \mathbb{M}^K & 0\\
0 & -\mathbb{M}^K\, \sigma & 0 & 0 & \mathbb{M}^K
\end{pmatrix}, \tag{G.24}$$

and

$$\mathbb{B}^K = \begin{pmatrix}
-\mathbb{Q}_y^{\beta(K,1)} & -\mathbb{Q}_y^{\beta(K,2)} & -\mathbb{Q}_y^{\beta(K,3)}\\
\mathbb{Q}_x^{\beta(K,1)} & \mathbb{Q}_x^{\beta(K,2)} & \mathbb{Q}_x^{\beta(K,3)}\\
\gamma_5\, \mathbb{F}^{\beta(K,1)} & \gamma_5\, \mathbb{F}^{\beta(K,2)} & \gamma_5\, \mathbb{F}^{\beta(K,3)}\\
0 & 0 & 0\\
0 & 0 & 0
\end{pmatrix}. \tag{G.25}$$

Transmission condition Now, we present the discretization of the transmission condition (G.19). We consider a face $F = \partial K \cap \partial K'$ in the interior of the mesh. On F, we can express the transmission condition as:

$$\int_F (\boldsymbol{n} \times \boldsymbol{E}_h)\, \nu - \int_F \gamma_5\, (\mathrm{H}_h - \lambda_3)\, \nu \,=\, 0\,.$$

We discretize the above equation and we replace the test function ν by $\psi_i^{\beta(K,f)}$, to give:

$$\int_F (n_x \boldsymbol{E}_y - n_y \boldsymbol{E}_x)\, \psi_i^{\beta(K,f)} - \int_F \gamma_5\, \left(H_h^K - \lambda_3\right)\, \psi_i^{\beta(K,f)} \,=\, 0\,,$$

and we express this equation in terms of local unknowns and elementary matrices defined respectively in (G.22) and (G.23):

$$(\mathbb{Q}_x^F)^T\, \underline{E}_y^K \,-\, (\mathbb{Q}_y^F)^T\, \underline{E}_x^K \,-\, (\mathbb{F}^F)^T \gamma_5\, \underline{\mathrm{H}}^K \,+\, \mathbb{G}^F \gamma_5 \underline{\lambda}_3 \,=\, 0\,.$$

This equation is summed for the all the faces of the mesh to obtain a global system, with $\underline{W}^K$ and $\underline{\Lambda}^K$ defined in (G.22):

$$\sum_{K \in \mathcal{T}_h} (\mathcal{A}_{HDG}^K)^T \left(\mathbb{P}^K \underline{W}^K + \mathbb{T}^K \mathcal{A}_{HDG}^K \underline{\Lambda}\right) = \mathbb{S}_{\mathrm{inc}}\,,$$

and with the elementary matrices:

$$\mathbb{P}^K = \begin{pmatrix} -(\mathbb{Q}_y^{\beta(K,1)})^T & (\mathbb{Q}_x^{\beta(K,1)})^T & -\gamma_5\, (\mathbb{F}^{\beta(K,1)})^T \\ -(\mathbb{Q}_y^{\beta(K,2)})^T & (\mathbb{Q}_x^{\beta(K,2)})^T & -\gamma_5\, (\mathbb{F}^{\beta(K,2)})^T \\ -(\mathbb{Q}_y^{\beta(K,3)})^T & (\mathbb{Q}_x^{\beta(K,3)})^T & -\gamma_5\, (\mathbb{F}^{\beta(K,3)})^T \end{pmatrix} \quad \text{and} \quad \mathbb{T}^K = \begin{pmatrix} \gamma_5\, \mathbb{G}^{\beta(K,1)} & 0 & 0 \\ 0 & \gamma_5\, \mathbb{G}^{\beta(K,2)} & 0 \\ 0 & 0 & \gamma_5\, \mathbb{G}^{\beta(K,3)} \end{pmatrix}. \tag{G.26}$$

G.3.3 Boundary conditions for a bounded domain

On the boundary of a bounded domain, we can impose two kinds of boundary conditions:

$$\boldsymbol{n} \times \boldsymbol{E} = \boldsymbol{n} \times \mathbf{e}^{\mathrm{inc}}\,, \quad \text{or} \quad \mathrm{H} = h^{\mathrm{inc}}\,,$$

where $\mathbf{e}^{\mathrm{inc}}$ and h^{inc} are incident fields. In the first case, the matrices $\mathbb{P}^K$ and $\mathbb{T}^K$ in the transmission condition on the boundary faces are not modified. However, when we impose a condition on the magnetic field, we impose directly

$$\lambda_3 \,=\, h^{\mathrm{inc}}\,,$$

on the boundaries of the mesh. In this case, $\mathbb{P}^K$ and $\mathbb{T}^K$ are modified. Let us consider an element K whose first face is on the boundary of the mesh. Then, the matrices $\mathbb{P}^K$ and $\mathbb{T}^K$ are expressed as follows:

$$\mathbb{P}^K = \begin{pmatrix} 0 & 0 & 0 \\ -(\mathbb{Q}_y^{\beta(K,2)})^T & (\mathbb{Q}_x^{\beta(K,2)})^T & -\gamma_5\, (\mathbb{F}^{\beta(K,2)})^T \\ -(\mathbb{Q}_y^{\beta(K,3)})^T & (\mathbb{Q}_x^{\beta(K,3)})^T & -\gamma_5\, (\mathbb{F}^{\beta(K,3)})^T \end{pmatrix} \quad \text{and} \quad \mathbb{T}^K = \begin{pmatrix} \mathbb{I} & 0 & 0 \\ 0 & \gamma_5\, \mathbb{G}^{\beta(K,2)} & 0 \\ 0 & 0 & \gamma_5\, \mathbb{G}^{\beta(K,3)} \end{pmatrix}. \tag{G.27}$$

G.4 HDG method in three dimensions

In this section, we apply the HDG method to the three-dimensional electromagnetic equations (G.3). We consider the following unknowns: $\boldsymbol{E} = (E_x, E_y, E_z)$, $\boldsymbol{J} = (J_x, J_y, J_z)$ and $\boldsymbol{H} = (H_x, H_y, H_z)$. We base our development on the HDG methods described in [87, 102].

G.4.1 Formulation of the HDG method

We consider a triangulation $\mathcal{T}_h$ of a three-dimensional domain $\mathcal{D}$, and we will use the notations given in (G.14) and (G.15). We recall that K denotes an element of the triangulation $\mathcal{T}_h$, F a face of the element K, and $\boldsymbol{n}$ the unit normal vector to F. We consider equations (G.3) on an element K of $\mathcal{T}_h$, and multiply the equation by test functions $(\tilde{\boldsymbol{e}}, \tilde{\boldsymbol{h}}, \tilde{\boldsymbol{j}}) \in (\boldsymbol{V}^p(K) \times \boldsymbol{V}^p(K) \times \boldsymbol{V}^p(K))$ and integrate on the element K:

$$\begin{aligned}
&\int_K \mathbf{curl}\, \boldsymbol{E} \,\cdot\, \tilde{\boldsymbol{e}} + \int_K \mathrm{i}\, \omega\, \mu_0\, \boldsymbol{H} \,\cdot\, \tilde{\boldsymbol{e}} \,=\, 0\,, \\
&\int_K \mathbf{curl}\, \boldsymbol{H} \cdot \tilde{\boldsymbol{h}} \,-\, \int_K \mathrm{i}\, \omega\, \epsilon_0\, \boldsymbol{E} \cdot \tilde{\boldsymbol{h}} \,-\, \int_K \boldsymbol{J} \cdot \tilde{\boldsymbol{h}} \,=\, \int_K \mathbf{f}_C \,\cdot\, \tilde{\boldsymbol{h}}\,, \\
&\int_K \boldsymbol{J} \cdot \tilde{\boldsymbol{j}} - \int_K \sigma\, \boldsymbol{E} \cdot \tilde{\boldsymbol{j}} \,=\, 0\,,
\end{aligned}$$

and we integrate by parts the above equations to obtain:

$$\begin{aligned}
&\int_K \boldsymbol{E}_h \cdot \mathbf{curl}\, \tilde{\boldsymbol{e}} - \int_{\partial K} \hat{\boldsymbol{E}} \cdot (\boldsymbol{n} \times \tilde{\boldsymbol{e}}) + \int_K \mathrm{i}\,\omega\,\mu_0\, \boldsymbol{H}_h \cdot \tilde{\boldsymbol{e}} = 0\,,\\
&\int_K \boldsymbol{H}_h \cdot \mathbf{curl}\, \tilde{\boldsymbol{h}} - \int_{\partial K} \hat{\boldsymbol{H}} \cdot (\boldsymbol{n} \times \tilde{\boldsymbol{h}}) - \int_K \mathrm{i}\,\omega\,\epsilon_0\, \boldsymbol{E}_h \cdot \tilde{\boldsymbol{h}} - \int_K \boldsymbol{J} \cdot \tilde{\boldsymbol{h}} = \int_K \mathbf{f}_C \cdot \tilde{\boldsymbol{h}}\,,\\
&\int_K \boldsymbol{J} \cdot \tilde{\boldsymbol{j}} - \int_K \sigma\, \boldsymbol{E} \cdot \tilde{\boldsymbol{j}} = 0\,.
\end{aligned} \tag{G.28}$$

Introduction of the trace variables: The numerical traces $\hat{\boldsymbol{H}}_h^t$ and $\hat{\boldsymbol{E}}_h$ are defined as:

$$\hat{\boldsymbol{H}}_h^t = \boldsymbol{\lambda}_3\,, \qquad \hat{\boldsymbol{E}}_h = \boldsymbol{E}_h - \gamma_5 \left(\boldsymbol{H}_h^t - \boldsymbol{\lambda}_3\right) \times \boldsymbol{n}\,,$$

with $\boldsymbol{H}_h^t = \boldsymbol{n} \times \boldsymbol{H}_h$ the tangential component of $\boldsymbol{H}_h$.

Remark G.2. We choose to stabilize only the tangential component of the magnetic field $\boldsymbol{H}$. This is similar to what is done in [87, 102]. In this way, the second term of equation (G.28) is:

$$-\int_{\partial K} \hat{\boldsymbol{E}} \cdot (\boldsymbol{n} \times \tilde{\boldsymbol{e}}) = -\int_{\partial K} \boldsymbol{E}_h \cdot (\boldsymbol{n} \times \tilde{\boldsymbol{e}}) + \int_{\partial K} \left(\gamma_5 \left(\boldsymbol{H}_h^t - \boldsymbol{\lambda}_3\right) \times \boldsymbol{n}\right) \cdot (\boldsymbol{n} \times \tilde{\boldsymbol{e}})\,.$$

We also have:

$$\left(\left(\boldsymbol{H}_h^t - \boldsymbol{\lambda}_3\right) \times \boldsymbol{n}\right) \cdot (\boldsymbol{n} \times \tilde{\boldsymbol{e}}) = \left(\left(\left(\boldsymbol{H}_h^t - \boldsymbol{\lambda}_3\right) \times \boldsymbol{n}\right) \times \boldsymbol{n}\right) \cdot \tilde{\boldsymbol{e}} = \left(\boldsymbol{H}_h^t - \boldsymbol{\lambda}_3\right) \cdot \tilde{\boldsymbol{e}} - \left(\left(\left(\boldsymbol{H}_h^t - \boldsymbol{\lambda}_3\right) \cdot \boldsymbol{n}\right) \boldsymbol{n}\right) \cdot \tilde{\boldsymbol{e}} = \left(\boldsymbol{H}_h^t - \boldsymbol{\lambda}_3\right) \cdot \tilde{\boldsymbol{e}}\,,$$

because $\boldsymbol{H}_h^t$ and $\boldsymbol{\lambda}_3$ are tangential components, which means that $\boldsymbol{H}_h^t \cdot \boldsymbol{n} = 0$ and $\boldsymbol{\lambda}_3 \cdot \boldsymbol{n} = 0$.

We replace in (G.28) the numerical traces $\hat{\boldsymbol{H}}$ and $\hat{\boldsymbol{E}}$ by their expressions (G.17), and we obtain:

$$\begin{aligned}
&\int_K \boldsymbol{E}_h \cdot \mathbf{curl}\, \tilde{\boldsymbol{e}} - \int_{\partial K} \boldsymbol{E}_h \cdot (\boldsymbol{n} \times \tilde{\boldsymbol{e}}) - \int_{\partial K} \gamma_5 \left(\boldsymbol{H}_h^t - \boldsymbol{\lambda}_3\right) \cdot \tilde{\boldsymbol{e}} + \int_K \mathrm{i}\,\omega\,\mu_0\, \boldsymbol{H}_h \cdot \tilde{\boldsymbol{e}} = 0\,,\\
&\int_K \boldsymbol{H}_h \cdot \mathbf{curl}\, \tilde{\boldsymbol{h}} - \int_{\partial K} \boldsymbol{\lambda}_3 \cdot (\boldsymbol{n} \times \tilde{\boldsymbol{h}}) - \int_K \mathrm{i}\,\omega\,\epsilon_0\, \boldsymbol{E}_h \cdot \tilde{\boldsymbol{h}} - \int_K \boldsymbol{J} \cdot \tilde{\boldsymbol{h}} = \int_K \mathbf{f}_C \cdot \tilde{\boldsymbol{h}}\,,\\
&\int_K \boldsymbol{J} \cdot \tilde{\boldsymbol{j}} - \int_K \sigma\, \boldsymbol{E} \cdot \tilde{\boldsymbol{j}} = 0\,.
\end{aligned}$$

Finally, after an integration by parts of the first equation, we obtain the following local problem:

$$\begin{aligned}
&\int_K \mathbf{curl} \boldsymbol{E}_h \cdot \tilde{\boldsymbol{e}} - \int_{\partial K} \gamma_5 \left(\boldsymbol{H}_h^t - \boldsymbol{\lambda}_3\right) \cdot \tilde{\boldsymbol{e}} + \int_K \mathrm{i}\,\omega\,\mu_0\, \boldsymbol{H}_h \cdot \tilde{\boldsymbol{e}} = 0\,,\\
&\int_K \boldsymbol{H}_h \cdot \mathbf{curl}\, \tilde{\boldsymbol{h}} - \int_{\partial K} \boldsymbol{\lambda}_3 \cdot (\boldsymbol{n} \times \tilde{\boldsymbol{h}}) - \int_K \mathrm{i}\,\omega\,\epsilon_0\, \boldsymbol{E}_h \cdot \tilde{\boldsymbol{h}} - \int_K \boldsymbol{J} \cdot \tilde{\boldsymbol{h}} = \int_K \mathbf{f}_C \cdot \tilde{\boldsymbol{h}}\,,\\
&\int_K \boldsymbol{J} \cdot \tilde{\boldsymbol{j}} - \int_K \sigma\, \boldsymbol{E} \cdot \tilde{\boldsymbol{j}} = 0\,.
\end{aligned}$$

As for the two-dimensional problem, we add a transmission condition between the elements to the local problem. We hence impose the physical condition given in (G.1). Using a test-function $\boldsymbol{\nu} \in \boldsymbol{M}_h$, the transmission condition is:

$$\sum_{F \in \mathcal{F}_h} \int_F [\![\boldsymbol{n} \times \hat{\boldsymbol{E}}_h]\!]\, \nu = \sum_{F \in \mathcal{F}_{\mathrm{ext}}} \int_F \boldsymbol{h}_{\mathrm{inc}} \cdot \boldsymbol{\nu}\,,$$

where $\boldsymbol{h}_{\mathrm{inc}}$ is an incident magnetic field. This can be written equivalently

$$\sum_{K \in \mathcal{T}_h} \int_{\partial K} (\boldsymbol{n} \times \hat{\boldsymbol{E}}_h)\, \boldsymbol{\nu} = \sum_{F \in \mathcal{F}_{\mathrm{ext}}} \int_F \boldsymbol{h}_{\mathrm{inc}} \cdot \boldsymbol{\nu}\,. \tag{G.29}$$

G.4.2 Discretization of the HDG method

In the following, we detail the three-dimensional discretization of the HDG method. In the formulation, the test functions are decomposed in the basis functions of V_p as φ_i^K for $\tilde{\boldsymbol{e}}, \tilde{\boldsymbol{h}}, \tilde{\boldsymbol{j}}$ and ψ_j^F for ν. The local solutions are expressed

along x, y and z directions:

$$\boldsymbol{E}_h^K = \begin{pmatrix} E_x^K \\ E_y^K \\ E_z^K \end{pmatrix}, \qquad \boldsymbol{E}_h^K = \begin{pmatrix} H_x^K \\ H_y^K \\ H_z^K \end{pmatrix}, \qquad \boldsymbol{J}_h^K = \begin{pmatrix} J_x^K \\ J_y^K \\ J_z^K \end{pmatrix}.$$

They are decomposed as:

$$E_l^K = \sum_{j=1}^{d_i^K} \underline{E}_{l,j}^K \varphi_j^K, \quad H_l^K = \sum_{j=1}^{d_i^K} \underline{H}_{l,j}^K \varphi_j^K, \quad \text{and } J_l^K = \sum_{j=1}^{d_i^K} \underline{J}_{l,j}^K \varphi_j^K, \tag{G.30}$$

where d_i^K denotes the number of degrees of freedom of an element, and with $l = x, y, z$. The local Lagrange unknowns are also decomposed as:

$$\lambda_{3,l}^F = \sum_{j=1}^{d_i^F} \underline{\lambda_3}_{l,j}^F \psi_j^F, \tag{G.31}$$

where d_i^F denotes the number of degrees of freedom of an edge. In (G.30), each component is considered as a vector of the form $\underline{E}_l^K = (\underline{E}_{l,1}^K, \ldots, \underline{E}_{,d_i^K}^K)^T$ for $l = x, y, z$. We define the two unknown vectors $\underline{W}^K$ and $\underline{\Lambda}^K$ respectively of size $9\, d_i^K$ and $12\, d_i^F$ as:

$$\underline{W}^K = (\underline{\mathrm{E}}_x^K, \underline{\mathrm{E}}_y^K, \underline{\mathrm{E}}_z^K, \underline{\mathrm{H}}_x^K, \underline{\mathrm{H}}_y^K, \underline{\mathrm{H}}_z^K, \underline{J}_x^K, \underline{J}_y^K, \underline{J}_z^K)^T,$$

and

$$\underline{\Lambda}^K = (\underline{\lambda}_{3x}^{\beta(K,1)}, \underline{\lambda}_{3x}^{\beta(K,2)}, \underline{\lambda}_{3x}^{\beta(K,3)}, \underline{\lambda}_{3x}^{\beta(K,4)}, \underline{\lambda}_{3x}^{\beta(K,1)}, \underline{\lambda}_{3y}^{\beta(K,2)}, \underline{\lambda}_{3y}^{\beta(K,3)}, \underline{\lambda}_{3y}^{\beta(K,4)}, \underline{\lambda}_{3z}^{\beta(K,1)}, \underline{\lambda}_{3z}^{\beta(K,2)}, \underline{\lambda}_{3z}^{\beta(K,3)}, \underline{\lambda}_{3z}^{\beta(K,4)})^T,$$

where $\beta(K, f)$ is the global index of the f-th face of the element K. Moreover, we also recall the following elementary matrices (*cf.* (3.18)): $\mathbb{M}^K$, $\mathbb{D}_v^K$, $\mathbb{E}^F$, $\mathbb{J}_v^F$ of size $d_i^K \times d_i^K$, $\mathbb{F}^F$, $\mathbb{Q}_v^F$ of size $d_i^K \times d_i^F$, and $\mathbb{G}^F$, $\mathbb{H}_v^F$ of size $d_i^F \times d_i^F$:

$$\begin{aligned}
&\mathbb{M}_{ij}^K = \int_K \varphi_i^K \varphi_j^K dX, && \mathbb{D}_{vij}^K = \int_K \varphi_j^K \frac{\partial \varphi_i^K}{\partial v} dX, \quad \mathbb{E}_{ij}^F = \int_F \varphi_i^K \varphi_j^K dS, && \mathbb{J}_{vij}^F = \int_F \varphi_i^K \varphi_j^K n_v \, dS, \\
&\mathbb{F}_{ij}^F = \int_F \psi_j^F \varphi_i^K dS, && \mathbb{Q}_{vij}^F = \int_F \psi_j^F \varphi_i^K n_v \, dS, \quad \mathbb{G}_{ij}^F = \int_F \psi_j^F \psi_j^F dS, && \mathbb{H}_{vij}^F = \int_F \psi_i^F \psi_j^F n_v \, dS,
\end{aligned} \tag{G.32}$$

with $v = x, y, z$. Finally, we define the elementary source vectors of size d_i^K

$$\left(\mathbb{C}_x^K\right)_i = \int_K f_{C,x}^K \varphi_i^K, \qquad \left(\mathbb{C}_y^K\right)_i = \int_K f_{C,y}^K \varphi_i^K, \qquad \left(\mathbb{C}_z^K\right)_i = \int_K f_{C,z}^K \varphi_i^K.$$

The discretization of the local problem is:

$$\begin{aligned}
&\int_K \left(\frac{\partial E_z^K}{\partial y} - \frac{\partial E_y^K}{\partial z}\right) \varphi_i^K - \int_{\partial K} \gamma_5 H_x^K \varphi_i^K + \int_{\partial K} \gamma_5 \lambda_{3x} \varphi_i^K + \int_K \mathrm{i}\omega\mu_0 H_x^K \varphi_i^K = 0, \\
&\int_K \left(\frac{\partial E_x^K}{\partial z} - \frac{\partial E_z^K}{\partial x}\right) \varphi_i^K - \int_{\partial K} \gamma_5 H_y^K \varphi_i^K + \int_{\partial K} \gamma_5 \lambda_{3y} \varphi_i^K + \int_K \mathrm{i}\omega\mu_0 H_y^K \varphi_i^K = 0, \\
&\int_K \left(\frac{\partial E_y^K}{\partial x} - \frac{\partial E_x^K}{\partial y}\right) \varphi_i^K - \int_{\partial K} \gamma_5 H_z^K \varphi_i^K + \int_{\partial K} \gamma_5 \lambda_{3z} \varphi_i^K + \int_K \mathrm{i}\omega\mu_0 H_z^K \varphi_i^K = 0,
\end{aligned}$$

$$\begin{aligned}
&\int_K H_y^K \frac{\partial \varphi_i^K}{\partial z} - \int_K H_z^K \frac{\partial \varphi_i^K}{\partial y} - \int_{\partial K} \lambda_{3y} n_z \varphi_i^K + \int_{\partial K} \lambda_{3z} n_y \varphi_i^K - \int_K \mathrm{i}\omega\epsilon_0 E_x^K \varphi_i^K - \int_K \boldsymbol{J}_x \varphi_i^K = \int_K f_{C,x}^K \varphi_i^K, \\
&-\int_K H_x^K \frac{\partial \varphi_i^K}{\partial z} + \int_K H_z^K \frac{\partial \varphi_i^K}{\partial x} + \int_{\partial K} \lambda_{3x} n_z \varphi_i^K - \int_{\partial K} \lambda_{3z} n_x \varphi_i^K - \int_K \mathrm{i}\omega\epsilon_0 E_y^K \varphi_i^K - \int_K \boldsymbol{J}_y \varphi_i^K = \int_K f_{C,y}^K \varphi_i^K, \\
&\int_K H_x^K \frac{\partial \varphi_i^K}{\partial y} - \int_K H_y^K \frac{\partial \varphi_i^K}{\partial x} - \int_{\partial K} \lambda_{3x} n_y \varphi_i^K + \int_{\partial K} \lambda_{3y} n_x \varphi_i^K - \int_K \mathrm{i}\omega\epsilon_0 E_z^K \varphi_i^K - \int_K \boldsymbol{J}_z \varphi_i^K = \int_K f_{C,z}^K \varphi_i^K,
\end{aligned}$$

and

$$\int_K \boldsymbol{J}_x\,\varphi_i^K - \int_K \sigma E_x^K\,\varphi_i^K = 0\,,$$
$$\int_K \boldsymbol{J}_y\,\varphi_i^K - \int_K \sigma E_y^K\,\varphi_i^K = 0\,,$$
$$\int_K \boldsymbol{J}_z\,\varphi_i^K - \int_K \sigma E_z^K\,\varphi_i^K = 0\,.$$

This gives, using the matrices defined in (G.32):

$$(\mathbb{D}_y^K)^T\underline{E}_z^K - (\mathbb{D}_z^K)^T\underline{E}_y^K - \sum_{f=1}^4\gamma_5\,\mathbb{E}^{\beta(K,f)}\underline{H}_x^K + \sum_{f=1}^4\gamma_5\,\mathbb{F}^{\beta(K,f)}\lambda_{3x} + \mathbb{M}^K\mathrm{i}\omega\mu_0\underline{H}_x^K = 0\,,$$
$$(\mathbb{D}_z^K)^T\underline{E}_x^K - (\mathbb{D}_x^K)^T\underline{E}_z^K - \sum_{f=1}^4\gamma_5\,\mathbb{E}^{\beta(K,f)}\underline{H}_y^K + \sum_{f=1}^4\gamma_5\,\mathbb{F}^{\beta(K,f)}\lambda_{3y} + \mathbb{M}^K\mathrm{i}\omega\mu_0\underline{H}_y^K = 0\,,$$
$$(\mathbb{D}_x^K)^T\underline{E}_y^K - (\mathbb{D}_y^K)^T\underline{E}_x^K - \sum_{f=1}^4\gamma_5\,\mathbb{E}^{\beta(K,f)}\underline{H}_z^K + \sum_{f=1}^4\gamma_5\,\mathbb{F}^{\beta(K,f)}\lambda_{3z} + \mathbb{M}^K\mathrm{i}\omega\mu_0\underline{H}_z^K = 0\,,$$

$$\mathbb{D}_z^K\underline{H}_y^K - \mathbb{D}_y^K\underline{H}_z^K - \sum_{f=1}^4\mathbb{Q}_z^{\beta(K,f)}\lambda_{3y} + \sum_{f=1}^4\mathbb{Q}_y^{\beta(K,f)}\lambda_{3z} - \mathbb{M}^K\mathrm{i}\omega\epsilon_0\underline{E}_x^K - \mathbb{M}^K\underline{J}_x^K = \mathbb{C}_x^K\,,$$
$$-\mathbb{D}_z^K\underline{H}_x^K + \mathbb{D}_x^K\underline{H}_z^K + \sum_{f=1}^4\mathbb{Q}_z^{\beta(K,f)}\lambda_{3x} - \sum_{f=1}^4\mathbb{Q}_x^{\beta(K,f)}\lambda_{3z} - \mathbb{M}^K\mathrm{i}\omega\epsilon_0\underline{E}_y^K - \mathbb{M}^K\underline{J}_y^K = \mathbb{C}_y^K\,,$$
$$\mathbb{D}_y^K\underline{H}_x^K - \mathbb{D}_x^K\underline{H}_y^K - \sum_{f=1}^4\mathbb{Q}_y^{\beta(K,f)}\lambda_{3x} + \sum_{f=1}^4\mathbb{Q}_x^{\beta(K,f)}\lambda_{3y} - \mathbb{M}^K\mathrm{i}\omega\epsilon_0\underline{E}_z^K - \mathbb{M}^K\underline{J}_z^K = \mathbb{C}_z^K\,,$$

and

$$\mathbb{M}^K\underline{J}_x^K - \mathbb{M}^K\sigma\underline{E}_x^K = 0\,,$$
$$\mathbb{M}^K\underline{J}_y^K - \mathbb{M}^K\sigma\underline{E}_y^K = 0\,,$$
$$\mathbb{M}^K\underline{J}_z^K - \mathbb{M}^K\sigma\underline{E}_z^K = 0\,.$$

The linear system can be written as:

$$\mathbb{A}^K\underline{W}^K + \mathbb{B}^K\underline{\Lambda}^K = \mathbb{C}_{\text{source}}^K\,.$$

where $\underline{W}^K$, $\underline{\Lambda}^K$ are defined in (G.30) and (G.31), and the elementary matrices $\mathbb{A}^K$ and $\mathbb{B}^K$ are given below:

$$\mathbb{A}^K = \begin{pmatrix}
-\mathbb{M}^K\mathrm{i}\omega\epsilon_0 & 0 & 0 & 0 & \mathbb{D}_z^K & -\mathbb{D}_y^K & -\mathbb{M}^K & 0 & 0\\
0 & -\mathbb{M}^K\mathrm{i}\omega\epsilon_0 & 0 & -\mathbb{D}_z^K & 0 & \mathbb{D}_x^K & 0 & -\mathbb{M}^K & 0\\
0 & 0 & -\mathbb{M}^K\mathrm{i}\omega\epsilon_0 & \mathbb{D}_y^K & -\mathbb{D}_x^K & 0 & 0 & 0 & -\mathbb{M}^K\\
0 & -(\mathbb{D}_z^K)^T & (\mathbb{D}_y^K)^T & \mathbb{M}^K\mathrm{i}\omega\mu_0 - \sum_{f=1}^4\gamma_5\,\mathbb{E}^{\beta(K,f)} & 0 & 0 & 0 & 0 & 0\\
(\mathbb{D}_z^K)^T & 0 & -(\mathbb{D}_x^K)^T & 0 & \mathbb{M}^K\mathrm{i}\omega\mu_0 - \sum_{f=1}^4\gamma_5\,\mathbb{E}^{\beta(K,f)} & 0 & 0 & 0 & 0\\
-(\mathbb{D}_y^K)^T & (\mathbb{D}_x^K)^T & 0 & 0 & 0 & \mathbb{M}^K\mathrm{i}\omega\mu_0 - \sum_{f=1}^4\gamma_5\,\mathbb{E}^{\beta(K,f)} & 0 & 0 & 0\\
-\mathbb{M}^K\sigma & 0 & 0 & 0 & 0 & 0 & \mathbb{M}^K & 0 & 0\\
0 & -\mathbb{M}^K\sigma & 0 & 0 & 0 & 0 & 0 & \mathbb{M}^K & 0\\
0 & 0 & -\mathbb{M}^K\sigma & 0 & 0 & 0 & 0 & 0 & \mathbb{M}^K
\end{pmatrix} \tag{G.33}$$

and

$$\mathbb{B}^K = \begin{pmatrix} 0 & 0 & 0 & 0 & -\mathbb{Q}_z^{\beta(K,1)} & -\mathbb{Q}_z^{\beta(K,2)} & -\mathbb{Q}_z^{\beta(K,3)} & -\mathbb{Q}_z^{\beta(K,4)} & \mathbb{Q}_y^{\beta(K,1)} & \mathbb{Q}_y^{\beta(K,2)} & \mathbb{Q}_y^{\beta(K,3)} & \mathbb{Q}_y^{\beta(K,4)} \\ \mathbb{Q}_z^{\beta(K,1)} & \mathbb{Q}_z^{\beta(K,2)} & \mathbb{Q}_z^{\beta(K,3)} & \mathbb{Q}_z^{\beta(K,4)} & 0 & 0 & 0 & 0 & -\mathbb{Q}_x^{\beta(K,1)} & -\mathbb{Q}_x^{\beta(K,2)} & -\mathbb{Q}_x^{\beta(K,3)} & -\mathbb{Q}_x^{\beta(K,4)} \\ -\mathbb{Q}_y^{\beta(K,1)} & -\mathbb{Q}_y^{\beta(K,2)} & -\mathbb{Q}_y^{\beta(K,3)} & -\mathbb{Q}_y^{\beta(K,4)}) & \mathbb{Q}_x^{\beta(K,1)}) & \mathbb{Q}_x^{\beta(K,2)}) & \mathbb{Q}_x^{\beta(K,3)} & \mathbb{Q}_x^{\beta(K,4)} & 0 & 0 & 0 & 0 \\ \gamma_5\mathbb{F}^{\beta(K,1)} & \gamma_5\mathbb{F}^{\beta(K,2)} & \gamma_5\,\mathbb{F}^{\beta(K,3)} & \gamma_5\mathbb{F}^{\beta(K,4)} & 0 & 0 & 0 & 0 & 0 & 0 & 0 & 0 \\ 0 & 0 & 0 & 0 & \gamma_5\mathbb{F}^{\beta(K,1)} & \gamma_5\mathbb{F}^{\beta(K,2)} & \gamma_5\mathbb{F}^{\beta(K,3)} & \gamma_5\mathbb{F}^{\beta(K,4)} & 0 & 0 & 0 & 0 \\ 0 & 0 & 0 & 0 & 0 & 0 & 0 & 0 & \gamma_5\mathbb{F}^{\beta(K,1)} & \gamma_5\mathbb{F}^{\beta(K,2)} & \gamma_5\mathbb{F}^{\beta(K,3)} & \gamma_5\mathbb{F}^{\beta(K,4)} \\ 0 & 0 & 0 & 0 & 0 & 0 & 0 & 0 & 0 & 0 & 0 & 0 \\ 0 & 0 & 0 & 0 & 0 & 0 & 0 & 0 & 0 & 0 & 0 & 0 \\ 0 & 0 & 0 & 0 & 0 & 0 & 0 & 0 & 0 & 0 & 0 & 0 \end{pmatrix}. \tag{G.34}$$

Next, we discretize the transmission condition. We consider a face F in the interior of the mesh. Then, we replace the expression of the numerical trace $\hat{\boldsymbol{E}}_h$ in (G.29), and as for the local problem we only penalize the tangential components. We hence have

$$\int_F (\boldsymbol{n}\times\hat{\boldsymbol{E}})\cdot\nu = \int_F (\boldsymbol{n}\times\boldsymbol{E}_h)\cdot\nu - \int_F \left(\gamma_5\left(\boldsymbol{H}_h^t - \boldsymbol{\lambda}_3\right)\right)\cdot\nu\,.$$

We then replace $\tilde{\boldsymbol{e}}$ by the basis functions $\psi^{\beta(,f)}i$,

$$\begin{aligned}
\int_F \left(E_z^K n_y - E_y^K n_z\right)\,\psi^{\beta(,f)}i \,+ \int_F \gamma_5\, H_x^K\,\psi^{\beta(,f)}i \,- \int_F \gamma_5\,\lambda_{3x}\,\psi^{\beta(,f)}i \;&= 0\,,\\
\int_F \left(E_x^K n_z - E_z^K n_x\right)\,\psi^{\beta(,f)}i \,+ \int_F \gamma_5\, H_y^K\,\psi^{\beta(,f)}i \,- \int_F \gamma_5\,\lambda_{3y}\,\psi^{\beta(,f)}i \;&= 0\,,\\
\int_F \left(E_y^K n_x - E_x^K n_y\right)\,\psi^{\beta(,f)}i \,+ \int_F \gamma_5\, H_z^K\,\psi^{\beta(,f)}i \,- \int_F \gamma_5\,\lambda_{3z}\,\psi^{\beta(,f)}i \;&= 0\,,
\end{aligned}$$

and we express the above equations in terms of the elementary matrices (G.32):

$$\begin{aligned}
-(\mathbb{Q}_z^{\beta(K,f)})^T\underline{E}_y^K + (\mathbb{Q}_y^{\beta(K,f)})^T\underline{E}_z^K \,- \gamma_5\,(\mathbb{F}^{\beta(K,f)})^T\underline{H}_x^K + \gamma_5\;(\mathbb{G}^{\beta(K,f)})^T\underline{\lambda}_{3x} \;&= 0\,,\\
-(\mathbb{Q}_x^{\beta(K,f)})^T\underline{E}_z^K + (\mathbb{Q}_z^{\beta(K,f)})^T\underline{E}_x^K \,- \gamma_5\,(\mathbb{F}^{\beta(K,f)})^T\underline{H}_y^K + \gamma_5\,(\mathbb{G}^{\beta(K,f)})^T\underline{\lambda}_{3y} \;&= 0\,,\\
-(\mathbb{Q}_y^{\beta(K,f)})^T\underline{E}_x^K + (\mathbb{Q}_x^{\beta(K,f)})^T\underline{E}_y^K \,- \gamma_5\,(\mathbb{F}^{\beta(K,f)})^T\underline{H}_z^K + \gamma_5\,(\mathbb{G}^{\beta(K,f)})^T\underline{\lambda}_{3z} \;&= 0\,.
\end{aligned}$$

Finally, the elementary matrices are:

$$\mathbb{P}^K = \begin{pmatrix}
0 & -(\mathbb{Q}_z^{\beta(K,1)})^T & (\mathbb{Q}_y^{\beta(K,1)})^T & -\gamma_5\,(\mathbb{F}^{\beta(K,1)})^T & 0 & 0 & 0 & 0 & 0 \\
0 & -(\mathbb{Q}_z^{\beta(K,2)})^T & (\mathbb{Q}_y^{\beta(K,2)})^T & -\gamma_5\,(\mathbb{F}^{\beta(K,2)})^T & 0 & 0 & 0 & 0 & 0 \\
0 & -(\mathbb{Q}_z^{\beta(K,3)})^T & (\mathbb{Q}_y^{\beta(K,3)})^T & -\gamma_5\,(\mathbb{F}^{\beta(K,3)})^T & 0 & 0 & 0 & 0 & 0 \\
0 & -(\mathbb{Q}_z^{\beta(K,4)})^T & (\mathbb{Q}_y^{\beta(K,4)})^T & -\gamma_5\,(\mathbb{F}^{\beta(K,4)})^T & 0 & 0 & 0 & 0 & 0 \\
(\mathbb{Q}_z^{\beta(K,1)})^T & 0 & -(\mathbb{Q}_x^{\beta(K,1)})^T & 0 & -\gamma_5\,(\mathbb{F}^{\beta(K,1)})^T & 0 & 0 & 0 & 0 \\
(\mathbb{Q}_z^{\beta(K,2)})^T & 0 & -(\mathbb{Q}_x^{\beta(K,2)})^T & 0 & -\gamma_5\,(\mathbb{F}^{\beta(K,2)})^T & 0 & 0 & 0 & 0 \\
(\mathbb{Q}_z^{\beta(K,3)})^T & 0 & -(\mathbb{Q}_x^{\beta(K,3)})^T & 0 & -\gamma_5\,(\mathbb{F}^{\beta(K,3)})^T & 0 & 0 & 0 & 0 \\
(\mathbb{Q}_z^{\beta(K,4)})^T & 0 & -(\mathbb{Q}_x^{\beta(K,4)})^T & 0 & -\gamma_5\,(\mathbb{F}^{\beta(K,4)})^T & 0 & 0 & 0 & 0 \\
-(\mathbb{Q}_y^{\beta(K,1)})^T & (\mathbb{Q}_x^{\beta(K,1)})^T & 0 & 0 & 0 & -\gamma_5\,(\mathbb{F}^{\beta(K,1)})^T & 0 & 0 & 0 \\
-(\mathbb{Q}_y^{\beta(K,2)})^T & (\mathbb{Q}_x^{\beta(K,2)})^T & 0 & 0 & 0 & -\gamma_5\,(\mathbb{F}^{\beta(K,2)})^T & 0 & 0 & 0 \\
-(\mathbb{Q}_y^{\beta(K,3)})^T & (\mathbb{Q}_x^{\beta(K,3)})^T & 0 & 0 & 0 & -\gamma_5\,(\mathbb{F}^{\beta(K,3)})^T & 0 & 0 & 0 \\
-(\mathbb{Q}_y^{\beta(K,4)})^T & (\mathbb{Q}_x^{\beta(K,4)})^T & 0 & 0 & 0 & -\gamma_5\,(\mathbb{F}^{\beta(K,4)})^T & 0 & 0 & 0
\end{pmatrix} \tag{G.35}$$

and

$$\mathbb{T}^K = \begin{pmatrix} \mathbb{T}_{\mathbb{T}}^K & 0 & 0 \\ 0 & \mathbb{T}_{\mathbb{T}}^K & 0 \\ 0 & 0 & \mathbb{T}_{\mathbb{T}}^K \end{pmatrix} \qquad \text{with} \qquad \mathbb{T}_{\mathbb{T}}^K = \begin{pmatrix} \gamma_5\mathbb{G}^{\beta(K,1)} & 0 & 0 & 0 \\ 0 & \gamma_5\mathbb{G}^{\beta(K,2)} & 0 & 0 \\ 0 & 0 & \gamma_5\mathbb{G}^{\beta(K,3)} & 0 \\ 0 & 0 & 0 & \gamma_5\mathbb{G}^{\beta(K,4)} \end{pmatrix}. \tag{G.36}$$

G.4.3 Boundary conditions for a bounded domain

We can impose on the boundary: $\boldsymbol{E} \times \boldsymbol{n} = \boldsymbol{e}^{\text{inc}} \times \boldsymbol{n}$, or $\boldsymbol{H} = \boldsymbol{h}^{\text{inc}}$. In the first case, the matrices are not modified. We consider the second case. Suppose that the first face of the considered element in on the boundary, the elementary matrices $\mathbb{P}^K$ and $\mathbb{T}^K$ are:

$$\mathbb{P}^K = \begin{pmatrix}
0 & 0 & 0 & 0 & 0 & 0 & 0 & 0 & 0 \\
0 & -(\mathbb{Q}_z^{\beta(K,2)})^T & (\mathbb{Q}_y^{\beta(K,2)})^T & -\gamma_5\,(\mathbb{F}^{\beta(K,2)})^T & 0 & 0 & 0 & 0 & 0 \\
0 & -(\mathbb{Q}_z^{\beta(K,3)})^T & (\mathbb{Q}_y^{\beta(K,3)})^T & -\gamma_5\,(\mathbb{F}^{\beta(K,3)})^T & 0 & 0 & 0 & 0 & 0 \\
0 & -(\mathbb{Q}_z^{\beta(K,4)})^T & (\mathbb{Q}_y^{\beta(K,4)})^T & -\gamma_5\,(\mathbb{F}^{\beta(K,4)})^T & 0 & 0 & 0 & 0 & 0 \\
0 & 0 & 0 & 0 & 0 & 0 & 0 & 0 & 0 \\
(\mathbb{Q}_z^{\beta(K,2)})^T & 0 & -(\mathbb{Q}_x^{\beta(K,2)})^T & 0 & -\gamma_5\,(\mathbb{F}^{\beta(K,2)})^T & 0 & 0 & 0 & 0 \\
(\mathbb{Q}_z^{\beta(K,3)})^T & 0 & -(\mathbb{Q}_x^{\beta(K,3)})^T & 0 & -\gamma_5\,(\mathbb{F}^{\beta(K,3)})^T & 0 & 0 & 0 & 0 \\
(\mathbb{Q}_z^{\beta(K,4)})^T & 0 & -(\mathbb{Q}_x^{\beta(K,4)})^T & 0 & -\gamma_5\,(\mathbb{F}^{\beta(K,4)})^T & 0 & 0 & 0 & 0 \\
0 & 0 & 0 & 0 & 0 & 0 & 0 & 0 & 0 \\
-(\mathbb{Q}_y^{\beta(K,2)})^T & (\mathbb{Q}_x^{\beta(K,2)})^T & 0 & 0 & 0 & -\gamma_5\,(\mathbb{F}^{\beta(K,2)})^T & 0 & 0 & 0 \\
-(\mathbb{Q}_y^{\beta(K,3)})^T & (\mathbb{Q}_x^{\beta(K,3)})^T & 0 & 0 & 0 & -\gamma_5\,(\mathbb{F}^{\beta(K,3)})^T & 0 & 0 & 0 \\
-(\mathbb{Q}_y^{\beta(K,4)})^T & (\mathbb{Q}_x^{\beta(K,4)})^T & 0 & 0 & 0 & -\gamma_5\,(\mathbb{F}^{\beta(K,4)})^T & 0 & 0 & 0
\end{pmatrix} \tag{G.37}$$

and

$$\mathbb{T}^K = \begin{pmatrix} \mathbb{T}_{\mathbb{T}}^K & 0 & 0 \\ 0 & \mathbb{T}_{\mathbb{T}}^K & 0 \\ 0 & 0 & \mathbb{T}_{\mathbb{T}}^K \end{pmatrix} \qquad \text{with} \qquad \mathbb{T}_{\mathbb{T}}^K = \begin{pmatrix} \mathbb{I} & 0 & 0 & 0 \\ 0 & \gamma_5 \mathbb{G}^{\beta(K,2)} & 0 & 0 \\ 0 & 0 & \gamma_5 \mathbb{G}^{\beta(K,3)} & 0 \\ 0 & 0 & 0 & \gamma_5 \mathbb{G}^{\beta(K,4)} \end{pmatrix}.$$

G.5 HDG method with radiation boundary conditions

Here, we present the development of the HDG method applied to the electromagnetic equations, in the case of a domain with absorbing boundary conditions. We consider a domain $\mathcal{D}$ with the boundary $\Gamma = \Gamma_l \cup \Gamma_{\text{abs}}$. On Γ_l, we impose either a condition on $\boldsymbol{H}$ or on $\boldsymbol{n} \times \boldsymbol{E}$. On Γ_{abs}, we impose a radiation boundary condition. In the following, we first focus on the two-dimensional case, then we develop the method in three dimensions.

G.5.1 HDG method with RBC in two dimensions

On the absorbing boundaries Γ_{abs}, we impose the Silver-Müller condition:

$$\sqrt{\epsilon_0}\, \boldsymbol{E} \times \boldsymbol{n} + \sqrt{\mu_0}\, \mathrm{H} = 0\,.$$

In the HDG method, imposing such a condition is equivalent to replace the transmission condition with:

$$\sum_{F \in \mathcal{F}_{\text{abs}}} \int_F \left(\sqrt{\epsilon_0}\, \hat{\boldsymbol{E}} \times \boldsymbol{n} + \sqrt{\mu_0}\, \hat{\mathrm{H}} \right) \nu = 0\,.$$

By using the expression of the numerical traces $\hat{\boldsymbol{E}}$ and $\hat{\mathrm{H}}$ given in (G.17), the above equation becomes:

$$\sum_{F \in \mathcal{F}_{\text{abs}}} \int_F \left(\sqrt{\epsilon_0}\, \boldsymbol{E}_h \times \boldsymbol{n} + \gamma_5 \left(\mathrm{H}_h - \lambda_3 \right) + \sqrt{\mu_0}\, \boldsymbol{\lambda}_3 \right) \nu = 0\,,$$

We discretize the above condition by decomposing the local unknowns using (G.20) and (G.21) and by replacing the test function ν by the basis function ψ_j^F:

$$\sum_{F \in \mathcal{F}_{\text{abs}}} \int_F \left(\sqrt{\epsilon_0} \left(\underline{E}_x^K\, \varphi_j^K n_y - \underline{E}_y^K\, \varphi_j^K\, n_x + \gamma_5 \left(\underline{H}_z^K \varphi_j^K - \underline{\lambda}_3\, \psi_j^F \right) \right) + \sqrt{\mu_0}\, \underline{\lambda}_3\, \psi_j^F \right) \psi_i^F = 0\,,$$

which gives in terms of elementary matrices defined in (G.23):

$$\sum_{F \in \mathcal{F}_{\text{abs}}} \left(\sqrt{\epsilon_0}\, (\mathbb{Q}_y^{\beta(K,f)})^T \underline{E}_x^K - \sqrt{\epsilon_0}\, (\mathbb{Q}_x^{\beta(K,f)})^T \underline{E}_y^K + \sqrt{\epsilon_0}\, (\mathbb{F}^{\beta(K,f)})^T \gamma_5\, \underline{H}_z^K - \sqrt{\epsilon_0}\, \mathbb{G}^{\beta(K,f)} \gamma_5 \underline{\lambda}_3 + \sqrt{\mu_0}\, \mathbb{G}^{\beta(K,f)} \underline{\lambda}_3 \right) = 0\,.$$

Let us consider an element K of $\mathcal{T}_h$, whose first local face is on Γ_{abs}. In this case, the elementary matrices of K are modified as:

$$\mathbb{P}^K = \begin{pmatrix} \sqrt{\epsilon_0}\, (\mathbb{Q}_y^{\beta(K,1)})^T & -\sqrt{\epsilon_0}\, (\mathbb{Q}_x^{\beta(K,1)})^T & \sqrt{\epsilon_0}\, \gamma_5\, (\mathbb{F}^{\beta(K,1)})^T \\ -(\mathbb{Q}_y^{\beta(K,2)})^T & (\mathbb{Q}_x^{\beta(K,2)})^T & -\gamma_5\, (\mathbb{F}^{\beta(K,2)})^T \\ -(\mathbb{Q}_y^{\beta(K,3)})^T & (\mathbb{Q}_x^{\beta(K,3)})^T & -\gamma_5\, (\mathbb{F}^{\beta(K,3)})^T \end{pmatrix},$$

and

$$\mathbb{T}^K = \begin{pmatrix} (-\sqrt{\epsilon_0}\, \gamma_5 + \sqrt{\mu_0}) \mathbb{G}^{\beta(K,1)} & 0 & 0 \\ 0 & \gamma_5\, \mathbb{G}^{\beta(K,2)} & 0 \\ 0 & 0 & \gamma_5\, \mathbb{G}^{\beta(K,3)} \end{pmatrix}.$$

G.5.2 HDG method with RBC in three dimensions

On the absorbing boundaries, we impose the Silver-Müller condition:

$$\sqrt{\epsilon_0}\, \boldsymbol{E} \times \boldsymbol{n} - \sqrt{\mu_0}\, (\boldsymbol{H} \times \boldsymbol{n}) \times \boldsymbol{n} = 0\,.$$

If we consider a face F on the absorbing boundary $\Gamma_{\rm abs}$, we have to impose the following condition:

$$\int_F \Big(\sqrt{\epsilon_0}\, \hat{\boldsymbol{E}}_h \times \boldsymbol{n} \,-\, \sqrt{\mu_0}\, (\hat{\boldsymbol{H}}_h^t \times \boldsymbol{n}) \times \boldsymbol{n} \Big) \cdot \nu \,=\, 0\,, \tag{G.38}$$

with

$$\begin{cases} \hat{\boldsymbol{H}}_h^t & = \boldsymbol{\lambda}_3\,, \\ \hat{\boldsymbol{E}}_h & = \hat{\boldsymbol{E}}_h - \gamma_5 \left(\boldsymbol{H}_h^t - \boldsymbol{\lambda}_3 \right) \times \boldsymbol{n}\,. \end{cases}$$

By replacing the expression of the trace variables, equation (G.38) becomes:

$$\int_F \sqrt{\epsilon_0}\, (\boldsymbol{E}_h \times \boldsymbol{n}) \cdot \nu + \int_F \sqrt{\epsilon_0}\, \gamma_5\, \boldsymbol{H}_h \cdot \nu + \int_F (-\sqrt{\epsilon_0}\, \gamma_5 + \sqrt{\mu_0})\, \boldsymbol{\lambda}_3 \cdot \nu \,=\, 0\,.$$

We discretize this equation along the directions x, y, z by decomposing the components of $\boldsymbol{E}_h$, $\boldsymbol{H}_h$ and of the test function ν, to obtain:

$$\begin{aligned}
&\int_F \sqrt{\epsilon_0}\, (\boldsymbol{E}_y\, n_z - \boldsymbol{E}_z\, n_y) \psi_i^{\beta(K,f)} + \int_F \sqrt{\epsilon_0}\, \gamma_5\, \boldsymbol{H}_x\, \psi_i^{\beta(K,f)} + \int_F (-\sqrt{\epsilon_0}\, \gamma_5 + \sqrt{\mu_0})\, \underline{\lambda}_{3x}\, \psi_i^{\beta(K,f)} \,=\, 0\,, \\
&\int_F \sqrt{\epsilon_0}\, (\boldsymbol{E}_z\, n_x - \boldsymbol{E}_x\, n_z) \psi_i^{\beta(K,f)} + \int_F \sqrt{\epsilon_0}\, \gamma_5\, \boldsymbol{H}_y\, \psi_i^{\beta(K,f)} + \int_F (-\sqrt{\epsilon_0}\, \gamma_5 + \sqrt{\mu_0})\, \underline{\lambda}_{3y}\, \psi_i^{\beta(K,f)} \,=\, 0\,, \\
&\int_F \sqrt{\epsilon_0}\, (\boldsymbol{E}_x\, n_y - \boldsymbol{E}_y\, n_x) \psi_i^{\beta(K,f)} + \int_F \sqrt{\epsilon_0}\, \gamma_5\, \boldsymbol{H}_z\, \psi^{\beta(K,f)} + \int_F (-\sqrt{\epsilon_0}\, \gamma_5 + \sqrt{\mu_0})\, \underline{\lambda}_{3z}\, \psi_i^{\beta(K,f)} \,=\, 0\,.
\end{aligned}$$

This gives, using the elementary matrices defined in (G.32):

$$\begin{aligned}
&\sqrt{\epsilon_0}\, (\mathbb{Q}_z^{\beta(K,f)})^T \underline{E}_y^K - \sqrt{\epsilon_0}\, (\mathbb{Q}_y^{\beta(K,f)})^T \underline{E}_z^K + \sqrt{\epsilon_0}\, \gamma_5\, (\mathbb{F}^{\beta(K,f)})^T\, \underline{H}_x^K + (-\sqrt{\epsilon_0}\, \gamma_5 + \sqrt{\mu_0})\, \mathbb{G}^{\beta(K,f)} \underline{\lambda}_{3x} \,=\, 0\,, \\
&\sqrt{\epsilon_0}\, (\mathbb{Q}_x^{\beta(K,f)})^T \underline{E}_z^K - \sqrt{\epsilon_0}\, (\mathbb{Q}_z^{\beta(K,f)})^T \underline{E}_x^K + \sqrt{\epsilon_0}\, \gamma_5\, (\mathbb{F}^{\beta(K,f)})^T\, \underline{H}_y^K + (-\sqrt{\epsilon_0}\, \gamma_5 + \sqrt{\mu_0})\, \mathbb{G}^{\beta(K,f)} \underline{\lambda}_{3y} \,=\, 0\,, \\
&\sqrt{\epsilon_0}\, (\mathbb{Q}_y^{\beta(K,f)})^T \underline{E}_x^K - \sqrt{\epsilon_0}\, (\mathbb{Q}_x^{\beta(K,f)})^T \underline{E}_y^K + \sqrt{\epsilon_0}\, \gamma_5\, (\mathbb{F}^{\beta(K,f)})^T\, \underline{H}_z^K + (-\sqrt{\epsilon_0}\, \gamma_5 + \sqrt{\mu_0})\, \mathbb{G}^{\beta(K,f)} \underline{\lambda}_{3z} \,=\, 0\,.
\end{aligned}$$

The above three scalar equations are integrated in the global system of the transmission and boundary conditions that is written as:

$$\sum_{K \in \mathcal{T}_h} (\mathcal{A}_{HDG}^K)^T \left(\mathbb{P}^K \underline{W}^K + \mathbb{T}^K \mathcal{A}_{HDG}^K \underline{\Lambda} \right) = \mathbb{S}_{\rm inc}\,,$$

If, in the local numbering, the first face of the element is on the absorbing boundary $\Gamma_{\rm abs}$, the elementary matrices $\mathbb{P}^K$ and $\mathbb{T}^K$ become:

$$\mathbb{P}^K = \begin{pmatrix}
0 & \sqrt{\epsilon_0}\, (\mathbb{Q}_z^{\beta(K,1)})^T & -\sqrt{\epsilon_0}\, (\mathbb{Q}_y^{\beta(K,1)})^T & \sqrt{\epsilon_0}\, \gamma_5\, (\mathbb{F}^{\beta(K,1)})^T & 0 & 0 & 0 & 0 & 0 \\
0 & (\mathbb{Q}_z^{\beta(K,2)})^T & -(\mathbb{Q}_y^{\beta(K,2)})^T & -\gamma_5\, (\mathbb{F}^{\beta(K,2)})^T & 0 & 0 & 0 & 0 & 0 \\
0 & (\mathbb{Q}_z^{\beta(K,3)})^T & -(\mathbb{Q}_y^{\beta(K,3)})^T & -\gamma_5\, (\mathbb{F}^{\beta(K,3)})^T & 0 & 0 & 0 & 0 & 0 \\
0 & (\mathbb{Q}_z^{\beta(K,4)})^T & -(\mathbb{Q}_y^{\beta(K,4)})^T & -\gamma_5\, (\mathbb{F}^{\beta(K,4)})^T & 0 & 0 & 0 & 0 & 0 \\
-\sqrt{\epsilon_0}\, (\mathbb{Q}_z^{\beta(K,1)})^T & 0 & \sqrt{\epsilon_0}\, (\mathbb{Q}_x^{\beta(K,1)})^T & 0 & \sqrt{\epsilon_0}\, \gamma_5\, (\mathbb{F}^{\beta(K,1)})^T & 0 & 0 & 0 & 0 \\
-(\mathbb{Q}_z^{\beta(K,2)})^T & 0 & (\mathbb{Q}_x^{\beta(K,2)})^T & 0 & -\gamma_5\, (\mathbb{F}^{\beta(K,2)})^T & 0 & 0 & 0 & 0 \\
-(\mathbb{Q}_z^{\beta(K,3)})^T & 0 & (\mathbb{Q}_x^{\beta(K,3)})^T & 0 & -\gamma_5\, (\mathbb{F}^{\beta(K,3)})^T & 0 & 0 & 0 & 0 \\
-(\mathbb{Q}_z^{\beta(K,4)})^T & 0 & (\mathbb{Q}_x^{\beta(K,4)})^T & 0 & -\gamma_5\, (\mathbb{F}^{\beta(K,4)})^T & 0 & 0 & 0 & 0 \\
\sqrt{\epsilon_0}\, (\mathbb{Q}_y^{\beta(K,1)})^T & -\sqrt{\epsilon_0}\, (\mathbb{Q}_x^{\beta(K,1)})^T & 0 & 0 & 0 & \sqrt{\epsilon_0}\, \gamma_5\, (\mathbb{F}^{\beta(K,1)})^T & 0 & 0 & 0 \\
(\mathbb{Q}_y^{\beta(K,2)})^T & -(\mathbb{Q}_x^{\beta(K,2)})^T & 0 & 0 & 0 & -\gamma_5\, (\mathbb{F}^{\beta(K,2)})^T & 0 & 0 & 0 \\
(\mathbb{Q}_y^{\beta(K,3)})^T & -(\mathbb{Q}_x^{\beta(K,3)})^T & 0 & 0 & 0 & -\gamma_5\, (\mathbb{F}^{\beta(K,3)})^T & 0 & 0 & 0 \\
(\mathbb{Q}_y^{\beta(K,4)})^T & -(\mathbb{Q}_x^{\beta(K,4)})^T & 0 & 0 & 0 & -\gamma_5\, (\mathbb{F}^{\beta(K,4)})^T & 0 & 0 & 0
\end{pmatrix}$$

and

$$\mathbb{T}^K = \begin{pmatrix} \mathbb{T}_{\mathbb{T}}^K & 0 & 0 \\ 0 & \mathbb{T}_{\mathbb{T}}^K & 0 \\ 0 & 0 & \mathbb{T}_{\mathbb{T}}^K \end{pmatrix} \qquad \text{with} \qquad \mathbb{T}_{\mathbb{T}}^K = \begin{pmatrix} (-\sqrt{\epsilon_0}\gamma_5 + \sqrt{\mu_0})\mathbb{G}^{\beta(K,1)} & 0 & 0 & 0 \\ 0 & \gamma_5\mathbb{G}^{\beta(K,2)} & 0 & 0 \\ 0 & 0 & \gamma_5\mathbb{G}^{\beta(K,3)} & 0 \\ 0 & 0 & 0 & \gamma_5\mathbb{G}^{\beta(K,4)} \end{pmatrix}.$$

G.6 Application of PML in the HDG method

In the following section, we include a Perfectly Matched Layer (PML) to the discretization of the electromagnetic equations using HDG method. The perfectly matched layer is an artificial absorbing layer on the borders of the computational domain. It absorbs the outgoing waves and prevents from reflections.

G.6.1 Application of PML in the HDG method in two dimensions

In two dimensions, we use two absorbing functions α and β that represent the attenuation of the wave in the absorbing layer. The attenuation functions α and β are taken equal to zero outside the absorbing layers, and the further the considered points in the layers are from the part with no attenuation, the more the values of the attenuation functions grow. In practice, we replace the derivatives

$$\frac{\partial}{\partial x} \to \frac{i\,\omega}{i\,\omega + \alpha(x)}\frac{\partial}{\partial x}, \qquad \text{and} \qquad \frac{\partial}{\partial y} \to \frac{i\,\omega}{i\,\omega + \beta(y)}\frac{\partial}{\partial y}.$$

With PML, the transmission conditions and the boundary conditions are not modified, contrary to the local problem. In the following, we detail the discretization of the electromagnetic equations (G.4) with PML. Considering an element K of $\mathcal{T}_h$, we multiply the equation by test functions $(\tilde{e}, \tilde{\boldsymbol{h}}, \tilde{\boldsymbol{j}}) \in (V^p(K) \times \boldsymbol{V}^p(K) \times \boldsymbol{V}^p(K))$ and integrate on the element K:

$$\int_K \left(\frac{i\,\omega}{i\,\omega + \alpha(x)}\frac{\partial\, E_y^K}{\partial x} - \frac{i\,\omega}{i\,\omega + \beta(y)}\frac{\partial\, E_x^K}{\partial y} \right) \tilde{e} + \int_K \mathrm{i}\,\omega\,\mu_0\, H^K\, \tilde{e} = 0,$$

$$\int_K \frac{i\,\omega}{i\,\omega + \beta(y)}\frac{\partial\, H^K}{\partial y}\,\tilde{h}_x - \int_K \frac{i\,\omega}{i\,\omega + \alpha(x)}\frac{\partial\, H^K}{\partial x}\,\tilde{h}_y - \int_K \mathrm{i}\,\omega\,\epsilon_0\,\boldsymbol{E}\cdot\tilde{\boldsymbol{h}} - \int_K \boldsymbol{J}\cdot\tilde{\boldsymbol{h}} = \int_K \mathbf{f}_C\cdot\tilde{\boldsymbol{h}},$$

$$\int_K \boldsymbol{J}\cdot\tilde{\boldsymbol{j}} - \int_K \sigma\,\boldsymbol{E}\cdot\tilde{\boldsymbol{j}} = 0.$$

We integrate by parts the above equations:

$$\int_K E_y^K \frac{i\,\omega}{i\,\omega + \alpha(x)}\frac{\partial\tilde{e}}{\partial x} - \int_K E_x^K \frac{i\,\omega}{i\,\omega + \beta(y)}\frac{\partial\tilde{e}}{\partial y} + \int_{\partial K} \hat{E}_y^K \frac{i\,\omega}{i\,\omega + \alpha(x)} n_x \tilde{e} - \int_{\partial K} \hat{E}_x^K \frac{i\,\omega}{i\,\omega + \beta(y)} n_y \tilde{e} + \int_K \mathrm{i}\omega\,\mu_0 H_h^K \tilde{e} = 0,$$

$$- \int_K H_h^K \frac{i\,\omega}{i\,\omega + \beta(y)}\frac{\partial\,\tilde{h}_x}{\partial y} + \int_{\partial K} \frac{i\,\omega}{i\,\omega + \beta(y)} \hat{H}^K\, n_y \tilde{h}_x + \int_K H_h^K \frac{i\,\omega}{i\,\omega + \alpha(x)}\frac{\partial\,\tilde{h}_y}{\partial x} - \int_{\partial K} \frac{i\,\omega}{i\,\omega + \alpha(x)} \hat{H}^K\, n_x \tilde{h}_y$$
$$- \int_K \mathrm{i}\omega\epsilon_0 \boldsymbol{E}_h\cdot\tilde{\boldsymbol{h}} - \int_K \boldsymbol{J}_h\cdot\tilde{\boldsymbol{h}} = \int_K \mathbf{f}_C\cdot\tilde{\boldsymbol{h}},$$

$$\int_K \boldsymbol{J}\,\tilde{\boldsymbol{j}} - \int_K \sigma\,\boldsymbol{E}\cdot\tilde{\boldsymbol{j}} = 0.$$

Then, we replace the numerical traces by their expressions given in (G.17), and we obtain

$$\int_K \left(\frac{i\,\omega}{i\,\omega + \alpha(x)}\frac{\partial E_y^K}{\partial x} - \frac{i\,\omega}{i\,\omega + \beta(y)}\frac{\partial E_x^K}{\partial y} \right) \tilde{e} - \int_{\partial K} \gamma_5 \left(H_h^K - \lambda_3\right) \left(\frac{i\,\omega}{i\,\omega + \alpha(x)} n_x^2 + \frac{i\,\omega}{i\,\omega + \beta(y)} n_y^2 \right) \tilde{e} + \int_K \mathrm{i}\omega\mu_0 H_h^K \tilde{e} = 0,$$

$$- \int_K H_h^K \frac{i\,\omega}{i\,\omega + \beta(y)}\frac{\partial\,\tilde{h}_x}{\partial y} + \int_{\partial K} \frac{i\,\omega}{i\,\omega + \beta(y)} \lambda_3\, n_y \tilde{h}_x + \int_K H_h^K \frac{i\,\omega}{i\,\omega + \alpha(x)}\frac{\partial\,\tilde{h}_y}{\partial x} - \int_{\partial K} \frac{i\,\omega}{i\,\omega + \alpha(x)} \lambda_3\, n_x \tilde{h}_y$$
$$- \int_K \mathrm{i}\omega\epsilon_0 \boldsymbol{E}_h\cdot\tilde{\boldsymbol{h}} - \int_K \boldsymbol{J}_h\cdot\tilde{\boldsymbol{h}} = \int_K \mathbf{f}_C\cdot\tilde{\boldsymbol{h}},$$

$$\int_K \boldsymbol{J}\,\tilde{\boldsymbol{j}} - \int_K \sigma\,\boldsymbol{E}\cdot\tilde{\boldsymbol{j}} = 0.$$

Now, we discretize the local problem, by decomposing the unknowns as given in (G.22):

$$\int_K \left(\frac{i\,\omega}{i\,\omega+\alpha(x)} \frac{\partial E_y^K}{\partial x} - \frac{i\,\omega}{i\,\omega+\beta(y)} \frac{\partial E_x^K}{\partial y} \right) \varphi_i^K - \int_{\partial K} \gamma_5 \, \left(H_h^K - \lambda_3 \right) \left(\frac{i\,\omega}{i\,\omega+\alpha(x)} n_x^2 + \frac{i\,\omega}{i\,\omega+\beta(y)} n_y^2 \right) \varphi_i^K + \int_K \mathrm{i}\omega\mu_0 H_h^K \varphi_i^K = 0\,,$$

$$- \int_K \frac{i\,\omega}{i\,\omega+\beta(y)} \, H_h^K \, \frac{\partial \varphi_i^K}{\partial y} + \int_{\partial K} \frac{i\,\omega}{i\,\omega+\beta(y)} \, \lambda_3 \, n_y \varphi_i^K - \int_K \mathrm{i}\,\omega\,\epsilon_0 \, E_x^K \, \varphi_i^K - \int_K J_x^K \, \varphi_i^K = \int_K f_{C,x} \, \tilde{h}_x \,,$$

$$\int_K \frac{i\,\omega}{i\,\omega+\alpha(x)} \, H_h^K \, \frac{\partial \varphi_i^K}{\partial x} - \int_{\partial K} \frac{i\,\omega}{i\,\omega+\alpha(x)} \, \lambda_3 \, n_x \varphi_i^K - \int_K \mathrm{i}\,\omega\,\epsilon_0 \, E_y^K \, \varphi_i^K - \int_K J_y^K \, \varphi_i^K = \int_K f_{C,y} \, \tilde{h}_y \,, \,,$$

$$\int_K J_x^K \, \varphi_i^K - \int_K \sigma E_x^K \, \varphi_i^K = 0\,,$$

$$\int_K J_y^K \, \varphi_i^K - \int_K \sigma E_y^K \, \varphi_i^K = 0\,.$$

We can express the above expression in terms of local unknowns and elementary matrices defined in (G.22) and (G.23):

$$\begin{aligned}
(\mathbb{D}_x^K)^T \, \frac{i\,\omega}{i\,\omega+\alpha(x)} \underline{E}_y^K - (\mathbb{D}_y^K)^T \, \frac{i\,\omega}{i\,\omega+\beta(y)} \underline{E}_x^K - \sum_{f=1}^{3} \gamma_5 \, \underline{\mathrm{H}}^K \mathbb{E}^{\beta(K,f)} \left(\frac{i\,\omega}{i\,\omega+\alpha(x)} n_x^2 + \frac{i\,\omega}{i\,\omega+\beta(y)} \, n_y^2 \right) \\
+ \sum_{f=1}^{3} \mathbb{F}^{\beta(K,f)} \left(\frac{i\,\omega}{i\,\omega+\alpha(x)} n_x^2 + \frac{i\,\omega}{i\,\omega+\beta(y)} \, n_y^2 \right) \gamma_5 \, \underline{\lambda}_3 + \mathbb{M}^K \mathrm{i}\,\omega\,\mu_0 \, \underline{\mathrm{H}}^K = 0\,, \\
-\mathbb{D}_y^K \, \frac{i\,\omega}{i\,\omega+\beta(y)} \underline{\mathrm{H}}^K - \sum_{f=1}^{3} \mathbb{Q}_y^{\beta(K,f)} \frac{i\,\omega}{i\,\omega+\beta(y)} \, \underline{\lambda}_3 - \mathbb{M}^K \, \mathrm{i}\,\omega\,\epsilon_0 \, \underline{E}_x^K - \mathbb{M}^K \, \underline{J}_x^K = \int_K f_{C,x} \, \tilde{h}_x \,, \\
\mathbb{D}_x^K \, \frac{i\,\omega}{i\,\omega+\alpha(x)} \underline{\mathrm{H}}^K + \sum_{f=1}^{3} \mathbb{Q}_x^{\beta(K,f)} \frac{i\,\omega}{i\,\omega+\alpha(x)} \underline{\lambda}_3 - \mathbb{M}^K \, \mathrm{i}\,\omega\,\epsilon_0 \, \underline{E}_y^K - \mathbb{M}^K \, \underline{J}_y^K = \int_K f_{C,y} \, \tilde{h}_y \,, \\
\mathbb{M}^K \underline{J}_x^K - \mathbb{M}^K \, \sigma \, \underline{E}_x^K = 0\,, \\
\mathbb{M}^K \underline{J}_y^K - \mathbb{M}^K \, \sigma \, \underline{E}_y^K = 0\,.
\end{aligned}$$

Recall that the above equation is written as a system:

$$\mathbb{A} \, \underline{W}^K + \mathbb{B} \, \underline{\Lambda}^K = \mathbb{C}_{\mathrm{source}}^K \,,$$

where $\underline{W}^K$ and $\underline{\Lambda}^K$ have been defined in (G.22). The matrices $\mathbb{A}^K$ and $\mathbb{B}^K$ are:

$$\mathbb{A}^K = \begin{pmatrix}
-\mathbb{M}^K \mathrm{i}\omega\epsilon_0 & 0 & -\mathbb{D}_y^K \frac{i\,\omega}{i\,\omega+\beta(y)} & -\mathbb{M}^K & 0 \\
0 & -\mathbb{M}^K \mathrm{i}\omega\epsilon_0 & \mathbb{D}_x^K \frac{i\,\omega}{i\,\omega+\alpha(x)} & 0 & -\mathbb{M}^K \\
-(\mathbb{D}_y^K)^T \frac{i\,\omega}{i\,\omega+\beta(y)} & (\mathbb{D}_x^K)^T \frac{i\,\omega}{i\,\omega+\alpha(x)} & \mathbb{M}^K \mathrm{i}\,\omega\,\mu_0 - \sum_{f=1}^{3} \gamma_5 \, \mathbb{E}^{\beta(K,f)} \left(\frac{i\,\omega}{i\,\omega+\alpha(x)} n_x^2 + \frac{i\,\omega}{i\,\omega+\beta(y)} \, n_y^2 \right) & 0 & 0 \\
-\mathbb{M}^K \, \sigma & 0 & 0 & \mathbb{M}^K & 0 \\
0 & -\mathbb{M}^K \, \sigma & 0 & 0 & \mathbb{M}^K
\end{pmatrix},$$

and

$$\mathbb{B}^K = \begin{pmatrix}
-\mathbb{Q}_y^{\beta(K,1)} \frac{i\,\omega}{i\,\omega+\beta(y)} & -\mathbb{Q}_y^{\beta(K,2)} \frac{i\,\omega}{i\,\omega+\beta(y)} & -\mathbb{Q}_y^{\beta(K,3)} \frac{i\,\omega}{i\,\omega+\beta(y)} \\
\mathbb{Q}_x^{\beta(K,1)} \frac{i\,\omega}{i\,\omega+\alpha(x)} & \mathbb{Q}_x^{\beta(K,2)} \frac{i\,\omega}{i\,\omega+\alpha(x)} & \mathbb{Q}_x^{\beta(K,3)} \frac{i\,\omega}{i\,\omega+\alpha(x)} \\
\gamma_5 \, \mathbb{F}^{\beta(K,1)} \left(\frac{i\,\omega}{i\,\omega+\alpha(x)} n_x^2 + \frac{i\,\omega}{i\,\omega+\beta(y)} \, n_y^2 \right) & \gamma_5 \, \mathbb{F}^{\beta(K,2)} \left(\frac{i\,\omega}{i\,\omega+\alpha(x)} n_x^2 + \frac{i\,\omega}{i\,\omega+\beta(y)} \, n_y^2 \right) & \gamma_5 \, \mathbb{F}^{\beta(K,3)} \left(\frac{i\,\omega}{i\,\omega+\alpha(x)} n_x^2 + \frac{i\,\omega}{i\,\omega+\beta(y)} \, n_y^2 \right) \\
0 & 0 & 0 \\
0 & 0 & 0
\end{pmatrix}.$$

G.6.2 Application of PML in the HDG method in three dimensions

In three dimensions, we use two absorbing functions α and β that represent the attenuation of the wave in the absorbing layer. The attenuation functions α and β are taken equal to zero outside of the absorbing layers. The value of the

attenuation functions increases with the distance of the point in the layer. In practice, we replace the derivatives

$$\partial_x \to \frac{i\,\omega}{i\,\omega+\alpha(x)}\partial_x\,,\quad \partial_y \to \frac{i\,\omega}{i\,\omega+\beta(y)}\partial_y\,,\quad \partial_z \to \frac{i\,\omega}{i\,\omega+\gamma(z)}\partial_z\,.$$

As before, we multiply equation (G.3) with test functions $(\tilde{\boldsymbol{e}},\tilde{\boldsymbol{h}},\tilde{\boldsymbol{j}}) \in (\boldsymbol{V}^p(K)\times\boldsymbol{V}^p(K)\times\boldsymbol{V}^p(K))$ and integrate on an element K. Next, we integrate by part the equations and replace the numerical traces $\hat{\boldsymbol{E}}$ and $\hat{\boldsymbol{H}}$ by their expressions (G.17). After that, the equations are integrated by parts to obtain the local problem. The local problem is discretized along x, y, and z components, by decomposing the local unknowns (G.30) and the Lagrange unknowns (G.31), and expressing the system with the elementary matrices (G.32). The matrices $\mathbb{A}^K$ and $\mathbb{B}^K$ are:

$$\mathbb{A}^K = \begin{pmatrix}
\mathbb{M}^K \mathrm{i}\omega\mu_0 & 0 & 0 & 0 & \mathbb{D}_z^K \frac{i\,\omega}{i\,\omega+\gamma(z)} & -\mathbb{D}_y^K \frac{i\,\omega}{i\,\omega+\beta(y)} & 0 & 0 & 0\\
0 & \mathbb{M}^K \mathrm{i}\omega\mu_0 & 0 & -\mathbb{D}_z^K \frac{i\,\omega}{i\,\omega+\gamma(z)} & 0 & \mathbb{D}_x^K \frac{i\,\omega}{i\,\omega+\alpha(x)} & 0 & 0 & 0\\
0 & 0 & \mathbb{M}^K \mathrm{i}\omega\mu_0 & \mathbb{D}_y^K \frac{i\,\omega}{i\,\omega+\beta(y)} & -\mathbb{D}_x^K \frac{i\,\omega}{i\,\omega+\alpha(x)} & 0 & 0 & 0 & 0\\
0 & -(\mathbb{D}_z^K)^T \frac{i\,\omega}{i\,\omega+\gamma(z)} & (\mathbb{D}_y^K)^T \frac{i\,\omega}{i\,\omega+\beta(y)} & -\mathbb{M}^K \mathrm{i}\omega\epsilon_0 - \sum_{f=1}^{4} \mathbb{N}_{\mathrm{pml}}^{\beta(K,f)}\gamma_5 & 0 & 0 & \mathbb{M}^K & 0 & 0\\
(\mathbb{D}_z^K)^T \frac{i\,\omega}{i\,\omega+\gamma(z)} & 0 & -(\mathbb{D}_x^K)^T \frac{i\,\omega}{i\,\omega+\alpha(x)} & 0 & -\mathbb{M}^K \mathrm{i}\omega\epsilon_0 - \sum_{f=1}^{4} \mathbb{N}_{\mathrm{pml}}^{\beta(K,f)}\gamma_5 & 0 & 0 & \mathbb{M}^K & 0\\
-(\mathbb{D}_y^K)^T \frac{i\,\omega}{i\,\omega+\beta(y)} & (\mathbb{D}_x^K)^T \frac{i\,\omega}{i\,\omega+\alpha(x)} & 0 & 0 & 0 & -\mathbb{M}^K \mathrm{i}\omega\epsilon_0 - \sum_{f=1}^{4} \mathbb{N}_{\mathrm{pml}}^{\beta(K,f)}\gamma_5 & 0 & 0 & \mathbb{M}^K\\
0 & 0 & 0 & -\mathbb{M}^K\sigma & 0 & 0 & \mathbb{M}^K & 0 & 0\\
0 & 0 & 0 & 0 & -\mathbb{M}^K\sigma & 0 & 0 & \mathbb{M}^K & 0\\
0 & 0 & 0 & 0 & 0 & -\mathbb{M}^K\sigma & 0 & 0 & \mathbb{M}^K
\end{pmatrix},$$

with $\mathbb{N}_{\mathrm{pml}}^{\beta(K,f)} = \mathbb{E}^{\beta(K,f)}\left(\frac{i\,\omega}{i\,\omega+\alpha(x)}n_x^2 + \frac{i\,\omega}{i\,\omega+\beta(y)}\,n_y^2 + \frac{i\,\omega}{i\,\omega+\gamma(z)}\,n_z^2\right)$, and $\mathbb{B}^K$ of the form

$$\mathbb{B}^K = \begin{pmatrix} B_{\lambda_{3x},1} & B_{\lambda_{3x},2} & B_{\lambda_{3x},3} & B_{\lambda_{3x},4} & B_{\lambda_{3y},1} & B_{\lambda_{3y},2} & B_{\lambda_{3y},3} & B_{\lambda_{3y},4} & B_{\lambda_{3z},1} & B_{\lambda_{3z},2} & B_{\lambda_{3z},3} & B_{\lambda_{3z},4}\end{pmatrix},$$

with

$$B_{\lambda_{3x},f} = \begin{pmatrix} 0\\ \mathbb{Q}_z^{\beta(K,f)} \frac{i\,\omega}{i\,\omega+\gamma(z)}\\ -\mathbb{Q}_y^{\beta(K,f)} \frac{i\,\omega}{i\,\omega+\beta(y)}\\ \gamma_5\,\mathbb{L}_{\mathrm{pml}}^{\beta(K,f)}\\ 0\\ 0\\ 0\\ 0\\ 0\end{pmatrix},\quad B_{\lambda_{3y},f} = \begin{pmatrix} -\mathbb{Q}_z^{\beta(K,f)} \frac{i\,\omega}{i\,\omega+\gamma(z)}\\ 0\\ \mathbb{Q}_x^{\beta(K,f)} \frac{i\,\omega}{i\,\omega+\alpha(x)}\\ 0\\ \gamma_5\,\mathbb{L}_{\mathrm{pml}}^{\beta(K,f)}\\ 0\\ 0\\ 0\\ 0\end{pmatrix},\quad B_{\lambda_{3z},f} = \begin{pmatrix} \mathbb{Q}_y^{\beta(K,f)} \frac{i\,\omega}{i\,\omega+\beta(y)}\\ -\mathbb{Q}_x^{\beta(K,f)} \frac{i\,\omega}{i\,\omega+\alpha(x)}\\ 0\\ 0\\ 0\\ \mathbb{L}_{\mathrm{pml}}^{\beta(K,f)}\gamma_5\\ 0\\ 0\\ 0\end{pmatrix},$$

with $f = 1,2,3,4$, and $\mathbb{L}_{\mathrm{pml}}^{\beta(K,f)} = \mathbb{F}^{\beta(K,f)}\left(\frac{i\,\omega}{i\,\omega+\alpha(x)}n_x^2 + \frac{i\,\omega}{i\,\omega+\beta(y)}\,n_y^2 + \frac{i\,\omega}{i\,\omega+\gamma(z)}\,n_z^2\right)$.

G.7 Numerical results

We present in this section the validation of the HDG method to solve the electromagnetic equations. We consider the electromagnetic equations on a domain $\mathcal{D}$ defined later, with $\mu_0 = 12.566\,10^{-7}$ N/A^2, $\epsilon_0 = 8.8595\,10^{-12}$ F.m-1, and

$\sigma = 10^{-9}$ S.m^{-1}. To validate the method, we use the relative numerical error $e_h(\mathfrak{U})$, which is computed from the knowledge of the numerical solution denoted by $\mathfrak{U}_{\text{numeric}}$ and the reference solution $\mathfrak{U}_{\text{reference}}$, following the formula:

$$e_h(\mathfrak{U}) = \frac{||\mathfrak{U}_{\text{numeric}} - \mathfrak{U}_{\text{reference}}||_2}{||\mathfrak{U}_{\text{reference}}||_2}, \quad \text{with} \quad ||\mathfrak{U}||_2 = \left(\sum_{K \in \mathcal{T}_h} \int_K |\mathfrak{U}|^2 \right)^{\frac{1}{2}}.$$

G.7.1 Numerical results in two dimensions

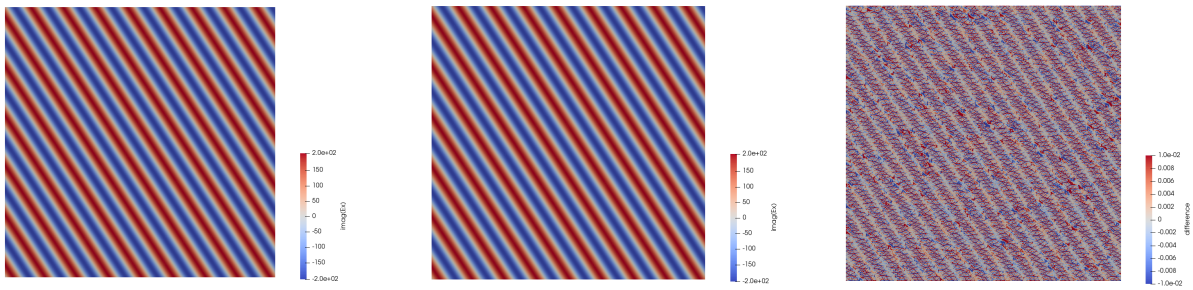

(a) Numerical solution (b) Reference solution (c) Difference

Figure G.2: Propagation of an EM plane wave in a two-dimensional homogeneous medium.

We consider a two-dimensional squared domain $\mathcal{D}$ of size $[0:1000] \times [0:1000]$m. On the boundary of the domain Γ, we first impose the propagation of an EM plane wave, see Section G.1.1, and we solve the electromagnetic equations using the HDG method described in Section G.3. We consider the frequency $f = 3$MHz, and we solve the equations for several meshes and several orders of interpolation of the HDG method. We give in Figure G.2 the result obtained for a mesh composed of 7750 elements and an order of interpolation 4. In this configuration, the relative errors are small: $e_h(E_x) = 5.6e-3$ %, $e_h(E_y) = 4.2e-3$ %, and $e_h(H_z) = 5.78e-2$ %. We plot in Figure G.3 the convergence curves of the method for different orders of interpolation. This shows that the method has an order of convergence equal to $p+1$, which is the optimal order of convergence for the HDG methods.

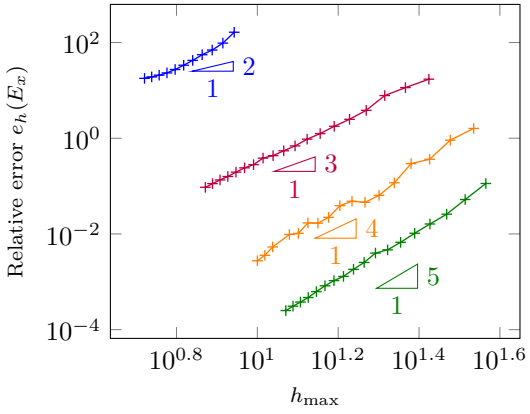

Figure G.3: Convergence curves of HDG method (component u_x) for several orders of interpolation. Results for order 1 are plotted in blue, for order 2 in purple, for order 3 in orange and for order 4 in green.

Next, we consider an infinite two-dimensional domain. We consider a point-source at the coordinate $\boldsymbol{x} = (500, 500)$m. The point-source is modeled as a Dirac distribution, denoted δ, along the x-axis. In the computation, we consider the two truncation methods presented in Sections G.5 and G.6, see Figure G.4.

We present the results for the two truncation methods in Figure G.5. Both the RBC and the PML seem to absorb well the reflections.

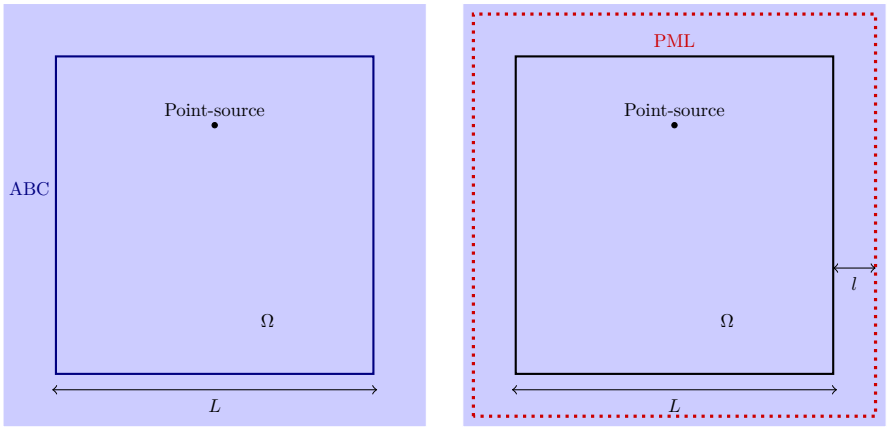

(a) Domain with RBC (b) Domain with PML

Figure G.4: Infinite domain used for the numerical tests, in which we set artificial boundaries, either RBC or PML. In the tests, we have: $L = 1000$m and $l = 100$m.

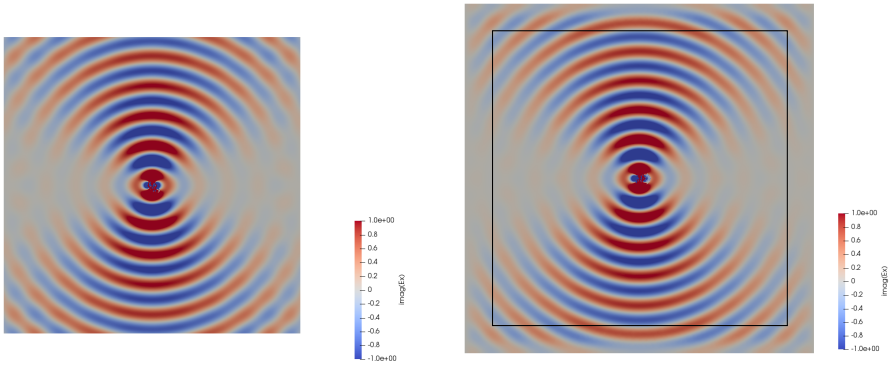

(a) E_x with RBC (b) E_x with PML

Figure G.5: Electric field E_x (V.m^{-1}) for a domain truncated with radiation boundary condition and a domain with PML.

G.7.2 Numerical results in three dimensions

We now move on to the three-dimensional case. We consider a domain $\mathcal{D}$ of size $[0:1000] \times [0:1000] \times [0:200]$m. We impose on the boundary of the domain Γ the propagation of an EM plane wave, see Section G.1.1, and the electromagnetic equations are solved on $\mathcal{D}$ by using the HDG method developed in Section G.3, for several meshes and several orders of interpolation of the HDG method at frequency $f = 1.5$MHz. Figure G.6 shows the result for a mesh composed of 14983 tetrahedra and an order of interpolation 4. The relative errors are small for all components (around 10^{-2} %). We show in Figure G.7 the convergence curves of the method for different orders of interpolation. With the curves, we observe that the method converges with an order $p+1$, which is the optimal order of convergence for the HDG methods.

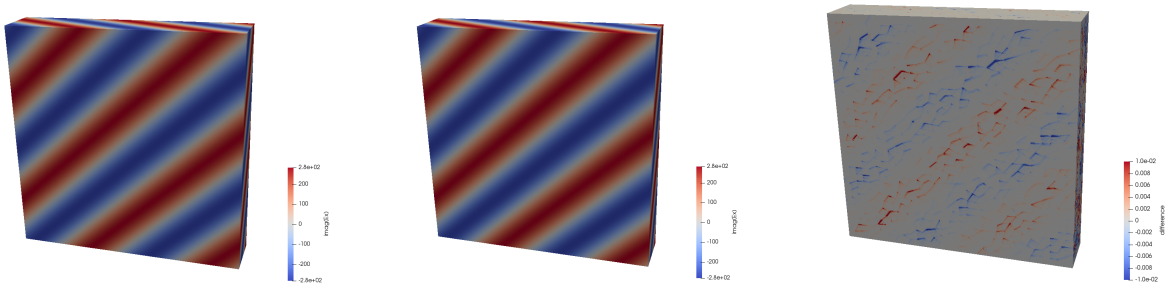

(a) Numerical solution (b) Reference solution (c) Difference

Figure G.6: Propagation of an EM plane wave in a three-dimensional homogeneous medium.

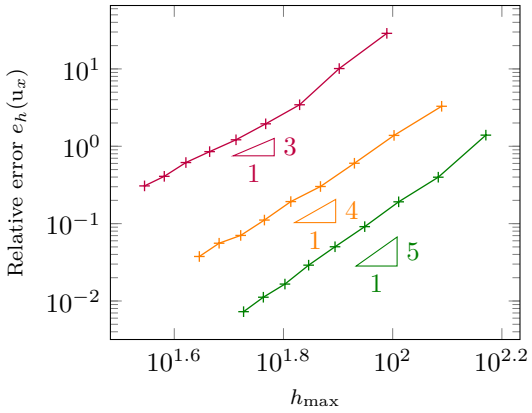

Figure G.7: Convergence curves of HDG method (component u_x) for several orders of interpolation. Results for order 1 are plotted in blue —+—, for order 2 in purple —+—, for order 3 in orange —+— and for order 4 in green —+—.

We now consider an infinite domain, and we use the truncation methods introduced in Sections G.5 and G.6 in the numerical computation. We consider a point-source located at the coordinate $\boldsymbol{x} = (500, 500, 100)$m. The point-source is modeled as a Dirac distribution, denoted δ, along the x-axis. The domain is truncated to the domain Ω, see Figure G.8.

The results for the two truncation methods are given in Figure G.9. This is presented as a clip along the (x, y) plane. There is no visible reflections due to the RBC or the PML.

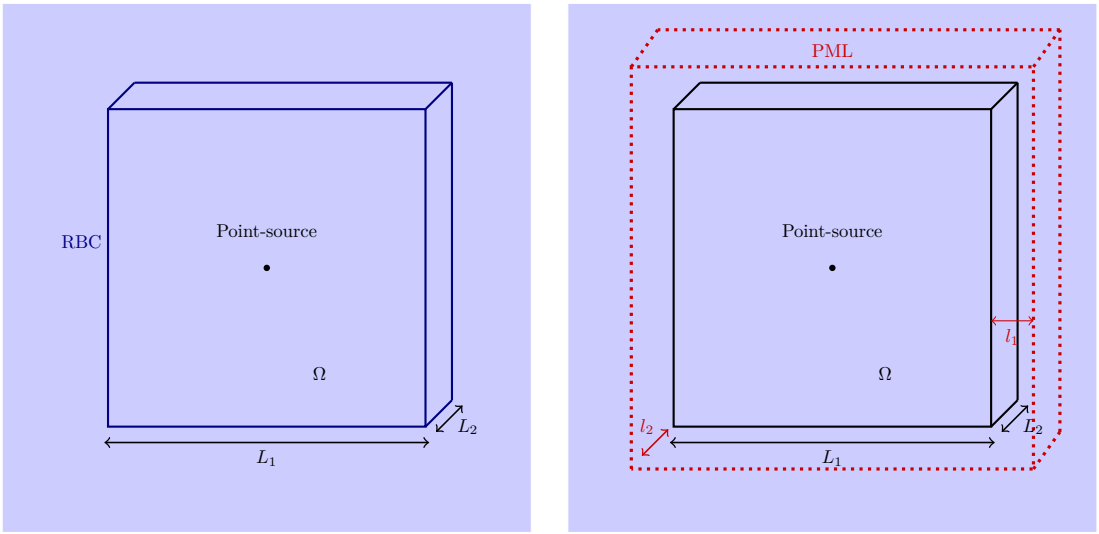

(a) Domain with RBC

(b) Domain with PML

Figure G.8: Infinite domain used for the numerical tests, in which we set artificial boundaries, either RBC or PML. In the tests, we have: $L_1 = 1000\text{m}$, $L_2 = 200\text{m}$, $l_1 = 100\text{m}$ and $l_2 = 20\text{m}$.

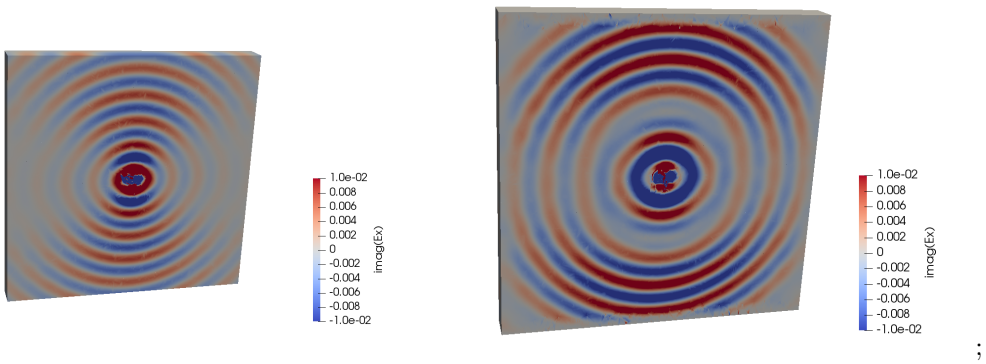

;

(a) E_x with RBC

(b) E_x with PML

Figure G.9: Electric field E_x (V.m^{-1}) for a domain truncated with radiation boundary condition and a domain with PML.

Conclusion

The objective of this thesis was to provide a piece of software for simulating waves in porous conducting media. These waves are governed by Pride's model which is based upon the coupling of Biot's and Maxwell equations. The model is characterized by parameters that depend non linearly on the frequency. Hence, for convenience, the work has been carried out in the frequency regime. All the numerical developments have been hosted by the software Hou10ni, which, at the beginning, was only prepared for solving elastic wave equations with HDG method. The work has been organized around three milestones:

• Definition of a convenient mathematical modeling by constructing analytical solutions that have been of great utility for validating the numerical method. The well-posedness of the solutions has been studied numerically and it has been shown that in presence of viscosity, the problems are well posed while there are some resonances corresponding to specific modes as Jones modes in elasticity when there is no viscosity.

• Development of a HDG formulation for Pride's equations. For this, the first step has been to develop a HDG method for solving Biot's equations in anisotropic porous media. A HDG formulation of Maxwell's equations has also been developed, following existing works. Convergence curves have been obtained for illustrating the optimal order of convergence (p+1) of the methods that guarantee a very good accuracy. It is worth noting that in two dimensions, the HDG formulations are stable in the sense that the condition number of both the global and local matrices stay in a correct range for linear solvers.

• Construction of a radiation boundary conditions (RBC). The RBCs have been constructed from the characterization of outgoing solutions in an infinite domain and are easy to integrate in the HDG formulation. Regarding the computations in truncated domains, we have also considered Perfectly Matched Layers. We have observed that their efficiency is limited with Pride's equations. This is due to the clear difference between the characteristic wavelengths of seismic and electromagnetic waves.

The final achievement of this Ph.D. work is the simulation of converted waves that appear in a conducting porous medium with interfaces. However, it is worth mentioning that the amplitude of the converted waves are small, and hence they can be difficult to detect. This has also been observed experimentally.

This work paves the way to multiple perspectives, whether from a theoretical or numerical point of view:

• Regarding analytical solutions, we have performed a numerical study of the corresponding eigenvalues that raises the interesting question of existing resonances (such as Jones modes) in presence of viscosity or not. Their extension to 3D is not that obvious, due to the difficulty to establish an adequate decomposition into potentials.

• The HDG methods could be improved by computing the HDG fluxes in a more precise way and by automating the values of the stabilization parameters. Another idea could be to consider a HDG+ formulation in which the unknowns are approximated with different polynomial orders [76]. For example, for poroelasticity, one way to do that could be to consider the solid velocity $\mathbf{u}$ and the pressure p in a polynomial space of one degree larger $(p+1)$ than the spaces used for the relative fluid velocity $\mathbf{w}$ and the stress $\boldsymbol{\tau}$ (degree p). The hybrid unknowns would be considered of degree p, which would not modify the size of the global system. In this way, we could obtain a more precise solution for the solid velocity $\mathbf{u}$ and the pressure p with no significant additional cost. This method also requires a precise adjustment of the numerical fluxes.

• Concerning the truncation methods, the performance of the RBC can be improved by increasing its order of approximation. This represents a significant work of development, because the construction of outgoing solutions is difficult.

• The main perspective is about the use of the method for more complex settings, in particular to simulate electrokinetic conversions in three dimensions. We can extend the study carried in the last chapter to three dimensions, but this is quite difficult, due to the large size of the global system that we need to inverse for each frequency. The main problem is that we use a direct solver for the inversion of the matrix, which requires a very large amount of

memory. Hence we need to have access to large computational resources. However, the use of a direct solver is essential, in particular for fields experiments where we consider several sources, where the multi right-hand side functionality of the direct solver MUMPS could be well suited for instance. To improve the performance of the solver in three dimensions, we could study the Block-Low-Range (BLR) functionality, which allows to decrease the memory needed for the inversion of the system.

• The extension to three dimensions could also allow the comparison with physical experiments carried in laboratory, or field experiments, to compare the difference in amplitude. In complex media, with many kinds of materials, we could enhance the strengths of the HDG method, as exploiting p-adaptivity of the method. We could also widen the comparison that we have done with Gar6more [45] to layered domains and compare the results of our code with the semi-analytical software developed by Garambois [62] or the software based upon Spectral Element method (SEM) developed by Morency [97]. The last step towards geophysical exploration will be to integrate the code by using it in an inverse problem software.

Acknowledgments

Experiments presented in this document were carried out using the PlaFRIM experimental testbed, supported by Inria, CNRS (LABRI and IMB), Université de Bordeaux, Bordeaux INP and Conseil Régional d'Aquitaine (see https://www.plafrim.fr/).

This project has received funding from the European Union's Horizon 2020 research and innovation program under the Marie Sklodowska-Curie grant agreement No 777778 (MATHROCKS).

This work has been funded by E2S-UPPA.

Bibliography

[1] T. Akiyoshi, K. Fuchida, and H. Fang, *Absorbing boundary conditions for dynamic analysis of fluid-saturated porous media*, Soil Dynamics and Earthquake Engineering, 13 (1994), pp. 387–397.

[2] T. Akiyoshi, X. Sun, and K. Fuchida, *General absorbing boundary conditions for dynamic analysis of fluid-saturated porous media*, Soil Dynamics and Earthquake Engineering, 17 (1998), pp. 397–406.

[3] P. R. Amestoy, I. S. Duff, J.-Y. L'Excellent, and J. Koster, *A fully asynchronous multifrontal solver using distributed dynamic scheduling*, SIAM Journal on Matrix Analysis and Applications, 23 (2001), pp. 15–41.

[4] E. Anderson, *LAPACK users' guide*, Society for Industrial and Applied Mathematics, Philadelphia, 1999.

[5] F. Assous, P. Degond, E. Heintze, P.-A. Raviart, and J. Segré, *On a finite-element method for solving the three-dimensional maxwell equations*, Journal of Computational Physics, 109 (1993), pp. 222–237.

[6] I. Azpiroz, H. Barucq, R. Djellouli, and H. Pham, *Characterization of partial derivatives with respect to material parameters in a fluid–solid interaction problem*, Journal of Mathematical Analysis and Applications, 465 (2018), pp. 903–927.

[7] H. Barucq, J. Diaz, R.-C. Meyer, and H. Pham, *Analytic solutions and transmission eigenvalues in isotropic poroelasticity for bounded domain, scattering of obstacles and fluid-solid interaction problems in 2D*, Research Report RR-9312, Inria, Dec. 2019.

[8] ——, *Implementation of HDG method for 2D anisotropic poroelastic first-order harmonic equations*, Research Report RR-9326, Inria, Feb. 2020.

[9] ——, *Implementation of HDG method for 2D anisotropic poroelastic first-order harmonic equations*, tech. rep., Inria, 2020.

[10] ——, *Low-order absorbing boundary condition for two-dimensional isotropic poroelasticity*, tech. rep., Inria, 2020.

[11] ——, *Implementation of hybridizable discontinuous Galerkin method for time-harmonic anisotropic poroelasticity in two dimensions*, International Journal for Numerical Methods in Engineering, (2021).

[12] H. Barucq, R. Djellouli, and E. Estecahandy, *On the existence and the uniqueness of the solution of a fluid–structure interaction scattering problem*, Journal of Mathematical Analysis and applications, 412 (2014), pp. 571–588.

[13] H. Barucq, F. Faucher, and H. Pham, *Outgoing solutions to the scalar wave equation in helioseismology*, Research Report RR-9280, Inria Bordeaux Sud-Ouest ; Project-Team Magique3D, August 2019.

[14] J.-P. Bérenger, *A perfectly matched layer for the absorption of electromagnetic waves*, Journal of computational physics, 114 (1994), pp. 185–200.

[15] M. A. Biot, *General solutions of the equations of elasticity and consolidation for a porous material*, Journal of Applied Mechanics, (1956).

[16] ——, *Theory of propagation of elastic waves in a fluid-saturated porous solid. I. Low-frequency range*, The journal of the Acoustical Society of America, 28 (1956), pp. 168–178.

[17] ——, *Theory of propagation of elastic waves in a fluid-saturated porous solid. II. Higher frequency range.*, Journal of the Acoustical Society of America, 28 (1956), pp. 179–191.

[18] ——, *Mechanics of deformation and acoustic propagation in porous media*, Journal of Applied Physics, 33 (1962), pp. 1482–1498.

[19] L. Boillot, *Contributions à la modélisation mathématique et à l'algorithmique parallèle pour l'optimisation d'un propagateur d'ondes élastiques en milieu anisotrope*, PhD thesis, Pau, 2014.

[20] M. Bonnasse-Gahot, *High order discontinuous Galerkin methods for time-harmonic elastodynamics*, theses, Université Nice Sophia Antipolis, Dec. 2015.

[21] M. Bonnasse-Gahot, H. Calandra, J. Diaz, and S. Lanteri, *Hybridizable discontinuous Galerkin method for the 2-D frequency-domain elastic wave equations*, Geophysical Journal International, 213 (2018), pp. 637–659.

[22] E. Bonnetier, F. Triki, and Q. Xue, *An inverse problem for an electroseismic model describing the coupling phenomenon of electromagnetic and seismic waves*, Inverse Problems, 35 (2019), p. 045002.

[23] C. Bordes, L. Jouniaux, S. Garambois, M. Dietrich, J.-P. Pozzi, and S. Gaffet, *Evidence of the theoretically predicted seismo-magnetic conversion*, Geophysical Journal International, 174 (2008), pp. 489–504.

[24] C. Boutin, G. Bonnet, and P.-Y. Bard, *Green functions and associated sources in infinite and stratified poroelastic media*, Geophysical Journal International, 90 (1987), pp. 521–550.

[25] R. Burridge and C. Vargas, *The fundamental solution in dynamic poroelasticity*, Geophysical journal international, 58 (1979), pp. 61–90.

[26] J. M. Carcione, *Wave fields in real media: Wave propagation in anisotropic, anelastic, porous and electromagnetic media*, vol. 38, Elsevier, 3 ed., 2015.

[27] J. M. Carcione, J. E. Santos, and S. Picotti, *Anisotropic poroelasticity and wave-induced fluid flow: harmonic finite-element simulations*, Geophysical Journal International, 186 (2011), pp. 1245–1254.

[28] N. Chaabane and B. Rivière, *A splitting-based finite element method for the Biot poroelasticity system*, Computers & Mathematics with Applications, 75 (2018), pp. 2328–2337.

[29] A. H.-D. Cheng, *Fundamentals of poroelasticity*, Analysis and Design Methods: Comprehensive Rock Engineering: Principles, Practice and Projects, 113 (2014).

[30] A. H.-D. Cheng, *Poroelasticity*, vol. 27, Springer, 2016.

[31] A. Christophe, S. Descombes, and S. Lanteri, *An implicit hybridized discontinuous Galerkin method for the 3d time-domain maxwell equations*, Applied Mathematics and Computation, 319 (2018), pp. 395–408.

[32] B. Cockburn, *Static condensation, hybridization, and the devising of the HDG methods*, in Building bridges: connections and challenges in modern approaches to numerical partial differential equations, Springer, 2016, pp. 129–177.

[33] B. Cockburn, B. Dong, J. Guzmàn, M. Restelli, and R. Sacco, *A Hybridizable Discontinuous Galerkin Method for steady-state convection-diffusion-reaction problems*, SIAM Journal on Scientific Computing, 31 (2009), pp. 3827–3846.

[34] B. Cockburn, J. Gopalakrishnan, and J. Guzmàn, *A new elasticity element made for enforcing weak stress symmetry*, Mathematics of Computation, 79 (2010), pp. 1331–1349.

[35] B. Cockburn, J. Gopalakrishnan, and R. Lazarov, *Unified hybridization of discontinuous Galerkin, mixed, and continuous Galerkin methods for second order elliptic problems*, SIAM Journal on Numerical Analysis, 47 (2009), pp. 1319–1365.

[36] B. Cockburn, F. Li, and C.-W. Shu, *Locally divergence-free discontinuous Galerkin methods for the Maxwell equations*, Journal of Computational Physics, 194 (2004), pp. 588–610.

[37] B. Cockburn and V. Quenneville-Bélar, *Uniform-in-time superconvergence of the HDG methods for the acoustic wave equation*, Mathematics of Computation, 83 (2014), pp. 65–85.

[38] O. Dazel and G. Gabard, *Discontinuous Galerkin methods for poroelastic materials*, Proceedings of Meetings on Acoustics, 19 (2013), p. 065004.

[39] J. de la Puente, M. Dumbser, M. Käser, and H. Igel, *Discontinuous Galerkin methods for wave propagation in poroelastic media*, Geophysics, 73 (2008), pp. T77–T97.

[40] J. de la Puente, M. Dumbser, M. Käser, and H. Igel, *Discontinuous Galerkin methods for wave propagation in poroelastic media*, Geophysics, (2008).

[41] G. Degrande and G. De Roeck, *An absorbing boundary condition for wave propagation in saturated poroelastic media—Part I: Formulation and efficiency evaluation*, Soil Dynamics and Earthquake Engineering, 12 (1993), pp. 411–421.

[42] ——, *An absorbing boundary condition for wave propagation in saturated poroelastic media—Part II: Finite element formulation*, Soil Dynamics and Earthquake Engineering, 12 (1993), pp. 423–432.

[43] A. I. Denneman, G. G. Drijkoningen, D. M. Smeulders, and K. Wapenaar, *Reflection and transmission of waves at a fluid/porous-medium interface*, Geophysics, 67 (2002), pp. 282–291.

[44] J. Diaz, *Approches analytiques et numériques de problèmes de transmission en propagation d'ondes en régime transitoire. Application au couplage fluide-structure et aux méthodes de couches parfaitement adaptées*, PhD thesis, ENSTA ParisTech, 2005.

[45] J. Diaz and A. Ezziani, *Analytical solution for waves propagation in heterogeneous acoustic/porous media. part i: the 2d case*, Communications in Computational Physics, 7 (2010), p. 171.

[46] ——, *Analytical solution for waves propagation in heterogeneous acoustic/porous media. part ii: the 3d case*, Communications in Computational Physics, 7 (2010), pp. 445–472.

[47] V. Dolean, H. Fol, S. Lanteri, and R. Perrussel, *Solution of the time-harmonic Maxwell equations using discontinuous Galerkin methods*, Journal of computational and applied mathematics, 218 (2008), pp. 435–445.

[48] N. Dudley Ward, T. Lähivaara, and S. Eveson, *A discontinuous Galerkin method for poroelastic wave propagation: The two-dimensional case*, Journal of Computational Physics, 350 (2017), pp. 690–727.

[49] M. Dumbser, D. S. Balsara, E. F. Toro, and C.-D. Munz, *A unified framework for the construction of one-step finite volume and discontinuous Galerkin schemes on unstructured meshes*, Journal of Computational Physics, 227 (2008), pp. 8209–8253.

[50] B. Dupuy, L. De Barros, S. Garambois, and J. Virieux, *Wave propagation in heterogeneous porous media formulated in the frequency-space domain using a discontinuous Galerkin method*, GEOPHYSICS, 76 (2011), pp. N13–N28.

[51] E. Estecahandy, *Contribution à l'analyse mathématique et à la résolution numérique d'un problème inverse de scattering élasto-acoustique*, PhD thesis, Pau, 2013.

[52] A. Ezziani, *Mathematical and Numerical modeling of Wave propagation in Viscoelastic and Poroelastic Media*, theses, ENSTA ParisTech, Feb. 2005.

[53] X. Feng, P. Lu, and X. Xu, *A hybridizable discontinuous Galerkin method for the time-harmonic Maxwell equations with high wave number*, Computational Methods in Applied Mathematics, 16 (2016), pp. 429–445.

[54] P. Fernandez, A. Christophe, S. Terrana, N. C. Nguyen, and J. Peraire, *Hybridized discontinuous Galerkin methods for wave propagation*, Journal of Scientific Computing, 77 (2018), pp. 1566–1604.

[55] L. Fezoui, S. Lanteri, S. Lohrengel, and S. Piperno, *Convergence and stability of a discontinuous Galerkin time-domain method for the 3d heterogeneous maxwell equations on unstructured meshes*, ESAIM: Mathematical Modelling and Numerical Analysis, 39 (2005), pp. 1149–1176.

[56] J. Frenkel, *On the theory of seismic and seismoelectric phenomena in a moist soil*, Journal of Engineering Mechanics, 131 (2005), pp. 879–887.

[57] G. Fu, *A high-order HDG method for the Biot's consolidation model*, Computers & Mathematics with Applications, 77 (2019), pp. 237–252.

[58] G. Fu, B. Cockburn, and H. Stolarski, *Analysis of an HDG method for linear elasticity*, International Journal for Numerical Methods in Engineering, 102 (2015), pp. 551–575.

[59] Y. Gao and H. Hu, *Seismoelectromagnetic waves radiated by a double couple source in a saturated porous medium*, Geophysical Journal International, 181 (2010), pp. 873–896.

[60] Y. Gao, F. Huang, and H. Hu, *Comparison of full and quasi-static seismoelectric analytically based modeling*, Journal of Geophysical Research: Solid Earth, 122 (2017), pp. 8066–8106.

[61] Y. Gao, D. Wang, C. Yao, W. Guan, H. Hu, J. Wen, W. Zhang, P. Tong, and Q. Yang, *Simulation of seismoelectric waves using finite-difference frequency-domain method: 2-d SHTE mode*, Geophysical Journal International, 216 (2019), pp. 414–438.

[62] S. Garambois, *Etudes expérimentales et théoriques des conversions d'ondes sismo-électriques dans les milieux poreux superficiels*, PhD thesis, Université Joseph-Fourier-Grenoble I, 1999.

[63] S. Garambois and M. Dietrich, *Seismoelectic wave conversions in porous media: Field measurements and transfer function analysis.*, Geophysics, (2001).

[64] S. Garambois and M. Dietrich, *Full waveform numerical simulations of seismoelectromagnetic wave conversions in fluid-saturated stratified porous media*, Journal of geophysical research, (2002).

[65] G. Giorgiani, S. Fernández-Méndez, and A. Huerta, *Hybridizable discontinuous Galerkin p-adaptivity for wave propagation problems*, International Journal for Numerical Methods in Fluids, 72 (2013), pp. 1244–1262.

[66] P. W. Glover and M. D. Jackson, *Borehole electrokinetics*, The Leading Edge, 29 (2010), pp. 724–728.

[67] R. Griesmaier and P. Monk, *Error analysis for a hybridizable discontinuous Galerkin method for the Helmholtz equation*, Journal of Scientific Computing, 49 (2011), pp. 291–310.

[68] ——, *Discretization of the wave equation using continuous elements in time and a hybridizable discontinuous Galerkin method in space*, Journal of Scientific Computing, 58 (2014), pp. 472–498.

[69] W. Guan and H. Hu, *Finite-difference modeling of the electroseismic logging in a fluid-saturated porous formation*, Journal of computational physics, 227 (2008), pp. 5633–5648.

[70] M. W. Haartsen, W. Dong, and M. Toksöz, *Dynamic streaming currents from seismic point sources in homogeneous poroelastic media*, Geophysical Journal International, 132 (1998), pp. 256–274.

[71] M. W. Haartsen and S. R. Pride, *Electroseismic waves from point sources in layered media*, Journal of Geophysical Research: Solid Earth, 102 (1997), pp. 24745–24769.

[72] S. S. Haines and S. R. Pride, *Seismoelectric numerical modeling on a grid*, Geophysics, 71 (2006), pp. N57–N65.

[73] Q. Han and Z. Wang, *Time-domain simulation of sh-wave-induced electromagnetic field in heterogeneous porous media: A fast finite-element algorithm*, Geophysics, 66 (2001), pp. 448–461.

[74] Y. He, T. Chen, and J. Gao, *Unsplit perfectly matched layer absorbing boundary conditions for second-order poroelastic wave equations*, Wave Motion, 89 (2019), pp. 116–130.

[75] H. Hu and Y. Gao, *Electromagnetic field generated by a finite fault due to electrokinetic effect*, Journal of Geophysical Research: Solid Earth, 116 (2011).

[76] A. Hungria, *Using HDG+ to Compute Solutions of the 3D Linear Elastic and Poroelastic Wave Equations*, PhD thesis, University of Delaware, 2019.

[77] T. Huttunen, J. Kaipio, and P. Monk, *An ultra-weak method for acoustic fluid–solid interaction*, Journal of Computational and Applied Mathematics, 213 (2008), pp. 166–185.

[78] L. Jouniaux and T. Ishido, *Electrokinetics in earth sciences: a tutorial*, International Journal of Geophysics, 2012 (2012).

[79] L. Jouniaux and F. Zyserman, *A review on electrokinetically induced seismo-electrics, electro-seismics, and seismo-magnetics for earth sciences*, Solid Earth, 7 (2016), pp. 249–284.

[80] G. Kanschat and B. Riviere, *A Finite Element Method with strong mass conservation for Biot's linear consolidation model*, Journal of Scientific Computing, 77 (2018), pp. 1762–1779.

[81] R. M. Kirby, S. J. Sherwin, and B. Cockburn, *To CG or to HDG:a comparative study*, Journal of Scientific Computing, 51 (2012), pp. 183–212.

[82] V. D. Kupradze, *Three-dimensional problems of elasticity and thermoelasticity*, vol. 25, Elsevier, 2012.

[83] G. Lefeuve-Mesgouez, A. Mesgouez, G. Chiavassa, and B. Lombard, *Semi-analytical and numerical methods for computing transient waves in 2d acoustic/poroelastic stratified media*, Wave Motion, 49 (2012), pp. 667–680.

[84] G. I. Lemoine, M. Y. Ou, and R. J. LeVeque, *High-resolution finite volume modeling of wave propagation in orthotropic poroelastic media*, SIAM Journal on Scientific Computing, 35 (2013), pp. B176–B206.

[85] L. Li, S. Lanteri, and R. Perrussel, *Numerical investigation of a high order hybridizable discontinuous Galerkin method for 2d time-harmonic Maxwell's equations*, COMPEL - The international journal for computation and mathematics in electrical and electronic engineering, 32 (2013), pp. 1112–1138.

[86] L. Li, S. Lanteri, and R. Perrussel, *A class of locally well-posed hybridizable discontinuous Galerkin methods for the solution of time-harmonic maxwell's equations*, Computer Physics Communications, 192 (2015), pp. 23–31.

[87] L. Li, S. Lanteri, and R. Perussel, *A hybridizable discontinuous Galerkin method combined to a Schwarz algorithm for the solution of 3d time-harmonic maxwell's equation*, Journal of computational physics, (2014).

[88] X. Li, D. Yao, and R. W. Lewis, *A discontinuous Galerkin finite element method for dynamic and wave propagation problems in non-linear solids and saturated porous media*, International Journal for Numerical Methods in Engineering, 57 (2003), pp. 1775–1800.

[89] A. Lozinski, *A primal discontinuous Galerkin method with static condensation on very general meshes*, Numerische Mathematik, 143 (2019), pp. 583–604.

[90] M. Markov, *Low-frequency Stoneley wave propagation at the interface of two porous half-spaces*, Geophysical Journal International, 177 (2009), pp. 603–608.

[91] P. A. Martin, *Multiple scattering: interaction of time-harmonic waves with N obstacles*, no. 107, Cambridge University Press, 2006.

[92] J. A. Martínez, S. Imperiale, P. Joly, and J. Rodríguez, *Solving 2D linear isotropic elastodynamics by means of scalar potentials: a new challenge for finite elements*, Journal of Scientific Computing, 77 (2018), pp. 1832–1873.

[93] V. Mattesi, M. Darbas, and C. Geuzaine, *A high-order absorbing boundary condition for 2d time-harmonic elastodynamic scattering problems*, Computers & Mathematics with Applications, 77 (2019), pp. 1703–1721.

[94] J. C. Maxwell, *A treatise on electricity and magnetism*, vol. 1, Oxford: Clarendon Press, 1873.

[95] L. B. Monachesi, F. I. Zyserman, and L. Jouniaux, *An analytical solution to assess the SH seismoelectric response of the vadose zone*, Geophysical Journal International, 213 (2018), pp. 1999–2019.

[96] L. Monforte, P. Navas, J. M. Carbonell, M. Arroyo, and A. Gens, *Low-order stabilized finite element for the full Biot formulation in soil mechanics at finite strain*, International Journal for Numerical and Analytical Methods in Geomechanics, 43 (2019), pp. 1488–1515.

[97] C. Morency, *Electromagnetic wave propagation based upon spectral-element methodology in dispersive and attenuating media*, Geophysical Journal International, 220 (2020), pp. 951–966.

[98] C. Morency and J. Tromp, *Spectral-element simulations of wave propagation in porous media*, Geophysical Journal International, 175 (2008), pp. 301–345.

[99] C.-C. Mow and Y.-H. Pao, *Diffraction of elastic waves and dynamic stress concentrations*, RAND, 1971.

[100] M. N'Diaye, *On the study and development of high-order time integration schemes for ODEs applied to acoustic and electromagnetic wave propagation problems*, PhD thesis, Université de Pau et des pays de l'Adour, 2017.

[101] N. C. Nguyen, J. Peraire, and B. Cockburn, *High-order implicit hybridizable discontinuous Galerkin methods for acoustics and elastodynamics*, Journal of Computational Physics, 230 (2011), pp. 3695–3718.

[102] ——, *Hybridizable discontinuous Galerkin methods for the time-harmonic maxwell's equations*, Journal of Computational Physics, 230 (2011), pp. 7151–7175.

[103] F. Olver, A. Olde Daalhuis, D. Lozier, B. Schneider, R. Boisvert, C. Clark, B. Miller, B. Saunders, H. Cohl, and e. M.A. McClain, *NIST Digital Library of Mathematical Functions*. http://dlmf.nist.gov/, Release 1.0.24 of 2019-09-15.

[104] C. Pain, J. Saunders, M. Worthington, J. Singer, W. Stuart-Bruges, G. Mason, and A. Goddard, *A mixed finite-element method for solving the poroelastic biot equations with electrokinetic coupling*, Geophysical Journal International, 160 (2005), pp. 592–608.

[105] Pride, *Governing equations for the coupled elctromagnetics and acoustics of porous media*, American Physical Society, (1994).

[106] S. R. Pride, *Governing equations for the coupled electromagnetics and acoustics of porous media*, Physical Review B, 50 (1994), p. 15678.

[107] ——, *Relationships between seismic and hydrological properties*, in Hydrogeophysics, Springer, 2005, pp. 253–290.

[108] S. R. Pride, A. F. Gangi, and F. D. Morgan, *Deriving the equations of motion for porous isotropic media*, The Journal of the Acoustical Society of America, (1992).

[109] S. R. Pride and S. Garambois, *Electroseismic wave theory of frenkel and more recent developments*, Journal of Engineering Mechanics, 131 (2005), pp. 898–907.

[110] S. R. Pride and M. W. Haartsen, *Electroseismic wave properties*, The Journal of the Acoustical Society of America, 100 (1996), pp. 1301–1315.

[111] S. R. Pride and F. D. Morgan, *Electrokinetic dissipation induced by seismic waves*, Geophysics, (1991).

[112] H. Ren, Q. Huang, and X. Chen, *A new numerical technique for simulating the coupled seismic and electromagnetic waves in layered porous media*, Earthquake Science, 23 (2010), pp. 167–176.

[113] A. Revil, A. Jardani, P. Sava, and A. Haas, *The Seismoelectric Method: Theory and Application*, John Wiley & Sons, 2015.

[114] C. Rodrigo, X. Hu, P. Ohm, J. Adler, F. Gaspar, and L. Zikatanov, *New stabilized discretizations for poroelasticity and the Stokes' equations*, Computer Methods in Applied Mechanics and Engineering, 341 (2018), pp. 467–484.

[115] J. E. Santos, *Finite element approximation of coupled seismic and electromagnetic waves in fluid-saturated poroviscoelastic media*, Numerical Methods for Partial Differential Equations, 27 (2011), pp. 351–386.

[116] M. Schakel and D. Smeulders, *Seismoelectric reflection and transmission at a fluid/porous-medium interface*, The Journal of the Acoustical Society of America, 127 (2010), pp. 13–21.

[117] M. Schakel, D. Smeulders, E. Slob, and H. Heller, *Laboratory measurements and theoretical modeling of seismoelectric interface response and coseismic wave fields*, Journal of Applied Physics, 109 (2011), p. 074903.

[118] M. Schanz, *Wave propagation in viscoelastic and poroelastic continua: a boundary element approach*, Springer, Berlin; London, 2011.

[119] C. Schwarzbach, *Stability of finite element solutions to maxwell's equations in frequency domain*, (2009).

[120] T. B. A. Senior and J. L. Volakis, *Approximate boundary conditions in electromagnetics*, Institution of Electrical Engineers, London, 1995.

[121] Q. Serra, M. Ichchou, and J.-F. Deü, *Wave properties in poroelastic media using a Wave Finite Element Method*, Journal of Sound and Vibration, 335 (2015), pp. 125–146.

[122] K. Shukla, J. S. Hesthaven, J. M. Carcione, R. Ye, J. de la Puente, and P. Jaiswal, *A nodal discontinuous Galerkin finite element method for the poroelastic wave equation*, Computational Geosciences, 23 (2019), pp. 595–615.

[123] E. Slob and M. Mulder, *Seismoelectromagnetic homogeneous space green's functions*, Geophysics, 81 (2016), pp. F27–F40.

[124] S. C. Soon, B. Cockburn, and H. K. Stolarski, *A hybridizable discontinuous Galerkin method for linear elasticity*, International Journal for Numerical Methods in Engineering, 80 (2009), pp. 1058–1092.

[125] I. Terrasse, *Résolution mathématique et numérique des équations de Maxwell instationnaires par une méthode de potentiels retardés*, PhD thesis, Palaiseau, Ecole polytechnique, 1993.

[126] M. Tohti, Y. Wang, E. Slob, Y. Zheng, X. Chang, and Y. Yao, *Seismoelectric numerical simulation in 2d vertical transverse isotropic poroelastic medium*, Geophysical Prospecting, 68 (2020), pp. 1927–1943.

[127] K. N. van Dalen, G. Drijkoningen, and D. Smeulders, *On wavemodes at the interface of a fluid and a fluid-saturated poroelastic solid*, The Journal of the Acoustical Society of America, 127 (2010), pp. 2240–2251.

[128] H. M. W and S. R. Pride, *Electroseismic waves from point sources in layered media*, Journal of American Geophysical Union, (1997).

[129] S. Warden, S. Garambois, L. Jouniaux, D. Brito, P. Sailhac, and C. Bordes, *Seismoelectric wave propagation numerical modelling in partially saturated materials*, Geophysical Journal International, 194 (2013), pp. 1498–1513.

[130] G. Wei, Y. Ze-Xin, and H. Heng-Shan, *Finite-difference modeling of seismoelectric logs*, Chinese Journal of Geophysics - Chines Edition, 60 (2017), pp. 4516–4526.

[131] F. Wenzlau and T. M. Müller, *Finite-difference modeling of wave propagation and diffusion in poroelastic media*, Geophysics, 74 (2009), pp. T55–T66.

[132] B. S. White and M. Zhou, *Electroseismic prospecting in layered media*, SIAM Journal on Applied Mathematics, 67 (2006), pp. 69–98.

[133] L. C. Wilcox, G. Stadler, C. Burstedde, and O. Ghattas, *A high-order discontinuous galerkin method for wave propagation through coupled elastic–acoustic media*, Journal of Computational Physics, 229 (2010), pp. 9373–9396.

[134] Q. Xue, *Mathematical and numerical study of the inverse problem of electro-seismicity in porous media*, PhD thesis, Université Grenoble Alpes, 2017.

[135] K. S. Yee and J. S. Chen, *The finite-difference time-domain (fdtd) and the finite-volume time-domain (fvtd) methods in solving maxwell's equations*, IEEE Transactions on Antennas and Propagation, 45 (1997), pp. 354–363.

[136] Y. Zeng, J. He, and Q. Liu, *The application of the perfectly matched layer in numerical modeling of wave propagation in poroelastic media*, Geophysics, 66 (2001), pp. 1258–1266.

[137] C. Zhi-Wen, W. Ke-Xie, H. Heng-Shan, and S. Jian-Guo, *Acousto-electric well logging by eccentric source and extraction of shear wave*, Chinese Physics, 16 (2007), p. 746.

[138] F. I. Zyserman, P. M. Gauzellino, and J. E. Santos, *Finite element modeling of SHTE and PSVTM electroseismics*, Journal of applied geophysics, 72 (2010), pp. 79–91.

[139] F. I. Zyserman, L. Jouniaux, S. Warden, and S. Garambois, *Borehole seismoelectric logging using a shear-wave source: possible application to CO2 disposal?*, International Journal of Greenhouse Gas Control, 33 (2015), pp. 89–102.

Abstract

We consider the time-harmonic waves propagation in poroelastic and conducting poroelastic media. The poroelastic materials are composed of an elastic solid frame and pores filled with fluid. Wave propagation in poroelastic materials is described by Biot's model. In geophysical media, due to the polarization of the fluid in the pores, we can observe the conversions between electromagnetic and seismic fields, which are called electrokinetic effects and are modeled using Pride's equations, a coupling between Maxwell's and Biot's equations. The electrokinetic coupling has been observed in natural geophysical media both in laboratory experiments and on the field. The converted waves are very interesting because they are heavily sensitive to the medium properties, and the seismoelectric conversions could for example help to locate interfaces in the material that seismic waves could not detect. The characterization of poroelastic or conducting poroelastic media is complex and involves many physical parameters. Some of these parameters depend non-linearly on the frequencies. In addition, the seismic and electromagnetic velocities are significantly different, which is complicated to handle for time domain simulations. Hence, we have chosen to solve the equations in the frequency domain and to use a Fourier transform to generate the seismograms in time domain. The main drawback to this is that we must invert one global linear system for each frequency, and this has a large computational cost because of the complexity of the equations and hence the high number of unknowns. We present the development and implementation of a HDG method for solving the poroelastic, the electromagnetic and Pride's equations. We validate the code in two dimensions in circular geometry thanks to analytical solutions that we have developed. Using these analytical solutions, we will show that the methods have an optimal order of convergence. In addition, to extend the method to infinite domains, we propose new radiation boundary condition for poroelastic equations and electrokinetic equations. We also use Perfectly Matched Layers. Finally, we present results of the electrokinetic conversions in time domain.

Résumé

Dans cette thèse, nous étudions la propagations d'ondes dans des milieux poroélastiques et poro-conducteurs. Les matériaux poroélastiques sont composés d'un squelette solide élastique et de pores remplis de fluide. La propagation des ondes dans les matériaux poroélastiques est décrite par le modèle de Biot. Dans les milieux géophysiques, en raison de la polarisation du fluide dans les pores, nous pouvons observer des conversions entre les champs électromagnétiques et sismiques. C'est ce qu'on appelle effets électrocinétiques, modélisés par le système d'équations de Pride, qui est écrit comme le couplage entre les équations de Maxwell et de Biot. Le couplage électrocinétique a été observé dans les milieux géophysiques naturels à la fois dans des expériences de laboratoire et sur le terrain. Les ondes converties sont intéressantes car elles sont très sensibles aux propriétés du milieu, et les conversions sismoélectriques pourraient par exemple aider à localiser des interfaces que les ondes sismiques ne pourraient pas détecter. La caractérisation des milieux poroélastiques ou poro-conducteurs est complexe et fait intervenir de nombreux paramètres physiques. Certains de ces paramètres dépendent de la fréquence de manière non linéaire. De plus, les vitesses sismiques et électromagnétiques sont fortement différentes, ce qui est compliqué à gérer pour les simulations dans le domaine temporel. Nous avons donc choisi de résoudre les équations dans le domaine fréquentiel et d'utiliser une transformée de Fourier pour générer des sismogrammes dans le domaine temporel. Le principal inconvénient de cette méthode est que nous devons inverser un système linéaire global pour chaque fréquence, ce qui entraîne un coût de calcul important en raison de la complexité des équations et donc du nombre élevé d'inconnues. Nous présentons le développement et l'implémentation d'une méthode HDG pour résoudre les équations poroélastiques, électromagnétiques et de Pride. Nous validons le code en deux dimensions en géométrie circulaire grâce aux solutions analytiques que nous avons développées. En utilisant ces solutions analytiques, nous montrons que les méthodes ont un ordre de convergence optimal. De plus, afin d'étendre la méthode aux domaines infinis, nous proposons de nouvelles conditions aux limites de radiation pour les équations poroélastiques et les équations électrocinétiques. Nous utilisons également des couches parfaitement adaptées (PML). Enfin, nous présentons les résultats des conversions électrocinétiques dans le domaine temporel.